ECAMP 12

12th European Conference on
Atoms Molecules and Photons

Extended Abstracts

Frankfurt am Main, Germany
September 5th to 9th, 2016

Photon Entanglement: Fundamentals and Applications

Anton Zeilinger
Austrian Academy of Sciences & University of Vienna

Abstract for the 12th European Conference on Atoms, Molecules and Photons (ECAMP 12)

After the discovery by Einstein, Podolsky and Rosen [1] that quantum mechanics is at variance with local realism and locality, John Bell [2] had found that some predictions of quantum mechanics are actually in contradiction with the local-realistic viewpoint. Many experiments followed, confirming more and more the quantum predictions, but some loopholes had been left open. That is, in experiments, assumptions were necessary to make them valid tests of Bell's theorem. In the last year, four experiments were performed [3, 4, 5, 6] which closed significant loopholes. I will report on these experiments and also give an outlook for the future. This will include experiments over increasingly large distances and experiments involving cosmic sources of randomness.

Besides such fundamental experiments, an interesting development is the realization that quantum entanglement can be used as a resource in quantum communication. Besides entanglement-based quantum cryptography, a very likely application in the future will be the use of entanglement swapping to connect future quantum computers. In the talk, I will also comment on some of the experimental and technological challenges.

Citations

[1] A. Einstein, B. Podolsky and N. Rosen, *Can Quantum-Mechanical Description of Physical Reality Be Considered Complete?*, Phys. Rev. **47**, 777 (1935).

[2] J. Bell, *On the Einstein Podolsky Rosen Paradox*, Physics **1**, 195–200 (1964).

[3] B. Hensen, H. Bernien, A. E. Dréau, A. Reiserer, N. Kalb, M. S. Blok, J. Ruitenberg, R. F. L. Vermeulen, R. N. Schouten, C. Abellán, W. Amaya, V. Pruneri, M. W. Mitchell, M. Markham, D. J. Twitchen, D. Elkouss, S. Wehner, T. H. Taminiau and R. Hanson, *Loophole-free Bell inequality violation using electron spins separated by 1.3 kilometres*, Nature **526**, 682–686 (2015).

[4] L. K. Shalm, E. Meyer-Scott, B. G. Christensen, P. Bierhorst, M. A. Wayne, M. J. Stevens, T. Gerrits, S. Glancy, D. R. Hamel, M. S. Allman, K. J. Coakley, S. D. Dyer, C. Hodge, A. E. Lita, V. B. Verma, C. Lambrocco, E. Tortorici, A. L. Migdall, Y. Zhang, D. R. Kumor, W. H. Farr, F. Marsili, M. D. Shaw, J. A. Stern, C. Abellán, W. Amaya, V. Pruneri, T. Jennewein, M. W. Mitchell, P. G. Kwiat, J. C. Bienfang, R. P. Mirin, E. Knill and S. W. Nam, *Strong Loophole-Free Test of Local Realism*, Phys. Rev. Lett. **115**, 250402 (2015).

[5] M. Giustina, M. A. M. Versteegh, S. Wengerowsky, J. Handsteiner, A. Hochrainer, K. Phelan, F. Steinlechner, J. Kofler, J.-Å. Larsson, C. Abellán, W. Amaya, V. Pruneri, M. W. Mitchell, J. Beyer, T. Gerrits, A. E. Lita, L. K. Shalm, S. W. Nam, T. Scheidl, R. Ursin, B. Wittmann and A. Zeilinger, *Significant-Loophole-Free Test of Bell's Theorem with Entangled Photons*, Phys. Rev. Lett. **115**, 250401 (2015).

[6] W. Rosenfeld, D. Burchardt, R. Garthoff, M. Krug, N. Ortegel, M. Rau, K. Redeker and H. Weinfurter, presentation at the PQE 2016 conference, Snowbird, Utah, USA (2016).

Sputtering of Fe surfaces by D and Ar ions

R. Stadlmayr, D. Blöch, B. M. Berger, S. Kaser, D. Mayer and F. Aumayr
Institute of Applied Physics, TU Wien, Fusion@ÖAW, Wiedner Hautpstraße 8-10, E134, 1040 Vienna, Austria

The lifespan of plasma facing materials highly depends on the plasma induced erosion caused by ion bombardment. Due to this bombardment the surface gets sputtered and surface modifications are the consequence. These modifications can appear e.g. as a change in the surface compositions (preferential sputtering) or as quasi-periodic height modulations which are often called "ripples" [1-3].

We investigated the erosion of 400 nm thick Fe films deposited onto polished quartz crystals under impact of mono-energetic D and Ar ion projectiles (500 eV/atom and 250 eV/atom). The experiments were performed at 465 K using a highly sensitive quartz crystal microbalance (QCM) technique [4]. The evolution of the mass change rate of the Fe model films under D and Ar ion irradiation was investigated under a specific angle of incident (0° - 70°) and as a function of the ion fluence. After predefined fluence steps, AFM investigations were performed, to investigate the change in surface morphology (for an example see fig 1.) and to correlate it with the observed fluence dependce of the measured erosion yield.

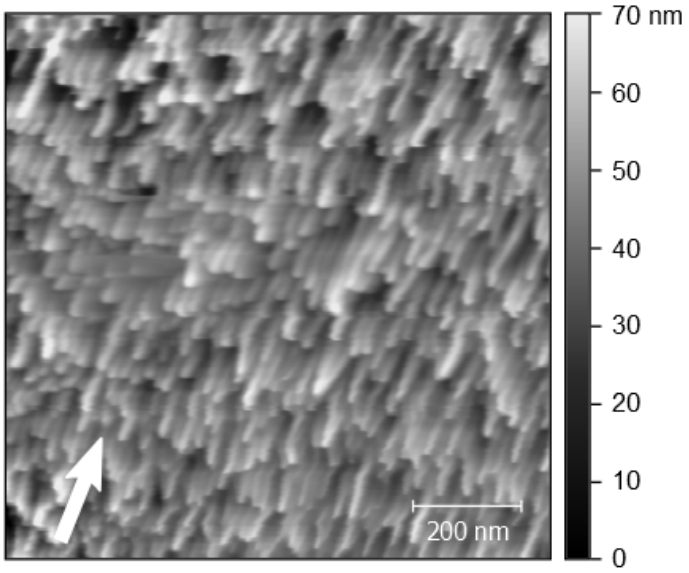

Fig. 1 AFM image of an Fe model film (contianing 1.5 at% W) after irradiation with 250 eV/D D projectiles under 60° angle (with respect to the surface normal, the white arrow indicates the direction of the ion beam on the surface) up to a fluence of $3{\cdot}10^{23}$ D/m^2. The observed structures are similar to the ones reported in ref. [2], called Perpendicular Mode Ripples (PeMR).

References

[1] S. Facsko, T. Dekorsy, C. Koerdt, C. Trappe, H. Kurz, A. Vogt, H. L. Hartnagel. *Formation of Ordered Nanoscale Semiconductor Dots by Ion Sputtering* Science **285** (1999) 1551

[2] T. Skeren, K. Temst, W. Vandervorst and A. Vantomme, *Ion-induced roughening and ripple formation on polycrystalline metallic films*, New J. Phys. **15**(2013) 093047

[3] M.A. Makeev and A.L. Barabasi, *Effect of surface morphology on the sputtering yields. II. Ion sputtering from rippled surfaces*, Nucl. Instr. Meth. B **222**(2004) 335

[4] G. Hayderer, M. Schmid, P. Varga, HP. Winter, and F. Aumayr., *A highly sensitive quartz-crystal microbalance for sputtering investigations in slow ion–surface collisions*, Rev. Sci. Instrum. **70** (1999) 3696

Density Functional Theory study on the adsorption of acrylonitrile, acrylamide and acrolein on Cu(100): importance of weak interactions.

Fernando Aguilar-Galindo[1], Sergio Díaz-Tendero[1, 2], Manuel Alcamí[1, 3]

1. *Departamento de Química.Universidad Autónoma de Madrid, Madrid E-28049 (Spain)*
2. *Condensed Matter Physics Center (IFIMAC) Universidad Autónoma de Madrid (Spain)*
3. *Instituto Madrileño de Estudios Avanzados en Nanociencia, Cantoblanco (Spain)*

The Density Functional Theory (DFT) has been widely used in the study of isolated molecules in the gas phase and in the solid state with great success. However, the main interactions in the adsorption processes of organic molecules on metal surfaces are the dispersion forces, as the Van der Waals forces (see e.g.[1]), which are not included in the most popular functionals (as PBE, PW91 or B3LYP). Several ways to take into account these forces have been developed, as the Grimme D2[2] and D3[3] corrections, or the inclusion of the interactions explicitly in the functional, proposed by Dion et al[4].
In this communication, we present a DFT study of the adsorption of three molecules with high technological importance as acrylonitrile, acrylamide and acrolein on a metallic surface, Cu(100). We compare the results obtained using some of these alternatives to treat the dispersion and we analyze their effects on the different functional groups of these molecules.
The way the molecules are adsorbed on the surface and the strength and nature of this interaction are important aspects to predict the behaviour of these systems in processes as the formation of self-assembling monolayers or heterogeneous catalysis.

References

[1] K. Berland, V. R. Cooper, K. Lee, E. Schröder, T. Thonhauser, P. Hyldgaard and B. I. Lundqvist: Rep. Prog. Phys. 2015, **78**:066501
[2] S. Grimme: J. Comp. Chem. 2006, **27**:1787-1799.
[3] S. Grimme, J. Antony, S. Ehrlich and S. Krieg: J. Chem Phys. 2010, **132**:154104
[4] M. Dion, H. Rydberg, E. Schröder, D. C. Langreth and B. I. Lundqvist: Phys. Rev. Lett. 2004, **92**,246401

Quantum interference between virtual paths in laser-dressed helium: Energetic-electron impact excitation

H. Agueny[1], A. Makhoute[2], A. Dubois[3], and L. Kocbach[1]
1.Department of Physics and Technology, Allegt. 55, University of Bergen, N-5007 Bergen, Norway
2.Physique du Rayonnement et des Interactions Laser-Matière, Faculté des Sciences.
Université Moulay Ismail, B.P. 11201, Zitoune, Meknes, Morocco
3.Sorbonne Universités, UPMC Univ Paris 06, CNRS, Laboratoire de Chimie Physique-Matière et Rayonnement,
F-75231 Paris Cedex 05, France

The scattering processes of electrons on atoms in the presence of a laser field, also called laser-assisted electron-atom scattering, have long been recognized as an useful tool to make evident the multiphoton signals. The characteristic that distinguishes this class of elementary collision physics is the presence of the laser photon, which plays a role of a "third body", in addition to the electron projectile and target atom. In this context, electronic transitions induced by a laser field can lead to new effects, which may emerge in the angular distribution of the scattered electron [1].

In the conference we shall present a study of quantum interference in energetic electron-impact excitation of helium atom embedded in a resonant low-frequency laser field. The process under investigation is dealt with a nonperturbative approach based on Born-Floquet method [2,3]. Under the framework of this approach, the dressed atomic states are first obtained via the Floquet theory. The incoming and scattered dressed-electron projectile are described using non-relativistic Volkov solutions; while their interactions with the target are treated within the first Born approximation. Here, we will show that the observed peak in the angular distribution of the scattered electron (cf. Fig. 1) is a signature of quantum interference between different virtual pathways that the excitation may follow in order to end up in a common final channel. These findings are supported by additional calculations based on Kroll-Watson approximation and perturbation theory, in which no quantum interferences are accounted for.

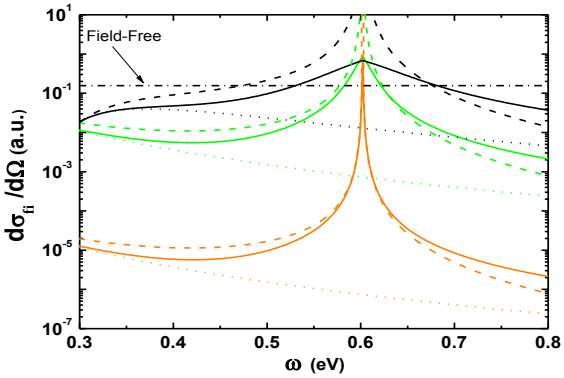

Figure 1: (Color online) Differential cross sections of the excitation of the dressed and field-free states $1s2s$ for one-photon emission (i.e., photon transferred between the colliding system and laser field) as a function of the photon energy ω. The incoming electron energy is fixed at 50 eV, the scattering angle is 0.3°, and the polarization of the laser field is kept along the momentum transfer. The results are shown for three peak intensities: 2 10^{10} W/cm^2 (Black color), 10^9 W/cm^2 (Green color) and 10^6 W/cm^2 (Orange color). Solid lines: Born-Floquet theory. Dashed lines: Perturbation theory. Dotted lines: Kroll-Watson approximation. Dot-dashed lines: Field-free calculations.

References

[1] H. Agueny, A. Makhoute, A. Dubois, and L. Kocbach *Dynamic Stark effect induced coherent mixture of virtual-paths in laser-dressed helium: Energetic electron-impact excitation*, submitted to Phys. Rev. A.
[2] H. Agueny, A. Makhoute, A. Dubois, I. Ajana, and G. Rahali, *Laser-assisted inelastic scattering of electrons by helium atoms*, Phys. Rev. A **92**, 013423 (2015).
[3] M. Dörr, C. J. Joachain, R. M. Potvliege, and S. Vučić, *Born-Floquet theory of laser-assisted electron-atom collisions*, Phys. Rev. A **49**, 4852 (1994).

The broadening and narrowing of the high gain parametric down conversion spectrum

P.R. Sharapova[1,2], O.V. Tikhonova[1,3], A.M.Perez[4], M.V.Chekhova[1,4], G. Leuchs[4]

1. Physics Department, Lomonosov Moscow State University, 119991, Moscow, Russia,
2. Department of Physics University of Paderborn Warburger Straße 100 D-33098 Paderborn Germany
3. Skobeltsyn Institute of Nuclear Physics, Lomonosov Moscow State University, Leninskie Gory, 1, 119234, Moscow, Russia
4. Max-Planck Institute for the Science of Light, Guenther-Scharowsky-Str. 1 / Bau 24, Erlangen D-91058, Germany

The Bright Squeezed Vacuum (BSV) is macroscopic non-classical state of light which can be created in the high gain parametric down conversion process. The BSV is very promising object for different application of quantum optics and quantum information due to its non-classical features such as macroscopic correlations, huge photon number per mode, noise reduction below the standard quantum limit etc. That's why such state of light requires of the correct theoretical description.

Such attempts were made by different theoretical groups and represent by itself the solution of integro-differential equations [1-3] or analytical solution in terms of the Schmidt modes [4,5] but with some restrictions. The analytical Schmidt modes approach allows one to explain many features of BSV, including different correlation characteristics, intensity profile and narrowing of the spectrum with increasing of parametric gain in scheme with two non-linear crystals and air gap between them (spatial domain) or two non-linear crystals and group velocity dispersive medium between them (frequency domain). But due to some restrictions the description of the broadening of the single crystal spectrum with increasing of pump power, which is well known experimental effect, never can be done by such approach. In contradiction, the solution of integro-differential equations catches the effect of the single spectrum broadening but can not explain the narrowing process.

In this work we present the method based on the exact numerical solution of the systems of integro-differential equations for the plane wave and frequency operators. Such method is general, did not contain any assumptions and allows one to explain simultaneously the broadening of the single crystal spectrum and the narrowing of the spectrum in two crystal configuration case with air (group velocity dispersion medium) gap between them. The calculation was performed for the spatial and frequency domain, all obtained results are in the good agreement with an experimental data.

References

[1] B. Dayan, Phys. Rev. A **76**, 043813 (2007)
[2] A.Christ, B.Brecht, W.Mauerer and Christine Silberhorn, "Theory of quantum frequency conversion and type-II parametric down-conversion in the high-gain regime", New Journ. of Phys. **15**, 053038 (2013)
[3] E. Brambilla, A.Gatti, M.Bache and L.A. Lugiato, "Simultaneous near-field and far-field spatial quantum correlations in the high-gain regime of parametric down-conversion", Phys. Rev. A **69**, 023802 (2004)
[4]PR Sharapova, AM Perez, OV Tikhonova, MV Chekhova, *Physical Review A* **91**, (2015) 043816
[5]AM Perez, T Sh Iskhakov, P Sharapova, S Lemieux, OV Tikhonova, MV Chekhova, G Leuchs, *Optics Letters* **39**, 2403-2406, (2014)

Electron Localization in Dissociating H_2^+ by Retroaction of a Photoelectron onto Its Source

Markus Waitz[1], Derya Aslitürk[1], Natascha Wechselberger[1], Haramrit K. Gill[1], Jonas Rist[1], Florian Wiegandt[1], Christoph Goihl[1], Gregor Kastirke[1], Miriam Weller[1], Tobias Bauer[1], Daniel Metz[1], Felix P. Sturm[1,3], Jörg Voigtsberger[1], Stefan Zeller[1], Florian Trinter[1], Gregor Schiwietz[2], Thorsten Weber[3], Joshua B. Williams[1], Markus S. Schöffler[1], Lothar Ph. H. Schmidt[1], Till Jahnke[1], and Reinhard Dörner[1]

1. Institut für Kernphysik, J. W. Goethe Universität, Max-von-Laue-Straße 1, 60438 Frankfurt, Germany

2. Helmholtz-Zentrum Berlin für Materialien und Energie, Institut G-ISRR, Hahn-Meitner-Platz 1, 14109 Berlin, Germany

3. Chemical Sciences Division, Lawrence Berkeley National Laboratory, Berkeley, California 94720, USA

We investigate the dissociation of H_2^+ into a proton and a H^0 after single ionization with photons of an energy close to the threshold. We find that the p^+ and the H^0 do not emerge symmetrically in case of the H_2^+ dissociating along the $1s\sigma_g$ ground state. Instead, a preference for the ejection of the p^+ in the direction of the escaping photoelectron can be observed, corresponding to a positive asymmetry parameter $\delta = \frac{n_p - n_H}{n_p + n_H}$ (see figure below). n_p and n_H are the count rate for break of the p-H bond with the proton towards and opposite to the electron respectively. Thus, $\delta > 0$ corresponds to the case of the proton emerging in the same hemisphere as the electron.

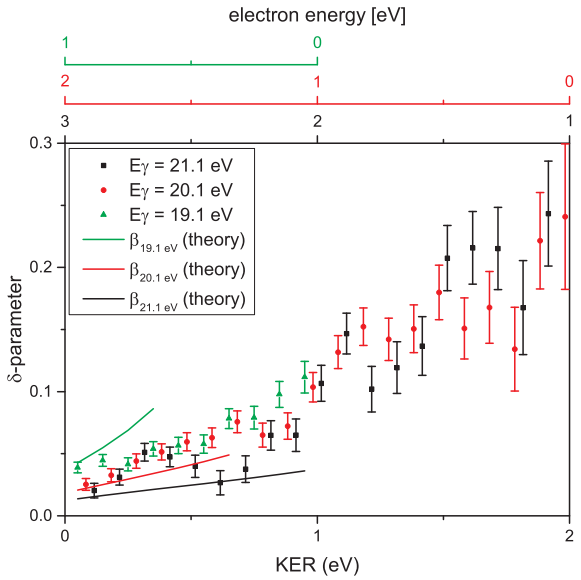

Fig. 1 The asymmetry parameter δ as a function of kinetic energy release KER for three different photon energies. Experiment: $E_\gamma = 19.1$ eV (green triangles), 20.1 eV (red circles) and 21.1 eV (black squares). Lines: corresponding predictions from [1], color coding as for the experiment. The theoretical curves are shown for $E_e > 2 * KER$ as the validity range of the calculation is $E_e >> KER$.

The observed symmetry breaking is strongest for very small electron energies. Our experiment is consistent with a recent prediction by Serov and Kheifets [1]. In their model, which treats the photoelectron classically, the symmetry breaking is induced by the retroaction of the long range Coulomb potential onto the dissociating H_2^+.

References

[1] Vladislav Serov and Anatoli S. Kheifets, *p-H symmetry breaking in dissociative photoionization of H_2 due to the molecular ion interacting with the ejected electron*, Phys. Rev. A **89**, 031402 (2014).

On fullerene anions as sources of spin-polarized electrons

Valeriy K. Dolmatov
Department of Physics and Earth Science, University of North Alabama, 35632 Florence, Alabama, U.S.A.

Production of spin-polarized electron beams is an important problem from the point of view of both basic and applied sciences. The present work provides a rough insight into spin-polarization of photoelectrons due to photodetachment of fullerene anions, C_n^-. It is predicted that, and interpreted why, the degree of spin-polarization of the photoelectron flux can be large, even 100%, depending on the photon frequency ω.

To meet the goal, a fullerene cage C_n is modelled by an attractive spherical potential of certain depth U_0, inner radius r_0 and thickness Δ (see, e.g., [1]). A fullerene anion is then formed due to binding of the electron by this potential into a $n\ell$-state. To evaluate spin-polarization of $n\ell$-photoelectrons from such modelled fullerene anions, the study exploits the Cherepkov's theory [2] of spin polarization of photoelectrons ejected from atoms with a single electron in the outer $n\ell$-subshell with $\ell \geq 1$ and a definite total angular momentum $j = \ell \pm 1/2$. According to [2], the angular-dependent cross section $I_j(\omega,\theta,\mu)$ of emission of a $n\ell$-photoelectron with a definite value of the spin projection μ on the direction of the angular momentum of a circularly polarized photon is given by

$$I_j(\omega,\theta,\mu) = [\sigma^j_{\rm tot}(\omega)/8\pi]\{1+(\boldsymbol{es})A_j(\omega) - [\beta(\omega)/2+(\boldsymbol{es})\gamma_1(\omega)]P_2(cos\theta)\}, \quad (1)$$

where $\boldsymbol{s}$ and $\boldsymbol{e}$ are unit vectors directed along the electron spin and photon polarization, respectively, $\sigma^j_{\rm tot}(\omega)$ is the total photodetachment cross section, $\beta(\omega)$ is the dipole photoelectron angular-asymmetry parameter, $\gamma_1(\omega)$ is due to accounting for electron spin polarization, $A_j(\omega)$ is the total angle-integrated degree of spin polarization of the electron flux and θ is the angle between the momenta of the photon (directed along the Z-axis) and photoelectron.

In the present study, calculations are performed for $2p$-photodetachment of fullerene anions C_n^- ($n = 60$, 240 and 540). A significant resonance enhancement of the photoelectron spin polarization along with its drastic change with increasing size of C_n^- is unravelled. This is exemplified by figure 1, where calculated $A_j(\omega)$ for $2p_{1/2}$-photodetachment of $C^-_{60}(2p_{j=1/2})$ and $C^-_{540}(2p_{j=1/2})$ is plotted. The photoelectron flux is seen to become 100% spin-polarized ($A_j = 1$) regardless of the direction of motion, at some resonance peaks. The resonances are due to a standing photoelectron wave formed inside the C_n cage-resonator known as "confinement resonances" [1].

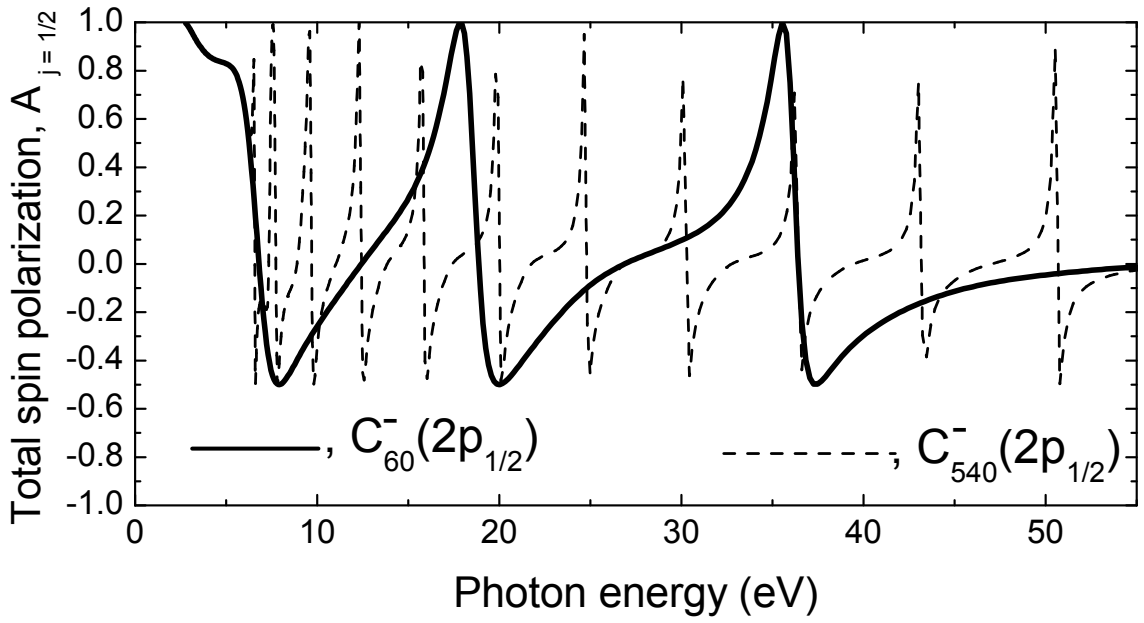

Fig. 1 Calculated angle-integrated degree of spin polarization of the photoelectron flux, $A_j(\omega)$, upon $2p_{1/2}$-photodetachment of $C^-_{60}(2p_{1/2})$ ($r_0 = 5.262$, $U_0 = 0.2958$ and $\Delta = 2.9102$ a.u.) and $C^-_{540}(2p_{1/2})$ ($r_0 = 5.262$, $U_0 = 0.404$ and $\Delta = 2.9102$ a.u.).

The support of NSF under the grant No. PHY-1305085 and a travel grant from CAS at UNA are acknowledged.

References

[1] V. K. Dolmatov, A. S. Baltenkov, J. P. Connerade, and S. T. Manson, *Structure and photoionization of confined atoms*, Radiat. Phys. Chem. **70**, 417 (2004).
[2] N. A. Cherepkov, *Angular distribution of photoelectrons with a given spin orientation*, Sov. Phys. - JETP **38**, 463 (1974).

Stepwise Contraction of the nf Rydberg Shells in the 3d Photoionization of Multiply-Charged Xenon Ions

Stefan Schippers[1,2], Alexander Borovik Jr.[1,2], Ticia Buhr[3], Jonas Hellhund[2], Kristof Holste[1], A. L. David Kilcoyne[4], Stephan Klumpp[5], Michael Martins[5], Alfred Müller[2], Sandor Ricz[6], and Stephan Fritzsche[7,8]

1. I. Physikalisches Institut, Justus-Liebig-Universität Gießen, 35392 Giessen, Germany
2. Institut für Atom- und Molekülphysik, Justus-Liebig-Universität Gießen, 35392 Giessen, Germany
3. Physikalisch-Technische Bundesanstalt, 38116 Braunschweig, Germany
4. Advanced Light Source, MS 7-100, Lawrence Berkeley National Laboratory, Berkeley, California 94720, USA
5. Institut für Experimentalphysik, Universität Hamburg, 22761 Hamburg, Germany
6. Institute for Nuclear Research, Hungarian Academy of Sciences, Debrecen, H-4001, Hungary
7. Helmholtz-Institut Jena, 07743 Jena, Germany
8. Theoretisch-Physikalisches Institut, Friedrich-Schiller-Universität Jena, 07743 Jena, Germany

Recently, first low-resolution results for 3d multiple photoionization of Xe^{q+} ($1 \le q \le 5$) from the photon-ion spectrometer PIPE at the Hamburg PETRA III synchrotron light source have been reported [1]. Here, new high-resolution measurements with an experimental energy spread of 160 meV are presented for $3 \le q \le 5$ [2] (Fig. 1). Pronounced resonance structures are observed for all ions but with an increasing number of resonances as the charge state of the ions is increased. In contrast to the usually rather complex cross sections for outer shell ionization of atoms and ions, the present inner-shell ionization cross sections can be interpreted straight-forwardly. The strongest resonances are associated with the photoexcitation of a $3d$ electron to an atomic nf subshell ($n = 4,5,6,...$) and the subsequent multiple autoionization of the associated hole states. The $3d_{3/2}^{-1} - 3d_{5/2}^{-1}$ fine structure splitting (~ 13 eV) of the $3d$ hole leads to two distinct Rydberg series of resonances in each spectrum. For Xe^{3+}, for example, resonances with principal quantum numbers n from 4 to 7 can be clearly discerned. For Xe^{5+} the series of nf resonances could be observed up to $n = 9$. This progression of resonance structure with increasing charge state clearly visualizes the re-ordering of the εf continuum into a regular series of (bound) Rydberg orbitals as the ionic core becomes more attractive. The energies and strengths of the resonances are extracted from the experimental data and are further analyzed by relativistic atomic-structure calculations.

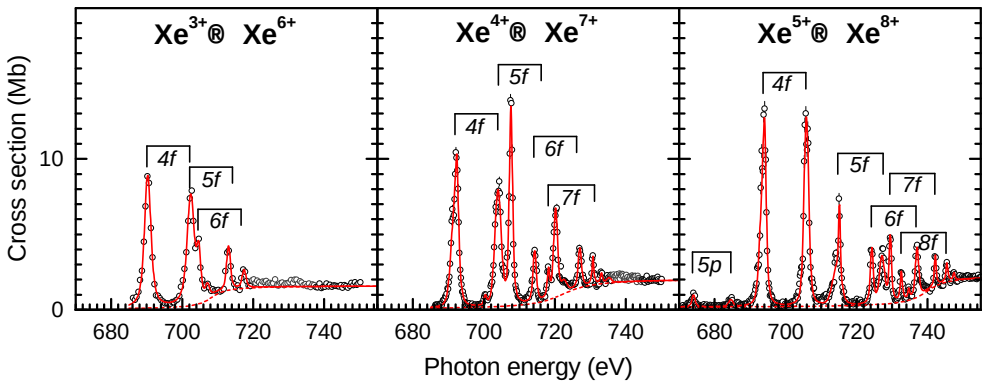

Fig. 1 Measured (symbols) and fitted (full lines) absolute cross sections for triple ionization of Xe^{3+}, Xe^{4+}, and Xe^{5+} ions. Resonances are labeled by the $n\ell$ subshell to where the $3d$ electron is excited.

References

[1] S. Schippers, S. Ricz, T. Buhr, A. Borovik Jr., J. Hellhund, K. Holste, K. Huber, H.-J. Schäfer, D. Schury, S. Klumpp, K. Mertens, M. Martins, R. Flesch, G. Ulrich, E. Rühl, T. Jahnke, J. Lower, D. Metz, L. P. H. Schmidt, M. Schöffler, J. B. Williams, L. Glaser, F. Scholz, J. Seltmann, J. Viefhaus, A. Dorn, A. Wolf, J. Ullrich, and A. Müller, *Absolute cross sections for photoionization of Xe^{q+} ions ($1 \le q \le 5$) at the 3d ionization threshold (J. Phys. B Highlight 2014)*, J. Phys. B **47**, 115602 (2014).

[2] S. Schippers, A. Borovik Jr., T. Buhr, J. Hellhund, K. Holste, A. L. D. Kilcoyne, S. Klumpp, M. Martins, A. Müller, S. Ricz, and S. Fritzsche, *Stepwise contraction of the nf Rydberg shells in the 3d photoionization of multiply-charged xenon ions (J. Phys. B Highlight 2015)*, J. Phys. B **48**, 144003 (2015).

Dissociative ionization of H_2 by 400 eV circularly polarized photons

Vladislav Serov[1] **and Anatoli Kheifets**[2]
1. Department of Theoretical Physics, Saratov State University, 83 Astrakhanskaya, Saratov 410012, Russia
2. Department of Theoretical Physics, Australian National University, Canberra ACT 2601, Australia

Single photoionization of H_2 becomes dissociative via a small overlap of the Frank-Condon region with the dissociative continuum of the H_2^+ ion. This allows to determine the photoelectron angular distribution (PAD) in the molecular frame by detecting the photoelectrons in coincidence with the dissociating fragments. Such a measurement may reveal the same interference and delocalization effects that were studied previously in the naturally dissociative double photoionization [1,2]. In the present work, we consider ionization-dissociation process $\hbar\omega + H_2 \to e^- + H + p$ by high-energy circularly polarized photons $\hbar\omega = 400$ eV. Such experiments have been conducted recently at the PETRA III synchrotron radiation source [3]. Particular emphasis in these experiments was on the role of the electron recoil on the nuclear motion and a possible breaking of the p – H symmetry in PAD. To elucidate these effects, a full account for the nuclear motion has to be included in our theoretical model [4].

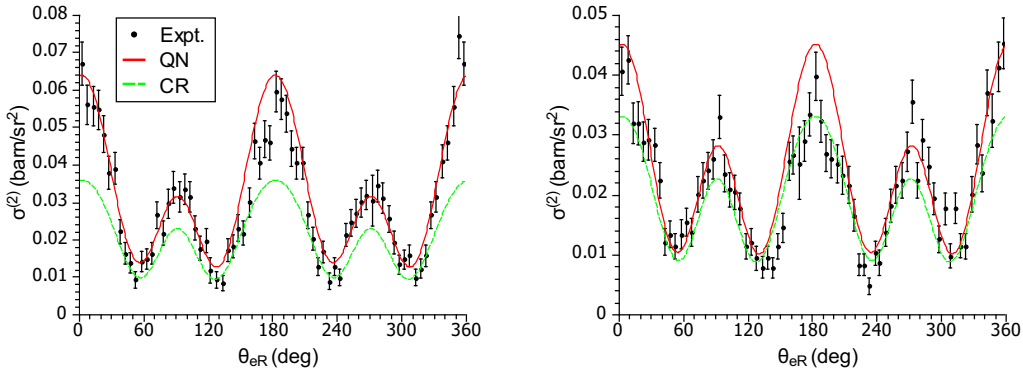

Fig. 1 The angle-averaged differential cross-section integrated over KER in the ranges of 0-0.2 eV (left) and 0.4-0.8 (right) are plotted as functions of the electron detection angle θ_{eR} measured relative to the molecular axis. The experimental data are shown with error bars. The theoretical results with quantum description of the nuclear motion (QN) are displayed with solid lines while the classical reflection (CR) calculations are visualized with dashed lines.

In our earlier work [4], we reported the PAD for the fully determined kinematics in which both the electron ejection angles and the kinetic energy release (KER) were fixed. However, in the experiment [3], to increase the count rate, both the electrons and protons were discriminated in energy within a finite range of KER and detected within the angular cone of 20°. To account for these experimental conditions, we calculate the differential cross-section integrated over KER $\sigma^{(2)} = \int_{E_1}^{E_2} \frac{d^3\sigma}{dE_R d\Omega_e d\Omega_R} dE_R$ and averaged over electron and proton ejection directions within a window of 20°. In Fig. 1, the samples of our new results are shown in comparison with the experimental data [3]. The experimental data, originally on an arbitrary scale, are normalized to the best visual fit to the theoretical curves. The two sets of calculations are shown. One is with a correct Quantum description of the Nuclear motion (QN). In another calculation, the nuclear motion is described within the Classical Reflection (CR) model. The experimental data clearly discriminate between these two calculations. The experiment is much closer to the QN calculation which takes into account the effect of the electron recoil on the nuclear motion in comparison with the CR calculation which does not account for this effect.

References

[1] D. Akoury *et al*, *The simplest double slit: Interference and entanglement in double photoionization of H_2*, Science **318**, 949 (2007).
[2] K. Kreidi *et al*, *Interference in the collective electron momentum in double photoionization of H_2*, Phys. Rev. Lett. **100**, 133005 (2008).
[3] Markus Waitz and Reinhard Dörner, private communication (2015).
[4] V. V. Serov and A. S. Kheifets, *Dissociative ionization of H2 by 400 eV circularly polarized photons*, J. Phys. B **47**, 115006 (2014).

Bound-free electron transitions in the H + H^- quasi-molecules

Alla Dadonova[1]***, Alexander Devdariani***[1,2]
1. Department of Theoretical Physics and Astronomy, A.I.Herzen University, St.Petersburg 191186, Russia
2. Department of Optics and Spectroscopy, St.Petersburg University, St.Petersburg 198904, Russia

The processes of photo-detachment or ionization of stable molecules are widely investigated in modern atomic physics. But the present work deals with the calculation of the photo-detachment cross-sections in the case of negative quasi-molecules formed during collisions. We took the reaction $H+H^-+\hbar\omega \to H+H+e$ as an example of bound-free transitions in single-active-electron quasi-molecules. For simplicity, we discuss the one-dimensional case in the frame of the zero-range potential model [1,2].

The cross-section of photo-detachment is proportional to the density of oscillator strengths:

$$\sigma(\omega) = \frac{2\pi^2}{c}\frac{df_{bc}}{d\omega} = \frac{4\pi^2}{c}\omega_{bc}\left|X_{bc}\right|^2. \tag{1}$$

The matrix element

$$X_{bc} = \int \langle \Psi_b \left|x\right| \Psi_c \rangle \, dx. \tag{2}$$

In the LCAO approximation quasimolecular gerade and ungerade wave functions in the frame of the zero-range potentials model are written as

$$\Psi_b^{gu} = \sqrt{\alpha_u}\left[exp(-\alpha_u\left|x+R/2\right|) \pm exp(-\alpha_u\left|x-R/2\right|)\right], \tag{3}$$

$$\Psi_c^{gu} = \frac{1}{\sqrt{2\pi k}}\left[sin(k\left|x+R/2\right|) \pm sin(k\left|x-R/2\right|)\right]. \tag{4}$$

Then the matrix element dipole moments can be expressed by the formula:

$$X_{b=g,c=u} = \sqrt{\frac{\alpha_u k}{\pi}}\frac{\alpha_u}{\omega^2}cos^2\left(\frac{kR}{2}\right) + \sqrt{\frac{\alpha_u}{\pi k}}\frac{\alpha_u R}{4\omega}sin\left(kR\right), \tag{5}$$

$$X_{b=u,c=g} = \sqrt{\frac{\alpha_u k}{\pi}}\frac{\alpha_u}{\omega^2}sin^2\left(\frac{kR}{2}\right) - \sqrt{\frac{\alpha_u}{\pi k}}\frac{\alpha_u R}{4\omega}sin\left(kR\right), \tag{6}$$

where $\omega = (\alpha_u^2 + k^2)/2$, that is the sum of the binding energy and kinetic energy of the free electron.

Although the quasi-molecular matrix elements increase with increasing R it does not lead to difficulties at large R. In this case potential energy curves $U_u = U_g$, and it is obligatory to use the sum of amplitudes of two different ways of detachment [1].

Collisions result in a lowering of the threshold of the electron detachment compared with the single ion H^- because ungerade quasi-molecular term is repulsive.

References

[1] Devdariani A.Z. *Radiative transitions in quasi-molecules,* Opt.spektr. **119(3)**, 333-337 (2015).
[2] Demkov Yu.N., Ostrovskii V.N. *Zero-Range Potentials and Their Applications in Atomic Physics,* Plenum Pub Corp, 288 (1988).

Laser polarization effects in laser-assisted electron-hydrogen inelastic collisions

Gabriela Buica

Institute of Space Sciences-INFLPR, P.O. Box MG-23, Ro 77125, Bucharest-Măgurele, Romania

buica@spacescience.ro

The purpose of this work is to study the laser polarization effects in *inelastic* scattering of fast electrons by hydrogen atoms in the presence of a circularly polarized (CP) laser field. We consider the excitation of hydrogen to an arbitrary state accompanied by one- and two-photon absorption. It is important to evaluate the contribution of the laser-assisted *inelastic* electron-atom scattering to the total electron energy spectrum since in experimental studies it might be quite difficult to separate the signal of elastic and inelastic scattering channels.[1]

Because the scattering process under investigation is a very complex problem, the theoretical approach presents considerable difficulties and several assumptions are made. (i) Moderate field strengths below 10^7 V/cm and fast projectile electrons are considered in order to safely neglect the second-order Born approximation in the scattering potential as well the exchange scattering.[2] (ii) The interaction between the projectile electrons and the laser field is described by a Gordon-Volkov wave function. (iii) The dressing of the hydrogen atom by the laser field, i.e., the modification of the target atom in the laser field, is described within the first-order time-dependent perturbation theory in the field.[3] Using the approach described for linearly polarized (LP) fields[4,5] we have obtained an *analytical formula* for the differential cross section (DCS) in the laser-assisted inelastic e-H($1s$) scattering that is valid for both circular and linear polarization. We analyze the angular distributions and the resonance structure of the DCSs for the excitation of the $n = 2$ and $n = 4$ subshells and we discuss the influence of the laser polarization on the angular distribution of the scattered electrons.

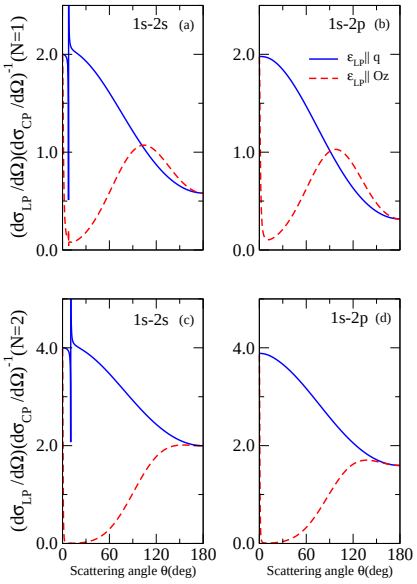

Figure 1: Ratios of the DCSs by the $\mathbf{LP}_{z(q)}$ and $\mathbf{CP}_x$ fields for *inelastic* laser assisted scattering, e(E_i)+H($1s$) +$N\omega$ $\rightarrow$ e(E_f)+H($2l$), with the excitation of the $2l$ subshells as a function of the scattering angle for $N = 1$ in (a) and (b), and $N = 2$ in (c) and (d). The full lines represent the results for $\mathbf{LP}_q$, while the dashed lines denote the $\mathbf{LP}_z$ fields.

We focus our discussion on three particular laser field polarizations denoted as: (a) $\mathbf{CP}_x$, where the laser beam is circularly polarized in the (y, z)-scattering plane and the laser beam propagates in the x-axis direction, $\boldsymbol{\varepsilon}_{\boldsymbol{CP_x}} = (\mathbf{e}_y + i\mathbf{e}_z)/\sqrt{2}$, (b) $\mathbf{LP}_q$, where the laser beam is linearly polarized and the polarization vector is parallel the momentum transfer vector $\boldsymbol{q}$, $\boldsymbol{\varepsilon}_{\boldsymbol{LP_q}} \parallel \mathbf{q}$, and (c) $\mathbf{LP}_z$, where the laser beam is linearly polarized with the polarization vector is parallel to the z-axis, $\boldsymbol{\varepsilon}_{\boldsymbol{LP_z}} = \mathbf{e}_z$. A comparison between the linear and circular polarizations of the laser field is made for the excitation of the $2l$ subshells and important differences appear between the angular distributions of DCSs depending on the type of polarization. In Figure 1 we show the ratios of the DCSs with excitation of the $2s$ and $2p$ subshells by the LP and CP fields for one- and two-photon absorption as a function of the scattering angle θ. The DCSs are calculated at the incident projectile energy of 200 eV, the laser field strength $\mathcal{E}_0 = 10^7$ V/cm, the photon energy 2 eV, and the azimuthal angle $\varphi = 90^\circ$. Depending of the laser parameters, projectile energies, and scattering geometry the CP scattering signal can be larger than the LP signal.

[1] C. J. Joachain, N. J. Kylstra, and R. M. Potvliege, Atoms in Intense Laser Fields (Cambridge University Press, UK) (2012).

[2] F. W. Byron Jr. and C. J. Joachain, Electron-atom collisions in a strong laser field, *J. Phys. B,* **17**, L295 (1984).

[3] V. Florescu and T. Marian, First-order perturbed wave functions for the hydrogen atom in a harmonic uniform external electric field, *Phys. Rev. A,* **34**, 4641 (1986).

[4] A. Cionga and V. Florescu, One-photon excitation in the e-H collision in the presence of a laser field, *Phys. Rev. A,* **45**, 5282 (1992).

[5] G. Buica, Inelastic scattering of electrons by metastable hydrogen atoms in a laser field, *Phys. Rev. A,* **92**, 033421 (2015).

Photo-dissociation Dynamics of Laser-Aligned Halogenated Organic Molecules.

E.Savelyev[1], R. Boll[1], K. Amini [2], L. Christensen[3], F. Brauße[4], B. Erk[1], C. Bomme[1], N. Berrah[5], S. Düsterer[1], H. Höppner[1], P. Johnsson[6], T. Kierspel[1,7], F. Krecinic[4], E. Müller[1], M. Müller[8], T. Mullins[1,7], P. Rudawski[6], N. Schirmel[1], J. Thorgersen[3], S. Toleikis[1], R. Treusch[1], S. Trippel[1,7], A. Ulmer[8], J. Wiese[1,7], A. Rouzée[4], J. Küpper[1,7], A. Lauer[2], M. Burt[2], A. Rudenko[9], H. Stapelfeldt[3], M. Brouard[2], S. Techert[1,10], D. Rolles[1,9]

1. *Deutsches Elektronen Synchrotron (DESY), 22607 Hamburg, Germany*
2. *Department of Chemistry, University of Oxford, United Kingdom*
3. *Aarhus University, 8000 Aarhus C, Denmark*
4. *Max-Born-Institut, 12489 Berlin, Germany*
5. *University of Connecticut, Storrs, CT 06269, USA*
6. *Department of Physics, Lund University, 22100 Lund, Sweden*
7. *Center for Free-Electron Laser Science (CFEL), DESY, 22607 Hamburg, Germany*
8. *Technical University of Berlin, 10623 Berlin, Germany*
9. *J.R. Macdonald Laboratory, Kansas State University, Manhattan, KS 66506, USA*
10. *Georg-August-University Göttingen, 37073 Göttingen, Germany*

Complex molecular systems are one of the next steps in future technology. To be able to control single molecules, we need to understand processes occurring on the molecular-atomic scale. For this purpose the charge transfer in the molecule is important for understanding the bond breaking and atomic dynamics in the molecule.

To this end, we have performed an experiment at FLASH using the CAMP endstation in order to investigate the UV-induced dissociation of various halogenated hydrocarbon molecules, such as iodomethane (CH_3I) and 2,6 difluoroiodobenzene ($C_6H_3F_2I$, DFIB). The target molecules were prepared as a cold supersonic molecular beam, and adiabatically aligned with a Nd:YAG laser. Inner-shell photoionization of the halogen atom is used as probe. To provide the necessary temporal resolution, we sorted our data according to the FLASH "beam arrival monitor" (BAM) and used a "timing-tool" downstream of the experiment to perform a direct measurement of the relative arrival time of the FEL and optical pulses. We present the time-resolved kinetic energy distributions of various iodine fragments as well as time-resolved photoelectron angular distributions of laser-aligned, dissociating DFIB molecules measured with a double-sided Velocity Map Imaging (VMI) spectrometer.

Time resolved radial distributions of triply charged iodine fragments reveal different kinetic energy dynamics. From that information the charge transfer dynamics between the iodine and the rest fragment can be observed together with Coulomb explosion dynamics.

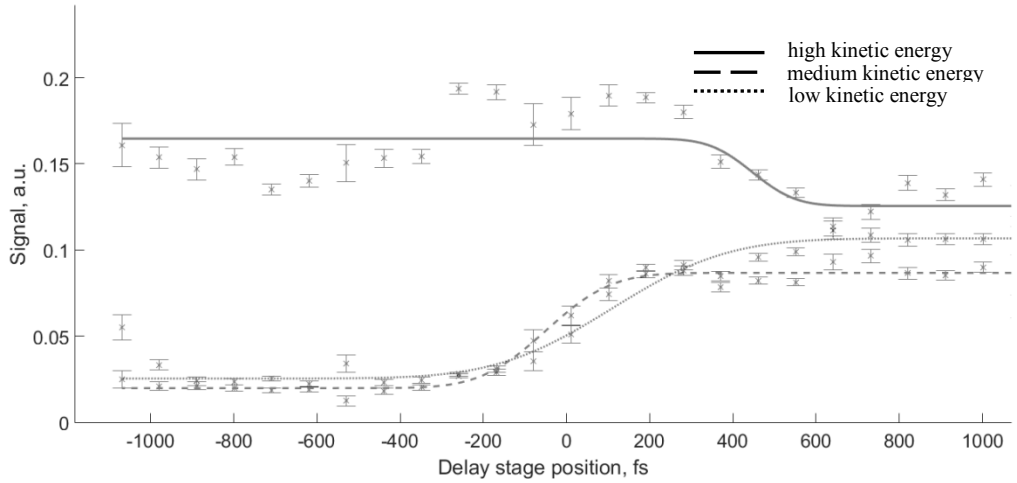

Fig. 1 Preliminary data on the dynamics of three distinct kinetic-energy channels of triply charged iodine occurring after the photo-dissociation of DFIB. The low-kinetic energy channel occurs when charge transfer between the iodine fragment and the residual molecule is no longer allowed for large distances between the fragments. The high-kinetic energy channel represents the total signal of Coulomb explosion of non-pumped molecules. The nature of the medium-kinetic energy channel is still to be clarified.

Comparing Coulomb explosion dynamics of triply charged OCS after soft x-ray initiated direct and Auger ionization processes

Ali Ramadhan[1], Benji Wales[1], Yiming Cai[1], Isabelle Gauthier[2], Reza Karimi, Mike MacDonald[2], Lucia Zuin[2], Joseph Sanderson[1]

1. Department of Physics and Astronomy, University of Waterloo, 200 University Ave W, Waterloo, Ontario, Canada N2L 3G1

2. Canadian Light Source, 44 Innovation Boulevard, Saskatoon, Saskatchewan, Canada S7N 2V3

3 Department of Energy Engineering and Physics, Amirkabir University of Technology 424 Hafez Avenue Tehran, Iran 15875-4413

Soft X-rays (90-173 eV) from the 3rd generation Canadian Light Source [1] have been used in conjunction with a multi coincidence time and position sensitive detection apparatus to observe the dissociative ionization of OCS. By varying the X-ray energy, we can compare dynamics from direct (90eV) and Auger ionization [2] (173eV) processes and access ionization channels which result in two or three body breakup, from 2+ to 4+ ionization states. We make several new observations for the 3+ state such as kinetic energy release limited by photon energy, and using Dalitz plots we can see evidence of timescale effects between the direct and Auger ionization process for the first time.

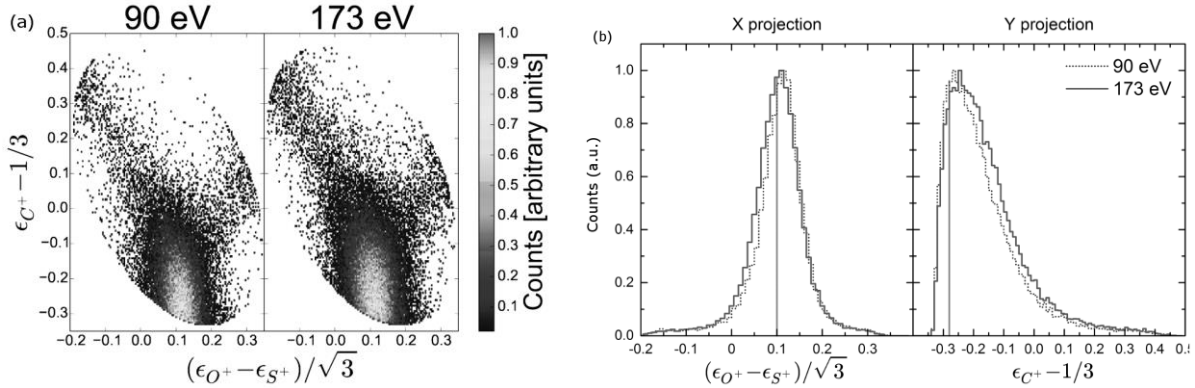

Fig. 1 (a) Dalitz plots for the (1,1,1) fragmentation channel of OCS^{3+}. The x-axis indicates the difference between the fraction of total energy released by the O and S ions, and the y-axis is the fraction of energy released by the C ion. The projections onto the x and y-axes are plotted in (b). The vertical lines in (b) indicate the expected peak value for Coulombic breakup from the ground state geometry.

In order to categorise the possible break up channels for the OCS^{3+} states in more detail we use the Dalitz plot method, a well-established technique for displaying the possible molecular dissociation geometries in a two dimensional histogram. Dalitz plots for the (1,1,1) channel are shown in Fig. 1a. The concerted process offers us the best opportunity to see differences due to the slower (10 fs) ionization speed associated with the Auger process, which therefore affords increased time between ionization steps and so more time is spent on the singly and doubly ionized potentials than is possible for the direct ionization process (<1 fs). The result of these increased residence times would include a greater degree of stepwise nature and increased bending exhibited in the Dalitz plots for 173 eV compared to the direct process best exemplified by 90 eV. There are indeed small but discernible differences between the direct and Auger ionization plots, but these differences can be seen more clearly by integrating over the horizontal and vertical axes and constructing two new plots shown in Fig1 b. As expected, the 173 eV data shows both more bending in the form of a peak which is at higher Y value and a wider distribution than the 90 eV data. The shift of the peak although small is significant as the 90 eV distribution is peaked very close to the predicted equilibrium value, marked by the vertical line, indicating that for the fastest ionization events at 90 eV, very little motion is possible for the molecule during the ionization process whereas for 173 eV even the fastest ionization allows time for some bending to occur. In order to confirm the exact timescales, with which the processes proceed, in the range of few femtoseconds to sub femtosecond, pump probe studies might be carried out utilising pulses from a free electron laser with sub femtosecond pulse length, or a high harmonic attosecond source with high flux.

References

[1] Y. F. Hu, L. Zuin, G. Wright, et. al. *Commissioning and performance of the variable line spacing plane grating monochromator beamline at the Canadian Light Source*, Rev. Sci. Instrum. **78**, 083109 (2007).

[2] T. Masuoka and H. Doi, *single-photoionization, double-photoionization, and triple-photoionization cross-sections of carbonyl sulfide (OCS) and ionic fragmentation of OCS+, OCS2+, AND OCS3+*, Phys. Rev. A. **47**, 278 (1993).

Simulation of Level Crossing Optically Detectable Magnetic Resonance Signals in Nitrogen - Vacancy Centres in Diamond

Marcis Auzinsh, Andris Berzins, Laima Busaite, Ruvin Ferber, Florian Gahbauer, Linards Kalvans, Reinis Lazda, Janis Smits

Laser Centre, University of Latvia, 19 Rainis Boulevard, Riga, Latvia, LV-1586

Nitrogen-vacancy (NV) centers are powerful instruments in many areas of reasearch, including quantum information, magnetometry and nanoscale sensing. They have been used to detect individual electron spins and spin ensembles, measure the magnetic field distributions in biological signals and measure temperature and electric fields [1].

NV centres are defects in diamond crystal consisting of paired nitrogen (N) and vacancy (V). The NV centre has a triplet ground state with a zero-field splitting between the $m_s = 0$ and $m_s = \pm 1$ ground state sublevels of 2.87 GHz. Due to nonradiative decay path from the excited state via singlet state that preferentially populates the $m_s = 0$ ground-state sublevel, the NV centre can be polarized optically, and the fluorescence from exciting $m_s = 0$ sublevel is more intense than the fluorescence from exciting the $m_s = \pm 1$ sublevels. In presence of microwave field population of $m_s = 0$ can be transferred to $m = \pm 1$ levels, decreasing the total detected fluorescence. However, if the magnetic field is applied along NV centre axis (which defines quantization axis in the system), the $m_s = \pm 1$ energies are shifted by $g_e \mu_B B_z$ or 2.8 MHz/G. At around 1025 G a crossing of sublevels $m_s = 0$ and $m_s = -1$ appear and due to nuclear spin interaction of ^{14}N, the hyperfine states of $m_s = 0$ and $m_s = -1$ are mixed and anticrossing is formed, creating complex energy level system (Fig. 1).

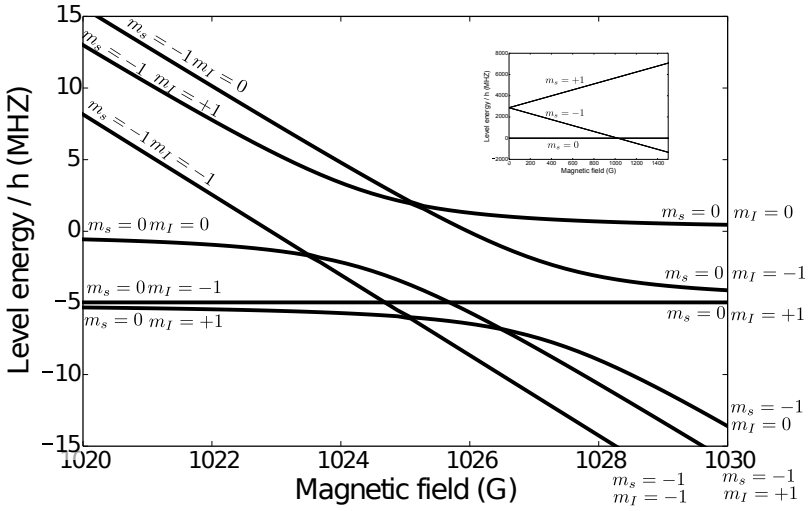

Fig. 1 Anticrossing of ground state hyperfine sublevels of $m_s = 0$ and $m_s = -1$ levels.

At the point of the anticrossing the wave functions of the ground state $m_s = 0$ and $m_s = -1$ hyperfine sublevels are mixed, modifying the probabilities for magnetic-dipole transition of microwave field.

To simulate the ODMR signals, including interaction of nuclear spin, magnetic field at the range of level crossing and microwave field, we calculated optical rate equations for ground state system, describing system Hamiltonian of NV centre ground state as [2]

$$\hat{H} = g_e \mu_B \vec{B} \hat{\vec{S}} + \hat{\vec{S}} \hat{D} \hat{\vec{S}} + \hat{H}_{HFI},$$

where $g_e \mu_B \vec{B} \hat{\vec{S}}$ describes interaction with magnetic field, $\hat{\vec{S}} \hat{D} \hat{\vec{S}}$ - describes spin - spin interaction of two unpaired electrons of NV centre and $\hat{H}_{HFI}$ - describes the hyperfine interaction of ^{14}N ($I_N = 1$). Microwave interaction was described as spin step-up and step-down operators for magnetic-dipole transitions.

This research was kindly supported by the M-ERA.NET project MyND no. Z/15/1366.

References

[1] L. Rondin et al., *Magnetometry with nitrogen-vacancy defects in diamond, Reports on Progress in Physics*, **77**, 056503 (2014), arXiv:1311.5214

[2] G. D. Fuchs et al., *A quantum memory intrinsic to single nitrogenvacancy centres in diamond* Nature Physics **7**, 789793 (2011)

Internal dynamics in small anionic carbon clusters

K. Saha[1], V. Chandrasekaran[1], B. Kafle[1], A. Prabhakaran[1], O. Heber[1], M. L. Rappaport[1], H. Rubinstein[1], D. Schwalm[1,2], Y. Toker[1,3], and D. Zajfman[1]

[1]*Faculty of Physics, Weizmann Institute of Science, Rehovot, 7610001, Israel*
[2]*Max-Planck-Institut für Kernphysik, D-69117 Heidelberg, Germany*
[3]*Department of Physics, Bar-Ilan University, Ramat-Gan 5290002, Israel*

Internal relaxation processes in molecules and clusters are of fundamental interest in such fields as interstellar medium (ISM), atmospheric science, plasmas and nanosciences. The question that is common to all of them is, what happens to a system after a sudden excitation e.g., photon absorption? In recent years, much progress has been achieved in the ultrashort time scales of attoseconds to femtoseconds. However, a fundamental question about the relaxation processes remains: What are the longer time scales' contributions to the processes? For example, how can the infrared emission from the ISM be explained? Is it from large polycyclic aromatic hydrocarbon (PAH) clusters? In our research, we study small negatively charged carbon cluster ions in order to understand their internal relaxation processes on longer time scales as a paradigm for many-body internal processes.

Cluster anions are generated in different ion sources in order to control their initial internal energy distributions and are then stored in an electrostatic ion beam trap (EIBT) to study their vibrational relaxation. After a given storage time, a laser pulse intersects the ion beam and one or two photons are absorbed. The relaxation of these excited clusters occurs on time scales ranging from microseconds to milliseconds. These relaxation processes are investigated by measuring the rate of delayed electron emission (or neutral production) for different photon energies and initial internal energy distributions. Using a statistical model, we are able to model the various relaxation mechanisms for all the clusters studied.

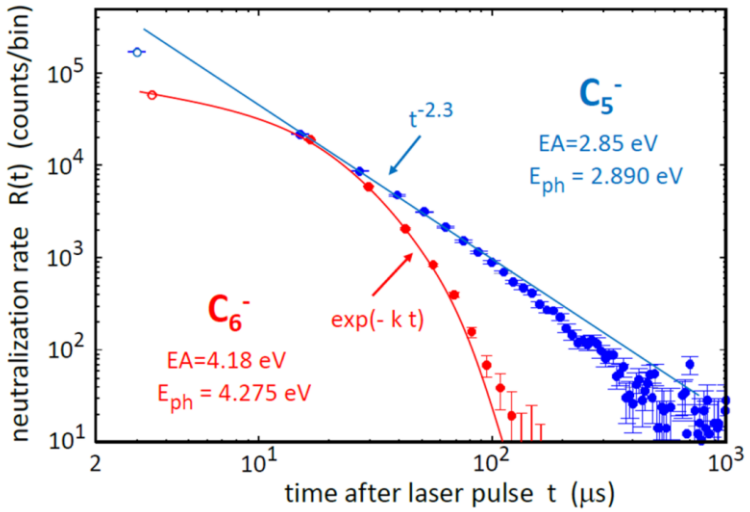

Fig 1 Neutral production after laser excitation and 190 ms trapping time. The lines are the result of model calculations. EA=adiabatic electron detachment energy; E_{ph}= photon energy.

While vibrational autodetachment was observed to dominate the relaxation process in C_5^-, in C_6^- it is recurrent fluorescence (RF) that was found to dominate for photon energies at and above the adiabatic electron detachment threshold [1,2]. Figure 1 shows the decay curves for both ions indicating the different dominant process. We determined the absolute rates of the RF process in C_6^- and showed that they are two orders of magnitude faster than the cooling rates due to infrared transitions. For C_{10}^-, where linear and cyclic isomers coexist, we have seen that vibrational autodetachment of the linear structure proceeds via adiabatic electron detachment to the cyclic isomer, which lies lower in energy.

References

[1] V. Chandrasekaran et al. J. Phys. Chem.Lett. **5,** 4078 (2014).
[2] Ito et al. Phys. Rev. Lett. **112**, 183001 (2014).

Charge transfer dynamics in halomethane molecules ionized by intense femtosecond X–ray pulses

Rebecca Boll[1,2*], Benjamin Erk[1], Ryan Coffee[3], Sebastian Trippel[4], Thomas Kierspel[4,5], Cédric Bomme[1], John D. Bozek[3], Mitchell Burkett[6], Sebastian Carron[3], Ken R. Ferguson[3], Lutz Foucar[7], Jochen Küpper[4,5,8], Tatiana Marchenko[9], Catalin Miron[10,11], Minna Patanen[10,12], Timur Osipov[3], Sebastian Schorb[3], Marc Simon[9], Michelle Swiggers[3], Simone Techert[1,13,14], Kiyoshi Ueda[15], Christoph Bostedt[3,16,17], Daniel Rolles[1,6], Artem Rudenko[6,2]

1. Deutsches Elektronen–Synchrotron (DESY), 22607 Hamburg, Germany
2. Max Planck Institute for Nuclear Physics, 69117 Heidelberg, Germany
3. SLAC National Accelerator Laboratory, Menlo Park, CA 94025, USA
4. Center for Free-Electron Laser Science, DESY, 22607 Hamburg, Germany
5. Center for Ultrafast Imaging, University of Hamburg, 22761 Hamburg, Germany
6. J.R. Macdonald Laboratory, Kansas State University, Manhattan, KS 66506, USA
7. Max Planck Institute for Medical Research, 69120 Heidelberg, Germany
8. Department of Physics, University of Hamburg, 22761 Hamburg, Germany
9. Sorbonne Universités, UPMC Univ Paris 06, CNRS, Laboratoire de Chimie Physique–Matiere et Rayonnement, F-75005 Paris, France
10. Synchrotron SOLEIL, L'Orme des Merisiers, Saint–Aubin, BP 48, F–91192 Gif-sur–Yvette Cedex, France
11. Extreme Light Infrastructure, Horia Hulubei National Institute for Physics and Nuclear Engineering, RO–077125 Magurele, Romania
12. Molecular Materials Research Community, P.O. BOX 3000, FIN–90014 University of Oulu
13.Max Planck Institute for Biophysical Chemistry, 37077 Göttingen, Germany
14. Institute of X–ray Physics, 37077 Göttingen University, Germany
15. IMRAM, Tohoku University, 980-8577 Sendai, Japan
16. Argonne National Laboratory, Lemont, IL 60439, USA
17. Department of Physics and Astronomy, Northwestern University, Evanston, IL 60208, USA
[*] *email: rebecca.boll@desy.de*

Electron transfer processes induced by photoabsorption play a central role in a broad range of physical, chemical, and biological reactions. Charge transfer phenomena involve electronic as well as nuclear motion and are, therefore, closely related to molecular bond formation and breaking. The microscopic understanding of their dynamics is crucial for emerging photosynthetic, photocatalytic, and photovoltaic applications.

Here, the results of a femtosecond pump–probe experiment conducted at the LCLS free–electron laser are presented, aimed at studying electron transfer dynamics initiated by inner–shell ionization of a halogen atom in gas–phase iodomethane (CH_3I) and fluoromethane (CH_3F) molecules [1]. Through inner–shell ionization followed by (local) Auger decay, multiple charges can be induced with a high degree of spatial localization at a heavy element with a large X–ray absorption cross section. The subsequent electron dynamics are strongly influenced by the initial positions of the nuclei, and by the interplay between electronic and nuclear motion. Depending on the internuclear distance at the time of the X–ray absorption, the charge either remains on the absorbing halogen or spreads over to the molecular environment. By measuring the charge state and the kinetic energy distributions of the created ionic fragments, the charge rearrangement between the two molecular centers can be traced as a function of their internuclear separation.

Iodomethane can be efficiently broken up into two neutral fragments, and its UV–induced photolysis in the A band is a prototypical photodissociation process which is well studied experimentally and theoretically. Fluoromethane is known to exhibit intriguing electron transfer dynamics upon fluorine (1s) photoabsorption, and fluorine as the most electronegative element is a predestined candidate to initiate charge transfer to the molecular environment. The experimental results are complementary, due to the qualitatively different reactions of the two species to UV irradiation, as well as the considerably different electronegativities of the two halogen atoms.

Signatures of long–distance intramolecular charge transfer are observed for both molecules, and a quantitative analysis of its distance dependence in iodomethane is carried out for charge states up to I^{21+}. The reconstructed critical distances for electron transfer are in good agreement with a classical over–the–barrier model and with an earlier experiment employing a near–infrared pump pulse [2]. Combined with coincident electron spectroscopy and upcoming attosecond soft X–ray pulses, this approach will allow tracing local charge propagation dynamics with Ångstrom spatial and sub–femtosecond temporal resolution.

References

[1] R. Boll, B. Erk, R. Coffee, S. Trippel, T. Kierspel, C. Bomme, J. D. Bozek, M. Burkett, S. Carron, K. R. Ferguson, L. Foucar, J. Küpper, T. Marchenko, C. Miron, M. Patanen, T. Osipov, S. Schorb, M. Simon, M. Swiggers, S. Techert, K. Ueda, C. Bostedt, D. Rolles, and A. Rudenko, *Charge transfer in dissociating iodomethane and fluoromethane molecules ionized by intense femtosecond X–ray pulses*, Struct. Dyn. **3**, 00000 (2016) DOI: 10.1063/1.4944344.

[2] B. Erk, R. Boll, S. Trippel, D. Anielski, L. Foucar, B. Rudek, S. W. Epp, R. Coffee, S. Carron, S. Schorb, K. R. Ferguson, M. Swiggers, J. D. Bozek, M. Simon, T. Marchenko, J. Küpper, I. Schlichting, J. Ullrich, C. Bostedt, D. Rolles, and A. Rudenko, *Imaging charge transfer in iodomethane upon x-ray photoabsorption*, Science **345**, 288 (2014).

Strong-Field Ionisation with Tailored Two-Color Laser Fields

Sebastian Eckart, Martin Richter, Maksim Kunitski, Alexander Hartung, Jonas Rist, Kevin Henrichs, Nikolai Schlott, Huipeng Kang, Tobias Bauer, Hendrik Sann, Lothar Ph. H. Schmidt, Markus Schöffler, Till Jahnke, Reinhard Dörner

Institut für Kernphysik, J. W. Goethe-Universität, Max-von-Laue-Str. 1, 60438 Frankfurt am Main, Germany

Strong-field ionization in linear and circular laser pulses shows features related to electron dynamics which make it different from single photon ionization. The recent introduction of two-color laser fields opens up new opportunities for the investigation and control of the related dynamic processes. Ellipticites, intensities and the relative phase can be tuned to tailor the combined electric field. In the past, such tailored laser pulses have been used to generate high harmonics of variable ellipticity [1, 2]. The 3D-momenta of the fragments will be recorded for selected combinations of this huge parameter space using Cold Target Recoil Ion Momentum Spectroscopy (COLTRIMS) as experimental technique.

Here we report on our results on studying single ionization in tailored two-colour (780 nm & 390 nm) laser fields with overall intensities of up to $5*10^{14}$ W/cm^2. We present technical aspects of the experimental setup including active stabilization of the relative phase as well as preliminary results (see Fig 1). Such studies allow to gain new insights into different aspects of ionization processes as recollision dynamics, single photoelectron interferences [3], nonsequential double ionization (NSDI), high harmonic generation (HHG) as well as the production of tailored monoenergetic electron beams.

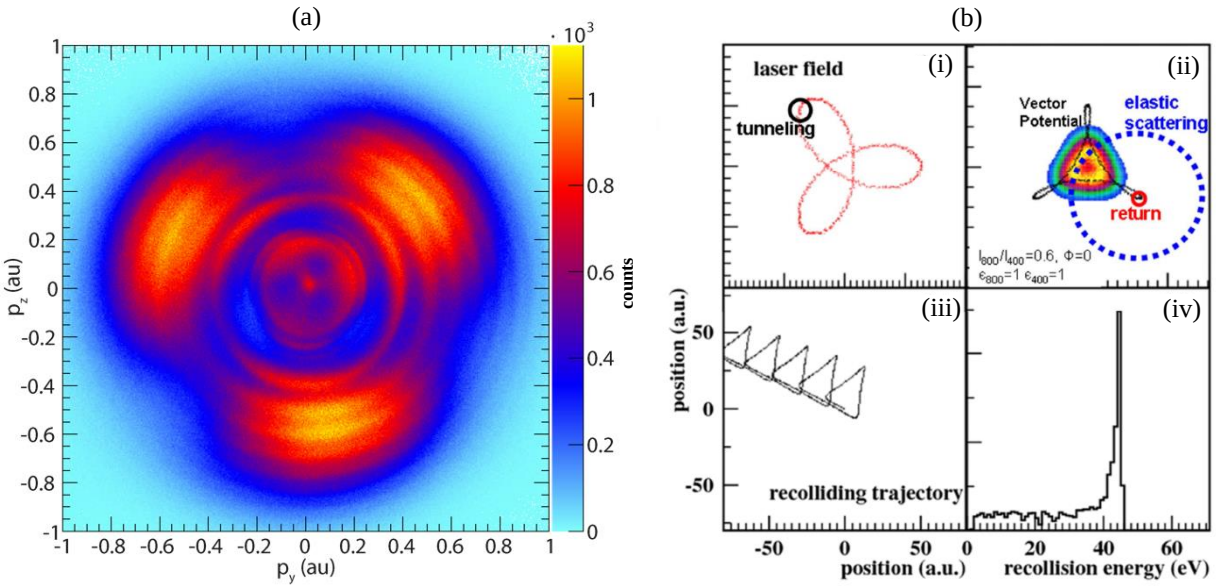

Fig. 1 (a) Electron momentum distribution obtained for a counter rotating two-color laser field with circular polarization and an intensity ratio I_{780nm}/I_{390nm}=9 of the fundamental wavelength I_{780nm} to the intensity of the second harmonic I_{390nm}. The used target is a supersonic argon jet. (Compare to [4].) **(b)** Illustration of a recollision scenario: **(i)** Combined electric field of a counter rotating two-color field. The black line in **(ii)** shows the corresponding vector field. Color: electron trajectories from simple-man model using ADK rates and transverse momentum distributions from ADK theory. Trajectories starting at the black circle marked "tunnelling" (panel (i)) will return (if they have the right transverse momentum) at the vector potential marked "return" (panel (ii)). If the electrons loose the energy in an inelastic collision they show up at the red circle, if they are elastically scattered at the core they end on the blue dotted circle. **(iii)** Shows recolliding trajectory (starting at field marked in (i)). Calculated energy distribution of returning electron trajectories (3-dim simple-man model with ADK neglecting the coulomb field) are shown in **(iv)**.

References

[1] Wilhelm Becker, Boris N. Chichkov, and Bernd Wellegehausen, *Schemes for the generation of circularly polarized high-order harmonics by two-color mixing*, Phys. Rev. A **60**, 1721-1722 (1999).

[2] Avner Fleischer, Ofer Kfir, Tzvi Diskin, Pavel Sidorenko and Oren Cohen, *Spin angular momentum and tunable polarization in high-harmonic generation*, Nature Photonics **8**, 543-549 (2014).

[3] Martin Richter, Maksim Kunitski, Markus Schöffler, Till Jahnke, Lothar Ph. H. Schmidt, Min Li, Yunquan Liu and Reinhard Dörner, *Streaking temporal double slit interference by an orthogonal two-color laser field*, Phys. Rev Lett. **114**, 143001 (2015).

[4] Christopher A. Mancuso et al., *Strong-field ionization with two-color circularly polarized laser fields*, Phys. Rev A **91**, 031402(R) (2015).

Excited State Distribution and Spin-Effects in Strong-Field Excitation of Neutral Helium

H. Zimmermann, U. Eichmann
Max-Born-Institute, 12489 Berlin, Germany

Excitation of neutral atoms and molecules by frustrated tunneling ionization [1] has recently been found to be an important channel in the tunneling regime, besides the well known processes of non-sequential double ionization (NSDI), high order above threshold ionization (HATI) and high harmonic generation (HHG). FTI naturally evolves from the semi classical tunneling picture, if one considers the quasi-classical electron dynamics in the combined laser and Coulomb field after tunneling. FTI helps to understand strong-field phenomena such as extreme acceleration of neutral atoms in intense focused laser fields [2] and Coulomb explosion without double ionization in strong laser field fragmentation of H_2 [3]. While predictions on the laser polarization dependent excited He* yield are well backed up by experiments [1], we present here the experimental confirmation of the important prediction on the Rydberg state distribution, which was still pending.

In our experiments we excite neutral Helium atoms in the strong-field tunneling regime using femto second pulses from a Ti:Sapphire laser at 800nm and employ the method of pulsed field ionization in conjunction with direct detection of excited neutral atoms to analyze the distribution of excited Rydberg states. This approach enables us to obtain a measurement signal proportional to the amount of initially excited atoms with a detection efficiency of approximately 30 %. Our measurements basically confirm the predictions [4] of the FTI model as well as quantum mechanical calculations [4,5] using the single-active electron (SAE) approximation (see Fig. 1). We conclude that excitation in the tunneling regime can be understood in terms of a quasi-classical process.

Moreover, we find that the excitation process also results in an efficient population of excited triplet states of Helium [4], which results from the fact that states with high orbital angular momentum $l > 3$ are accessible for our experimental conditions. For these high l states the strict separation into singlet and triplet states is removed due to the breakdown of the Russel-Saunders coupling scheme. The direct excitation of triplet states is then possible via the admixture of their singlet component, which we could directly prove using a Stern-Gerlach setup.

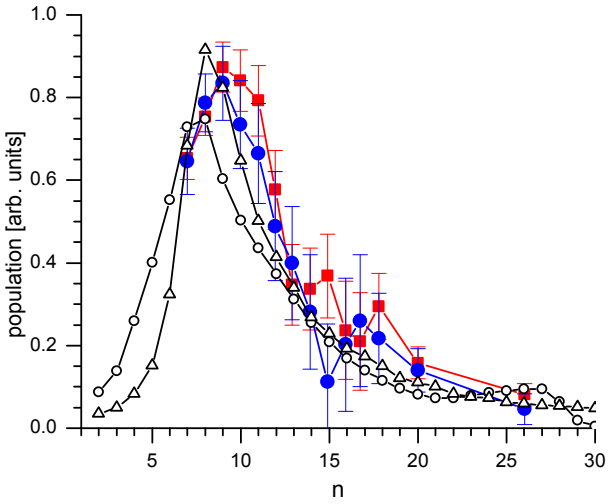

Fig. 1 Comparison of the theoretically and experimentally obtained n-distributions in Helium. The intensities used in the experiments are 3×10^{15} Wcm^{-2} (red squares) and 2×10^{15} Wcm^{-2} (blue dots). The intensity for the theoretical calculations performed using the semiclassical FTI model (triangles) and a qm. SAE approximation (circles) [5] is 10^{15} Wcm^{-2}.

References

[1] T. Nubbemeyer *et al*, Phys. Rev. Lett., **101** 233001 (2008).
[2] U. Eichmann *et al*, Nature**461**, 1261 (2009); S Eilzer *et al*, Phys. Rev. Lett. **112**, 113001 (2014).
[3] B. Manschwetus *et al*, Phys. Rev. Lett. **102**, 113002 (2009).
[4] H. Zimmermann *et al*, Phys. Rev. Lett. **114**, 123003 (2015).
[5] E. Khosravi and A. Saenz , *unpublished* 2015.

Electron Energy Discretization in Strong Field Double Ionization

K. Henrichs[α], M. Waitz[α], F. Trinter[α], H.-K. Kim[α], A. Menssen[α], H. Gassert[α], H. Sann[α], T. Jahnke[α], J. Wu[β], M. Pitzer[α], M. Richter[α], M. S. Schöffler[α], M. Kunitski[α], R. Dörner[α]

[α] *Institut für Kernphysik, Universität Frankfurt, Max-von-Laue-Str. 1, 60438 Frankfurt, Germany*
[β] *State Key Laboratory of Precision Spectroscopy, East China Normal University, Shanghai 200062, China*
henrichs@atom.uni-frankfurt.de

Abstract: We study the double ionization of Argon and Helium at a wavelength of 394 nm. We found discretization in the sum energy of those ionized electrons for Argon. Additionally the individual energies of both electrons also show ATI-like structures. Therefore we propose that a doubly excited intermediate state has to be present. For Helium only weak discretization was visible at low intensities at 394 nm. Nevertheless, our highly differential data and high resolution allows for the study of the impact of parity and angular momentum transferred by the field.

Ionization by a strong electromagnetic field leads to so-called ATI peaks (Above-Threshold-Ionization) in the energy spectrum of electrons. These ATI peaks are well known and have been observed several times. However, discretized energy transfer should also lead to a similar peak structure in the sum energy spectrum of electrons that belong to the same double ionization event. Previous experiment couldn't find those structures and attributed that to a smearing of the spectrum by focal averaging.

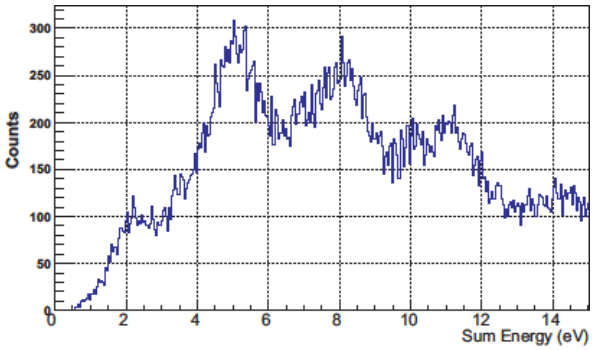

Fig. 1: Sum energy of both emitted electrons originating from double ionization of Ar at 394 nm and 1.3x10^{14} W/cm^2.

Therefore, we doubly ionized Argon atoms in a COLTRIMS [2] setup by 394 nm laser pulses at peak intensity 1.3x10^{14} W/cm^2. By using 394 nm the energy spacing of the ATI peaks is doubled and the ponderomotive potential U_p is lowered to reduce the influence of focal averaging. For the first time clear structures are visible in the sum energy spectrum of both electrons as shown in Fig. 1 [1]. The peaks are spaced by the photon energy of 3.14 eV. Furthermore we unexpectedly found that the energy spectra of both individual electrons show discretization structures as well (see Fig. 2). These findings are consistent with a doubly excited intermediate state. This state is created via recollision and both electrons get ionized independently afterwards.

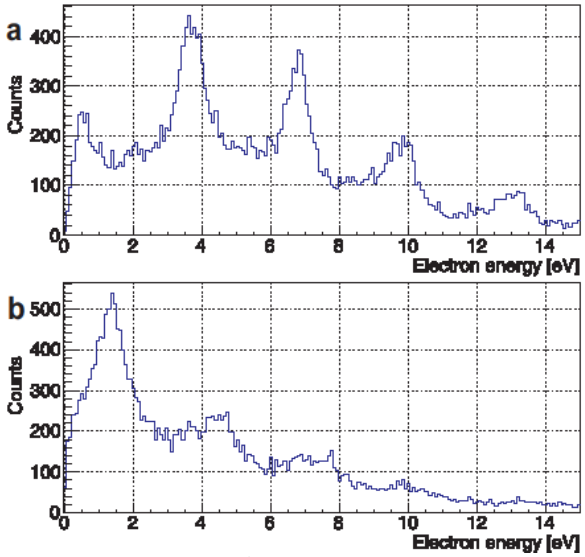

Fig. 2: Energy spectrum of (a) one and (b) the other electron at same conditions as in Fig. 1.

The counting of photons enables to make a statement about the parity that is transferred to the system and, thus, about the parity of the final state. Ni et al. [3] proposed several selection rules for the continuum wave function of both electrons. With the knowledge of the parity it should be possible to find those signatures. Since those symmetry considerations only apply for exactly two electrons Argon as a target is not suitable.

Hence, for the first time we doubly ionized Helium atoms by 394 nm laser pulses at various intensities. At high intensities (>5x10^{14} W/cm^2) no peaks were visible in the electron sum energy spectrum at all. But for the lowest measured intensity (3x10^{14} W/cm^2) weak peaks could be observed. Now we are able to study the influence of angular momentum and parity in strong field double ionization.

References

[1] K. Henrichs et al., *Observation of Electron Energy Discretization in Strong Field Double Ionization*, Phys. Rev. Lett. **111**, 113003 (2013).
[2] J. Ullrich et al., *Recoil-ion and electron momentum spectroscopy : reaction-microscopes*, Rep. Prog. Phy. **66**, 1463 (2003).
[3] H. C. Ni et al., *Selection rules in the few-photon double ionization of the helium atom*, J. Phys. B. **44**, 175601 (2011).

Resonance-Enhanced Two-Photon Ionisation of Helium Atoms with Femtosecond Free Electron Laser Pulses

Andrej Mihelič[1], **Mateja Hrast**[2]
1. Jožef Stefan Institute, Jamova cesta 39, Ljubljana, Slovenia
2. Faculty of mathematics and physics, University of Ljubljana, Jadranska ulica 19, Ljubljana, Slovenia

We present a theoretical study of resonance-enhanced two-photon ionisation of the ground-state helium atoms with intense ($\sim 10^{14}$ W/cm^2) femtosecond free electron laser (FEL) pulses with photon energies in the region of the resonance states lying below the second ionization threshold (65.4 eV). Contrary to single-photon ionisation (autoionisation), two-photon ionisation may in this case result in helium ions in excited states. We determine the population of the excited ionic species and assess the photon yields due to the decay of the excited ionic states. This work represents an extension of our past activities dealing with radiative decay of resonance states studied with intense coherent FEL light [1, 2].

References

[1] Matjaž Žitnik, Andrej Mihelič, Klemen Bučar, Matjaž Kavčič, Jan-Erik Rubensson et al., *High resolution multipohoton spectroscopy by a tunable free-electron-laser light*, Phys. Rev. Lett. **113**, 193201 (2014).
[2] Andrej Mihelič and Matjaž Žitnik, *Two-photon excitation to autoionizing states of He detected via radiative cascades to the metastable states*, Phys. Rev. A **91**, 063409 (2015).

Transport of intense photon pulse through dense helium gas at 60-65 eV

Matjaž Žitnik[1,2], **Špela Krušič**[2], **Andrej Mihelič**[1], **Klemen Bučar**[1]
1. J. Stefan Institute, Jamova 39, Ljubljana, SI-1000, Slovenia
2. Faculty of Mathematics and Physics, University of Ljubljana, Jadranska 19, Ljubljana, SI-1000, Slovenia

Following our previous studies of two-photon excitation of doubly excited states (DES) of He observed by detection of metastable states [1,2] we now study the transport of short (100 fs FWHM Gaussian) and intense (up to 10^{14} W/cm^2 peak power density) light pulses through a layer of a dense helium gas (up to $\approx$ 1 mm length and 500 mbar pressure). The photon probe energy is varied in the 60-65 eV region coinciding with the lowest lying DES of helium atoms. The physical process is simulated by the three-level lambda system governed by the Maxwell-Bloch equations where the upper state is one of the $n^+\ ^1P$ DES below the N=2 ionization threshold with n going up to 10.

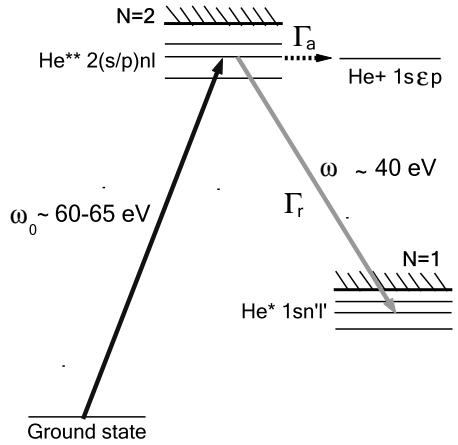

Fig. 1 Scheme of the lambda system in case of the resonant excitation of He DES by the free electron laser light with photon energy ω_0.

The model includes leakage of the upper and of the final singly excited state of He due to two-photon ionization, autoionization decay and absorption of light by ions. At the highest values of target pressure and probe intensity the simulations show that resonantly tuned probe pulse is followed by noise-induced stimulated emission signal at $\approx$ 40 eV photon energy which saturates at distances comparable to the probe beam diameter ($\approx$ 50 μm). The model allows to compute the 60 $\rightarrow$ 40 eV light conversion efficiency and to generate the secondary light spectra for different target pressure/length parameters and for a wide range of probe intensity/detuning, considering DES with different autoionization rates. While the prompt emission of light is governed by collective effects emerging from coherent excitation of densely packed atoms, a delayed fluorescence signal due to decay of excited ionic states may be produced at later times because of the electron collisions with ions and atoms in the ground state.

References

[1] Matjaž Žitnik et al., *High Resolution Multiphoton Spectroscopy by a Tunable Free-Electron-Laser Light*, Phys. Rev. Lett. **113**, 193201 (2014).
[2] Andrej Mihelič in Matjaž Žitnik, *Two-photon excitation to autoionizing states of He detected via radiative cascades to the metastable states*, Phys. Rev. A **91**, 063409 (2015).

Streaking Temporal Double-Slit Interference by an Orthogonal Two-Color Laser Field

Martin Richter[1], Maksim Kunitski[1], Markus Schöffler[1], Till Jahnke[1], Lothar P. H. Schmidt[1], Min Li[2], Yunquan Liu[2,3] and Reinhard Dörner[1]

1. Institut für Kernphysik, J. W. Goethe-Universität, Max-von-Laue-Str. 1, 60438 Frankfurt am Main, Germany
2. State Key Laboratory for Mesoscopic Physics and Department of Physics, Peking University, Beijing 100871, China
3. Collaborative Innovation Center of Quantum Matter, Beijing 100871, China

When indistuingishable electron wave packets are launched from a sample at different times interferences occur in the final electron momentum distribution. Any which-way information will destroy the interference. The which-way information can either be stored in another particle by entanglement of the electron with the particle or in the electron itself, more precisely in a spin degree of freedom or in a motional degree of freedom like one of the momentum components.

The interfering electron wave packets are launched by strong-field tunnel ionization whereby the most prominent interference fringes are the equidistant peaks in the electron energy distribution. These above-threshold ionization (ATI) peaks result from the interference of wave packets born periodically in time at subsequent laser cycles [1]. 2005 additional fringes were discovered resulting from the interference between wave packets released within one cycle at times where the vector potential is the same but the direction of the electric field is opposite [2]. In this work we show that orthogonally polarized two-color pulses can be used to turn these typically faint intracycle interference fringes into a dominating structure in the electron momentum distribution (Fig. 1) and, at the same time, can be used as a controllable which way marker.

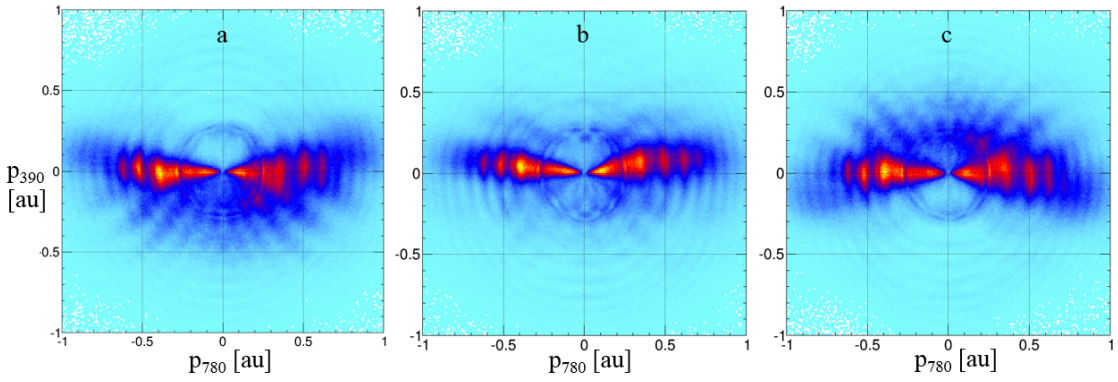

Fig. 1 Electron momentum spectra in the polarization plane for the relative phase ϕ between the streaking field and ionizing field. At the phases $\phi = \pi/2$ (a) and $\phi = 3\pi/2$ (c) the intracycle interference pattern is clearly visible while at the phase $\phi = \pi$ (b) the interferences are switched off almost completely.

References

[1] P. Agostini, *Intensity dependence of non-perturbative above-threshold ionisation spectra: experimental study*, Phys. Rev. Lett. **42**, 1127 (1979).

[2] F. Lindner, M. G. Schätzel, H. Walther, A. Baltuška, E. Goulielmakis, F. Krausz, D. B. Milošević , D. Bauer, W. Becker, and G. G. Paulus, *Attosecond Double-Slit Experiment*, Phys. Rev. Lett. **95**, 040401 (2005).

Few body break-up spectra using the time dependent surface flux method

Vinay Pramod Majety, Alejandro Zielinski and Armin Scrinzi
Ludwig Maximimilians University, Munich, Germany

Computation of differential spectra poses a major challenge in theoretical modeling of strong field induced break-up phenomena. At common visible and near IR wave length, pulse durations are very long on the natural time scales of atomic and molecular systems and the interaction is non-perturbative. As a result, the system extends to very large volumes before spectral information can be obtained by standard stationary analysis. The ensuing large demands on computational resources have so far strongly limited theoretical access to break-up spectra.

The time dependent surface flux (tSurff) method introduced in [1,2] overcomes this limitation by containing the numerical simulation on a small volume and recovering the time-dependent asymptotic solutions by the use of Volkov functions. The drastic reduction of problem size allows the computation of singly and multiply differential break-up spectra of few-body systems with relative errors below the 10% level for many physically relevant observables.

Here we present applications of tSurff and its extension to the molecular break-up problem.

(1) We studied strong field ionization of CO_2, using a multi-channel description for the electronic structure [3]. Previously we had demonstrated that *dynamic exchange* strongly affects ionization rates in CO_2 [4], here we will discuss the role of multi-electron effects in spectra, Fig.1a.

(2) Doubly energy differential and angularly resolved spectra for the double ionization of Helium at 800 nm [5] and at 400 nm are presented. The spectra show unexpected structure, Fig.1b, that is tentatively ascribed to intermediate resonances.

(3) Finally, an extension of the original formulation [1,2] to breakup of molecular systems will be presented. This, for the first time, allows a complete quantum mechanical description of electron-nuclear correlation in such processes.

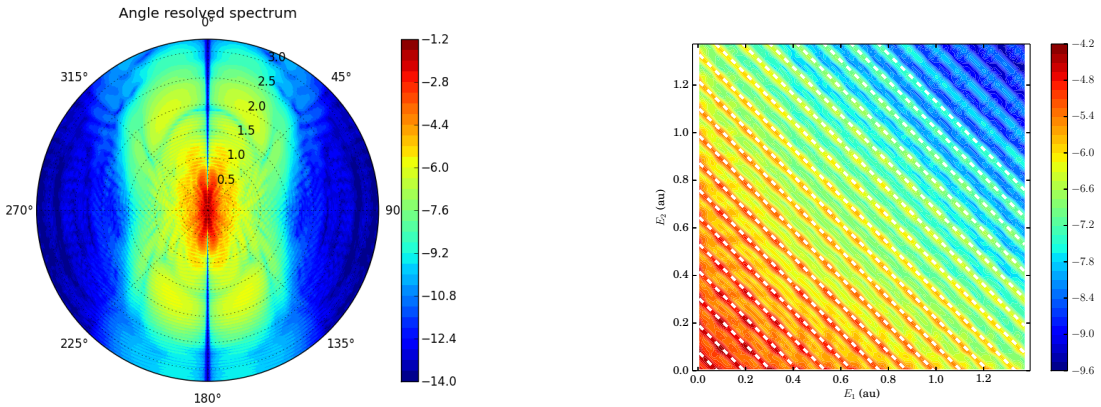

(a) Single ionization of CO_2 molecule

(b) Double ionization of Helium

Figure 1: (1a): Single ionization spectra for CO_2 ionized by a 3-cycle, 800 nm pulse with a peak intensity of 10^{14} W/cm^2. The polarization axis is parallel to the molecular axis. The nodal structure along the polarization axis is a result of the nodal structure in the highest occupied molecular orbital of the molecule. (1b): Energy resolved double ionization spectra for Helium ionized by a 3-cycle, 400 nm pulse with a peak intensity of 5×10^{14} W/cm^2. The colorbars are logarithmically scaled.

References

[1] L. Tao, and A. Scrinzi, *Photo-electron momentum spectra from minimal volumes: the time-dependent surface flux method*, New J. Phys., **14**, 013021, 2012.
[2] A. Scrinzi, *tSurff: fully differential two-electron photo-emission spectra*, New Journal of Physics, **14**, 085008, 2012.
[3] V. P. Majety, A. Zielinski, and A. Scrinzi, *Photoionization of few electron systems: a hybrid coupled channels approach*, New J. Phys., **17**, 063002, 2015.
[4] V. P. Majety and A. Scrinzi *Dynamic exchange in the strong field ionization of molecules*, Phys. Rev. Lett. **115**, 103002, (2015).
[5] A. Zielinski, V. P. Majety, and A. Scrinzi, *Double photo-electron momentum spectra of Helium at infrared wavelength*, Phys. Rev. A **93**, 023406 (2016).

Mapping molecular nitrogen photodissociation with attosecond temporal resolution

Andrea Trabattoni [1,2], Markus Klinker[3], Jesus González-Vázquez[3], Candong Liu[4], Giuseppe Sansone[1], Roberto Linguerri[5], Majdi Hochlaf[5], Jesse Klei[6], Marc J. J. Vrakking[6], Fernando Martín[3], Mauro Nisoli[1,7], and Francesca Calegari[7]

1. Dipartimento di Fisica, Politecnico di Milano, Piazza Leonardo da Vinci 32, I-20133 Milano, Italy

2. Center for Free-Electron Laser Science (CFEL), DESY, Notkestrasse 85, 22607, Hamburg, Germany

3. Departamento de Química, Módulo 13. Universidad Autónoma de Madrid, 28049 Madrid, Spain

4. State Key Laboratory of High Field Laser Physics, Shanghai Institute of Optics and Fine Mechanics, Shanghai 201800, China

5. Université Paris-Est, Laboratoire Modélisation et Simulation Multi Echelle, 5 bd Descartes, 77454 Marne-La-Vallée, France

6. Max-Born-Institut, Max Born Strasse 2A, D-12489 Berlin, Germany

7. Institute for Photonics and Nanotechnologies, IFN-CNR, Piazza Leonardo da Vinci 32, I-20133 Milano, Italy

Molecular nitrogen is the most abundant species in the Earth's atmosphere, and the investigation of the ultrafast dissociative mechanisms triggered by the absorption of XUV photons is of crucial importance for understanding the radiative-transfer processes occurring in nature[1]. In this work we used isolated attosecond pulses to disclose the dissociative photoionization of N_2 with extremely high temporal resolution and retrieve precise information on the shape of the potential energy curves (PECs) involved in the dissociative process[2].

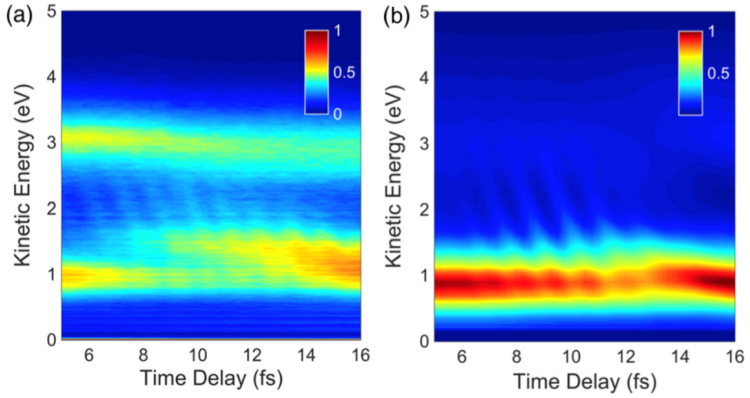

Fig. 1 (a) Kinetic energy distribution of N^+ ions as a function of the delay between pump and probe pulses, in the 5-16 fs delay range. (b) Simulation of time-dependent N^+ kinetic energy spectra in the same delay interval.

In the experiment, sub-300-as XUV pulses were used in combination with 4-fs visible/near-infrared (VIS/NIR) pulses to photoionize the N_2 molecule and trigger the following ultrafast dynamics occurring in N_2^+, leading to molecular dissociation. The process was studied by recording the three-dimensional momentum distribution of N^+ ions in a Velocity Map Imaging spectrometer, as a function of the delay between the attosecond pulse (pump pulse) and the 4-fs VIS/NIR pulse (probe pulse). The delay-dependent ion yield (Fig. 1(a)) shows two main features: a strong depletion of the signal at 1eV in the 5-16 fs delay range, and the appearance of a fast tilted modulation with a periodicity of 1.22 fs in the same delay interval. In order to understand the underlying physical process, the Time- Dependent Schrödinger Equation has been solved for a set of 616 diabatic excited states of N_2^+ , taking into account the couplings induced by the VIS/NIR probe pulse. The numerical results are in excellent agreement with the experimental data, as reported in Fig. 1(b), and allowed us to understand all the features shown in the experiment. In particular, the tilt in the modulation pattern is caused by the dispersion of the nuclear wavepacket during propagation along the populated PECs, thus carrying important information on the shape of the N_2^+ potential energy curves involved in the ultrafast dissociative process. At the same time, the theoretical model provided accurate values for the dissociative ionization yields, revealing important contributions coming from channels that were not considered so far in the modelling of nitrogen chemistry in planetary atmospheres[1,3]. A realistic modelling should also incorporate the presence of nitrogen atoms or ions in various excited states, which are likely to have a different reactivity.

This work combined for the first time attosecond technology with a sophisticated theoretical model to access photodissociation of molecular nitrogen with an unprecedented accuracy, giving new perspectives in the investigation of ultrafast chemical reactions of small molecules.

References

[1] R.R. Meier, *Ultraviolet Spectroscopy and Remote Sensing of the Upper Atmosphere*, Space Sci. Rev. **58**,1 (1991).

[2] A. Trabattoni et al., *Mapping the Dissociative Ionization Dynamics of Molecular Nitrogen with Attosecond Time Resolution*, Phys. Rev. X **5** 041053 (2015).

[3] V. A. Krasnopolsky, *A Photochemical Model of Titan's Atmosphere and Ionosphere*,Icarus **201**, 226 (2009).

Laser-driven attosecond dynamics in hydrogenic molecules using XUV+IR schemes

Alicia Palacios[1], **Roger Y. Bello**[1], **Fernando Martín**[1,2,3]

1. Departamento de Química, Módulo 13, Universidad Autónoma de Madrid, Cantoblanco, 28049, Madrid, Spain
2. Instituto Madrileño the Estudios Avanzados (IMDEA) en Nanociencia, Cantoblanco, 28049, Madrid, Spain
3. Condense Matter Physics Center (IFIMAC), Universidad Autónoma de Madrid, Cantoblanco, 28049, Madrid, Spain

Electron dynamics in matter can be monitored by means of ultrashort light pulses with durations in the sub-femtosecond regime. We investigate the laser-induced coupled electron-nuclear dynamics in the smallest molecules in the context of XUV-IR pump-probe protocols. Significant progresses have been made in photoionization experiments performed in atomic [1,2] and small molecular targets [3,4], where an attosecond pulse triggers ionization and an IR field drives the photoelectron, thus gaining a certain control of the ionization events. A main topic of interest is the role of electron correlation in the IR-induced dynamics, in particular through the population of doubly excited states [2,3]. In this work, we present ab initio calculations performed on H_2/D_2 to investigate the role of highly excited states and the coupled nuclear motion in XUV photoionization driven and/or traced by a IR-probe field.

We obtain fully differential probabilities in both electron and nuclear kinetic energies (see Fig. 1), which already reveal the main XUV+IR ionization pathways. We then discuss the signal of electron correlation in the electron streaking patterns, i.e. in the photoelectron momentum as a function of the time delay between the pulses. The streaking signal is commonly described in the context of a semiclassical approach using a single-active electron picture that invariably breaks down when these doubly excited states come into play [6]. We thus analyze the signature of autoionization in the streaking patterns associated to the dissociative and non-dissociative ionization channels. Furthermore, we explore the fully differential angular distributions obtained upon XUV photoionization and those obtained in the presence of a the combined XUV+IR scheme. Asymmetric electron angular distributions can be obtained as a consequence of coherently populating states of different symmetry with respect to the inversion center of the molecule, gerade and ungerade states that can be associated to the same [3] or to different ionic states left behind [5]. In either case, when using an XUV-IR scheme, the asymmetry can be solely induced by the IR-field or mediated by the delayed autoionization event. We will show the dependence of the relative contribution of these two mechanisms in the resulting asymmetry with the time-delay between the XUV and the IR field, and thus the level of control that could be expected for different laser parameters.

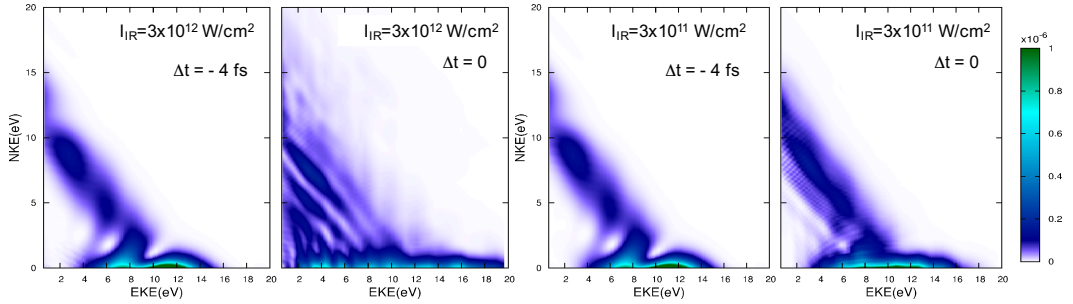

Fig. 1 Electron-ion coincident maps. Density of ionization probability as a function of both electronic (EKE) and nuclear kinetic energy (NKE) for different time delays and IR intensities. Ionization with NKEs above 2-3 eV is mostly due to the autoionization events. Results obtained for a XUV pulse of 28 eV (reaching doubly excited states), 1 fs duration and I=10^9 W/cm^2 combined with different intensities for the a 750 nm IR pulse of 9 fs. For time delays below 4 fs (IR pulse arrives first), we find the distribution due to the interaction of the XUV pulse alone. When both pulses efficiently overlap (0 delay), we find total absorption lines for the absorption of the XUV plus up to three IR photons whose profiles strongly depend on the IR intensity.

References

[1] T. Remetter *et* al., *Attosecond electron wave packet interferometry*, Nat. Phys. **2**, 323 (2006)
[2] S. Gilbertson, M. Chini, X. Feng, S. Khan, Y. Wu and Z. Chang, *Monitoring and controlling the electron dynamics in helium with isolated attosecond pulses*, Phys. Rev. Lett. **105**, 263003 (2010)
[3] G. Sansone *et* al., *Electron localization following attosecond molecular photoionization*, Nature **465**, 763 (2010)
[4] P. Ranitovic *et* al., *Attosecond vacuum UV coherent control of molecular dynamics*, PNAS **111**, 912 (2014)
[5] A. González-Castrillo, A. Palacios, H. Bachau and F. Martín, *Clocking ultrafast wave packet dynamics in molecules through UV-induced symmetry*, Phys. Rev. Lett. **108**, 063009 (2012)
[6] A. Palacios, A. González-Castrillo and F. Martín, *Electron streaking and dissociation in laser-assisted of molecular hydrogen*, J. Phys. B **47**, 124013 (2014)

Initial phase space dependent tunnel ionization of the hydrogen atom

Viktor Ayadi[1], Péter Földi[2,3], Péter Dombi[1,3], Károly Tőkési[4]

1. MTA "Lendület" Ultrafast Nanooptics Group, Wigner Research Centre for Physics, Konkoly-Thege M. út 29-33, H-1121 Budapest, Hungary

2. Department of Theoretical Physics, University of Szeged, Tisza Lajos kör út 84, H-6720 Szeged, Hungary

3. ELI-ALPS, ELI-HU Non-pro_t Ltd., Dugonics tér 13, H-6720 Szeged, Hungary

4. Institute for Nuclear Research, Hungarian Academy of Sciences, H-4001 Debrecen, P.O. Box 51, Hungary

Understanding the ionization process during atomic collisions is fundamental both from the experimental and theoretical points of view. Especially, it is a challenging task for theory to describe the ionization cross sections near the threshold region. It was shown that the interaction of a short, few-cycle infrared laser pulse with an atom characterized initially by superposition of two stationary states exhibits strong signatures of atomic coherence [1]. Along this line, we calculate the above threshold ionization (ATI) spectra and the angular distribution of electrons ejected from the hydrogen atom in the tunneling regime for single states (1s, 2s 3s) and for superposition of stationary states (2s+3s).

In the present work, we use both a full quantum mechanical and a semiclassical method to describe the tunnel ionization of hydrogen atom. As quantum treatment, we applied the direct integration of the time dependent Schrödinger equation (TDSE). In the semiclassical approximation (SCA), it is assumed that wavepacket propagation in the post-tunneling process can be well described within the classical framework [2-4]. The method is similar to the Classical Trajectory Monte Carlo (CTMC) method based on the inclusion of the classical phase information of the motion.

With these two methods, we analyze the similarities and deviations for ionization of the hydrogen atom (see Fig. 1). We found that the 3 dimensional semi-classical method can describe reasonably well the momentum correlation pattern of the ATI peak. We also show good agreement between the results obtained by TDSE method and the semi-classical method for the ground state. Semiclassical simulations have many advantages. First, these methods can be easily applied to systems with nontrivial geometries. Second, semiclassical simulations can help to identify the specific mechanism responsible for the relevant phenomena, and provide an illustrative picture of this mechanism in terms of classical trajectories. Therefore, we analyzed the different regions of Fig 1. We sorted the events according to the certain part of (p_z-p_ρ) as a function of initial velocities and tunnel exit points. We clearly identify and separate the regions in momentum distributions of the ejected electrons according to initial conditions.

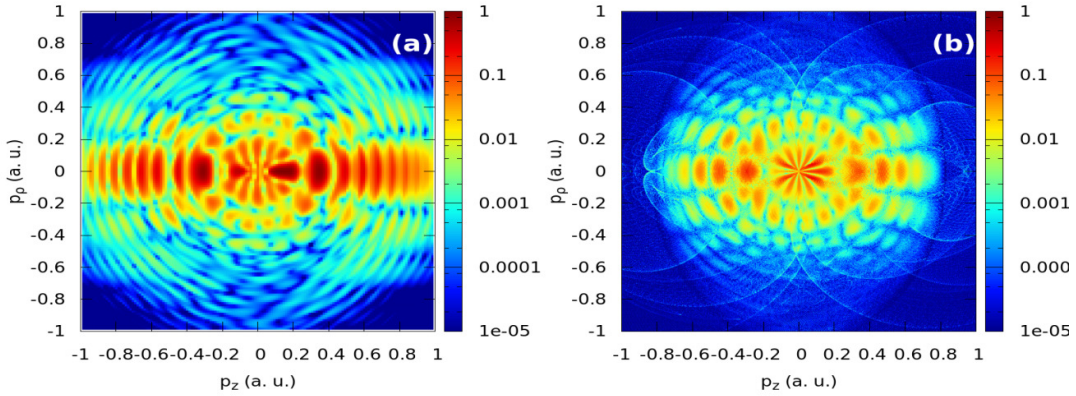

Fig.1. Ionization probability densities for the H atom as a function of the electron parallel and perpendicular momentum measured from the polarization vector ε, which coincides with the Oz axis. a) TDSE, b) SCA. The vector potential of the external laser pulse is: $A(t)=A_0\sin(\omega t)\sin^2(\pi t/\tau)$, where $A_0 = 0.05$ a.u., $\omega = 0.056$ a.u., and $\tau = 885$ a.u..

References

[1] V. Ayadi, M. G. Benedict, P. Dombi, P. Földi, submitted for publication
[2] M. Li, J. W. Geng, H. Liu, Y. Deng., C. Wu, L. Y. Peng, Q. Gong, Y. Liu, Phys Rev Lett. **112**, 113002 (2014)
[3] B. Hu, J. Liu, S. G. & Chen, Phys. Lett. A **236**, 533 (1997)
[5] R. P. Feynman, Rev. Mod. Phys. **20**, 367 (1948)

RMT Two-Electron outer region for ab-initio modelling of Ultrafast Dynamics

Jack Wragg[1], **Hugo van der Hart**[1]
1. Centre for Theoretical Atomic, Molecular, and Optical Physics,
Queens University Belfast, University Rd, Belfast, BT7 1NN, Northern Ireland

R-matrix with time-dependence (RMT) is an ab-initio method for solving the Schrödinger equation for many-electron atoms in the presence of short intense laser pulses on the attosecond timescale [1, 2]. RMT makes use of the traditional R-Matrix division of configuration space into (i) a many-electron inner region and (ii) a region describing single-ionisation states, where the ionised electron is represented using finite-difference (FD) techniques. Previous applications of RMT include calculation of rates and spectra for single electron ionisation, and investigation of HHG in many-electron atoms.

The RMT formalism has been extended to include a third region (iii) where double-ionisation states are represented through the inclusion of a two-dimensional finite difference grid. This double-ionisation grid is connected to single-ionised states (region (ii)) through standard RMT Bloch operator techniques. Recent research has demonstrated an application of region (iii) by the study of two-electron photoionisation of a He atom with RMT. Cross sections for the one-photon two-electron ionisation process were calculated (which were previously unobtainable with RMT), and show good agreement with benchmark data [3].

More recently, this extended RMT has further been applied to a three-electron system - S-wave electron impact of a He atom. This added complexity makes necessary the consideration of differing spin couplings, and residual ion states for region (iii). An example He electron impact result is shown in figure 1, where the resulting time-dependent wavefunction (1a) is seperated into components where the two outer electrons are coupled to S=1 and S=0 (1b and 1c respectively). A range of physical processes is seen and measurable in the RMT model, including elastic scattering, impact excitation and impact ionisation. Cross sections may be calculated for all of these processes and show agreement with benchmark data. RMT also provides insight into the spin dynamics during the collision, and evidence of autoionising states is also present. Calculated decay rates of these autoionising states are again found to be in agreement with benchmark data. Work is ongoing to apply this RMT formalism to attosecond two-electron photoionisation in three electron systems, with the expectation that RMT will soon enable the ab-initio study of two-electron ionisation of general atoms.

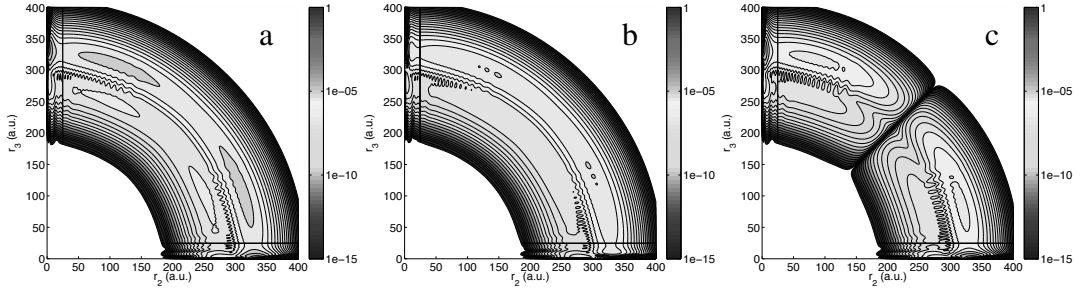

Fig. 1 Probability densities according to the radial position of the outer two electrons (r2 and r3 - the impact electron and the ejected electron) after S-Wave electron impact ionisation of a He atom. (a) Full wavefunction density. (b, c) Contribution of outer two electrons coupled to S=1 and S=0 respectively.

References

[1] Nikolopoulos, L. A. A., J. S. Parker, and K. T. Taylor., *Combined R-matrix eigenstate basis set and finite-difference propagation method for the time-dependent Schrödinger equation: The one-electron case*, Phys. Rev. A. **78**, 063420 (2008).

[2] Moore, L. R., Lysaght, M. A., Nikolopoulos, L. A. A., Parker, J. S., *The RMT method for many-electron atomic systems in intense short-pulse laser light*, Journal of Modern Optics. **58**, 1132-1140 (2011).

[3] Wragg, Jack, J. S. Parker, and H. W. van der Hart., *Double ionization in R-matrix theory using a two-electron outer region*, Phys. Rev. A. **92** 022504 (2015)

Carrier-Wave Rabi Flopping Signatures in HHG for Alkali Species

M. F. Ciappina[1], J. A. Pérez-Hernández[2], A. S. Landsman[3], T. Zimmermann[4], L. Roso[2], F. Krausz[1,5] and M. Lewenstein[6,7]

1. Max-Planck Institut für Quantenoptik, Hans-Kopfermann-Str. 1, D-85748 Garching, Germany
2. Centro de Láseres Pulsados (CLPU), Parque Científico, E-37008 Villamayor, Salamanca, Spain
3. Max-Planck Institut für Physik complexer Systeme, Nöthnitzer-Str. 38, D-01187 Dresden, Germany
4. Physics Department, ETH Zurich, CH-8093 Zurich, Switzerland
5. Fakultät für Physik, Ludwig-Maximilians-Universität München, Am Coulombwall 1, D-85748 Garching, Germany
6. ICFO-Institut de Ciènces Fotòniques, The Barcelona Institute of Science and Technology, 08860 Castelldefels (Barcelona), Spain
7. ICREA-Institució Catalana de Recerca i Estudis Avançats, Lluis Companys 23, 08010 Barcelona, Spain

We present a theoretical study of the carrier-wave Rabi flopping (CWRF) phenomenon in real atoms by employing numerical simulations of high-order harmonic generation (HHG) in alkali species [1]. Given the short HHG cutoff, closely related to the low saturation intensity of the targets under study, we concentrate on the features of the third harmonic of sodium (Na) and potassium (K) atoms. For pulse areas of 2π and Na atoms, a unique peak appears, which, after analyzing the ground state population, we correlate it with the conventional Rabi flopping behavior. On the other hand, and for larger pulse areas, CWRF occurs, and emerges as a more complex structure in the around the third harmonic frequency, i.e. $\omega/\omega_0 = 3$, where ω_0 is the central frequency of the driven laser pulse. This new feature is identified with rapid changes in the ground state population, in a time scale much shorter than the conventional one. This new characteristics observed in K atoms indicates the breakdown of the area theorem, as was already demonstrated under similar circumstances in narrow band gap semiconductors [2]. We observe that HHG spectra of K atoms present a drastic change around the third harmonic, as pulse envelope area increases. Our results are directly analogous to the manifestation of CWRF behavior observed in GaAs [2]. It is worth noting the marked contrast to the HHG spectra of Na, where a single peak is present in the third harmonic regardless of the envelope pulse area (see Fig. 1).

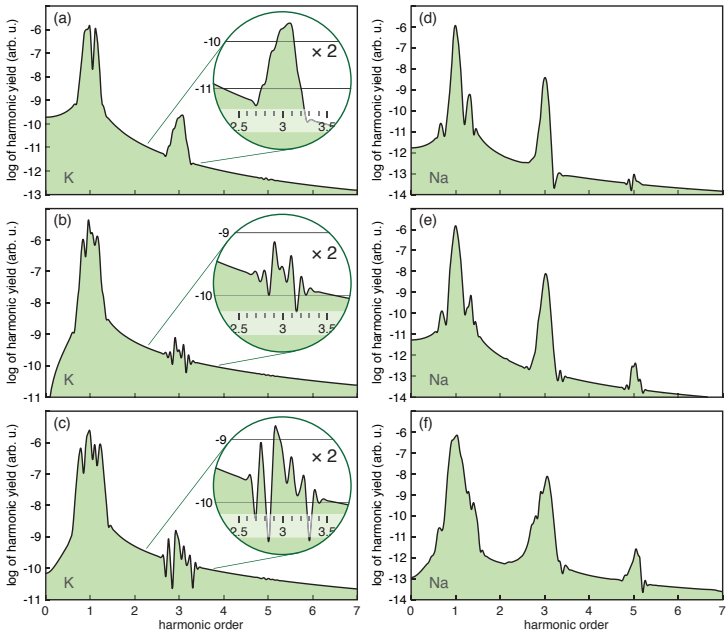

Fig. 1 3D-TDSE harmonic spectra in K for the corresponding laser intensities $I = 3.158 \times 10^{11}$ W/cm^2 (panel a), $I = 5.6144 \times 10^{11}$ W/cm^2 (panel b) and $I = 1.108 \times 10^{12}$ W/cm^2 (panel c) and an 18 fs (FWHM) driving pulse. Panels (d), (e) and (f) represent the HHG in Na for the same laser parameters. The insets of panels (a), (b) and (c) show a zoom around the region of the third harmonic $\omega/\omega_0 = 3$.

Our model uses accurate values for the atomic wavefunction of both ground and excited states as well as typical laser parameters, easily achievable with the current laser technology. As a consequence, the experimental confirmation of our results appears straightforward. Moreover, the CWRF phenomenon in atoms could emerge as a robust alternative for carrier-envelope phase (CEP) characterization for long pulses and in a plausible way to control the strong field ionization, considering it is governed by the population of the atomic bound states.

References

[1] M.F. Ciappina et al., *Carrier-wave Rabi Flopping Signatures in High-order Harmonic Generation for Alkali Atoms,* Phys. Rev. Lett. **114**, 143902 (2015).
[2] O. D. Mücke et al., *Signatures of Carrier-Wave Rabi Flopping in GaAs,* Phys. Rev. Lett. **87**, 057401 (2001).

Angular distributions of photoelectrons ejected from Neon in the presence of XUV and IR laser fields

R. Morgan[1*] and H. W. van der Hart[1]

[1] *Centre for Theoretical Atomic Molecular and Optical Physics*
[*] *Corresponding author:* rmorgan12@qub.ac.uk

The rapid development of both high intensity and ultrashort light sources, e.g. free electron lasers (FELs) have led to some great breakthroughs in atomic science, unlocking the potential for experimental observation of electron dynamics with attosecond timescale resolution [1, 2, 3] and even control of these dynamics [4].

These advances however do come at a cost: the need for powerful theoretical methods which can describe and interpret experimental results on the dynamics of an atomic system that are simultaneously accurate and computationally feasible.

Theoretical models of varying complexity can be used to solve problems in these areas. These range from simple models which can cost very little in terms on computational power to complex models which describe the whole dynamics of an atomic system with high precision but are, in general, far more costly in terms of computing power. The latter contains ab initio calculations, such as the R-matrix with time-dependence (RMT) [5, 6, 7].

Recent experimental results of angular dependence of neon irradiated by intense two-colour fields have highlighted some interesting modulations in emission angle [8]. These experimental findings were compared to strong-field approximation calculations (SFA). However, the comparison showed some qualitative differences.

Using RMT we can investigate this system from first principles and compare outcomes to both experimental and theoretical model findings. Photoelectron angular distribution spectra are obtained for a range of intensities showing an increase in angular modulation and sideband formation as intensity increases. Our ab initio results are in very good agreement with experimental results for the central line; however for the second side band, our calculations compare better to the SFA model. We also compare RMT calculations with the soft-photon approximation [9].

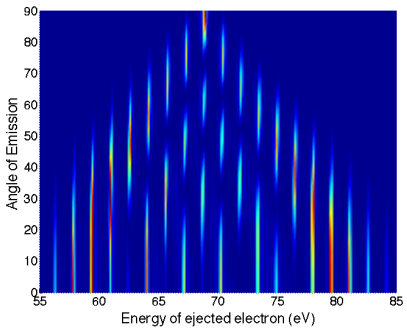

Figure 1: Photoelectron angular distribution spectra for the photoionisation of Neon irradiated by a combination of an XUV laser at 90.5 eV photon energy and an IR laser operating at 800 nm and intensity of 5×10^{12} W/cm^2.

References

[1] M. Hentschel *et al.*, Nature **414**, 509 (2001)
[2] M. Drescher *et al.*, Nature **419**, 803 (2002)
[3] M. Uiberacker *et al.*, Nature **446**, 627 (2007)
[4] A. Landsman *et al.*, Optica **1** 545 (2014)
[5] H. W. van der Hart, M. A. Lysaght and P.G. Burke Phys. Rev. A **76**, 043405 (2007)
[6] M. A. Lysaght, H. W. van der Hart and P. G. Burke, Phys. Rev. A **79**, 053411 (2009)
[7] M. A. Lysaght, *et al.*, Quantum Dynamic Imaging, Springer, 107 (2011)
[8] S. Düsterer *et al.*, J. Phys. B **46** 164026 (2014)
[9] A. Maquet *et al.*, Journal of Modern Optics **54** 1847 (2007)

Towards multidimensional spectroscopy with ultrashort XUV and soft-x-ray pulses

Thomas Ding, Alexander Blättermann, Christian Ott, Veit Stooß, Kristina Meyer, Marc Rebholz, Lennart Aufleger, Paul Birk, Maximilian Hartmann, Andreas Kaldun, and Thomas Pfeifer

Max-Planck-Institut für Kernphysik, Saupfercheckweg 1, 69117 Heidelberg, Germany

Ultrafast multidimensional coherent spectroscopy at infrared (IR), visible (VIS), and ultraviolet (UV) frequencies has been widely used to map the (time-dependent) couplings between vibrational and electronic states, typically in complex molecules. However, the extension to the extreme ultraviolet (XUV) and (soft)-x-ray spectral range has not yet been realized partly due to the failure of standard optical elements at these photon energies. The XUV spectral range is of particular interest as it contains the photo-excitation region of spatially localized inner-valence electrons in atoms. Thus, ultrashort laser pulses at appropriately tuned XUV frequencies allow to selectively excite a specific atom within a molecule and then to probe the initiated charge migration or transfer to different atoms in the molecule.

As a first step towards implementing such multidimensional spectroscopy with XUV [1] light, we present time-resolved four-wave-mixing (FWM) spectroscopy on 2s inner-valence transitions in neon [2]. In this scheme, the nonlinear atomic response is stimulated from the combined action of a perturbative XUV- and a VIS-pump pulse together with a strong time-delayed VIS-probe pulse. The first two coinciding pulses (attosecond XUV and femtosecond VIS) form a two-colour pump step for the coherent excitation of both dipole-allowed and dipole-forbidden transitions to final states ($2s^{-1}$np) and ($2s^{-1}$3s, $2s^{-1}$3d), respectively. The third pulse (high-intensity femtosecond VIS) can be varied in time delay with respect to the pump and thus plays the role of a dynamical control or probe field by inducing coupling between dipole-allowed and dipole-forbidden states. Observed as a function of time delay and VIS intensity, the nonlinear spectral response reveals the dynamical pathways along which the system is driven (cf. fig.1). This method allows to perform time-resolved XUV spectroscopy on dipole-forbidden states and to study their coupling to other excited states.

Furthermore, we present the experimental design and current status of a multidimensional XUV and soft-x-ray spectroscopy setup applicable for both attosecond high-harmonic sources and ultra-intense free-electron lasers (FEL). The heart of the setup is a dynamical soft-x-ray-compatible four-segment split mirror to generate temporally well-controlled multi-pulse sequences for four-wave mixing. First experiments will again target benchmark systems such as helium, neon and small molecules. In the near future, one key application with FEL pulses will be the femtosecond-time-resolved multidimensional site-specific spectroscopy of molecules to follow charge migration as a function of time.

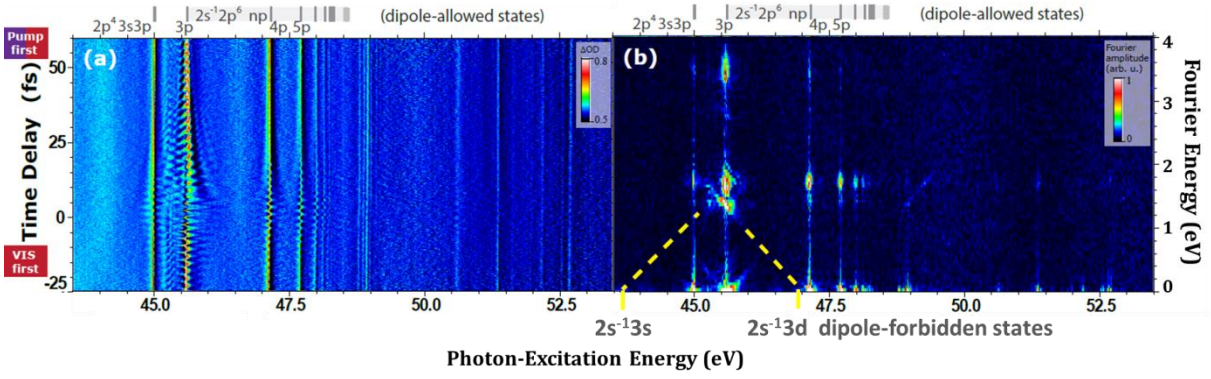

Fig. 1(a) XUV Transient absorption spectroscopy of 2s-hole states in neon with ~10^{12} W/cm^2 VIS pulses. The key mechanism to observing spectral modulations as a function of delay is the two-pulse/two-colour pump step coherently exciting both dipole-allowed and -forbidden transitions. (b) Fourier transform along the time-delay axis. Transient forbidden/allowed level-couplings give rise to directed diagonal Fourier features pointing towards the coupling partner (dashed lines as guide to the eye).

References

[1] I. Schweigert, S. Mukamel, *Coherent Ultrafast Core-Hole Correlation Spectroscopy: X-Ray Analogues of Multidimensional NMR*, Phys. Rev. Lett. **99**, 163001 (2007).

[2] T. Ding et al., *Time-resolved four-wave-mixing spectroscopy for inner-valence transitions*, Opt. Lett. **41**, 709-712 (2016).

Computation of high harmonic generation spectra using time-dependent configuration interaction

Marie Labeye, Jérémie Caillat, Richard Taïeb
Sorbonne Universités, UPMC Univ Paris 06, CNRS, LCPMR, 11 rue Pierre et Marie Curie 75231 Paris Cedex 05, France

High-harmonic generation (HHG) is a highly nonlinear optical phenomenon [1] that can provide coherent XUV and soft X-ray radiation with attosecond (10^{-18} s) durations. This property makes it of increasing interest because it offers the opportunity to investigate unexplored research areas in atoms and molecules with unprecedented time resolution [2-4]. The HHG process arises when a gas of atoms or molecules interacts with a strong infrared femtosecond laser pulse and can be understood by means of semi-classical pictures, such as the celebrated three-step model [5]: (1) an electron escapes from the atom through tunnel ionization induced by the strong laser field, (2) it is accelerated away by the laser field until the sign of the field changes, whereupon the electron is reaccelerated back to the nucleus, (3) where it emits a photon as it recombines to the ground state.

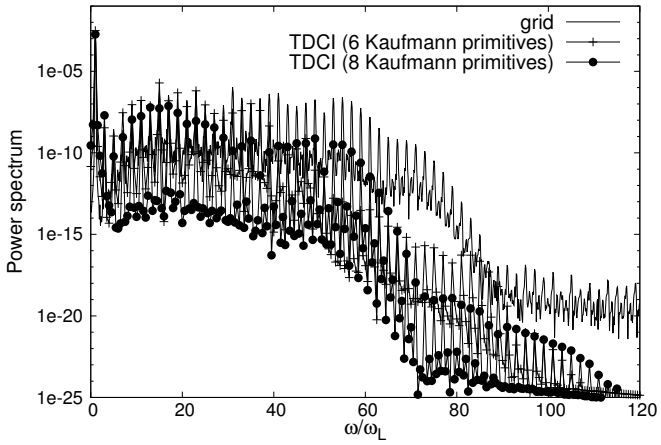

Fig. 1 HHG spectrum of a 1D Helium at λ = 800 nm and I = $3x10^{14}$ W.cm^{-2}

The ab initio calculation of high harmonic generation spectra is a real computational challenge for large systems, since it requires to solve the time dependent Schrödinger equation, which is impossible, even in the near-future, when the number of electrons exceeds two. To tackle this issue, we explore the computation of HHG spectra of multi-electronic systems using time dependent configuration interaction (TDCI) i.e. solving the Schrödinger equation projected on a CI basis. To build the latter, one has to choose a basis of single electron primitives to properly represent the bound and continuum states of the system, the delocalized continuum states being a real challenge for the commonly used localized function such as gaussians. Following the work already done in [6] on a single electron atom (the hydrogen), we investigate the efficiency of Gaussian functions specifically designed for the description of the continuum proposed by Kaufmann et al. [7]. We assess the range of applicability of this approach by studying one dimensional systems with two electrons, for which exact calculations on a grid can be performed and then be used as a reference to test the TDCI method (see Fig. 1). We believe that if the results obtained with two electrons are in reasonable agreement with the grid reference, then it will allow us to extend this method to bigger systems for which no accurate methods of calculations are known.

References

[1] P. Antoine, A. L'Huiller, and M. Lewenstein, *Attosecond Pulse Trains Using High–Order Harmonics*, Phys. Rev. Lett. **77**, 1234 (1996).
[2] J. Itatani, J. Levesque, D. Zeidler, H. Niikura, H. Pepin, J. C. Kieffer, P. B. Corkum, and D. M. Villeneuve, *Tomographic imaging of molecular orbitals*, Nature **432**, 867 (2004).
[3] E. Goulielmakis, Z.-H. Loh, A. Wirth, R. Santra, N. Rohringer, V. S. Yakovlev, S. Zherebtsov, T. Pfeifer, A. M. Azzeer, M. F. Kling, S. R. Leone, and F. Krausz, *Real-time observation of valence electron motion*, Nature **466**, 739 (2010).
[4] S. Haessler, J. Caillat, W. Boutu, C. Giovanetti-Teixeira, T. Ruchon, T. Auguste, Z. Diveki, P. Breger, A. Maquet, B. Carré, R. Taëb, and P. Salières, *Attosecond imaging of molecular electronic wavepackets*, Nature Phys. **6**, 200 (2010).
[5] M. Lewenstein, P. Balcou, M. Y. Ivanov, A. L'Huillier, and P. B. Corkum, *Theory of high-harmonic generation by low-frequency laser fields*, Phys. Rev. A **49**, 2117 (1994).
[6] E. Coccia, B. Mussard, M. Labeye, J. Caillat, R. Taïeb, J. Toulouse, and E. Luppi, *Gaussian continuum basis functions for calculating high-harmonic generation spectra*, Int. J. Quantum Chem. (accepted).
[7] K. Kaufmann, W. Baumeister, and M. Jungen, *Universal Gaussian basis sets for an optimum representation of Rydberg and continuum wavefunctions*, J. Phys. B: At. Mol. Opt. Phys.**22**, 2223 (1989).

Ultrafast VUV-Photodissociation of H_2O Isotopologues Traced by Single-shot Autocorrelation

Arne Baumann[1], **Oliver Schepp**[1], **Dimitrios Rompotis**[1], **Marek Wieland**[1,2,3], **Markus Drescher**[1,2,3]
1. Institut für Experimentalphysik, Universität Hamburg, Luruper Chaussee 149, 22761 Hamburg, Germany
2. The Hamburg Centre for Ultrafast Imaging (CUI), Luruper Chaussee 149, 22761 Hamburg, Germany
3. Centre for Free-Electron-Laser Science, Universität Hamburg, Luruper Chaussee 149, 22761 Hamburg, Germany

The VUV-induced photodissociation of water in the excited $\tilde{A}$ ($^1B_1$) state is a prototypical example of a barrierless dissociation reaction taking place on a sub 10 fs time scale. A detailed knowledge of the pulse properties in a pump-probe experiment, where the pulse duration is comparable to the reaction time of the system, is necessary to extract the time constants of molecular processes. To achieve this, we combine single-shot pulse metrology with pump-probe measurements in a colliding-pulse autocorrelation experiment.

The scheme is based on wave-front splitting of high-harmonic pulses created by a Ti:Sa laser system in a loose-focusing geometry [1,2]. The fifth harmonic (161.0 nm, 7.70 eV) is selected, focused into a gas target and ions created by the radiation are imaged onto a position-sensitive detector, thus mapping the temporal delay between both pulses onto a spatial coordinate (Fig. 1 a). Compared to traditional delay-scanning approaches this dramatically decreases acquisition time, thus increasing the statistical precision of the measurement.

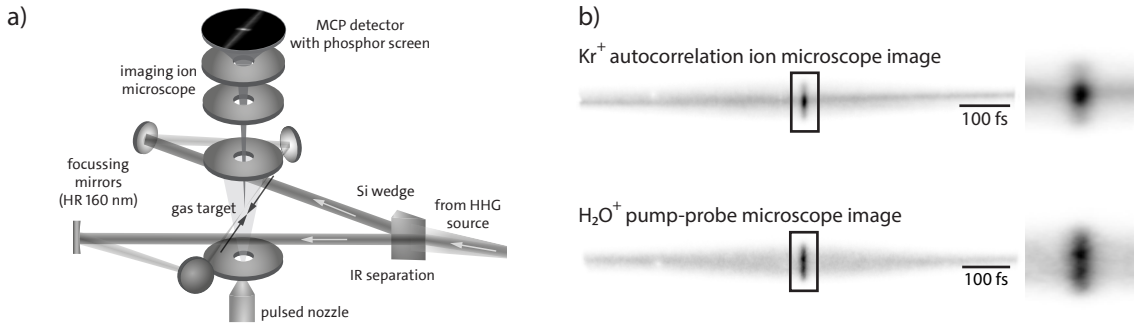

Fig. 1 (a) Experimental setup for the VUV single-shot autocorrelation experiment. (b) The ion microscope image recorded for the direct two-photon ionization of Krypton corresponds to the intensity autocorrelation of the 161.0 nm pulse, while the second image shows the pump-probe ion signal for the VUV-induced photodissociation of H_2O.

The photodissociation of water in the $\tilde{A}$ ($^1B_1$) state has been studied for the first time in a VUV+VUV approach, excluding the effects of strong IR radiation as a probe, such as bond-softening and intermediate resonances. In this scheme a time constant of less than 7 fs has been observed. Furthermore, isotope substitution has been utilized to study the primary and secondary kinetic isotope effects on the reaction dynamics. Depending on the degree of hydrogen substitution the observed dynamics take place in 10 ± 2 fs and less.

References

[1] D. Rompotis, T. Gebert, M. Wieland, F. Karimi, and M. Drescher, *Efficient generation of below-threshold harmonics for high-fidelity multi-photon physics in the VUV spectral range*, Opt. Let. **40**, 1675 (2015).
[2] T. Gebert, D. Rompotis, M. Wieland, F. Karimi, A. Azima, and M. Drescher, *Michelson-type all-reflective interferometric autocorrelation in the VUV regime*, New J. Phys. **16**, 073047 (2014)

Non-perturbative quantum-path effects in the generation of attosecond extreme-ultraviolet vortices

Laura Rego[1], Antonio Picón[2], Julio San Román[1], Luis Plaja[1], and Carlos Hernández-García[1]

1. Grupo de Investigación en Aplicaciones del Láser y Fotónica, University of Salamanca, E-37008, Salamanca, Spain

2. Argonne National Laboratory, Argonne, Illinois 60439, USA

Helical phased beams, also called optical vortices, are structures of the electromagnetic field with a spiral phase ramp about a point-phase singularity. The spiral phase imprints an orbital angular momentum (OAM) to the beam, in addition to the intrinsic angular momentum associated with the polarization. These beams, commonly generated in the optical regime, present a well-defined OAM during the beam propagation and have a wide range of applications: classical and quantum communications, micromanipulation, microscopy, among others [1]. The production of OAM beams in the extreme-ultraviolet (XUV) and x-ray regimes is of great interest, as it will allow extending the applications of optical vortices down to the nanometric scale. Phase singularities can be imprinted to short-wavelength light using high-order harmonic generation (HHG), producing XUV vortices [2]. When driving HHG by an optical OAM beam, highly-charged harmonic vortices with unprecedented spatio-temporal properties are emitted in the form of helical attosecond beams [3]. It has been theoretically [3] and experimentally [4] shown that OAM is conserved in HHG, i.e., each harmonic is generated with a topological charge of $q\ell$, being q the harmonic order and ℓ the topological charge of the driving optical beam.

In this contribution we explore, through numerical simulations, the contribution of different quantum paths to the generation of XUV beams through HHG. We study the role of the non-perturbative atomic phase in the generation of harmonic vortices. To this end, we present a detailed analysis of OAM-HHG driven by single or multiple infrared OAM beams. In particular, if driven by a combination of infrared vortices with different topological charges, HHG leads to the emission of unprecedented vortex beam structures whose topological charge is affected by the non-perturbative atomic phase of the HHG process itself [5]. We know that the transverse phase matching [6] plays a fundamental role in the macroscopic emission of XUV vortices. We show how to take advantage of the transverse phase matching to select helical attosecond beams generated from short or long quantum paths, and thus, exhibiting positive or negative temporal chirp [7].

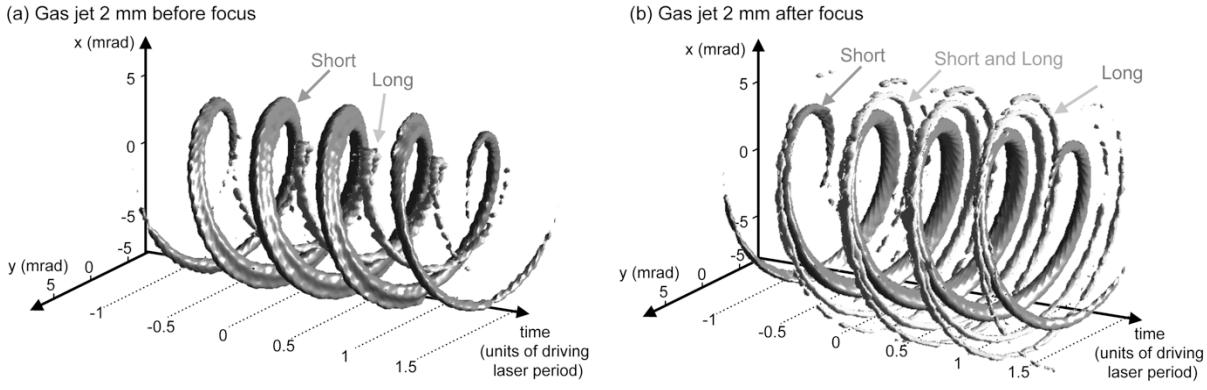

Fig. 1. Helical structure of attosecond pulses showing the threaded contributions of short and long quantum paths for a HHG simulation where the argon gas jet is placed 2 mm before (a) and after (b) the focus position. The driving field is modelled as an infrared (800 nm) vortex beam with ℓ=1, with a temporal $\sin^2$ envelope of 15.4 fs at full-width-half-maximum and $1.4\text{x}10^{14}$ Wcm^{-2} peak intensity [6].

References

[1] A. M. Yao, and M. J. Padgett, *Orbital angular momentum: origins, behavior and applications*, Adv. Opt. Photonics. **3**, 161-204 (2011).

[2] M. Zürch, C. Kern, P. Hansinger, A. Dreischuh, and Ch. Spielmann, *Strong-field physics with singular light beams*, Nature Phys. **8**, 743-746 (2012).

[3] Carlos Hernández-García, Antonio Picón, Julio San Román, and Luis Plaja, *Attosecond Extreme Ultraviolet Vortices from High-Order Harmonic Generation*, Phys. Rev. Lett. **111**, 083602 (2013).

[4] Genevieve Gariepy, Jonathan Leach, Kyung Taec Kim, T. J. Hammond, E. Frumker, Robert W. Boyd, and P. B. Corkum, *Creating High-Harmonic Beams with Controlled Orbital Angular Momentum*, Phys. Rev. Lett. **113**, 153901 (2014).

[5] Laura Rego, Antonio Picón, Julio San Romám, Luis Plaja, and Carlos Hernández-García, in preparation.

[6] C. Hernández-García, I. J. Sola, and L. Plaja, *Signature of the transversal coherence length in high-order harmonic generation Phys. Rev. A*. **88**, 043848 (2013).

[7] Carlos Hernández-García, Julio San Román, Luis Plaja, Antonio Picón, *Quantum-path signatures in attosecond helical beams driven by optical vortices,* New J. Phys. **17**, 093029 (2015).

Harmonic Spectra of Neon in Mixed Laser Pulse Schemes

Kathryn Hamilton[1], Andrew Brown[1], Hugo van der Hart[1]

1. Centre for Theoretical Atomic, Molecular and Optical Physics, Queen's University Belfast, University Road, Belfast, BT7 1NN, Northern Ireland

High harmonic generation (HHG) is the fundamental process of attosecond science, providing us the means to observe some of the fastest dynamics known to man. Analysis of the spectra produced by HHG can give us an insight on the motion of electrons on their own characteristic attosecond timescale (10^{-18} s) [1] and the high energy harmonic light produced from the process can be used to create ultrashort ($T < 10^{-15}$ s) laser pulses [2].
However, the description of HHG is a computationally challenging task as electrons are not simple, separable particles, but are in fact strongly correlated. Therefore determining the response of a many-electron atom to a laser pulse typically requires the use of massively parallel computers. At Queen's University Belfast, through the use of the R-matrix with time-dependence method (RMT), we have successfully described the response of general, multielectron atoms in short, intense laser fields. RMT applies the basic principles of R-matrix theory, in which all interactions between all electrons are taken into account close to the nucleus, but exchange interactions are neglected when one electron has become distanced from the parent ion.
This poster presents the latest results from a study of HHG in Neon. Included are spectra produced in a mixed (800nm + time-delayed 400nm) laser pulse scheme. The introduction of the second harmonic laser pulse allows the control of electron trajectories, and the identification of time-dependent features in the spectra.

a) **b)**

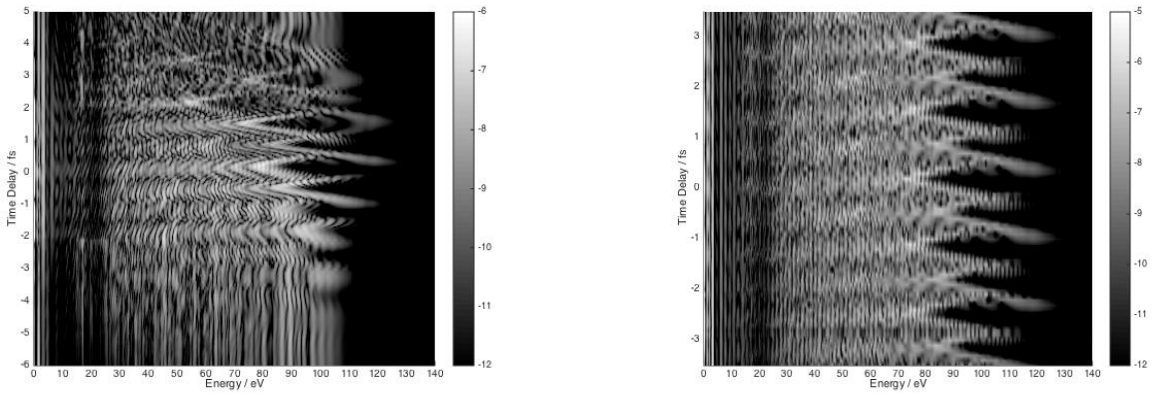

Fig. 1 Harmonic spectra produced when Neon is subjected to a 6 cycle (3 $\sin^2$ ramp-on 3 $\sin^2$ ramp-off) 800nm pulse at $4x10^{14}$ W/cm^2 mixed with **a)** a 6 cycle (3 on - 3 off) 4 $x10^{13}$ W/cm^2 time-delayed 400mn pulse and **b)** a 12 cycle (3-6-3) $4x10^{13}$ W/cm^2 time-delayed 400mn pulse.

References

[1] Olga Smirnova et al, *High Harmonic Interferometry of Multi-electron Dynamics in Molecules*, Nature **460**, 972 (2009).
[2] P. M Paul et al, *Observation of a Train of Attosecond Pulses from High Harmonic Generation*, Science **312**, 1689 (2001).

Near-Forward Rescattering Photoelectron Holography in Strong-Field Ionization: Extraction of the Phase of the Scattering Amplitude

Yueming Zhou[1,2], **Oleg I. Tolstikhin**[3], **Toru Morishita**[4,2]

1. School of Physics, Huazhong University of Science and Technology, Wuhan 430074, China

2. Department of Engineering Science, The University of Electro-Communications, 1-5-1 Chofu-ga-oka, Chofu-shi, Tokyo 182-8585, Japan

3. Moscow Institute of Physics and Technology, Dolgoprudny 141700, Russia

4. Institute for Advanced Science, The University of Electro-Communications, 1-5-1 Chofu-ga-oka, Chofu-shi, Tokyo 182-8585, Japan

Electrons produced in tunneling ionization of atoms and molecules by intense laser fields being driven by the field may fly directly to a detector without interacting with the parent ion or may first undergo rescattering by the ion. The interference of direct and near-forward rescattered electrons with the same final momenta results in a distinct strong-field photoelectron holography (SFPEH) pattern [1] in photoelectron momentum distributions (PEMD) observed experimentally for various targets. It was suggested [1] that this pattern should encode some structural information, but what kind of information and how to decode it remained unknown. These most important for target imaging questions have been answered in our recent paper [2].

Our analysis is based on the adiabatic theory [3]. In the adiabatic approximation, the interference phase determining a near-forward rescattering SFPEH pattern produced by a linearly polarized laser pulse is $\Delta\phi_{\rm AA} = \frac{1}{2}k_\perp^2\Delta t + \alpha$, where Δt is the time between the ionization and rescattering events for a forward rescattered electron, which depends only on the component k_z of the photoelectron momentum along the laser field, and α is the phase of the scattering amplitude, which additionally depends on the perpendicular component $k_\perp$. On the other hand, the interference phase can be extracted from a given PEMD by fitting the SFPEH pattern with predictions of the adiabatic theory. This enables one to find α as a function of $(k_\perp, k_z)$, which can then be converted into a function of the incident momentum and scattering angle. We demonstrate this imaging procedure by applying it to PEMDs calculated by solving the time-dependent Schrödinger equation (TDSE) for a model potential. Figure 1(a) shows such a PEMD. The low-contrast nearly horizontal interference fringes represent an SFPEH pattern of the type discussed above. Figure 1(b) demonstrates that the interference minima extracted from the TDSE results closely follow the predictions of the adiabatic theory. Figure 1(c) compares the phase α of the scattering amplitude extracted from the TDSE results with that obtained from scattering calculations. The agreement is good and even the relatively small difference between the two potentials considered is clearly resolved.

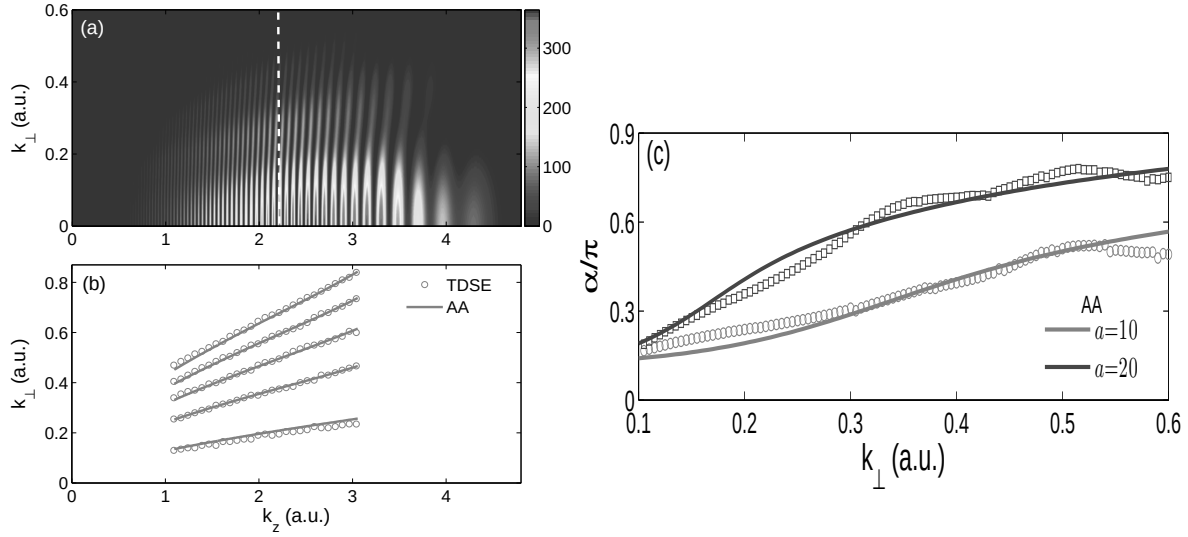

Fig. 1 (a) TDSE results for the PEMD produced in ionization from a potential $V(r) = -\exp[-(r/a)^2]/r$ with $a = 10$ by a one-cycle pulse with $\lambda = 800$ nm and $I = 3.5\times10^{14}$ W/cm^2. (b) Interference minima of the near-forward rescattering SFPEH pattern extracted from the TDSE results (open circles) and obtained in the adiabatic approximation from $\Delta\phi_{\rm AA} = (2n+1)\pi$ with $n = 0, 1, \ldots, 4$ (solid lines). (c) The phase α of the scattering amplitude for potentials with $a = 10$ and 20 as a function of $k_\perp$ at $k_z = 2.2$ extracted from the TDSE results (symbols) and obtained from scattering calculations (solid lines).

References

[1] Y. Huismans *et al.*, *Time-Resolved Holography with Photoelectrons*, Science **331**, 61 (2011).

[2] Y. Zhou, O. I. Tolstikhin, and T. Morishita, *Near-Forward Rescattering Photoelectron Holography in Strong-Field Ionization: Extraction of the Phase of the Scattering Amplitude*, Phys. Rev. Lett., accepted for publication (2016).

[3] O. I. Tolstikhin and T. Morishita, *Adiabatic theory of ionization by intense laser pulses: Finite-range potentials*, Phys. Rev. A **86**, 043417 (2012).

High-Order Parametric Amplification in Intense Laser Field

V V Strelkov[1], M A Khokhlova[1,2]

1. A.M.Prokhorov General Physics Institute of RAS, Moscow 119991, Russia

2. M.V.Lomonosov Moscow State University, Moscow 119991, Russia

Usually nonlinear optics deals with processes involving few photons and describes the matter response in the terms of nonlinear susceptibilities $\chi^{(m)}$. If the laser field perturbatively interacts with matter, this approach allows description for numerous nonlinear effects. However, in the case of intense laser field the perturbation approach fails. The only process which is well-understood in this case is high-order harmonic generation (HHG). The study of the other nonlinear optical processes in the nonperturbative regime is limited, among other factors, by poorly developed methods of their description. In particular, experimental [1] and numerical [2] observation of the exponential growth of the harmonic signal lead to active discussion [3,4].

In this paper we develop an approach describing matter response in the presence of a given pump laser field and a weaker field (this could be a weak external field or the HH field generated in the target). The interaction of the latter field with matter can be described in terms of the *induced susceptibilities* $\kappa_q^{(m)}$, where q and m are numbers of the photons from the pump and the weak field, respectively. We study the permutation symmetry of the induced susceptibilities, which is to some extent analogous to such symmetry of $\chi^{(m)}$. The technique of the induced susceptibilities allows understanding of number of published results, for instance, the properties of the ultrahigh-order wave mixing in noncollinear HHG [5] or properties of the two-color laser-plasma generation of terahertz radiation [6]. The propagation equations for the weak field is similar to such equations in the "usual" nonlinear optics. Thus we can describe high-order frequency mixing, high-order parametric amplification and generation, high-order Raman scattering. In some cases these equations have solutions which are well-known in the nonlinear optics, for instance, the exponential growth for the parametric amplification, and in other cases they provide new types of solutions, for instance, the super-exponential (namely, hyperbolic) growth. Using numerical solution of the 3D time-dependen Schrodinger equation (TDSE) we calculate the induced susceptibilities for the laser intensities typically used for HHG. The found susceptibilities are high enough to provide parametric amplification of the seeding XUV. This seeding is generated in the process of high-order wave-mixing.

Our analytical findings are confirmed by results of the numerical propagation equation solution. This solution is done simultaneously for the laser and generated fields and uses the nonlinear polarization calculated via 3D TDSE for every slice of the generating medium.

Experimentally the process of high-order parametric amplification can be realized in high-pressure gas filled capillaries. This can be a perspective way of intense coherent XUV generation.

References

[1] J. Seres et al., *Nature Phys.* **6**, 455 (2010)
[2] Carles Serrat, *Phys. Rev. Lett.* **111**, 133902 (2013)
[3] S. Kazamias et al., *Nature Phys*. **6**, 927 (2010)
[4] J. Seres et al., *Nature Phys*. **6**, 928 (2010)
[5] J. B. Bertrand et al., *Phys. Rev. Lett.* **106**, 023001 (2011)
[6] N. V. Vvedenskii et. al, *Phys. Rev. Lett.* **112**, 055004 (2014)

Influens of Defects in Regular Nanosystems on Interference Processes at the Reemission of Attosecond Electromagnetic Pulses

V.I. Matveev and D.N. Makarov

Northern (Arctic) Federal University, Severnaya Dvina Emb. 17, 163002 Arkhangelsk, Russia

Crystals and nanostructured targets are natural diffraction gratings for X rays. The diffraction of X rays by various periodic structures is usually described as the scattering of plane waves with infinite time duration [1]. The scattering of attosecond electromagnetic pulses from such structures has been poorly studied to date. At the same time, such processes can supplement the X-ray diffraction analysis by the capabilities of high time resolution spectroscopy, including attosecond spectroscopy and attosecond metrology [2–6]. Nevertheless, the processes of interference at the scattering of attosecond pulses from various regular targets have been studied only in a few works. The theory of the reemission of attosecond electromagnetic pulses by arbitrary multiatomic systems consisting of isolated complex atoms was developed in [7–9]. Interference effects become dominant in the rescattering spectra when targets are regular structures with a large number of atoms. In this case, the angular distributions of the incident and scattered radiations can be significantly separated by choosing the spatial structure of targets and their various combinations. The theory of the reemission of attosecond electromagnetic pulses by arbitrary regular multiatomic systems consisting of identical complex atoms was developed in [10] with allowance for chaotic thermal vibrations. However, interference processes at the reemission of attosecond electromagnetic pulses by arbitrary regular multiatomic systems containing various defects have not yet been considered.

In this work, the effect of defects in nanostructured targets on interference spectra at the reemission of attosecond electromagnetic pulses is considered. General expressions were obtained for calculations of spectral distributions for one-, two-, and threedimensional multiatomic nanosystems consisting of identical complex atoms with defects such as bends, vacancies, and breaks. Changes in interference spectra by a linear chain with several removed atoms (chain with breaks) and by a linear chain with a bend have been calculated as examples allowing a simple analytical representation. Generalization to two- and threedimensional nanosystems has been developed. The proposed approach can be directly expanded to more general types of defects.

References

[1] J. M. Cowley, Diffraction Physics (North-Holland, Amsterdam, 1975).
[2] P. Agostini, Rep. Prog. Phys. 67, 813 (2004).
[3] P. V. Corkit and F. Krausz, Nature Phys. 3, 381 (2007).
[4] F. Krausz and M. Ivanov, Rev. Mod. Phys. 81, 163 (2009).
[5] A. M. Zheltikov, Phys. Usp. 54, 29 (2011).
[6] J. Fink, E. Schierle, E. Weschke, and J. Geck, Rep. Prog. Phys. 76, 056502 (2013).
[7] V. I. Matveev and D. U. Matrasulov, JETP Lett. 96, 628 (2012).
[8] D. N. Makarov and V. I. Matveev, J. Exp. Theor. Phys. 117, 784 (2013).
[9] D. N. Makarov and V. I. Matveev, Opt. Spectrosc. 116, 163 (2014).
[10] D. N. Makarov and V. I. Matveev, JETP Lett. 101, 603 (2015).

Superfluid in helical container as a sensor of metric disturbances.

A.Yu.Okulov*
Russian Academy of Sciences, 119991, Moscow, Russian Federation.

Gravitational waves emitted by coalescent black holes produce tiny changes of space intervals. Current experimental sensitivity of long base laser interferometers [1] offers a possibility to detect strains of the order of $10^{-21}Hz^{1/2}$ [2]. Next generation of LIGO/LISA detectors [3] is expected to be a matter wave interferometers known currently as a sensors of gravity, rotations and magnetic fields. The inherent advantage of atomic interferometers compared to optical Sagnac [4] and Michelson [1] sensors is of the order of ratio of the atomic rest mass to photon energy $mc^2/\hbar\omega \sim 10^{10}$.This feature had been demonstrated for atomic Mach-Zehnder and Sagnac configurations.

Recently the alternative quantum interference device with twisted interference fringes had been proposed [5]. The atomic interference fringes are formed inside helical waveguide produced by two phase-conjugated optical vortices [6]. Waveguide profile is given in cylindrical coordinates z, r, θ by:

$$V_{twist}(z,r,\theta) \sim \exp\left[\frac{-2r^2}{D_0^2(1+z^2/k^2D_0^4)}\right][1+\cos(2kz+2\ell\theta)]\cdot\frac{r^{2|\ell|}}{D_0^{2|\ell|}}, \quad (1)$$

where Rayleigh-range $L_R \cong D_0^2/\lambda$ of LG (Laguerre-Gaussian) vortex beams [7] with topological charge ℓ depends on beam waist radius D_0, wavenumber $2\pi/\lambda$. Noteworthy this helical potential had been realized experimentally with phase conjugating photorefractive mirror [8]. The exact solution for macroscopic wavefunction in this potential [9] predicts that atomic cloud will move along $\vec{z}$ (interferometer axis) with translational velocity $V_z = \pm|\vec{\Omega}_\oplus|\ell/k$, where $\vec{\Omega}_\oplus$ is angular velocity of reference frame.

In a more general case when matter wave interferometer is placed on rotating sphere the interferometer axis $\vec{z}(t)$ moves around frame rotation axis $\vec{\Omega}_\oplus$ thus Gross-Pitaevskii equation for matter wavefunction Ψ has the form [10]:

$$i\hbar\frac{\partial\Psi}{\partial t} = -\frac{\hbar^2}{2m}\Delta\Psi + V_{twist}(z,r,\theta)\,\Psi + g|\Psi|^2\Psi - \vec{\Omega}_\oplus\cdot\hat{\vec{L}}\Psi + m\vec{g}\cdot\vec{z}\,[1+\epsilon\cos(\Omega_{gr}t)], \quad (2)$$

where $\hat{\vec{L}}$ is angular momentum operator, m is the mass of trapped atom, $\vec{g}$ is free-fall acceleration, Ω_{gr} is frequency of gravitational wave, ϵ is small parameter. In this case the matter wave vortices [9] inside helical waveguide experience the splitting of energy δE due to Coriolis effect:

$$\delta E(t) = -\hbar\ell\vec{z}(t)\cdot\vec{\Omega}_\oplus,\ \ \alpha(t) = \int_0^t d\tau\,\delta E(t)/\hbar, \quad (3)$$

where geometric phase $\alpha(t)$ [11] had been acquired via transport of rotating matter wave vortices along a closed trajectory (fig.1). When axes $\vec{z}$ and $\vec{\Omega}_\oplus$ are parallel to each other the geometric phase gives frequency shift via angular Doppler effect [12].

[1] B.P.Abbott et al., "LIGO: the Laser Interferometer Gravitational-Wave Observatory ", Rep. Prog. Phys.,**72(7)**, 076901 (2009).
[2] B.P. Abbott et al., "Observation of Gravitational Waves from a Binary Black Hole Merger", Phys.Rev.Lett., **116**, 061102 (2016).
[3] M.Kasevich et al., "Gravitational wave detection with atom interferometry", Phys.Lett., B **678**, 37-40 (2009).
[4] M.O.Scully, M.S.Zubairy,*"Quantum optics"*, (Cambridge University Press) (1997).
[5] A.Yu.Okulov, "Superfluid rotation sensor with helical laser trap", Journ.Low.Temp.Phys., **171**, 397-407 (2013).
[6] A.Yu.Okulov, "Phase-conjugation of the isolated optical vortex using a flat surfaces", J. Opt. Soc. Am. B, **27**, 2424-2427 (2010).
[7] L.Allen, M.W.Beijersbergen, R.J.C.Spreeuw and J.P.Woerdman, "Orbital angular momentum of light and the transformation of Laguerre-Gaussian laser modes," Phys.Rev.A, **45**,8185-8189 (1992).
[8] M.Woerdemann, C.Alpmann and C.Denz, Opt. Express, **17**, 22791(2009).
[9] A.Yu.Okulov, "Cold matter trapping via slowly rotating helical potential", Phys.Lett.A, **376**, 650-655 (2012).
[10] A.L.Fetter, Rev.Mod.Phys. **81**, 647 (2009).
[11] K. Y. Bliokh, Y. Gorodetski, V.Kleiner, and E. Hasman, "Coriolis Effect in Optics: Unified Geometric Phase and Spin-Hall Effect" Phys.Rev.Lett., **101**, 030404 (2008).
[12] A.Yu.Okulov, "Rotational Doppler shift of the phase-conjugated photons", J. Opt. Soc. Am. B **29**, 714-718 (2012).

*Electronic address: alexey.okulov@gmail.com; URL: https://sites.google.com/site/okulovalexey

Towards Measuring Parity Violation in Cold Chiral Molecules Using Vibrational Spectroscopy

S.K. Tokunaga[1], B. Argence[1], M. Pierens[1], D.B.A. Tran[1], R. Santagata[1], A. Shelkovnikov[1], O. Lopez[1], C. Daussy[1], C. Chardonnet[1], A. Amy-Klein[1], D. Nicolodi[2], M. Abgrall[2], Y. Le Coq[2], R.J. Hendricks[3], J.D. Tandy[3], E.A. Hinds[3], M.R. Tarbutt[3], B. Darquié[1]

1. Laboratoire de Physique des Lasers, Université Paris 13, Sorbonne Paris Cité, CNRS, F-93430, Villetaneuse, France

2. LNE-SYRTE, Observatoire de Paris, PSL Research Univ, CNRS, Sorbonne Univ, UPMC Univ. Paris 06, Paris 75014, France

3. Centre for Cold Matter, Blackett Laboratory, Imperial College London, London SW7 2AZ, UK

Parity violation (PV) effects have so far never been observed in chiral molecules. Caused by the weak nuclear force, PV should lead to frequency differences in the rovibrational spectra of the two enantiomers of a chiral molecule. However the effect is small, making its observation a very difficult experimental challenge. There are many reasons for attempting this difficult measurement. A successful PV measurement will undoubtedly shed light on the origins of biomolecular homochirality. It can also constitute a test of the standard model of the universe in the low-energy regime or, in fact, a probe of physics beyond it, and will serve as a stringent benchmark for computational protocols used in relativistic quantum chemistry. We have been working towards measuring this difference using Ramsey interferometry in the mid-infrared (at around 10 μm) using ultra-narrow linewidth CO_2 lasers referenced to atomic clocks in Paris via an optical link. We expect to reach a fractional sensitivity at around 10^{-15} (~10 mHz) on the frequency difference between enantiomers [1].

We present the results of preliminary investigations conducted on methyltrioxorhenium (MTO), an achiral test molecule whose chiral derivatives, which have recently been synthesized, are expected to show a $\sim 10^{-14}$ level PV effect [2]. We report on the high-resolution spectroscopy of MTO [3,4,5], both in cells and in molecular beams. This work has enabled us to identify several key elements of the current experiment needing improvement prior to making a PV measurement.

The first is the lack of tuneability of our CO_2 lasers. We present our on-going work towards their replacement with quantum cascade lasers (QCLs) [5,6] the very latest mid-IR laser technology which offers broad and continuous tuning. We have developed a method to lock any mid-IR radiation to a frequency comb stabilized to a near-IR reference. This frequency reference, generated at the French national metrology institute, is monitored against atomic frequency standards and transferred via an optical fibre. Stabilizing a QCL this way provides the ultimate frequency accuracy (potentially the 3×10^{-16} of the Cs fountain clock) and stability ($\sim 10^{-15}$ after 1s of integration) indispensable for the PV test. It results in the narrowest (0.2-Hz linewidth) and most accurate QCL to date [6], paving the way towards 'atomic physics' types of precision measurements on molecules.

Secondly, our current molecular beam source only yields a modest flux for species such as MTO and its chiral derivatives which are solid at room temperature. We plan to overcome this by developing a buffer-gas-beam source and report on our latest efforts to implement buffer-gas cooling on polyatomic species. Gas phase MTO is produced by ablating a solid target in a cryogenic buffer gas cell containing helium at ~5 K. MTO molecules cool by colliding with the cold helium. The light from a QCL is used to perform absorption spectroscopy of the Re=O stretching mode of MTO from which we estimate a temperature of ~6 K. Furthermore, the resolution demonstrated (~3 MHz) allows the hyperfine structure in the excited vibrational state to be unravelled, quite a feat for such a complex molecule, showing that precision spectroscopic measurements are already possible with this first setup. This is an essential step towards creating a cold intense beam of organometallic molecules to observe weak-force induced PV in chiral molecules.

PV aside, the technological developments proposed in this project will allow complex polyatomic molecules to be studied at an unprecedented level of precision. With such techniques, we envision new possibilities for using polyatomic molecules to perform further precision measurements of importance for fundamental physics.

References

[1] B. Darquié, C. Stoeffler, A. Shelkovnikov, C. Daussy, A. Amy-Klein, C. Chardonnet, S. Zrig, L. Guy, J. Crassous, P. Soulard, P. Asselin, T.R. Huet, P. Schwerdtfeger, R. Bast and T. Saue, *Progress Toward the First Observation of Parity Violation in Chiral Molecules by High-Resolution Laser Spectroscopy*, Chirality **22**, 870 (2010).

[2] N. Saleh, S. Zrig, T. Roisnel, L. Guy, R. Bast, T. Saue, B. Darquié and J. Crassous, *A chiral rhenium complex with predicted high parity violation effects: synthesis, stereochemical characterization by VCD spectroscopy and quantum chemical calculations*, Phys. Chem. Chem. Phys. **15**, 10952 (2013).

[3] C. Stoeffler, B. Darquié, A. Shelkovnikov, C. Daussy, A. Amy-Klein, C. Chardonnet, L. Guy, J. Crassous, T.R. Huet, P. Soulard and P. Asselin, *High resolution spectroscopy of methyltrioxorhenium: towards the observation of parity violation in chiral molecules*, Phys. Chem. Chem. Phys. **13**, 854 (2011).

[4] S.K. Tokunaga, C. Stoeffler, F. Auguste, A. Shelkovnikov, C. Daussy, A. Amy-Klein, C. Chardonnet and B. Darquié, *Probing weak force induced parity violation by high resolution mid-infrared molecular spectroscopy*, Mol. Phys. **111**, 2363 (2013).

[5] P.L.T. Sow, S. Mejri, S.K. Tokunaga, O. Lopez, A. Goncharov, B. Argence, C. Chardonnet, A. Amy-Klein, C. Daussy and B. Darquié, *A widely tunable 10-μm quantum cascade laser phase-locked to a state-of-the-art mid-infrared reference for precision molecular spectroscopy*, App. Phys. Lett. **104**, 264101 (2014).

[6] B. Argence, B. Chanteau, O. Lopez, D. Nicolodi, M. Abgrall, C. Chardonnet, C. Daussy, B. Darquié, Y. Le Coq and A. Amy-Klein, *Quantum cascade laser frequency stabilization at the sub-Hz level*, Nature Photon. **9**, 456 (2015).

Precision Atomic Calculations for Clocks Based on Highly-Charged Ions and Electron-Hole Transitions

Julian Berengut

School of Physics, University of New South Wales, Sydney, NSW 2052, Australia

Several recent proposals have necessitated new methods of calculation of atomic spectra and properties in systems where holes play an important role. Interesting systems include highly charged ions, where hole transitions can form the basis of optical atomic clocks with extraordinarily high accuracy [1, 2]. In cases where the transitions are available due to level crossings, the clocks can have extremely high sensitivity to variation of the fine-structure constant α, potentially improving current limits on time-variation of α by up to two orders-of-magnitude.

The experimental spectroscopy of one such candidate, the Ir^{17+} ion which has two holes in the otherwise closed $4f^{14}\,5s^2$ valence shells, has shown that current theoretical methods have severe limitations in accurately describing the spectrum [3]. That study included (along with the experimental spectrum) the results of several calculations including different variants of configuration interaction (CI), multiconfigurational Dirac-Fock, and Fock-space coupled cluster. None of the theories tested were able to unambiguously identify the entire observed spectrum. Furthermore many existing methods of calculation – such as the combined configuration interaction and many-body perturbation theory (CI+MBPT), correlation potential methods, and coupled-cluster methods – are designed to work well in one- or two-valence-electron atoms and particularly in near-neutral systems.

We have developed an *ab initio* method of calculating atomic spectra and properties in systems where holes play an important role. Based on the CI+MBPT method [4], implemented in AMBiT, we have employed Wick's theorem to allow the inclusion of configurations with arbitrary numbers of valence holes, electrons, and any combinations thereof concurrently (of course, the total number of electrons should be conserved). The method can treat valence-hole systems like Ir^{17+}, electron-hole excitations in, e.g. noble gases, and can be used to add important hole configurations to improve the accuracy of transitions of valence electrons.

As a first test case, we have performed calculations of spectra and sensitivity to α-variation for the Hg^+ ion, where the clock transition $6s \to 5d^{-1}\,6s^2$ has been compared with an Al^+ clock to get the best current limit on time-variation of α [5]. Previously, this ion has been treated as an 11-valence-electron system ($5d^{10}\,6s \to 5d^9\,6s^2$) using configuration interaction [6]. We present results of the full CI+MBPT method with holes, and updated limits on time-variation of α based on the existing experiment [5].

References

[1] J. C. Berengut, V. A. Dzuba, V. V. Flambaum, and A. Ong, *Hole Transitions in Multiply-Charged Ions for Precision Laser Spectroscopy and Searching for α-variation*, Phys. Rev. Lett. **106**, 210802 (2011).

[2] A. Derevianko, V. A. Dzuba, and V. V. Flambaum, *Highly-Charged Ions as a Basis of Optical Atomic Clockwork of Exceptional Accuracy*, Phys. Rev. Lett. **109**, 180801 (2012).

[3] A. Windberger *et al.*, *Identification of the Predicted 5s–4f Level Crossing Optical Lines with Applications ?to Metrology and Searches for the Variation of Fundamental Constants*, Phys. Rev. Lett. **114**, 150801 (2015).

[4] V. A. Dzuba, V. V. Flambaum and M. G. Kozlov, *Combination of the Many-body Perturbation Theory with the Configuration-Interaction Method*, Phys. Rev. A **54**, 3948 (1996)

[5] T. Rosenband *et al.*, *Frequency Ratio of Al+ and Hg+ Single-Ion Optical Clocks; Metrology at the 17th Decimal Place*, Science **319**, 1808 (2008).

[6] V. A. Dzuba, *Correlation Potential and Ladder Diagrams*, Phys. Rev. A **78**, 042502 (2008).

Spectroscopy of H_2^+ and HD^+ Near Their Dissociation Thresholds: Shape and Feshbach Resonances

Maximilian Beyer and Frédéric Merkt
ETH Zürich, Laboratorium für Physikalische Chemie, Vladimir-Prelog-Weg 2, 8093 Zürich, Switzerland

We use high Rydberg states to measure the properties of H_2^+ and HD^+ in the vicinity of their dissociation limits H^++H, H^++D and H+D^+, with particular emphasis on the spectral positions and widths of the quasibound rovibrational levels above the dissociation threshold of the $X^+\ ^2\Sigma_g^+$ ground state [1].
Although the existence of these quasibound levels has been predicted a long time ago, they have never been observed. Positions and widths of the lowest resonances have not been calculated either. Given the role that such states play in the three-body and radiative recombination of H(1s) and H^+ to form H_2^+, this lack of data may be regarded as one of the largest unknown aspects of this otherwise accurately known fundamental molecular cation.
We present measurements of the positions and widths of the lowest-lying quasibound rotational levels of H_2^+, located close to the top of the centrifugal barriers and which decay by quantum-mechanical tunneling. These states are also refered to as shape resonances. For HD^+ we present measurements of rovibrational levels of the $A^+\ ^2\Sigma_u^+$ state, located between the two dissociation limits. Because of the g-u-symmetry breaking in HD^+, these levels are coupled to the H^++D continuum by nonadiabatic interactions and can be regarded as Feshbach resonances.
The experimental results will be compared with the positions and widths we calculate for these levels using a potential model for the X^+ and the A^+ state of H_2^+ and HD^+ which includes adiabatic, nonadiabatic, relativistic and radiative corrections to the Born-Oppenheimer potential energies.

References

[1] Maximilian Beyer, and Frédéric Merkt, *Observation and Calculation of the Quasibound Rovibrational Levels of the Electronic Ground State of H_2^+*, Phys. Rev. Lett. **116**, 093001 (2016).

Fourier transform spectroscopy with resolution beyond the optical path limit

Piotr Maslowski[1], Kevin F. Lee[2], Alexandra C. Johannson[3], Amir Khodabakhsh[3], Grzegorz Kowzan[1], Lucile Rutkowski[3], Andrew A. Mills[2], Christian Mohr[2], Jie Jiang[2], Martin E. Fermann[2] and Aleksandra Foltynowicz[3]

1. Institute of Physics, Faculty of Physics, Astronomy and Informatics, Nicolaus Copernicus University in Toruń, Grudziadzka 5, 87-100 Toruń, Poland

2. IMRA America, Inc., 1044 Woodridge Ave., Ann Arbor, MI, USA 48105

3. Department of Physics, Umeå University, 901 87 Umeå, Sweden

Fourier transform spectrometers (FTS) based on optical frequency combs (OFC) allow detection of broadband molecular spectra with high signal-to-noise ratios within acquisition times orders of magnitude shorter than traditional FTIRs based on thermal sources [1]. Moreover, high absorption sensitivity for absorption and low detection limits can be obtained using optical enhancement cavities [2]. Due to the pulsed nature of OFCs the interferogram consists of a series of bursts rather than a single burst at zero optical path difference (OPD). The comb mode structure can be resolved by acquiring multiple bursts [3]. However, the measurement of molecular lines narrower than the resolution limit set by the maximum OPD has not been demonstrated.

We show that it is sufficient to acquire an interferogram in a symmetric range around a single burst with a length precisely matched to the comb line spacing in order to exceed the spectrometer's OPD-limited resolution and measure accurately the intensity change of the individual comb lines. Our method allows measurements of broadband spectra with absorption lines narrower than the OPD-limited resolution without any loss of accuracy due to the instrumental lineshape function. It reduces the acquisition time of high-resolution measurements and interferometer length by orders of magnitude. We demonstrate this by measuring undistorted low pressure CO_2 and CO absorption lines with linewidths narrower than the OPD-limited resolution using OFC-based mechanical FTS in the near- and mid-infrared wavelength ranges [4]. The near-infrared system is based on an Er:fiber femtosecond laser locked to a high finesse cavity, while the mid-infrared system is based on a fully-stabilized Tm:fiber-laser-pumped optical parametric oscillator coupled to a multi-pass cell.

References

[1] J. Mandon, G. Guelachvili and N. Picqué, *Fourier transform spectroscopy with a laser frequency comb*, Nature Photonics **3**, 99–102 (2009).

[2] A. Foltynowicz, T. Ban, P. Masłowski, F. Adler, and J. Ye, *Quantum-Noise-Limited Optical Frequency Comb Spectroscopy*, Phys. Rev. Lett. **107**, 233002 (2011).

[3] M. Zeitouny, P. Balling, P. Kren, P. Masika, R.C. Horsten, S. T. Persijn, H. P. Urbach, and N. Bhattacharya, *Multi-correlation Fourier transform spectroscopy with the resolved modes of a frequency comb laser,* Ann. Phys. **525**, 437 (2013).

[4] P. Maslowski, K. F. Lee, A.C. Johansson, A. Khodabakhsh, G. Kowzan, L. Rutkowski, A. A.Mills, C. Mohr, J. Jiang, M. E.Fermann and A. Foltynowicz, *Surpassing the path-limited resolution of Fourier-transform spectrometry with frequency combs*, Phys. Rev. A **93**, 021802 (2016).

Continuously Tunable Mid-infrared Frequency Comb Spectrometer

Vinicius Silva de Oliveira[1], Piotr Maslowski[2], Axel Ruehl[1], and Ingmar Hartl[1]

[1]*Deutsches Elektronen – Synchrotron, Notkestrasse 85, 20251 Hamburg, Germany*

[2]*Institute of Physics, Faculty of Physics, Astronomy and Informatics, Nicolaus Copernicus University in Toruń, ul. Grudziadzka 5, 87-100 Toruń, Poland*

The ability to control the phase of the electric field in ultrashort laser pulses revolutionized many aspects of fundamental and applied science. In such a frequency comb (FC), a train of phase-stabilized pulses results in a set of equally spaced narrow spectral "comb" modes, whose absolute position can be controlled by reference oscillators. In the field of Fourier-transform spectroscopy, the usage of frequency comb sources led to a remarkable progress in terms of sensitivity, accuracy and the resolution is not limited by the optical path delay (OPD) [1,2].

We report on a frequency comb based Fourier-transform spectrometer (FTS) operating in the mid-infrared (MIR) spectral region, where molecules exhibit their strongest absorption features and signatures of their dynamics. A schematic of the setup is shown in Fig. 1 (a). The MIR frequency comb is based on a stabilized 2 W Yb:fiber laser and difference frequency generation. The laser output is split into pump and signal field whereas the signal is spectrally shifted in a highly nonlinear fiber [3]. An idler field corresponding to the difference between the incident fields is generated in a periodically-poled lithium niobate nonlinear crystal with fan-out structure. The optical spectrum can be continuously tuned from 1900 to 3300 cm^{-1} as shown in Fig. 1 (b). The average output power was 500 µW – 1.5 mW, corresponding to a power-per-comb-mode of up to 200 nW. Details of the FC system and the possibility to extend its spectral coverage to 1000 cm^{-1} can be found in Ref. [4]. The spectral read out of the FC was realized by a home-built scanning FTS. The optical path delay is measured with a frequency stabilized helium-neon laser and it is sufficient to resolve individual FC lines at 150 MHz or 0.005 cm^{-1} spacing.

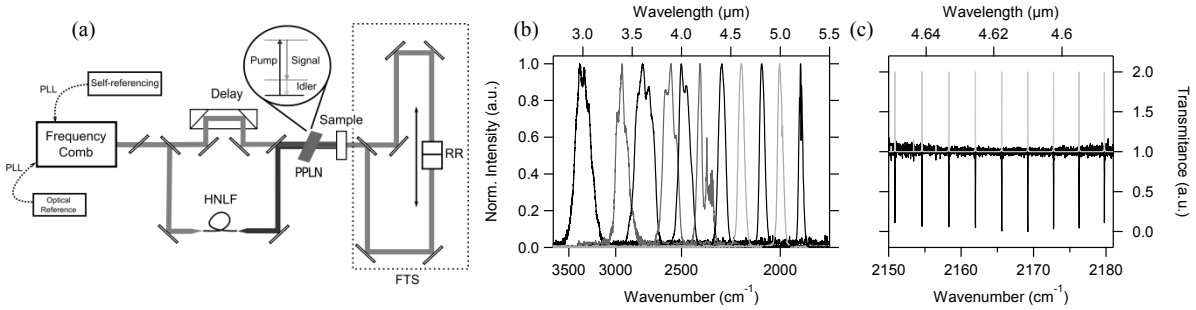

Fig. 1: (a) Schematic of the frequency comb spectrometer. PPL: phase-locked loop. HNLF: highly-nonlinear fiber. RR: retro-reflectors. (b) MIR spectra generated with a PPLN crystal. (c) Measured CO spectrum (black) and comparison with HITRAN database (gray)

For an initial demonstration of the capability of the instrument, the FC source was tuned to 4.6 µm to measure the fundamental absorption band of CO. Fig. 1(c) shows a single scan spectrum (125 cm OPD in 4 s) of the R-branch with a resolution of 0.008 cm^{-1} measured in a 45 mm long gas cell filled with 15 mbar. Fig. 1 (c) also shows the comparison with a HITRAN based model calculated for our measurement conditions.

The presented spectroscopy setup is ideally suited for applications such as trace gas detection and lineshape analysis. It can be used throughout the important MIR spectral region to probe the vibration bands of molecules with the qualities of a frequency comb.

Vinicius Silva de Oliveira acknowledges the support from CNPq, Conselho Nacional de Desenvolvimento Científico e Tecnologico - Brasil.

References

[1] A. Foltynowicz et al., *Optical frequency comb spectroscopy*, Faraday Discuss. **150**, 23 (2011).

[2] P. Maslowski et al., *Surpassing the path-limited resolution of Fourier-transform spectrometry with frequency combs,* Phys. Rev. A **93**, 021802(R) (2016).

[3] A. Ruehl et al., *Ultrabroadband coherent supercontinuum frequency comb,* Phys. Rev. A **85**, 011806(R) (2011).

[4] A. Ruehl et al., *Widely-tunable mid-infrared frequency comb source based on difference frequency generation*, Opt. Lett. **37**, 2232 (2012).

Nature mechanism-force origin

Zheng sheng ming

Physics research yuquan19(jia) Beijing China 100049

In the process of mankind investigate natural rule: people know well many interactions in the nature, today all interactions in the nature are classed by four kinds of force: electromagnetic force, gravitation, weak force, and strong force. Since Einstein declared his next idea was to unify these four kinds force. This idea has been attracting many people to make great efforts to answer! For solve this question and find its mechanism of origin, I do some experiments and discover that the moving photons produce gravitation. My experiments reveal the origin of gravitation. Moreover I apply this discovery in the electromagnetic phenomena reveal the origin of electromagnetic force. In this book describe the detail of my experiment and all calculate. Base on this I first unify the electromagnetic force and gravitation: their essence is same and their size is equally. From this we can know the meaning of gravitational mass which Newton and Einstein defined and the meaning of electric charge which Coulomb and Franklin defined; moreover I further reveal the essence of caloric, and reveal the mechanism of chemical reaction, demonstrate the quantum and General theory of Relativity are all wrong. Along this way, I reveal the mechanism of motion in optics, thermal, electromagnet, and gravitation. This shows the mechanism of natural motion. Namely I find the essence natural rule that the nature how moving in atomic world and in the heavenly body world, and reveal what is the elementary particle in nature, the matter how to compose. That is to say the elementary particle in the Nature is photon; the moving photons produce electromagnetic force and gravitation. Meanwhile the photon also transmit these forces in space, from this engender chemical interaction, heat phenomenon, and other many natural phenomena, in the end come to being cosmos[1].

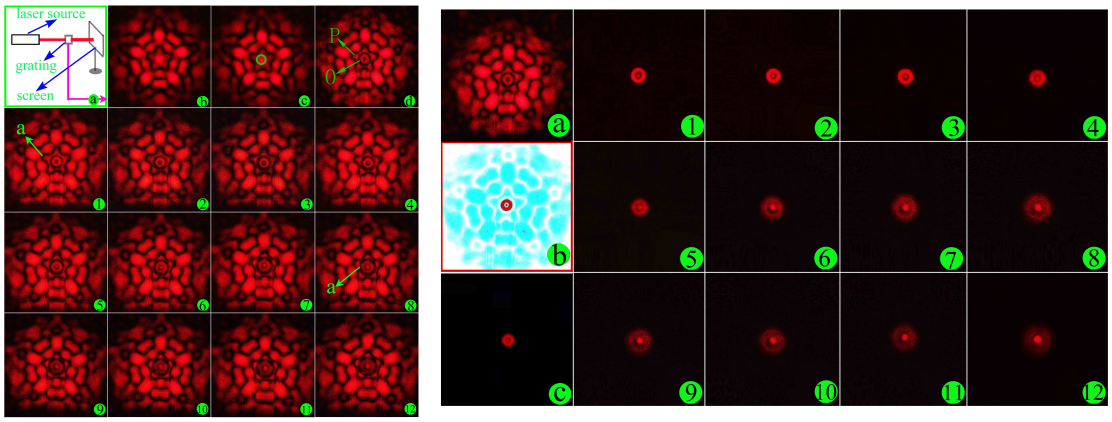

Figure 1. Picture **a** is the device of the experiment. Picture **c** is the ring site in light beam O, and pictures **1-12** are photographs showing that light beam O changed form from a circle to a pentagon when the other light beam accompany moving forward.
Figure 2. This experiment demonstrates that light beam O does not change its circular shape when there are no other light beams accompany moving forward.

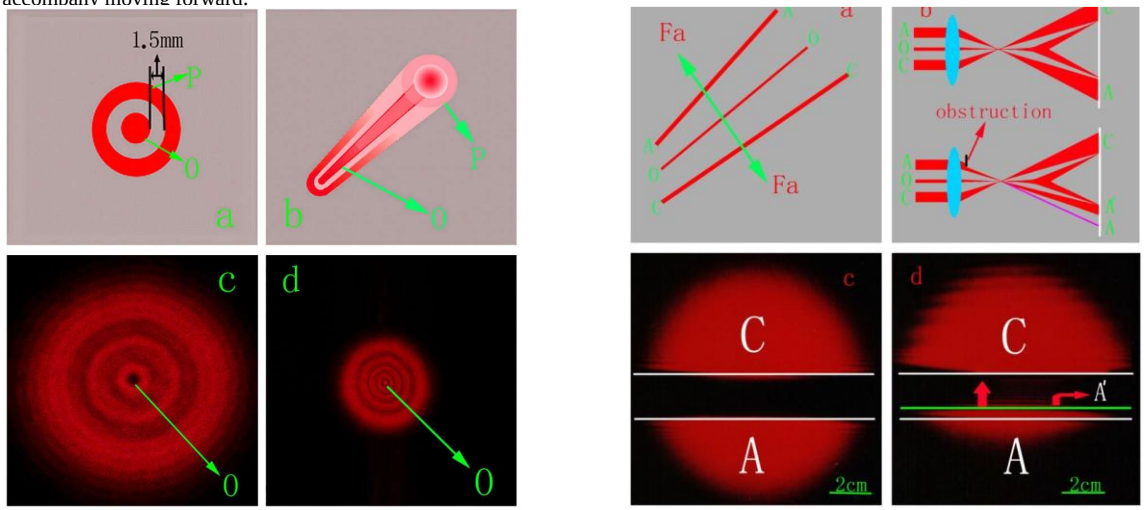

Figure 3. Picture **a** shows sectional state of the two light beams O, P. Picture **b** is the state of the moving track of light beams O, P; picture **c** is the photograph in the screen when light beams O, P are all moving forward; and picture **d** is the photograph of the screen when only light beam O moves forward.
Figure 4. Picture **a** is the state of force in the three light beams A, O, and C; picture **b** shows the section of movement of light beams A, O, and C; picture **c** is the photograph of light beams A, and C when they are first on he screen; picture **d** is the photograph when the outer part of light beam A is removed. In picture **d,** the white line is the original site of light beam A when outside light beam has not been removed; the green line is the site of light beam A when outside fringe has been removed, the red arrow shows the direction of the light beam A accepting this force; The purple line in picture **b** is the moving track of light beam A when outer light beam has not been removed.

References

[1] *Nature mechanism-force origin* see below website: https://www.amazon.com/Nature-Mechanism-force-Origin-zheng-sheng/dp/9881986869/ref=sr_1_1?ie=UTF8&qid=1470836833&sr=8-1&keywords=9789881986863

Searches for exotic transient signals with a Global Network of Optical Magnetometers for Exotic physics

S. Pustelny
Institute of Physics, Jagiellonian University, 30-383 Kraków, Poland
On behalf of the GNOME collaboration

Synchronous monitoring of spin dynamics in distant experiments offers new means of searching for physics beyond the Standard Model [1]. Here, we discuss application of a network of synchronized optical magnetometers, separated by hundreds or even thousands of kilometers, to search for transient exotic spin couplings [2]. Such couplings would manifest as temporal disturbances of magnetometers' operation and abrupt, yet brief, changes of their readouts. However, due to uncontrollable nature of the couplings, identification of such signals and their distinction from ordinary (e.g., magnetic) noise is, in an isolated experiment, particularly difficult. Therefore, we propose to correlate readouts of distant magnetometers, which limits local noise and makes the network sensitive to global spin disturbances. Appropriate experimental arrangements (e.g., magnetic shielding) and careful analysis of magnetometers' signals (e.g., vetoing techniques) allow to strongly reduce contribution from magnetic couplings, making the network sensitive to hypothetical (exotic) couplings. Such exotic couplings may be induced by hitherto undiscovered exotic particles or fields, which opens the possibility to test various theoretical model, including the ones that have not been yet unexplored experimentally.

References

[1] Derek F. Kimball, Steve K. Lamoreaux, Timothy E. Chupp, *Tests of fundamental symmetry with optical magnetometers*, In Dmitry Budker and Derek F. Jackson Kimball, Eds., *Optical Magnetometry* (Cambridge University Press, Cambridge, 2013).

[2] Szymon Pustelny, Derek F. Jackson Kimball, Chris Pankow, Micah P. Ledbetter, Przemyslaw Wlodarczyk, Piotr Wcislo, Maxim Pospelov, Joshua R. Smith, Jocelyn Read, Wojeciech Gawlik, and Dmitry Budker *The Global Network of Optical Magnetometers for Exotic physics (GNOME): A novel scheme to search for physics beyond the Standard Model*, Ann. Phys. **525**, 659 (2013).

Theory of Interfering One-Photon and Resonant Two-Photon Ionization of Neon by Femtosecond XUV Pulses

Alexei N. Grum-Grzhimailo[1], Elena V. Gryzlova[1], Nicolas Douguet[2], Klaus Bartschat[2]

1. Skobeltsyn Institute of Nuclear Physics, Lomonosov Moscow State University, 119991 Moscow, Russia

2. Department of Physics and Astronomy, Drake University, Des Moines, Iowa 50311, USA

The quantum coherent control, originally developed for optical lasers, is now extending into the XUV range due to development of new radiation sources. The seeded free-electron laser FERMI [1] is suitable for the corresponding experiments because of its high temporal coherency. Here we theoretically consider and further develop a scheme of coherent control in the XUV regime based on interference between one-photon and resonant two-photon ionization pathways in atomic ionization. This scheme was recently realized at FERMI [2]. When the frequencies of the two fields are ω and 2ω, respectively, the same configuration of electric field vectors is repeated each optical cycle. Thus a memory regarding the initial phase between the fields is kept, even if the pulses are infinitely long [3]. In our principal example, the frequency ω scans the vicinity of the $2p^5 4s$ and $2p^5 3d$ states in the neon atom, leading to resonant two-photon ionization, whereas the photon with the doubled frequency causes direct single-photon ionization. The resonant mode was selected in order to increase the probability of the two-photon ionization pathway. For fields with parallel linear polarizations, the interference of photoelectron continuum waves with different parities results in a 'left-right' asymmetry of the photoelectron angular distribution. This asymmetry depends on the photon frequency, the phase shift between the harmonics (ϕ), the ratio of the harmonic amplitudes (η), and the pulse duration. It can thus serve as a good marker of the coherent control [2].

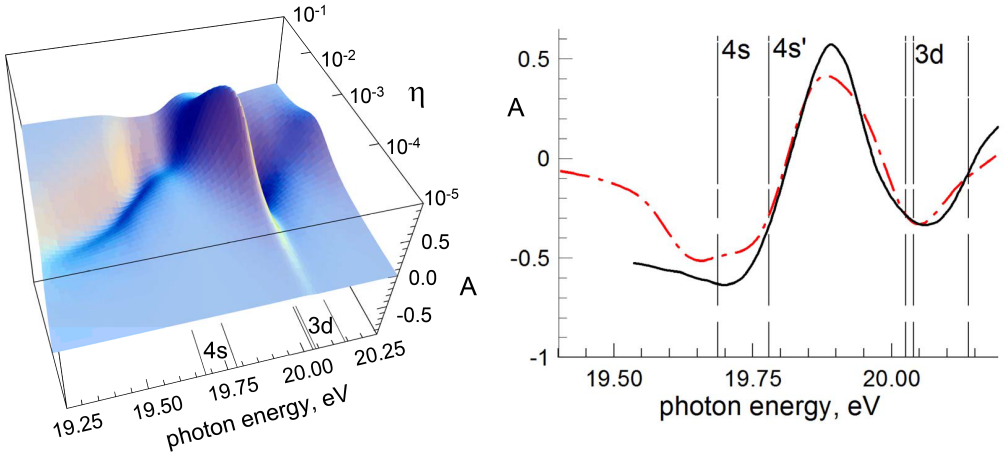

Fig. 1 (Left) PT results for the photoelectron left-right asymmetry A = [(I(ϑ=0) - I(ϑ=π)] / [(I(ϑ=0) + I(ϑ=π)], where ϑ is the electron emission direction with respect to the electric field, as function of the photon energy and the ratio of the amplitudes of the first and the second harmonics η for a peak field of intensity 10^{12} W/cm^2, a sin^2 pulse envelope covering 250 optical cycles, and a phaseshift ϕ=π/2 between the harmonics. (Right) Same as on the left as function of the photon energy for η=0.02155 (chain line) compared with the TDSE prediction (solid line). The positions of the intermediate fine-structure resonant states are marked by lines.

We calculated the photoelectron angular distribution within time-dependent perturbation theory (PT) and by solving the time-dependent Schrödinger equation (TDSE) [4]. Some of the results are shown in Fig. 1. When either the first or second harmonic is weak, the interference and, consequently, the asymmetry are suppressed. In our case the one-photon ionization is very strong compared to two-photon ionization, and thus the largest asymmetry is achieved already with a small admixture of the second harmonic. Results for other field parameters, including the case of circularly polarized fields, together with a detailed analysis of the effect will be presented at the conference.

This work is supported, in part, by the United States National Science Foundation under grant No. PHY-1430245 and the XSEDE allocation No. TG-PHY-090031 (ND and KB).

References

[1] http://www.elettra.trieste.it/lightsources/fermi/fermi-machine/general-description.html

[2] Kevin C. Prince et al., *Coherent control with a short-wavelength free-electron laser*, Nature Photonics **10**, 176 (2016).

[3] Nadezhda B. Baranova and Boris Ya. Zel'dovich, *Physical effects in optical fields with nonzero average cube,* $\langle E^3 \rangle \neq 0$, J. Opt. Soc. Am. B **8**, 27 (1991).

[4] Alexei N. Grum-Grzhimailo et al., *Interfering one-photon and two-photon ionization by femtosecond VUV pulses in the region of an intermediate resonance,* Phys. Rev. A **91**, 063418 (2015).

Building an Optical Centrifuge for Spinning of Molecules Embedded in Helium Nanodroplets

Anders Vestergaard[1], **Lauge Christensen**[2] **and Henrik Stapelfeldt**[2]
1. Institut for Fysik og Astronomi, Aarhus University, Ny Munkegade 120, 8000 Aarhus C, Denmark
2. Institut for Kemi, Aarhus University, Langelandsgade 140, 8000 Aarhus C, Denmark

We present our work on building an optical centrifuge for use in experiments on isolated molecules and molecules inside helium nanodroplets. A laser pulse consisting of two counter-rotating electric fields with chirp of opposing signs is created by passing an input pulse into a custom version of a 4f pulse shaper. In the Fourier plane of the pulse shaper, half the spectrum is send to one arm and the other half of the spectrum to another arm [1,2]. The resulting pulse's polarisation rotates and accelerates to a maximum angular frequency of half the bandwidth of the input pulse $\sim$ 10 THz. The 500 µJ, 70 ps (FWHM) centrifuge pulse will then be used to trap and rotate molecules adiabatically to high-lying rotational states. The final rotational speed can be controlled by limiting the spectrum of either arm in the pulse shaper.

Helium nanodroplets is an exciting medium to study in itself and for its properties as a quantum solvent. By expanding pre-cooled 12 K helium at 30 bar through a 5 µm orifice one can create droplets consisting of around 10^4 helium atoms. The number of Helium atoms can be controlled by varying the helium temperature and backing pressure. In our setup, these droplets travel through a pickup cell in which the partial pressure of a molecular gas is carefully controlled to optimize the conditions such that each droplet pick up a single molecule. In the target area, the droplet beam is, in the standard pump-probe fashion, overlapped with the centrifuge beam and a probe, consisting of 35 fs intense pulse at 800 nm used for Coulomb exploding the molecules inside the droplets. The resulting ionic fragments are then imaged using a 2D VMI-spectrometer.

The same setup allows for comparison with gas-phase molecules in which a mixture of the molecule along with Helium used as carrier gas, is loaded into a Even Lavie-Valve, which then in turn expands and cools the mixture into the target chamber.

This work presents the preliminary results on using the experimental setup with the centrifuge pulse on CS_2-molecules in both the gas-phase and in helium-droplets. We also present new results of laser-induced alignment of molecules in helium-droplets using a recently constructed vacuum chamber setup.

References

[1] Karczmarek Joanna, James Wright, Paul Corkum and Misha Ivanov, *Optical Centrifuge for Molecules*, Phys. Rev. Lett. **82**, 17 (1999).
[2] Aleksey Korobenko, Alexander A. Milner, John W. Hepburn and Valery Milner, *Rotational spectroscopy with an optical centrifuge*, Phys.Chem.Chem.Phys. **16**, 4071 (2014).

Quantum control of photoassociation: a comparative study of two pathways for the formation of heteronuclear molecules

Emanuel F. de Lima[1]
1. Departamento de Física, Universidade Federal de São Carlos, São Paulo 13565-905, Brazil

The obtainment of samples of ultracold polar molecules has been attracting considerable interest due to their potential applications, such as the precision measurement of physical constants, the elaboration of quantum computing methodologies, and the study of ultracold chemistry [1,2]. One route for the formation of ultracold molecules is photoassociation, in which two colliding atoms are bind together through the interaction with an external electromagnetic field. In the laboratory, photoassociation is usually achieved by a laser-induced transition from the free atomic pair to a molecule in a electronic excited state. In order to obtain molecules in the electronic ground state, the excited molecule is transferred by either spontaneous or induced emission. However, the existence of a permanent dipole moment in heteronuclear molecules offers an alternative pathway for photoassociation, in which all transitions take place in the electronic ground state [3,4]. This approach, though restricted to heteronuclear molecules, has the advantage of not depending on the structure and lifetime of electronic excited states.

In the present work, we investigate the photoassociation of ultracold atoms occurring through two distinct pathways. In the first one, the colliding atoms are photoassociated into the excited electronic state. In the second one, photoassociation takes place within the electronic molecular ground state. In each case, shaped control pulses are sought through the application of the TBQCP quantum control algorithm combined with a frequency filtering [5]. The optimization goal is to maximized the photoassociation probability. We perform a comparative investigation of the obtained control fields and the corresponding system dynamics.

References

[1] Juris Ulmanis, Johannes Deiglmayr, Marc Repp, Roland Wester and Mathias Weidermüller *Ultracold molecules Formed by Photoassociation: Heteronuclear Dimers, Inelastic Collisions, and Interactions with Ultrashort Laser Pulses*, Chem. Rev. **112**, 4890 (2012).
[2] Christiane P. Koch and Moshe Shapiro *Coherent Control of Ultracold Photoassociation*, Chem. Rev. **112**, 4928 (2012).
[3] Svetlena Kotochigova, *Prospects for Making Polar Molecules with Microwave Fields*, Nature Phys. **123**, 1234 (2007).
[4] Emanuel F. de Lima, Tak-San Ho and Herschel Rabitz *Optimal Laser Control of Molecular Photoassociation along with Vibrational Stabilization*, Chem. Phys. Lett. **501**, 267 (2011).
[5] Tak-San Ho and Herschel Rabitz, *Accelerated Monotonic Convergence of Optimal Control over Quantum Dynamics*, Phys. Rev. E **82**, 026703 (2010).

Correction of Arbitrary Field Errors in Population Inversion of Quantum Systems by Universal Composite Pulses

Genko T. Genov[1], Daniel Schraft[1], Thomas Halfmann[1], Nikolay V. Vitanov[2]

1. Institute of Applied Physics, Technical University of Darmstadt, Hochschulstr. 6, 64289 Darmstadt, Germany

2. Department of Physics, St. Kliment Ohridski University of Sofia, 5 James Bourchier boulevard, 1164 Sofia, Bulgaria

Performing high-fidelity and robust population transfer by external fields remains an important challenge in various areas of physics, e.g., atomic and molecular physics, nuclear magnetic resonance, and quantum information processing. Most of the available techniques provide either high population transfer efficiency or robustness against variations in the field parameters, but not both. For example, resonant techniques deliver high efficiency but are not robust. Adiabatic passage techniques are robust, but in nearly all of them population transfer is incomplete because of demanding adiabaticity criteria. Optimal control techniques achieve high fidelity but their implementation is challenging due to the complicated time dependence of the applied fields.

The technique of **composite pulses** (CPs) [1], i.e., sequences of pulses with suitably chosen relative phases, is far easier to implement and has been applied in nuclear magnetic resonance, quantum information processing, and quantum optics for highly accurate and robust qubit rotation. However, essentially all existing CPs compensate errors in a single or at most two interaction parameters, usually assuming a rectangular pulse shape.

We **theoretically develop and experimentally demonstrate** [2] universal broadband composite pulse sequences for robust high-fidelity population inversion in two-state quantum systems, which **compensate systematic errors in any parameter** of the driving field (e.g., pulse amplitude, duration, detuning, Stark shifts, unwanted frequency chirp). Our novel composite pulses are also applicable with any pulse shape.

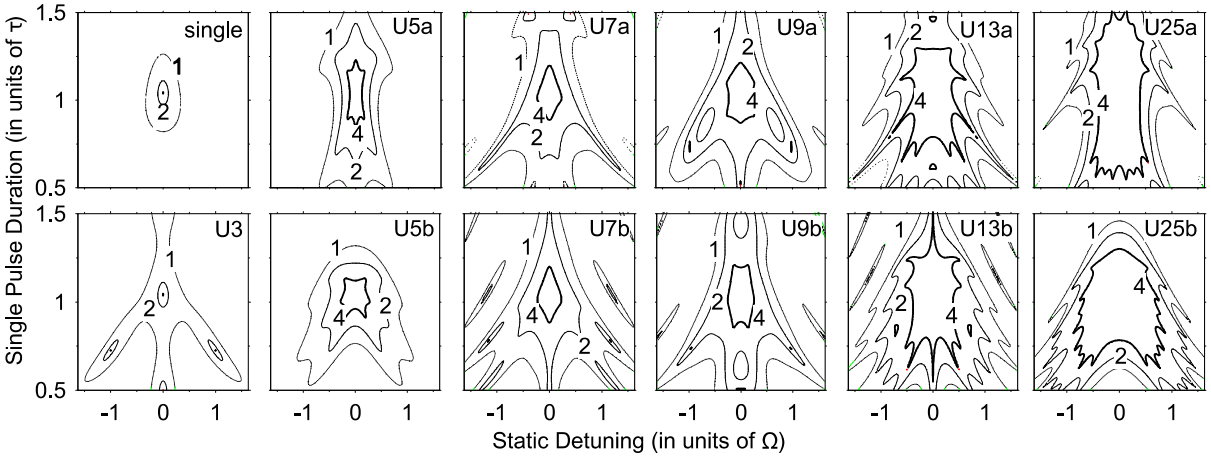

Fig. 1 Numerically simulated infidelity vs static detuning and duration of each constituent pulse for a single pulse and several universal CPs (with rectangular shapes). As it is well known, the transition probability for a rectangular pulse quickly drops when it is not resonant or its pulse area differs from $\Omega\tau = \pi$. The universal composite pulses expand significantly the 10^{-4} error parameter range (the labels m = 1, 2, 4 indicate the error level 10^{-m}).

We demonstrate the efficiency and universality of these composite pulses by experimental data on **rephasing of atomic coherences** in a Pr^{3+}:Y_2SiO_5 crystal. In particular, our data demonstrate robust rephasing in a broad range of experimental parameters and for different pulse shapes. The efficiency and operation bandwidth of universal CPs are significantly larger compared to conventional π pulses or nonuniversal CPs. The universal CPs are a highly accurate and robust tool for quantum control, particularly valuable in the presence of significant experimental uncertainties.

References

[1] M. H. Levitt, *Composite pulses*, Prog. Nucl. Magn. Reson. Spectrosc. **18**, 61 (1986).

[2] G. T. Genov, D. Schraft, T. Halfmann, N. V. Vitanov, *Correction of Arbitrary Field Errors in Population Inversion of Quantum Systems by Universal Composite Pulses*, Phys. Rev. Lett. **113**, 043001 (2014).

Atomic control with low frequency electromagnetic radiation: fine structure under strong bichromatic driving

German A. Sinuco Leon, Barry M. Garraway
Department of Physics and Astronomy, University of Sussex, Brighton, BN1 9QH, United Kingdom

Low frequency electromagnetic radiation constitutes a superb tool for coherent control of the internal state of a wide variety of quantum systems (e.g. NV centres, superconducting circuits and trapped atoms and ions). It is usual to describe the dynamics of such systems neglecting their multilevel nature via perturbative expansions and applying the rotating wave approximation (RWA). However, modern experimental implementations let us explore the regime of strong matter-radiation coupling where all relevant energy scales can be of the same order of magnitude, which renders inaccurate the standard simplifications. In this work, we present a study of the dynamics of a multilevel quantum system coupled to strong fields in the context of ultracold alkali atoms under the influence of radio-frequency and microwave radiation.

To set the stage, we first describe a typical atom-chip configuration and highlight the range of relevant energy scales achievable with state-of-the-art technology. Then, we discuss effects associated with non-equal energy spacing between internal states (corresponding to non-linear Zeeman shifts) and its utility to reduce the sensitivity of atomic clock transitions via RF and MW dressing [1-3], and to implement addressed manipulation of atomic qubits trapped in a lattice [4,5]. Following this, we consider qubits encoded by atomic RF dressed states and evaluate beyond RWA effects on its transition frequency and coupling to microwave radiation. Finally, we explore a strategy to design microwave pulses for implementing fast and accurate single qubit control, taking into consideration the interplay between strong driving and the multilevel nature of the the system. This work is of particular relevance for atomic interferometry [6,7] and quantum information processing with trapped ultracold atomic ensambles.

References

[1] G. A. Sinuco-Leon and B.M. Garraway, *Radio-frequency dressed atoms beyond the linear Zeeman effect*, New Journal of Physics **14**, 123008 (2012).
[2] G.A. Kazakov and T. Schumm, *"Magic" radio-frequency dressing for trapped atomic microwave clocks*, Phys. Rev. A. **91**, 023404 (2015)
[3] L. Sarkany, P. Weiss, H. Hattermann and J. Fortagh. *Controlling the magnetic field sensitivity of atomic clock states by microwave dressing*, Phys. Rev. A **90**, 053416 (2014)
[4] G. A. Sinuco-Leon and B.M. Garraway, *Radio-frequency dressed lattices for ultracold alkali atoms*, New Journal of Physics **17**, 053037 (2015).
[5] G. A. Sinuco-Leon and B.M. Garraway, *Addressed qubit manipulation in radio- frequency dressed lattices*, New Journal of Physics **18** 035009 (2016).
[6] G.A. Sinuco-Leon, K.A., Burrows, A.S. Arnold A.S. and B.M. Garraway, *Inductively coupled circuits for ultracold dressed atoms.* Nature Communications **5**, 5289 (2014)
[7] R. Stevenson, M. R. Hush, T. Bishop, I. Lesanovsky, and T. Fernholz, *Sagnac Interferometry with a Single Atomic Clock.* Physical Review Letters **115**, 163001 (2015)

Förster Resonances Between Cold Rydberg Atoms in a Time-Varying Electric Field and Their Applications in Quantum Information

I.I.Ryabtsev[1, 2], D.B.Tretyakov[1, 2], V.M.Entin[1, 2], I.I.Beterov[1, 2], M.Saffman[3], E.A.Yakshina[1, 2], and C.Andreeva[4]

1. Rzhanov Institute of Semiconductor Physics SB RAS, Pr. Lavrentyeva 13, 630090 Novosibirsk, Russia

2. Novosibirsk State University, Ul. Pirogova 2, 630090 Novosibirsk, Russia

3. University of Wisconsin, Madison, Wisconsin, 53706, USA

4. Institute of Electronics, Tsarigradsko Shosse 72, 1784 Sofia, Bulgaria

Long-range interactions between cold Rydberg atoms are being investigated for neutral-atom quantum computing, quantum simulations, phase transitions in cold Rydberg gases and other applications. Fine tuning of the interaction strength can be implemented using Förster resonances between Rydberg atoms controlled by an electric field. Observation of the Stark-tuned Förster resonances between Rydberg atoms excited by narrowband cw laser radiation requires the use of a Stark-switching technique to excite the atoms first in a constant electric field and then to induce the interactions in a varied electric field, which is scanned across the Förster resonance.

In our experiments with cold Rb Rydberg atoms we have found that the transients at the edges of the electric pulses strongly affect the line shapes of the Förster resonances, since the resonance occurs on a time scale of ~100 ns being comparable with the duration of the transients. For example, a short-term ringing at certain frequency causes additional radio-frequency (rf) assisted Förster resonances, while non-sharp edges lead to an asymmetry. An intentional application of the radio-frequency field induces transitions between collective states whose line shape depends on the interaction strengths and time. In this report we present the experimental and theoretical analysis of the line shapes of the Förster resonances $\mathrm{Rb}(nP_{3/2}) + \mathrm{Rb}(nP_{3/2}) \rightarrow \mathrm{Rb}(nS_{1/2}) + \mathrm{Rb}((n+1)S_{1/2})$ for a few cold Rb Rydberg atoms in a time-varying electric field [1]. In particular, we studied the rf-assisted Förster resonances between N=2-5 cold Rb Rydberg atoms [2] (Fig.1). We have shown that they can be induced both for the "accessible" Förster resonances which can be tuned by the dc field alone [Fig.1(a)] and for those which cannot be tuned and are "inaccessible" [Fig.1(b)]. The van der Waals interaction of almost arbitrary high Rydberg states can thus be tuned to resonant dipole-dipole interaction.

This can be especially useful for improving the fidelity of quantum gates implemented with Rydberg atoms [3]. We have studied theoretically various Förster resonances in Rb and Cs Rydberg atoms and calculated interspecies Rydberg-Rydberg interaction strengths for generation of long-range entanglement and quantum nondemolition measurements [4]. We have also developed schemes of two-qubit quantum gates based on adiabatic passage of the Stark-tuned Förster resonances in a swept electric field [5]. These are based on deterministic phase accumulation during double adiabatic passage of the Stark-tuned Förster resonance.

This work was supported by the RSF Grant No. 16-12-00028, RFBR Grants No. 14-02-00680 and 16-02-00383, Novosibirsk State University and Russian Academy of Sciences.

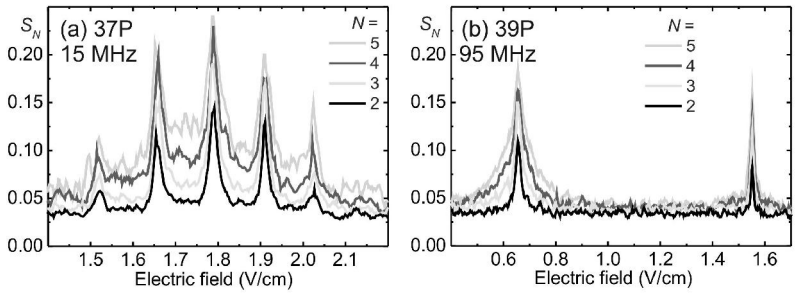

Fig. 1 Radio-frequency (rf) assisted Förster resonances for N=2-5 detected cold Rb Rydberg atoms: (a) "accessible" resonance in Rb(37P) atoms can be tuned by dc field alone at 1.79 V/cm, while rf-field induces additional resonances; (b) "inaccessible" resonance in Rb(39P) atoms can be induced only by the rf field.

References

[1] E.A.Yakshina, D.B.Tretyakov, I.I.Beterov, V.M.Entin, C.Andreeva, A.Cinins, Z.Iftikhar, and I.I.Ryabtsev (2016, in preparation).
[2] D.B.Tretyakov, V.M.Entin, E.A.Yakshina, I.I.Beterov, C.Andreeva, and I.I.Ryabtsev, Phys. Rev. A **90**, 041403(R) (2014).
[3] I.I.Beterov, M.Saffman, E.A.Yakshina, S.Bergamini, D.B.Tretyakov, V.M.Entin, G.N.Hamzina, and I.I.Ryabtsev, J. Phys. B (2016, in press); arXiv:1601.07282.
[4] I.I.Beterov and M.Saffman, Phys. Rev. A **92**, 042710 (2015).
[5] I.I.Beterov, S.Bergamini, M.Saffman, E.A.Kuznetsova, D.B.Tretyakov, V.M.Entin, E.A.Yakshina, and I.I.Ryabtsev (2016, in preparation).

Excitation of high orbital angular momentum Rydberg states with twisted photons

J.D. Rodrigues
Instituto de Plasmas e Fusão Nuclear, Instituto Superior Técnico, Universidade de Lisboa, 1049-001 Lisbon, Portugal

L.G. Marcassa
Instituto de Física de São Carlos, Universidade de São Paulo, Caixa Postal 369, 13560-970, São Carlos, São Paulo, Brasil

J.T. Mendonça
Instituto de Plasmas e Fusão Nuclear, Instituto Superior Técnico, Universidade de Lisboa, 1049-001 Lisbon, Portugal

Rydberg atoms [1-5] are amongst the most exciting and promising research topics nowadays. Much of this interest arises from the particularities of these systems, such as strong dipole-dipole interactions and long lifetimes. Until now and in most experiments, the Rydberg atoms were excited using dipole allowed transitions, either from the ground state or from an intermediate excited state. Only recently, electric dipole-forbidden transitions to Rydberg *nD* states were observed in Rubidium atoms [6]. In a recent work, Schmiegelow and co-workers have used Laguerre-Gauss laser beams to study a quadrupole transition in a Calcium ion [7]. In principle such a technique could be applied to cold Rydberg atoms as well.

In this work we investigate the excitation of Rydberg states using orbital angular momentum (OAM) carrying photons, namely with Laguerre-Gauss (LG) laser beams. As Allen and co-workers discovered in 1992, LG light fields carry a discrete amount of orbital angular momentum per photon [8, 9]. We begin by revisiting the standard dipole selection rules for plane wave excitations. We then introduce the Laguerre-Gauss modes as an appropriate set of solutions of the Helmholtz equation in the paraxial approximation. We show, in a particular geometry setting, that a relaxation of the standard selection rules occurs, thus increasing the number of accessible states through a single photon excitation process. The transition matrix element is decomposed into an angular and radial coupling and we show how the later is corrected by the spacial profile of the LG laser beam. Explicit numerical calculations are presented for an hydrogen-like atom, which captures the essential ingredients of the OAM. We also discuss the nature of the angular momentum coupling between the LG photon and the atom in a hyperfine structure basis.

With this work we contribute to the further understanding of the interaction of orbital angular momentum bearing laser beams with matter. We considered the excitation of Rydberg states using LG laser beams and demonstrated that, in the case an atomic ground state centered at the optical vortex, the orbital angular momentum from the Laguerre-Gauss beam, $\ell_0\hbar$, can be transferred to the electron internal degrees of freedom. This is the mechanism responsible for the relaxation of the standard dipole selection rules and allowing for the excitation of higher orbital angular momentum atomic states, at much higher rates than the ones expected for usual dipole-forbidden transitions.

References

[1]T. F. Gallagher, Rydberg atoms (Cambridge University Press, 1994).
[2]L. G. Marcassa and J. P. Shaffer, Advances In Atomic, Molecular, and Optical Physics, 63, 47 (2014).
[3]M. Saffman, T. G. Walker, and K. Molmer, Rev. Mod. Phys. 82, 2313 (2010).
[4]R. Low, H. Weimer, J. Nipper, J. B. Balewski, B. Butscher, H. P. Buchler, and T. Pfau, Journal of Physics B: Atomic, Molecular and Optical Physics 45, 113001 (2012).
[5]J. S. Cabral, J. M. Kondo, L. F. Gonçalves, V. A. Nascimento, L. G. Marcassa, D. Booth, J. Tallant, A. Schwettmann, K. R. Overstreet, J. Sedlacek, and J. P. Shaffer, Journal of Physics B: Atomic, Molecular and Optical Physics 44, 184007 (2011).
[6]D. Tong, S. M. Farooqi, E. G. M. van Kempen, Z. Pavlovic, J. Stanojevic, R. Cote, E. E. Eyler, and P. L. Gould, Phys. Rev. A 79, 052509 (2009).
[7]C. T. Schmiegelow, J. Schulz, H. Kaufmann, T. Ruster, U. G. Poschinger, and F. Schmidt-Kaler, arxiv:1511.07206 (2015).
[8]L. Allen, M. W. Beijersbergen, R. J. C. Spreeuw, and J. P. Woerdman, Phys. Rev. A 45, 8185 (1992).
[9]M. Beijersbergen, L. Allen, H. van der Veen, and J. Woerdman, Optics Communications 96, 123 (1993).

RYDBERG EXCITATION OF LASER-COOLED ATOMS IN THE AC-MOT

John Agomuo [1,2,*], Matthew Harvey[2] and Andrew James Murray[2]
[1] Department of Physics, Nigerian Defence Academy Kaduna, Nigeria
[2] Photon Science Institute, School of Physics and Astronomy, University of Manchester, Manchester M13 9PL, UK.

Corresponding Author: jcagomuo@nda.edu.ng

Abstract

Precise energy levels of high-n Rydberg states of potassium have been measured using stepwise-excitation of cooled, trapped atoms in the AC-MOT [1], with the intermediate state being the $4^2P_{1/2}$ state that was excited by resonant laser radiation at 389,286,368.12 MHz. Excitation from the $4^2P_{1/2}$ state to the $n^2S_{1/2}$ states was carried out using blue radiation from a dye laser, for transitions to Rydberg states with principal quantum numbers in the range $18 \le n \le 200$. For excitation to the $n^2D_{3/2}$ states, energy levels of states with principal quantum numbers n ranging from 18 to 167 were measured. Due to strong interaction between Rydberg atoms [3], the measured energy levels deviated from the predicted theoretical values at high principal quantum numbers $n \ge 130$ for the S-states, and $n \ge 100$ for the D-states. For principal quantum numbers greater than these values, the spectral lines were found to both broaden and shift in energy and new features in the Rydberg spectra were observed. These new features have been attributed to the dipole-forbidden $n^2P_{1/2}$ and $n^2P_{3/2}$ states, which cannot be excited directly by the laser. These states must hence be excited due to interplay between the highly excited Rydberg atoms that is occurring due to the large effective size and close proximity of the atoms in the AC-MOT, however further work is required to ascertain the exact mechanism of their excitation.

References

[1] Harvey, M., & Murray, A. J. (2008). *Cold atom trap with zero residual magnetic field: The ac magneto-optical trap.* Physical Review Letters, 101(17), 173201.

[2] Harper, C. D., Wheatley, S. E., & Levenson, M. D. (1977). Two-photon absorption spectroscopy of potassium Rydberg states. *JOSA*, *67*(5), 579-583.

[3] Singer, K., Reetz-Lamour, M., Amthor, T., Marcassa, L. G., & Weidemüller, M. (2004). *Suppression of excitation and spectral broadening induced by interactions in a cold gas of Rydberg atoms*. Physical Review Letters, 93(16), 163001.

Ionization of Rydberg atoms by single-cycle THz pulses: Scaling properties

M. Chovancova, H. Agueny, J. P. Hansen and L. Kocbach
Department of Physics and Technology, Allegt. 55, University of Bergen, N-5007 Bergen, Norway

Recently, it has been experimentally discovered [1] that the threshold fields necessary to ionize 10% of the sodium Rydberg (nd) atoms with principal quantum number $n \in 6,15$ scale as n^{-3} rather than the expected n^{-4} scaling. The ionization mechanism has been identified in THz spectral region [2]. On the theoretical side, the mechanism was considered by Yang and Robicheaux in [3,4] based on both classical and quantum calculations. However, their calculations were limited to shorter pulses. Such calculations in the low-frequency and long-pulse regimes are a real challenge, in particular when the momentum or the angular distributions of the ejected electrons are considered. This, indeed, requires very large grids to simulate the ionization dynamics since the electron displacement during the pulse can extend up to 10^5 a.u. in combination with a pulse duration also of the magnitude of the order 10^5 a.u. as well.

In the conference we shall present our preliminary results of the scaling law of field ionization of Rydberg hydrogen-like atoms in a long single-cycle THz pulse (field period $T = 5$ ps). The results stem from a semiclassical approach to solve the time-dependent Schrödinger equation. Due to the computational challenge we restrict ourselves to a one-dimensional model. The scaling properties will be discussed for the ionization probabilities (cf. Fig. 1) with principal initial quantum number ranging from $n = 6$ to 15. As shown in Fig. 1, all the ionization probabilities fall onto an almost common curve, when multiplying the electric peak field intensity with the factor n^3/n_{max}^3. The scaling behavior is reproduced by classical simulations based on a Classical Trajectory Monte-Carlo method. We will also report an extension to the ionization dynamics by studying the momentum distribution of the ejected electron, which reveals additional interesting effects. Their origin will be also addressed.

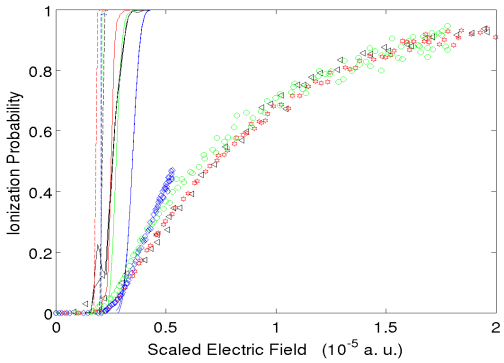

Figure 1: . (Color online) Experimental points for ionization probabilities replotted from Ref. [1] on a scaled common max intensity axis of $n/(n_{max} = 15)^3 E_0$. Here, the fields period is $T = 5$ ps and frequency is $\omega = 1.05$ THz. The full lines show scaled quantum ionization probabilities from the $n = 6, 9, 12, 15$ levels. The dashed lines show scaled CTMC probabilities for the microcanonical distribution pertaining to the same initial energy as the quantum calculations. $n = 6$ (blue), $n = 9$ (green), $n = 12$ (red), $n = 15$ (black).

References

[1] S. Li and R. R. Jones, *Ionization of Excited Atoms by Intense Single-Cycle THz Pulses*, Phys. Rev. Lett. **112**, 143006 (2014).
[2] R. R. Jones, D. You, and P. H. Bucksbaum, *Ionization of Rydberg atoms by subpicosecond half-cycle electromagnetic pulses*, Phys. Rev. Lett. **70**, 1236 (1993).
[3] B. C. Yang and F. Robicheaux, *Field ionization of Rydberg atoms in a single-cycle pulse*, Phys. Rev. A **91**, 043407 (2015).
[4] B. C. Yang and F. Robicheaux, *Field-ionization threshold and its induced ionization-window phenomenon for Rydberg atoms in a short single-cycle pulse*, Phys. Rev. A **90**, 063413 (2014).

Microwave spectroscopy in interacting gases of polar Rydberg atoms as a probe of mean-field energy shifts

Valentina Zhelyazkova and Stephen D. Hogan

University College London, Department of Physics and Astronomy, Gower Street, WC1E 6BT, London, United Kingdom

As an electron in a Rydberg state (with high principal quantum number n) is very far from the core and experiences a much weaker Coulomb attraction, the atom can be easily polarized by an external electric field. It is possible to prepare a Rydberg atom in a quantum state in which the electron density distribution resembles a classical electric dipole μ. Dense ensembles of Rydberg atoms can be used as model systems with which to explore the classical dipole-dipole interactions, characterized by the interaction energy $V_{\rm dd} \simeq \mu^2/(4\pi\varepsilon_0 R^3)$, where R is the interatomic separation. These interactions differ from (i) the resonant dipole-dipole interactions arising from large transition moments [1], and (ii) the second-order van der Waals interactions exploited in Rydberg excitation blockade experiments [2], giving rise to measurable mean-field energy shifts of the atomic levels.

Here, we present the results of experiments in which helium atoms produced in a supersonic source are excited to $n = 70$ Rydberg state and subsequently polarized by a small ($0.1 - 0.7$ V/cm) dc electric field so that they acquire large classical electric dipole moments ranging from 110 to 12 260 D. After photoexcitation, the atoms interact with a microwave field at a frequency of ~ 38 GHz, which drives transitions to the higher lying $n = 72$ state. Following interaction with the microwave field the atoms are detected by state-selective electric field ionization with the resulting electrons collected on a microchannel plate detector.

Using this approach, mean-field energy shifts [3] arising as a result of electric dipole-dipole interactions can be probed by driving microwave transitions between states of different electric dipole moment. Electric dipole moments of μ =12 260 D correspond to an average dipole-dipole interaction energy of 10 MHz for a mean interatomic separation of $R = 10$ μm. Because of the high particle number densities in the supersonic beam ($\sim 10^9$ cm^{-3}), such dipole moments can be exploited to probe the mean-field shifts. We demonstrate that the measured transition frequencies are dependent on the density of Rydberg atoms which can be varied by adjusting the intensity of the excitation lasers, and for the highest density ($\sim 2\times10^9$ cm^{-3}), the transition frequency is shifted to higher values by approximately 5 MHz (Fig. 1). In addition, the lineshape of the microwave transition exhibits an asymmetric shape and a steep decline at higher frequencies which is indicative of the Rydberg excitation blockade effects.

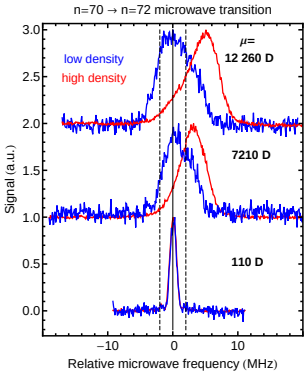

Fig. 1 Microwave spectra of transitions between the $n = 70$ and $n = 72$ Rydberg-Stark states that evolve adiabatically to the respective *ns* states in zero electric field. Measurements were performed at low densities (blue) and high densities (red) in selected electric field.

References

[1] I. Mourachko, D. Comparat, F. de Tomasi, A. Fioretti, P. Nosbaum, V. M. Akulin, and P. Pillet, *Many-body Effects in a Frozen Rydberg Gas*, Phys. Rev. Lett. **80**, 253 (1998).

[2] D. Tong, S. M. Farooqi, J. Stanojevic, S. Krishnan, Y. P. Zhang, R. Côté, E. E. Eyler, and P. L. Gould, *Local Blockade of a Rydberg Excitation in an Ultracold Gas*, Phys. Rev. Lett. **93**, 063001 (2004).

[3] A. Gaj, T. Krupp, J. B. Balewski, R. Löw, S. Hofferberth, and T. Pfau, *From molecular spectra to a density shift in dense Rydberg gas*, Nature Commun. **5**, 4546 (2014).

Light Shift in Three-Level Λ System Driven by the Periodically Phase-Modulated Field

Maksim Basalaev[1,2], **Valery Yudin**[1,2,3], **Aleksey Taichenachev**[1,2]
1. Novosibirsk State University, ul. Pirogova 2, Novosibirsk 630090, Russia
2. Institute of Laser Physics SB RAS, pr. Akademika Lavrent'eva 13/3, Novosibirsk 630090, Russia
3. Novosibirsk State Technical University, pr. Karla Marksa 20, Novosibirsk 630073, Russia

Currently, coherent population trapping (CPT) resonances at the hyperfine structure of the alkali-metal atoms underlie atomic clocks [1], which have a great practical importance. CPT can occur in a Λ system in which two hyperfine components of the ground state are coupled to a common excited state by two laser fields with frequency difference equal hyperfine splitting. In miniature atomic clocks the harmonic phase modulation of vertical cavity surface emitting laser (VCSEL) is ordinarily used. In this case the field can be written as

$$E(t) = E_0 e^{-i[\omega t + \varphi(t)]} + \text{c.c.}, \quad \varphi(t) = A\sin(\nu t), \tag{1}$$

where E_0 is the field amplitude, ω is the central frequency of laser, A and ν are the amplitude and frequency of phase modulation, respectively. It is obvious that this field is polychromatic, in which the frequency difference between the adjacent components equals ν. The phase modulation at full or half of the hyperfine splitting is usually used. For theoretical description of this problem the Fourier expansion of the field is traditionally employed. In this case, to solve the density matrix equation one can extract two resonant components, which are involved in the absorption and directly form the dark resonance. While the remaining frequency components are taken into account only from the viewpoint of field-induced shifts of the clock transition. The field-induced shift is one of the major sources of long-term instability of CPT atomic clocks.

In this work for three-level Λ system we investigate the line shape and field-induced shift of the dark resonance formed by the field with a periodically modulated phase. In our calculations we use the conception of dynamic steady state [2], which in contrast to Fourier formalism automatically guarantees a full account of all frequency components. Figure 1 displays the dependence of the field shift of the dark resonance δ_{shift} on the modulation amplitude A. There is the value set of A, for which the field shift vanishes.

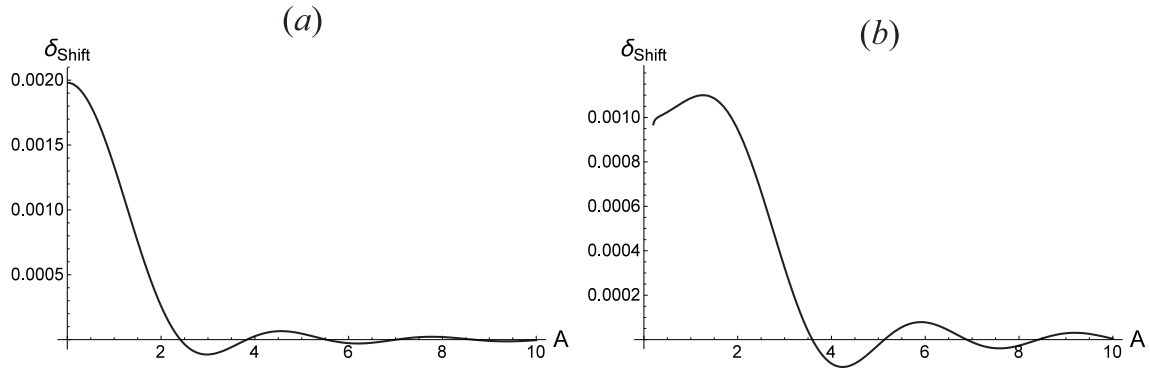

Fig. 1 The dependence of the dark resonance position δ_{shift} on parameter A: (*a*) the case when ν is varied near $\Delta/2$ and (*b*) the case when ν is varied near $\Delta/4$, where Δ is the frequency of hyperfine splitting.

The work was supported by the Ministry of Education and Science of the Russian Federation (State Assignment No. 2014/139, Project No. 825), by the Russian Foundation for Basic Research (Grants No. 16-32-60050, 16-32-00127, 14-02-00712, 14-02-00939).

References

[1] V. Shah and J. Kitching, *Advances in coherent population trapping for atomic clocks*, Adv. At. Mol. Opt. Phys. **59**, 21-74 (2010).
[2] V. I. Yudin, A. V. Taichenachev, and M. Yu. Basalaev, *Dynamic steady state of periodically driven quantum systems*, Phys. Rev. A **93**, 013820 (2016).

Polarizing Effects In Recoil-induced Resonances

***David Lazebny*[1,2], *Alexey Taichenachev*[1,2], *Valery Yudin*[1,2,3]**

1. Institut of Laser Physics SB RAS, Lavrent'eva 13/1, Novosibirsk 630090, Russia

2. Novosibirsk State University, Pirogova 2, Novosibirsk 630090, Russia

3. Novosibirsk State Technical University, Karla Marksa 20, Novosibirsk 630073, Russia

Laser cooling of atoms using magneto optical trap is an essential part of modern atomic physics [1,2]. In order to measure temperature of cold atoms and their function of distribution methods of nonlinear spectroscopy are widely used. One of such methods is based on the so-called recoil-induced resonances which were predicted in the work [3] for the first time and were observed in this work [4]. In our work we describe theoretically the most general case of recoil-induced resonances for arbitrary polarization of fields and for arbitrary dipole allowed transition (^{85}Rb), since in previous works all analysis was down to either simplified two-level models or transition for certain values of momenta for ground and excited states or for concrete polarizations of fields. The main results of the work are:

1. For any closed dipole transition we got explicit analytical expressions for polarizing dependence of magnitude of recoil-induced resonances as for the case of free atoms and for atoms in the magneto optical trap. Max and min values was got.
2. In working trap contributions associated with orientation and alignment are suppressed because of averaging over parameters of local polarization vector of field of trap. One can easily retrieve information about an average value of multipole momenta of atom in magneto optical trap from polarizing measurements.
3. Theory can be generalized subject to real hyperfine structure.

The work was supported by the Ministry of Education and Science of the Russian Federation (State Assignment No. 2014/139, Project No. 825), by the Russian Foundation for Basic Research (Grants No. 14-02-00712, 14-02-00939, 15-02-08377, 15-32-20330) and by the grant of President of RF (NSH-4096.2014.2).

References

[1] H. J. Metcalf and P. Straten, J. Opt. Soc. Am. B **20**, 887 (2003).
[2] V.I. Balykin, V.G. Minogin, and V.S. Letokhov, Rep. Progr. Phys. **63**, 1429 (2000).
[3] J. Guo, P. R. Berman, B. Dubetsky, and G. Grynberg, Phys. Rev. A **46**, 1426 (1992).
[4] J. Courtois, G. Grynberg, B. Lounis, and P. Verkerk, Phys. Rev. Lett. **72**, 3017 (1994)

Investigation of Hyperfine Structure of Atomic Holmium

Gönül Başar[1], Nadia Al-Labady[1],Berin Yapıcı[1], Feyza Güzelçimen[1], Alev Er[1], İpek K. Öztürk[1], Sophie Kröger[2], Artis Kruzins[3], Maris Tamanis[3], Ruvin Ferber[3]

1. Istanbul University, Faculty of Science, Physics Department, Tr-34134 Vezneciler, Istanbul, Turkey

2. Hochschule für Technik und Wirtschaft Berlin, Fachbereich 1, Wilhelminenhofstr. 75A, D-12459 Berlin, Germany

3. Laser Centre, The University of Latvia, Rainis Bulevard 19, LV-1586 Riga, Latvia

In this work we present the 34 new magnetic dipole and 25 new electric quadrupole hyperfine structure constants of atomic Holmium. An emission spectra of a Holmium (Ho) hollow cathode discharge lamp have been recorded in the UV spectral range from 24500 up to 31500 cm^{-1} (315 to 400 nm) using a high-resolution Bruker IFS-125 HR Fourier transform (FT) spectrometer with a resolution of 0.05 cm^{-1} at the Laser Centre of the University of Latvia in Riga. Two Ho spectra are measured with Neon and Argon as buffer gas, respectively.

With the atomic number 67 Ho is the eleventh element of the so-called lanthanide or rare earth element group. Due to the unfilled 4f electron shell the spectrum of Ho is very dense and complex as for all lanthanides. Ho is the only rare earth element which has only one stable isotope, i.e.^{165}Ho. This isotope has a nuclear spin of I = 7/2 and a very large nuclear magnetic dipole moment of μ_I = 4.125 μ_N causing a very broad hyperfine structure. The electric quadrupole moment with Q = 2.64 barn is very large as well, resulting in a noticeable deviation from the Landé interval rule of the hyperfine structure for many Ho lines.

Lines with unknown hyperfine structure constants and sufficient signal to noise ratio were analysed. For the classification of the spectra we used the classification program CLASS_LW [1]. The program Fitter was used in order to fit the line profile and to determine the magnetic dipole and electric quadrupole hyperfine structure constants *A* and *B* of energy levels. The hyperfine structure of spectral lines was fitted by using a Voigt profile function. Most lines are only partly resolved and many of them could be fitted only if the *A* and *B* constants of one of the two levels were fixed during the fit. It was possible in cases where these constants were well-known from literature [2-6] or from other lines investigated in this work. For totally unresolved lines the *B* constants could not be determined.

We have determined for the first time the *A* constants for 10 energy levels of even parity as well as for 24 levels of odd parity. In spite of the Doppler limitation of our spectra we were able to determine new *B* constants for 8 energy levels of even parity and for 17 energy levels of odd parity.

References

[1] Windholz, L., & Guthöhrlein, G. H., *Classification of Spectral Lines by Means of their Hyperfine Structure. Application to Ta I and Ta II Levels*, Phys. Scr., **T 105**, 55 (2003)

[2] Merzyn, G., et.al.,*The Hyperfine Structure of the Ground State of Ho^{165}*, Zeitschrift fr Physik, **252**, 5 (1972)

[3] Reddy, M., N., et.al., *Laser optogalvanic spectroscopy of holmium*, J. Opt. Soc. Am. B, **9**, 1 (1992)

[4] Wyart, J., F., et.al., *Etude du spectre de l'holmium atomique-I*, Physica, **92C**, 377 (1977)

[5] Childs, W., J., et.al., *New line classifications in Ho I based on high-precision hyperfine-structure measurement of low levels*, Optical Society of America, **73**, 2 (1983)

[6] Gurell, J., et.al., *Wavelengths, energy levels and hyperfine structure constants in Ho II*, Phys. Scr., **79**, 1 (2009)

Ground State Hyperfine Splitting in Lithiumlike and Hydrogenlike Bismuth

Johannes Ullmann[a,b], Jonas Vollbrecht[d], Zoran Andelkovic[c], Andreas Dax[h], Wolfgang Geithner[c], Christopher Geppert[b], Christian Gorges[b], Michael Hammen[e,g], Volker Hannen[d], Kristian König[b,c], Simon Kaufmann[b], Yuri Litvinov[c], Matthias Lochmann[b], Bernhard Maass[b,c], Johann Meisner[f], Tobias Murböck[k], Rodolfo M. Sánchez[c], Stefan Schmidt[b,g], Matthias Schmidt[f], Markus Steck[c], Thomas Stöhlker[a,c], Richard C. Thompson[i], Christian Weinheimer[d], Wilfried Nörtershäuser[b]

[a] *Helmholtz Institut Jena, Jena, Germany*
[b] *Institut für Kernphysik, Technische Universität Darmstadt, Germany*
[c] *GSI Helmholtzzentrum für Schwerionenforschung, Darmstadt, Germany*
[d] *Institut für Kernphysik, Universität Münster, Germany*
[e] *Helmholtz Institut Mainz, Universität Mainz, Germany*
[f] *Physikalisch-Technische Bundesanstalt, Braunschweig, Germany*
[g] *Institut für Kernchemie, Universität Mainz, Germany*
[h] *Paul Scherrer Institute, Villigen, Switzerland*
[i] *QOLS Group, Department of Physics, Imperial College London, UK*
[k] *Institut für Angewandte Physik, Technische Universität Darmstadt, Germany*

While quantum electrodynamics (QED) is usually referred to as the most accurately tested theory, its validity for electrons in very strong fields is still not tested with high accuracy. The strongest magnetic fields available in the laboratory are experienced by electrons in the ground-state of highly charged heavy ions which can be probed by hyperfine spectroscopy. Even though the ground state M1 hyperfine transition in hydrogen-like bismuth was observed already in 1994 [1], its ability to test QED was limited by the unknown magnetic moment distribution inside the nucleus. However, it was suggested that a so-called specific difference between the hyperfine splitting in hydrogen-like and lithium-like ions of the same isotope can be used to cancel nuclear structure effects and provide an accurate test of QED [2]. The transition in Li-like Bismuth was observed for the first time in 2011 at the experimental storage ring ESR located at the GSI Helmholtz-Center for heavy ion research in Darmstadt [3]. Yet the accuracy of the result was limited by the calibration of the electron cooler voltage, determining the ion velocity. We now report an improved measurement of the hyperfine splitting in hydrogen-like bismuth ($^{209}Bi^{82+}$) at the Experimental Storage Ring ESR at GSI by laser spectroscopy on a coasting beam. Accuracy was improved by about an order of magnitude compared to the first observation in 1994 [1]. The most important new feature was an *in-situ* high voltage measurement at the electron cooler platform with an accuracy at the 10-ppm level provided by the Physikalisch-Technische Bundesanstalt. Furthermore, the space charge effect of the electron cooler current on the ion velocity was determined with two independent techniques that provided consistent results. The result of $\lambda_0 = 243.821(6)$ nm provides an important reference value for experiments testing bound-state QED in the strong magnetic field regime by evaluating the specific difference between the splittings in the hydrogen-like and lithium-like ions. Further measurements of hydrogen-like and lithium-like ^{209}Bi with bunched beams are currently under analysis.

References

[1] I. Klaft et al. Phys. Rev. Lett **73**, 2428 (1994)

[2] V. Shabaev et al., Phys. Rev. Lett. **86**, 3959 (2001)

[3] M. Lochmann et al., Phys. Rev. A **90**, 030501 (2014)

Paschen-Back Effect and Transition Probabilities at Fields up to 7 kG in Caesium Atoms

Andris Erglis
Laser Centre, University of Latvia, Rainis blvd. 19, Riga, Latvia, LV-1586

Marcis Auzinsh[1], Andris Berzins[1], Ruvin Ferber[1], Janis Smits[1]
1. Laser Centre, University of Latvia, Rainis blvd. 19, Riga, Latvia, LV-1586

Alkali metal atoms are hydrogen-like atoms that are easily accessible to laboratory experiments, which makes them convenient systems for demonstrating fundamental interactions between atoms and magnetic fields for fundamental research as well as teaching. We have designed an experiment that simple enough to carry out in the context of an advanced undergraduate or master's level laboratory course, while illustrating important atomic physics principles, which the students would be able to calculate. At the same time, these effects can be also used to measure magnetic field in a wide range of magnetic field values.

The development of distributed feedback laser diodes has enabled frequency scanning over several hundred GHz without mode hops. As a result it is possible to record an entire Caesium D line spectrum even at magnetic fields up to one tesla and to compare easily the positions and relative amplitudes of the peaks corresponding to the different allowed transitions. Together with the simple theoretical model based on estimating transition probabilities from the eigenvector coefficients and the Wigner-Eckart theorem, such measurements are suitable for illustrating the Paschen-Back effect with good didactic potential at the advanced undergraduate or master's student level.

In the experiment we used a diode laser with low output power (approximately 2 μW) to make absorption measurements, which is convenient for many applications. To split hyperfine energy levels of Caesium, we used an electromagnet which can produce a homogeneous magnetic field up to 7 kG. We excited the atoms by means of linearly polarised radiation in two ways (σ and π): for σ excitation the polarisation vector of the exciting radiation is perpendicular to the magnetic field vector, whereas for π excitation they are parallel.

Figure 1 shows absorption spectra measured on the D_1 transition of Caesium for a) π excitation and b) σ excitation at several magnetic field values up to 7 kG.

We measured signals for the D_1 and D_2 transitions and present these experimental results together with predictions based on a theoretical model.

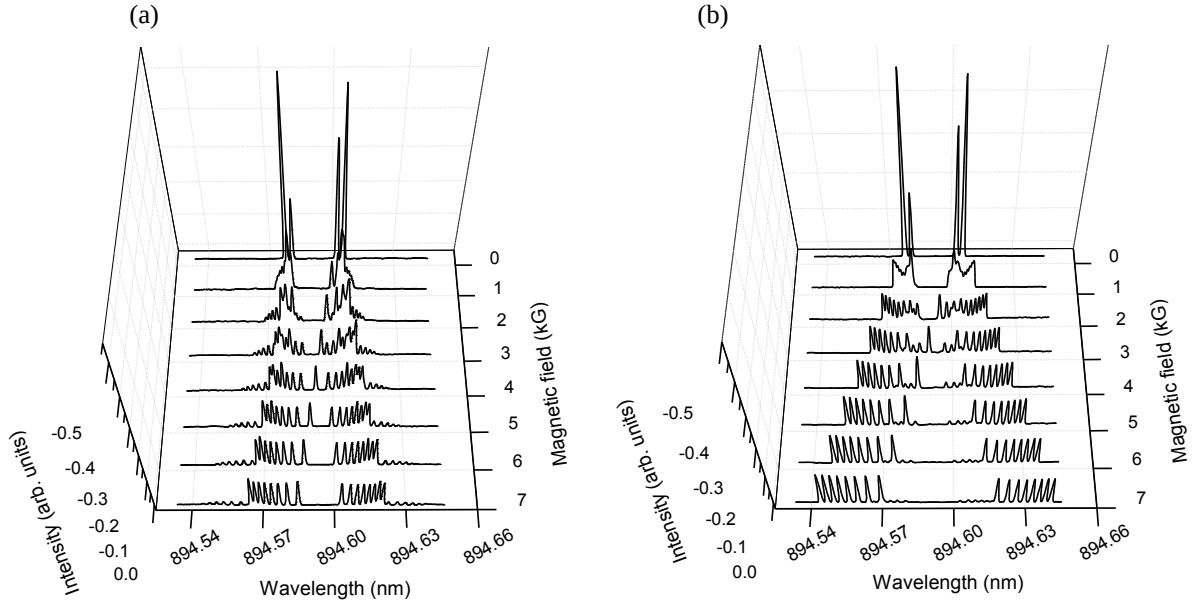

Fig. 1 a) π excitation; b) σ excitation

Dynamical strong-field effects in the XFEL spectroscopy of astrophysically relevant highly charged Fe ions

Natalia S. Oreshkina, Stefano M. Cavaletto, Zoltán Harman, Christoph H. Keitel
Max Planck Institute for Nuclear Physics, Saupfercheckweg 1, 69117 Heidelberg, Germany

Line intensities and oscillator strengths for the controversial 3C and 3D astrophysically relevant x-ray lines in neonlike Fe^{16+} ions are calculated [1,2]. First, a large-scale configuration-interaction calculation of oscillator strengths is performed with the inclusion of higher-order electron-correlation effects. Also, quantum electrodynamic effects to the transition energies were calculated. Further considered dynamical effects give a possible resolution of discrepancies of theory and experiment found by recent x-ray free electron laser measurements [3] of these controversial lines. We find that for strong x-ray sources, the modeling of the spectral lines by a peak with an area proportional to the oscillator strength is not sufficient and non-linear dynamical effects have to be taken into account. Thus we advocate the use of light-matter interaction models also valid for strong light fields in the analysis and interpretation of certain astrophysical and laboratory spectra. We also investigate the system distinguishing between the coherent and incoherent parts of the emission spectrum. An influence of the spectrum of Fe^{15+}, an ion which was also present in the recent laboratory experiment, is considered in addition.

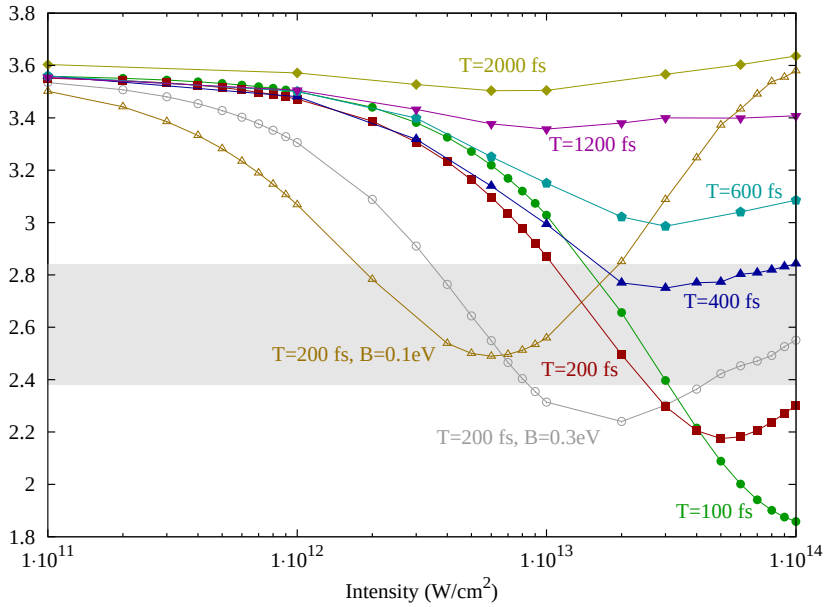

Fig. 1 The line strength ratio S_{3C}/S_{3D} as a function of the intensity and duration T of the incoherent pulse [2]. For the shortest pulses, results with three different bandwidths (B) are shown. The gray shaded area shows the experimental ratio 2.61 with its error bar of 0.23 from the experiment [3].

References

[1] N. S. Oreshkina, S. M. Cavaletto, C. H. Keitel and Z. Harman, Phys. Rev. Lett. **113**, 143001 (2014).
[2] N. S. Oreshkina, S. M. Cavaletto, C. H. Keitel and Z. Harman, J. Phys. B., *in print* (2016).
[3] S. Bernitt, G. V. Brown, J. K. Rudolph, R. Steinbrügge *et al.*, Nature **492**, 225 (2012).

Transition Probabilities and lifetimes for Y III

Şule Ateş
Selcuk University, Faculty of Science, Department of Physics, 42075 Konya, Turkey

The one-electron systems such as Rb-like yttrium ions because of their relatively simple electronic structure can be served for testing theoretical methods and comparing with experimental values to results [1]. Transition probabilities in yttrium ions are needed for the determination of the chemical composition of the sun and the stars in astrophysics [2]. Also, Y III can also be used for the diagnostics and modelling of the stellar plasma [3,4]. Thus, the spectra of Y III in both atomic physics and astrophysics should not be ignored.

The present study includes to some results of electric dipole transition probability and lifetime for doubly-ionized yttrium (Y III). For calculations the weakest bound electron potential model (WBEPM) theory and the quantum defect orbital (QDO) theory have been used. It has been employed both the numerical Coulomb approximation (NCA) method and numerical non-relativistic Hartree–Fock (NRHF) wave functions for expectation values of radii in the WBEPM theory. The energy values required for calculations in both The WBEPM theory and the QDO theory are taken from NIST [5].The calculated transition probabilities and lifetimes have been compared with available results [1,2,4,6-8]. A good agreement with results in literature has been obtained.

References

[1]U.I. Safronova and M. S. Safronova, Phys. Rev. A **87**, 032501 (2013).
[2]E. Biemont, K. Blagoev, L. Engstrom, H. Hartman, H. Lundberg et al Mon. Not. R. Astron. Soc. (2011). doi:10.1111/j.1365-2966.2011.18637.x
[3]M. S. Dimitrijevic and S. J. Sahal-Brechot, Appl.Spectrosc. **65,** 49 (1998). Dimitrijevic M S and Sahal-Brechot S 1997 Joint Europeanand National Meeting
[4]B. K. Sahoo, H. S. Nataraj, B. P. Das, R. K. Chaudhuri and D. Mukherjee, J. Phys. B: At. Mol. Opt. Phys. **41,** 055702 (2008).
[5]A. Kramida, Yu, Ralchenko, J.Reader and NIST ASD Team (2015) http://physics.nist.gov/asd
[6]A. Redfors, Astron. Astrophys. **249**, 589 (1991).
[7]T. Brage, G. M. Wahlgren, S.G. Johansson, D. S. Leckrone and C. R. Proffitt , The Astophysical Journal **496,** 1051È1057 (1998).
[8]T.Zhang and N. Zheng, Chin. J. Chem. Phys. **22**, 246 (2009)

Excitation of Nitrous Oxide by Electron Impact

Marián Danko, Juraj Országh, Michal Ďurian, Štefan Matejčík

Department of Experimental Physics, Comenius University in Bratislava, Mlynská dolina F2, 842 48 Bratislava

The electron impact excitation of nitrous oxide was studied using the crossed beams electron induced fluorescence apparatus (EIFA). Nitrous oxide has been the aim of studies for many years for wide variety of reasons. Its role in the chemistry of the upper atmosphere is considered to be significant due to its contribution to ozone decomposition [1]. It is significant in the field of astrophysics [2] as well as used in many technological applications [3].

The experimental apparatus used for this study was described in detail in [4] and [5]. The electron beam was generated by trochoidal electron monochromator with heated tungsten filament used as electron source [6]. The energetic resolution of the electron beam was approximately 400meV and the electron current measured by the faraday cup was 900nA and was within 5% of this value in the range from 4eV up to 100eV. The electron beam was perpendicular to the molecular beam formed by effusive capillary. Due to the conditions in the reaction chamber all the reactions were binary i.e. there were no three body collisions present. The optical system of mirror and lenses guides and focuses the photons emitted in the deexcitation processes onto the entrance slit of the optical monochromator and photomultiplier working in the photon counting regime serves as a detector.

The emission spectrum was measured at the incident electron energy of 50eV. At this energy most of the excitation reactions lead to production of the electronically excited positive ion N_2O^+ $A^2\Sigma$. These species emit photons with wavelengths between 330 and 410nm during deexcitation to the electronic ground state $X^2\Pi$ (see Fig. 1.) The vibration states were determined according to the [7].

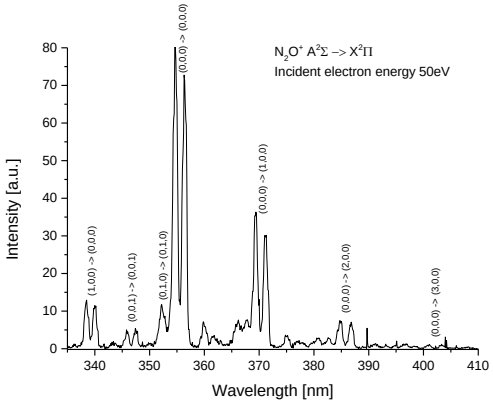

Fig. 1. Emission spectrum of nitrous oxide induced by electrons with kinetic energy of 50eV.

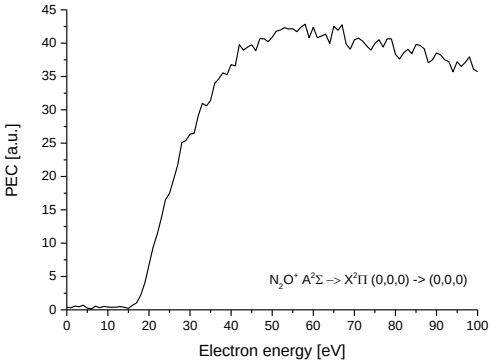

Fig. 2. PEC of the most intense transition N_2O^+ $A^2\Sigma$ -> $X^2\Pi$ (0,0,0) -> (0,0,0).

The photon efficiency curves (PEC) (see Fig. 2.) correspond to the relative cross sections of the processes of electron impact excitation and subsequent deexcitation of the species. They were measured for the transitions detected in the emission spectra and the threshold energies were determined by fitting the measured curves.

This work was supported by the Slovak Research and Development Agency, project Nr. APVV-0733-11 and the grant agency VEGA, project Nr. 1/0417/15. This project has received funding from the European Union's Horizon 2020 research and innovation programme under grant agreement No 692335.

References

[1] R.P. Waye, *Chemistry of Atmospheres*, 2nd ed., Oxford Science Publications, Oxford (1991).
[2] L.M. Ziurys, A.J. Apponi, et al., *Detection of interstellar N2O: A new molecule containing an N-O bond*, Astrophys. J. **436**, L181 (1994).
[3] M. Kitajima, Y. Sakamoto, R.J. Gulley, et al., *Electron scattering from N_2O: absolute elastic scattering and vibrational excitation*, J. Phys. B **33**, 1687 (2000).
[4] M. Danko, J. Országh, M. Ďurian et al., *Electron impact excitation of methane: determination of appearance energies for dissociation products*, J. Phys. B: At. Mol. Opt. Phys. **46**, 045203 (2013).
[5] A. Ribar, M. Danko, J. Országh, et al., *Dissociative excitation study of iron pentacarbonyl molecule*, Eur. Phys. J. D **69**, 4 (2015).
[6] J. Matúška, D. Kubala, Š. Matejčík, *Numerical simulation of a trochoidal electron monochromator*, Measurement Science and Technology **20**, 015901 (2009).
[7] J.H. Callomon, F. Creutzberg, *The electronic emission spectrum of ionized nitrous oxide, N_2O^+: $A^2\Sigma$-$X^2\Pi$*, Phil. Trans. R. Soc. Lond. A **277** (1974).

Thermal Mass Spectrometry of Fructose

Anatoly Zavilopulo, Otto Shpenik, Anatoly Mylymko, Larysa Prots, Olha Pylypchynets

Institute of Electron Physics, National Academy of Sciences of Ukraine, 88017, Uzhgorod, Ukraine
E-mail: gzavil@gmail.com

Glucose and fructose are isomers with the same gross formula $C_6H_{12}O_6$, but different position of the carbonyl group [1]. Using an experimental setup with an MX 7304A monopole mass spectrometer with mass resolution better than ΔM = 1 Da [2], we performed a series of studies of fructose molecule mass spectra in the mass range 10-190 a.m.u. at different temperatures and energies of the ionizing electrons. The obtained mass spectrum of the fructose molecule at the energy E_i = 70 eV is characterized by high fragmentation depth and lack of the molecular ion peak as the parent molecule breaks down almost at the moment of ionization. The molecular ion and the initial dissociation products are easily dehydrated, as most of the fragment ions are formed at the elimination of one or two molecules of water. Fragments resulting from dissociative ionization of the molecular ion, except $[CH3O]^+$, contain from 2 to 4 carbon atoms and an aldehyde group $[CHO]^+$. Relative intensities of the ion peaks in the mass spectrum are highly dependent of the fructose molecule evaporation temperature. Figure 1a shows the mass spectrum of the fructose molecule consisting of a series of mass with ± 1 a.m.u. increment due to the detachment of hydrogen atoms at different temperatures. As can be seen, besides the $[CH_3O]^+$ (m/z=31), $[C_2H_3O]^+$ (m/z=43), $[C_2H_4O_2]^+$ (m/z=60), $[C_3H_5O_2]^+$ (m/z=73), $[C_4H_7O_3]^+$ (m/z=103) fragment peaks, characteristic of fructose which are the most intense in the series, an intense peak of water $[H_2O]^+$ (m/z=18) is observed. To find out the reason for its appearance we carried out thermal gravimetric analysis (TGA) of the fructose molecule (Fig. 1b). The TGA curves show the presence of two phase transitions at 322 and 357 K, and as can be seen from Fig. 1a, at these temperatures an intense mass peak of molecular water is observed.

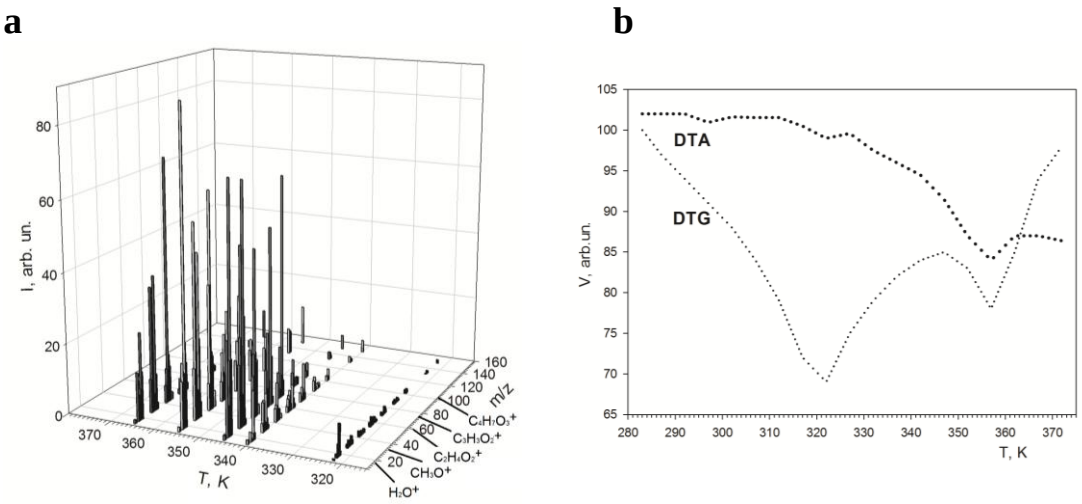

Fig. 1 Mass spectrum of fructose molecule at different temperatures (**a**) and thermal gravimetric analysis DTA and DTG (**b**)

Noted that the crystalline fructose melting point is 103 ± 2º C and at T > 125º C the process of irreversible decomposition of fructose begins with transition to the solid state (caramel). The thermal gravimetric analysis enabled us to specify the optimal temperature range for the measurements and to develop a methodology for the mass spectra measurements.

References

[1] Vivien F. Taylora, Raymond E. Marchb, Henry P. Longerichc, Christopher J. Stadeyb, *A Mass Spectrometric Study of Glucose, Sucrose, and Fructose Using an Inductively Coupled Plasma and Electrospray Ionization*, Intern. J. Mass Spectrometry 243 (2005) 71–84

[2] A.N. Zavilopulo, P.P. Markush, O.B. Shpenik and M.I. Mykyta, *ElectronImpact Ionization and Dissociative Ionization of Sulfur in the Gas Phase*, Technical Physics, **59**, No. 7, pp. 951–958. (2014).

Circular dichroism in photoionization of chiral systems by laser pulses

Anne D. Müller[1], **Anton N. Artemyev**[1], **and Philipp V. Demekhin**[1]
1. Institut für Physik und CINSaT, Universität Kassel, Heinrich-Plett Str. 40, 34132 Kassel, Germany

It is well known, that chiral molecules exhibit a circular dichroism (CD) phenomenon, which can be used to identify different enantiomers. The CD occurs due to the fact that chiral molecules interact with left and right circularly polarized light in different ways. In the absorption spectra of the randomply oriented chiral molecules, CD usually ranges between $10^{-6} - 10^{-3}$ of the total absorption. This value is very small, since CD is governed here by the electric-dipole-magnetic-dipole interference terms. It has been predicted theoretically [1], that the photoelectron circular dichroism (PECD) in the angular-resolved photoionization spectra of chiral molecules is significantly larger, because it emerges already in the electric-dipole approximation. For one-photon ionization, PECD has already been studied systematically in a number of theoretical and experimental works. Most of those results are reviewed in the book [2].

Recently, experiments on the 2+1 resonantly enhanced multiphoton ionization (REMPI) of bicyclic ketones [3,4] have been reported. It was shown that CD in the velocity map images of the photoelectron angular distribution may achieve values of up to $\pm 10\%$. The theoretical interpretation of these experiments is much more complicated than that for the one-photon ionization [5]. Up to now, only a few theoretical results have been published on this topic and those experiments on multiphoton PECD are still uninterpreted. Here, we would like to close this gap. Therefore, we first investigate the one- and two-photon ionization of a simple model chiral system by a circular polarized laser pulse [6]. We compute the angular resolved photoelectron spectra and analyse the corresponding PECD effect. Secondly, we discuss our results for the multiphoton PECD in the 2+1 REMPI of the camphor molecule.

To this end, we have developed a theoretical approach which is based on the time-dependent single center (TDSC) method [7]. In the method, the time-dependent Schrödinger equation for a single active electron, moving in an effective molecular potential and driven by an arbitrary laser pulse, is solved numerically. The method uses the TDSC expansion, which describes the one-particle wave function in spherical coordinates, as well as the subsequent description of the radial functions by the finite-element discrete-variable representation (FEDVR). The basis function in each finite element is represented by the normalized Lagrange interpolating polynomials which are constructed over a Gauss-Lobatto grid. The short-interactive Lanczos method is used to propagate the resulting system of equations for the time-dependent expansion coefficients.

For some orientations of a fixed-in-space model chiral system we achieve PECD values of up to 50% for the PECD. For randomly oriented systems, the PECD is much smaller, on the order of 10%, which agrees with the experimental results from [3,4]. For camphor, theoretical PECD reproduces the experimental one: both in the magnitude and sign, as well as in the nodal structure [4]. Our study of the multiphoton PECD for bicyclic ketones pave the way to a deeper understanding of this fundamental effect.

References

[1] B. Ritchie, *Phys. Rev. A* **13**, 1411 (1976).
[2] *Chiral Recognition in the Gas Phase*, edited by A. Zehnacker (CRC Press, Boca Raton, 2010).
[3] C. Lux, M. Wollenhaupt, T. Bolze, Q. Liang, J. Köhler, C. Sarpe, T. Baumert, *Angew. Chem. Int. Ed.* **51**, 5001 (2012).
[4] C. Lux, M. Wollenhaupt, C. Sarpe, and T. Baumert, *ChemPhysChem* **16**, 115 (2015).
[5] M. H. M. Janssen and I. Powis, *Phys. Chem. Chem. Phys.* **16**, 856 (2014).
[6] A. N. Artemyev, A. D. Müller, D. Hochstuhl, and P. V. Demekhin, *J. Chem. Phys.* **142**, 244105 (2015).
[7] P. V. Demekhin, D. Hochstuhl, and L. S. Cederbaum, *Phys. Rev. A* **88**, 023422 (2003).

Theoretical *ab-initio* study of inner shell excited molecular ions

Puglisi, Alessandra[1] , Sisourat, Nicolas[1] , Carniato, Stéphane[1]

1. Sorbonne Universités, UPMC Univ. Paris 06, CNRS, Laboratoire de Chimie Physique Matiére et Rayonnement, F-75005, Paris, France

Molecular ions play an important role in the interstellar chemistry since they act as precursors in the formation of larger molecule [1]. Molecular ions containing carbon are well known and have been identified in the interstellar medium (ISM) a long time ago [2], conversely the observation of oxygen- and silicium-based moleculear ions is much more recent [3,4]. The interest toward the first two categories of molecule comes from their capability to form hydrocarbons or small organic acid and water respectively. For what concern the silicum-based molecules, the detection of the Silylidyne (SiH) from Schilke, P. *et al.* [4] in the 2001 brings back the spotlight to the possibility formation of silicon hydride from photodissociation of larger molecule in the ISM [5].

X-ray photoabsorption spectroscopy provides a powerful tool to study the chemical environment of different types of systems going from small to more complex molecular ions and molecules. The spectroscopic studies of these ions provide unique identification of atomic/molecular species and their relative abundances in astrophysical environments.

In this context, we are interested in the simulation of K and L-shell photoabsorption spectra of molecular ions containing the afore mentioned elements Carbon, Oxygen and Silicium. The calculations were carried out using a combination of post Hartree-Fock and nuclear dynamics wavepacket propagation. In detail, we use the Configuration Interaction (CI) method to compute the potential energy surfaces of hundred of inner shell excited states. In our calculations, the spin orbit coupling is taken into account through the Breit-Pauli operator. The photoabsoption spectra were computed with a time dependent nuclear wave packet propagation which includes the core-hole lifetime. In order to understand the spectra structure of the studied systems, we investigate the nature of the electronic dipolar transitions.

The theoretical results compare quantitatively with the experimental ones and allow the attribution of the experimental spectroscopic lines [6]. The proposed combined approach can readily be applied to other molecular ions and opens new perspectives in the nascent field of the photoionization of molecular ions in gas phase.

References

[1] Smith, D, *Phil. Trans. R. Soc. Lond.*, **A324** 257-273 (1988)
[2] Yamada, K. M. T., Winneweisser, G., Interstellar Molecules –Springer Tracts in Modern Physics 241 2011
[3] Wyrowski,F., Menten, K.M., Güsten, R., Belloche, A., Astron. Astroph., 518, 2010
[4] Schilke, P., Benford, D.J., Hunter, T.R., Lis, D.C., Phillips, T.G.; Astrophys. J. Suppl. S. 2001132, 281-364
[5] Gharaibeh, M. F., Cubaynes, D., Guilbaud, S., Hassan, N. E., Shorman, M. M. A. , Miron, C., Nicolas, C., Robert, E., Blancard, C., McLaughlin, B. M. and Bizau, J. M., J. Phys. B At. Mol. Opt. Phys. 201144,175-208
[6] Mosnier, J-P, Kennedy, E.T., van Kampen, P., Cubaynes, D., Guilbaud, S., Sisourat, N., Puglisi, A., Carniato, S. and Bizau, J.-M., submitted to Phys. Rev. Lett.

Positive ion detection from multiphoton dissociation of nitromethane at 532nm and 355nm laser radiation

Denhi Martínez, Alfonso Guerrero, Ignacio Álvarez, Carmen Cisneros

Instituto de Ciencias Físicas, Universidad Nacional Autónoma de México, Av. Universidad s/n, Chamilpa, 62210 Cuernavaca, Morelos.

Nitromethane is still being an important molecule to analyze due to their intrinsic complex dynamic and its study is yet incomplete. Also this molecule is quite gentle, in the sense, that with UV radiation from a commercial laser it can be obtained an extensive dissociation and the formation of several ionic fragments by multiphoton ionization. In the present work, high resolution mass spectrometry: Reflectron and TOF technique is used to analyze dissociation channels of nitromethane. Nanosecond laser pulses of 2.33 eV and 3.49 eV are used for the production of ions by multiphoton absorption, the density power (irradiation) range is in 10^9 – 10^{10} W * cm^{-2} regime. The identification of 20 ions is presented; some of them not were being reported before.
In particular, the observation of masses, 1, 12, 15, 30, 31, 43 and 45 corresponding to the ions of H^+, C^+, CH_3^+, NO^+, CH_3O^+, $CHNO^+$ and CH_3NO^+, is discussed with more detail.
The figure 1 shows the mass spectra for two different wavelengths: 532nm and 355nm. Selected significant ions appear in bold. According with our results, some of the different dissociation paths which give raise these ions are proposed.

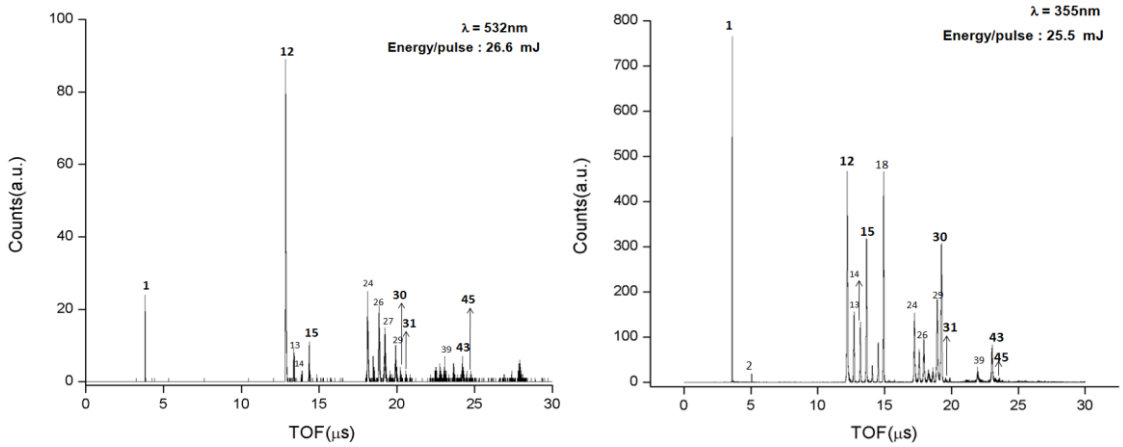

Fig. 1 Mass spectra at two different wavelengths

Using a different technique Masataka [1] suggests the existence of competing photodissociation pathways for the formation of CH_3O^+ mainly, however he points out that it is necessary the direct observation by spectroscopy methods as it is done in the present work. On the other hand Kilic [2], using laser pulses at 375nm and 10ns reports the observation of only large quantities of NO^+, where the irradiation condition was 6 x10^{10} W * cm^{-2}. Only with a fs laser pulse and irradiation of 1.8 x10^{13} W * cm^{-2}, he observes several ions including H^+, C^+, CH_3^+, NO^+ and NO_2^+. In contrast to these results using 355nm and 6.5ns our spectra show larger number of ions than in [2] including NO^+. It is convenient to emphasize that in the range of irradiation 2.8 - 3.08 x10^9 W * cm^{-2}, there is a substantial production of NO^+.
Regarding to 532nm, the two main features are: first for the production of NO^+ more resolution is needed, higher than in the case 355nm, and the intensity of the signal is lower; second, the formation of ionic fragments with large mass (30-57 amu) is more evident.
For the appearance of CH_3O^+, we suggest that the formation of such ion is related with the roaming mechanism, that has been propose by Arghya [3], and moreover in the work of Bowman [4] where a detailed study confirms this probable pathway.

References

[1] M. Sumida, Y. Kohge, K.Yamasaki, and H. Kohguchi, *Multiple product pathways in photodisocciation of nitromethane at 213nm,* J. Chem. Phys., **144**, 064304 (2016).
[2] H. S. Kilic et al., *Multiphoton Ionization and dissociation of Nitromethane Using Femtosecond Laser Pulses at 375and 750nm,* J. Phys. Chem A, **101**, 817-823 (1997).
[3] D. Arghya et al., *Photodissociation dynamics of nitromethane and methyl nitrite by infrared multiphoton dissociation imaging with quasiclassical trajectory calculations : Signatures of the roaming pathway,* J. Chem. Phys., **140**, 054305 (2014).
[4] J. M. Bowman, *TOPICAL REVIEW:Roaming,* Molecular Physics, **112**, 2516-2528 (2014).

Spin–Orbit Coupling and Rovibrational Structure in the Iododiacetylene Cation by PFI-ZEKE Photoelectron Spectroscopy

Katrin Dulitz[1], **Elias Bommeli**[1], **Daniel Zindel**[1], **Frédéric Merkt**[1]
1. Laboratory of Physical Chemistry, ETH Zürich, Vladimir-Prelog-Weg 2, 8093 Zürich, Switzerland

Haloacetylenes, H–C≡C–X, and dihalodiacetylenes, H–C≡C–C≡C–X (with X = F, Cl, Br, I), are of interest for the study of charge migration processes in molecules, because they contain both conjugated π-type molecular orbitals along the $(C{\equiv}C)_2$ molecular axis and $2p_{x,y}$-type atomic orbitals at the halogen end groups. Photoelectron spectroscopy allows for a systematic study of the charge distribution in halogen-containing molecular cations, because the observed spin–orbit coupling is a direct measure of the electron-hole density on the halogen atom [1, 2]. In a previous study by our group, the rotationally resolved photoelectron spectrum of iodoacetylene, HC_2I, was obtained using pulsed-field-ionization zero-kinetic-energy (PFI-ZEKE) photoelectron spectroscopy [2]. In the $X^+\,^2\Pi$ electronic ground state of the HC_2I^+ cation, the spin–orbit coupling is much stronger than the Renner-Teller effect and effectlively quenches its vibronic interactions. A two-state charge-transfer model was applied to haloacetylenes, HC_2X, and provided a semi-quantitative description of the structure of the photoelectron spectra. Here, we report on the measurement of the PFI-ZEKE photoelectron spectrum of the $X^+\,^2\Pi \leftarrow X\,^1\Sigma^+$ photoionizing transition in iododiacetylene, HC_4I, which has been recorded with partial resolution of the rotational structure. The first adiabatic ionization energy of HC_4I and the spin–orbit splitting of the $X^+\,^2\Pi$ state of HC_4I^+ are determined as $E_I^{ad}/(hc) = 74470.7\ \mathrm{cm}^{-1}$ and $\Delta\tilde{\nu}_{SO} = -1916.7\ \mathrm{cm}^{-1}$, respectively. The fundamental vibrational wave numbers of several vibrational modes of the $X^+\,^2\Pi$ electronic ground state of the HC_4I^+ cation have been identified. We show that a simple three-state charge-transfer model allows for a qualitative description of the change in bond lengths upon ionization, and of the electronic structure and spin–orbit coupling in HC_4I^+.

References

[1] Monika Grütter, Ximei Qian, and Frédéric Merkt, *Photoelectron Spectroscopic Study of the E⊗e Jahn-Teller Effect in the Presence of a Tunable Spin–Orbit Interaction. III. Two-State Excitonic Model Accounting for Observed Trends in the $\tilde{X}^2E$ Ground State of CH_3X^+ (X=F, Cl, Br, I) and CH_3Y (Y=O, S)*, J. Chem. Phys. **137**, 084313 (2012).

[2] Bérenger Gans, Guido Grassi, and Frédéric Merkt, *Spin–Orbit and Vibronic Coupling in the Ionic Ground State of Iodoacetylene from a Rotationally Resolved Photoelectron Spectrum*, J. Phys. Chem. A **117**, 9353 (2013).

Forbidden Electric Dipole Transitions in Hydrogen Molecule Ion

Petar Danev[1], **Vladimir Korobov**[2], **Dimitar Bakalov**[1]
1. Institute for Nuclear Research and Nuclear Energy, Bulgarian Academy of Sciences, blvd. Tsarigradsko ch. 72, Sofia 1142, Bulgaria
2. Joint Institute for Nuclear Research, 141980, Dubna, Russia

The spectrum of the lower ro-vibrational excitations of the hydrogen molecular ion H_2^+ has been recently evaluated with a very high precision [1,2]. It has been shown that the small natural width and the suppressed sensitivity to external fields makes this ion suitable for a high precision time standard. In [3] the most appropriate E1 and two-photon transition lines for such purposes were selected.

In the present work we extend the class of possible candidates with a detailed study of the so-called "forbidden transitions", i.e. transitions that are due to mixing of states with opposite parity under exchange in spite of being forbidden by selection rules in the non-relativistic limit. The intensity of the forbidden lines is suppressed in comparison to the allowed ones, but their study gives better and more complete knowledge of H_2^+ spectrum as well as a precise description of the lifetime and population of low excited ro-vibrational states of the hydrogen molecular ion. The corrections to the wave function were calculated in first order of perturbation theory using the Breit three particle Hamiltonian. Laser induced electric dipole transition rates between H_2^+ hyperfine levels were computed and their possible use in metrology was analysed.

The authors (P.D. and D.B.) are gratefully acknowledging the support of grant No. DFNP 47/21.04.2016 of the program for support of young scientists at BAS.

References

[1] V.I. Korobov, J.C.J. Koelemeij, J.-Ph. Karr, and L. Hilico, *Theoretical hyperfine structure of the molecular hydrogen ion at the 1 ppm level* Phys. Rev. Lett. **116**, 053003 (2016).
[2] V.I. Korobov, L. Hilico, and J.-P. Karr, *Relativistic corrections of ma6(m/M) order to the hyperfine structure of the H2+ molecular ion*, Phys. Rev. **A 79**, 012501 (2009)
[3] S. Schiller, D. Bakalov, and V.I. Korobov, *Simplest molecules as Candidates for Precise Optical Clocks*, Phys. Rev. Lett. **113**, 023004 (2014).

X-ray Photoelectron Spectroscopy Study Spectra and Electron Structure of Mono- and Binuclear Cu and Ni Complexes with "Non-Innocent" Ligands

Tatiana Ivanova[1], Aleksei Sidorov[1], Stanislav Nikolaevskii[1], Michail Kiskin[1], Serguei Savilov[1,2], Roman Linko[3], Gennady Sapozhnikov[4], Vladimir Novotortsev[1], Igor Eremenko[1]

1. Kurnakov Institute of General and Inorganic Chemistry of RAS, 31 Leninskii pr., 119991 Moscow, Russia
2. Department of Chemistry, M. V. Lomonosov Moscow State University, 1-3 Leninskie Goru, 119991 Moscow Russia,
3. Peoples' Friendship Universty, Moscow, 6 Mikluho-Maklaya st., 117198 Moscow, Russia
4. Physico-Technical Institute, Ural Branch, of RAS, Izhevsk, 85-31 Dzerzhinskogo Str., 426039 Izhevsk, Russia

X-ray photoelectron spectroscopy (XPS) method was used for the identification and study the charge state of the metal center of the mono- and binuclear complexes of copper (I, II) and nickel (II) with "non-innocent" ligands. The spectra M2p, M3s and M3p (M=Cu, Ni) and electron structure of the mono- and binuclear complexes of copper (I, II) and nickel (II) were investigated. The difference between the states of metal atoms had been determined both from the chemical shift and from the distinction of the satellite structure M2p, M3s, M3p lines. Were discussed the results of comparative analysis of the binding energy of the inner levels M2p, M3s and M3p and N1s nitrogen atoms and the effects of the electron density distribution in the free ligand and complexes. An intense satellite structure was most noticeable for the Cu2p lines in the case of paramagnetic complex, but not for nickel (II) the diamagnetic complex. It was determined that mononuclear complex is a high-spin paramagnetic and diamagnetic complex there is binuclear. Mononuclear complex can be represented as different types of resonant structures. XP-spectra of the samples at room temperature were registered with Axis Ultra DLD spectrometer (Kratos Analytical) (non-monochromatic MgKα radiation, 150 W). The spectra were calibrated using C1s-line energy which refers to the C C/C H bonds; it was taken equal to 285.0 eV. Measurements were done at least two times at a pressure of ~10–9 Torr. Spectral fitting was accomplished using the Kratos Analytical package. The XPS data are in good agreement with the X-ray structure analysis (XSA).

ACKNOWLEDGMENTS
This work was supported by the Russian Foundation of Basic Research (project 16-03-00047) and Russian Scientific Foundation (14-23-00176).

Proposal for the formation of ultracold paramagnetic polar molecules in their absolute ground state

D. Borsalino, E. Luc, N. Bouloufa-Maafa, P. Zuchowski and O. Dulieu

1 Laboratoire Aimé Cotton, CNRS, Université Paris-Sud, ENS Cachan, Université Paris-Saclay, 91405 Orsay Cedex, France

2 Instytut Fizyki. Uniwersytet Mikolaja Kopernika, Torun, Poland

Alkali-alkaline-earth dimers, such as RbCa and RbSr, possess (in their ground electronic state) both a permanent magnetic and electric dipole moment in the molecular frame, allowing their manipulation with external fields at ultracold temperatures. Such molecules have been proposed as candidates for quantum simulators. We propose an efficient method combining a photoassociation step and a stimulated Raman process to create ultracold RbSr and RbCa molecules in their absolute ground state, suitable for studying dipolar interactions in quantum gases. Our model is based on new accurate quantum chemistry computations [1,2] of potential energy surfaces of ground and excited molecular states and of relevant transition dipole moments of these molecules. The results are in good agreement with recent low-resolution spectroscopic data recorded with Helium nanodroplets [3].

In addition we determined the dynamic dipole polarizabilities for RbSr and RbCa, relevant for the optical trapping of such molecules.

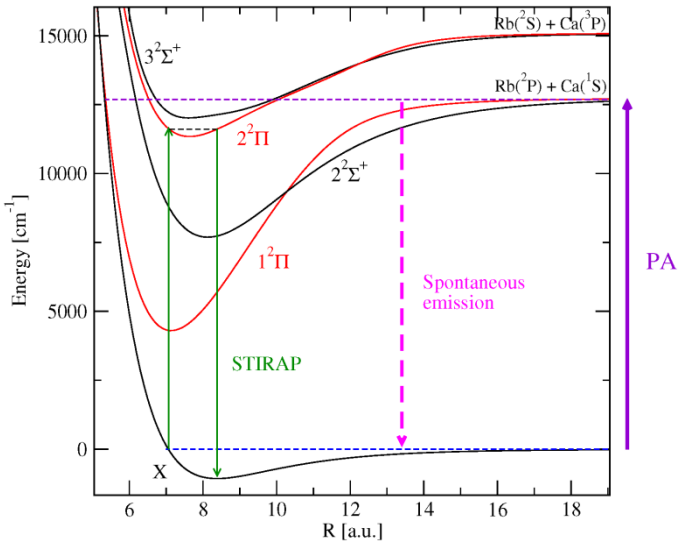

Fig. 1 Scheme of the proposed scheme for creating ultracold RbCa molecules in their absolute ground state level : photoassociation (PA) step followed by spontaneous emission, and stimulated Raman adiabatic passage (STIRAP) to transfer the population of the weakly-bound level down to the lowest ground state level.

References

[1] P. Zuchowski, R. Guérout and O. Dulieu, Phys. Rev. A **90**, 012507 (2014)
[2] D. Borsalino, P. Zuchowski, N. Bouloufa-Maafa and O. Dulieu, submitted
[3] J. V. Pototschnig, G. Krois, F. Lackner, and W. E. Ernst, J. Mol. Spectrosc. **310**, 126 (2015)

Cold Ion-Neutral Reactions in Next-Generation Ion-Atom Hybrid Traps

Pascal Eberle[1], Alexander Dörfler[1], Claudio von Planta[1], Humberto da Silva Jr.[2], Maurice Raoult[2], Olivier Dulieu[2], Stefan Willitsch[1]

1. Department of Chemistry, University of Basel, Klingelbergstrasse 80, 4056 Basel, Switzerland
2. Laboratoire Aimé Cotton, CNRS, Université Paris-Sud XI, 91405 Orsay Cedex, France

Recent advances in the simultaneous ("hybrid") trapping of cold ions and atoms enabled the study of ion-atom interactions and reactions at very low collision energies. Details of the mechanism of chemical reactions and the nature of molecular interaction potentials could be studied [1-4]. But so far, insufficient control over the collision energy distributions impeded the study of effects with narrow dependencies on collision energy such as shape resonances [5]. Here we present results from the extension of our hybrid trap setup with increased control over the collision energies. Our hybrid trap consists of a linear Paul trap for atomic and molecular ions overlapped with a magneto-optical trap for neutral rubidium atoms.

In the original setup, control over the energy of the ion-atom collisions was achieved by changing the number of ions and shape of the ion crystal. Heating of the ions due to micromotion lead to large spreads of the collision energies. In a new approach, we use a modified magneto-optical trap which allows the use of a dynamic atom cloud. Radiation pressure differences in the cooling laser beams along one axis create atom clouds in off-center positions. On-resonance push laser beams accelerate the atoms through the ion crystal after which the atoms are recaptured in the opposite off-center position. By carefully tuning the cooling and push beam sequence and intensities we are able to produce moving atom clouds with well-defined velocities in the lab frame. Using this approach with ion strings on the rf null line of the ion trap, the collision energy resolution can be greatly improved.

A detailed characterization of the setup and analysis of the moving atom cloud with results from experiments and Monte Carlo trajectory simulations are shown. We also present results from velocity-controlled collisions between Ca^+ ions and neutral Rb atoms. In a next step, following our pioneering study to introduce molecular species in the hybrid trap [4], sympathetically cooled molecular ions will be studied using the new hybrid trap. Starting with N_2^+ as a first test system, we will move on to state-selectively produced O_2^+ ions, for which we have coupled the setup with a molecular beam machine.

References

[1] Felix H. J. Hall, Mireille Aymar, Nadia Bouloufa-Maafa, Olivier Dulieu, and Stefan Willitsch, *Light-Assisted Ion-Neutral Reactive Processes in the Cold Regime: Radiative Molecule Formation versus Charge Exchange*, Phys. Rev. Lett. **107**, 243202 (2011).

[2] Felix H.J. Hall, Pascal Eberle, Gregor Hegi, Maurice Raoult, Mireille Aymar, Olivier Dulieu and Stefan Willitsch, *Ion-neutral chemistry at ultralow energies: dynamics of reactive collisions between laser-cooled Ca^+ ions and Rb atoms in an ion-atom hybrid trap*, Mol. Phys. **111**, 14-15, 2020 (2013).

[3] Felix H.J. Hall, Mireille Aymar, Maurice Raoult, Olivier Dulieu and Stefan Willitsch *Light-assisted cold chemical reactions of barium ions with rubidium atoms*, Mol. Phys. **111**, 12-13, 1683 (2013).

[4] Felix H. J. Hall and Stefan Willitsch, *Millikelvin Reactive Collisions between Sympathetically Cooled Molecular Ions and Laser-Cooled Atoms in an Ion-Atom Hybrid Trap*, Phys. Rev. Lett. **109**, 233202 (2012).

[5] Humberto da Silva Jr, Maurice Raoult, Mireille Aymar and Olivier Dulieu, *Formation of molecular ions by radiative association of cold trapped atoms and ions*, New J. Phys. **17**, 045015 (2015)

Towards Continuous Trap Loading of Helium in Rydberg States

Ondřej Tkáč, Matija Žeško, Frédéric Merkt

Laboratory of Physical Chemistry, ETH Zurich, CH-8093 Zurich, Switzerland

Deceleration of atoms and molecules in pulsed supersonic beams using time-dependent inhomogeneous electric and magnetic fields is an attractive method to generate cold samples [1,2]. Following deceleration, the cold samples can be stored in traps for investigation by spectroscopy or for use as targets in scattering experiments.

The ability to load cold atoms or molecules in the trap from successive gas pulses would enable one to achieve a higher phase-space density of trapped species. We present work pursuing this goal based on Rydberg-Stark deceleration and trapping. The atoms or molecules are deflected from the original beam propagation direction while being decelerated and are then loaded into an off-axis electric trap [3]. The radiative decay of the Rydberg atoms or molecules then populates the ground electronic state or a metastable state. Superimposing a magnetic trap onto the electric trap enables one increase the density of trapped species pulse after pulse. Since the trap consists of combined electric and magnetic fields, the effects of these fields on the Rydberg states and the Rydberg-Stark deceleration must be characterized.

We present experiments on triplet helium Rydberg states carried out to realise the trap-loading scheme described above. We measured the spectra of transitions to Rydberg states of He around n = 30 in pure electric (Stark effect) and magnetic (Zeeman effect) fields as well as in combined electric and magnetic fields at various relative angles and strengths. The spectra were also calculated by diagonalization of the Hamiltonian matrix and the avoided crossings between Rydberg states in the range of electric- and magnetic-field strengths relevant for Rydberg-Stark deceleration and magnetic trapping were characterized. The results of Rydberg-Stark deceleration experiments of triplet helium in the presence of a quadrupole magnetic field will be presented.

References

[1] Sebastiaan Y. T. van de Meerakker, Hendrick L. Bethlem, Nicolas Vanhaecke, and Gerard Meijer, *Manipulation and Control of Molecular Beams*, Chem. Rev. **112**, 4828 (2012).

[2] Stephen D. Hogan, Michael Motsch, and Frederic Merkt, *Deceleration of supersonic beams using inhomogeneous electric and magnetic fields*, Phys. Chem. Chem. Phys. **13**, 18705 (2011).

[3] Ch Seiler, S. D. Hogan, H. Schmutz, J. A. Agner, and F. Merkt, *Collisional and Radiative Processes in Adiabatic Deceleration, Deflection, and Off-Axis Trapping of a Rydberg Atom Beam*, Phys. Rev. Lett. **106**, 073003 (2011).

A buffer gas cooled beam of Barium Monohydride for laser cooling experiments

Geoffrey Iwata, Marco Tarallo, Rees McNally, and Tanya Zelevinky
Department of Physics, Columbia University, 538 West 120th Street, New York, NY 10027-5255, USA

We present a cryogenic beam source of barium monohydride (BaH), and study laser ablation of solid precursor targets as well as helium buffer gas cooling dynamics [1]. Such a molecular beam is amenable to laser slowing and cooling, and we cover progress towards a molecular magneto-optical trap (MOT), with spectroscopic studies of relevant cooling transitions in the $B^2\Sigma^+ \leftarrow X^2\Sigma$ manifold in laser ablated molecules. We include resolution of hyperfine structure and precision measurements of the vibrational Frank-Condon factors. The $B^2\Sigma^+ \leftarrow X^2\Sigma$ can be combined with the first excited state transition ($A^2\Pi \leftarrow X^2\Sigma$) for complementary laser cooling and trapping advantages: the former has a large magnetic moment that can result in stronger magneto-optical trapping forces [2], while the latter is predicted to have more favorable decay branching ratios [3,4]. Finally, we examine the feasibility of photodissociation of trapped BaH molecules to yield optically accessible samples of ultracold hydrogen for precision spectroscopic measurements [4].

References

[1] M. Tarallo, G.Z. Iwata, and T. Zelevinsky, *BaH molecular spectroscopy with relevance to laser cooling*, Phys. Rev. A (accepted).
[2] M. R. Tarbutt, and T. C. Steimle, *Modeling magneto-optical trapping of CaF molecules*, Phys. Rev. A **92**, 053401 (2015).
[3] M. D. Di Rosa, *Laser-cooling molecules: Concept, candidates, and supporting hyperfine-resolved measurements of rotational lines in the A–X(0,0) band of CaH*, Eur. Phys. J. D 31, 395 (2004).
[4] I. C. Lane, *Production of ultracold hydrogen and deuterium via Doppler-cooled Feshbach molecules*,Phys. Rev. A **92**, 022511 (2015).

Equation of state and generalized Lane-Emden models with laser cooled gases

J.A. Rodrigues
Departamento de Física, Faculdade de Ciências e Tecnologia, Universidade do Algarve, Faro, Portugal
Instituto de Plasmas e Fusão Nuclear, Instituto Superior Técnico, Universidade de Lisboa, 1049-001 Lisbon, Portugal

J.D. Rodrigues
Instituto de Plasmas e Fusão Nuclear, Instituto Superior Técnico, Universidade de Lisboa, 1049-001 Lisbon, Portugal

O.L. Moreira
Instituto de Plasmas e Fusão Nuclear, Instituto Superior Técnico, Universidade de Lisboa, 1049-001 Lisbon, Portugal

H. Terças
Physics of Information Group, Instituto de Telecomunicações, Lisbon, Portugal

J.T. Mendonça
Instituto de Plasmas e Fusão Nuclear, Instituto Superior Técnico, Universidade de Lisboa, 1049-001 Lisbon, Portugal

The concept of an equation of state, the relationship between thermodynamic state variables such as pressure, P, temperature, T, and volume, V, has evolved beyond the original formulation of Clapeyron for an ideal gas, $PV = NK_BT$. In astrophysics, the equation-of-state plays a central role in the study of stellar structure, where hydrostatic equilibrium condition of a polytropic gas under the gravitational field and thermodynamic pressure leads to the celebrated Lane-Emden equation [1, 2].

Here we extend the Lane-Emden formalism to experimentally determine the equation of state of a laser cooled gas, by directly measuring the atomic density profiles of large magneto-optical traps. In our experiment, the hydrostatic equilibrium condition is provided (in first order) by the balance between the harmonic confinement - the analog of the gravitational force - and the thermodynamic pressure, cast in the form of a polytropic equation of state. However, when the cooling lasers tuned close to the atomic resonance, multiple scattering of light occurs and an additional collective interaction appears, due to the exchange of scattered photons with nearby atoms [3, 4]. In this regime, the atoms experience a Coulomb-like long-range interaction [5], therefore allowing to regard the system as an effective one-component trapped plasma [6]. Thus, the condition of hydrostatic equilibrium results in a generalized Lane-Emden equation, which encompasses the joint effects of harmonic confinement, thermodynamics and radiation pressure due to multiple scattering of light. Here, we provide the experimental evidence of the multiple scattering of light in the equation of state of a laser cooled gas and extracting the polytropic exponent by fitting the density profiles to our theory.

The Lane-Emden formalism is, to the best of our knowledge, for the first time applied outside the context of astrophysics. The results obtained here pave the way to the subsequent experimental investigation of more exotic plasma-like processes in non degenerate cold gases. We have previously introduced the possibility of observing effects like phonon-lasing [7], classical rotons [8], plasmon modes and Tonks-Dattner resonances [6, 9], photon bubbles [10], the dynamical Casimir-effect [11] and twisted excitations carrying orbital angular momentum [12].

References

[1]J. P. Cox and R. T. Giuli, Principles of Stellar Structure (Gordon and Breach, New York, 1968).
[2]A. R. Choudhuri, Astrophysics for Physicists (Cambridge University Press, New York, 2010).
[3]D. W. Sesko, T. G. Walker, and C. E. Wieman, J. Opt. Soc. Am. B 8, 946 (1991).
[4]J. Dalibard, Optics Communications 68, 203 (1988).
[5] L. Pruvost, I. Serre, H. Duong, and J. Jortner, Phys. Rev. A 61, 053408 (2000).
[6] J. T. Mendonça and H. Terças, Physics of Ultra-Cold Matter (Spring Series on Atomic, Optical and Plasma Physics Vol. 70, Berlin, 2012).
[7]J. T. Mendonça, H. Terças, G. Brodin, and M. Marklund, EPL (Europhysics Letters) 91, 33001 (2010).
[8]H. Terças, J. T. Mendonça, and V. Guerra, Phys. Rev. A 86, 053630 (2012).
[9]J. Mendonça, R. Kaiser, H. Terças, and J. Loureiro, Phys. Rev. A 78, 013408 (2008).
[10]J. T. Mendonça and R. Kaiser, Phys. Rev. Lett. 108, 033001 (2012).
[11]V. V. Dodonov and J. T. Mendonça, Physica Scripta 2014, 014008 (2014).
[12]J.D. Rodrigues, H. Terças, and J.T. Mendonça, EPL (Europhysics Letters) 113 (1), 13001

Photoassociation of $NaCa^+$ molecular ions in the electronic ground state from cold atom-ion mixtures

Marko Gacesa
NASA Ames Research Center, Moffett Field, California 94035, USA

John A. Montgomery, H. Harvey Michels, Robin Côté
Department of Physics, University of Connecticut, Storrs, Connecticut 06269, USA

We present a theoretical study of feasibility of using photoassociation - via one or more intermediate states - for production of $(NaCa)^+$ molecular ions in its electronic ground state. We rely on post-Hartree-Fock methods and effective core potential approach to determine the electronic structure of excited singlet states and transition dipole moments. For the initial setup, we assume a mixture of cold trapped Ca^+ ions immersed into an ultracold gas of Na atoms. The $(NaCa)^+$ molecular ions are first photoassociated in the excited $E^1\Sigma^+$ electronic state and allowed to spontaneously decay, either directly to the ground electronic state or to an intermediate state from which the population is transferred to the ground state by the second laser. Our analysis of all possible optical pathways suggests that the efficiency of two-photon photoassociation approach, with either $B^1\Sigma^+$ or $C^1\Sigma^+$ intermediate state, is sufficient to produce significant quantities of ground state $(NaCa)^+$ molecular ions. A single-step process results in lower formation rates and would require either a high density sample or a very intense photoassociation laser to be realistic [1]. The analyzed molecule is often considered a benchmark system in experiments involving diatomic molecular ions. Consequently, positive results of our study suggest that photoassociation, as an optical method of production of neutral ultracold dimers, could be extended to a number of molecular ions species.

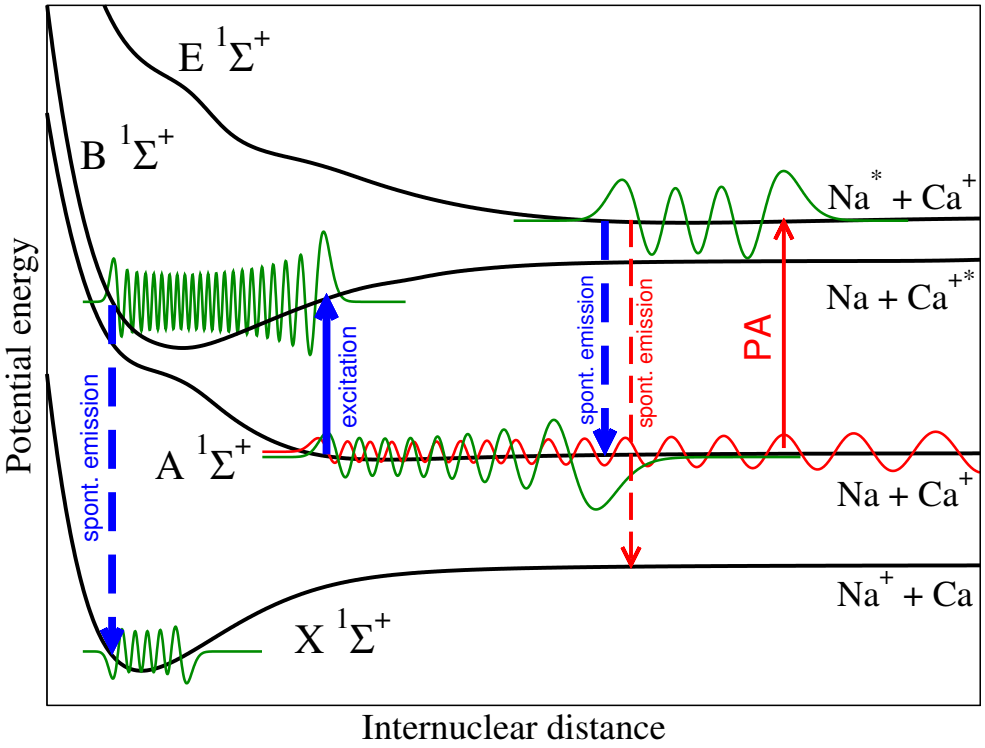

Fig. 1 Schematics of the optical pathways suggested for production of $NaCa^+$ dimers in the electronic ground state.

References

[1] M. Gacesa, J. A. Montgomery, H. H. Michels, R. Côté, *Production of $NaCa^+$ molecular ions in the ground state from cold atom-ion mixtures by photoassociation via an intermediate state*, Phys. Rev. A. **94**, 013407 (2016).

Rotation of quantum impurities in the presence of a many-body environment

Mikhail Lemeshko,[1] **Richard Schmidt**[2,3]

1. Institute of Science and Technology (IST) Austria, Am Campus 1, 3400 Klosterneuburg, Austria
2. ITAMP, Harvard-Smithsonian Center for Astrophysics, 60 Garden Street, Cambridge, Massachusetts 02138, USA
3. Physics Department, Harvard University, 17 Oxford Street, Cambridge, Massachusetts 02138, USA

We present the first systematic treatment of quantum rotation coupled to a many-particle environment. We approach the problem by introducing the quasiparticle concept of an "angulon" – a quantum rotor dressed by a quantum field – and reveal its properties using a combination of variational and diagrammatic techniques. The theory [1,2] can be applied to a wide range of systems described by the angular momentum algebra, from Rydberg atoms immersed into Bose-Einstein Condensates, to cold molecules solvated in helium droplets, to ultracold molecular ions.

In particular, the theory sheds light on experiments on non-adiabatic molecular dynamics inside superfluid helium nanodroplets [3], which lacked even a qualitative explanation so far. Furthermore, we predict new features in the rotational spectra of ultracold molecules and molecular ions due to their interaction with a Bose-Einstein Condensate.

References

[1] Richard Schmidt, Mikhail Lemeshko, "Rotation of Quantum Impurities in the Presence of a Many-Body Environment," Phys. Rev. Lett. **114**, 203001 (2015)
[2] Richard Schmidt, Mikhail Lemeshko, "Deformation of a Quantum Many-Particle System by a Rotating Impurity," Phys. Rev. X **6**, 011012 (2016)
[3] Dominik Pentlehner, Jens H. Nielsen, Alkwin Slenczka, Klaus Mølmer, and Henrik Stapelfeldt, Phys. Rev. Lett. **110**, 093002 (2013)

Rotational state thermometry with OH^- at the Heidelberg Cryogenic Storage Ring (CSR)

Christian Meyer[1], Arno Becker[1], Klaus Blaum[1], Christian Breitenfeldt[1,2], Sebastian George[1], Jürgen Göck[1], Manfred Grieser[1], Florian Grussie[1], Robert von Hahn[1], Philipp Herwig[1], Jonas Karthein[1], Claude Krantz[1], Holger Kreckel[1], Sunil Kumar[1], Jorrit Lion[1], Svenja Lohmann[1], Preeti M. Mishra[1], Oldřich Novotný[1], Aodh P. O'Connor[1], Roland Repnow[1], Kaija Spruck[1,3], Stefan Schippers[3], Dirk Schwalm[1,4], Lutz Schweikhard[2], Stephen Vogel[1], Andreas Wolf[1]

1. Max-Planck-Institut für Kernphysik, Saupfercheckweg 1, 69117 Heidelberg, Germany
2. Institut für Physik, Ernst-Moritz-Arndt Universität Greifswald, Felix-Hausdorff-Straße 6, 17487 Greifswald, Germany
3. Institut für Atom- und Molekülphysik, Justus-Liebig-Universität Gießen, Leihgesterner Weg 217, 35392 Gießen, Germany
4. Weizmann Institute of Science, Herzl St 234, Rehovot, 7610001, Israel

The Cryogenic Storage Ring (CSR) [1] located at the Max-Planck-Institut für Kernphysik in Heidelberg is an electrostatic storage ring with a circumference of 35 m in a fully cryogenic environment. Planned experiments aim at investigating ground state properties and collisions of molecular and cluster ions with neutral particles or electrons in the gas phase. By cooling the experimental chambers down to 6 K a residual gas density below 140 cm^{-3} ($< 10^{-14}$ mbar rte) can be reached which enables storage times of fast ion beams of several hours [1]. In addition, stored molecules in the CSR can equilibrate with the cryogenic environment by radiative cooling via infrared modes. First measurements on resonant photodissociation of CH^+ ions in low-J rotational levels were recently reported [2]. During the first cryogenic beam time the radiation field of CSR was measured by monitoring the internal state populations of OH^- up to 1200 by observing the near-threshold photodetachment signal, similar to previous ion trap studies [3]. For this measurement, a 60 keV OH^- ion beam was overlapped with a continuous wave HeNe laser (633 nm) and a pulsed, wavelength tunable OPO laser using wavelengths between 680 to 709 nm. Neutral particles created by laser-induced photodetachment leave the closed orbit of the ring and are recorded by a microchannel-plate detector in the cryogenic zone. To correct for the ion-beam lifetime and other ring effects the neutral rate induced by the OPO laser is normalized by the rate induced by the HeNe laser. By varying the wavelength of the OPO different rotational states are detached. The normalized neutral count rates for various wave numbers $\tilde{\nu}$ (see Fig. 1) are then fitted by a cooling model combined with a probing model. The fits shown include spontaneous and induced radiative transitions between rotational levels in the vibrational ground state only. The model reveals the evolution of the rotational level populations in J=2, 1 and 0, showing a J=0 equilibrium population of >90%. The determination of the relative photodetachment cross sections from this measurement is under study.

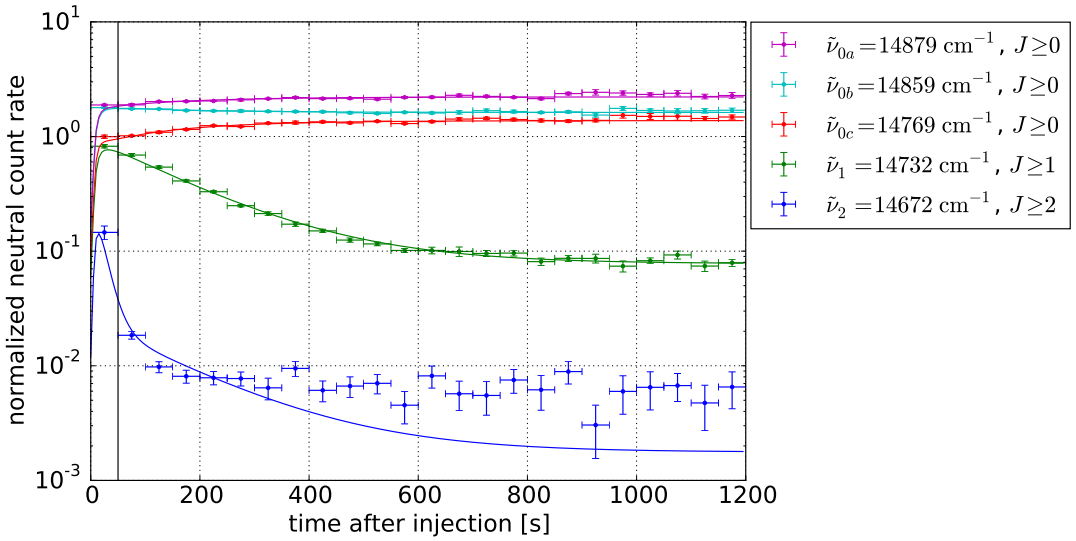

Fig. 1 Normalized neutral count rate of photodetached OH measured over storage time at different wavenumbers. The data were fitted after 50 s (black vertical line) by a model indicating a J=0 equilibrium population of >90%.

References

[1] R. von Hahn *et. al.*, *The Cryogenic Storage Ring CSR* (submitted)
[2] A. P. O'Connor *et. al.*, *Photodissociation of an Internally Cold Beam of CH^+ Ions in a Cryogenic Storage Ring*, PRL. **116**, 113002 (2016)
[3] R. Otto *et. al.*, *Internal state thermometry of cold trapped molecular anions*, Phys. Chem. Chem. Phys. **15**, 612 (2013)

Diffraction of polar biomolecules at nanomechanical gratings

Christian Brand[1], Christian Knobloch[1], Benjamin Stickler[2], Lisa Wörner[1], Michele Sclafani[1,3], Thomas Juffmann[1,4], Yigal Lilach[5], Ori Cheshnovsky[5,6], Klaus Hornberger[2], and Markus Arndt[1]

1. University of Vienna, Faculty of Physics, VCQ, Boltzmanngasse 5, 1090 Vienna, Austria
2. University of Duisburg-Essen, Faculty of Physics, Duisburg, Germany
3. ICFO - Institut de Ciències Fotòniques, 08860 Castelldefels (Barcelona), Spain.
4. Physics Department, Stanford University, 382 Via Pueblo Mall, Stanford, California 94305-4060, USA.
5. The Center for Nanosciences and Nanotechnology at Tel Aviv University
6. Tel Aviv University, School of Chemistry, The Raymond and Beverly Faculty of Exact Sciences, Tel Aviv 69978, Israel

The high complexity of molecular matter-waves makes them very sensitive to external perturbations originating, for instance, from electric fields or single photons. These can be exploited to study internal properties of the molecules and differentiate between constitutional isomers [1,2]. However, in order not to bias the results it is crucial to characterize the interaction between the matter-wave and the beamsplitter very precisely. This is especially true for mechanical gratings.

Here, we study the diffraction of polar and non-polar molecules at nano-mechanical gratings. The velocity-dependent broadening of the individual diffraction orders is explained by phase averaging due to the interaction between a permanent dipole moment and charges in the grating. While this effect is moderate for a conducting membrane made of amorphous carbon, it leads to complete decoherence of the matter-wave diffracted at insulating silicon dioxide. The results explain the partial decoherence of the biomolecule hypericine in molecular far-field diffraction and set constraints to matter-wave experiments with molecules of biological interest.

References

[1] Sandra Eibenberger, Xiaxi Cheng, Joseph Cotter, and Markus Arndt, *Absolute Absorption Cross Sections from Photon Recoil in aMatter-Wave Interferometer*, Phys. Rev. Lett. **112**, 4145 (2014).

[2] Jens Tüxen, Stefan Gerlich, Sandra Eibenberger, Markus Arndt, and Marcel Mayor, *Quantum interference distinguishes between constitutional isomers*, Chem. Comm. **46**, 4145 (2010).

Fragmentation of Doubly Charged L-Alanine: A Comparison Among Theoretical Methods.

E. Rossich[1], D.G. Piekarski[2], Y. Wang[2,3], S. Díaz-Tendero[2,4], E. Tapavicza[5], F. Martín[2,3,4], M. Alcamí [2,3]

1. LAMBE UMR8587, Université d'Evry val d'Essonne, 91025 EVRY, France

2. Departamento de Química, Facultad de Ciencias M-13, Universidad Autónoma de Madrid,, 28049 Madrid, Spain.

3. IMDEA Nanociencia, Cantoblanco, 28049 Madrid, Spain

4. Condensed Matter Physics Center (IFIMAC), Universidad Autónoma de Madrid, 28049 Madrid, Spain

5 Department of Chemistry and Biochemistry, California State University, Long Beach, 1250 Bellflower Boulevard, CA 90840, USA

The study of fragmentation dynamics of charged biomolecules, and in particular amino acids, is of great interest to better understand the processes of biological damage by irradiations. Theoretical methods combining both a full exploration of the potential energy surface and ab initio Molecular Dynamics (MD) have been recently carried out [1-3] and are able to reproduce the observed fragmentation patterns and to get insight in the different competing mechanisms (coulomb explosion, isomerization, emission of neutral fragments...).

In this work we will present a comparison of different methodologies that can be used to describe the dynamical processes: from very expensive Time-Dependent Density Functional Theory (TD-DFT) calculations based in Ehrenfest dynamics, where electrons are extracted from specific inner orbitals[4], to ab initio MD in the ground state based in the Car-Parrinello method (CPMD)[5] or Atom Centred Density Matrix Propagation (ADMP)[6] as well as Self-Consistent Charge Density Functional Tight-Binding approach (SCC-DFTB)[7], we have also considered the role of different excited states using Non-Adiabatic Molecular Dynamics (NAMD)[8].

For this study we have chosen L-alanine as the simplest amino acid. Due to the small size of the system it is possible in the case of the computationally less expensive methods, as DFTB or ADMP, to run hundreds of trajectories lasting up to some hundreds of femtoseconds and consider different internal energies. From these calculations most of the channels observed in the experiments can be reproduced and a full simulation of the coincidence spectra can be obtained. We will also analyse the importance of the initial conformation of the amino acid and its spin state (singlet or triplet). These results will be compared with the ones obtained with more expensive methods such as CPMD. The role of specific orbital excitation will be analysed by comparing with the TD-DFT results.

References

[1] M. Capron, S. Díaz-Tendero, S. Maclot, A. Domaracka, E. Lattouf, A. Lawicki, R. Maisonny, J.Y. Chesnel, A. Méry, J.C. Poully, J. Rangama, L. Adoui, F. Martín, M. Alcamí, P. Rousseau and B. A. Huber Chem. Eur. J. **18** 9321 (2012)

[2] S. Maclot, D. G. Piekarski, A. Domaracka, A. Méry, V. Vizcaino, L. Adoui, F. Martín, M. Alcamí, B.A. Huber, P. Rousseau and S. Díaz-Tendero J. Phys. Chem. Lett., **4** 3903 (2013)

[3] D. T. Ha, Y. Wang, M. Alcamí, E. Itala, K. Kooser, S. Urpelainen, M. A. Huels, E. Kukk and F. Martín J. Phys. Chem. A **118**, 1374 (2014)

[4] I. Tavernelli, U.F. Röhrig and U. Rothlisberger Mol. Phys. **103**, 963 (2005)

[5] R. Car and M. Parrinello Phys. Rev. Lett. **55**, 2471 (1985)

[6] H. B. Schlegel, J. M. Millam, S. S. Iyengar, G. A. Voth, G. E. Scuseria, A. D. Daniels, and M. J. Frisch, J. Chem. Phys. **114**, 9758 (2001)

[7] B. Aradi, B. Hourahine, and Th. Frauenheim, J. Phys. Chem. A, 111, 5678 (2007)

[8] E. Tapacviza, G.D. Bellchambers, J.C. Vincent and F. Furche. Phys. Chem. Chem. Phys., **15**, 18336 (2013)

Unusual fragmentation mechanisms of excited doubly-positively charged amino acids in the gas phase

Sergio Díaz-Tendero[1,2], Dariusz G. Piekarski[1], Manuel Alcamí[1,3], Fernando Martín[1,2,3], Sylvain Maclot[4,5], Rudy Delaunay[4,5], Alicja Domaracka[5], Patrick Rousseau[4,5], Lamri Adoui[4,5], and Bernd A. Huber[5]

1. Departamento de Química, Módulo 13, Universidad Autónoma de Madrid, Cantoblanco 28049, Madrid, Spain

2. Condensed Matter Physics Center (IFIMAC), Universidad Autónoma de Madrid, Cantoblanco 28049, Madrid, Spain

3. Instituto Madrileño de Estudios Avanzados en Nanociencia (IMDEA-Nanociencia), Cantoblanco 28049, Madrid, Spain

4. Université de Caen Basse-Normandie, Esplanade de la Paix, CS 14032, 14032 Caen cedex 5, France

5. CIMAP (UMR 6252) - CEA,CNRS,ENSICAEN,Blvd. Henri Becquerel, BP 5133, 14070 Caen cedex 5, France

Hadron therapy is radiation therapy using strongly interacting particles [1]. A better depth dose profile of the energetic ion beam (Bragg peak) has proven its superiority over gamma radiation for killing cancer cells selectively [2]. With the advent of these ion-beam cancer treatments [3,4], the interaction of biomolecules with ionising particles (X- rays, electrons, ions) in the gas phase has become a fundamental technique to investigate the radiation damage of biological tissues at the molecular level [5-7]. In biological tissues the damages produced in the biomolecules are not only caused directly by the particle-matter collision but also by radicals and secondary particles created after the fragmentation of different chemical species along the ionisation path [8,9]. This underlines the importance of a proper description of the fragmentation mechanisms after electron removal. Thus, studying the behavior of the amino acids after interaction with highly charged ions gives valuable information for the hadron therapy treatment based on ion beams at a molecular level.

In this communication we present recent results on fragmentation of small lineal amino acids, doubly-positively charged in the gas phase, $NH_2{-}(CH_2)_n{-}COOH$: n=1 glycine [10]; n=2 b−alanine [11] and n=3 g−aminobutyric acid GABA [12,13]. Experimentally, we obtain the data in the gas phase for neutral molecules in collisions with low-energy highly charged ions. State-of-the-art multi-coincidence detection mass spectrometric techniques are used to determine the charge state of the molecule before fragmentation. The experimental data are analyzed by means of quantum chemistry calculations. In particular, *ab initio* molecular dynamics simulations of the excited and charged species provide valuable information on the fragmentation mechanisms; further exploration of the potential energy surfaces with the density functional theory calculations allows us to obtain energetic and structural information on the most populated dissociation channels.

Our results [10-13] have shown that in competition with the expected Coulomb explosion, the doubly positively charged lineal amino acids present several de-excitation mechanisms. In particular, hydrogen migration and hydroxyl group migration, together with ring formation, are mechanisms that appear in the femtosecond timescale, and lead to unusual fragmentation products.

References

[1] Petti and Lennox, Hadronic Radiotherapy, *Ann. Rev. Nuclear & Particle Science* **44,** 154 (1994)
[2] H. Kaur *et al. AIP Conf. Proc.* **205,** 1530 (2013).
[3] D. Schardt *et al. Rev. Mod. Phys.* **82,** 383 (2010).
[4] M. Durante and J.S. Loeffler *Nat. Rev. Clin. Oncol.* **7,** 37 (2010).
[5] P.Swiderek *Angew.Chem.Int.Ed.* **45,** 4056 (2006).
[6] B.Boudaïffa *et al*. *Science* **287,** 1658 (2000).
[7] M.H. Holzscheiter *et al*. *Radiother.Oncol.* **105** ,1 (2012).
[8] L. Sanche *Eur. Phys. J. D* **35**, 367 (2005).
[9] C. V. Parast *et al*. *Biochemistry* **34,** 2393 (1995).
[10] S. Maclot *et al*. *J.Phys.Chem.Lett.* **4,** 3903 (2013).
[11] D.G. Piekarski *et al. Phys.Chem.Chem.Phys.* **17,** 16767 (2015).
[12] M. Capron *et al*., *Chem. Eur. J.* **18** 9321 (2012)
[13] D.G. Piekarski *et al.* (in preparation).

Inelastic electron interaction with biomolecular clusters: pathways to radiation damage of DNA

Michael Neustetter,[1] Bea Haslwanter,[1] Julia Aysina [1], Filipe Ferreira da Silva[2], Stephan Denifl[1]

1. Institut für Ionenphysik und Angewandte Physik, Universität Innsbruck, Technikerstrasse 25, 6020-Innsbruck, Austria

2. Laboratório de Colisões Atómicas e Moleculares, CEFITEC, Departamento de Física, Faculdade de Ciências e Tecnologia, Universidade NOVA de Lisboa, 2829-516 Caparica, Portugal

In recent years there has been a significant interest in the understanding of damage processes of DNA, also induced by low energy electrons (LEEs). Ionizing radiation releases a large amount of secondary electrons in human cells. These electrons possess kinetic energies up to a few of tens of eV [1]. In this energy range electron ionization as well as electron attachment could cause chemical transformation in biological tissue. Investigations by Sanche and co-workers [1] indicated that these LEEs can induce single and double strand breaks in a film of plasmid DNA upon dissociative electron attachment (DEA). In the process of DEA an electron attaches resonantly to a molecule leading to the formation of a transient negative ion which then may decay into a stable anion and neutral(s) upon the fragmentation of the molecule. This dissociation can be fast and often has only spontaneous electron emission as competitive channel. A large number of studies on electron ionization and electron attachment to various simple biomolecules (e.g. DNA bases, sugars, amino acids) in the gas phase have been carried out [2]. Thereby, it turned out that single biomolecules in the gas phase often substantially decompose upon electron collisions. In addition, DEA is a site selective process, i.e. only certain bonds are cleaved in a molecule after capture of an electron with specific kinetic energy [3].

However, in order to understand radiation damage of complex matter it is highly important to understand how the fragmentation process of biomolecules is modified by a surrounding environment.
In the present study we used biomolecular clusters to observe electron induced reactions in DNA [4]. We chose biomolecules as pyrimidine ($C_4H_4N_2$), tetrahydrofuran (C_4H_8O) and triethylphosphate ($C_6H_{15}O_4P$) as model compounds of DNA building blocks. Clusters of these compounds were produced via supersonic expansion of the biomolecules into vacuum and crossed with a low energy electron beam. Adding water vapour to the expansion led to efficient formation of micro-hydrated biomolecules. Cations and anions formed were analysed by mass spectrometry. Our cluster studies with pyrimidine [4] confirmed a recent postulate [1] how a single LEE can induce a double strand break in DNA.

Acknowledgment: This work was partially supported by FWF(I1015,M1145).

References

[1] Elahe Alizadeh, Thomas M. Orlando, and Leon Sanche, Biomolecular Damage Induced by Ionizing Radiation: The Direct and Indirect Effects of Low-Energy Electrons on DNA, Annual Rev. of Phys. Chem. **66**, 379 (2015).
[2] Isabella Baccarelli, Ilko Bald, Franco A. Gianturco, Eugen Illenberger, Janina Kopyra, Electron-induced damage of DNA and its components: experiments and theoretical models, Phys. Rep. **508**, 1 (2011).
[3] Sylwia Ptasinska, Stephan Denifl, Verena Grill, Tilmann D. Märk, Eugen Illenberger, Paul Scheier, Bond- and Site-Selective Loss of H from Pyrimidine Bases, Phys. Rev. Lett. **24**, 093201 (2005).
[4] Michael Neustetter, Julia Aysina, Filipe Ferreira da Silva, Stephan Denifl, The Effect of Solvation on Electron Attachment to Pure and Hydrated Pyrimidine Clusters, Angew. Chem. Int Ed. **127**, 9252 (2015).

Electron-impact ionization of Xe^{24+} ions: Theory versus experiment

Pengfei Liu[1], **Jiaolong Zeng**[1,2], **Alexander Borovik, Jr.**[3,4], **Stefan Schippers**[4], **and Alfred Müller**[3]
1. Department of Physics, College of Science, National University of Defense Technology, Changsha Hunan 410073, PR China
2. IFSA Collaborative Innovation Center, Shanghai Jiao Tong University, Shanghai 200240, PR China
3. Institut für Atom- und Molekülphysik, Justus-Liebig Universität Gießen, 35392 Giessen, Germany
4. I. Physikalisches Institut, Justus-Liebig Universität Gießen, Giessen, 35392 Germany

Electron-impact ionization of ions is an important atomic collision process in many plasma environments. For many-electron systems, ionization results from a complicated pattern of ionization mechanisms involving electrons from many atomic subshells. Even today, this makes the task of its correct theoretical description and, therefore, adequate modeling of corresponding plasma environments challenging. Besides the widespread use in numerous applications xenon ions with their many-electron atomic structure are attractive objects of experimental and theoretical studies for detailed investigations of the roles of the various ionization mechanisms.

Previous studies on ionization of xenon ions revealed that the main mechanisms contributing to the single-ionization cross section are direct ionization (DI) and non-resonant excitation-autoionization (EA). For intermediate charge states, resonant processes such as resonant-excitation double autoionization (REDA) yield significant contributions, in addition. The relative importance of these processes was found to increase with increasing charge state up to 17+ [1,2]. Here, we report on experimental measurements and theoretical calculations of the cross section for electron-impact single-ionization of Xe^{24+} ions [3]. The measurements were performed using the crossed-beams method. For the cross-section calculations the fine-structure level-to-level distorted-wave approach was used as implemented in the Flexible Atomic Code (FAC). The calculations comprised DI, EA, as well as REDA processes. A special effort was made to assess the roles of resonant and non-resonant excitations to high n,ℓ subshells with the goal to include all relevant partial cross-section contributions. The total ionization cross section turned out to be dominated by the indirect ionization processes. Figure 1 shows the comparison of the experimental and the theoretical results in the energy range where significant contributions by REDA occur.

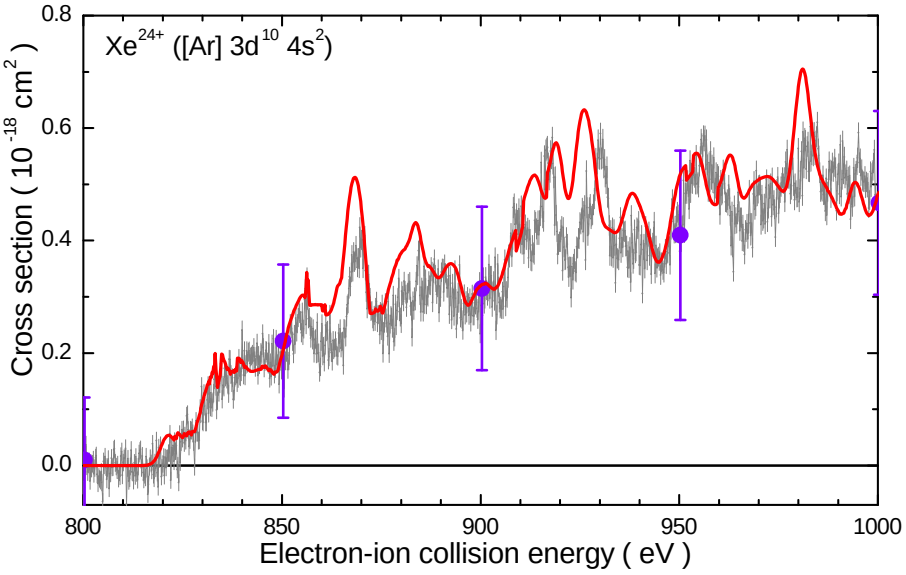

Fig. 1 Cross section for electron-impact ionization of Xe^{24+} ions in the energy range where REDA processes make significant contributions [3]. Symbols represent the experimental data. The solid (red) curve is the result of the theoretical calculation.

References

[1] M. S. Pindzola, S. D. Loch, A. Borovik Jr., M. F. Gharaibeh, J. K. Rudolph, S. Schippers, and A. Müller, *Electron-impact ionization of moderately charged xenon ions*, J. Phys. B **46**, 215202 (2013).
[2] A. Borovik Jr., M. F. Gharaibeh, S. Schippers, and A. Müller, *Plasma rate coefficients for electron-impact ionization of Xe^{q+} ions (q = 8, . . . , 17)*, J. Phys. B **48**, 035203 (2015).
[3] P. Liu, J. Zeng, A. Borovik, Jr., S. Schippers, and A. Müller, *Electron-impact ionization of Xe^{24+} ions: Theory versus experiment*, Phys. Rev. A, **92**, 012701 (2015).

Prospects for Electron-Ion Collision Studies at the Upcoming CRYRING@ESR Storage-Ring Facility

C. Brandau[1,2], S. Geyer[3], M. Lestinsky[2], A. Borovik, Jr.[1], B. Ebinger[1], O. Kester[2,3], C. Kozhuharov[2], O. Meusel[3], A. Müller[4], S. Schippers[1], and Th. Stöhlker[2,5,6]
for the SPRAC Working Group Electron Targets
1. I. Physikalisches Institut, Justus-Liebig-Universität Giessen, 35392 Giessen, Germany
2. GSI-Helmholtzzentrum für Schwerionenforschung, 64291 Darmstadt, Germany
3. Institut für Angewandte Physik, Goethe Universität, 60438 Frankfurt am Main, Germany
4. Institut für Atom- und Molekülphysik, Justus-Liebig-Universität Giessen, 35392 Giessen, Germany
5. Institut für Optik und Quantenelektronik, Friedrich-Schiller-Universität Jena, 07743 Jena, Germany
6. Helmholtz-Institut Jena, 07743 Jena, Germany

Within the scope of the FAIR project, i.e., the extension of the present accelerators at the GSI-Helmholtzzentrum für Schwerionenforschung in Darmstadt one of the first new installations will be the low-energy heavy-ion storage ring CRYRING@ESR. CRYRING was formerly located at the Manne-Siegbahn laboratory in Stockholm, and was recently transferred to Darmstadt [1]. The combination of the powerful accelerator chain at GSI/FAIR that can deliver highly charged heavy ions up to bare uranium as well as artificially synthesized radioisotopes with a dedicated low-energy cooler storage ring allows a long list of fascinating physics topics in the realms of nuclear physics, biophysics, material science and atomic physics to be addressed. In atomic physics, experiments at an internal gas-jet target, at a MOT target, with laser spectroscopy and ion-ion collisions are envisaged [1,2].

In addition, for collision studies between circulating ions and free electrons two main experimental sites that complement each other are envisaged at CRYRING@ESR: Firstly, the CRYRING electron cooler (Fig. 1) used as merged-beams electron target for precision collision spectroscopy utilizing the resonant process of dielectronic recombination [3,4]. The main advantage of the CRYRING electron cooler over the setup at the ESR is an electron beam that is substantially colder, in particular in the transverse direction. As a consequence, a boost in resolution, accuracy and sensitivity is expected [2,3,4]. Secondly, a dedicated electron target that operates in transverse collision geometry and that will be optimized with respect to photon and electron spectroscopy is presently being constructed [5,6,7]. In contrast to the cooler setup, a crossed-beams arrangement allows one to easily access the interaction region for spectroscopy. The transverse target thus opens new opportunities to study electron-impact phenomena such as excitation, ionization or recombination. Observations are not influenced by the presence of a target nucleus, as is the case for gas-jet targets. Processes like kinematic electron capture (”non-radiative capture”, NRC) or proton-impact excitation are absent by design.

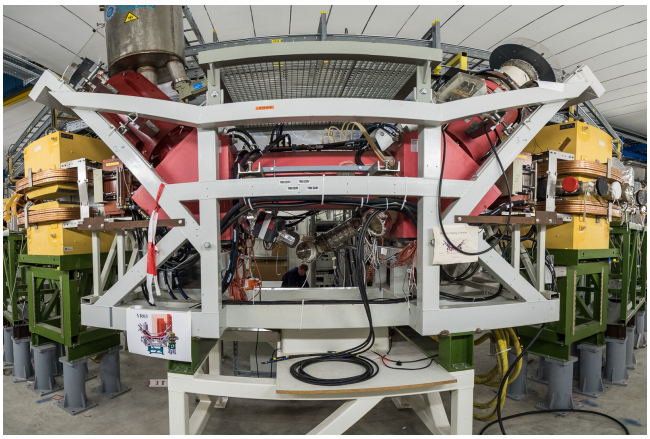

Fig. 1 Electron cooler at the CRYRING@ESR facility.

References

[1] M. Lestinsky, A. Bräuning-Demian et al., *CRYRING@ESR: present status and future research*, Phys. Scr. **T166**, 014075 (2015).
[2] M. Lestinsky et al., *Physics book: CRYRING@ESR*, in preparation.
[3] A Müller, *Electron–ion collisions: Fundamental processes in the focus of applied research* Adv. At. Mol. Opt. Phys. **55**, 293-417 (2008).
[4] C. Brandau, C. Kozhuharov, M. Lestinsky et al., *Storage-ring experiments on dielectronic recombination at the interface of atomic and nuclear physics*, Phys. Scr. **T166**, 014022 (2015).
[5] W. Shi, J. Jacobi, H. Knopp, et al., *A high-current electron gun for electron–ion collision physics*, Nucl. Instrum. Meth. B **205**, 201 (2003).
[6] S. Geyer, O. Meusel, and O. Kester, *A transverse electron target for the investigation of electron–ion interaction processes*, Phys. Scr. **T156**, 014093 (2013).
[7] A. Borovik Jr, W. Shi, J. Jacobi et al., *High-power electron gun for electron-ion crossed-beams experiments*, J. Phys.: Conf. Ser. **488**, 142007 (2014).

Multipole magnetic shielding constants of the ground state of the relativistic hydrogenlike atom: application of the Sturmian expansion of the generalized Dirac–Coulomb Green function

Grzegorz Łukasik, Radosław Szmytkowski

Atomic Physics Division, Department of Atomic, Molecular and Optical Physics, Faculty of Applied Physics and Mathematics, Gdańsk University of Technology, Narutowicza 11/12, 80-233 Gdańsk, Poland

The knowledge of the Dirac–Coulomb Green function is required for many physical problems. Among several well-known representations of that function, a particularly convenient one is that in the form of the Sturmian expansion, constructed in [1]. It has been already used to derive closed-form expressions for various electromagnetic properties of relativistic hydrogenlike atoms in electric or magnetic multipole fields (see, for instance, [2,3]).

Consider a relativistic hydrogenlike atom. Within the framework of the perturbation theory, one can calculate the magnetic field at the nucleus:

$$\boldsymbol{B} \simeq \boldsymbol{B}^{(0)} + \boldsymbol{B}^{(1)}, \tag{1}$$

where $\boldsymbol{B}^{(0)}$ is the magnetic field in the unperturbed atom, while

$$\boldsymbol{B}^{(1)} = -\sigma_L \boldsymbol{B}_L^{ext} \tag{2}$$

is the first-order approximation to the induced magnetic field, proportional to the perturbing external 2^L-pole magnetic field $\boldsymbol{B}_L^{ext}$. The factor σ_L is the multipole magnetic shielding constant.

Using the Sturmian expansion of the generalized Dirac–Coulomb Green function [1], we derive a closed-form expression for the multipole magnetic shielding constant of the ground state of the Dirac one-electron atom placed in a weak, static, 2^L-pole magnetic field. For $L = 1$ (the magnetic dipole field), we obtain

$$\sigma_1 = -\alpha^2 Z \frac{2(4\gamma_1^3 + 6\gamma_1^2 - 7\gamma_1 - 12)}{27\gamma_1(\gamma_1+1)(2\gamma_1-1)}, \tag{3}$$

while for $L \geqslant 2$ we find

$$\begin{aligned} \sigma_L \;=\; & -\alpha^2 Z \frac{2}{(2L+1)^2} \left[\frac{(L+1)(\gamma_L+\gamma_1)}{(L-1)(\gamma_L+\gamma_1-L)} {}_3F_2\left(\begin{matrix} -L,\, 1,\, \gamma_L-\gamma_1-L \\ \gamma_L-\gamma_1+1,\, \gamma_L+\gamma_1-L+1 \end{matrix} ;1 \right) \right. \\ & \left. - \frac{L(\gamma_{L+1}+\gamma_1)}{(L+2)(\gamma_{L+1}+\gamma_1-L)} {}_3F_2\left(\begin{matrix} -L,\, 1,\, \gamma_{L+1}-\gamma_1-L \\ \gamma_{L+1}-\gamma_1+1,\, \gamma_{L+1}+\gamma_1-L+1 \end{matrix} ;1 \right) \right], \end{aligned} \tag{4}$$

where $\gamma_\kappa = \sqrt{\kappa^2 - (\alpha Z)^2}$ (α is the Sommerfeld's fine structure constant) and ${}_3F_2$ is the generalized hypergeometric function. Equation (3) confirms previous results [4-6], while Eq. (4) is much simpler than its counterpart in [4]. It is worth to emphasize that the ${}_3F_2$ functions in Eq. (4) are truncating ones and consequently for each particular value of $L \geqslant 2$ the formula for σ_L may be expressed in terms of elementary functions.

References

[1] Radosław Szmytkowski, *The Dirac–Coulomb Sturmians and the series expansion of the Dirac–Coulomb Green function: application to the relativistic polarizability of the hydrogenlike atom*, J. Phys. B **30**, 825 (1997) [erratum: J. Phys. B **30**, 2747 (1997); addendum: arXiv:physics/9902050]

[2] Radosław Szmytkowski, Grzegorz Łukasik, *Static electric and magnetic multipole susceptibilities for Dirac one-electron atoms in the ground state*, At. Data Nucl. Data Tables, doi: 10.1016/j.adt.2016.02.002

[3] Radosław Szmytkowski, Grzegorz Łukasik, *Static electric multipole susceptibilities of the relativistic hydrogen-like atom in the ground state: Application of the Sturmian expansion of the generalized Dirac–Coulomb Green function*, arXiv:1602.00613

[4] Sergey A. Zapryagaev, Nikolai L. Manakov, Lev P. Rapoport, *Multipole screening of nuclei of hydrogenlike atoms*, Yad. Fiz. **19**, 1136 (1974) [English translation: Sov. J. Nucl. Phys. **19**, 582 (1974)]

[5] Vladimir G. Ivanov, Savely G. Karshenboim, Roman N. Lee, *Electron shielding of the nuclear magnetic moment in a hydrogen atom*, Phys. Rev. A **79**, 012512 (2009)

[6] Patrycja Stefańska, Radosław Szmytkowski, *Electric and magnetic dipole shielding constants for the ground state of the relativistic hydrogen-like atom: Application of the Sturmian expansion of the generalized Dirac–Coulomb Green function*, Int. J. Quantum Chem. **112**, 1363 (2012)

Multiple Electron Processes in Helium impacted by H^+, He^{2+} and Li^{3+} Ions

Pavel Nikolaevich Terekhin[1,2], Pablo Raúl Montenegro[1], Michele Arcangelo Quinto[1], Juan Manuel Monti[1], Omar Ariel Fojón[1], Roberto Daniel Rivarola[1]

1. Instituto de Física Rosario (CONICET-UNR), Bv 27 de Febrero, 2000 Rosario, Argentina

2. NRC Kurchatov Institute, Kurchatov Sq. 1, 123182 Moscow, Russia

Collisions of bare ion projectiles impacting on He atoms are the simplest systems for investigation of single and multiple electron transitions. The study of these collisional systems is crucial to fully understand the mechanisms underlying these basic reactions. Moreover, they are of interest in several fields such as heavy-ion therapy [1], thermonuclear fusion [2], hot plasmas [3], etc.

In this work, multiple electron processes (single and multiple ionization, single capture, transfer-ionization) of He targets impacted by H^+, He^{2+} and Li^{3+} projectiles are analyzed theoretically in detail at intermediate and high collision energies. Absolute cross sections for these processes are obtained by computation of transition probabilities as a function of the impact parameter in the framework of the Continuum Distorted Wave-Eikonal Initial State theory (CDW-EIS) [4]. A binomial analysis is employed to calculate exclusive probabilities using the independent electron (IEL) model, where static and dynamic correlations are neglected [5], as well as the independent event (IEV) model, in which the ionization is viewed as a two step process [6]. It is worthy to note that only exclusive probabilities are able to describe properly the measured cross sections taking into account all possible processes. Total single electron ionization cross sections as a function of the incident projectile energy for H^+ impacting on He targets are displayed in figure 1.

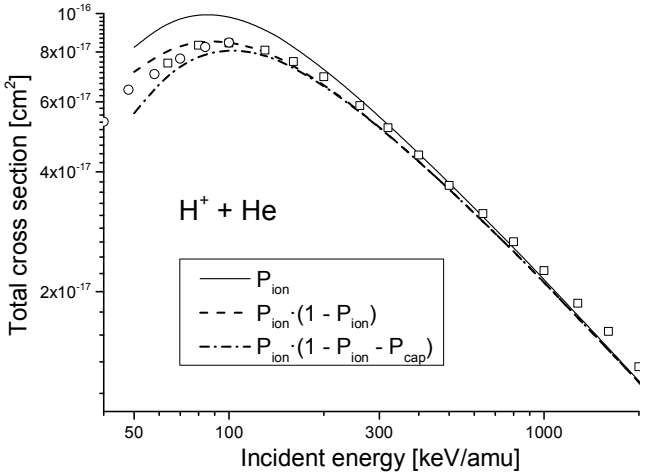

Fig. 1. Total single electron ionization cross sections as a function of the incident energy for H^+ impacting on He targets.

The comparison with the available theoretical and experimental results shows that exclusive probabilities are needed for a reliable description of the experimental data. The total cross sections within the IEV model and using exclusive probabilities are in better agreement with the experimental results than previous IEV calculations. The developed approach may be used to obtain the input database for modeling multiple electron processes of energetic charged particles passing through matter.

References

[1] Ugo Amaldi and Gerhard Kraft, *Radiotherapy with beams of carbon ions*, Rep. Prog. Phys. **68**, 1861 (2005).

[2] Simon S. Yu, B.G. Logan, J.J. Barnard, F.M. Bieniosek, R.J. Briggs, R.H. Cohen, J.E. Coleman, R.C. Davidson, A. Friedman, E.P. Gilson, L.R. Grisham, D.P. Grote, E. Henestroza, I.D. Kaganovich, M. Kireeff Covo, R.A. Kishek, J.W. Kwan, E.P. Lee, M.A. Leitner, S.M. Lund, A.W. Molvik, C.L. Olson, H. Qin, P.K. Roy, A. Sefkow, P.A. Seidl, E.A. Startsev, J.L. Vay, W.L. Waldron, D.R. Welch, *Heavy-ion-fusion-science: summary of US progress*, Nucl. Fusion **47**, 721 (2007).

[3] I. Murakami, J. Yan, H. Sato, M. Kimura, R. K. Janev, and T. Kato, *Excitation, ionization, and electron capture cross sections for collisions of Li^{3+} with ground state and excited hydrogen atoms*, At. Data Nucl. Data Tables **94**, 161 (2008).

[4] Pablo D. Fainstein, Victor H. Ponce and Roberto D. Rivarola, *Two-centre effects in ionization by ion impact*, Phys. B: At. Mol. Opt. Phys. **24**, 3091 (1991).

[5] J. Bradley, R. J. S Lee, M. McCartney and D. S. F. Crothers, *Multi-ionization of helium and lithium using the independent electron and independent event models with intrinsic CDW*, J. Phys. B: At. Mol. Opt. Phys. **37**, 3723 (2004).

[6] D. S. F. Crothers and R. McCarroll, *Correlated continuum distorted-wave resonant double electron capture in He^{2+} - He collisions*, J. Phys. B: At. Mol. Phys. **20**, 2835 (1987).

Studying plasmonic effects in diamondoid-metal hybrid systems with ion yield spectroscopy

Tobias Zimmermann[1], Andre Knecht[1], Andrea Merli[1], Vicente Zamudio-Bayer[2], Tobias Lau[2], Thomas Möller[1], Torbjörn Rander[1]

1. Institut für Optik und Atomare Physik, Technische Universität Berlin, Hardenbergstr. 36, 10623 Berlin, Germany

2. Institut Methoden und Instrumentierung der Forschung mit Synchrotronstrahlung, Helmholz- Zentrum Berlin, Albert-Einstein-Str. 15, 12489 Berlin, Germany

Plasmon resonance effects can enhance radiative emission rates in fluorophores in the vicinity of metal surfaces. Applications such as surface enhanced Raman spectrosopy make use of this effect [1]. The combination of metallic nanoparticles with molecules enables tailoring of hybrid systems with optical properties optimized for such purposes.

Diamondoids are UV luminescent sp3 hybridized carbon nanostructures that are perfectly size- and shape-selectable in their neutral form [2,3]. Due to their sizes and structures being well defined, diamondoids enable direct comparison of experimental investigations with theoretical calculations. The optical properties of small metal clusters in a size regime where every atom counts largely depend on electronic and geometric shell closures. As a result, characteristics like absorption onset and electronic resonances can strongly vary between sizes. The combination of both diamondoids and small metal clusters gives the opportunity to study resonance effects in small hybrid systems. By this means, fundamental aspects like the influence of the matching between plasmon resonances of the metal particles with electronic transitions of a luminescent molecule can be analyzed.

We synthesized hybrid systems of diamondoids and metal clusters and studied their absorption in a linear trap, using ion yield spectroscopy. With this technique, the absorption of both the hybrid cluster and the isolated constituents can be compared. First results will be presented.

References

[1] M. Moskovits, *Surface-enhanced spectroscopy*, Rev. Mod. Phys. **57**, 783 (1985).

[2] J. E. Dahl, S. G. Liu, R. M. K. Carlson, *Isolation and Structure of Higher Diamondoids, Nanometer-Sized Diamond Molecules*, Science **299**, 96 (2003).

[3] R. Richter, M. I. S. Röhr, T. Zimmermann *et al.*, *Laser-induced fluorescence of free diamondoid molecules*, Phys. Chem. Chem. Phys. **17**, 4739 (2015).

Interatomic Coulombic decay in small helium clusters: a diatomics-in-molecule approach

Sévan Kazandjian, Tsveta Miteva, Nicolas Sisourat.
Sorbonne Universités, UPMC Univ Paris 06, CNRS, Laboratoire de Chimie Physique Matière et Rayonnement, F-75005, Paris, France

Interatomic Coulombic decay (ICD) is an ultrafast non-radiative electronic decay process which can occur in many polyatomics systems (such as rare gas clusters [1] or hydrogen bonded clusters [2,3]). In the case of helium clusters, one atom is both excited and ionized and its excess energy is transferred to a neighboring atom, ionizing it, as shown on **Fig. 1**. After the decay, the cluster contains two He^+ ions, and dissociates due to Coulombic repulsion. This process was predicted in 1997 by Cederbaum *et al* [4], and experimentally demonstrated in 2003 for neon clusters, by Marburger *et al* [5] and Jahnke *et al* [6].

Our work focuses on ICD in small helium clusters which are peculiar quantum systems: owing to the weak interactions between the atoms and their low mass these systems exhibit remarkable interatomic distance distributions. For example, the pair distribution function of the helium trimer spreads up to 15 Å and the mean interatomic distance is predicted to be around 9.6 Å. Small helium clusters thus allow to gain insight into the ICD process over a considerable range of distances and geometries.

We have developed a diatomics-in-molecules approach for the description of ICD in rare-gas clusters [7-10]. Combined with a surface-hopping algorithm specifically designed for ICD, this method is used to compute the nuclear dynamics (before and after the decay) and the decay rates (inverse of the lifetime of the excited state). The latter depend strongly on the distance between the atoms and consequently on the geometry of the cluster. We will illustrate the method on the example of the helium trimer [11]. Additionally, the kinetic energy distribution of the ionic fragments and the lifetime of the excited helium ion within the cluster will be presented for clusters containing up to ten atoms.

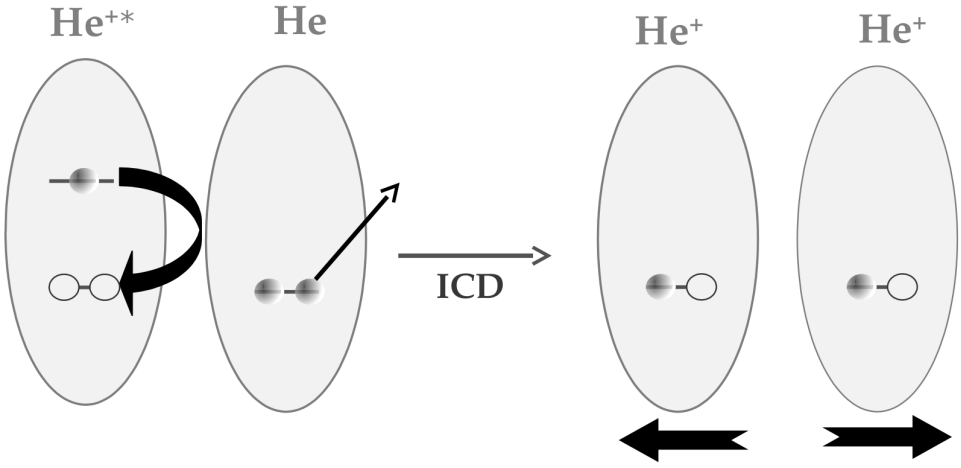

Fig. 1 ICD in helium dimer. After simultaneous ionization and excitation of one helium atom, this excited ion relaxes and transfers its excess energy to a neighboring helium atom, ionizing it. Due to Coulombic repulsion, the system fragments.

References

[1] V. Averbukh et al. *Dynamical Processes in Atomic and Molecular Physics* **29**, Bentham Science Publishers (2012).
[2] M. Mucke et al. *A hitherto unrecognized source of low-energy electrons in water*, Nature Physics,**6**, 143 (2010).
[3] T. Jahnke et al. *Ultralong-range energy transfer by interatomic Coulombic decay in an extreme quantum system*, Nature Physics, **6**, 139 (2010).
[4] L. S. Cederbaum et al, *Giant Intermolecular Decay and Fragmentation of Clusters*, Phys. Rev. Lett. **79**, 4778 (1997).
[5] S. Marburger et al, *Experimental Evidence of Interatomic Coulombic Decay in Ne Clusters*, Phys. Rev. Lett. **90**, 203401 (2003).
[6] T. Jahnke et al. *Experimental Observation of Interatomic Coulombic Decay in Neon Dimers*, Phys. Rev. Lett. **93**, 163401 (2004).
[7] F.O. Ellison, J. Am. Chem. Soc. *A Method of Diatomics in Molecules. I. General Theory and Application to H_2O*, **85**, 3540 (1963).
[8] P.J. Kuntz and J. Valldorf, *A DIM model for homogeneous noble gas ionic clusters*, Z. Phys. D - Atoms, Molecules and Clusters **8**, 185 (1988).
[9] R.B. Gerber, D. Shemesh, M.E. Varner, J. Kalinowski and B. Hirshberg, *Ab initio and semi-empirical Molecular Dynamics simulations of chemical reactions in isolated molecules and in clusters* , Phys. Chem. Chem. Phys. **16**, 9760 (2014) (and references therein).
[10] D. Bonhommeau, A. Viel and N. Halberstadt, *Fragmentation dynamics of ionized neon trimer inside heliu m nanodroplets: A theoretical study*, J. Chem. Phys. **120**, 11359 (2004).
[11] N. Sisourat, S. Kazandjian, A. Randimbiarisolo and P. Kolorenč, *Interatomic Coulombic decay widths of helium trimer: A diatomics-in-molecules approach*, J. Chem. Phys, **144**, 084111 (2016)

The Impact of the Guest-Water Interaction on the Cage Occupation and Spectra of the sI CO_2 Clathrate Hydrates

Rita Prosmiti[1], **Álvaro Valdés**[2], **Daniel J. Arismendi-Arrieta**[1]
1. Institute of Fundamental Physics (IFF-CSIC), CSIC, Serrano 123, 28006 Madrid, Spain
2. Departamento de Física, Universiadad Nacional de Colombia, Calle 26, Cra 39, Edif. 404, Bogotá, Colombia

The interest in CO_2 hydrate is driven in part by the possibility of trapping and storage of this greenhouse gas from the atmosphere and control climate change, as well as due to its interest in astrophysics. Thus, quantitative understanding of physical and chemical properties, on both macroscopic and microscopic levels, is essential in several areas of physical science. The confinement of a molecule into a cage leads to the quantization of the translational (T) degrees of freedom of its center of mass, and well as to its rotational (R) and vibrational (V) states. This allows the investigation of the dynamics of the guest molecule, and the effect of the size, shape, and composition of the host cavity, as well as the occupancy and identity of the trapped molecule/s. The occupancy of the sI and sH CO_2 clathrate hydrates has been studied experimentally by X-ray, powder X-ray, and neutron diffraction methods [1], while spectroscopic characterization of the sI and sII CO_2 clathrate hydrates has been reported via Raman, solid-state NMR, and the infrared (IR) spectroscopy [2].

These experimental studies motivated us to develop quantum methodology for rigorous calculations of T-R-V energies of a nanoconfined CO_2 molecule inside the polyhedral cavities of simple clathrate hydrates [3] within the multi configuration time-dependent Hartree (MCTDH) framework [4]. We employed semiempirical and *ab initio*-based potential surfaces evaluating their quality by direct comparison with the available experimental data. It was found that the rotational ability of the CO_2 is hindered in the small cavities (5^{12}), while in the large cage ($5^{12}6^2$) translational and rotational degrees of freedom are highly coupled. By analyzing the corresponding T-R eigenstates, we established a connection with experimental X-ray measurements on the orientation of the CO_2 molecule in each cage [1]. Further, vibrational excitations of the fundamental symmetric (ν_1) and antisymmetric (ν_3) stretch modes, their overtones, and combination bands are computed from 7D quantum calculations. We found significant frequency shifts, which are comparable to those observed in the double-peak profile of the experimentally recorded infrared spectra, for the $^{12}CO_2$, $^{13}CO_2$, and ^{18}OCO isotopes trapped in the small and large cages of the sI clathrate hydrate (see Fig. 1). The agreement with the measurements from recent spectroscopic studies of carbon dioxide clathrate hydrate at low temperatures supports a CO_2 single occupation of the sI structure cages, allowing an assessment of the theoretical approaches employed. As the results obtained from a quantum mechanical treatment, the differences can be understood in terms of the nature of the interactions, and the insights gained are applicable in other clathrate hydrates or inclusion compounds.

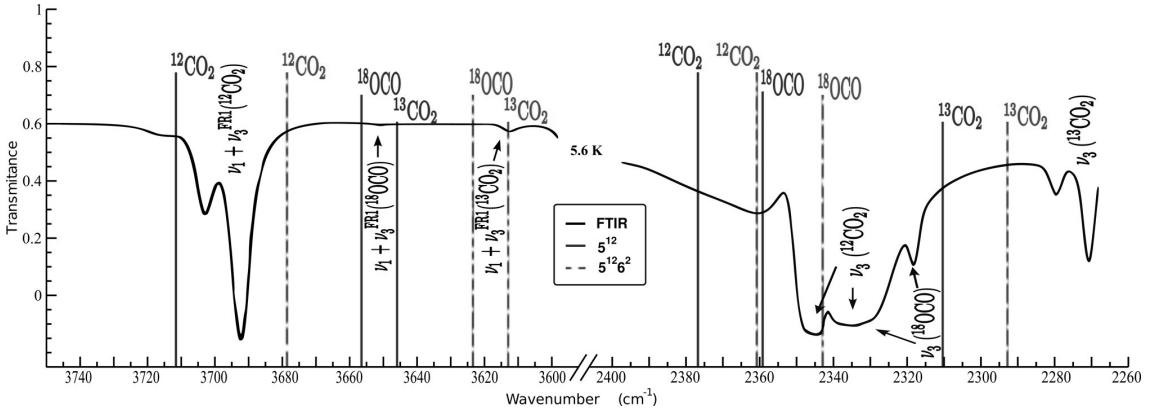

Fig. 1 Comparison between the FTIR spectra [2] for the sI CO_2 clathrate hydrate with the corresponding energy levels from the 7D MCTDH calculations [3] (see vertical sticks) for the indicated CO_2 isotope in the small (5^{12}) and large ($5^{12}6^2$) cages.

References

[1] S. Takeya, K.A. Udachin, I. Moudrakovski, R. Susilo, and J.A. Ripmeester, *Direct Space Methods for Powder X-ray Diffraction for Guest-Host Materials: Applications to Cage Occupancies and Guest Distributions in Clathrate Hydrates*, J. Am. Chem. Soc. **132**, 524 (2010).
[2] E. Dartois and B. Schmitt, *Carbon Dioxide Clathrate Hydrate FTIR Spectrum: Near Infrared Combination Modes for Astrophysical Remote Detection*, A&A **504**, 869 (2009).
[3] Á. Valdés, D.J. Arismendi-Arrieta, and R. Prosmiti, *Quantum Dynamics of Carbon Dioxide Encapsulated in the Cages of the sI Clathrate Hydrate: Structural Guest Distributions and Cage Occupation*, J. Phys. Chem. C **119**, 3945 (2015).
[4] H.-D. Meyer, *The MCTDH Package, version 8.4*, (2007) http://mctdh.uni-hd.de.

Production of polyanionic lead and tin clusters and study of their electron emission, dissociation and fission upon photoexcitation

Stephan König, Paul Fischer, Gerrit Marx, Lutz Schweikhard, Markus Wolfram, Albert Vass

Institut für Physik, Ernst-Moritz-Arndt Universität Greifswald, Felix-Hausdorff-Str. 6, 17489 Greifswald, Germany

During the last couple of years the Penning-trap setup ClusterTrap [1,2] has been further extended for studies of the production and properties of poly-anionic metal clusters [3,4], focusing mainly on the elements aluminum and gold [5, 6]. Recent experiments reached out to further elements including lead and tin.

Mono-anionic clusters were produced in a laser vaporization source and were transferred and captured in a 12-Tesla Penning trap. As previously for other elements, the clusters were size selected and exposed to an "electron bath": By shooting primary electrons axially through the trap, argon buffer-gas atoms are ionized. The argon cations immediately leave the trap while the secondary electrons stay stored and can attach to the clusters, thus forming polyanions – provided they overcome the repulsing Coulomb barrier [3]. The reaction products are analyzed by ejection from the Penning trap and time-of-flight mass spectrometry.

The measurements as a function of cluster size yield the appearance sizes for doubly and triply charged anionic clusters. In addition, and unlike the clusters of other metals, the small lead and tin clusters show distinct dissociation patterns, with very prominent peaks at specific cluster sizes, e.g. the (monoanionic) decamer and the clusters with ten atoms less than the precursors.

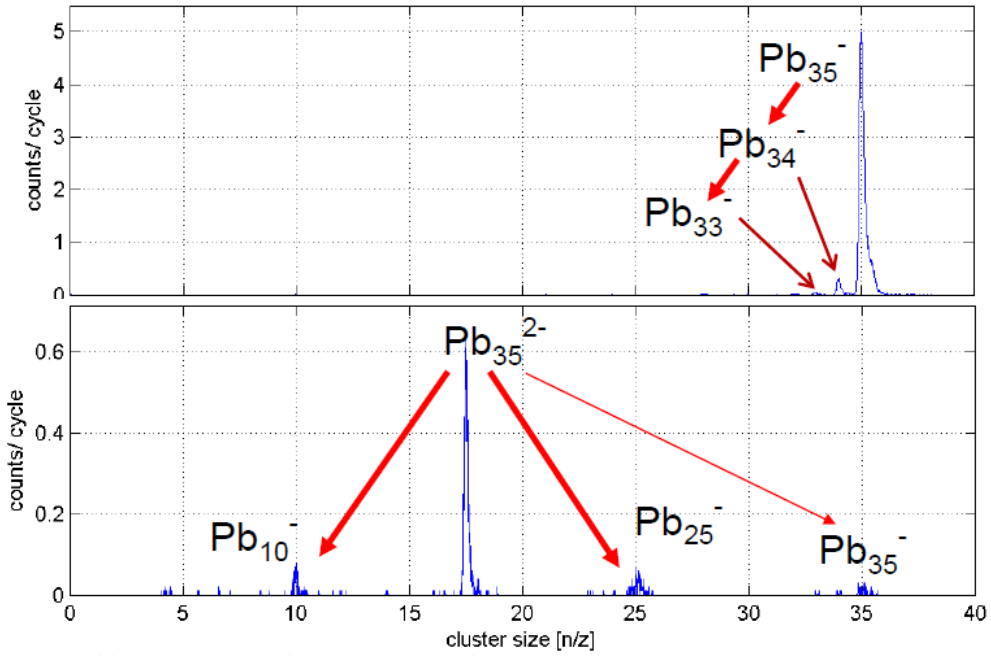

Fig. 1. Time-of-flight mass spectra after photoexcitation of mass selected mono- (top) and dianionic lead clusters (bottom).

These clusters are also dominant in photodissociation spectra of small dianions, e.g. Pb_{35} (Fig. 1 bottom) where the monoanion decays by evaporation of neutral monomers (Fig. 1, top). Apparently, there is a third decay pathway of polyanionic lead and tin clusters, in addition of electron emission and neutral atom evaporation: Fission into two (charged) smaller clusters. The experiments are still ongoing and will be extended with respect to further charge states, including cationic species.

References

[1] F. Martinez, G. Marx, L. Schweikhard, A. Vass, F. Ziegler, *The new ClusterTrap setup*, Eur. Phys. J. D **63**, 255 (2011).
[2] F. Martinez, S. Bandelow, C. Breitenfeldt, G. Marx, L. Schweikhard, A. Vass, F. Wienholtz, *Upgrades at ClusterTrap and Latest Results*, Int. J. Mass Spectrom. **365-366**, 266 (2014).
[3] A. Herlert, S. Krückeberg, L. Schweikhard, M. Vogel, C. Walther, *First Observation of Doubly Charged Negative Gold Cluster Ions*, Physica Scripta **T80**, 200 (1999).
[4] C. Yannouleas, U. Landman, A. Herlert, L. Schweikhard, *Multiply Charged Metal Cluster Anions*, Phys. Rev. Lett. **86**, 2996 (2001).
[5] F. Martinez, S. Bandelow, G. Marx, L. Schweikhard, *Production of multiply-charged metal-cluster anions in Penning and radio-frequency traps*, AIP Conf. Proc. **1521**, 230 (2013).
[6] F. Martinez, S. Bandelow, G. Marx, L. Schweikhard, A. Vass, *Abundances of Tetra-, Penta- and Hexa-Anionic Gold Clusters*, J. Phys. Chem. C **119**, 10949 (2015).

Confinement-Induced Off-Center Displacement in Endohedral Fullerenes within the Zero-Range Potential and the Dirac "Bubble" Models

Galina Schrange

St. Petersburg Polytechnical University, Russia; e-mail: gkashenock@yahoo.de

The object is "endohedron": a fullerene with an atom (confined atom) trapped inside the carbon spatial hollow cage. Some experiments and calculations have demonstrated that the geometry of an endohedral system with an atom guest positioned at the center is not energetically preferable. The physical mechanisms leading to the off-center displacement of an endohedral atom are still under discussion. In the work [1] it has been shown that the equilibrium position of an atom in a impenetrable spherical cavity, which was mimicked by a Zero-Range Potential (ZRP), is off-center positioned as soon as the attractive interaction of an active electron with an atom core occurs to be strong enough. In the present study a more realistic description of the carbon fullerene shell are used - the Dirac "bubble" potential ($V_{conf}(r) = -\frac{\beta}{R}\,\delta(r-R)$; β is the strength parameter, R is the fullerene radius, and the ZRP approximation for the interaction of an active electron with an endohedral atomic core is kept. The question is: does the tendency to take the off-center equilibrium position under the some strength parameters conditions survive?

Mathematically the ZRP model casts the boundary condition on the electron Green's function [2] at the point $\vec{r}_0$ where the interaction potential is located: $\left[2\pi G(\vec{r},\vec{r}_0;k) - \frac{1}{|\vec{r}-\vec{r}_0|}\right]_{\vec{r}\to\vec{r}_0} = -\alpha$. The parameter α characterizes the interaction strength. This is the transcendental equation that defines spectral parameter k, i.e. the active electron state energy $E = \frac{1}{2}k^2$. The latter is a function of the system parameters: $E(r_0, R, \alpha, \beta)$. Note, the energy E might be positive (for real k) or negative (for imaginary k).

In the present work the Green's function of an active electron is constructed for the model, and it is obtained that the transcendental equation in terms of spherical Bessel functions of the first and third kinds - $j_l(z), h_l^{(1)}(z)$ - takes form:

$$\sum_{l=0}^{\infty}\left[ik\,j_l(kr_0)h_l^{(1)}(kr_0) + \beta R\,\frac{2(ik)^2 j_l^2(kr_0)\,{h_l^{(1)}}^2(kR)}{1-2ik\beta R\,j_l(kR)h_l^{(1)}(kR)} - \frac{1}{2l+1}\,\frac{1}{r_0}\right] = -\alpha\ .$$

This provides a required potential curve $E_{\rm ad}(r_0)$, the effective potential in which an endohedral nucleus moves in the spirit of the Born-Oppenheimer, or, more exactly, the adiabatic approximation. It is shown (fig.1) that the potential curves for imaginary k have a minima at at the $r_0 > 0$ for some parameters α, β. The equilibrium position of an endohedral nucleus is shifted from the geometrical centre of a fullerene (*off-center displacement*). Since the both models accepted here (ZRP and Dirac "bubble") dictate only the exact boundary conditions (for construction of a spherical cage geometry) and two strength parameters (α and β, for characterization of the interaction forces) they grasp the only main features of the system. When the off-center displacement occurs, we can speak about "spontaneuos breaking of symmetry" in the sense that it has been introduced in [1]. The effect is induced directly by the confinement existence and by its existence itself.

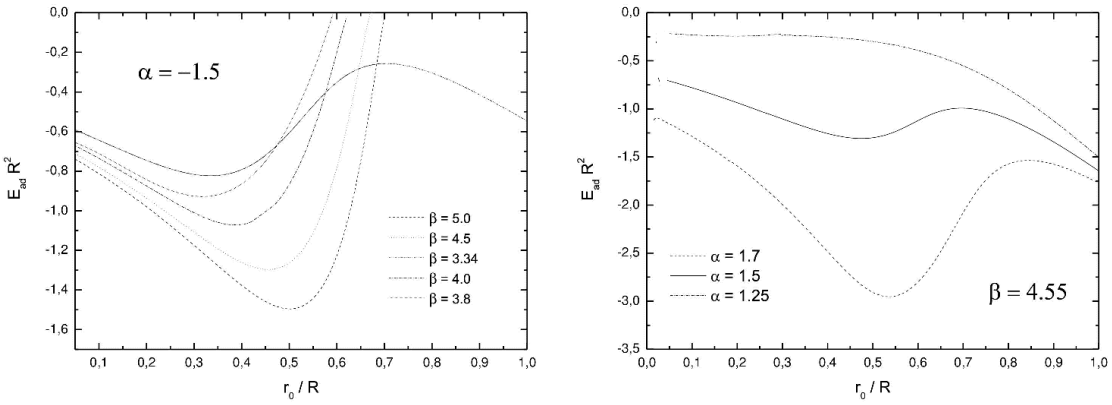

Fig. 1 Adiabatical potential curves as function of strength parameters.

References

[1] V. N. Ostrovsky, *An atom in a impenetrable spherical cavity within the ZRP approach*, J.Phys.B **39**, L367 (2006).
[2] Yu. N. Demkov and V. N. Ostrovsky, *Zero-Range Potentials and Their Application in Atomic Physics.* NY: Plenum Press (1998).

Coincidence spectroscopy of water and water-ammonia clusters upon soft X-ray absorption.

Bart Oostenrijk[1], Noelle Walsh[2], Anna Sankari[1], Shabnam Oghbaie[1], Erik P. Månsson[3], Stacey Sorensen[1], Mathieu Gisselbrecht[1]

[1]*Department of Physics, Lund University, 221 00 Lund, Sweden,* [2]*MAX IV Laboratory, Fotongatan 2, 225 94 Lund, Sweden,* [3]*Institute of photonics and nanotechnology-CNR, Polytechnical University of Milan, Milan, Italy*

Molecular clusters are known to exist and nucleate in the atmosphere [1-3], where small water clusters contribute to light absorption [4]. Molecules such as NH_3, H_2SO_4 and organic molecules form small mixed clusters with water, and these act as condensation centers in the upper atmosphere [5]. We study hydrogen-bonded clusters as a prototype for chemical processes in the atmosphere. In the literature these clusters are mainly reported to exist in protonated form as cations [6], whose origin is likely the result of fast proton transfer following ionization, before fragmentation has time to occur [7]. Previous experimental work reported the observation of protonated mixed ammonia/water clusters ((NH3)m(H2O)nH+) in three distinct $(m, compositions)$ n, and a shell structure was proposed for these binary clusters [8].

In this work, we investigate the fragmentation of singly and multiply charged clusters of pure water or water-ammonia prepared by soft X-ray ionization. The experiments were performed at the I411 beamline, at the MAX-lab synchrotron facility in Lund, Sweden. The cluster beam was produced via adiabiatic expansion, which allows us to tailor both the cluster composition and size distribution. The cluster beam intersected the photon beam in the interaction region of a 3D ion momentum imaging spectrometer [9]. Charged photofragments were measured over a 4π solid angle, and the (coincident) mass spectra analyzed after core-electron ionization at the nitrogen and oxygen 1s absorption edges.

The experimental results indicate that the fragment (m,n) composition depends on the expansion conditions of the cluster source. Under certain conditions, this fragment composition differs from that in the previous work using a corona discharge source [8]. A higher photon energy leads to an increase of internal energy within the cluster, thus opening more fragmentation channels and decreasing the average fragment size. The photon energy can be tuned close to either the Nitrogen or Oxygen ionization edges, creating an element-selective localized hole state that rapidly evolves to multiple ionization via electronic relaxation. We study the charge separation processes after core ionization by looking at the Coulomb explosion of small mixed clusters. The cluster size dictates the maximum possible distance between two charges. At a critical dication size, the inter-molecular binding force exceeds the repulsive Coulomb interaction. This critical size has been reported for pure water clusters [10] and pure ammonia clusters [11], but not for mixed clusters. We compare the experimentally observed critical size of the mixed cluster with both values.

References

[1] Arnold, et al., *Growth of atmospheric cluster ions at the cold mesopause*, Geoph. Res. Lett., **6**, 763 (1979).
[2] Arijs, E., et al., *Negative ion composition measurements in the stratosphere*, Geoph. Res. Lett., **8**, 121 (1981).
[3] Kulmala M., *How Particles Nucleate and Grow*, Science, **302**, 302 (2003)
[4] P. Chýlek and D. J. W. Geldart, *Water vapor dimers and atmospheric absorption of electromagnetic radiation* Geophys. Res. Lett., **24** 2015 (1997).
[5] M. Kulmala et al. Science 318, *Toward Direct Measurement of Atmospheric Nucleation* 89 (2007).
[6] Belau et al., *Vacuum Ultraviolet (VUV) Photoionization of Small Water Clusters*, J. Phys. Chem. A, **111**, 10075 (2007).
[7] Hiroto Tachikawa, *Ionization Dynamics of the Small Sized Water Clusters: A Direct Ab Initio Trajectory Study*, J. Phys. Chem. A, **108**, 7853, (2004).
[8] Hvelplund et al., *Stability and Structure of Protonated Clusters of Ammonia and Water,* $H^+(NH3)_m\ (H2O)_n$, J. Phys. Chem. A, **114**, 7301, (2010).
[9] J. Laksman et al., *Development and characterization of a multiple-coincidence ion-momentum imaging spectrometer*, Rev. Sci. Inst., **84**, 123113 (2013).
[10] Stace, A. J., *Evidence of Two Stable Forms of Doubly and Triply Charged Water Cluster*, Phys. Rev. Lett., **61**, 306 (1988).
[11] A.K. Shukla, C. Moore and A.J. Stace, *Doubly charged ion clusters*, Chem. Phys. Lett., **109**, 324 (1984).

Modelling ion/atom impact on complex molecules and their clusters: prompt atom knockouts and molecular growth processes

Giovanna D'Angelo[1], Michael Gatchell[1], Henrik Cederquist[1], and Henning Zettergren[1]

1. Department of Physics, Stockholm University, AlbaNova University Center, S-10691 Stockholm, Sweden

Recent combined experimental and theoretical studies have demonstrated that prompt atom knockout is important in Rutherford-like scattering processes when PAHs, fullerenes, or their clusters are exposed to energetic ions/atoms [1,2,3]. Such processes yield highly reactive fragments, which can efficiently form new covalent bonds with other molecules, e.g. in a cluster environment [4,5]. This type of energetic processing of molecular systems by atoms or ions can be of importance for our understanding of e.g. the origin and evolution of molecules in space [6].

Here we will present an overview on how we model such impulse driven reactions in isolated molecules and their clusters [6]. As part of this we will show recent results for keV-ion impact on butadiene clusters and low energy collisions between porphyrin ions and noble gas atoms.

We have performed classical Molecular Dynamics simuations with the LAMMPS software to model entire collision sequences, i.e. the initial knockout event and the subsequent fragmentation or molecular growth processes inside molecules and molecular clusters. Results for isolated coronene are showed in Fig. 1, where the color and size of each point represents the angular dependent threshold displacement energy calculated with the Tersoff potential [7] for the four unique atom positions in coronene [8]. We are currently performing such calculations for porphyrin ions, which will be presented at the conference.

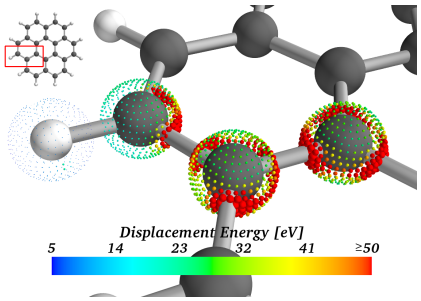

Fig. 1 Displacement energies for three unique carbon-, and one unique hydrogen-, positions in coronene as calculated with the Tersoff potential [7].

References

[1] M H Stockett, H Zettergren, L Adoui, J D Alexander, U Bērziņš, T Chen, M Gatchell, N Haag, B A Huber, P Hvelplund, A Johansson, H A B Johansson, K Kulyk, S Rosén, P Rousseau, K Støchkel, H T Schmidt and H Cederquist, *Nonstatistical fragmentation of large molecules*, Phys. Rev. A **89**, 032701 (2014)

[2] M Gatchell, M H Stockett, P Rousseau, T Chen, K Kulyk, H Schmidt, J Y Chesnel, A Domaracka, A Méry, S Maclot, L Adoui, K Stöchkel, P Hvelplund, Y Wang, M Alcamí, B A Huber, F Martín, H Zettergren and H Cederquist, *Non-statistical fragmentation of PAHs and fullerenes in collisions with atoms*, Int. J. Mass Spectrom. **365**, 260 (2014).

[3] M H Stockett, M Gatchell, T Chen, N de Ruette, L Giacomozzi, M Wolf, H T Schmidt, H Zettergren and H Cederquist, *Threshold* Energies for Single-Carbon Knockout from Polycyclic Aromatic Hydrocarbons, J. Phys. Chem. Lett. **6**, 4504 (2015)

[4] R Delaunay, M Gatchell, P Rousseau, A Domaracka, S Maclot, Y Wang, M H Stockett, T Chen, L Adoui, M Alcamí, F Martín, H Zettergren, H Cederquist, and B A. Huber Delaunay, *Molecular Growth Inside of Polycyclic Aromatic Hydrocarbon Clusters Induced by Ion Collisions*, J. Phys. Chem Lett **6**, 1536 (2015)

[5] H Zettergren, P Rousseau, Y Wang, F Seitz, T Chen, M Gatchell, J D Alexander, M H Stockett, J Rangama, J Y Chesnel, M Capron, J C Poully, A Domaracka, A Méry, S Maclot, H T Schmidt, L Adoui, M Alcamí, A G G M Tielens, F Martín, B A Huber and H Cederquist, *Formations of Dumbbell C118 and C119 inside Clusters of C60 Molecules by Collision with a Particles*, Phys. Rev. Lett. **110**, 185501 (2013)

[6] A G G M Tielens, *The Molecular Universe*, Rev. Mod. Phys. **85**, 1021–1081 (2013)

[7] J Tersoff, *New empirical approach for the structure and energy of covalent systems*, Physical Review B **39(8)**, 5566– 5568 (1989)

[8] M Gatchell, H Zettergren, *Knockout driven reactions in complex molecules and their clusters*, J. Phys. B: At. Mol. Opt. Phys. (2016)

Theoretical Study of the $5p^5nln'l'n''l''$ *LSJ* Autoionizing States of Ba

Gintaras Kerevičius[1], Alicija Kupliauskienė[1], Alexander Borovik[2,3]

1. *Institute of Theoretical Physics and Astronomy, Vilnius University, Saulėtekio Ave. 3, 10222 Vinius, Lithuania*
2. *Department of Electron Processes, Institute of Electron Physics, Universitetska 21, 88017 Uzhgorod, Ukraine*
3. *Faculty of Physics, Uzhgorod National University, Voloshina 54, 88000 Uzhgorod, Ukraine*

The calculations of excitation energies, electron impact excitation cross sections, autoionization probabilities and Auger decay yields of $5p^5nln'l'n''l''$ *LSJ* autoionizing states of Ba atoms are performed for the first time by using large scale configuration interaction (CI) approach. For the basis of radial orbitals in CI, the numerical solutions of Dirac-Fock-Slater equations were used [1]. In order to optimize the local central potential including the approximated exchange part, singly excited configurations $5p^6 6snl$ (nl = 4f, 5d, 6p, 6d, 7s – d) were used. The following singly excited $5p^6 6snl$ (nl = 4f, 5d – g, 6p – g, 7f, 7g and n = 7 – 10, l = 0 – 2) and 5p-core excited $5p^5nln'l'n''l''$ (nl = 5d, 6s; $n'l'$ = 4f, 5d, 6s – d, 7s – d) states were used to take into account the correlation effects. The total number of both even and odd states included into calculation was 10199. The same basis set was used to calculate excitation cross sections. For the calculation of autoionization probabilities, it was supplemented with $5p^6nl$ (nl = 5d, 6s – d, 7s, 7p) configurations of Ba^+ to include the most important Auger decay channels. In the case of autoionizing states with excitation energy greater than 21.04 eV, the $5p^55d^2$ and $5p^55d6s$ configurations of Ba^+ were also added to include additional energetically allowed decay channels.

For comparison of present data with other spectroscopic data, a transformation of the expansion coefficients of wave functions from *jjJ* to *LSJ* coupling scheme of angular momenta was performed [2]. The classification of calculated levels was performed by using the largest expansion coefficient of the *LSJ* coupling scheme. As the first expansion coefficient of particular states was used for other levels, the second or even third coefficient was chosen. Calculated results were used for the identification of measured ejected-electron spectra from electron impact excited Ba atoms [3]. For a number of lowest excited states, the comparison of calculated and measured excitation energies is presented in Table 1.

Table 1. Comparison of calculated E_{cal} and experimental E_{exp} [3] excitation energies (in eV) of the $5p^5nln'l'n''l''$ *LSJ* states of Ba.

$nln'l'n''l''$ *LSJ*	E_{cal}	E_{exp}	$nln'l'n''l''$ *LSJ*	E_{cal}	E_{exp}
$5d6s^2\ ^3P_0$	15.603	15.61	$5d^2(^3F)(^2F)6s\ ^3F_3$	16.822	16.72
$5d6s^2\ ^3P_1$	15.790	15.81	$5d^2(^3P)(^4P)6s\ ^5P_1$	17.109	16.84
$5d^2(^3F)(^4D)6s\ ^5D_1$	15.820	15.90	$5d^2(^1D)(^2D)6s\ ^3D_3$	17.178	16.92
$5d^2(^3F)(^4D)6s\ ^5D_2$	15.858	15.91	$5d^2(^3F)(^4F)6s\ ^5F_1$	17.221	17.01
$5d^2(^3F)(^4D)6s\ ^5D_4$	16.091	16.09	$5d^2(^1D)(^2P)6s\ ^3P_2$	17.280	17.10
$5d6s^2\ ^3P_2$	16.121	16.17	$5d6s^2\ ^3D_3$	17.698	17.19
$5d6s^2\ ^3F_4$	16.267	16.26	$5d^2(^1D)(^2P)6s\ ^3P_1$	17.852	17.34
$5d6s^2\ ^3F_3$	16.350	16.31	$5d^2(^1D)(^2F)6s\ ^3F_3$	17.875	17.44
$5d6s^2\ ^1D_2$	16.477	16.40	$6s^26p\ ^3P_2$	17.970	17.61
$5d^2(^3F)(^4D)6s\ ^3D_1$	16.633	16.51	$5d^2(^1D)(^2F)6s\ ^1F_3$	18.136	17.71
$5d^2(^3P)(^4D)6s\ ^3D_3$	16.683	16.61	$5d^2(^3P)(^4P)6s\ ^3P_1$	18.145	17.81

The results of Table 1 show that the accuracy of calculations is high enough to be used for an accurate identification of experimental ejected-electron spectra.

References

[1] M. F. Gu, *The flexible atomic code*, Can. J. Phys. **86**, 675 (2008).
[2] O. Zatsarinny (private communication).
[3] V. Hrytsko, G. Kerevičius, A. Kupliauskienė, and A. Borovik, *The 5p autoionization spectra of Ba atoms excited by electron impact: Identification of lines*, J. Phys. B: At. Mol. Opt. Phys. (2016, submitted).

Stochastic cooling at the low-energy ion-beams storage ring DESIREE

Gustav Eklund, Ansgar Simonsson, Anders Källberg, Samuel Silverstein, Stefan Rosén, Henrik Cederquist and Henning T. Schmidt.
Stockholm University, Department of Physics, SE-106 91 Stockholm, Sweden

Stochastic cooling is one of the most important methods for improving the beam quality in an ion storage ring. Stochastic cooling uses a pickup element to detect the weak signals from the circulating beam known as Schottky signals. These signals are processed by the electronics for the ion-beam phase-space cooling system and sent to a kicker element that corrects the beam. Stochastic cooling can be used for reducing the beam size or emittance and also for reducing the momentum spread of the beam. While stochastic cooling is widely used for high energy storage rings with beam energies in the MeV or GeV range it has not yet been applied to ion beams stored at keV energies [1].

We are currently developing a stochastic cooling system for the DESIREE ion-beams storage rings at Stockholm University in Sweden [2]. DESIREE is a cryogenically cooled electrostatic ion-beams storage ring with beam energies ranging from about 5 keV to 100 keV. This is many orders of magnitude lower than the high energy storage rings that have applied stochastic cooling so far. For low energy beams it is difficult to obtain a low noise pickup signal and this limits the available bandwidth of the cooling system. The bandwidth for the cooling system for DESIREE is expected to be several orders of magnitudes lower than the bandwidth of typical high energy stochastic cooling systems. Low bandwidth implies slow cooling but the effect is compensated by the low ion beam current used in the ring. The cooling time is estimated to be on the order of 100 seconds which is shorter than typical ion beam storage lifetimes due to excellent vacuum of the cryogenic storage ring [3].

The stochastic cooling system for DESIREE is designed for momentum cooling of the beam using the filter method [4]. The filter method makes use of a longitudinal pickup [5]. The Schottky signals detected by the pickup are observed as bands at the harmonics of the revolution frequency with a width proportional to the momentum distribution of the ion beam. The signal is filtered using a periodic notch filter that attenuates the signal at the harmonics of the revolution frequency. This signal is sent to the kicker which corrects the momentum of the beam. Because of the notch filter only the ions with incorrect momentum are effected by the kicker, thus the low momentum ions are accelerated and the high momentum ions are decelerated.

The main part of the stochastic cooling electronics is a digital notch filter which is based on an earlier design [6]. The notch filter is implemented using an FPGA board which allows for the settings of the filter to be controlled directly. This is essential for the stochastic cooling system to work for different ion energies and masses. Other electronics include a high gain amplifier for the pickup, noise filters, an ADC/DAC board for the FPGA and a delay element for the signal also implemented using the FPGA board.

References

[1] Caspers, Fritz, and D. Möhl. *History of stochastic beam cooling and its application in many different projects.* EPJ H **36.4**, 601-632 (2012).
[2] Thomas, Richard D., et al. *The double electrostatic ion ring experiment: A unique cryogenic electrostatic storage ring for merged ion-beams studies.* Rev. Sci. Instrum. **82.6**, 065112 (2011).
[3] Schmidt, Henning T., et al. *First storage of ion beams in the Double Electrostatic Ion-Ring Experiment: DESIREE.* Rev. Sci. Instrum. **84.5** (2013): 055115.
[4] Carron, G and Thorndahl, L. *Stochastic cooling of momentum spread by filter techniques* Int. report CERN-ISR-RF-78-12 (1978)
[5] Forck, Peter. *Lecture notes on beam instrumentation and diagnostics.* JUAS (2015).
[6] Chanel, M., J. Perrier, and R. MacCaferri. *Momentum stochastic cooling with digital notches.* Int. report CERN-PS-90-33-AR (1990).

Quasi-Equilibrium in Charge-State Evolution for S and C Ions after C-Foil Penetration

Alex M Imai[1], Masao Sataka[2,3], Satoru Okayasu[2], Makoto Matsuda[2], Kiyoshi Kawatsura[4], Katsumi Takahiro[5], Ken-ichiro Komaki[6], Hiromi Shibata[7], Katsuhisa Nishio[2]

1. Department of Nuclear Engineering, Kyoto University, Nishikyo, Kyoto 615-8540, Japan

2. Japan Atomic Energy Agency (JAEA), Tokai, Ibaraki 319-1195, Japan

3. Research Facility Center for Science and Technology, University of Tsukuba, Tsukuba, Ibaraki 305-8573, Japan

4. Theoretical Radiation Research Laboratory, Sakyo, Kyoto 606-0966, Japan

5. Kyoto Institute of Technology, Sakyo, Kyoto 606-8585, Japan

6. RIKEN, Wako, Saitama 351-0198, Japan

7. The Institute of Scientific and Industrial Research, Osaka University, Ibaraki, Osaka 567-0047, Japan

After a series of measurements of pre-equilibrium and equilibrium charge-state distribution for 2.0 MeV/u S^{q+} (q = 6-16) and C^{q+} (q = 2-6) ions after penetrating C-foils of 0.9-200 μg/cm^2 in thickness [1–4], we claim that quasi-equilibrium in charge-state evolution has been systematically observed, *i.e.*, charge-state distributions, mean charge-sates, and distribution widths for projectile ions without K-shell holes, S^{q+} (q = 6-14) and C^{q+} (q = 2-4), once merge at target thickness of 6.9 and 5.7 μg/cm^2 respectively, showing quasi-equilibrium, and simultaneously evolve to establish the real-equilibrium as the foil thickness is increased. On the other hand, those for projectile ions with K-shell hole(s), $S^{15+,16+}$ and $C^{5+,6+}$, evolve differently and directly to the real equilibrium established at ~150 μg/cm^2 for S ions and over 10 μg/cm^2 for C ions. The quasi- and real-equilibrium mean charge-states for 2.0 MeV/u S ions were 12.3 and 12.68, respectively [3], whereas those for 2.0 MeV/u C ions were 5.48 and 5.57 [4].

A calculation of rate-equations taking only single-electron capture and loss processes into account as well as simulations with ETACHA code [5,6] have shown that the quasi-equilibrium is brought by differences between reaction-rates of K- and L-shell processes, *i.e.*, difficulties in removing K-shell electrons for projectile ions with filled K-shells and in filling K-shell hole(s) for projectile ions with K-shell hole(s). Thus, the quasi-equilibrium can be treated as equilibrium of L-shell processes leaving K-shell processes untouched, and more number of collisions is required for the real-equilibrium including K-shell processes. The fact that 2.0 MeV/u S ions in the equilibrium wear 1.3 L-shell electrons with filled K-shell in the ground state was favorable for observing the quasi-equilibrium for L-shell processes. Measurements for C projectile ions still suggested there was a difficulty in removing the final K-shell electron in the case exiting-ions have less than one electron in average, which resulted in weak quasi-equilibrium observed for C^{q+} (q = 2-4) initial ions.

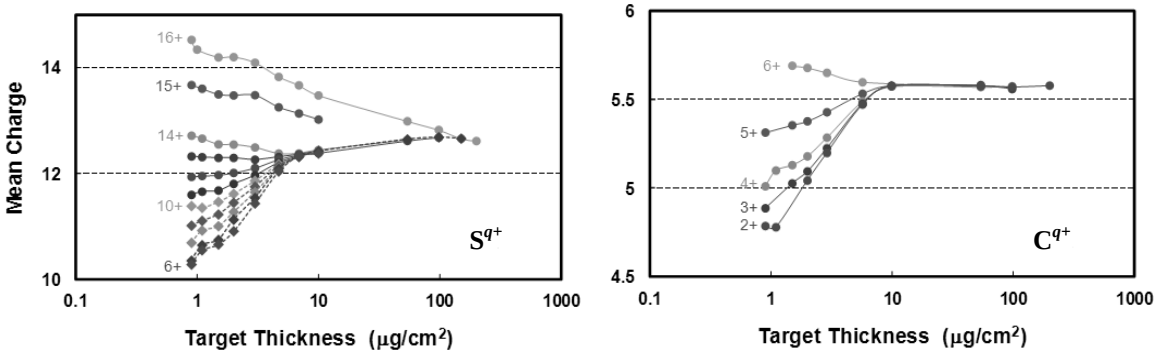

Fig. 1 Evolution of mean charge-states for 2.0 MeV/u S^{q+} (q = 6-16) and C^{q+} (q = 2-6) ions after C-foil penetration.

References

[1] M. Imai, *et al.*, *Charge state distribution and its equilibration of 2 MeV/u sulfur ions passing through carbon foils*, Nucl. Instr. Meth. B **230**, 63 (2005)

[2] M. Imai, *et al.*, *Charge state evolution of 2 MeV/u sulfur ion passing through thin carbon foil*, Nucl. Instr. Meth. B **256**, 11 (2007).

[3] M. Imai, *et al.*, *Equilibrium and non-equilibrium charge-state distributions of 2 MeV/u sulfur ions passing through carbon foils*, Nucl. Instr. Meth. B **267**, 2675 (2009).

[4] M. Imai, *et al.*, *Equilibrium and non-equilibrium charge-state distributions of 2.0 MeV/u carbon ions passing through carbon foils*, Nucl. Instr. Meth. B **354**, 172 (2015).

[5] J.P. Roset *et al.*, *Charge-state distributions of few-electron ions deduced from atomic cross sections*, J. Phys. B **22**, 33 (1989).

[6] E. Lamour *et al.*, *Extension of charge-state-distribution calculations for ion-solid collisions towards low velocities and many-electron ions*, Phys. Rev. A **92**, 042703 (2015).

Anion Emission from Molecular Species Following Cation Impact

Z. Juhász[1], J.-Y. Chesnel[2], E. Lattouf[2], S. T. S. Kovács[1], E. Bene[1], P. Herczku[1], B. A. Huber[2], A. Méry[2], J.-C. Poully[2], J. Rangama[2], J. A. Tanis[3] and B. Sulik[1]

1. Institute for Nuclear Research, Hungarian Academy of Sciences, H-4001 Debrecen, Hungary

2. Centre de Recherche sur les Ions, les Matériaux et la Photonique (CIMAP), 6 Bd Mar. Juin, F-14000 Caen, France

3. Department of Physics, Western Michigan University, Kalamazoo, Michigan 49008 USA

It has been recently shown that negative ions can be ejected from gas-phase molecular species in different collision systems involving atoms and positive ions at a few keV impact energies [1-3]. These findings are relevant for studies of interstellar media and ionospheres, as well as for radiolysis and radiobiology since slow anions are efficient agents for charge transfer and chemical reactions.

We have observed that an H^- ion can be formed from an OH^+ ion when the H center is removed by collision on an Ar target atom [1-2]. The angular distribution of the so-created H^- ions has been found to be proportional to the one calculated for H scattering on the target atom. A similar result is found for the emitted H^+ ions. Also, the kinetic energy distribution of the H^+ fragments shows strong similarities with that of the ejected H^- ions. These findings indicate that the final charge state distribution of the emitted H centers does not depend on how closely the atomic centers approach each other during the collision. Rather, it seems to follow simple statistical laws. A statistical model will be presented.

Also, in 6.6-keV $^{16}O^+ + H_2O$ collisions, emission of both H^- and heavier (O^- and OH^-) anions has been observed, with a larger yield for H^- [3]. Figure 1 shows the experimental double-differential cross sections (DDCS) for anion emission in these collisions. The main component of each spectrum is a broad, slowly decreasing structure. There, the relative contribution of H^- anions was derived from complementary time-of-flight (TOF) measurements. At forward angles (< 90°), pronounced peaks are observed at higher energies. These peaks are due to recoil anions formed in hard binary collisions occurring at small impact parameters, while the broad contribution results from soft many-body processes. Spectral features can be well reproduced by model calculations that include kinetic energy release (KER) due to electronic excitation and ionization processes (see Fig. 1). This indicates that these processes play a decisive role in H^- formation.

This work was supported by the Hungarian National Science Foundation OTKA (Grant No. K109440), the French-Hungarian Cooperation Program PHC Balaton (No. 27860ZL/TéT_11-2-2012-0028), and the French-Hungarian CNRS-MTA Cooperation (ANION project).

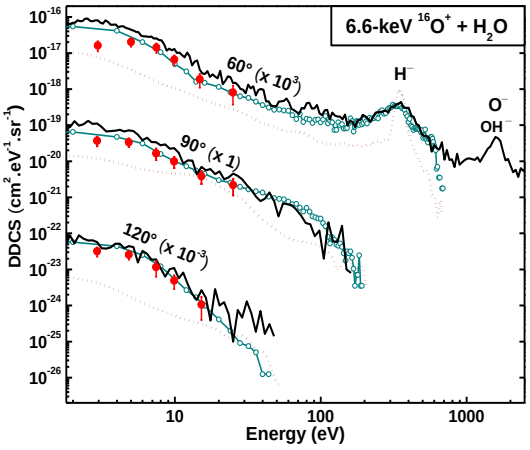

Fig. 1 Full curve: Experimental DDCS for anion emission in 6.6-keV $^{16}O^+ + H_2O$ collisions; Full circles: H^- contribution from TOF measurements. Open circles: Simulated DDCS for H^- emission at different angles with KER; Dotted curve: Same without KER. Each spectrum is multiplied by the indicated factor.

References

[1] Z. Juhász, B. Sulik, J. Rangama, E. Bene, B. Sorgunlu-Frankland, F. Frémont, and J.-Y. Chesnel, *Formation of negative hydrogen ions in 7-keV OH^+ + Ar and OH^+ + acetone collisions: A general process for H-bearing molecular species*, Phys. Rev. A **87**, 032718 (2013).

[2] E. Lattouf, Z. Juhász, J.-Y. Chesnel, S. T. S. Kovács, E. Bene, P. Herczku, B. A. Huber, A Méry, J.-C. Poully, J. Rangama, and B. Sulik, *Formation of anions and cations via a binary-encounter process in OH^+ + Ar collisions: The role of dissociative excitation and statistical aspects*, Phys. Rev. A **89**, 062721 (2014).

[3] J.-Y. Chesnel, Z. Juhász, E. Lattouf, J. A. Tanis, B. A. Huber, E. Bene, S. T. S. Kovács, P. Herczku, A. Méry, J.-C. Poully, J. Rangama, and B. Sulik, *Anion emission from water molecules colliding with positive ions: Identification of binary and many-body processes*, Phys. Rev. A **91**, 060701(R) (2015).

Electron emission mechanisms in ion-induced ionization of small molecules

S. T. S. Kovács, P. Herczku , L. Sarkadi, L. Gulyás, Z. Juhász and B. Sulik
Institute for Nuclear Research, Hungarian Academy of Sciences (MTA Atomki), Bem tér 18/c, H-4026 Debrecen,Hungary

Ion-impact ionization of small molecules was investigated both experimentally and theoretically. Ionization of atoms and molecules is of fundamental interest in atomic and molecular physics [1-3]. Besides that, ionization is important in many applications, for instance plasma physics, industrial irradiations and radiotherapy. In this work, electron energy spectra were taken by an energy dispersive electrostatic spectrometer at different observation angles. The obtained absolute electron emission cross sections were compared with the results of CDW-EIS and CTMC calculations. Both theories are in a reasonable agreement with the experimental data.

In the experiment, beams of H^+, He^+, C^+ and N^+ ions were provided by a 5 MV VdG accelerator in the 46-1000 keV/u energy range. The ion beams crossed gas jets of CH_4, H_2O and N_2. By applying a rotatable energy dispersive electrostatic spectrometer we determined double differential electron emission cross sections (DDCSs) in the 20°-160° observation angle range.

In figure 1 we compare the energy spectrum of the electrons ejected in 46 keV/u $N^+ + H_2O$ collisions at 160° observation angle with CTMC (figure 1a) and CDW-EIS [4] (figure 1b) calculations. The main interest here is how can the different theoretical approaches treat a dressed projectile (and dressed target) as collision agent at strong perturbations.The calculated total electron yields (comparable with the experimental data) originates from both projectile and target ionization. The calculated contribution from the target ionization is also shown.

In the CTMC calculations we used a multi-center approach with a full three-body dynamics. A good overall agreement was found between the experimentally observed DDCS and that obtained by the CTMC calculations in the entire electron energy range. Fig. 1a shows that except a slight overestimation between 30 and 140 eV, the agreement is almost perfect. The quantum mechanical CDW-EIS calculations have also been extended for dressed projectiles and molecular targets [4]. Fig. 1.b shows that CDW-EIS also provide a reasonable qualitative description, though it overestimates both the projectile and target contributions at lower energies. Moreover, above ~80 eV the calculated CDW-EIS results fall off significantly faster then the experimental data.

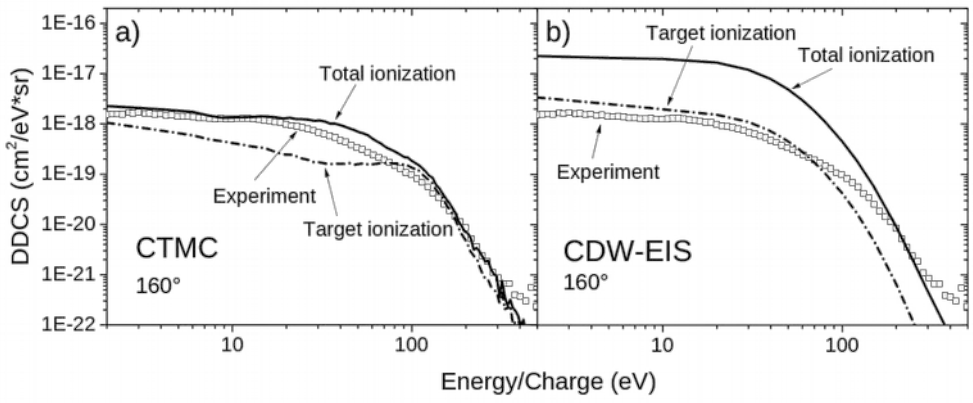

Fig. 1 Comparison of the experimental electron spectrum with the results of CTMC (a) and CDW-EIS (b) calculations at 160° observation angle for 650 keV $N^+ + H_2O$ collisions.

We interpret the results that the nonperturbative character of CTMC allows it to account for all the significant mechanisms in this collision regime including two-center effects. We note that the peak around 100 eV in the target ionization contribution belongs to a four-fold accelerating scattering of the target electrons (Fermi-shuttle) [5]. The perturbetive CDW-EIS method can not treat this latter process, this is the most likely reason of the much faster fall off of the theory there.

This work was supported by the Hungarian National Science Foundation OTKA (Grant No. K109440).

References

[1] W. E. Wilson and L. H. Toburen, *Electron emission from proton-hydrocarbon-molecule collisions at 0.3-2.0 MeV,* Phys. Rev. A **11**, 1303 (1975).
[2] A. N. Agnihotri et al., *Doubly differential distribution of electron emission in ionization of uracil in collision with 3.5 MeV/u bare C ions*, Phys. Rev. A **87**, 032716 (2013).
[3] A.V. Solov'yov et al., *Physics of ion beam cancer therapy: a multiscale approach*, Phys. Rev. E **79,** 011909 (2009).
[4] L. Gulyas, I. Tóth and L. Nagy, *CDW-EIS calculation for ionization and fragmentation of methane impacted by fast protons*, J. Phys. B **46**, 075201 (2013).
[5] B. Sulik et al., *Evidence for Fermi-Shuttle Ionization in Intermediate Velocity C^+ + Xe Collisions*, Phys. Rev. Lett. **88**, 073201 (2002).

Carbon backbone stability of hydrogenated and native pyrene

Michael Wolf[1], Hjalte V. Kiefer[2], Linda Giacomozzi[1], Michael Gatchell[1], Jeppe Langeland[2], Nathalie de Ruette[1], Lars H. Andersen[2], Henning T. Schmidt[1], Henrik Cederquist[1], Mark H. Stockett[1,2], and Henning Zettergren[1]

1. Department of Physics, Stockholm University, Stockholm, SE–106 91, Sweden
2. Department of Physics and Astronomy, Aarhus University, DK–8000 Aarhus C, Denmark

Polycyclic Aromatic Hydrocarbons (PAHs) are believed to be abundant within the interstellar medium [1]. In astrophysical environments PAHs may be excited through photoabsorption processes, or in collisions with electrons or heavy particles like ions or atoms. One interesting issue in this context is the effect of hydrogenation on the PAH carbon-backbone stability. On one hand, hydrogenation converts unsaturated C-C bonds to single bonds, which weakens the carbon backbone. On the other hand, the additional hydrogen atoms allows for cooling of the PAH carbon skeleton through H-loss, which thus may *protect* the carbon backbone from fragmentation. Pioneering experiments by Reitsma *et al.* [2] indicated such a protective effect following core electron excitation using an x-ray light source. There the coronene molecule ($C_{24}H_{12+m}$, $m = 0$–7) lost fewer of its native hydrogen atoms when it was hydrogenated, with a stronger protective effect for a higher degrees of hydrogenation. From this Reitsma *et al*. inferred that hydrogenation always has a net protective effect on the carbon backbone for PAHs [2].

We have performed two experiments that lead to the opposite conclusion. The first experiment, concerning collision-induced dissociation of hydrogenated pyrene ($C_{16}H^+_{10+m}$, $m = 0, 6,$ or 16) cations, was carried out at Stockholm University. Here, we measured increases in the absolute carbon backbone fragmentation cross section for increasing degrees of hydrogenation [3], as shown to the left in Fig. 1. Furthermore, measurements of absolute CH_x-loss cross sections down to very low collision energies also indicated a weakening of the carbon backbone for hydrogenated pyrene [4].

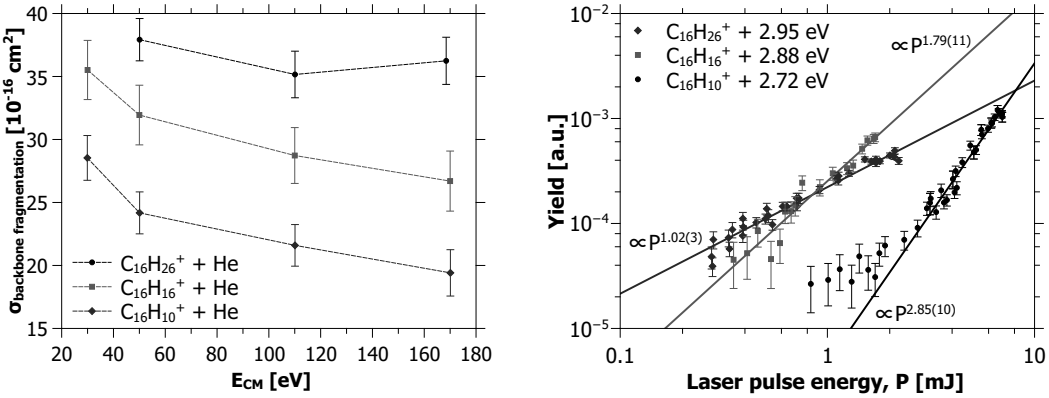

Fig. 1 The left graph shows absolute carbon backbone fragmentation cross sections in He + $C_{16}H^+_{10+m}$ ($m = 0, 6,$ or 16) collisions as a function of center-of-mass energy E_{CM}. The right graph shows the total fragmentation yield as a function of laser pulse energy, P. The lines are power fits, where the exponents (see insets) give the number of photons absorbed.

We have recently investigated photo-induced dissociation of the same molecules at the ELISA (Electrostatic Ion Storage Ring in Aarhus) facility at Aarhus University. The graph to the right in Fig. 1 shows preliminary laser-power dependencies for fragmentation of $C_{16}H^+_{10+m}$ ($m = 0, 6,$ or 16). From the slope in the log-log diagram the photon dependency, i.e. the number of photons needed for fragmentation, can be deduced. The number decreases from three 2.72 eV photons (total of 8.16 eV) for $C_{16}H^+_{10}$, to two 2.88 eV photons (total of 5.76 eV) for $C_{16}H^+_{16}$, and only one 2.95 eV photon for $C_{16}H^+_{26}$. This shows that hydrogenation leads to larger tendencies of carbon-backbone fragmentation also when the molecules are photo-excited.

References

[1] A. G. G. M. Tielens, *The molecular universe*, Rev. Mod. Phys. **85**, 1021 (2013).

[2] G. Reitsma, L. Boschman, M. J. Deuzeman, O. González-Magaña, S. Hoekstra, S. Cazaux, R. Hoekstra, and T. Schlathölter, *Deexcitation Dynamics of Superhydrogenated Polycyclic Aromatic Hydrocarbon Cations after Soft-x-Ray Absorption*, Phys. Rev. Lett. **113**, 053002 (2014).

[3] M. Gatchell, M. H. Stockett, N. de Ruette, T. Chen, L. Giacomozzi, R. F. Nascimento, M. Wolf, E. K. Anderson, R. Delaunay, V. Vizcaino, P. Rousseau, L. Adoui, B. A. Huber, H. T. Schmidt, H. Zettergren, and H. Cederquist, *Failure of hydrogenation in protecting polycyclic aromatic hydrocarbons from fragmentation*, Phys. Rev. A **92**, 050702(R) (2015).

[4] M. Wolf, L. Giacomozzi, M. Gatchell, N. de Ruette, M. H. Stockett, H. T. Schmidt, H. Cederquist, and H. Zettergren, *Hydrogenated pyrene: Statistical single-carbon loss below the knockout threshold*, Eur. Phys. J. D, (in press).

Theoretical study of laser-assisted $(e,2e)$ collisions on He and H_2^+ at large momentum transfer

Andrew A. Bulychev[1], **Konstantin A. Kouzakov**[2]

1. Laboratory of Theoretical Physics, Joint Institute for Nuclear Research, Moscow Region, 141980 Dubna, Russia

2. Department of Nuclear Physics and Quantum Theory of Collisions, Faculty of Physics, Lomonosov Moscow State University, 119991 Moscow, Russia

In this contribution, we present a theoretical analysis of the laser-assisted $(e,2e)$ scattering in the He atom and in the hydrogen molecular ion H_2^+. A low-frequency laser field of relatively weak strength is considered, such that the Keldysh parameter is $\gamma \gg 1$. We focus on the kinematical regime of high impact energy and large momentum transfer, which is typical for electron momentum spectroscopy (EMS).

In the chosen kinematics, an S-matrix of the scattering reaction is described with the use of the binary-encounter and first Born approximations. This strongly simplifies theoretical treatment of ionization dynamics, both in the absence and in the presence of a laser field. In our theoretical analysis of laser-assisted EMS of atomic helium with excitation of the residual He^+ ion, we found that the cross section exhibits much highe sensitivity to electron-electron correlations in the target than in the field-free case [1]. Fig. 1 shows numerical results for different number of photons N when the laser electric field with frequency $\hbar\omega = 1.55\,\mathrm{eV}$ and intensity $I = 1.55 \times 10^{11}\,\mathrm{W/cm^2}$ is parallel to the incident electron momentum (LP$\|$). The cross sections calculated with different correlated ground-state wave functions of He (SPM, BK, and CI) appear to be well distinguishable from each other, while in the absence of a laser field they are practically identical.

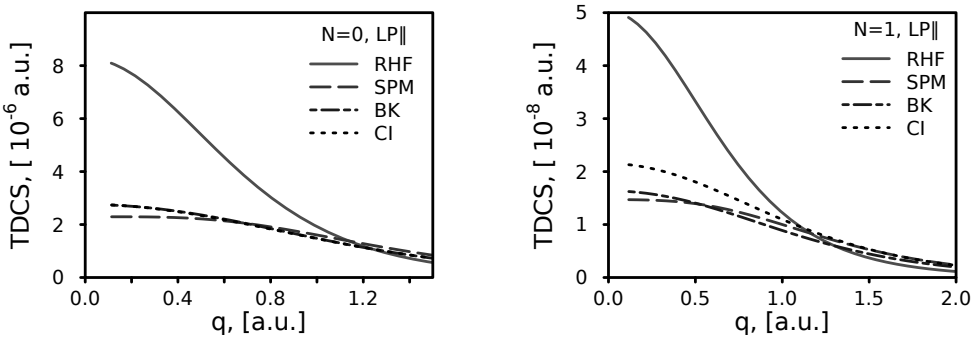

Fig. 1 Laser-assisted triply differential cross sections in the case of He^+ ion transition to the first excited state for the net number of emitted photons $N = 0, 1$.

In the case of molecular targets, a number of various effects of a laser field on the target can be expected, ranging from a laser-induced molecular axis alignment to a laser-induced molecular dissociation. Employing the so-called quasiadiabatic model to describe laser-dressed states of the molecular ion H_2^+, we show that using the laser-assisted EMS method [2] one can get access to the electron momentum distribution in the $1\sigma_u$ state, which remains inaccessible in the field-free case.

References

[1] Andrew A. Bulychev and Konstantin A. Kouzakov, *Laser-assisted ionization-excitation of helium by electron impact at large momentum transfer*, Eur. Phys. J. D **68**, 354 (2014).

[2] Konstantin A. Kouzakov, Yuri V. Popov, and Masahiko Takahashi, *Laser-assisted electron momentum spectroscopy*, Phys. Rev. A **82**, 023410 (2010).

Resonance Contribution to the $6s^26d\ ^2D_{5/2}\rightarrow 6s^26p\ ^2P^o_{3/2}$ Transition of the Pb^+ Ion at Electron-Impact Excitation

Anna Gomonai, Yuriy Hutych, Aleksandr Gomonai

Institute of Electron Physics, Ukrainian National Academy of Sciences, 21 Universitetska str., 88017 Uzhgorod, Ukraine

First measurements of emission cross section for electron-impact excitation of the $6s^26d\ ^2D_{5/2}\rightarrow 6s^26p\ ^2P^o_{3/2}$ transition of the Pb^+ ion are reported:

$$e + Pb^+(5d^{10}6s^26p)\ ^2P^o_{1/2} \rightarrow e + Pb^{+*}(5d^{10}6s^26d)\ ^2D_{5/2}$$
$$\downarrow$$
$$Pb^+(5d^{10}6s^26p)\ ^2P^o_{3/2} + h\nu\ (\lambda 182.2\ nm).$$

The experiment was carried out by a photon VUV spectroscopy method using a crossed electron and ion beam technique. The crossed-charged-beams apparatus and technique applied were described in detail in [1]. The ion-beam current in the collision region was $(0.5–1.0)\times10^{-6}$ A at 800 eV. The electron beam current in the energy region 6 ÷ 50 eV was $(5\div10)\times10^{-5}$ A, the energy spread (FWHM) of the electron beam was 0.6 eV.

The electron-impact excitation function of the Pb^+ ion λ182.2 nm line is shown in Fig. 1. Strong resonance features were observed in the near-threshold excitation region, below and above the Pb^+ ion ionization potential.

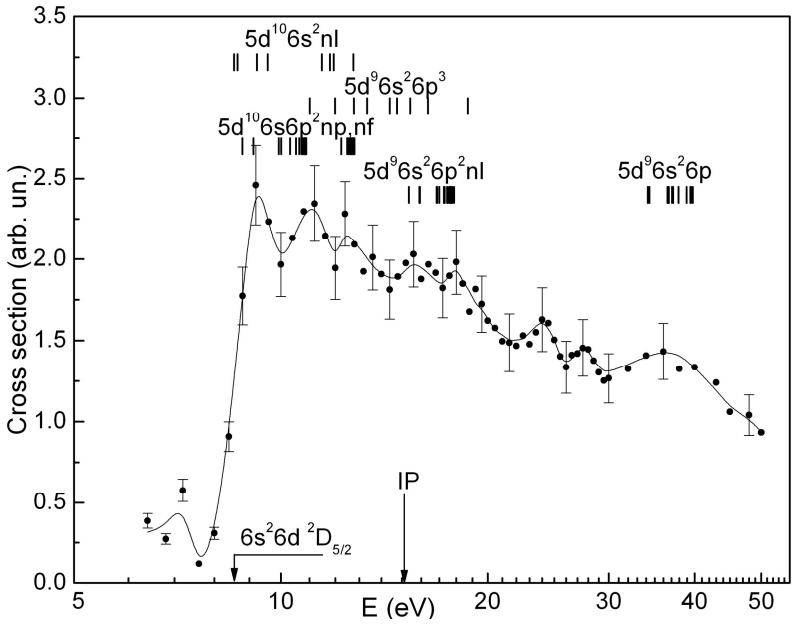

Fig. 1 Electron-impact excitation emission cross-sections of the Pb^+ ion $6s^26d\ ^2D_{5/2}\rightarrow 6s^26p\ ^2P^o_{3/2}$ (λ182.2 nm) transition

Analysis of the results obtained using the data on the energy position of the single- and double-charged lead ion levels [2] as well as of atomic and ionic autoionizing states [3-4] enabled us to explain the nature of the structure found. Near-threshold excitation of the emission is complicated not only by the resonance excitation via autoionizing states but also by dielectronic recombination which is the principal mechanism of the dielectronic satellites excitation. The structure above 9.2 eV is due both to the cascade transitions from $5d^{10}6s^2nl$ levels and to the electronic decay of $5d^{10}6s^2nln_1l_1$, $5d^{10}6s6p^2np,nf$, $5d^96s^26p^3$ and $5d^96s^26p^2np,nf$ autoionizing states resulted from the sequential multi-step processes. This is due to the fact that the electron correlations play an essential role in this process because the two-electron transitions are possible only provided the electron–electron interaction is taken into account.

References

[1] E.V. Ovcharenko, A.I. Imre, A.N. Gomonai, and Yu.I. Hutych, *Emission cross-sections of the In^{2+} ion VUV laser transitions at electron–In^+ ion collisions*, J. Phys. B. **43**, 175206 (2010).

[2] J.E. Sansonetti, and W.C. Martin, *Handbook of Basic Atomic Spectroscopic Data*, J. Phys. Chem. Ref. Data. **34**, 1559 (2005).

[3] J.P. Connerade, W.R.S. Garton, M.W.D. Mansfield, and M.A.P. Martin, *Interchannel Interactions and Series Quenching in the 5d and 6s Spectra of Pb I*, Proc. R. Soc. Lond. A. **357**, 499 (1977).

[4] V. Pejcev, C.G. Back, K.J. Ross, and M. Wilson, *High-resolution ejected-electron spectrum of Pb I and Pb II autoionising levels excited by low-energy electron impact*, J. Phys. B. **14,** 4649 (1981).

Two-channel model for cold collisions of metastable neon atoms

Christian Cop[1], **Reinhold Walser**[1]
Institut für Angewandte Physik, Technische Universität Darmstadt, Schlossgartenstr. 7, 64289 Darmstadt

Metastable noble gas cooling began in the 1980's for various species. At the Technical University of Darmstadt, the group of Gerhard Birkl investigates experimentally the prospects to condense metastable neon atoms (Ne*) to degeneracy. The high internal energy of Ne* ($\sim$16 eV) allows for single-ion detection, however, it stands in contrast to the low kinetic energies in cold collision experiments $\sim 10^{-10}$ eV and may lead to loss rates through Penning ionization (PI) and Associative ionization (AI), given by

$$\mathrm{Ne^*} + \mathrm{Ne^*} \longrightarrow \mathrm{Ne} + \mathrm{Ne^+} + e^- \quad \text{(PI)},$$
$$\mathrm{Ne^*} + \mathrm{Ne^*} \longrightarrow \mathrm{Ne_2^+} + e^- \quad \text{(AI)}.$$

For samples of atoms where the total electronic spins of the atoms are aligned the AI and PI loss channels are forbidden due to conservation ot total electronic spin during the collision. This suppression of losses due to spin polarization of the atoms has been demonstrated in the experiment [1]. Extended experimental data is now also available on scattering lengths, relaxation cross sections and two-body loss rates of different isotope- and spin-mixtures of the three stable isotopes of Ne* [1,2]. The data suggests that different isotopes of Ne* behave very differently in the collision process.

In order to model and explain these interesting experimental results we set up a two-channel model, where a single interaction potential for Ne* is coupled to an arbitrary loss channel via an internal-state-dependent coupling. The loss channel represents AI and PI. Suppression of AI and PI is modeled by introducing a weaker coupling for atoms colliding in the spin-aligned states than for collisions of atoms colliding in other states.

Figure 1 shows the internal-spin-state dependent two-body loss rates β of homonuclear collisions and the experimental data points. It can be seen that the numerical results are in good agreement with the experiment.

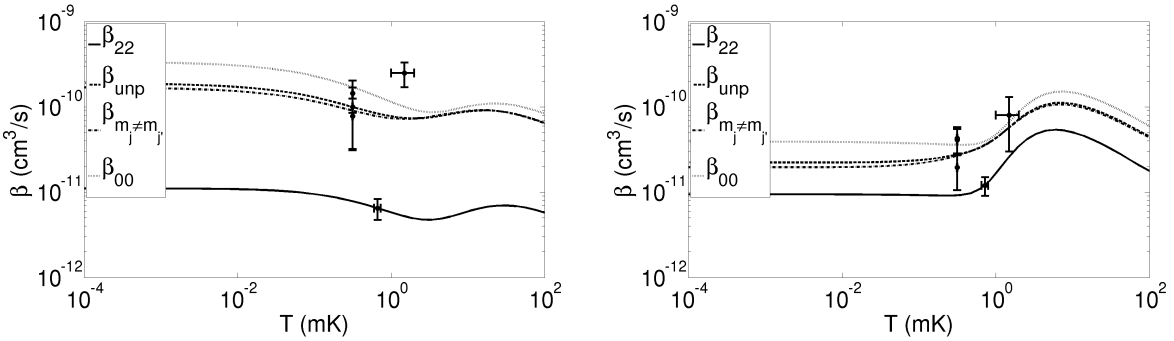

(a) ^{20}Ne collisions (b) ^{22}Ne collisions

Fig. 1: Two-body loss rates β as functions of temperature T for homonuclear Ne* collisions. Numerical results for loss rates where the atoms collide (i) in the spin-stretched $m_j = 2$ states are indicated by the solid lines (ii) in the same state but not the spin-stretched state $m_j = m_{j'} \neq 2$ by the dotted lines (iii) in different internal states $m_j \neq m_{j'}$ by the dash-dotted lines. Numerical results for loss rates for unpolarized samples where all the internal states of the atoms are uniformly populated are indicated by the dashed lines. The dots and error bars are given by the experiment.

Further numerical results of homonuclear ^{20}Ne and ^{22}Ne collisions will be presented as well as of heteronuclear collisions between ^{20}Ne, ^{21}Ne, ^{22}Ne. It will be shown that the numerical results agree very well with the experiment [3]. Thus, the two-channel model gives a consistent explanation of the available *isotope-sensitive* scattering data of metastable neon and extends existing quantum reflection models which explain collisions of metastable noble gases with *no isotope-sensitive* scattering properties [4].

References

[1] P. Spoden, N. Herrschbach, W.J. van Drunen, W. Ertmer, and G. Birkl, *Collisional properties of cold spin-polarized metastable neon atoms*, Phys. Rev. Lett. **94**, 223201 (2005).
[2] J. Schütz, T. Feldker, H. John, and G. Birkl, *Heteronuclear collisions between laser-cooled metastable neon atoms*, Phys. Rev. A **86**, 022713 (2012).
[3] C. Cop, A. Martin, G. Birkl, and R. Walser, *Penning ionization and elastic scattering in cold collisions of metastable neon atoms*, to be published.
[4] C. Orzel, M. Walhout, U. Sterr, P.S. Julienne, S.L. Rolston, *Spin polarization and quantum-statistical effects in ultracold ionizing collisions*, Phys. Rev. A **59**, 1926 (2016)

Reactive collisions with conformationally controlled molecules

Daniel Rösch[1], **Ardita Kilaj**[1], **Hong Gao**[1], **Stefan Willitsch**[1]
1. Department of Chemistry, University of Basel, 4056 Basel, Switzerland)

Yuan-Pin Chang[2], **Jochen Küpper**[2,3]
2. Center for Free-Electron Laser Science, DESY, 22607 Hamburg, Germany
3. Department of Physics, University of Hamburg, 22761 Hamburg, Germany

Many molecules have multiple conformations (rotational isomers), which can exhibit different reactivites, opening up perspectives to manipulate chemical reactions by selecting specific molecular conformations [1]. However, a detailed understanding of the role of conformations in gas-phase chemical reactions still has to be established.
We have developed an apparatus to separate molecular conformations and study their reactivity with cold ions. This was demonstrated in a recent experiment where we studied reactive collisions between conformationally selected 3-aminophenol and Coulomb crystals of laser-cooled Ca^+ ions [2,3].

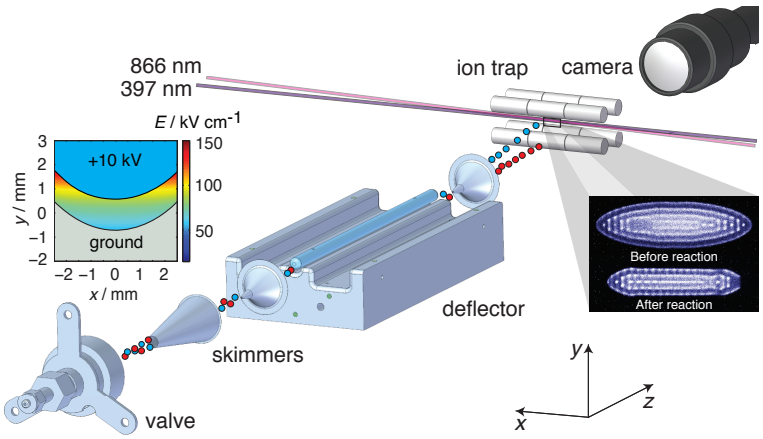

Fig. 1 Experimental setup for studying conformationally controlled chemical reactions.

A cold molecular beam of 3-aminophenol is guided through an electrostatic deflector. The two different conformations (cis and trans) are spatially separated due to different permanent dipole moments and thus different resulting Stark shifts in an inhomogeneous electric field. By tilting the molecular beam machine mechanically with respect to the ion trap, conformationally pure components of the molecular beam are overlapped with the ion trap. The progress of the reaction is monitored by imaging the laser-induced fluorescence of unreacted ions. We recently upgraded the apparatus with a time-of-flight mass spectrometer which is coupled to the ion trap and enables reaction product analysis with high mass resolution ($m/\Delta m \approx 700$).
In future experiments we want to study reactions that are relevant for organic synthesis. A particular interesting class of reactions are Diels-Alder reactions. These are pericyclic reactions between a dien and a dienophile, forming a cyclic product in a stereo and regioselective reaction. The mechanism is generally believed to be concerted with a cyclic transition state. However, for polar cycloadditions, in which one reaction partner is charged, the mechanism is not necessarily concerted anymore.
2,3-dibromobutadiene has two conformations and only one should undergo a Diels-Alder reaction with maleic anhydride. We will investigate the polar cycloaddition with charged maleic anhydride on this setup and are at the moment also setting up a crossed beam machine to study reactive collisions with neutral maleic anhydride.
Our electrostatic deflector also intrinsically acts as a rotational state selector, since the effective dipole moments differ between different rotational states. We want to exploit this to study ion-molecule reactions with the neutral reaction partner in selected rotational quantum states.
On the poster we give an overview over the 3-aminophenol + Ca^+ experiment, the new ion trap coupled to a TOF-MS and present preliminary results of ongoing experiments.

References

[1] F. Filsinger, U. Erlekam, G. von Helden, J. Küpper, and G. Meijer, Phys. Rev. Lett. 100, 133003 (2008)
[2] Y.-P. Chang, K. Dlugolecki, J. Küpper, D. Rösch, D. Wild and S. Willitsch, Science 342, 98 (2013)
[3] D. Rösch, S. Willitsch, Y.-P. Chang and J. Küpper, JCP 140, 124202 (2014)

Mutual Neutralization Studies at Subthermal Collision Energies

Nathalie de Ruette[1], Rodrigo F. Nascimento[1,3], Arnaud Dochain[2], Magdalena Kaminska[1,4], Mark H. Stockett[1,5], Henning T. Schmidt[1], Henrik Cederquist[1], and Xavier Urbain[2]

1. Department of Physics, Stockholm University, Stockholm, SE-106 91, Sweden

2. Institute of Condensed Matter and Nanosciences, Université catholique de Louvain, B-1348 Louvain-la-Neuve, Belgium

3. Centro Federal de Educação Tecnológica Celso Suckow da Fonseca, Petrópolis, 25620-003, RJ, Brazil

4. Institute of Physics, Jan Kochanowski University, 25-369 Kielce, Poland

5. Department of Physics and Astronomy, Aarhus University, Ny Munkegade 120, DK 8000 Aarhus C, Denmark

Anions play important roles in the chemistry of various astrophysical environments ranging from planetary and stellar atmospheres to interstellar clouds [1-5]. A key reaction for the ionization balance in those media is the Mutual Neutralization (MN) of atomic or molecular anions and cations [5,6]:

$$A^+ + B^- \rightarrow A + B. \quad (1)$$

Such reactions have been included in models of chemical reaction networks in astrophysical environments ever since 1973 [7-9]. Measurements of MN rate coefficients are thus urgently needed, especially at subthermal energies. Until now, few rate coefficients have been measured due to the complexity of this type of experiments [10].

MN studies with atomic ions have so far mainly been limited to collision energies down to a few eV, which is higher than the range of energies relevant for cold astrophysical environments. Moreover, these experiments could not resolve the electronic (n), angular momentum (L), and spin (S) states, i.e. the LS-terms, of the neutral products [11,12].

We recently upgraded the merged beam setup in Louvain-la-Neuve to reach 5 meV collision energies, and incorporated three-dimensional momentum imaging using two position sensitive detectors located 3.25 meters downstream from the 7 cm long region where the A^+ and B^- beams overlap. Besides providing clear coincidence signals between A and B, this technique gives unambiguous identification of LS-terms of the products via the measurement of the Kinetic Energy Release (KER). The KER-resolution (50 meV FWHM at 1 eV) is mainly limited by the finite length of the interaction region. Measuring the momentum distribution of both products yields the total and the energy and angular differential cross sections. The absolute cross section scale is defined by the simultaneous measurement of associative ionization $A^+ + B^- \rightarrow AB^+ + e^-$ cross sections by means of a 180° bending magnet, a 30° electrostatic deflector, and a channeltron detector.

We present absolute MN cross sections for N^+ colliding with O^- in the 0.005-10 eV energy range and KER-spectra at subthermal energies for C^+ on P^-, C^-, Si^-, O^- or S^-. The latter leads to identifications of the capture states (n, L, and S) of the products. While several of the $A^+ + B^-$ systems that we have studied give results well accounted for by means of simple multi-channel Landau-Zener calculations, there are striking exceptions. For the $C^+ + O^-$ and $C^+ + P^-$ systems, there are final states populated that require much stronger couplings to the initial $A^+ + B^-$ channel than expected.

The present study will also serve to benchmark merged ion beams studies at the double electrostatic storage ring DESIREE now in operation at Stockholm University [13]. With DESIREE it will be possible to study MN between molecular ions with very low internal energies (down to 10 K).

References

[1] R. Wildt, *Molecular Bands in Stellar Spectra*, Astrophys. J. **89**, 295 (1939).

[2] H. Massey, *Negative Ions*, 3rd ed. (Cambridge University Press, 1976).

[3] D. Smith & P. Spanel, *Ions in the Terrestrial Atmosphere and in Interstellar Clouds*, Mass Spectrom. Rev. **14**, 255 (1995).

[4] P. Chaizy, H. Rème, J. A. Sauvaud, C. d'Uston, R. P. Lin, D. E. Larson, D. L. Mitchell, K. A. Anderson, C. W. Carlson, A. Korth, and D. A. Mendis, *Negative Ions in the Coma of Comet Halley*, Nature **349**, 393 (1991).

[5] M. Larsson, W. D. Geppert, and G. Nyman, *Ion Chemistry in Space*, Rep. Prog. Phys. **75**, 066901 (2012).

[6] N. Harada and E. Herbst, *Modeling Carbon Chain Anions in L1527*, Astrophys. J. **685**, 272 (2008).

[7] A. Dalgarno and R. A. McCray, *The Formation of Interstellar Molecules from Negative Ions*, Astrophys. J. **181**, 95 (1973).

[8] V. Wakelam, E. Herbst, J. C. Loison, I. W. M. Smith, V. Chandrasekaran, B. Pavone, N. G. Adams, M. C. Bacchus-Montabonel, A. Bergeat, K. Béroff, V. M. Bierbaum, *et al.*, *A Kinetic Database for Astrochemistry (KIDA)*, Astrophys. J. Suppl. Ser. **199**, 21 (2012).

[9] D. McElroy, C. Walsh, A. J. Markwick, M. A. Cordiner, K. Smith, and T. J. Millar, *The UMIST Database for Astrochemistry 2012*, Astron. & Astrophys. **550**, A36 (2013), arXiv:1212.6362 [astro-ph.SR].

[10] N. G. Adams, L. Babcock, and C. Molek, *The Encyclopedia of Mass Spectrometry*, edited by P. Armentrout (Elsevier Amsterdam, 2003) pp. 555–561.

[11]M. Terao, S. Szücs, M. Cherkani, F. Brouillard, R. J. Allan, C. Harel, and A. Salin, *Experimental and Theoretical Study of Electron Transfer in the He_2^+-H^- Collision*, Europhys. Lett. **1**, 123 (1986).

[12] S. M. Nkambule, N. Elander, Å. Larson, J. Lecointre, and X. Urbain, *Differential and total cross sections of mutual neutralization in low-energy collisions of isotopes of $H^+ + H^-$*, Phys. Rev. A **93**, 032701 (2016).

[13] R. D. Thomas, H. T. Schmidt, G. Andler, M. Björkhage, M. Blom, L. Brännholm, E. Bäckström, H. Danared, S. Das, N. Haag, *et al.*, *The double electrostatic ion ring experiment: A unique cryogenic electrostatic storage ring for merged ion-beams studies*, Rev. Sci. Instrum. **82**, 065112 (2011)

Suppression of spin-exchange relaxation in tilted magnetic fields within the geophysical range

Theo Scholtes[1,2], Szymon Pustelny[3], Stephan Fritzsche[4,5], Volkmar Schultze[1], Ronny Stolz[1], Hans-Georg Meyer[1]

1. Leibniz Institute of Photonic Technology, Albert-Einstein-Straße 9, 07745 Jena, Germany
2. Department of Physics, University of Fribourg, Chemin du Musée 3, 1700 Fribourg, Switzerland
3. Marian Smoluchowski Institute of Physics, Jagiellonian University, Łojasiewicza 11, 30-348 Cracow, Poland
4. Helmholtz-Institut Jena, Fröbelstieg 3, 07743 Jena, Germany
5. Theoretisch-Physikalisches Institut, Friedrich-Schiller-Universität Jena, D-07743 Jena, Germany

We investigate experimentally and theoretically the spin-exchange mechanism acting on the electronic ground states of alkali metal vapor atoms. By comparing the experimentally determined intrinsic relaxation rate of the cesium ground state spin coherence to the results of a detailed density-matrix simulation we prove, that the relaxation due to spin-exchange collisions can be reduced substantially even in a tilted, large magnetic field of geomagnetic strength. By this we explain one side of the observed improved sensitivity of the light-narrowed M_x (LN) optically pumped magnetometer (OPM) [1], which is based on an adapted hyperfine-selective optical pumping scheme and can operate without being restricted to a longitudinal magnetic field geometry or to near-zero magnetic field.
The hyperfine-resolved optical repumping of the lower cesium ground state manifold leads to a reduction of the intrinsic coherence relaxation rate γ_{20}. Its dependence on the cell temperature, the magnetic field orientation with respect to the laser beam direction and the repumping power is inferred by measurements of the optically detected magnetic resonance signals in the transmitted laser light. Fitted linewidths are extrapolated to vanishing probe and rf-field power [2].
To simulate the dynamical action of the spin-exchange relaxation mechanism on the atomic spin $\mathbf{S}$ we employed the formula introduced firstly by F. Grossetete [3]

$$\frac{\hat{\Gamma}_{SE}(\rho)}{R_{SE}} = -\frac{3}{4}\rho + \mathbf{S}\cdot\rho\mathbf{S} + \langle\mathbf{S}\rangle\left(\{\mathbf{S},\rho\} - 2i\mathbf{S}\times\rho\mathbf{S}\right), \tag{1}$$

into our model based on the density matrix ρ. In this way we were to describe all the relevant phenomena in our cesium D_1-line system, such as the Zeeman effect in the tilted external field, the Larmor precession driven by an rf field, the optical pumping on the ground state level structure and the relaxation of the atomic polarization. We demonstrate that the narrowing of the magnetic resonance occurs already when the lower ground state manifold $F = I - 1/2$ gets depleted, but the effect gets maximized when additionally a significant orientation is generated within the upper ground state $F = I + 1/2$.

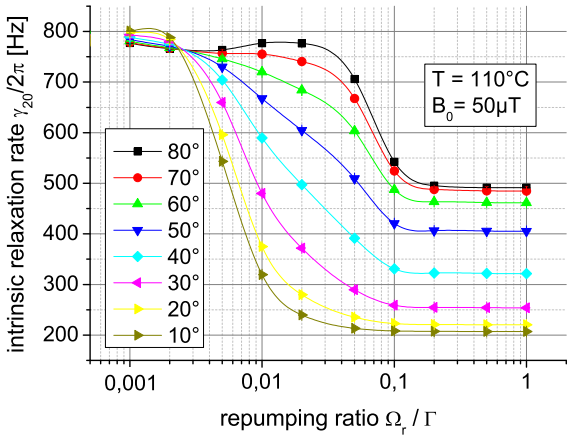

Fig. 1 Calculated dependence of the intrinsic relaxation rate γ_{20} on the tilting angle θ of the static magnetic field with respect to the laser beam for different values of repumping power (in terms of the ratio of the excited state relaxation rate Γ to repumping laser Rabi frequency Ω_r) at 110°C. Each data point is the result of an extrapolation to zero probe power.

References

[1] T. Scholtes, V. Schultze, R. IJsselsteijn, S. Woetzel, and H.-G. Meyer, *Light-narrowed optically pumped M_x magnetometer with a miniaturized Cs cell*, Phys. Rev. A **84**, 043416 (2011); A **86**, 059904(E) (2012).
[2] T. Scholtes, S. Woetzel, R. IJsselsteijn, V. Schultze, and H.-G. Meyer, *Intrinsic relaxation rates of polarized Cs vapor in miniaturized cells*, Appl. Phys. B **107**, 211 (2014).
[3] F. Grossetête, *Relaxation par collisions d'échange de spin*, J. Phys. (Paris) **25**, 383 (1964).

Double Differential Cross Sections of Simple Hydrocarbon Molecules with 50 and 100 eV Electron Impact

Zehra Nur Ozer[1], Murat Yavuz[1] Christophe Champion[2], Mevlut Dogan[1]

1. Afyon Kocatepe University, Department of Physics, e-COL Laboratory, Afyon, Turkey

2. Centre d'Etudes Nucléaires de Bordeaux Gradignan, Université Bordeaux, CNRS/IN2P3, Gradignan, France

Double differential cross sections (DDCSs) for electron impact ionisation of methane and acetylene have been measured in a crossed-beam experiment for primary energies of 50 and 100 eV. Angular distributions of the cross sections are presented for one of the outgoing electron after electron-molecule collision. Although it is impossible to determine with one detector which electrons of detected is the scattered or ejected one, DDCS experiments give very important results about the ionization process [1]. DDCS measurements are the fundamental studies to which other measurements may be related. The results are compared with the theoretical calculations obtained from the first Born approximation, using the one Coulomb wave model. The good agreement of experimental measurements with the theoretical calculations at intermediate energies demonstrates that the first Born Approximation is appropriate to describe the electron-methane molecule collisions at sufficiently high incident energies. For relatively small energies of the ejected electron the theory show a shift from the experiment. We assume that a more accurate description of the slower electrons make the theoretical formalism more accurate.

This work was supported by the AKU-BAP through grant 15.HIZ.DES.131.

References

[1] M. Dogan, M. Ulu, Z. N. Ozer, M. Yavuz, G. Bozkurt, *Double differential cross-sections for electron impact ionization of atoms and molecules*. Journal of Spectroscopy, **2013**,(2013).

E1-M2 interference effect on the polarization of the U^{91+} Lyman-α_1,β_1 lines emission following radiative recombination

Latifa Bettadj*[1], *Mohammed Réda Boufatah*[1], *Kemal Mokhtar Inal [1]

1. Laboratoire de Physique Théorique, Département de Physique, Universié de Tlemcen, 13000 Tlemcen, Algeria

We discuss, in this work, the E1-M2 multipole mixing effect on the polarization of each of the Lyman-α_1 ($2p_{3/2} \rightarrow 1s_{1/2}$) and Lyman-$\beta_1$ ($3p_{3/2} \rightarrow 1s_{1/2}$) lines emitted by the highly charged H-like U^{91+} ions after radiative recombination (RR) of U^{92+} with unidirectional, unpolarized electrons.
The calculations have been performed for incident-electron kinetic energies ε ranging from 0.01 to 10 times the electron binding energy in the $1s_{1/2}$ ground state E_{1s} and the radiative cascades following recombination into states with principal quantum number up to n=6 were included. Furthermore, the data for the effective RR cross sections used to get the degree of polarization of Lyman-α_1 and Lyman-β_1 lines were evaluated using two treatments. The first one is based on the electric-dipole approximation with nonrelativistic coulomb electron wavefunctions for both the continuum and bound states, where we have derived an original expression for the partial RR cross sections [1]. In the second treatment, we have used the exact relativistic formalism for the electron wavefunctions with all multipoles of the radiation field [2]. The figure below shows the obtained results of the degree of polarization of Ly-α_1 and Ly-β_1 lines as a function of reduced energy X for the emitting ions U^{91+}. One notes that the relativistic and multipole effects lead to an increase in the degree of polarization of the lines by about the same factor as in the pure E1 decay approximation. It can also be seen that the E1-M2 interference effect leads to a reduction in the degree of polarization estimated by about 11% to 15% for Ly-α_1 and 13% to 17% for Ly-β_1, depending slightly on the value of X and the treatment used (nonrelativistic dipole or exact relativistic).

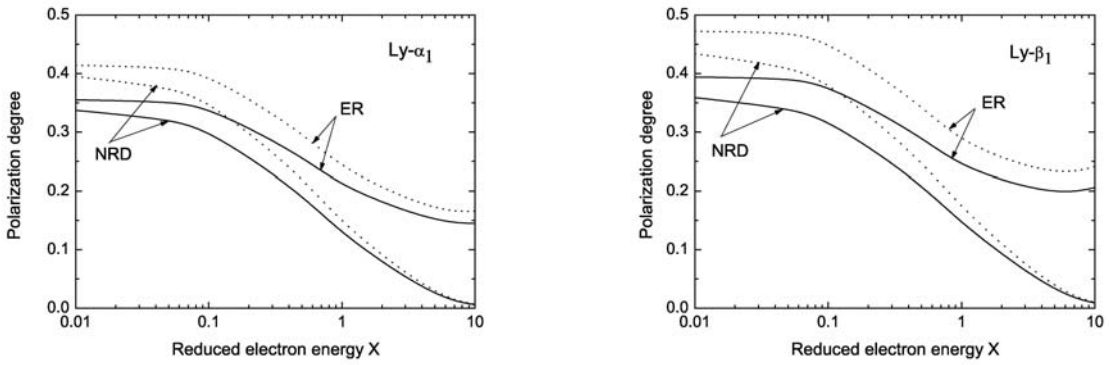

Fig. 1 Polarization degrees of the Ly-α_1 and Ly-β_1 lines emitted by the recombined H-like ions U^{91+} plotted against the reduced electron energy $X=\varepsilon/E_{1s}$ in the range 0.01-10. The results obtained using the nonrelativistic dipole (NRD) and exact relativistic (ER) calculations of the effective RR cross sections are shown. The dotted and solid lines correspond to values of the polarizations obtained assuming a pure E1 transition and those including E1-M2 multipole mixing, respectively.

References

[1] Latifa Bettadj, Mokhtar Kemal Inal and Mustapha. Benmouna, *Polarization of the Lyman line emission following radiative recombination of bare ions: effects of relativity and radiation multipoles*, J. Phys. B: At. Mol. Opt. Phys. **47**, 105205 (2014).

[2] Latifa Bettadj, Mokhtar Kemal Inal, Andrew Surzhykov and Stephan Fritzsche, *Effects of the radiative recombination on the intensity and polarization of the Ly-α emission of hydrogen-like ions*, Nuclear. Methods Phys. Res. B. **268**, 3509 (2010).

Potential Electron Scattering by the Sb_2 and Sb_4 Antimony Molecules

Shandor Demesh[1,2], Vladimir Kelemen[1], Eugene Remeta[1]

1. *Institute of Electron Physics, National Academy of Sciences of Ukraine, Universitetska St. 21, 88017 Uzhhorod, Ukraine*
2. *Institute for Nuclear Research of the Hungarian Academy of Sciences (ATOMKI), Bem tér 18/c, 4026 Debrecen, Hungary*

We used the optical potential approach [1] to calculate various cross-sections for e+Sb_n ($n = 2,4$) elastic scattering in the independent atom model (IAM) [2,3]. The local relativistic parameter-free real optical potential approximation (RSEP LA) is used for e+Sb scattering. It contains static, relativistic local exchange, polarization (local correlation-polarization), scalar-relativistic and spin-orbit potentials [1].

The differential cross section (DCS) for potential electron scattering by homonuclear molecules in the IAM framework is given: for a two-atomic molecule – $d\sigma_{\text{el}}/d\Omega = (2d\sigma_{\text{el,A}}/d\Omega)[1+\sin(sr_{nm})/sr_{nm}]$; for a four-atomic molecule (with the same interatomic distances $r_{nm} = r_0$) – $d\sigma_{\text{el}}/d\Omega = (4d\sigma_{\text{el,A}}/d\Omega)[1+3\sin(sr_0)/sr_0]$. Here $s = 2k\sin(\theta/2)$, θ – scattering angle, $k = \sqrt{2E}$ (in a.u.), E – electron energy, r_{nm} – distance between the atoms, $d\sigma_{\text{el,A}}/d\Omega$ – DCS for electron scattering by an individual atom. The r_{nm} interatomic distances are calculated by the GAMESS code (HF/CCSD method). Their values (in Å) for Sb_2: r_{12} = 2.5627 (NIST value – 2.3415); for Sb_4: $r_0 = r_{12} = r_{13} = r_{14} = r_{23} = r_{24} = r_{34}$ = 2.9081. Worth noting, that static-exchange approximation with the SMC method is used with pseudopotentials in [4] to calculate integral and differential cross sections for e+Sb_2 scattering.

We present the DCSs at 10, 20, 30 and 75 eV impact energies in Fig. 1, compared with the available theoretical [4] and experimental data [5]. Note, that the obtained DCSs at 20 and 30 eV have more structured angular dependencies then [4], while at 75 eV they agree well with the experimental data [5].

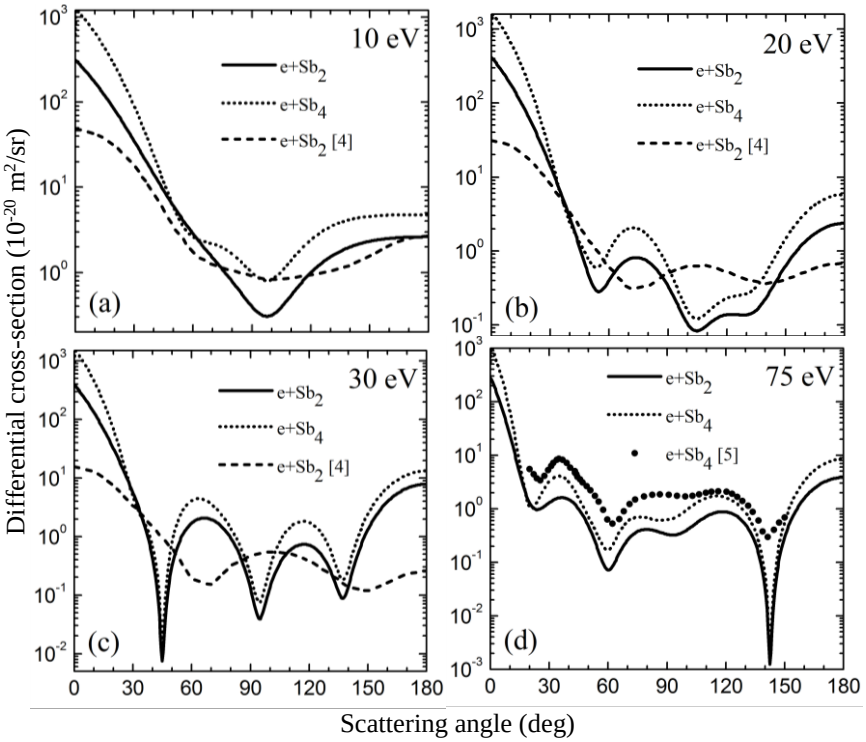

Fig. 1 Differential elastic cross sections for e+Sb_2 and e+Sb_4 scattering at 10 (a), 20 (b), 30 (c) and 75 (d) eV.

References

[1] Sh. Demesh, E. Remeta and V. Kelemen, *Elastic Electron Scattering on Molecule in Optical Potential Approach*, CEPAS-6 (Bratislava, Slovakia) 65 (2014).

[2] D. Raj, *A Note of the Use of the Additivity Rule for Electron-Molecule Elastic Scattering*, Phys. Lett. A **160**, 571 (1991).

[3] P. Możejko, B. Żywicka-Możejko and C. Szmytkowski, *Elastic Cross-Section Calculations for Electron Collisions with XY_4 (X=Si, Ge; Y=H, F, Cl, Br, I) molecules*, Nucl. Instr. Meth. B. **196**, 245 (2002).

[4] M.H.F. Bettega, M.A.P. Lima and L.G. Ferreira, *Low-Energy Electron Scattering by N_2, P_2, As_2 and Sb_2*, J. Phys. B. **31**, 2091 (1998).

[5] J. Kessler, H. Lorenz, H. Rempp und W. Büring, *Differentiele Wirkugsquerschnitte und Spinpolarisation für Elastische Streuung Langsamer Elektronen an Sb_4-Molekülen*, Z. Physik. **246**, 348 (1971).

Ionization by Electron Impact of CH_4, H_2O and NH_3 : A Sturmian Approach

Carlos M. Granados–Castro[1,2], **Lorenzo Ugo Ancarani**[1]
1. Équipe TMS, SRSMC UMR 7565, *Université de Lorraine,* 57078 *Metz, France*
2. Departamento de Física, Universidad Nacional del Sur, 8000 *Bahía Blanca, Argentina*

The Sturmian approach [1], using Generalized Sturmian Functions (GSF), has been applied successfully to study $(e,3e)$ [2] and $(\gamma,2e)$ [3] processes in helium. A first extension of the method to molecular systems has been developed in order to study single photoionization [4, 5]. In this contribution, we use the tool to look at ionization by electron impact of small molecules. In particular, we are interested in $(e,2e)$ processes on CH_4, NH_3 and H_2O under sufficiently asymmetrical kinematical conditions as to ignore exchange between the two escaping electrons.

One difficulty arising in the description of molecular ionization processes is the construction of accurate continuum states of the highly non-central target Hamiltonian. Contrary to bound states, which can be obtained with well established methods, continuum electrons are represented by functions oscillating up to infinity with specific boundary conditions. At large distances, an electron ejected from a molecule feels a positive unit charge, and this can be easily described using a GSF basis set having exactly that Coulomb outgoing behavior [5].

In this work we study $(e,2e)$ on molecules making the single active-electron approximation. The initial state is described by a one-electron wave function in the one-center expansion, calculated by Moccia [6]. A non-central molecular model potential [7] is used as scattering potential. The projectile-target interaction is described with a Coulomb potential, using the first-Born approximation. We solve the time-independent, first-order perturbative, Schrödinger equation, expanding the scattering wave function in a GSFs basis set. The adequate asymptotic behavior of all basis elements allows us to extract the transition amplitudes directly from the expansion coefficients [5], without requiring any evaluation of a matrix element. From the amplitudes, we calculate the triply-differential cross sections (TDCSs) for $(e,2e)$ processes. The random orientation of the target molecule is taken into account through an angular average of TDCSs over all possible spatial orientations of the molecule.

Our calculated TDCSs are compared with theoretical and relative experimental data. An example is shown in Figure 1 where all data are internormalized.

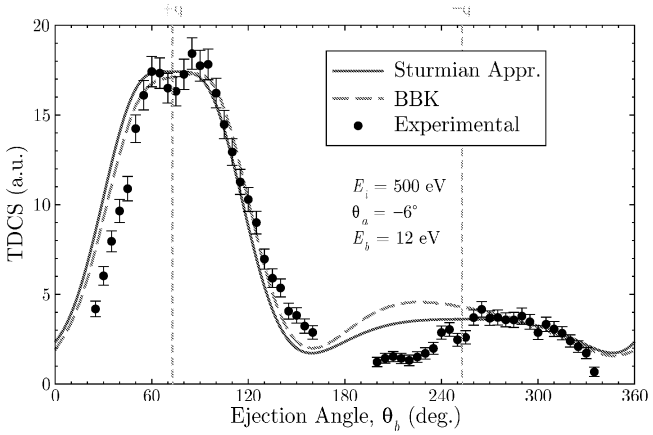

Fig. 1 Coplanar geometry TDCS for ionization from the $1t_2$ orbital of CH_4, for an incident energy $E_i = 500$ eV, an ejected electron with $E_b = 12$ eV, and a fast scattered electron in the $\theta_a = -6^0$ direction. Our results, using the Sturmian approach (solid line), are compared with a BBK calculation (dashed line) [8] and experimental data (points) [8].

References

[1] G. Gasaneo *et al*, *Three-Body Coulomb Problems with Generalized Sturmian Functions*, Adv. Quantum Chem. **57**, 153 (2013).
[2] M. J. Ambrosio *et al*, *Double Ionization of Helium by Fast Electrons with the Generalized Sturmian Functions Method*, J. Phys. B: At. Mol. Opt. Phys. **48**, 055204, (2015).
[3] J. M. Randazzo *et al*, *Double Photoionization of Helium: a Generalized Sturmian Approach*, Eur. J. Phys. D **69**, 189 (2015).
[4] C. M. Granados–Castro *et al*, *A Sturmian Approach to Photoionization of Molecules*, Adv. Quantum Chem. **73**, 3 (2016).
[5] C. M. Granados-Castro, *Application of Generalized Sturmian Basis Functions to Molecular Systems*, Ph.D. thesis, Université de Lorraine, Metz (2016).
[6] R. Moccia, *One-Center Basis Set SCF MO's. I. HF, CH_4 and SiH_4*, J. Chem. Phys. **40**, 2164 (1964); *[. . .] II. NH_3, NH_4^+, PH_3, PH_4^+* **40**, 2176 (1964); *[. . .] III. H_2O, H_2S and HCl* **40**, 2186 (1964).
[7] L. Fernández–Menchero and S. Otranto, *Single Ionization of CH_4 by bare ions: Fully Differential Cross Sections*, Phys. Rev. A **82**, 022712 (2010).
[8] A. Lahmam–Bennani *et al*, *Dynamics of Electron Impact Ionization of the Outer and Inner Valence ($1t_2$ and $2a_1$) Molecular Orbitals of CH_4 at Intermediate and Large Ion Recoil Momentum*, J. Phys. B: At. Mol. Opt. Phys. **42**, 165201 (2009)

Quasi Sturmian Basis for the Two-electron Continuum

Alexander S. Zaytsev[1], **Lorenzo Ugo Ancarani**[2], **Sergey A. Zaytsev**[1]
1. Pacific National University, Khabarovsk, 680035, Russia
2. Equipe TMS, SRSMC, UMR CNRS 7565, Université de Lorraine, 57078 Metz, France

The Coulomb three-body scattering problem is one of the most fundamental outstanding problems in theoretical atomic and molecular physics. Several *ab initio* methods have been and are being developed for constructing solutions (see, e.g., the review [1], and Introduction of (2]), the primary mathematical and numerical difficulty being the cumbersome boundary conditions the wave function should obey.

Some of the methods convert the problem into an inhomogeneous Schrödinger equation with a spatially confined driven term. This equation is solved within a box $\{r_1, r_2 \leq R\}$ with a sufficiently large length R (here r_1 and r_2 represent the electronic coordinates in, e.g., the two-electron continuum which arises as a final state in ionization processes). The exterior complex scaling method [3] allows the problem to be solved without explicit use of the asymptotic form of the wave function by recasting the original problem into a boundary problem with zero boundary conditions. In the generalized Sturmian appproach [4], one uses an expansion in terms of products of two one-particle generalized Sturmian functions with outgoing-wave boundary conditions set at the box border. The angular coupling builds up a three-body scattering solution with an hyperspherical wave front in the region Ω_0 where all interparticle distances are large.

The ionization problem also admits a formulation such that the transition amplitude calculations are performed with a finite set of square integrable one-particle functions of r_1 and r_2 (which corresponds to a box $\{r_1, r_2 \leq R\}$). In so doing accurate boundary conditions need not be imposed. For example, the convergent close coupling [1] method provides a correct result for the wave function in an 'internal' region in coordinate space. An alternative way to obtain the ionization amplitude is to calculate the two-electron continuum wave function in the asymptotic domain Ω_0. For example, the Coulomb-Sturmian separable expansion [5] and the J-matrix [6] methods deal with the wave function in the entire space using a Laguerre basis representation.

Recently [2], we proposed to describe a Coulomb three-body system continuum with a set of two-particle functions, which are built using so called Quasi Sturmian (QS) functions [7]. The latter satisfy a two-body inhomogeneous Schrödinger equation with a Coulomb potential and an outgoing-wave boundary condition, and possess the merit of having a closed form. The proposed two-particle basis functions, that we name Convoluted Quasi Sturmian (CQS) functions, are obtained, by analogy with Green's function of two non-interacting hydrogenic atomic systems, as a convolution integral of two one-particle QS functions (the analytic form of QS allows us to find an appropriate integration path that is useful for numerical calculations). The CQS have the following important characteristic: unlike a simple product of two one-particle functions, by construction, they look asymptotically (i.e., as the hyperradius $\rho \to \infty$) like a six-dimensional outgoing spherical wave.

In order to test the capacity of CQS basis functions to describe a Coulomb three-body scattering problem, we apply them to the double ionization of helium by high-energy electron impact in the framework of the Temkin-Poet model. Specifically, we endeavor to solve the $(e, 3e)$ driven equation proposed in [8] by expanding the solution in terms of CQS functions. Unlike the above mentioned *ab initio* methods, in our approach, the three-body problem is solved in the entire space rather than in a box. The Coulomb interelectronic interaction is not taken into account when constructing the CQS functions, so that they do not possess the correct asymptotic behavior in the region Ω_0. Such a formal inconsistency between the boundary conditions and the basis functions leads to a divergent expansion as the basis size increases. At the same time, we show that quite rapid convergence of the expansion can be obtained by multiplying the basis functions by an appropriate logarithmic-like phase factor corresponding to the interelectronic potential.

References

[1] I. Bray *et al.*, *Electron- and photon-impact atomic ionisation*, Phys. Rep. **520**, 135 (2012).
[2] A. S. Zaytsev, L.U. Ancarani, and S.A. Zaytsev, *Quasi Sturmian basis for the two-electron continuum*, Eur. Phys. J. Plus **131**, 48 (2016).
[3] C. W. McCurdy, M. Baertschy and T. N. Rescigno,*Solving the three-body Coulomb breakup problem using exterior complex scaling*, J. Phys. B **37**, R137 (2004).
[4] G. Gasaneo *et al.*, *Three-Body Coulomb Problems with Generalized Sturmian Functions*, Adv. Quantum Chem. **57**, 153 (2013).
[5] Z. Papp, C.-Y. Hu, Z. T. Hlousek, B. Kónya, and S. L. Yakovlev,*Three-potential formalism for the three-body scattering problem with attractive Coulomb interactions*, Phys. Rev. A **63**, 062721 (2001).
[6] M. S. Mengoue, M. G. Kwato Njock, B. Piraux, Yu. V. Popov, and S. A. Zaytsev,*Electron-impact double ionization of He by applying the Jacobi matrix approach to the Faddeev-Merkuriev equations*, Phys. Rev. A **83**, 052708 (2011).
[7] J. A. Del Punta, M. J. Ambrosio, G. Gasaneo, S. A. Zaytsev and L. U. Ancarani, *Non-homogeneous solutions of a Coulomb Schrödinger equation as basis set for scattering problems*, J. Math. Phys. **55**, 052101 (2014).
[8] G. Gasaneo, D. M. Mitnik, J. M. Randazzo, L. U. Ancarani and F. D. Colavecchia, *S-model calculations for high-energy-electron-impact double ionization of helium*, Phys. Rev. A **87**, 042707 (2013).

Evaluation of Cross Sections for Electron-atom Ionization Using the Quantum Flux and Bohm's Velocity Field

Juan Martín Randazzo[1,2], **Lorenzo Ugo Ancarani**[3], **Flavio Darío Colavecchia**[1,2]
1. División Física Atómica, Molecular y Óptica, Centro Atómico Bariloche, 8400 S. C. de Bariloche, Río Negro, Argentina.
2. Consejo Nacional de Investigaciones Científicas y Técnicas (Conicet), 8400 S. C. de Bariloche, Río Negro, Argentina.
3. Equipe TMS, SRSMC, UMR CNRS 7565, Université de Lorraine, 57078 Metz, France.

The quantum mechanical flux formula derived by R. Peterkop [1] for electron-hydrogen ionization cross sections is defined as the ratio between the emitted and incident particle flux. The incident one corresponds to the flux of the projectile in the prepared state, and is taken as known. The emitted flux is the one corresponding to the two final (projectile and "ionized") electrons, and is evaluated using the scattering state through the flux functional. The flux depends on the position of the two electrons' coordinates which locate them with respect to the atomic nucleus. While numerical scattering solutions are necessarily built on finite domains, cross sections are defined in the asymptotic region where the interaction between the electrons is weak. To obtain the ionization cross section as a function of the electrons final momenta, one makes the kinematical assumption $\mathbf{r} \to t\mathbf{k}$ (here t is time). This can be physically interpreted as a mapping from the quantum regime to the classical one which occurs in measurements [2].

The use of the flux procedure to evaluate Single Differential Cross Sections (SDCSs) in numerical calculations for s-wave models [3] showed good results except at the very unequal kinematical situations $k_i/k_j = r_i/r_j \to 0$ ($i \neq j$), where it has been said that contamination of the flux by discrete channels occurs. Thereafter, the flux formula has been abandoned for practical purposes.

In a classical investigation [4], we observed that at finite distances from the nucleus the kinematical assumption is not correct; the continuum electrons have to overcome the remaining potential energy to be completely free. We then proposed a finite distance reinterpretation of the standard energy fraction definition, and obtained well-behaved SDCSs.

In a more recent work [5], we explored an alternative way of defining the local momenta of the electrons by using the Bohm's velocity field. It was found that, for finite domains, the zero energy value for the velocity of one of the electrons is located in a region very different to the one predicted by the kinematical relation. Results for the SDCS with a new definition of the energy fraction are well behaved on the whole range, showing that the quantum mechanical flux formula can indeed be used.

In this contribution, we apply the modified quantum flux approach with local momenta to the electron impact ionization of hydrogen by considering the problem in its whole dimensionality, i.e., not only the s-wave term. We present results for the triple differential cross section, and compare results with other theories and experimental data for several incident energies.

References

[1] R. Peterkop, *Theory of ionization of atoms by electron impact* (Colorado Associated University Press, Boulder, 1977).
[2] John S. Briggs and James M. Feagin, *The generalised imaging theorem: autonomous quantum to classical transitions*, arXiv:1601.02588v1 (2016).
[3] M. Baertschy, T. N. Rescigno, W. A. Isaacs and C. W. McCurdy, *Benchmark single-differential ionization cross section results for the s-wave model of electron-hydrogen scattering*, Phys. Rev. A **60**, R13 (1999).
[4] Lorenzo Ugo Ancarani and Juan M. Randazzo, *SDCS quantum mechanical flux formula revisited for electron-hydrogen ionization*, J. At. Mol. Sci. **4**, 193 (2013).
[5] Juan M. Randazzo and Lorenzo Ugo Ancarani, *Modification of the quantum mechanical flux formula for electron-hydrogen ionization through Bohm's velocity field*, Phys. Rev. A **92**, 062706 (2015).

Ionization-excitation of Helium by Fast Electrons Using Generalized Sturmian Functions

Antonio I. Gómez[1,2], **Gustavo Gasaneo**[1,2], **Darío M. Mitnik**[2,3], **Marcelo J. Ambrosio**[2,3], **Lorenzo Ugo Ancarani**[4]

1. Departamento de Física, Universidad Nacional del Sur, 8000 Bahía Blanca,Buenos Aires, Argentina
2. Consejo Nacional de Investigaciones Científicas y Técnicas (CONICET), Argentina
3. Instituto de Astronomía y Física del Espacio (IAFE) and Universidad de Buenos Aires, C1428EGA Buenos Aires, Argentina
4. Equipe TMS, SRSMC, UMR CNRS 7565, Université de Lorraine, 57078 Metz, France.

In recent years the ionization–excitation process of Helium by fast electron impact has provided great challenges both for experimentalists and for theoreticians. In spite of significant advances in the understanding of this strongly correlated process, important discrepancies between the experimental data and theoretical calculations still can not be explained satisfactorily.

Recently the Generalized Sturmian Functions (GSF) method [1,2] helped towards resolving the controversy [3] for the Helium $(e,3e)$ process in the fast projectile and small momentum transfer regimes [4,5], presenting fully differential cross sections in complete agreement with those obtained by the Convergent Close Coupling [6] approach. This led us to explore other kinematic conditions.

In this contribution, we calculate the triply differential cross section (TDCS) of ionization–excitation of Helium in the strongly asymmetric kinematics used in the experiment performed by Dupré *et al.* [7] leaving the residual ion in the $n = 2$ excited state. In their coplanar experiment, the scattered electron energy was fixed at 5.5 keV and the values of the ejected electron energy were 5, 10, or 75 eV, with scattering angles 0.35° , 0.32° and 1°, respectively. In these kinematics, the amount of momentum transferred to the target is very small (large impact parameter), meaning that the dipolar or quasiphoton limit is approached.

The accurate solution of the corresponding four–body Schrödinger equation remains a formidable task from a numerical point of view. However, in the high-energy regime it is possible to reduce this problem to a three–body one, by keeping the first order of a series expansion of the exact solution. In previous works, we have shown that the three–body equivalent problem for the $(e,3e)$ ionization can be described by the time–independent Schrödinger equation [5,8,9]:

$$[E_a - h_{He}]\,\Phi^+_{sc}(\mathbf{r}_2,\mathbf{r}_3) = \frac{4\pi}{q^2}\frac{1}{(2\pi)^3}\left(-2 + e^{i\mathbf{q}\cdot\mathbf{r}_2} + e^{i\mathbf{q}\cdot\mathbf{r}_3}\right)\Phi_i(\mathbf{r}_2,\mathbf{r}_3). \tag{1}$$

Here the wave function $\Phi^+_{sc}(\mathbf{r}_2,\mathbf{r}_3)$ dictates the ionized electron dynamics, while $\Phi_i(\mathbf{r}_2,\mathbf{r}_3)$ is the $1s^2$ state of He, with Hamiltonian h_{He}, E_a is the energy of the ejected electrons and $\mathbf{q}$ is the momentum transferred to the target by the projectile. In order to calculate the wave function of the ground state of Helium, the single–continuum state and the scattering wave function, we use GSFs basis sets generated with their respective, adequate, asymptotic conditions. Thereafter, as it is typical of the GSF methodology, scattering amplitudes can be extracted directly from the asymptotic limit of each partial wave and, finally, TDCSs are calculated without requiring a matrix element evaluation.

References

[1] G. Gasaneo, L.U. Ancarani, D.M. Mitnik, J.M. Randazzo, A.L. Frapiccini and F.D. Colavecchia, *Three-Body Coulomb Problems with Generalized Sturmian Functions*, Adv. Quantum Chem. **67**, 153 (2013).
[2] D.M. Mitnik, F.D. Colavecchia, G. Gasaneo and J.M. Randazzo, *Computational Methods for Generalized Sturmians Basis*, Comp. Phys. Comm. **45**, 1145 (2011).
[3] L.U. Ancarani, C. Dal Cappello and G. Gasaneo, *Double Ionization of Two–Electron Systems*, J. Phys.: Conf. Ser. **212**, 012025 (2010).
[4] M.J. Ambrosio, F.D. Colavecchia, D.M. Mitnik and G. Gasaneo, *Discrepancy Between Theory and Experiment in Double Ionization of Helium by Fast Electrons*, Phys. Rev. A **91**, 012704 (2015).
[5] M.J. Ambrosio, F.D. Colavecchia, G. Gasaneo, D.M. Mitnik, and L.U. Ancarani *Double ionization of helium by fast electrons with the Generalized Sturmian Functions method*, J. Phys. B **48**, 055204 (2015).
[6] A. Kheifets, I. Bray, L. Bennani, A. Duguet and I. Taouil, *A comparative experimental and theoretical investigation of the electron-impact double ionization of He in the keV regime*, J. Phys. B **32** 5047 (1999).
[7] C. Dupré, A. Lahmam-Bennani, A. Duguet, F. Mota-Furtado, P.F. O'Mahony and C. Dal Cappello, *(e,2e) Triple Differential Cross Sections for the Simultaneous Ionization and Excitation of Helium*, J. Phys. B **25**, 259 (1992).
[8] G. Gasaneo, D.M. Mitnik, J.M. Randazzo, L.U. Ancarani and F.D. Colavecchia, *S-Model Calculations for High–Energy–Electron–Impact Double Ionization of Helium*, Phys. Rev. A **87**, 042707 (2013).
[9] M.J. Ambrosio, G. Gasaneo and F.D. Colavecchia, *Insights From the Zero–Angular–Momentum Wave in Single and Double Ionization of He by Fast Electrons*, Phys. Rev. A **89**, 012713 (2014).

À la carte sculpted potential energy surfaces based on purine and pyrimidine cores: from photostable DNA nucleobases to UVA chemotherapeutic agents

Inés Corral[1]

1. Departamento de Química, Universidad Autónoma de Madrid, Campus de Cantoblanco, C/ Francisco Tomás y Valiente, 7, 28049 Madrid, Spain

Canonical DNA and RNA nucleobases are naturally engineered biomolecules, sharing a common internal conversion mechanism that reverts the UV excited systems to the ground state, in ultrafast timescales. These systems owe their photostable properties to the characteristic topology of their excited potential energy surfaces, which lack of minima along the spectroscopic excited state minimum energy path connecting the Franck Condon region and the funnel for internal conversion. These sloped potentials minimize the time spent by the system in excited electronic states and therefore the probability of undergoing photochemical reactions or radiative emission. The landscape of the excited and ground potential energy surfaces is, however, very sensitive to both the nature and the pattern of substitution of the purine and pyrimidine aromatic cores. For instance, the positional isomer of canonical adenine, 2-aminopurine, or the thiosubstituted analogue of natural guanine, are respectively strongly fluorescent [1,2], and efficiently populate long-lived triplet states from which chemistry can occur [3].

In an attempt to understand how do electronic and structural factors imprint potential energy surfaces' topography and ultimately govern the photophysics and/or photochemistry of nucleobase derivatives, we have investigated the excited state dynamics of selected modified purine and pyrimidine bases, including purine heterocyclic core [4] and a series of thiosubstituted nucleobase analogues, among others [5,6]. Purine free base is a logical starting model to investigate whether the common core to all purine nucleobases is the structural key to ultrafast internal conversion and thus to photostability in guanine and adenine monomers, whilst carbonyl-by-thiocarbonyl substitution transposes the original photostable behavior of natural thiobases into a phototoxic response of which triplet states are responsible.

This presentation will overview the underlying deactivation mechanisms of a selected group of DNA nucleobase monomer derivatives and their correlation with the position and nature of the substituents of the core aromatic rings, supported by static and full dimensional photodynamical nonadiabatic surface-hopping simulations incorporating spin orbit couplings and femtosecond broadband transient absorption experiments.

References

[1] Edward L. Rachofsky, Roman Osman, and J. B. Alexander Ross, *Probing Structure and Dynamics of DNA with 2-Aminopurine: Effects of Local Environment on Fluorescence*, Biochemistry **40**, 946 (2001).

[2] Luis Serrano-Andrés, Manuela Merchán, and Antonio C. Borin, *Adenine and 2-aminopurine: Paradigms of modern theoretical photochemistry*, Proc. Nat. Acad. Sci. **103**, 8691 (2006)

[3] Christian Reichardt, Cao Guo, and Carlos E. Crespo-Hernández, *Excited-State Dynamics in 6-Thioguanosine from the Femtosecond to Microsecond Time Scale*, J. Phys. Chem. B **115**, 3263 (2011)

[4] Carlos E. Crespo-Hernández, Lara Martínez-Fernández, Clemens Rauer, Christian Reichardt, Sebastian Mai, Marvin Pollum, Philipp Marquetand, Leticia González, and Inés Corral, *Electronic and Structural Elements That Regulate the Excited-State Dynamics in Purine Nucleobase Derivatives*, J. Am Chem. Soc. **137**, 4368 (2015).

[5] Lara Martínez-Fernández, Inés Corral, Giovanni Granucci, and Maurizio Persico, *Competing ultrafast intersystem crossing and internal conversion: a time resolved picture for the deactivation of 6-thioguanine*, Chem. Sci. **5**, 1336 (2014).

[6] Lara Martínez-Fernández, Leticia González, and Inés Corral, *An ab initio mechanism for efficient population of triplet states in cytotoxic sulfur substituted DNA bases: the case of 6-thioguanine*, Chem. Comm. **48**, 2134 (2012).

Using Picosecond Photoelectron Imaging to Probe Intramolecular Dynamics in Polyatomic Molecules

Laura Whalley, Julia A. Davies, Katharine L. Reid
School of Chemistry, University of Nottingham, Nottingham NG7 2RD, United Kingdom

We have pioneered the use of picosecond time-resolved photoelectron imaging as a means of studying intramolecular dynamics [1-5]. This technique has a unique capability to provide insight into mechanisms of energy flow in a number of small aromatic molecules, as a consequence of an optimal combination of laser pulse duration and bandwidth. These not only exactly suit the processes under study, but also provide a good match with the best achievable photoelectron energy resolution. This energy resolution is optimised through use of the slow electron velocity map imaging (SEVI) technique pioneered by Neumark and coworkers [6]. Particular insight derives from comparative studies, which help us to establish the key factors that determine and control energy flow. These factors might include density of states, mode character, and unique characteristics of the vibrational energy level structure. Of further interest is the role of flexible side groups, such as methyl rotors, in facilitating dynamics [7-9].

In earlier work we studied excited-state intramolecular vibrational energy redistribution (IVR) dynamics following the excitation of a mode with predominantly C-CH_3 stretching character, and an internal energy of ~1200 cm^{-1}, in the three related molecules toluene, toluene-d_3 and *p*-fluorotoluene [5]. Temporal changes in the intensities of spectral features in each molecule showed the clear involvement of so-called "doorway" states in mediating the dynamics in toluene and toluene-d_3, but not in *p*-fluorotoluene.

In this talk we will explore these questions further, and will describe how the picosecond time-resolved photoelectron imaging technique has been used to study and compare the IVR dynamics that ensue following the excitation of two near-isoenergetic vibrational states in S_1 *p*-fluorotoluene. These states are labelled $13^1 1^1$ (lying at 1990 cm^{-1}) and $7a^1 1^1$ state (lying at 2026 cm^{-1}), where mode 1 has ring breathing character, mode 13 has C-CH_3 stretching character, and mode 7a has C-F stretching character. In both cases IVR lifetimes have been determined, and the dynamics are found to be mediated by a single strongly-coupled doorway state. These dynamics contrast with those observed following the preparation of the $7a^1 1^1$ state in the analogous *p*-difluorobenzene molecule, which lies at 2068 cm^{-1} [5]. Further comparison is made with studies of dynamics at lower internal energy in *p*-fluorotoluene by our group [2,3,5] and others [7].

References

[1] J. A. Davies, A. M. Green and K. L. Reid, *Deducing Anharmonic Coupling Matrix Elements from Picosecond Time-resolved Photoelectron Spectra*, Phys. Chem. Chem. Phys. **12**, 9872 (2010).
[2] J. A. Davies and K. L. Reid, *Elucidating Quantum Number-Dependent Coupling Matrix Elements Using PicosecondTime-Resolved Photoelectron Spectroscopy*, Phys. Rev. Lett. **109**, 193004 (2012).
[3] J. A. Davies and K. L. Reid, *Intramolecular Vibrational Dynamics in S_1 p-Fluorotoluene: Direct Observation of Doorway States*, J. Chem. Phys. **135**, 124305 (2011).
[4] J. Midgley, J. A. Davies and K. L. Reid, *Complex and Sustained Quantum Beating Patterns in a Classic IVR System: The $3^1 5^1$ Level in S_1 p-Difluorobenzene*, J. Phys. Chem. Lett. **5**, 2484 (2014).
[5] J. A. Davies, A. M. Green, A. M. Gardner, C. D. Withers, T. G. Wright and K. L. Reid, *Critical Influences on the Rate of Intramolecular Vibrational Redistribution: A Comparative Study of Toluene, Toluene-d_3 and p-Fluorotoluene*, Phys. Chem. Chem. Phys. **16**, 430 (2014).
[6] A. Osterwalder, M. J. Nee, J. Zhou and D. M. Neumark, *High Resolution Photodetachment Spectroscopy of Negative Ions via Slow Photoelectron Imaging*, J. Chem. Phys. **121**, 6317 (2004).
[7] D. B. Moss and C. S. Parmenter, *Acceleration of Intramolecular Vibrational Redistribution of Methyl Internal-Rotation - a Chemical Timing Study of p-Fluorotoluene and p-Fluorotoluene- d_3*, J. Chem. Phys. **98**, 6897 (1993).
[8] D.R. Borst, D.W. Pratt, *Toluene: Structure, Dynamics, and Barrier to Methyl Group Rotation in its Electronically Excited State. A Route to IVR*, J. Chem. Phys. **113**, 3658 (2000).
[9] D.S. Perry, G.A. Bethardy, X.-L. Wang, *The Effect of the Torsional Barrier Height on the Acceleration of Intramolecular Vibrational Relaxation (IVR) by Molecular Flexibility*, Ber. Bunsenges. Phys. Chem. **99**, 530 (1995).

Ethane, carbon tetrafluoride and 1,1-difluoroethylene illuminated via molecular frame photoelectron angular distributions following core ionization

A. Menssen[1], C.S. Trevisan[2], M.S. Schöffler[1], T. Jahnke[1], I. Bocharova[3], F. Sturm[3], N. Gehrken[1], B. Gaire[3], H. Gassert[1], S. Zeller[1], J. Voigtsberger[1], A. Kuhlins[1], A. Gatton[4], J. Sartor[4], D. Reedy[4], C. Nook[4], B. Berry[5], M. Zohrabi[5], A. Kalinin[1], A. Belkacem[3], R. Dörner[1], Th. Weber[3], A.L. Landers[4], T.N. Rescigno[3], C.W. McCurdy[3,6], J.B. Williams[1,7]

1. Institut für Kernphysik, J. W. Goethe Universität, Max-von-Laue-Str. 1, 60438 Frankfurt, Germany
2. Department of Sciences and Mathematics, California Maritime Academy, Vallejo, California 94590, USA
3. Lawrence Berkeley National Laboratory, Chemical Sciences, Berkeley, California 94720, USA
4. Department of Physics, Auburn University, Auburn, Alabama 36849, USA
5. JRM Laboratory, Kansas State University, Manhattan, KS 66506, USA
6. Department of Chemistry, University of California, Davis, California 95616, USA
7. Departnent of Physics, University of Nevada, Reno, Nevada, 89557, USA

Molecular frame photoelectron angular distributions (MFPADs) are measured in electron-ion momentum imaging experiments and compared with complex Kohn variational calculations for carbon K-shell ionization of carbon tetrafluoride (CF_4), ethane (C_2H_6) and 1,1-difluoroethylene ($C_2H_2F_2$)[1]. While in ethane the polarization averaged MFPADs show a tendency at low energies for the photoelectron to be emitted in the directions of the bonds, the opposite effect is seen in CF_4, as seen in Figure 1. A combination of these behaviors is seen in difluoroethylene where ionization from the two carbons can be distinguished experimentally because of their different K-shell ionization potentials, shown in Figure 2. Excellent agreement is found between experiment and simple static-exchange or coupled two-channel theoretical calculations.

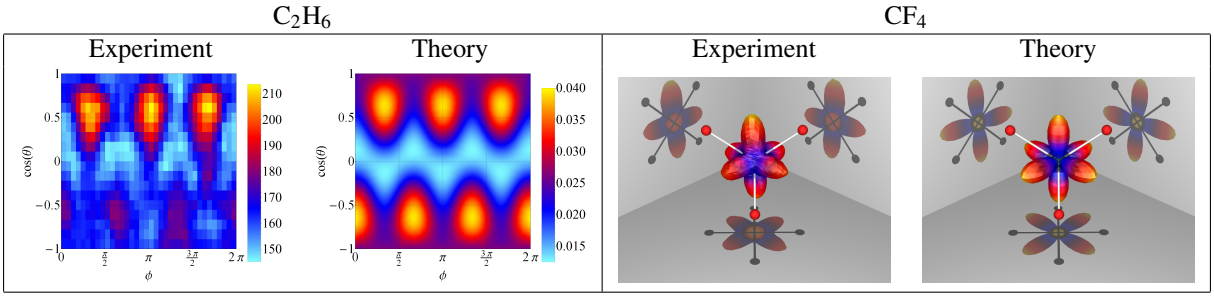

Figure 1: MFPAD for C_2H_6 (left panel) at 4.5 eV above the C 1s threshold from analysis of the experimental data assuming the three protons in the breakup channel $C_2H_6 + h\nu \rightarrow H^+ + H^+ + H^+ + \text{neutrals} + 3e^-$ originated from the same carbon atom and complex Kohn calculations at 4.35 eV. MFPAD for K-shell ionization of CF_4 (right panel). Experiment shows the observed photoelectron distribution measured in coincidence with $F^+ + F^+$ following Auger decay. Theory shows the MFPAD calculated using the complex Kohn variational method. Data and theory are integrated over all orientations of the polarization vector. The equilibrium molecular geometry is represented by the ball and stick models.

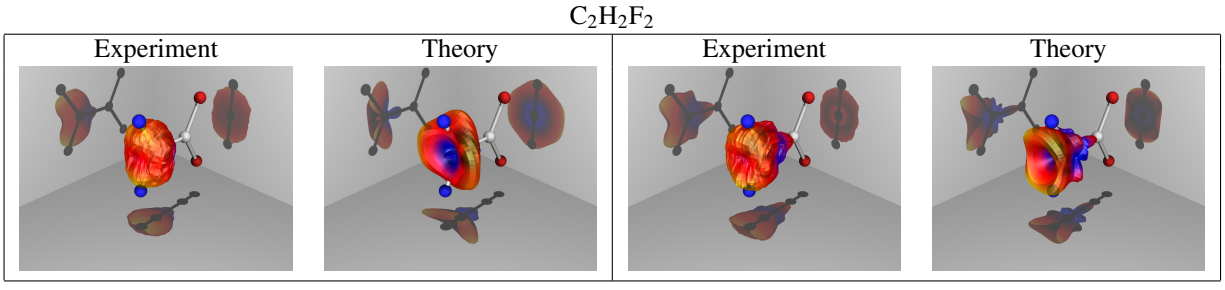

Figure 2: $C_2H_2F_2$ MFPADs of $C_2H_2F_2$ where the carbon on H_2 side was ionized in experiments performed at two different photon energies: $h\nu = 296$ eV and $h\nu = 301$ eV. Experiment: 4-6 eV (left) and 8-12 eV (right) photoelectrons. Theory: complex Kohn results at photoelectron energies of 5.44 eV (left) and 10.88 eV (right).

References

[1] Menssen, A, C S Trevisan, et al. *Molecular Frame Photoelectron Angular Distributions for Core Ionization of Ethane, Carbon Tetrafluoride and 1,1-Difluoroethylene.* J. Phys. B: 49, no. 5 (2016)

Electron Emission Processes in Atoms, Molecules, and Clusters upon Single-Photon Interaction: The Fluorescence Spectrometry View

Arno Ehresmann, Andreas Hans, Christian Ozga, Ltaief BenLtaief, Catmarna Küstner-Wetekam, Martin Pitzer, Martin Wilke, Xaver Holzapfel, Philipp Reiß, and Andre Knie

Institut für Physik and Center for Interdisciplinary Nanostructure Science and Technology (CINSaT), Universität Kassel, Heinrich- Plett-Str.40, 34132 Kassel, Germany

Electron emission following the interaction of single photons with atoms, molecules, and clusters, is considerably influenced by electron-electron interactions and by decay path and particle indistinguishability aspects. Related phenomena in the corresponding elementary processes have been experimentally investigated in the past mainly by a multitude of variants of photoelectron and photoion spectrometries (including different variants of coincidence spectrometries) after excitation by monochromatized synchrotron radiation. The spectrometry of electrons gives direct access to the relevant elementary electron emission processes. When such elementary processes have to be identified and quantified in denser systems (dense gases, clusters, liquids), however, the detection of electrons is less advantageous due to increasing electron-scattering events at surrounding matter after the elementary process has taken place.

Although the spectro- and polarimetry of dispersed fluorescence emitted from an excited ion state after an electron emission process is less straight forward experimentally as compared to electron spectrometry for the interpretation of electron emission processes, its application to identify elementary electron emission processes in denser systems seems to be promising as the escape depth of photons from dense media is longer than the one for electrons. Here we present examples of investigations on elementary electron emission processes initiated by photon interaction using dispersed fluorescence spectro- and polarimetry. Starting from comparably simple examples of elementary processes in individual-atom systems initiated by photon interaction the use of fluorescence spectrometry of target systems after interaction with monochromatized synchrotron radiation (one-photon experiments) will be demonstrated on increasingly complex target systems (molecules, clusters, liquids). In the experiments a focus is laid on quantitative results enabling a comparison to modern theoretical descriptions. In a prototype atomic system we will show the effect of a correlative suppression of "normal" photoelectron emission from a particular shell. The well-known Fano-resonance shape due to the interference of an autoionizing resonant state and a photoelectron continuum will then be shown as seen from fluorescence spectro-polarimetry [1]. A further degree of complexity is added in experiments with individual molecules, where the nuclear motion adds additional degrees of freedom. Examples of experiments on individual diatomic molecules will demonstrate interferences of electron emission from different electronic states, benchmark experiments on molecular hydrogen [2], and electron emission after resonant excitation of innershell states which do overlap due to their lifetime vibrational broadening [3].

Recent experiments on clusters will demonstrate that "(resonant) Interatomic/ Intermolecular Coulombic Decay" (rICD), an elementary electron emission process not present in individual atoms or molecules, may be also investigated by fluorescence spectrometry even on a quantitative basis [4]. The combination of electron and fluorescence spectrometry enables the determination of quantitative photon emission probabilities as functions of cluster size. Finally first efforts towards investigations of elementary electron emission processes in liquids using fluorescence spectrometry will be shown [5].

References

[1] Boris M Lagutin, Ivan D Petrov, Victor L Sukhorukov, Sven Kammer, Sascha Mickat, Rüdiger Schill, Karl-Heinz Schartner, Arno Ehresmann, Yuri A Shutov, and Hans Schmoranzer, *Raman Regime Energy Dependence of Alignment and Orientation of KrII States Populated by Resonant Auger Effect*, Phys. Rev. Lett. **90**, 073001 (2003)

[2] Michele Glass-Maujean, Christian Jungen, Hans Schmoranzer, Andre Knie, Irina Haar, Rainer Hentges, Witoslaw Kielich, Kari Jänkälä, and A. Ehresmann, *H_2 Superexcited States: Experimental and Theoretical Characterization of their Competing Decay-Channel Fluorescence, Dissociation, and Ionization*, Phys. Rev. Lett. **104**, 183002 (2010).

[3] Arno Ehresmann, Witoslaw Kielich, Lutz Werner, Philipp V Demekhin, Dmitri V Omel'yanenko, Victor L Sukhorukov, K.-H. Schartner, and H. Schmoranzer, *Lifetime vibrational interference during the NO $1s^{-1}\pi^*$ resonant excitation studied by the $NO^+(A\,^1\Pi \rightarrow X\,^1\Sigma^+)$ fluorescence,* Europ. J. Phys. D **45**, 235 (2007)

[4] André Knie, Andreas Hans, Marko Förstel, Uwe Hergenhahn, Philipp Schmidt, Philipp Reiß, Christian Ozga, Benjamin Kambs, Florian Trinter, Jörg Voigtsberger, Daniel Metz, Till Jahnke, Reinhard Dörner, Alexander I Kuleff, Lorenz S Cederbaum, Philipp V Demekhin and Arno Ehresmann, *Detecting ultrafast interatomic electronic processes in media by fluorescence*, New. J. Phys. **16**, 102002 (2014).

[5] Andreas Hans, Andre Knie, Philipp Schmidt, Ltaief Ben Ltaief, Christian Ozga, Philipp Reiß, Henning Huckfeldt, Marko Förstel, Uwe Hergenhahn, and Arno Ehresmann, *Lyman-series emission after valence and core excitation of water vapor*, Phys. Rev. A. **92**, 032511 (2015).

Light storage based on Coherent Population Oscillations

Marie-Aude Maynard[1], Pascal Neveu[1], Jasleen Lugani[1], Chitram Banerjee[1], Rupamanjari Ghosh[2,3], Fabien Bretenaker[1], Etienne Brion[1], Fabienne Goldfarb[1]

1. Laboratoire Aimé Cotton, CNRS, Univ. Paris-Sud, ENS Cachan, Université Paris-Saclay, 91405 Orsay Cedex, France
2. Shiv Nadar University Gautam Buddha Nagar, UP 201 314, India
3. School of Physical Sciences, Jawaharlal Nehru University, New Delhi 110067, India

In recent years, a great effort has been put to design different types of quantum memories. Most of the techniques developed so far – such as Electromagnetically Induced Transparency (EIT) storage – rely on the excitation of a long lived coherence between two atomic levels [1]. As the signal is mapped onto a coherence, these existing memories are very sensitive to dephasing effects.

Coherent population oscillations (CPO) is a phenomenon very different from EIT. It is a dynamical saturation, which occurs in a two level system (TLS) and gives rise to a resonance with a width limited by the decay rate of populations of the upper level. In a Λ system (where two ground states are optically coupled to the same excited level), a ultranarrow CPO resonance due to population exchanges between the two lower levels can appear. The width is then limited by the population decay rates of these ground states [2]. We report here the experimental demonstration of CPO based storage in such a Λ system. The experiment is performed with metastable helium atoms at room temperature [3]. As CPO storage does not rely on the excitation of atomic coherence, it is robust to magnetic field gradients. Storage efficiencies are much higher than what was expected from a theoretical proposal in a two-level system that decays via a shelving state [4]. CPO based storage was later observed in Cesium vapor [5] and then used to store orbital angular momenta [6].

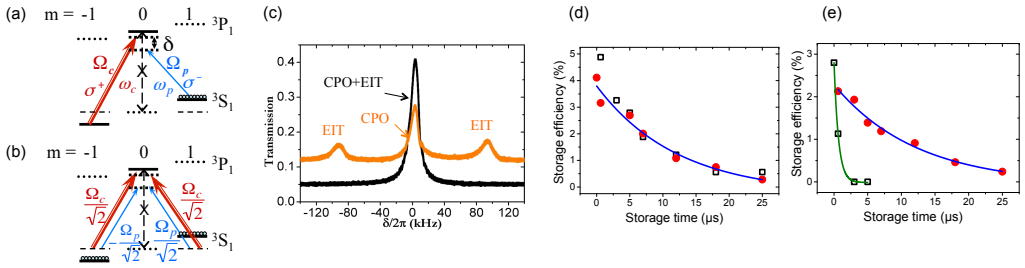

Fig. 1 On the D1 line of metastable helium, two configurations can be studied with circular (a) or linear (b) coupling and probe beams. In the first case, δ is the Raman detuning, while in the latter $\delta = \omega_c - \omega_p$ is the coupling-probe frequency detuning. (c): Resonances obtained without (black) and with (orange) a magnetic field that can lift the Zeeman sub level degeneracy. In the latter cas, both transmission resonances at $\delta \simeq \pm 90$ kHz are Raman resonances for Λ subsystems. But the central resonance does not correspond to any Raman resonance: it is due to the transfer of coherent population oscillations in CPOs between the ground state levels of the Λ-system. (d): experimental EIT (black open squares) and CPO (red circles) storage efficiencies obtained with a magnetic shielding, which protects the cell from stray fields. (e): experimental EIT (black open squares) and CPO (red circles) storage efficiencies obtained with magnetic field inhomogeneities. The EIT memory lifetime is strongly decreased, while the CPO memory lifetime remains similar to the previous case.

We have recently performed numerical simulations based on optical Bloch equations and wave propagation equations, which show that the signal is mapped onto population oscillations during the storage time. These simulations confirm the robustness of CPO-based storage to dephasing effects: we analyzed the evolution of storage efficiencies versus storage time in CPO and EIT storage configurations and we obtained exactly the same values of CPO storage efficiencies in both experimental cases whereas, as expected and observed experimentally, the time constant associated with the decay rate of EIT storage efficiencies is much smaller in the presence of magnetic field gradients.

References

[1] Novikova, R. L. Walsworth, and Y.Xiao, *Electromagnetically induced transparency-based slow and stored light in warm atoms*, Laser Photonics Rev. **6**, 333–353 (2012).
[2] T. Lauprêtre, S. Kumar, P. Berger, R. Faoro, R. Ghosh, F. Bretenaker, and F. Goldfarb, *Ultranarrow resonance due to coherent population ooscillations in a Λ-type atomic system*, Phys. Rev. A **85**, 051805 (2012).
[3] A. Eilam, I. Azuri, A. V. Sharypov, A. D. Wilson-Gordon, and H. Friedmann, *Spatial optical memory based on coherent population oscillations*, Science Optics Lett.**35**, 772 (2010).
[4] M.-A. Maynard, F. Bretenaker, and F. Goldfarb, *Light storage in a room-temperature atomic vapor based on coherent population oscillations*, Phys. Rev. A **90**, 061801(R) (2014).
[5] A.J.F. de Almeida, J. Sales, M.-A. Maynard, T. Lauprêtre, F. Bretenaker, F. Goldfarb, and J. W. R. Tabosa, *Light storage via coherent population oscillation in a thermal cesium vapor*, Phys. Rev. A **90**, 043803 (2014).
[6] A.J.F. de Almeida, S. Barreiro, W. S. Martins, R. A. de Oliveira, D. Felinto, L. Pruvost, and J. W. R. Tabosa, *Storage of orbital angular momenta of light via coherent population oscillation*, Opt. Lett. **90**, 2545–2548 (2015).

Quantum optimal control theory with realistic laser pulses

Esa Räsänen[1], **Janne Solanpää**[1], **Marcelo Ciappina**[2]
1. Department of Physics, Tampere University of Technology, FI-33101 Tampere, Finland
2. Max-Planck-Institut für Quantenoptik, DE-85748 Garching, Germany

Laser pulses can be tailored in the optimal control framework to achieve a desired effect in the system of interest. Several different systems have been studied ranging from atoms and molecules to nanostructures with applications from molecular bond breaking to qubits [1]. The optimized driving lasers have usually been constrained by some maximum frequency and either by the maximum peak intensity or fluence. However, experimental synthesis of tailored pulses is usually done by mixing a few different spectral bands [2].

Here we propose an optimization scheme [3] to produce experimentally realizable laser pulses. We take up to three component pulses each with a certain (possibly overlapping) spectral shape. The components are combined by optimizing their amplitudes, carrier-envelope phases, and time delays. In addition, we set constraints to the peak amplitude and fluence of the total pulse.

We demonstrate our scheme for the optimization of photoelectron emission in a one-dimensional hydrogen model. As shown in Fig. 1, The fully optimized driving laser (blue) with a moderately low fluence and peak intensity achieves a major cutoff extension and yield enhancement. We also test the strategy for the optimization of the high-harmonic generation, which previously has been studied with less strict constraints [4].

Our optimization code can use any existing software for the time propagation and for the physical quantities to be optimized. In the future, this will make it easy to extend to three-dimensional and many-electron models, and to other targets in strong-field physics and femtochemistry.

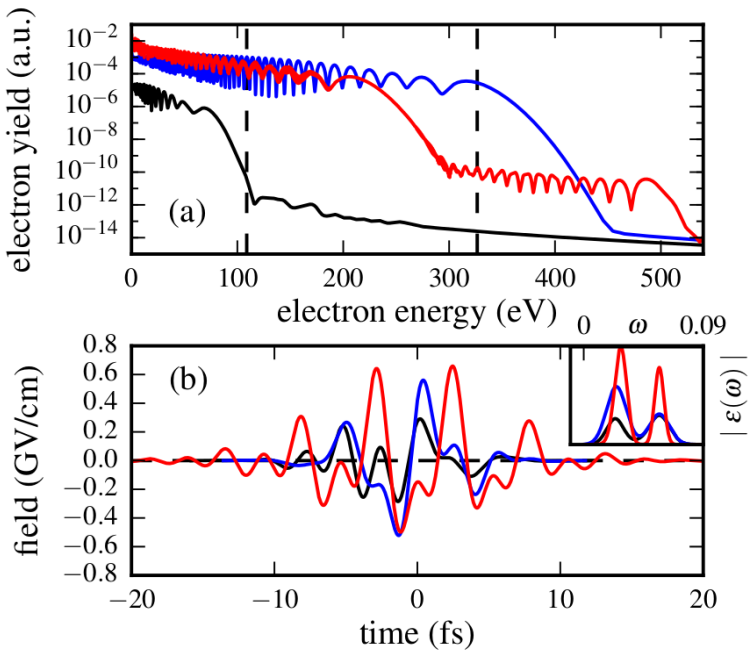

Fig. 1 Photoelectron spectra (a) and the corresponding laser pulses (b) and their spectral composition [inset of (b)] for the initial (black) and two optimized pulses (blue and red). The optimized pulse plotted in blue reaches completely the target range indicated by vertical dashed lines in (a), even though it has a lower fluence and peak intensity than the pulse plotted in red.

References

[1] For a review, see, e.g., C. Brif, R. Chakrabarti, and H. Rabitz, New J. Phys. **12**, 075008 (2010).
[2] A. Wirth *et al.*, Science **334**, 195 (2011); H. Fattahi *et al.*, Optica **1**, 45 (2014).
[3] J. Solanpää, M. Ciappina, and E. Räsänen, submitted (2016).
[4] J. Solanpää, J. A. Budagosky, N. I. Shvetsov-Shilovski, A. Castro, A. Rubio, and E. Räsänen, Phys. Rev. A **90**, 053402 (2014).

Direct Excitation of Butterfly States in Rydberg Molecules

Carsten Lippe[1], **Oliver Thomas**[1,2], **Thomas Niederprüm**[1], **Tanita Eichert**[1], **Herwig Ott**[1]

1. Department of Physics and Research Center OPTIMAS, Technische Universität Kaiserslautern, Erwin-Schrödinger-Straße 46, 67663 Kaiserslautern, Germany

2. Graduate School Materials Science in Mainz, Gottlieb-Daimler-Straße 47, 67663 Kaiserslautern, Germany

Since their first theoretical prediction Rydberg molecules have become an increasing field of research. These exotic states originate from the binding of a ground state atom in the electronic wave function of a highly-excited Rydberg atom mediated by a Fermi contact type interaction. A special class of long-range molecular states, the butterfly states, were first proposed by Greene et al. [1]. These states arise from a shape resonance in the p-wave scattering channel of a ground state atom and a Rydberg electron and are characterized by an electron wavefunction whose density distribution resembles the shape of a butterfly.

We report on the direct observation of deeply bound butterfly states of Rydberg molecules of ^{87}Rb. The butterfly states are studied by high resolution spectroscopy of UV-excited Rydberg molecules. We find states bound up to $-50\,\mathrm{GHz}$ from the $25\mathrm{P}_{1/2}, F = 1$ state, corresponding to binding lengths of $50\,a_0$ to $500\,a_0$ and with permanent electric dipole moments of up to 500 Debye. This distinguishes the observed butterfly states from the previously observed long-range Rydberg molecules in rubidium.

References

[1] Chris H. Greene, A. S. Dickinson, H. R. Sadeghpour, *Creation of Polar and Nonpolar Ultra-Long-Range Rydberg Molecules*, Phys. Rev. Lett. **85**, 2458 (2000).

Antiproton energy loss distribution in He gas

Sándor Borbély[1], Iva Brezinova[2], Stefan Nagele[2], Fabian Lackner[2], Ladislau Nagy[1], Károly Tőkési[3,4], Joachim Burgdörfer[2]

1. Faculty of Physics, Babeş-Bolyai University, 400084 Cluj-Napoca, Romania, EU
2. Institute for Theoretical Physics, Vienna University of Technology, 1040 Vienna, Austria, EU
3. Institute of Nuclear Research, Hungarian Academy of Sciences (ATOMKI), P.O. Box 51, H-4001 Debrecen, Hungary, EU
4. ELI-ALPS, ELI-HU Non-profit Ltd., Dugonics tér 13, H-6720 Szeged, Hungary, EU

Several aspects of the penetration of charged particles in matter have been studied over the last more then hundred years. Triggered by the pioneering work of Bohr [1-2] the energy loss mechanisms of charged particles penetrating matter were investigated extensively both theoretically and experimentally. A comprehensive overview of these studies can be found in reference [3]. The primary parameter describing the stopping of charged particles in matter is the mean energy loss per traveled path-length (or alternatively by the stopping cross section). Additional information on the stopping process is provided by the straggling, which is the mean squared deviation of the energy loss per traveled path-length (or straggling cross section). Even at the level of these integrated quantities the discrepancies between the experiments and theoretical calculations are quite large (see in [4]). In order to resolve the existing discrepancies new high precision calculations for prototypical systems are required. A good starting point for such a calculation is our *ab initio* approach [5], which solves the fully-correlated two-electron time-dependent Schrödinger equation for the antiproton-He collision. At fixed $E_{\bar{p}}$ antiproton impact energies and b impact parameters our calculation provides high precision $P_{i\to f}(E_{\bar{p}},b)$ transition probabilities from the Ψ_i ground state to the Ψ_f final state. As final channels the single excitation, single ionization and double ionization are considered. From these probabilities the antiproton energy, and impact parameter dependent stopping power is calculated as

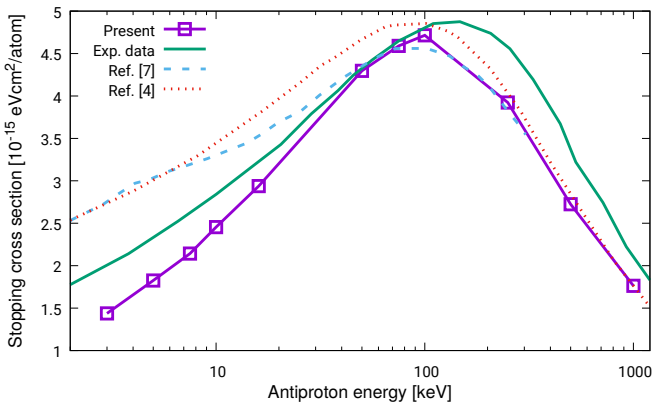

Fig. 1 The present stopping cross sections compared to the experimental data by Agnello *et al.* [6] and to other theoretical data by Lühr *et al.* [4] and Schiwietz *et al.* [7].

$$S(b,E_{\bar{p}}) = \sum_f P_{i\to f}(E_{\bar{p}},b)\left[E_f - E_i\right], \tag{1}$$

while the straggling as

$$T(b,E_{\bar{p}}) = \sum_f P_{i\to f}(E_{\bar{p}},b)\left[E_f - E_i - S(b,E_{\bar{p}})\right]^2. \tag{2}$$

Total stopping and straggling cross sections are calculated by performing the impact parameter integrations. Calculations were performed for antiproton impact energies ranging from 3keV up to 1MeV, and the obtained stopping cross sections are shown in Fig.1 along with the experimental data of Agnello *et al.* [6] and the theoretical predictions of Lühr *et al.* [4] and Schiwietz *et al.* [7]. At high antiproton energies the agreement between the theories and the experimental data is good, while at low antiproton energies notable discrepancies are present. Since the present results are based on fully-correlated two-electron *ab initio* calculations, they can provide a benchmark for approximate calculations.

References

[1] Niels Bohr, *On the theory of the decrease of velocity of moving particles on passing through matter*, Philos. Mag. **25**, 10 (1913).
[2] Niels Bohr, *On the decrease of velocity of swiftly moving electrified particles is passing through matter*, Philos. Mag. **30**, 581 (1915).
[3] Peter Sigmund *Particle penetration and radiation effects*, Springer Series in Solid-State Sciences, Vol. 151 (Springer, Berlin, 2006).
[4] Armin Lühr and Alejandro Saenz, *Stopping power of antiprotons in H, H_2 and He targets* Phys. Rev. A **79** 042901 (2009).
[5] S. Borbély, J. Feist, K. Tőkési, S. Nagele, L. Nagy, and J. Burgdörfer, *Ionization of helium by slow antiproton impact: Total and differential cross sections* Phys. Rev. A **90** 052706 (2014).
[6] M. Agnello et al., *Antiproton slowing down in H_2 and He and evidence of nuclear stopping power* Phys. Rev. Lett. **74** 371 (1995).
[7] G. Schiwietz, U. Wille, R. Díez Muino, P. D. Fainstein and P. L. Grande, *Comprehensive analysis of the stopping power of antiprotons and negative muons in He and H_2 gas targets* J. Phys. B **29** 307 (1996).

Quantum Cheshire Cat

Daniel Rohrlich
Physics Department, Ben-Gurion University of the Negev, Beersheba 8410501, Israel

Weak values, conceived and developed by Yakir Aharonov and co-workers [1], show us a quantum world that is both stranger and freer than we ever imagined – a world in which particles can carry negative kinetic energy [2] or travel faster than light [3], and in which a cat and its grin [4] (or a neutron and its magnetic moment [5]) can part ways. Yet there is nothing fanciful or subjective about weak values: they are actual results of non-intrusive measurements on pre- and post-selected ensembles (ensembles that manifest microscopic time-reversal symmetry) [6]. Experiments have shown practical applications of weak values, such as amplification and noise reduction [7]. I will focus on three weak value effects: the quantum Cheshire Cat (in which the smile of the Cat takes one arm of an interferometer while the Cat itself takes the other); an analysis of the Cat's current (in which a quantum current carries spin but not mass); and quantum violation of the pigeonhole principle (showing how three charges can pass through the two arms of an interferometer without ever taking the same arm) [8]. These effects take us by surprise, but they are just the more unexpected examples of weak values that may arise in the most mundane ways in *series* of measurements.

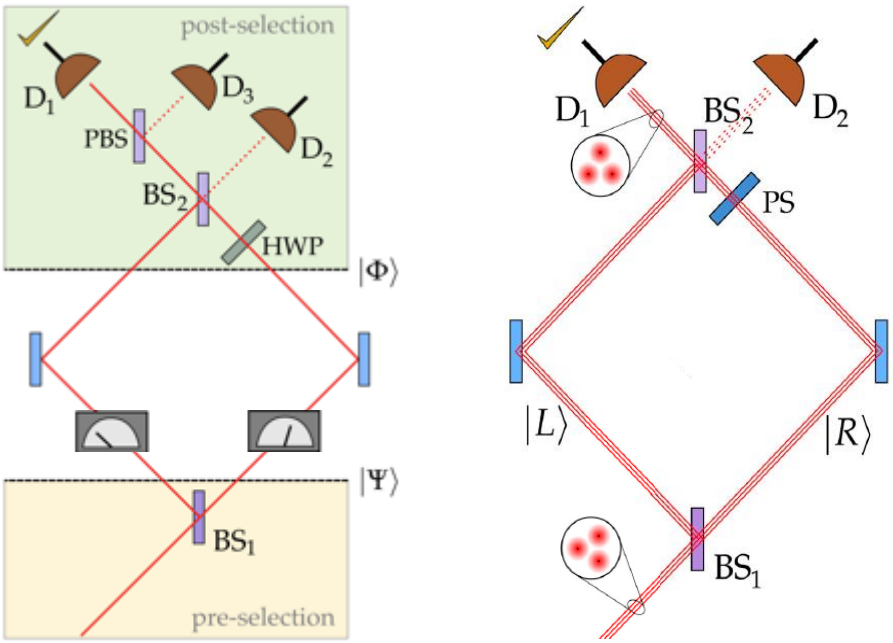

Fig. 1(a) The Quantum Cheshire Cat with pre- and post-selected photon states. The dials check for the intermediate smile (polarization) and passage of Cats (photons). **(b)** Quantum violation of the pigeonhole principle. At least two of the three charged particles must take the same arm of the interferometer, yet they do not repel each other.

References

[1] Y. Aharonov, D. Z. Albert and L. Vaidman, *How the result of a measurement of a component of the spin of a spin- 2 particle can turn out to be 100*, Phys. Rev. Lett. **60**, 1351 (1988).
[2] Y. Aharonov, S. Popescu, D. Rohrlich and L. Vaidman, *Measurements, errors, and negative kinetic energy*, Phys. Rev. A **48**, 4084 (1993).
[3] D. Rohrlich and Y. Aharonov, *Cherenkov radiation of superluminal particles*, Phys. Rev. A **66**, 042102 (2002).
[4] Y. Aharonov, S. Popescu, D. Rohrlich and P. Skrzypczyk, *Quantum Cheshire Cats*, New J. Phys. 15, 113015 (2013); Y. Aharonov, E. Cohen and S. Popescu, *A current of the Cheshire Cat's smile: dynamical analysis of weak values*, arXiv:1510.03087v1.
[5] T. Denkmayr et al. *Observation of a quantum Cheshire Cat in a matter-wave interferometer experiment*, Nat. Commun. **5**, 4492 (2014).
[6] Y. Aharonov and D. Rohrlich, Quantum Paradoxes: Quantum Theory for the Perplexed (Wiley VCH, Weinheim), 2005.
[7] O. Hosten and P. G. Kwiat, *Observation of the spin Hall effect of light via weak measurements*, Science **319**, 787 (2008); P. B. Dixon, D. J. Starling, A. N. Jordan and J. C. Howell, *Ultrasensitive beam deflection measurement via interferometric weak value amplification*, Phys. Rev. Lett. **102**, 173601 (2009).
[8] Y. Aharonov, F. Colombo, S. Popescu, I. Sabadini, D. C. Struppa and J. Tollaksen, *Quantum violation of the pigeonhole principle and the nature of quantum correlations*, Proc. Nat. Acad. Sci. **113**, 532 (2016).

Photon and Ion Collisions with Complex Molecular Systems

Paola Bolognesi*[1], Antonella Cartoni[2,1], AnnaRita Casavola[1], Mattea C. Castrovilli[1], Rudy Delaunay[3], Alicja Domaracka[3], Bernd A. Huber[3], Jaroslav Kocisek[3], Sylvain Maclot[3], Pal Markus[1], Bratislav Marinkovic[4], Patrick Rousseau[3], Sanja Tosic[4], Lorenzo Avaldi[1]

1. *CNR-ISM, Area della Ricerca di Roma 1, 00015 Monterotondo Scalo (Roma), Italy*
2. *Dipartimento di Chimica, Sapienza Università di Roma, 00185 Roma, Italy*
3. *Normandie Université - CIMAP - UMR 6252 CEA/CNRS/ENSICAEN/UNICAEN, - 14070 Caen cedex 5 – France*
4. *Institute of Physics, University of Belgrade, Belgrade, Serbia*

Gas phase studies of molecules of biological interest [1] represent the most suitable approach to disentangle the intrinsic properties of the molecules from those due to the interaction with the environment. Electron and ion spectroscopic techniques combined with ab-initio calculations and DFT methods provide detailed information on the molecular structure and the dynamics of interaction with the ionising radiation. This approach allows to probe and to understand the basic mechanisms of radiation damage in elementary biomolecules, for example DNA/RNA bases, as well as how radiosensitiser molecules that, used in conjunction with radiotherapy, provide a more selective approach for cancer treatment.

Tunable synchrotron radiation at Elettra (Trieste) [2-4] and multiply charged ion beams at GANIL (Caen) [4,5] have been used to perform electron photoemission, mass spectrometry, electron-ion and ion-ion coincidence experiments on biomolecules of increasing complexity. This has been achieved either moving from simple targets as DNA bases [4] to larger biomolecules, as for example nucleosides, or embedding the biomolecule in a cluster or hydrated cluster (see Fig. 1, ref. 5) to mimick a 'realistic' environment which affects its properties and behaviour.
The results of these experiments together with theoretical calculations that support their interpretation will be reviewed in the presentation.

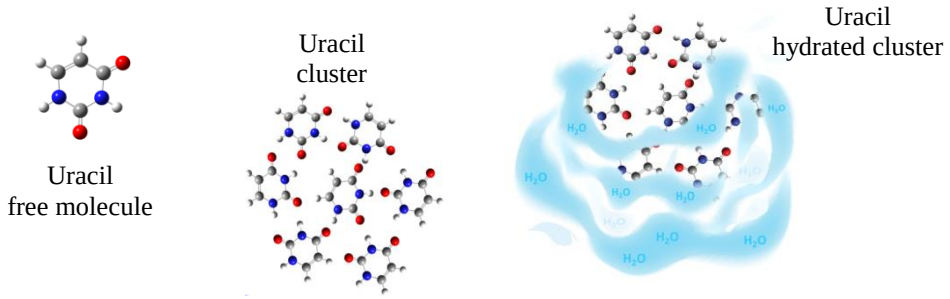

Fig. 1 A biological system of increasing complexity, moving from isolated Uracil to a pure and nano-hydrated cluster of Uracil molecules [5], allows to assess the role played by the environment on the intrinsic properties of the single biomolecule.

Acknowledgements.
This work is partially supported by the Serbia – Italy (PGR00220) Joint Research Project '*A nanoview of radiation-biomatter interaction*', the COST Action XLIC (CM1204) and the MIUR FIRB No. RBFR10SQZI project 2010. The staff of GasPhase and CiPo beamlines of ELETTRA as well as at the ARIBE beamline of GANIL is acknowledged for technical support.

References

[1] Prince Kevin C. et al., *J. Electron Spectrosc. Relat. Phenom.* **204**, 335 (2015).
[2] Castrovilli Mattea C. et al., *J. Am. Soc. Mass Spectrom*. **25**, 351 (2014).
[3] Bolognesi Paola et al., *Phys.Chem.Chem.Phys*.**17**, 24063 (2015).
[4] Maclot Sylvain et al, submitted to *Phys Rev. Lett.* (2016).
[5] Markus Pal et al, submitted to *Phys. Chem. Chem. Phys.* (2016).

Quantification of electron and photon induced DNA Damage using DNA Nanotechnology

Ilko Bald[1,2], Jenny Rackwitz[1], Robin Schürmann[1,2], Stefanie Vogel[1], Kenny Ebel[1]

1. *University of Potsdam, Institute of Chemistry – Physical Chemistry, Karl-Liebknecht-Str. 24-25, 14476 Potsdam, Germany*
2. *BAM Federal Institute of Materials Research and Testing, Richard-Willstätter-Straße 11, 12489 Berlin, Germany*

High-energy radiation is routinely used to treat cancer in combination with radiosensitizing therapeutics such as halogenated nucleosides. The treatment relies on an accurate modeling of DNA radiation damage, which is to a large extent ascribed to the indirect damage by low-energy electrons [1]. To accurately quantify DNA strand breakage induced by low-energy radiation in terms of absolute cross sections for DNA strand breakage we have developed an approach using AFM analysis of target DNA arranged on DNA origami platforms [2-5]. In this way we can effectively study the dependence of DNA strand breakage on the sequence and higher-order structure and assess the effect of radiosensitizers used or proposed for cancer radiation therapy. The main advantages of the technique are (i) the analysis and comparison of multiple sequences at the same time, (ii) the analysis of more complex higher-order structures [6], and (iii) a rather simple determination of absolute cross sections for strand breakage at specific irradiation conditions.

We have applied the DNA origami technique to DNA strand breaks induced by low-energy electrons (0.5 - 18 eV) [2-4], and vacuum UV photons (5 – 9 eV) [7]. In this presentation the following aspects in electron-induced DNA strand breakage will be discussed: (i) The dependence of the strand break cross section on the DNA sequence and the electron energy, (iii) the effect of radiosensitizers such as halogenated Adenines incorporated into the DNA sequences, and (iii) the role of the secondary structure by comparing linear telomeric DNA with folded G quadruplex structures. Furthermore, the effect of gold nanoparticles on DNA damage will be demonstrated [8].

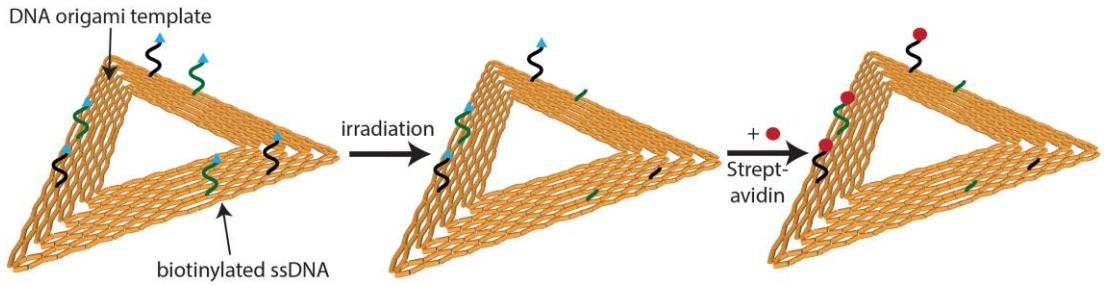

Fig. 1 Scheme of the procedure to quantify DNA strand breakage using triangular DNA origami substrates. The streptavidin labeled target sequences can be identified by AFM.

References

[1] I. Baccarelli et al., *Electron-induced damage of DNA and its components*, Phys. Rep. **508**, 1 (2011).
[2] A. Keller et al., *Sequence dependence of electron-induced DNA strand breakage revealed by DNA nanoarrays*, Sci. Rep. **4**, 7391 (2014).
[3] A. Keller et al., *Probing Electron-Induced Bond Cleavage at the Single-Molecule Level Using DNA Origami Templates*, ACS Nano **6**, 4302 (2012).
[4] A. Keller et al., *Electron-induced damage of biotin studied in the gas phase and in the condensed phase at a single-molecule level*, New J. Phys. **15**, 083045 (2013).
[5] I. Bald, A. Keller, *Molecular Processes Studied at a Single-Molecule Level Using DNA Origami Nanostructures and Atomic Force Microscopy*, Molecules **19**, 13803 (2014).
[6] L. Olejko, P. Cywinski, I. Bald, *Ion-Selective Formation of a Guanine Quadruplex on DNAOrigami Structures*, Angew. Chem. Int. Ed. **54**, 673 (2015).
[7] S. Vogel et al., *Using DNA Origami Nanostructures To Determine Absolute Cross Sections for UV Photon-Induced DNA Strand Breakage*, J. Phys. Chem. Lett. **6**, 4589 (2015).
[8] R. Schürmann, I. Bald, *Decomposition of DNA Nucleobases by Laser Irradiation of Gold Nanoparticles Monitored by Surface-Enhanced Raman Scattering*, J. Phys. Chem. C **120**, 3001 (2016).

Electron-Induced Chemistry in Molecular Solids

Leo Sala, Justine Houplin, Céline Dablemont, Lionel Amiaud, Anne Lafosse
Institut des Sciences Moléculaires d'Orsay (ISMO), CNRS, Univ. Paris Sud, Université Paris-Saclay, F-91405 Orsay (France)

Electron-induced chemical modifications are ubiquitous processes, which are of interest to various scientific communities, for instance dealing with beam assisted lithography [1] or with radiation processing of interstellar ice analogues [2]. Exposure of molecular solids (resist/ice layers) to energetic particles (electrons, ions or photons) leads to the release of bunches of secondary low-energy electrons (LEE, E ≤ 20-25 eV). LEEs initiate efficient reactive processes and definitely contribute to the overall chemical transformation induced by irradiation. Different primary interaction mechanisms are involved with relative probabilities which strongly depend on the incident electron energy [3,4]. After electron attachment, electronic excitation or ionization, different dissociative pathways open and the reactive fragments created within the molecular solids further contribute to the chemistry.

In dealing with electron chemistry induced in molecular films, the resulting chemical modifications have to be identified, the associated cross sections should be evaluated when possible, and the primary interaction mechanisms and elementary reaction steps involved should be investigated. To address these questions, molecular film irradiation experiments at tunable temperature (28-750 K) are performed at Orsay in the dedicated experimental setup "electrons-solids". High Resolution Electron Energy Loss Spectroscopy (HREELS) and Electron Stimulated Desorption (ESD) of neutral fragments are combined as main characterization techniques. Molecular solids in the form of Self-Assembled Monolayers (SAMs) of *p*-terphenylthiol HS-$(C_6H_4)_2$-C_6H_5 (TPT) deposited onto gold will be considered as an illustrative example in this lecture (Fig. 1). Such SAMs were considered in a recent series of studies [5]. They are organized surface-confined monolayers of aromatic compounds, often used to develop sensors [6] and functionalized carbon nanomembranes [7]. Electron-induced chemistry in these model aromatic organic platforms were investigated with special emphasis on their hydrogen contents:

- a strong electron attachment resonance was identified at about 6 eV as evidenced by its clear contribution to the vibrational excitation of the ν(CH) stretching modes under electron impact,
- the global chemical modifications undergone by the layers under electron processing were observed to be strongly dependent on the incident energy in the range 1-50 eV,
- the primary electron interactions and possible subsequent reaction mechanisms were discussed as a function of the incident energy, including the eventual contribution of secondary electrons,
- and finally, the cross sections for chemical modifications were estimated at 6 end 50 eV.

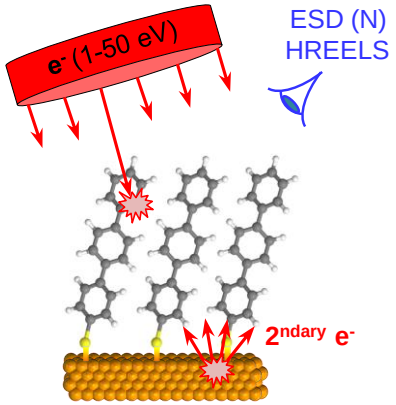

Fig. 1 Low-energy electron chemistry in Self-Assembled Monolayers of TPT.

References

[1] Rachel M. Thorman, Ragesh Kumar, D. Howard Fairbrother, Oddur Ingólfsson, Beilstein J. Nanotechnol. **6**, 1904 (2015).
[2] Kristal K. Sullivan, Mavis D. Boamah, Katie E. Shulenberger, Sitara Chapman, Karen E. Atkinson, Michael C. Boyer, Christopher R. Arumainayagam, MNRAS **460,** 664 (2016)
[3] Anne Lafosse, Mathieu Bertin, Roger Azria, Prog. Surf. Sci. **84**, 177 (2009).
[4] Esther Böhler, Jonas Warneke, Petra Swiderek, Chem. Soc. Rev. **42**, 9219 (2013).
[5] Justine Houplin, Céline Dablemont, Leo Sala, Anne Lafosse, Lionel Amiaud, Langmuir **31**, 13528 (2015); Justine Houplin, Lionel Amiaud, Céline Dablemont, Anne Lafosse, Phys. Chem. Chem. Phys. **17**, 30721 (2015); Justine Houplin, Lionel Amiaud, Thomas Sedzik, Céline Dablemont, Dominique Teillet-Billy, Nathalie Rougeau, Anne Lafosse, Eur. Phys. J. D **69**, 217 (2015); Lionel Amiaud, Justine Houplin, Marion Bourdier, Vincent Humblot, Roger Azria, Claire-Marie Pradier, Anne Lafosse, Phys. Chem. Chem. Phys. **16**, 1050 (2014).
[6] J. Christopher Love, Lara A. Estroff, Jennah K. Kriebel, Ralph G. Nuzzo, George M. Whitesides, Chem. Rev. **105**, 1103 (2005).
[7] Andrey Turchanin, Armin Gölzhäuser, Prog. Surf. Sci. **87**, 108 (2012).

Why are leaves green? Action spectroscopy of chlorophyll molecules and dimers *in vacuo*.

Mark H. Stockett[1*], Jørgen Houmøller[1], Christina Kjær[1], Bruce F. Milne[2,3], Lihi Musbat[4], Angel Rubio[2,5], Yoni Toker[4], and Steen Brøndsted Nielsen[1]

1. Department of Physics and Astronomy, Aarhus University, Denmark
2. Department of Materials Physics, University of the Basque Country, Donostia, Spain
3. Centre for Computational Physics, Department of Physics, University of Coimbra, Portugal
4. Institute of Nanotechnology and Advanced Materials, Bar-Ilan University, Ramat-Gan, Israel
5. Max Planck Institute for the Structure and Dynamics of Matter, Hamburg, Germany

Chlorophyll (Chl) *a* and *b* are the main light-absorbing pigments found in green plants. It is nontrivial to predict the absorption spectra of these molecules or what effect the protein environment may have. As a starting point, we have measured the absorption spectra of gas-phase Chl a and b using photodissociation action spectroscopy of Chl molecules tagged with quaternary ammonium ions [1,2]. These experimental data were used to calibrate time-dependent density functional theory (TDDFT) calculatons and determine the transition energies of the bare Chls in the absence of the charge tag. Chl *a* and *b* differ only on one peripheral substituent, but their absorption band maxima are shifted relative to each other by more than 30 nm. These shifts were reproduced in our gas-phase data, meaning that they are intrinsic effects and not due to interactions with the micro-environment. On the other hand, the bands of both Chl *a* and *b* were significantly blue-shifted relative to those in solution and in proteins. Interactions with the protein and solvent environments are thus crucial to understanding the absorption of chlorophylls.

One key mechanism by which the absorption spectrum of Chl is tuned in proteins is exciton coupling of two or more Chl pigments. This purely quantum mechanical effect gives rise to a splitting of the energy levels (and thus a color shift) of the collectively excited multi-Chl complex. It is difficult to disentangle this effect from shifts due to interactions the protein microenvironment such as axial ligation. With the absorption spectra of bare Chl now well established, we can begin to ask the question of which of these effects is more significant for color tuning. Furthermore, these interactions govern the mechanism for energy transfer to the reaction centers of photosynthetic proteins. For funnelling via localised states on the energy landscape, the protein environment is most important whereas so-called supertransfer requires fully delocalized states where all pigments are excitonically coupled [3]. We have measured the intrinsic strength of exciton coupling by applying our action spectroscopy technique to charge tagged dimers of Chl *a* [4]. Compared to our baseline measurements of Chl *a* monomers, the absorption band maximum is red-shifted by 50-70 meV, in good agreement with our TDDFT calculations.

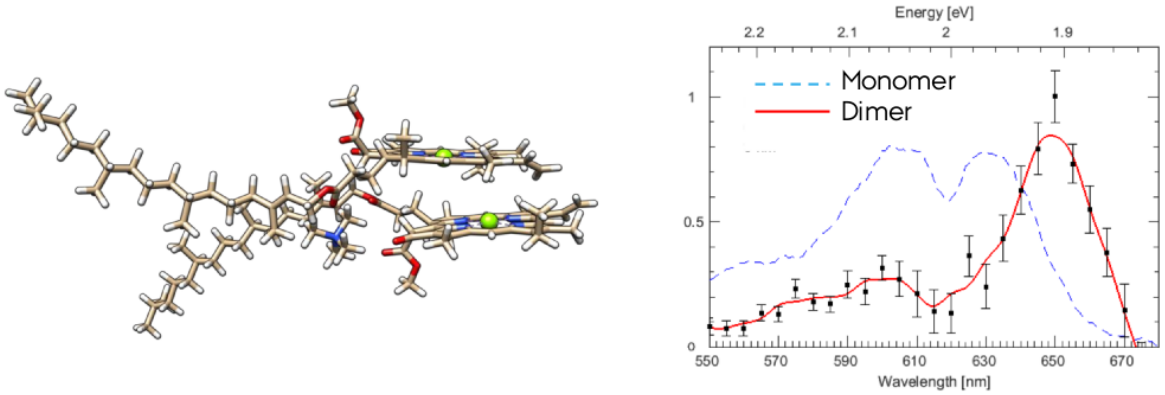

Fig. 1 Left: Optimized structure of Chl *a* dimer tagged with a quaternary ammonium cation. Right: Measured action spectra of charge tagged Chl *a* monomers (dashed line) and dimers (solid line and symbols).

References

[1] Bruce F. Milne, Yoni Toker, Angel Rubio, and Steen Brøndsted Nielsen, *Unraveling the Intrinsic Color of Chlorophyll* Angew. Chem. Int. Ed. **54**, 2170 (2015).

[2] Mark H. Stockett, Lihi Musbat, Christina Kjær, Jørgen Houmøller, Yoni Toker, Angel Rubio, Bruce F. Milne and Steen Brøndsted Nielsen, *The Soret absorption band of isolated chlorophyll a and b tagged with quaternary ammonium ions* Phys. Chem. Chem. Phys. **17**, 25793 (2015).

[3] Sima Baghbanzadeh and Ivan Kassal, *Distinguishing the roles of energy funnelling and delocalization in photosynthetic light harvesting*, Phys. Chem. Chem. Phys. **18**, 7459 (2016).

[4] Bruce F. Milne, Christina Kjær, Jørgen Houmøller, Mark H. Stockett, Yoni Toker, Angel Rubio, and Steen Brøndsted Nielsen, *On the exciton coupling between two chlorophyll pigments in the absence of a protein environment: Intrinsic effects revealed from theory and experiment*, Angew. Chem. Int. Ed. (Submitted).

Isomerization and Fragmentation of Retinal Chromophore Derivatives

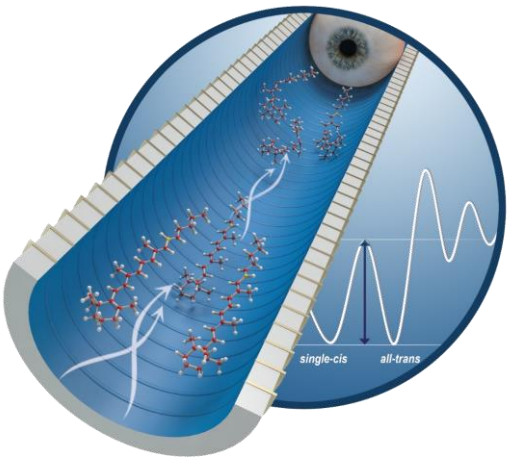

Yoni Toker
Department of Physics, Bar Ilan University, Ramat Gan 5290002, Israel

L. Musbat[1], J. Dilger[2], M. Nihamkin[1], S. Assis[1], S. Itzhak[1], A. V. Bochenkova[3], M. Sheves[4], D. Clemmer[5]

1. Department of Physics, Bar Ilan University, Ramat Gan 5290002, Israel
2. Spectrum Warfare Systems Department, NSWC Crane Division, Crane, IN 47522, USA
3. Department of Chemistry, Moscow State University, 119991 Moscow, Russia
4. Chemistry Department, Weizmann Institute of Science, Rehovot 978007, Israel.
5. Department of Chemistry, Indiana University, Bloomington, Indiana 47405, USA.

All known forms of vision rely on one specific chromophore as their photon detector- the retinal protonated Schiff base (RPSB). The RPSB, located in the centre of Opsin proteins, acts as an optical switch – whereby following the absorption of a photon it undergoes a photoisomerization. One approach to understand what makes this molecule so unique is by studying derivatives of the chromophore and thus examining how the photo properties of the chromophore depend on its exact structure.

Recently our group and others have used two stages of ion-mobility spectroscopy to study isomerization and gas phase fragmentation of the RPSB, and have shown that the barrier energy for isomerization is much lower than within the protein. Here we extend these studies to derivatives of the chromophore and show how minute changes to the structure of the chromophore have dramatic effects on its isomerization properties.

References

[1] J. Dilger, L. Musbat, M. Sheves, A. B. Bochenkova, D. E. Clemmer, Y. Toker, Ang Chemie Int. Ed. 127 (2015), 4830.
[2] Coughlan, Bieske et al. PCCP 17 (2015), 22623
[3] Y. Toker, D. B. Rahbek, H. V. Kiefer, J. Rajput, R. Antoine, P. Dugourd, S. Brønsted Nielsen, A. V. Bochenkova, L. H. Andersen PCCP 15 (2013), 19566.
[4] N. Coughlan, E. Bieske et al., JPCL 5 (2015), 3195.
[5] N. A. Pierson and D Clemmer Int. J. Mass. Spec **377** (2014), 646.

Measurement and control of a nanomechanical oscillator at the thermal decoherence rate

Dal Wilson, Vivishek Sudhir, Nicolas Piro, Ryan Schilling, Tobias J. Kippenberg (PhD)
Institute of Condensed Matter Physics
EPFL, Switzerland

In real-time quantum feedback protocols (*1*), the record of a continuous measurement is used to stabilize a desired quantum state. Recent years have seen spectacular advances in a variety of well-isolated micro-systems, including microwave photons(*2*) and superconducting qubits(*3*). By contrast, the ability to stabilize the quantum state of a tangibly massive object, such as a nano-mechanical oscillator, remains a difficult challenge. The main obstacle is environmental decoherence, which places stringent requirements on the timescale in which the state must be measured. Using cavity optomechanical coupling we report on a position sensor that is capable of resolving the zero-point motion of a solid-state, 4.3 MHz frequency nanomechanical oscillator in the timescale of its thermal decoherence(*4*), a basic requirement for preparing its ground-state using feedback as well as (Markovian) quantum feedback. The sensor is based on evanescent coupling to a high-Q optical microcavity(*5*), and achieves an imprecision 40 dB below that at the standard quantum limit for a weak continuous position measurement(*6*), a 100-fold improvement over previous reports, while maintaining an imprecision-back-action product within a factor of 5 of the Heisenberg uncertainty limit. As a demonstration of its utility, we use the measurement as an error signal with which to feedback cool the oscillator. Using radiation pressure as an actuator, the oscillator is cold-damped(*7*) with unprecedented efficiency: from a cryogenic bath temperature of 4.4 K to an effective value of 1.1 mK, corresponding to a mean phonon number of 5.3 (i.e., a ground state probability of 16%). Our results set a new benchmark for the performance of a linear position sensor, and signal the emergence of mechanical oscillators as practical subjects for measurement-based quantum control.

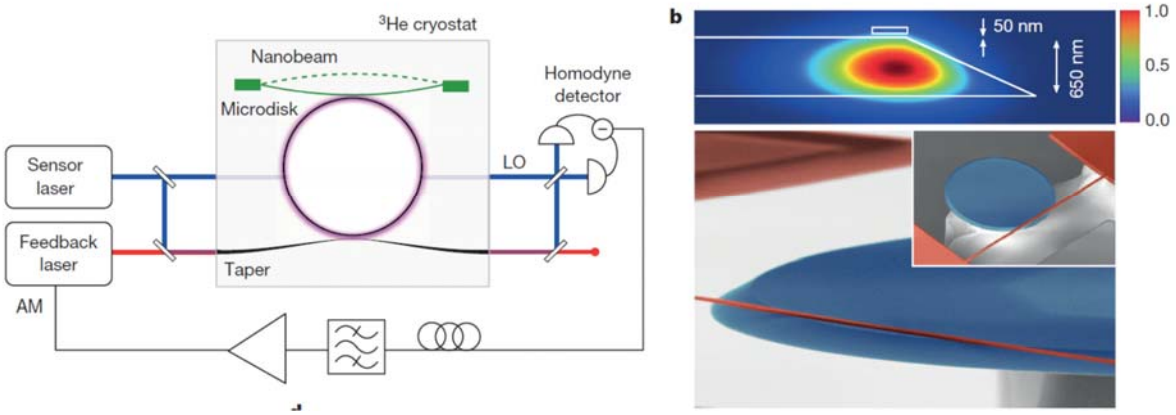

References:

1. H. Wiseman, Quantum theory of continuous feedback. *Physical Review A* **49**, 2133 (1994).
2. C. Sayrin *et al.*, Real-time quantum feedback prepares and stabilizes photon number states. *Nature* **477**, 73 (Sep 1, 2011).
3. R. Vijay *et al.*, Stabilizing Rabi oscillations in a superconducting qubit using quantum feedback. *Nature* **490**, 77 (Oct 4, 2012).
4. D. J. Wilson *et al.*, Measurement and control of a mechanical oscillator at its thermal decoherence rate. *arXiv:1410.6191 (Nature, in press)*, .
5. E. Gavartin, P. Verlot, T. J. Kippenberg, A hybrid on-chip optomechanical transducer for ultrasensitive force measurements. *Nature nanotechnology* **7**, 509 (Aug, 2012).
6. A. A. Clerk, M. H. Devoret, S. M. Girvin, F. Marquardt, R. J. Schoelkopf, Introduction to quantum noise, measurement, and amplification. *Reviews of Modern Physics* **82**, 1155 (2010).
7. M. Pinard, P. Cohadon, T. Briant, A. Heidmann, Full mechanical characterization of a cold damped mirror. *Physical Review A* **63**, (2000).

Chiral Quantum Optics

Arno Rauschenbeutel
Vienna Center for Quantum Science and Technology, Atominstitut, TU Wien, Stadionallee 2, 1020 Wien, Austria

Controlling the interaction of light and matter is the basis for diverse applications ranging from light technology to quantum information processing. Nowadays, many of these applications are based on nanophotonic structures. Remarkably, it turns out that the confinement of light in such nanostructures imposes an inherent link between its local polarization and its propagation direction, also referred to as spin–momentum locking of light [1]. This leads to chiral, i.e., propagation direction-dependent effects in the emission and absorption of light, and elementary processes of light–matter interaction are fundamentally altered. For example, when coupling plasmonic particles or atoms to evanescent fields, the intrinsic mirror symmetry of the particles' emission can be broken. With optical photons, this effect was first observed in the interaction between single rubidium atoms and the evanescent part of a light field that is confined by continuous total internal reflection in a whispering-gallery-mode microresonator [2]. In the following, this allowed us to realize chiral nanophotonic interfaces in which the emission direction of light into the structure is controlled by the polarization of the excitation light [3] or by the internal quantum state of the emitter [4], respectively. Moreover, we employed this chiral interaction to demonstrate an integrated optical isolator [5] as well as an integrated optical circulator [6] which operate at the single-photon level and which exhibit low loss. The latter are the first two examples of a new class of nonreciprocal nanophotonic devices which exploit the chiral interaction between single quantum emitters and transversally confined photons.

References

[1] K. Y. Bliokh, F. J. Rodríguez-Fortuño, F. Nori, and A. V. Zayats, *Spin-orbit interactions of light*, Nat. Photon. **9**, 796 (2015).
[2] C. Junge, D. O'Shea, J. Volz, and A. Rauschenbeutel, *Strong coupling between single atoms and non-transversal photons*, Phys. Rev. Lett. **110**, 213604 (2013).
[3] J. Petersen, J. Volz, and A. Rauschenbeutel, *Chiral nanophotonic waveguide interface based on spin-orbit coupling of light*, Science **346**, 67 (2014).
[4] R. Mitsch, C. Sayrin, B. Albrecht, P. Schneeweiss, and A. Rauschenbeutel, *Quantum state-controlled directional spontaneous emission of photons into a nanophotonic waveguide*, Nature Commun. **5**, 5713 (2014).
[5] C. Sayrin, C. Junge, R. Mitsch, B. Albrecht, D. O'Shea, P. Schneeweiss, J. Volz, and A. Rauschenbeutel, *Nanophotonic Optical Isolator Controlled by the Internal State of Cold Atoms*, Phys. Rev. X **5**, 041036 (2015).
[6] M. Scheucher, A. Hilico, E. Will, J. Volz, and A. Rauschenbeutel, *Programmable integrated optical circulator controlled by a single spin-polarized atom*, in preparation (2016).

Scalable quantum computing with atomic qubit arrays

M. Saffman
Department of Physics, University of Wisconsin-Madison, 1150 University Avenue, Madison, WI, 53706 USA

Recent years have witnessed substantial progress in using interactions between Rydberg excited atoms for quantum gates and entanglement generation[1]. The strong Rydberg interaction enables entanglement between identical atoms, between atoms of different species, and in hybrid settings of atomic and photonic qubits. Quantum logic experiments with a two-dimensional array of optically trapped Cs atoms will be described. New gate protocols with shaped Rydberg excitation pulses have the potential for very high fidelity entangling gates[2]. We will also present an architecture for scalable magnetic trap arrays with rare earth atom qubits.

References

[1] M. Saffman, *Quantum computing with atomic qubits and Rydberg interactions: Progress and challenges*, arXiv:1605.05207 (2016).
[2] L. S. Theis, F. Motzoi, F. K. Wilhelm, and M. Saffman, *A high ?delity Rydberg blockade entangling gate using shaped, analytic pulses*, arXiv:1605.08891 (2016).

Bell correlations in a Bose-Einstein condensate

Roman Schmied[1], Jean-Daniel Bancal[1,2], Baptiste Allard[1], Matteo Fadel[1], Valerio Scarani[2], Philipp Treutlein[1], and Nicolas Sangouard[1]

[1]*Department of Physics, University of Basel, Switzerland*
[2]*Centre for Quantum Technologies, National University of Singapore*

The parts of a composite system can share correlations that are stronger than any classical theory allows. These so-called Bell correlations can be confirmed by violating a Bell inequality and represent the most profound departure of quantum from classical physics. We report experiments where we detect Bell correlations between the spins of 480 atoms in a Bose-Einstein condensate [1]. We derive a Bell correlation witness from a recent many-particle Bell inequality [2] involving one- and two-body correlation functions only. Our measurement on a spin-squeezed state [3] exceeds the threshold for Bell correlations by 3.8 standard deviations. Concluding the presence of Bell correlations is unprecedented for an ensemble containing more than a few particles. Our work shows that the strongest possible non-classical correlations are experimentally accessible in many-body systems, and that they can be revealed by collective measurements. This opens new perspectives for using many-body systems in quantum information tasks.

[1] R. Schmied, J.-D. Bancal, B. Allard, M. Fadel, V. Scarani, P. Treutlein, N. Sangouard, Science, in press (2016)
[2] J. Tura, R. Augusiak, A.B. Sainz, T. Vértesi, M. Lewenstein, A. Acín, Science 344, 1256 (2014)
[3] M.F. Riedel, P. Böhi, Y. Li, T.W. Hänsch, A. Sinatra, P. Treutlein, Nature 464, 1170 (2010)

Ultracold atoms as quantum simulators for new materials –optical lattices, synthetic magnetic fields and topological phases

Wolfgang Ketterle

Research Laboratory for Electronics, MIT-Harvard Center for Ultracold Atoms, and Department of Physics, Massachusetts Institute of Technology, 77 Massachusetts Ave., Cambridge, MA 02139-4307, USA

When atoms are cooled to nanokelvin temperatures, they can easily be confined and manipulated with laser beams. Crystalline materials are simulated by placing the atoms into an optical lattice, a periodic interference pattern of laser beams. Recently, synthetic magnetic fields and spin-orbit coupling have been realized [1-4]. With the help of laser beams, neutral atoms move around in the same way as charged particles subject to the magnetic Lorentz force. These developments should allow the realization of quantum Hall systems and topological insulators with ultracold atoms.

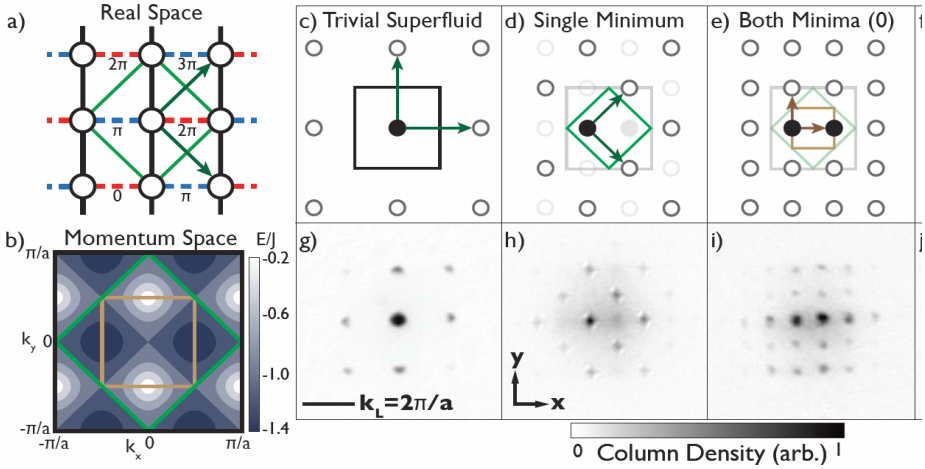

Fig. 1 Observation of Bose-Einstein condensation in the HH model with one half flux quantum per unit cell. (a) Spatial structure of the cubic lattice with the synthetic vector potential, which generates a lattice unit cell that is twice as large as the bare cubic lattice (green diamond). (b) The band structure of the lowest band of the HH Hamiltonian shows a twofold degeneracy of the ground state and two Dirac points. The magnetic Brillouin zone (green diamond) has half the area of the original Brillouin zone and has a primitive cell that is even smaller (doubly reduced Brillouin zone, brown square). These lattice symmetries are both revealed in time-of-flight pictures showing the momentum distribution of the wavefunction. (c,d,e) Schematics of the momentum peaks of a superfluid. The dominant momentum peak (filled circle) is equal to the quasimomentum of the ground state. Due to the spatial periodicity of the wavefunction, additional momentum peaks (empty circles) appear, separated by reciprocal lattice vectors (green arrows) or vectors connecting degenerate states in the band structure (brown arrows). (g,h,i) Time-of-flight images. The superfluid ground state of the normal cubic lattice is shown in (g) in comparison to the superfluid ground state of the HH lattice (h,i). In (h), only one minimum of the band structure is filled, directly demonstrating the fundamental symmetry of the HH Hamiltonian in our chosen gauge. The number of momentum components in (i) is doubled again due to population of both degenerate ground states.

References

[1]. C.J. Kennedy, G.A. Siviloglou, H. Miyake, W.C. Burton, and W. Ketterle, *Spin-orbit coupling and spin Hall effect for neutral atoms without spin flips,* Phys. Rev. Lett. **111**, 225301 (2013), http://link.aps.org/doi/10.1103/PhysRevLett.111.225301

[2] H. Miyake, G.A. Siviloglou, C.J. Kennedy, W.C. Burton, and W. Ketterle, *Realizing the Harper Hamiltonian with Laser-Assisted Tunneling in Optical Lattices,* Phys. Rev. Lett. **111**, 185302 (2013), http://link.aps.org/doi/10.1103/PhysRevLett.111.185302

[3] C.J. Kennedy, W.C. Burton, W.C. Chung, and W. Ketterle, *Observation of Bose-Einstein Condensation in a Strong Synthetic Magnetic Field,* Nature Physics **11**, 859–864 (2015), http://dx.doi.org/10.1038/nphys3421

[4]. J. Li, W. Huang, B. Shteynas, S. Burchesky, F.C. Top, E. Su, J. Lee, A.O. Jamison, and W. Ketterle, *Spin-Orbit Coupling and Spin Textures in Optical Superlattices*, preprint, arXiv:1606.03514 (2016), http://arxiv.org/abs/1606.03514

Steering and Visualizing Proton Migration using Few-Cycle Pulses

M. Kübel[1], C. Burger[1], R. Siemering[2], Nora G. Kling[1], A.S. Alnaser[3,4], I. Ben-Itzhak[5], R. Moshammer[6], R. de Vivie-Riedle[2], M.F. Kling[1,3]

[1] *Department of Physics, Ludwig-Maximilians-Universität Munich, D-85748 Garching, Germany*
[2]*Department of Chemistry and Biochemistry, Ludwig-Maximilians-Universität Munich, D-81377 München, Germany*
[3]*Max Planck Institute of Quantum Optics, D-85748 Garching, Germany*
[4]*Physics Department, American University of Sharjah, POB26666, Sharjah, UAE*
[5]*J.R. Macdonald Laboratory, Physics Department, Kansas State University, Manhattan, KS 66506, USA*
[6]*Max Planck Institute of Nuclear Physics, D-69117 Heidelberg, Germany*

Chemical reactions involving the rearrangement of C-H bonds are ubiquitous in nature. The capability to steer such rearrangements towards a desired outcome is key to controlling complex reactions in organic molecules. Recently, it has been demonstrated that waveform controlled few-cycle laser pulses can be used to selectively break C-H bonds in acetylene [1].

Here, we go beyond simple dissociation reactions and demonstrate control over the direction of proton migration in hydrocarbons (acetylene and allene) by means of phase-controlled few-cycle pulses. Charged fragments originating from the interaction of a molecule with an intense laser pulse are detected in coincidence using a reaction microscope. We find that the preferential direction of hydrogen migration can be steered with the carrier-envelope phase (CEP) of the driving laser pulse, see Fig. 1 (a).

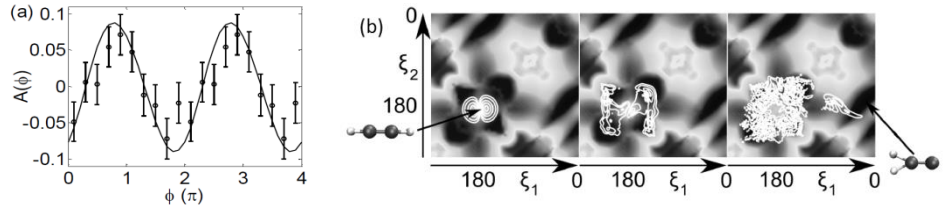

Fig. 1 CEP-dependence of the proton migration direction in acetylene. Shown in (a) is the measured (symbols) and calculated (solid line) asymmetry parameter $A(\phi) = (N_+ - N_-) / (N_+ + N_-)$, where N_+ (N_-) is the yield of carbon ions emitted from vinylidene with positive (negative) momentum. (b) Propagation of a vibrational wavepacket on the potential energy surface of the reactive A^3P state of the acetylene dication along two reactive coordinates (specifically, the C-H bond angles). The contour lines display snapshots of the calculated nuclear wavepacket whose propagation leads to isomerization of the acetylene dication towards the "left" vinylidene configuration.

The experimental results are interpreted in terms of a quantum mechanical model [1,2] in which the laser prepares a CEP-dependent vibrational wavepacket. Propagation of this wavepacket (Fig. 1(b)) on a reactive state is found to lead to a preferential direction of the hydrogen migration, which therefore depends on the CEP.

In a second step, we follow the temporal evolution of hydrogen migration by Coulomb explosion imaging with a time-delayed probe pulse, reconstructing the transient molecular structure from the detected ion momenta. The isomerization of acetylene to vinylidene is tracked by breakage of both C-H bonds in the trication and coincident detection of all three fragments. This allows for capturing a "movie" of the isomerization (see Fig. 2) and following intermediate states of the isomerization in real time.

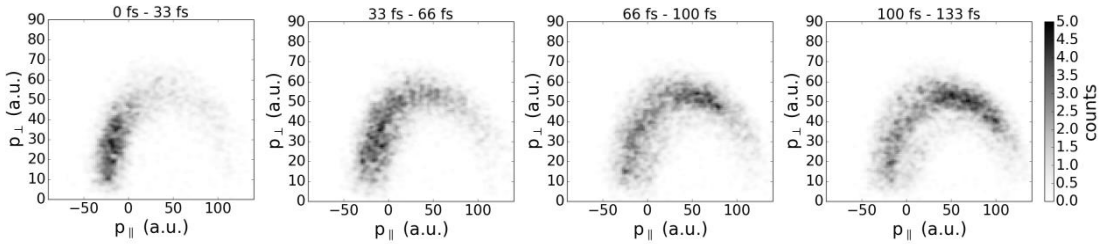

Fig. 2 Molecular Newton plots visualizing the isomerization of acetylene to vinylidene. The transient molecular structures are imaged by detecting all ions arising from the Coulomb explosion channel $C_2H_2^{3+} \rightarrow H^+ + H^+ + C_2^+$ in coincidence. The momentum distributions of one proton is displayed in the co-moving frame of the C_2^+ ion with the momentum of the other proton (not shown) fixed along the positive $p_\parallel$. The snapshots were obtained for different time delays, as indicated.

References

[1] A.S. Alnaser *et al.*, Nat. Commun. **5**, 3800 (2014), S. Miura, *et al.*, Chem. Phys. Lett. **595**, 61 (2014).
[2] M. Kübel *et al.*, arXiv:1508.04018
[3] C. Burger *et al.*, *in preparation.*

A molecular movie of Interatomic Coulombic Decay

Florian Trinter[1], Tsveta Miteva[2], Miriam Weller[1], Sebastian Albrecht[1], Alexander Hartung[1], Martin Richter[1], Joshua Williams[1], Averell Gatton[3], Bishwanath Gaire[3], Thorsten Weber[3], James Sartor[4], Allen Landers[4], Ben Berry[5], Vasili Stumpf[2], Kirill Gokhberg[2], Reinhard Dörner[1], and Till Jahnke[1]

1. *Institut für Kernphysik, Goethe-Universität, 60438 Frankfurt am Main, Germany*
2. *Theoretische Chemie, Physikalisch-Chemisches Institut, Universität Heidelberg, 69120 Heidelberg, Germany*
3. *Lawrence Berkeley National Laboratory, Chemical Sciences Division, Berkeley, California 94720, USA*
4. *Department of Physics, Auburn University, Auburn, Alabama 36849, USA*
5. *J. R. MacDonald Laboratory, Department of Physics, Kansas State University, Manhattan, Kansas 66506, USA*

During the last 15 years a novel decay mechanism of excited atoms has been discovered and investigated. This so called "Interatomic Coulombic Decay" (ICD) [1,2] involves the chemical environment of the electronically excited atom or molecule: the excitation energy is transferred to a neighbor of the initially excited particle usually ionizing that neighbor. It turned out that ICD is a very common decay route in nature as it occurs across van der Waals and hydrogen bonds. The time evolution of ICD is predicted to be highly complex, as its efficiency strongly depends on the distance of the atoms involved and this distance typically changes during the decay.

Here we present a direct measurement of the temporal evolution of ICD using a novel experimental approach [3] as well as theoretical results. The results show the evolution of the vibrational wavepacket of a NeKr dimer during the decay. So we gain insight into the complex behavior of ICD in the time domain.

Figure 1 shows the norm of the wavepacket as a function of the IC-decay time, i.e. temporal behavior of the survival probability of the intermediate state prior to ICD. Two photon energies as well as theory are included. The data points are extracted from two datasets employing two different photon energies in order to access different decay times: for the black points a photoelectron kinetic energy of 120 meV was chosen while the red points belong to a dataset with a photoelectron energy of 200 meV.

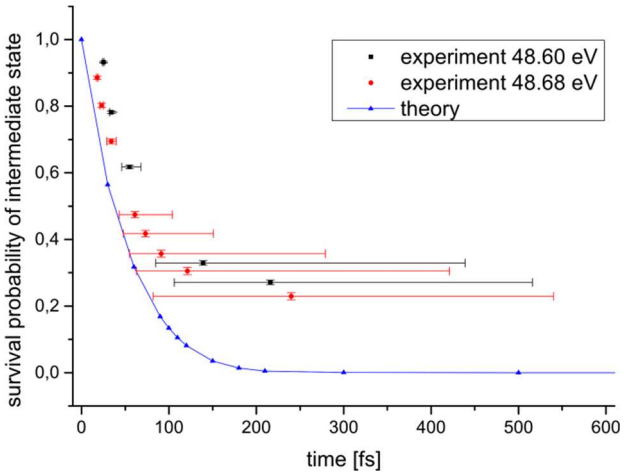

Fig. 1 Results NeKr: Norm of the wavepacket as a function of the IC-decay time, i.e. temporal behaviour of the survival probability of the intermediate state prior to ICD.

References

[1] L. S. Cederbaum, J. Zobeley, and F. Tarantelli, *Giant Intermolecular Decay and Fragmentation of Clusters*, Phys. Rev. Lett. **79**, 4778 (1997).
[2] T. Jahnke et al., *Experimental Observation of Interatomic Coulombic Decay in Neon Dimers*, Phys. Rev. Lett. **93**, 163401 (2004).
[3] F. Trinter et al., *Evolution of Interatomic Coulombic Decay in the Time Domain*, Phys. Rev. Lett. **111**, 093401 (2013).

Hamiltonian Algorithm Study of Aromatic Oxidative Cyclization on *N*-Methoxy-*N*-Prenylbenzamide

Hiroyuki Teramae*[1], Kousuke Hayashi[2], Jun Takayama[2], and Takeshi Sakamoto[2]

1. Department of Chemistry, Faculty of Science, Josai University,1-1 Keyakidai, Sakado 3500295, Japan

2. Faculty of Pharmaceutical Sciences, Josai University, 1-1 Keyakidai, Sakado 3500295, Japan

Hamiltonian algorithm (HA) is one of the general optimization method and it resembles the molecular dynamics calculations when applied to the optimization of the molecular structures except for the kinetic energy term[1]. We combined it to ab initio molecular orbital method to calculate the energy and the force acting on the nuclei. We have applied HA in the present paper on the geometry optimizations of the phenomxenium cation.

Recently, many examples of the syntheses of 1-azaspiro ring compounds have been reported[2], however, little examples of 2-azaspiro ring compounds have been reported. We have examined the syntheses of the 2-azaspiro ring compounds by aromatic oxidative cyclization of the benzanilide derivatives using hypervalent iodine compounds, $PhI(OCOCF_3)_2$[3]. We also examined the same reaction of the compounds **1a-d** incorporating an allyl group on the nitrogen atom of *N*-methoxybenzamide (Table 1). It is very significant that the reaction can proceed only when using **1a** having an prenyl group ($R^1 = R^2 = Me$) as starting materials.

Table 1. Aromatic oxidative cyclization of *N*-allyl-*N*-methoxybenzamides using $PhI(OCOCF_3)_2$

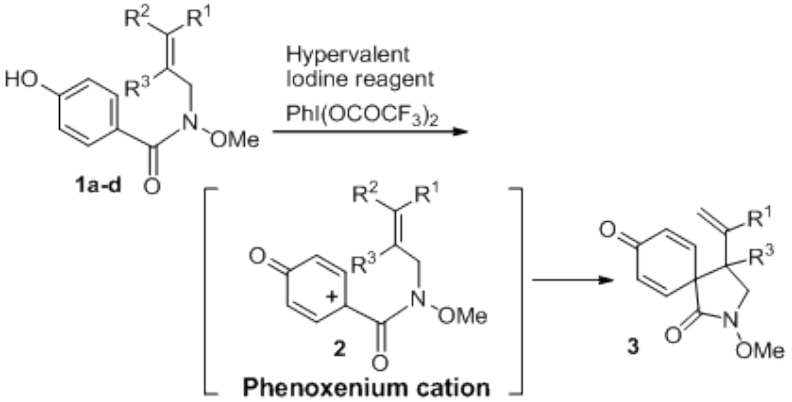

Entry	Starting Material	R^1	R^2	R^3	Product Yield (%)
1	**1a**	Me	Me	H	**3** (54)
2	**1b**	H	H	H	28[a]
3	**1c**	H	H	Me	12[a]
4	**1d**	H	Me	H	8[a]

[a] Recovery of starting materials.

In the present study, therefore, the geometric structures of the phenoxenium cation which is a cation intermediates of 2-azaspiro ring compounds (2-azaspiro[4.5]decane) from *N*-allyl-*N*-methoxy- benzamides are studied by means of the Hamiltonian algorithm with ab intio molecular orbital calculations at HF/3-21G level. The geometries are further refined with MP2/6-311G** level. We tried four substituted compounds with methylated allyl groups. Among them, *N*-prenyl derivative **1a** with two methyl group only gives ring-closure intermediate, which is well agreed with the experimental results

References

[1] K. Ohtawara, H. Teramae, *Chem. Phys. Lett.*, **390**, 84 (2004).
[2] Y. Kikugawa, *Heterocycles*, **78**, 571 (2009).
[3] T. Sakamoto, *et al*., unpublished results.

Imaging the Complex Influence of the Leaving Group on Nucleophilic Substitution Reactions

Martin Stei[1], Eduardo Carrascosa[1], Jennifer Meyer[1], Tim Michaelsen[1], Björn Bastian[1], Martin A. Kainz[1], Aditya H. Kelkar[1], István Szabó[2,3], Gábor Czakó[3], Roland Wester[1],

1. Institut für Ionenphysik und Angewandte Physik, Universität Innsbruck, Technikerstraße 25, 6020 Innsbruck, Austria
2. Laboratory of Molecular Structure and Dynamics, Institute for Chemistry, Eötvös Univeristy, PO Box 32, Budapest 112 1518, Hungary
3. Department of Physical Chemistry and Materials Science, University of Szeged, Rerrich Béla tér 1, Szeged H-6720, Hungary

Predicting the outcome of a reactive encounter is of fundamental importance for processes in synthetic chemistry, catalysis or astrochemistry. A deep understanding of the factors influencing the thermodynamics and the kinetics of a given reactive system is necessary to reliably predict the product distribution. On a molecular level this means that the dynamics of the system during the reaction have to be understood. One of the most investigated organic reactions in chemical physics is the bimolecular nucleophilic substitution reaction S_N2. Classic textbook knowledge predicts it to proceed via a collinear geometry under inversion of the stereo center. Our group has investigated the dynamics of several gas phase S_N2 reactions of the type $X^- + CH_3Y$ where X (nucleophile) and Y (leaving group) are halide atoms and has identified a number of distinct dynamical features [1]. The dynamics of the classic S_N2 mechanism have been found to be much more complex than the expected back side attack alone.

Here, we report on the influence of the leaving group on the dynamics of S_N2 reactions [2]. Our experimental approach combines crossed beam scattering with 3D velocity map imaging. This allows us to record differential scattering cross sections which contain the full three dimensional velocity information [3]. Specifically, we have studied the reaction of F^- with CH_3Cl. We expected similar dynamics as for $F^- + CH_3I$ because both systems show very similar energetics in the entrance channel. However, we found a significantly different dynamical behavior in case of chlorine as leaving group. The system mostly follows the classic direct S_N2 mechanism and only shows indirect dynamics at low collision energies. In contrast, the reaction with iodine as leaving group shows a major contribution of indirect dynamics even at high collision energies [4]. These differing dynamics are not due to the lower mass of the chlorine compared to iodine. High level chemical dynamics simulations, performed in the group of G. Czakó, revealed that the differences in interaction of the nucleophile F^- and the respective leaving group leads to this distinct differences in the dynamics [2]. Our experimental results in combination with theory show how subtle differences influence the dynamics of gas phase S_N2 reactions and the relative importance of different mechanisms. Additionally, a number of further reaction products besides the S_N2 product can be observed in the reaction with methyl iodine but not with methyl chloride [5].

Recently, we extended our investigations of gas phase organic reactions to the competition of based induced elimination E2 with bimolecular nucleophilic substitution S_N2 reactions. These two reaction channels are in constant competition, if the molecule contains at least two carbon atoms in its backbone. To disentangle both channels by experimental methods is challenging because the same ionic product is formed in both S_N2 and E2 reactions. This makes the application of mass spectroscopic methods almost impossible. We used ion imaging to identity the dynamical fingerprint of the E2. First results will be shown on the transition from S_N2 to E2 dynamics.

References

[1] Jing Xie, Rico Otto, Jochen Mikosch, Jiaxu Zhang, Roland Wester, and William L. Hase, *Identification of Atomic-Level Mechanisms for Gas-Phase* $X^- + CH3_Y$ *S_N2 Reactions by Combined Experiments and Simulations*, Acc. Chem. Res. **47**, 2960 (2014)

[2] Martin Stei, Eduardo Carrascosa, Martin A. Kainz, Aditya H. Kelkar, Jennifer Meyer, István Szabo, Gábor Czakó, and Roland Wester, *Influence of the Leaving Group on the Dynamics of Gas-Phase S_N2 Reactions*, Nature Chem. **8**, 151 (2016).

[3] Roland Wester, *Velocity Map Imaging of Ion Molecule Reactions*, Phys. Chem. Chem. Phys., **16**, 396 (2014)

[4] Jochen Mikosch, Jiaxu Zhang, Sebastian Trippel, Christoph Eichhorn, Rico Otto, Rui Sun, Wibe A. de Jong, Matthias Weidemüller, William L. Hase, Roland Wester *Indirect Dynamics in a Highly Exoergic Substitution Reaction*, J. Am. Chem. Soc. **135**, 4250 (2013).

[5] Eduardo Carrascosa, Tim Michaelsen, Martin Stei, Björn Bastian, Jennifer Meyer, Jochen Mikosch, Roland Wester, *Imaging Proton Transfer and Dihalide Formation Pathways in Reactions of* $F^- + CH_3I$, J. Phys. Chem. A. **in press**, doi:10.1021/acs.jpca.5b11181 (2016)

Predissociation of rotationally and vibrationally excited dimer anions studied in the Heidelberg Cryogenic Storage Ring (CSR)

Jürgen Göck[1], Arno Becker[1], Klaus Blaum[1], Christian Breitenfeldt[1,2], Sebastian George[1], Manfred Grieser[1], Florian Grussie[1], Robert von Hahn[1], Philipp Herwig[1], Jonas Karthein[1], Claude Krantz[1], Holger Kreckel[1], Sunil Kumar[1], Jorrit Lion[1], Svenja Lohmann[1], Christian Meyer[1], Preeti M. Mishra[1], Oldřich Novotný[1], Aodh P. O'Connor[1], Roland Repnow[1], Kaija Spruck[1,3], Stefan Schippers[3], Dirk Schwalm[1,4], Lutz Schweikhard[2], Stephen Vogel[1], Andreas Wolf[1]

1. Max-Planck-Institut für Kernphysik, Saupfercheckweg 1, 69117 Heidelberg, Germany
2. Institut für Physik, Ernst-Moritz-Arndt Universität Greifswald, Felix-Hausdorff-Straße 6, 17487 Greifswald, Germany
3. I. Physikalisches Institut, Justus-Liebig-Universität Gießen, Heinrich-Buff-Ring 16, 35392 Gießen, Germany
4. Department of Particle Physics and Astrophysics, Weizmann Institute of Science, Herzl St 234, Rehovot, 76100, Israel

The newly developed Cryogenic Storage Ring (CSR) [1] is located at the Max-Planck-Institut für Kernphysik in Heidelberg. It is designed for storing and investigating cationic and anionic ion beams of up to 300 keV kinetic energy per unit charge in a cryogenic environment that leads to extremely low vacuum and a low level of thermal blackbody radiation. The vacuum chambers, ion optical elements and detection systems of the fully electrostatic storage ring with a circumference of 35 m are cooled by a closed-cycle liquid helium system. Temperatures of < 6 K lead to a residual-gas density found to be below 140 particles per cm^3, which is equivalent to a room-temperature pressure below 10^{-14} mbar. Under these conditions a storage time constant of about 45 min was demonstrated for an ion beam of Ag_2^- at an energy of 60 keV. The capability of storing ion beams for long periods in a cryogenic environment offers new experimental prospects for quasi background-free gas-phase spectroscopy in atomic, molecular, and cluster physics.

Beams of anionic cobalt and silver dimers, Co_2^- and Ag_2^-, produced in a sputter ion source, were stored in the CSR at a beam energy of 60 keV and investigated over times up to 1000 s. On a single-particle counting detector [2] installed behind a storage-ring deflector in the cryogenic vacuum, a continuously decreasing signal of fast ions at half the mass of the beam ions (assigned to Co^- and Ag^-, respectively) was observed up to several hundreds of seconds after the injection. The counted ion signal is interpreted as being due to predissociation of quasi-stable, highly excited vibrational states (v) of the molecule above the ground-state dissociation limit. States of this type exist for molecules with high rotational excitation (J) behind the rotational barrier and predisssociate by quantum mechanical tunneling. Depending on the energetic position of the various levels below the rotational barrier, vastly different tunneling rates can occur. Previous measurements at a room-temperature electrostatic ion storage ring [3] showed that the decay signal, resulting from a broad range of excited v and J states, decreases with the storage time t approximately as a power law t^n with $n \approx$ -1. These experiments, however, faced considerable background from collisional dissociation of the ions in the residual gas and, therefore, could track the decay for times up to ~ 0.1 s, only.

At the extremely low background in our measurements, we can track the predissociation signal up to storage times several thousand times longer. We find that the predissociation signals as a function of time roughly continue as a power law with a similar exponent as observed earlier. In addition to this overall dependence, modulations in the signal intensity occur, which will be discussed in more detail in this contribution.

References

[1] R. von Hahn *et. al.*, *The Cryogenic Storage Ring CSR* (submitted)
[2] K. Spruck *et. al.*, *An efficient, movable single-particle detector for use in cryogenic ultra-high vacuum environments*, Rev. Sci. Instrum. **86**, 023303 (2015)
[3] J. Fedor *et. al.*, *Nonthermal Power Law Decay of Metal Dimer Anions*, Phys. Rev. Lett. **94**, 113201 (2005)

Probing O_2^+ potential curves with an XUV–IR pump–probe experiment

Philipp Cörlin[1], Andreas Fischer[1], Tomoya Mizuno[1], Michael Schönwald[1], Uwe Thumm[2], Thomas Pfeifer[1], Robert Moshammer[1]

1. Max-Planck-Institut für Kernphysik, Heidelberg, Germany

2. J.R. Macdonald Laboratory, Department of Physics, Kansas State University, Manhattan, Kansas, USA

In an XUV–IR pump–probe experiment, an extreme ultraviolet (XUV) pulse initiates an oscillating nuclear vibrational wave packet in the binding $O_2^+(a\,^4\Pi_u)$ potential by single-photon ionization. After a variable time delay population is transferred to the weakly repulsive $O_2^+(f\,^4\Pi_g)$ state by an infrared (IR) pulse [Duration ≈ 12 fs (FWHM), Intensity $\approx 3\times10^{12}$ W/cm^2] (Fig. 1, left panel). The initial three-dimensional momenta of the created photoions and photoelectrons are determined using a reaction microscope.

The experimental yield of O^+ ions with KER < 0.08 eV is plotted as a function of the pump–probe delay in Fig. 1 (right panel). Clearly visible is an oscillation with a period of 40 fs. The anharmonicity of the $a\,^4\Pi_u$ PEC causes the originally well localized wave packet to dephase over a period of approximately 640 fs before it revives after 1270 fs .

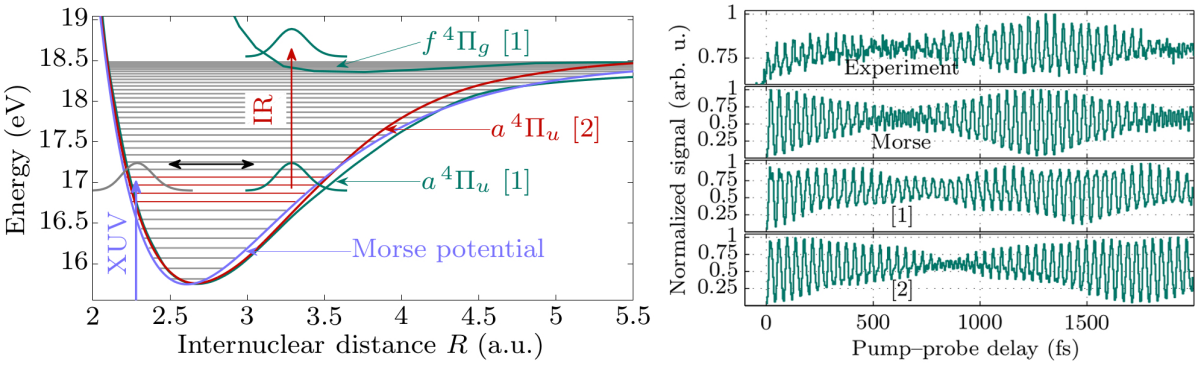

Fig. 1 Left panel: Illustration of the pump–probe scheme with O_2^+ PECs calculated in Refs. [1, 2] as well as a Morse potential adjusted to the experimental data.
Right panel: O^+ yield as a function of the pump–probe delay. Experimental data (top) [3] and three simulated spectra using a Morse potential as well as the PECs calculated in Refs. [1, 2].

With a coupled-channel calculation, we simulate the wave-packet oscillation and the probing process for different sets of PECs. The results are shown in the three lower graphs of Fig. 1 (right panel). The revival time of the wave packet is overestimated in the simulations using the PECs calculated in Refs. [1, 2]. If the wave-packet is propagated within a Morse potential adjusted to the experimental data, the revival time is in very good agreement with the experimental data.

The close resemblance between the Morse potential and the predicted PECs in Fig. 1 demonstrates that the revival time and our experimental method is sensitive to small variations in the shape of the binding PEC. Additionally, the KER distribution of the O^+ ions contains information about the shape of the repulsive PEC. This allows us to distinguish between the $O_2^+(f\,^4\Pi_g)$ PECs calculated in Refs. [1, 2].

References

[1] Christel M. Marian, Ralf Marian, Sigrid D. Peyerimhoff, Bernd A. Hess, Robert J. Buenker, Georg Seger, Mol. Phys. **46**, 779 (1982)
[2] Maia Magrakvelidze, Christine M. Aikens, and Uwe Thumm, Phys. Rev. A **86**, 023402 (2012)
[3] Philipp Cörlin, Andreas Fischer, Michael Schönwald, Alexander Sperl, Tomoya Mizuno, Uwe Thumm, Thomas Pfeifer, Robert Moshammer, Phys. Rev. A. **91**, 043415 (2015)

Theoretical Study of Sulphur Cluster Fragmentation

Shandor Demesh[1,2], Eugene Remeta[1]

1. *Institute of Electron Physics, National Academy of Sciences of Ukraine, Universitetska St. 21, 88017 Uzhhorod, Ukraine*
2. *Institute for Nuclear Research of the Hungarian Academy of Sciences (ATOMKI), Bem tér 18/c, 4026 Debrecen, Hungary*

Detailed theoretical calculations of energy and vibrational characteristics of neutral and positively charged sulphur clusters S_n^{q+} ($n=1-6$, $q=0-1$) were carried out by density functional theory (DFT). The B3PW91 exchange-correlation functional along with the augmented correlation-consistent polarized valence double-zeta (aug-cc-pVDZ) basis-set were used for the calculations by the GAMESS [1] software package. From these simulations there were evaluated several properties, such as adiabatic and vertical ionization energies and dissociation energies of several fragmentation channels [2]. There were found and studied theoretically 43 different S_n^{q+} cluster structures in total.

The results of the provided *ab initio* calculations, such as total energies, relaxed geometries and the vibrational frequencies of normal modes of the molecules then served as the starting point for further calculations. On the basis of the mentioned simulations, statistical calculations were also performed in a collaboration with the research group of N. Aguirre *et al*. by using the M3C (microcanonical Metropolis Monte-Carlo) package [3] in order to obtain the fragmentation branching ratios of the observed species and the breakdown curves for the several fragmentation channels.

In particular, the first results for the singly charged clusters were compared with the available mass-spectroscopic data from the NIST mass-spectra database [4] (see Fig.1).

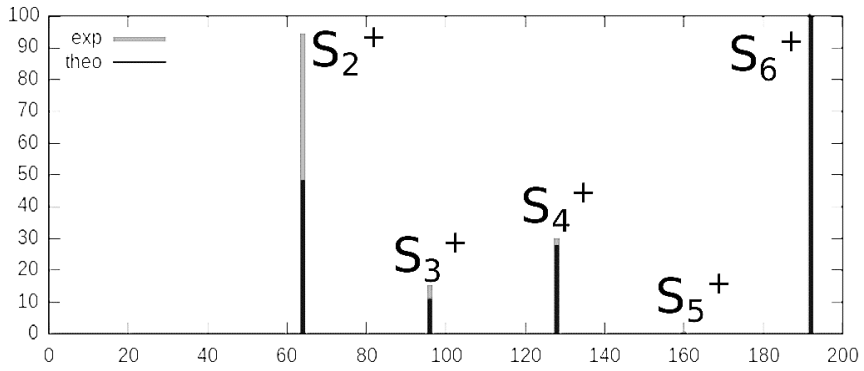

Fig. 1 Theoretical and experimental mass spectra for the S_6 molecule.

We can see that, in general, there is a good agreement between theory and experiment, except of the case of S_2^+ ion, where probably there seems to be a factor, which we might not take into consideration. There should be several possible reasons to explain the deviation from the experiment: for example, one of these is that for some channels there might be a barrier in the reaction (principally a high-lying transition state) along the reaction path, which we did not take into account. Another explanation is due to the fact that DFT is a coarse approximation. Then some energies at DFT level have much lower values, than we expect from the higher level variational methods (e.g. CCSD(T), CASSCF), which could invert the energetic trends for some reactions. For this reason, we provide further *ab initio* calculations on the sulphur clusters on higher theory levels and then correct the M3C simulaions with this new results.

References

[1] M.W. Schmidt et al., *General Atomic and Molecular Electronic Structure System*, J. Comput. Chem. **14,** 1347 (1993).
[2] Sh. Sh. Demesh and E. Yu. Remeta, *Appearance Energies of S_k^+ Ions from S_n Molecules Studied Ab Initio*, XLIC 3rd General meeting, (Debrecen, Hungary) 33 (2015).
[3] N. Aguirre, S. Díaz-Tendero, P-A. Hervieux, M. Alcamí and F. Martín, *M3C: A software package designed to describe statistical fragmentation of excited molecules*. In preparation (2016).
[4] P. J. Linstrom and W. G. Mallard, editors. NIST Chemistry WebBook, NIST Standard Reference Database Number **69**. NIST, Gaithersburg MD, 20899 (2005) (http://webbook.nist.gov/cgi/cbook.cgi?ID=C13798237&Units=SI&Mask=200#Mass-Spec)

Enhanced Ionization of Embedded Clusters by Electron Transfer Mediated Decay in Helium Nanodroplets

A. C. LaForge[1], V. Stumpf[2], K. Gokhberg[2], J. von Vangerow[1], F. Stienkemeier[1], N. V. Kryzhevoi[2], P. O'Keeffe[3], A. Ciavardini[3], M. Coreno[3], K. C. Prince[4], R. Richter[4], R. Moshammer[5], T. Pfeifer[5], L. S. Cederbaum[2], and M. Mudrich[1]

1. *Physikalisches Institut, Universität Freiburg, 79104 Freiburg, Germany*
2. *Physikalisch-Chemisches Institut, Universität Heidelberg, 69120 Heidelberg, Germany*
3. *CNR - Istituto di Struttura della Materia, CP10, 00016 Monterotondo Scalo, Italy*
4. *Elettra-Sincrotrone Trieste, 34149 Basovizza, Trieste, Italy*
5. *Max-Planck-Institut für Kernphysik, 69117 Heidelberg, Germany*

The interplay between electrons after single photon absorption has been a stimulating topic for studying electron correlation in atomic physics since its foundation. Systems consisting of many weakly-interacting atoms or molecules additionally offer a unique environment for studying said correlation where new decay mechanisms become accessible between the constituents. In particular, Cederbaum and coworkers [1] predicted a new decay mechanism, known as interatomic Coulombic decay (ICD), available in electronically excited weakly bound systems where energy is exchanged with a neighboring atom leading to its ionization. Electron transfer mediated decay (ETMD) is another interatomic decay mechanism, typically much weaker than ICD, where electron transfer from the neighbor to the ion releases energy leading to an additional ionization event [2]. A new variant of ETMD has been was reported which does not require the aforementioned excess energy and can even occur for a ground state ion [3]. Recently, Stumpf et al. [4] predicted ETMD to dramatically enhance the single photon double ionization of a Mg atom in the vicinity of a He atom. Surprisingly, due to ETMD, the theoretical cross section for double ionization of Mg is even higher than that of direct single ionization and is comparable to that of He. Overall, the decay path and its predicted enhancement is not limited to Mg in He clusters, but can be applied to any embedded atoms or molecules which have a lower double ionization potential than the single ionization potential of the environment. Thus, the phenomenon is considered to be of quite general relevance and can be used in He droplets as a new pathway to the formation of doubly-ionized cold species which are difficult to form otherwise.

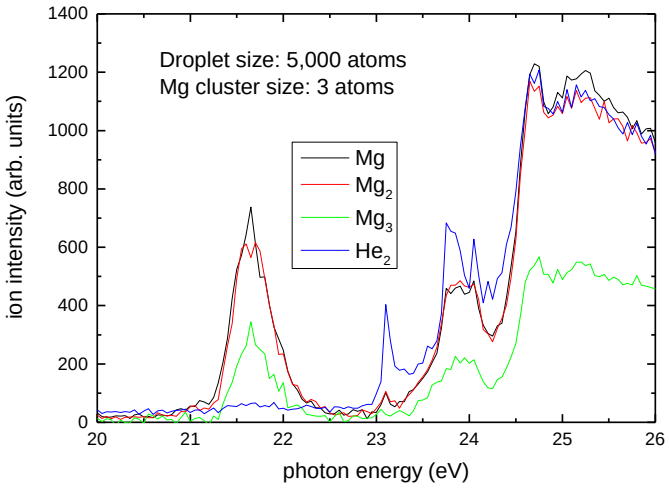

Fig. 1 Ion signal intensity of Mg (black), Mg_2 (red), Mg_3 (green), and He_2 (blue) as a function of photon energy. The droplet size is 5 000 He atoms with an average of 2-3 Mg atoms attached.

Here, we will report on the first experimental observation of this new variant ETMD for particles embedded in superfluid He nanodroplets[5]. Following the initial ionization of a He atom within the droplet, ETMD leads to double ionization of the embedded Mg clusters. Fig. 1 shows the ion signal intensities for several Mg oligomers and the He dimer. From the spectrum, one can see that the relative intensities of Mg ionization is comparable even to that of He. Furthermore, the electron kinetic energy spectra reveal a low energy ETMD peak at about 1 eV agreeing well with theory. We will additionally show that the ETMD mechanism turns out to be the dominant means to doubly ionize Mg clusters and even produce stable doubly ionized clusters. We will further discuss more recent results where we have extended our studies to new molecular systems.

References

[1] L. S. Cederbaum, J. Zobeley, and F. Tarantelli, Phys. Rev. Lett. 79, 4778 (1997).
[2] J. Zobeley, R. Santra, and L. S. Cederbaum, J. Chem. Phys. 115, 5076 (2001).
[3] V. Stumpf, P. Kolorenc, K. Gokhberg, and L. S. Cederbaum, Phys. Rev. Lett. 110, 258302 (2013).
[4] V. Stumpf, N. Kryzhevoi, K. Gokhberg, and L. Cederbaum, Phys. Rev. Lett. 112, 193001 (2014).
[3] A. C. LaForge et al., Accepted as a Phys. Rev. Lett.

Ionisation processes of Rubidium in strong electromagnetic fields

Mihály András Pocsai[1] **and Imre Ferenc Barna**[1,2]

1. Wigner Research Center of the Hungarian Academy of Sciences, Konkoly-Thege Miklós út 29-33, 1121 Budapest, Hungary

2. ELI-ALPS Nonprofit Ltd. Dugonics tér 13, 6720 Szeged, Hungary

We investigate the photoionisation processes of rubidium in strong infra-red laser fields and ionisation processes in the electromagnetic field of a 400 GeV energy proton beam via ab initio calculations. We reduce the latter phenomena to photoionisation by applying the Weizsäcker–Williams method. The time-dependent one-active electron Schrödinger equation is solved using a coupled-channel method. The bound and the continuum states are described with Slater orbitals and Coulomb wavepackets, respectively. Large number of the bound states has been calculated with the variational method with a satisfactory accuracy. Orbitals with anguar momenta l=0,1,2,3,4 have been considered. This approach has been proven to be succesful for studying various ionisation processes of He atom [1-3]. We investigate the effects of the pulse shape and pulse parameters to the photoionisation cross section. These calculations may provide valuable contributions ot the design of laser and plasma based novel accelerators, e.g. the CERN AWAKE experiment [4]. Our future aim is to include our results in plasma propagation models or in Partice-In-Cell studies.

References

[1] Imre Ferenc Barna, Norbert Grün and Werner Scheid, Eur. Phys. J. D **25,** 239 (2003).
[2] Imre Ferenc Barna and Jan-Michael Rost, Eur. Phys. J. D **27,** 287 (2003).
[3] Imre Ferenc Barna, Jianyi Wang and Joachim Bugrdörfer, Phys. Rev. A **73,** 023402 (2006).
[4] Edda Gschwendtner *et. al: The AWAKE Experimental Facility at CERN*, Proceedings of IPAC 2014, Dresden, Germany.

Parametric Amplification in Metastable Helium at Room Temperature

Chitram Banerjee[1],Jasleen Lugani[1], Marie-Aude Maynard[1], Pascal Neveu[1],R.Soorat[2],Rupamanjari Ghosh[2],Fabien Bretenaker[1], Fabienne Goldfarb[1]

1. Laboratoire Aime Cotton, CNRS-Universite Paris-Sud 11-ENS Cachan, 91405 Orsay Cedex, France

2. Shiv Nadar University Gautam Buddha Nagar, UP 201 314, India

Phase Sensitive Amplification can amplify a signal without degrading the signal to noise ratio, it has been widely studied for applications in optical communication, imaging industry, quantum optics and quantum information experiments. This parametric process has been mainly implemented in non-linear crystals ($\chi^{(2)}$) and fibers ($\chi^{(3)}$)and recently in alkali vapors such as rubidium [1, 2].In this work, we present our work on phase sensitive amplification performed in metastable helium at room temperature. The maximum obtainable gain is close to 6 with a bandwidth of 100 kHz.

Motivated by our recent works on successful implementation of optical storage [3] in metastable helium, we have used $2^3S_1 \rightarrow 2^3P_1$ (D1) transition of He. In comparison to alkali atoms, helium is free of hyperfine levels resulting in (a) a simplified level structure, (b) eliminating the need of repumping lasers (c) remove the possibility of extraneous FWM processes which may add noise and degrade squeezing as affected in rubidium [2]. Through our measurements, we have shown that contrary to rubidium, we can achieve better gains close to resonance and within the Doppler width. The gains obtained for the PIA case and the PSA case correspond well, illustrating that we have pure PSA without any other FWM processes.

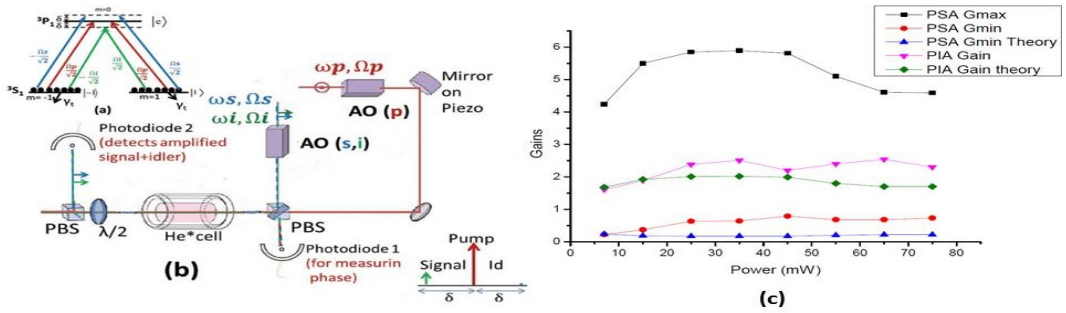

Figure 1: (a) Double Λ structure in helium, both arms are excited by pump (Ω_p, red), signal ((Ω_s), blue) and idler (Ω_i, green) beams (b) Experimental setup: Pump, signal and idler derived from the same laser, their frequencies and amplitudes controlled by two acousto optics (AO). Signal and idler follow the same path. Polarizing beam splitter (PBS) recombine the beams before the cell. The piezo-actuator in the pump path enables to scan the phase. (c) The results obtained: experimental maximum gain and the minimum gain for PSA and the gain from PIA and the theoretically calculated minimum gain for PSA and the gain for PIA.

Such large gains in the absence of a cavity have been possible because of inherent large χ^3 offered by the system. Since optical storage has already been performed on this system [3], using it as a PSA would serve as a noiseless preamplifier of the stored/retrieved signal and also in the generation of non-classical states for quantum information experiments.

References

[1] R. C Pooser, A. M Marino, V. Boyer, K.M Jones, P.D. Lett, "Quantum correlated light beams from non-degenerate four-wave mixing in an atomic vapor: the D1 and D2 lines of 85 Rb and 87 Rb," Optics express **17**, 16722-16730 (2009).

[2] N.V. Corzo, A.M. Marino, K.M. Jones, P.D. Lett, "Noiseless Optical amplifier operating on hundreds of spatial modes," Phys. Rev. Lett. **109**, 043602 (2012).

[3] M.-A. Maynard, F. Bretenaker, F. Goldfarb, "Light storage in a room temperature atomic vapor based on coherent population oscillations," Phys. Rev. A **90**, 061801 (2014).

Statistical regimes and 'extreme events' in Random Laser emission

Federico Tommasi[1], Emilio Ignesti[1], Lorenzo Fini[1], Stefano Lepri[2], Stefano Cavalieri[1]
1.Dipartimento di Fisica e Astronomia, Università di Firenze, via G. Sansone 1, I-50019 Sesto Fiorentino, Italy
2. Istituto dei Sistemi Complessi, Consiglio Nazionale delle Ricerche, via Madonna del Piano 10, I-50019 Sesto Fiorentino, Italy

Random laser [1] is an optical source constituted of a scattering active medium where the light is amplified by stimulated emission along random paths. If gain overcomes losses, a laser-like output emission, without the requirement of an optical cavity, is generated [2].

Since '90s several experimental and theoretical works devoted to the investigation on the characteristics of this new optical system have been reported. In particular, the random laser shows peculiar and exotic behaviours that are due to the combined effects of the chaotic propagation of light in the disorder medium, the non-linearity of the amplification mechanism and the complex modes coupling. In such a system large fluctuations can appear in the emission spectrum that deeply alter the shot-to-shot output emission with the same starting conditions. Lévy statistics have been successfully applied to characterize such statistical fluctuations [3]. Narrow spikes at random frequencies have been reported in random laser emission spectra and we have identified three statistical regimes both in experimental data [4] and in the numerical simulations, as well as modifications in the output directionality [5].

Our theoretical model describes a 'mode' as a possible path of the light inside the disordered medium, whereas an incoherent feedback mechanism has been identified as responsible of the laser action in weakly scattering samples. A Monte Carlo simulation of the propagation of random walkers within the active diffusive medium has shown that gain competition for the available gain is the coupling mechanism for the optical modes. This work has lead to a clear link between the experimental behaviour and the theoretical framework.

In addition, we also explored the possibility to study random laser systems in the light of the recent growing interest about the statistics of extreme events that appear as 'outliers' in the tail of a statistical distribution. These events, due to their huge size and catastrophic impact, appear as beyond the normal expectation and it could be of great importance form many different fields to understand the underlying mechanisms that are able to trigger them. Hence, we have also investigated the random laser in a new approach to analyse when this system can be driven to an unexpected behaviour by its complex dynamics, that can also trigger extreme rare events with a 'catastrophic' impact [6,7]. Experimental and theoretical investigations are currently in progress.

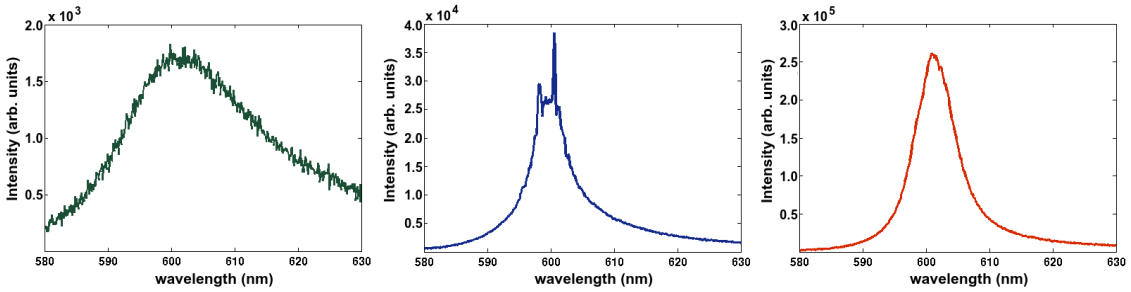

Fig. 1 Three typical experimental spectra of random laser emission for the same weakly scattering sample at different pumping energies.

References

[1] V. S. Letokhov, *Generation of light by a scattering medium with negative resonance absorption*, Zh. Eksp. Teor. Fiz. **53**, 1442 (1967); Sov. Phys. JETP **26**, 835 (1968).
[2] Diederik S. Wiersma, *The physics and applications of random lasers*, Nature Phys. **4**, 359 (2000).
[3] Stefano Lepri, Stefano Cavalieri, Gian-Luca Oppo, Diederik S. Wiersma, *Statistical regimes of random laser fluctuactions*, Phys. Rev. A **75**, 063820 (2007)
[4] Emilio Ignesti, Federico Tommasi, Lorenzo Fini, Stefano Lepri, Vivekananthan Radhalakshmi, Diederik S. Wiersma, Stefano Cavalieri, *Experimental and theoretical investigation of statistical regimes in random laser emission*, Phys. Rev. A **88**, 033820 (2013)
[5] Federico Tommasi, Emilio Ignesti, Lorenzo Fini, Stefano Cavalieri, *Controlling directionality and the statistical regime of the random laser emission*, Phys. Rev. A **91**, 033820 (2015)
[6] Nassim N. Taleb, *The Black Swan: The Impact of Highly Improbable*, Random House, New York (2007)
[7] Hugo L. D. de S. Cavalcante, Marcos Oriá, Dieder Sornette, Edward Ott, Daniel J. Gauthier, *Predictability and Suppression of Extreme Events in a Chaotic System*, Phys. Rev. Lett. **111**, 198701 (2013)

Single Photon Hot Electron Ionisation of Molecules

Klavs Hansen
Tianjin International Center of Nanoparticles and Nanosystems, Tianjin University, P.R.China

Robert Richter[1], Michele Alagia[2], Stefano Stranges[2,3], Luca Schio[2], Peter Salén[4], Vasyl Yatsyna[5], Raimund Feifel[5], and Vitali Zhaunerchyk[5]
1 Elettra - Sincrotrone Trieste, Trieste, Italy
2 IOM-CNR Tasc, Trieste, Italy
3 Dipartimento di Chimica e Tecnologie del Farmaco, Universitá Sapienza, Roma, Italy
4 Department of Physics, Stockholm University, Sweden
5 Department of Physics, University of Gothenburg, Sweden

One photon molecular ionization is conventionally understood as emission of an electron in state-to-state processes, involving only a few and well defined electronic states. In contrast, multiphoton ionization may proceed *via* several different mechanisms, such as above threshold ionization, field ionization and thermionic emission. In addition, electrons can be emitted in a quasi-thermal process where the electronic degrees of freedom act as a thermal subsystem which is heated by e.g. laser pulses while the vibrational motion remains cold for a good fraction of a picosecond [1].

This mechanism has been shown to be responsible for the ionization of a number of large polycyclic aromatic hydrocarbons exposed to light with photon energy far below the ionization energy [2]. The ionization requires a laser pulse of duration on the order of the electron-vibration coupling time or shorter, to avoid the premature dissipation of excitation energy into the vibrational motion.

We have recently shown that C_{60} also ionizes with this mechanism after absorption of a *single* photon [3]. The measurements were performed at the ELETTRA Synchrotron Light Source in Trieste (Italy) with photons of energies between 13.5 and 60 eV. The primary experimental evidence is a persistent and strong component of low kinetic energy electrons in the photoelectron spectra. The electron momenta are spherically distributed with no remaining sign of the light polarization and can be described with a Boltzmann factor with a temperature of 1-2 eV, or 1-2 $\cdot 10^4$ K. Additionally, the threshold and channel (viz. single and double C_2 loss from C_{60}^+) for subsequent fragmentation of the produced cation agrees quantitatively with the previously measured thermal behavior. The presence of this type of ionization for photon energies above 30 eV which reach beyond the valence band requires that the photon creates a particle-hole state with at least two particles and two holes.

The observation of this process expands the picture of light-matter interaction with a fundamentally new type of ionization process. It will be of special and immediate importance in astrophysics, e.g. by providing a novel mechanism for producing low energy electrons in the dense interstellar medium close to nascent stars.

References

[1] E.E.B. Campbell, K. Hansen, K. Hoffmann, G. Korn, M. Tchaplyguine, M. Wittmann, I.V. Hertel, *From Above Threshold Ionization to Statistical Electron Emission: The Laser Pulse Duration Dependence of C_{60} Photoelectron Spectra* Phys. Rev. Lett. **8**4 2128 (2000).

[2] M. Kjellberg, A.V. Bulgakov, M. Goto, O. Johansson, and K. Hansen, *Femtosecond electron spectroscopy of coronene, benzo[GHI]perylene and anthracene* J. Chem. Phys. **1**33 074308 (2010).

[3] Klavs Hansen, Robert Richter, Michael Alagia, Stefano Stranges, Luca Schio, Peter Salén, Vasyl Yatsyna, Raimund Feifel, and Vitali Zhaunerchyk, *Single Photon Thermal Ionisation of Molecules* To be published

A New Detection System for photodetachment studies of Negative Ions

Jakob Welander[1], Tobias Leopold[1,2], Johan Rohlén[1], Felipe Ademir Alemán Hérnandez[1,3] and Dag Hanstorp[1]
1. Department of physics, Gothenburg University, Kemivägen 9, SE 412 58 Göteborg, Sweden
2. University of Mainz, Saarstraße 21, 55122 Mainz, Germany
3. National Autonomous University of Mexico, Mexico City, Federal District, Mexiko

Negative ions are unique quantum mechanical systems, where the outermost electron is very weakly bound. Independent particle model fails to describe the most basic properties Instead many body theory including the effect of electron correlations is needed to understand the ion property. Therefore, there is a strong demand to perform experimental investigations which can be used to test theories which include the electron correlation effect.

At GUNILLA (Gothenburg University Negative Ion Laser LAb) we use the Laser Photodetachment Threshold Spectroscopy to measure energy dependent interactions between ions and light of a laser. A Pelletron Cesium Sputter Ion Source [1], is used to generate a beam of negative ions and several high power pulsed lasers to generate the wavelength adjustable laser light. The PLTS is performed in a colinear geometry as shown in figure 1.

We will present a new experimental detection system where we can detect Rydberg atoms produced in the photodetachment process. Different Rydberg atoms will be ionized at different position in the field ionizer and will therefore be produce at different electric potentials. Hence, they will obtained different kinetic energies, and can therefore be separated in the electrostatic spectrometer where they hit the detector at different positions. First, we will use the system to measure the branching into the different Rydberg states.

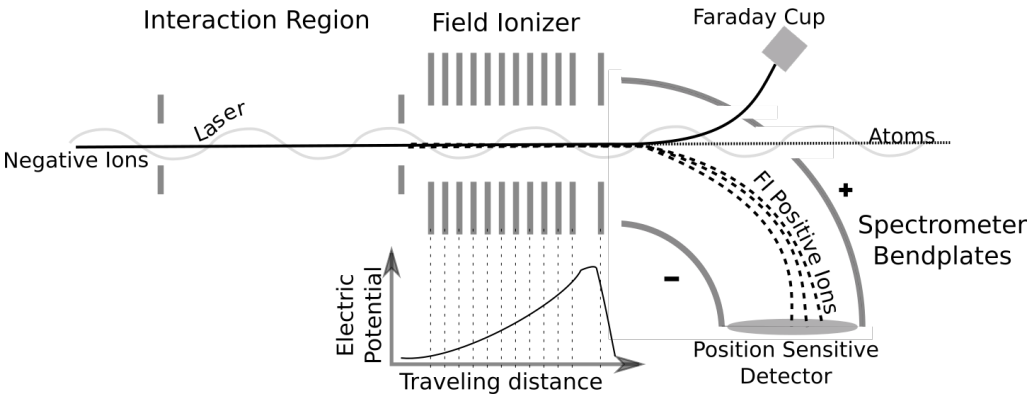

Fig. 1 A schematic view of the interaction region. The field ionizer consists of twelve coaxial plates. The plates can be individually adjusted, and it is hence possible to produce a longitudoal gradient field. Ions with different energies will follow different trajectories and hence strike the position sensitive detector at different positions.

We will also investigate the threshold behavour around the doubly photodetachment. The behaviour of this three body interaction has been described theoretically by both Wannier [2] and Temkin [3]. The diversity of the theoretical prediction makes it even more intriguing to analyse the results from such experiments.

References

[1] Roy Middleton, *A Negative-Ion Cookbook*, Dep. Of Physics, Univ. of Pennsylvania Phil. (1990).
[2] G. H. Wannier, *Threshol Law for Single Ionization of Atoms or Ions by Electrons*, Phys. Rev. **90** 817-825, (1953).
[3] A. Temkin, *The Energy Distribution Cross Section in Threshold Electron-Atom Impact Ionization*, Journal of Phys. B **7** L450-L453, (1974).

UV emission spectrum of liquid water after excitation with photons with exciting-photon energies of 530 eV to 600 eV

Andreas Hans[1], Christian Ozga[1], Robert Seidel[2], Philipp Schmidt[1], Xaver Holzapfel[1], Marvin Pohl[2], Petr Slavíček[3], Bernd Winter[2], Arno Ehresmann[1] and André Knie[1]

1. Institute for Physics and CINSaT, University of Kassel, Heinrich-Plett Straße 40, 343312 Kassel, Germany

2. Helmholtz-Zentrum für Materialen und Energie, Albert-Einstein Straße 15, 12489 Berlin, Germany

3. Department of Physical Chemisry, University of Chemistry and Technology, Technická 5, 16628 Prague, Czech Republic

With the introduction of the liquid microjet technique in the late 1980s [1] the investigation on liquids with considerably high vapor pressure like water by synchrotron radiation became accessible for the first time. This technique meets the vacuum conditions for both synchrotron radiation and photoelectron spectroscopy and thereby allows intense research of the electronic structure of the liquid phase [2,3]. Within the last 20 years several intermolecular interaction schemes like the recently discovered Intermolecular Coulombic Decay (ICD) and non-local de-excitation pathways were found [4]. Additionally the influence of the pH-value of the solution on the solvent could be shown for different nucleobases [5]. However, due to the low escape length of charged particles within dense media these techniques are restricted to the outermost layers of the liquid [6].

To overcome this limitation we propose a new experimental approach for the investigation of the electronic structure of liquids based photon induced fluorescence spectrometry (PIFS) after excitation with synchrotron radiation. This technique was developed mainly for gas-phase experiments using static pressure cells [7,8] but is also feasible for investigations of supersonic cluster jets [9] and the aforementioned liquid microjet technique. Here, we want to present our recent results of an experimental set-up as sketched in Fig.1 which combines the PIFS set-up with the liquid microjet. Due to the significantly higher escape length of emitted photons it is possible to probe regions of the liquid microjet which were not accessible before.

We will show fluorescence spectra of a liquid water microjet for two different energies of the exciting-photons and the fluorescence yield dependency of two of the visible features in the vicinity of the O1s edge as showcase example of the technique.

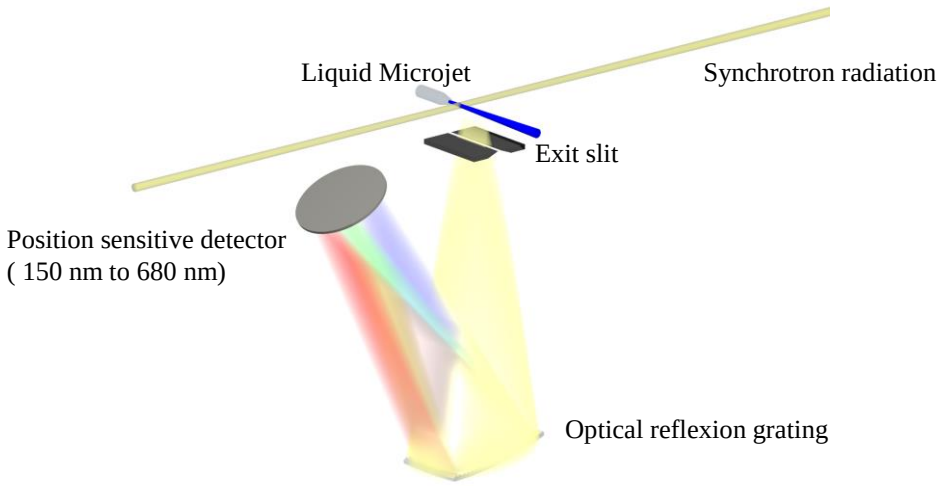

Fig. 1 Scheme of the experimental set-up.

References

[1] M. Faubel, S. Schlemmer, J.P. Toennies, *A molecular beam study of the evaporation of water from a liquid microjet*, Z. Phys. D **10**, 269 (1988).
[2] B. Winter and M. Faubel, *Photoemission from Liquid Aqueous Solutions*, Chem. Rev. **106**, 1176 (2006).
[3] B. Winter, *Liquid microjet for photoelectron spectroscopy*, Nucl. Instrum. Meth. A **601**, 139 (2009).
[4] S. Thürmer, M. Ončak et al., *On the nature and origin of dicationic, charge-separated species formed in liquid water on X-ray irradiation*, Nature Chem. **5**, 590 (2013).
[5] H. Shimada, T. Fukao et al., *Nitrogen K-edge X-ray absorption near edge structure (XANES) spectra of purine-containing nulceotides in aqueous solution*, Chem. Phys. Lett. **591**, 137 (2014).
[6] S. Thürmer, R. Seidel et al., *Photoelectron Angular Distribution from Liquid Water: Effects of Electron Scattering*, PRL **111**, 1 (2013).
[7] A. Knie, M. Ilchen et al., *Angle-resolved study of resonant Auger decay and fluorescence emission processes after core excitations of the terminal and central nitrogen atoms in N_2O*, Phys. Rev. A **90**, 013416 (2014).
[8] A. Hans, A. Knie et al., *Lyman-series emission after valence and core excitation of water vapor*, Phys. Rev A **92**, 032511 (2015).
[9] A. Knie, A. Hans et al. , *Detecting ultrafast interatomic electronic processes in media by fluorescence*, New J. Phys. **16**, 102002 (2014).

Spectral characterization of SASE bunch trains

Philipp Schmidt, Martin Wilke, André Knie and Arno Ehresmann
Institut für Physik und Center for Interdisciplinary Nanostructures Science and Technology, Universität Kassel, Heinrich-Plett-Straße 40, 34132 Kassel, Germany

The recent availability of short wavelength Free-Electron-Lasers (FELs) enabled the investigations of the nonlinear response of matter in the X-ray wavelength regime, i.e. at photon energies where the dominant interaction involves the strongly bound core electrons. The unique temporal, coherence and intensity properties of such devices can therefore be used to monitor the charge and energy flow in highly correlated electron systems and molecular complexes with strong coupling between the electronic and nuclear degrees of freedom [1].
Streak camera-type detectors are ideally suited to analyze the spontaneous and stimulated emissions of such systems after an excitation driven by FELs. After converting a photon signal into electrons, they use a very rapidly changing electric field to deflect these electrons depending on their arrival time in the streak tube, thus projecting the original time information on a spatial axis. In combination with a spectrometer that disperses along another axis, they are able to spectrally and temporally resolve a single x-ray flash on the picosecond time scale.
But for FEL sources like the FLASH facility in Hamburg as well as the upcoming European XFEL that employ bunch trains of up to 3000 individual bunches [2] to achieve very high repetition rates, it also allows recording the SASE (self-amplified spontaneous emission) spectra of all the individual bunches in the very long trains at the same time and for each shot as shown in Fig. 1. Due to the statistical nature of the SASE process [3], this allows for an explicit selection of desired beam parameters and investigations into the correlations between the SASE bunches in these bunch trains in realtime.

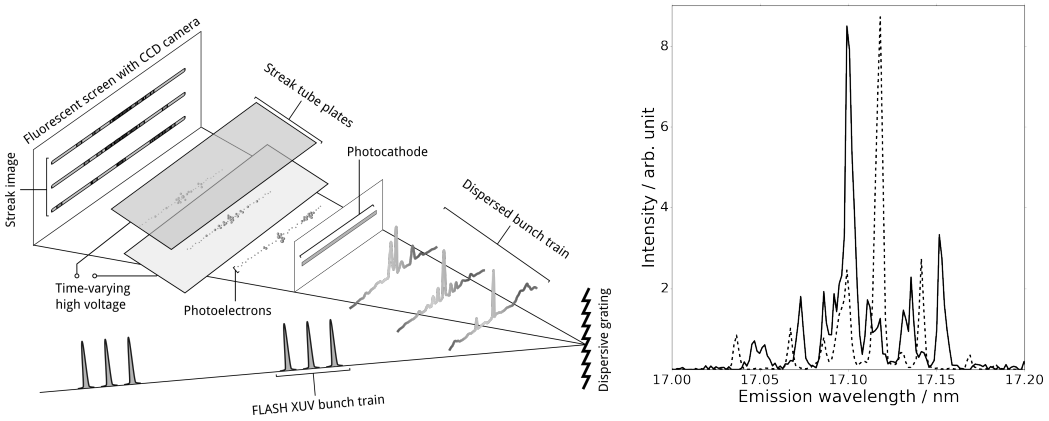

Fig. 1 A schematic of the set-up used to spectrally resolve individual bunches in FLASH bunch trains. Each bunch train is dispersed by a grating in the spectrometer and subsequently converted to electrons by the slit-shaped photocathode. The streaking is performed in perpendicular direction to the dispersion, hence resulting in a picture resolved in time and energy. The resulting single bunch spectra (right) are shown for two exemplary bunches.

Here we want to present first results recently acquired at the FLASH facility as well as future applications and experimental methods using an x-ray streak camera in this manner at FELs.

References

[1] Brian W. J. McNeil and Neil R. Thompson, *X-ray free-electron lasers*, Nature Photonics **4**, 814 (2010)
[2] DESY XFEL Project Group, *European XFEL Technical Design Report* (2007)
[3] S. V. Milton et al, *Exponential Gain and Saturation of a Self-Amplified Spontaneous Emission Free-Electron Laser*, Science **292**, 5524 (2001)

Dynamic Interference in the Photoionization of Helium by Coherent Intense High-Frequency Laser Pulses

Anton N. Artemyev[1], Anne D. Müller[1], David Hochstuhl[2], Lorenz S. Cederbaum[3], and Philipp V. Demekhin[1]
1. Institut für Physik, Universität Kassel, Heinrich-Plett-Str. 40, 34132 Kassel, Germany
2. Institut für Theoretische Physik und Astrophysik, 24098 Kiel, Germany
3. Physikalisch-Chemisches Institut, Universität Heidelberg, Im Neuenheimer Feld 229, 69120 Heidelberg, Germany

Photoionization is one of the basic processes occurring during the interaction between light and matter. The presently available free electron laser (FEL) pulse sources allow to investigate this process in the completely new regime of short intense coherent pulses with carrier frequencies far beyond the ionization threshold. Many new effects become accessible in this regime.

Here, we theoretically investigate the direct ionization of the He atom by an intense coherent high-frequency laser pulse. In particular, we consider photon energies which are nearly resonant for the $1s \rightarrow 2p$ excitation transition in the He^+ ion. This photon energy is enough for the direct ionization of the neutral helium atom, but not sufficient for the one-photon ionization of the remaining He^+ ion. On the other hand, the nearly resonant photon energy couples the $1s$ and $2p$ states of the ion and makes the dynamic interference possible. The scheme of the investigated process is shown in Fig. 1. The effect is exclusively produced by the dynamics of the electron remaining in the He^+ ion. One can describe the process as the repulsion of two ionization thresholds (corresponding to minimal energy, needed for the production of the final singly-ionized states $He^+(1s)$ and $He^+(2p)$), which are seen by the photoelectron. This results in the emission of photoelectrons with different kinetic energies when the pulse arrives, and, symmetrically, the same set of energies when the pulse expires. The photoelectron wave packets with equal kinetic energies superimpose, which results in the dynamic interference phenomenon [1].

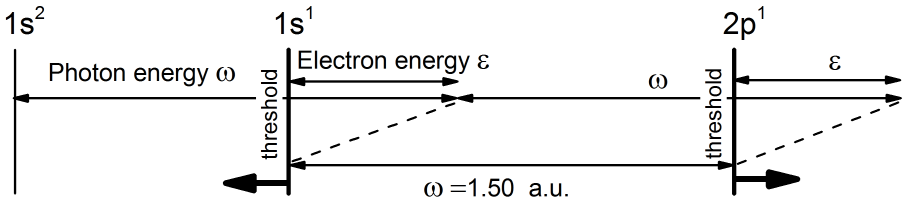

Fig. 1 Scheme of the presently studied process, in which one photon from the high-frequency linearly polarized pulse brings the photoelectron in the ionization continuum, whereas absorption of another near-resonant photon from the same pulse couples 1s and 2p states of the remaining electron in the He^+ ion. The photoelectron sees these states of the ion as the photoionization thresholds, which repel each other and shift in opposite directions following the laser pulse.

In order to describe this process we solve numerically the time-dependent Schrödinger equation for the two-electron wave-function using the efficient time-dependent restricted-active-space configuration-interaction method (TD-RASCI, [2]). Since sequential double-ionization within the selected regime is possible only via absorption of three and more photons, we restrict the active space for one of the electrons by few bound states, describing important relevant orbitals in the neutral atom and remaining ion. The active space of the second electron allows ionization. As a result, the present calculations completely describe all processes, involving absorption of one and two photons, and partially those with three photons. In order to enable observation of the dynamic interference patterns in the computed photoionization spectrum, the two-electron wave-packets were propagated on large spatial grids over long times.

The calculated energy spectra of photoelectron demonstrate clear patterns due to the dynamic interference. We show, how the form of the pattern can be controlled by carrier frequency as well as the pulse intensity. Our results pave the way for future experiments on verification of the dynamic interference by currently available FELs, e.g., FERMI@Elettra.

References

[1] Ph. V. Demekhin, L. S. Cederbaum, Phys. Rev. Lett. **108**, 253001 (2012).
[2] D. Hochstuhl, M. Bonitz, Phys. Rev. A **86**, 053424 (2012).

Multiphoton Ionization and High-order Harmonic Generation from Quasi-periodic Systems in the Terawatt Intensity Regime

Henri Bachau and Fabrice Catoire
Centre des Lasers Intenses et Applications, Université de Bordeaux-CNRS-CEA, 33405 Talence Cedex, France

We have considered the theoretical study of the single ionization of a quasi-periodic system interacting with an infra-red (IR) laser. A large increase of the photoelectron cut-off is observed and goes well beyond what is expected when one consider an atomic or molecular system [1].

In this work, the target is simulated by a one-active electron system plunged in a potential that is composed of a finite number of identical wells submitted to an intense long-wavelength laser. When an infinite number of wells is considered, the model is the so-called Kroenig-Penney model. The time-dependent schrödinger Equation is solved numerically in the velocity gauge and the dimensionality has been reduced to one, along the polarization axis, for the sake of simplification. The initial state is chosen to be the ground state of the system which has a momentum component essentially centered around $k = 0$. The results are compared with a Kroenig-Penney model for a periodic crystal using Bloch functions [2]. Figure 1 shows the ionization probability for a potential reproducing the CsI crystal [3]. A clear change of the cut-off law is observed when the number of wells is increased. The classical atomic/molecular $10U_p$ cut-off is, for the considered laser parameters, 6 eV [4]. In this work we show that the main mechanism responsible for the strong increase of the plateau cut-off is an inter-band non-perturbative dynamics involving a resonance like transition so that high values of energy in the continuum is reached that goes well beyond $10U_p$. The change of regime from perturbative to non-perturbative is characterized by the Keldysh parameter $\gamma = \sqrt{\frac{I_p}{2U_p}}$ for atomic/molecular systems. When $\gamma << 1$ the non-perturbative tunnelling regime is defined and when $\gamma >> 1$ the perturbative multi-photon ionization occurs [5]. For quasi-periodic systems, we show that this transition is defined by a new parameter $\Gamma = \frac{\omega_B}{\omega_0}$, where ω_B is the so-called Bloch frequency [6] and ω_0 is the laser central frequency. $\omega_B = aE_0$ where a is the lattice constant and E_0 the electric field value. When $\Gamma \geq \pi$ then the inter-band resonance is favorable describing the non-perturbative regime, while $\Gamma < \pi$ characterises the perturbative regime.

High-order harmonic generation (HHG) is also investigated as a function of the number of wells. In particular the HHG yield as a function of the number of wells is studied and compared with available experiments [7]. Results will be presented at the conference.

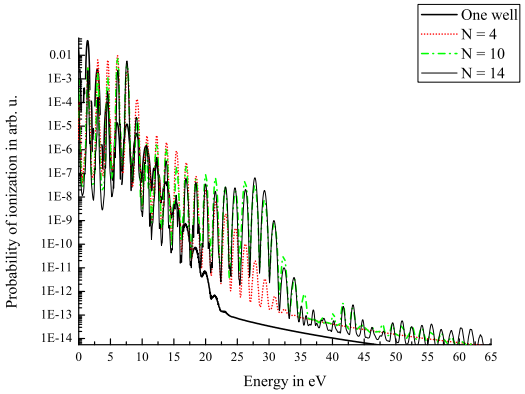

Fig. 1 Plot of the probability ionization as a function of the number of wells (N) [3]. The laser parameters are a peak intensity of I = 10 TW/cm^2, a central wavelength of 800 nm and a pulse duration of 20 fs described a sin^2 envelope. The ponderomotive energy is $U_p = 0.6$ eV.

References

[1] A.N. Belsky, P. Martin, H. Bachau, A.N. Vasil'ev, B.N. Yatsenko, S. Guizard, and G. Petite, Eurphys. Lett. **67**, 301 (2004).
[2] H. Bachau, A.N. Belsky, P. Martin, A.N. Vasil'ev and B.N. Yatsenko, Phys. Rev. B **74**, 235215 (2006).
[3] F. Catoire and H. Bachau, Phys. Rev. Lett. **115**, 163602 (2015).
[4] P. Colosimo *et al.*, Nat. Phys. **4**, 386 (2008).
[5] L.V. Keldysh, Sov. Phys. JETP **20**, 1307 (1965).
[6] F. Bloch, Z. Phys. **52**, 555 (1928).
[7] H. Park, Z. Wang, H. Xiong, S.B. Schoun, J. Xu, P. Agostini and L.F. DiMauro, Phys. Rev. Lett. **113**, 263401 (2014).

Ionization of Aligned and Oriented OCS Molecules with Few-Cycle Mid-IR Laser Pulses

Rasmus Johansen[1], Lauge Christensen[2], Darko Dimitrovski[1], Lars Madsen[1] and Henrik Stapelfeldt[2]
1. Department of Physics and Astronomy, Aarhus University, Ny Munkegade 120, 8000 Aarhus, Denmark
2. Department of Chemistry, Aarhus University, Langelandsgade 140, 8000 Aarhus, Denmark

We present new results on the ionization of aligned or oriented OCS molecules with few-cycle mid-IR (1850nm, 12fs) laser pulses. The pulses originate from a recently established setup following the design in ref. [1]. The pulses are passively carrier-envelope phase (CEP) stabilized and the CEP can be controlled by a pair of fused-silica wedges.

Two experiments are presented. In the first OCS molecules were adiabatically aligned with a 10-nanosecond laser pulse and singly ionized by the linearly polarized mid-IR pulse. The ionization process produces solely OCS+ cations with negligible fragmentation. The yield of ions was measured as a function of the angle between the polarization of the mid-IR pulse and the molecular axis determined by the polarization of the alignment pulse. The results are displayed in Fig. **1a** and show that the ion yield reaches a maximum when the mid-IR polarization is at an angle of $\theta = 60^\circ$ or $\theta = 120^\circ$ with respect to the molecular axes. Our measurements differ qualitatively from previous measurements at 800 nm [1]. Calculations in the tunneling regime are used to rationalize the experimental findings.

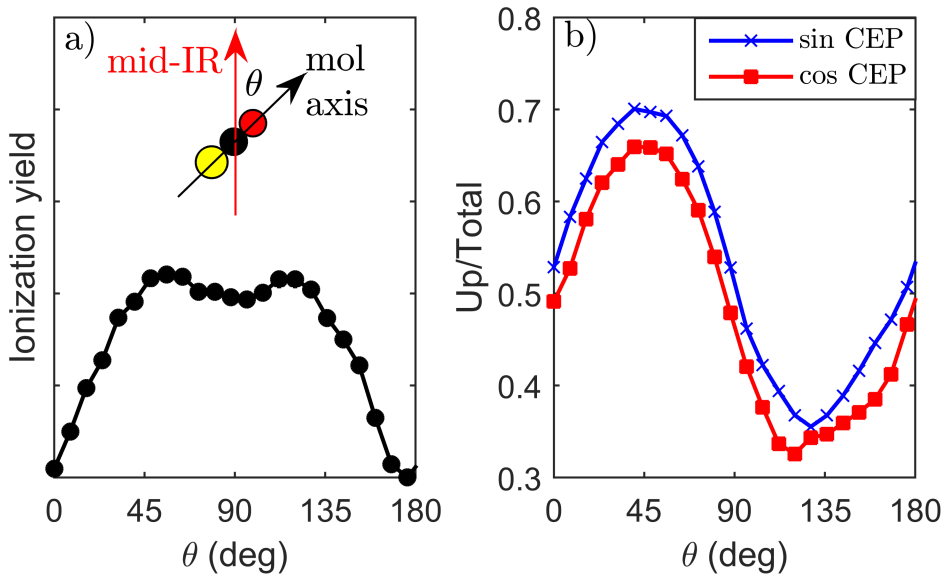

Fig. 1 a) The measured OCS ionization yield as a function of the angle between the ionizing laser polarization and the molecular axis, θ, as defined in the insert. **b)** The result of measuring electron VMI images and calculating the up/total ratio for different orientation angles and for both a sine- and cosine like CEP value.

In the second experiment the molecules were oriented by the combined interactions of the 10-nanoscond laser pulse and a weak static electric field using OCS molecules selected in the absolute ground state [3]. Again the molecules were singly ionized by the mid-IR pulses and the photoelectrons were detected. The number of electrons emitted in the forward direction of the mid-IR field compared to the total number of electrons emitted, Up/Total, was determined. The result, presented in Fig. **1b** for three different CEPs, shows a strong dependence on the molecular orientation. The experimental results are compared to theoretical calculations and reveal details on the laser-field induced distortion of molecular orbitals.

References

[1] Bruno Schmidt, Pierre Béjot, Mathieu Giguére, Andrew Shiner, Carlos Trallero-Herrero et al., *Compression of* 1.8 μm *laser pulses to sub two optical cycles with bulk material*, Appl. Phys. Lett. **96**, 121109 (2010).

[2] Jonas Hansen, Lotte Holmegaard, Jens Nielsen, Henrik Stapelfeldt, Darko Dimitrovski and Lars Madsen, *Orientation-dependent ionization yields from strong-field ionization of fixed-in-space linear and asymmetric top molecules*, J. Phys. B: At. Mol. Opt. Phys. **45**, 015101 (2012).

[3] Jens Nielsen, Henrik Stapelfeldt, Jochen Küpper, Bretislav Friedrich, Juan Omiste and Rosario González-Férez *Making the Best of Mixed-Field Orientation of Polar Molecules: A Recipe for Achieving Adiabatic Dynamics in an Electrostatic Field Combined with Laser Pulses*, Phys. Rev. Lett. **108**, 193001 (2012).

Trapping of Neutral Atoms in Structured Light: Role of the light orbital angular momentum

Dominik Schulze[1], **Anita Thakur**[1,2], **A. S. Moskalenko**[1,3], **Jamal Berakdar**[1]
[1] *Institut für Physik, Martin-Luther-Universität Halle-Wittenberg, Karl-Freiherr-von-Fritsch-Straße 3, 06120 Halle/Saale, Germany*
[2] *ELI - extreme light infrastructure, Prague, Czech Republic*
[3] *Department of Physics and Center for Applied Photonics, University of Konstanz, 78457 Konstanz, Germany*

The ponderomotive force plays a key role in laser-induced particle acceleration [1,2] and trapping [3,4]. The direction of the force is independent of the sign of the particle charge acting in the direction of the intensity gradient. Acceleration of the center of mass of a neutral atom by an intense Gaussian laser beam were demonstrated in Ref. [2].
We study here the dynamics of neutral atoms focused, high-intensity spatially structured laser beams, in particular those carrying orbital angular momentum OAM (optical vortices). We find (cf. Fig.1) that the trapping potential can be spatially structured by an appropriate superposition OAM beams. The topological charge of the beams controls the spatial inhomogeneity. The atom can be trapped or scattered by the potential, which maybe exploited for atom guiding and for lithographic applications.

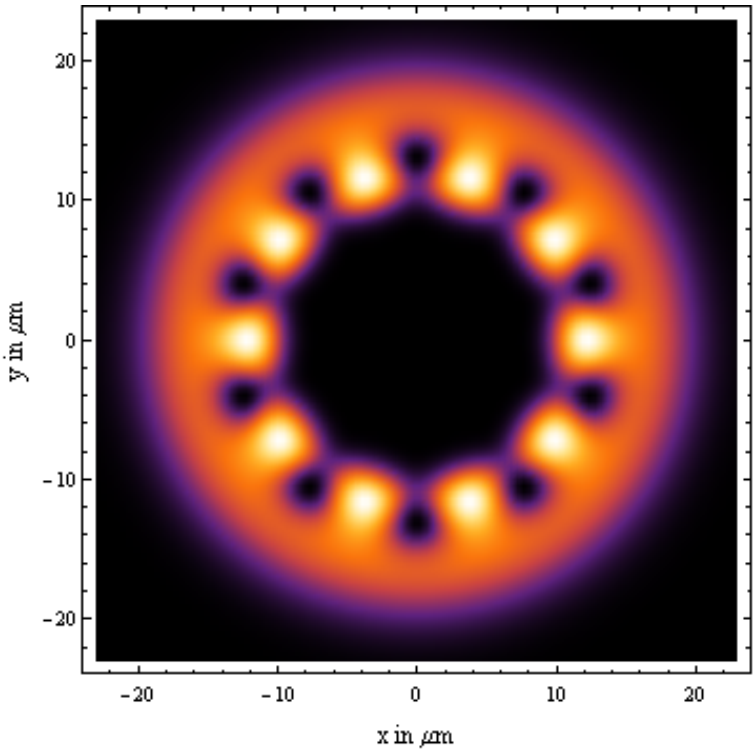

Fig. 1 The ponderomotive potential of a superposition of two counter propagating Laguerre-Gaussian beams that carry orbital momentum.

References

[1] T. Tajima, and J.M. Dawson, *Laser electron accelerator*, Phys. Rev. Lett. **43**, 267–270 (1979).
[2] U. Eichmann, T. Nubbemeyer, H. Rottke and W. Sandner, *Acceleration of neutral atoms in strong short-pulse laser fields*, Nature **461**, 1261 (2009).
[3] H.A.H. Boot, and R.B.R.-S. Harvie, *Charged particles in a non-uniform radiofrequency field*, Nature **180**, 1187 (1957).
[4] H.G. Dehmelt, *Radio-frequency spectroscopy of stored ions*, Adv. At. Mol. Phys. **3**, 53–72 (1967).

Circularly polarized high harmonics from Ne atoms

Lukas Medišauskas
Max Planck Institute for the Physics of Complex Systems, Nöthnitzer Str. 38, 01187 Dresden, Germany

Jack Wragg[1], Hugo van der Hart[1], Misha Yu. Ivanov[2,3,4]
1. Centre for Theoretical Atomic, Molecular and Optical Physics, School of Mathematics and Physics, Queen's University Belfast, Belfast BT7 1NN, UK
2. Department of Physics, Imperial College London, South Kensington Campus, SW7 2AZ London, United Kingdom
3. Max-Born-Institute, Max-Born Strasse 2A, D-12489 Berlin, Germany
4. Department of Physics, Humboldt University, Newtonstr. 15, D-12489 Berlin, Germany

To extend the applicability of High Harmonic Generation (HHG) process as a light source for ultrafast spectroscopy, it is important to control the polarization of emitted XUV light. An elegant solution to generate circularly polarized harmonics relies on combining circularly polarized fundamental with counter-rotating second harmonic [1,2]. The harmonic spectra generated by such driving field consists of pairs of left- and right- circularly polarized harmonics. This approach was used in recent experiments [3,4] where bright, phase matched high harmonic radiation was produced. However, Ar and Ne atoms, which were used in these experiments, have a ground state with non-vanishing angular momentum. Up to now its role in the HHG process with counter-rotating bi-chromatic fields was little investigated.

In this work [5], we numerically investigate the HHG process with bi-chromatic counter rotating circularly polarized laser fields by solving the Time-Dependent Schödinger Equation for a 2D model of Neon atom. We demonstrate that the harmonic spectra is distinctively different when atomic orbitals with non-zero angular momentum, e.g., 2p, and orbitals with zero angular momentum, e.g., 1s, are considered. Namely, the height of left- and right- circularly polarized harmonics is different by an order of magnitude when 2p orbitals are used (see Figure 1). The effect is due to the suppression of the contribution from orbitals counter-rotating with the driving field, i.e., $2p_-$, and involves an interplay of ionization, recombination and continuum electron propagation dynamics.

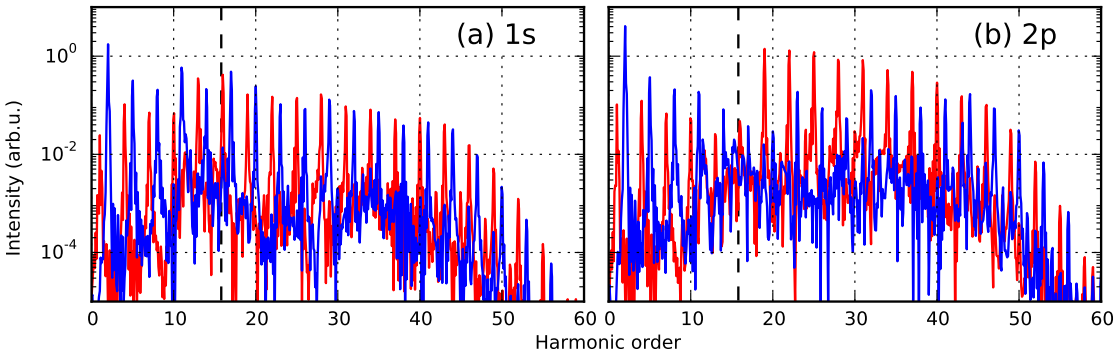

Fig. 1 Spectra for (a) 1s and (b) superposition of $2p_+$ and $2p_-$ states split into contributions that are co-rotating (red) and counter-rotating (blue) with the driving IR field. Vertical dashed line marks the energy of ionization potential I_p

In the time domain, the generated harmonics from Ne correspond to a train of attosecond pulses with close to circular polarization. Hence, we demonstrate an amplitude gating scheme that allows to isolate a single attosecond radiation burst and thus attain highly elliptical isolated attosecond pulses.

References

[1] Eichmann, H. and Egbert, A. and Nolte, S. and Momma, C. and Wellegehausen, B. and Becker, W. and Long, S. and McIver, J. K., *Polarization-dependent high-order two-color mixing*, Phys. Rev. A. **51**, R3414(R) (1995).
[2] Long, S. and Becker, W. and McIver, J. K., *Model calculations of polarization-dependent two-color high-harmonic generation*, Phys. Rev. A **52**, 2262 (1995).
[3] Avner Fleischer, Ofer Kfir, Tzvi Diskin, Pavel Sidorenko and Oren Cohen, *Spin angular momentum and tunable polarization in high-harmonic generation*, Nature Photon.. **8**, 543–549 (2014).
[4] Kfir, O., Grychtol, P., Turgut, E., Knut, R., Zusin, D., Popmintchev, D., Popmintchev, T., Nembach, H., Shaw, J.M., Fleischer, A. and Kapteyn, H., *Generation of bright phase-matched circularly-polarized extreme ultraviolet high harmonics*, Nature Photon.. **9**, 99–105 (2015).
[5] Medišauskas, L., Wragg, J., van der Hart, H. and Ivanov, M.Y., *Generating Isolated Elliptically Polarized Attosecond Pulses Using Bichromatic Counterrotating Circularly Polarized Laser Fields*, Phys. Rev. Lett. **115**, 153001 (2015).

Laser-sub-cycle Fragmentation Dynamics of Argon Dimers

S. Erattupuzha[1], V. Kunnummel[1], S. Larimian[1], V. Hanus[1], M. Koch[2], M. Schöffler[3], X. Xie[1], A. Baltuska[1], G. Paulus[4,5], C. Lemell[6], J. Burgdörfer,[6] and M. Kitzler[1]

1. Photonics Institute, Vienna University of Technology, Gusshausstrasse 27, A-1040 Vienna, Austria
2. Institute of Experimental Physics, Graz University of Technology, Petersgasse 16, A-8010 Graz, Austria
3. Institut für Kernphysik, Goethe-Universität Frankfurt, Max-von-Laue-Str. 1, D-60438 Frankfurt am Main, Germany
4. Friedrich-Schiller-Universität Jena, Max-Wien-Platz 1, D-07743 Jena, Germany
5. Helmholtz Institute Jena, Fröbelstieg 3, D-07743 Jena, Germany
6. Institute for Theoretical Physics, Vienna University of Technology, Wiedner Hauptstrasse 8, A-1040 Vienna, Austria

We experimentally investigate the fragmentation of multiply ionized argon dimers with sub-5 fs laser pulses with a known carrier envelope offset phase (CEP). The overall goal of our experiments is to obtain insight into the sub-laser-cycle dynamics leading to the trapping of an emitted electron into Rydberg states by the so-called process of frustrated tunnel ionization (FTI) [1], and, furthermore, to investigate the amenability of this process to strong-field-control.

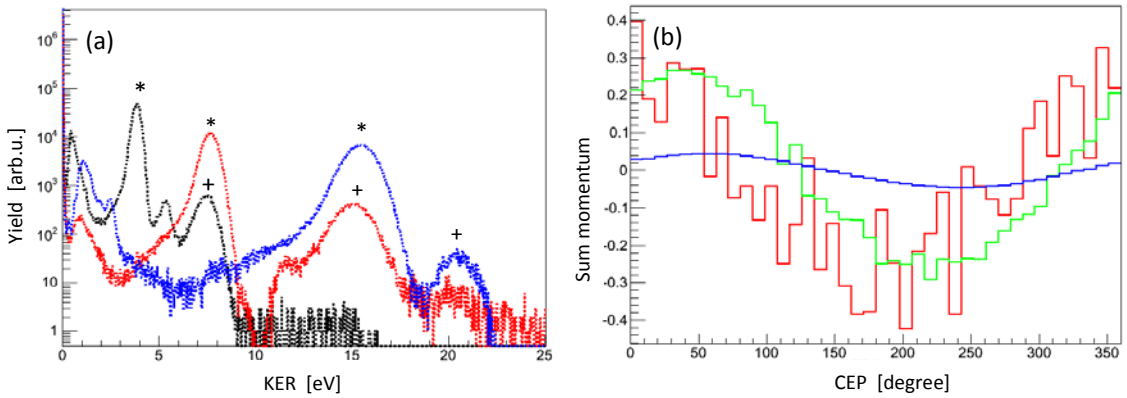

Fig. 1: (a) Kinetic energy release (KER) spectra for different fragmentation channels. The plot in black gives the KER of channel Ar^{+}/Ar^{+}, the red plot corresponds to Ar^{2+}/Ar^{+} and the blue plot to Ar^{2+}/Ar^{2+}. (b) Sum momentum of fragments for fragmentation channel Ar^{2+}/Ar^{+} plotted over CEP for Coulomb explosion (green curve), frustrated tunneling ionization (red curve) and argon monomer (blue curve).

Measured kinetic energy release (KER) distributions of different fragmentation channels of argon dimers, Ar^{+}/Ar^{+}, Ar^{2+}/Ar^{+} and Ar^{2+}/Ar^{2+} are shown in Fig.1 (a). The distributions feature several peaks. The peaks marked by **'*'** are due to Coulomb explosions of multiply ionized argon dimers at their equilibrium geometry into ion pairs Ar^{+n}/Ar^{+m}, while the peaks marked by **'+'** are due to explosions after FTI. The fragments resulting from Coulomb explosion after a FTI process feature a higher KER than the corresponding dimers in the ground (or only weakly excited) state with the same initial charge state (n+m). The reason is that the trapped electrons are in highly excited ionic states and therefore, due to the large spatial extension of the corresponding electronic states, do not shield the nuclear charge efficiently. As a result, the corresponding Ar^{+n}/Ar^{+m} pairs feature almost the same KER values as pairs with ions in their ground state but a charge state (n+m+1). Fig. 1(a) shows that the measured KER distribution for the Ar^{2+}/Ar^{+} fragmentation channel (red) features an additional peak at even higher KER. This peak can be attributed to the recapture of two electrons [2]. These results are qualitatively very similar to those obtained with significantly longer pulses (~40 fs) [2-4]. However, interestingly, in our experiments performed with few cycle laser pulses we measure a higher yield for the trapped Rydberg electrons.

To obtain insight into the sub-cycle evolution of the trapping process we analyzed its dependence on the CEP. Fig. 1(b) shows the sum momentum of the Ar^{2+}/Ar^{+} ion pairs as a function of CEP. To obtain the CEP-dependence we applied the phase-tagging method with a stereo ATI- phase meter. As in this scheme the absolute phase is not known, the CEP-dependence of the argon monomer can serve as a reference, cf. blue line in Fig. 1(b). Because the sum momentum of the Ar^{2+}/Ar^{+} ion pairs is equivalent to the momentum sum imparted to the dimer by the electrons during emission and recapture, comparison of its CEP-dependence for pairs where an electron has been trapped with pairs for which no trapping has occurred can give insight into the laser-sub-cycle dependence of the trapping process. By comparison of the measured CEP-dependence with that simulated by the Classical trajectory Monte Carlo method we gain insight into the electron trajectory dynamics that leads to the trapping process.

References

[1] T. Nubbemeyer et al., *"Strong-Field Tunneling without Ionization"*, Phys. Rev. Lett. **101**, 233001 (2008).
[2] J. Wu et al., *"Multiple Recapture of Electrons in Multiple Ionization of the Argon Dimer by a Strong Laser Field"*, Phys. Rev. Lett. **107**, 043003 (2011).
[3] B. Manschwetus et al., *"Mechanisms underlying strong-field double ionization of argon dimers"*, Phys. Rev. A **82**, 013413 (2010).
[4] B. Ulrich et al., *"Double-ionization mechanisms of the argon dimer in intense laser fields"*, Phys. Rev. A **82**, 013413 (2010).

Coincidence Spectroscopy of Strong Laser Field Induced Rydberg States

Seyedreza Larimian[1], Sonia Erattupuzha[1], Raffael Maurer[1], Christoph Lemell[2], Stefan Nagele[2], Shuhei Yoshida[2], Joachim Burgdörfer[2], Andrius Baltuška[1], Markus Kitzler[1], and Xinhua Xie[1]

1. Photonics Institute, Vienna University of Technology, A-1040 Vienna, Austria

2. Institute for Theoretical Physics, Vienna University of Technology, A-1040 Vienna, Austria

Ionization of atoms and molecules by strong laser fields is starting point for many strong field phenomena [1]. In a strong laser field, atoms and molecules are ionized via tunneling ionization, i.e., an electron passes through the potential barrier of the combined Coulomb and the laser field. After tunneling, electrons are steered by the laser field and most of them will eventually escape the Coulomb field of the remaining ion core. However, a fraction of them are recaptured into highly excited states by the ionic Coulomb field. This process frequently referred to as frustrated field ionization leads to the formation of high-lying Rydberg states [2].

In this submission, we report on the experimental observation of high-lying Rydberg states with principal quantum number up to $n > 120$ populated during strong field interaction of atoms and molecules with a reaction microscope [3]. Laser pulses with a center wavelength of 795 nm, a pulse duration of 25 fs and a peak laser intensity on the order of $I \sim 10^{14}$ W/cm^2 are exploited in the measurements. A weak homogeneous dc field is applied in the time-of-flight spectrometer to accelerate charged particles to the detectors and to induce field ionization of high-lying Rydberg states populated during the strong field interaction of atoms and molecules.

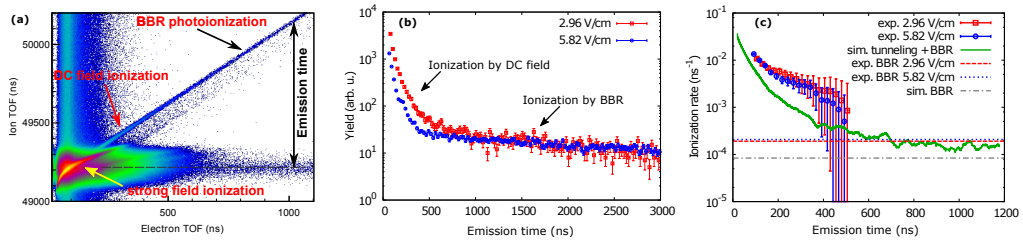

Fig. 1 (a) PEPICO spectrum for argon atoms interacting with laser pulses with peak intensity $I = 1.5 \times 10^{14}$ W/cm^2 and a dc field strength of $F_{\rm dc} = 3$ V/cm. (b) Measured signal intensity of post-pulse ionized argon Rydberg states as a function of the emission time for two field strength $F_{\rm dc}$ with the same laser interaction condition. (c) Ionization rate of Rydberg states derived from measurements and simulated tunneling ionization rates for $F_{\rm dc} = 3$ V/cm and black-body radiation rates.

A typical photoelectron-photoion-coincidence (PEPICO) spectrum for argon atoms (laser intensity $I = 1.5 \times 10^{14}$ W/cm^2, $F_{\rm dc} = 3$ V/cm) features a main peak at electron time-of-flight of TOF$_e = 85$ ns and ion time-of-flight of TOF$_i = 49205$ ns (Fig. 1(a)) due to strong field ionization. Post-pulse ionization events, i.e., an electron and its parent ion being separated after the conclusion of the exciting laser pulse are registered along the diagonal with unit slope from which the ionization times of the excited argon atoms can be read off directly. The post-pulse ionization yield strongly depends on the field strength $F_{\rm dc}$ of the external dc field (Fig. 1(b)). As expected, stronger dc fields initially lead to faster field ionization of the excited Ar* atoms. By contrast, the corresponding ionization rates $\Gamma = -d\ln[I(\tau)]/d\tau$ (Fig. 1(c)) derived from the data in Fig. 1(b) appear to be rather insensitive to the value of $F_{\rm dc}$. The rate decreases from about $\Gamma \approx 0.01$ ns^{-1} at $\tau = 100$ ns to about $\Gamma \approx 0.001$ ns^{-1} at $\tau = 500$ ns. For emission times longer than one microsecond the ionization rate becomes nearly constant at $\Gamma \approx 2 \times 10^{-4}$ ns^{-1}.

In order to identify processes underlying the delayed emission on the nano- to microsecond scale, over-the-barrier and tunneling ionization induced by the dc field and black-body radiation induced photoionization is considered. We determine the effective time-dependent ionization rate by Monte-carlo sampling of alternative decay channels starting with an energy-dependent spectral excitation density formed by frustrated field ionization [4]. The simulated tunneling ionization rate of the Rydberg state with $n = 121$ are shown in Fig. 1(c). Summing over the range $20 < n < 121$ the BBR ionization rate is estimated as $R_{\rm BBR}(n) = 8.4 \times 10^{-5}$ ns^{-1}. Total ionization rates $\sim 2 \times 10^{-4}$ ns^{-1} including tunneling and BBR-induced ionization yield good agreement with the measurements for times approaching one microsecond. The simulation suggests that present time-delayed PEPICO spectra provide for the first time direct access to long-lived Stark resonances in very high Rydberg states and to the population of the Rydberg manifolds extending from $n_{\rm BBR} \approx 20$ to $n_F \approx 120$ formed by frustrated field ionization.

References

[1] T. Brabec and F. Krausz, *Intense few-cycle laser fields: Frontiers of nonlinear optics*, Rev. Mod. Phys. **72**, 545 (2000).

[2] T. Nubbemeyer, K. Gorling, A. Saenz, U. Eichmann, and W. Sandner, *Strong-Field Tunneling without Ionization*, Phys. Rev. Lett. **101**, 233001 (2008).

[3] R. Dörner, V. Mergel, O. Jagutzki, L. Spielberger, J. Ullrich, R. Moshammer, H. Schmidt-Böcking, *Cold Target Recoil Ion Momentum Spectroscopy: A 'Momentum Microscope' to View Atomic Collision Dynamics*, Physics Reports **330**, 95 (2000).

[4] B. Wolter, C. Lemell, M. Baudisch, M. G. Pullen, X.-M. Tong, M. Hemmer, A. Senftleben, C. D. Schröter, J. Ullrich, R. Moshammer, J. Biegert, and J. Burgdörfer, *Formation of very-low-energy states crossing the ionization threshold of argon atoms in strong mid-infrared fields*, Phys. Rev. A **90**, 063424 (2014).

Angular dependence of the attosecond time delay in the H_2^+ molecular ion

Vladislav Serov[1] **and Anatoli Kheifets**[2]
1. Department of Theoretical Physics, Saratov State University, 83 Astrakhanskaya, Saratov 410012, Russia
2. Department of Theoretical Physics, Australian National University, Canberra ACT 2601, Australia

Angular dependence of attosecond time delay relative to polarization of light can now be measured using a combination of the RABBITT (Reconstruction of Attosecond Beating By Interference of Two-photon Transitions) and the COLTRIMS (Cold Target Recoil Ion Momentum Spectroscopy) techniques [1]. This dependence brings particularly useful information in molecules where the angular dependent time delay is sensitive to the orientation of the molecular axis [2]. Here we extend our previous work [2] and consider a molecular H_2^+ ion exposed to an attosecond pulse train (APT) and a dressing IR field which is a characteristic configuration of external electromagnetic fields in a RABBIT measurement. This configuration becomes particularly challenging for theoretical treatment of non-spherically symmetric targets like molecules or molecular ions. To meet this challenge, we solve the time-dependent Schrödinger equation using a fast spherical Bessel transformation (SBT) for the radial variables [3], a discrete variable representation for the angular variables and a split-step technique for the time evolution. The use of SBT ensures correct phase of the wave function for a long time evolution which is especially important in time delay calculations. To speed up computations, we implement an expanding coordinate system [4] which allows us to reach space sizes and propagation times unattainable by other techniques.

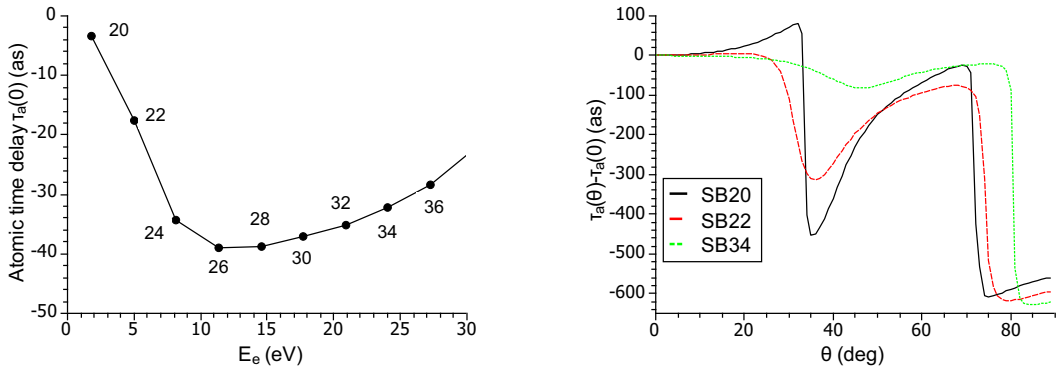

Fig. 1 The atomic time delay $\tau_a(E_e,\theta)$ as a function of the photoelectron energy E_e for fixed $\theta = 0$ (left) and the angular variation of the time delay $\tau_a(E_e,\theta) - \tau_a(E_e,0)$ as for several different E_e values (right). The corresponding sideband indices are marked by integers on both panels..

Results of our investigation are illustrated in Fig. 1 where we show the atomic time delay τ_a in H_2^+ extracted from the side band intensity oscillation $S_{2q}(\tau) = A + B\cos[2\omega(\tau - \tau_a)]$ as a function of the time delay τ between the APT and the IR pulse. The APT is modeled by a series of 11 Gaussian XUV pulses with the central frequency $\omega_{\rm XUV} = 43\omega_{\rm IR}$ and the width $\tau_{\rm XUV} = 120$ as, whereas an long IR pulse is modeled by a continuous wave with frequency $\omega_{\rm IR} = 1.59$ eV ($\lambda = 780$ nm) and the electric field strength $\mathscr{E}_{\rm IR} = 1.5\times10^9$ V/m (field intensity 3×10^{11} W/cm^2). A polarization of the field is parallel to the molecular axis. The time delay τ_a as a function of the photoelectron ejection energy E_e at a fixed ejection angle $\theta = 0$ and the angular variation of the time delay $\tau_a(E_e,\theta) - \tau_a(E_e,0)$ for several fixed photoelectron energies E_e are shown on the left and right panels, respectively. The corresponding side band indices $2q$ are marked on both panels.

References

[1] S. Heuser *et al*, *Time delay anisotropy in photoelectron emission from the isotropic ground state of helium*, arxiv:1503.08966 (2015), Nature Communications, submitted.
[2] V. V. Serov *et al*, *Interpretation of time delay in the ionization of two-center systems*, Phys. Rev. A, **87**, 063414 (2013).
[3] V. V. Serov, *Orthogonal fast spherical Bessel transform on uniform grid*, arXiv:1509.07115 (2015).
[4] V. V. Serov *et al*, *Wave-packet-evolution approach for single and double ionization of two-electron systems by fast electrons*, Phys. Rev. A, 75, 012715 (2007).

Role of nuclear dynamics in ultrafast charge migration

Manuel Lara-Astiaso[1], David Ayuso[1], Ivano Tavernelli[2], Piero Decleva[3], Alicia Palacios[1] and Fernando Martín[1,4,5]

1. Departamento de Química, Universidad Autónoma de Madrid, Cantoblanco, 28049 Madrid, Spain
2. IBM Research GmbH, Zurich Research Laboratory 8803 Rueschlikon, Switzerland.
3. Dipartimento di Scienze Chimiche e Farmaceutiche, Università di Trieste and CNR-Istituto Officina dei Materiali, 34127 Trieste, Italy
4. Instituto Madrileño de Estudios Avanzados en Nanociencia (IMDEA Nano), Campus Universitario de Cantoblanco, 28049 Madrid, Spain
5. Condensed Matter Physics Center (IFIMAC), Universidad Autónoma de Madrid, 28049 Madrid, Spain.

Electron dynamics can be nowadays observed with sub-femtosecond time resolution in ever-increasing molecular systems, from the simplest case of a hydrogen molecule [1] to the more complex amino acid phenylalanine [2]. The possibility of inducing ultrafast charge migration along the skeleton of large biological molecules upon their photoionization was already predicted more than 15 years ago [3], yet its experimental confirmation on phenylalanine has only been achieved very recently, being the first observation of ultrasfast charge migration induced by a single attosecond pulse. The experiment made use of a XUV-IR pump-probe scheme and measured the production of doubly charged species as a function of time-delay with unprecedented attosecond resolution to track the dynamics of the singly charged molecule. A theoretical method based on a density functional theory (DFT) approach, but properly accounting for the scattering states of the ionized biomolecule, was able to reproduce the beatings observed in the ion yields, by accurately describing the electronic wave packet created by the attosecond pulse. This wave packet, which involves more than thirty ionic states, describes the motion of a highly delocalized hole that gives rise to charge fluctuations occurring in less than 4-5 fs. Despite the breakthrough of this joint experimental and theoretical work, a number of questions remained open, in particular, what is the role of nuclear motion in the observed hole dynamics.

Here we explore a new approach to include the nuclear degrees of freedom combining our ab initio DFT-based methods [4] with time-dependent density functional theory plus Ehrenfest dynamics. We first apply it to the glycine molecule, for which there are previous theoretical work performed by assuming that the nuclei remain fixed during the whole process [5]. The latter assumption is based on the argument that nuclear motion should have a negligible effect at the early stages of this evolution, typically during the first tens of femtoseconds, since the shortest vibrational periods within the glycine molecule should exceed 10 fs and usually involve hydrogen atoms, which are not likely to play a major role in charge delocalization processes. The validity of this argument was proved in recent works [6]. However, it has also been shown that nuclear dynamics could strongly affect the coherence between two electronic states beatings in less than 10 fs in situations where the molecular state after photoionization falls not far from a conical intersection [7]. Since conical intersections are a common feature in large molecules, can we really assume that nuclear motion does not play any role in the early stages of the charge migration process? In this communication, we aim at theoretically answering this question.

References

[1] G. Sansone *et* al., *Electron localization following attosecond molecular photoionization*, Nature **465**, 763 (2010)
[2] F. Calegari *et* al., *Ultrafast electron dynamics in phenylalanine initiated by attosecond pulses*, Science **346**, 336 (2014)
[3] L. Cederbaum and J. Zobeley, *Ultrafast charge migration by electron correlation*, Chem. Phys. Lett. **307**, 205 (1999)
[4] M. Stener and P. Decleva, *Time-dependent density functional calculations of molecular photoionization cross sections: N_2 and PH_3*, J. Chem. Phys. **112**, 10871 (2000)
[5] A. I. Kuleff, Jörg Breidbach and L. S. Cederbaum, *Multielectron wave-packet propagation: General theory and application*, J. Chem. Phys. **123**, 044111 (2005)
[6] V. Despré *et* al., *Attosecond hole migration in benzene molecules surviving nuclear motion*, J. Phys. Chem. Lett. **6**, 426 (2015)
[7] M. Vacher *et* al., *Electron dynamics following photoionization: Decoherence due to the nuclear-wave-packet width*, Phys. Rev. A **92**, 040502 (2015)

Measurement and control of atomic phase shifts in ultrafast laser fields – A tool for pulse characterization & quantum dynamics investigations

Alexander Blättermann, Paul Birk, Veit Stooß, Christian Ott, Andreas Kaldun, Maximilian Hartmann, Thomas Ding and Thomas Pfeifer

Max-Planck-Institut für Kernphysik, Saupfercheckweg 1, 69117 Heidelberg, Germany

Attosecond transient absorption spectroscopy (ATAS) constitutes a powerful technique that – besides other advantages – allows for direct observation of bound-state quantum mechanics. Making use of attosecond extreme ultraviolet (XUV) light and intense femtosecond near-infrared (NIR) laser pulses, a multitude of light–matter interaction processes in highly excited atomic, molecular, and more complex systems can be accessed, investigated, and controlled on ultrashort time scales.

Here, we demonstrate a method that allows to extract dynamic phase shifts of the atomic or molecular dipole response from time-delay–resolved absorption spectra. The observed dipole response of the sample is initiated by the XUV pulse and subsequently manipulated by the strong field of the NIR pulse. Since interaction with the NIR pulse leaves its fingerprint in the XUV absorption line shape, and because this line shape is intrinsically tied to the phase of the dipole oscillation [1], we can recover the impact of the intense and short NIR laser pulse on the sample. The method is implemented using the dipole-control model, which allows us to analytically treat light–matter interaction in a general formalism [2]. Here, we focus on the non-resonant ac Stark effect, which is introduced by virtue of the NIR laser. While the NIR laser pulse acts on the sample, the resonance frequency ω_r

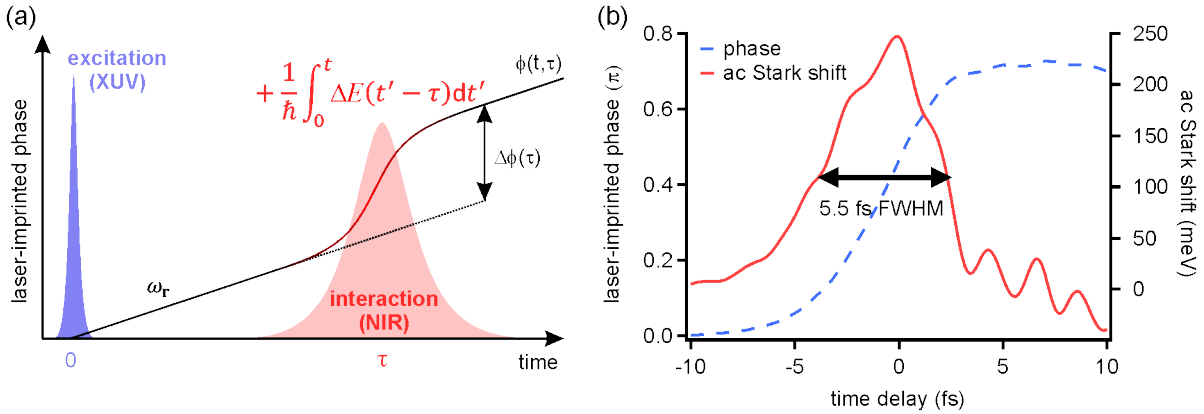

Fig. 1 (a) Schematic of phase evolution in the presence of a dressing NIR laser pulse. (b) Experimentally obtained phase evolution and corresponding Stark shift, which reveals the shape of the used 5.5 fs NIR pulse.

of a given state is effectively shifted leading to an accelerated phase evolution and in total to an additionally accumulated phase $\Delta\phi$ (see Fig. 1(a)). Around the temporal overlap of both pulses, the state experiences only the fraction of the NIR driving pulse that is present after the XUV excitation. Therefore, the NIR pulse shape is directly mapped onto the amount of additional phase or onto the spectral line shape, respectively. The derivative of the phase directly yields the time-resolved ac Stark shift ΔE. Besides information on the sample, this quantity reveals the pulse shape as depicted in Fig. 1(b) for the measurement of a 5.5 fs laser pulse. This pulse characterization scheme can be exploited even further: studying loosely bound states, the ac Stark shift becomes the ponderomotive potential, which is directly linked to the pulse intensity allowing for a complete characterization of the pulse envelope [3]. Most importantly, the pulse characterization is done *in situ*, since we investigate the effect of the NIR laser on the XUV-excited target atoms. Therefore, quantum dynamics and pulse properties are investigated simultaneously so that the knowledge on the laser pulse can directly be used to conduct quantitative studies, control dynamics, and for high-precision tests of quantum-dynamics theory.

References

[1] Christian Ott, Andreas Kaldun, Philipp Raith, Kristina Meyer, Martin Laux, Jörg Evers, Christoph H. Keitel, Chris H. Greene, Thomas Pfeifer, *Lorentz Meets Fano in Spectral Line Shapes: A Universal Phase and Its Laser Control*, Science **340** 716 (2013)

[2] Alexander Blättermann, Christian Ott, Andreas Kaldun, Thomas Ding, and Thomas Pfeifer, *Two-dimensional spectral interpretation of time-dependent absorption near laser-coupled resonances*, J. Phys. B: At. Mol. Opt. Phys. **47** 124008 (2014)

[3] Alexander Blättermann, Christian Ott, Andreas Kaldun, Thomas Ding, Veit Stooß, Martin Laux, Marc Rebholz, and Thomas Pfeifer, *In situ characterization of few-cycle laser pulses in transient absorption spectroscopy*, Opt. Lett. **40** 3464 (2015)

Asymmetric Wigner Time Delay in CO Photoionization

J. Vos*, L. Cattaneo*, S. Heuser, M. Lucchini, C. Cirelli, U. Keller
Institute of Quantum Electronics, ETH Zurich, 8093 Zurich, Switzerland

Energy streaking and RABBITT techniques are now used to measure relative time delays between valence electrons emitted from different energy levels within the same atomic system [1,2], or distinct atoms [3]. It is well established that these techniques give access to the scattering phase shift φ_W accumulated by the outgoing electron wave packet (EWP) in the presence of the atomic potential. In scattering theory, such phase shift is traditionally referred to as Wigner delay [4], defined as $\tau_W = \hbar\,\partial\varphi_W/\partial E$. In molecular systems however, this topic remains relatively unexplored [5,6]. Photoionization of molecular systems is a much more complex phenomenon since the outgoing EWP released upon absorption of an XUV photon will experience a highly anisotropic scattering potential. Here, we present the first experimental estimation of the Wigner time delay in photoionization of one of the simplest hetero-nuclear molecules, CO.

We measure the photoionization time delay based on the RABBITT technique combined with coincidence detection using a COLTRIMS apparatus. An attosecond pulse train (APT) is created by a strong IR-field focussed in an argon gas target. A cold jet of CO molecules is ionized by this pump-pulse, yielding photoelectrons at kinetic energies dictated by the harmonics present in the spectrum. In the presence of a relatively weak IR-field two-photon transitions will be induced, yielding electrons with a kinetic energy centred between successive harmonics in the RABBITT trace. Due to quantum path interference these sideband signals oscillate as a function of pump-probe delay (τ).

Detection of the ion-electron pair in coincidence allows for the reconstruction of the molecular axis upon photoionization. Reconstruction of the molecular axis requires dissociation, as we do not align the molecules. If we know the orientation of the molecule prior ionization, we can distinguish between electrons emitted on either side of the molecule and measure a difference in photoionization time delay referred to as the Stereo Wigner time delay $\Delta\tau^{LR}$ [7].

RABBITT traces with the electron escaping either anti-parallel or parallel to the C-side of the molecule can thus be reconstructed. The oscillating sideband signals are approximated with $SB(\tau) \cong \cos(2\omega_{IR}\tau - \Delta\varphi_{XUV} - \Delta\varphi_{molecule})$ [8], showing that the measured photoionization time delays are composed of two contributions, i.e. a measurement induced time delay that is the attochirp τ_{XUV} and a molecular term $\tau_{molecule}$. Like in the atomic case, the molecular term contains the coupling between the laser field and the Coulomb potential τ_{CC} and the actual molecule specific Wigner time delay τ_W [2]. We compare sidebands at equal energies to extract a photoemission time delay difference free of τ_{XUV} and τ_{CC} since the two terms at equal energy are affected equally i.e. we measure a pure Wigner time delay difference [8].

The integration of the sideband signal as a function of pump-probe delay for electrons emitted anti-parallel and parallel to the C-side of the molecule reveal a clear phase shift. Electrons emitted on either side of the hetero-nuclear molecule will experience a distinct Coulomb potential, being more attractive at the O-side of the molecule. This leads to a stronger retardation of the transmitted wave relative to the electron wave-packet originating from the C-side of the molecule. This left-right asymmetry is characteristic for non-symmetric Coulomb potentials and will not manifest itself in homo-nuclear diatomic molecules as shown in figure 1.

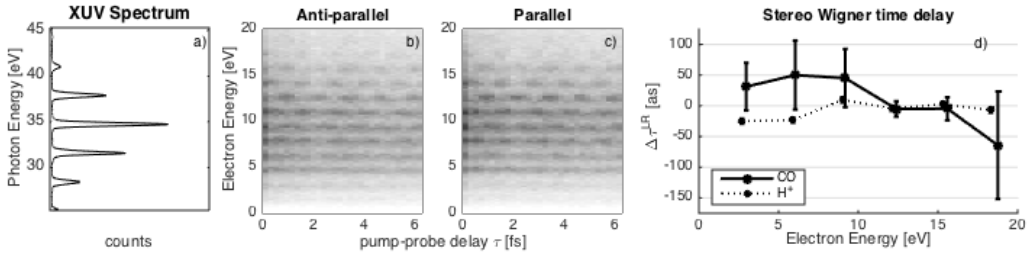

Fig. 1 Principle of RABBITT technique. High harmonics a) create oscillating sidebands in the photoelectron spectrum in the presence of an IR-field. A phase shift is visible for electrons escaping anti-parallel b) and parallel c) to the C-side of the molecule, therewith revealing a asymmetry in the Wigner time delay d).

References

[1] M. Schulze, et al., *Delay in Photoemission,* Science **328**, 1658 (2010).
[2] K. Klünder, et al., *Probing Single-Photon Ionization on the Attosecond Time Scale,* Phys. Rev. Lett. **106,** 143002 (2011).
[3] M. Sabbar, et al., *Resonance Effect in Photoemission Time Delays,* Phys. Rev. Lett. **115,** 133001 (2015).
[4] E. P. Wigner, *Lower Limit for the Energy Derivative of the Scattering Phase Shift,* Phys. Rev. **98,** 145 (1955).
[5] E. Frumker, et al., *Probinf Polar Molecules with High Harmonic Spectroscopy,* Phys. Rev. Lett. **109,** 233904 (2012).
[6] S Haessler, et al., *Phase-Resolved Attosecond Near-Threshold Photoionization of Molecular Nitrogen,* Phys. Rev. A **80,** 011404 (2009).
[7] A. Chacon, et al., *Asymmetry of Wigner's Time Delay in a small Molecule,* Phys. Rev. A **89,** 0553427 (2014).
[8] J. M. Dahlström, et al., *Introduction to Attosecond Delays in Photoionization,* J. Phys. B: At. Mol. Opt. Phys. **45** 183001 (2012).

Double-electron Re-combination in High-Order Harmonic Generation Driven by Spatially Inhomogeneous Fields

A. Chacón[1], M. F. Ciappina[2], M. Lewenstein[1,3]

1. ICFO-Institut de Ciències Fotòniques, The Barcelona Institute of Science and Technology, 08860 Castelldefels (Barcelona), Spain
2. Max-Planck Institut für Quantenoptik, Hans-Kopfermann-Str. 1, D-85748 Garching, Germany
3. ICREA-Institució Catalana de Recerca i Estudis Avançats, Lluis Companys 23, 08010 Barcelona, Spain

The fundamental mechanism of high-order harmonic generation (HHG) in atoms driven by spatially inhomogeneous plasmonics fields can be briefly summarized as follows: a femtosecond low-intensity pulse is coupled to the plasmon mode inducing a collective oscillation of free charges within the metal. These free charges redistribute the electric field around each of the metallic nanostructures, thereby forming a hot spot - a tiny region of highly enhanced electric field. The enhanced field exceeds then the threshold of HHG, thus by injection of a noble gas onto the spot of the enhanced field, HHG are generated [1]. All the numerical and semiclassical approaches to study HHG in atoms and molecules are largely based on the assumption that the laser electric field is spatially homogeneous in the region where the electron dynamics takes place. Due to the strong confinement of plasmonic hot spots, the laser electric field is clearly no longer spatially constant, and consequently important changes in the laser-matter-processes would occur. Up to now several theoretical studies of HHG driven by plasmonic fields have been made (see e.g. [2]) in atomic or molecular systems by considering a Single Active Electron (SAE) approximation model. However, in the case of multielectronic atoms or molecules, it is known the electron-electron (e-e) correlation plays an instrumental role both in the laser ionization process and, consequently, the HHG. In this contribution we study e-e correlation effects in the HHG process driven by plasmonic fields. The description of the laser-matter interaction of the multielectron system is given by the time dependent Schrödinger equation (TDSE) in reduced dimensions, which allows us to include the e-e interaction. We develop a 1Dx1D model for the calculation of the HHG spectrum driven by spatially inhomogeneous fields in the He atom and the H^- ion, two prototypical examples of two active electron (TAE) systems. Furthermore, and in order to investigate the role of the e-e correlation in the HHG process, the SAE is also invoked and compared to the full e-e correlated model. As it is clearly observed in Fig. 1, we demonstrate that a new mechanism, a double non-sequential two-electron re-combination process, is the main responsible of the extension of the HHG spectra in the H^- ion [3].

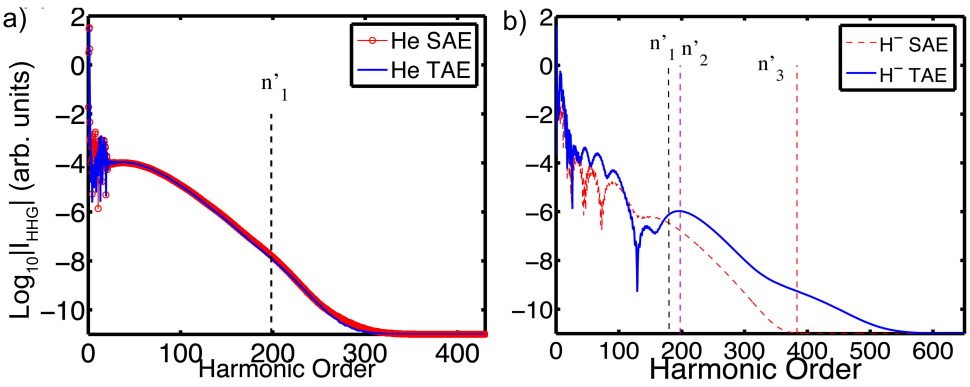

Fig. 1 The harmonic emission from the He atom and the H^- ion driven by a spatially inhomogeneous field are depicted in (a) and (b), respectively. The laser peak intensity is $I = 2\times10^{14}$ W/cm^2, with central frequency $\omega_0 = 0.057$ a.u. (wavelength $\lambda = 800$ nm, photon energy 1.55 eV). The pulse envelope has a sin^2-shape with 3 cycles of total time duration. The spatial inhomogeneity is linear with $\varepsilon = 0.02$ a.u (see e.g. [2] for more details). Red (blue) line denotes the HHG spectra calculated by the SAE (TAE) approach. n_1' is the 'conventional' HHG cutoff, i.e. $n_1' = (E_k + I_p)/\omega_0$, n_2' is the cutoff corresponding to a double sequential recombination process $n_2' = (E_k + I_{p_1} + I_{p_2})/\omega_0$ and n_3' is the cutoff for a non-sequential double recombination mechanism $n_3' = (E_{k_1} + E_{k_2} + I_{p_1} + I_{p_2})/\omega_0$.

References

[1] S. Kim, et al., *High-harmonic generation by resonant plasmon field enhancement*, Nature **453**, 757 (2008).
[2] M. F. Ciappina, et al., *High-order harmonic generation from inhomogeneous fields*, Phys. Rev. A **85**, 033828 (2012).
[3] A. Chacón, et al., *Double-electron recombination in high-order harmonic generation driven by spatially inhomogeneous fields*, Phys. Rev. A, (submitted) (2016).

Theoretical study of time delays in $(\omega, 2\omega)$ above threshold ionization

Sebastián D. López[1], Stefan Nagele[2], Diego G. Arbó[1], and Joachim Burgdörfer[2]
1. Institute for Astronomy and Space Physics, IAFE (CONICET-UBA), 1428 Buenos Aires, Argentina
2. Institute for Theoretical Physics, Vienna University of Technology, Vienna, Austria, EU

Recent experiment employing either attosecond streaking or the complementary interferometric RABBIT technique have allowed to study photoemission from rare gas atoms and surfaces in the time-domain with attosecond precision. The experimental progress has triggered considerable theoretical efforts to understand photoionization from a time-dependent perspective (see [1] and references therein).

A recent experiment in atomic ionization by two-color $(\omega, 2\omega)$ lasers by Zipp *et al.* [2] has revealed that a pump-probe scheme can be used to characterize time delays in the emission of electrons in the above-threshold ionization regime for visible frequency of the pump. In this work, we perform a theoretical analysis of the time delays in Ar ionization by two-color laser for a typically $(\omega, 2\omega)$ configuration of Ti:sapphire laser (800 nm). To shed more light in ionization process we perform simulations with the time dependent Schödinger equation and compare this results with the strong field and Coulomb-Volkov approximations. We find that time delays depend on the definition from electron momentum distributions. Besides, we also find a large discrepancy between the results predicted by the strong field approximation (zero delay for sidebands) and numerical solutions of time-dependent Schrödinger equation at the highest simulation energies. We also find that the strong assumption of additive time delays adopted in streaking or RABBITT techniques [3], needs to be revisited when applied to the case of $(\omega, 2\omega)$ lasers due to the multiplicity of coherent quantum paths leading to a final multiphoton peak.

As an example, we show in Fig. 1 time delays obtained from asymmetries and forward emission (considering integrations over $\pm$z hemispheres).

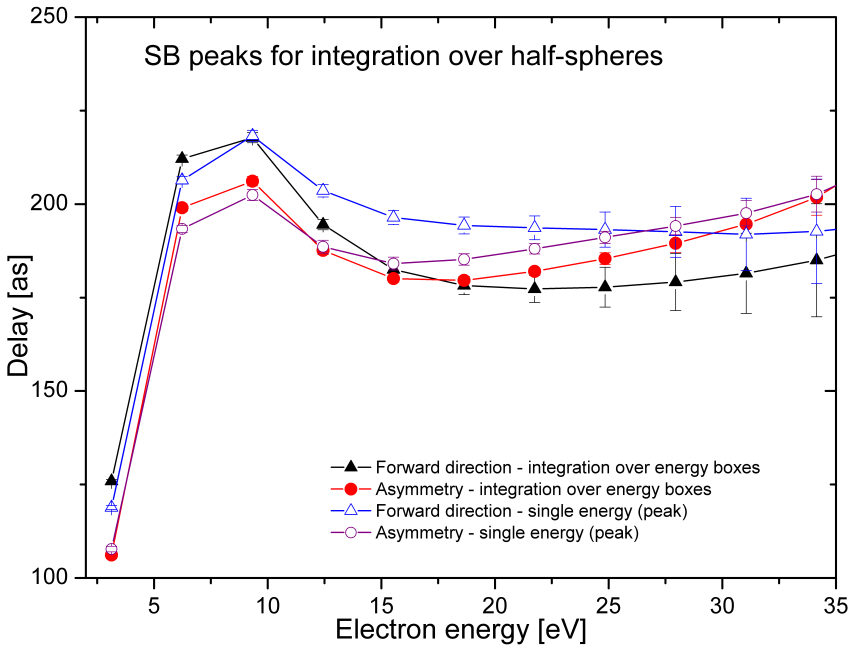

Fig. 1 Delays calculated as function of the emission energy for sidebands wothin TDSE. The delays are calculated for forward emission (triangles) and asymmetry (circles). The calculations were performed integrating around peak energy (solid symbols) or considering only the peak energy (open symbols). The 2ω component intensity is 8×10^{13} W/cm^2 and the ω component is 4×10^{11} W/cm^2.

This work was supported by the FWF-Austria (SFB NEXTLITE, SFB VICOM), by CONICET (PIP100386), University of Buenos Aires (UBACyT0617), by ANPCYT (PICT-2014-2363), by the OeAD (WTZ AR 03/2013), by the NSF through XSEDE resources (TG-PHY090031), and through computational resources at the Vienna Scientific Cluster (VSC).

References

[1] R. Pazourek, S. Nagele, and J. Burgdörfer, *Attosecond chronoscopy of photoemission*, Rev. of Mod. Phys., **87**, 765, (2015).
[2] L. J. Zipp, A. Natan, and P. H. Bucksbaum, *Probing electron delays in above-threshold ionization*, Optica **1**, 361-364 (2014).
[3] J. Feist, O. Zatsarinny, S. Nagele, R. Pazourek, J. Burgdörfer, X. Guan, K. Bartschat and B. I. Schneider, *Time delays for attosecond streaking in photoionization of neon*, Phys. Rev. A, **89**, 033417, (2014).

Attosecond Interferometry with Self-Amplified Spontaneous Emission of a Free-Electron Laser

Sergey Usenko[1], Andreas Przystawik[1], Markus Jakob[1], Leslie Lamberto Lazzarino[2], Günter Brenner[1], Sven Toleikis[1], Christian Haunhorst[3], Detlef Kip[3], and Tim Laarmann[1, 4]

1. Deutsches Elektronen-Synchrotron DESY, Notkestr. 85, 22607 Hamburg, Germany

2. Department of Physics, University of Hamburg, 22761 Hamburg, Germany

3. Faculty of Electrical Engineering, Helmut Schmidt University, Hamburg 22043, Germany

4. The Hamburg Centre for Ultrafast Imaging CUI, Luruper Chaussee 149, 22761 Hamburg, Germany

Science with short-wavelength free-electron lasers (FELs) has enabled multiple breakthroughs covering the broad range from basic research in life sciences to applications in material science and catalysis. Particularly, the high degree of spatial coherence of the light field allows for key applications such as serial-femtosecond X-ray crystallography using the well-established and robust self-amplified spontaneous emission (SASE) of FELs [1]. Recently, temporal coherence provided by seeded FELs moved into the focus of interest [2-4]. It has been shown that full control over the light phase allows for a new class of light-phase sensitive experiments in the short-wavelength limit [5-7], such as non-linear four-wave mixing [8] and attosecond (1 as = 10^{-18} s) coherent control [9]. These give novel opportunities to study and possibly control energy and charge migration in molecular systems of increasing complexity with unprecedented spatial and temporal resolution. Here, we demonstrate phase control on the attosecond timescale in a Michelson-type all-reflective interferometric autocorrelator using monochromatic SASE pulses at a central wavelength of 38 nm. The carrier frequency of the light wave shown in Fig.1 is sampled with attosecond precision (preliminary data).The study paves the way towards utilization of advanced nonlinear methodologies even at partial coherent soft X-ray SASE FEL sources.

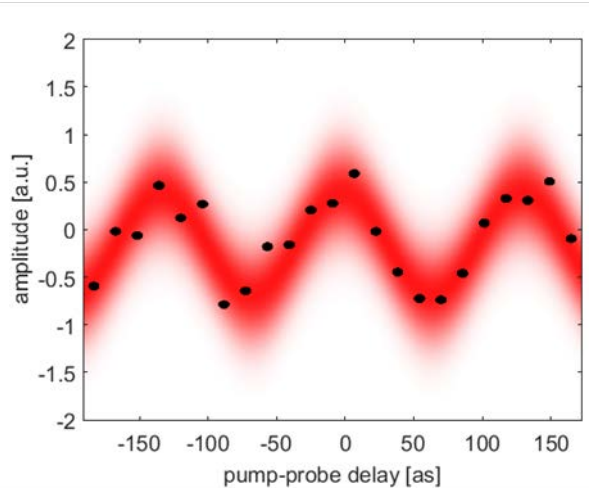

Fig. 1 Interferometric autocorrelation recorded with FLASH (SASE) pulses.

References

[1] Henry Chapman et al., *Femtosecond diffractive imaging with a soft-X-ray free-electron laser*, Nature Physics **2**, 839 (2006).
[2] Enrico Allaria et al., *Highly coherent and stable pulses from the FERMI seeded free-electron laser in the extreme ultraviolet*, Nature Photonics **6**, 699 (2012).
[3] Enrico Allaria et al., *Two-stage seeded soft-X-ray free-electron laser*, Nature Photonics **7**, 913 (2013).
[4] Sven Ackermann et al., *Generation of Coherent 19- and 38-nm Radiation at a Free-Electron Laser Directly Seeded at 38 nm*, Phys. Rev. Lett. **111**, 114801 (2013).
[5] David Gauthier et al., *Spectrotemporal Shaping of Seeded Free-Electron Laser Pulses*, Phys. Rev. Lett. **115**, 114801 (2015).
[6] David Gauthier et al., *Generation of Phase-Locked Pulses from a Seeded Free-Electron Laser*, Phys. Rev. Lett. **116**, 024801 (2016).
[7] Giovanni De Ninno et al., *Single-shot spectro-temporal characterization of XUV pulses from a seeded free-electron laser*, Nature Communications **6**, 8075 (2015).
[8] Filippo Bencivenga et al., *Four-wave mixing experiments with extreme ultraviolet transient gratings*, Nature **520**, 205 (2015).
[9] Kevin Charles Prince et al., *Coherent control with a short-wavelength free-electron laser*, Nature Photonics **10**, 176 (2016).

Strong-field photoelectron holography with the two-color fields

Yueming Zhou,[1] Oleg I. Tolstikhin,[2] Toru Morishita[3], Yang Li[1] and Peixiang Lu[1]

1. *Huazhong University of Science and Technology, Wuhan 430074, China*
2. *Moscow Institute of Physics and Technology, Dolgoprudny 141700, Russia*
3. *The University of Electro-Communications, Chofu-shi, Tokyo 182-8585, Japan*

It is believed that strong-field photoelectron holography originating from the interference of the direct and rescattered electrons encodes structural information. However, it is still unknown what type of structural information is encoded there and how to extract this information. Recently, with the adiabatic theory, we have shown that this structural information is the phase of the scattering amplitude and we demonstrated how this information is encoded and how it can be read out from the corresponding interference pattern in photoelectron momentum distributions (PEMDs) produced in the ionization of atoms and molecules by intense laser pulses. Here, we will show how the holographic structures could be enhanced with the scheme of the two-color fields and how they could be separated from other types of interference structures in the photoelectron momentum spectra. This is very important for extracting structural information and ultrafast dynamics with the concept of holography.

Dissociative Photoionization Dynamics of O_2 at High-order Harmonics Photon Excitation Energies

Marius Hervé[1], Kévin Veyrinas[1], Sonia Marggi Poullain[1], Nicolas Saquet[1], Mogens Lebech[2], Danielle Dowek[1]

1. Institut des Sciences Moléculaires d'Orsay (ISMO), CNRS, Univ. Paris-Sud, Université Paris-Saclay, F-91405 Orsay (France)
2. Niels Bohr Institute, DK-2100 Copenhagen, Denmark

The study of rapid electron and nuclear dynamics in molecular systems at a femtosecond or sub-femtosecond time scale nowadays relies on advanced light sources such as high-order harmonic generation (HHG) or free electron lasers. Attosecond control of dissociative photoionization (DPI), which is a major channel in the XUV photon energy range, has been demonstrated for simple molecules in two-color XUV + infrared (IR) pump-probe experiments on e.g., H_2, D_2 [1] or O_2 [2]. In the context of such studies, the most advanced knowledge of the DPI processes induced for each harmonic energy in an attosecond pulse train (APT) is needed for the interpretation of the observed dynamics. With this motivation, we report a complete study of DPI of the O_2 molecule induced at the selected photon energies corresponding to the H15-H21 harmonics of a 800 nm IR laser, combining electron-ion coincidence 3D momentum spectroscopy [3] and circularly polarized synchrotron radiation on the DESIRS beamline at SOLEIL [4]. The (E_{O+},E_e) kinetic energy correlation diagrams (KECD) enable us to identify each process in terms of the populated molecular ionic state and dissociation limit, while molecular frame photoelectron angular distributions (MFPADs) for each channel characterize the electronic wave function in the continuum. In addition to PI into the $O_2^+(B^2\Sigma_g^-, 3^2\Pi_u, c^4\Sigma_u^-)$ states [5], new processes are observed, in particular population of the ($O^+(^4S)$ + $O(^1D)$) L_2 dissociation limit at H15 photon energy, characterized both by a continuous distribution and discrete structures amounting to about 8% of all DPI processes, unobserved at the other energies (Fig 1.a). These structures can be assigned to resonant autoionization of Rydberg states converging to the $O_2^+(3^2\Pi_u)$, which may involve both autoionization of O*(nl) atomic states at large internuclear distances, as studied in pump-probe experiments for molecular Rydberg states converging to the $O_2^+(c^4\Sigma_u^-)$ state [6,7], or autoionization occurring during dissociation leading to a continuous energy sharing between electron and nuclei. Further results as well as angular analysis will be presented.

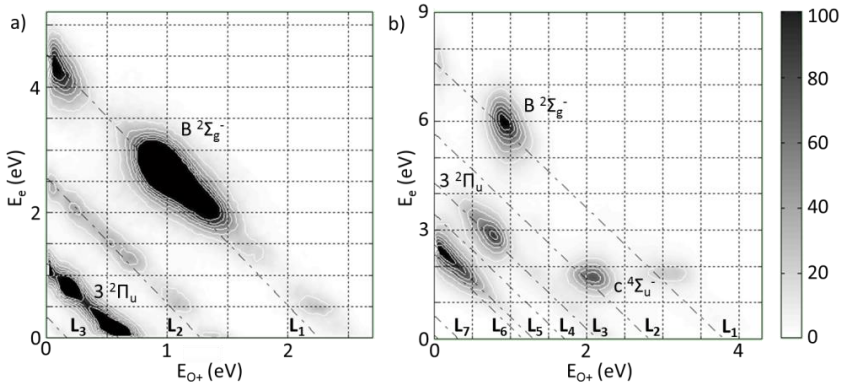

Fig. 1 (E_{O+},E_e) KECDs at a) 23,25 eV (H15), autoionization populates the L_2 dissociation limit; b) 26,35 eV (H17).

References

[1] M. F. Kling, Ch. Siedschlag, A. J. Verhoef, J. I. Khan, M. Schultze, Th. Uphues, Y. Ni, M. Uiberacker, M. Drescher, F. Krausz, M. J. J. Vrakking, *Control of Electron Localization in Molecular Dissociation*, Science **312**, 246 (2006).

[2] W. Siu, K. Kelkensberg, G. Gademann, A. Rouzée, P. JoD hnsson, D. Dowek, M. Lucchini, F. Calegari, U. De Giovannini, A. Rubio, R. R. Lucchese, H. Kono, F. Lépine and M. J. J. Vrakking, *Attosecond control ionization of O_2 molecules*, Phys. Rev. A **84**, 063412 (2011).

[3] A. Lafosse, M. Lebech, J. C. Brenot, P. M. Guyon, O. Jagutzki, L. Spielberger, M. Vervloet, J. C. Houver and D. Dowek, *Vector Correlations in Dissociative Photoionization of Diatomic Molecules in the VUV Range: Strong Anisotropies in Electron Emission from Spatially Oriented NO Molecules*, Phys. Rev. Lett. **84**, 5987 (2000).

[4] L. Nahon and C. Alcaraz, *SU5: a calibrated variable-polarization synchrotron radiation beam line in the vacuum-ultraviolet range*, Appl. Opt. **43**, 1024 (2004).

[5] A. Lafosse, J. C. Brenot, A. V. Golovin, P. M. Guyon, K. Hoejrup, J. C. Houver, M. Lebech and D. Dowek, *Vector correlations in dissociative photoionization of O_2 in the 20-28 eV range. I. Electron-ion kinetic energy correlations*, J. Chem. Phys. **114**, 6605 (2001).

[6] H. Timmers, N. Shivaram and A. Sandhu, *Ultrafast Dynamics of Neutral Superexcited Oxygen: A Direct Measurement of the Competition between Autoionization and Predissociation*, Phys. Rev. Lett. **109**, 173001 (2012).

[7] B. Doughty, C. J. Koh, L. H. Haber, S. R. Leone, *Ultrafast decay of superexcited $c^4\Sigma_u^-$ $nl\sigma_g$ $v=0,1$ states of O_2 probed with femtosecond photoelectron spectroscopy*, J. Chem. Phys. **136**, 214303 (2012).

Real tunneling time in attosecond experiments from the time-energy uncertainty relation, and time in quantum mechanics

Ossama Kullie

Theoretical Physics, Institute for Physics, Department of Mathematics and Natural Science, University of Kassel, Germany. kullie@uni-kassel.de

Tunneling time in attosecond and strong field experiments is one of the most controversial issues in today's research, because of its importance to the theory of time, the time operator and the time-energy uncertainty relation in quantum mechanics. In this work [1] we present a theoretical model of the tunneling time and the tunneling process (in attosecond experiment for the He atom). Our model is supported with physical reasoning leading to a relation which performs an excellent estimation for the tunneling time in attosecond and strong-field experiments of the He atom [2, 3]. Our tunneling time estimation is found by utilizing the time-energy uncertainty relation and represents a quantum clock.

The tunneling time is also featured as the time of passage through the barrier similar to Einsteins photon-box Gedanken experiment. Our work tackles an important case study for the theory of time in quantum mechanics and is very promising for the search for a (general) time operator in quantum mechanics. The work can be seen as a fundamental step in dealing with the tunneling time in strong-field and ultrafast science and is appealing for more elaborate treatments using quantum wave-packet dynamics and especially for complex atoms and molecules.

We showed that the important question is a more general one: How to understand the time and the measurement of the time of a quantum system?. In respect to our result, the time in quantum mechanics can be, in more general fashion, classifed in two types, intrinsic dynamically connected, and external dynamically not connected to the system, and consequently (perhaps only) the classical Newtonian time remains as a parametric type of time.

[1] O Kullie 2015 *Phys. Rev. A* **92** 052118. O Kullie 2016 *J. Phys. B*, acccepted.
[2] A S Landsman and Keller U 2014 *Optica* **1** 343.
[3] P Eckle, Smolarski M, Schlup F, Biegert J, Staudte A, Schöffler M, Muller H G, Dörner R and Keller U 2008 *Nat. phys.* **4** 565. P Eckle, Pfeiffer A N, Cirelli C, Staudte A, Dörner R, Muller H G, Büttiker M and Keller U 2008 *Sience* **322** 1525.

Ultrafast photodissociation dynamics of molecular oxygen in the vacuum ultraviolet studied with a single-color pump-probe scheme

Oliver Schepp[1], Arne Baumann[1], Dimitrios Rompotis[2], Thomas Gebert,[3] Marek Wieland[1,3,4], and Markus Drescher[1,3,4]

1. *Institut für Experimentalphysik, Universität Hamburg, Luruper Chaussee 149, 22761 Hamburg, Germany*
2. *Deutsches Elektronen Synchrotron DESY, Notkestraße 85, 22607 Hamburg, Germany*
3. *Center for Free-Electron Laser Science CFEL, Luruper Chaussee 149, 22761 Hamburg, Germany*
4. *The Hamburg Centre for Ultrafast Imaging CUI, Luruper Chaussee 149, 22761 Hamburg, Germany*

Molecular wavepacket dynamics of oxygen is studied in the time domain, using a single-color VUV pump/ VUV probe scheme. 17 fs VUV pulses, centered at 161nm with pulse energies up to 1.1 μJ created as the 5th harmonic of a 800nm laser are split by two moveable interdigitated double comb mirrors into two collinearly propagating replicas with a variable delay. Focusing the beam into a gas target creates ions in the interaction region which are mapped onto a 2D ion-mass sensitive detector [1,2]. This Michelson-type all-reflective interferometric autocorrelation scheme is used for recording the time-dependent yield of oxygen ions with simultaneous non-resonant two-photon ionization of krypton as a precise timing-reference.
The photoreaction dynamics of molecular oxygen is initiated with an excitation into the Schumann-Runge continuum and the subsequent evolution is probed by ionization via absorption of additional VUV photons. A decay time for the O_2^+-signal is extracted and identified as the molecule-specific time-window for delay-dependent two-photon ionization. This ionization window is extended by delay-dependent three-photon ionization, generating O^+ as an additional observable.

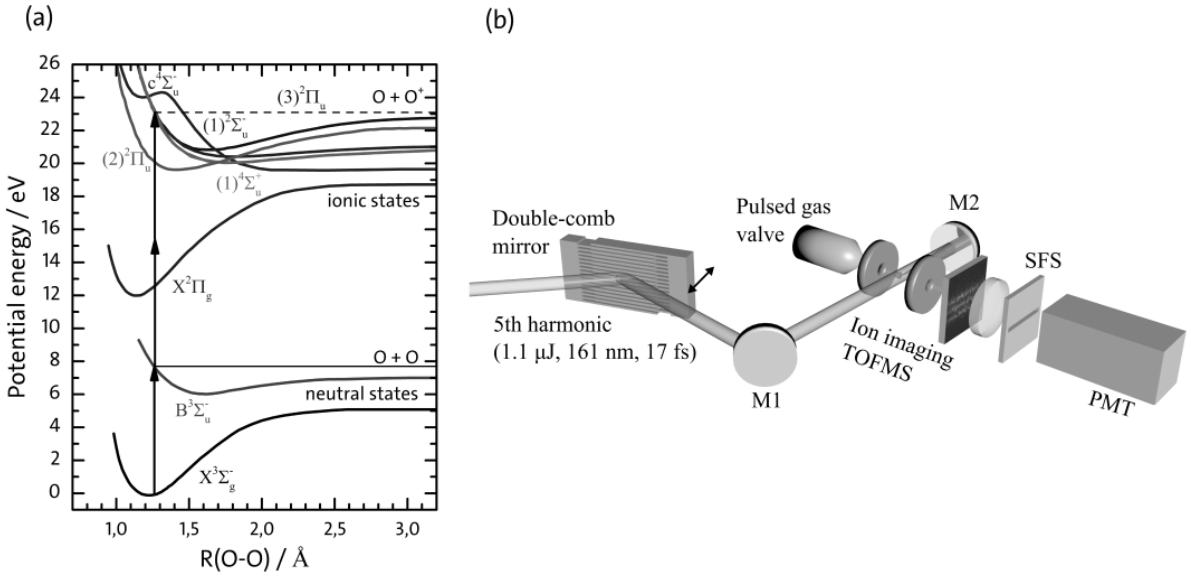

Fig. 1 (a) Potential energy curves of molecular oxygen for a two- and three-photon absorption process adopted from [3] and [4]. (b) Michelson-type all-reflective interferometric autocorrelation scheme.

References

[1] Dimitrios Rompotis, Thomas Gebert, Marek Wieland, Fawad Karimi, and Markus Drescher, *Efficient generation of below-threshold harmonics for high-fidelity multi-photon physics in the VUV spectral range*, Opt. Let. **40**, 1675 (2015) .
[2] Thomas Gebert, Dimitrios Rompotis, Marek Wieland, Fawad Karimi, Armin Azima, and Markus Drescher, *Michelson-type all-reflective interferometric autocorrelation in the VUV regime*, New J. Phys. **16**, 073047 (2014).
[3] Paul H. Krupenie, *The Spectrum of Molecular Oxygen*, J. Phys. Chem. Ref. Data **1**, 423 (1972).
[4] Kouichi Takeshita, Yosiki Sadamatu, and Kiyoshi Tanaka , *A theoretical study on the inner-valence photoelectron spectra lying between 21 and 26 eV of the O2 molecule*, J. Chem. Phy. **122**, 44302 (2005).

Intense XUV Attosecond Physics at the Lund Laser Centre

Sylvain Maclot[1] Linnea Rading[1], Hampus Wikmark[1], Jan Lahl[1], Filippo Campi[1], Hélène Coudert-Alteirac[1], Bastian Manschwetus[1], Piotr Rudawski[1], Christoph M. Heyl[1], Miguel Miranda[1], Anne L'Huillier[1] and Per Johnsson[1]

1. Department of Physics, Lund University, Box 118, SE-22100 Lund, Sweden

The stability of ionized and excited complex molecular systems is mainly driven by fundamental processes such as electron dynamics, charge transfer/migration and nuclear motion [1-3]. They can lead to chemical reactions and specific dissociations through, for instance, intramolecular rearrangements [4]. That is why, in this context of radiation damage, it is of prime importance to understand and characterize the effects of these processes on the molecular behaviour.

In order to follow the dynamics of these processes occurring from attosecond to femtosecond timescales, specific time-resolved tools are required [5]. An efficient technique involves pump-probe experiments using high-order harmonic pulses (XUV) produced after the focusing of an intense infrared (IR) femtosecond laser pulse in a gas. Most of the recent works have employed two color XUV/IR pump-probe experiments giving sub-femtosecond resolution. The limitation of this method lies in the fact that the IR pulse, most of the time, controls the dynamics rather than making an observation of the dynamics intrinsic to the molecule. A solution to this problem, is to use XUV-pump XUV-probe experiments.

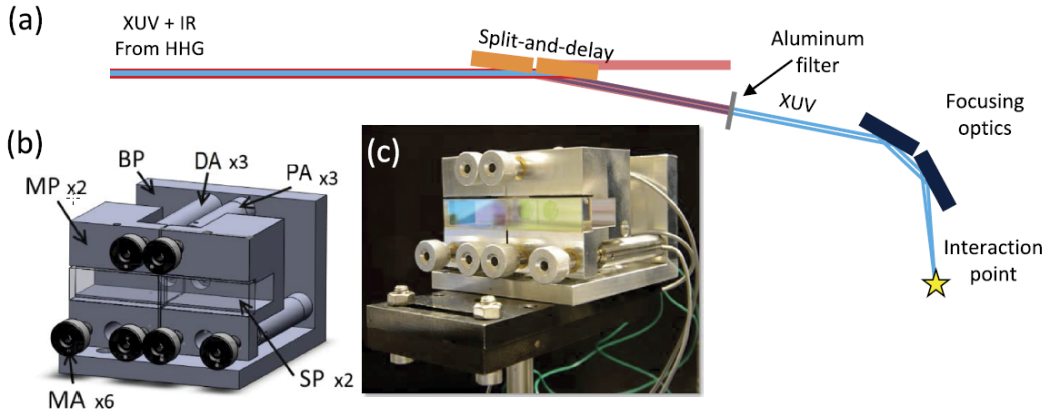

Fig. 1 (a) Sketch of the intended use of the split-and-delay unit in the existing high-intensity XUV beamline. (b) 3D-model of the split-and-delay unit with mounted silica plates. The two movable parts (MPs) are connected to the base plate (BP) by either real piezo-actuators (PA) or dummy actuators (DA), three for each MP. For each connection point there is also a manual actuator (MA) for coarse adjustments. The silica plates (SPs) are held in place by set screws from the top. (c) Photograph of the split-and-delay unit mounted on an optical post for the tests.

At the Lund Laser Centre, using the high-order harmonic generation (HHG) technique with a Ti:Sapphire laser at 800 nm and a repetition rate of 10 Hz [6-7], we will perform XUV-pump XUV-probe experiments using a newly designed split and delay unit (Fig. 1) [8]. That will allow us to study time-dependent fragmentation of small molecules from attosecond to femtosecond timescales. The target will be produced in the gas phase by an Even-Lavie pulsed valve and the products of the interaction will be recorded by a double-sided velocity map imaging detector (VMI) allowing to have access simultaneously to both electron and ion information. Experiments are currently in progress starting with atoms and small molecules and then moving towards more complex systems such as biomolecules.

References

[1] L.S. Cederbaum *et al Chem. Phys. Lett.* **307**, 205 (1999)
[2]F. Remacle *et al Proc. Natl. Acad. Sci.* **103**, 6793 (2006)
[3] F. Calegari *et al Science* **346**, 336 (2014)
[4] Y.H. Jiang *et al Phys. Rev. Lett.* **05**, 263002 (2010)
[5] F. Lépine *et al Nat. Photonics* **8**, 195 (2014)
[6] P. Rudawski *et al Rev. Sci. Instrum.* **84**, 073103 (2013)
[7] B. Manschwetus *et al* submitted, arXiv 1603.05439 (2016)
[8] F. Campi *et al Rev. Sci. Instrum.* **87**, 023106 (2016)

Femtosecond to Nanosecond Dynamics of Dipolar and Octupolar Light Harvesting Molecules Based on Benzothiazole e⁻ Acceptors

Kostas Seintis[1], Dafni Chroni[1], Veronika Hrobáriková[2], Ivica Sigmundová[2], Peter Hrobárik,[2,3] Mihalis Fakis[1,*]

1. Department of Physics, University of Patras, 26504 Patras, Greece

2. Department of Organic Chemistry, Comenius University, Mlynská dolina, SK-84215 Bratislava, Slovakia

3. Institute of Chemistry, Technical University of Berlin, D-10623 Berlin, Germany

**email:fakis@upatras.gr*

Light-harvesting organic molecules exhibiting directional energy transfer attract an increased scientific interest because of their potential applications in photovoltaics, light emitting diodes and lasers [1-3]. Octupolar or multipolar systems are considered promising as artificial light-harvesting systems. Understanding how energy is transferred and delocalized in such systems is the challenge to be addressed. A successful approach towards this goal is to comparatively study their properties with those of their dipolar-linear analogues.

In this work, the excited state dynamics of six three-branched molecules are compared with those of their dipolar counterparts using fs to ns fluorescence spectroscopy. The three-branched compounds bear triphenylamine as the core and benzothiazole moieties as electron acceptors at the periphery while additional electron withdrawing groups (EWG) are added in some compounds (Fig. 1a). Besides, the effect of the orientation of the benzothiazole group is also examined. Benzothiazole is an attractive building block for the construction of dyes with enhanced two photon absorption and for application in photovoltaics [4,5].

Fig. 1b shows the early excited state dynamics of compounds D1-D6 and T1-T6 in toluene. It is observed that increasing the strength of the EWG leads to the appearance of a fast decay mechanism in both linear and tri-branched systems. Besides, in compounds D1-D3 and T1-T3 having the non-common orientation of the benzothiazole, the initial decay is faster pointing to a more efficient ICT formation.

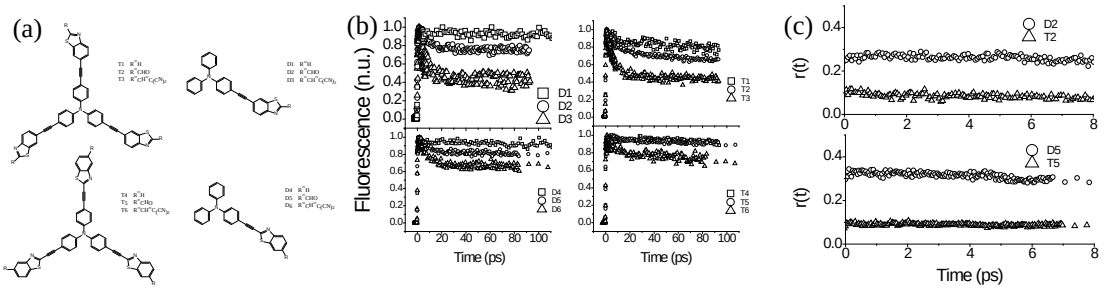

Fig. 1 (a) Chemical structures of the studied molecules, (b) Early fluorescence dynamics of the studied molecules in toluene, (c) Early anisotropy dynamics of the D2, T2 and D5, T5 in toluene.

Fig. 1c shows the early anisotropy dynamics of compounds D2, T2 and D4 and T4 probing the nature and amount of coupling among branches and excitation delocalization. The linear compounds exhibit an initial anisotropy value of 0.3-0.37 as expected for compounds with small angle between the absorption and emission dipoles. In the three-branched compounds, an initial anisotropy value of 0.1 is observed which is exactly the predicted value for planar molecules with equally distributed energy among chromophores [6] pointing to an ultrafast energy redistribution in the studied multichromophoric systems.

Acknowledgements: This work was supported by Grant E0.28 from the Research Committee of the University of Patras (Programme K. Karatheodori).

References

[1] Xiaohui Zhang, Yi Zeng, Tianjun Yu, Jinping Chen, Guoqiang Yang, and Yi Li, *Advances in Photofunctional Dendrimers for Solar Energy Conversion*, J. Phys. Chem. Lett. **5**, 2340 (2014).

[2] Tianshi Qin, Wolfgang Wiedemair, Sebastian Nau, Roman Trattnig, Stefan Sax, Stefanie Winkler, Antje Vollmer, Norbert Koch, Martin Baumgarten, Emil J. W. List, and Klaus Müllen, *Core, Shell, and Surface-Optimized Dendrimers for Blue Light-Emitting Diodes*, J. Am. Chem. Soc. **133**, 1301 (2011).

[3] Georgios Tsiminis, Jean-Charles Ribierre, Arvydas Ruseckas, Homar S. Barcena, Garry J. Richards, Graham A. Turnbull, Paul L. Burn, and Ifor D. W. Samuel, *Two-Photon Absorption and Lasing in First-Generation Bisfluorene Dendrimers*, Adv. Mater. **20**, 1940 (2008).

[4] Peter Hrobárik, Veronika Hrobáriková, Ivica Sigmundová, Pavol Zahradník, Mihalis Fakis, Ioannis Polyzos, and Peter Persephonis, *Benzothiazoles with Tunable Electron-Withdrawing Strength and Reverse Polarity: A Route to Triphenylamine-Based Chromophores with Enhanced Two-Photon Absorption*, J. Org. Chem. **76**, 8726 (2011).

[5] Mihalis Fakis, Peter Hrobárik, Oleksandr Yushchenko, Ivica Sigmundová, Marius Koch, Arnulf Rosspeintner, Elias Stathatos, and Eric Vauthey, *Excited State and Injection Dynamics of Triphenylamine Sensitizers Containing a Benzothiazole Electron-Accepting Group on TiO_2 and Al_2O_3 Thin Films*, J. Phys. Chem. C **118**, 28509 (2014).

[6] Oleg Varnavski, Xingzhong Yan, Olivier Mongin, Mireille Blanchard-Desce and Theodore Goodson, *Strongly Interacting Organic Conjugated Dendrimers with Enhanced Two-Photon Absorption*, J. Phys. Chem. C **111**, 149 (2007).

The Magnetic Moment of the Proton and a High-Precision Comparison of the Proton to Antiproton Charge-To-Mass Ratio

Andreas Mooser[1], Klaus Blaum[2], James Harrington[1], Takashi Higuchi[1,3], Nathan Leefer[4], Yasuyuki Matsuda[3], Hiroki Nagahama[1,3], Georg Schneider[1,5], Stefan Sellner[1], Christian Smorra[1,6], Toya Tanaka[1,3], Wolfgang Quint[7], Jochen Walz[4,5], Yasunori Yamazaki[8], Stefan Ulmer[1]

1. Ulmer Initiative Research Unit, RIKEN, 2-1 Hirosawa, Wako, Saitama 351-0198, Japan
2. Max-Planck-Institut für Kernphysik, Saupfercheckweg 1, 69117 Heidelberg, Germany
3. Graduate School of Arts and Science, University of Tokyo, 3-8-1 Komaba, Meguro-ku, Tokyo 153-8902 Japan
4. Helmholz-Institut Mainz, Johann-Joachim-Becher-Weg 36, 55128 Mainz, Germany
5. Institut für Physik, Johannes Gutenberg-Universität Mainz, Staudingerweg 7, 55128 Mainz, Germany
6. CERN, CH-1211 Geneva 23, Switzerland
7. Atomphysik, GSI-Helmholzzentrum für Schwerionenforschung, Planckstraße 1, 64291 Darmstadt, Germany
8. Atomic Physics Laboratory, RIKEN, 2-1 Hirosawa, Wako, Saitama 351-0198, Japan

The Standard Model (SM) of particle physics is known to be incomplete. This inspires various searches for physics beyond the SM, among those, direct high-precision tests of the invariance under the simultaneous transformations of charge conjugation, parity inversion and time reversal (CPT). The goal of the BASE collaboration is to perform such CPT-tests by comparing with highest precision the magnetic moment $\mu_{p,\bar{p}}$ and the charge-to-mass ratio of single protons and antiprotons stored in cryogenic Penning traps at low energy [1].
In a Penning trap the measurement of $\mu_{p,\bar{p}}$ is based on the determination of two frequencies, the Larmor and the cyclotron frequency. Based on a statistical detection of spin transitions we measured the Larmor frequency on a single proton for the first time [2], which resulted in a direct determination of μ_p with a fractional precision at the parts-per-million level [3]. The precision was improved significantly by using a double Penning-trap technique [4]. This required the detection of single spin flips, which was achieved with an improved apparatus and by using Bayesian data analysis [5]. Our developments ultimately culminated in the most precise and first direct high-precision measurement of the proton magnetic moment with a relative precision of 3.3 parts per billion [6].
This method can be directly applied to measure the magnetic moment of the antiproton, to provide one of the most stringent tests of CPT invariance using baryons. Thus we constructed the BASE experiment at the antiproton decelerator of CERN. In our first experimental campaign with the newly implemented apparatus we developed a novel fast measurement procedure for cyclotron frequency comparisons of two individual particles. This enabled us to compare the charge-to-mass ratio of the proton and the antiproton with a fractional precision of 69 parts per trillion, which is the most precise test of CPT-invariance using baryons [7]. Our measurements were performed at cyclotron frequencies of about 30 MHz, which means that in this case CPT symmetry holds at the atto-electronvolt scale. Currently the apparatus is beeing prepared for magnetic moment measurements. A major part of the required techniques has been implemented. In the contribution I will summarize the achievements and give an outlook on future perspectives.

References

[1] Christian Smorra *et al.*, *BASE - The Baryon Antibaryon Symmetry Experiment*, Eur. Phys. J. ST **224**, 14 (2015).
[2] Stefan Ulmer *et al.*, *Observation of Spin Flips with a Single Trapped Proton*, Phys. Rev. Lett **106**, 253001 (2011).
[3] Cricia Rodegheri *et al.*, *An experiment for the direct determination of the g-factor of a single proton in a Penning trap*, New J. Phys. **14**, 063011 (2012).
[4] Andreas Mooser *et al.*, *Demonstration of the Double Penning Trap Technique with a Single Proton*, Phys. Lett. B **723**, 78 (2013).
[5] Andreas Mooser *et al.*, *Resolution of Single Spin-Flips of a Single Proton*, Phys. Rev. Lett **110**, 140405 (2013).
[6] Andreas Mooser *et al.*, *Direct high-precision measurement of the magnetic moment of the proton*, Nature **509**, 596 (2014).
[7] Stefan Ulmer *et al.*, *High-precision comparison of the antiproton-to-proton charge-to-mass ratio*, Nature **524**, 196 (2015).

Broadband and ultra-broadband polarisation rotators made by composite stacks of ordinary wave plates

Emiliya Dimova[1], Andon Rangelov[2], Elica Kyoseva[3]
1. Institute of Solid State Physics, BAS, 72 Tzarigradsko Chaussee Blvd., 1784 Sofia, Bulgaria
2. Department of Physics, Sofia University, 5 James Bourchier blvd., 1164 Sofia, Bulgaria
3. Engineering Product Development, Singapore University of Technology and Design, 8 Somapah Road, 487372 Singapore, Singapore

We experimentally demonstrate two types of broadband and ultra-broadband spectral bandwidth polarization rotators with modular design.
The first type presented polarization rotators comprise arrays of half-wave plates rotated at different angles. [1] We give the general recipe to determine the exact values of the rotation angles as follows: align the fast polarization axis of the first half-wave plate with the incoming polarized light, and then rotate each subsequent half-wave plate at a gradually increasing angle until the fast polarization axis of the last half-wave plate is parallel with the desired polarization rotation angle. We show that the broadband and ultra-broadband performance of the polarization rotators is due to the adiabatic nature of the evolution of the light polarization.
We also propose and experimentally demonstrate a novel type of polarization rotator that is capable of rotating the polarization plane of a linearly polarized light at any desired angle in either broad or narrow spectral bandwidth [2]. The rotator comprises an array of standard half-wave plates rotated at specific angles with respect to their fast-polarization axes. The performance of the rotator depends on the number of individual half-wave plates, and in this paper we experimentally investigate the performance of two composite rotators comprising 6 and 10 half-wave plates.

This work is supported by project INERA 316309.

References:
[1] E Dimova, A Rangelov, E Kyoseva, *Broadband and ultra-broadband polarization rotators with adiabatic modular design*, Journal of Optics, **17** (7), 075605 (5pp) (2015)
[2] E Dimova, A Rangelov, E Kyoseva, *Tunable bandwidth optical rotator*, Photon. Res **3** (4) pp. 177-179 (2015)

Precision description of the atomic structure. Example of the even configuration system of La I

Jerzy Dembczyński[1], Magdalena Elantkowska[2], Jarosław Ruczkowski[1], Laurentius Windholz[3]
1. Institute of Control and Information Engineering, Poznan University of Technology, Piotrowo 3A, 60-965 Poznan, Poland
2. Institute of Materials Research and Quantum Engineering, Poznan University of Technology, Piotrowo 3, 60-965 Poznan, Poland
3. Institut für Experimentalphysik, Technische Universität Graz, Petersgasse 16, 8010 Graz, Austria

The way to obtain information regarding the structure of an atom, the mechanisms of interaction between the electrons, and the interactions of the electron shell with the nucleus is to find the most accurate wave function describing the state of the atom. The knowledge of the exact wave function allows to specify, according to the quantum mechanics rules, the expected values of observables, which are the attributes of the atomic structure that are measurable, thus making an experimental verification possible.

In order to describe precisely the atomic structure we developed a method, which allows to analyze a complex electronic system composed of up to four open shells, taking into account all electromagnetic interactions expected in an atom, in accordance with the second-order perturbation theory. Within this theory, all possible combinations following the excitation of one or two electrons from closed shells to particular open shells were considered. The appropriate formulae and computer codes have been developed over many years by our research group. The scheme of the computational procedures was presented in a previous paper [1]. By using of this code, both the electronic and atomic wave functions were produced on the basis of experimentally determined energy levels. The quality of these wave functions was proved by a comparison of the experimental g_J-factors, hyperfine structure (hfs) A- and B constants and oscillator strengths with those calculated with the use of the wave functions obtained by our computer code.The application of this method to the even configurations system $(5d + 6s)^3$ of lanthanum atom in 2010 [2].

Recently this procedure was applied to the analysis of the electronic structure of the thorium ion [3]. Since for this ion only a very limited number of experimental data, especially concerning the hfs are available, not all contributions from one- and two electron excitation to the atomic structure can be determined. In order to show the effectiveness of our method better, we decided to choose lanthanum, as an atom with a complex structure and with a huge amount of experimental data concerning energy levels and hyperfine structure constants [4-8].

Currently the La level list contains ca. 430 even La I levels, all of them with known hyperfine constants A (sometimes also B constants are known). 167 odd La levels are known, but few of them may not really exist. It provides an excellent test confirming the correctness of our method and the complex formulae derived, which in the case of consideration.

For the study of La, we considered the system of 100 even configurations: $4f^25d + 4f^26s + 4f\,5d5f + 4f\,5f6s + \sum_{n'=6}^{12} 4f5dn'p + \sum_{n'=6}^{12} 4f6sn'p + 5d^3 + \sum_{n'=6}^{15} 5d^2n's + \sum_{n'=6}^{15} 5d^2n'd + \sum_{n'=5}^{14} 5d^2n'g + 5d6s^2 + \sum_{n'=7}^{15} 5d6sn's + \sum_{n'=6}^{15} 5d6sn'd + \sum_{n'=5}^{14} 5d6sn'g + 5d6p^2 + 6s6p^2 + \sum_{n'=7}^{15} 6s^2n's + \sum_{n'=6}^{15} 6s^2n'd.$

In our procedure we use all the experimental data known so far. Very good agreement between experimental and calculated values of energy and hyperfine structure constants was achieved. The energy values and hfs constants for the levels up to approx. 45 000 cm^{-1} were also predicted.

This work was supported by the Research Projects of the Polish Ministry of Sciences and Higher Education: 04/45/DSPB/0135 (JD and JR) and 06/65/DSPB/0516 (ME).

References

[1] M. Elantkowska, J. Ruczkowski, and J. Dembczyński, Eur Phys J Plus **130**, 14 (2015).
[2] J. Dembczyński, M. Elantkowska, B. Furmann, J. Ruczkowski, and D. Stefańska, Journal of Physics B: Atomic, Molecular and Optical Physics **43**, 065001 (2010).
[3] J. Dembczyński, M. Elantkowska, and J. Ruczkowski, Phys. Rev. A **92**, 012519 (2015).
[4] W. C. Martin, R. Zalubas, and L. Hagan, *Atomic Energy Levels: The Rare-Earth Elements. NSRDS-NBS 60*, Tech. Rep. (Washington, DC: National Bureau of Standards, U.S. Department of Commerc, 1978).
[5] F. Güzelçimen, I. Siddiqui, G.Başar, S. Kröger, L. Windholz, Journal of Physics B: Atomic, Molecular and Optical Physics **45**, 135005 (2012).
[6] F. Güzelçimen, G. Başar, M. Tamanis, A. Kruzins, R. Ferber, L. Windholz, and S. Kröger, The Astrophysical Journal Supplement Series **208**, 18 (2013).
[7] I. Siddiqui, S. Khan, B. Gamper, J. Dembczyński, and L. Windholz, Journal of Physics B: Atomic, Molecular and Optical Physics **46**, 065002 (2013).
[8] B. Gamper, P. Głowacki, I. Siddiqui, J. Dembczyński, and L. Windholz, Journal of Physics B: Atomic, Molecular and Optical Physics **47**, 165001 (2014).

Multi-Photon Entanglement in High Dimensions

Mehul Malik,[1,2] **Manuel Erhard,**[1,2] **Marcus Huber,**[3]
Mario Krenn,[1,2] **Robert Fickler,**[1,2] **Anton Zeilinger**[1,2]
1. Institute for Quantum Optics and Quantum Information (IQOQI), Austrian Academy of Sciences, Vienna, Austria
2. Faculty of Physics, University of Vienna, Boltzmanngasse 5, 1090 Vienna, Austria
3. Universitat Autonoma de Barcelona, 08193 Bellaterra, Barcelona, Spain

Entanglement lies at the heart of quantum mechanics—as a fundamental tool for testing its deep rift with classical physics, while also providing a key resource for quantum technologies such as quantum computation and cryptography. The entanglement of many quantum particles has been demonstrated in physical systems as diverse as ions, photons, and superconducting circuits. However, all these experiments have remained in a two-dimensional space for each particle. Here we show the experimental generation of the first multipartite entangled state where both—the number of particles and the number of dimensions—are greater than two [1]. Our method relies on combining two pairs of photons, high-dimensionally entangled in their orbital angular momentum (OAM), in such a way that information about their origin is erased. As depicted in Fig. 1a), a UV laser pulse creates two OAM-entangled photon pairs in two nonlinear crystals (NL1 and NL2). Both pairs are spatially separated via polarising beam splitters (PBS). A moving trombone prism ensures that a photon from each pair arrives simultaneously at the OAM beam splitter, which is an interferometric device containing two dove-prisms (DP1 and DP2). Considered as a whole, the OAM beam splitter reflects odd OAM quanta and transmits even ones, mixing the OAM quanta of two input photons. A coincidence at detectors B and C can only arise when both detected photons have the same OAM parity. A trigger photon at detector T projects photons at detectors A, B, and C into an asymmetric three-photon entangled state that is entangled in $3 \times 3 \times 2$ dimensions of its OAM. Interestingly, this asymmetric entanglement structure is only possible when one considers multi-particle entangled states in dimension greater than two [2].

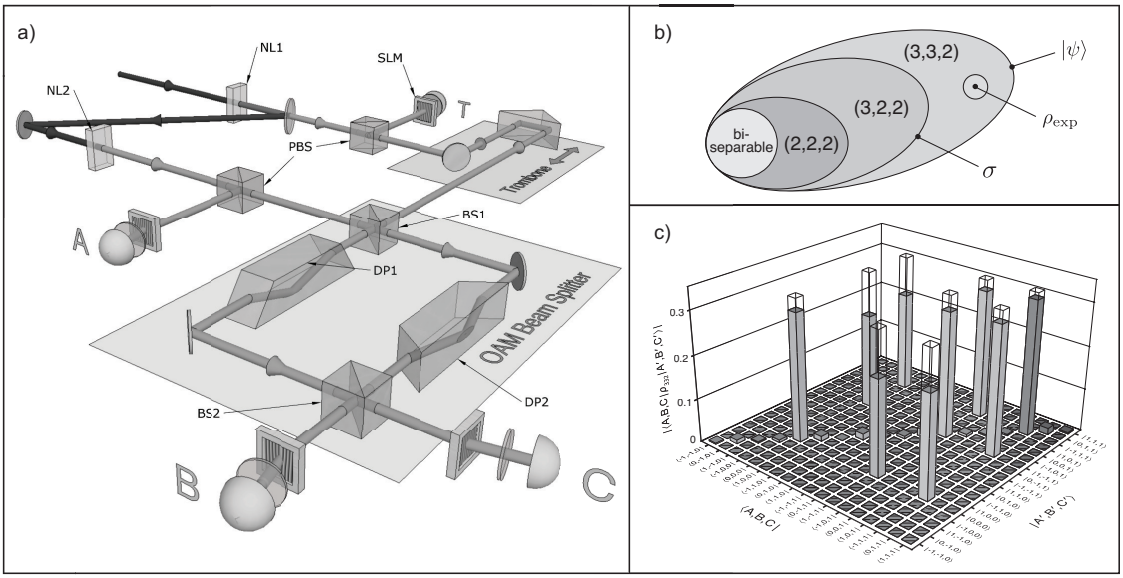

Fig. 1 a) Schematic of the experimental setup (details in the text), b) Russian nesting-doll-like structure of high-dimensional three-particle states showing our measured state $\rho_{\rm exp}$, and c) Density matrix elements of $\rho_{\rm exp}$ measured for verifying the presence of (3,3,2) entanglement.

In order to verify that our three-photon state is entangled in $3 \times 3 \times 2$ dimensions, we have to show that it cannot be decomposed into entangled states of a smaller dimensionality structure (Fig. 1b). We construct an entanglement witness that requires us to calculate the overlap of our state $\rho_{\rm exp}$ with an ideal target $(3,3,2)$-state $|\Psi\rangle$. This is done by measuring the 18 diagonal and 3 unique off-diagonal elements in its density matrix (Fig. 1c) with the help of spatial light modulators (SLMs). Next, we show that this overlap is significantly greater than the best achievable overlap of an ideal state σ from the next lower dimensionality structure (3,2,2), thus verifying the presence of (3,3,2) entanglement. Finally, we show how this state enables a new type of layered quantum cryptographic protocol where two parties share an additional layer of secure information over that already shared by all three parties [1]. In addition to their application in novel quantum communication protocols, such asymmetric entangled states serve as a manifestation of the complex dance of correlations that can exist within quantum mechanics.

References

[1] Mehul Malik et al, *Multi-photon entanglement in high dimensions*, Nat. Photonics (2016), doi:10.1038/nphoton.2016.12.
[2] Marcus Huber and Julio de Vicente, *Structure of multidimensional entanglement in multipartite Systems*, Phys. Rev. Lett. **110**, 030501 (2013).

Determination of Molecular Line Positions in Reference to an Optical Atomic Clock

Katarzyna Bielska, Szymon Wójtewicz, Piotr Morzyński, Piotr Ablewski, Agata Cygan, Marcin Bober, Michał Zawada, Roman Ciuryło, Piotr Masłowski, Daniel Lisak

Institute of Physics, Faculty of Physics, Astronomy and Informatics, Nicolaus Copernicus University in Toruń, Grudziadzka 5, 87-100 Toruń, Poland

We have measured position of the P7P7 oxygen B-band transition occurring near 690 nm in reference to the strontium optical clock. The experimental setup (shown in Fig.1) consisted of three important sub-systems: the first was Pound-Drever-Hall locked frequency stabilised cavity ring-down spectrometer (PDH-locked FS-CRDS) which was used for recording molecular spectra, see [1] and references therein for details of spectrometer's operation. The second system component was ^{88}Sr optical clock working on $^1S_0$-$^3P_0$ transition [2,3]. This transition is the practical realisation of the metre. Finally, the third one was a link between them made with an Er:fibre optical frequency comb (OFC), frequency shifted to 1390 nm range and subsequently frequency doubled. During measurements, two heterodyne beat-note signals were measured simultaneously at each point: one between the spectrometer's probe beam and OFC, and the other between the clock laser beam and OFC. All counters and frequency generator were referenced with the same 10 MHz reference signal from hydrogen maser [4] transferred by 330 km fibre link [3,5], recently used in spectroscopic experiment [6]. Such procedure enables to refer each point of the spectrum to the frequency of the strontium clock transition.
Several spectra were collected at multiple sample pressures. Preliminary results indicate that the uncertainty of line position extrapolated to zero pressure is below 30 kHz. This is a proof–of–principle experiment which demonstrates the use of optical atomic clocks as a frequency reference in molecular spectroscopy.

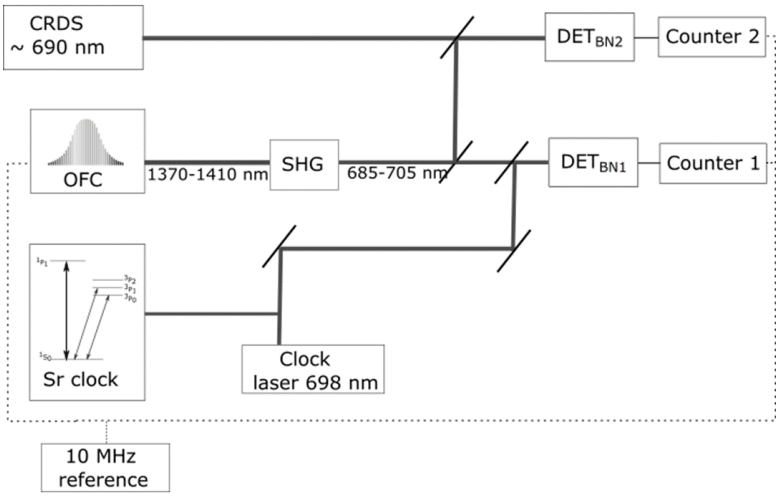

Fig. 1 Schematic diagram of experimental setup: OFC is optical frequency comb, DET$_{BN1}$ and DET$_{BN2}$ are detectors used for heterodyne beat-note signals between the probe beam and the OFC as well as clock laser beam and OFC. See other explanations in the text.

References

[1] J. Domysławska et. al., *Spectral lines hapes and frequencies of molecular oxygen B-band R-branch transitions*, J. Quant. Spectrosc. Radiat. Transf. **155**, 22 (2015)
[2] M. Bober et. al., *Strontium optical lattice clocks for practical realization of the metre and secondary representation of the second*, Meas. Sci. Technol. **26**, 0075201 (2015)
[3] P. Morzyński et. al., *Absolute measurement of the $^1S_0 - {}^3P_0$ clock transition in neutral 88Sr over the 330 km-long stabilized fibre optic link*, Sci. Rep. **5**, 17495 (2015)
[4] Z. Jiang et.al,. *Comparing a GPS time link calibration with an optical fibre self-calibration with 200 ps accuracy*, Metrologia **52**, 384 (2015)
[5] P. Krehlik et. al., *Ultrastable long-distance fibre-optic time transfer: active compensation over a wide range of delays*, Metrologia **52**, 82 (2015)
[6] A. Cygan et.al., *Absolute molecular transitions frequencies measured by three cavity-enhanced spectroscopy techniques*, submitted to J. Chem. Phys.

High-Precision Spectroscopy of the 1557 nm Magnetic Dipole Transition in a BEC of Metastable Helium

R.P.M.J.W. Notermans, R.J. Rengelink, W. Vassen
LaserLaB, Dept. of Physics and Astronomy, Vrije Universiteit Amsterdam, de Boelelaan 1081, 1081 HV Amsterdam, the Netherlands

QED theory allows extraction of nuclear charge radii from high-precision spectroscopy in simple atomic systems. This recently led to a significant discrepancy in the proton charge radius determined from normal and muonic hydrogen, now known as the 'proton size puzzle'. Spectroscopy in helium can provide additional insight by comparing extracted charge radii of the alpha and helion (^{3}He nucleus) particles with spectroscopy of muonic $^4He^+$ and $^3He^+$ ions, recently performed at the muon facility of the Paul Scherrer Institute in Switzerland.

Our group previously measured the 1557 nm $2\ ^3S \rightarrow 2\ ^1S$ magnetic dipole transition ($\Gamma = 2\pi \times 8$ Hz) to 1.5 kHz accuracy in a quantum degenerate (T ~ 0.2 μK) gas of metastable ^{4}He and ^{3}He atoms in a 1.56 μm crossed dipole trap, allowing a 1% accurate determination of the charge radius difference between the alpha and helion particle [1]. Measurements in muonic He^+ aim for a precision of 3×10^{-4} [2]. In order to provide a similar accuracy, we aim to remeasure the 1557 nm transition with ~0.1 kHz precision by reducing the linewidth of the spectroscopy laser and by implementing a magic wavelength ($\lambda = 319.8$ nm) dipole trap [3]. As a first step we have observed the $2\ ^3S \rightarrow 2\ ^1S$ transition in a BEC, contained in a 1.56 μm crossed-dipole trap, with a 4-5 kHz linewidth spectroscopy laser and now see a ~10 kHz wide asymmetric line profile (Fig. 1). We think this is caused by mean-field effects, similar to the work on the 1S → 2S transition in atomic hydrogen at MIT [4-6], as well as the AC Stark effect in the trap. This allows for the first determination of the unknown triplet-singlet scattering length a_{31} as the mean field causes a frequency shift $\Delta\nu_{2\,^3S-2\,^1S} = (a_{31} - a_{33})\,2\hbar n/m$, where $n(r)$ is density of metastable helium atoms in the trap (the triplet-triplet scattering length $a_{33} = 7.512(5)$ nm [7]).

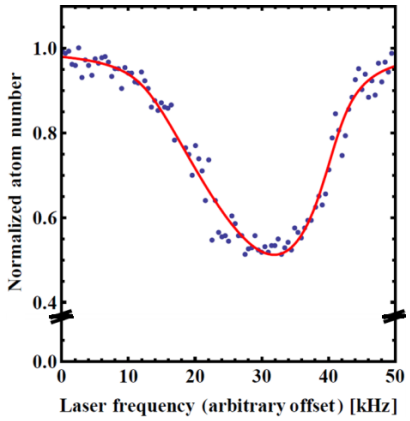

Fig. 1 Asymmetric line profile of the $2\ ^3S \rightarrow 2\ ^1S$ transition in a BEC of metastable ^{4}He atoms in a 1.56 μm crossed dipole trap. The experimental points show the remaining fraction of atoms after a 1s excitation with a narrowband laser. The line is a fit to the data using the Killian model developed for hydrogen in a magnetic trap [6], adapted to include AC Stark broadening and shifts in a dipole trap, and convoluted with a 4-5 kHz Lorentzian laser line profile.

For the magic wavelength trap we have built a laser system, consisting of sum frequency mixing of 1085.5 nm and 1557.3 nm fibre laser/amplifiers, followed by frequency doubling of the 639.6 nm output. We produce >2 W narrowband radiation in this way and have demonstrated trapping of ultracold metastable ^{4}He, both thermal (~0.2 μK) and in a BEC [8].

References

[1] R. van Rooij, J.S. Borbely, J. Simonet, M.D. Hoogerland, K.S.E. Eikema, R.A. Rozendaal and W. Vassen, *Frequency Metrology in Quantum Degenerate Helium: Direct Measurement of the $2\ ^3S_1 \rightarrow 2\ ^1S_0$ Transition,* Science **333**, 198 (2011).
[2] A. Antognini *et al.*, *Illuminating the Proton Radius Conundrum: the μHe^+ Lamb Shift,* Can. J. Phys. **89**, 47 (2011).
[3] R.P.M.J.W. Notermans, R.J. Rengelink, K.A.H. van Leeuwen, W. Vassen, *Magic Wavelengths for the $2\ ^3S_1 \rightarrow 2\ ^1S_0$ Transition in Helium*, Phys. Rev. A **90**, 042508 (2014).
[4] T.C. Killian, D.G. Fried, L. Willmann, D. Landhuis, S.C. Moss, T.J. Greytak, D. Kleppner, *Cold Collision Frequency Shift of the 1S- 2S Transition in Hydrogen*, Phys. Rev. Lett. **81**, 3807 (1998).
[5] D.G. Fried, T.C. Killian, L. Willmann, D. Landhuis, S.C. Moss, D. Kleppner, T.J. Greytak, *Bose-Einstein Condensation of Atomic Hydrogen*, Phys. Rev. Lett. **81**, 3811 (1998).
[6] T.C. Killian, *1S- 2S Spectrum of a Hydrogen Bose-Einstein Condensate*, Phys. Rev. A **61**, 033611 (2000).
[7] S. Moal, M. Portier, J. Kim, J. Dugué, U.D. Rapol, M. Leduc, C. Cohen-Tannoudji, *Accurate Determination of the Scattering Length of Metastable Helium Atoms Using Dark Resonances between Atoms and Exotic Molecules*, Phys. Rev. Lett. **96**, 023203 (2006).
[8] R.J. Rengelink, R.P.M.J.W. Notermans, W. Vassen, *A Simple 2 W Continuous-Wave Laser System for Trapping Ultracold Metastable Helium Atoms at the 319.8 nm Magic Wavelength*, arXiv:1511.00443 (2015).

Phase Sensitive 2DAtom Localization Via Probe Absorption measurement For Closed Loop Quantum Systems

Hamid Reza Hamedi and Gediminas Juzeliunas

Institute of Theoretical Physics and Astronomy, Vilnius University, A. Goštauto 12, Vilnius 01108, Lithuania

A scheme of high- precision **two dimensional (2D) atom localization** is proposed and analyzed by using the density matrix method in a five-level atom-light coupling scheme (Fig. 1(a)). In this system four strong laser components couple a pair of atomic internal states to another pair of states to form a closed loop diamond- shape configuration of the atom-light interaction [1]. We consider various situations in which the atom could interact with the position-dependent standing-wave fields (Fig. 1(b)-(d)).

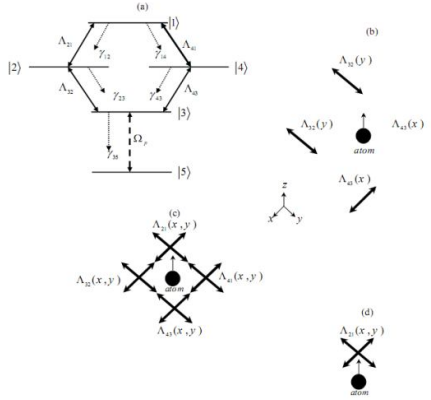

Fig. 1 Schematic diagram of the five level quantum system. Here the atomic states are denoted by $|1\rangle,|2\rangle,|3\rangle,|4\rangle$ and $|5\rangle$, the coherent probe and driving fields are Ω_p and Λ_{ij}, respectively. The spontaneous decay rates from the upper level $|i\rangle$ to the lower level $|k\rangle$ are denoted by γ_{ik}. (b), (c), and (d) Different situations considered in which the atom could interact with the position- dependent standing-wave fields.

By systematically solving the density matrix equations of the motion, we show that the imaginary part of the susceptibility for the weak probe field is position-dependent. As a result, we can obtain information about the position of the atom by measuring the resulting absorption spectra. Focusing on the signatures of the relative phase of the applied fields providing the closed- loop structure of the diamond- shape subsystem, we present analytical solutions to elucidate the phase- control of spatial- distribution of the atom passing through the standing waves. We find out that there exists a significant phase dependence of the eigenvalues leading to the phase dependence of the probe absorption spectra. By properly choosing the amplitudes and phases of the driving fields, the atom-light Hamiltonian can contain three, four, and two absorption peaks, resulting in different localization patterns for the atom. However, we show that the first two situations shown in Fig. 1(b) and Fig. 1(c) are not suitable for achieving high-resolution and perfect precision of 2D atom localization. In the last situation where the atom is coupled to a single standing wave (Fig. 1(d)), a nearly perfect 2D atom localization can be obtained. In this case, the detection probability of finding the atom at a particular position will be increased, and the precision of localization of the atom will be improved [2].

The atom localisation is detected here by measuring the probe-absorption spectra of the system. The absorption measurement is much easier to perform in a laboratory compared to the spontaneous emission measurement [3,4]. Moreover, here the atom is prepared in the ground state, which is very easy to implement in atomic physics experiments. These advantages suggests a relatively easy experimental implementation of our 2D atom localization scheme.

References

[1] H. R. Hamedi and G. Juzeliūnas, *Phase-sensitive Kerr nonlinearity for closed-loop quantum systems*, Phys. Rev. A **91**, 053823 (2015)
[2] H. R. Hamedi and G. Juzeliūnas, *Phase-sensitive atom localization for closed-loop quantum systems*, Submitted to Phys. Rev. A (2015)
[3] Sajid Qamar, Shi-Yao Zhu, and M. Suhail Zubairy, *Atom localization via resonance fluorescence*, Phys. Rev. A **61**, (2000)
[4] Chunling Ding and Jiahua Li and Zhiming Zhan and Xiaoxue Yang, *Two-dimensional atom localization via spontaneous emission in a coherently driven five-level M-type atomic system*, Phy. Rev. A **83**, 063834 (2011).

Case Studies for Coherent Control of Chaotic Molecular Systems

Johannes Floß and Paul Brumer
Chemical Physics Theory Group, Department of Chemistry and Centre for Quantum Information and Quantum Control, University of Toronto, Ontario M5S 3H6, Canada

A major aim of coherent control is the steering of complex chemical reactions towards a desired product. However, until today the success of this approach has been limited to rather simple processes, most of them are unimolecular. Even moderately sized molecular systems reveal chaotic behaviour, extreme sensitivity of the phase space trajectories on the initial conditions [1]. Using simple model systems for which the underlying classical dynamics are chaotic, we will present theoretical case studies on the prospects of coherent control of such systems. Based on these model systems, simple experimental schemes to test the relationship between chaos and coherent control are suggested.

We will show how the chaotic dynamics of the underlying classical system can manifest itself in the quantum dynamics of the coherent control scheme. For example, we have found that the excited wave packet can show Wigner ("chaotic") or Poisson ("regular") nearest level spacing distributions for a system that has an underlying Poisson distribution – the coherent control scheme "picks" either distribution depending on whether the excitation is into a classically chaotic or regular region of the phase space. Another manifestation can be found in the quantum revivals. A chaotic region of the phase-space may prevent the excitation of a reviving wave packet, even if the underlying level structure would support revivals.

For illustration, we present in Fig. 1 the case of laser-assisted alignment of the asymmetric top molecule SO_2. This is a well established coherent control scenario [2, 3]. However, if an external field is applied, the classical motion becomes chaotic, as illustrated by the Poincaré maps shown in Figs. 1(a,b). This chaotic motion affects the control scheme: If the excited wave packet is in a classically regular region of the phase-space [Figs. 1(c,e)], strong alignment as well as quantum revivals can be observed. For the chaotic case on the other hand [Fig. 1(d)], one may still observe alignment, but the quantum revivals are gone.

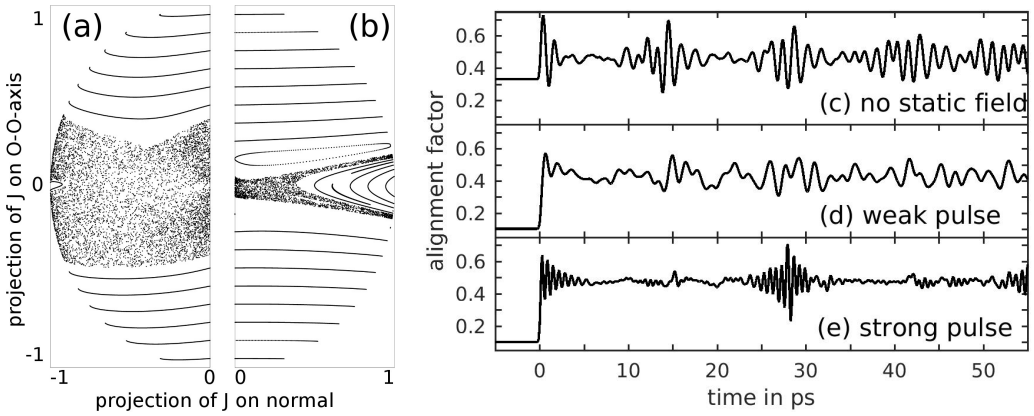

Fig. 1 (a,b): Classical dynamics of SO_2 molecules in a static electric field, for (a) strong and (b) weak fields, illustrated by Poincaré maps. Shown are the normalised projections of the angular momentum J on the O-O-axis and the normal of the molecular plane, respectively, at the crossings of the surface of section (defined by the dipole moment being perpendicular to the electric field). (c,d,e): Quantum dynamics of SO_2 molecules in a static electric field, interacting with a 250 fs long laser pulse which is linearly polarised in the same direction as the static field. Shown is the alignment of the O-O-axis – measured as $\langle \cos^2 \alpha \rangle$, where α is the angle between the O-O-axis and the static electric field – for different strengths E_0 of the electric field and peak intensities I_0 of the laser pulse. The parameters are: (c) $E_0 = 0$ MV/m, $I_0 = 20$ TW/cm^2; (d) $E_0 = 50$ MV/m, $I_0 = 20$ TW/cm^2; (e) $E_0 = 50$ MV/m, $I_0 = 50$ TW/cm^2.

References

[1] Meishan Zhao, Jiangbin Gong, and Stuart A. Rice, *Classical, Semiclassical, and Quantum Mechanical Unimolecular Reaction Rate Theory*, Adv. Chem. Phys. **130**, 1 (2005).

[2] Emmanuel Péronne, Mikael D. Poulsen, Christer Z. Bisgaard, Henrik Stapelfeldt, and Tamar Seideman, *Nonadiabatic Alignment of Asymmetric Top Molecules: Field-Free Alignment of Iodobenzene*, Phys. Rev. Lett. **91**, 043003 (2003).

[3] Stefan Pabst, *Atomic and molecular dynamics triggered by ultrashort light pulses on the atto- to picosecond time scale*, Eur. Phys. J. Spec. Top. **221**, 1 (2013).

Stopped Light at High Storage Efficiency in a $Pr^{3+}:Y_2SiO_5$ Crystal

Marcel Hain[1], Daniel Schraft[1], Nikolaus Lorenz[1], Thomas Halfmann[1]

1. Institut für Angewandte Physik, Technische Universität Darmstadt, Hochschulstraße 6, 64289 Darmstadt, Germany

Storage of photonic qubits typically requires atomic media (i.e. quantum memories) of large optical depth - no matter which light storage protocol is applied to convert the photons to atomic excitations. The larger the optical depth OD = -ln(T), with the transmission T through the medium, the larger the storage and retrieval efficiency. A typical approach to reach high optical depth beyond 1000 is based on spatially confined cold atomic gases, e.g. atoms in a magneto-optical-trap [1]. However, due to atomic motion the maximal storage times and spatial multiplexing capacities are still very limited in gaseous media. Solid media, such as rare-earth ion-doped crystals, do not suffer from atomic motion, permit very long storage times and multiplexing. Moreover, they are easy to handle, integrate and scale. However, the drawback in such solids compared to cold atomic gases is their rather low optical depth, leading to rather low light storage efficiencies. As an example, in our recent work on light storage by electromagnetically induced transparency (EIT) in a $Pr^{3+}:Y_2SiO_5$ crystal, we obtained ultra-long storage times up to one minute, but storage efficiencies in the regime of 1 % only [2]. Among others, this was limited by a small optical depth OD ≈ 3 in the $Pr^{3+}:Y_2SiO_5$ crystal.

A straightforward concept to increase the optical depth and storage efficiency is to use the medium in multipass configuration, i.e. to let the data pulse pass the medium N times. Though conceptionally simple, this is technologically often a rather tricky approach, as the dimensions of the media are typically rather small, and dense optical and control setups impose further geometrical constraints.

In our EIT experiment in $Pr^{3+}:Y_2SiO_5$, we implemented now a multipass setup to increase the efficiency of "stopped light" in the solid-state memory. The optical multipass setup is based on a ring configuration with two 4f-imaging systems (see Fig. 1 (a), depicted for N=8 passes).

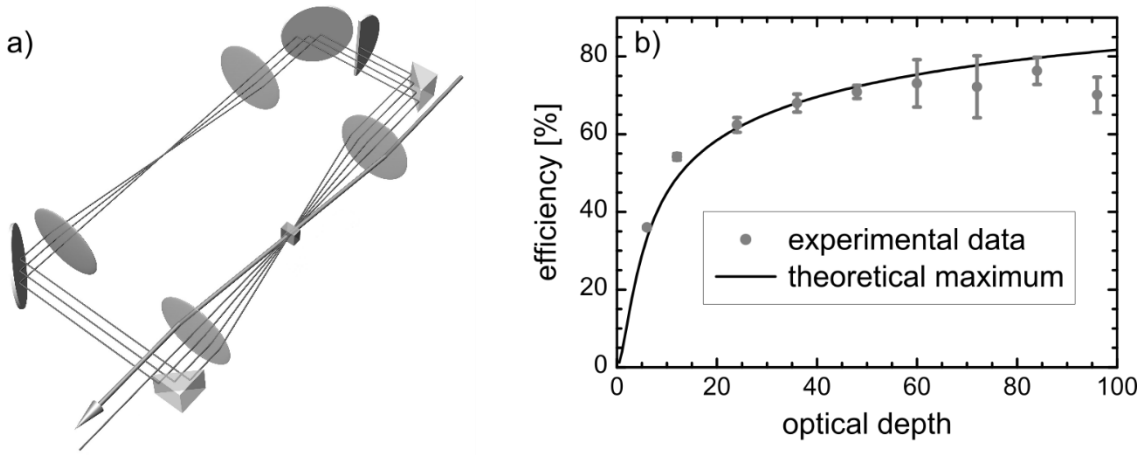

Fig. 1 a) Optical multipass setup for the data pulse shown for N=8 passes together with the control beam needed for the EIT protocol. b) Experimental light storage efficiency and theoretical maximum efficiency [3] versus optical depth.

Back reflection of one of the beams in the ring allows an easy variation of the number of passes up to N=16. Implementation of control techniques (e.g. dynamical decoupling, ZEFOZ) required to prolong the storage time remains possible also in the complex multipass setup. Using our setup we obtained an optical depth up to OD≈96. In combination with pulse shaping approaches, this enabled us to reach EIT storage efficiencies for classical light pulses up to 76 % (see Fig. 1 (b)) [4]. This exhibits the largest value reported so far in the available literature for solid state systems and protocols related to EIT.

We will present the technical implementation of the multipass configuration, optimization procedures for efficient light storage by EIT, and dependencies of the storage efficiency with regard to relevant experimental parameters.

References:

[1] F. Blatt, T. Halfmann, and T. Peters, *One-dimensional ultracold medium of extreme optical depth*, Opt. Lett. **39**, 446 (2014)

[2] G. Heinze, C. Hubrich, and T. Halfmann, *Stopped Light and Image Storage by Electromagnetically Induced Transparency up to the Regime of One Minute*, Phys. Rev. Lett. **111**, 033601 (2013)

[3] A. Gorshkov, A. André, M. Lukin, and A. Sørensen, *Photon storage in Λ-type optically dense atomic media. II. Free-space model*, Phys. Rev. A **76**, 033805 (2007)

[4] D. Schraft, M. Hain, N. Lorenz, and T. Halfmann, *Stopped Light at High Storage Efficiency in a $Pr^{3+}:Y_2SiO_5$ Crystal*, Phys. Rev. Lett. **116**, 073602 (2016)

Selective Excitation of Uncorelated Sets of Adiabatic States in Non-degenerate Hyperfine Level Systems

Teodora Kirova[1], Arturs Cinins[1,2], Martins Bruvelis[2], Dmitry K. Efimov[3], Kaspars Miculis[1], Nikolai N. Bezuglov[3,1], Marcis Auzinsh[2], and Aigars Ekers[4]

1. Institute of Atomic Physics and Spectroscopy, University of Latvia, 4 Skunu street, Riga, LV-1586, Latvia
2. Department of Physics, University of Latvia, 8 Zellu street, Riga, LV-1002, Latvia
3.St. Petersburg State Unviersity, 7/9 Universitetskaya nab., St. Petersburg, 199034, Russia
4.King Abdullah University of Science and Technology (KAUST), Computer, Electrical and Mathematical Science and Engineering Division (CEMSE), Thuwal, 23955-6900, Saudi Arabia

We study the formation of adiabatic states upon strong laser coupling of two levels with non-degenerate hyperfine (HF) structure. We examine a typical Autler-Townes (AT) [1] type of experiment in the ladder excitation scheme $3S_{1/2}-3P_{3/2}-4D_{5/2}$, which is conveniently accessible by visible laser radiation sources. The strong field couples the $3P_{3/2}$ and $4D_{5/2}$ states, creating adiabatic (laser-dressed) states [2], which are then probed by a weak laser field on the $3S_{1/2}-3P_{3/2}$ transition. Both laser fields are linearly polarized, implying the selection rule $\Delta M_F = 0$ for Zeeman sublevels, which allows us to consider each subset of mutually coupled HF levels with the same M_F as an independent multilevel system. The probe laser intensity is chosen week enough, in order to avoid optical pumping and mixing of the ground state HF components. Doppler broadening due to atomic velocity distribution is not taken into account, which is justified in laser-atom interactions in supersonic atomic beams [5].
We investigate numerically the population of state $4D_{5/2}$ as a function of the probe laser detuning for different values of the coupling field strength and detuning. Our numerical calculations are based on the Optical Bloch equations (OBEs) formalism [3] for the density matrix equations of motion. The system of OBEs for the diagonal (Zeeman coherences) and the off-diagonal (optical coherences) elements is readily solved numerically using the Split Operator Technique [4]. Analysis of the non-resonant adiabatic mixing of HF levels by the strong laser field reveals some intuitively unexpected features of the AT spectra. First, the intensities of the bright peaks diminish with the increase of the coupling field strength, such that the peak ratio is inversely proportional to the coupling Rabi frequency squared. Second, and most interesting from applications point of view, it is possible to excite two uncorrelated (orthogonal) configurations of adiabatic states, by using the appropriate choice of probe laser detuning for excitation from $F = 1$ or $F = 2$ HF ground state components. Simultaneous use of two probe fields pulses leads to interesting perspectives to form a two-component bichromatic polariton [6], where a single strong control laser field can drive the independent propagation of the two uncoupled probe field pulses.
We acknowledge support from the Trilateral grant of the Latvian, Lithuanian, and Taiwanese Research Councils FP-20174-ZF-N-100.

References

[1] S. H. Autler and C. H. Townes, *Stark Effect in Rapidly Varying Fields*, Physical Review **100 (2)**, 703 (1955).
[2] S. Reynaud and C. Cohen-Tannoudji, *Dressed Atom Approach to Collisional Redistribution*, J. Physique **43 (7)**, 1021 (1982).
[3] F. Bloch, *Nuclear Induction*, Phys. Rev., **70**, 460 (1946).
[4] A. K. Kazansky, N. N. Bezuglov, A. F. Molisch, F. Fuso, and M. Allegrini, *Direct Numerical Method to Solve Radiation Trapping Problems with a Doppler-Broadening Mechanism for Partial Prequency Redistribution*, Phys. Rev. A **64**, 022719 (2001).
[5] M. Bruvelis, J. Ulmanis, N. N. Bezuglov, K. Miculis, C. Andreeva, B. Mahrov, D. Tretyakov, and A. Ekers, *Analytical Model of Transit Time Broadening for Two-Photon Excitation in a Three-Level Ladder and its Experimental Validation*, Phys. Rev. A **86**, 012501 (2012).
[6] M. Fleischhauer and M. D. Lukin, *Quantum Memory for Photons: Dark-State Polaritons*, Phys. Rev. A **65**, 022314 (2002).

Controlling spin-dependent directed transport in a bipartite lattice

Wenhua Hai, Yunrong Luo
Department of Physics and Key Laboratory of Low-dimensional Quantum Structures and Quantum Control of Ministry of Education, Hunan Normal University, Changsha 410081, China

The theoretical model of synthetic gauge field for neutral atoms has been widely studied [1]. Recently, such a model was realized experimentally in spinor Bose-Einstein condensates (BECs) [2]. Consequently, spin-orbit-coupled (SO-coupled) atomic system became an ideal platform and attracted great interest in studying novel quantum phenomena. On the other hand, it has been demonstrated that a quantum ratchetlike effect in a bipartite lattice of the form *ABABAB*... can be induced by an amplitude-modulated periodic field to alternately decouple the two nearest-neighbour sites with lattice separations $\overline{AB}$ and $\overline{BA}$ [3-5]. Therefore, it is expectable to seek novel control strategies and applications for the spin-dependent dynamical localization (DL) and directed transport (DT) of single atoms in a bipartite lattice based on the combined effects of the SO-coupling and the quantum ratchetlike.

In this paper, we study coherent control of spin-dependent DL and DT of a SO-coupled single atom loaded in a driven optical bipartite lattice. Under the high-frequency limit and nearest-neighbour tight binding approximation, by combining the two effects of SO-coupling and quantum ratchetlike, we find a new decoupling mechanism between states with the same (or different) spins, which leads to two sets of analytical solutions describing DL and DT with (or without) spin flipping, and the approximate coherent destruction of tunneling (CDT) [3-5]. The analytical results are numerically confirmed and perfect agreements are found. By extending the results to the case of non-adjacent SO-coupled single atoms, we find the different DT forms which can be applied to control the propagation speed and distance of the spin-Hall-like effect and to transport the quantum information carried by a few atoms to an arbitrary predetermined position with adjustable velocity, as shown schematically in Fig. 1. The results can be experimentally tested in the current setups [6]. Particularly, making use of the approximate CDT, we can obtain the stationary single atoms held in the desired write port and read port [7] labeled by the big dashed circles in Fig. 1. Such a system has the advantage that the quantum information is localized in individually addressable particles that can be manipulated and controlled in a straightforward way. We expect possible application of the scheme in quantum information processing and in design of quantum logic gate device.

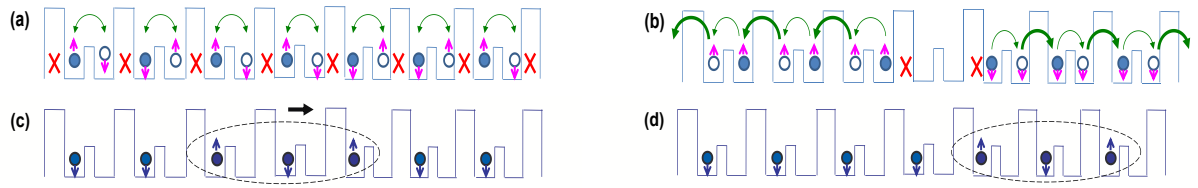

Fig. 1 Schematic diagrams for (a) the DL and (b) the DT of single atoms loaded in a driven optical bipartite lattice, and (c, d) the quantum information transport via a spin chain of three single atoms carrying quantum qubits. Here, the filled circles represent the initial state of the single atoms with different spin ↑ and ↓, and the empty circles denote the next state. In (a), the driving field is adjusted to make one of the two effective couplings vanishing, then the synchronous Rabi oscillations with spin flipping of single atoms occur between the initial sites and their right neighbor sites. In (b), by alternately decoupling the two nearest-neighbour sites with different lattice separations, the spin-Hall-like effect with controllable propagation speed and distance is shown, where two different spin trains perform the DT without spin flipping toward different directions, respectively. In (c), a short spin train labeled by the big dashed circle (write port) is initially imprinted quantum qubits, and starts to transport toward the right. In (d), the quantum information carried by the spin train is transported to a desired read port by selecting the number of adjustments to the driving field, then letting both the two effective couplings vanish.

Acknowledgments: This work was supported by the NNSF of China under Grant Nos. 11175064 and 11475060, and the Construct Program of the National Key Discipline of China.

References

[1] R. Dum and M. Olshanii, *Gauge structures in atom-laser interaction: Bloch oscillations in a dark lattice*, Phys. Rev. Lett. **76**, 1788 (1996)
[2] Y. J. Lin, K. Jiménez-García, and I. B. Spielman, *Spin–orbit-coupled Bose–Einstein condensates*, Nature (London) **471**, 83 (2011).
[3] C. E. Creffield, *Quantum control and entanglement using Periodic driving fields*, Phys. Rev. Lett. **99**, 110501 (2007).
[4] K. Hai, W. Hai, and Q. Chen, *Controlling transport and entanglement of two particles in a bipartite lattice*, Phys. Rev. A **82**, 053412 (2010).
[5] K. Hai, Y. Luo, G. Lu, and W. Hai, *Phase-controlled localization and directed transport in an optical bipartite lattice*, Opt. Express **22**, 4277 (2014).
[6] Y. A. Chen, S. Nascimbène, M. Aidelsburger, M. Atala, S. Trotzky, and I. Bloch, *Controlling correlated tunneling and superexchange interactions with ac-driven optical lattices*, Phys. Rev. Lett. **107**, 210405 (2011).
[7] O. Romero-Isart and J. J. García-Ripoll, *Quantum ratchets for quantum communication with optical superlattices*, Phys. Rev. A **76**, 052304 (2007).

Direct Excitation of Butterfly States in Rydberg Molecules

Carsten Lippe[1], **Oliver Thomas**[1,2], **Thomas Niederprüm**[1], **Tanita Eichert**[1], **Herwig Ott**[1]

1. Department of Physics and Research Center OPTIMAS, Technische Universität Kaiserslautern, Erwin-Schrödinger-Straße 46, 67663 Kaiserslautern, Germany

2. Graduate School Materials Science in Mainz, Gottlieb-Daimler-Straße 47, 67663 Kaiserslautern, Germany

Since their first theoretical prediction Rydberg molecules have become an increasing field of research. These exotic states originate from the binding of a ground state atom in the electronic wave function of a highly-excited Rydberg atom mediated by a Fermi contact type interaction. A special class of long-range molecular states, the butterfly states, were first proposed by Greene et al. [1]. These states arise from a shape resonance in the p-wave scattering channel of a ground state atom and a Rydberg electron and are characterized by an electron wavefunction whose density distribution resembles the shape of a butterfly.

We report on the direct observation of deeply bound butterfly states of Rydberg molecules of ^{87}Rb. The butterfly states are studied by high resolution spectroscopy of UV-excited Rydberg molecules. We find states bound up to $-50\,\mathrm{GHz}$ from the $25\mathrm{P}_{1/2}, F = 1$ state, corresponding to binding lengths of $50\,a_0$ to $500\,a_0$ and with permanent electric dipole moments of up to 500 Debye. This distinguishes the observed butterfly states from the previously observed long-range Rydberg molecules in rubidium.

References

[1] Chris H. Greene, A. S. Dickinson, H. R. Sadeghpour, *Creation of Polar and Nonpolar Ultra-Long-Range Rydberg Molecules*, Phys. Rev. Lett. **85**, 2458 (2000).

Interatomic Förster Resonance and Anomalous Low Spontaneous Decay of p-Series States in Na

Arturs Cinins[1], Kirill Arefieff[2], Kaspars Miculis[1], Nikolai Bezuglov[2], Andrei Klyucharev[2], Aigars Ekers[3]
1. Institute of Atomic Physics and Spectroscopy, University of Latvia, Riga, LV-1586, Latvia
2. Saint Petersburg State University, St. Petersburg State University, 7/9 Universitetskaya nab., St. Petersburg, 198904, Russia
3. King Abdullah University of Science and Technology (KAUST), Computer, Electrical and Mathematical Science and Engineering Division (CEMSE), Thuwal, 23955-6900, Kingdom of Saudi Arabia

The situation when one of the levels of Rydberg l-series of an atom is located more or less exactly between two levels of adjacent $l' = (l+1)$ or $l' = (l-1)$ series corresponds to the so called Förster resonance [1]. Rydberg levels can be shifted into a Förster resonance using external fields [2], which is a way for achieving tunable interaction strength between atoms. The coherent nature of dipole-dipole interaction between Förster tuned Rydberg states has also been demonstrated in a recent experiment [3]. Another recent study [4] has pointed towards a strong blockade of dipole matrix elements for transitions between l' and l-series in the vicinity of a Förster resonance. The latter occurs when the difference of quantum defects $\Delta\delta = \delta_{l'} - \delta_l$ between the l' and l-series is 0.5 (Förster configuration). In that case the atom can be considered to a good approximation as an ideal 3D oscillator with frequency ω, the energy levels of which are given by $\varepsilon = \omega \times (2n_r + l + 3/2)$, where n_r is the radial quantum number. The energy levels of l and l' series of such oscillator exactly meet the Förster resonance condition. Selection rules of the 3D oscillator allow for optical transitions only between the levels with energy difference matching ω (atomic units are used). In accordance with the correspondence principle, "long" optical transitions (i.e., transitions with frequency corresponding to multiples of ω) are forbidden; hence one would expect anomalous increase of the radiative lifetime in the vicinity of a Förster resonance, when the behaviour of an atom is akin to that of a 3D oscillator.

l	Li	Na	K	Rb	Cs	H
s	0.40	1.35	2.19	3.13	4.06	0
p	0.04	0.85	1.71	2.66	3.59	0

Table 1 Quantum defects δ_l for s-, p-series of alkali and hydrogen atoms [5].

Consider the lifetimes of hydrogen-like alkali atoms. As can be seen from Table 1, the $l = 0$ and $l = 1$ (i.e., s and p) series are close to the Förster configuration of energy levels, while sodium is a special case because it fulfils the condition $\Delta\delta = \delta_s - \delta_p = 0.5$.

l	Li	Na	K	Rb	Cs	H
s	0.005	0.015	0.017	0.017	0.018	0.013
p	0.069	**0.014**	0.051	0.075	0.061	1.00

Table 2 The C_l-coefficient for s-, p-series of alkali and hydrogen atoms [6].

According to the conclusions made in the review of alkali lifetimes [6], the spontaneous decay rates $A_{nl} = 1/\tau_{nl}$ for alkali Rydberg series obey the power law $A_{nl} = \alpha C_l n_{eff}^{-3}/(l+0.5)$, where $n_{eff} = n - \delta_l$ is the effective quantum number, the parameter $\alpha = 1.18 \cdot 10^{10} s^{-1}$, while the C_l-coefficients are provided in Table 2. The p-states of sodium have the $C_{l=1}$ value nearly five times smaller than the respective values of other alkali atoms. Another interesting observation is that for Na the coefficients $C_{l=0}$ and $C_{l=1}$ are nearly equal; such equality is another characteristic feature of 3D oscillators. In this presentation we shall explain the occurrence of this anomaly in the spontaneous emission rates of Na p-states by closeness of the levles of s- and p- series to the Förster configuration. We shall also demonstrate how the transition matrix elements are significantly reduced (blockaded) using the example of a single-parameter model potential.

We acknowledge partial support by the Trilateral grant of the Latvian, Lithuanian, and Taiwanese Research Councils FP-20174-ZF-N-100.

References

[1] T. Forster, Ann. Phys. **437**, 55 (1948).
[2] I. I. Ryabtsev, D. B. Tretyakov, I. I. Beterov, and V. M. Entin, Phys. Rev. Lett. **104**, 073003 (2010).
[3] S. Ravets, H. Labuhn, D. Barredo, L. Beguin, T. Lahaye, and A. Browaeys, Nature Physics **10**, 914 (2014).
[4] Mihail Y Zakharov, Nikolai N. Bezuglov, Andrei N. Klyucharev, et al, Russian J. Phys. Chem. B, **5**, 537 (2011).
[5] T. P. Hezel, C. E. Burkhardt, M. Ciocca, L.-W. He, & J. J. Leventhal, Am. J. Phys., **60**, 329 (1992).
[6] Nikolai N Bezuglov, Evgenij N. Borisov, Ya. F. Verolainen, Sov. Phys. Usp , **34**, 3 (1991).

Ionization energy of optically cooled Li7 atoms measured by using allowed and forbidden Rydberg transitions

B. B. Zelener, S. A. Saakyan, V. A. Sautenkov, B.V. Zelener, V.E. Fortov

Joint institute for high temperature RAS, Izhorskaya st. 13 Bd.2, 125412 ,Moscow, Russia

The Li7 is very close to hydrogen and antihydrogen atoms. Therefore ionization energy of Li7 atom is very important parameter for atomic physics. We applied resonance two photon technique for excitation Rydberg states of Li7 atoms in magneto-optical trap. The direct observation of resonance fluorescence increases sensitivity and allows to record allowed and forbidden transition in the same set of measurements. In our work we used allowed and forbidden Rydberg transition for evaluation of lithium7 ionization energy. The highly-excited states of atoms have been studied by tunable UV-laser. The results of measurements for different Rydberg states nS, nP, nD, nF with quantum numbers n from 38 to 161 will be presented. Obtained ionization energy is in a good agreement with previous experimental and theoretical data. The work is supported by the Russian Science Foundation, project no. 14–12–01279.

Rydberg atoms of Ytterbium

Henri Lehec[1] , Alexandre Zuliani[1], Wilfried Maineult[1], Pierre Pillet[1] et Patrick Cheinet[1]

[1] Laboratoire Aimé Cotton, CNRS UMR 9188, Université Paris Sud, ENS Cachan
Batiment 505 Campus d'Orsay 91405 Orsay Cedex

Physical properties of Rydberg atoms pave the way to experimental control of the quantum state of mesoscopic ensemble of particles. Interactions between Rydberg atoms are large for interparticle distances in the micrometer range. They can be used to induce Rydberg blockade and generate entanglement between two[1,2] or even larger ensemble [3] of atoms. Nevertheless, Rydberg atoms lack some of the ressources used with neutral atoms, especially techniques such as imaging and optical dipole traps .

In this poster, I'll describe the experimental scheme under development and present the status of the experiment. Ytterbium atoms have two valence electrons which should allow applying optical manipulation on the Rydberg states. The idea is first to promote one electron to a long lived Rydberg state. The system can then be approximated as a free electron orbiting around an ionic core. The latter has still a valence electron that can be used for optical manipulation (i.e. imaging or trapping)

We are currently able to have Ytterbium atoms held inside a magneto-optical trap on the intercombinaison transition between $^1S_0$ and $^3P_1$ around 556nm. We performed the spectrocopy of the *ns* and *nd* Rydberg states from n=35 to n=80, increasing by two orders of magnitude the precision of their energy levels. By means of a Multi-Channel Quantum Defect Theory (MQDT) analysis we are able to fit the levels and deduce a new value of the ionization energy. The next step will be to complete the spectroscopy and compute the Stark map of the Rydberg states.

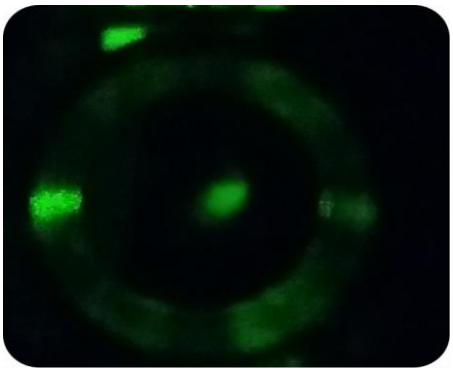

Fig 1 : Photograph of the Yb M.O.T.

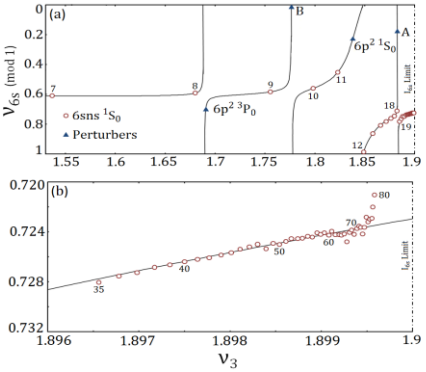

Fig 2 : Lu-Fano plot of the *6sns* $^1S_0$ serie

[1] Urban, E., Johnson, T. A., Henage, T., Isenhower, L., Yavuz, D. D., Walker, T. G., & Saffman, M. (2009). Observation of Rydberg blockade between two atoms. *Nature Physics*, *5*(2), 110-114.

[2] Gaëtan, A., Miroshnychenko, Y., Wilk, T., Chotia, A., Viteau, M., Comparat, D., ... & Grangier, P. (2009). Observation of collective excitation of two individual atoms in the Rydberg blockade regime. *Nature Physics*, *5*(2), 115-118.

[3] Peter Schauß, Johannes Zeiher, Takeshi Fukuhara, Sebastian Hild, Marc Cheneau, Tommaso Macrì, Thomas Pohl, Immanuel Bloch, and Christian Gross. *Dynamical crystallization in alow-dimensional Rydberg gas.* Science 347, 1455 (2015)

Helium atoms in 'circular' Rydberg states for hybrid cavity QED experiments

Valentina Zhelyazkova and Stephen D. Hogan

University College London, Department of Physics and Astronomy, Gower Street, WC1E 6BT, London, United Kingdom

Until recently, efforts directed towards the development of architectures for quantum information processing have typically focused on individual quantum systems, e.g., atoms, ions, superconducting qubits, etc. However, it is challenging to achieve in one single system all the criteria required for a scalable quantum computer, and new attempts have increasingly been directed towards hybrid approaches to quantum computation [1], in which two complimentary systems are combined to exploit the most favourable aspects of each. Inspired by cavity QED experiments [2], in which atoms in the gas phase are coupled to three-dimensional microwave resonators, promising prospect is to couple atomic systems to chip-based superconducting circuits [3].

Circular Rydberg states (states in which the excited electron is in an orbital with maximum angular momentum, i.e., $|m_l| = l = n-1$) have properties which make them particularly well-suited for the above applications [4]. These include (i) long lifetimes (46 ms for the circular state with $|n,l,m_l\rangle = |55,54,54\rangle$ in helium), (ii) large transition dipole moments and quasi-two-level character of $\Delta n = 1$ circular-state-to-circular-state transitions (e.g., $|\langle 55,54,54|\mu|56,55,55\rangle| = 2148\ ea_0$), and (iii) their low sensitivity to stray electric fields, including those emanating from surfaces. Together we expect these properties to offer long coherence times and narrow transition line-widths in hybrid cavity QED experiments.

Here, we describe experiments in which helium atoms from a supersonic beam are excited to a low-angular momentum Rydberg state with $n = 55$ and subsequently transferred to the $n = 55$ circular state using the crossed electric and magnetic fields method, as proposed by Delande and Gay [5]. The atoms are probed by ramped electric-field ionization and high-resolution microwave spectroscopy. The successful preparation of these circular states paves the way for future experiments in which we aim to coherently couple them to microwave fields in chip-based superconducting microwave circuits.

References

[1] M. Wallquist, K. Hammerer, P. Rabl, M. Lukin and P. Zoller, *Hybrid quantum devices and quantum engineering*, Phys. Scr. **T137**, 014001 (2009).

[2] S. Gleyzes, S.Kuhr, C. Guerlin, J. Bernu, S. Deléglise, U. Busk Hoff, M. Brune, M. Raimond and S. Haroche, *Quantum jumps of light recording the birth and death of a photon in a cavity*, Nature **446**, 297 (2007).

[3] A. Blais, R.-S. Huang, A. Wallraff, S. M. Girvin, and R. J. Schoelkopf, *Cavity quantum electrodynamics for superconducting electrical circuits: An architecture for quantum computation*, Phys. Rev. A **69**, 062320 (2004).

[4] M. Saffman, T. G. Walker, and K. Mølmer, *Quantum information with Rydberg atoms*, Rev. Mod. Phys. **82**, 2313 (2010).

[5] D. Delande and J. C. Gay, *A new method for producing circular Rydberg states*, Europhys. Lett. **5**(4), 303-308 (1988).

Electrostatic trapping Rydberg atoms above microwave transmission lines

Patrick Lancuba and Stephen D. Hogan
Department of Physics and Astronomy, University College London, Gower Street, WC1E 6BT, UK.

The very large electric dipole moments associated with high Rydberg states of atoms and molecules ($>$ 10000 D for states with principal quantum numbers, n, greater than 51) make gas-phase samples in these states very well suited to deceleration and trapping using inhomogeneous electric fields [1-5]. With the aim of developing a Rydberg laboratory on a chip in which cold Rydberg atoms and molecules can be transported, manipulated and non-destructively detected while being exploited in collision and spectroscopic studies [6,7], and in hybrid approaches to quantum information processing [8], we have implemented a chip-based Rydberg-Stark decelerator [9,10] that allows us to electrostatically trap cold Rydberg atoms directly above two-dimensional microwave transmission lines. In these experiments helium atoms in Rydberg-Stark states with $n = 48$ were decelerated from 2000 m/s to zero mean velocity in the laboratory-fixed frame-of-reference in the travelling electric traps of a transmission-line decelerator. When brought to rest above the transmission line of the decelerator the trapped atoms were detected *in situ* by pulsed electric field ionisation with the resulting He^+ ions collected on a microchannel plate detector. The experimental results have been compared with the results of numerical calculations of particle trajectories during the deceleration and trapping process, and offer insights into sources of trap loss.

References

[1] E. Vliegen, H. J. Wörner, T. P. Softley and F. Merkt, *Nonhydrogenic Effects in the Deceleration of Rydberg Atoms in Inhomogeneous Electric Fields*, Phys. Rev. Lett. **92**, 033005 (2004).
[2] S. D. Hogan, Ch. Seiler, and F. Merkt, *Rydberg-State-Enabled Deceleration and Trapping of Cold Molecules*, Phys. Rev. Lett. **103**, 123001 (2009).
[3] S. D. Hogan, P. Allmendinger, H. Saßmannshausen, H. Schmutz and F. Merkt, *Surface-Electrode Rydberg-Stark Decelerator*, Phys. Rev. Lett., **108**, 063008 (2012).
[4] P. Allmendinger, J. Deiglmayr, J. A. Agner, H. Schmutz, and F. Merkt, *Surface-electrode decelerator and deflector for Rydberg atoms and molecules*, Phys. Rev. Lett., **90**, 043403 (2014).
[5] S. D. Hogan, *Rydberg-Stark deceleration of atoms and molecules*, EPJ Techniques and Instrumentation, **3**, 1 (2016).
[6] J. A. Gibbard, M. Dethlefsen, M. Kohlhoff, C. J. Rennick, E. So, M. Ford, and T. P. Softley, *Resonant Charge Transfer of Hydrogen Rydberg Atoms Incident on a Cu(100) Projected Band-Gap Surface*, Phys. Rev. Lett., **115**, 093201 (2015).
[7] T. E. Wall, A. M. Alonso, B. S. Cooper, A. Deller, S. D. Hogan, and D. B. Cassidy, *Selective Production of Rydberg-Stark States of Positronium*, Phys. Rev. Lett., **114**, 173001 (2015).
[8] S. D. Hogan, J. A. Agner, F. Merkt, T. Thiele, S. Filipp and A. Wallraff, *Driving Rydberg-Rydberg Transitions from a Coplanar Microwave Waveguide*, Phys. Rev. Lett., **108**, 063004 (2012).
[9] P. Lancuba and S. D. Hogan, *Guiding Rydberg atoms above surface-based transmission lines*, Phys. Rev. A, **88**, 043427 (2013).
[10] P. Lancuba and S. D. Hogan, *Transmission-line decelerators for atoms in high Rydberg states*, Phys. Rev. A, **90**, 053420 (2015).

Isotope shift of the electron affinity of carbon

Christophe Blondel, David Bresteau and **Cyril Drag**
Laboratoire Aimé-Cotton, Centre national de la recherche scientifique, université Paris-sud, F-91405 Orsay cedex, France

The electron affinity of carbon has been measured on a C^- beam by **photodetachment microscopy**, with a precision increased by one order of magnitude with respect to the last measurement, made in 1998 [1]. Isotopes 12 and 13 are used in succession, which makes it possible to determine the **isotope shift** of the electron affinity of carbon. The obtained result, about -7.3(6) m^{-1}, corroborates recent calculations of this shift [2]. The electron affinities of ^{12}C and ^{13}C are 1 017 970.5(10) and 1 017 963.3(10) m^{-1}, i.e., 1.262 122 6(11) and 1.262 113 6(12) eV, respectively [3].

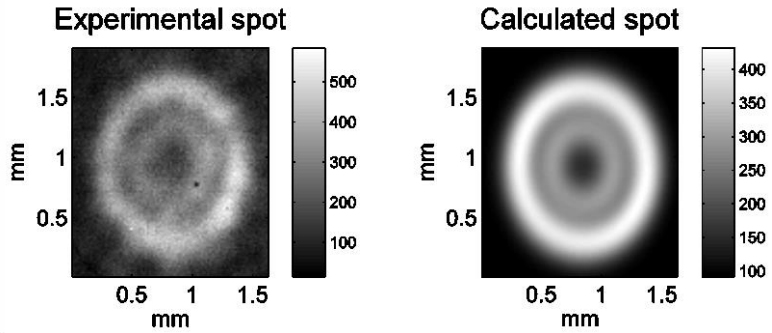

Fig. 1 An electron interferogram obtained experimentally by photodetachment of $^{13}C^-$ in an electric field F=356(5) Vm^{-1} at a distance 0.563 m of the electron imaging detector. The laser wave number is set at 1 022 366.45 m^{-1}, i.e. about 60 m^{-1} above the $^3P_2$ threshold. The best fitting synthetic image (right) provides a measurement of the kinetic energy ε of the photodetached electron, numerically 55.97(30) m^{-1} if we assume the electric field to be exactly 355.9 Vm^{-1}. The method, however, essentially relies on fitting the phase of the interferogram, which is proportional to $\varepsilon^{3/2}/F$. The uncertainty of the electric field value can thus make the uncertainty of the photoelectron energy significantly larger. The error made with the electric field measurement can be revealed by plotting the apparent threshold value as a function of the mean electron kinetic energy (figure 2).

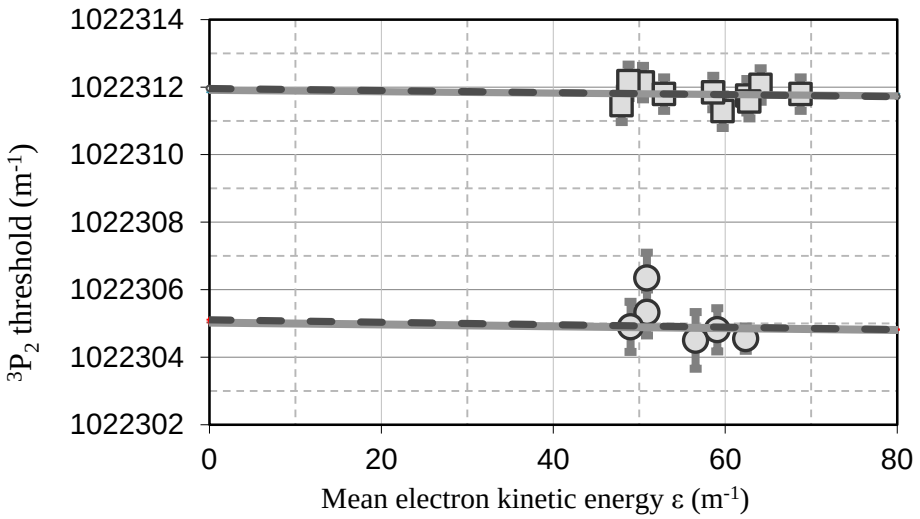

Fig. 2 Apparent $^3P_2$ (excited) detachment thresholds of $^{12}C^-$ (squares) and $^{13}C^-$ (circles) as functions of the mean photoelectron kinetic energy. A linear regression down to zero electron kinetic energy is made to take a possible relative error on the electric field into account. The intercepts are 1 022 311.96(95) and 1 022 305.11(105) m^{-1} for isotope 12 and isotope 13, respectively. Fine structure subtraction provides the electron affinity ($^3P_0$ threshold).

References

[1] M. Scheer, R.C. Bilodeau, C.A. Brodie and H.K. Haugen, *Systematic study of the stable states of C^-, Si^-, Ge^-, and Sn^- via infrared laser spectroscopy*, Phys. Rev. A **58**, 2844 (1998).

[2] T. Carette and M.R. Godefroid, *Theoretical study of the C^- $^4S^o_{3/2}$ and $^2D^o_{3/2,5/2}$ bound states and C ground configuration: Fine and hyperfine structures, isotope shifts, and transition probabilities*, Phys. Rev. A **83**, 062505 (2011).

[3] D. Bresteau, C. Drag and C. Blondel, *Isotope shift of the electron affinity of carbon measured by photodetachment microscopy*, Phys. Rev. A **93**, 013414 (2016).

Laser Induced Fluorescence spectroscopy applied to metallic atoms for investigations of solid propellant flames

Gautier Vilmart, Nelly Dorval, Mikaël Orain, Brigitte Attal-Tretout, Alexandre Bresson

ONERA, the French Aerospace lab, F-91761 Palaiseau France

We are interested in studying the combustion of solid composite aluminized propellants by means of LIF (Laser Induced Fluorescence) diagnostics. Composite propellants are composed of an oxidizer (ammonium perchlorate), a fuel (aluminium particles) and an inert polymeric binder. Metallic atoms such as iron atoms may be present when burning rate catalysts are used in the propellant formulations. Our idea is to use gaseous Fe and Al atoms as fluorescent markers in order to record their spatial distributions atoms above the burning surface of the propellant. The strong line strengths of the electronic transitions of the atoms should be an advantage to improve the sensitivity of the LIF technique for probing this harsh combustion environment (high-pressure, high-luminosity, heavily particle laden medium). Spectral investigations are performed in the UV range in order to avoid the strong interference with the blackbody radiation. Furthermore the fluorescence signal is detected far away from the excitation wavelength in order to get rid of the spurious laser scattering (e.g. Mie scattering).

Figure 1 shows a dispersed fluorescence spectrum using KrF laser excitation at 248 nm of Fe (a^5D-x^5F transition) which is composed of the prominent resonance fluorescence and direct fluorescence lines at 248 nm, 300 nm and 304 nm. Weaker spectral features are also observed at 250/255 nm, 272/274 nm, 278/285 nm and 305/310 nm. In order to assign properly these latter features to stepwise fluorescence lines due to collisional energy transfer between the excited state and the lower energy states, we have developed a simple theoretical model that takes into account the different fluorescence pathways. The model is based on the kinetic equations of the LIF process which takes into account the electronic collisional transfer rates. The collisional transfer coefficients Q_{if} ($cm^3.s^{-1}$) are approximately calculated by the kinetic theory of gases: $Q_{i\to f} = q \cdot N_{pert} \cdot v \cdot \sigma \cdot e^{-\frac{\Delta E_a}{k_B \cdot T}}$, where q is a steric factor, v ($cm.s^{-1}$) is the thermal velocity, N_{pert} (cm^{-3}) the collisional partner concentration, σ (cm^{-2}) the cross section of the collisional reaction, ΔE_a (cm^{-1}) the activation energy of the collisional reaction, k_B ($cm^{-1}.K^{-1}$) the Boltzmann constant and T (K) the temperature. The simulation which involved 490 levels is compared to the experiment in Fig 1.a. The model successfully predicts which electronic levels are populated by collisions namely, y^5G, x^5D, y^5P (Fig 1.b). Good agreement is found between the calculated coefficients Q_{if} and the measured ones given in [1].The experimental spectrum is fitted quite well, although some discrepancies remain which are certainly due to the simple model used to calculate the Q_{if} coefficients. We will present the structure of the code and fine comparisons with experimental data.

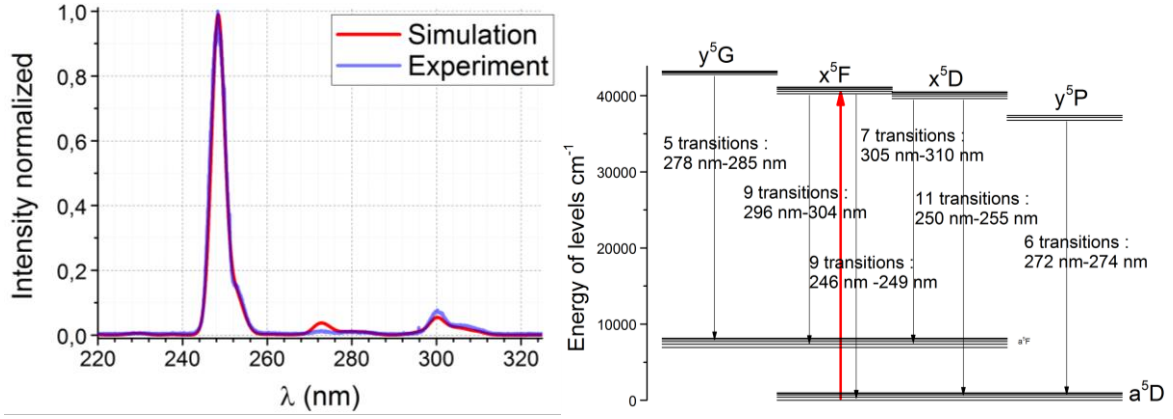

Fig. 1 a. Comparison of calculated and experimental dispersed fluorescence spectrum of Fe at 300 mbar and 2000 K in He for laser excitation at 248 nm. b. Diagram of the transitions involved in the fluorescence spectrum of Fe.

For the Al atom, two excitation/detection schemes are being investigated 308-309 nm/396 nm and 257 nm/309 nm. An evaporation chamber has been specifically developed and instrumented for in situ optical diagnostics. Metal evaporation parameters are readily controllable which enable spectroscopic analysis. Laser excitation is provided by nanoseconde-pulsed tunable dye laser. Both excitation and dispersed fluorescence spectra are recorded. The radiative lifetimes of different involved levels and the rate of collisional transfers are determined. The saturation threshold and the line spectral shapes depending on the laser intensity are also measured.

References

[1] Boris Nizamov, Paul J. Dagdigian. *Collisional Quenching and Energy Transfer of the z^5 D_J o States of the Fe Atom*. J Phys Chem A **104,** 6345–6350 (2000).

Lamb Shifts and Many-Body Effects in Neutral Atoms

Jacinda Ginges, Julian Berengut
School of Physics, University of New South Wales, Sydney NSW 2052, Australia

We use the radiative potential method [1] to study many-body effects on the Lamb shifts in neutral alkali atoms [2,3]. The effects of core relaxation and valence-core correlations are considered. Calculations are performed for the lowest valence s, p, and d waves for the series of alkali atoms Na to E119. We demonstrate the reliability of the method by performing calculations of Lamb shifts in frozen atomic potentials and comparing with the results of rigorous quantum electrodynamics calculations [4]; the results for s-wave binding energies agree at the level of 1%. Overall, the many-body effects act to increase the size of the shifts. For s waves, consideration of many-body effects is important for obtaining high accuracy. For p and d waves, account of these effects is crucial for obtaining the correct size and sign of the shifts. The many-body enhancement for the d-wave shifts is so sizeable that these shifts are only an order of magnitude smaller than the s-wave shifts for the atoms K to E119. High-precision spectroscopic studies for neutral alkali atoms could provide sensitive tests of combined many-body and quantum electrodynamics effects.

References

[1] V. V. Flambaum and J. S. M. Ginges, *Radiative Potential and Calculations of QED Radiative Corrections to Energy Levels and Electromagnetic Amplitudes in Many-Electron Atoms*, Phys. Rev. A **72**, 052115 (2005).
[2] J. S. M. Ginges and J. C. Berengut, *QED Radiative Corrections and Many-Body Effects in Atoms: Vacuum Polarization and Binding Energy Shifts in Alkali Metals*, accepted to J. Phys. B; arxiv:1511.01459v1 (2015).
[3] J. S. M. Ginges and J. C. Berengut, *Atomic Many-Body Effects and Lamb Shifts in Alkali Metals*, submitted to Phys. Rev. A; arxiv:1603.09116v1 (2016).
[4] J. Sapirstein and K. T. Cheng, *Calculation of the Lamb Shift in Neutral Alkali Metals*, Phys. Rev. A **66**, 042501 (2002).

Ground State Calculations for Coulomb Three-body Systems with Different Masses using Adjustable Sturmian Functions

Juan Martín Randazzo[1] **and Lorenzo Ugo Ancarani**[2]
1. División Físca Atómica, Molecular y Óptica, Centro Atómico Bariloche, 8400 S. C. de Bariloche, Río Negro, Argentina
2. Equipe TMS, SRSMC, UMR CNRS 7565, Université de Lorraine, 57078 Metz, France

In this work we test a configuration interaction method implemented with Sturmian Functions (SF) to obtain ground state energies of several Coulomb three-body systems with different masses and charges. The one-particle basis functions come from a fictitious two-body problem where the energy is fixed and the eigenvalue is the magnitude of one of the potentials included in a Sturmian equation.

By optimizing the Sturmian basis [1], it has been shown that it is possible to improve the expansion convergence, reaching the best known energy value of the helium ground state with a fixed number of radial and angular basis functions. Contrary to the well-known Coulomb Sturmian Functions, Generalized Sturmian Functions map to a Sturm-Liouville eigenvalue problem to which one can impose exact two-body Kato cusp conditions in the radial coordinate, and the asymptotic fall-off behavior associated to the case where one of the particles is far away from the other two. Although the method was shown to be very efficient, a full optimization of the basis becomes cumbersome because one has to vary on the functional space of generating potentials [1]. In other publications [2,3] we opted for a simplified approach by using one general potential with variational parameters.

It is the aim of this work to present a more friendly recipe to define the Sturmian basis, which are ultimately used to find energies of different systems in a more practical way. This recipe is based on a simple and general way to define the parameters and potentials of the Sturmian equation. Still with a focus on simplicity and practicality, to generate the basis we remove from the radial equation the centrifugal barrier included in previous works [1-3]. In other words, for a given coordinate, instead of using a complete set of SF for each partial wave, we use always the one corresponding to $l = 0$ for every partial wave term. While this slightly reduces the basis efficiency (i.e., finally, the energy accuracy for a fixed number of basis functions), it provides a substantial gain in memory and computational time resources; in practice, this gain is used to recover, and surpass, the lost accuracy.

We build three-body ground state wave functions for general masses and charges with a configuration interaction scheme with products of two of such one-particle SF (i.e., we use two of the three inter-particle coordinates). Since all three particles are treated quantum mechanically on equal footing, we have the choice amongst three different pairs. When two particles are much lighter than the third one, the natural choice consists in taking as radial coordinates the two distances from the heavy center. When considering systems with two equal masses, such as H_2^+ and Ps^- ($e^- - e^- - e^+$), we have a choice, and we explore the convergence rates when choosing the two possible options.

We calculated ground state energies for a large number of known and exotic systems, and compared them with those obtained with correlated basis functions or with the hyperspherical harmonics expansion (see [4,5] and earlier references therein). Very good precision can be achieved with a relatively moderate number of basis functions.

References

[1] Juan M. Randazzo, Lorenzo. U. Ancarani, Gustavo Gasaneo, Ana L. Frapiccini, and Flavio D. Colavecchia, *Generating optimal Sturmian basis functions for atomic problems*, Phys. Rev. A **81**, 042520 (2010).
[2] Juan M. Randazzo, Ana L. Frapiccini, Flavio D. Colavecchia and Gustavo Gasaneo, *Discrete sets of Sturmian functions applied to two-electron atoms*, Phys. Rev. A **79**, 022507 (2009).
[3] Gustavo Gasaneo *et al.*, *Three-Body Coulomb Problems with Generalized Sturmian Functions*, Adv. Quantum Chem. **57**, 153 (2013).
[4] Lorenzo U. Ancarani, Karina V. Rodriguez and Gustavo Gasaneo, *Correlated $n^{1,3}S$ States for Coulomb Three-Body Systems*, Int. J. Quant. Chem. **111**, 4255 (2011).
[5] Md. A. Khan, *Hyperspherical three-body calculation for muonic atoms*, Eur. Phys. J. D **66**, 83 (2012).

Theoretical Hyperfine Structures of excited levels in ^{17}O I and ^{19}F I

Messaoud Nemouchi[1], Nouria Aourir[1], Michel Godefroid[2], Per Jönsson[3]
1. Laboratoire d'Électronique Quantique, Faculté de Physique, USTHB, BP32, El-Alia, Algiers, Algeria
2. Chimie Quantique et Photophysique, Université libre de Bruxelles, B-1050 Brussels, Belgium
3. Center for Technology Studies, Malmö University, 205-06 Malmö, Sweden

Multiconfiguration Hartree-Fock (MCHF) [1] and multiconfiguration Dirac-Hartree-Fock (MCDHF) [2] calculations are performed on $2p^5\ ^2P^o$, $2p^4(^3P)3s\ ^4P$ and $2p^4(^3P)3s\ ^2P$ of fluorine to determine their hyperfine constants. Several computing strategies are considered to include correlation and relativistic effects. In the MCHF non relativistic approach, first-order correlation effects are investigated through multiconfiguration expansions built by allowing single (S) and double (D) excitations from the reference configuration state function (CSF) to orbitals of increasing active sets [3]. Higher-order correlation effects are included through SD-multireference MCHF calculations based on a careful selection of the largest components of the single reference MCHF wave functions to define the multireference sets. Relativistic effects are evaluated using the Breit-Pauli approximation. A similar strategy is used for the calculation of MCDHF relativistic wave functions and hyperfine parameters.
We observe that correlation and relativistic effects are rather small for the ground state. We highlight however some significant effect of relativity on the $A_{1/2}$ hyperfine constants of $2p^4(^3P)3s\ ^4P$. For all other states, correlation effects are, as expected, the most important contribution to the hyperfine interaction.
We also revisit the hyperfine constants of $2p^3(^4S)3s\ ^5S^o$ and $2p^3(^4S)3p\ ^5P^o$ in ^{17}O I [4] using similar strategies. The results are found to be in excellent agreement with experiment [5].

References

[1] C. Froese Fischer, G. Tashiev, G. Gaigalas and M. Godefroid, *An MCHF atomic-structure package for large-scale calculations*, Comp. Phys. Comm. **176**, 559 (2007).
[2] P. Jönsson, G. Gaigalas, J. Bieroń, C. Froese Fischer and I.P. Grant, *New version: Grasp2K relativistic atomic structure package*, Comp. Phys. Comm. **184**, 2197 (2013).
[3] C. Froese Fischer, T. Brage and P. Jönsson, *Computational Atomic Structure - An MCHF Approach*, Institute of Physics Publishing, (1997).
[4] M. Godefroid, G. Van Meulebeke, P. Jönsson and C. Froese Fischer, *Large-scale MCHF calculations of hyperfine structures in nitrogen and oxygen* Z. Phys. D. Atoms, Molecules and Clusters, **42**, 193 (1997).
[5] R. Jennerich and D. Tate, *Hyperfine-structure intervals and isotope shifts in the* $2p^3 3s\ ^5S_2 \rightarrow 3p^3 3p\ ^5P_{J'}$ *in the transitions of atomic oxygen* Phys. Rev. A, **62**, 042506 (2000).

Magnetic shielding constant for relativistic hydrogenlike atom in an arbitrary discrete energy eigenstate

Patrycja Stefańska

Atomic Physics Division, Department of Atomic, Molecular and Optical Physics, Faculty of Applied Physics and Mathematics, Gdańsk University of Technology, Narutowicza 11/12, 80-233 Gdańsk, Poland

Analytical calculations of electric and magnetic properties of the relativistic one-electron atoms, performed within the perturbation theory combined with the Green function technique, require the knowledge of the Dirac–Coulomb Green function (DCGF). One of the most useful form of that function is its expansion in the Sturmian basis proposed by Szmytkowski in [1]. It has been used in calculations of many electromagnetic parameters of Dirac one-electron atom in the ground state (cf. e.g. [2, 3]). Recently, we have shown that utility of this method goes beyond the study of the atomic ground state. Using it, we derived analytically the expressions for the magnetizability [4, 5] and the magnetic-dipole-to-electric-quadrupole cross susceptibility [6] of the atom being in an arbitrary discrete energy eigenstate. Both results are of the form of double finite sum of the hypergeometric function ${}_3F_2$ with the unit argument and agree with every single result obtained by other authors for some particular states of the atom.

In this work, we present an application of the DCGF Sturmian expansion technique to obtain closed-form expression for the magnetic dipole shielding constant (σ) of the relativistic hydrogenlike atom in an arbitrary discrete energy eigenstate [7]. In contrast to the final results from [4-6], the formula for σ was found to be possible to transform it into an elementary form with the use of the theory of hypergeometric functions. The final expression for the magnetic shielding constant of Dirac one-electron atom being in the state characterized by the set of quantum numbers $\{n_r, \kappa, \mu\}$, in which n_r denotes the radial quantum number, κ is an integer different from zero (related to the principal quantum number n through $n = n_r + |\kappa|$), μ is the magnetic quantum number, reads

$$\sigma = \frac{\alpha^2 Z}{(4\kappa^2-1)N_{n_r\kappa}^2}\left\{\kappa^2 - \frac{\eta_{n_r\kappa}^{(+)}}{4} - \frac{\eta_{n_r\kappa}^{(-)}}{4} + \frac{\mu^2}{4\kappa^2-1}\left[\frac{2\kappa+1}{2\kappa-1}\eta_{n_r\kappa}^{(+)} + \frac{2\kappa-1}{2\kappa+1}\eta_{n_r\kappa}^{(-)} + \frac{4\kappa^2(4\kappa^2-5)}{4\kappa^2-1} + \frac{32\kappa^3\,[2\kappa(n_r+\gamma_\kappa)-N_{n_r\kappa}]\,(\alpha Z)^2}{\gamma_\kappa(4\gamma_\kappa^2-1)N_{n_r\kappa}^2}\right]\right\},$$

where $\eta_{n_r\kappa}^{(\pm)} = N_{n_r\kappa}(2\kappa \pm 1)/(n_r + \gamma_\kappa \pm N_{n_r\kappa})$, with $N_{n_r\kappa} = \pm\sqrt{n_r^2 + 2n_r\gamma_\kappa + \kappa^2}$ and $\gamma_\kappa = \sqrt{\kappa^2 - (\alpha Z)^2}$. For states with zero radial quantum number, the above formula reduces to the one obtained by Moore [8]. In turn, by substituting $\kappa = -1$ into the above equation, we reconstruct the result provided by Ivanov *et al.* in [9]. For very special case, i.e. the atomic ground state, our general expression for σ is in agreement with the formulas derived earlier by Zapryagaev *et al.* [10], Cheng *et al.* [11], and also by us [12]. Moreover, for states with $n = 2$ we get the same results as Pyper and Zhang [13].

References

[1] Radosław Szmytkowski, *The Dirac–Coulomb Sturmians and the series expansion of the Dirac–Coulomb Green function: application to the relativistic polarizability of the hydrogen-like atom*, J. Phys. B **30**, 825 (1997); Erratum: J. Phys. B **30**, 2747 (1997).

[2] Radosław Szmytkowski, Patrycja Stefańska, *Magnetic field-induced electric quadrupole moment in the ground state of the relativistic hydrogenlike atom: Application of the Sturmian expansion of the generalized Dirac–Coulomb Green function*, Phys. Rev. A **85**, 042502 (2012).

[3] Radosław Szmytkowski, Patrycja Stefańska, *Electric field-induced magnetic quadrupole moment in the ground state of the relativistic hydrogenlike atom: Application of the Sturmian expansion of the generalized Dirac–Coulomb Green function*, Phys. Rev. A **89**, 012501 (2014).

[4] Patrycja Stefańska, *Magnetizability of the relativistic hydrogenlike atom in an arbitrary discrete energy eigenstate: Application of the Sturmian expansion of the generalized Dirac–Coulomb Green function*, Phys. Rev. A **92**, 032504 (2015).

[5] Patrycja Stefańska, *Magnetizabilities of relativistic hydrogenlike atoms in some arbitrary discrete energy eigenstates*, At. Data Nucl. Data Tables **108**, 193 (2016).

[6] Patrycja Stefańska, *Magnetic-field-induced electric quadrupole moments for relativistic hydrogenlike atoms: Application of the Sturmian expansion of the generalized Dirac–Coulomb Green function*, Phys. Rev. A **93**, 022504 (2016).

[7] Patrycja Stefańska, *Closed-form expression for the dipole magnetic shielding constant of the relativistic hydrogenlike atom in an arbitrary discrete energy eigenstate: Application of the Sturmian expansion of the generalized Dirac–Coulomb Green function*, in preparation.

[8] Elaine A. Moore, *Relativistic chemical shielding: formally exact solutions for one-electron atoms of maximum total angular momentum for any principal quantum number*, Mol. Phys. **97**, 375 (1999).

[9] Vladimir G. Ivanov, Savely G. Karshenboim, Roman N. Lee, *Electron shielding of the nuclear magnetic moment in a hydrogenlike atom*, Phys. Rev. A **79**, 012512 (2009).

[10] Sergey A. Zapryagaev, Nikolai L. Manakov, Lev P. Rapoport, *Multipole screening of nuclei of hydrogen-like atoms*, Yad. Fiz. **19**, 1136 (1974) (in Russian).

[11] Lan Cheng, Yunlong Xiao, Wenjian Liu, *Four-component relativistic theory for NMR parameters: Unified formulation and numerical assessment of different approaches*, J. Chem. Phys. **130**, 144102 (2009).

[12] Patrycja Stefańska, Radosław Szmytkowski, *Electric and magnetic dipole shielding constants for the ground state of the relativistic hydrogen-like atom: Application of the Sturmian expansion of the generalized Dirac–Coulomb Green function*, Int. J. Quantum Chem. **112**, 1363 (2012).

[13] Nick C. Pyper, Zongchao C. Zhang, *Relativistic theory of nuclear shielding in one-electron atoms II: Analytical and numerical results*, Mol. Phys. **97**, 391 (1999).

Calculation of Ar Photoelectron Satellites to Double Core Hole States in Hard X-ray Region

***Miron Ya. Amusia*[1,2], *Victor G. Yarzhemsky*[3, 4]**

1. Racah Institute of Physics, the Hebrew University, 91904 Jerusalem, Israel
2. A. F. Ioffe Physical-Technical Institute, 194021 St Petersburg, Russia
3. N. S. Kurnakov Institute of General and Inorganic Chemistry, 119991 Moscow, Russia
4. .Moscow Institute of Physics and Technology, Dolgoprudny, 141700 Moscow Region, Russia

Recent experiments in hard X-ray photoelectron spectroscopy (HARPES) resulted in an essentially new type of photoelectron satellites, corresponding to final double core hole (DCH) states and one excited electron [1]. In the case of Ar ionization, the excited states have configurations $1s^{-1}2p^{-1}(^{2S+1}P)np(^2S)$ and $1s^{-1}2p^{-1}(^{2S+1}P)4s(^2P)$. The first series corresponds to As1s ionization with excitation $2p \rightarrow np$ and the second series corresponds to Ar2p ionization with excitation $1s \rightarrow 4s$. Due to a very large excitation energy, intensities of these satellite peaks are two orders of magnitude smaller than that, corresponding to the excitation from valence shells [2].

We demonstrate in this presentation that the results of [1] can be understood in the frame of a rather simple theoretical approaches – shake-up for the high intensity lines with a big contribution of knock-up for lines with low intensities.

Calculations were performed in the frame of the shake-up model, using many-body perturbation theory in a basis of Hartree-Fock one-electron functions [3]. Since in the excitation $1s \rightarrow 4s$ the energy transfer to the satellite is very large, the correction of photoionization cross-section due to satellite energy of the main line according to the results of [3] was performed. The data obtained are presented in the Table.

TABLE Theoretical and experimental shake-up intensities (in 10^{-4}) of Ar 1*s* photoelectron line

Final state	Spectroscopic factor	Including the correction due to satellite energy	Experiment [1, 2]
$1s^{-1}3p^{-1}4p(^2S)$	680[a)]	680	~600
$1s^{-1}2p^{-1}(^1P_1)4p(^2S)$	2.6	3.0	~2.75
$1s^{-1}2p^{-1}(^1P_1)5p(^2S)$	1.0	1.18	~0.75
$1s^{-1}2p^{-1}(^1P_1)6p(^2S)$	0.48	0.57	~0.37
$1s^{-1}2p^{-1}(^3P_{0,1,2})4p(^2S)$	4.5	5.3	~2.08
$1s^{-1}2p^{-1}(^3P_{0,1,2})5p(^2S)$	1.7	2.0	~0.79
$1s^{-1}2p^{-1}(^1P_1)4s(^2P)$	$0.30\ 10^{-5}$ [b)]	$0.60\ 10^{-3}$ [c)]	~0.33
$1s^{-1}2p^{-1}(^3P_{0,1,2})4s(^2P)$	$0.96\ 10^{-3}$ [b)]	0.19 [c)]	~0.23

a) The sum of $1s^{-1}3p^{-1}(^1P)4p$ and $1s^{-1}3p^{-1}(^3P)4p$ states, whose theoretical intensities equal to 0.025 and 0.043 of Ar 1*s* line intensity, respectively

b) Spectroscopic factors were multiplied by the ratio of photoionization cross-sections σ_{2p}/σ_{1s} =0.0383 (photon energy 3900 eV for both shells).

c) Spectroscopic factors were multiplied by the ratio of photoionization cross-sections σ_{2p}/σ_{1s} =7.63 (photon energy 700 eV for 2*p* –shell and photon energy 3900 eV for 1*s*-shell).

It is seen from the Table, that theoretical results for the most intense series $1s^{-1}2p^{-1}(^{2S+1}P)np(^2S)$ are in good agreement with the experiment [1].

It is also seen that for the $1s^{-1}2p^{-1}(^1P_1)4s(^2P)$ line the shake-up model used is not sufficient to explain experimental intensity. However, close to this configuration another one, $1s^{-1}2p^{-1}(^1P)3d(^2P)$, is located. It was obtained, that for this case the direct knock-up of an electron by outgoing electron should be taken into account. In this approach the latter state was interpreted as $1s^{-1}2p^{-1}(^1P_1)3d(^2P)$ satellite of 2p ionization leading to results that are in reasonable agreement with experiment.

References

[1] R. Püttner, G. Goldsztejn, D. Céolin, J.-P. Rueff, T. Moreno, R. K. Kushawaha, T. Marchenko, R. Guillemin, L. Journel, D. W. Lindle, M. N. Piancastelli, and M. Simon. Phys. Rev. Lett. **114**, 093001 (2015).
[2] S. H. Southworth, T. LeBrun, Y. Azuma, and K. G. Dyal, J. Electron Spectrosc. Relat. Phenom., 94, 33 (1998).
[3] M. Ya. Amusia, L. V. Chernysheva, and V. G. Yarzhemsky, *Handbook of Theoretical Atomic Physics*, Data for Photon Absorption, Electron Scattering, and Vacancies Decay, Springer-Verlag, Berlin, Heidelberg, 2012.

Ambiguity in determination of interatomic potential of diatomic molecule

Tomasz Urbańczyk[1], Jarosław Koperski[1], Asen Pashov[2]

1. Smoluchowski Institute of Physics, Jagiellonian University, prof. Stanisława Łojasiewicza 11, 30-348 Kraków, Poland

2. Department of Physics, Sofia University, 5 James Bourchier Boulevard, 1164 Sofia, Bulgaria

A theoretical study of ambiguity of determination of interatomic potential of diatomic molecule in case of spectrum with unresolved, or partially resolved, rotational structure will be presented. As an example we have analyzed an excitation spectrum of the $B^31 \leftarrow X^10^+$ electronic transition in CdAr van der Waals complex [1]. It has been shown, that when the experimental spectrum is measured only with vibrational resolution, *i.e.*, without resolved rotational structure, one can find several significantly different representations of the upper-state interatomic potential that provide proper simulations of the experimental spectrum.

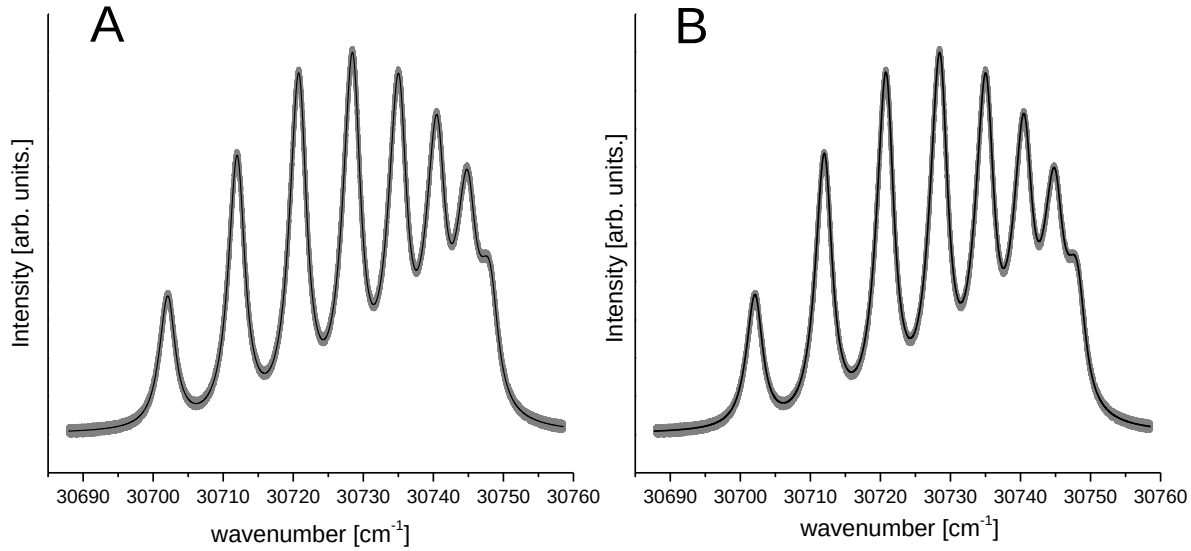

Fig. 1 (A) Reference spectrum (grey) and simulation (black) performed under an assumption that the B^31-state interatomic potential is represented with a Morse function with parameters R_e' = 5.05[Å], D_e' = 55.0[cm^{-1}] β' = 0.988[1/Å^{-1}] and transition dipole moments determined for the following points: 2[Å] = 2.0, 3[Å] = 2.0, 5[Å] = 1.0, 8[Å] = 1.0. (B) Reference spectrum (grey) and simulation (black) performed under the same assumption as in (A) but with the following parameters R_e' = 5.1[Å], D_e' = 54.97[cm^{-1}] β' = 0.988[1/Å^{-1}] and for transition dipole moments determined for the following points: 2[Å] = 2.0, 3[Å] = 2.2, 5[Å] = 3.0, 8[Å] = 1.0 For both simulations, parameters for the X^10^+ state were as in [1].

This work was supported by the National Science Centre Poland under grant number UMO-2015/17/B/ST4/04016.

References

[1] T. Urbańczyk, J. Koperski, *Rotational profiles of vibrational bands recorded at the $B^31(5^3P_1)\leftarrow X^10^+(5^1S_0)$ transition in CdAr complex*, Chem. Phys. Lett. **591**, 64 (2014).

Why are leaves green? Action spectroscopy of chlorophyll molecules and dimers *in vacuo*.

Mark H. Stockett[1*], Jørgen Houmøller[1], Christina Kjær[1], Bruce F. Milne[2,3], Lihi Musbat[4], Angel Rubio[2,5], Yoni Toker[4], and Steen Brøndsted Nielsen[1]

1. Department of Physics and Astronomy, Aarhus University, Denmark
2. Department of Materials Physics, University of the Basque Country, Donostia, Spain
3. Centre for Computational Physics, Department of Physics, University of Coimbra, Portugal
4. Institute of Nanotechnology and Advanced Materials, Bar-Ilan University, Ramat-Gan, Israel
5. Max Planck Institute for the Structure and Dynamics of Matter, Hamburg, Germany

Chlorophyll (Chl) *a* and *b* are the main light-absorbing pigments found in green plants. It is nontrivial to predict the absorption spectra of these molecules or what effect the protein environment may have. As a starting point, we have measured the absorption spectra of gas-phase Chl a and b using photodissociation action spectroscopy of Chl molecules tagged with quaternary ammonium ions [1,2]. These experimental data were used to calibrate time-dependent density functional theory (TDDFT) calculatons and determine the transition energies of the bare Chls in the absence of the charge tag. Chl *a* and *b* differ only on one peripheral substituent, but their absorption band maxima are shifted relative to each other by more than 30 nm. These shifts were reproduced in our gas-phase data, meaning that they are intrinsic effects and not due to interactions with the micro-environment. On the other hand, the bands of both Chl *a* and *b* were significantly blue-shifted relative to those in solution and in proteins. Interactions with the protein and solvent environments are thus crucial to understanding the absorption of chlorophylls.

One key mechanism by which the absorption spectrum of Chl is tuned in proteins is exciton coupling of two or more Chl pigments. This purely quantum mechanical effect gives rise to a splitting of the energy levels (and thus a color shift) of the collectively excited multi-Chl complex. It is difficult to disentangle this effect from shifts due to interactions the protein microenvironment such as axial ligation. With the absorption spectra of bare Chl now well established, we can begin to ask the question of which of these effects is more significant for color tuning. Furthermore, these interactions govern the mechanism for energy transfer to the reaction centers of photosynthetic proteins. For funnelling via localised states on the energy landscape, the protein environment is most important whereas so-called supertransfer requires fully delocalized states where all pigments are excitonically coupled [3]. We have measured the intrinsic strength of exciton coupling by applying our action spectroscopy technique to charge tagged dimers of Chl *a* [4]. Compared to our baseline measurements of Chl *a* monomers, the absorption band maximum is red-shifted by 50-70 meV, in good agreement with our TDDFT calculations.

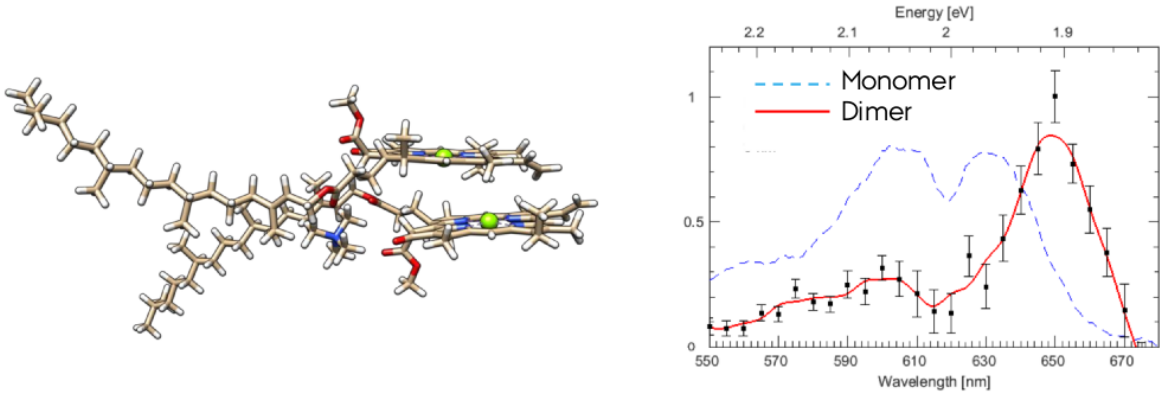

Fig. 1 Left: Optimized structure of Chl *a* dimer tagged with a quaternary ammonium cation. Right: Measured action spectra of charge tagged Chl *a* monomers (dashed line) and dimers (solid line and symbols).

References

[1] Bruce F. Milne, Yoni Toker, Angel Rubio, and Steen Brøndsted Nielsen, *Unraveling the Intrinsic Color of Chlorophyll* Angew. Chem. Int. Ed. **54**, 2170 (2015).

[2] Mark H. Stockett, Lihi Musbat, Christina Kjær, Jørgen Houmøller, Yoni Toker, Angel Rubio, Bruce F. Milne and Steen Brøndsted Nielsen, *The Soret absorption band of isolated chlorophyll a and b tagged with quaternary ammonium ions* Phys. Chem. Chem. Phys. **17**, 25793 (2015).

[3] Sima Baghbanzadeh and Ivan Kassal, *Distinguishing the roles of energy funnelling and delocalization in photosynthetic light harvesting*, Phys. Chem. Chem. Phys. **18**, 7459 (2016).

[4] Bruce F. Milne, Christina Kjær, Jørgen Houmøller, Mark H. Stockett, Yoni Toker, Angel Rubio, and Steen Brøndsted Nielsen, *On the exciton coupling between two chlorophyll pigments in the absence of a protein environment: Intrinsic effects revealed from theory and experiment*, Angew. Chem. Int. Ed. (Submitted).

Path integral simulation on muoniated acetone radical

Yuki Oba, Tsutomu Kawatsu, and Masanori Tachikawa

Graduate School of NanoBioScience, Yokohama City Unviersity, 22-2, Seto, Kanazawa-ku, Yokohama 236-0027, Japan

A considerable amount of knowledge for muonium (Mu; complex of positive muon and electron) chemistry has been accumulated for over 30 years [1]. Compared with a proton, positive muon (μ^+) has a smaller mass and larger magnetic moment. Because of these unique features, Mu is used as the muon spin resonance/rotation/relaxation (μSR), where hyperfine coupling constant (HFCC) is a good index for the magnetic interaction between electron and muon spins.

The HFCC value of muoniated acetone radical (Mu-ACE, Figure 1) is measured by Percival et al [2] as 10.27 MHz at 300 K (reduced using the proton magnetic moment). However, the reduced HFCC value for Mu-ACE is calculated as -5.8 MHz with the conventional DFT calculation [3], where the quantum effect of nuclei and thermal effect are excluded. In this study, thus, we performed *on-the-fly ab initio* path integral molecular dynamics (PIMD) simulation [5], which can include these effects, to reproduce the reduced HFCC value of Mu-ACE. We also calculated hydrogenated acetone radical (H-ACE) to compare with Mu-ACE.

Table 1 shows the results of the reduced HFCC values with experimental ones. Our reduced HFCC values for Mu-ACE and H-ACE are calculated as 32.1 and 3.97 MHz, respectively, which are in reasonable agreement with the corresponding experimental values of 10.3 and 1.51 MHz. Such mass-dependence on the reduced HFCC values is due to the large quantum effect of muon.

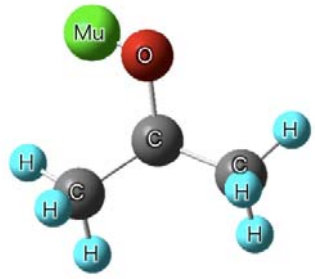

Figure 1: Structure of Mu-ACE.

Table 1: Reduced HFCC values for Mu-ACE and H-ACE. [in MHz]

	Mu-ACE	H-ACE
Exptl.	10.27[2]	1.51[4]
This study	32.1	3.97

References

[1] P. W. Percival, Radiochemica Acta, **26**, 1 (1979).
[2] P. W. Percival, J.-C. Brodovitch, K. Ghandi, B. M. McCollum and I. McKenzie, J. Am. Chem. Soc. **127**, 13715 (2005).
[3] R. M. Macraea and I. Carmichael, Physica B, **326**, 81 (2003).
[4] H. Zeldes and R. Livingston, J. Chem. Phys., **44**, 1245 (1966).
[5] K. Yamada, Y. Kawashima, and M. Tachikawa, J. Chem. Theory Comput., **10**, 2005 (2014).

Structure-resolved ultrafast dynamics in complex molecules by laser induced electron diffraction

Andrea Trabattoni[1], Joss Wiese[1], Evangelos Karamatskos[1], Terence Mullins[1], Arnaud Rouzée[2], Sebastian Trippel[1,3], Jochen Küpper[1,3,4]

1. Center for Free-Electron Laser Science (CFEL), DESY, Notkestrasse 85, 22607, Hamburg, Germany

2. Max-Born-Institut, Max-Born-Strasse 2A, 12489 Berlin, Germany

3. The Hamburg Center for Ultrafast Imaging (CUI), Universität Hamburg, Luruper Chaussee 149, 22761 Hamburg, Germany

4. Department of Physics, Universität Hamburg, Luruper Chaussee 149, 22761 Hamburg, Germany

One of the ultimate goals of molecular physics is the possibility of manipulating the structural dynamics of molecules through external fields. To this end, one first has to image the molecular structure and dynamics with an extremely high temporal resolution and atomic spatial resolution simultaneously. In this perspective, laser-induced electron diffraction (LIED) is an excellent candidate to this end [1]. In this work we describe the development of a novel implementation of mid-infrared-laser-induced diffraction for the investigation of ultrafast structure-resolved dynamics occurring in controlled complex molecules.

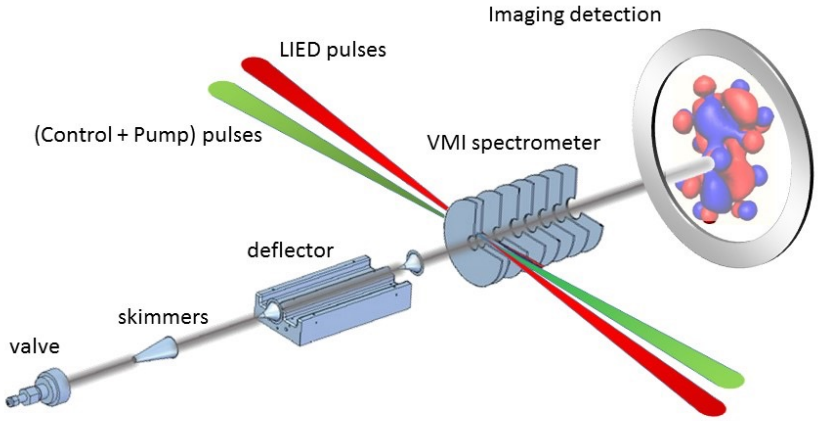

Fig. 1 Experimental setup of pump-probe LIED experiments.

The experimental setup for pump-probe LIED experiments is reported in Fig. 1. Strongly 3D aligned molecules are prepared in the interaction area by exploiting a combination of quantum-state-selected molecular beams and pulse-shaped laser fields (both adiabatic and field-free alignment are used, alternatively) [2]. Molecular orientation can also be achieved by the application of a moderately strong DC electric field. The controlled molecules are then excited by 30-fs UV pulses (230–400nm) generated by an IR-pumped optical parametric amplifier (OPA), and the dynamics induced by the pump pulses is triggered and investigated by LIED. The LIED driving field consists of linearly polarised 50-fs pulses, with a tunable wavelength in the range 1.8-2.5 μm and an energy of few hundreds μJ (at 2.5 μm).

The photoelectron angular distribution is recorded in a high-energy velocity map imaging spectrometer, with a maximum detectable photoelectron kinetic energy up to 500 eV. The rescattering part, e.g., the very-high-kinetic-energy electrons, is analysed by exploiting Quantitative Rescattering (QRS) theory in combination with independent atom modelling, in order to retrieve the time-dependent structure of the molecule under study.

With increasing complexity of the molecular system, a strong support by simulations might be of fundamental importance to disclose the signature of molecular structure imprinted in the photoelectron diffraction patterns. In particular, TD-DFT calculations are good candidates for the simulation of laser induced diffraction [3]. At the same time, the full calculation of photoionisation and rescattering processes in the presence of long-wavelength fields is still extremely challenging. In our work we aim to push the state of the art of experimental tools and theoretical models in the field of laser-induced diffraction, to reach an unprecedented insight in the time-dependent structural dynamics of complex molecules.

References

[1] T. Zuo et al., Chem. Phys. Lett. **259**, 313–320 (1996).
[2] Y-P Chang et al, International reviews in physical chemistry **34**(4), 557-590 (2015).
[3] S.-K. Son and S.-I Chu, Phys. Rev. A **80**, 011403 R (2009).

Wavelength dependence of Photoelectron Circular Dichroism in Femtosecond Multiphoton Ionization

Alexander Kastner, Stefanie Züllighoven, Tom Ring, Cristian Sarpe, Christian Lux, Arne Senftleben and Thomas Baumert

Institut für Physik, Universität Kassel, D-34132 Kassel, Germany

The asymmetry of photoelectron angular distributions (PADs) from randomly oriented enantiomers of chiral molecules in the ionization with circularly polarized light arises in forward/backward direction with respect to the light propagation. This effect was termed Photoelectron Circular Dichroism (PECD) and so far investigated using synchrotron radiation [1] and recently also by using high harmonic generation [2]. We observed highly structured asymmetries in the range of $\pm$ 10% on bicyclic Ketones [3, 4]. Due to the multi photon ionization (MPI), high order Legendre polynomials appear in the measured PADs in the threshold as well as the above threshold ionization [5]. We recently tested the sensitivity of femtosecond PECD on enantiomeric excess [6]. In the case of Resonance Enhanced MPI (REMPI) using femtosecond laser pulses, the observed Legendre polynomial distribution is determined through the intermediate resonance and can be influenced by the laser wavelength. In this contribution we show our recent findings on wavelength dependence of the PECD effect of bicyclic Ketones. Between the ionization threshold for 3 photons to the region slightly below our previous measurement point at 398 nm, a single intermediate dominates the PAD images while for even shorter wavelengths the contribution from a second intermediate resonance arises.

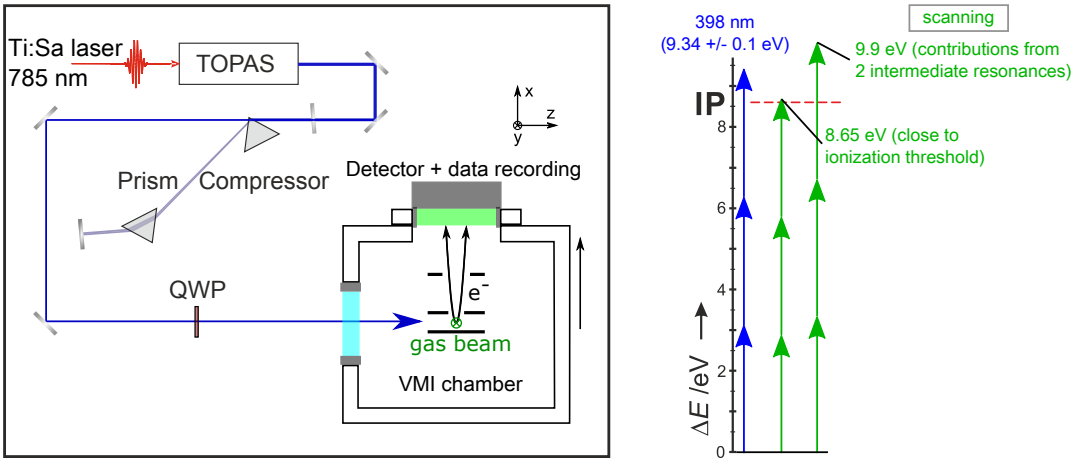

Figure 1: Experimental setup and excitation scheme

Financial support by the State Initiative for the Development of Scientific and Economic Excellence (LOEWE) in the LOEWE-Focus ELCH is gratefully acknowledged.

[1] I. Powis in S. A. Rice (Ed.): *Photoelectron Circular Dichroism in Chiral Molecules*, Adv. Chem. Phys. 138, 267-329 (2008)
[2] A. Ferré et al.: *A table-top ultrashort light source in the extreme ultraviolet for circular dichroism experiments*, Nature Photonics, 9, 93–98, (2015).
[3] C. Lux et al.: *Circular Dichroism in the Photoelectron Angular Distributions of Camphor and Fenchone from Multiphoton Ionization with Femtosecond Laser Pulses*, Angew. Chem. Int. Ed. 51, 5001-5005 (2012)
[4] C. Lux et al.: *Photoelectron Circular Dichroism of Bicyclic Ketones from Multiphoton Ionization with Femtosecond Laser Pulses*, Chem. Phys. Chem, 16, 115 – 137, (2015)
[5] C. Lux et al.: *Photoelectron circular dichroism observed in the above-threshold ionization signal from chiral molecules with femtosecond laser pulses*, J. Phys. B: At. Mol. Opt. Phys. 49, doi:10.1088 / 0953-4075 / 49 / 2 / 02LT01, (2016)
[6] A. Kastner et al.: *Enantiomeric Excess Sensitivity to Below One Percent by Using Femtosecond Photoelectron Circular Dichroism*, Chem. Phys. Chem, DOI: 10.1002/cphc.201501067, (2016)

Interatomic Coulombic Decay in Benzene dimer

Nicolas Sisourat[1], **Sévan Kazandjian**[1], **Tsveta Miteva**[1]

1. Sorbonne Universités, UPMC Univ Paris 06, CNRS, Laboratoire de Chimie Physique Matière et Rayonnement, F-75005, Paris, France

Aromatic π-π interactions are ubiquitous in chemistry, biology and engineering: these non-convalent interactions play a vital role in molecular recognition processes [1], in the tertiary and quaternary structures of proteins and DNA [2,3] as well as in organic crystal growth [4].

Benzene dimer is the simplest prototype system to study aromatic interactions and as such it has been studied for decades (see [5] for a recent review). Owing to the small binding energy between the two molecules, the dimer may exist in different conformational geometries, even at low temperature. Theory predicts three low and nearly isoenergetic conformers, namely the T-shaped (T), the tilted T-shaped (TT) and the Parallel-Displaced (PD) geometries (see Fig.1). The binding energy of these conformers is around 2.8 kcal/mol. Among the other conformers lying above these lowest configurations the sandwich (S) geometry has been widely investigated since it represents a model for stacked structures. The T-shaped conformers have been confirmed experimentally using microwave spectroscopy [6]. However, other configurations are more challenging to identify because they lack permanent dipole moments.

In this work, we theoretically investigate a spectroscopic method based on the Intermolecular Coulombic Decay (ICD) effect [7-10] in order to probe the various conformers of benzene dimer. ICD is an efficient and ultrafast energy transfer process: after inner-valence ionization of a molecule embedded in a chemical environment this molecular ion transfers its excess energy to a neighboring molecule which is then ionized. The timescale for the energy transfer and the kinetic energy distribution of the secondary electron (so-called ICD electron) depend strongly on the environment and in particular on the distance between the molecules.

We have computed the kinetic energy distributions of the photoelectron in coincidence with that of the ICD electron for the lowest benzene dimer conformers. Subtanstial differences between these electron-electron spectra may be used to identify the various configurations.

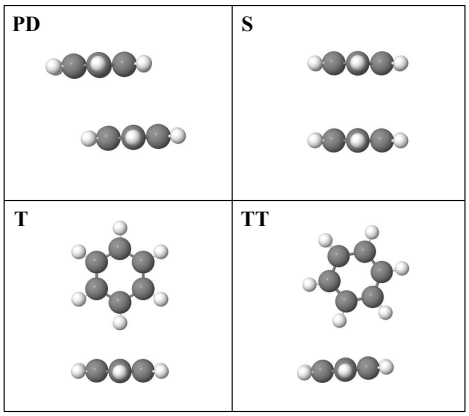

Fig. 1 Geometry of the lowest conformers of benzene dimer.

References

[1] C.A. Hunter, *Meldola Lecture. The role of aromatic interactions in molecular recognition*, Chem. Soc. Rev. **23**, 101 (1994).
[2] S.K. Burley and G.A. Petsko, *Aromatic-aromatic interaction: a mechanism of protein structure stabilization*, Science **229**, 23 (1985).
[3] K.E. Riley and P. Hobza, *On the Importance and Origin of Aromatic Interactions in Chemistry and Biodisciplines*, Journal of Physical Organic Chemistry **10**, 254 (1997).
[4] C.G. Claessens and J.F. Stoddart, $\pi - \pi$ *interactions in self-assembly*, Accounts of Chemical Research **46**, 927 (2013).
[5] S.R. Gadre and S.D. Yeole and N. Sahu, *Quantum Chemical Investigations on Molecular Clusters*, Chemical Reviews **24**, 12132 (2014).
[6] E. Arunan and H.S. Gutowsky, *The rotational spectrum, structure and dynamics of a benzene dimer*, J. Chem. Phys. **98**, 4294 (1993).
[7] L.S. Cederbaum, J. Zobeley and F. Tarantelli, *Giant Intermolecular Decay and Fragmentation of Clusters*, Phys. Rev. Lett. **79**, 4778 (1997).
[8] S. Marburger, O. Kugeler, U. Hergenhahn and T. Möller, *Experimental Evidence for Interatomic Coulombic Decay in Ne Clusters*, Phys. Rev. Lett. **90**, 203401 (2003).
[9] T. Jahnke, A. Czasch, M.S. Schöffler, S. Schössler, A. Knapp, M. Käsz, J. Titze, C. Wimmer, K. Kreidi, R.E. Grisenti, A. Staudte, O. Jagutzki, U. Hergenhahn, H. Schmidt-Böcking and R. Dörner, *Experimental Observation of Interatomic Coulombic Decay in Neon Dimers*, Phys. Rev. Lett. **93**, 163401 (2004).
[10] See http://www.pci.uni-heidelberg.de/tc/usr/icd/ICD.refbase.html for the complete list of ICD papers

Cd_2 and Hg_2 Interatomic Potentials: a "Test-Bed" for Theory-to-Experiment Agreement

Tomasz Urbańczyk[1], Marek Krośnicki[2], Marcin Strojecki[3], Asen Pashov[4], Andrzej Kędziorski[5] Jarosław Koperski[1]

1. Smoluchowski Institute of Physics, Jagiellonian University, prof. Stanisława Łojasiewicza 11, 30-348 Kraków, Poland

2. Institute of Theoretical Physics and Astrophysics, University of Gdansk, Wita Stwosza 57, 80-952 Gdańsk, Poland

3. Jerzy Haber Institute of Catalysis and Surface Chemistry, Polish Academy of Sciences, Niezapominajek 8, 30-239 Kraków, Poland

4. Department of Physics, Sofia University, 5 James Bourchier Boulevard, 1164 Sofia, Bulgaria

5. Institute of Physics, Nicolaus Copernicus University, Grudziądzka 5/7, 87-100 Toruń, Poland

New all-electron *ab initio* and experimental studies of the interatomic potentials of *ungerade* excited and ground electronic energy states of the heavy van der Waals dimers Cd_2 and Hg_2 were used as a "test-bed" for theory-to-experiment comparisons. Representations of the lowest excited- and ground-state Cd_2 and Hg_2 interatomic potentials were proposed, by using a new analytical approach as well as by using an inverted perturbation approach. The comparison of the new *ab-initio* calculated potentials with the results of the analyses illustrates an improved theory-to-experiment agreement for demanding heavy systems such as Cd_2 or Hg_2.

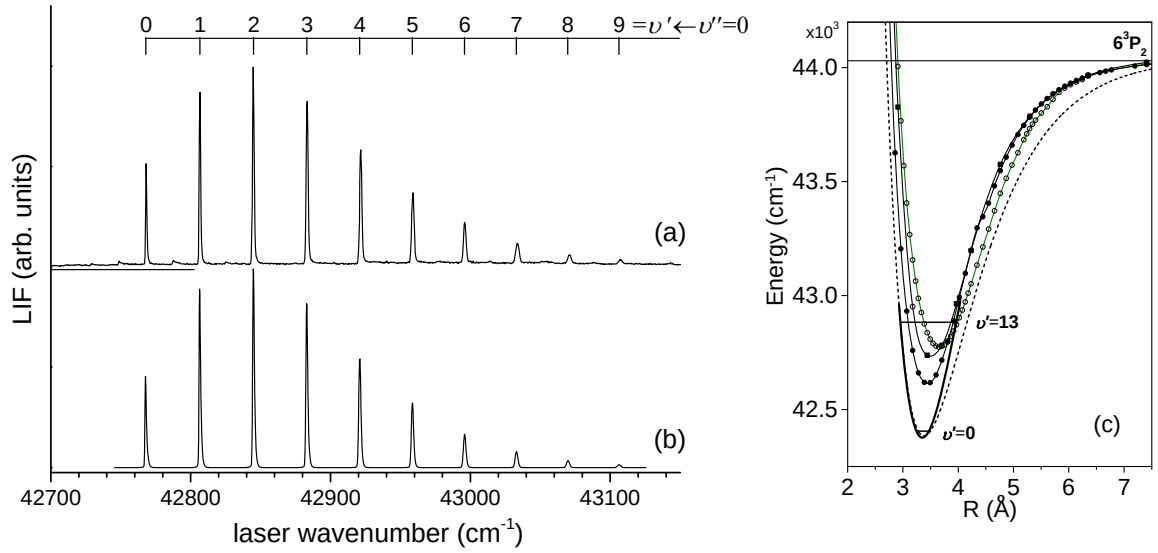

Fig. 1 (a) LIF excitation spectrum recorded [1] using the $E^3\Pi_u(6^3P_2)\leftarrow X^1\Sigma_g^+$ transition in Hg_2. (b) Simulation [2,3,4] performed assuming a Morse representation for the $E^3\Pi_u$- and $X^1\Sigma_g^+$-state potentials. (c) Interatomic potential of the $E^3\Pi_u$ state of Hg_2. The scheme shows *ab-initio* calculated potentials of Czuchaj *et al.* [5] (full squares), Kullie [6] (empty circles) and of this work (full circles), as well as those obtained experimentally [1] (dashed line) and in this study from simulation of the LIF excitation spectrum (solid line). Positions of υ'=0 and υ'=13 vibrational levels show the energy region within which the characterizations were performed.

This work was supported by the National Science Centre Poland under grant number UMO-2015/17/B/ST4/04016.

References

[1] J. Koperski, J.B. Atkinson, L. Krause, *Molecular Beam Spectroscopy of the $1_u(6^3P_2)$-$X0_g^+$ and $1_u(6^3P_1)$-$X0_g^+$ Transitions in Hg_2*, Can. J. Phys. **72**, 1070 (1994).

[2] R.J. LeRoy, *LEVEL 8.0. A Computer Program for Solving the Radial Schrodinger Equation for Bound and Quasibound Levels*. University of Waterloo. The source code: http://leroy.uwaterloo.ca.

[3] C. M. Western, *PGOPHER version 8.0, a Program for Simulating Rotational Structure*, University of Bristol. The source code: http://pgopher.chm.bris.ac.uk.

[4] T. Urbańczyk, *LEVEL-to-PGOPHER 2.0 Computer Program*, Krakow, 2013.

[5] E. Czuchaj, F. Rebentrost, H. Stoll, H. Preuss, *Calculation of ground- and excited-state potential energy curves for the Hg_2 molecule in a pseudopotential approach*, Chem. Phys. **214**, 277 (1997).

[6] O. Kullie, *A relativistic time-dependent density functional study of the excited states of the mercury dimer*, J. Chem. Phys. **140**, 024304 (2014).

Dependence of D_2 Continuum Radiation on Electron Beam Energy in Electron Induced Fluorescence Experiment

Marián Danko, Michal Ďurian, Juraj Országh, Štefan Matejčík

Faculty of Mathematics, Physics and Informatics, Comenius University in Bratislava, Mlynská dolina F2, 842 48 Bratislava, Slovakia

Hydrogen and deuterium molecules have been extensively studied in the past, partly because of need for high-quality kinetic data necessary for modelling of plasmas, particularly in fusion [1, 2]. Our work in this field concentrates on studying excitation-emission processes using electron induced fluorescence (EIF). Within the experiment it is possible to measure emission spectra induced by electron impact and photon efficiency curves (PEC), which after calibration correspond to excitation-emission cross-sections of specific processes.

In this abstract we present results of our recent experiments studying D_2 continuum radiation originating from $a^3\Sigma_g^+ \rightarrow b^3\Sigma_u^+$ transition. The hydrogen continuum spectrum is a superposition of narrower continua origination from the decay of different vibrational levels in the upper electronic state to the lower unbound state [1, 3]. The result is strong emission spanning from VUV to VIS range that has found its application in deuterium calibration lamp or other radiation sources.

The electron induced fluorescence apparatus is described in detail in [4]. In present experiment we have used electron beam with electron energy resolution of 0.5eV FWHM at few hundreds nA of electron current. Photon emission was measured using optical system comprising of Cornerstone 260 grating monochromator, focusing optics and photon-counting Hamamatsu H4220P photomultiplier module sensitive in the spectral range from 200 to 670nm. Background signal level was 0.3 photon/s and constituted predominantly by intrinsic noise of PMT. Optical resolution was about 1 nm with 500μm monochromator slits. Optical system was calibrated for spectral sensitivity by measuring tungsten filament emission and taking gray body radiation model above 500nm and using known H_2 continuum radiation shape for wavelengths above 200nm [5]. Optical filter was used to cut off radiation below 420nm in order to rule out second order diffraction from our grating.

In Fig. 1 we present D_2 fluorescence spectra at five discrete electron beam energies ranging from 12 to 15eV in 200 – 650nm spectral region. With increasing electron energy we can observe the evolution of the emission spectra. Spectral structures appear as their respective excitation thresholds are exceeded, the continuum is visible at 12.5eV already and Fulcher bands appear at 15eV. The structures of the continuum, especially in 230 – 350nm region are in agreement with earlier studies [3, 5]. Uniqueness of present spectra lies in observation of the continuum radiation up to 650nm, which is much higher than commonly reported 500nm limit. Similar results have been achieved with H_2 molecule.

To verify that the signal at 650nm originates from the $a^3\Sigma_g^+ \rightarrow b^3\Sigma_u^+$ transition, we have measured the PEC of D_2 continuum at this wavelength (Fig. 2), which was selected to avoid any signal from nearby spectral lines. The shape of this curve is in agreement with PEC measured at 230nm.

This work was supported by the Slovak Research and Development Agency, project Nr. APVV-0733-11 and the grant agency VEGA, project Nr. 1/0417/15. This project has received funding from the European Union's Horizon 2020 research and innovation programme under grant agreement No 692335.

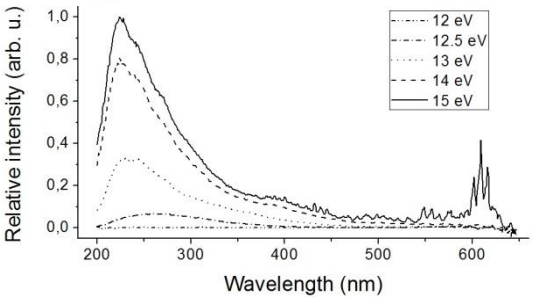

Fig. 1 D_2 fluorescence spectra at various energies.

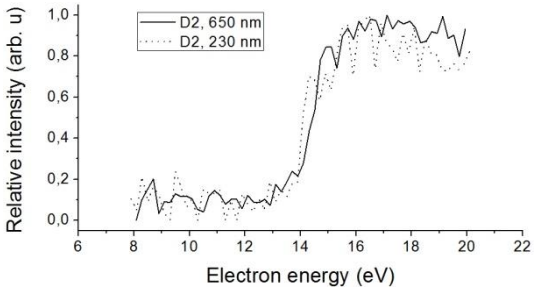

Fig. 2 D_2 PECs at 230nm and 650nm.

References

[1] Boris Pavlovich Lavrov, Alexei Sergeevich Melnikov, Marko Käning and Jürgen Röpcke, *Phys. Rev. E**59***, 3526 (1999).
[2] Marco Ajello and Donald E. Shemansky, *The Astrophysical Journal* **407**, 820 (1993).
[3] Hubert M. James and Albert S. Coolidge, *Phys. Rev.* **55**, 184 (1939).
[4] Marián Danko, Juraj Országh, Michal Ďurian, Jaroslav Kočíšek, Matthias Daxner, Samuel Zöttl, Jelena B. Maljković, Juraj Fedor, Paul Scheier, Stephan Denifl and Štefan Matejčík, *J. Phys. B: At. Mol. Opt. Phys.* **46**, 045203 (2013)
[5] Geoffrey K. James, Joseph M. Ajello and Wayne R. Pryor, *J. Geophys. Res.* **103**, 20113 (1998)

Circular Dichroism in the O 1s photoionization of fixed-in-space methyloxirane enantiomers

Maurice Tia[1], Martin Pitzer[1], Gregor Kastirke[1], Janine Gatzke[1], Hong-Keun Kim[1], Florian Trinter[1], Jonas Rist[1], Alexander Hartung[1], Daniel Trabert[1], Juliane Siebert[1], Kevin Henrichs[1], Jasper Becht[1], Stefan Zeller[1], Helena Gassert[1], Florian Wiegandt[1], Robert Wallauer[1], Andreas Kuhlins[1], Carl Schober[1], Tobias Bauer[1], Natascha Wechselberger[1], Phillip Burzynski[1], Jonathan Neff[1], Miriam Weller[1], Daniel Metz[1], Max Kircher[1], Markus Waitz[1], Joshua B. Wlliams[2], Lothar Schmidt[1], Anne D. Müller[3], André Knie[3], Andreas Hans[3], Ltaief Ben Ltaeif[3], Arno Ehresmann[3], Robert Berger[4], Hironobu Fukuzawa[5], Kiyoshi Ueda[5], Horst Schmidt-Böcking[1], Reinhard Dörner[1], Till Jahnke[1], Philipp V. Demekhin[3], and Markus Schöffler[1]

1. Institut für Kernphysik, Johann Wolfgang Goethe Universität, Max-von-Laue-Straße 1, 60438 Frankfurt am Main, Germany
2. Department of Physics, University of Nevada, Reno, Nevada 89557, USA
3. Institut für Physik und CINSaT, Universität Kassel, Heinrich-Plett-Str. 40, 34132 Kassel, Germany
4. Theoretical Chemistry, Department of Chemistry, Philipps-Universität Marburg, Hans-Meerwein-Strasse, 35032 Marburg
5. Institute of Multidisciplinary Research for Advanced Materials, Tohoku University, Sendai 980-8577, Japan

It is well known that chiral (optically active) molecules interact in different ways with right- and left-handed circular polarized light. This phenomenon is known as circular dichroism (CD), and it is routinely used to distinguish different enantiomers of a chiral molecule by observing their total photoabsorption spectra [1]. Here, CD is governed by the electric-dipole – magnetic-dipole interference and it is on the order of about $10^{-3} - 10^{-5}$ of the total absorption. In the angular-resolved photoelectron spectra, CD exists already in electric-dipole approximation [2], and it is, therefore, much stronger. At present, a series of independent experiments has confirmed that in the angular-resolved spectra of randomly oriented molecules photoelectron circular dichroism (PECD) can be seen as a few percent forward-backward asymmetry in the emission of a photoelectron. Here, we prove that orienting a chiral molecule in space additionally enhances the PECD by about a factor of 10.

The present experiment on the O 1s-photoionization of the methyloxirane molecules was performed by the well-established COLTRIMS (Cold Target Recoil Ion Momentum Spectroscopy, [3]) with synchrotron radiation provided by the variable polarization undulator-based beamline SEXTANTS at the Synchrotron SOLEIL (Saint-Aubin, France). Before the nuclei start to rearrange in response to the creation of the O 1s-hole, an ultrafast Auger decay takes place, which is finally followed by a Coulomb fragmentation of the doubly-charged ion. We have observed and analyzed the molecular break-up into two different fragment combinations: $C_2H_2^+ - COH^+$ and $CH_3^+ - C_2H_2O^+$. The electronic structure and dynamics calculations were carried out by the Single Center method and code [4], which provides an accurate description of the partial photoelectron continuum waves in molecules. The photoionization transition amplitudes were computed in the Relaxed-Core Hartree-Fock approximation at the equilibrium internuclear geometry of the ground electronic state of methyloxirane.

The PECD measured for the O 1s photoionization of the randomly oriented metyloxirane molecules shows maximum values between 3 and 4%, whereas the PECD obtained after fixing the fragmentation axes in space (angle between the molecular axis and the light propagation axis) shows a much higher effect. We observe an asymmetry of up to 15% for the $C_2H_2^+ - COH^+$ breakup and even higher asymmetries of up to 30% for the fragmentation channel $CH_3^+ - C_2H_2O^+$. The presently computed PECDs show a good overall agreement with the experimental data. For the fragmentation channel $C_2H_2^+ - COH^+$, the present calculations show asymmetries of up to 30%, whereas PECD of about 35% is computed for the fragmentation channel $CH_3^+ - C_2H_2O^+$. We also observe the generally expected change of sign of PECD with respect to the interchange of the enantiomers for both, randomly oriented and fixed-in-space molecules. Further analysis is performed by selecting molecular orientations to be perpendicular to the light propagation direction and looking at the circular dichroism in angular distribution (CDAD) as a function of the azimuthal emission angle in the polarization plane.

References

[1] *Chiral Recognition in the Gas Phase*, edited by A. Zehnacker (CRC Press, Boca Raton, 2010).

[2] B. Ritchie, *Theory of the angular distribution of photoelectrons ejected from optically active molecules and molecular negative ions*, Phys. Rev. A **13**, 1411 (1976).

[3] R. Dörner , V. Mergel, O. Jagutzki, L. Spielberger, J. Ullrich, R. Moshammer, H. Schmidt-Böcking, *Cold Target Recoil Ion Momentum Spectroscopy: a 'momentum microscope' to view atomic collision dynamics*, Physics Reports **330**, 95 (2000).
J. Ullrich, R. Moshammer, A. Dorn, R. Dörner, L.Ph.H. Schmidt and H. Schmidt-Böcking, *Recoil-ion and electron momentum spectroscopy: reaction-microscopes*, Rep. Prog. Phys. **66**, 1463 (2003).

[4] Ph.V. Demekhin, A. Ehresmann, V.L. Sukhorukov, *Single Center method: A computational tool for ionization and electronic excitation studies of molecules*, J. Chem. Phys. **134**, 024113 (2011).
S.A. Galitskiy, A.N. Artemyev, K. Jänkälä, B.M. Lagutin, and Ph.V. Demekhin, *Hartree-Fock calculation of the differential photoionization cross sections of small Li clusters*, J. Chem. Phys. **142**, 034306 (2015).

Proposal for laser-cooling of rare-earth ions

Maxence Lepers[1], Ye Hong[1], Jean-François Wyart[1,2] and Olivier Dulieu[1]

1. *Laboratoire Aimé Cotton, CNRS, Université Paris-Sud, ENS Cachan, Université Paris-Saclay, 91405 Orsay Cedex, France*
2. *LERMA, UMR8112, Observatoire de Paris-Meudon, Université Pierre et Marie Curie, 92195 Meudon, France*

The efficiency of laser-cooling relies on the existence of an almost closed optical-transition cycle in the energy spectrum of the considered species. In this respect rare-earth elements exhibit many transitions which are likely to induce noticeable leaks from the cooling cycle. In this work, to determine whether laser-cooling of singly-ionized erbium Er^+ is feasible, we have performed accurate electronic-structure calculations of energies and spontaneous-emission Einstein coefficients of Er^+, using a combination of *ab initio* and least-square-fitting techniques [1]. We identify five weak closed transitions suitable for laser-cooling, the broadest of which is in the kilohertz range. For the strongest transitions, by simulating the cascade dynamics of spontaneous emission, we show that repumping is necessary, and we discuss possible repumping schemes. We expect our detailed study on Er^+ to give a good insight into laser-cooling of neighbouring ions like Dy^+.

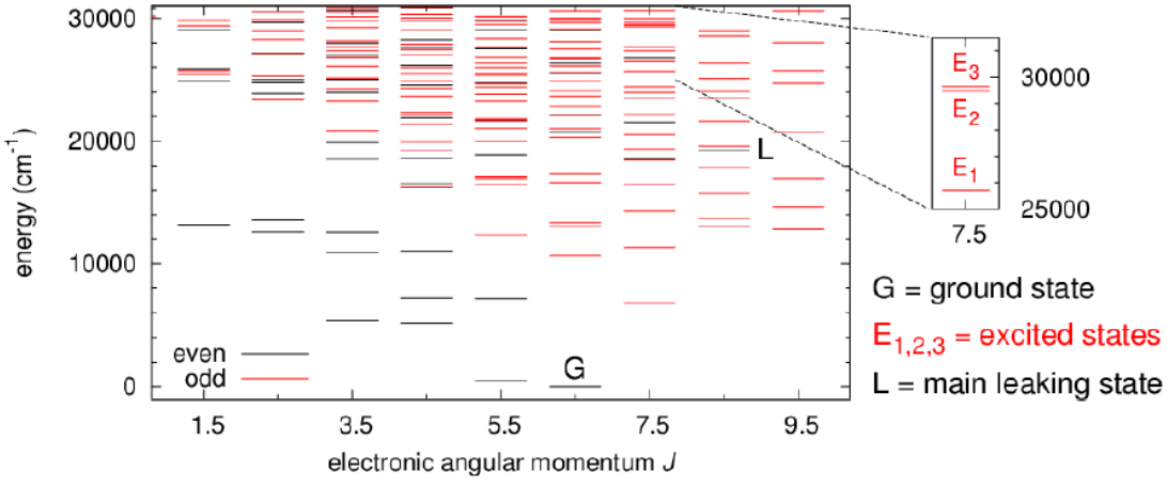

Fig. 1: scheme of the Er+ energy levels sorted according to their parity. In the inset are shown three particular levels which are the most suitable for laser cooling.

References

[1] M. Lepers, Y. Hong, J.-F. Wyart, O. Dulieu, Phys. Rev. A **93**, 011401(R), 2016

Few-body physics with ultracold potassium rubidium mixtures

Ridha Horchani[1], L. Wacker[2], N. Winter[2] , J. Sherson[2] , J.J. Arlt[2]

[1] *College of applied sciences, Dhofar University, Salalah, Oman*

[2] *Institute of physics and astronomy, Aarhus university, Denmark*

Within the past decade, research on ultracold atoms has moved from the investigation of their fundamental properties to the application of ultracold samples in quantum simulation and precision metrology. The ability to tailor external potentials freely and to manipulate the interaction strength within the samples has led to numerous advances in the field. In particular, mixed quantum gases have attracted considerable interest, since they offer a wealth of research opportunities. These include the creation of deeply bound dipolar molecules [1], the investigation of few-particle physics [2, 3], the observation of quantum phases in optical lattices [4] and precision measurements [5]. Such mixed quantum gasses can generally be realized by using a single atomic species in multiple quantum states, by using multiple isotopes of the same species, or by using different atomic species. Thus it is possible to realize Bose-Fermi, Bose-Bose or Fermi-Fermi mixtures. Since cooling techniques to achieve ultracold temperatures have become available for an increasing number of atomic species, this leads to a considerable number of possible mixtures. Here, we present the production of dual-species Bose-Einstein condensates of ^{39}K and ^{87}Rb. Preparation of both species in the $|F = 1, mF = -1\rangle$ state enabled us to exploit a total of three Feshbach resonances which allows for simultaneous Feshbach tuning of the ^{39}K intraspecies and the ^{39}K-^{87}Rb interspecies scattering length. Thus dual-species Bose-Einstein condensates were produced by sympathetic cooling of ^{39}K with ^{87}Rb. A dark spontaneous force optical trap was used for ^{87}Rb, to reduce the losses in ^{39}K due to light-assisted collisions in the optical trapping phase, which can be of benefit for other dual-species experiments. The tunability of the scattering length was used to perform precision spectroscopy of the interspecies Feshbach resonance located at 117.56(2) G and to determine the width of the resonance to 1.21(5) G by rethermalization measurements. The transition region from miscible to immiscible dual-species condensates was investigated and the interspecies background scattering length was determined to 28.5 a0 using an empirical model. This paves the way for dual-species experiments with ^{39}K and ^{87}Rb BECs ranging from molecular physics to precision metrology.

.

References

[1] L. D. Carr, D. DeMille, R. V. Krems, and J. Ye, *New Journal of Physics* 11 (2009).
[2] N. Zinner, *Few-Body Systems* 55, 599 (2014).
[3] N. T. Zinner and A. S. Jensen, *Journal of Physics G: Nuclear and Particle Physics* 40, 053101 (2013).
[4] I. Bloch, *Nature Physics* 1, 23 (2005).
[5] D. Schlippert, J. Hartwig, H. Albers, L. L.
Richardson, C. Schubert, A. Roura, W. P. Schleich, W. Ertmer, and E. M. Rasel, Phys. Rev. Lett. 112, 203002 (2014).

Radiative Force to Laser-Cooled Atoms by Near Optical Resonant Trap

Shota Yonekawa[1] Tatsuhiko Hibino[1], Kosuke Shibata[1], Satoshi Tojo[1]

1. Department of Physics, Chuo University, 1-13-27, Kasuga, Bunkyo, 112-8551, Tokyo, Japan

For the purpose of precise manipulation for cold atoms, one of radiative forces, the dipole force, is usually applied as a typical manipulation technique. The dipole force is a conservative force based on stimulated emission and absorption of photons. On the other hand, another radiative force, the scattering force, is different possibility of realization of the manipulation for atoms by photon-atom interaction [1].

The scattering force results from photon collision against an atom and photon scattering in random directions, and dependent on detuning from a resonance line of the atom [2,3]. In general, the scattering force of an optical dipole trap is quite weak to effect on atoms because the laser detuning is far from the resonance in a typical Far-Off Resonant optical dipole Trap (FORT). On the other hand, in the case of a Near-Optical Resonant Trap (NORT) with the detuning being the range of several GHz to several THz from D1 line of rubidium atoms, the atoms cloud in NORT may be affected by the scattering force [1].

We measure the displacement of center-of-mass positions of the atoms in the NORT, with the dependence of the power and the detuning of NORT. The detuning of the laser from D1 line is in the range from 30 to 150 GHz. In order to measure the displacement precisely, we prepare the atom cloud in NORT-FORT crossed trap as shown as Fig. 1(a). The pre-cooled atoms are trapped in 42×42×200 μm region with 2×10^4 atoms at 70 μK. By turning off the FORT non-adiabatically, we can observe trap time dependence of atom cloud, and estimate the displacement of the center-of-mass of the atoms in NORT. Figure 1(b) shows the dependence of the displacement of the atoms on the trap time with the laser power being 172 mW, and the frequency detuning δ in the range from 50 to 100 GHz from a resonance of rubidium atoms. The displacements of the center-of-mass atoms positions increase in increasing of the trap time. The experimented displacement can be fitted by the parabolic curve in good agreement. This means that atoms behave as an uniformly accelerated motion. The acceleration of atoms tends to be inversely proportional to detuning from D1 line and proportional to laser power. We find that acceleration can be explained by the scattering force of NORT.

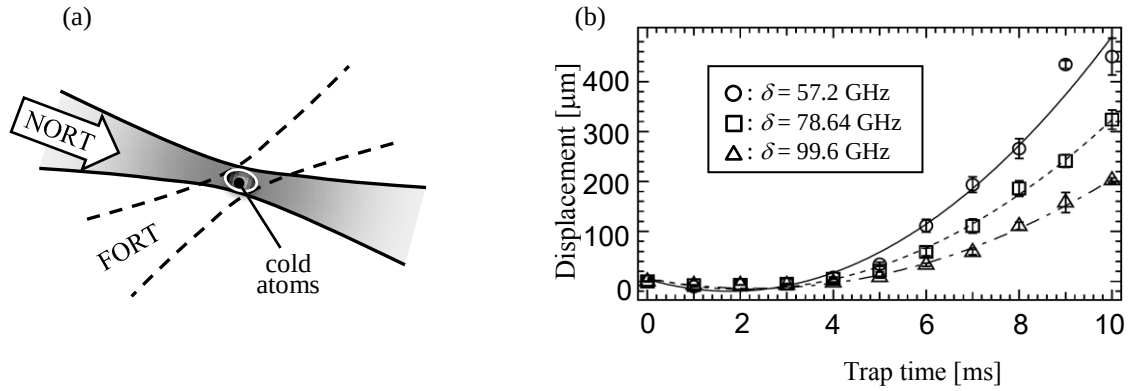

Fig. 1 (a) NORT-FORT crossed trap. (b) Displacement of the-center-of the mass positions of the atom cloud in NORT with the detuning δ.

References

[1] T. Bienaime, S. Bux, E. Lucioni, Ph. W. Courteille, N. Piovella, R. Kaiser, Phys. Rev. Lett. **104,** 183602 (2010).
[2] S.J.M. Kuppens, K.L. Corwin, K.W Miller, T.E. Chupp, C.E. Wieman, Phys. Rev. A **62**, 013406 (2000).
[3] A. Szczepkowicz, L. Krzemień, A. Wojciechowski, K. Brzozowski, M. Krüger, M. Zawada, M. Witkowski, J. Zachorowski, W. Gawlik, Phys. Rev. A **79**, 013408 (2009).

Cooperative emission of light in optically thick strontium cold cloud

Chang Chi Kwong[1], **Dominique Delande**[2], **Romain Pierrat**[3] **David Wilkowski**[1,4,5]
1. School of Physical and Mathematical Sciences, Nanyang Technological University, 637371 Singapore, Singapore.
2. Laboratoire Kastler Brossel, UPMC, CNRS, ENS, Collège de France, 4 Place Jussieu, F-75005 Paris, France.
3. ESPCI ParisTech, PSL Research University, CNRS, Institut Langevin, 1 rue Jussieu, F-75005 Paris, France.
4. Centre for Quantum Technologies, National University of Singapore, 117543 Singapore, Singapore.
5. MajuLab, CNRS-University of Nice-NUS-NTU International Joint Research Unit UMI 3654, Singapore.

We investigate the transient coherent transmission of light through an optically thick cold Strontium gas [1]. We observe a coherent superflash of light just after an abrupt probe extinction, with peak intensity, surprisingly, well above the incident intensity (see Fig. 1a). We show that this coherent superflash is a direct signature of the cooperative forward emission of the atoms [2]. Similarities between the superflash effect and the Dicke superradiance can be drawn where the optical thickness plays the role of the number of cooperative atoms. Taking advantage of the fast decay time of the cooperative emission, we create a pulse train of light with a repetition time shorter than the atomic lifetime (see Fig. 1b). In this regime single atom spontaneous emission can be quenched and the response of the cold gas is fully governed by cooperativity [3].

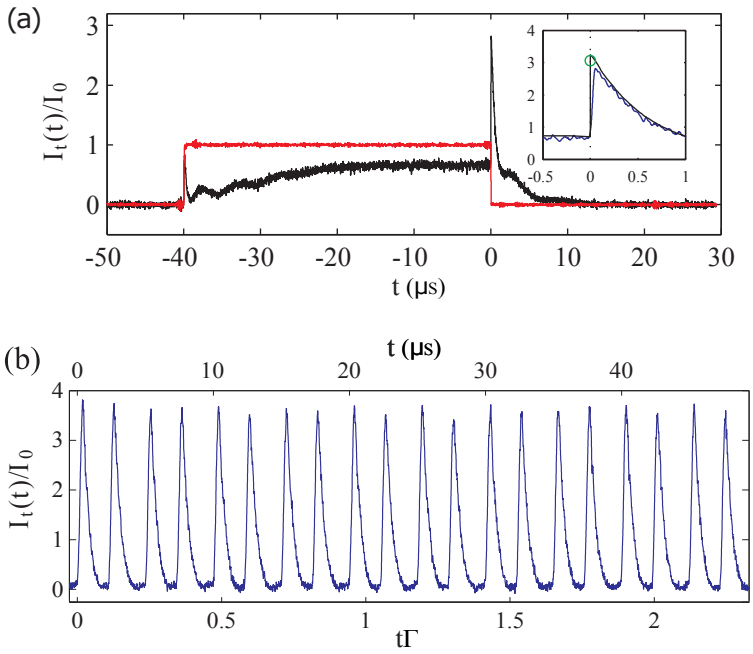

Fig. 1 (a) temporal evolution of the transmitted light into an optically thick cold cloud of atoms (black line). The red curve shows the normalized incident intensity. Inset: zoom at $t \sim 0$. The frequency detuning is $\delta = -11.2\Gamma$, where Γ is the atomic linewidth. (b) coherent transmission for a periodic abrupt change of the phase of the incident field. Here we have $\delta = 0$

The experiments were performed using the narrow intercombination line of Strontium. The long lifetime of the excited state was of key importance to resolve the temporal evolution of the system. More standard transitions on thermal vapors (with Rubidium for example) would lead to the same phenomena, but in the picosecond range. Potential applications for pulse generation can be proposed. On a more fundamental aspect, transient coherent transmission of light can be an interesting probing tool to reveals pair correlation in quantum gases.

References

[1] M. Chalony, R. Pierrat, D. Delande, and D. Wilkowski, Physical Review A **84**, 011401(R) (2011).
[2] C. C. Kwong, T. Yang, M. S. Pramod, K. Pandey, D. Delande, R. Pierrat, and D. Wilkowski, Physical review letters **113**, 223601 (2014).
[3] C. C. Kwong, T. Yang, D. Delande, R. Pierrat, and D. Wilkowski, Physical review letters **115**, 223601 (2015).

Experimental realization of a single-ion heat engine

J. Rossnagel[1], S. T. Dawkins[1], F. Schmidt-Kaler[2], G. Jacob[2], D. Criwelli[1], K. Singer[1]

1. Experimentalphysik I, Universität Kassel, Heinrich-Plett-Str. 40, D-34132 Kassel, Germany

2. Quantum, Institut für Physik, Universität Mainz, D-55128Mainz, Germany.

Thermodynamic machines can be reduced to the ultimate atomic limit [1], using a single ion as a working agent. The confinement in a linear Paul trap with tapered geometry allows for coupling axial and radial modes of oscillation. The heat-engine is driven thermally by coupling it alternately to hot and cold reservoirs, using the output power of the engine to drive a harmonic oscillation. From direct measurements of the ion dynamics, the thermodynamic cycles for various temperature differences of the reservoirs can be determined [2] and the efficiency compared with analytical estimates.

References

[1] O. Abah et al., Phys. Rev. Lett. 109, 203006 (2012).
[2] J. Rossnagel et al., "A single-atom heat engine", Science 352, 325 (2016).

Ac Stark Shifts for Ultracold Dysprosium and Holmium

H. Li[1], M. Lepers[1], J.-F. Wyart[1,2], O. Dulieu[1]

1. Laboratoire Aimé Cotton, CNRS, Université Paris-Sud, ENS Cachan, Université Paris-Saclay, 91405 Orsay, France
2. LERMA, UMR8112, Observatoire de Paris-Meudon, Université Pierre et Marie Curie, 92195 Meudon, France

Ultracold gases of dipolar particles have attracted tremendous interest during the past years, due to their application in exploring strongly correlated matter with the presence of the long-range, anisotropic dipole-dipole interaction [1]. Lanthanide atoms, which possess an electronic configuration with an unfilled inner 4f shell shielded by a closed 6s outer shell, are very promising candidates to study dipolar quantum gases. Among the lanthanides, dysprosium [2] and holmium [3] possess some of the largest magnetic moments, equal to 10 and 9 Bohr magnetons respectively.

The deep understanding of the optical trapping – trap depth and photon-scattering rate – of lanthanides is necessary to control them with laser fields. In this work, we investigate theoretically the complex dynamic dipole polarizability of dysprosium and holmium in their ground and first excited states. The calculations are performed with the sum-over-state formula, whose flexibility enables us to calculate both the real and imaginary parts of the scalar, vector and tensor polarizabilities for any trapping frequency, with the same set of atomic transition energies and transition dipole moments. The latter, which are computed using a combination of *ab initio* and least-square-fitting techniques, also give us precious information on the spectroscopy of dysprosium and holmium.

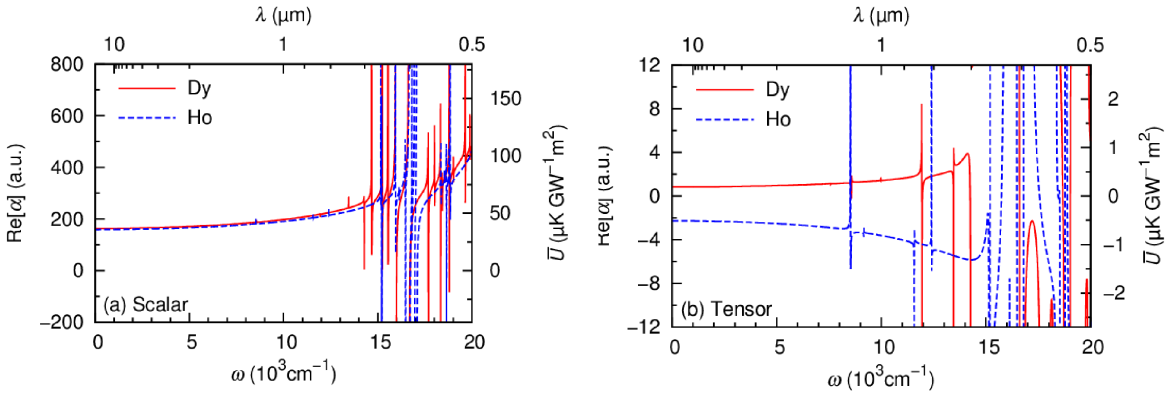

Fig. 1: Real part of the dynamic dipole polarizabilities (in atomic units) and corresponding trap depths obtained for an intensity of 1 GW.m^{-2}, for ground-state dysprosium (Dy) and holmium (Ho), as functions of the trapping frequency and wavelength. Panel (a) shows the scalar contribution, and panel (b) the tensor one.

Our results indicate that, for the real part of the polarizability, the vector and tensor contributions are extremely small compared to the scalar contribution (see Figure 1), whereas for the imaginary part, all the contributions have the same order of magnitude. These conclusions, which are valid for the ground and first excited states of Dy and Ho, are similar to our previous work on erbium [4]. For both atoms, the polarizability of the ground and the first excited are very close, which make them interesting candidates for metrology [5].

References

[1] T. Lahaye, C. Menotti, L. Santos, M. Lewenstein and T. Pfau, Rep ; Prog. Phys., **72**, 126401 (2009).
[2] M. Lu, N.Q. Burdick, S.H. Youn, and B.L. Lev, Phys. Rev. Lett., **107**, 190401 (2011).
[3] J. Miao, J. Hostetter, G. Stratis, and M. Saffman, Phys. Rev. A, **89**, 041401(R) (2014).
[4] M. Lepers, J.-F. Wyart and O. Dulieu, Phys. Rev. A, **89**, 022505 (2014).
[5] A. Kozlov, V.A. Dzuba and V.V. Flambaum, Phys. Rev. A, **88**, 032509 (2013).

Long ion chain in a octupole trap: local minimas on mutipolar RF traps

Jofre Pedregosa-Gutierrez, Marius Kamsap, Caroline Champenois, Marie Houssin, Martina Knoop
Aix Marseille Université, CNRS, PIIM, UMR 7345, 13397 Marseille, France

The radiofrequency linear ion trap is a widely used device in physics and chemistry. The quadrupole linear trap is a widespread tool for many fundamental physics experiments (quantum computing, metrology, etc). Compared to quadrupole trap, higher order traps present the interesting feature to generate an almost flat potential well, which induces a small RF-driven motion and a low RF-heating, compared to quadrupole trap. These traps have been widely used in the ultra cold collisions community with buffer gas cooled samples and to produce Coulomb crystals of a new kind thanks to laser cooling [1].

However, ions in a 22-pole trap showed the presence of 10 local minimums [2]. In fact it can be proven that a $2k$ trap will lead to $(k-1)$ minima unless the positioning of the $2k$ rods forming the trap are perfectly positioned. Such imperfection leads to a symmetry breaking, responsible for the appearance of the $(k-1)$ minima. While for hot ions, such local minimums do not play a relevant role, they become important when the ion temperatures become comparable to the local minimum depth, which can go from some 1 to 100 Kelvin, depending of the degree of misalignment of the rods.

In ECAMP12 we will report in recent experiments where we have obtained three chains of ions with temperatures lower than 10mK in an octopole trap. We will present the longest chain to date > 150 ions and show how it follows the theory developed by Dubin et al.[3].

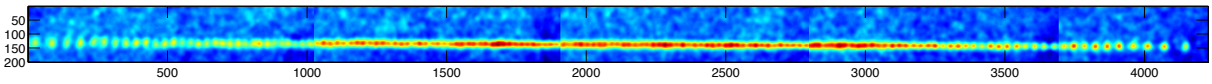

Figure 1: Picture of the whole chain built from 5 pictures taken with a translated objective. Axes are in pixels.

In addition, it will presented a proof of principle showing that it is possible to correct for imperfections in the case of multipolar radio-frequency trap [4].

References

[1]M. Marciante, C. Champenois, A. Calisti, and M. Knoop, *Structural phase transitions in multipole traps*, Appl. Phys. B **107**, 1117 (2012).
[2] R. Otto, P. Hlavenka, S. Trippel, J. Mikosch, K. Singer, M. Weidemüller, and R. Wester, *How can a 22-pole ion trap exhibit ten local minima in the effective potential?* J. Phys. B: At. Mol. Opt. Phys. **42**, 154007 (2009).
[3] D. H. E. Dubin,*Theory of structural phase transitions in a trapped Coulomb crystal*, Phys. Rev. Lett. **71**, 2753 (1993).
[4] J. Pedregosa-Gutierrez et al. in preparation

Cold Reactive Collisions between Neutral Molecules and Cold, Trapped Ions

Lorenzo S. Petralia[1], Frederick J. J. Cascarini[1], Katharina A. E. Meyer[1], Chris J. Rennick[1], Brianna R. Heazlewood[1], Tim P. Softley[1]

1. *Department of Chemistry, University of Oxford, Chemistry Research Laboratory, 12 Mansfield Road, Oxford, OX1 3TA, United Kingdom*

We study ion-molecule reactions under cold conditions, where quantum effects become important. By controlling the properties of both the ionic and neutral reactants, we can examine state-selected reaction dynamics and kinetics as a function of collision energy [1]. Cold neutral molecules are introduced into the reaction chamber through a Stark decelerator [2]; the ionic reactants are held in a linear Paul ion trap. The ensemble of laser-cooled atomic ions within the trap undergoes a phase transition, adopting an ordered structure called a Coulomb crystal [3]. Other non-laser cooled species can be sympathetically cooled into the Coulomb crystal, enabling a range of ionic targets to be prepared.

Reactions are investigated by monitoring the change in the morphology of the crystal over time (observed via laser-induced fluorescence) and by performing time-of-flight mass spectrometry. In particular, a charge exchange reaction between sympathetically cooled Xe^+ ions and deuterated isotopologues of ammonia is studied using a novel damped cosine ion trap [4].

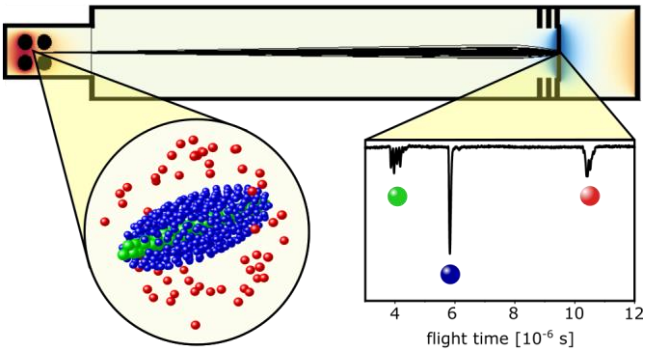

Fig. 1 Pictorial view of the detection process. Coulomb crystals are formed within the ion trap and subsequently ejected towards an MCP detector in order to perform time-of-flight mass-spectrometry.

References

[1] B. R. Heazlewood and T. P. Softley, *Low-Temperature Kinetics and Dynamics with Coulomb Crystals*, Annu. Rev. Phys. Chem. 66 475-495 (2015).

[2] H.L. Bethlem, G. Berden, G. Meijer, *Decelerating Neutral Dipolar Molecules*, Phys. Rev. Lett., 83 1558–61 (1999).

[3] S. Willitsch, M. T. Bell, A. Gingell, S. R. Proctor, T. P. Softley, *Cold Reactive Collisions between Laser-Cooled Ions and Velocity-Selected Neutral Molecules*, Phys. Rev. Lett.,100 043203 (2008).

[3] K. A. E. Meyer, L. L. Pollum, L. S. Petralia, A. Tauschinsky, C. J. Rennick, T. P. Softley, and B. R. Heazlewood, *Ejection of Coulomb Crystals from a Linear Paul Ion Trap for Ion–Molecule Reaction Studies*, J. Phys. Chem. A, 119 (50), (2015)

Lifetime measurements of bound metastable levels in the carbon-group anions: Si^-, Ge^-, Sn^-

O. M. Hole[1], M. Kaminska[1], KC Chartkunchand[1], R. Nascimento[1], H. Hartman[3,4], A. Pehlivan[3], H. Nilsson[4], A. Engqvist[1], E. Bäckström[1], M. Gatchell[1], A. Källberg[1], P. Löfgren[1], P. Reinhed[1], S. Rosén[1], A. Simonsson[1], R. D. Thomas[1], D. Hanstorp[2], S. Mannervik[1], H. T. Schmidt[1], and H. Cederquist[1]

1. Department of Physics, Stockholm University, SE-106 91 STOCKHOLM, Sweden
2. Department of Physics, Göteborg University, SE-412 96 GÖTEBORG, Sweden
3. Material Sciences and Applied Mathematics, Malmö University, 205 06 MALMÖ, Sweden
4. Lund Observatory, Lund University, Box 43, 221 00 LUND, Sweden

The Double ElectroStatic Ion Ring ExpEriment (DESIREE) is a tool with the primary goal of investigating interactions between internally cold anions and cations at very low center-of-mass energies [1,2]. The storage rings are situated within a cooled chamber (∼13 K) which limits the amount of black-body radiation. This enables the storage of loosely bound atomic and molecular ions – ions that would rapidly photo-detach at ambient temperatures. The low temperature also enables the rings to have excellent vacuum conditions (10^{-14} mbar) which means that beams can be stored for long periods of time before they are lost due to collisions with the residual gas – 1/e lifetimes of more than 10^3 seconds have been measured for several anions [1,3].

Here, we present preliminary measurements of the lifetimes of excited, metastable states for Si^-, Ge^- and Sn^-. These ions all have two bound excited states with ^{2}D character with J=3/2 and J=5/2, respectively. The Si^- ion, only, has in a addition a third bound excited state - a $^2P_{1/2}$ state. These excited states all have the same parity as the $^4S_{3/2}$ ground state and therefore electric-dipole transitions are forbidden and they decay slowly to the ground state. The corresponding lifetimes range from seconds to several minutes. We will present preliminary results of the measured intrinsic lifetimes of these metastable states using a similar method as established in earlier measurements of lifetimes of metastable bound states based on the time and wavelength dependencies of photodetachment signals in S^- [3] and Ni^- [4].

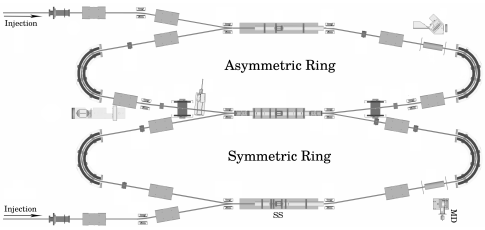

Fig. 1 A schematic of the DESIREE ion optics [1,2]. The measurements were done by probing the stored ion beam with a short laser pulse at the straight section, "SS", of the symmetric ring. This photo-detaches a small fraction of the ions which can then be detected by the detector (MD). By using a laser wavelength either above or below the photo-detachment threshold for the ground state anions, we could selectively detach either from all bound states or just the metastable bound states. This allows for the determination of the lifetimes of the metastable states.

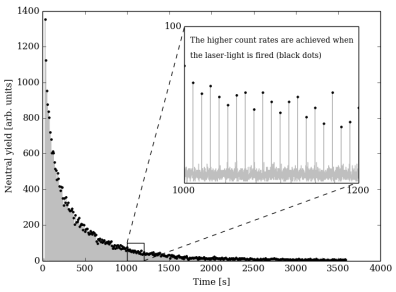

Fig. 2 A typical dataset for measurements detaching all bound states in Sn^- - the two bound (^{2}D) finestructure levels and the $^4S_{3/2}$ ground state with the probing laser set to 532 nm. As can be seen in the inset the data points (black dots) are well above the background level. The main contributions to the background are detector noise and ion neutralization due to rest-gas collisions.

References

[1] H. T. Schmidt et al., *First storage of ion beams in the Double Electrostatic Ion-Ring Experiment: DESIREE*, Rev. Sci. Instrum. **84**, 055115 (2013).

[2] R. D. Thomas et al., *The double electrostatic ion ring experiment: A unique cryogenic electrostatic storage ring for merged ion-beams studies*, Rev. Sci. Instrum. **82**, 065112 (2011).

[3] E. Bäckström et al., *Storing keV Negative Ions for an Hour: The Lifetime of the Metastable $^2P^o_{1/2}$ level in $^{32}S^-$*, Phys. Rev. Lett. **114**, 143003 (2015).

[4] M. Kaminska et al., *The lifetime of the bound excited level in Ni^-*, Phys. Rev. A **93**, 012512 (2016).

Centrifuge Deceleration of Internally Cold Polyatomic Molecules from a Cryogenic Buffer-Gas Cell

T. Gantner[1], X. Wu[1], M. Koller[1], M. Zeppenfeld[1], S. Chervenkov[1], and G. Rempe[1]
1. Max-Planck-Institut für Quantenoptik, Hans-Kopfermann-Str. 1, D-85748 Garching, Germany

Beams of translationally slow and internally cold polar molecules offer an indispensable tool for studying collision dynamics and reaction pathways in the cold regime, and open new avenues for controlled chemistry, precision spectroscopy, and exploration of fundamental physics, e.g., measurement of the dipole moment of the electron. The production of bright beams of slow molecules with high internal-state purity, however, still presents a challenge.

To measure the rotational temperature of the molecules cooled in a cryogenic buffer-gas cell [1], we developed a radio-frequency depletion method for guided molecules [2], which yields accurate information on their internal-state distribution. Using this technique together with Monte-Carlo trajectory simulations, we can determine the rotational temperature of the molecules leaving the buffer-gas cell. Exploring the process of buffer-gas cooling in both the effusive and the supersonic regime showed rotational temperatures down to 4.1 K and 1.6 K, respectively.

Furthermore, we demonstrated the deceleration of molecules from the buffer-gas cell in the effusive regime, employing the centrifugal force in a rotating frame [2]. We optimized the system to maximize the flux of slow molecules, achieving intense continuous beams with fluxes of about $7 * 10^9$ molecules/s at velocities below 20 m/s. To demonstrate the generality of these methods, we implemented the thermometry as well as the deceleration technique for two different molecules, CH_3F and CF_3CCH.

References

[1] L. D. van Buuren, C. Sommer, M. Motsch, S. Pohle, M. Schenk, J. Bayerl, P. W. H. Pinkse, and G. Rempe, *Electrostatic Extraction of Cold Molecules from a Cryogenic Reservoir*, Phys. Rev. Lett. **102**, 033001 (2009).

[2] S. A. Rangwala, T. Junglen, T. Rieger, P. W. H. Pinkse, and G. Rempe, *Continuous source of translationally cold dipolar molecules*, Phys. Rev. A **67**, 043406 (2003).

[3] S. Chervenkov, X. Wu, J. Bayerl, A. Rohlfes, T. Gantner, M. Zeppenfeld, and G. Rempe, *Continuous Centrifuge Decelerator for Polar Molecules*, Phys. Rev. Lett. **112**, 013001 (2014).

On the VUV Emission Spectrum Excited by Electron Impact on the Gas-Phase Alanine

H. G. Bohachov, R. V. Tymchyk

Institute of Electron Physics, Universitetska 21, Uzhhorod, 88000 Ukraine

Biomolecule fragmentation under the low-energy electron influence is being studied extensively using the mass-spectrometry technique [1]. However, in this case the role of the fragments produced due to excitation remains not clarified. This paper is devoted to studying the VUV-emission spectra produced in the electron collisions with the alanine molecules that could be useful for understanding the fragment excitation role.

Present work was carried out using the crossed electron and molecular beam technique applying the concave diffraction grating vacuum monochromator described in detail elsewhere [2]. The beam of the molecules under study was formed from the fine-crystalline alanine powder by means of heating in the oven provided with a cylindrical channel. The oven was kept at the 100–120^{o}C temperature, i.e. substantially below the alanine decomposition temperature (297^{o}C).

The emission spectra were recorded in the 112–180 nm region at the electron energies from 20 to 100 eV. The above spectrum measured at the 100 eV energy is shown in Fig. 1. Note that at the electron energies above 40 eV the resonance atomic hydrogen 121.6 nm line dominates. A number of more long-wavelength emissions are observed in the above spectra (see Fig. 1). It is easy to state that, using the compilation data [3], some of them could be assigned to the atomic oxygen (115.0, 130.0, 135.5 nm), carbon (127.5, 156.1 nm) and nitrogen (120.0, 124.3 nm) spectra.

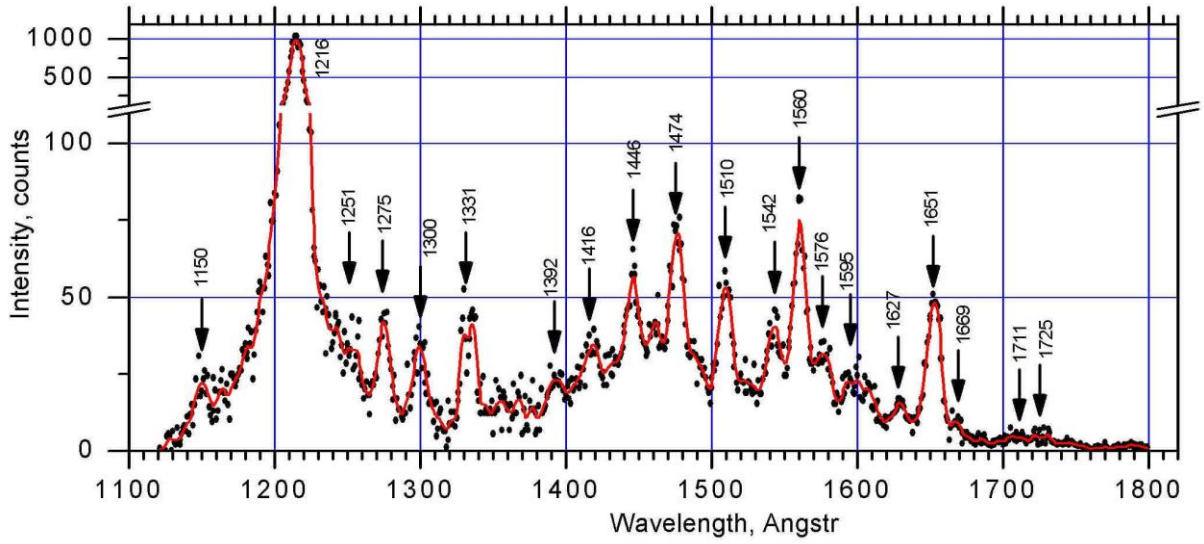

Fig. 1 Emission spectra recorded at the 100 eV electron energy.

The mechanisms of the appearance of the other emissions in the spectrum are analyzed.

References

[1] L. Sanche, *Eur. Phys. J.* **D 35**, 367 (2005).
[2] I. S. Aleksakhin, G. G. Bogachev, I. P. Zapesochnyi, S. Yu. Ugrin, *Sov. Phys. JETP* **53**, 1140 (1981).
[3] P. J. M. van der Burgt, W. B. Westerveld, J. S. Risley, *J. Phys. Chem. Ref. Data* **18**, 1757 (1989).

Stabilities of porphyrin ions

Linda Giacomozzi[1], Nathalie de Ruette[1], Michael Gatchell[1], Giovanna D'Angelo[1], Henning Zettergren[1], Henning T. Schmidt[1] and Henrik Cederquist[1]

1. Department of Physics, Stockholm University, Stockholm, SE-106 91, Sweden

The importance of porphyrin derivatives is not only connected to biological functions, like respiration or photosynthesis, their presence in the interstellar medium has also been suggested [1, 2]. This raises questions on how they are formed and respond to energetic processing by e.g. photons, electrons, and ions/atoms. Studies of their inherent stabilities may help to shed light on these intriguing issues.

Ionisation and fragmentation of Metallo-TetraPhenyl Porphyrin MTPP (M=metal like Fe or Mn) and TPP have been studied with various mass spectrometric techniques such as e.g. electron impact excitations [3] and two-step laser mass spectrometry [4]. Here, we have studied the stability of MTPP and TPP cations using a Collision Induced Dissociation (CID) type setup which is part of the DESIREE facility at Stockholm University. Briefly, this setup consists of an electrospray ionization source followed by a quadrupole mass filter and a collision gas cell. After the collisions, the ionic fragments are analysed by two pairs of electrostatic deflectors and recorded with a position-sensitive microchannel plate detector. This setup allows us to measure fragment mass spectra at different collision energies (1-13 keV in the laboratory frame) and absolute total fragmentation cross sections from attenuation measurements of the primary ion beam as a function of the gas (e.g. He, Ne, Ar, or Xe) pressure in the cell.

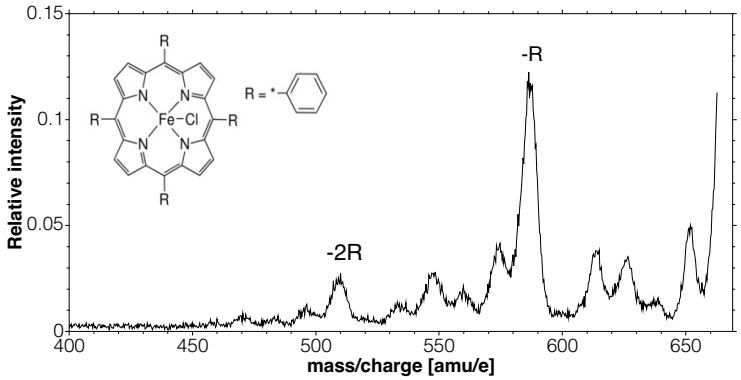

Fig. 1 CID mass spectrum due to collisions between FeTPP cations and He at 80 eV center-of-mass energy.

In Fig. 1, we show the mass spectrum for FeTPP cations colliding with He atoms at a center of mass energy of 80 eV. The spectrum display similar features as those from electron impact studies [3], but the branching ratios are markedly different. The peak corresponding to the intact ion is located at 668 amu in Fig. 1 (off scale). The most prominent fragment mass peak corresponds to the loss of the phenyl group (-R, see the inset in Fig. 1). In between these peaks there are peaks which are significantly stronger compared to those reported in Ref. 3. The reason for this difference is still an open question. To aid in the interpretations of the experimental results, we are currently performing molecular dynamics simulations of the entire collision process. Here, we use a similar approach as was successfully used for studies of PAHs and fullerenes [5-7], which showed that prompt carbon atom knockout is a prominent fragmentation pathway. This gives highly reactive fragments which may not be formed by e.g. photon impact [5-7]. The present simulations will thus provide information on the fragmentation products and reveal if knockout processes are important for porphyrins.

References

[1] F. M. Johnson, *Diffuse interstellar bands: A comprehensive laboratory study*, Spectrochim. Acta A **65** 1154-1179 (2006)

[2] U. J. Meierhenrich, G. M. Muñoz Caro,*et al.*, *Precursor of Biological Cofactors from Ultraviolet Irradiation of Circumstellar/Interstellar Ice Analogues*, Chem. Eur. J. **11** 4895-4900 (2005)

[3] S. Feil, M. Winkler,*et al.*, *Single, double and triple ionization of tetraphenyl iron (III) poprhyrine chloride*, Int. J. Mass Spectr. **255-256** 232-238 (2006)

[4] M. J. Dale, K. F. Costello,*et al.*, *Investigation of Porphyrins and metallo Porphyrins using Two-Step Laser Mass Spectrometry*, J. of Mass. Spectrom. **31** 590-601 (1996)

[5] M. H. Stockett, H. Zettergren,*et al.*, *Nonstatistical fragmentation of large molecules*, Phys. Rev. A. **89**, 032701 (2014).

[6] M. H. Stockett, M. Gatchell,*et al.*, *Fragmentation of anthracene $C_{14}H_{10}$, acridine $C_{13}H_9N$ and phenazine $C_{12}H_8N_2$ ions in collisions with atoms*, Phys. Chem. Chem Phys. **16** 21980 (2014).

[7] M. Gatchell, M.H. Stockett,*et al.*, *Non-statistical fragmentation of PAHs and fullerenes in collisions with atoms*, Int. J. Mass Spectrom. **366(0)** 260-265 (2014)

Spectroscopic Study on Interaction of Tricationic Porphyrin with poly(G)·poly(C) and poly(A)·poly(U) Polynucleotides

Olga Ryazanova[1], Victor Zozulya[1], Igor Voloshin[1], Igor Dubey[2], Larysa Dubey[2], Victor Karachevtsev[1]

1. B. Verkin Institute for Low Temperature Physics and Engineering, Natl. Acad. Sci. of Ukraine, 47 Lenin ave, 61103 Kharkov, Ukraine

2. Institute of Molecular Biology and Genetics, Natl. Acad. Sci. of Ukraine, 150 Zabolotnogo str., 03680 Kyiv, Ukraine

Water soluble porphyrin dyes are compounds having unique photophysical properties and great biological significance. They play a key role in photosynthesis, oxygen transport, redox reactions. Porphyrins and their metallated derivatives, conjugates and supramolecular assemblies are efficiently applied in the medicine and in the nanoelectronics (solar cells etc.). One of them, TMPyP4 porphyrin, is well-known as efficient anti-viral agent, photo sensitizer for PDT, DNA binder and stabilizer of G-quadruplex structures. Its tricationic derivative, $TMPyP^{3+}$ (Fig. 1), was synthesized. It bears the flexible carboxyalkyl linker which greatly facilitates its conjugation with another dyes, oligonucleotides, fullerenes or carbon nanotubes. High biological activity of this compound necessitates careful study not only of its properties themselves, but also of its complexes with biological molecules, one of whose most important representatives are nucleic acids (NA).

Interaction of a tricationic water soluble porphyrin, $TMPyP^{3+}$ with polyribonucleotide duplexes poly(G)·poly(C) and poly(A)·poly(U) has been studied in aqueous buffered solutions, pH 6.9, of low ionic strength in a wide range of molar phosphate-to-dye ratios (*P/D*). To clarify the binding modes of $TMPyP^{3+}$ to the biopolymers the various spectroscopic techniques, including absorption and polarized fluorescence spectroscopy, Raman spectroscopy, and resonance light scattering were used.

The dependence of normalized fluorescence intensity of $TMPyP^{3+}$ porphyrin on *P/D* ratio (Fig. 2) is strongly dependent on the polymer base composition. So upon titration by poly(G)·poly(C) the curve is biphasic. At *P/D* = 0÷3 the porphyrin fluorescence quenching was observed being accompanied by the splitting of emission band, and increase of fluorescence polarization degree, *p*. The porphyrin Soret absorption band (SAB) exhibits 43 % hypochromism and 5 nm red shift;. The linear dependence of fluorescence intensity on *P/D* indicates external electrostatic binding of the cationic porphyrin to negatively charged phosphate backbone of NA with self-stacking of nearest dye molecules. The minimal emission level, 52% from initial, was fixed at *P/D* = 3 corresponding to the stoichiometric binding. Rise of resonance light scattering (RLS) signal evidence formation of extended aggregates (Fig. 3). Further increase of *P/D* results in the enhancement of porphyrin emission, rise of *p* up to 0.08, 15 nm red shift of SAB, small red shifts of fluorescence peaks, as well as the reduction of the light scattering. In such a way, another competitive binding mode predominated at high *P/D* ratios was identified as embedding of the porphyrin *J*-dimers into the groove of poly(G)·poly(C). For $TMPyP^{3+}$ bound to poly(A)·poly(U) substantially different behavior was observed at *P/D* < 3. There is sharp increase in its emission intensity (Fig. 2), splitting of fluorescence band and rise of *p*, 49 % hypochromism and 14 nm red shift of SAB, and more significant enhancement of RLS signal (Fig. 3). So at low *P/D* ratios outside electrostatic binding without the porphyrin self-stacking was assumed, but with formation of large unordered aggregates. At high *P/D* the same groove binding mode is suggested as in the case of poly(G)·poly(C). It manifests itself by gradual enhancement of the porphyrin emission, red shifts of absorption/fluorescence bands and rise of *p* up to 0.1. RLS signal remains high throughout all *P/D* range (Fig. 3) indicating existence of large aggregates in solution. These findings provide new insight into the features of molecular interactions between porphyrins and nucleic acids.

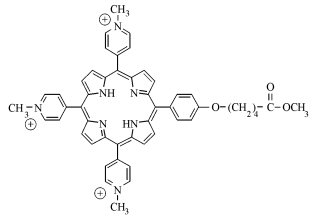

Fig. 1. Molecular structure of tricationic *meso*-porphyrin, $TMPyP^{3+}$.

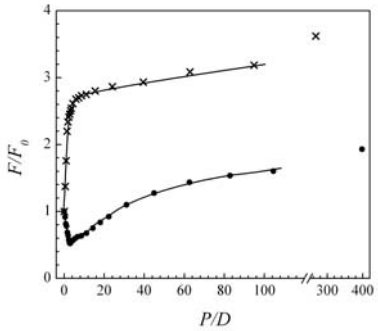

Fig. 2 Dependence of relative $TMPyP^{3+}$fluorescence intensity of on *P/D* ratio upon titration by poly(A)·poly(U) (×) and poly(G)·poly(C) (●) in 5 mM phosphate buffer pH6.9, C_{dye}= 10 μM, λ_{exc}=500 nm, λ_{obs}= 680 nm.

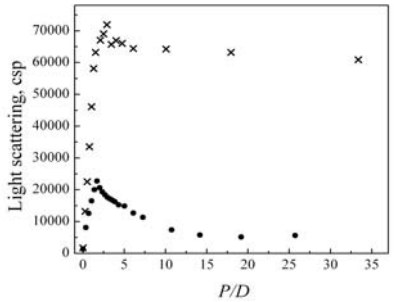

Fig. 3 Dependence of the resonance light scattering intensity at λ = 500 nm on *P/D* ratio for $TMPyP^{3+}$ complex with poly(A)·poly(U) (×) and poly(G)·poly(C) (●) in 5 mM phosphate buffer, pH6.9, [$TMPyP^{3+}$] = 10 μM

Isomerization and Fragmentation of Retinal Chromophore Derivatives

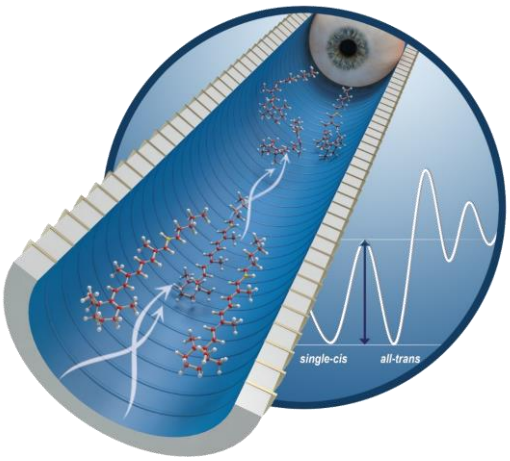

Yoni Toker
Department of Physics, Bar Ilan University, Ramat Gan 5290002, Israel

L. Musbat[1], J. Dilger[2], M. Nihamkin[1], S. Assis[1], S. Itzhak[1], A. V. Bochenkova[3], M. Sheves[4], D. Clemmer[5]

1. Department of Physics, Bar Ilan University, Ramat Gan 5290002, Israel
2. Spectrum Warfare Systems Department, NSWC Crane Division, Crane, IN 47522, USA
3. Department of Chemistry, Moscow State University, 119991 Moscow, Russia
4. Chemistry Department, Weizmann Institute of Science, Rehovot 978007, Israel.
5. Department of Chemistry, Indiana University, Bloomington, Indiana 47405, USA.

All known forms of vision rely on one specific chromophore as their photon detector- the retinal protonated Schiff base (RPSB). The RPSB, located in the centre of Opsin proteins, acts as an optical switch – whereby following the absorption of a photon it undergoes a photoisomerization. One approach to understand what makes this molecule so unique is by studying derivatives of the chromophore and thus examining how the photo properties of the chromophore depend on its exact structure.

Recently our group and others have used two stages of ion-mobility spectroscopy to study isomerization and gas phase fragmentation of the RPSB, and have shown that the barrier energy for isomerization is much lower than within the protein. Here we extend these studies to derivatives of the chromophore and show how minute changes to the structure of the chromophore have dramatic effects on its isomerization properties.

References

[1] J. Dilger, L. Musbat, M. Sheves, A. B. Bochenkova, D. E. Clemmer, Y. Toker, Ang Chemie Int. Ed. 127 (2015), 4830.
[2] Coughlan, Bieske et al. PCCP 17 (2015), 22623
[3] Y. Toker, D. B. Rahbek, H. V. Kiefer, J. Rajput, R. Antoine, P. Dugourd, S. Brønsted Nielsen, A. V. Bochenkova, L. H. Andersen PCCP 15 (2013), 19566.
[4] N. Coughlan, E. Bieske et al., JPCL 5 (2015), 3195.
[5] N. A. Pierson and D Clemmer Int. J. Mass. Spec **377** (2014), 646.

maXs: Micro-calorimeter Arrays for High Resolution X-Ray Spectroscopy in Atomic Physics

D.Hengstler[1], C.Schötz[1], M.Krantz[1], J.Geist[1], M. Keller[1], P.Schneider[1], L.Gamer[1], A.Fleischmann[1], S.Kempf[1], L.Gastaldo[1], C.Enss[1], T.Gassner[2], R.Märtin[2], G.Weber[2], T.Stöhlker[2]

1. Kirchhoff Institute for Physics, Heidelberg University, INF 227, 69120 Heidelberg, Germany
2. Helmhotz Institut Jena, Fröbelstieg 3, 07743 Jena, Germany

We recently started the development of 2-dimensional arrays of metallic magnetic calorimeters (MMCs) for x-ray spectroscopy on highly charged heavy ions stored in EBITs and storage rings. MMCs are energy dispersive particle detectors operated at temperatures below 50 mK, which use a paramagnetic temperature sensor to convert the temperature upon the absorption of a single x-ray photon into a change of magnetic flux in a SQUID [1,2].
The detector system maXs uses a dry dilution refrigerator with long side arm as common cryogenic platform for 3 detector arrays, each consisting of 8x8 x-ray absorbers with optimized size and thickness for 20/30/200 keV x-rays having an energy resolution below 2/5/50eV. The detector geometry shares many details with the successful one-dimensional predecessors maXs-20/200, where the one for soft x-rays has an instrumental linewidth of 1.6 eV(FWHM) in the investigated energy range up to 6 keV.
We believe to be able to further enhance this energy resolution and push the resolving power of MMCs beyond 10000 by implementing: i) overhanging absorbers on small cross-section stems to reduce the loss of hot phonons and to eliminate position dependencies, ii) paramagnetic sensors made of Ag:Er instead of Au:Er to eliminate the hanging heat capacity carried by Au nuclei in the vicinity of Er ions, iii) a novel fast high resolution susceptibility thermometer to stabilize the operating temperature of the detector platform and allow for unprecedented total gain stability.
We discuss the physics of MMCs and the considerations that went into the design of our 2d-arrays. We present recent results on first maXs-30 arrays, including the linearity, the crosstalk between pixels and the improvement of the signal shapes introduced by the new sensor material Ag:Er. In addition, we show first results of measurements at the experimental storage ring ESR at GSI (Darmstadt, Germany), where we used the linear 1x8 pixel array maXs-200, optimized for hard x-rays, for the high resolution x-ray spectroscopy of H- and He-like Xe [3]. The demonstrated combination of stopping power, energy resolution, linearity and dynamic range will trigger numerous novel approaches in high precision atomic physics experiments with stored ion beams.

References

[1] Cryogenic Particle Detection ed. C. Enss, Topics Appl. Phys. 99 (2005)
[2] Metallic magnetic calorimeters, A. Fleischmann et al.: AIP Conf. Proc. 1185, 571 (2009)
[3] Towards FAIR: first measurements of metallic magnetic calorimeters for high-resolution x-ray spectroscopy at GSI, D. Hengstler, M. Keller, C. Schötz, J. Geist, M. Krantz, S. Kempf, L. Gastaldo, A. Fleischmann, T. Gassner, G. Weber, R. Märtin, Th. Stöhlker, and C. Enss, Physica Scripta 2015, 014054 (2015)

Dominant higher-order resonant contributions to Fe K_α x-ray line polarization in anisotropic ∼7 MK plasmas

Chintan Shah[1,2], Pedro Amaro[1], René Steinbrügge[2], Sven Bernitt[2,3], Christian Beilmann[1,2], Stephan Fritzsche[3], Andrey Surzhykov[4], José R. Crespo López-Urrutia[2], and Stanislav Tashenov[1]

[1]*Physikalisches Institut, Im Neunheimer feld 226, 69120 Heidelberg, Germany*
[2]*Max–Planck–Institut für Kernphysik, Saupfercheckweg 1, 69117 Heidelberg, Germany*
[3]*Friedrich-Schiller-Universität Jena, Fürstengraben 1, 07743 Jena, Germany*
[4]*Helmholtz-Institut, Helmholtzweg 4, 07743 Jena, Germany*

Resonantly captured electrons with energies below the excitation threshold are the strongest source of x-ray line formation in plasmas at $2 \leq T_e \leq 20$ MK containing highly charged Fe ions. The angular distribution and polarization of x rays emitted due to these processes were experimentally studied using an electron beam ion trap. Polarization due to dielectronic recombination of $Kr^{28+..34+}$ was measured using Compton polarimetry [1]. Later, the electron-ion collision energy was scanned over the *KLL* dielectronic, trielectronic and quadruelectronic recombination resonances of Fe and Kr ions with a resolution of ∼ 6 eV. The angular distribution of x rays was measured along and perpendicular to the electron beam propagation direction.

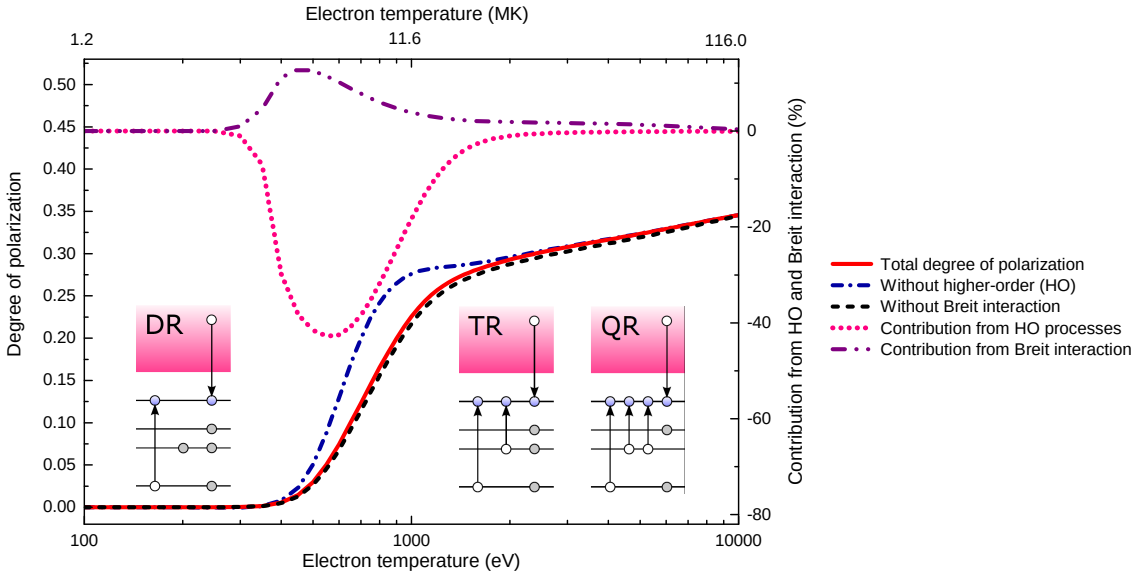

Fig. 1 Maximum polarization of iron K_α x rays due to resonant recombination as a function of the plasma temperature. Higher-order trielectronic and quadroelectronic recombination transitions dominate total polarization in the temperature range of 500–1500 eV (or 7–14 MK).

The data reveal the alignment of the populated excited states and show a high sensitivity of these parameters to the relativistic Breit interaction [1, 2]. We found that most of the transitions lead to polarization, including hitherto neglected trielectronic and quadruelectronic resonances. These channels dominate not only the ionization balance but also the polarization of the prominent K_α x rays emitted by hot anisotropic plasmas in a broad range temperature range (see Fig. 1). Our results comprehensively benchmark full-order atomic calculations done with the FAC [3] and RATIP [4] codes. We conclude that accurate polarization diagnostics of hot anisotropic plasmas, e. g., of solar flares and active galactic nuclei, and laboratory fusion plasmas of tokamaks can only be obtained under the premise of inclusion of relativistic and higher-order resonances which were neglected in previous work.

References

[1] C. Shah, H. Jörg, S. Bernitt, S. Dobrodey, R. Steinbrügge, C. Beilmann, P. Amaro, Z. Hu, S. Weber, S. Fritzsche, A. Surzhykov, J. R. Crespo López-Urrutia and S. Tashenov, *Polarization measurement of dielectronic recombination transitions in highly charged krypton ions*, Phys. Rev. A. **92**, 042702 (2015).

[2] H. Jörg, Z. Hu, H. Bekker, M. A. Blessenohl, D. Hollain, S. Fritzsche, A. Surzhykov, J. R. Crespo López-Urrutia, and S. Tashenov, *Linear polarization of x-ray transitions due to dielectronic recombination in highly charged ions*, Phys. Rev. A **91**, 042705 (2015).

[3] M. F. Gu, *The flexible atomic code*, Can. J. Phys. **86**, 675 (2008).

[4] S. Fritzsche, *The Ratip program for relativistic calculations of atomic transition, ionization and recombination properties*, Comput. Phys. Commun. **183**, 1525-1559 (2012).

A new setup for studying the interaction of slow highly charged ions with 2D materials

D. Melinc[1], J. Schwestka[1], R. A. Wilhelm[1], and F. Aumayr[1]

1. Institute of Applied Physics, TU Wien, Wiedner Hauptstraße. 8-10/E134, 1040 Vienna, Austria

Since its discovery [1] the unique electronic properties of ultimately thin single layer graphene (SLG), made of sp^2-hybridized carbon atoms, has attracted enormous attention as an excellent candidate for future nanoelectronics. Disorder, as caused e.g. by collisions with energetic electrons or ions, alter the electronic structure and therefore allow to modify and tailor the properties of this true 2D material. Collision studies between ions and freestanding SLG are also of fundamental interest, because they bridge the gap between atomic collisions in gaseous and those in solid targets [2]. To learn more about the microscopic interaction mechanism we have built a new experimental setup (figure 1) based on the time-of-flight (TOF) technique, which allows us to study electron emission, energy loss and charge exchange associated with highly charged ion impact on SLG simultaneously.

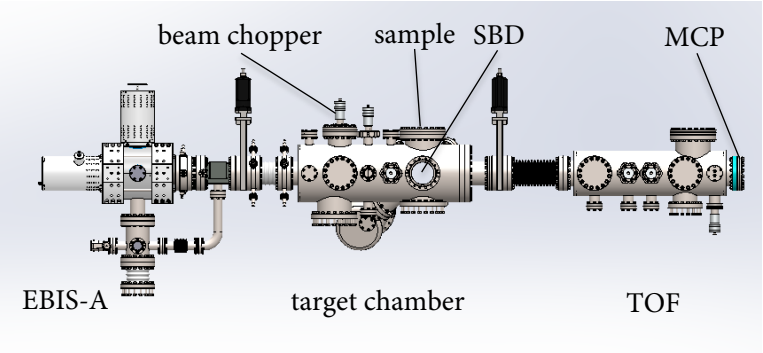

Fig. 1 New experimental setup based on the time-of-flight technique

A room-temperature electron beam ion source (Dreebit EBIS-A), which is equipped with a Wien filter and mounted on a high voltage platform provides highly charged ions of different charge states Q (Xe^{1+} to Xe^{46+}) at kinetic energies ranging from 100eVxQ to 12keVxQ. The ion beam is extracted in a continuous (DC) mode. To generate a start signal in our TOF setup the beam is blanked by a pulsed voltage applied to electric field plates. A set of collimators with an acceptance of <0.5° allows us to use blanking voltages of <50V with a rise/fall time of less then 1ns (GBS Spezialelektronik) [3]. Ions traversing through a SLG sample are recorded by an imaging multi channel plate (MCP) located at the end of the 1.7m long flight path. The MCP signal serves as a stop for the TOF measurement and another electrostatic beam deflector in front of the MCP allows a charge state separation. With this setup we plan to achieve an energy resolution of $\Delta E/E<2\%$, which will be sufficient to measure charge state enhanced kinetic energy loss [2].

In parallel to the TOF a Vienna electron statistics detector is mounted [4]. Electrons emitted from the SLG are attracted by a weak electric field applied to a highly transparent grid mounted as close as possible to the target. This grid shields a surface barrier detector (SBD) biased at 25-30 kV. The quantity of emitted electrons per impact is obtained from the pulse height of the SBD which shows discrete peaks that can clearly be assigned to a certain number of emitted electrons.

With this setup we aim on measure not only energy loss for charged and neutral transmitted ions/atoms, but also on coincidence measurements of charge exchange and electron emission.

References

[1] A. K. Geim and K. S. Novoselov, Nature Mat. **6**, 183 (2007)
[2] R.A. Wilhelm, E. Gruber, R. Ritter, R. Heller, S. Facsko, F. Aumayr, Phys. Rev. Lett., 112, 153201 (2014)
[3] N. Klingner, R. Heller, G. Hlawacek, J. von Borany, J. A. Notte, J. Huang, and S. Facsko, Ultramicroscopy **162**, 91-97 (2015)
[4] G. Lakits, F. Aumayr, and H. Winter, Rev. Sci. Instrum. **60**, 3151 (1989)

Compact 0.86 T room-temperature electron beam ion traps

Peter Micke[1,2], Sven Bernitt[1,3], Klaus Blaum[1], Lisa F. Buchauer[1], Thore M. Bücking[1], André Cieluch[1], Alexander Egl[1], James Harries[4], Daniel Hollain[1], Steven A. King[2], Sandro Kraemer[1], Steffen Kühn[1], Tobias Leopold[2], Thomas Pfeifer[1], Thomas Stöhlker[3], Sven Sturm[1], Joachim Ullrich[2], Robert Wolf[1], Piet O. Schmidt[2,5], José R. Crespo López-Urrutia[1]

1. Max-Planck-Institut für Kernphysik, Saupfercheckweg 1, D-69115, Heidelberg, Germany
2. Physikalisch-Technische Bundesanstalt, Bundesallee 100, D-38116, Braunschweig, Germany
3. Friedrich-Schiller-Universität Jena, D-07737, Germany
4. SPring-8, Hyogo, Japan
5. Leibniz Universität Hannover, D-30167, Germany

Research on multiply and highly charged ions (HCIs) is of great interest not only for atomic physics but also for fundamental studies. Electron beam ion traps (EBITs) have proven to be versatile and indispensable tools for HCI production and study. In an EBIT, an electron beam is compressed by a strong, inhomogeneous magnetic field to breed and trap these ions efficiently. Usually, the magnetic field is generated by superconducting coils, but room-temperature models also exist.

To ease operation we have built a novel room-temperature EBIT based on permanent magnets whereby their magnetic field is guided and focused at the trap center, reaching a value of 0.86 T. Our prototype EBIT can provide a continuous beam of Xe ions up to charge state 29+, and a total ion current of 100 pA, with a 4 mA 2 keV electron beam. Charge states of Xe as high as 36+ were also produced. Pulsed extraction of Ar ions up to charge state 16+ was demonstrated. Following this design we recently started to construct a second generation of four new EBITs. While the protoype currently serves as a HCI source for the Penning trap ALPHA-TRAP, dedicated to high-precision g-factor determinations, the new-generation EBITs will serve as HCI sources for Paul or Penning traps, where precision measurements are performed at low HCI temperatures. In particular, at PTB in Braunschweig we are currently setting up an experiment aiming at quantum logic spectroscopy in a cryogenic Paul trap based on CryPTEx [1, 2] to probe a possible variation of the fine-structure constant and with the ultimate goal to create a novel optical atomic clock based on HCIs. A fourth EBIT will be constructed to provide HCIs for X-ray laser spectroscopy at synchrotron and free-electron laser light sources. This EBIT features a novel off-axis electron gun, which will enable the trap to be used for energy calibration at such facilities. The photon beam then can pass through the EBIT and remains available for beamline users downstream.

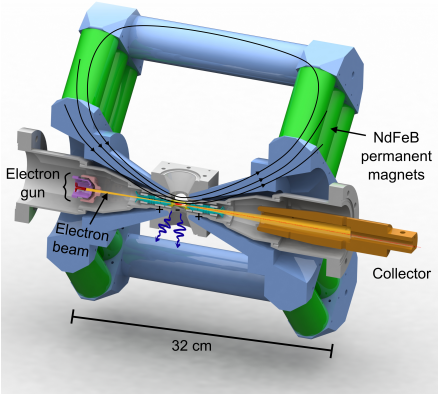

Fig. 1 A cross section of the EBIT showing vacuum chamber, magnetic system, and electrode configuration. The design gives a measured magnetic field of 0.86 T at the trap center. Four ports for optical access with an opening angle of 60° are available.

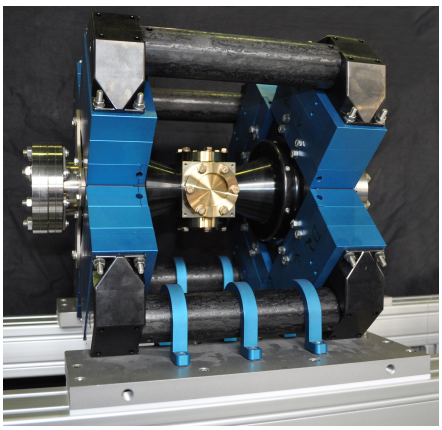

Fig. 2 Magnetic structure of one of the second-generation compact EBITs.

References

[1] Maria Schwarz et al., *Cryogenic linear Paul trap for cold highly charged ion experiments*, Rev. Sci. Instrum. **83**, 083115 (2012).
[2] Lisa Schmöger et al., *Coulomb crystallization of highly charged ions*, Science **347**, 1233-1236 (2015).

Ions collisions to suppress the thermal hysteresis in magnetocaloric thin films

Sophie Cervera[1], Martino Trassinelli[1], Louis Bernard Carlsson[1], Mahmoud Eddrief[1], Victor Etgens[1], Vasilica Gafton[1,2], Emily Lamour[1], Anna Lévy[1], Stéphane Macé[1], Massimiliano Marangolo[1], Christophe Prigent[1], Jean-Pierre Rozet[1], Sébastien Steydli[1] and Dominique Vernhet[1]

1. Institut des NanoSciences de Paris (INSP), Sorbonne Universités, UPMC Univ. Paris 06, CNRS, UMR 7588, 4 Place Jussieu, 75005 Paris, France
2. Alexandru Ioan Cuza University, Faculty of Physics, 11 Carol I Blv, Iasi 700506, Romania

Magnetic materials with giant magnetocaloric effect are promising for application in magnetic refrigeration. But they all exhibit a first-order phase transition and suffer from a large thermal hysteresis which reduces significantly the efficiency of the refrigeration cycle. Several studies aimed at getting rid of the thermal hysteresis but it was to the detriment of the other magnetic properties, inducing for instance a collapse of the refrigerant power [1,2]. Another approach consists of using ion collisions to modify material properties. Nevertheless, most of those studies were focused on magnetic materials with second-order phase transition and using singly charged ions.
Recently, our group demonstrated that the thermal hysteresis of the MnAs thin film can be entirely suppressed by impact of Ne^{9+} at 90 keV whereas other structural and magnetic properties are barely affected [3]. In addition, we show this modification to be stable in time [4], but mechanisms at the origin of the thermal hysteresis suppression were not completely understood.

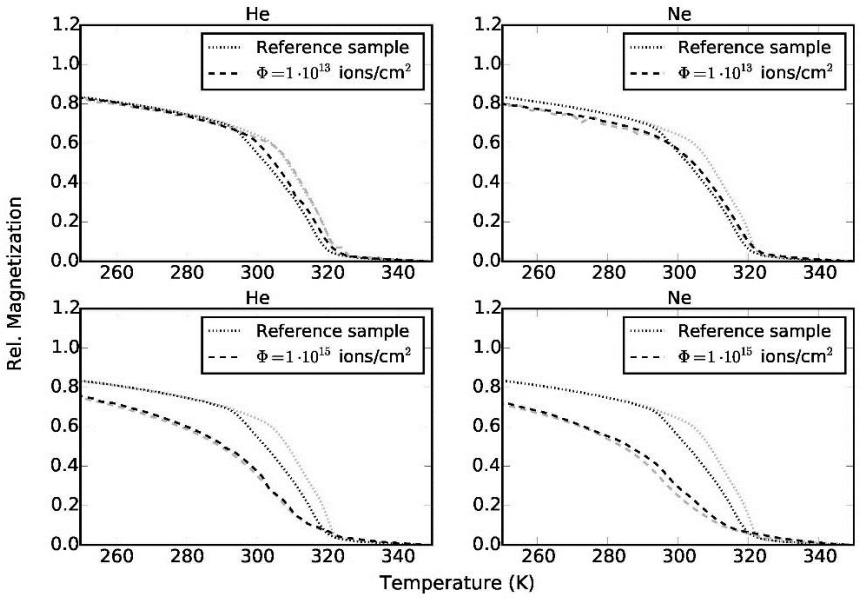

Fig. 1 Relative magnetization of MnAs thin film as a function of temperature for the reference (dotted lines) and for the irradiated samples (dashed lines) with He and Ne ions at two fluences. Data obtained by a temperature increase (grey) and decrease (black).

Trying to disentangle ion implantation effect from and ion collision-induced defects, we investigated the role of different parameters like the projectile mass and energy, and the ion fluence. As displayed in figure 1, comparing helium and neon ion impact at different fluences but with the same penetration depth, the ion mass is playing the major role. This indicates that the binary collision kinematics, at the origin of induced-defects, seems to be the key parameter responsible for the thermal hysteresis suppression. Further investigations are in progress and will be presented at the conference.

References

[1] Jian Liu, et. al., *Giant magnetocaloric effect driven by structural transitions*, Nat. Mater. **11**, 620-626 (2012)
[2] Ariana De Campos, et. al. *Ambient pressure colossal magnetocaloric effect tuned by composition in Mn1-xFexAs*, Nat. Mater. **10**, 802-804 (2006)
[3] Martino Trassinelli, et. al. , *Suppression of the thermal hysteresis in magnetocaloric MnAs thin film by highly charged ion bombardment*, Appl. Phys. Lett. **104**, 081906 (2014)**.**
[4] Sophie Cervera, et.al., *Hints on the origin of the thermal hysteresis suppression in giant magnetocaloric thin films irradiatied with highly charged ions*, J. Phys.: Conf. Ser. **635**, 012028 (2015).

Size determination of neon clusters by fluorescence spectrometry

Xaver Holzapfel[1], Andreas Hans[1], Philipp Schmidt[1], Florian Wiegandt[2], Ltaief ben Ltaief[1], Philipp Reiss[1], Reinhard Dörner[2], Arno Ehresmann[1], André Knie[1]

1. Institut für Physik, Universität Kassel, Heinrich-Plett-Str. 40, 34132 Kassel, Germany

2. Institut für Kernphysik, J. W. Goethe-Universität, Max-von-Laue-Str. 1, 60438 Frankfurt am Main, Germany

Noble gas clusters bound by van-der-Waals forces are well suited to illuminate the size dependent changes of the electronic structure from isolated atoms to bulk material [1]. A usual method for cluster generation is an adiabatic expansion through a nozzle, which yields a distribution of different cluster sizes. The resulting mean cluster size can be calculated from stagnation conditions by using scaling laws, which empirically connect the experimental parameters to the mean cluster size [2]. Yet discrepancies have been reported as different scaling laws differ by factors of two or more [3]. Resonant excitation of outer valence electrons in noble gas clusters by synchrotron radiation yield characteristic informations in the resulting fluorescence yield about the mean cluster size. Here we present a novel way of cluster size determination of clusters by photon induced fluorescence spectrometry (PIFS) [4].

There are different techniques which are used to get a handle on cluster sizes. Usage of electron spectrometry yields information about the degree of condensation, but no detailed information about the cluster sizes. Additionally, the escape probability of electrons is lowered for increasing cluster sizes, due to the small mean free path in dense media. For a direct measurement by mass spectrometry clusters are ionized and often immediately fragment into smaller clusters. Therefore just the mass-to-charge-ratio of the fragmented clusters are achievable and not the initial cluster size itself. Resonant fluorescence measurements are well suited to probe clusters properties as the large mean free path of photons allows an adequate measuring of bulk states.

The binding energies of electrons in a cluster are depending on the total number of particles per cluster and on the position where the excited particle is located, either on the surface or in the bulk. The size information itself is given by the intensity ratios of the surface and bulk states, as sketched in fig. 1. Thereby, the resonance energies of surface and bulk excitations can be measured and the intensity ratios of these determined. Using geometrical approximations for the shape of the clusters, the ratio of the measured intensities can be connected to fixed mean cluster sizes and their calculated ratios of surface and bulk. These characteristic informations are necessary to verify the existing scaling laws and can be used furthermore as a basis for corrections. Experimental results of measurements on neon cluster for different sizes will be discussed in this contribution.

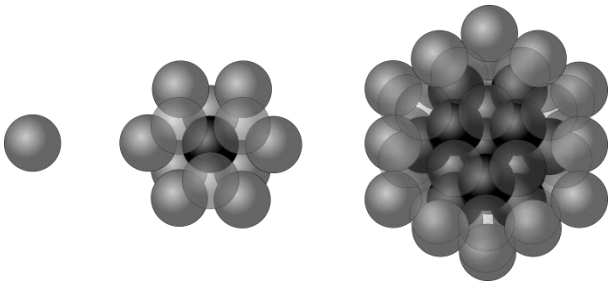

Fig. 1 Schematic noble gas clusters ranging from small (left) to big (right) cluster sizes. The ratio between the number of bulk (black) and the number of surface (grey) particles has certain values for different cluster sizes. Hence, the bulk to surface ratios containes the cluster size informations.

References

[1] Joshua Jortner, *Cluster size effects*, Z. Phys. D **24**, 247 (1992).

[2] Udo Buck, and Reinhard Krohne, *Cluster size determination from diffractive He atom scattering*, JCP **105**, 5408 (1996).

[3] Henrik Bergersen, et al., *Size of neutral argon clusters from core-level photoelectron spectroscopy*, Phys. Chem. Chem. Phys., **8**, 1891 (2006).

[4] André Knie, et al., *Detecting ultrafast interatomic electronic processes in media by fluorescence*, New J. Phys. **16**, 102002 (2014).

X-Ray Photoelectron Spectra and the Electron Structure of the Nanosize Nickel and Cobalt Ferrites

Tatiana Ivanova[1], Michail Kiskin[1], Serguei Savilov[1,2], Roman Linko[3], Gennady Sapozhnikov[4], Vladimir Novotortsev[1], Igor Eremenko[1]

1. Kurnakov Institute of General and Inorganic Chemistry of RAS, 31 Leninskii pr., 119991 Moscow, Russia
2. Department of Chemistry, M. V. Lomonosov Moscow State University, 1-3 Leninskie Goru, 119991 Moscow, Russia
3. Peoples' Friendship Universty, Moscow, 6 Mikluho-Maklaya st., 117198 Moscow, Russia
4. Physico-Technical Institute, Ural Branch, of RAS, Izhevsk, 85-31 Dzerzhinskogo Str., 426039 Izhevsk, Russia

The spectra, electron structure and composition of ferrites nanoparticles MFe_2O_4 (M = Co, Ni) was investigated by X-ray photoelectron spectroscopy (XPS). Ferrites nanoparticles were obtained by thermolysis of the molecular heterometallic complexes $[M^{II}Fe^{III}_2O(Piv)_6(HPiv)_3]$ (M = Co, Ni; Piv is anion pivalic acid). Their thermolysis was carried out on air at 400 ºC. Averaged size of ferrite nanoparticles was 13.3 nm and 19.3 nm according to XPD data. XP-spectra of the samples at room temperature were registered with Axis Ultra DLD spectrometer (Kratos Analytical) (non-monochromatic MgKα radiation, 150 W). The spectra were calibrated using C1s-line energy which refers to the C C/C H bonds; it was taken equal to 285.0 eV. Measurements were done at least two times at a pressure of ~10^{-9} Torr. The binding energies of the M2p, M3s, C1s and O1s levels and satellite lines; the spin-orbit and the multiplet splitting of the M2p, M3s levels were identified. Spectral fitting was accomplished using the Kratos Analytical package. The difference between the states of metal atoms had been determined both from the chemical shift and from the distinction of the satellite structure M2p, M3s, M3p lines. The analysis of nanoparticles consisting of different iron oxides is a serious problem because of their complicated crystalline structure. XPS method may be useful for determining the oxidation state of iron in nanoparticles because the XPS spectra of ions Fe^{II} and Fe^{III} are different. XPS data was suggested that the thermolysis of heterometallic complexes results in compounds of iron oxide with oxides of nickel or cobalt. We revealed features in the spectra of the $Fe2p_{3/2}$ of nickel and cobalt nanoferrites, and inverse spinels $NiFe_2O_4$ and $CoFe_2O_4$. The magnetic states of cobalt and nickel ferrites are different. It was shown amount of $cobalt^{II}$ ions is 60% and they occupy octahedral sites, 40% of cobalt atoms are associated with diamagnetic ions Co^{III} in tetrahedral sites. The obtained values of the binding energy of the metal atoms, the spin-orbit splitting and the relative intensities of the satellites, let to identify the products of thermolysis as oxides with metal ions Co^{II}, Co^{III}, Ni^{II} and Fe^{III}.

ACKNOWLEDGMENTS

This work was supported by the Russian Foundation of Basic Research (project 16-03-00047) and Russian Scientific Foundation (14-23-00176).

Transverse Spin in Structured Light

Martin Neugebauer[1,2], Peter Banzer[1,2,3], Gerd Leuchs[1,2,3]

1. Max Planck Institute for the Science of Light, Guenther-Scharowsky-Straße 1, D-91058 Erlangen, Germany

2. Institute of Optics, Information and Photonics, University Erlangen-Nuremberg, Staudtstraße 7/B2, D-91058 Erlangen, Germany

3. Department of Physics, University of Ottawa, 25 Templeton Street, Ottawa ON K1N 6N5, Canada

A circularly polarized paraxial beam of light carries spin angular momentum either parallel or anti-parallel to its propagation direction, since the electric and magnetic fields are predominately transverse and spin only around the longitudinal axis. In contrast, highly confined fields like guided modes, surface plasmon polaritons or tightly focused beams exhibit longitudinal field components that actually result in electric and/or magnetic fields spinning around a transverse axis [1-4]. Particularly noteworthy is the direct link between propagation direction and the sense of the transverse spin, which can be used for designing novel nano-optcial devices based on spin-orbit coupling [3-7].

Here, we demonstrate how the transverse components of the spin density $s_E^x \propto Im[E_y^* E_z]$ and $s_E^y \propto Im[E_z^* E_x]$ can be measured in the focal plane of highly confined polarization tailored beams [2]. For illustration, Fig. 1a shows the occurrence of transverse spin in a tightly focused radially polarized beam.

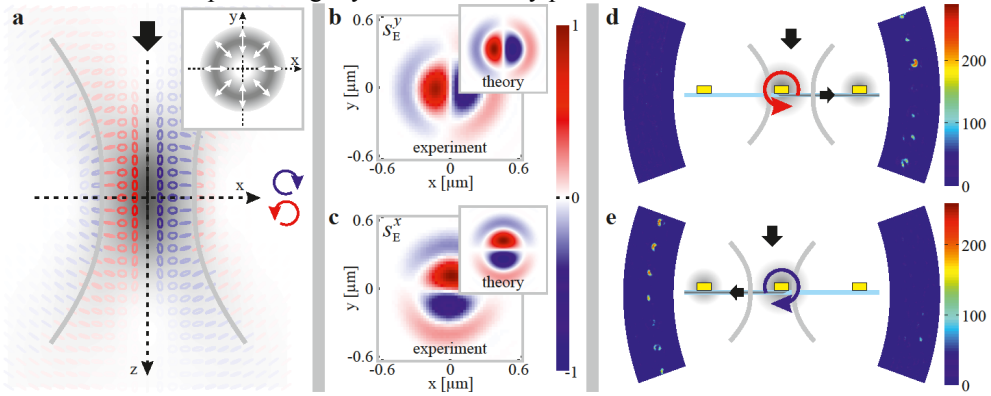

Fig. 1 Measurement and utilization of the transverse spin density of light. (a) Side view of a focused radially polarized beam propagating along *z*. The far-field is locally purely linearly polarized (see inset). The polarization ellipses close to the focal region are indicated in blue (clockwise spinning) and red (counter-clockwise spinning). (b-c) Corresponding measured and calculated focal distributions of the transverse spin density parameters s_E^x and s_E^y. (d-e) Application of the transverse spin density for directional coupling to dielectric waveguides. Probe particles to the left and right of the nano-antenna in the centre light up depending on the local spinning sense of the excitation beam.

The locally purely linear polarization in the far-field (see inset) yields transversely spinning fields in the focal region as indicated by the polarization ellipses in blue (clockwise spinning) and red (counter-clockwise spinning). The corresponding focal distributions of s_E^x and s_E^y are measured with a nano-probe scanning technique (see experimental and theoretical results depicted in Figures 1b-c and ref. 2). The precise knowledge of those distributions allows for the application of the transverse spin for directional coupling to dielectric waveguides [7]. For example, by proper lateral positioning a single gold nano-antenna with respect to the radially polarized excitation beam, the orientation of the induced spinning dipole moment can be controlled. In the experimental scheme as sketched in Figures 1d-e, the counter-clockwise spinning dipole yields coupling to the right side and clockwise spinning yields coupling to the left. For verification of the coupling directivity, we image probe particles to the left and right of the central nano-antenna.

References

[1] Peter Banzer, Martin Neugebauer, Andrea Aiello, Christoph Marquardt, Norbert Lindlein, Thomas Bauer, and Gerd Leuchs, *The photonic wheel - demonstration of a state of light with purely transverse angular momentum*, J. Eur. Opt. Soc, Rapid Publ. **8**, 13032 (2013).

[2] Martin Neugebauer, Thomas Bauer, Andrea Aiello, and Peter Banzer, *Measuring the Transverse Spin Density of Light*, Phys. Rev. Lett. **114**, 063901 (2015).

[3] Andrea Aiello, Peter Banzer, Martin Neugebauer, and Gerd Leuchs, *Beyond beam optics – From transverse angular momentum to photonic wheels*, Nat. Photon. **9**, 789 (2015).

[4] Konstantin Y. Bliokh, Francisco J. Rodríguez-Fortuño, Franco Nori, and Anatoly V. Zayats, *Spin-orbit interactions of light*, Nat. Photon. **9**, 796 (2015).

[5] Francisco J. Rodríguez-Fortuño, Giuseppe Marino, Pavel Ginzburg, Daniel O'Connor, Alejandro Martínez, Gregory A. Wurtz, and Anatoly V. Zayats, *Near-Field Interference for the Unidirectional Excitation of Electromagnetic Guided Modes*, Science **340**, 328 (2013).

[6] Christian Junge, Danny O'Shea, Jürgen Volz, and Arno Rauschenbeutel, *Strong Coupling between Single Atoms and Nontransversal Photons*, Phys. Rev. Lett. **110**, 213604 (2013).

[7] Martin Neugebauer, Thomas Bauer, Peter Banzer, and Gerd Leuchs, *Polarization Tailored Light Driven Directional Optical Nanobeacon*, Nano Lett. **14**, 2546 (2014).

Photoelectron spectroscopic view to the structure of binary clusters

Kari Jänkälä[1], Lauri Hautala[1], Esko Kokkonen[1], Mikko-Heikki Mikkelä[2], Maxim Tchaplyguine[2], Marko Huttula[1]

1. Centre for molecular materials research, University of Oulu, Box 3000, 90014 University of Oulu, Finland
2. MAX IV Laboratory, Lund University, Box 118, 22100 Lund, Sweden

Clusters constitute an intermediate phase between single atoms and the solid state, and their properties evolve from atomic and molecular to bulklike as a function of size. In addition to exhibiting characteristics of these two extremes, clusters have unique features not seen in other forms of matter. For unravelling these properties, research of clusters has grown to an active area of science at many different fields of spectroscopy.

Small clusters constituting atoms in the range of few to few hundred atoms made from elements that are solid at room temperature are notoriously difficult to produce at large quantities, which is why most photoelectron spectroscopic studies of clusters have been carried out using laser ionization. The use of synchrotron radiation, however, opens new possibilities for clusters studies. For example, one may look at site specific core-shell ionization and resonant excitations, study X-ray scattering and different Auger decay processes. These studies give a different viewpoint to cluster physics and provide new challenges for the theory describing the observed phenomena.

Recently researchers at Oulu University, Finland, in collaboration with researchers from Lund and Uppsala Universities, have carried out studies on initially neutral clusters produced by an exchange pick-up source [1]. These experimental and theoretical studies have concentrated on valence [1,2] and core ionization of metallic clusters [4], doped water clusters [5] and molecular clusters made from different salts [6]. The focus of the studies has varied from the research of developing fundamental understanding of jellium and conduction sphere models for metal clusters [3,4] to solubility of salt at nanoscale environments [5] and investigation of site specific photoionization of salt clusters [6]. The studies have combined experimental measurements at synchrotron radiation sources to theoretical modelling done at *ab initio* and semi-empirical levels. As an example, our recent investigation on the site-specific inner-shell ionization of RbCl and CsCl cluster as a function of mean size combined with theoretical calculations for the chemical shifts provided a way to study the cluster geometry via variations in the intensity profiles of the observed photoelectron spectra [6].

The presentation at ECAMP12 will provide an overview to our present and recent research on initially neutral clusters. The focus will be put to the theoretical means and methods used to understand the experimental photoelectron spectroscopic data collected at synchrotron radiation sources [3,7,8] and as showcase a recent studies on RbCl, RbBr, CsCl and CsBr clusters will be presented. In addition, our recent developments in producing binary clusters from liquid and solid samples will be discussed. A new cluster source capable of producing mixed liquid clusters at freely variable concentration, a modified exchange pick-up source that can be used to make clusters from two different solid at room temperature elements will be described and a reaction chamber source providing the possibility to study reactivity of nanoscale particles will be presented.

References

[1] M. Huttula, M.-H. Mikkelä, M. Tchaplyguine, and O. Björneholm, *Size-varied photoelectron spectroscopy of metal clusters using the Exchange Metal Cluster Source*, J. Electron Spectrosc. Relat. Phenom. **181**, 145 (2010).

[2] K. Jänkälä, M. Tchaplyguine, M.-H. Mikkelä, O. Björneholm, and M. Huttula, *Photon Energy Dependent Valence Band Response of Metallic Nanoparticles*, Phys. Rev. Lett. **107**, 183401 (2011).

[3] K. Jänkälä, M.-H. Mikkelä, and M. Huttula *Valence photoionization of free, neutral, and size-varied alkali metal clusters*, J. Phys. B: At. Mol. Opt. Phys. **44**, 105101 (2011).

[4] M.-H. Mikkelä, M. Tchaplyguine, S. Urpelainen, K. Jänkälä, O. Björneholm, and M. Huttula, *Photoelectron spectroscopy of unsupported bismuth clusters: Size related effects of metallic properties*, J. Appl. Phys. **112**, 084326 (2012).

[5] L. Partanen, M.-H. Mikkelä, M. Huttula, M. Tchaplyguine, C. Zhang, T. Andersson, and O. Björneholm, *Solvation at nanoscale: Alkali-halides in water clusters*, J. Chem. Phys. **138**, 044301 (2013).

[6] L. Hautala, K. Jänkälä, M.-H. Mikkelä, M. Tchaplyguine, and M. Huttula, *Surface site coordination dependent responses resolved in free clusters: applications for neutral sub-nanometer cluster studies*, Phys. Chem. Chem. Phys. **17**, 7012 (2015).

[7] T. Löytynoja, J. Niskanen, K. Jänkälä, O. Vahtras, Z. Rinkevicius, and H. Ågren *Quantum Mechanics/Molecular Mechanics Modeling of Photoelectron Spectra: The Carbon 1s Core–Electron Binding Energies of Ethanol–Water Solutions*, J. Phys. Chem. B **118**, 13217 (2014).

[8] S. A. Galitskiy, A. N. Artemyev, K. Jänkälä, and Ph. V. Demekhin, *Hartree-Fock calculation of the differential photoionization cross sections of small Li clusters* J. Chem. Phys. **142** 034306 (2015).

Internal energy measurement of small anionic metal clusters

Sebastian George[1], Klaus Blaum[1], Christian Breitenfeldt[1,2], Jürgen Göck[1], Jonas Karthein[1], Thomas Kolling[3], Christian Meyer[1], Jennifer Mohrbach[3], Gereon Niedner-Schatteburg[3], Dirk Schwalm[1,4], Lutz Schweikhard[2], Andreas Wolf[1]

1. Max-Planck-Institut für Kernphysik, 69117 Heidelberg, Germany
2. Institut für Physik, Ernst-Moritz-Arndt-Universität, 17487 Greifswald, Germany
3. Fachbereich Chemie, Universität Kaiserslautern, 67663 Kaiserslautern, Germany
4. Department of Particle Physics, Weizmann Institute of Science, Rehovot 76100, Israel

The Cryogenic Trap for Fast ion beams (CTF) [1] located at the Max-Planck-Institut für Kernphysik (MPIK) is an electrostatic ion beam trap (EIBT) setup. It is well suited to investigate dynamical processes of stored ion beams and can be operated at temperatures ranging from room temperature down to 10 K. Vibrational electron autodetachment, also called delayed electron detachment, is monitored by recording the rate of neutralized particles escaping from the EIBT as a function of storage time and, in case of laser-induced electron loss processes, as a function of the time after laser excitation.

Ro-vibrationally excited ions with internal temperatures of several hundred Kelvin are produced in a caesium ion sputter source and stored in the CTF at room temperature for several seconds. The ions' internal energy distribution was probed by measuring the change in the laser-induced delayed electron detachment rate as a function of the photon energy. The internal energy distribution could be followed over the storage time of 6 s until equilibrium with the room-temperature environment was almost reached.

The CTF was constructed as the test facility for the new Cryogenic Storage Ring (CSR) [2] commissioned at the MPIK. At the CSR ground-state spectroscopy on molecular and cluster ions employing photons, electrons and neutral atoms as interaction partners is a fundamental part of the physics program. As a consequence, ion sources producing ions close to their ro-vibrational ground state are needed to avoid waiting times while the ions cool down. Therefore, a laser vaporization source was installed at the CTF. By employing a supersonic helium expansion the ions were cooled during production. Their internal energies were probed by laser-induced delayed electron detachment experiments as described before. Recent results will be presented.

References

[1] M. Lange *et. al., A cryogenic electrostatic trap for long-time storage of keV ion beams*, Rev. Sci. Instrum. **81**, 055105 (2010).
[2] R. von Hahn *et. al., The Cryogenic Storage Ring CSR* (submitted)

Antiproton energy loss distribution in He gas

Sándor Borbély[1], Iva Brezinova[2], Stefan Nagele[2], Fabian Lackner[2], Ladislau Nagy[1], Károly Tőkési[3,4], Joachim Burgdörfer[2]

1. Faculty of Physics, Babeş-Bolyai University, 400084 Cluj-Napoca, Romania, EU
2. Institute for Theoretical Physics, Vienna University of Technology, 1040 Vienna, Austria, EU
3. Institute of Nuclear Research, Hungarian Academy of Sciences (ATOMKI), P.O. Box 51, H-4001 Debrecen, Hungary, EU
4. ELI-ALPS, ELI-HU Non-profit Ltd., Dugonics tér 13, H-6720 Szeged, Hungary, EU

Several aspects of the penetration of charged particles in matter have been studied over the last more then hundred years. Triggered by the pioneering work of Bohr [1-2] the energy loss mechanisms of charged particles penetrating matter were investigated extensively both theoretically and experimentally. A comprehensive overview of these studies can be found in reference [3]. The primary parameter describing the stopping of charged particles in matter is the mean energy loss per traveled path-length (or alternatively by the stopping cross section). Additional information on the stopping process is provided by the straggling, which is the mean squared deviation of the energy loss per traveled path-length (or straggling cross section). Even at the level of these integrated quantities the discrepancies between the experiments and theoretical calculations are quite large (see in [4]). In order to resolve the existing discrepancies new high precision calculations for prototypical systems are required. A good starting point for such a calculation is our *ab initio* approach [5], which solves the fully-correlated two-electron time-dependent Schrödinger equation for the antiproton-He collision. At fixed $E_{\overline{p}}$ antiproton impact energies and b impact parameters our calculation provides high precision $P_{i\to f}(E_{\overline{p}},b)$ transition probabilities from the Ψ_i ground state to the Ψ_f final state. As final channels the single excitation, single ionization and double ionization are considered. From these probabilities the antiproton energy, and impact parameter dependent stopping power is calculated as

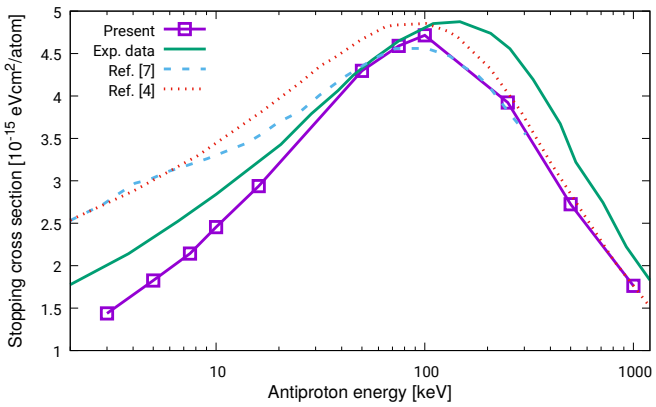

Fig. 1 The present stopping cross sections compared to the experimental data by Agnello *et al.* [6] and to other theoretical data by Lühr *et al.* [4] and Schiwietz *et al.* [7].

$$S(b,E_{\overline{p}}) = \sum_f P_{i\to f}(E_{\overline{p}},b)\left[E_f - E_i\right], \tag{1}$$

while the straggling as

$$T(b,E_{\overline{p}}) = \sum_f P_{i\to f}(E_{\overline{p}},b)\left[E_f - E_i - S(b,E_{\overline{p}})\right]^2. \tag{2}$$

Total stopping and straggling cross sections are calculated by performing the impact parameter integrations. Calculations were performed for antiproton impact energies ranging from 3keV up to 1MeV, and the obtained stopping cross sections are shown in Fig.1 along with the experimental data of Agnello *et al.* [6] and the theoretical predictions of Lühr *et al.* [4] and Schiwietz *et al.* [7]. At high antiproton energies the agreement between the theories and the experimental data is good, while at low antiproton energies notable discrepancies are present. Since the present results are based on fully-correlated two-electron *ab initio* calculations, they can provide a benchmark for approximate calculations.

References

[1] Niels Bohr, *On the theory of the decrease of velocity of moving particles on passing through matter*, Philos. Mag. **25**, 10 (1913).
[2] Niels Bohr, *On the decrease of velocity of swiftly moving electrified particles is passing through matter*, Philos. Mag. **30**, 581 (1915).
[3] Peter Sigmund *Particle penetration and radiation effects*, Springer Series in Solid-State Sciences, Vol. 151 (Springer, Berlin, 2006).
[4] Armin Lühr and Alejandro Saenz, *Stopping power of antiprotons in H, H_2 and He targets* Phys. Rev. A **79** 042901 (2009).
[5] S. Borbély, J. Feist, K. Tőkési, S. Nagele, L. Nagy, and J. Burgdörfer, *Ionization of helium by slow antiproton impact: Total and differential cross sections* Phys. Rev. A **90** 052706 (2014).
[6] M. Agnello et al., *Antiproton slowing down in H_2 and He and evidence of nuclear stopping power* Phys. Rev. Lett. **74** 371 (1995).
[7] G. Schiwietz, U. Wille, R. Díez Muino, P. D. Fainstein and P. L. Grande, *Comprehensive analysis of the stopping power of antiprotons and negative muons in He and H_2 gas targets* J. Phys. B **29** 307 (1996).

Electron Impact Excitation Cross Section of the $4p^5 5s5p\ ^4S_{3/2}$ State in Rb

Viktoriya Roman[1], Gintaras Kerevičius[2], Alicija Kupliauskienė[2], Alexander Borovik[1,3]

1. Department of Electron Processes, Institute of Electron Physics, Universitetska 21, 88017 Uzhgorod, Ukraine

2. Institute of Theoretical Physics and Astronomy, Vilnius University, Saulėtekio Ave. 3, 10222 Vilnius, Lithuania

3. Faculty of Physics, Uzhgorod National University, Voloshina 54, 88000 Uzhgorod, Ukraine

In alkali atoms there exists a subclass of quartet levels (they are termed "quasimetastable") which due to their mixing with autoionizing and non-autoionizing doublets of a given *J* retains relative metastability against autoionization, and which also radiates in the extreme ultraviolet spectral region [1]. The electron impact excitation of the lowest quasimetastable state $4p^5 5s5p\ ^4S_{3/2}$ at 16.64 eV in Rb atoms was studied earlier by observation of its radiative decay channel $4p^5 5s5p\ ^4S_{3/2} \rightarrow 4p^6 5p\ ^2P_{3/2}$ (λ = 82.4 nm) [2].

In the present work we report the first data on electron impact excitation cross section of the $4p^5 5s5p\ ^4S_{3/2}$ state obtained by observing its radiationless decay in ejected-electron spectra measured at different impact energies. The measurements were performed at an observation angle of 54.7° and incident electron energy resolution of 0.12 eV by using the apparatus and procedure described in detail earlier [3]. The measured cross section for electron impact excitation of the $4p^5 5s5p\ ^4S_{3/2}$ state with subsequent decay by electron emission is presented in Fig. 1 together with the optical excitation function for the $4p^5 5s5p\ ^4S_{3/2} \rightarrow 4p^6 5p\ ^2P_{3/2}$ transition measured with an energy resolution of 1.5 eV [2]. The cross sections were normalized at 45.5 eV impact energy.

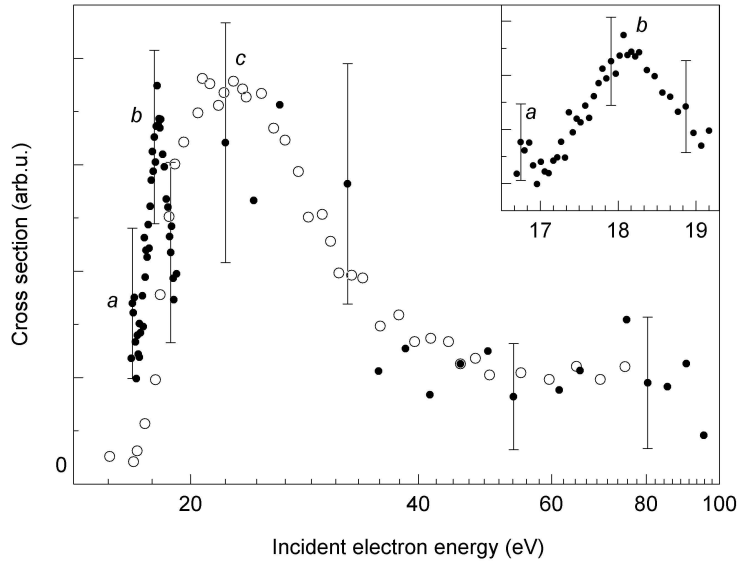

Fig. 1 The electron impact excitation cross section of the $4p^5 5s5p\ ^4S_{3/2}$ state in Rb. ● - present data; ○ - optical data [2].

As can be seen, both excitation functions are similar in shape at impact energies above 20 eV. The main maximum *c* at approximately 25 eV reflects the spin-exchange excitation character of the $4p^5 5s5p\ ^4S_{3/2}$ state. The difference between the data exists at near-threshold impact energies where, due to a better energy resolution of the present measurements two resonance features *a* and *b* are observed at 16.8 and 18.1 eV, respectively (see inset in Fig. 1). By analogy with data for the $3p^5 4s4p\ ^4S_{3/2}$ quasimetastable state in potassium [4], this structure can be due to core-excited Rb^- resonances predominantly of the $4p^5 4s4p^2$ configuration. Extensive *R*-matrix calculations are needed for a detailed description of these resonances.

References

[1] A. J. Mendelsohn, C. P. J. Barty, M. H. Sher, J. F. Young, and S. E. Harris, *Emission spectra of quasimetastable levels of alkali-metal atoms*, Phys. Rev. A **35**, 2095 (1987).

[2] I. S. Aleksakhin, G. G. Bogachev, I. P. Zapesochnyi, and S. Yu. Ugrin, *Experimental investigations of radiative decay of autoionizing states of alkali and alkaline earth elements*, Sov. Phys. JETP **53**, 1140 (1981).

[3] A. A. Borovik, A. N. Grum-Grzhimailo, K. Bartschat, and O. Zatsarinny, *Electron impact excitation of the $(3p^5 4s^2)^2P_{3/2,1/2}$ autoionizing states in potassium*, J. Phys. B: At. Mol. Opt. Phys. **38,** 1081 (2005).

[4] A. A. Borovik Jr., A. A. Borovik, O. Zatsarinny, and K. Bartschat, *Near-threshold electron-impact excitation of the $(3p^5 4s4p)\ ^4S_{3/2}$ quasimetastable state in potassium*, Phys. Rev. A **73**, 062701 (2006).

Velocity distribution of molecules sequentially evaporated from $H^+(H_2O)_4$

F. Berthias*, L. Feketeová*, H. Abdoul-Carime*, F. Calvo[$], B. Farizon*, M. Farizon*, and T. D. Märk[#]

[*] Université de Lyon; Université Claude Bernard Lyon1; Institut de Physique Nucléaire de Lyon, CNRS/IN2P3 UMR 5822, 69622 Villeurbanne Cedex, France
[$] Univ Grenoble 1, CNRS, LIPhy UMR 5588, F-38041 Grenoble, France
[#] Institut für Ionenphysik und Angewandte Physik, Leopold Franzens Universität, 6020 Innsbruck, Austria

The velocity of molecules evaporated from $H^+(H_2O)_4$ is measured by velocity map imaging in combination with the correlated ion and neutral time-of-flight mass spectrometry technique [1-3] (COINTOF MS). A single high-velocity collision with an Ar atom leads to energy deposition in the droplet via the electronic excitation of one of the molecules. After excitation, the out-of-equilibrium nanodroplet relaxes via the sequential evaporation of one or several molecules. The protonated residue is mass analysed at least 80 ns after the collision allowing for a quantitative comparison among the velocity distributions measured for the evaporation of one, two and three molecules. The measured Boltzmann velocity distribution of the evaporated molecules demonstrates that a large amount of energy can be evenly redistributed over the droplet prior to molecular evaporation. The velocity distribution clearly shows two contributions corresponding to a total redistribution of the deposited energies and to non-ergodic events, i.e., evaporation before complete energy redistribution.

References

[1] F. Berthias *et al* 2014 *Phys. Rev. A* **89** 062705
[2] C. Teyssier *et al* 2014 *Rev. Sci. Instrum.* **85** 015118
[3] G. Bruny *et al* 2012 *Rev. Sci. Instrum.* **83** 013305
[4] H. Abdoul-Carime *et al* 2015 Angewandte Chemie International Edition: DOI: 10.1002/anie.201505890, Angew. Chem. Int. Ed., **54**, 14685 –14689

Coplanar (e, 2e) ionization of CH_4 at 250 eV impact energy

István Tóth[1], **Ladislau Nagy**[1]
1. Faculty of Physics, Babeş-Bolyai University, 400084 Cluj Napoca, Romania

(e, 2e) ionization of molecules by electron impact has attracted much interest in recent years. These studies provide the most complete set of information about the ionization process through the TDCS (triple differential cross section). Compared to atomic ionization, molecular targets pose several difficulties both experimentally and in the theoretical calculations. One of these difficulties is the separation of molecular orbitals with very close energies. The theoretical treatment should take into account the multi-center nature of the molecular target. The random orientation of the molecules in experiments requires the averaging of the cross sections over these orientations in the calculations.

Studying the ionization of methane is particularly important, given its status as the simplest organic molecule. Often, methane is employed as a testing target for the assessment of damage produced to organic matter by the irradiation. The ionization of methane is important also from the perspective of other fields, like atmospheric physics (methane is an important greenhouse gas) or space related sciences.

Both experimental and theoretical studies have been performed [1-8] in order to investigate the ionization of methane by electron impact. These studies were performed for different kinematical conditions and geometrical arrangements. Coplanar and non-coplanar studies as well as symmetrical and non-symmetrical ionization have been investigated for different impact energies of the projectile. Nevertheless, the theoretical description of these processes is still incomplete.

Previously, we have performed calculations for the ionization of methane at higher (above 500 eV) [6] and lower (below 70 eV) [7] impact energies. In the present study the cross sections are determined for a coplanar geometry, where the momenta of the incident, scattered and ejected electrons are in the same plane. We extend our calculations for impact energies of 250 eV and scattering angles of 10 and 20 degrees, respectively. The TDCSs are calculated for the ionization of the $1t_2$ and $2a_1$ orbitals of the methane molecule. In the calculations we use a distorted wave approach, where all free particles are described by wave functions calculated in the spherically averaged potential field of the target molecule or the molecular ion. The initial state of the target is described by Gaussian-type multi-center wavefunctions. The molecular wavefunctions are given as a linear combination of atomic wavefunctions, which are contractions of Gaussian primitives. The calculated TDCSs for the $1t_2$ orbital are compared to the very recent experimental data of [8].

The post collision interaction between the outgoing electrons is taken into account through the Coulomb distortion factor of [9]. We perform the calculations both with this factor and without it in order to assess the effect of the post collision interaction on the cross section. Our detailed results will be presented at the conference.

References

[1] A. Lahmam-Bennani et al, *Dynamics of electron impact ionization of the outer and inner valence ($1t_2$ and $2a_1$) molecular orbitals of CH_4 at intermediate and large ion recoil momentum*, J. Phys. B: At. Mol. Opt. Phys. **42**, 165201 (2009)
[2] K. L. Nixon et al, *Low energy (e,2e) studies from CH_4: Results from symmetric coplanar experiments and molecular three-body distorted wave theory*, J. Chem. Phys. **134**, 174304 (2011)
[3] K. L. Nixon et al, *Low energy (e,2e) measurements of CH_4 and neon in the perpendicular plane*, J. Chem. Phys. **136**, 094302 (2012)
[4] C. Y. Lin, C. W. McCurdy and T. N. Rescigno, *Theoretical study of (e,2e) from outer- and inner-valence orbitals of CH_4: A complex Kohn treatment*, Phys. Rev. A **89**, 052718 (2014)
[5] H. Chaluvadi, C. G. Ning and D. H. Madison, *Theoretical triple-differential cross sections of a methane molecule by a proper-average method*, Phys. Rev. A **89**, 062712 (2014)
[6] I. Tóth and L. Nagy, *Triple-differential cross-section calculations for the ionization of CH_4 by electron impact*, J. Phys. B: At. Mol. Opt. Phys. **43**, 135204 (2010)
[7] I. Tóth, R. I. Campeanu and L. Nagy, *Ionization of NH_3 and CH_4 by electron impact*, Eur. Phys. J. D, **69**, 2 (2015)
[8] N. Işik, M. Dogan and S. Bahçell, *Triple differential cross section measurements for the outer valence molecular orbitals ($1t_2$) of a methane molecule at 250 eV electron impact*, J. Phys. B: At. Mol. Opt. Phys. **49**, 065203 (2016)
[9] S. J. Ward and J. H. Macek, *Wave functions for continuum states of charged fragments*, Phys. Rev. A, **49**, 1049 (1994)

Theoretical investigations on projectile coherence effects in fast ion-atom collisions

Ferenc Járai-Szabó, Ladislau Nagy
Faculty of Physics, Babeş-Bolyai University, Kogălniceanu Street No. 1, 400084 Cluj, Romania

Fully differential ionization cross sections (FDCS) give us the most complete information about an ionization process. After the development of the reaction microscopes [1] a great interest has been focused on measuring and calculating this quantity for different ionization processes. Regarding this topic, one of the most discussed processes is the ionization of helium by fast charged projectiles [2]. It has been observed significant difference between experimental data and theoretical continuum distorted wave (CDW) results. These, and other similar theoretical calculations were not able to reproduce the experimentally observed structures in the perpendicular plane. However, our semiclassical calculations [3] and the convolution of the first Born approximation with elastic scattering [4] described fairly well these structures.

On one hand, the discrepancy between these calculations and their relationship with the experimental data was solved, when it has been shown the importance of the projectile coherence in the details of the FDCs [5]. There have been obtained significant differences in the FDCSs for the ionization of helium, using projectiles causing the same perturbation, but different transversal coherence lengths. If the coherence length was larger than the atomic dimensions, the results were closer to the CDW calculations, which assumes a plane wave for the projectile, while for smaller coherence lengths the results were closer to the convoluted [6] and our semiclassical results. On the other hand, very recently, new measurements have been realized with high momentum resolution on the single ionization of helium induced by 1-MeV protons [7]. In these experimental data no indication has been found that the ionization process could be influenced by the coherence length of the projectile.

In a recent paper we have shown how the projectile coherence may be treated theoretically [6]. Here, starting from the same transition amplitude, we have calculated the FDCS in the two extreme cases. First, we used the semiclassical approach which assumes a straight-line trajectory for the projectile. Second, the full quantum method has been used in constucting FDCS which considers the projectile a plane wave.

In the present work we investigate theoretically the transition between these two extreme approaches. In these calculations the projectile is considered a wave packet with a given, finite coherence width. As a first step we calculate in the framework of the first order, semiclassical, impact parameter approximation the transition amplitude $a(\mathbf{b},\mathbf{p}_{\rm el})$, where $\mathbf{p}_{\rm el}$ is the ejected electron momentum and $\mathbf{b}$ is the impact parameter. The scattering amplitude $R(\mathbf{q}_\perp,\mathbf{p}_{\rm el})$ which depend on the perpendicular momentum transfer $\mathbf{q}_\perp$ is calculated by an inverse Fourier transform [6]. Here, we have the possibility to consider the finite coherence length Δb of the projectile wave packet by a Gaussian profile centered to the impact parameter b_0

$$R(q_\perp,p_{\rm el})=\frac{C}{2\pi}\int d\mathbf{b}\,a(\mathbf{b},\mathbf{p}_{\rm el})\,e^{i\mathbf{b}\cdot\mathbf{q}_\perp}\,b^{2i\frac{Z_pZ_t}{v}}\,e^{-\frac{(b_0-b)^2}{2\Delta b^2}}\,.$$

Here C is a normalization constant and $b^{2i\frac{Z_pZ_t}{v}}$ is an eikonal phase accounting for the internuclear interaction, Z_p and Z_t being the charges of the projectile and the target nucleus, respectively, and v the projectile velocity. The impact parameter b_0 which depends on the momentum transfer $\mathbf{q}_\perp$ is calculated based on classical potential scattering theory. The FDCSs are then obtained as the square of modulo of the scattering matrix element $R(q_\perp,p_{\rm el})$.

By the above described theoretical approach we investigate, how the projectile coherence length affects the FDCSs in case of the experimentally studied kinematical conditions [5,7]. By analizing the obtained results we can conclude that our calculations show significant differences in FDCS when different projectile coherence lengths are considered.

References

[1] J. Ullrich *et* al., *Recoil-ion momentum spectroscopy*, J. Phys. B: At. Mol. Opt. Phys. **30**, 2917 (1997).
[2] M. Schultz *et* al., *Three-dimensional imaging of atomic four-body processes*, Nature **422**, 48 (2003).
[3] F. Járai-Szabó, L.Nagy, *Impact parameter method calculations for fully differential ionization cross sections*, Nucl. Instrum. Methods B **267**, 292 (2009).
[4] M. Schulz, M. Dürr, B. Najjari, R. Moshammer and J. Ullrich, *Reconciliation of measured fully differential single ionization data with the first Born approximation convoluted with elastic scattering*, Phys. Rev. A **76**, 032712 (2007).
[5] Wang X *et* al., *Projectile coherence effects in single ionization of helium*, J. Phys. B: At. Mol. Opt. Phys. **45**, 211001 (2012).
[6] F. Járai-Szabó and L. Nagy, *Theoretical investigations on the projectile coherence effects in fully differential ionization cross sections*, Eur. Phys. J. D **69**, 4 (2015).
[7] H. Gassert, *et* al., *Agreement of Experiment and Theory on the Single Ionization of Helium by Fast Proton Impact*, Phys. Rev. Lett. **116**, 073201 (2016).

Experimental Evidence of the Low-Lying Triplet States of Halothane As Studied by Electron Energy Loss Spectroscopy Method

E. Lange[1], J. Ameixa[1], P. Limão-Vieira,[1] F. Ferreira da Silva[1]

1. Faculdade de Ciência e Tecnologia,, Universidade Nova de Lisboa, 2829-516 Caparica, Portugal.

Halothane ($CF_3CHBrCl$) was widely used in the past as an halogenated anaesthetic in medicine and although there are not precise data on the amount used, an estimate of 10 kilotons/year [1], where 80% of the gas used is exhaled by the patient unchanged was reported [2]. The interaction of halothane with UV radiation has raised environmental concerns since it is delivered to the Earth lower atmospheric layers has an estimated lifetime of about 7 years, which allows it to reach the troposphere and the lower layers of the stratosphere [1].

In this study we present the first experimental evidence of the low-lying triplet states of halothane as probed by electron energy loss spectroscopy measurements. Were obtained the spectrum of electron collisions with halothane in both dipolar and non-dipolar conditions. For the former, it is compared with de VUV photoabsorption spectrum of halothane [3] whilst for the latter we have obtained experimental evidence showing the spin forbidden transitions. The role of spin-orbit effects have been considered in recent calculations of the electronic states of halothane [3] to explain the broad natures of the 6.1 eV and 7.5 eV features assigned to excitation of Br and Cl lone pairs to σ*(C–Br) and σ*(C–Cl) transitions. Electron-halothane collisions were performed in the High Resolution Electron Energy Loss Spectrometer (HREELS) in our laboratory, VG-SEELS 400 [4]. The VUV photoabsorption spectrum was recorded at the UV1 beam line of the ASTRID synchrotron facility, ISA at the Aarhus University, Denmark [5].

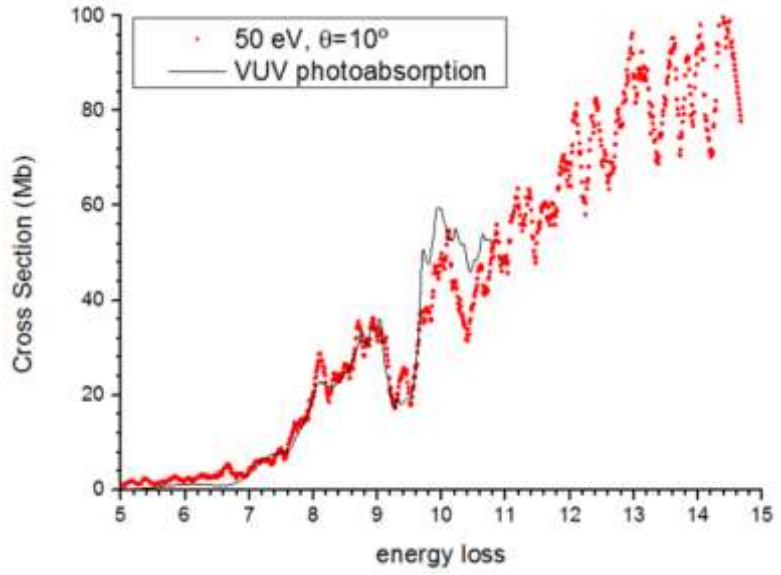

Fig. 1: The VUV photoabsorption cross section of Halothane (black line) compared with the electron energy loss spectrum (red dots) in dipolar conditions.

References

[1] Y. Shiraishi and K. Ikeda, *Uptake and biotransformation of sevof lurane in humans: A comparative study of sevof lurane with halothane, enflurane, and isoflurane*, J. Clin. Anesth.,. **2,**. 381 (1990).

[2] T. Langbein, H. Sonntag, D. Trapp, a Hoffmann, W. Malms, E. P. Röth, V. Mörs, and R. Zellner, *Volatile anaesthetics and the atmosphere: atmospheric lifetimes and atmospheric effects of halothane, enflurane, isoflurane, desflurane and sevoflurane.*, Br. J. Anaesth. **82**, 66 (1999).

[3] F. Ferreira. Da Silva, D. Duflot, S. V. Hoffmann, N. C. Jones, F. N. Rodrigues, A. M. Ferreira-Rodrigues, G. G. B. De Souza, N. J. Mason, S. Eden, and P. Limão-Vieira, *Electronic State Spectroscopy of Halothane As Studied by ab Initio Calculations, Vacuum Ultraviolet Synchrotron Radiation, and Electron Scattering Methods* J. Phys. Chem. A, **119**, 8503 (2015).

[4] F. Motte-Tollet, M.-J. Hubin-Franskin, and J. E. Collin, *Vibrational excitation of methylamine by electron impact in the 4.5–30 eV energy range*, J. Chem. Phys., **97**, 7314 (1992).

[5] S. Eden, P. Limão-Vieira, S. V. Hoffmann, and N. J. Mason, *VUV photoabsorption in CF3X (X=Cl, Br, I) fluoro-alkanes*, Chem. Phys., **323**,. 313 (2006).

Merged-Beam Study of Mutual Neutralization of $Li^+ + D^-$

Thibaut Launoy[1,2], Xavier Urbain[2], Nathalie Vaeck[1]

1. Service de Chimie quantique et Photophysique (CQP), Faculté des Sciences, Université Libre de Bruxelles, 50, av. F. Roosevelt, CP160/09, 1050 Bruxelles, Belgium

2. Institute of Condensed Matter and Nanosciences (IMCN), Université catholique de Louvain, chemin du cyclotron 2, 1348 Louvain-la-Neuve, Belgium

Modelling of stellar atmospheres requires various detailed and accurate data on different processes such as the mutual neutralization (MN) of cation-anion pairs that can affect atomic species of interest. Indeed, neutralization reactions play an important role in atmospheric and astrophysical processes. Furthermore, there is a strong demand from the astrochemical community for information about the low-energy cross section of processes involving H^- (or D^-).

Our merged-beam setup [1] was modified in order to be able to study the mutual neutralization of $^7Li^+ + ^2D^- \rightarrow Li^*(nl) + D(1s)$ and determine which states of the lithium neutral atom are predominant in the total cross section. Preliminary measurements at ~7 meV have been performed and compared with theoretical calculations [2]. As seen in Fig.1, our apparatus gives access to the branching ratio among accessible neutral channels of the lithium atom and could discriminate the Li(3p) and Li(3d) channels separated by only 44 meV.

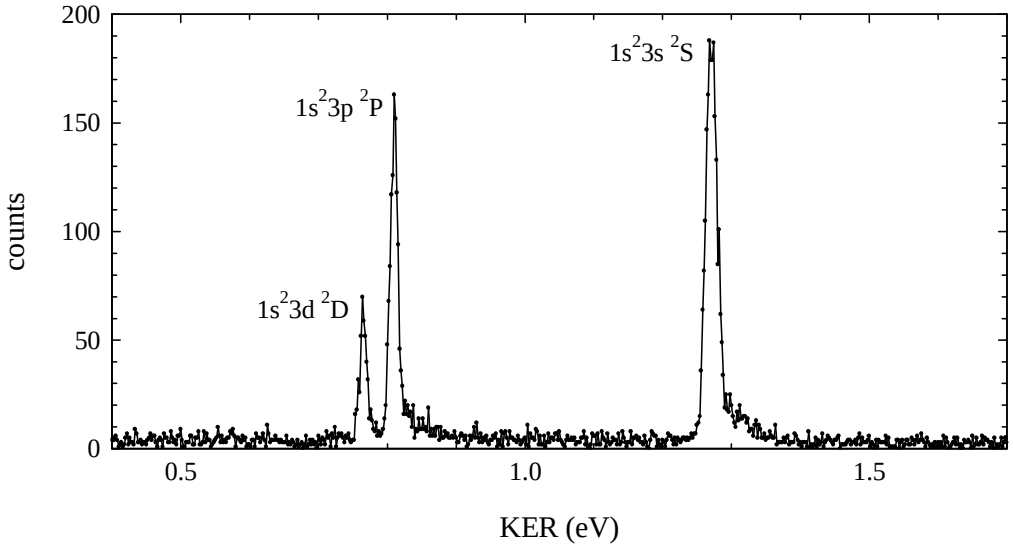

Fig. 1 Kinetic energy release resulting from the mutual neutralization between Li^+ and D^- at 7 meV average collision energy.

The measured total cross section of this study agrees with the results of Croft *et al*. However, our measured branching ratio suggests higher proportions of the 3d (by approximately 6%) and 3s (by approximately 5%) channels at the expense of Li(3p).

Further experiments at higher collision energies are still needed to completely compare our results with the experimental study of Pear and Hayton [3] which was restricted to higher collision energies in the range of 0.7 to 316 eV or with theoretical calculations.

References

[1] Nkambule, S. M., Elander, N., Larson, Å., Lecointre, J. and Urbain, X., *Differential and total cross sections of mutual neutralization in low-energy collisions of isotopes of $H^+ + H^-$*, Phys. Rev. A **93**, 032701 (2016).

[2] Croft, H., Dickinson, A. S. and Gadéa, F. X., *A theoretical study of mutual neutralization in Li + H collisions.* J. Phys. B: At. Mol. Opt. Phys. **32,** 81 (1999).

[3] Peart, B. and Hayton, D. A., *Merged beam measurements of the mutual neutralization of He^+/H^- and Li^+/D^- ions.* J. Phys. B: At. Mol. Opt. Phys. **27,** 2551 (1994).

Search for Young-Type Interferences in (e,2e) Reactions on H_2 Molecules with Known Spatial Alignment

Xueguang Ren[1], Khokon Hossen[1], Xingyu Li[2,3], Xiangjun Chen[2,3] and Alexander Dorn[1]

1. *Max Planck Institute for Nuclear Physics, 69117 Heidelberg, Germany*
2. *Hefei National Laboratory for Physical Sciences at Microscale and Department of Modern Physics, University of Science and Technology of China, Hefei, Anhui, 230026, China*
3. *Synergetic Innovation Center of Quantum Information and Quantum Physics, University of Science and Technology of China, Hefei, Anhui, 230026, China*

An experimental and theoretical (e,2e) study is performed for H_2 at 500 eV impact energy. The molecular alignment is determined experimentally by measuring the emitted proton momentum for ground state dissociation of the residual H_2^+ ion. We observe oscillations in the cross section as function of the molecular alignment angle which can be reproduced using a Multi-Center Distorted Wave method (MCDW) while the standard two-center interference treatment using a coherent sum of two effective atomic amplitudes fails completely**.**

Interferences of coherent electron waves emitted from multicenter systems or traveling along several indistinguishable paths are ubiquitous in physics. One prominent example is their observation for electron emission from gas phase molecules induced by photo-absorption or particle impact. Often analogies are drawn to Young's double slit experiment and the simplest models describing molecular ionization are based on this scenario by using single center outgoing waves which are coherently summed up for all emission centers in the molecule. Two center interferences were also considered for the (e,2e) reaction where, so far, most experiments have averaged over the molecular axis alignment in space which is one essential parameter determining the interference pattern.

Here we present fully differential cross sections (FDCS) for fast (500 eV) electron impact on H_2 with the H_2^+ ($^2\Sigma^+_g$) final ionic ground state. A small fraction of ions dissociates such that the measurement of the proton momentum vector allows to determine the spatial alignment of the molecular axis in space during the collision. Experimentally a reaction microscope is used to detect both outgoing electrons and the proton in a triple coincidence measurement. Theoretically a Multi-Center Distorted Wave method (MCDW) is used and, alternatively, the standard interference factor $(1 + \cos(\boldsymbol{\chi}\cdot\boldsymbol{\rho}))$ is multiplied with the atomic hydrogen FDCS. Here $\boldsymbol{\rho}$ in the phase of the cosine function is the internuclear vector. $\boldsymbol{\chi}$ is the ejected electron wave number $\mathbf{k}$ in case of photoionization. For particle impact ionization (treated in plane wave first Born approximation) $\boldsymbol{\chi} = \mathbf{k} - \mathbf{q}$ where $\mathbf{q}$ is the momentum transferred by the projectile. The additional phase contribution originates from the different phases of the scattered projectile wave at the two atomic centers.

In Fig. 1b we see strong alignment dependent variations of the FDCS which are well reproduced by MCDW (c) while the pure interference description (d) fails clearly. This is most likely due to the rather low energy of the ejected electron of $E_2 = 10$ eV which does not justify a spherical wave description as it is used in the derivation of the interference factor.

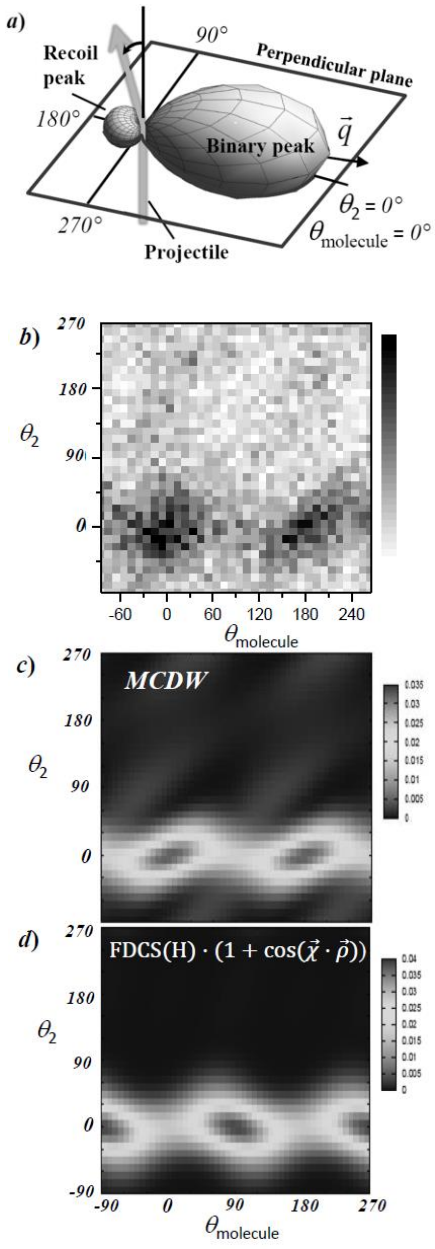

Fig. 1 FDCS as function of the molecular alignment angle $\theta_{molecule}$ and the ejected electron angle θ_2 both in the plane perpendicular to the incoming projectile beam (θ_2 = 0° is roughly the direction along the momentum transfer). Projectile scattering angle θ_1 = -20°, ejected electron energy E_2 = 10 eV. a) Coordinate frame. b) experimental data. c) MCDW calc. d) interference factor.

Formation of Positron-Atom Bound States in Collisions Between Rydberg Ps and Neutral Atoms

A. R. Swann[1], D. B. Cassidy[2], A. Deller[2], G. F. Gribakin[1]
1. School of Mathematics and Physics, Queen's University Belfast, University Road, Belfast BT7 1NN, United Kingdom
2. Department of Physics and Astronomy, University College London, Gower Street, London WC1E 6BT, United Kingdom

Though predicted twenty years ago [1–3], positron binding to neutral atoms has not yet been observed experimentally. We propose a new scheme to detect positron-atom bound states by colliding Rydberg (highly excited) positronium (Ps) with neutral atoms. Theoretical estimates of the cross section for the charge-transfer reaction $\mathrm{Ps}(nl) + A \to e^+A + e^-$ are made for a selection of neutral target atoms A across a wide range of incident Ps energies and principal quantum numbers n. By comparing the experimental measurements with these theoretical predictions, it may be possible to infer a postitron-atom binding energy and compare it with existing predictions [4].

For the theoretical calculations we work in the Born approximation, taking the motion of the incident Ps and the outgoing electron as plane waves with momenta **K** and **k** respectively. The positron-atom binding energy ε_b is typically small (a fraction of an electronvolt), so we describe the wave function of the bound positron using the zero-range potential model. From Fermi's golden rule, the cross section (averaged over the magnetic quantum number of the Ps) is found (after some analytical work) to be

$$\sigma(K) = \frac{8\pi^2\kappa}{K^2}\int_{|k-K/2|}^{k+K/2} p|F_{nl}(p)|^2\,dp, \tag{1}$$

where $\kappa = \sqrt{2\varepsilon_b}$ and F_{nl} is the radial part of the momentum-space internal Ps wave function. Experimentally produced Rydberg Ps is mostly in s or d states, so we perform calculations for $l = 0$ and 2. Figure 1(a) shows the cross section for the Cu atom ($\varepsilon_b = 0.170$ eV [4]) for $l = 0$ and select values of n.

On the side of experiment, recent technological developments have made efficient Rydberg Ps production much more feasible [5]. A time-focused positron pulse will be implanted into a mesoporous SiO_2 film, resulting in the production of Ps($^3S_1$) atoms. These will subsequently be excited via $n = 2$ to levels $n = 3$–30 using nanosecond-pulsed UV ($\lambda = 243.0$ nm) and IR ($\lambda = 729$–1312 nm) laser radiation. Ps atoms in varying Rydberg states and having kinetic energies in the range of 10–1000 meV will collide with neutral target atoms in a scattering cell, enabling the charge-transfer reaction to take place. Figure 1(b) shows a schematic of the experimental apparatus.

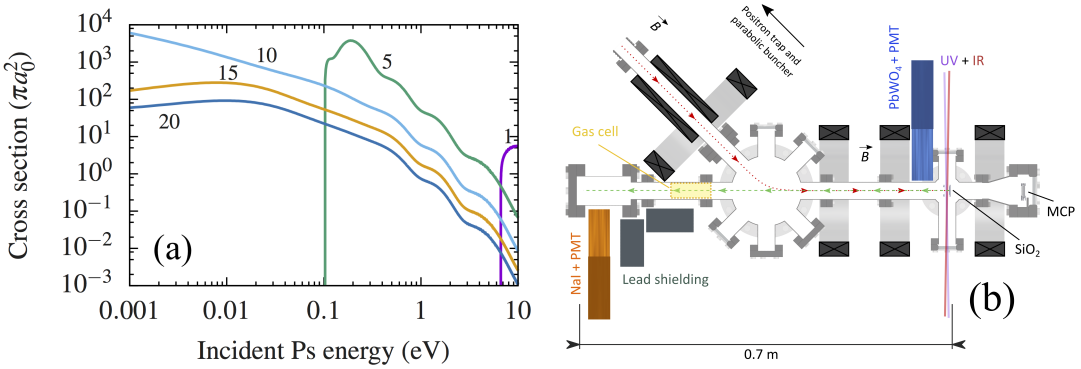

Fig. 1 (a) Charge-transfer reaction cross section for the Cu atom, for $l = 0$ and various n (labelled); (b) experimental apparatus.

Though our theoretical calculations have neglected both the interaction of the electron in Ps with the atom and the Coulomb interaction between the outgoing electron and the positron-atom complex, these should be unimportant for Rydberg states of Ps. The presence of electric fields in the experimental setup will lead to Stark mixing of the Ps states, but we have also found that cross sections for different l agree to within an order of magnitude.

References

[1] V. A. Dzuba, V. V. Flambaum, G. F. Gribakin, and W. A. King, *Bound States of Positrons and Neutral Atoms*, Phys. Rev. A **52**, 4541 (1995).
[2] G. G. Ryzhikh and J. Mitroy, *Positronic Lithium, an Electronically Stable Li-e^+ Ground State*, Phys. Rev. Lett. **79**, 4124 (1997).
[3] K. Strasburger and H. Chojnacki, *Quantum Chemical Study of Simple Positronic Systems Using Explicitly Correlated Gaussian Functions—PsH and PsLi$^+$*, J. Chem. Phys. **108**, 3218 (1997).
[4] C. Harabati, V. A. Dzuba, and V. V. Flambaum, *Identification of Atoms that Can Bind Positrons*, Phys. Rev. A **89**, 022517 (2014).
[5] D. B. Cassidy, T. H. Hisakado, H. W. K. Tom, and A. P. Mills, Jr., *Efficient Production of Rydberg Positronium*, Phys. Rev. Lett. **108**, 043401 (2012).

Model Approach for Theoretical Investigations of Inelastic Processes in Collisions of Heavy-Particles with Hydrogen

Svetlana A. Yakovleva, Yaroslav V. Voronov, Andrey K. Belyaev
Department of Theoretical Physics, Herzen University, St. Petersburg 191186, Russia

Information on inelastic collision processes is important for non-local thermodynamic equilibrium (non-LTE) modelling of stellar atmospheres. One of the main sources of uncertainties for non-LTE studies is atomic data on collisions of atoms and positive ions of different chemical elements with hydrogen atoms and negative ions. A full quantum treatment of these processes is laborious and required data for many atoms of interest are still unavailable. For these reasons, the so-called Drawin formula is still used for estimates of inelastic collision rate coefficients although it has been shown [1] that it does not provide a reliable data and moreover cannot be applied to charge transfer processes, which have been found to be the most important in astrophysical applications.

The model approach within the framework of the Born-Oppenheimer formalism has been recently proposed [2] in order to evaluate physically reliable data of cross sections and rate coefficients for inelastic collision processes. The approach is based on the asymptotic method for electronic structure calculations and on the branching probability current method for a non-adiabatic nuclear dynamics treatment. The method has been recently applied to aluminium-hydrogen [3] and cesium-hydrogen [4] collisions.

Proposed electronic structure modelling allows one to describe long-range non-adiabatic regions due to ionic-covalent interaction and obtain adiabatic potential curves for high-lying excited states that can also be combined with available *ab initio* data for low-lying states.

Non-adiabatic transition probabilities between adjacent molecular states are calculated using the Landau-Zener model, see Ref.[2] for the new Landau-Zener formula. When non-adiabatic regions are passed in a particular order (which is the case of regions formed by an ionic-covalent interaction), the multichannel formula can be used to calculate the total transition probability [5]. When adjacent states form several non-adiabatic regions (which is typical for *ab initio* potentials), the branching probability current method should be applied. The advantage of the multichannel formulas is that it is analytical in contrast to the branching probability current method, which is numerical. The multichannel formulas have been applied in inelastic process studies for silicon-hydrogen [5], calcium-hydrogen [6] and beryllium-hydrogen [in press] collisions.

The proposed model approach has been tested on different collisional systems that were treated by quantum methods before and the analysis of the calculated data shows that the treated processes can be divided into three groups. Processes of the first two groups have high or medium cross sections and rate coefficients and can affect non-LTE effects. The rate coefficients for these two groups are in a good agreement with the results of quantum studies. For the third group, that consist of processes with very small cross sections and rate coefficients, results can deviate substantially, but both quantum and model methods give negligible values that are unlikely to play any role in astrophysical applications. The details of the approach and calculations will be presented at the conference.

This work has been partly supported by the Ministry of Education and Science of the Russian Federation and by the Dynasty Foundation.

References

[1] Paul S. Barklem *et al*, *On inelastic hydrogen atom collisions in stellar atmospheres*, Astron. Astrophys. **530**, A94 (2011).
[2] Andrey K. Belyaev, *Model approach for low-energy inelastic atomic collisions and application to Al + H and $Al^+ + H^-$*, Phys. Rev. A **88**, 052704 (2013).
[3] Andrey K. Belyaev, *Inelastic aluminium-hydrogen collision data for non-LTE applications in stellar atmospheres*, Astron. Astrophys. **560**, A60 (2013).
[4] Andrey K. Belyaev, Bruno Lepetit, and Florent X. Gadeá, *Theoretical study of electronic excitation, ion-pair formation, and mutual neutralization in cesium-hydrogen collisions*, Phys. Rev. A **90** 062701(2014).
[5] Andrey K. Belyaev, Svetlana A. Yakovleva, Paul S. Barklem, *Inelastic silicon-hydrogen collision data for non-LTE applications in stellar atmospheres*, Astron. Astrophys. **572**, A103 (2014).
[6] Andrey K. Belyaev *et al*, *Model estimates of inelastic calcium-hydrogen collision data for non-LTE stellar atmospheres modelling*, Astron. Astrophys. **587**, A114 (2016).

Signature of Concerted and sequential break up processes in ion impact fragmentation of CO_2 molecular ions

Arnab Khan, Lokesh C. Tribedi, and Deepankar Misra

Tata Institute of Fundamental Research, Homi Bhabha Road, Colaba, Mumbai 400005, India

Carbon dioxide (CO_2) has long been used as a prototype system to study the fragmentation dynamics upon the impacts of heavy ions [1], electrons [2], and photons [3]. However, for ion projectiles, the detailed study of fragmentation dynamics of CO_2^{q+} in the intermediate velocity regime is clearly lacking in the literature. In addition, most of the earlier works mainly concentrated on the decay dynamics of CO_2^{3+} or were only limited to the kinetic energy release (KER) distribution studies. In present experiment, we have investigated the three-body breakup dynamics of carbon dioxide molecular ion (CO_2^{q+} where q = 3-5) in collision with 1-MeV Ar^{8+} ions using a Recoil Ion Momentum Spectrometer (RIMS) [4]. The motivation behind this study is to answer whether the bond breakup in CO_2^{q+} happens in a concerted manner, i.e. one-step, or sequential manner, i.e. two-step and to gain further insight about these processes. The study shows, among the various possible fragmentation channels of CO_2^{q+} (q = 3-5), where all fragments are charged, only three channels [(1,1,1), (2,1,1), and (3,1,1)] show the signature of a sequential breakup process. The similarity between all these three channels is that, in each case, the ejection of an O^{n+} (n = 1-3) ion leaves a metastable CO^{2+} ion which successively decays into C^+ + O^+. The signatures of the concerted and sequential channels have been exemplified with the help of three-body Dalitz plots [5] and Newton diagrams [1,4]. Further, it is seen that in the sequential processes most of the KER comes from the motion of the center-of-mass of the CO^{2+} moiety and the first O^{n+} ion leaving only a small amount of internal excitation energy in the CO^{2+} moiety which eventually dissociates. For sequential decay it is observed that, irrespective of the charge state of the parent molecular ion, the internal energy of the CO^{2+} fragment is always around the same value. The detection of all the three fragments in coincidence allows us to construct the instantaneous molecular structure prior to the Coulomb explosion and it is also observed that molecular bending is preferred as the charge on the precursor molecular ion increases. Moreover, it is seen that the energy deposition to the system plays an indispensable role to decide whether a sequential or a concerted channel will be dominant during the fragmentation. In Fig. 1 we show the Dalitz plots for the three-body decay of CO_2^{4+}, and CO_2^{5+}. In each plots the intense region near x = 0.1, and y = -0.33 corresponds to the concerted decay and the wing-like structure in the right side stands for the sequential decay.

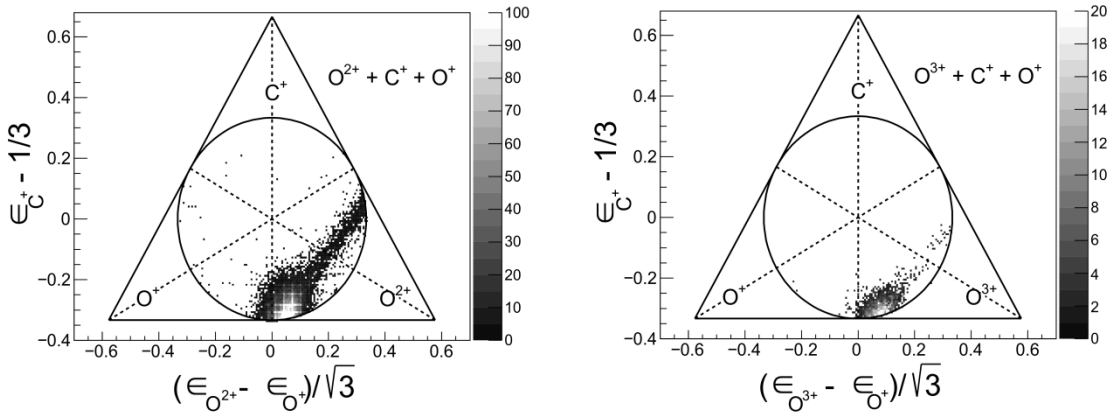

Fig. 1 Dalitz plots for the three-body decay of CO_2^{4+} (left panel) and CO_2^{5+} (right panel).

References

[1] N. Neumann, D. Hant, L. P. H. Schmidt, J. Titze, T.Jahnke, A. Czasch, M. S. Schöffler, K. Kreidi, O. Jagutzki, H. Schmidt-Böcking, and R. Dörner, *Fragmentation Dynamics of CO_2^{3+} Investigated by Multiple Electron Capture in Collisions with Slow Highly Charged Ions*, Phys. Rev. Lett.**104**, 103201 (2010).

[2] C. Tian and C. R. Vidal**,** *Single to quadruple ionization of CO_2 due to electron impact*, Phys. Rev. A **58**, 3783 (1998).

[3] C. Wu, C. Wu, D. Song, H. Su, Y. Yang, Z. Wu, X. Liu, H. Liu, M. Li, Y. Deng, Y. Liu, L.-Y. Peng, H. Jiang, and Q.Gong, *Nonsequential and Sequential Fragmentation of CO_2^{3+} in Intense Laser Field*, Phys. Rev. Lett. **110**, 103601 (2013).

[4] A. Khan, L. C. Tribedi, and D. Misra, *Observation of a sequential process in charge-asymmetric dissociation of CO_2^{q+} (q = 4,5) upon the impact of highly charged ions*, Phys. Rev. A **92**, 030701(R) (2015).

[5] R. Dalitz, *On the analysis of τ-meson data and the nature of the τ-meson*, London Edinburgh Dubl. Philos. Mag. J. Sci. **44**, 1068 (1953).

The Magnetic Toroidal Sector: A broad-band Electron-Positron Pair Spectrometer

S. Hagmann[1], P.M. Hillenbrand[1, 3], Y. A Litvinov[1], U. Spillmann[1], K. Stiebing[2], Th. Stöhlker[1, 4, 5]

[1] GSI Helmholtzzentrum Darmstadt, [2] Inst. für Kernphysik, Universität Frankfurt, [3] Universität Giessen,[4]Helmholtz Institut Jena, [5]Fakultät für Physik, Universität Jena

Electron–positron pair production has evolved into a central topic of QED in extreme fields as the coupling between the lepton field and the electromagnetic field is close to one[1, 2]. Most recently the surprisingly high cross sections observed for pair production in relativistic heavy-ion atom collisions have aroused new interest in this process even in the accelerator design community as capture from pair production has been identified as a critical, potentially luminosity limiting process in relativistic heavy ion colliders. The enormous cross sections observed can be traced[1] to the large transverse electric fields $E_{transv}\sim\gamma$. Theory predicts a scaling of the total cross section for free-free pair production [1,3] $\sigma_{free\text{-}free}\sim(Z_{proj})^2(Z_{tar})^2\ln^3\gamma$ and a very complex relation between the angular emission patterns of electron and positron[4]. The future relativistic storage ring HESR at FAIR with a collision energy range up to $\gamma\sim6$ will be best suited to study for ion-induced pair-production all channels which may be distinguished experimentally[3]. A corresponding future experimental investigation of the dynamics of the heavy-ion induced free-free pair creation up to $\gamma\sim6$

$$X^{Z+}+A\longrightarrow X^{Z+}+\{A^*\}+e^+ + e^- \qquad (1)$$

is the motivation for the current spectrometer design study: a coincident detection of both outgoing leptons and their vector momenta as is constitutive in a complete description of free-free pair production, is not practically possible with instruments covering only a small solid angle for each lepton.

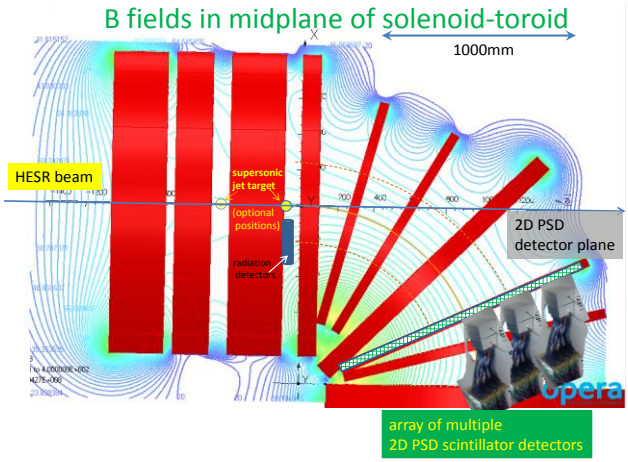

Fig. 1 Cut through midplane of coil assembly of a toroidal magnetic lepton spectrometer for lepton energies up to 20 MeV

We have therefore employed OPERA-3D[5] to study the electro-optical properties of a magnetic toroidal spectrometer with very large effective solid angle enabling coincident detection of the vector momenta of electrons and positrons from a free-free pair (see fig. 1). In a toroidal B-field e^- and e^+ are momentum-dispersed perpendicular to the bend plane of the toroid.

For a given B-field one can find lepton momenta $\beta_0\gamma_0/n$, $n\geq1$, for which all trajectories independent of their forward laboratory emission angle will intersect in a point X_n on the detector plane (fig. 2). For all other lepton momenta $\beta\gamma$ the parallel and perpendicular momenta can be determined by 2D-PSD detectors.

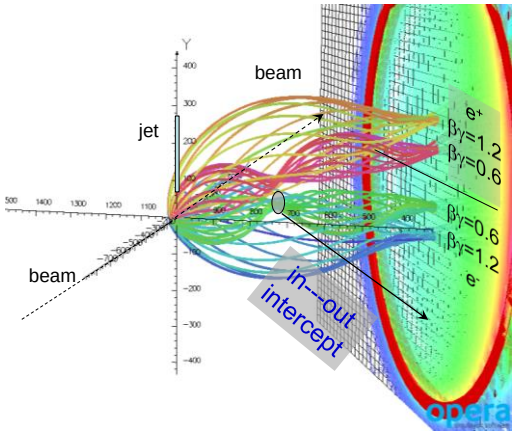

Fig. 2 Vertical dispersion of leptons in the toroidal field

The complete emitter frame emission pattern of a lepton pair may thus be determined by coincident detection of leptons in the detector plane for a choice of a few appropriate B-field settings.

References

[1] Ionescu, D. Habilitationsschrift, FU-Berlin (1997).
[2] A. Voitkiv, J. Ullrich, Relativistic Collisions, Springer Series AOPP, Vol. 49 (2008)
[3] D. Ionescu et al. Phys. Rev. A54 4960 (1996)
[4] R. Tenzer et al. Eur. Phys. J. D 11 347-353 (2000)
[5] OPERA-3D User Guide, Vector Fields Limited, 24 Bankside, Kidington, Oxford OX5 1JE, UK

A Quantitative Study of Capillary Charging and Discharging During Ion Beam Guiding

E. Giglio[1], K. Tőkési[2] and R.D. DuBois[3]

[1] Centre de Recherche sur les Ions, les Matériaux et la Photonique (CIMAP), F-14000, Caen, France, EU

[2]Institute for Nuclear Research, Hungarian Academy of Sciences, 4026 Debrecen Bem tér 18/c, Hungary, EU

[3] Misssouri University of Science and Technology, Rolla, MO 65409 USA

Since the original discovery of ion beam guiding by insulating capillaries, numerous studies have been performed. The vast majority of these provide qualitative information about the transmitted intensity as a function of time and/or angle between the capillary axis and the original beam direction. Models of the stochastic buildup of charge on the capillary surfaces have been used to simulate these properties [1]. However, quantitative information about the charge buildup, i.e., the deposition and redistribution, is needed for testing and improving these models.

In an earlier study of low energy ion beam guiding by a cylindrical glass capillary, we provided some experimental information about how rapidly the charge decayed away plus simulated the beam transmission [2]. Also, a highly charged ion beam was guided and then moved to pass close by the outside of the charged capillary. The beam was observed to have a time dependent deflection as the capillary charge decayed away. However, in both studies, the geometries plus the data acquired were incompatible with providing information about the spacial and temporal behavior of the capillary charge.

Here, a new study employing well defined geometry is described. The experimental setup at the Missouri University of Science and Technology used a 1 keV Ar^+ beam guided by two parallel glass microscope slides (approximately 58 mm long, 25 mm high and 1 mm thick). The beam was collimated by three 0.5 mm apertures, one centered between the plates, the other two positioned to transmit beams between the outer surface of one of the glass plates and a parallel metal plate. One of the bypass beams was at the same height as the "guided" beam, the other was 3 beam diameters lower.

Several quantitative studies were performed for capillary rotations of a few degrees. They include 1) absolute measurements of the currents that were transmitted and that impacted the glass plates as a function of time; 2) measurement of the initial transmitted current after the beam was blocked for various times; 3) 2D images of the intensities and positions of the "guided" and "bypass" beams as functions of the charging and discharging times. From these data, quantitative information about the charging and discharging times as well as the special and temporal charge distributions on the plates is being extracted and simulations describing these features are in progress.

References

[1] K. Schiessl, W. Palfinger, K. Tőkési, H. Nowotny, C. Lemell, and J. Burgdörfer, Phys. Rev. A.**72** (2005) 062902.
[2] E. Giglio, R.D. DuBois, A. Cassimi, K.Tőkési, Nucl. Instr. and Meth. Phys. Res. B**354** (2015) 82.

Interference Effects in the Electron Impact Ionization of Diatomic Molecules at Intermediate Energies

Zehra Nur Ozer[1], Sadek Amami[2], Don Madison[2] ,Mevlut Dogan[1]

1. Afyon Kocatepe University, Science and Literature Faculty, Physics Department,e-COL Laboratory, Afyonkarahisar,Turkey

2. Missouri University of Science and Technology, Rolla MO 65409, USA

Wave-particle duality is the basis of elementary quantum physics. This phenomenon has been seen for photons, electrons, neutrons and atoms and likened to the famous double slit light experiment. It is desirable to obtain a better understanding of basic quantum phenomena and one way to do that is to study collision processes in which the kinematical details of all the particles are determined. One of the experimental techniques that determines all the kinematical parameters is the measurement of the triple differential cross sections (TDCS) using the so called (e,2e) spectrometer. Electron impact ionization of diatomic molecule studies using the (e,2e) method have shown existence of interference effects in the TDCS measurements in combination with theoretical studies obtained using different models [1-3].

The most sensitive way to search for possible interference effects is to look at the so called I-factor which is the ration of the TDCS for a diatomic molecule to the equivalent TDCS for one of the atoms in the pair since it is not obvious how the interference could be seen directly in the TDCS for the molecule. The ratio of molecule/atom, on the other hand, should show directly the two-center effects. In this work, we will discuss how the interference factor for diatomic molecules may exhibit young-type interference patterns which depend on scattering angle, initial and ejected electron energy for 350 eV electron impact. We will discuss the significance of interference effects and interpret the experimental data from e-COL laboratory by comparing with theoretical results of the distorted wave Born approximation and the 3-body distorted wave approximation.

This work was supported by the AKU-BAP through grant 15.HIZ.DES.131.

References

[1] Z. N. Ozer, H. Chaluvadi, M. Ulu, M. Dogan, B. Aktas, D. Madison, *Young's double-slit interference for quantum particles.* Physical Review A, **87(4)**, 042704, (2013).

[2] H. Chaluvadi, Z.N. Ozer, M. Dogan, C. Ning, J. Colgan, D. Madison, *Observation of two-center interference effects for electron impact ionization of N2*. Journal of Physics B: Atomic, Molecular and Optical Physics, **48**(15), 155203, (2015).

[3] Z. N. Ozer, H. Chaluvadi, D. Madison, M. Dogan, *Interference effects for intermediate energy electron-impact ionization of H2 and N2 molecules.* In Journal of Physics: Conference Series (**Vol. 601**, **No. 1**, p. 012003). IOP Publishing, (2015).

Electron-Impact Ionization of Beryllium-Like Carbon Ions

Benjamin Ebinger[1,2], Alexander Borovik Jr.[1,2], Stefan Schippers[1,2], Alfred Müller[2]
1. I. Physikalisches Institut, Justus-Liebig-Universität Gießen, Leihgesterner Weg 217, 35392 Giessen, Germany
2. Institut für Atom- und Molekülphysik, Justus-Liebig-Universität Gießen, Leihgesterner Weg 217, 35392 Giessen, Germany

Reliable atomic data are of crucial importance for the modeling of environments where matter is ionized. Cross sections for electron-impact ionization of atoms and ions are particularly important. Besides the fairly well understood direct-ionization process, indirect ionization mechanisms such as excitation-autoionization (EA) and resonant-excitation double autoionization (REDA) can significantly contribute to net single-ionization [1]. Benchmark experiments uncovering fine structures that arise from indirect ionization processes in few-electron systems provide guidance for theoretical efforts to adequately describe total single ionization by electron collisions. Here, we present measurements of electron-impact single-ionization cross sections of the C^{2+} ion, i. e., of a fairly simple four-electron system. Complications arise, however, from the presence of both $1s^2\,2s^2\ {}^1S_0$ ground-level and $1s^2\,2s\,2p\ {}^3P_{0,1,2}$ metastable-level ions in the experiment. Employing the well-established fine-step energy-scan technique [2], contributions of indirect-ionization processes invoked by excitation of the K-shell were uncovered with a statistical uncertainty of less than 0.03% thus helping to disentangle the various cross-section contributions.

Figure 1a displays the measured total cross section together with earlier data [3]. Both data sets show a similar pattern with the difference on the absolute scale explainable by a higher fraction of metastable-level ions present in our experiment ($\sim$70% vs. $\sim$46% in Ref. [3]). The ionization thresholds are indicated by the numbered arrows: 1 (ground level) and 2 (metastable levels). Clearly evident onsets at both energies reveal the presence of significant fractions of both levels.

Figure 1b highlights the cross section features in the energy range 260 - 320 eV which are attributed to indirect ionization processes. A clear step in the cross section, which has been predicted by several calculational methods such as the distorted-wave (DW) and R-Matrix with Pseudostates (RMPS) approaches [3], could be experimentally observed for the first-time for C^{2+}. This feature originates from an EA process associated with $1s \rightarrow 2s$ (only for metastable ions) and $1s \rightarrow 2p$ excitations. Apparently, both theoretical methods estimate the strength of these EA processes correctly. In addition to the step-like feature, resonances are clearly visible in the cross section (Fig. 1b). These are due to REDA processes and could be experimentally observed in this system for the first-time as well.

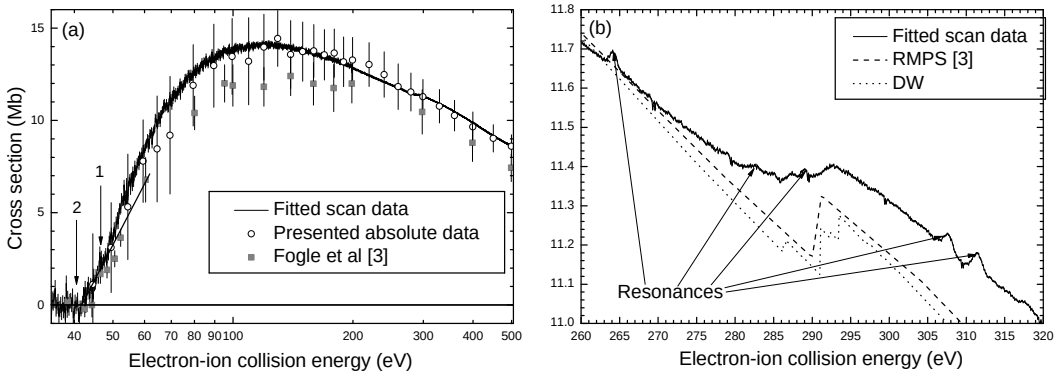

Fig. 1 (a) Measured cross section for electron-impact ionization of C^{2+} ions in comparison with earlier data. The numbers label the ionization threshold of the ground (1; $1s^2 2s^2$) and metastable level (2; $1s^2 2s 2p\ {}^3P$) respectively. (b) The measured cross section between 260 and 320 eV compared with theoretical calculations. A step (arising from EA) and several resonances (arising from REDA) can be seen clearly.

References

[1] P. Liu, J. Zeng, A. Borovik Jr., S. Schippers, and A. Müller, *Electron-impact ionization of Xe24+ ions: Theory versus experiment*, Phys. Rev. A. **92**, 012701 (2015).

[2] A. Müller, K. Tinschert, G. Hofmann, E. Salzborn, and G.H. Dunn, *Resonances in electron-impact single, double, and triple ionization of heavy metal ions*, Phys. Rev. Lett. **61**, 70-73 (1988).

[3] M. Fogle, E.M. Bahati, M.E. Bannister, C.R. Vane, S.D. Loch, M.S. Pindzola, C.P. Ballance, R.D. Thomas, V. Zhaunerchyk, P. Bryans, W. Mitthumsiri, and D.W. Savin, *Electron-impact ionization of Be-like C III, N IV and O V*, Astrophys. J. Suppl. Ser. **175**, 543-556 (2008).

PEGASUS: An Intense Spin-Polarized Electron-Beam Source

Daniel Schury[1,2], **Michael Lestinsky**[1], **Stefan Schippers**[2], **Siegbert Hagman**[1], **Christophor Kozhuharov**[1], **Thomas Stöhlker**[1,3]

1. GSI Helmholtzzentrum für Schwerionenforschung GmbH, 64291 Darmstadt, Germany
2. 1. Physikalisches Institut, Justus-Liebig-Universität Gießen, 35392 Giessen, Germany
3. Helmholtz-Institut Jena, 07443 Jena, Germany

The PEGASUS project at GSI aims at providing an intense and portable spin-polarized electron beam for experiments in crossed- and merged-beams arrangements at various ion-beam facilities. Electron energies will range from 1 to 10 keV at electron currents up to 100 μA. Laser induced electron emission from GaAs photocathodes [1] with a state of negative electron affinity [2] will be utilized for beam generation. The cathode is currently under construction. With a set of electrostatic lenses and benders [3], the electrons will be transported to the interaction zone. Wien-filters will be used for controlling the spin orientation.

The current status of the experiment is shown in Fig. 1. The experiment has been designed to be transportable such that it can be used in different places for different experiments, for example as a user experiment at storage rings or as a stand-alone installation coupled with diagnostic elements. Currently planned first experiments comprise the investigation of asymmetries in nonradiative electron capture to continuum at CRYRING at GSI [4] and the measurement of the circular dichroism in collisions of spin polarized electrons with chiral molecules using an ESA22 electron spectrometer [5].

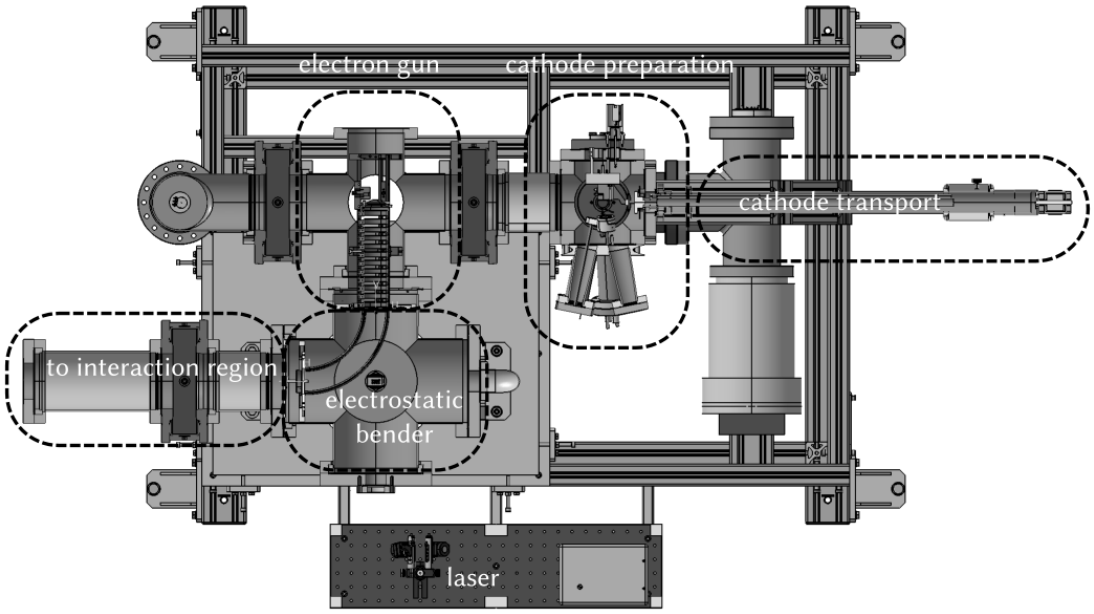

Fig. 1 Top view of PEGASUS in the current state of construction.

References

[1] Yu. A. Mamaev, L. G. Gerchikov, Yu. P. Yashin, D. A. Vasiliev, V. V. Kuzmichev, V. M. Ustinov, A. E. Zhukov, V. S. Mikhrin, and A. P. Vasiliev, *Optimized photocathode for spin-polarized electron sources*, Appl. Phys. Lett. **93**, 081114 (2008).

[2] H. Kreckel, H. Bruhns, K. A. Miller, E. Wåhlin, A. Davis, S. Höckh, and D. W. Savin, *A simple double-focusing electrostatic ion beam deflector*, Rev. Sci. Inst. **81**, 063304 (2010).

[3] D. T. Pierce, R. J. Celotta, G.-C. Wang, W. N. Unertl, A. Galejs, C. E. Kuyatt, and S. R. Mielczarek, *GaAs spin polarized electron source*, Rev. Sci. Inst. **51**, 478 (1980).

[4] P.-M. Hillenbrand, S. Hagman, D. H. Jakubassa-Amundsen, J. M. Monti, D. Banaś, K. H. Blumenhagen, C. Brandau, W. Chen, P. D. Fainstein, E. De Filippo, A. Gumberidze, D. L. Guo, M. Lestinsky, Yu. A. Litvinov, A. Müller, R. D. Rivarola, H. Rothard, S. Schippers, M. S. Schöffler, U. Spillmann, S. Trotsenko, X. L. Zhu, and Th. Stöhlker, *Electron-capture-to-continuum cusp in* $U^{88+}+N_2$ *collisions*, Phys. Rev. A **91**, 022705 (2015).

[5] L. Ábrók, T. Buhr, Á. Kövér, R. Balog, D. Hatvani, P. Herczku, S. Kovács, and S. Ricz, *A method for intensity calibration of an electron spectrometer with multi-angle detection*, Nucl. Instrum. Methods Phys. Res. B **369**, 24 (2016).

Electron interaction with Dicyclohexyl phthalate

Michal Lacko[1], Peter Papp[1], Štefan Matejčík[1]

1. Department of Experimental Physics, Faculty of Mathematics, Physics and Informatics, Comenius University in Bratislava, Mlynská dolina, 842 48 Bratislava, Slovakia

Esters of phthalatic acid ("phthalates") are molecules used in industrial manufacturing of plastic products as some plasticizers. Potential negative health effect of phthalates was investigated for many years. High amount of animal and human studies was carried out with focus on exposition of phthalates as well as on health effect [1-4]. The evidence of threat by exposition with the phthalates during evolution of human reproduction system is well known. Many techniques were developed for detection of phthalates in everyday products, among all LC-MS or GC-MS are the most used [5]. In case of positive ions, formation of protonated phthalate anhydride with *m/z* 149 can be observed frequently. This reaction represent a good confirmation of presence of phthalates in the sample, unfortunately information about phthalate type is suppressed.

In the present study we report electron ionization and electron attachment processes with corresponding dissociated pathways on Dicyclohexyl phthalate molecule (DCHP). Experiment [6] was performed by trochoidal electron monochromator interacting with gas phase molecular beam. Created ion products were analyzed by quadrupole mass spectrometer. In the mass spectrum we can observe two most dominant products, of the characteristic protonated phthalate anhydride (*m/z* 149) and the product with *m/z* 167 (trihydrogenated phthalate). Ions with *m/z* 231 (phthalate-O-R) and 249 (dihydrogenated cyclohexyl phthalate) contain information only about one cyclohexyl substituent. No parent ion was detected for DCHP molecule.

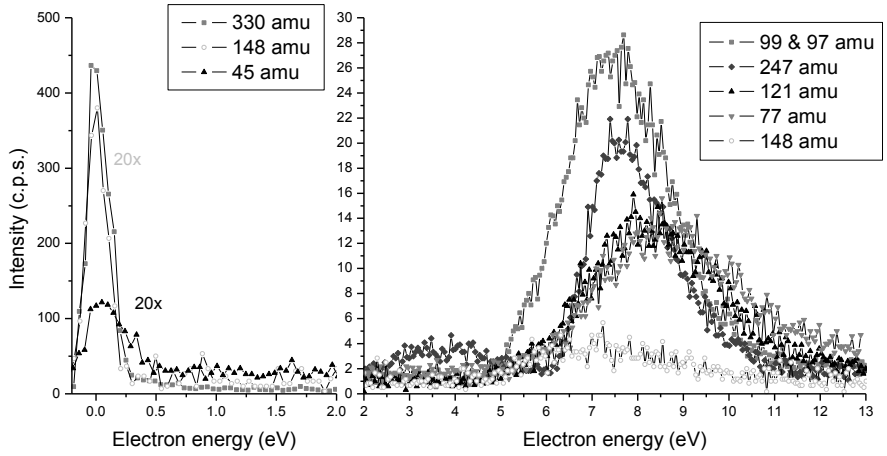

Fig. 1 The cross sections of creation of negative ions by EA and DEA on DCHP molecule.

In the case of creation of negative ions, cross sections of detected products are presented on fig. 1. Creation of parent anion *via* electron attachment is the most intensive process with resonance maximum close to 0 eV. Other anions are created by dissociative electron attachment process. At the same energy we can observe production of ions with *m/z* 148 and 45 represented by creation of phthalate anhydride anion and $COOH^-$ respectively. For these products a considerable positive electron affinity is evident. Resonances at higher electron energy are situated with respect of excited states of neutral DCHP. In this range resonances show the same character and can be localized in shorter range with dissociation threshold at ~ 4.5eV, except production of ion with *m/z* 247. It is represented by two resonances with thresholds at ~ 2 eV and ~ 6 eV.

This work was supported by the Slovak Research and Development Agency under Contract No. APVV-0733-11 and the Slovak grant agency VEGA 1/0417/15. This work was conducted within the framework of the COST Action CM1301 (CELINA). This project has received funding from the European Union's Horizon 2020 research and innovation programme under grant agreement No 692335.

References

[1] R.U. Halden, *Annual review of public health*, **31** (2010) 179-194.
[2] P.J. Lioy, R. Hauser, C. Gennings, H.M. Koch, P.E. Mirkes, B.A. Schwetz, A. Kortenkamp, *Journal of exposure science & environmental epidemiology*, **25** (2015) 343-353.
[3] S. Benjamin, S. Pradeep, M.S. Josh, S. Kumar, E. Masai, *Journal of hazardous materials*, **298** (2015) 58-72.
[4] V.M. Pak, L.A. McCauley, J. Pinto-Martin, *AAOHN Journal*, **59** (2011) 228-233.
[5] M.V. Russo, P. Avino, L. Perugini, I. Notardonato, *RSC Adv.*, **5** (2015) 37023-37043.
[6] M. Stano, S. Matejcik, J.D. Skalny, T.D. Märk, *Journal of Physics B: Atomic, Molecular and Optical Physics*, **36** (2003) 261.

Electron Impact Ionization of He(1s2s ^{3}S)

Matthieu Génévriez[1], Jozo J. Jureta[1], Pierre Defrance[1], Xavier Urbain[1]
1. Institute of Condensed Matter and Nanosciences, Université Catholique de Louvain, Louvain-la-Neuve B-1348, Belgium

The electron impact ionization of the metastable state 1s2s ^{3}S of helium is particularly important in the modeling of plasmas, and, as a simple system, is also a benchmark for theories. There are only a few absolute experimental determinations of the ionization cross section, the latest being that of Dixon *et al.* [1]. They are a factor of two higher than most, numerous theoretical calculations [2, 3], and therefore another absolute measurement is highly demanded by the community.

In previous experiments, metastable atoms were produced by charge exchange with alkali vapour and therefore yielded a mixture of singlet and triplet states (^{1,3}S). A precise knowledge of the blending was thus necessary to determine absolute cross sections. To overcome this difficulty, we designed a novel source for the production of a fast, intense beam of metastable helium atoms in the 1s2s ^{3}S state only. A duoplasmatron source produces He^+ ions, accelerated to 8 keV. They are sent into a sodium vapor cell, where double charge exchange produces He^- ions with an efficiency of the order of 1%. The He^- beam, cleaned from its neutral and positive components, interacts collinearly, for about 35 cm, with a CW CO_2 laser providing light at a wavelength of 10.6 μm and with a power of 7 W. A significant fraction ($\sim$40%) of the He^- ions is photodetached by the laser light, leaving neutral helium atoms in the 1s2s ^{3}S state. We are thus able to produce a fast beam of He(1s2s ^{3}S). The beam of neutral atoms is injected downstream in the setup for electron-ion collisions, described elsewhere [4], where the electron impact ionization cross section is measured following the animated-crossed-beam method of Defrance *et al.* [5].

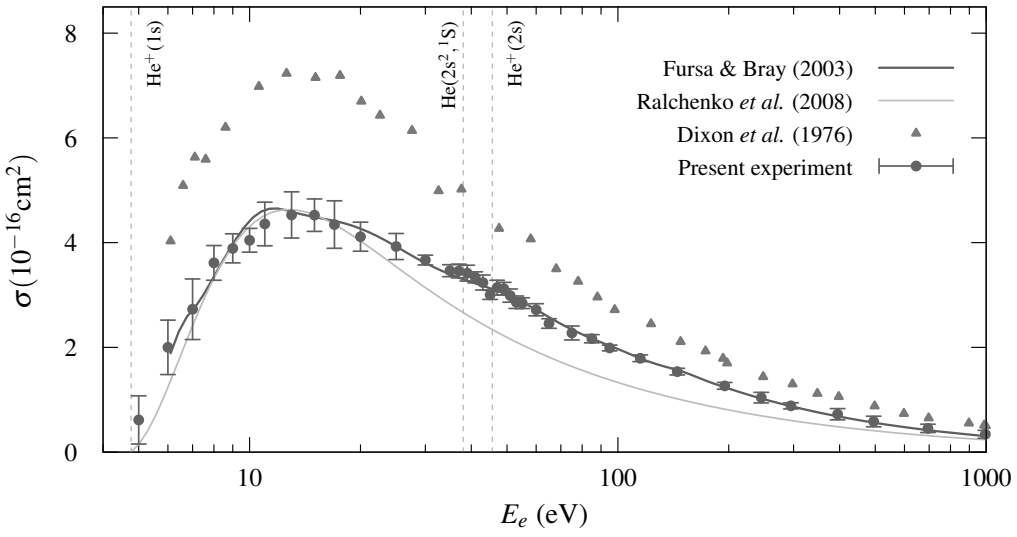

Fig. 1 Cross section for the electron impact ionization of He(1s2s ^{3}S).

The present results for He(1s2s ^{3}S) are presented in figure 1. They lie significantly lower than the previous experiments. They are also in very good agreement with the theoretical results of Fursa and Bray [2], who performed a frozen core convergent-close-coupling calculation combined, at high electron energies, with multi-core Born calculations. It thus accounted for the effect of doubly excited states, which indeed have a strong influence on the cross section. The cross sections reported more recently by Ralchenko *et al.* do not include doubly excited states [3], whence the pronounced dip in the cross section at higher electron energies.

References

[1] A. J. Dixon, M. F. A. Harrison and A. C. H. Smith, *A measurement of the electron impact ionization cross section of helium atoms in metastable states*, J. Phys. B **9**, 2617 (1976).
[2] D. V. Fursa and I. Bray, *Electron-impact ionization of the helium metastable 2 ^{3}Sstate* J. Phys. B **36**, 1663 (2003)
[3] Y. Ralchenko, R. K. Janev , T. Kato, D.V. Fursa, I. Bray and F.J. de Heer, *Electron-impact excitation and ionization cross sections for ground state and excited helium atoms*, At. Data Nucl. Data Tables **94**, 603 (2008)
[4] . Lecointre, S. Cherkani-Hassani, D.S. Belic, J.J. Jureta, K. Becker, H. Deutsch, T.D. Märk, M. Probst, R.K. Janev and P. Defrance, *Absolute cross sections and kinetic energy release distributions for electron impact ionization and dissociation of CD^+*, J. Phys. B **40**, 2201 (2007)
[5] P. Defrance, F. Brouillard, W. Claeys and G. Van Wassenhove, *Crossed beam measurement of absolute cross sections: an alternative method and its application to the electron impact ionisation of He^+*, J. Phys. B 14, 103 (1981)

Coherent Charge-Spin Coupled Transport in Two Dimensional Dirac Systems

Saber Rostamzadeh, Inanc Adagideli

Faculty of Engineering and Natural Sciences,
Sabanci University, Orhanli - Tuzla, 34956, Turkey

In this study we use the density matrix approach and attempt to derive a generalized Quantum Botlzmann transport equation for a 2D single cone Dirac system given by the Bloch Hamiltonian $\mathcal{H} = v_F\,\vec{\sigma}\cdot\mathbf{k}$. This model best describes the dynamics of carriers on the surface of a flat topological insulators, i.e,

$$\partial_t \mathfrak{g}_{\mathbf{k}} + i v_F[\sigma_{\mathbf{k}}, \mathfrak{g}_{\mathbf{k}}]_- + \frac{v_F}{2}[\vec{\sigma}, \nabla_r \mathfrak{g}_{\mathbf{k}}]_+ = \frac{i}{\tau}\Big(G^R(\mathbf{k},\varepsilon)\,\rho - \rho\,G^A(\mathbf{k},\varepsilon)\Big) - \frac{\mathfrak{g}_{\mathbf{k}}}{\tau} \tag{1}$$

We have established the exact same equation using the Keldysh formalism by deriving a kinetic equation in terms of the Greens' functions and Fourier transforming to obtain the generalized transport equation.

The extension into a double cone system to study Graphene or 3D systems to include 3D topological insulators and Weyl semimetals are straightforward and will not be presented here.

Following this expression and defining $\rho = \frac{\rho_0}{2} + \vec{s}\cdot\vec{\sigma}$, where $\vec{s} = (\mathbf{s}, s_3)$, and the diffusion constant as $D = \frac{v_F\tau}{2}$ we obtain a set of coupled spin charge diffusion equations

$$\begin{aligned} D\,\nabla^2\rho_0 - v_F\,\nabla\cdot\mathbf{s} &= 0, \\ D\,\nabla^2\mathbf{s} - D\,\nabla(\nabla\cdot\mathbf{s}) - v_F\,\nabla\rho_0 &= \tfrac{\mathbf{s}}{\tau/2}, \\ D\,\nabla^2 s_3 - v_F\,(\hat{\mathbf{z}}\times\nabla)\cdot\mathbf{s} &= \tfrac{s_3}{\tau/2}. \end{aligned} \tag{2}$$

In obtaining this equations we assume the large limit of spin-charge coupling hence shorter scattering time than spin relaxation time. In this limit spin polarizations vary slowly in the limit of mean free path. This particular features suggests some spin related effects which can lead to observable outcomes.

References

[1] E. G. Mishchenko, A. V. Shytov, and B. I. Halperin Phys. Rev. Lett. 93, 226602 (2004),

[2] Inanc Adagideli and Gerrit E. W. Bauer Phys. Rev. Lett. 95, 256602 (2005),

[3] A. A. Burkov and D. G. Hawthorn Phys. Rev. Lett. 105, 066802 (2010),

[4] A. A. Burkov, Alvaro S. Nez, and A. H. MacDonald Phys. Rev. B 70, 155308 (2004)

Electron-Ion Recombination of Ions with an Open 4f Shell: W^{19+}

Nigel Badnell[1], Kaija Spruck[2,3], Claude Krantz[3], Oldřich Novotný[3,4], Arno Becker[3], Dietrich Bernhardt[2], Manfred Grieser[3], Michael Hahn[4], Roland Repnow[3], Daniel Wolf Savin[4], Andreas Wolf[3], Alfred Müller[2], and Stefan Schippers[5]

1. Department of Physics, University of Strathclyde, Glasgow G4 0NG, United Kingdom
2. Institut für Atom- und Molekülphysik, Justus-Liebig-Universität Gießen, 35392 Giessen, Germany
3. Max-Planck-Institut für Kernphysik, Saupfercheckweg 1, 69117 Heidelberg, Germany
4. Columbia Astrophysics Laboratory, Columbia University, 550 West 120th Street, New York, NY 10027, USA
5. I. Physikalisches Institut, Justus-Liebig-Universität Gießen, 35392 Giessen, Germany

Atomic collision processes with tungsten ions are of current interest for understanding the role of tungsten impurities in fusion plasmas [1]. For example, the charge balance of tungsten is determined by the interplay of electron-impact ionization and electron-ion recombination. Most of the required cross sections come from theoretical calculations which often bear large uncertainties and, thus, require benchmarking by experiment. To this end, we have focussed on tungsten ions with a particulary complex atomic structure. The present study extends our previous work on electron-ion recombination of W^{20+} [2,3] and W^{18+} [4] to $W^{19+}([Kr]4d^{10}4f^{9})$.

The experiment was carried out by employing the electron-ion merged-beams technique at the Heidelberg heavy-ion storage ring TSR. As in the previous cases of W^{18+} and W^{20+}, an unusually large W^{19+} recombination rate coefficient has been observed at low electron-ion collision energies (Fig. 1a) leading to a plasma rate coefficient that is larger by up to almost three orders of magnitude than the rate coefficient from the ADAS [5] data base (Fig. 1b). According to our present understanding, this is caused by resonant recombination involving many-electron processes which cannot fully be treated by the standard theory for electron-ion recombination. Nevertheless, they can be accounted for in a coarse manner by statistical theory [6]. Different variants of statistical theory have already been applied successfully to electron-ion recombination of W^{20+} [3,7] and W^{18+} [4]. Also our present calculations for W^{19+} are in good agreement with the experimental findings (Fig. 1). This adds to the confidence that statistical theories will be able to provide reliable electron-ion recombination rate coefficients also for other complex ions.

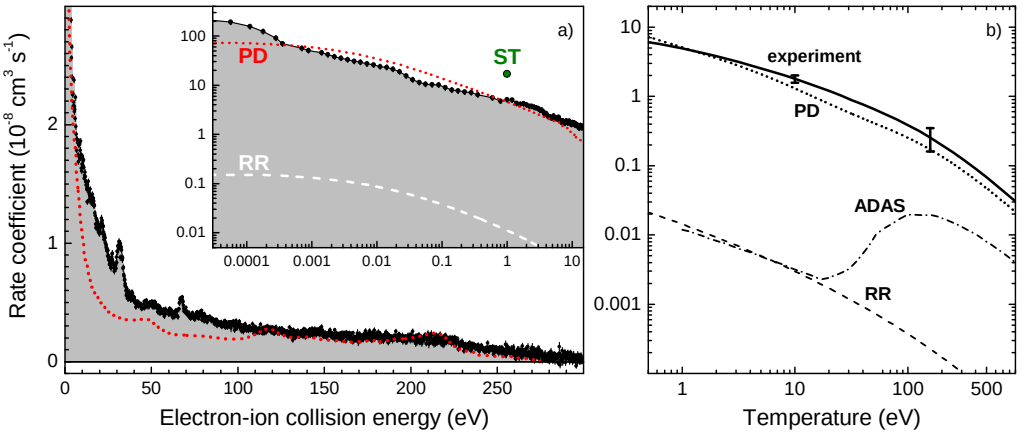

Fig. 1 Merged-beams (a) and plasma (b) rate coefficients for electron-ion recombination of W^{19+}. PD: present partitioned and damped statistical theory; ST: statistical theory [7]; ADAS: result from the ADAS [5] data base; RR: radiative recombination.

References

[1] A. Müller, *Fusion-related ionization and recombination data for tungsten ions in low to moderately high charge states*, Atoms **3**, 120 (2015).
[2] S. Schippers, D. Bernhardt, A. Müller, C. Krantz, M. Grieser, R. Repnow, A. Wolf, M. Lestinsky, M. Hahn, O. Novotný, and D. W. Savin, *Dielectronic recombination of xenonlike tungsten ions*, Phys. Rev. A **83**, 012711 (2011).
[3] N. R. Badnell, C. P. Ballance, D. C. Griffin, and M. O'Mullane, *Dielectronic recombination of W^{20+} ($4d^{10}4f^{8}$): Addressing the half-open f shell*, Phys. Rev. A **85** 052716 (2012).
[4] K. Spruck, N. R. Badnell, C. Krantz, O. Novotný, A. Becker, D. Bernhardt, M. Grieser, M. Hahn, R. Repnow, D. W. Savin, A. Wolf, A. Müller, and S. Schippers, *Recombination of W^{18+} ions with electrons: Absolute rate coefficients from a storage-ring experiment and from theoretical calculations*, Phys. Rev. A, **90** 032715 (2014).
[5] ADAS, *Atomic Data and Analysis Structure*, `http://www.adas.ac.uk`.
[6] V. Flambaum, A. A. Gribakina, G. F. Gribakin, and C. Harabati, *Electron recombination with multicharged ions via chaotic many-electron states*, Phys. Rev. A **66**, 012713 (2002).
[7] V. A. Dzuba, V. V. Flambaum, G. F. Gribakin, C. Harabati, and M. G. Kozlov, *Electron recombination, photoionization, and scattering via many-electron compound resonances*, Phys. Rev. A **88**, 062713 (2013).

Photorecombination of Berylliumlike and Boronlike Silicon Ions

Dietrich Bernhardt[1], Arno Becker[2], Carsten Brandau[3,4], Manfred Grieser[2], Michael Hahn[5], Claude Krantz[2], Michael Lestinsky[4], Oldřich Novotný[2,5], Roland Repnow[2], Daniel Wolf Savin[5], Kaija Spruck[1,2], Andreas Wolf[2], Alfred Müller[1], and Stefan Schippers[3]

1. Institut für Atom- und Molekülphysik, Justus-Liebig-Universität Gießen, 35392 Giessen, Germany
2. Max-Planck-Institut für Kernphysik, 69117 Heidelberg, Germany
3. I. Physikalisches Institut, Justus-Liebig-Universität Gießen, 35392 Giessen, Germany
4. GSI Helmholtzzentrum für Schwerionenforschung, 64291 Darmstadt, Germany
5. Columbia Astrophysics Laboratory, Columbia University, New York, NY 10027, USA

We report measured rate coefficients for electron-ion recombination of Si^{10+} forming Si^{9+} and of Si^{9+} forming Si^{8+}, respectively [1]. The measurements were performed using the electron-ion merged-beams technique at the Heidelberg heavy-ion storage ring TSR. Electron-ion collision energies ranged from 0 to 50 eV for Si^{9+} and from 0 to 2000 eV for Si^{10+}, thus extending previous measurements for Si^{10+} [2] to much higher energies (Fig. 1). Experimentally-derived rate coefficients for the recombination of Si^{9+} and Si^{10+} ions in a plasma are presented along with simple parameterizations. These rate coefficients are useful for the modeling of the charge balance of silicon in photoionized plasmas (Si^{9+} and Si^{10+}) and in collisionally ionized plasmas (Si^{10+} only). In the corresponding temperature ranges, the experimentally-derived rate coefficients agree with the latest corresponding theoretical results [3,4] within the experimental uncertainties.The storage-ring techniques allows for the preparation of ions in well defined energy levels by spontaneous relaxation of excited states. This has been exploited in particular for reducing the Si^{10+} ion beam contamination by long-lived $2s\,2p\ ^3P$ metastable levels to almost insignificance.

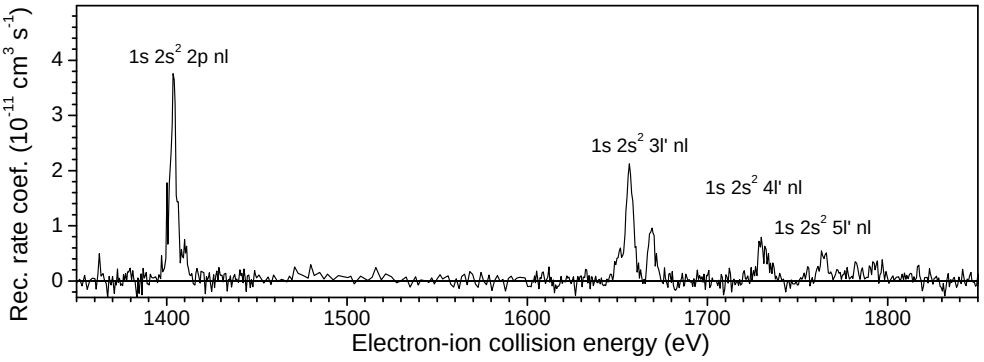

Fig. 1 High-energy part of the measured merged-beams rate coefficient (solid black line) for photorecombination of Si^{10+} in the energy range of dielectronic recombination resonances associated with K-shell excitations. Resonance groups are labelled by the according $1s^2\,2s^2 \rightarrow 1s\,2s^2\,N'l'$ core excitations. The figure has been taken from Ref. [1].

References

[1] D. Bernhardt, A. Becker, C. Brandau, M. Grieser, M. Hahn, C. Krantz, M. Lestinsky, O. Novotný, R. Repnow, D. W. Savin, K. Spruck, A. Wolf, A. Müller, and S. Schippers, *Absolute rate coefficients for photorecombination of berylliumlike and boronlike silicon ions*, J. Phys. B **49**, 074004 (2016).

[2] I. Orban S. D. Loch, S. Böhm, and R. Schuch, *Recombination rate coefficients of Be-like Si*, Astrophys. J. **721**, 1603 (2010).

[3] J. Colgan, M. S. Pindzola, A, D. Whiteford, N. R. Badnell, *Dielectronic recombination data for dynamic finite-density plasmas III. The beryllium isoelectronic sequence*, Astron. Astrophys. **412**, 597 (2003).

[4] Z. Altun, A. Yumak, N. R. Badnell, J. Colgan, and M. S. Pindzola, *Dielectronic recombination data for dynamic finite-density plasmas VI. The boron isoelectronic sequence*, Astron. Astrophys. **420**, 775 (2004).

Photoelectron Cicular Dichroism Measured by Multiphoton Ionization

Thomas Baumert
Institut für Physik and CINSaT, Universität Kassel, Heinrich-Plett-Str. 40, 34132 Kassel, Germany

The photo electron circular dichroism (PECD) [1,2], i.e. a striking forward / backward electron emission with respect to the light propagation of a light beam ionizing randomly oriented chiral molecules, was extended to the resonance enhanced multi photon ionization (REMPI) regime with femtosecond laser pulses [3,4] and studied as a function of absorbed photons [5]. As the effect is in the ten percent regime, sub one percent sensitivity to enantiomeric excess was demonstrated [6]. Besides a discussion of the published experiments I will highlight the current status of our experiments with a special focus on coherent control techniques to study and control the coupled electron nuclear motion [7,8] in chiral potentials also with the prospect to the development of laser-driven purification schemes.

References

1. I. Powis, "Photoelectron circular dichroism," in *Comprehensive chiroptical spectroscopy*, N. Berova, P. Polavarapu, K. Nakanishi, R. Woody, eds. (Wiley, 2012), pp. 407–432.
2. I. Powis, "Photoelectron Circular Dichroism in Chiral Molecules," Adv. Chem. Phys. **138**, 267–329 (2008).
3. C. Lux, M. Wollenhaupt, T. Bolze, Q. Liang, J. Köhler, C. Sarpe, and T. Baumert, "Circular Dichroism in the Photoelectron Angular Distributions of Camphor and Fenchone from Multiphoton Ionization with Femtosecond Laser Pulses," Angew. Chem. Int. Ed. **51**, 5001–5005 (2012).
4. C. Lux, M. Wollenhaupt, C. Sarpe, and T. Baumert, "Photoelectron Circular Dichroism of Bicyclic Ketones from Multiphoton Ionization with Femtosecond Laser Pulses," ChemPhysChem **16**, 115–137 (2015).
5. C. Lux, A. Senftleben, C. Sarpe, M. Wollenhaupt, and T. Baumert, "Photoelectron circular dichroism observed in the above-threshold ionization signal from chiral molecules with femtosecond laser pulses," J. Phys. B: At. Mol. Opt. Phys. **49**, 02LT01 (2016). doi:10.1088/0953-4075/49/2/02LT01
6. A. Kastner, C. Lux, T. Ring, S. Züllighoven, C. Sarpe, A. Senftleben, and T. Baumert, "Enantiomeric Excess Sensitivity to Below One Percent by Using Femtosecond Photoelectron Circular Dichroism" ChemPhysChem (2016). DOI : 10.1002/cphc.201501067
7. M. Wollenhaupt, and T. Baumert, "Ultrafast laser control of electron dynamics in atoms, molecules and solids," Faraday Discuss. Chem. Soc. **153**, 9–26 (2011).
8. T. Bayer, H. Braun, C. Sarpe, R. Siemering, P. von den Hoff, R. de Vivie-Riedle, T. Baumert, and M. Wollenhaupt, "Charge oscillation controlled molecular excitation," Phys. Rev. Lett. **110**, 123003 (2013).

X-ray magnetic circular dichroism spectroscopy in transition metal dimer cations

V. Zamudio-Bayer[1,2], K. Hirsch[1], A. Langenberg[1], A. Ławicki[1], C. Bülow[1], R. Lindblad[1,3], G. Leistner[1], A. Terasaki[4], B. v. Issendorff[2], J.T. Lau[1]

[1]*Institut für Methoden und Instrumentierung der Forschung mit Synchrotronstrahlung, Helmholtz-Zentrum Berlin, Germany*
[2]*Physikalisches Institut, Universität Freiburg, Germany*
[3]*Synkrotronljusfysik, Lunds Universitet, Sweden*
[4]*Department of Chemistry, Kyushu University, Japan*

Although they consist of only two atoms, 3d transition metal dimers possess a complex electronic structure making it challenging to correctly predict their electronic ground state. Experimentally they are not easily accessible due to their high reactivity and low sample densities. We have recently investigated spin and orbital angular momenta in the electronic ground states of 3d transition metal diatomic molecular cations by x-ray magnetic circular dichroism spectroscopy in a cryogenic ion trap. [1] We find that all investigated (chromium, manganese, iron, cobalt, and nickel) diatomic molecular cations tend to adopt the maximum spin multiplicity in their electronic ground states as a result of strong exchange. [2-4] Orbital angular momentum still is a good quantum number in diatomics because of symmetry and can lead to a strong coupling of the spin to the molecular axis. [2] Our results also show that the ground states of neutral and cationic transition metal dimers cannot be assumed to be linked by simple one-electron processes. [2-4] This behaviour is similar to the case of 3d transition metal atoms.

[1] M. Niemeyer *et al.*, Spin Coupling and Orbital Angular Momentum Quenching in Free Iron Clusters, *Phys. Rev. Lett.* **108**, 057201 (2012).
[2] V. Zamudio-Bayer *et al.*, Electronic Ground States of Fe_2^+ and Co_2^+ as Determined by X-ray Absorption and X-ray Magnetic Circular Dichroism Spectroscopy, *J. Chem. Phys.* **143**, 244318 (2015).
[3] V. Zamudio-Bayer *et al.*, Maximum Spin Polarization in Chromium Dimer Cations as Demonstrated by X-ray Magnetic Circular Dichroism Spectroscopy, *Angew. Chem. Int. Ed.* **54**, 4498 (2015).
[4] V. Zamudio-Bayer *et al.*, Direct Observation of High-Spin States in Manganese Dimer and Trimer Cations by X-ray Magnetic Circular Dichroism Spectroscopy in an Ion Trap, *J. Chem. Phys.* **142**, 234301 (2015).

Enantiomer differentiation using microwave three-wave mixing

Melanie Schnell
Max Planck Institute for the Structure and Dynamics of Matter at the Center for Free-Electron Laser Science, Luruper Chaussee 149, 22761 Hamburg, Germany

Microwave three-wave mixing is a new technique to analyse complex chiral mixtures in the gas phase, based on broadband rotational spectroscopy. It allows us to differentiate the enantiomers of chiral molecules in the gas phase, to determine the enantiomeric excess and, in an indirect way, the absolute configuration of the excess enantiomer.

Microwave three-wave mixing is based on broadband rotational spectroscopy and involves a closed cycle of three rotational transitions. The molecules are excited resonantly, so that the obtained information is like an unambiguous molecular fingerprint, even when the molecules are very similar. The phase of the acquired signal bares the signature of the enantiomers, as it depends upon the product of the transition dipole moments, and the signal amplitude is proportional to the ee.

In the lecture, I will introduce the technique and give an update on the recent developments. For example, we could recently apply it to the analysis of a commercially available essential oil and address molecules with several stereogenic centers. Furthermore, we are exploring if an extension of this technique can be used to separate the enantiomers.

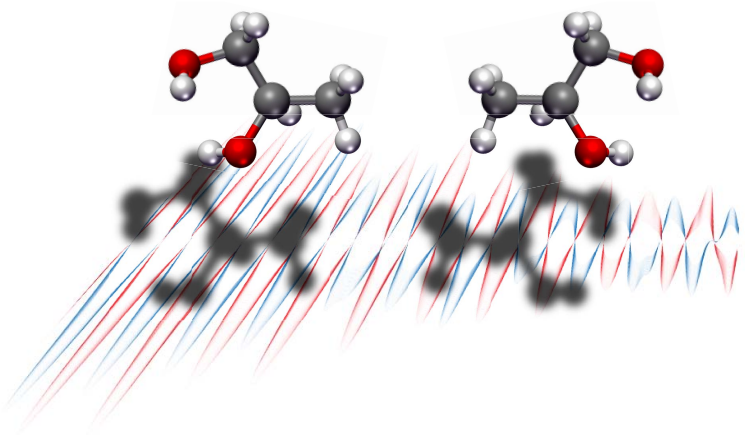

Fig. 1 The mirror-image character of the two enantiomers resulting in a π radian phase shift in the respective free-induction decay of the chiral sample, as indicated by the color code.

Exploring Dynamics in Chiral Systems with Free-Electron Lasers

Markus Ilchen[1,3,8], Sadia Bari[2], Ryan Coffee[3], Philipp Demekhin[4], Andreas Galler[1], Gregor Hartmann[5], Nick Hartmann[3], Zhirong Huang[3], Nikolay Kabachnik[6,1], Andrey Kazanski[7], André Knie[4], Zheng Li[2,8], Alberto Lutman[3], Timothy Maxwell[3], James MacArthur[3], Tommaso Mazza[1], Stefan Moeller[3], Heinz-Dieter Nuhn[3], Hirohito Ogasawara[3], Hendrik Ohldag[3], Timur Ospipov[3], Jones Rafipoor[1], Dipanwita Ray[3], Patrick Rupprecht[3,8,9], Philipp Schmidt[4], Jens Viefhaus[5], Peter Walter[5,3], Thomas Wolf[8], and Michael Meyer[1]

1. *European XFEL GmbH, Albert-Einstein-Ring 19, 22761 Hamburg, Germany*
2. *Center for Free-Electron Laser Science - CFEL, Notkestraße 85, 22607 Hamburg, Germany*
3. *SLAC National Accelerator Laboratory, 2575 Sand Hill Road, 94025 Menlo Park, USA*
4. *Institut für Physik, Universität Kassel, Heinrich-Plett-Str. 40, 34132 Kassel, Germany*
5. *Deutsches Elektronen-Synchrotron, Notkestraße 85, 22607 Hamburg, Germany*
6. *Departamento de Fisica de Materiales, UPV/EHU, Donostia International Physics Center, E-20018 San Sebastian/Donostia, Spain*
7. *IKERBASQUE, Basque Foundation for Science, E-48011 Bilbao, Spain*
8. *PULSE at Stanford, 2575 Sand Hill Road, 94025 Menlo Park, USA*
9. *Physik-Department, Technische Universität München, James-Franck-Strasse 1, D-85748 Garching, Germany*

The handedness, i.e. chirality, of life's molecular building blocks as well as of electronic spin is of large interest for practically all natural sciences. Spin control with applications in magnetism [1] as well as in fundamental atomic physics [2] and the stereochemistry of homo-chirality of life on earth with major implications for pharmaceuticals [3] are examples of state-of-the-art multidisciplinary science.

A very common technique to study chiral properties is to measure the absorption differences of opposing helicities of circularly polarized light, the so called circular dichroism. Only recently, free-electron lasers such as FERMI in Italy and LCLS in the USA have shown to provide very high degrees of circular polarization directly from the undulator light source while preserving the characteristic properties of ultrafast and ultraintense X-ray pulses [4,5]. This new capability unprecedentedly opens the door for studying chiral and magnetic properties via observation of "handed" dynamics of highly bound electrons on a femtosecond time scale.

We present preliminary as well as final results of synchrotron (SSRL, USA) and (X-ray) free-electron laser studies (FERMI, Italy and LCLS, USA) of circular dichroism in oriented and resonantly excited electronic states as well as core shell investigations of statics and dynamics in the chiral compound Trifluoro-epoxypropane ($C_3H_3F_3O$) (see Fig. 1). The results constitute a kick-off for transient as well as resonant chirality studies at (X)FELs.

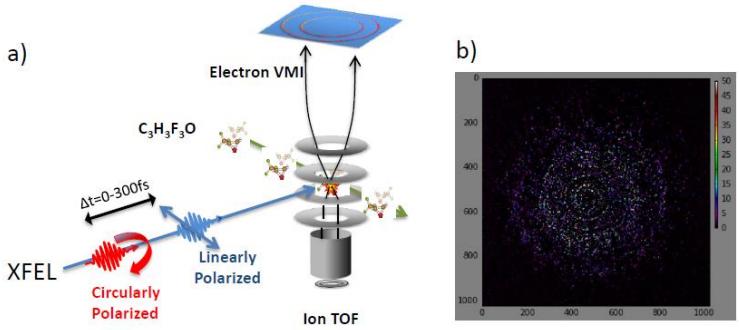

Fig. 1a) Pump-probe scheme with variable polarization provided by the new Delta undulator at LCLS. Here, the linearly polarized X-ray pulse triggers a molecular dissociation whereas the circularly polarized X-ray pulse with shifted photon energy and arrival time probes the remaining chirality of the system on a femtosecond time scale via photoelectron circular dichroism (PECD). The measurements were done with an electron velocity map imaging (VMI) and a simultaneously recorded ion time-of-flight (TOF) spectrometer. Fig 1b) depicts a raw single shot image of the electron emission of Trifluoro-epoxypropane 60 fs after the trigger pulse had arrived.

References

[1] Gunter Schütz, Wolfgang Wagner, W. Wilhelm, P. Kienle, R. Zeller, et al. *Absorption of circularly polarized x rays in iron.* Phys. Rev. Lett. **58**, 737–740 (1987).

[2] Tommaso Mazza, Markus Ilchen, Jones Rafipoor, Carlo Callegari, Paola Finetti, et al., *Determining the polarization state of an extreme ultraviolet free-electron laser beam using atomic circular dichroism*, Nat. Comms. **5**, 3648 (2014).

[3] Lien Ai Nguyen, Hua He, and Chuong Pham-Huy, *Chiral drugs: an overview.* Int J Biomed Sci **2**, 85–100 (2006).

[4] Enrico Allaria, Bruno Diviacco, Carlo Callegari, Paola Finetti, Benoît Mahieu, et al. *Control of the polarization of a vacuum-ultraviolet, high-gain, free-electron laser*, Phys. Rev. X **4**, 041040 (2014)

[5] Alberto Lutman, James MacArthur, Markus Ilchen, Anton Lindahl, Jens Buck, et al., *Polarization Control in an X-Ray Free-Electron Laser*, Nat. Phot. Accepted March 2016

Kinetic-energy release distributions of fragment anions from collisions of potassium atoms with D-ribose and tetrahydrofuran

A. Rebelo[1], T. Cunha[1], M. Mendes[1],
G. García[2], P. Limão-Vieira[1] and F. Ferreira da Silva[1]

[1] *Laboratório de Colisões Atómicas e Moleculares, CEFITEC, Departamento de Física, Faculdade de Ciências e Tecnologia, Universidade NOVA de Lisboa, 2829-516, Caparica, Portugal*

[2] *Instituto de Física Fundamental, Consejo Superior de Investigaciones Científicas (CSIC), Serrano 113-bis, 28006 Madrid, Spain*

Electron transfer in atom-molecule collision experiments is mediated by the crossing of the covalent (K + AB) and ionic (K^+ + AB^-) potential energy surfaces, where the electron donor is an alkali atom (K) and AB an electron acceptor molecule. At large atom-molecule distances, the ionic potential-energy surface lies above the covalent whilst at smaller distances, due to the Coulomb interaction, a crossing seam may be reached, meaning that both potential surfaces have the same value [1]. In this type of processes a positive ion K^+ and a temporary negative ion (TNI) (or molecular anion $(AB^-)^{\#}$) is formed, allowing access to states which are not attained by electron attachment experiments. In particular, states with a positive electron affinity can be formed, and the role of vibronic excitation can be studied [2], as well as the distribution of the translational energy of the fragment anions formed upon electron transfer in potassium molecule collisions.

In this communication we present Kinetic-energy release distributions obtained from the width and shapes of the time-of-flight (TOF) negative ion mass peaks in collisions of fast potassium atoms with D-Ribose and tetrahydrofuran (THF) molecules. In the case of D-Ribose the most intense signal is due to OH^- [3] whereas in the case of THF is due to O^- [4] formation. The kinetic energy release for a molecule dissociating into to fragments with masses m_1 and m_2, is obtained as

$$\varepsilon_d = \frac{1}{8\mu}\left(F.\Delta t\right)^2$$

were μ is the reduced mass of the m_1 and m_2 system, Δt the extraction time and F extracting field. The kinetic energy release distribution is obtained by

$$D(\varepsilon_d) = \frac{1}{A}\left[1 + \frac{3}{4}\frac{v_m^2}{v_o^2} + \ldots\right]\Delta t.I(\Delta t)$$

References

[1] A. W. Kleyn and A. M. C. Moutinho, *Negative ion formation in alkali-atom-molecule collisions,* J. Phys. B **34**, R1 (2001).
[2] A. W. Kleyn, J. Los, and E. A. Gislason, *Vibronic coupling at intersections of covalent and ionic states***,** Phys. Rep. **90**, 1 (1982).
[3] D. Almeida, F. Ferreira da Silva, G. García, and P. Limão-Vieira, *Dynamic of negative ions in potassium-D-ribose collisions*, J. Chem. Phys. **139**, 114304 (2013).
[4] D. Almeida, F. Ferreira da Silva, S. Eden, G. García, and P. Limão-Vieira, *New Fragmentation Pathways in K–THF Collisions As Studied by Electron-Transfer Experiments: Negative Ion Formation,* J. Phys. Chem. A **118**, 690 (2014).

Strong field physics with highly charged ions

Vladimir Shabaev
Departmant of Physics, St.Petersburg State University, 7/9 Universitetskaya nab., St. Petersburg, 199034 Russia

The present status of quantum electrodynamics (QED) theory of highly charged ions is reviewed. The theoretical predictions for the binding energies, the hyperfine splittings, and the bound-electron g factors are compared with available experimental data. These investigations provide tests of QED at strong fields and can also serve for determination of fundamental constants. Special attention is paid to study of the isotope shifts which can provide tests of nonperturbative QED methods at strong coupling regime beyond the Furry picture [1]. It is also demonstrated that the nonperturbative QED methods developed for calculations of highly charged ions [2] can be very efficient for light atomic systems [3]. The recent progress on calculations of various processes in low-energy heavy ion collisions is also reported [4,5].

References

[1] F. Köhler, K. Blaum, M. Block, S. Chenmarev, S. Eliseev, D.A. Glazov, M. Goncharov, J. Hou, A. Kracke, D.A. Nesterenko, Yu.N. Novikov, W. Quint, E. Minaya Ramirez, V.M. Shabaev, S. Sturm, A.V. Volotka, and G. Werth, *Isotope dependence of the Zeeman effect in lithium-like calcium*, Nature Communications **7**, 10246 (2016).

[2] V.A. Yerokhin and V.M. Shabaev, *Lamb Shift of n = 1 and n = 2 States of Hydrogen-like Atoms*, $1 \leq Z \leq 110$, Journal of Physical and Chemical Reference Data **44**, 033103 (2015).

[3] V.A. Yerokhin and V.M. Shabaev, *Nuclear Recoil Effect in the Lamb Shift of Light Hydrogenlike Atoms*, Physical Review Letters **115**, 233002 (2015).

[4] Y.S. Kozhedub, V.M. Shabaev, I.I. Tupitsyn, A. Gumberidze, S. Hagmann, G. Plunien, and Th. Stöhlker, *Relativistic calculations of x-ray emission following a Xe-Bi^{83+} collision*, Physical Review A **90**, 042709 (2014).

[5] I.A. Maltsev, V.M. Shabaev, I.I. Tupitsyn, A.I. Bondarev, Y.S. Kozhedub, G. Plunien, and Th. Stöhlker, *Electron-positron pair creation in low-energy collisions of heavy bare nuclei*, Physical Review A **91**, 032708 (2015).

Experimental Studies of Alignment and Polarization Phenomena in Energetic Atomic Collisions

Stanislav Tashenov
Physikalisches Institut der Universität Heidelberg, Im Neuenheimer Feld 226, 69120 Heidelberg, Germany

Collisions of energetic electrons with highly charged ions (HCI) and heavy atoms provide unique opportunities to investigate fundamental atomic processes in the extreme regime of strong Coulomb fields and hard x rays. The fields of HCIs approach the Schwinger limit of 1e16 V/cm, where the atomic interactions are affected by a host of previously unexplored relativistic and spin phenomena. Development of novel techniques of hard x-ray polarimetry opened broad possibilities to explore these phenomena in processes such as photoelectric effect, radiative and dielectronic recombination and bremsstrahlung.

In particular, by detecting correlated x rays for the first time in the relativistic atomic collisions, we were able to observe the coherence between the magnetic substates in a hydrogenlike uranium ion, populated by the process of radiative recombination (RR), the time-reverse of the photoelectric effect. This allowed identification of a strong contribution of the spin-orbit interaction to the photoelectric effect [1].

In studies of bremsstrahlung we focused on the effects of the electron spin on x-ray linear polarization. In these experiments, for the first time, the polarization properties of both the electron beam and the emitted x rays were controlled simultaneously [2,3]. The observed correlation between the incoming electron spin and x-ray linear polarization unambiguously revealed the precession of the electron spin in bremsstrahlung and indicated a striking effect of the electron spin on the electron motion in a strong Coulomb field [4].

Furthermore, we studied polarization and angular distributions of x rays emitted in resonant recombination of highly charged middle-Z ions, resolving dielectronic, trielectronic, and quadruelectronic channels. The measured emission asymmetries comprehensively benchmarked full-order atomic calculations revealing dominant contributions of the Breit interaction [5,6]. We also concluded that accurate polarization diagnostics of hot plasmas can only be obtained under the premise of inclusion of higher-order processes that were neglected in earlier work.

I will review these experiments performed in my research group and the instrumental developments which were essential to the success of these experiments.

References

[1] Stanislav Tashenov et al. *Observation of Coherence in the Time-Reversed Relativistic Photoelectric Effect*, Phys. Rev. Lett. **113**, 113001 (2014).
[2] Stanislav Tashenov et al. *Measurement of the Correlation between Electron Spin and Photon Linear Polarization in Atomic-Field Bremsstrahlung*, Phys. Rev. Lett. **107**, 173201 (2011).
[3] Stanislav Tashenov et al. *Bremsstrahlung Polarization Correlations and Their Application for Polarimetry of Electron Beams*, Phys. Rev. A **87**, 022707 (2013).
[4] Oleksiy Kovtun et al. *Spin-Orbit Interaction in Bremsstrahlung and its Effect on the Electron Motion in a Strong Coulomb Field*, Phys. Rev. A **92**, 062707 (2015).
[5] Holger Jörg et al. *Linear Polarization of X-Ray Transitions due to Dielectronic Recombination in Highly Charged Ions*, Phys. Rev. A **91**, 042705 (2015).
[6] Chintan Shah et al. *Polarization Measurement of Dielectronic Recombination Transitions in Highly Charged Krypton Ions*, Phys. Rev. A **92**, 042702 (2015).

Precision Deep–UV Ramsey-Comb Spectroscopy of Kr and H_2

R.K. Altmann[1], S. Galtier[1], L.S. Dreissen[1], K.S.E. Eikema[1]
1. LaserLaB Amsterdam, Vrije Universiteit, De Boelelaan 1081, 1081 HV Amsterdam, Netherlands

High-resolution spectroscopy of simple atomic and molecular systems is an excellent tool for testing Quantum-Electrodynamics (QED). Although many consider QED the best tested theory in physics, a comparison between 1S-2S spectroscopy in atomic-hydrogen and the 2S-2P transition in muonic-hydrogen has led to a sizeable discrepancy in 2010. This finding, which was confirmed in 2013, can be interpreted as a significant (>5 sigma) difference in proton size between both systems [1], or could point to e.g. issues with the Rydberg constant. Comparing spectroscopy of He^+ ions and the 'muonic' counterpart might provide new insights to solve this conundrum. Moreover, due to recent advances in theory by K. Pachucki and co-workers also H_2 has become a very interesting candidate for tests of QED [2, 3] and the proton size. The challenge is that ground-state electronic transitions in 'normal' He^+ and H_2 require extreme- or deep-ultraviolet radiation.

We developed an excitation method based on pairs of selectively amplified near-infrared frequency-comb laser pulses that enables high-resolution spectroscopy at such short wavelengths. The laser system for it parametrically amplifies any combination of two pulses from a Ti:sapphire frequency comb laser in a phase-coherent manner, with a pulse delay from nanoseconds to microseconds. The comb laser is locked to a cesium atomic clock, thereby providing the required accuracy and long-term phase coherence. After amplification of two pulses to the mJ level, efficient conversion to shorter wavelengths, e.g. by frequency doubling in crystals, or by high-harmonic generation is possible. These nonlinear processes conserve the coherence of the comb laser pulses to a high degree. When the converted pulses are then used to excite transitions, interference leads to an oscillation of the excited state population as a function of the delay (or phase) between the pulses. We record one or more oscillations of this Ramsey-like signal at several multiples (*N*) of the repetition time (~8 ns) of the comb laser (see Fig. 1). The frequencies of the exited transitions are then extracted by analyzing only the *phase differences* between such a series of Ramsey scans. In this manner any (constant) phase shifts from amplification or frequency conversion are eliminated, including the phase (and therefore frequency) effect of the AC-Stark effect.

Originally we demonstrated this form of "Ramsey-comb" spectroscopy with Rb on a two-photon transition in the near-infrared with 5 kHz accuracy [4, 5]. Now we sequentially frequency double the pulses to demonstrate deep-UV two-photon Ramsey-comb excitation in Kr (2×212 nm). We achieved an accuracy of 103 kHz, presenting a 34-fold improvement over previous measurements. It is only limited by the 27 ns lifetime of the excited state. We also report preliminary results of exciting the EF←X two-photon transition in molecular hydrogen at 2×202 nm. This transition is highly interesting for tests of QED and the proton size due to its 200 ns excited state lifetime. A preliminary analysis of a single Ramsey-comb measurement (which takes 30 minutes to record) shows a very promising statistical uncertainty of 15 kHz.

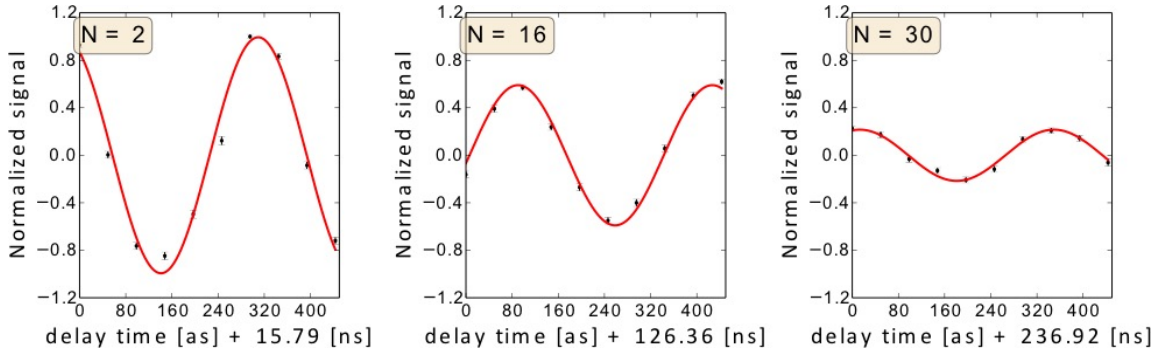

Fig. 1 Ramsey-comb excitation of H_2 in an atomic beam on the two-photon EF←X transition at 2x202 nm for macro delays of 15.8 ns, 126 ns and 237 ns between the pulses. The EF population is detected via ionization with 355 nm.

References

[1] A. Antognini, et. al., *Proton Structure from the Measurement of 2S-2P Transition Frequencies of Muonic Hydrogen*, Science **339**, 417-420 (2013).
[2] W. Ubachs et al., *Physics beyond the Standard Model from hydrogen spectroscopy*, J. Mol. Spec. **320**, 1 (2016).
[3] K. Pachucki and J. Komasa, *Schrödinger equation solved for the hydrogen molecule with unprecedented accuracy*, J. Chem. Phys. **144**, 164306 (2016).
[4] J. Morgenweg, I. Barmes, K.S.E. Eikemea, *Ramsey-comb spectroscopy with intense ultra-short laser pulses*, Nature Physics **10**, 30-33 (2014).
[5] J. Morgenweg, K.S.E. Eikema, *Ramsey-comb spectroscopy: Theory and signal analysis*, Phys. Rev. A **89**, 052510 (2014).

Molecular spectroscopy, based on laser frequency combs

Nathalie Picqué,[1,2,3]

1. Ludwig-Maximilians-Universität München, Fakultät für Physik, Schellingstr. 4/III, 80799 Munich, Germany

2. Max-Planck-Institut für Quantenoptik, Hans-Kopfermannstr. 1, 85748 Garching, Germany

3. Institut des Sciences Moléculaires d'Orsay, CNRS, Bâtiment 350, 91405 Orsay, France

At the moment of printing, no abstract was submitted

Ab-initio molecular dynamics with electronic friction: beyond the Born-Oppenheimer approximation in gas-surface processes

Maite Alducin[1,2]

1. Centro de Física de Materiales CFM/MPC (CSIC-UPV/EHU), P. Manuel de Lardizabal 5, 20018 Donostia-San Sebastián, Spain
2. Donostia International Physics Center DIPC, P. Manuel de Lardizabal 4, 20018 Donostia-San Sebastián, Spain

The challenge in present thermal and hyperthermal gas-surface simulations is to provide a reliable description of the two main energy exchange channels that may affect the dynamics and reactivity of gas-phase species on solid surfaces, namely, phonon excitations and electron-hole (e-h) pair excitations. In the end, these are the mechanisms that dictate the thermalization rate and, hence, the mean traveled length of the incipient adsorbates. Even more generally, these mechanisms are expected to contribute actively in any gas-surface process that involves strong and long-lasting interactions. In this respect, our recently developed ab-initio molecular dynamics methodology with electronic friction (AIMDEF) [1-3] that is based on the local density friction approximation (LDFA) [4] constitutes a promising and efficient tool to accurately provide a joint description of e-h pair and phonon excitations.

Using AIMDEF we have recently investigated the competition between e-h pairs and phonons in the adsorption and relaxation of atoms and molecules on metal surfaces and how this competition depends on two important factors: (i) the depth of the adsorption well and (ii) the mass ratio between the gas species and the surface atom. We demonstrate -using H/Pd(001), N/Ag(111), and N_2/Fe(110) as case studies- that, even if phonons increasingly dominate relaxation the heavier the hot species (see Fig. 1), electronic excitations rule the last stages of the process.

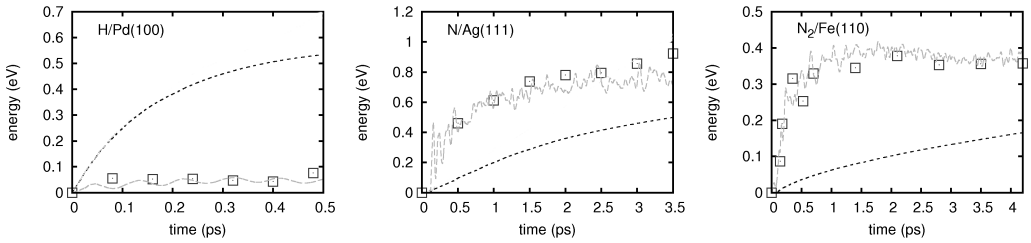

Fig. 1 Energy dissipated into e-h pairs (black dotted curves) and phonons (Squares and grey dashed curves) during the adsorption of H on Pd(100), N on Ag(111), and N_2 on Fe(110) as indicated in each panel.

As an additional example of the AIMDEF capabilities, I will also discuss our preliminary results on femtosecond-laser induced desorption processes, which are motivated by existing experiments on the recombinative desorption of H_2, HD, and D_2 from Ru(0001) with different mixed (H,D) saturation coverages [5].

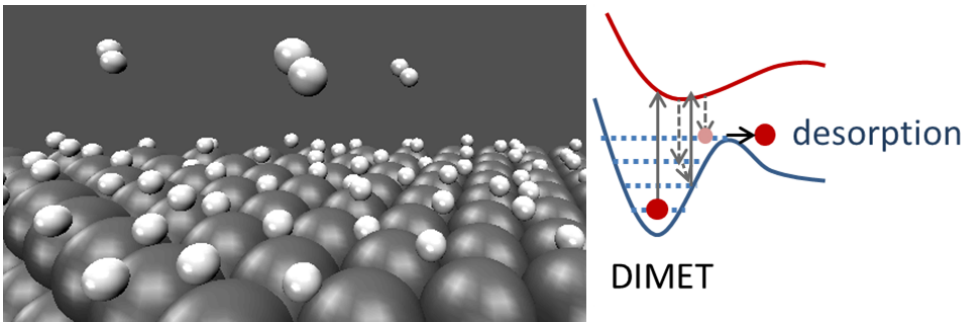

Fig. 2 AIMDEF simulation of the recombinative desorption of H_2, HD, and D_2 from (H,D)-saturated Ru(0001) induced by fs-laser pulses

References

[1] María Blanco-Rey, J.Iñaki Juaristi, Ricardo Díez Muiño, H.Fabio Busnengo, Geert-Jan Kroes, and Maite Alducin, Phys. Rev. Lett. **112**, 103203 (2014).
[2] Dino Novko, María Blanco-Rey, J.Iñaki Juaristi, and Maite Alducin Phys. Rev. B **92**, 201411 (2015).
[3] Dino Novko, María Blanco-Rey, J.Iñaki Juaristi, and Maite Alducin, Nucl. Instrum. Meth. B (2016), doi:10.1016/j.nimb.2016.02.031.
[4] J.Iñaki Juaristi, Maite Alducin, Ricardo Díez Muiño, H. Fabio Busnengo, and Antoine Salin, Phys. Rev. Lett. **100**, 116102 (2008).
[5] N. Denzler, C. Frischkorn, C. Hess, M. Wolf, and G. Ertl, Phys. Rev. Lett. **91**, 226102 (2003).

Fast Atom Diffraction : Bound State Resonances to probe the coherence of a crystal surface on the micron scale. A tribute to Otto Stern.

M. Debiossac, A. Zugarramurdi, P. Lunca-Popa, A. Momeni, H. Khemliche, A. G. Borisov, and P. Roncin*
Institut des Sciences Moléculaires d'Orsay (ISMO) CNRS-Univ. Paris Sud, université Paris Saclay,F-91405 Orsay, France

In 1930, Otto Stern discovered [1] the diffraction of molecular rays on surfaces demonstrating the wave nature of complex, many particles systems. In 1933 he observed [2] singularities on top of the smooth evolution of the population of these diffraction orders with incoming energy. This was rapidly interpreted [3] as due to resonance between the kinetic energy associated with the exchange of reciprocal lattice vectors $\delta k = 2n\pi/a$ with the binding energy E_i of discrete physisorption bound states in the on the surface Fig.1(c). The advent of supersonic expansions boosted the technique which became probably the most sensitive technique [4] to probe the Van der Waals forces, a quantity challenging the most accurate DFT descriptions of the atom surface interaction. More recently, atomic diffraction was observed at keV energies and grazing incidence (GIFAD). The geometry Fig.1(a) provides a high detection efficiency and a specific resistance to decoherence allowing application to high temperatures and to molecular beam epitaxy [5,6], a technique also credited to Otto Stern.

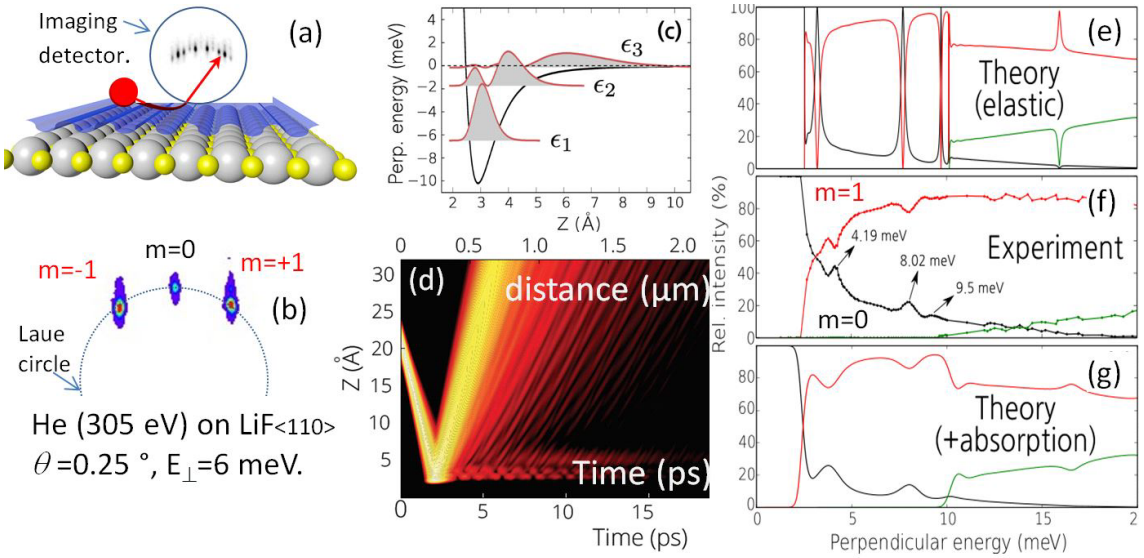

Fig. 1 (a) scheme of the grazing incidence setup, (b) typical image with three diffraction orders, (c) scheme of the He-LiF potential energy as a function of the distance to the surface. (d) image of wave packet showing multiple rebounds on the surface. (e,f,g) evolution of the diffracted intensities with $E_\perp$. (d) elastic theory, (f) experiment (g) theory with a lifetime τ=2ps.

The search for few meV bound states resonances at keV energies turned out to be more difficult than expected because it can only be observed if the projectile bumps on the surface without exciting phonons. Most important, due to the large parallel velocity v, the distance $L = v\tau$ spanned during the time τ of a typical oscillation in the potential well, is on the order of a micron. Maintaining coherence between the trapped and scattered waves requires that no singularity (defects; ad-atom, step edges etc...) is encountered on the surface in this distance. In this respect, the 0.5 meV width of the resonances observed in Fig.1(f) [7] seems to be a measure the surface coherence. This interpretation is supported by calculations based on a wave packet propagation method [8] where a good agreement could be reached by imposing a lifetime $\tau \sim 2.5ps$ on the surface corresponding to distance of 0.2 - 0.3 μm. By wobbling the beam energy around the resonance, this technique compatible with UHV and high temperatures, could help in situ monitoring of ultra high quality surfaces with very large distances between defects.

References

[1] I. Estermann and O. Stern, *Beugung von molekularstrahlen* Z. Phys. **61**, 95 (1930).
[2] Frisch and Stern, *Anomalien bei der spiegelnden Reflexion und Beugung von Molekularstrahlen an Kristallspaltflächen.* Z. Phys.**84**, (1933).
[3] J.E. Lennard-JonesS & A. F. Devonshire *Diffraction and Selective Adsorption of Atoms at Crystal Surfaces*, Nature **137**, 1069-1070 (1936).
[4] A.P. Jardine *et al*, *Ultrahigh-Resolution Spin-Echo Measurement of Surface Potential Energy Landscapes*, Science **304**, 5678,p1790 (2004).
[5] M. Debiossac *et al.Combined exp. and theo. study of fast atom diffraction on the* $\beta_2(2x4)$ *GaAs(001) surf.* Phys.Rev.B. **90**, 155308 (2014).
[6] P. Atkinson *et al*. *Dynamic grazing incidence fast atom diffraction during MBE growth of GaAs*.APL **105**, 021602 (2014).
[7] M. Debiossac *et al*, *Transient Quantum Trapping of Fast Atoms at Surfaces*, Phys. Rev. Lett. **112**, 023203 (2014).
[8] A Zugarramurdi *et al*. *Surface-grating deflection of fast atom beams*, Phys. Rev. A **88** 012904 (2013).

Highly charged ion interaction with graphene

Richard A. Wilhelm[1,2], Elisabeth Gruber[2], Valerie Smejkal[2], Janine Schwestka[2], Roland Kozubek[3], Anke Hierzenberger[3], Marika Schleberger[3], Stefan Facsko[1], Friedrich Aumayr[2]

1. Institute of Ion Beam Physics and Materials Research, Helmholtz-Zentrum Dresden-Rossendorf, Bautzner Landstr. 400, 01328 Dresden, Germany

2. Institute of Applied Physics, TU Wien, Wiedner Hauptstr. 8-10, 1040 Vienna, Austria

3. Faculty of Physics, University of Duisburg-Essen, Lotharstr. 1-21, 47057 Duisburg, Germany

Studying ion-solid interaction has a long standing tradition both in fundamental research and for technological applications. The main parameter in this respect is the ion stopping force, i.e. the kinetic energy loss per unit length in a solid. The stopping force depends on the kinetic energy of the ions as well as on the degree of ionization [1]. The latter fact is usually disregarded, because after a few nanometers in a solid the ion accommodates an equilibrium charge state independent of it's initial charge state. Stopping force in charge equilibrium is very well known.

Here we use slow ($v \ll v_0$) highly charged ions ($Q \lesssim Z$) to study stopping force far from charge equilibrium and the charge equilibration dynamics [2,3]. Using novel two-dimensional materials as target material allows us to limit the ion trajectory in the solid with monolayer precision and thus study non-equilibrium effects.

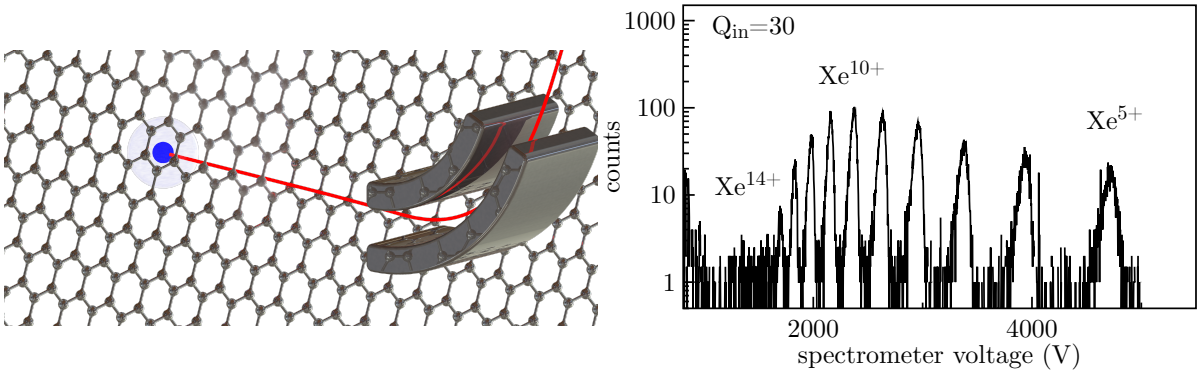

Figure 1: **Fig. 1** Left: Schematic view of the experimental conditions. Right: Exit charge state distribution of 40 keV Xe^{30+} transmitted through 1ML freestanding graphene. Charge states from 5 to 14 are visible.

The left side of fig. 1 shows schematically the experimental conditions with an ion beam transmitted under normal incidence through a freestanding single layer graphene sheet. The ion energy and charge state are measured with an electrostatic analyzer. A typical charge state distribution for Xe^{30+} ions at 40 keV (310 eV/amu) transmitted through graphene is also shown (right). Ions at this low velocity ($0.1v_0$) are not fully neutralized. Hence, they still capture and stabilize about 20 electrons within the collision time of only 1-3 fs. Especially stabilization of the electrons is surprising, since the classical-over-barrier model for charge exchange [4] predicts the population of highly excited states with principal quantum numbers of $n > 10$ and a subsequent Auger electron cascade. Such a cascade would lead to the reemission of electrons and thus to a recharging of the ion. Present results show the need for a model beyond classical-over-barrier.

This ultrafast charge exchange process is accompanied by a kinetic energy loss of up to $\Delta E/E \approx 10\,\%$, which is about 1 order of magnitude larger than predicted by the SRIM code. In this contribution, recent results on charge exchange and energy loss of highly charged ion at low velocities in graphene will be presented. A qualitative description of the processes involved will be given.

References

[1] Peter Sigmund, *Charge-dependent electronic stopping of swift nonrelativistic heavy ions*, Phys. Rev. A **56**, 3781–3793 (1997).

[2] Richard A. Wilhelm, Ayman S. El-Said, Franciszek Krok, René Heller, Elisabeth Gruber, Friedrich Aumayr, and Stefan Facsko, *Highly charged ion induced nanostructures at surfaces by strong electronic excitations*, Prog. Surf. Sci. **90**, 377-395 (2015).

[3] Richard A. Wilhelm, Elisabeth Gruber, Robert Ritter, René Heller, Stefan Facsko, and Friedrich Aumayr, *Charge Exchange and Energy Loss of Slow Highly Charged Ions in 1nm Thick Carbon Nanomembranes*, Phys. Rev. Lett. **112**, 153201 (2014).

[4] Joachim Burgdörfer, Peter Lerner, Fred W. Meyer, *Above-surface neutralization of highly charged ions: The classical over-the-barrier model*, Phys. Rev. A **44**, 5674-5685 (1991).

From a loophole-free Bell test to a global quantum network

Andreas Reiserer [1,2],

1. *Qutech and Kavli Institute of Nanoscience, Lorentzweg 1, 2628CJ Delft, The Netherlands*
2. *Max-Planck-Institute of Quantum Optics, Hans-Kopfermann-Str. 1, 85748 Garching, Germany*

Bas Hensen, Hannes Bernien, Anaïs Dréau, Norbert Kalb, Machiel S. Blok, Koen J.M. van Bemmelen, David Elkouss, Stephanie Wehner, Tim H. Taminiau, Ronald Hanson

Qutech and Kavli Institute of Nanoscience, Lorentzweg 1, 2628 Delft, The Netherlands

Entanglement is one of the most intriguing phenomena in quantum science. The outcomes of independent measurements of the quantum state of entangled objects are correlated, even if the objects are space-time separated. This property, often called quantum non-locality, cannot be explained by classical physics and is a unique resource for quantum information processing and quantum communication.

Fifty years after its derivation, many experiments have tested Bell's famous inequality [1]. However, all of these experiments relied on additional assumptions in order to obtain a violation, most prominently the absence of communication between the entangled particles, and fair sampling of the full dataset when using inefficient detectors. Closing the 'loopholes' that arise from these assumptions has been one of the major fundamental research goals of experimental quantum physics, with applications [2] such as device-independent quantum key distribution to the generation of provably random numbers.

In [3], we have demonstrated the first experiment that is free of any such additional assumption. We have entangled two electronic spins in diamond at a separation of 1.3 km via an optical fiber channel. We have used an event-ready scheme in combination with efficient and fast spin read-out (to avoid the fair-sampling assumption) and fast random basis-selection (to ensure the required locality conditions). A second run of the loophole-free Bell experiment has further improved statistical evidence [4].

To enable further fundamental tests, as well as numerous applications in quantum communication, computation and measurement, we plan to extend the separation as well as the number of entangled particles, aiming for the realization of a global-scale quantum network [5]. This will be feasible by embedding the diamond samples into high-quality optical resonators, as pioneered with cold atoms [6]. In addition, unavoidable inefficiencies in photon transmission require the implementation of a quantum memory that is robust under failed remote entanglement attempts.

We have demonstrated individual control and readout of five nuclear spin qubits via the hyperfine interaction with a close-by electronic spin. By encoding quantum states into a decoherence-protected subspace of two nuclear spins we show that quantum coherence can be maintained for over 1000 repetitions of a remote entangling protocol [7]. These results and insights pave the way towards remote entanglement purification [8] and the realization of a quantum repeater [9] using nitrogen-vacancy center quantum network nodes. I will present our recent results in this respect.

References

[1] J.S. Bell, *On the Einstein Podolsky Rosen Paradox*, Physics **1**, 195 (1964) .

[2] N. Brunner, D. Cavalcanti, S. Pironio, V. Scarani, and S. Wehner, *Bell nonlocality*, Rev. Mod. Phys. **86**, 419 (2014).
A. Ekert and R. Renner, *The ultimate physical limits of privacy*, Nature **507**, 443 (2014).

[3] B. Hensen, H. Bernien, A. E. Dréau, A. Reiserer, N. Kalb, M. S. Blok, J. Ruitenberg, R. F. L. Vermeulen, R. N. Schouten, C. Abellán, W. Amaya, V. Pruneri, M. W. Mitchell, M. Markham, D. J. Twitchen, D. Elkouss, S. Wehner, T. H. Taminiau, and R. Hanson, *Loophole-free Bell inequality violation using electron spins separated by 1.3 kilometres*, Nature **526**, 682 (2015).

[4] B. Hensen, N. Kalb, M. S. Blok, A. Dréau, A. Reiserer, R. F. L. Vermeulen, R. N. Schouten, M. Markham, D. J. Twitchen, K. Goodenough, D. Elkouss, S. Wehner, T. H. Taminiau, and R. Hanson, *Loophole-free Bell test using electron spins in diamond: second experiment and additional analysis*, arXiv:1603.05705 (2016).

[5] H. J. Kimble, *The quantum internet*, Nature **453**, 1023 (2008).

[6] A. Reiserer and G. Rempe, *Cavity-based quantum networks with single atoms and optical photons*, Rev. Mod. Phys. **87**, 1379 (2015).

[7] A. Reiserer, N. Kalb, M. S. Blok, K. J. M. van Bemmelen, D. J. Twitchen, M. Markham, T. H. Taminiau, and R. Hanson, *Robust quantum-network memory using decoherence-protected subspaces of nuclear spins*, arXiv:1603.01602 (2016).

[8] C. H. Bennett, G. Brassard, S. Popescu, B. Schumacher, J. A. Smolin, and W. K. Wootters, *Purification of Noisy Entanglement and Faithful Teleportation via Noisy Channels*, Phys. Rev. Lett. 76, 722 (1996).

[9] H.-J. Briegel, W. Dür, J. I. Cirac, and P. Zoller, *Quantum Repeaters: The Role of Imperfect Local Operations in Quantum Communication*, Phys. Rev. Lett. 81, 5932 (1998).

Laboratory study of VUV photodesorption processes of interstellar ice analogues

Mathieu Bertin[1], Xavier Michaut[1], Claire Romanzin[2], Laurent Philippe[1], Pascal Jeseck[1], N. Litgerink[3], Harold Linnartz[3] & Jean-Hugues Fillion[1]

1. LERMA, Sorbonne Universités, UPMC Univ. Paris 06, Observatoire de Paris, PSL Research University, CNRS, F-75252, Paris, France

2. LCP (UMR 8000), CNRS, Université Paris-Sud, F-91405 Orsay, France

3. Sackler Laboratory for Astrophysics, Leiden Observatory, Leiden University, P.O. Box 9513, NL-2300 RA Leiden, The Netherlands

In cold regions of the Interstellar Medium (ISM), like star-forming regions or protoplanetary disks, molecules form or accrete on the surface of dust grains. The resulting icy mantles represent the main reservoir of molecules beside H2. Through desorption processes, these ices can eventually enrich the gas phase with more or less complex species, and therefore influence observed gas phase abundance ratio and chemistry. In the vicinity of warm objects (protostar, edge of clouds…) thermal energy is high enough to trigger sublimation of the ices. This is not the case in the colder regions, but other mechanisms, such as cosmic-rays or UV photons impact on the ices, can stand at the origin of the ice desorption. In any case, both thermal and non-thermal desorption processes need to be quantified in order to get a better understanding of the observed molecular abundance ratio, and to bring trustable and relevant parameters for astrochemical models.

The efficiency of thermal desorption is usually linked to the strength of the interaction energy between the adsorbed molecule and the ice surface, so-called adsorption energy. Less is known concerning non-thermal desorption processes. Using energy-resolved studies at the synchrotron SOLEIL, we have focused our studies on UV photodesorption in the 7 – 13. 6 eV range, and obtained for the first time energy-resolved photodesorption rates for a collection of small, astrophysical-relevant, molecules [1-5]. Photodesorption of simple molecules (CO, H_2O…) have already been studied, but using broad band discharge lamps. In our case, the energy resolution allows us for extracting (i) absolute photodesorption rates as a function of the photon energy, applicable to any different UV field, and for (ii) identifying the molecular mechanism and the parameters involved in the desorption process.

I will summarize results we have obtained in the case of simple molecular ices such as CO, N_2 and CO_2 and show the crucial role played by the surrounding molecules (ice composition) and the photochemistry in the UV photodesorption. Finally, I will present very recent results obtained on the photodesorption of CH_3OH and H_2CO, pure and mixed in CO-rich ices.

References

[1] E.C. Fayolle, M. Bertin, C. Romanzin, X. Michaut, P. Jeseck, K.I. Öberg, H. Linnartz & J.-H. Fillion, Astrophysical Journal Letters 739 (2011), L36

[2] M. Bertin, E.C. Fayolle, C. Romanzin, K.I. Öberg, X. Michaut, A. Moudens, L. Philippe, P. Jeseck, H. Linnartz & J.-H. Fillion, Physical Chemistry Chemical Physics 14 (2012), 9929-9935

[3] M. Bertin, E.C. Fayolle, C. Romanzin, H.A.M. Poderoso, X. Michaut, L. Philippe, P. Jeseck, K.I. Öberg, H. Linnartz & J.-H. Fillion, Astrophysical Journal 779 (2013), 120

[4] J.-H. Fillion, E.C. Fayolle, X. Michaut, M. Doronin, L. Philippe, J. Rakovsky, C. Romanzin, N. Champion, K.I. Öberg, H. Linnartz & M. Bertin, Faraday Discussion 168 (2014), 533-552

[5] M. Bertin, C. Romanzin, M. Doronin, L. Philippe, N. Ligterinks, H. Linnartz, X. Michaut, & J.-H. Fillion, The Astrophysical Journal Letters 817 (2016), L12

Molecular Response to Ultra-Intense Femtosecond X-rays: Correlated Charge and Nuclear Dynamics in Soft and Hard X-ray Regimes

Artem Rudenko

J.R. Macdonald Laboratory, Department of Physics, Kansas State University, 116 Cardwell Hall, 66506, Manhattan KS, USA

The development of high-intensity, short-pulsed X-ray radiation sources promises revolutionary new techniques in diverse scientific fields, nurturing the vision of dynamic imaging of matter with angstrom spatial and femtosecond temporal resolution [1]. In particular, the start-up of the first hard X-ray free-electron laser, the Linac Coherent Light Source (LCLS), triggered a variety of imaging experiments on small molecules, clusters, nanocrystals, and isolated nano-scale particles. The basic prerequisite for designing these experiments is understanding the response of individual atoms, and tracing electronic and nuclear dynamics in the vicinity of the atom that absorbed X-ray photon(s), thus, revealing basic mechanisms of local radiation damage. Pursuing this goal, we performed a series of experiments on multiphoton multiple X-ray ionization of heavy atoms with high absorption cross sections embedded into an environment consisting of lighter elements.

For soft X-ray ionization of heavy rare gas atoms such as Xe and Kr [2], we observed the charge states well above the predictions of the simple sequential ionization model (up to 36+ instead of 26+ for Xe at 1500 eV), which was very successful in explaining results of the earlier LCLS experiments on lighter elements [3]. Comparing experimental data with theory (XATOM model [4]), studying the wavelength dependence and the fluorescence spectra, we found that intermediate resonant excitations are responsible for the extremely high charge states observed. Comparing the ionization of the isolated Kr and Xe atoms with the ionization of molecules containing single Se (CH_3SeH, C_2H_5SeH) or I (ICl, CH_3I) atom, which have the electronic structure very similar to Kr and Xe, respectively, we found signatures of efficient charge redistribution interweaved with ultrafast nuclear dynamics [5]. In a dedicated laser pump / X-ray probe experiment, we studied similar charge rearrangement reaction in a laser-dissociated CH_3I molecule, showed that its spatial range can be estimated from a classical over-the-barrier model and observed signatures of electron transfer up to internuclear separations of ~ 20 Å [6,7].

We complement the results in the soft X-ray domain with the data obtained using ultra-intense hard (5.5-8.3 keV) X-ray radiation. By focusing the LCLS beam to ~ 0.1 μm^2 spot, we achieve the unprecedented X-ray intensities of ~ 2-3x10^{19} W/cm^2. Under these conditions we were able to strip all 18 electrons from argon atoms, 34 (all but two 1s) electrons from krypton, and reached the record 48+ charge state for xenon at 8.3 keV. Although the highest charge states is reached at the highest photon energy (8.3 keV), the wavelength dependence of the spectra from 5.5 to 8.3 keV shows significant overall enhancement in the production of high charge states at the intermediate photon energies (around 6.5 keV). Similar to the soft X-ray regime, this behaviour results from the ionization enhanced or even enabled by intermediate resonance excitations [2].

However, the response of small polyatomic molecules to ultra-intense hard X-ray pulses is quite different compared to our earlier results in the soft X-ray regime [5-7], and to the outcome of recent experiments at SACLA XFEL in Japan performed with weaker hard X-rays [8]. In our LCLS experiment at 8.3 keV the presence of molecular partners does not significantly reduce the highest charge state observed for high-Z elements: we detected I^{47+} ions from CH_3I as compared to Xe^{48+}, and even for a larger system like C_6H_5I, the maximum charge state observed is ~ I^{45+}. Along with the presence of charged carbon fragments and protons this indicates that the total charge of the molecule considerably exceeds that of an isolated atom with a similar absorption cross section. This enhancement is due to efficient charge rearrangement from the absorbing atom to its neighbours, which is followed by the absorption of the next photon(s). At very high X-ray intensities this process is essentially limited by the number of electrons available from the molecular environment to fill the vacancies created at the iodine site. Interestingly, for both, CH_3I and C_6H_5I, the highest charge state of carbon observed is just C^{4+}. This highlights that in the vicinity of the high-Z element light atoms obtain their charge by charge transfer rather than by direct X-ray absorption. The absence of higher carbon charge states is in good agreement with the over-the-barrier charge transfer model used in [6,7]. Overall enhancement of molecular ionization as compared to a system of isolated atom can be quantitatively described using the newly extended version of the XMOLECULE toolkit [9] and is expected to be important for imaging experiments involving biological systems with heavy atom impurities [10].

References

[1] J. Ullrich, A. Rudenko and R. Moshammer, *Annu. Rev. Phys. Chem.* **63** 635 (2012).
[2] B. Rudek *et al Nature Photonics* **6** 858 (2012); *Phys. Rev. A* **87** 023413 (2013).
[3] L. Young *et al*, 2010 *Nature* **466** 56 (2010).
[4] S.K. Son and R. Santra, *Phys. Rev. A* **85** 063415 (2012).
[5] B. Erk *et al*, *Phys. Rev. Lett.* **110** 053003 (2013); *J. Phys. B* **46** 164031 (2013).
[6] B. Erk *et al*, *Science* **345** 288 (2014).
[7] R. Boll et al., *Structural Dynamic*s **3** 043207 (2016).
[8] K. Motomura et al., *J. Phys. Chem. Lett.* **6** 2944 (2015); K. Nagaya, et al., *Phys. Rev. X* **6** 021035 (2016).
[9] Y. Hao, L. Inhester, K. Hanasaki, S.-K. Son and R. Santra, *Structural Dynamics*. **2**, 041707 (2015).
[10] K. Nass et al., *J. Synchrotron Rad*. **22**, 225 (2015).

Tuneable polarization of bright high-order harmonics

Avner Fleischer, Ofer Kfir, Eliyahu Bordo, Gil Ilan, Gavriel Lerner, Ofer Neufeld and Oren Cohen

Solid State Institute and Physics Department, Technion – Israel Institute of Technology, Haifa 32000, Israel

Ultrashort pulses of extreme-UV and X-rays emerging from high harmonic generation (HHG) sources have been applied to many applications. For many years, the polarization of bright HHG-based sources was limited to linear region. I will present our recent work in which we learned to fully control the polarization of high harmonics within the generation process, from linear through elliptic to circular polarization, without compromising on the efficiency of the HHG process [1-4]. For example, I will present a novel, compact, and stable apparatus for inline generation of circular HHG which we name MAZEL-TOV for MAch-ZEhnder-Less for Threefold Optical Virginia spiderwort. The apparatus converts a standard linearly polarized ultrashort pulse into a co-propagating bi-chromatic field composed of the fundamental laser field and its second harmonic, which is required for generation of circularly polarized HHG. A single quarter-wave waveplate controls the polarization of both spectral components and tunes the polarization of the pump and the resulting HHG from linear, through elliptical to circular polarization.

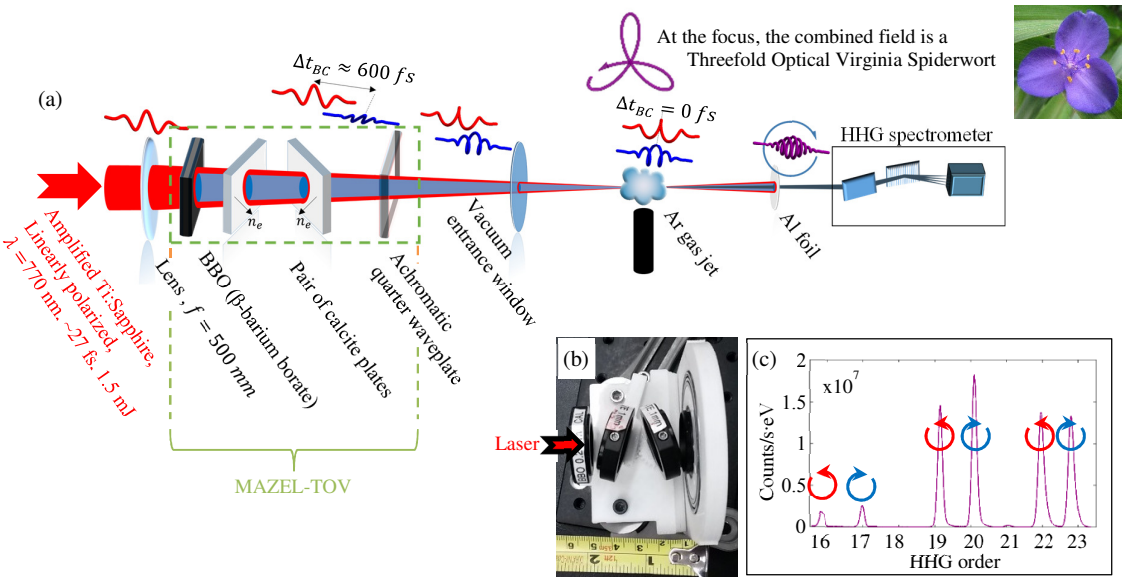

Figure 1 – (a) Scheme of for simple and robust generation of high harmonics with controllable polarization. Top right shows a threefold optical and a botanical Virginia Spiderwort. (b) A compact (2" long) implementation of a MAZEL-TOV apparatus including a BBO (left), a pair of calcite plates, and a rotatable achromatic quarter waveplate (right). We added a ruler for scale and marked the laser entrance direction by a red arrow. (c) A recorded spectrum typical for circularly polarized HHG. The MAZEL-TOV apparatus (dashed green in (a)) is simply inserted into a standard system for generating linearly polarized HHG, where a lens (f=500 mm) focuses a linear s-polarized fundamental beam onto a jet of argon gas in vacuum.

References

[1] A. Fleischer, O. Kfir, T. Diskin, P. Sidorenko, and O. Cohen, Spin angular momentum and tunable polarization in high harmonics generation, Nature Photonics 8, 543 (2014).

[2] O. Kfir, P. Grychtol, E. Turgut, R. Knut, D. Zusin, D. Popmintchev, T. Popmintchev, H. Nembach, J. M. Shaw, A. Fleischer, H. Kapteyn, M. Murnane and O. Cohen, Generation of bright phase-matched circularly-polarized extreme ultraviolet high harmonics. Nature Photonics, 9, 99 (2015).

[3] T. Fan, P. Grychtol, R. Knut, C. Hernández-García, D. D. Hickstein, D. Zusin, C. Gentry, F. J. Dollar, C. A. Mancuso, C. W. Hogle, O. Kfir, D. Legut, K. Carva, J. L. Ellis, K. M. Dorney, C. Chen, O. G. Shpyrko, E. E. Fullerton, O. Cohen, P. M. Oppeneer, D. B. Milošević, A. Becker, A. A. Jaroń-Becker, T. Popmintchev, M. M. Murnane, and H. C. Kapteyn, Bright circularly polarized soft x-ray high harmonics for x-ray magnetic circular dichroism, Proceedings of the National Academy of Sciences of the United States of America (PNAS) 112, 14206 (2015).

[4] O. Kfir, P. Grychtol, E. Turgut, R. Knut, D. Zusin, A. Fleischer, E. Bordo, T. Fan, D. Popmintchev, T. Popmintchev, H. Kapteyn, M. Murnane and O. Cohen, Helicity-selective phase-matching and quasi-phase matching of circularly polarized high-order harmonics: towards chiral attosecond pulses, J. Phys. B, 49, 123501 (2016).

High harmonic spectroscopy of polyatomic molecules

A. Ferré[1], A. E. Boguslavskiy[2,6], C. Bourassin-Bouchet[9], R. Canonge[1], F. Catoire[1], M. Dagan[3], V. Blanchet[1], B.D. Bruner[3], F. Burgy[1], A. Camper[4], D. Descamps[1], B. Fabre[1], N. Fedorov[1], J. Gaudin[1], G. Geoffroy[1], E. Mével[1], J. Mikosch[2,8], S. Patchkovskii[2,8], S. Petit[1], O. Pedatzur[3], B. Pons[1], T. Ruchon[4], H. Soifer[3], D. Staedter[5], I. Wilkinson[2], A. Stolow[2,6,7], N. Dudovich[3], Y. Mairesse[1]

[1] *Université de Bordeaux - CNRS - CEA, CELIA, UMR5107, F33405 Talence, France*
[2] *National Research Council Canada, 100 Sussex Dr, Ottawa, ON K1A 0R6, Canada*
[3] *Department of Physics of Complex Systems, Weizmann Institute of Science, Rehovot 76100, Israel*
[4] *CEA, IRAMIS, Lasers, Interactions and Dynamics Laboratory - LIDyL, CEA-SACLAY , F-91191 Gif-sur-Yvette, France*
[5] *Université de Toulouse - CNRS, LCAR-IRSAMC, Toulouse, France*
[6] *Department of Physics, University of Ottawa. 150 Louis Pasteur ON K1N 6N5, Canada*
[7] *Department of Chemistry, University of Ottawa. 10 Marie Curie ON K1N 6N5, Canada*
[8] *Max-Born-Institute, Max-Born-Strasse 2A, 12489 Berlin, Germany*
[8] *Synchrotron SOLEIL, Saint Aubin, BP 34, 91192 Gif-sur-Yvette, France*

High-harmonic spectroscopy consists in resolving the structure and dynamics of atoms and molecules from their response to a strong laser field. High-order harmonics are emitted via a subcycle recollision process: within one optical cycle an electron is removed from the molecule by strong field ionization, accelerated in the continuum and recollides with the parent ion to emit extreme ultraviolet radiation. This process is very sensitive to the ionization potential and structure of the contributing orbitals, as well as to possible couplings by the laser field. While this sensitivity to multiple parameters makes high-harmonic spectroscopy a promising tool to study ultrafast dynamics, disentangling the different degrees of freedom encoded in the emission is a major challenge.

High-order harmonic generation in polyatomic molecules generally involves multiple channels of ionization. Their relative contribution can be strongly influenced by the presence of resonances, whose assignment remains a major challenge for high-harmonic spectroscopy. We present a multi-modal approach for the investigation of unaligned polyatomic molecules, using SF_6 as an example [1,2]. We combine methods from extreme-ultraviolet spectroscopy, above-threshold ionization and attosecond metrology. Fragment-resolved above-threshold ionization measurements reveal that strong-field ionization opens at least three channels. A shape resonance in one of them is found to dominate the signal in the 20-26 eV range. This resonance induces a phase jump in the harmonic emission, a switch in the polarization state and different dynamical responses to molecular vibrations.

In a second experiement, we disentangle the two main steps in high harmonic generation – ionization and recombination – by combining two-dimensional control of the electron trajectories and vibrational control of the molecules. We introduce a new measurement scheme, Frequency-Resolved Opto-MoleculAr Gating (FROMAGe), which resolves the temporal amplitude and phase of the harmonic emission from excited molecules. Focusing on the study of vibrational motion in N_2O_4, we show that such advanced schemes provide a unique insight into the structural and dynamical properties of the underlying mechanism [3].

References

[1] A. Ferré, David Staedter, F. Burgy, M. Dagan, D. Descamps, N. Dudovich, S. Petit, H. Soifer, V. Blanchet, Y. Mairesse, *High-order harmonic transient grating spectroscopy of SF6 molecular vibrations*, Journal of Physics B **47** 124023 (2014)

[2] A. Ferré, A.E. Boguslavskiy, M. Dagan, V. Blanchet, B.D. Bruner, F. Burgy, A. Camper, D. Descamps, B. Fabre, N. Fedorov, J. Gaudin, G. Geoffroy, J. Mikosch, S. Patchkovskii, S. Petit, T. Ruchon, H. Soifer, D. Staedter, I. Wilkinson, A. Stolow, N. Dudovich and Y. Mairesse *Multi-channel electronic and vibrational dynamics in polyatomic resonant high-order harmonic generation*, Nature Communications **6**, 5952 (2015)

[3] A. Ferré, H. Soifer, O. Pedatzur, C. Bourassin-Bouchet, B. Bruner, R. Canonge, F. Catoire, D. Descamps, B. Fabre, E. Mével, S. Petit, N. Dudovich, Y. Mairesse, *Two-dimensional Frequency Resolved Opto-Molecular Gating of High-order Harmonic Generation*, Physical Review Letters 116, 053002 (2016)

Laser-induced alignment of molecules in He-nanodroplets: Revivals, long-time coherence and breaking-loose

Henrik Stapelfeldt

Department of Chemistry, Aarhus University, Denmark

High resolution infrared and microwave spectra of molecules dissolved in liquid helium nanodroplets display discrete rotational structure – a unique feature explained as the result of frictionless rotation of molecules adiabatically followed by a local solvation shell of He atoms [1].

The frictionless behavior did, however, not manifest itself in recent time-resolved experiments, based on femtosecond laser-induced molecular alignment techniques. In particular, the transient recurrences of alignment characteristic of freely rotating gas phase molecules was absent and the rotational dynamics was much slower than that expected from spectroscopy [2,3].

In this talk we present new experiments on femtosecond laser-induced alignment of iodine molecules embedded in helium nanodroplets showing striking new phenomena:

1) At low to moderate fluences the alignment pulse sets the molecule and a non-superfluid fraction of the He droplet into coherent motion. The coherence, although decaying, persists for many hundreds of picoseconds – long enough to allow the composite molecule-He-shell system to exhibit rotational revivals.

2) At larger fluences of the alignment pulse the molecule is accelerated to such large angular velocities that the binding to the surrounding He atoms in the droplet is broken due to the centrifugal force. Hereafter, the molecule rotates essentially freely for a few ps until the interaction with He atoms sets in again and slows the molecule down.

Our experimental observations are rationalized by classical and two-body time-dependent quantum simulations

References

[1] M. Y. Choi, *et al.*, *Infrared spectroscopy of helium nanodroplets: novel methods for physics and chemistry*, Int. Rev. Phys. Chem. **25**, 15 (2006).

[2] D. Pentlehner *et al.*, *Impulsive Laser Induced Alignment of Molecules Dissolved in Helium Nanodroplets*, Phys. Rev. Lett. **110,** 093002 (2013).

[3] L. Christiansen *et al.*, *Alignment enhancement of molecules embedded in helium nanodroplets by multiple laser pulses*, Phys. Rev. A. **92,** 053415 (2015).

Ion trap experiments to study the photophysics and stability of interstellar polycyclic aromatic hydrocarbons

***Christine Joblin*[1]**

1. Institut de Recherche en Astrophysique et Planétologie, Université de Toulouse (UPS), CNRS, 9 Av. colonel Roche, BP 44346, 31028 Toulouse cedex 4, France

Polycyclic aromatic hydrocarbons (PAHs) have been proposed 30 years ago to be a ubiquitous and abundant component of cosmic matter [1-3]. Interstellar PAHs absorb ultraviolet (UV) photons from stars and reemit this energy in the so-called Aromatic Infrared Bands (AIBs). Being involved in the heating of the gas by photoelectric effect, the ionisation balance, the attenuation of UV photons and the chemistry, PAHs play a key role in the physical and chemical evolution of many objects of interest for astronomers, such as star formation regions, protoplanetary disks or galaxies. However, our incomplete knowledge of their properties including the lack of identification of individual molecules limits our use of these species to probe astrophysical environments. This limitation becomes even more critical at the era of new astronomical instruments. In particular the forthcoming James Webb Space Telescope will allow us to observe at unprecedented spatial scales the evolution of PAH populations in relation with the physical conditions such as the UV radiation field, the hydrogen (H, H_2) and electron densities.

The photophysics/chemistry of PAHs in space is governed by long timescales. On one hand, extreme isolation conditions prevail there making slow events such as emission of infrared photons important in relaxing internal energy. Studying these processes in the laboratory requires therefore dedicated setups. On the other hand, the typical lifetime of astronomical environments is in the range 10^4-10^6 years. Therefore rare events have to be considered; for instance sequential absorption of UV photons is expected to govern the chemical evolution of large PAHs, which can eventually lead to the formation of C_{60} [4].

In my presentation, I will introduce our view of the chemical evolution of interstellar PAHs [5,6]. I will describe how studies in ion traps and storage rings can help us in describing PAH photophysics and dissociation in models [6]. More specifically, at the University of Toulouse/CNRS, we have developed the PIRENEA ("*Piège à Ions pour la Recherche et l'Etude de Nouvelles Espèces Astrochimiques*") setup, which is a home-built Fourier transform ion cyclotron resonance mass spectrometer with the additional characteristics of a cold environment generated by a set of cryogenic shields. The advantages and drawbacks of this setup have led us to design the next generation setup PIRENEA-2, which is currently being constructed in the frame of the ERC Synergy project Nanocosmos [7].

Finally, I will address the case of the identification of interstellar PAHs through spectral fingerprints. Information that can be derived from infrared emission spectroscopy is tricky since it involves band broadening due to e.g. vibrational anharmonicity in the hot emitting species. Electronic spectroscopy seems a more promising way to identify individual species in space as recently illustrated in the case of C_{60}^+ [8]. In PIRENEA, we are using action spectroscopy, which requires in general a multiple photon scheme to dissociate the trapped ions themselves [9,10]. We are trying to improve this scheme but the ultimate goal would be to perform absorption spectroscopy as was achieved by Campbell et al. in their cold ion trap [8].

References

[1] A. Léger, J. L. Puget, *Identification of the 'unidentified' IR emission features of interstellar dust?*, Astron. & Astrophys. **137**, L5 (1984).
[2] L. J. Allamandola, A. G. G. M. Tielens, J. R. Barker, *Polycyclic aromatic hydrocarbons and the unidentified infrared emission bands - Auto exhaust along the Milky Way*, Astrophys. J. **290**, L25 (1985).
[3] *PAHs and the Universe: A Symposium to Celebrate the 25th Anniversary of the PAH Hypothesis*, C. Joblin and A.G.G.M. Tielens eds, EAS Pub. Series, vol. **46**, (2011).
[4] O. Berné, J. Montillaud, C. Joblin, *Top-down formation of fullerenes in the interstellar medium: proof of concept by photochemical modeling*, Astron. & Astrophys. **577**, id.A133 (2015).
[5] P. Pilleri, J. Montillaud, O. Berné, and C. Joblin, *Evaporating Very Small Grains as tracers of the UV radiation field in Photo-dissociation Regions*, Astron. & Astrophys. **542**, id.A69 (2012).
[6] J. Montillaud, C. Joblin, D. Toublanc, *Evolution of PAHs in photodissociation regions. Hydrogenation and charge states*, Astron. & Astrophys. **552**, id.A15 (2013).
[7] http://www.icmm.csic.es/nanocosmos/
[8] E.K. Campbell, M. Holz, D. Gerlich, and J.P. Maier, *Laboratory confirmation of C_{60}^+ as the carrier of two diffuse interstellar bands*, Nature **523**, 322 (2015).
[9] F. Useli-Bacchitta, A. Bonnamy, G. Malloci, G. Mulas, D. Toublanc, C. Joblin, *Visible photodissociation spectroscopy of PAH cations and derivatives in the PIRENEA experiment*, Chem. Phys. **371**, 16 (2010).
[10] J. Zhen, A. Bonnamy, G. Mulas, C. Joblin, *The optical spectrum of a giant isolated gas-phase PAH cation: $C_{78}H_{26}^+$*, Mol. Astrophys. **2**, 12 (2016).

Cesium D_1 And D_2 Atomic Lines Pressure-Broadened By Ground Helium Atoms

***K. Alioua*[1,2], *A. Moussaoui* [1,2]**
1. Univerité Chérif Messaadia, Route de Annaba, B.P. 1553, Souk-Ahras 41000, Algeria
2. LPMR, Souk-Ahras University, B.P. 1553, Souk-Ahras 41000, Algeria

The spectral broadening of the alkali $D_1(np^2P_{1/2} - ns^2S_{1/2})$ and $D_2(np^2P_{3/2} - ns^2S_{1/2})$ lines, induced by atom-atom interactions, is of interest to the astrophysical community as a possible diagnostic of brown dwarf atmospheres and extrasolar giant planets, which exhibit strong alkali absorption features that are broadened by collisions with helium and hydrogen molecules. The spectra have appreciable values as they are very powerful tools to scan the environments of the brown dwarfs and extrasolar planets. They are even capable to identify their different chemical components and specify their physical properties [1].

Similarly, the spectral broadening of the D_1 and D_2 lines of alkali atoms induced by collisions has aroused a great interest among laser specialists. They have particularly paid attention to optically pumped alkali laser (OPAL) systems by providing a mechanism with which the D_2 alkali line can be broadened to more closely match the optical pump bandwidth [2]. Instead of pumping the D_2 line of the alkali atom, exciplex-pumped alkali laser (XPAL) systems pump a collisionally induced blue satellite [3]. The importance of the alkali-rare gas molecules, selected from the field of pumped molecular exciplex lasers, is robustly linked to their molecular structure that has bound and unbound excited states. Accordingly, the comprehension of the mechanisms of exciplex formation is mostly based on accurate potential-energy curves associated with ground and first excited states [4].

We are concerned by the quantal determination of the far-wing pressure broadening profiles generated by D_1 and D_2 atomic lines when perturbed by the presence of He atoms in both absorption and emission. In this framework the low-density limit will be taken into account for consider only the binary collisions between Cs and He pair of atoms. For this purpose, we have chosen to use the potential-energy curves (PECs) and transition dipole moments (TDMs) of the CsHe molecule which we have generated by ab initio calculations, where we adopted the state-averaged complete active space self consistent field (SA-CASSCF) with the multireference configuration interaction (MRCI) methods including the spin-orbit coupling effects (SO), as it is more significant than the lighter alkali-rare gas systems. Subsequently, we will characterize the potential-energy curves of the $X\ ^2\Sigma_{1/2}^+$, $A\ ^2\Pi_{1/2}$, $A\ ^2\Pi_{3/2}$, and $B\ ^2\Sigma_{1/2}^+$ molecular states by determining their spectroscopic parameters like the equilibrium distance Re and the well depth De.

We will then analyze the behavior of absorption and emission profiles versus temperatures, and determine the position of the eventual satellites in the wings and specify the type and the origin of the radiative transitions from which the satellites may arise. Finally, we compare the calculated pressure broadening profiles with other theoretical studies and also with measured experimental data.

References

[1] C. Sharp and A. Burrows, Astrophys. J., Suppl., **168**, 140 (2007).
[2] A. Chattopadhyay, J. Phys. B **45**, 035101 (2012).
[3] J.D. Readle, C.J. Wagner, J.T. Verdeyen, T.M. Spinka, D.L. Carroll, and J.G. Eden, Appl. Phys. Lett. **94**, 251112 (2009).
[4] L. Fechner, B. Gruner, A. Sieg, C. Callegari, F. Ancilotto, F. Stienkemeiera, and M. Mudricha, Phys. Chem. Chem. Phys. **14**, 3843 (2012).

Transition Probabilities of the Neutral Niobium in the Wavelength Region from 300 to 400 nm

Ipek Kanat Ozturk[1], Betul Atalay[2], Taha Yusuf Kebapcı[3], Sophie Kröger[4]

1. Istanbul University, Faculty of Science, Department of Physics, 34134 Istanbul, Turkey
2. Canakkale Onsekiz Mart University, Faculty of Art and Sciences, Department of Physics, Canakkale, Turkey,
3. Cankaya University, Faculty of Engineering, Materials Science and Engineering, Ankara, Turkey
4.Hochschule für Technik und Wirtschaft Berlin, Fachbereich 1, Wilhelminenhofstr. 75A, D-12459 Berlin, Germany

The atomic transition probabilities are very important fundamental parameters in the fields of physics and astrophysics. The atomic structure of niobium has been subject of several experimental and theoretical investigations [1-12]. However, there is especially need for further studies on the transition probability. The aim of the present work is to supply some more knowledge on this subject. Knowledge about transition probabilities can provide an effective support for the search for further unknown energy levels of atomic Niobium.

The electric dipole transition probabilities of neutral Niobium (Nb I) have been calculated using the Cowan code for the wavelength region from 300 to 400 nm in this study. The transition probability calculation is restricted to the three configurations of even parity $4d^3 5s^2$, $4d^4 5s$, and $4d^5$, and the three configurations of odd parity $4d^3 5s 5p$, $4d^4 5p$ and $4d^2 5s^2 5p$. The electric dipole transition probabilities have been calculated for 214 transitions of atomic niobium. Only transitions with $gA > 10^7\ s^{-1}$ are given in this study. The transition probability results obtained in this work are mostly in agreement with previous data available in the literature [1]. The transition probabilities for 63 transitions are given for the first time.

References

[1]Corliss C. H. and Bozman W. R. ,*Experimental Transition Probabilities for Spectral Lines of Seventy Elements*, National Bureau of Standards Monograph **53**, (1962)
[2]Kröger, S., Bouzed A., *Hyperfine structure in the atomic spectrum of niobium II: Theoretical analysis of the even configurations*, Eur. Phys. J. D **23,** 63–72 (2003)
[3]Bouzed A. Kröger S., Zimmermann D., Kronfeldt H.-D., Guthöhrlein G., Eur. Phys. J. D **23**, 57 (2003)
[4]Sansonetti J.E., Martin W.C., *Handbook of Basic Atomic Spectroscopic Data*, (2005)
[5]Kröger, S., Ozturk I. K., Acar F.G. Basar Gö., Basar Gü. ,b, and Wyart J.-F., *Fine and hyperfine structure in the atomic spectrum of niobium Theoretical analysis of the odd configurations and further new levels*, Eur. Phys. J. D **41**, 61–70 (2007)
[6]Malcheva, G.; Nilsson, Hampus; Engström, Lars; Lundberg, Hans, et al. *Radiative Parameters of Nb I Excited States* Monthly Notices of the Royal Astronomical Society, **412,** (3), 1823 – 1827 (2011)
[7]Er A., Öztürk İ., Başar G., Kröger S., Jarmola A., Ferber R., Tamanis M., "Hyperfine Structure Study Of Atomic Niobium With Enhanced Sensitivity Of Fourier Transform Spectroscopy", J. Phys. B: At. Mol. Opt. Phys., vol.44, pp.1-8, (2011)
[8]Kröger S., Er A., Öztürk İ., Başar G., Jarmola A., Ferber R., Tamanis M., Zacs L., "Hyperfine Structure Measurements Of Neutral With Fourier Transform Spectroscopy Niobium", Astronomy& Astrophysics, A70, pp.1-20, (2010)
[9]Başar G., Başar G., Öztürk İ., Er A., Güzelçimn F., Kröger S., Hyperfine Structure Investigations of Atomic Niobium With Optogalvanic And Laser-Induced Fluorescence Spectroscopy in the Near-Infrared Wavelength Range ", Astronomy& Astrophysics, **556,** (2013)
[10]Kanat Öztürk İ., Er A., Güzelçimen F., Başar G., Başar G., Kröger S., New Energy Levels Of Atomic Niobium By Laser İnduced Fluorescence Spectroscopy İn The Near İnfrared, Journal Of Physics B: Atomic, Journal Of Physics B-Atomic Molecular And Optical Physics, Vol.48, No.15005, Pp.1-7, (2015)
[11]Dembczynski J., Elantkowska M., Ruczkowski J., Kanat Öztürk İ., Er A., Güzelçimen F., et al., Parametric Study of the Fine and Hyperfine Structure for the Even Parity Configurations of Atomic Niobium, Journal Of Physics B-Atomic Molecular And Optical Physics, **48,** 15005, (2015)
[12]Er A., Güzelçimen F., Başar G., Kanat Öztürk İ., Tamanis M., Ferber R., Et Al., High-Resolution Fourier Transform Spectroscpoy Of Nb I in the Near-Infrared, Astronomy & Astrophysics Supplement Serıes, 221, **14,** (2015)

Structure and Fragmentation of $H_mC_n^{q+}$ (n=1-5; m=1-4; q=0-3) Clusters

J.P. Sánchez[1], N.F. Aguirre[1], S. Díaz-Tendero[1,2], M. Chabot[3], K. Béroff[4], P.-A. Hervieux[5], M. Alcamí[1,6], F. Martín[1,2,6]

[1] *Departamento de Química, Módulo 13,Universidad Autónoma de Madrid, 28049, Madrid, Spain*
[2] *Condensed Matter Physics Center (IFIMAC), Universidad Autónoma de Madrid, 28049 Madrid, Spain.*
[3] *Institut de Physique Nucléaire d'Orsay, Université Paris Sud and CNRS F-91406 Orsay Cedex, France*
[4] *Institut des Sciences Moléculaires d'Orsay, Université Paris Sud and CNRS F-91405 Orsay Cedex, France*
[5] *Institute de Physique et Chimie des Matériaux de Strasbourg, Université de Strasbourg, 67034 Strasbourg,France*
[6] *Instituto Madrileño de Estudios Avanzados en Nanociencias (IMDEA-Nanociencia), 28049 Madrid, Spain*

Partially hydrogenated carbon clusters have been widely but heterogeneously studied. Theoretical modeling of their properties and fragmentation behavior provides valuable information. This allows to study the evolution of new molecules and ions detected in the Interstellar Medium (ISM). It also helps to understand the composition and chemical processes taking place in the ISM [1].

Previously we have only considered bare carbon clusters [2]. When hydrogen atoms are added, the complexity of the studied systems increases. In general, only a few works have considered this family of molecules systematically but only on small sequences [3]. This work intents to homogenize all the sparse data available in bibliography for the hydrogenated carbon clusters [4]. From this study we obtain trends that may be extrapolated to bigger and more complex molecules of the same family. In this work, calculations of several properties for species of the $H_mC_n^{q+}$ family (for n=1-5; m=1-4; q=0-3) are carried out at DFT-B3LYP/6-311++G(3df,2p)//CCSD(T)/6-311++G(3df,2p) level of theory. The studied properties are: relative energies between isomers, ionization potentials, dissociation energies, vibrational frequencies and fragmentation reactions. Additionally, by using this information, we use the statistical model M3C [5] to study the fragmentation processes of the $H_mC_n^{q+}$ ($n = 1-4$, $m = 1$ and $q = 0, 1$) molecules. We present the obtained breakdown curves, branching ratios and deposited energy distribution functions. We obtain good agreement with the experiments [6]. In particular Fig. 1 shows the capabilities of M3C to describe the fragmentation of the HC_2^+ system with their associated breakdown-curves.

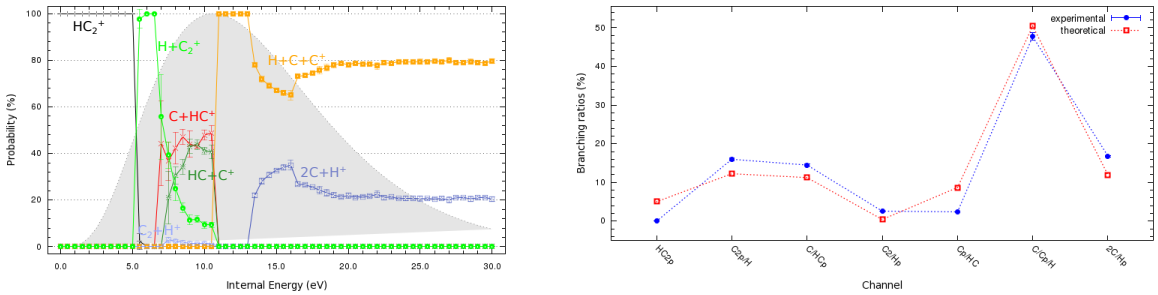

Fig. 1 Results for the fragmentation of HC_2^+ system. Left panel: Channel breakdown curves and deposited energy distribution function (gray). Right panel: Theoretical branching ratios compared to experimental values.

References

[1] M. Chabot, T. Tuna, K. Béroff, T. Pino, A. Le Padellec, P. Désequelles, G. Martinet, V. O. Nguyen-Thi, Y. Carpentier, F. Le Petit, E. Roueff, V. Wakelam, *Statistical Universal Branching Ratios for Cosmic Ray Dissociation, Photodissociation, and Dissociative Recombination of the C, CH and C_3H_2 Neutral and Cationic Species*, A&A **524**, A39 (2010).

[2] S. Díaz-Tendero, P.-A. Hervieux, M. Alcamí, F. Martín, *Statistical Fragmentation of Small Neutral Carbon Clusters*, Phys. Rev. A **71**,033202 (2005).

[3] K.-C Lau, C. Y. Ng, *Accurate Ab Initio Predictions of Ionization Energies of Hydrocarbon Radicals: CH_2, CH_3, C_2H, C_2H_3, C_2H_5, C_3H_3, and C_3H_5*, J. Chem. Phys. **122**, 224310 (2005).

[4] J. P. Sánchez, N. F. Aguirre, S. Díaz-Tendero, F. Martín, M. Alcamí, *Structure, Ionization, and Fragmentation of Neutral and Positively Charged Hydrogenated Carbon Clusters: $C_nH_m^{q+}$ ($n = 1-5$,m= $1-4$, q= $0-3$)* , J. Phys. Chem. A **120**, 588-605 (2016).

[5] N.F. Aguirre, S. Díaz-Tendero, P-A. Hervieux, M. Alcami and F. Martín. *M3C: A software package designed to describe statistical fragmentation of excited molecules*. In preparation (2016).

[6] T. Tuna, M. Chabot, T. Pino, P. Désesquelles, A. LePadellec, G. Martinet, M. Barat, B. Lucas, F. Mezdari, L. Montagnon, N. T. Van-Oanh, L. Lavergne, A. Lachaize, Y. Carpentier, K. Béroff, K., *Fragmentation Branching Ratios of Highly Excited Hydrocarbon Molecules C_nH and Their Cations C_nH^+($n \leq 4$)*, J. Chem. Phys. **128**, 124312 (2008).

Laboratory study of VUV photodesorption processes of interstellar ice analogues

Mathieu Bertin[1], Xavier Michaut[1], Claire Romanzin[2], Laurent Philippe[1], Pascal Jeseck[1], N. Litgerink[3], Harold Linnartz[3] & Jean-Hugues Fillion[1]

1. LERMA, Sorbonne Universités, UPMC Univ. Paris 06, Observatoire de Paris, PSL Research University, CNRS, F-75252, Paris, France

2. LCP (UMR 8000), CNRS, Université Paris-Sud, F-91405 Orsay, France

3. Sackler Laboratory for Astrophysics, Leiden Observatory, Leiden University, P.O. Box 9513, NL-2300 RA Leiden, The Netherlands

In cold regions of the Interstellar Medium (ISM), like star-forming regions or protoplanetary disks, molecules form or accrete on the surface of dust grains. The resulting icy mantles represent the main reservoir of molecules beside H2. Through desorption processes, these ices can eventually enrich the gas phase with more or less complex species, and therefore influence observed gas phase abundance ratio and chemistry. In the vicinity of warm objects (protostar, edge of clouds…) thermal energy is high enough to trigger sublimation of the ices. This is not the case in the colder regions, but other mechanisms, such as cosmic-rays or UV photons impact on the ices, can stand at the origin of the ice desorption. In any case, both thermal and non-thermal desorption processes need to be quantified in order to get a better understanding of the observed molecular abundance ratio, and to bring trustable and relevant parameters for astrochemical models.

The efficiency of thermal desorption is usually linked to the strength of the interaction energy between the adsorbed molecule and the ice surface, so-called adsorption energy. Less is known concerning non-thermal desorption processes. Using energy-resolved studies at the synchrotron SOLEIL, we have focused our studies on UV photodesorption in the 7 – 13. 6 eV range, and obtained for the first time energy-resolved photodesorption rates for a collection of small, astrophysical-relevant, molecules [1-5]. Photodesorption of simple molecules (CO, H_2O…) have already been studied, but using broad band discharge lamps. In our case, the energy resolution allows us for extracting (i) absolute photodesorption rates as a function of the photon energy, applicable to any different UV field, and for (ii) identifying the molecular mechanism and the parameters involved in the desorption process.

I will summarize results we have obtained in the case of simple molecular ices such as CO, N_2 and CO_2 and show the crucial role played by the surrounding molecules (ice composition) and the photochemistry in the UV photodesorption. Finally, I will present very recent results obtained on the photodesorption of CH_3OH and H_2CO, pure and mixed in CO-rich ices.

References

[1] E.C. Fayolle, M. Bertin, C. Romanzin, X. Michaut, P. Jeseck, K.I. Öberg, H. Linnartz & J.-H. Fillion, Astrophysical Journal Letters 739 (2011), L36

[2] M. Bertin, E.C. Fayolle, C. Romanzin, K.I. Öberg, X. Michaut, A. Moudens, L. Philippe, P. Jeseck, H. Linnartz & J.-H. Fillion, Physical Chemistry Chemical Physics 14 (2012), 9929-9935

[3] M. Bertin, E.C. Fayolle, C. Romanzin, H.A.M. Poderoso, X. Michaut, L. Philippe, P. Jeseck, K.I. Öberg, H. Linnartz & J.-H. Fillion, Astrophysical Journal 779 (2013), 120

[4] J.-H. Fillion, E.C. Fayolle, X. Michaut, M. Doronin, L. Philippe, J. Rakovsky, C. Romanzin, N. Champion, K.I. Öberg, H. Linnartz & M. Bertin, Faraday Discussion 168 (2014), 533-552

[5] M. Bertin, C. Romanzin, M. Doronin, L. Philippe, N. Ligterinks, H. Linnartz, X. Michaut, & J.-H. Fillion, The Astrophysical Journal Letters 817 (2016), L12

PROBING PHOTOELECTRON ANGULAR DISTRIBUTIONS IN MULTIPHOTON IONIZATION OF ATOMS, MOLECULES AND CLUSTERS

M. Nrisimhamurty[1], **P. C. Deshmukh**[1], **and G. Aravind**[1]
1. Indian Institute of Technology Madras, Chennai, Tamilnadu-600036, INDIA.

Studies of fundamental processes like photoexcitation, photoionization, photodetachment, photodissociation and dissociative ionization etc., are of paramount importance to explore the structure and dynamics of matter. The impact of electron-electron correlations and relativistic effects in exploring the structure and evolution of matter also lead to significance of these photon-matter and matter-matter interaction studies. In addition, requirement of accurate spectroscopic data to model the structure and dynamics of interstellar and intergalactic medium [1], development of x-ray free-electron lasers [2], attosecond physics [3], to understand hot-dense plasma dynamics [4] and the development of intense laser ionization sources [5], also resulted in the upsurge of these studies. To scrutinize the structure and dynamics of atoms, molecules and clusters, one requires information about various physical observables such as absolute total cross-section and product angular distribution (PAD) asymmetry (β).

Our motivation is to explore the physics of fundamental interactions which are responsible for the formation of multiphase interstellar medium (ISM) through the measurements of photoelectron angular distributions. The key underpinning the photoelectron angular distributions is that they yield the relative strength of the degenerate channels of the photodetachment or photoionization transition and the relative phase-shifts between them whereas the cross section measurements provide the relative strengths of the transition amplitudes alone. In that direction, state-of-the-art velocity-map imaging (VMI) spectrometer, based on Andrei Sanov's model [6] is designed, simulated and constructed to simultaneously measure the photoelectron kinetic energy and angular distributions. The basic principle is that, essentially, the charged particles with the same velocity vector will reach at the same point on the detector irrespective of the point of formation in the interaction region. The design and simulation of our VMI spectrometer is presented in the Fig. 1. Our simulations show that the resolution of VMI spectrometer is 4.5 meV at 1 eV electron kinetic energy and interaction volume diameter 1 mm.

Presently, multiphoton ionization (MPI) of xenon, argon, methyl iodide and ethyl alcohol is being carried out to calibrate the VMI. The laser wavelengths employed to perform MPI are 355 and 532 nm wavelengths, provided by nanosecond Nd:YAG laser. The results corresponding to these experiments will be presented and discussed.

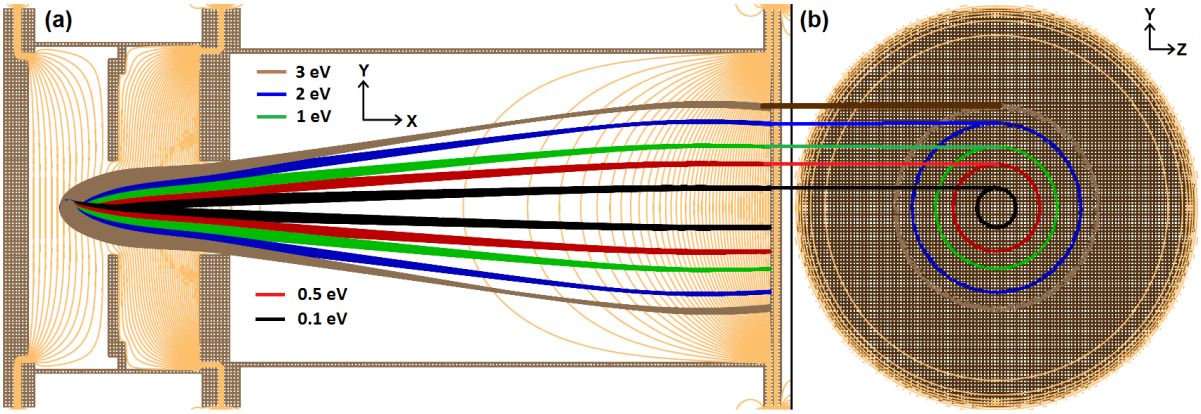

Figure 1: Simulations shown demonstrate the behaviour of photoelectrons traversing with different kinetic energies. Part (a) and part (b) corresponds to simulations recorded for the XY- and YZ-plane respectively. The radii of the circular rings corresponds to kinetic energy of photoelectrons.

References

[1] M. F. Hasoglu, T. W. Gorczyca, M. A. Bautista, Z.Felfli, and S. T. Manson, *Radiation damping in the photoionization of* Fe^{14+}, Phys. Rev. A **85**, 3 (2012).
[2] B. Rudek *et al.*, *Ultra-efficient ionization of heavy atoms by intense X-ray free-electron laser pulses*, Nature Photon. **6**, 858 (2012).
[3] W.-C. Chu, Toru Morishita, and C. D. Lin, *Probing dipole-forbidden autoionizing states by isolated attosecond pulses*, Phys. Rev. A **89**, 033427 (2014).
[4] K. B. Fournier *et al.*, *Observations of high-n transitions in the spectra of near-neon-like copper ions from laser-produced plasmas*, J. Phys. B: At. Mol. Opt. Phys. **4075**, 3347 (2002).
[5] A. Teigelhöfer, J. Lassen, Z. Abboud, P. Bricault, H. Heggen, P. Kunz and R. Li and T. Quenzel, and S. Raeder, *Yttrium ionization scheme development for Ti:Sa laser based RILIS*, Hyperfine Interact. **216**, 65 (2013).
[6] E. Surber, R. Mabbs, and A. Sanov, *Probing the electronic structure of small molecular anions by photoelectron imaging*, J. Phys. Chem. A **107**, 8215 (2003).

A new setup for sputtering experiments with Mercury and Moon analogues

Paul Szabo[1], Bernhard M. Berger[1], Reinhard Stadlmayr[1], André Galli[2], Helmut Lammer [3], Peter Wurz [2], Friedrich Aumayr[1]

1. Institut für Angewandte Physik (IAP), TU Wien, Wiedner Hauptstr. 8-10/134, 1040 Wien, Austria
2. Physikalisches Institut, University of Bern, Sidlerstrasse 5, CH-3012 Bern, Switzerland
3. Space Research Institute, Austrian Academy of Sciences, Schmiedlstrasse 6, A-8042 Graz, Austria

The surfaces of Mercury and Moon are not shielded by a thick atmosphere and therefore they are exposed to bombardment by charged particles, ultraviolet photons and micrometeorites. These influences lead to an alteration and erosion of the surface, and the emitted atoms and molecules form a thin atmosphere, an exosphere, around these celestial bodies [1]. Therefore, the composition of these exospheres is connected to the surface composition and has been subject to flyby measurements by satellites. Model calculations which include the erosion mechanisms can be used as a method of comparison for such exosphere measurements and allow conclusions about the surface composition. Surface sputtering induced by solar wind ions hereby represents a major contribution to the erosion of the surfaces of Mercury and Moon [1]. However, the experimental database for sputtering of respective analogue materials by solar wind ions, which would be necessary for exact modelling, is still in its infancy.

Sputtering experiments have been performed at TU Wien during the past years using a quartz crystal microbalance (QCM) [2]. Target material is deposited on the quartz surface as a thin layer and the quartz's resonance frequency is measured under ion bombardment. The sputter yield can then be calculated from the frequency change and the ion current [2]. In order to remove the restrictions of a thin layer QCM target and simplify experiments with composite targets, a new QCM catcher setup was developed (see Fig. 1a). In the new design, the QCM is placed beside the target holder and acts as a catcher for material that is sputtered from the target surface. By comparing the catcher signal to reference measurements and SDTrimSP simulations [3], the target sputter yield can be determined.

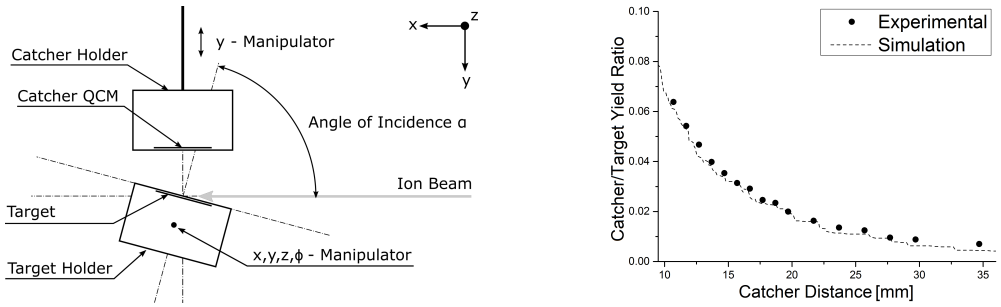

Fig. 1 (a) A sketch of the new catcher QCM setup. (b) An example reference measurement, which shows experimental and theoretical data of the ratio between the yields at the catcher QCM and a Au-coated QCM target for different distances between target and catcher.

As a first test, we have performed experiments with a Au-coated QCM target under 2 keV Ar^+-bombardment. Thus both the mass changes at the target and at the catcher could be obtained simultaneously. Experimental results have been found to be reproducible and the ratio between the two yields coincides with SDTrimSP predictions, with an example of such a reference measurement being shown in Fig. 1b. These results indicate the feasibility of sputtering measurements with the new design. Using the catcher setup, a wide array of targets becomes accessible and further influences such as the sample roughness can be investigated.

After final adjustments to the setup, sputtering experiments on Mercury and Moon analogues will be conducted with the QCM catcher setup and preliminary results will be presented at ECAMP12. Knowledge gained with this research will enhance the understanding of surface sputtering by solar wind ions. This will be used to improve theoretical models of the Mercury's and Moon's exosphere formation so that more insight about their surface composition can be obtained.

References

[1] Esa Kallio, Peter Wurz, Rosemary Killen, Susan McKenna-Lawlor, Anna Milillo, Alessandro Mura, Stefano Massetti, Stefano Orsini, Helmut Lammer, Pekka Janhunen andWing-Huen Ip, *On the impact of multiply charged heavy solar wind ions on the surface of Mercury, the Moon and Ceres*, Planetary and Space Science, **56(11)**, 1506 (2008).

[2] Günter Hayderer, Michael Schmid, Peter Varga, Hannspeter Winter and Friedrich Aumayr, *A highly sensitive quartz-crystal microbalance for sputtering investigations in slow ion–surface collisions*, Review of scientific instruments, **70(9)**, 3696 (1999).

[3] Andreas Mutzke, Ralf Schneider, Wolfgang Eckstein, Renate Dohmen, *SDTrimSP: Version 5.00*, IPP Report, **12/8**, (2011).

Reaction of NH^+ with molecular hydrogen at low temperatures – experimental study

Radek Plašil[1], Štěpán Roučka[1], Serhiy Rednyk[1], Thuy Dung Tran[1], Artem Kovalenko[1], Juraj Glosík[1]

1. Department of Surface and Plasma Science, Faculty of Mathematics and Physics, Charles University in Prague, V Holešovičkách 2, 18000 Prague, Czech Republic

A formation of nitrogen hydrides in interstellar space is of importance for astrophysical models. These molecules are studied as tracers of conditions in interstellar media [1]. The N^+ ion may be formed by reaction of N_2 with He^+ created by cosmic rays. In the series of reactions with molecular hydrogen NH_4^+ ion is formed and in consequent recombination ammonia is created.

We have already studied the formation of NH^+ in reaction $N^+ + H_2$ at low temperatures in range of 10 K to 100 K [2]. This reaction exhibits activation energy barrier and at low temperature conditions it poses a bottleneck of overall process. The amidogen ion, NH^+, still waits for its discovery in interstellar space [3]. Together with process of its formation also processes of its depletion need to be investigated. Apart from a dissociative recombination with electrons [4], NH^+ may reacts with molecular hydrogen. There is only limited number of measurements of the reaction $NH^+ + H_2$ mostly at 300 K; see Fig. 1.

We decided to study the reaction at low temperatures. The reaction is exoergic and may have the rate coefficient as high as theoretical Langevin value. In Fig. 1 we plotted preliminary results of this study between 10 K and 40 K. We have observed the formation of NH_2^+ and also H_3^+ as was reported also by Adams [5].

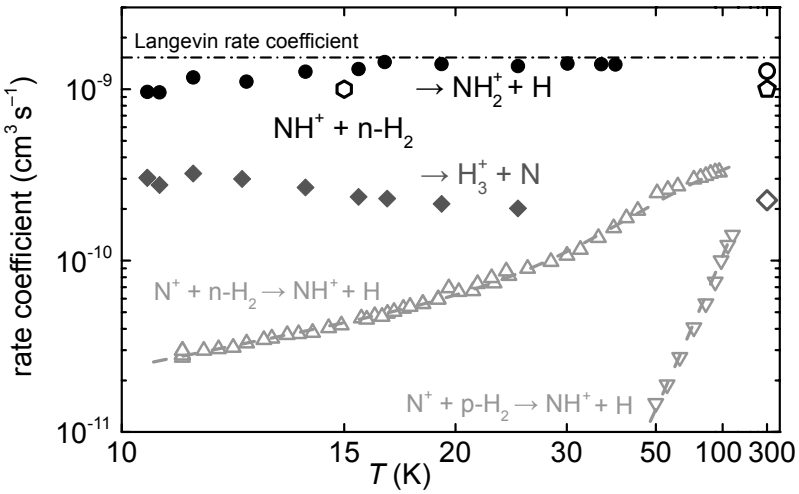

Fig. 1 Measured rate coefficient of the reaction $NH^+ + H_2$ (● product NH_2^+, ◆ product H_3^+) compared with reaction $N^+ + H_2$ (triangles [2]) at low temperatures. The horizontal reciprocal axis covers temperature range relevant for interstellar clouds from 10 K to 300 K. There are distinguished reactions with para hydrogen (p-H_2) and normal hydrogen (n-H_2) that consists of ¼ para and ¾ ortho H_2. Previous measurements of the title reaction are also depicted for a comparison (⬡ [6]; ⬠ [7]; ○, ◇ [5]). Dashed-dotted line shows Langevin rate coefficient for the reaction $NH^+ + H_2$.

The used apparatus is based on the ion-trapping technique developed by prof. D. Gerlich [8]. The ions are confined in the wide nearly field-free effective potential created by the inhomogeneous radio frequency field. The cooling of trapped ions is provided by collisions with neutral buffer gas while the trap is placed on closed-cycle helium cryostat.

References

[1] V. Dislaire, P. Hily-Blant, A. Faure, S. Maret, A. Bacmann and G. Pineau des Forêts, *Nitrogen hydrides and the H_2 ortho-to-para ratio in dark clouds*, Astronomy & Astrophysics **537**, A20 (2012).

[2] Illia Zymak, M. Hejduk, D. Mulin, R. Plašil, J. Glosík and D. Gerlich, *Low-temperature ion trap studies of $N^+(^3P_{ja}) + H_2(j) \rightarrow NH^+ + H$*, Astrophys. J. **768**, 86 (2013).

[3] Carina M. Persson, et al., *Upper limits to interstellar NH^+ and para-NH_2^- abundances: Herschel-HIFI observations towards Sgr B2 (M) and G10.6−0.4 (W31C)*, Astronomy & Astrophysics **567**, A130 (2014).

[4] Oldřich Novotný, et al., *Dissociative recombination measurements of NH^+ using an ion storage ring*, Astrophys. J. **792**, 132 (2014).

[5] Nigel G. Adams, D. Smith and J. F. Paulson, *An experimental survey of the reactions of NH_n^+ ions (n = 0 to 4) with several diatomic and polyatomic molecules at 300 K*, J. Chem. Phys. **72**, 288 (1980).

[6] Dieter Gerlich, *Experimental investigations of ion-molecule reactions relevant to interstellar chemistry*, J. Chem. Soc. Faraday Trans. **89**, 2199 (1993).

[7] Frederick C. Fehsenfeld, Arthur L. Schmeltekopf and Eldon E. Ferguson, *Thermal-Energy Ion-Neutral Reaction Rates. VII. Some Hydrogen-Atom Abstraction Reactions*, J. Chem. Phys. **46**, 2802 (1967).

[8] Dieter Gerlich, *Inhomogeneous Electrical Radio Frequency Fields: A Versatile Tool for the Study of Processes with Slow Ions*, Adv. Chem. Phys. LXXXII (Wiley, New York, 1992).

Gas phase PAH cations: Hydrogen attachment, abstraction and energetic processing

Thomas Schlathölter[1], Leon Boschman[1,2], Nolan Foley[1], Dmitrii Egorov[1], Geert Reitsma[4], Nathalie Rougeau[3], Dominique Teillet-Billy[3], Sabine Morisset[3], Ronnie Hoekstra[1], Stephanie Cazaux[2]

1. University of Groningen, Zernike Institute for Advanced Materials, Nijenborgh 4, 9747AG Groningen,The Netherlands
2. Kapteyn Astronomical Institute, University of Groningen, P.O. Box 800, NL 9700 AV Groningen, The Netherlands
3. Institut des Sciences Moléculaires d'Orsay, ISMO), CNRS, Univ Paris-Sud, Université Paris Saclay, F-91405 Orsay, France
4. Max-Born-Institute, Max Born Strasse 2A, D-12489 Berlin, Germany

Gas-phase PAH interactions with energetic photons and ions are the subject of intense study, on one hand because of the relevance of such processes in astrophysical environments and on the other hand because of the opportunities of PAH photoionization as a tool for analytical chemistry. In the astrophysical context, superhydrogenation of PAHs is of great relevance, as it might influence PAH lifetime in the harsh astrophysical environments and contribute to the formation of H_2, the most abundant molecule in the universe. Furthermore, graphene hydrogenation is known to cause electronic and structural changes, for instance allowing for opening up the graphene band gap in a tunable fashion and the investigation of similar processes in PAHs might yield deeper insights into the underlying physics.

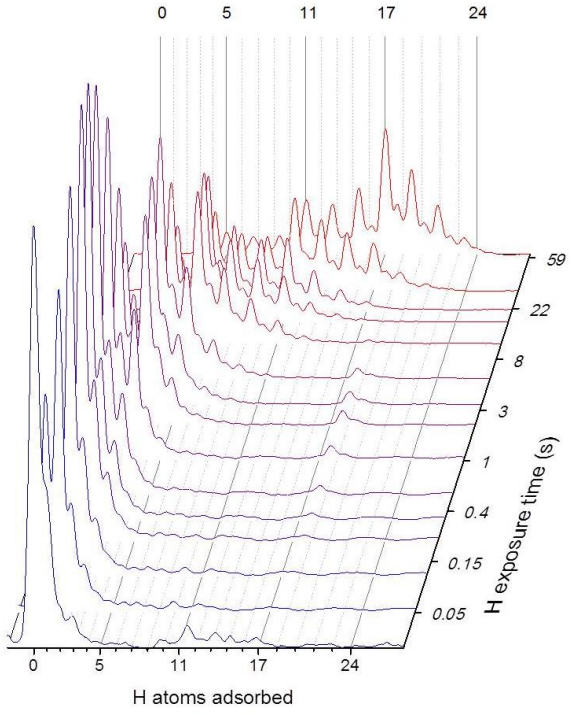

Fig. 1. Hydrogenation of coronene cations vs exposure time.

We have studied superhydrogenation of trapped gas-phase coronene cations [1] and the dehydrogenation of these systems upon photoionization [2] as well as the response of PAH cations upon impact of energetic ions and photons [2,3]. Hydrogenation was achieved by exposure of RF-trapped coronene cations to a thermal atomic H beam. Variation of H exposure time allowed for addition of 1-23 H and for the determination of the respective adsorption barriers. The observed magic numbers, i.e. hydrogenation states of particular stability, and the observed hydrogenation dynamics are in good agreement with preferred binding sites and chemisorption barriers as determined by means of density functional theory (DFT). Hydrogenation is concluded to proceed via a well defined sequence of adsorption sites [4]. Comparison of H and D attachment reveals, that hydrogen attachment is competing with hydrogen abstraction which in turn can lead to H_2 formation. The latter has profound consequences for the H_2 production in astrophysical environments.

Last but not least, we found that attachment of few H atoms to $C_{24}H_{12}^+$ stabilizes the molecule with respect to photofragmentation upon soft X-ray absorption. Quantification of photon induced H "evaporation" from hydrogenated PAHs even allows for determination of the deposited energy.

References

[1] L. Boschman, G. Reitsma, S. Cazaux, T. Schlathölter, M. Spaans, R. Hoekstra, O. Gonzalez-Magaña,, Astrophys. J. Lett. **761** L33 (2012)
[2] G. Reitsma, L. Boschman, M.J. Deuzeman, O. Gonzalez-Magaña, S. Hoekstra, S. Cazaux, R. Hoekstra, and T. Schlathölter, *Deexcitation dynamics of superhydrogenated polycyclic aromatic hydrocarbon cations after soft X-ray absorption*, Phys. Rev. Lett **113** (2014) 053002
[3] G. Reitsma, H. Zettergren, S. Martin, R. Brédy, L. Chen, J. Bernard, R. Hoekstra, T. Schlathölter, *Activation energies for fragmentation channels of anthracene dications—experiment and theory*, J. Phys. B **45** (2012) 215201; G. Reitsma, H. Zettergren, L. Boschman, E. Bodewits, R. Hoekstra, T. Schlathölter, *Ion-PAH collisions: kinetic energy releases for specific fragmentation channels*, J. Phys. B **46** (2013) 245201
[4] S. Cazaux, L. Boschman, N. Rougeau, G. Reitsma, R. Hoekstra, D. Teillet-Billy, S. Morisset, M. Spaans, T. Schlathölter, *The sequence to hydrogenate coronene cations: A journey guided by magic numbers*, Scientific Reports **6** 19835 (2016)

Theoretical Investigation of 2D Hydrogen in Magnetic Field

Eugene A. Koval [1,2], Oksana A. Koval[1]

1. *Bogoliubov Laboratory of Theoretical Physics, Joint Institute for Nuclear Research, Dubna, Moscow Region 141980, Russian Federation*
2. *Department of Fundamental Problems of Microworld Physics, University "Dubna", Dubna, Moscow Region 141980, Russian Federation*

The numerical algorithm for investigation of the energy spectrum and corresponding wave functions of a two-body system with the anisotropic interaction potential is developed.

We study the model of 2D hydrogen atom in the arbitrarily oriented magnetic field (see Fig.1). We have obtained good agreement of the numerical results of the energy spectrum, dipole moments and mean radius with known analytical ones for the 2D hydrogen model [1]. We reproduce the results for the 2D hydrogen in the magnetic field applied perpendicular to the plane of the motion, which were obtained recently by A. Soylu et.al. [1] and by A.V. Turbiner et.al. [2]. In contrast to variational methods used in [2] the convergence of our computational scheme is the same for the magnetic field of an arbitrary strength, which allowed refining results of work [2] for strong fields.

To the authors' knowledge the 2D hydrogen atom in the magnetic field $\boldsymbol{B} = \gamma \sin(\alpha)\, \boldsymbol{i} + \gamma \cos(\alpha)\, \boldsymbol{k}$, tilted to the plane of motion, has not been studied yet. The calculated ground state energy dependence on the magnetic field tilt angle α and field strength $\gamma = |\boldsymbol{B}|$, presented in Fig. 2, demonstrates the possibility to control the energy levels by the orientation of the magnetic field.

This work was supported by the Russian Foundation for Basic Research, Grant No. 16-32-00865.

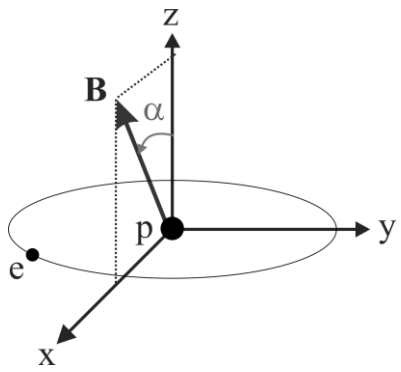

Fig. 1 The schematic representation of the 2D hydrogen atom in the magnetic field tilted into the plane of motion.

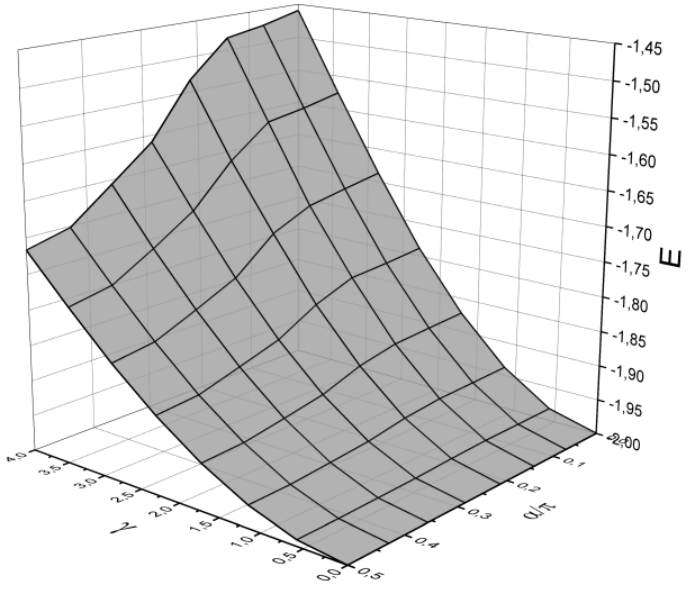

Fig. 2 The 2D hydrogen ground state energy as a function of the magnetic field tilt angle α and the magnetic field strength γ. All quantities are in atomic units.

References

[1] X. Yang, S. Guo, F. Chan, K. Wong, and W. Ching, *Analytic solution of a two-dimensional hydrogen atom. I. Nonrelativistic theory*, Phys. Rev. A **43**, 1186 (1991).

[2] A. Soylu, O. Bayrak and I. Boztosun, *The energy eigenvalues of the two dimensional hydrogen atom in a magnetic field*, International Journal of Modern Physics E **15**, No. 6, 1263–1271 (2006).

[3] M.A. Escobar-Ruiz and A.V. Turbiner, *Two charges on plane in a magnetic field I.''Quasi-equal'' charges and neutral quantum system at rest cases*, Annals of Physics **340**, 37–59 (2014).

[4] V. S. Melezhik, *New Method for Solving Multidimensional Scattering Problem*, J. Comput. Phys. **92**, 67-81 (1991)

[5] V. S. Melezhik and C.-Y. Hu, *Ultracold atom-atom collisions in a nonresonant laser field*, Phys. Rev. Lett. **90**, 8 (2003).

[6] M. Taut, *Two-dimensional hydrogen in a magnetic field: analytical solutions*, J. Phys. A **27**, 1045 (1994).

Unambiguous Observation of Triple-Auger Decay in Near-K-Edge Multiple Photoionization of C^+ Ions

A. Müller[1], A. Borovik Jr.[1,2], T. Buhr[1,3], J. Hellhund[1], K. Holste[1,2], A. L. D. Kilcoyne[4], S. Klumpp[5], M. Martins[5], S. Ricz[1,6], J. Viefhaus[7], S. Schippers[1,2]

1. Institut für Atom- und Molekülphysik, Justus-Liebig-Universität Giessen, Germany
2. I. Physikalisches Institut, Justus-Liebig-Universität Giessen, Germany
3. Physikalisch-Technische Bundesanstalt, Braunschweig, Germany
4. Advanced Light Source, Lawrence Berkeley National Laboratory, Berkeley, California, USA
5. Institut für Experimentalphysik, Universität Hamburg, Germany
6. Institute of Nuclear Research of the Hungarian Academy of Sciences, Debrecen, Hungary
7. FS-PE, DESY, Hamburg, Germany

Single, double and triple photoionization of C^+ ions by a single photon have been investigated in the energy range 286 to 326 eV. Absolute cross sections have been measured employing the photon-ion spectrometer PIPE [1] at the PETRA III synchrotron radiation source in Hamburg. Different from previous photoionization experiments involving the K shell [2] the present measurement covered a much broader energy range and multiple ionization was studied in detail. We were thus able to unambiguously observe triple-Auger decay processes [3] in which specific K-vacancy terms of C^+ were selectively excited from the ground state by irradiation with narrow-bandwidth VUV photons. Subsequent to the decay of the intermediate resonantly excited K-vacancy terms, product ions C^{2+}, C^{3+} and C^{4+} were recorded. Fig. 1 shows the experimental cross sections for processes in which a K-shell electron is excited to the L shell according to $\gamma + C^+(1s^2 2s^2 2p\ ^2P) \rightarrow C^+(1s2s^2 2p^2\ ^2D,^2P) \rightarrow C^{1+m+}(1s^2 2\ell^{3-m}) + me$ leading to net photoionization with $m = 1, 2, 3$. Net triple ionization resulted in the production of $C^{4+}(1s^2)$ (corresponding to $m = 3$), i. e., of a heliumlike ion with no electron left in the L shell. Clearly, the K vacancy produced by $1s \rightarrow 2p$ photoexcitation in the first step has to be filled during the subsequent production of C^{4+} because otherwise there would not be enough energy available to release even a single electron from C^+. The fact that no electrons are left in the L shell after the release of three electrons excludes the possibility of an Auger cascade.

By making use of the outstanding brightness of PETRA III and the sensitivity of our experimental setup PIPE the natural linewidths of the intermediate resonant states could be measured. By combining all the information obtained in the experiment, the absolute transition rates for radiative as well as single and multiple Auger decays were inferred [4]. The triple-Auger decay rate was found to be approximately 2×10^{10} s^{-1} for the $C^+(1s2s^2 2p^2\ ^2D)$ and 1×10^{10} s^{-1} for the $C^+(1s2s^2 2p^2\ ^2P)$ intermediate resonantly-excited terms investigated in this study. Both decay rates are estimated to have a 50% uncertainty. The ratios of single- to double- to triple-Auger rates of the ^2D and ^2P terms are about 100 : 2.7 : 0.013 and 100 : 3.3 : 0.013, respectively.

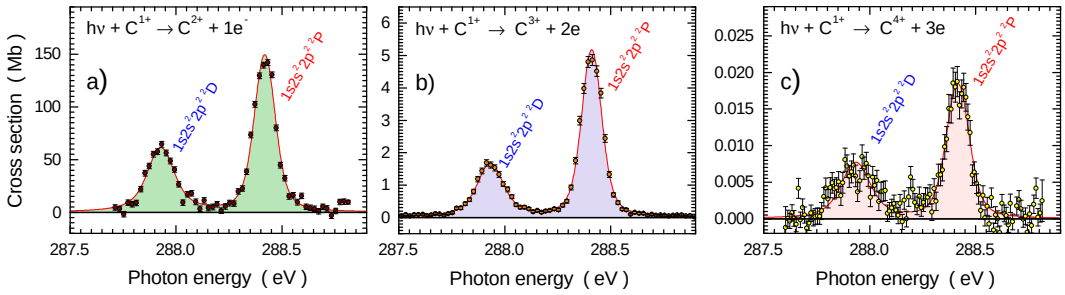

Fig. 1 Photoionization cross sections of C^+ ions associated with resonant excitations $\gamma + C^+(1s^2 2s^2 2p\ ^2P) \rightarrow C^+(1s2s^2 2p^2\ ^2D,^2P)$ from the ground term. The excited term can decay by single-Auger (a), double-Auger (b) and triple-Auger (c) decay.

References

[1] S. Schippers, S. Ricz, T. Buhr, A. Borovik Jr., J. Hellhund, K. Holste, K. Huber, H.-J. Schäfer, D. Schury, S. Klumpp, K. Mertens, M. Martins, R. Flesch, G. Ulrich, E. Rühl, T. Jahnke, J. Lower, D. Metz, L. P. H. Schmidt, M. Schöffler, J. B. Williams, L. Glaser, F. Scholz, J. Seltmann, J. Viefhaus, A. Dorn, A. Wolf, J. Ullrich, and A. Müller, *Absolute cross sections for photoionization of Xe^{q+} ions ($1 \le q \le 5$) at the 3d ionization threshold (J. Phys. B Highlight 2014)*, J. Phys. B **47**, 115602 (2014).

[2] A. Müller, *Precision studies of deep-inner-shell photoabsorption by atomic ions*, Phys. Scr. **90**, 054004 (2015).

[3] A. Müller, A. Borovik Jr., T. Buhr, J. Hellhund, K. Holste, A. L. D. Kilcoyne, S. Klumpp, M. Martins, S. Ricz, J. Viefhaus, S. Schippers, *Observation of a four-electron Auger process in near-K-edge photoionization of singly charged carbon ions (Editors's Suggestion)*, Phys. Rev. Lett. **114**, 013002 (2015);
see also *Making a four-body Auger process happen*, in DESY PHOTON SCIENCE 2015, Science Highlights, Deutsches Elektronen-Synchrotron, Hamburg, Editors: L. Bocklage et al., p.28.

[4] A. Müller, A. Borovik Jr., T. Buhr, J. Hellhund, K. Holste, A. L. D. Kilcoyne, S. Klumpp, M. Martins, S. Ricz, J. Viefhaus, S. Schippers, *Observation of four-electron Auger processes*, J. Phys.: Conf. Ser. **635** 012033 (2015).

Laser–Dressed Morse Potentials: An Exact Analytic Treatment

Sándor Varró[1,2], Imre Barna[1,2], Szabolcs Hack[2], Attila Czirják[2,3]

1. Wigner Research Centre for Physics, Hungarian Academy of Sciences, Konkoly-Thege Miklós út 29-33, 1121 Budapest, Hungary

2. ELI-HU Research & Development Nonprofit Ltd., Dugonics tér 13, 6720 Szeged, Hungary

3. Department of Theoretical Physics, University of Szeged, Tisza Lajos körút 84, 6720 Szeged, Hungary

The interaction of strong laser fields with atoms, molecules, solids or free charges has been extensively investigated [1–3] after the discovery and construction of the first lasers. Concerning possible non-perturbative theoretical descriptions of such strong-field phenomena, the method of space-translation, with the corresponding Floquet analysis, have been proved to be an important tool in treating various high-order processes like ionization or stabilization of atoms [4–5], as well as laser-assisted scattering [6]. This method relies on the Kramers-Henneberger transformation [4–6] leading to a Schrödinger equation, in which the original interaction potential between the charged particles aquires an oscillating shift induced by the interaction with the laser field. The Fourier series of this potential in this so-called Kramers-Henneberger oscillating reference frame contains all the multiphoton components up to infinite order, associated to the laser-atom interaction.

In the present contribution the exact analytic form of the laser-dressed internuclear potential of a heteronuclear diatomic molecule in the Kramers-Henneberger frame is given. It has been derived from the space-translated version of the original Morse potential [7], which represents the vibrational degree of freedom of a molecule. A numerical illustration of a special case for LiH of our general results is displayed in Figure 1. In this case the distortion effect due to the laser field can be represented by the zeroth Fourier component of the space-translated Morse potential, which has the same functional form as the original one, and expressed as

$$\overline{V}(u) = D_1[1-\exp(-a(u-u_1))]^2 - D_1 \,. \quad (1)$$

Here D_1 and u_1 denotes the laser-dressed dissociation energy and the shift of the equilibrium position, respectively. In the above equation u denotes the internuclear distance measured from the original equilibrium position r_0 (for the LiH molecule D=2.515eV, a=1.127Å^{-1}, and r_0=1.596 Å).

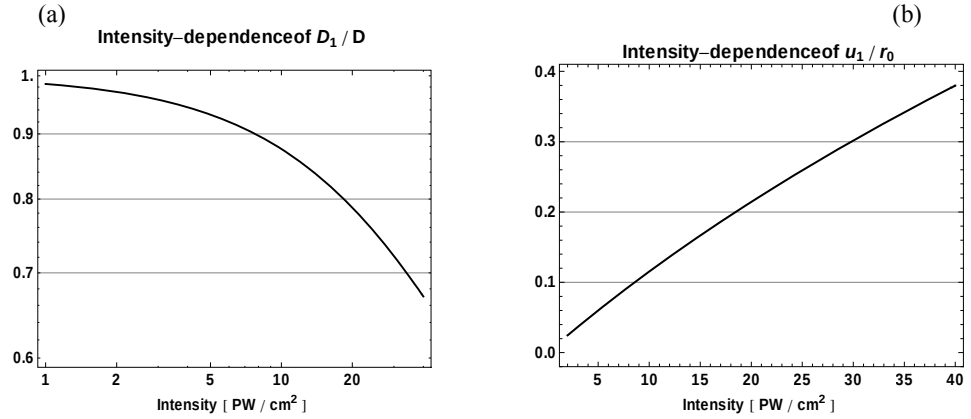

Fig. 1 The left figure (a) shows the intensity-dependence of the ratio D_1/D of the laser-dressed dissociation energy to the original one, in the case of the LiH molecule. The wavelength of the (mid-infrared) laser has been taken λ=3.4μm. Figure 1 (b) displayes the intensity-dependence of the relative change u_1/r_0 in the equilibrium position corresponding the laser-dressed Morse potential given by equation (1). We note that the relative change of the spacing of the vibrational levels $\nu_1/\nu_0=(D_1/D)^{1/2}$ behaves qualitatively similarly to the potential depth shown in (a).

We note that our considerations are realistic if the laser photon energy ($h\nu$=0.365eV) is much larger than the spacing of the vibrational levels ($h\nu_0$=0.071eV), and, at the same time, it is much smaller than the characteristic energy of the electronic excitations. In the above numerical example for LiH these conditions are satisfied.

References

[1] Faisal F H M, *Theory of Multiphoton Processes* (Plenum Press, New York and London, 1987)
[2] Fedorov M V, *Atomic and Free Electrons in a Strong Laser Field* (World Scientific, Singapore, 1997)
[3] Joachain Ch J, Kylstra N J and Potvliege R M, *Atoms in Intense Laser fields* (Cambridge University Press, Cambridge, UK, 2012)
[4] Gavrila M, *Atomic stabilization in superintense laser fields*, J. Phys. B **35**, R147-R193 (2002)
[5] Joachain Ch J, *High-intensity laser-atom interactions*, Europhysics Letters **108**, 4401-p1-p7 (2014)
[6] Varró S, Szabó L and Czirják A, *Laser-assisted electron scattering on a nano-sphere*, Nucl. Instr. Meth. Phys. Res. B **396**, 29-33 (2016)
[7] Morse P M, *Diatomic molecules according to the wave mechanics. II. Vibrational levels*, Phys. Rev. **34**, 57-64 (1929)

On electric dipole-quadrupole interference in photodetachment of a fullerene anion

Valeriy K. Dolmatov
Department of Physics and Earth Science, University of North Alabama, 35632 Florence, Alabama, U.S.A.

It is shown in the present work that one should expect large nondipole (electric dipole-quadrupole) effects to emerge in photoelectron angular distributions from C_n^- anions in the photon energy region of only few to tens eV. These effects become comparable to, and even greater than, generally dominant dipole effects. This is found to be because of "confinement resonances" due to a standing photoelectron wave formed inside the C_n cage-resonator.

To the best of the author's knowledge, nothing is really known to date about electric dipole-quadrupole effects in photodetachment spectra of C_n^- anions (similar studies have been performed for photoionization of only atoms encapsulated inside the hollow interior of a C_n fullerene, see, e.g., [1]). Noting that a fullerene anion is, in essence, a giant atom with a loosely bound outer electron, it becomes interesting to get insight into nondipole photoelectron angular distributions upon photodetachment of these "giant atoms" and learn how these distributions might depend on the size of C_n. The present study answers this question in a rough model approximation. There, a fullerene cage C_n is modelled by an attractive spherical potential of certain depth U_0, inner radius r_0 and thickness Δ (see, e.g., [1]). A fullerene anion is then formed due to binding of the electron by this potential into a $n\ell$-state.

For illustration, calculated dipole $\beta_{n\ell}(\omega)$ and dipole-quadrupole $\zeta_{n\ell}(\omega) = \gamma_{n\ell}(\omega) + 3\delta_{n\ell}(\omega)$ angular-asymmetry parameters (in the definitions of [2]) upon photodetachment of $C_{60}^-(2p)$ and $C_{540}^-(2p)$ are depicted in figure 1. Clearly, results are indicative of resonantly enhanced (due to "confinement resonances") low-energy nondipole effects in photodetachment angular distributions from fullerene anions which, at ceratin energies, are comparable to, or even greater than, the dipole effects, and both effects undergo drastic changes with increasing size of C_n^-.

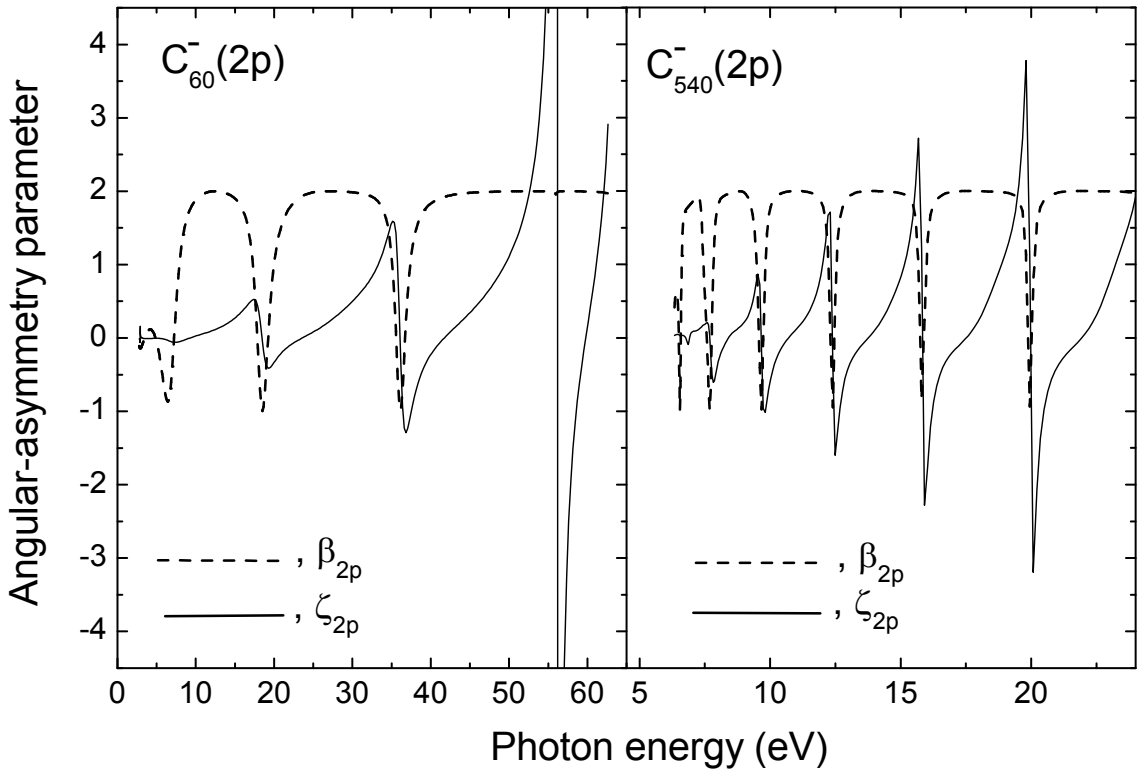

Fig. 1 Calculated β_{2p} and ζ_{2p} upon $2p$-photodetachment of $C_{60}^-(2p)$ ($r_0 = 5.262$, $U_0 = 0.2958$ and $\Delta = 2.9102$ a.u.) and $C_{540}^-(2p)$ ($r_0 = 5.262$, $U_0 = 0.404$ and $\Delta = 2.9102$ a.u.) (see text for the utilized notations).

The support of NSF under the grant No. PHY-1305085 and a travel grant from CAS at UNA are acknowledged.

References

[1] M. Ya. Amusia, A. S. Baltenkov, V. K. Dolmatov, S. T. Manson, and A. Z. Msezane, *Confinement resonances in photoelectron angular distributions from endohedral atoms*, Phys. Rev. A **70**, 023201 (2004).
[2] J. W. Cooper, *Photoelectron-angular-distribution parameters for rare-gas subshells*, Phys. Rev. A **47**, 1841 (1993).

Interatomic Coulombic Decay after Multiple Resonant Excitations

Ghazal Jabbari and Lorenz S. Cederbaum
Theoretische Chemie, Ruprecht-Karls-Universität, Im Neuenheimer Feld 229, D-69120 Heidelberg, Germany

The advent of intense and ultrashort extreme ultraviolate sources offers an exceptional opportunity to investigate fast electronic relaxation mechanisms. When multiple photons are absorbed in clusters, at moderate field intensities, multiple excitations in clusters can undergo processes such as autoionization or resonant interatomic Coulombic decay.

Since it's prediction in 1997, interatomic Coulombic decay (ICD) has been studied vastly in theoretical and experimental works[1]. Here we want to discuss a particular manifestation of the ICD process which is initiated by multiple photon absorption. The relaxation of the multiply excited states occurs through a very efficinet energy transfer, leading to the de-excitation of one atom and the ionization of the other species:

$$[Rg]_2 \xrightarrow{2\hbar\omega} [Rg^*...Rg^*] \xrightarrow{ICD} [Rg...Rg^+] + e^-_{ICD} \tag{1}$$

$$[Rg]_2 \xrightarrow{2\hbar\omega} [Rg^{**}...Rg] \xrightarrow{ICD} [Rg^*...Rg^+] + e^-_{ICD} \tag{2}$$

The process in Eq(1) has been studied before in rare gas dimers and clusters[2,3], and was shown to be an efficient relaxation mechanism (occurring on a femtosecond timescale) compared to other possible decay channels. The process in Eq(2), however, due to it's complicated nature and it's competition with autoionization has not been investigated. In this work, we study theoretically both processes in several homo- and hetroatomic rare gas dimers.

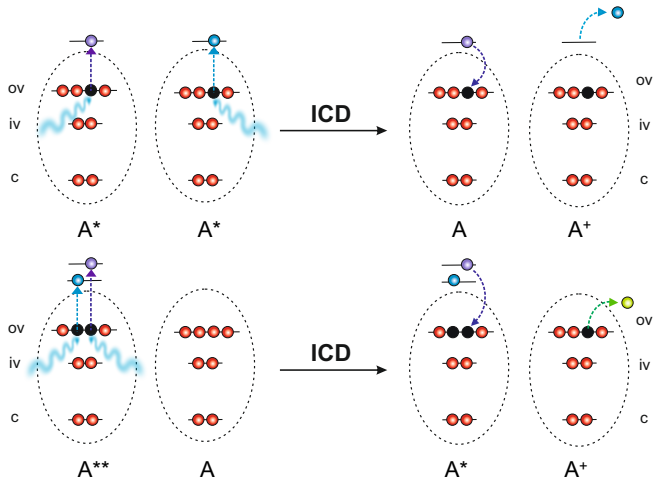

Figure 1: A schematic representation of the two ICD processes after double excitation in a rare gas dimer.

References

[1] L.S. Cederbaum, J. Zobeley, and F. Tarantelli, *Giant Intermolecular Decay and Fragmentation of Clusters*, Phys. Rev. Lett. **79**, 4778 (1997), T. Jahnke, *Interatomic and intermolecular Coulombic decay: the coming of age story*, J. Phys. B **48**, 082001 (2015).

[2] A.I. Kuleff, K. Gokhberg, S. Kopelke, and L.S. Cederbaum, *Ultrafast Interatomic Electronic Decay in Multiply Excited Clusters* , Phys. Rev. Lett. **105**, 043004 (2010), Ph.V. Demekhin, K. Gokhberg, G. Jabbari, S. Kopelke, A.I. Kuleff, and L.S. Cederbaum, *Overcoming blockade in producing doubly excited dimers by a single intense pulse and their decay*, J. Phys. B: Atomic, Molecular and Optical Physics **46**, 021001 (2013).

[3] A.C. LaForge, M. Drabbels, N.B. Brauer, M. Coreno, M. Devetta, M. Di Fraia, P. Finetti, C. Grazioli, R. Katzy, V. Lyamayev, T. Mazza, M. Mudrich, P. O'Keeffe, Y. Ovcharenko, P. Piseri, O. Plekan, K.C. Prince, R. Richter, S. Stranges, C. Callegari, T. Möller, and F. Stienkemeier, *Collective Autoionization in Multiply-Excited Systems: A novel ionization process observed in Helium Nanodroplets*, Sci. Rep. **4**, 3621 (2014), B. Schütte, M. Arbeiter, T. Fennel, G. Jabbari, A.I. Kuleff, M.J.J. Vrakking, and A. Rouzée, *Observation of correlated electronic decay in expanding clusters triggered by near-infrared fields*, Nat. Commun. **6**, 8596 (2015).

Optomagnetism Based on Light Carrying Orbital Angular Momentum

***Jonas Wätzel*[1], *Jamal Berakdar*[1]**

1. Institut für Physik, Martin-Luther Universität Halle-Wittenberg, Karl-Freiherr-von-Fritsch Str.3, 06112 Halle, Germany

Endohedral molecular magnets are promising candidates for quantum information processing and sensing as well as molecular electronics [1,2]. For their utilization a control of the local magnetization and spin dynamics on an ultrafast time scale is favourable. We suggest here to photo-trigger current loops on a fullerene sphere by initiating resonant transitions to the virtual, (super) atomic-like molecular orbitals (SAMOs) [3,4,5]. These current loops produce localized magnetic pulses which steer the magnetic properties of the fullerene.

The use of inhomogeneous light carrying orbital angular moment (OAM) provides an effective method for this purpose, as SAMOs are effectively optically dark when starting from HOMO for homogeneous optical pump fields. The spatial profile of the employed structured light exhibits a singularity at its centre. The phase front associated with the light forms a helical shape characterized by the amount of OAM which can be transferred to charge carriers and leads to a torque generating the current loop. In principle in presence of the spin-orbit coupling one may drive the spin channels directly with such a beam [6] but here we generate a magnetic moment that Zeeman-couples to the well isolated spin active states associated with the endohedral structure.

We present results showing that UV OAM pulse with a moderate intensity of 10^{13} W/cm² generates nA current loops with an associated magnetic field on the scale of a few hundred μT in the center of the fullerene [7]. We found that this current is highly controllable scale by the frequency (different resonant transitions to SAMOs possible) and the topological charge (sets the amount of transferable OAM) of the light.

References

[1] J. Crose *et al*., *Tunneling spectra of individual magnetic endofullerene molecules*, Nat. Mater. **7**, 884 (2008).
[2] R. Westerström *et al.*, *An Endohedral Single-Molecule Magnet with Long Relaxation Time*, J. Am. Chem. Soc. **134**, 9840 (2012).
[3] M. Feng, J. Zhao, and H. Petek, *Atomlike, Hollow-Core-Bound Molecular Orbtials in C60*, Science **320**, 359 (2008).
[4] Y. Pavlyukh and Jamal Berakdar, *Kohn-Sham potentials for fullerenes and spherical molecules*, Phys. Rev. A **81**, 042515 (2010).
[5] Y. Pavlyukh and Jamal Berakdar, *Communication: Superatom molecular orbitals: New types of long-lived electronic states*, J. Chem. Phys. **135**, 201103 (2011).
[6] G. F. Quinteiro, P. I. Tamborenea, and J. Berakdar, *Orbital and spin dynamics of intraband electrons in quantum rings driven by twisted light*, Opt. Expr. **19**, 26733 (2011).
[7] J. Wätzel *et al.*, *Optical vortex driven charge current loop and Optomagnetism in fullerenes*, Carbon **99**, 439 (2016).

Monitoring correlated electron dynamics by attosecond transient absorption spectroscopy

Maximilian Hollstein[1], **Robin Santra**[1,2] **and Daniela Pfannkuche**[1]
[1] Department of Physics, Universität Hamburg, Jungiusstraße 9, D-20355 Hamburg, Germany
[2] Center for Free-Electron Laser Science, DESY, Luruper Chaussee 149, D-22716 Hamburg, Germany

The dynamics of electrons govern elementary processes such as chemical reactions and charge transport in molecular systems. The observation and understanding of these processes is the central goal of ultrafast science. With the advent of attosecond pulses, it has become possible to steer and to probe these electron dynamics on their natural timescale [1]. In molecular systems, electron correlation is of significant importance. In fact, electron correlation is predicted [2] to drive an ultra-fast and efficient first step of a charge transfer even before the nuclear motion sets in. However, experimental evidence of this process is still missing. In this context, a particularly promising technique that might allow the evidence and the investigation of these correlation-driven dynamics is attosecond transient absorption spectroscopy (ATAS) [3-5]. So far, this technique has been applied predominantly to the electron dynamics in atomic systems, i.e. mostly nobel gas atoms, whereas an application to more complex systems where correlation driven charge migration can occur - to our best knowledge - has not yet been conducted. Here, we investigate theoretically to which extent ATAS can be employed to monitor correlated electron dynamics in polyatomic molecules. For this purpose, we determine theoretical time-resolved ATAS spectra for the C_2H_4BrI molecule after it has undergone prompt double ionization. Noteworthy, whereas for single ionization, correlation driven charge migration involving the population of shake-up states occurs predominantly after inner-valence ionization, we find that analogous processes occur already for outer-valence double ionization. Remarkably, we find that ATAS allows highly detailed insight into these dynamics that follow the ionization process and we observe that although the electron dynamics are strongly correlated, features in the ATAS spectra can be related to electron-hole populations thus providing surprisingly intuitive access to the electron-hole dynamics. With this, our findings highlight the outstanding role of ATAS to be one of the most promising techniques for monitoring ultrafast electron dynamics in complex molecular systems.

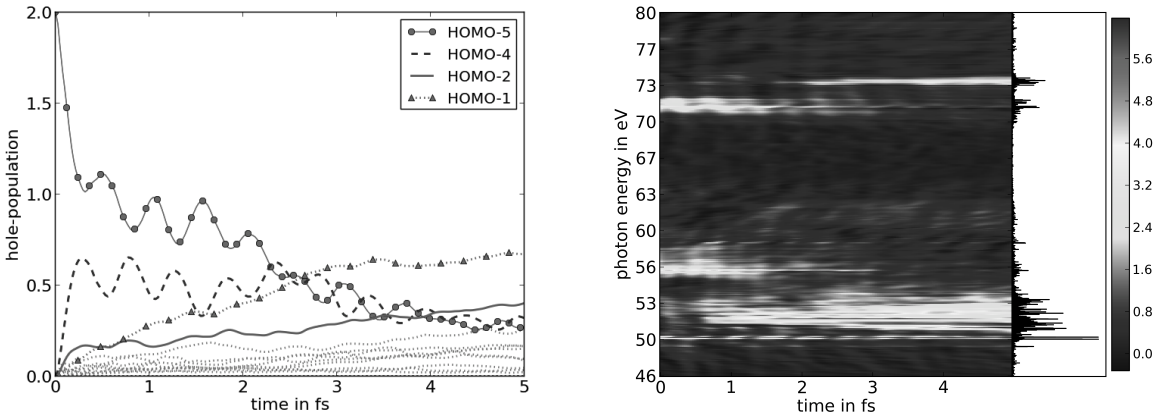

(a) (b)

a) The time-dependent hole populations following the prompt removal of two electrons from the HOMO-5 of the C_2H_4IBr molecule. b)The time-resolved absorption cross section in Mb. The (de)population of molecular orbitals is reflected in the absorption cross section.

References

[1]F. Krausz and M. Ivanov, Rev. Mod. Phys. 81, 163 (2009).
[2]L.S. Cederbaum and J. Zobeley, Chemical Physics Letters 307, 205 (1999)
[3]E. Goulielmakis et al, Nature 466, 739 (2010).
[4]H. Wang et al, Phys. Rev. Lett. 105, 143002 (2010).
[5]M. Holler et al, Phys. Rev. Lett. 106, 123601 (2011).

Photoionization of CH_4, H_2O and NH_3: A Sturmian Approach

Carlos M. Granados–Castro[1,2], **Lorenzo U. Ancarani**[1], **Gustavo Gasaneo**[2,4], **Darío M. Mitnik**[3,4]
1. Équipe TMS, SRSMC UMR 7565, *Université de Lorraine,* 57078 *Metz, France*
2. Departamento de Física, Universidad Nacional del Sur, 8000 *Bahía Blanca, Argentina*
3. Instituto de Astronomía y Física del Espacio (IAFE) and Universidad de Buenos Aires, Argentina
4. Consejo Nacional de Investigaciones Científicas y Técnicas (CONICET), Argentina

Study of ionization processes plays a central role in quantum mechanics. Different theoretical methods have been proposed in the past, particularly to study photoionization (PI) of atoms (see [1], and references therein). When studying PI in molecular systems, several challenges appear: the spatial orientation of the target (not resolved experimentally), the description of the Hamiltonian (highly noncentral) and the corresponding continuum states. Finding an accurate representation of such states for molecules is not an easy task. The Sturmian approach [2], which uses Generalized Sturmian Functions (GSF), has been applied successfully for the study of $(e,3e)$ [3] and $(\gamma,2e)$ [4] in He, but the extension of the method to molecular systems is under development. In this contribution, we use such Sturmian approach to study PI of molecules, in particular of CH_4, NH_3 and H_2O.

We use the single active-electron approximation and the one-center expansion (OCE). The initial state is described by the OCE wave functions calculated by Moccia [5]. In order to calculate the PI cross sections, we solve the time-independent, first-order perturbative, Schrödinger equation, expanding the scattering wave function in a GSFs basis set. Their adequate asymptotic behavior (in this case outgoing Coulomb behavior, corresponding to a $+1$ charge felt at large distances by the escaping photoelectron) [2] allows us to extract the transition amplitudes directly from the expansion coefficients [1]. The random spatial orientation of the target is included in our calculations in two different ways: (a) in the post-averaged scheme we use a noncentral molecular model potential [6], calculated for each individual spatial orientation, and an angular average of the cross sections is performed at the end; (b) in the pre-averaged scheme we use an angular averaged molecular model potential. Results for both schemes are compared in order to investigate whether the second option (which is computationally much lighter) is acceptable or not.

The calculated cross sections are compared with theoretical and experimental data. Figure 1 provides an example, for ionization from the outer valence orbital $3a_1$ of NH_3.

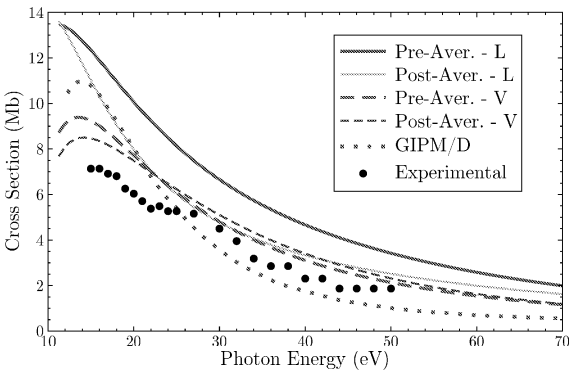

Fig. 1 PI cross section in Mbarns, versus photon energy in eV, for ionization from the $3a_1$ orbital of NH_3. Our results with the Sturmian approach, in length gauge, in the pre- (thick solid line) and the post-averaged (thin solid) schemes, and in velocity gauge, in the pre- (thick dashed) and post-averaged (thin dashed) schemes, are compared with GIPM/D calculations (dotted) [7] and experimental data (points) [8].

References

[1] C. M. Granados–Castro *et al*, *A Sturmian Approach to Photoionization of Molecules*, Adv. Quantum Chem. **73**, 3 (2016).
[2] G. Gasaneo *et al*, *Three-Body Coulomb Problems with Generalized Sturmian Functions*, Adv. Quantum Chem. **57**, 153 (2013).
[3] M. J. Ambrosio *et al*, *Double Ionization of Helium by Fast Electrons with the Generalized Sturmian Functions Method*, J. Phys. B: At. Mol. Opt. Phys. **48**, 055204, (2015).
[4] J. M. Randazzo *et al*, *Double Photoionization of Helium: a Generalized Sturmian Approach*, Eur. J. Phys. D **69**, 189 (2015).
[5] R. Moccia, *One-Center Basis Set SCF MO's. I. HF, CH_4 and SiH_4*, J. Chem. Phys. **40**, 2164 (1964); *[. . .] II. NH_3, NH_4^+, PH_3, PH_4^+* **40**, 2176 (1964); *[. . .] III. H_2O, H_2S and HCl* **40**, 2186 (1964).
[6] L. Fernández–Menchero and S. Otranto, *Single Ionization of CH_4 by bare ions: Fully Differential Cross Sections*, Phys. Rev. A **82**, 022712 (2010).
[7] D. A. L. Kilcoyne, S. Nordholm and N. S. Hush, *Diffraction Analysis of the Photoionisation Cross Sections of Water, Ammonia and Methane*, Chem. Phys. **107**, 213 (1986).
[8] C. Brion, A. Hamnett, G. Wight and M. van der Wiel, *Branching Ratios and Partial Oscillator Strengths for the Photoionization of NH_3 in the* 15-50 *eV Region*, J. Electron Spectros. Relat. Phenomena **12**, 323 (1977).

Two–photon ionization as a benchmark for scattering problems with nondecaying sources

Antonio Ilan Gómez[1,2], Gustavo Gasaneo[1,2], Darío M. Mitnik[2,3], Marcelo J. Ambrosio[2,3], Lorenzo Ugo Ancarani[4]

1. Departamento de Física, Universidad Nacional del Sur, 8000 Bahía Blanca, Buenos Aires, Argentina
2. Consejo Nacional de Investigaciones Científicas y Técnicas (CONICET), Argentina
3. Instituto de Astronomía y Física del Espacio (IAFE) and Universidad de Buenos Aires, Buenos Aires, Argentina
4. Equipe TMS, SRSMC, UMR CNRS 7565, Université de Lorraine, 57078 Metz, France

The description with traditional methods of single or multiple ionization of atoms and molecules by two or more successive photons requires some special treatment (see, e.g., [1]). Difficulties occur when a spatially non-decaying driven term appears in the Schrödinger-like non-homogeneous equation for the scattering wave function. The simplest of such situations is the non-sequential two-photon double ionization of Helium which has been studied extensively during the last decade, both theoretically [2] and experimentally [3]. Nevertheless, there are still large discrepancies between the different theoretical approaches, and with experimental data; as such, the process is not considered as fully understood. Two major theoretical difficulties are the imposition of adequate asymptotic conditions and how to extract the ionization amplitude from the solution.

Before addressing the full Helium problem within a Generalized Sturmian Functions (GSF) approach [4,5], we study here the two-photon ionization of Hydrogen that presents the main characteristics we want to emphasize. This benchmark case allows us to understand how the methodology [6] works and to delve into some of the numerical aspects of the general method we propose to address, i.e., the multiphoton double ionization problem in two–electron atoms. The GSF used to solve the first and second order equations are constructed possessing appropriate asymptotic conditions (outgoing Coulomb behavior). The treatment of the second order equation is particular due to the fact that its driven term does not vanish for large distances r, as can be seen on Fig. 1(a). This non-vanishing behavior enforces on the second order scattering wave function a "beat" type asymptotic behavior, as shown in Fig. 1(b). Within the methodology we propose, a suitable set of GSFs can be easily constructed possessing, at large distances, exactly that "beat" behavior (see Fig. 1(c)).

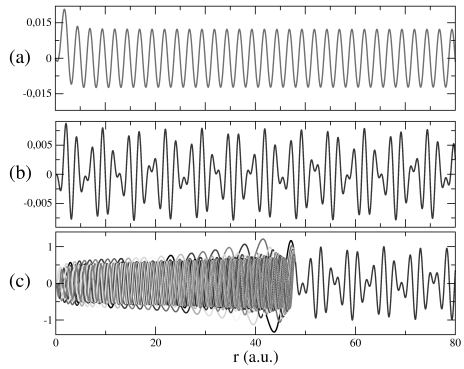

Fig. 1 For an Hydrogen atom interacting with a monochrome laser, we plot as a function of the emitted electron distance r: (a) the second order driven term; (b) the second order scattering wavefunction; (c) a suitable set of Generalized Sturmian Functions.

When solving the second order equation using this adequate basis set, convergence is naturally increased. Moreover, in contrast to other approaches, our methodology provides a practical way to extract the ionization amplitude directly from the asymptotic behavior of the scattering wave function, not as a matrix element, that is to say without the need for any *ad hoc* approach. We also briefly illustrate how similar situations are encountered, for example, in the multiphoton double ionization of helium.

References

[1] D.A. Horner, F. Morales, T.N. Rescigno, F. Martín and W. McCurdy, *Two-photon double ionization of helium above and below the threshold for sequential ionization*, Phys. Rev. A, **76**, 030701(R) (2007).
[2] L.Malegat *et al.*, *A novel estimate of the two-photon double-ionization cross section of helium*, J. Phys. B, **45**, 175601 (2012).
[3] Sh.A. Abdel-Naby *et al.*, *Nuclear-recoil differential cross sections for the two-photon double ionizatio of helium*, Phys. Rev. A **87**, 063425 (2013).
[4] G. Gasaneo, L.U. Ancarani, D.M. Mitnik, J.M. Randazzo, A.L. Frapiccini and F.D. Colavecchia, *Three-Body Coulomb Problems with Generalized Sturmian Functions*, Adv. Quantum Chem. **67**, 153 (2013).
[5] D.M. Mitnik, F.D. Colavecchia, G. Gasaneo and J.M. Randazzo, *Computational methods for Generalized Sturmians basis*, Comp. Phys. Comm. **45**, 1145 (2011).
[6] A.I. Gómez, G. Gasaneo, D.M. Mitnik, M.J. Ambrosio and L.U. Ancarani, *submitted*

Subcycle resolved interference effects in self-diffraction

Christoph G. Leithold, Jan Reislöhner, Adrian N. Pfeiffer

Institut für Optik und Quantenelektronik, Friedrich Schiller Universität Jena, Max-Wien-Platz 1, 07743 Jena, Germany

We investigate subcycle resolved interference effects using a self-diffraction pump-probe setup. While interference in between self-diffraction orders is readily understood and connected to a close-to-collinear beam geometry, we also present a new kind of subcycle sensitive interference which concerns the self-diffraction orders themselves.

Two laser pulses from a mode-locked Ti:Sa laser with pulse duration of about 20 fs and central wavelength of 700 nm are focused into a 145 µm thick borosilicate glass target. The two beams intersect each other under a shallow angle inside the bulk solid forming an interference pattern with a few fringes. The phase of this interference pattern (GEP: groove-envelope-phase) can be adjusted by means of the delay τ between the two pulses. The nonlinear interaction within the target leads to self-diffraction, which can be described by four/multi-wave-mixing or self-focusing. If half the crossing angle is comparable to the divergence angles of two adjacent beams, they do not separate in the far field and thus they share spatial frequency components. In this case the beams are double octave spanning in the spatial frequency domain: This is the third order (Kerr) spatial analogue to a second order (SHG) f-2f interferometer, which can be used for CEP stabilization. Since stability of the GEP is typically ensured by a stable interferometric setup, further stabilization is unnecessary. The interference between adjacent self-diffraction orders could be used to examine phase contributions that originate from the non-instantaneous nature of self-diffraction.

Surprisingly not only interferences between adjacent diffracted beams after the sample are observed. At sufficiently high intensities of around 25 TW/cm^2 distinct modulations of the self-diffraction orders themselves are visible when changing the pump-probe delay (Fig. 1 top). We present a simplified model which phenomenologically explains this new kind of interference (Fig. 1 bottom). It is based on the occurrence of a narrow, strongly localized change in the transmission properties of the solid. These localized transmission changes (LTC) are assumed to occur at the very peaks of the grating which start to filament as the light propagates through the bulk solid. Each intensity maximum with sufficiently high intensity (to build up LTC) introduces an additional, broad, spatial frequency distribution (corresponding to a narrow real space distribution). Hence the electrical field of the introduced LTC term will significantly overlap in the far field with neighbouring self-diffraction orders, explaining the experimentally observed interferences on the self-diffraction orders. Our model suggests that this effect cannot be explained by the third order nonlinearity.

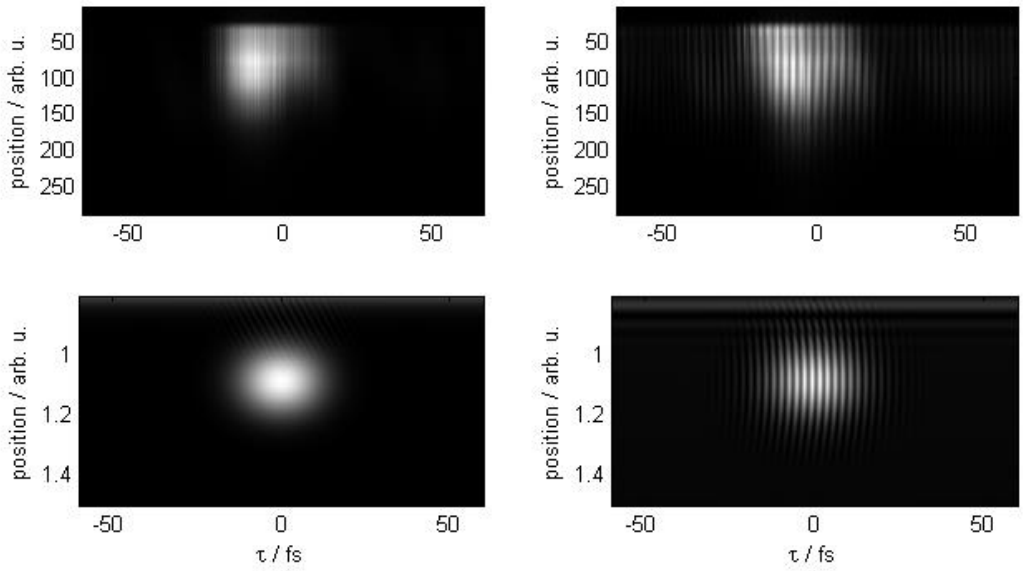

Fig. 1 First self-diffraction order over pump-probe delay τ. Top: measurement raw data at low intensity (left) and higher intensity (right). Bottom: model calculation without (left) and with LTC (right).

Electron Spin Polarization In Strong-Field Ionization Of Xenon Atoms

Alexander Hartung[1], Felipe Morales[2], Maksim Kunitski[1], Kevin Henrichs[1], Alina Laucke[1], Martin Richter[1], Till Jahnke[1], Anton Kalinin[1], Markus Schöffler[1], Lothar Ph. Schmidt[1], Misha Ivanov[2], Olga Smirnova[2] & Reinhard Dörner[1]

1. Institut für Kernphysik, J. W. Goethe-Universität, Max-von-Laue-Str. 1, 60438 Frankfurt am Main, Germany
2. Max-Born-Institut, Max-Born-Straße 2A, D-12489 Berlin, Germany

As a fundamental property of the electron, the spin plays a decisive role in the electronic structure of matter from solids to molecules and atoms, e.g. causing magnetism. Hence studying effects regarding the spin is highly interesting. Even 90 years after the famous Stern-Gerlach experiment was carried out new questions concerning the spin arise consistently. In 2013 I. Barth and O. Smirnova predicted theoretically that electrons, which were created by ionization of noble gas atoms by an intense infrared laser, are spin polarized [1]. Yet, until today no experimental investigation of the spin dynamics of electrons released during the interaction of atoms with strong ultrashort laser pulses were released.

Here we report on the experimental detection of electron spin polarization by strong-field ionization of Xenon atoms and support our results by theoretical analysis [2]. We found up to 30% spin polarization changing its sign with electron energy, see Fig 1. This work opens the new dimension of spin to strong-field physics. It paves the way to production of sub-femtosecond spin polarized electron pulses with applications ranging from probing magnetic properties of matter at ultrafast time scales to testing chiral molecular systems with sub-femtosecond temporal and sub-Ångström spatial resolution.

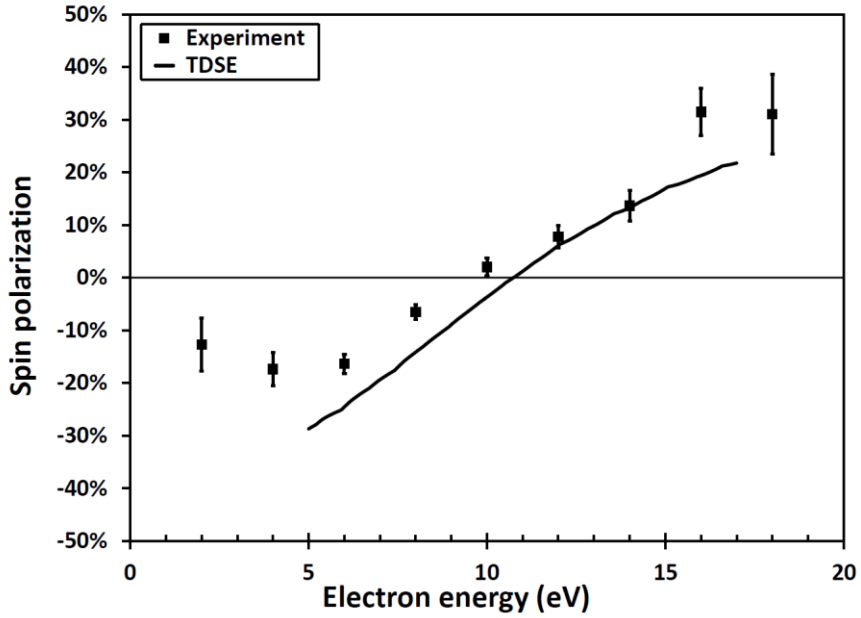

Fig. 1: spin polarization of electrons ejected by strong field ionization of Xe parallel to the light propagation direction by circularly polarized laser pulses. The spin polarization is defined as the weighted difference between spin-up and spin-down electrons. Consequential positive values correspond to a surplus of electrons with spin parallel to the propagation axis of the laser. Rectangles show experimental data for 40 fs, 780 nm pulses. Solid curve shows results of numerical simulations. Error bars show statistical errors only.

References

[1] Ingo Barth & Olga Smirnova, *Spin-polarized electrons produced by strong-field ionization*, Phys. Rev. A **88**, 013401 (2013).
[2] Alexander Hartung et al., *Electron spin polarization in strong-field ionization of Xenon atoms*, submitted to Nat. Phot. (2016).

Double-slit electron interference in strong-field ionization of neon dimer

Pia Huber[1], Maksim Kunitski[1], Jonas Köhler[1], Kevin Henrichs[1], Nikolai Schlott[1], Hendrik Sann[1], Florian Trinter[1], Till Jahnke[1], Markus Schöffler[1], Stefan Zeller[1], Lothar Schmidt[1] and Reinhard Dörner[1]

[1]*Institut für Kernphysik, Goethe University Frankfurt,*
Max-von-Laue-Str. 1, D-60438 Frankfurt am Main, Germany
E-mail: huber@atom.uni-frankfurt.de

Abstracts: *Two types of double-slit interference have been experimentally identified in the molecular frame angular distribution of photo-electrons upon strong-field ionization of neon dimer.*

Wave-like behavior of particles, e.g. interference, is "the mystery", as stated by Feynman, ''which is impossible, *absolutely* impossible, to explain in any classical way, and which has in it the heart of quantum mechanics''. The double-slit experiment has been widely utilized in order to learn different aspects of this "mystery", as, for instance, in famous Bohr-Einstein debates. In the 1960s it was realized that the double-slit experiment can be performed at the molecular level by exploiting two sites of a diatomic molecule as coherent electron emitters (*1*). Several such experiments have been reported so far (*2–6*).

Here we report the observation of photo-electron double-slit interference in single ionization of neon dimer by a strong ultra-short laser field (40 fs, 790 nm, $6.0 \cdot 10^{14}$ W/cm^2). An electron and a single Ne ion resulting from break-up of Ne_2^+ along the repulsive $II(1/2)_g$ potential were measured in coincidence by means of COLd Target Recoil Ion Momentum Spectroscopy (COLTRIMS) (*7*). The molecular axis of Ne_2 upon ionization was deduced from the momentum direction of the detected Ne ion. The interference pattern in the angular distribution has been found to be governed by the parity of the molecular orbital from which the electron is freed. The electron removed from an *ungerade* orbital shows constructive interference perpendicular to the molecular axis, whereas the one from a *gerade* orbital shows destructive interference.

References

1. H. D. Cohen, U. Fano, *Phys Rev* **150**, 30–33 (1966).
2. D. Rolles *et al.*, *Nature* **437**, 711–715 (2005).
3. X.-J. Liu *et al.*, *J. Phys. B At. Mol. Opt. Phys.* **39**, 4801 (2006).
4. D. Akoury *et al.*, *Science* **318**, 949–952 (2007).
5. Z. Ansari *et al.*, *New J. Phys.* **10**, 093027 (2008).
6. S. E. Canton *et al.*, *Proc. Natl. Acad. Sci.* **108**, 7302–7306 (2011).
7. J. Ullrich *et al.*, *Rep. Prog. Phys.* **66**, 1463 (2003).

Tunneling delay time within the Coulomb-corrected strong-field approximation

Michael Klaiber, Karen Z. Hatsagortsyan, and Christoph H. Keitel[1]

[1]*Max-Planck-Institut für Kernphysik, Saupfercheckweg 1, 69117 Heidelberg, Germany*

(Dated: March 31, 2016)

Signatures of the ionization delay time in the photoelectron final momentum distribution during the laser-induced ionization of atoms or ions in tunneling [1] and multiphoton [2] regimes are investigated analytically. A modified Coulomb corrected strong-field approximation (SFA) is applied, where the exact continuum state in the S-matrix is approximated by the eikonal Coulomb-Volkov state. We simplify the known Perelomov-Popov-Terentev (PPT) and the analytical R-matrix (ARM) theories. Instead of matching the eikonal Coulomb-Volkov wave function with the bound state one, we calculate the ionization differential probability via the saddle point integration method by time as well as by coordinate, and in this way avoiding the Coulomb singularity. The Coulomb momentum shift in the photoelectron momentum distribution and the Coulomb correction factor to the probability in addition to the standard SFA results for short-range potentials are derived. Comparison with PPT and ARM theories are carried out, differences are analyzed, and the question of the tunneling delay time is discussed.

[1] M. Klaiber, E. Yakaboylu, H. Bauke, K.Z. Hatsagortsyan, and C.H. Keitel, Phys.Rev. Lett. **110**, 063417 (2013).

[2] M. Klaiber, K.Z. Hatsagortsyan, and C.H. Keitel, Phys.Rev. Lett. **114**, 083001 (2015).

High-Order Harmonic Generation from Ultrathin Ionic Layers Supported on Metal Surfaces: NaCl/Cu(111)

Néstor F. Aguirre[1], Fernando Martín[1,2,3]

1. Departamento de Química, Módulo 13,Universidad Autónoma de Madrid, 28049, Madrid, Spain

2. Instituto Madrileo de Estudios Avanzados en Nanociencias (IMDEA-Nanociencia), 28049 Madrid, Spain

3. Condensed Matter Physics Center (IFIMAC), Universidad Autónoma de Madrid, 28049 Madrid, Spain.

It has been demonstrated that solid-state samples can be used as generators of high-order-harmonic (HHG) radiation [1]. The interest of this phenomenon resides in the fact that HHG represents one of the most reliable ways to generate coherent ultraviolet to extreme ultraviolet light, with the possibility to observe strong-field physics with modest laser-fields strengths, in contrast with atoms.

In this work we present a theoretical study of HHG from a ultrathin ionic layers of NaCl supported on a Cu(111) surface, by using a quantum-mechanical model within the single-active-electron (SAE) approximation by using a wave packet propagation scheme. We used the laterally averaged potential of the model published by Díaz-Tendero *et al.* [2]. This model includes the potential of Cu(111) published by Chulkov *et al.* [3] to represent the bulk and an electrostatic model to describe the electron interaction with the Cu(111) surface coated with adsorbate layers of NaCl. We investigate theoretically the origin behind the formation of the plateau and cutoff as a function of the laser field intensity and the number of NaCl layers.

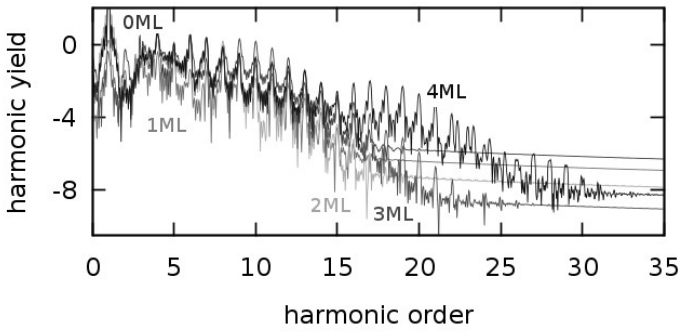

Fig. 1 Harmonic spectra for the 1D model of NaCl/Cu(111) for up to four layers of NaCl. irradiated by a 26.7 fs laser pulse (I_0 = 50 TW/cm^2, λ = 800 nm).

References

[1] Shambhu Ghimire, Anthony D. DiChiara, Emily Sistrunk, Pierre Agostini, Louis F. DiMauro and David A. Reis, *Observation of high-order harmonic generation in a bulk crystal*, Nature Phys. 7, 138 (2011)

[2] Sergio Díaz-Tendero, Andrey G. Borisov and Jean-Pierre Gauyacq, *Theoretical study of the electronic excited states in ultrathin ionic layers supported on metal surfaces: NaCl/Cu(111)*, Phys. Rev. B, **83**, 115453 (2011).

[3] Evgueni V. Chulkov, Vyacheslav M. Silkin and Pedro .M. Echenique, *Image potential states on metal surfaces: binding energies and wave functions*, Surf. Sci. **437**, 330 (1999).

Single attosecond pulse generation via nonlinear Thomson scattering

Szabolcs Hack [1], Sándor Varró[1,2], Attila Czirják[1,3]

1. ELI-ALPS, ELI-HU Non-Profit Ltd., Dugonics tér 13, H-6720 Szeged, Hungary

2. Wigner Research Center for Physics, SZFI, PO Box 49, H-1525 Budapest, Hungary

3. Department of Theoretical Physics, University of Szeged, Tisza L. krt. 84-86, H-6720 Szeged, Hungary

Nonlinear Thomson scattering [1], i.e. classical electromagnetic radiation of a relativistic electron beam driven by an intense laser pulse, is a promising method for the generation of high-order harmonics and attosecond light pulses. In our recent work [2], we already demonstrated the possibility of single attosecond pulse generation in the XUV – soft X-ray regime, see Fig. 1, assuming the head-on collision of a mono-energetic non-interacting electron bunch [3] with a high-intensity near-infrared laser pulse, based on a new analytical formula for the relativistic electron's motion in the field of a 3-cycle laser pulse with sine-squared envelope. We also emphasised the importance of the correct treatment of the initial values [4], especially in the case of several electrons.

In the present contribution, we report about our new results regarding the feasibility of single attosecond pulses. We investigate how do the characteristics of nonlinear Thomson scattering depend on the laser parameters, using a new analytical solution of the Newton-Lorentz equations, assuming a few-cycle laser pulse with sine-squared envelope, arbitrary number of cycles and carrier envelope phase difference. Regarding the more realistic modelling of the electron bunch, we consider finite energy spread and we account also for the electron-electron interaction by a mean field method [5]. Our calculations of the angular dependence of the emitted spectrum, shown in Fig. 2, suggest that single attosecond XUV – soft X-ray pulse generation via nonlinear Thomson scattering is possible in a narrow beam around the direction of the initial velocity of the electron bunch.

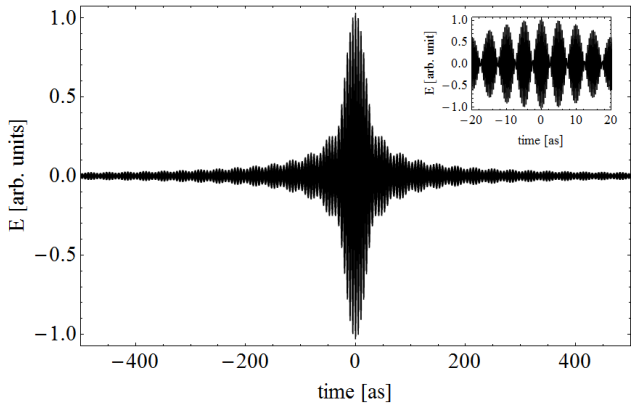

Fig. 1. Electric field vs. time of the single attosecond pulse (along the direction of the initial velocity of the electron) that can composed by suitable spectral filtering of the radiation of a relativistic electron bunch in head-on collision with a high-intensity near-infrared laser pulse.

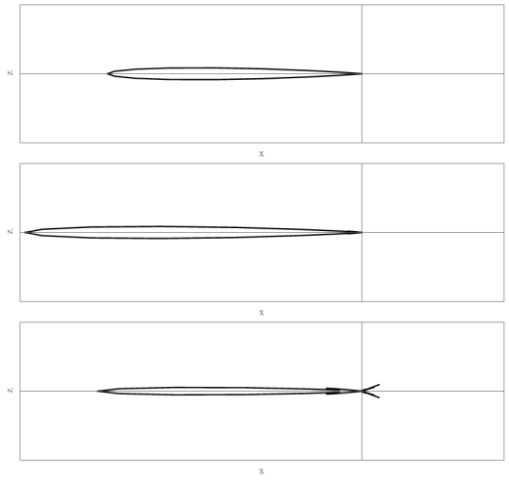

Fig. 2. Polar diagrams of the angular distribution of the spectral intensity at the following harmonic orders: 260th harmonic (top), 286th harmonic (middle), 320th harmonic (bottom). Radiation in this spectral range creates the attosecond pulse of Fig. 1.

S. V. has been supported by the National Scientific Research Foundation OTKA, Grant No. K 104260. Partial support by the ELI-ALPS project is also acknowledged. The ELI-ALPS project (GOP-1.1.1-12/B-2012-000, GINOP-2.3.6-15-2015-00001) is supported by the European Union and co-financed by the European Regional Development Fund.

References

[1] M. V. Fedorov: *Atomic and Free Electrons in a Strong Laser Field* (World Scientific, Singapore, 1997)

[2] Sz. Hack, S. Varró, and A. Czirják, *Interaction of relativistic electrons with an intense laser pulse: HHG based on Thomson scattering*, NIM Phys. B: Beam interaction with Materials and Atoms. **369**, 45-49 (2016).

[3] N. Naumova, et al., *Attosecond electron bunches*, Phys. Rev. Lett. **93**, 195003 (2004).

[4] S. Varró and F. Ehlotzky, *Thomson scattering in strong external fields*, Zeitschrift für Physik D, Atoms, Molecules and Clusters. **22**, 619-628 (1992).

[5] E. Esarey, S.K. Ride, P. Sprangle, *Nonlinear Thomson scattering of intense laser pulses from beams and plasmas*, Phys. Rev. E **48** 3003 (1993).

Angular asymmetry of Wigner time delay in the CO molecule

Serguei Patchkovskii[1] **and Anatoli Kheifets**[2]
1. Max-Born-Institute, Max-Born Strasse 2A, D-12489 Berlin, Germany
2. Department of Theoretical Physics, Australian National University, Canberra ACT 2601, Australia

Photoelectron group delay, also known as Wigner time delay [1], refers to the delay, or advance, of the photoelectron wave packet receding in the field of the ionized target relative to its propagation in free space. The Wigner time delay is a prominent marker of the attosecond molecular dynamics and its accurate determination is an important goal of attosecond science.

A very crude one-dimensional model predicted a noticeable asymmetry of the time delay in heteronuclear molecules [2]. This asymmetry has indeed been observed experimentally in the CO molecule when the photoelectrons were receding in the direction of the C or O atoms [3]. For quantitative analysis of the experimental data, we model time delay using the technique of time-dependent resolution in ionic states (TD-RIS) [4,5]. We start from highly-accurate, correlated wave functions $|I_m\rangle$ for the target molecular-ion states, calculated using standard *ab initio* codes [6]. Each static, bound-state ion wave function is combined with an active-electron wave function $|\chi_m(t)\rangle$ represented on a three-dimensional spatial grid, forming an ionization channel. The total, time-dependent wave function of the system is then written as [4]

$$|\Psi(t)\rangle = a(t)|N\rangle + \sum_m b(t)|I_m\rangle|\phi_m^d\rangle + \sum_m |I_m\rangle|\chi_m(t)\rangle \,, \tag{1}$$

where $|N\rangle$ is the correlated wave function of the initial neutral state, and $|\phi_m^d\rangle \propto \langle I_m|N\rangle$ is the Dyson orbital associated with the ionization channel $N \to I_m$. Laser field-driven and electronic correlations between the channels are incorporated using the appropriate transition matrix elements.

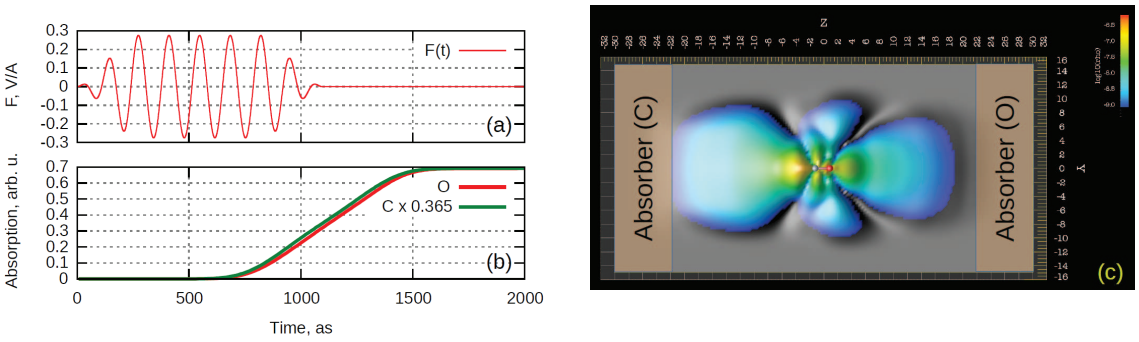

Fig. 1 Electron time-of-flight simulation for the ground-state ionization channel of CO. (a) Electric field profile for the 9-cycle flat-top XUV pulse. The pulse is polarized along the Z direction. (b) Probability of an electron reaching the absorber as a function of time, in arbitrary units. Green (upper) curve: probability of reaching the absorber at negative Z (carbon end). Red (lower) curve: probability of reaching the absorber at positive Z (oxygen end). The carbon curve has been scaled by a factor $\times 0.365$. (c) Probability density of the active electron ($|\chi_1(t)|^2$) at time $t = 650$ as. The probability density (in Bohr^{-3}) is measured in the YZ plane, 0.18 Bohr below the plane containing the nuclei. Note that the wave function on the negative-Z (carbon) end of the molecule is already being absorbed. The wave function on the positive-Z (oxygen) end still have not reached the absorber.

Our methodology is illustrated in Fig. 1. A more detailed analysis of our data will be presented at the conference.

References

[1] Eugene P. Wigner, *Lower limit for the energy derivative of the scattering phase shift*, Phys. Rev. **98**, 145 (1955).
[2] A. Chacon, M. Lein, and C. Ruiz, *Asymmetry of Wigner's time delay in a small molecule*, Phys. Rev. A **89**, 053427 (2014).
[3] J. Vos, L. Cattaneo, S. Heuser, M. Lucchini, C. Cirelli, and U. Keller, *Asymmetric Wigner time delay in CO photoionization*, ECAMP 12 (2016).
[4] M. Spanner and S. Patchkovskii, *One-electron ionization of multielectron systems in strong nonresonant laser fields*, Phys. Rev. A **80**, 063411 (2009).
[5] M. Spanner and S. Patchkovskii, *Molecular strong field ionization and HHG*, Chem. Phys. **414**, 10 (2013).
[6] M. W. Schmidt *et al*, *General atomic and molecular electronic structure system*, J. Comp. Chem. **14**, 1347 (1993).

XUV-initiated high-harmonic generation in Ne and Ar

Andrew C. Brown
Centre for Theoretical Atomic, Molecular and Optical Physics, Queen's University Belfast, BT7 1NN

High harmonic generation (HHG) is now a well established tool both for the generation of attosecond laser pulses [1], and as a measurement technique for atomic and molecular structure and ultrafast electron dynamics [2-4]. The well-known 'three-step' or 'simple-man's' model captures well the gross dynamics of process: an electron is 1) ionised and then 2) driven by a strong laser field before 3) recolliding with its parent ion, and releasing its energy in the form of a high-harmonic photon [5].

For some time now, researchers have been concerned with both the *optimization* of the process, and its *application* to measurement in so called high-harmonic spectroscopy. Both of these considerations have led to the same conclusion: the initial step of the three-step model (tunnel ionization) limits both the conversion efficiency and the ability of HHG to probe general electron dynamics, restricted as it is to the emission of the outermost valence electron. Hence, it has been proposed that by subjecting the target to both the strong driving field and a short XUV pulse, the HHG process can be initiated by photoionization rather than tunnel-ionization. This has the advantage of being significantly more efficient, and also opening the possibility of driving more deeply bound electrons [6-8]. Several theoretical studies have explored the first aspect by utilising simple model calculations to describe the three-step process.

However, there are only a handful of computational methods capable of describing the multielectron dynamics necessary for an exploration of the second aspect- HHG with inner-valence and core electrons. Among them, the R-matrix with time-dependence (RMT) technique holds significant promise for the description of ultrafast processes in general multielectron systems [9,10]. Here we present results from a recent study with RMT into XUV-initiated HHG in argon and neon– two common targets for HHG studies– and discuss both the optimization problem and the possibility of driving inner-valence electron dynamics.

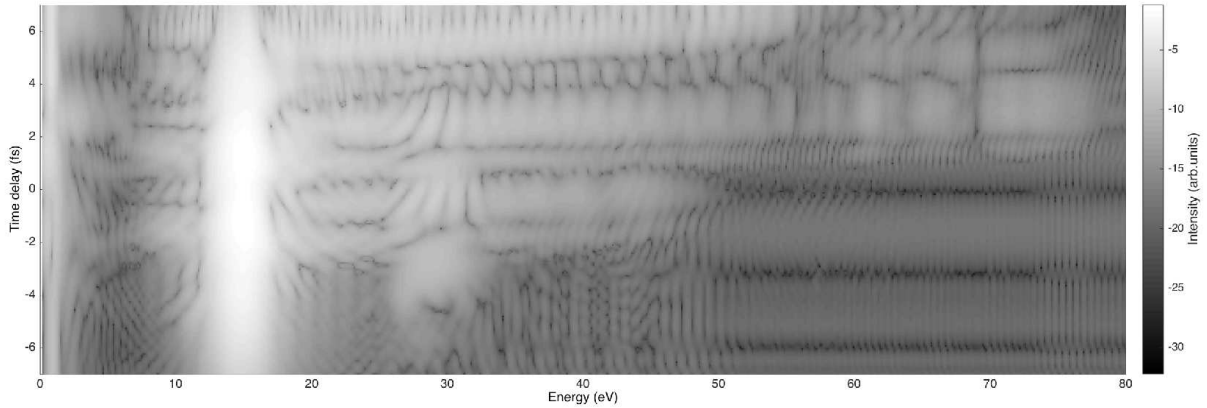

Fig. 1 The harmonic yield from argon subjected to a 4-cycle, 1.8 μm, 6×10^{13} Wcm^{-2} laser pulse with a time-delayed 2fs, 14eV pulse initiating the high-harmonic generation process. A significant yield enhancement is observed when the XUV pulse aligns with the optimal emission time for HHG ($\approx$ 2fs before the peak of the IR driving pulse).

References

[1] K. Zhao *et al.*, "*Tailoring a 67 attosecond pulse through advantageous phase-mismatch*," Opt. Lett., **37**, 3891, (2012).
[2] P. B. Corkum, "*Recollision physics*," Phys. Today, **64**, 36, (2011).
[3] O. Smirnova *et al.*, "*High harmonic interferometry of multi-electron dynamics in molecules*," Nature, **460**, 972, (2009).
[4] A. D. Shiner *et al.* "*Probing collective multi-electron dynamics in xenon with high-harmonic spectroscopy*," *Nat. Phys.*, **7**, 464, (2011).
[5] P. B. Corkum, "*Plasma perspective on strong field multiphoton ionization*," Phys. Rev. Lett., **71**, 1994, (1993).
[6] J. Biegert *et al.* , "*Control of high-order harmonic emission using attosecond pulse trains*," J. Mod. Optics., **53**,
[7] G. Gademann *et al.*, "*Attosecond control of electron–ion recollision in high harmonic generation*," New J. Phys., **13**, 033002, (2011).
[8] J. Leeuwenburgh, B. Cooper, V. Averbukh, J. P. Marangos, and M. Ivanov, "*High-order harmonic generation spectroscopy of correlation-driven electron hole dynamics*," Phys. Rev. Lett., **111**, 123002, (2013).
[9] L. R. Moore *et al.*, "*The RMT method for many-electron atomic systems in intense short-pulse laser light*," J. Mod. Optics, **58**, 1132, (2011).
[10] T. Ding, *et al.*, "*Time-resolved four-wave-mixing spectroscopy for inner-valence transitions*," Opt. Lett., **41**, 709, (2016).

Resonant photoionization of atoms and molecules using quantum chemistry packages: the XCHEM approach.

Carlos Marante[1], Jesús González-Vázquez[1], Inés Corral[1], Markus Klinker[1], Luca Argenti[1], Fernando Martín[1,2,3]

1. Departamento de Química, Universidad Autónoma de Madrid, Cantoblanco 28049, Madrid, Spain
2. Instituto Madrileño de Estudios Avanzados en Nanociencia (IMDEA-Nanociencia), Cantoblanco 28049, Madrid, Spain
3. Condensed Matter Physics Center (IFIMAC), Universidad Autónoma de Madrid, Cantoblanco 28049, Madrid, Spain

Current quantum chemistry packages (QCP), such as MOLCAS [1], implement sophisticated methods to describe electronic correlation in bound states of atoms and molecules. Recent advances in the generation of extreme ultraviolet (XUV) and x-ray attosecond pulses have now made it possible to follow correlated electron dynamics in real time [2, 3]. Such pulses, however, can also liberate one electron from the atoms and molecules with which they interact, a process whose theoretical interpretation goes beyond the capabilities of QCPs, as it requires to represent the ionization continuum of the target in a wide energy range. So far, this representation has only been achieved with *ad hoc* codes for selected small systems, such as He and H_2 [4-7]. For more complex systems, however this approach is impractical, and it disregards the advanced methods already available for bound-state calculations.

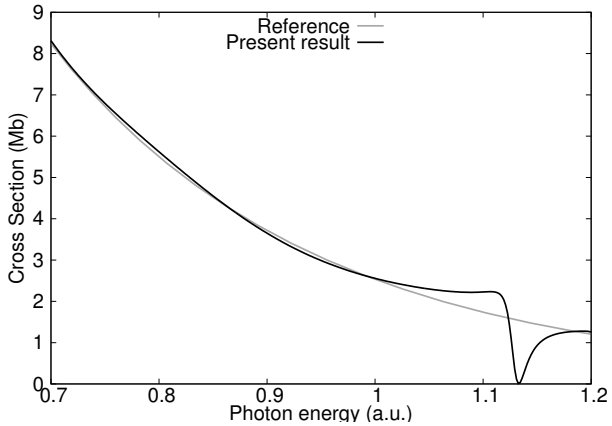

Fig. 1 Photoionization cross section from the ground state of the H_2 molecule, oriented along the field polarisation, computed with the xchem approach, compared with the reference theoretical prediction for the non-resonant background, obtained from the H_2 codes described in [10].

To overcome the limitations of QCP and of *ad hoc* codes for molecular ionization, we follow a novel approach based on the merge between existing QCPs and state-of-the-art numerical scattering methods. As customary in close-coupling methods, the electronic configuration space is divided in a short-range and a long-range region. The wave function in the short-range region is fully described in terms of Gaussian functions, which are compatible with standard QCPs. In the long-range region, a single electron interacts with a finite number of correlated parent ions. The state of this electron is expressed in terms of a hybrid basis which combines mono centric Gaussian functions with B-splines (GABS)[8], which are appropriate to represent the continuum. Here we present the results for the resonant multichannel ionization of the He atom and of the H_2 molecule, as a first step towards more complex systems. The scattering parameters we obtain are in excellent agreement with accurate benchmarks [9-10]. These positive results, together with the great flexibility of QCPs, position our method as a strong candidate for the theoretical study of the ionization of poly-electronic systems.

References

[1] Gunnar Karlström, et al, *MOLCAS: a program package for computational chemistry*, Comput. Mater. Sci. **28**, 222 (2003).
[2] Michael Chini, Kun Zhao, and Zenghu Chang, *The generation, characterization and applications of broadband isolated attosecond pulses*, Nature Photonics **8**, 178 (2014).
[3] Tenio Popmintchev, et al, *The attosecond nonlinear optics of bright coherent X-ray generation*, Nature Photonics **4**, 822 (2010).
[4] Álvaro Jiménez-Galán, Luca Argenti, Fernando Martín, *Modulation of Attosecond Beating in Resonant Two-Photon Ionization*, Phys. Rev. Lett. **113**, 263001 (2014).
[5] Christian Ott, et al, *Reconstruction and control of a time-dependent two-electron wave packet*, Nature **516**, 374 (2014).
[6] Giuseppe Sansone, et al, *Electron localization following attosecond molecular photoionization*, Nature **465**, 763 (2010).
[7] D. Dowek, et al, *Circular Dichroism in Photoionization of H_2*, Phys. Rev. Lett. **104**, 233003 (2010).
[8] Carlos Marante, Luca Argenti, Fernando Martín, *Hybrid Gaussian–B-spline basis for the electronic continuum: Photoionization of atomic hydrogen*, Phys. Rev. A **90**, 012506 (2014).

Time development of the cusp in lateral momentum distributions for the process of strong field ionization.

I.A.Ivanov[1,3], **Chang Hee Nam**[1,2], **Kyung Taec Kim**[1,2]

1. Center for Relativistic Laser Science, Institute for Basic Science, Gwangju 500-712, Republic of Korea
2. Advanced Photonics Research Institute, GIST, Gwangju 500-712, Republic of Korea
3. Research School of Physics and Engineering, The Australian National University, Canberra ACT 0200, Australia

Tunneling theories of photo-ionization proved to be of great value for understanding atomic or molecular ionization by strong infrared (IR) laser field for which the so-called Keldysh parameter $\gamma = \omega\sqrt{2|\varepsilon_0|}/E$ is small (here ω, E and $|\varepsilon_0|$ are the frequency, field strength and ionization potential of the target system in atomic units). By tunneling theories we mean the theories following the approach proposed in the work [1]. In the picture of the tunneling ionization process offered by these theories electron emerges into the continuum as a result of the under-the-barrier tunelling. Tunneling theories provide quantum mechanical distributions (in particular momenta distributions) at the moment of the ionization event, predicting simple Gaussian-like structures for these initial distributions. If the after-ionization-event motion is guided by the laser field only (ionic core potential is neglected), the momentum distributions at the detector should retain this Gaussian character. Of particular interest, therefore, is the so-called transverse or lateral electron momentum distribution (TEMD), which describes the distribution of the electron momenta measured at the detector in the direction perpendicular to the polarization plane of the driving pulse. Contrary to the predictions of the tunneling theories, for the case of the linearly polarized laser pulse, the TEMD exhibits a sharp cusp-like peak at zero transverse momentum, which was attributed to the Coulomb focussing effect [2]. We studied this transition from the cusp-like to the Gaussian-like structure in TEMD with varying ellipticity of the laser pulse experimentally [3], and theoretically [4], using the *ab initio* solution of the time-dependent Schrödinger equation (TDSE). Using the numerical procedure described in [4], we study presently the process of the dynamical formation of the cusp in TEMD for a linearly polarized pulse. As a model we consider hydrogen atom driven by a short laser pulse (800 nm wavelength, 3.5×10^{14} W/cm^2 the peak intensity, 3 optical cycles total duration). Velocity distributions are computed by Fourier transforming the TDSE wave-function at different moments of time during and after the end of the laser pulse (a care was taken to remove the contribution form the bound states population). Results are shown in Fig.1.

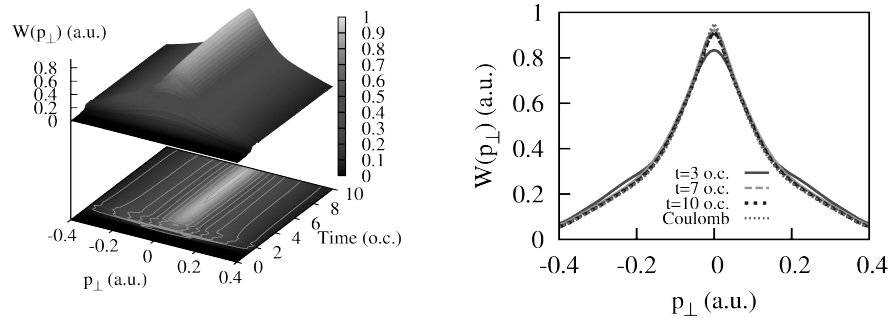

Fig. 1 Left panel: evolution of TEMD in time. Right panel: Lateral velocity distributions computed at various moments of time after the end of the laser pulse. "Coulomb" stands for the projection on the Coulomb continuum spectrum wave-functions.

As one can see, the TEMD distribution gradually evolves with time from the Gaussian structure predicted by the tunelling theories to a cusp-like behavior at zero transverse momenta. At the large time limit the velocity distribution coincide with the results obtained by projecting TDSE solution on the set of the Coulomb ingoing scattering states (which corresponds mathematically to taking the infinite time limit).

References

[1] L.V. Keldysh, *Ionization in the Field of a Strong Electromagnetic Wave*, Sov. Phys. -JETP **20**, 1307 (1965).
[2] A. Rudenko, K. Zrost, Th. Ergler, A.B.Voitkiv, B. Najjari, V.L.B. de Jesus, B. Feuerstein, C.D. Schröter, R. Moshammer, and and J. Ullrich, *Coulomb singularity in the transverse momentum distribution for strong-field single ionization*, J. Phys. B **38**, L191 (2005).
[3] I. A. Ivanov, A.S. Kheifets, J.E. Calvert, S. Goodall, X. Wang, Han Xu, A. J. Palmer, D. Kielpinski, I. V. Litvinyuk, and R. T. Sang *Transverse electron momentum distribution in tunneling and over the barrier ionization by laser pulses with varying ellipticity*, Scientific Reports **6**, 19002 (2016).
[4] I.A.Ivanov, *Evolution of the transverse photoelectron-momentum distribution for atomic ionization driven by a laser pulse with varying ellipticity*, Phys. Rev. A **90**, 013418 (2014).

Attosecond Multi-Dimensional Spectroscopy

Michael Krüger[1], Doron Azoury[1], Gal Orenstein[1], Henrik R. Larsson[2], Sebastian Bauch[2], Barry D. Bruner[1], Nirit Dudovich[1]

1. Department of Physics of Complex Systems, Weizmann Institute of Science, 76100 Rehovot, Israel

2. Christian-Albrechts-Universität zu Kiel, D-24098 Kiel, Germany

Attosecond science has revolutionized our ability to resolve electron dynamics on its natural time scale. Two main approaches for time-resolved pump-probe measurements have been pursued very successfully, attosecond pump-probe spectroscopy [1] and attosecond self-imaging [2]. The first approach combines a strong IR laser pulse and an attosecond pulse into a pump-probe pair, whereas the second approach uses high harmonic generation (HHG) itself as a natural pump-probe scheme. Although self-imaging offers excellent temporal and spatial resolution, the interpretation of these experiments is challenging; the observable, the HHG spectrum, contains information on all steps of the strong-field light matter interaction that need to be disentangled.

In this work, we demonstrate XUV-initiated high harmonic generation (XiHHG, [3-5]), combining the two approaches. Here, photoionization by attosecond XUV pulses replaces tunnelling ionization as the first step in HHG (see Fig. 1(a)). The liberated electron is driven back to the parent ion by a strong IR laser field, leading to re-emission of attosecond radiation bursts. XiHHG allows for independent measurement and control of photoionization and the dynamics of the liberated electron, hence naturally disentangling the two main steps of the strong-field light matter interaction inherent to attosecond self-imaging. In our experiment, we observe XiHHG from helium and neon atoms by combining an attosecond XUV pulse train and an IR pulse and show that the XUV-IR delay controls the timing of ionization.

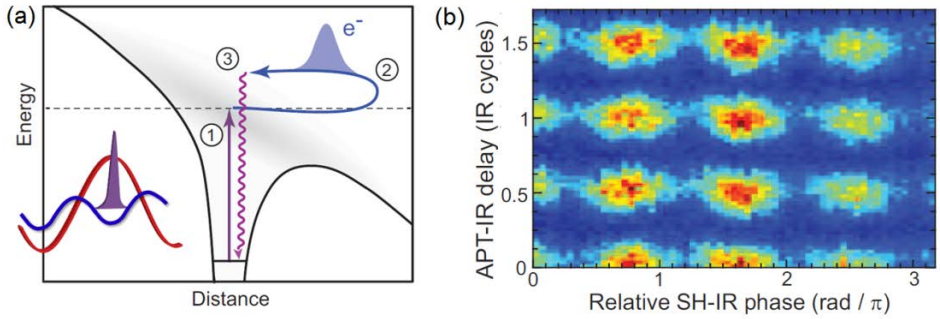

Fig. 1 (a) Illustration of XiHHG. Step 1: Photoionization by an XUV attosecond pulse (purple) instead of tunnelling ionization. Step 2: Propagation of the liberated electron wavepacket (blue) driven by a strong IR field (red). Step 3: Recombination and emission of an XUV photon. The dimensionality of the experiment can be increased further by adding a weak second harmonic field (blue). (b) Two-dimensional measurement of XiHHG. The intensity of harmonic 18 is shown as a function of XUV-IR delay (vertical axis) and second harmonic-IR delay (horizontal axis). We observe oscillations of the signal in both dimensions with the half the periodicity of the IR field.

We increase the dimensionality of the experiment by adding a weak second harmonic field and scan its phase relative to the IR, implementing two-dimensional spectroscopy (see Fig. 1(b)). We retrieve even-numbered harmonics that oscillate completely out of phase with the odd-numbered harmonics [6]. These observations unambiguously reveal the involvement of electron trajectories and the insignificance of tunnelling in the process, showing that ionization and propagation are decoupled and can be controlled independently. Furthermore, we are able to reconstruct the wavepacket of the liberated electron in amplitude and phase from our measurements. A strong-field model and *ab-initio* calculations corroborate our findings.

XiHHG holds the potential for investigations of much more complex phenomena within the self-imaging approach. For example, unlike tunnelling ionization, XUV-driven photoionization enables access to inner-shell electrons [5]. We expect that XiHHG can both launch and clock electronic processes ranging from Auger decay to charge migration in complex molecules, allowing new and exciting experiments in ultrafast spectroscopy.

References

[1] R. Kienberger, et al., *Attosecond Transient Recorder*, Nature **427**, 817 (2004).
[2] K. T. Kim, D. M. Villeneuve, and P. B. Corkum, *Manipulating Quantum Paths for Novel Attosecond Measurement Methods*, Nature Photonics **8**, 187 (2014).
[3] Kenneth Schafer, et al., *Strong Field Quantum Path Control Using Attosecond Pulse Trains*, Phys. Rev. Lett. **92**, 023003 (2004).
[4] Georg Gademann, et al., *Attosecond Control of Electron-Ion Recollision in High Harmonic Generation*, New J. Phys. **13**, 033002 (2011).
[5] Jonathan Leeuwenburgh, et al., *High-Order Harmonic Generation Spectroscopy of Correlation-Driven Electron Hole Dynamics*, Phys. Rev. Lett. **111**, 123002 (2013).
[6] Oren Pedatzur, et al., *Attosecond Tunnelling Interferometry*, Nature Physics **11**, 815 (2015).

Spatial and temporal interference effects in the ionization of atoms by few-cycle laser pulses

Sándor Borbély[1], Attila Tóth[2], Károly Tőkési[3,4] and Ladislau Nagy[1]
1. Faculty of Physics, Babeş-Bolyai University, 400084 Cluj-Napoca, Romania, EU
2. Department of Theoretical Physics, University of Debrecen, H-4010 Debrecen, PO Box 5, Hungary, EU
3. Institute for Nuclear Research, Hungarian Academy of Sciences (ATOMKI), H-4026 Debrecen, P.O. Box 51, Hungary, EU
4. ELI-ALPS, ELI-HU Non-profit Ltd., Dugonics tér 13, H-6720 Szeged, Hungary, EU

As a result of the recent development of the laser technology, the generation of ultrashort laser pulses containing only a few optical cycles [1] became a routine task. When an atomic system interacts with such a laser pulse the dominant process is ionization, which is well documented and understood [2]. However, beside the dominant ionization secondary processes are also present, which leave their imprint on the ionization spectrum. One of the results of these secondary processes are the intra-pulse interference effects [3], which have the most pronounced impact on the ionization spectrum. As discussed in [3] these effects are the result of interference between electronic wave packets following different spatio-temporal paths. From the numerous possible scenarios [3], in most of the cases only two have a significant impact on the final momentum distribution of the continuum electrons.

In the first scenario, electronic wave packets emitted at different parts of the laser pulse (i.e., at different time moments) interfere, leading to a fringe structure in the electron energy spectrum, consisting of circular interference maxima and minima, which are perpendicular to the laser polarization [4]. This process can be interpreted as a double-(multi-) slit interference in time domain (temporal interference), and it was studied in detail by several groups both theoretically [5] and experimentally [4]. In the second scenario, electronic wave packets emitted at the same time (during the same quarter-pulse cycle) follow different paths accumulating different final phases, leading to a radial fringe structure in the electron spectra [6-7]. In a simplistic picture [6], the radial fringe structure is a result of the interference between the direct (i.e., unscattered) and the scattered wave packets, where the direct wave packet can be considered as a reference while the scattered wave packet as a signal wave. In this picture, the interference fringe structure can be interpreted as the holographic mapping (HM) of the target atom's or molecule's state. Before the application of the HM as a structure analysis tool we need to face the following challenges: first we need to understand in details all aspects of the HM process, and then we need to devise an efficient method for the extraction of the structural information encoded in the HM interference pattern. Due to the recent experimental and theoretical [7] works the physics behind the formation of the HM interference pattern is fairly understood.

The quantitative analysis of the HM patterns measured in experiments [6] or obtained as a result of *ab initio* calculations [7] is difficult due to the temporal interference (the HM patterns resulting from the scattering of electronic wave packets created during the different half-cycles are coherently added). Thus, before a rigouros analysis the spatial and temporal interference patterns should be separated. In order to achieve this we have implemented the following wave function analysis method in our *ab initio* [7] approach. We have started the numerical solution of the time-dependent Schrödinger equation at the begining of the external laser pulse and we have propagated our system in time until the first zero-point of the electric component was reached. At this time moment the time-dependent wave function was split into two parts containing the bound and continuum part of the wave function (we can do this separation since the eigenstates of the field-free Hamiltonian are known). After the separation the partial wave functions were propagated until the next zero-point was reached. Here from the bound part the newly ionized part was split and a new partial continuum wave function was created. We repeated this procedure until the end of the laser pulse was reached, where all electronic continuum wave packets created during each half-cycle of the laser pulse were stored in separate partial wave functions. By calculating the ionization spectrum separately for each partial wave function we have obtained the pure HM pattern created by each half-cycle of the driving laser field. The final electron spectrum is obtained by adding coherently the partial ionization amplitudes. During this coherent summing the temporal interference effects will emerge.

References

[1] A. Baltuška et. al, *Attosecond control of electronic processes by intense light fields* Nature **421** 611 (2003).
[2] C. J. Joachain et. al, *Atoms in Intense laser fields*, Cambridge University Press (2012).
[3] X.-B. Bian et. al, *Subcycle interference dynamics of time-resolved photoelectron holography with midinfrared laser pulses* Phys. Rev. A **84** 043420 (2011).
[4] F. Lindner et. al, *Attosecond Double-Slit Experiment* Phys. Rev. Lett. **95** 040401 (2005).
[5] D. G. Arbó et. al, *Time double-slit interferences in strong-field tunneling ionization* Phys. Rev. A **74** 063407 (2006).
[6] Y. Huismans et. al, *Time-Resolved Holography with Photoelectrons* Science **331** 61 (2011).
[7] S. Borbély et. al, *Spatial and temporal interference during the ionization of H by few-cycle XUV laser pulses* Phys. Rev. A **87** 013405 (2013); S. Borbély et. al, *Laser-induced electron diffraction in a pump-probe setup using half-cycle electric pulses* Phys. Scr. **T156** 014066 (2013); S. Borbély et. al, *Ionization of atoms by few-cycle EUV laser pulses: carrier-envelope phase dependence of the intra-pulse interference effects* Eur. Phys. J. D **68** 339 (2014).

Strong field assisted XUV lasing in atoms and molecules

Timm Bredtmann[1], **Szczepan Chelkowski**[2], **André D. Bandrauk**[2], **Serguei Patchkovskii**[1], **Misha Ivanov**[1,3]
1. Max-Born-Institut, Max-Born-Strasse 2A, D-12489 Berlin, Germany
2. Laboratoire de Chimie Théorique, Faculté des Sciences, Université de Sherbrooke, Sherbrooke, Québec, Canada
3. Department of Physics, Imperial College London, South Kensington Campus, SW7 2AZ, London, UK

Using ab-initio simulations, we demonstrate amplification of XUV radiation during transient absorption in a high-harmonic generation type process in atoms and molecules. The strong IR driving field rapidly depletes the initial ground state while populating excited electronic states through frustrated tunnelling [1,2], hence creating a population inversion. Concomitant XUV lasing is demonstrated by explicit inclusion of the XUV seed in our simulations, allowing a thorough analysis in terms of this transient absorption setup. Possibilities for increasing this gain, e.g. through preexcitation of excited states or through control of nuclear quantum dynamics [3], are discussed. Our findings should lead to a reinterpretation of recent experiments [4,5].

References

[1] T. Nubbemeyer, K. Gorling, A. Saenz, U. Eichmann, and W. Sandner, *Strong-Field Tunneling without Ionization*, Phys. Rev. Lett. **101**, 233001 (2008).
[2] U. Eichmann, A. Saenz, S. Eilzer, T. Nubbemeyer, and W. Sandner, *Observing Rydberg Atoms to Survive Intense Laser Fields*, Phys. Rev. Lett. **110**, 203002 (2013).
[3] T. Bredtmann, S. Chelkowski, A. D. Bandrauk, M. Ivanov, *XUV lasing during strong-field assisted transient absorption in molecules*, Phys. Rev. A, **93**, 021402(R), (2016).
[4] J. Seres, E. Seres, D. Hochhaus, B. Ecker, D. Zimmer, V. Bagnoud, T. Kuehl, C. Spielmann, *Laser-driven amplification of soft X-rays by parametric stimulated emission in neutral gases*, Nature Phys., **6**, 455 (2010).
[5] J. Seres, E. Seres, B. Landgraf, B. Ecker, B. Aurand, A. Hoffmann, G. Winkler, S. Namba, T. Kuehl, C. Spielmann, *Parametric amplification of attosecond pulse trains at 11 nm*, Scientific Reports, **4**, 4254 (2014).

Quenching Effect In Below-threshold High Harmonic Generation

Xiaosong Zhu[1], Xi Liu[1], Pengfei Lan[1], Qingbin Zhang[1], Yueming Zhou[1], Min Li[1], and Peixiang Lu[1,2]

1. School of Physics and Wuhan National Laboratory for Optoelectronics, Huazhong University of Science and Technology, Wuhan 430074, China

2. Laboratory of Optical Information Technology, Wuhan Institute of Technology, Wuhan 430205, China

Recently, increasing attentions are paid to the below-threshold high harmonic generation HHG, due to the potential application of generating extreme ultraviolet frequency combs for the precision spectroscopy and metrology. However, compared with the HHG above threshold, the process of below-threshold HHG is much more complex. The mechanism of below-threshold HHG has been much less explored and many questions still remain unclear. Moreover, in most studies on HHG, single active electron (SAE) approximation is routinely adopted. The effect of dynamical electron-electron interactions on HHG has seldom been investigated, except for only a few works. It was shown that the collective multi-electron dynamics lead to a characteristic giant resonant enhancement of HHG near the cutoff region in the high harmonic spectrum of Xe [1-4].

In our work, we theoretically demonstrate the quenching effect in below-threshold HHG from At, Kr, and Xe by using the TDDFT. It is found that, the HHG at particular harmonic orders is substantially suppressed when multi-electron interaction comes into play. The intensities of the quenched harmonics are 2-3 orders of magnitude lower than those in the plateau regions. [5] It is also shown that the positions where the quenching occurs are determined by the energy gaps between the highest occupied *n*p orbitals and the higher *(n+1)* s orbitals. The results are explained by a new class of dynamics involving the *e-e* energy transfer as illustrated in Fig. 1.

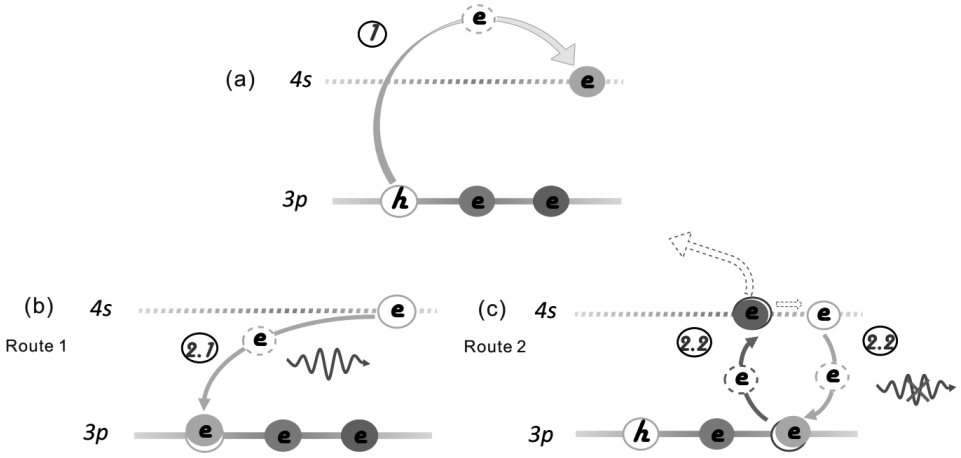

Fig. 1 Schematic illustration of the quenching effect in HHG taking the target Ar as an example.

We take Ar for example. The considered electron is ionized and accelerated by the laser field, and finally recombines with the energy equal to E_{4s}. This electron may recombine to the 3p orbital and release the accumulated energy in two ways. (b) In Route 1, it may release the energy in the form of a harmonic photon with energy ΔE. (c) In route 2, it may transfer the energy to another electron in the 3p orbital. The second electron may recombine to the 3p orbital again or be further excited/ionized. The overall effect of the dynamics in Route 2 is the loss of recombining electrons with energy E_{4s} and the decrease of emitted harmonic photons with energy of ΔE. The study will help people gain a deeper insight into the HHG process.

References

[1] A. D. Shiner, B. E. Schmidt, C. Trallero-Herrero et al., *Probing Collective Multi-electron Dynamics in xenon with High-harmonic Spectroscopy*, Nat. Phys. 7**,** 464 (2011).

[3] S. Pabst, and R. Santra, *Strong-Field Many-Body Physics and the Giant Enhancement in the High-Harmonic Spectrum of Xenon*, Phys. Rev. Lett. **111,** 233005 (2013).

[4] D. Facciala, S. Pabst, B. D. Bruner et al., *Probe of Multi-electron Dynamics in Xenon by Caustics in High Order Harmonic Generation*, arXiv:1603.01755v1

[5] X. Zhu, X. Liu, P Lan et al., arXiv:1512.04213

Exploring Dynamics in Chiral Systems with Free-Electron Lasers

Markus Ilchen[1,3,8], Sadia Bari[2], Ryan Coffee[3], Philipp Demekhin[4], Andreas Galler[1], Gregor Hartmann[5], Nick Hartmann[3], Zhirong Huang[3], Nikolay Kabachnik[6,1], Andrey Kazanski[7], André Knie[4], Zheng Li[2,8], Alberto Lutman[3], Timothy Maxwell[3], James MacArthur[3], Tommaso Mazza[1], Stefan Moeller[3], Heinz-Dieter Nuhn[3], Hirohito Ogasawara[3], Hendrik Ohldag[3], Timur Ospipov[3], Jones Rafipoor[1], Dipanwita Ray[3], Patrick Rupprecht[3,8,9], Philipp Schmidt[4], Jens Viefhaus[5], Peter Walter[5,3], Thomas Wolf[8], and Michael Meyer[1]

1. *European XFEL GmbH, Albert-Einstein-Ring 19, 22761 Hamburg, Germany*
2. *Center for Free-Electron Laser Science - CFEL, Notkestraße 85, 22607 Hamburg, Germany*
3. *SLAC National Accelerator Laboratory, 2575 Sand Hill Road, 94025 Menlo Park, USA*
4. *Institut für Physik, Universität Kassel, Heinrich-Plett-Str. 40, 34132 Kassel, Germany*
5. *Deutsches Elektronen-Synchrotron, Notkestraße 85, 22607 Hamburg, Germany*
6. *Departamento de Fisica de Materiales, UPV/EHU, Donostia International Physics Center, E-20018 San Sebastian/Donostia, Spain*
7. *IKERBASQUE, Basque Foundation for Science, E-48011 Bilbao, Spain*
8. *PULSE at Stanford, 2575 Sand Hill Road, 94025 Menlo Park, USA*
9. *Physik-Department, Technische Universität München, James-Franck-Strasse 1, D-85748 Garching, Germany*

The handedness, i.e. chirality, of life's molecular building blocks as well as of electronic spin is of large interest for practically all natural sciences. Spin control with applications in magnetism [1] as well as in fundamental atomic physics [2] and the stereochemistry of homo-chirality of life on earth with major implications for pharmaceuticals [3] are examples of state-of-the-art multidisciplinary science.

A very common technique to study chiral properties is to measure the absorption differences of opposing helicities of circularly polarized light, the so called circular dichroism. Only recently, free-electron lasers such as FERMI in Italy and LCLS in the USA have shown to provide very high degrees of circular polarization directly from the undulator light source while preserving the characteristic properties of ultrafast and ultraintense X-ray pulses [4,5]. This new capability unprecedentedly opens the door for studying chiral and magnetic properties via observation of "handed" dynamics of highly bound electrons on a femtosecond time scale.

We present preliminary as well as final results of synchrotron (SSRL, USA) and (X-ray) free-electron laser studies (FERMI, Italy and LCLS, USA) of circular dichroism in oriented and resonantly excited electronic states as well as core shell investigations of statics and dynamics in the chiral compound Trifluoro-epoxypropane ($C_3H_3F_3O$) (see Fig. 1). The results constitute a kick-off for transient as well as resonant chirality studies at (X)FELs.

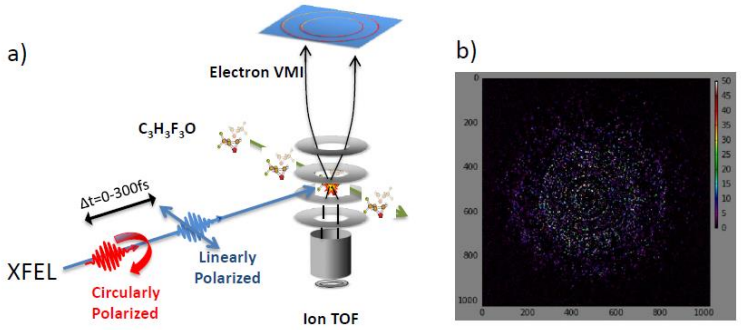

Fig. 1a) Pump-probe scheme with variable polarization provided by the new Delta undulator at LCLS. Here, the linearly polarized X-ray pulse triggers a molecular dissociation whereas the circularly polarized X-ray pulse with shifted photon energy and arrival time probes the remaining chirality of the system on a femtosecond time scale via photoelectron circular dichroism (PECD). The measurements were done with an electron velocity map imaging (VMI) and a simultaneously recorded ion time-of-flight (TOF) spectrometer. Fig 1b) depicts a raw single shot image of the electron emission of Trifluoro-epoxypropane 60 fs after the trigger pulse had arrived.

References

[1] Gunter Schütz, Wolfgang Wagner, W. Wilhelm, P. Kienle, R. Zeller, et al. *Absorption of circularly polarized x rays in iron.* Phys. Rev. Lett. **58**, 737–740 (1987).

[2] Tommaso Mazza, Markus Ilchen, Jones Rafipoor, Carlo Callegari, Paola Finetti, et al., *Determining the polarization state of an extreme ultraviolet free-electron laser beam using atomic circular dichroism*, Nat. Comms. **5**, 3648 (2014).

[3] Lien Ai Nguyen, Hua He, and Chuong Pham-Huy, *Chiral drugs: an overview.* Int J Biomed Sci **2**, 85–100 (2006).

[4] Enrico Allaria, Bruno Diviacco, Carlo Callegari, Paola Finetti, Benoît Mahieu, et al. *Control of the polarization of a vacuum-ultraviolet, high-gain, free-electron laser*, Phys. Rev. X **4**, 041040 (2014)

[5] Alberto Lutman, James MacArthur, Markus Ilchen, Anton Lindahl, Jens Buck, et al., *Polarization Control in an X-Ray Free-Electron Laser*, Nat. Phot. Accepted March 2016

Attosecond nonlinear polarization and light-matter energy transfer in solids

A. Sommer[1], E.M. Bothschafter[2], S. A. Sato[3], C. Jakubeit[1], T. Latka[4], O. Razskazovskaya[1], H. Fattahi[1], M. Jobst[4], W. Schweinberger[1], V. Shirvanyan[4],V. S. Yakovlev[5], R. Kienberger[4], K. Yabana[3], N. Karpowicz[1], M. Schultze[1,6], F. Krausz [1,6]

1.Max-Planck-Institut für Quantenoptik, Hans-Kopfermann-Str. 1, 85748 Garching, Germany
2. Paul Scherrer Institut, 5232 Villingen, Switzerland
3. Graduate School of Pure and Applied Sciences, University of Tsukuba, Tsukuba 305-8571, Japan
4. Physik-Department, Technische Universität München, James-Franck-Str. 1,85748 Garching, Germany
5. Center for Nano-Optics and Department of Physics and Astronomy, Georgia State University, Atlanta, GA 30303, USA
6. Fakultät für Physik, Ludwig-Maximilians-Universität, Am Coulombwall 1, 85748 Garching, Germany

Attosecond soft-X-ray pulses were first demonstrated a decade ago. Their routine availability facilitates time resolved spectroscopy in a wide range of atomic and molecular gas phase systems allowing to test standard assumptions of light-matter interaction [1]. More recently, solid state attosecond spectroscopy was employed to gain a time-domain understanding of the excitation of electrons across the band gap of semiconductors, the resulting band structure modifications and the nonlinear polarization response of dielectric materials [2].
The development of APS (Attosecond Polarization Spectroscopy) facilitates to observe the modifications of the electronic material properties of transparent materials under the influence of extreme visible fields with attosecond resolution. The observations provide a direct time-domain picture of the macroscopic nonlinear polarization wave and reveal the sub-100 attosecond response time of the optical Kerr nonlinearity and the energy transfer dynamics during the interaction (Fig. 1). APS presents an advancement of conventional pump-probe spectroscopy as it possesses attosecond temporal resolution independent of the temporal extent of the probe pulse. Its basic concept relies on the transmission of few cycle visible laser pulses through the sample under scrutiny at two different intensities and their subsequent temporal characterizing in an attosecond streak camera [3]. Comparison of the electric field evolution of the two transmitted pulses provides access to the nonlinear polarization wave and the excitation energy transfer as a function of time (i.e. the number of carriers excited into the conduction band). It reveals a significant transient and fully reversible conduction band population which appears to be suitable for signal manipulation at optical frequencies.

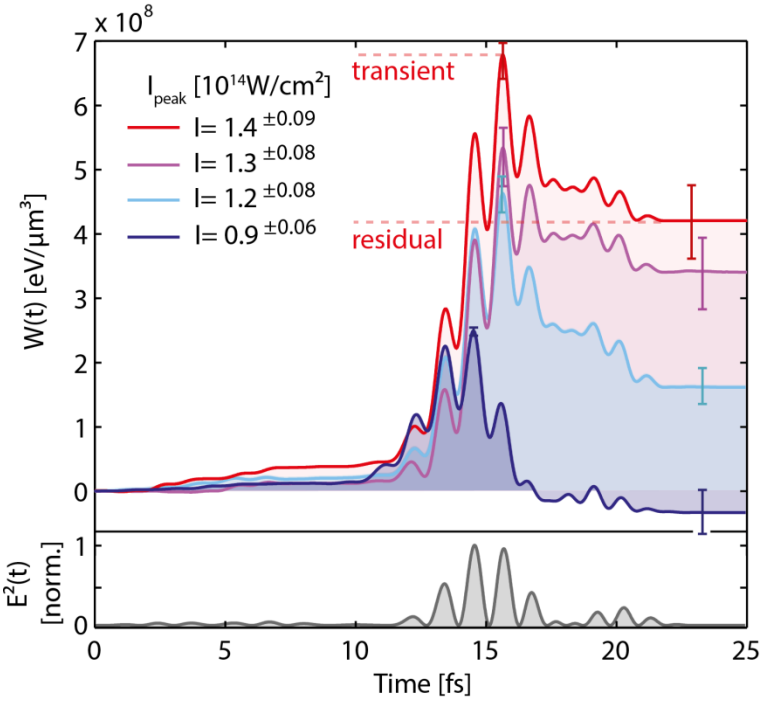

Fig. 1 Ultrafast Energy Transfer Dynamics
The amount of energy few-cycle NIR laser fields transfer into fused silica is obtained from the nonlinear polarization measured with APS. The signal shows signatures of a significant transient virtual conduction band population (transient energy transfer) oscillating in synchrony with the driving electric field. The amount of energy irreversibly deposited in the sample after the interaction (residual) depends critically on the maximum applied field intensity. While the recordings for a peak intensity of the applied electric field of I_{peak} = 1.2 to $1.4 \cdot 10^{14}$ W/cm² show significant residual absorption, the dissipated energy becomes immeasurably small for I_{peak} = $0.9 \cdot 10^{14}$ W/cm².
Lower panel: The squared electric field evolution of the reference wave

References

[1] F. Krausz, M. Ivanov, *Attosecond physics*, Rev. Mod. Phys. **81,** 163–234 (2009).
[2] M. Schultze et al., *Controlling dielectrics with the electric field of light*, Nature **493,** 75–8 (2013).
[3] J. Itatani et al., *Attosecond streak camera***,** Phys. Rev. Lett. **88**, 173903 (2002).

Coherent diffractive imaging of individual nanoparticles in free flight with intense XUV pulses from a high-order harmonic generation source

Daniela Rupp[1], Bruno Langbehn[1], Mario Sauppe[1], Nils Monserud[2], Anatoli Ulmer[1], Julian Zimmermann[1], Thomas Möller[1], Fabio Frassetto[3], Andrea Trabattoni[3], Francesca Calegari[3], Katharina Sander[4], Thomas Fennel[4], Marc Vrakking[2], and Arnaud Rouzée[2]

1. Institut für Optik und atomare Physik, Technische Universität Berlin, Germany

2. Max-Born-Institut für nichtlineare Optik und Kurzzeitspektroskopie, Berlin, Germany

3. Dipartimento di Fisica, Politecnico di Milano, Italy

4. Institut für Physik, Universität Rostock, Germany

Single-shot coherent diffractive imaging (CDI) of individual nanoparticles in free flight has become possible in the last years using high-intensity femtosecond short-wavelength pulses from extreme ultraviolet (XUV) or X-ray free electron lasers (X-FELs). Capturing the elastically scattered light from a single non-periodic specimen allows investigating its morphology and making light-induced dynamics visible, such as changes in the electronic properties after pulsed laser excitation. Up to now, X-FELs were seen as the only light sources capable of delivering sufficiently intense, short-wavelength radiation for single-shot imaging applications. Therefore, with only four operating X-FEL-facilities worldwide, this exciting field of research has so far been constrained to a few experiments only.

For the first time we performed single-shot imaging of individual gas-phase nanoparticles with a table-top light source. Single superfluid helium nanodroplets were imaged using intense XUV pulses from high-order harmonic generation (HHG) with up to 1μJ pulse energy. Most of the scattering patterns generated in this proof-of-principle experiment exhibit clear ring structures up to scattering angles of 45° revealing spherical droplet shapes with radii of several hundred nanometers. With a smaller abundance also nonspherical patterns were captured which could be clearly assigned to prolate, pill-shaped droplet shapes.

Combining HHG-CDI with the attosecond capabilities and the high degree of control over the delay between the XUV pulses and the optical driver laser(s) given at HHG sources promotes exciting future prospects such as using the phase stable multicolor pulses from HHG and even attosecond XUV flashes to create, steer, and follow ultrafast coherent plasma dynamics.

Laser-induced Ultrafast Melting of metallic samples Investigated by X-rays

A. Lévy [1], S. Cervera[1], E. Lamour[1], S. Macé[1], C. Prigent[1], J.P. Rozet[1], S. Steydli[1], M. Trassinelli[1], D. Vernhet[1]

J. Gaudin[2], B. Chimier[2], N. Fedorov[2], P. Martin[2], I. Papagiannouli[2]

R . Grisenti[3]

K. Ueda[4], Y. Ito[4]

M. Patanen[5]

P. Combis[6], V. Recoules[6], L. Soulard[6], L. Videau[6]

1. Institut des NanoSciences de Paris, Sorbonne Universités UPMC Paris 6, 75252 Paris Cedex 05, France

2. Université de Bordeaux, CEA, CNRS, CELIA, 33400 Talence, France

3. Institut für Kernphysik, J. W. Goethe Universität Max-von-Laue-Str. 1, 60438 Frankfurt (M), Germany

4. Tohoku University, Sendai 980-8577, Japan

5. University of Oulu, Department of Physics, 90014 Oulu, Finland

6. CEA, DAM, DIF, 91297 Arpajon, France

The aim of this research study is to understand phase transitions occurring in metallic materials irradiated by femtosecond laser pulses [1-4]. This specific interaction is characterized by the ultrafast energy deposition timescale related to the very short duration of these laser pulses. In these conditions, the laser pulse energy is, in the first stage, deposited in the electronic population while the lattice sub-system remains cold and unperturbed. This leads to the creation of the so-called out-of-equilibrium regime of matter owing to specific properties of matter which remain poorly described by theoretical models [5]. This prevents the prediction and control of the matter relaxation.

Improving our understanding of the underlying mechanisms during the matter relaxation is crucial since the development of powerful and reliable femtosecond lasers has attracted numerous academic and industrial interests [6]. This growing use of femtosecond lasers together with the difficulty of theoretically describe this regime of laser-matter interaction appeals for the development of experimental measurements able to retrieve the matter relaxation after irradiation.

Preliminary results of this research project together with the long-term strategy will be presented. It is based on the matter relaxation probing thanks to time-resolved photoemission electron spectroscopy (PES) measurements [7]. This has been achieved on laser-induced XUV sources (High order Harmonic Generation) for bulk samples of gold in the pump fluence range of few hundreds of J/m^2. This proof-of-principle experiment paves the way for time-resolved PES measurements on free-standing nanoparticles [8-10] which are of great interest for a large amount of technological applications. Such long-term development is dedicated to be performed on large-scale Free Electron Laser facilities.

References

[1] J. Chen et al., *Time-resolved structural dynamics of thin metal films heated with femtosecond optical pulses*, PNAS **108**, 18887 (2011).
[2] W. L. Chan et al., *Solidification Velocities in Deeply Undercooled Silver*, Phys. Rev. Lett. **102**, 095701 (2009).
[3] J. N. Clark et al., *Imaging transient melting of a nanocrystal using an X-ray laser*, PNAS **112**, 7444 (2015).
[4] N. Wang et al., *Ultrafast laser melting of Au nanoparticles: atomistic simulations*, J. Nanopart. Res. **13**, 4491 (2011).
[5] Z. Lin and L. V. Zhigilei, *Electron-phonon coupling and electron heat capacity of metals under conditions of strong electron-phonon nonequilibrium*, Phys. Rev. B **77**, 075133 (2008).
[6] S. Hashimotoa, et al., *Studies on the interaction of pulsed lasers with plasmonic gold nanoparticles toward light manipulation, heat management, and nanofabrication*, J. Photochem. Photobio. C **13**, 28 (2012).
[7] D. E. Eastman, *Photoemission Spectra for Liquid and Crystalline Au*, Phys. Rev. Lett. **26**, 1108 (1971).
[8] O. Sublemontier, et al., *X‑ray Photoelectron Spectroscopy of Isolated Nanoparticles*, J. Phys. Chem. Lett. **5**, 3399 (2014).
[9] M. Tchaplyguine, et al., *Gold Oxide Nanoparticles with Variable Gold Oxidation State*, J. Phys. Chem. C **119**, 8937 (2015).
[10] A. Lindblad, et al., *A multi purpose source chamber at the PLEIADES beamline at SOLEIL for spectroscopic studies of isolated species: Cold molecules, clusters, and nanoparticles*, Rev. Sci. Instrum. **84**, 113105 (2013).

Femtosecond Spin Dynamics in a Molecular Magnet

J. Olof Johansson[1], Ji-Wan Kim[2], Emily Allwright[1], David M. Rogers[1], Neil Robertson[1], Jean-Yves Bigot[2]

1. EaStCHEM, School of Chemistry, University of Edinburgh, David Brewster Road, EH9 3FJ, UK

2. Institut de Physique et Chimie des Matériaux de Strasbourg (IPCMS), UMR 7504, CNRS, Université de Strasbourg, BP 43, 23 rue du Loess, 67034 Strasbourg, France

There are very few experimental methods available that can explicitly measure spin dynamics with femtosecond time-resolution in molecular systems. This provides an interesting challenge for current research in molecular photophysics. Recent developments in ultrafast magnetism has enabled optical studies in solid-state systems of fundamental magnetic interactions from a new perspective such as the spin-orbit, spin-phonon and exchange interactions [1–3]. Molecular magnets are promising candidate systems for exploring these interactions in environments with reduced dimensionality, which can be chemically tuned due to the vast library of structures accessible with synthetic chemistry. We have carried out an ultrafast magneto-optical (MO) study of a molecule-based magnet. This technique is one of very few methods that can directly probe the spin state of electrons on time scales relevant for photoexcitation.

Femtosecond pump-probe spectroscopy was used to measure the MO and transient transmission dynamics of thin films of the $V^{II/III}Cr^{III}$ Prussian Blue Analogue (PBA) [4,5], which is a room-temperature molecule-based magnet. The MO signal is obtained by carefully measuring the change in polarisation state of the probe pulse (Fig. 1 (a)). We demonstrate that exciting the films at the ligand-to-metal charge-transfer band (Fig. 1 (b)) leads to a sub-ps change in the MO signal, as seen in Fig. 1 (c). This is attributed to a modification of the super-exchange interaction between the metal ions caused by a change in spin configuration on the Cr ions after the optical excitation [6].

These measurements open up new possibilities to study the spin dynamics in novel magnetic molecular materials. The results provide a stringent test of the theoretical models being developed to study spin dynamics in molecular systems. Switching the spin configuration of molecular magnets to metastable states using ultrashort laser pulses would provide an attractive route for developing future high-density data storage devices operating at high switching speeds.

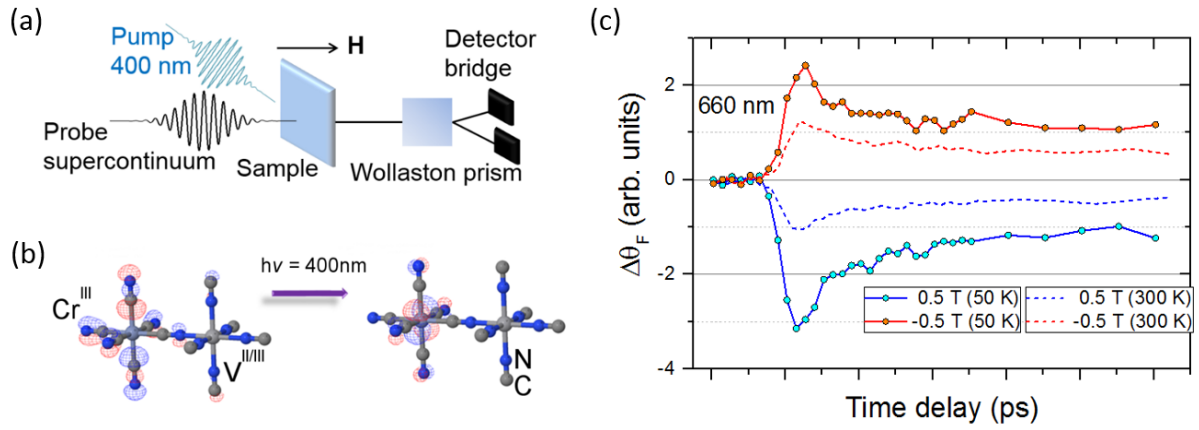

Fig. 1 (a) The films were excited with 60 fs, 400 nm laser pulses, which spectrally overlapped with the broad ligand-to-metal (LMCT) bands in the UV (b). A white-light supercontinuum spanning 480 – 690 nm, and generated by the fs pulses, was used to monitor the changes in transmission and MO signal (Faraday rotation and ellipticity) as a function of time delay between the pump and probe. Measurements were carried out at 50 and 300 K and in ± 0.5 T external magnetic fields in order to separate the optical and magnetic dynamical response. (c) The change in Faraday rotation $\Delta\theta_F$ for $\lambda = 660$ nm as a function of pump probe delay for two different sample temperatures and external magnetic field directions.

References

[1] E. Beaurepaire, J.-C. Merle, A. Daunois, and J.-Y. Bigot, Phys. Rev. Lett. **76**, 4250 (1996).
[2] J.-Y. Bigot and M. Vomir, Ann. Phys. **525**, 2 (2013).
[3] A. Kirilyuk, A. V. Kimel, and T. Rasing, Rep. Prog. Phys. **76**, 026501 (2013).
[4] S. Ferlay, T. Mallah, R. Ouahès, P. Veillet, and M. Verdaguer, Nature **378**, 701 (1995).
[5] S. Ohkoshi, M. Mizuno, G. Hung, and K. Hashimoto, J. Phys. Chem. B **104**, 9365 (2000).
[6] J. O. Johansson, J.-W. Kim, E. Allwright, D. Rogers, N. Robertson, and J.-Y. Bigot, Submitted (2016).

Molecular pathway control in sequential double ionization of CO_2 using two-pulse sequences

Sonia Erattupuzha[1], Seyedreza Larimian[1], Andrius Baltuška[1], Xinhua Xie[1], and Markus Kitzler[1]
1. Photonics Institute, Vienna University of Technology, Gusshausstrasse 27, A-1040 Vienna, Austria

Using a double-pulse scheme we visualize and control molecular dynamics taking place on intermediately populated states during different sequential double ionization pathways of CO_2. We demonstrate that exchanging the sequence of two differently intense pulses can almost completely switch the pathways. Fig. 1(a) shows the measured yields of CO_2^+ and CO_2^{2+}, as well as the yield of the fragmentation channel CO^+/O^+ as a function of the delay between 25 fs (FWHM) laser pulses from a Titanium-Sapphire laser amplifier system, in the range of Δt=−1.3…+2.6 ps, where negative (positive) delays mean that the stronger (weaker) pulse arrives earlier. The delay between the pulses (Δt) was varied in steps of 4 fs using a Mach-Zehnder interferometer. Electrons and ions emerging from the interaction of the two pulses with CO_2 molecules were detected in coincidence using a reaction microscope. The intensity of the two pulses was 1.7×10^{14} W/cm^2 and 3×10^{14} W/cm^2, respectively.

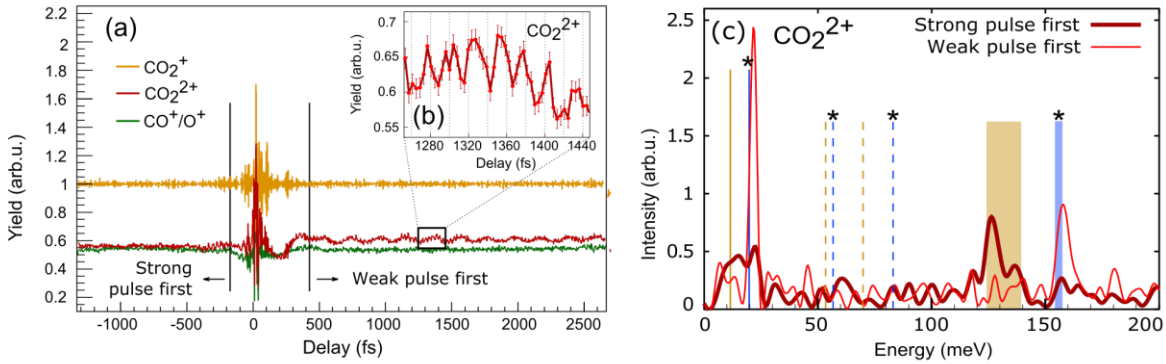

Figure 1: (a) Measured yields of CO_2^+, CO_2^{2+} and CO^+/O^+ as a function of the delay between the two pulses, normalized to the one of CO_2^+ at large delays. (b) Zoom into a short delay-range of the CO_2^{2+}-yield with statistical error bars added. (c) Fourier transforms of the yield modulations from Fig.1 (a) for CO_2^{2+} for negative/positive pulse delays separately, encoded by thick/thin lines, respectively. Literature values [1, 2] of electronic and vibrational transition energies of CO_2^+ are marked by lines and filled areas. Transitions on the X-state (A-state) are marked in blue (yellow) and with (without) an asterisk. Full and dashed lines indicate transitions due to electronic and bending dynamics, respectively. The range of transition energies corresponding to symmetric C–O stretch vibrational dynamics on both the X and A-states is indicated by filled areas.

Measured traces of the ionization and fragmentation yields, shown in Fig. 1(a), exhibit several interesting signatures on top of the dominant delay-independent signals that are mostly caused by the stronger of the two pulses. It can be seen that the yields are weakly modulated with various frequencies that are different for positive and negative delays. This is exemplified by the zoom into the yield of CO_2^{2+} shown in Fig. 1(b). In the delay region around Δt=0, where the two pulses overlap, the ionization and fragmentation yields exhibit very strong modulations due to field-extinction and -enhancement effects. To obtain insight into the dynamics involved, we analyzed the various weak modulations present in the yields in Fig. 1(a). To this end, we performed a Fourier analysis of the yields in Fig. 1(a) for Δt<−200 fs and Δt>+500 fs, respectively. The resulting spectra for CO_2^{2+} are shown in Fig. 1(c). Similar spectra were obtained for the fragmentation channel CO^+/O^+ [1]. The following features are apparent in the Fourier spectra: (i) the position and strength of the peaks strongly depend on whether the strong or weak pulse interacts with the molecule first. (ii) Both the CO_2^{2+} and CO^+/O^+ signals contain the same Fourier components; however, the relative intensities of the peaks strongly differ.

Comparison of the spectral features to published frequencies [2,3] allowed us to conclude that the features in the positive (negative) time delay region are dominantly due to electronic and nuclear dynamics on the $X^2\Pi_g$ ($A^2\Pi_u$) state of CO_2^+ [1]. We thus conclude that during the multiple ionization process the final molecular ionic states can be reached via different pathways along intermediately populated ionic potential energy surfaces, thus opening up opportunities for strong-field fragmentation control on extended time scales [1].

References

[1] Erattupuzha, S., Larimian, S., Baltuška, A., Xie, X. & Kitzler, M. *Two-Pulse Control over Double Ionization Pathways in CO2*. J. Chem. Phys. **144,** 024306 (2016).
[2] Liu, J., Hochlaf, M. & Ng, C. Y. *Pulsed field ionization–photoelectron bands for CO2+ in the energy range of 17.2–19.0 eV: An experimental and theoretical study*. J. Chem. Phys. **113**, 7988 (2000).
[3] Liu, J., Chen, W., Hsu, C.-W., Hochlaf, M., Evans, M., Stimson, S. & Ng, C. Y. *High resolution pulsed field ionization–photoelectron study of CO2+ in the energy range of 13.6–14.7 eV*. J. Chem. Phys. **112**, 10767 (2000).

Signatures of Intramolecular Interference in Strong-Field Ionization of Homonuclear Diatomics in a Circularly Polarized Laser Field

Vladimir Usachenko [1], ***Pavel Pyak*** [1,2]

1. *Institute of Applied Physics, National University of Uzbekistan, Tashkent, 100174, Uzbekistan*
2. *Physics Department, National University of Uzbekistan, Tashkent, 100174, Uzbekistan*

We report about the results of our theoretical study of strong-field (multiphoton) *above-threshold ionization* (ATI) in laser-irradiated molecular species (viz. N_2, O_2 and H_2) under conditions of recent experiment [1] using mid-infrared laser wavelengths ($\lambda \sim 1.0$ μm), for which the typical values of the so-called *Keldysh parameter* $\gamma \leq 1$. The problem is addressed within the *velocity-gauge* (VG) formulation of conventional *strong-field approximation* (SFA) suggesting only the *direct ATI process* as a solely contributing and sufficient underlying physical mechanism. Moreover, the *density-functional-theory* (DFT) is also essentially exploited as a complementary method [2] for numerical composition of initial (laser-free) molecular state using the routines of GAUSSIAN-03 code [3].

Fig.1 demonstrates a sample of our DFT-SFA calculation results for angle-resolved photoelectron energy spectra (PES) calculated for N_2 molecule corresponding to photoelectron emission from predominantly contributing $3\sigma g$ *highest-occupied molecular orbital* (HOMO) along the internuclear molecular axis, which is supposed to have a spatial orientation within the polarization plane of circularly polarized laser radiation field. The spectra are calculated for laser field of various different wavelengths λ (800 *nm* and 2.0 μm) and peak intensities I (500 and 1000 $TW \cdot cm^{-2}$) corresponding to three different values of the *Keldysh parameter* γ (0.205, 0.362 and 0.512).

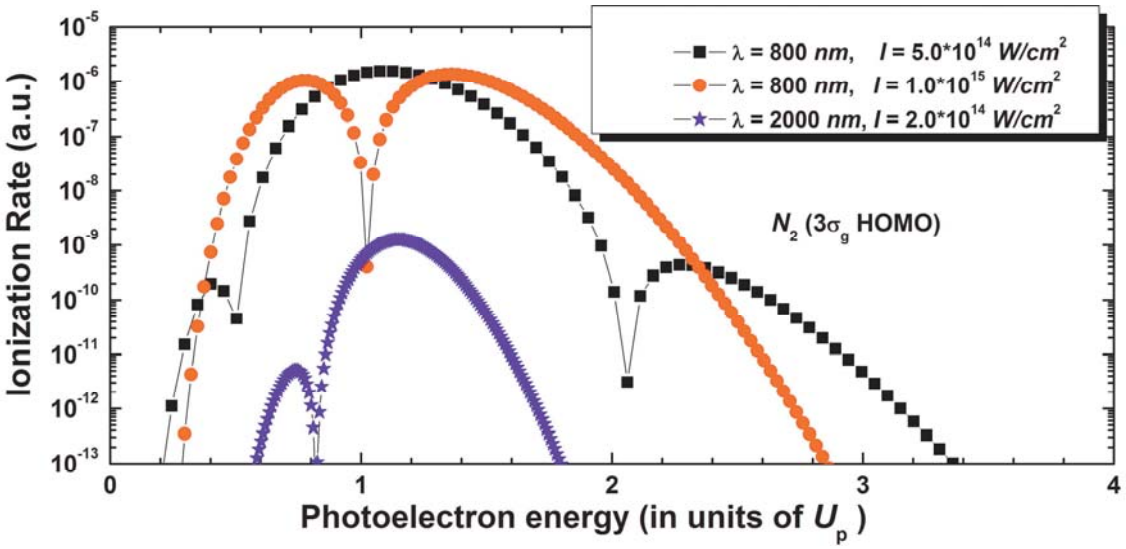

Fig. 1 Angle-resolved photoelectron energy spectra due to ATI in laser-irradiated N_2 calculated for three different combinations of laser wavelength λ and peak intensity I (as indicated in picture inset).

As expected [4], for circular laser field polarization the calculated PES proved to demonstrate a high suppression in ionization rates within the low-energy domain $E_p << U_p$ (here U_p is the *ponderomotive energy* of photoelectron oscillating motion in incident laser field). Another remarkable feature present in all calculated PES is a clear signature of the so-called *intramolecular* quantum interference manifested as a distinct and pronounced minimum(a) arising in high-energy spectra domain due to superposition of multiphoton transition amplitudes of ATI corresponding to photoelectron emission from two different (identical) atomic centers in molecule. Accordingly, the position (location) of the minimum(a) in calculated spectra proved to be very sensitive to the value of laser wavelength λ and molecular internuclear separation R_0.

References

[1] C. I. Blaga *et al.*, Nature Phys. **5**, 335 (2009).
[2] V. I. Usachenko, P. E. Pyak and V. V. Kim, Phys. Rev. A **79**, 023415 (2009).
[3] M. J. Frisch and J A Pople, **Gaussian-03**, Revision A.1 (Gaussian, Inc., Pittsburgh, PA 2003).
[4] T. J. McIlrath *et al*., Phys. Rev. A **35**, 4611 (1987).

Extreme-Scale Nonlinear Optics in Gases

C. M. Heyl[1,2], H. Coudert-Alteirac[1], M. Miranda[1], M. Louisy[1], K. Kovacs[3,4], V. Tosa[3,4], E. Balogh[4,5], K. Varjú[4,5], A. L'Huillier[1], A. Couairon[6], and C. L. Arnold[1]

[1]Department of Physics, Lund University, P. O. Box 118, SE-221 00 Lund, Sweden
[2]JILA, University of Colorado, Boulder, CO 80302 Boulder, USA
[3]National Institute for R&D Isotopic and Molecular Technologies, Cluj-Napoca, Romania
[4]ELI-ALPS, ELI-Hu Nkft, Dugonics ter 13, Szeged 6720, Hungary
[5]Department of Optics and Quantum Electronics, University of Szeged, Dom ter 9, 6720 Szeged, Hungary
[6]Centre de Physique Théorique, École Polytechnique, CNRS, F-91128, Palaiseau, France
Author e-mail address: christoph.heyl@fysik.lth.se

Nonlinear interactions of energetic ultrashort laser pulses with gases form the basis behind a wealth of interesting phenomena, such as multiphoton ionization, plasma formation, spectral broadening, as well as the creation of attosecond pulses and the formation of electron or ion beams. While optimum conditions for certain nonlinear processes are often well explored within rather narrow parameter ranges, the rapid advances in femtosecond laser technology, driven by the desire to access, e.g., faster times scales or to reach higher intensities, demand the extension of nonlinear optical methods to new parameter regimes. Important attempts in this direction include the extension of high harmonic and attosecond sources to higher repetition rates and higher pulse energies [1,2] as well as the power-scaling of pulse-post compression techniques [3] and filamentation [4].

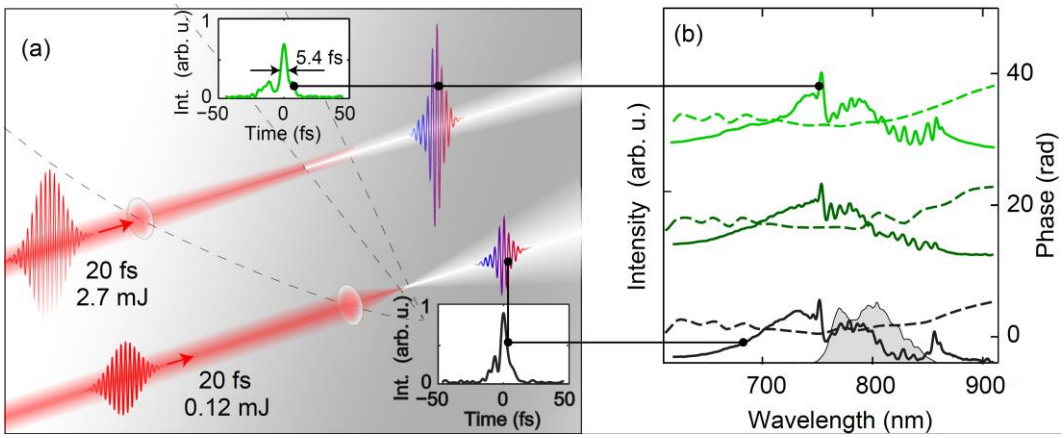

Figure 1: (a) Illustration of filament scaling: a filament is created by focusing a 20 fs-laser pulse into an Argon gas medium. (b) Spectral intensity and spectral phase for three different input pulse energies measured after recompressing the center of the filament output. The grey shaded area denotes the input spectrum. An arbitrary offset was added to the displayed data for better visualization. The retrieval yields pulse duration around 5.4 fs for all cases (see insets in a).

Here, we present a general methodology that allows the invariant scaling of various nonlinear light-matter interactions in gases. We identify a fundamental principle of nonlinear optics showing that even highly complex nonlinear propagation phenomena in gases are scale-invariant, if appropriate scaling relations for gas density, laser pulse energy and spatial dimensions are employed [5]. We present the concept of our scaling model and its limitations as well as the application to two important phenomena of nonlinear optics: high-order harmonic generation and filamentation (see Figure 1). We believe that our results are of fundamental interest for ultrafast science and provide routes for scaling various nonlinear optics phenomena to completely unexplored parameter regimes.

References

[1] C. Heyl *et al*., "High-order harmonic generation with μj laser pulses at high repetition rates," J. Phys. B, **45**, 074020 (2012).
[2] J. Rothhardt *et al*., "Absorption-limited and phasematched high harmonic generation in the tight focusing regime," New Jour. Phys., **16**, 033022 (2014).
[3] C. Fourcade *et al*., "Post-compression of high-energy femtosecond pulses using gas ionization", Opt. Lett. 35 253 (2010).
[4] P. A. Zhokhov *et al*., "Scaling laws for laser-induced filamentation", Phys. Rev. A, **89**, 043816 (2014)
[5] C. M. Heyl *et al*., "Scale-invariant nonlinear optics in gases", Optica **3**, 75 (2016).

Towards Antihydrogen Synthesis With Sympathetically Laser-Cooled Positrons

D. Maxwell[1], M. Sameed[1], J. Segal[1], N. Madsen[1]
1. Swansea University, Singleton Park, Swansea, Wales, SA2 8PP, UK

The ALPHA experiment at CERN aims to perform precise comparisons of the properties of matter with those of antimatter, and has been consistently trapping antihydrogen atoms since 2010 [1]. However, only about two antihydrogen atoms can be trapped per seven-minute experimental cycle, putting considerable restrictions on the precision the experiment is likely to achieve. The positron temperature is thought to play a vital role in both the rate of antihydrogen formation, and on the trapping rate of antihydrogen [2,3]. Currently, positron temperatures reach $\sim$50 K. By lowering the positron temperature, significantly more antihydrogen atoms should be trapped. We propose to sympathetically cool the positrons using laser-cooled beryllium ions, $^{9}Be^{+}$, a technique that has previously been demonstrated [4]. Simulations in ALPHA have shown that the temperature of the positrons could potentially be reduced to less than 5K if cooling is maintained during antihydrogen formation [5].

A source of $^{9}Be^{+}$ ions, operational under significant constraints imposed by the ALPHA apparatus, is currently being tested. A major constraint is the UHV environment of the ALPHA apparatus, which requires that the source minimise vacuum contamination. As such, the source will rely on laser ablation to produce a low flux, low energy source of ions. The aim is to directly trap the low energy ions in the Penning-Malmberg trap currently used to trap and mix positron and anti-proton plasmas [6]. The geometry of the ALPHA apparatus also requires that the source can be moved in and out of the beamline to allow the passage of particles. To achieve this the source and diagnostic equipment, including optical elements for fluorescence collection, are mounted on a linear translator.

We present preliminary results showing that the desired properties of the ion source can be achieved through a careful choice of laser ablation pulse parameters. An ablation source for the main ALPHA apparatus has been designed and will be installed in 2016.

References

[1] ALPHA Collaboration, *Trapped antihydrogen*, Nature **468**, 673 (2010).
[2] G. Gabrielse et al, *Antihydrogen production using trapped plasmas*, Physics Letters A **129**, 38 (1988).
[3] ATHENA Collaboration, *Antihydrogen production temperature dependence,* Physics Letters B **583**, 59 (2004).
[4] B. M. Jelenkovic et al, *Sympathetically cooled and compressed positron plasma,* Phys. Rev. A **67**, 063406 (2003).
[5] N. Madsen et al, *Antihydrogen trapping assisted by sympathetically cooled positrons*, New J. Phys **16**, 063046 (2014).
[6] ALPHA Collaboration, *The ALPHA antihydrogen trapping apparatus,* Nucl. Inst. Meth. Phys. Res. A **735**, 319 (2014).

Bound-Electron *g*-Factor Measurements for a Stringent Test of QED and the Determination of Fundamental Constants

Florian Köhler-Langes[1], Fabian Heiße[1,2], Wolfgang Quint[2], Günter Werth[3], Sven Sturm[1], Klaus Blaum[1]

1. *Max-Planck-Institut für Kernphysik, Saupfercheckweg 1, 69117 Heidelberg, Germany*
2. *GSI Helmholtzzentrum für Schwerionenforschung, Planckstraße 1, 64291 Darmstadt, Germany*
3. *Institut für Physik, Johannes Gutenberg-Universität Mainz, Staudingerweg 7, 55128 Mainz, Germany*

High-precision measurements of the gyromagnetic factor (*g*-factor) of highly-charged ions provide the opportunity to determine fundamental constants with highest precision [1,2] and to test the underlying theory of quantum electrodynamics of bound systems (BS-QED) [3-5]. In 2011 the most stringent test of BS-QED has been performed by measuring the *g*-factor of hydrogenlike silicon with a relative uncertainty of 0.07 ppb [3]. The ensuing comparison of the measured *g*-factor of lithiumlike silicon with its theoretical prediction enabled the most stringent test of electron-electron interaction in 2013 [4].

In a recent experiment the atomic mass of the electron has been determined with a relative uncertainty of 0.03 ppb by the measurement of the bound-electron *g*-factor of a single hydrogenlike carbon ion [1,2]. In that way, the former literature value recommended by the CODATA (Committee on Data for Science and Technology) 2010 adjustment has been improved by a factor of 13 [6,7].

In our most recent measurement campaign, we measured the *g*-factors of two different lithiumlike calcium isotopes, ^{40}Ca and ^{48}Ca [5]. Despite their 20% mass difference, they have an almost identical nuclear charge radius, thus providing a unique system across the entire nuclear chart to test the pure relativistic nuclear recoil effect by measuring the *g*-factor difference $\Delta g = g(^{40}Ca^{17+}) - g(^{48}Ca^{17+})$. The corresponding theoretical prediction requires BS-QED but goes beyond the standard formalism, the so-called Furry picture, where the nucleus is considered as a classical source of the Coulomb field.

We determine the bound-electron *g*-factor by measuring the ratio between the spin-precession frequency (Larmor frequency) of the bound electron to the cyclotron frequency of the singly trapped ion. The spin-state is determined via the continuous Stern-Gerlach effect. The cyclotron frequency is measured by a novel phase-sensitive detection techniques, working at ultra-low temperatures. In this contribution, I will present the apparatus including the triple Penning-trap setup as well as all detection techniques. The focus will be set on the electron mass results and the recently published *g*-factor measurements on the two lithiumlike calcium isotopes.

References

[1] Sven Sturm, Florian Köhler et al., *High-precision measurement of the atomic mass of the electron*, Nature **506**, 467-470 (2014)
[2] Florian Köhler et al., *The electron mass from g-factor measurements on hydrogen-like carbon* $^{12}C^{5+}$, J. Phys. B: At. Mol. Opt. Phys. **48**, 144032 1-20 (2015)
[3] Sven Sturm et al., *g Factor of Hydrogenlike* $^{28}Si^{13+}$, Phys. Rev. Lett. **107**, 023002 (2011)
[4] Anke Wagner et al., *g Factor of Lithiumlike Silicon* $^{28}Si^{11+}$, Phys. Rev. Lett. **110**, 033003 (2013)
[5] Florian Köhler et al., *Isotope dependence of the Zeeman effect in lithium-like calcium*, Nature Communications **7**, 10246 (2016)
[6] Peter J. Mohr et al., *CODATA recommended values of the fundamental physical constants: 2010*, Rev. Mod. Phys. **84**, 1527-1605 (2012)
[7] Peter J. Mohr et al., *CODATA recommended values of the fundamental physical constants: 2014*, arXiv:1507.07956v1 (2015)

Dispersion forces on extended and rotating particles

Johannes Fiedler[1,2], **Stefan Scheel**[2], **Stefan Y. Buhmann**[1]
1. Physikalisches Institut, Albert-Ludwig-Universität, Hermann-Herder-Str. 3, 79104 Freiburg, Germany
2. Institut für Physik, Universität Rostock, Albert-Einstein-Str. 23, 18059 Rostock, Germany

Dispersion forces, such as Casimir-Polder forces between a microscopic particle and a macroscopic surface or van-der-Waals force between two microscopic particles, arise from the ground-state fluctuations of the quantized electromagnetic field. Commonly, the theoretical description of this interaction assumes the electric-dipole approximation in which the particle is represented by a point dipole [1,2]. However, recent interference experiments use large organic molecules at relatively high velocities which interfere on very thin material gratings [3]. A consequence of this set of parameters is that the molecules approach the grating surface very closely, at typical distances in the range of only a few nanometers, which implies that the molecules cannot be treated as point dipoles any longer.

In order to account for this experimental situation, we have developed a theory describing the interaction of large (i.e. spatially extended) molecules very close to surfaces. We employ the idea of Gaussian polarisability densities to include the size and shape of the molecule while retaining the dipole approximation [4]. We will investigate the effect of molecular rotation on the Casimir-Polder interaction during transit through the grating [5]. In addition, we will investigate the influence of an atomic extension due to a particle in a microspherical cavity, as it is circumstanced by the solution of a van-der-Waals molecule [6].

References

[1] Stefan Scheel and Stefan Y. Buhmann, *Macroscopic quantum electrodynamics - concepts and applications*, Acta Phys. Slov. **58**, 675 (2008).
[2] Stefan Y. Buhmann, *Dispersion Forces I: Macroscopic Quantum Electrodynamics*, Vol. **247** of Springer Tracts in Modern Physics (Springer, Heidelberg, 2012).
[3] Christian Brand, Johannes Fiedler *et al. A Green's function approach to modeling molecular diffraction in the limit of ultra-thin gratings*, Ann. Phys. (Berlin) **527**, 580 (2015).
[4] Drew F. Parsons and Barry W. Ninham, *Ab Initio Molar Volumes and Gaussian Radii*, J. Chem. Phys. A **113**, 1141 (2009).
[5] Johannes Fiedler and Stefan Scheel, *Casimir–Polder potentials on extended molecules*, Ann. Phys. (Berlin) **527**, 570 (2015).
[6] Alexander Held and Michael Walter, *Simplified continuum solvent model with a smooth cavity based on volumetric data*, J. Chem. Phys. **141**, 174108 (2014).

$\alpha^6 m$ corrections to the ground state of H_2

Mariusz Puchalski[1], **Jacek Komasa**[1], **Paweł Czachorowski**[2], **Krzysztof Pachucki**[2]
1. Faculty of Chemistry, Adam Mickiewicz University, Umultowska 89b, 61-614 Poznań, Poland
2. Faculty of Physics, University of Warsaw, Pasteura 5, 02-093 Warsaw, Poland

The hydrogen atom and various hydrogenic systems like positronium, muonium, muonic hydrogen, He^+, due to highly accurate theoretical predictions, are the cornerstone for precision spectroscopy, for the determination of fundamental physical constants and for the low energy tests of the Standard Model. The $1S-2S$ transition in H is an exceptional example where the high precision measurement $f(1S-2S) = 2\,466\,061\,413\,187\,035(10)$ Hz [1] exceeds by orders of magnitude any theoretical predictions. This is because of the insufficient precision of fundamental physical constants and because of the uncertainties in the proton structure. The lack of the other calculable sharp transition in the hydrogen and the lack of the continuous wave laser for $He^+(1S-2S)$ transition makes the determination of the Rydberg constant much less accurate as it would be, if the other such transition is available. Here we point out that the molecular transitions in H_2 can serve for this purpose, as they can be calculated with sufficient precision to resolve the proton charge radius puzzle and to improve determination of the Rydberg constant.

The calculations for the hydrogen molecule has never been considered to be as accurate as for hydrogen due to lack of the analytic solution of the Schrödinger equation. Nevertheless the numerical solution, as it has been shown recently, can be as accurate as 10^{-11} for the dissociation energy [2]. An excellent agreement of theoretical results with experimental values achieved for the hydrogen molecule H_2 [3] indicates good understanding of all physical effects up to the 10^{-8} precision level. There are obviously various corrections, such as relativistic and quantum electrodynamic (QED) ones. These have been calculated up to $\alpha^5 m$ order in the adiabatic approximation.

Here we calculate the leading unknown $\alpha^6 m$ correction using the so called nonrelativistic QED approach [4] and give improved results for the dissociation and the fundamental vibrational energies [5]. These results open the window for the high precision spectroscopy of H_2 and related accurate tests of fundamental interactions models.

References

[1] Christian G. Parthey, Arthur Matveev, Janis Alnis, Birgitta Bernhardt, Axel Beyer, Ronald Holzwarth, Aliaksei Maistrou, Randolf Pohl, Katharina Predehl, Thomas Udem, Tobias Wilken, Nikolai Kolachevsky, Michel Abgrall, Daniele Rovera, Christophe Salomon, Philippe Laurent, and Theodor W. Hänsch, Phys. Rev. Lett. **107**, 203001 (2011).
[2] K. Piszczatowski, G. Lach, M. Przybytek, J. Komasa, K. Pachucki and B. Jeziorski, J. Chem. Theory Comput. 5, 3039 (2009).
[3] J. Liu, E. J. Salumbides, U. Hollenstein, J. C. J. Koelemeij, K. S. E. Eikema, W. Ubachs, and F. Merkt, J. Chem. Phys. 130, 174306 (2009).
[4] W. E. Caswell and G. P. Lepage, Phys. Lett. B **167**, 437 (1986).
[5] M. Puchalski, J. Komasa, P. Czachorowski and K. Pachucki, unpublished yet.

QED in an external Coulomb field

Daniel Šimsa[1], **Jaroslav Zamastil**[1], **Vojtěch Patkóš**[1]
1. Department of Chemical Physics and Optics, Faculty of Mathematics and Physics, Charles University, Ke Karlovu 3, 121 16 Prague 2, Czech Republic

In recent years the so called proton radius puzzle [1] has sparked discussion about the possible error in the computation of standard QED effects. Regarding this problem it is important to check the known results and verify them by independent calculations. Another part of our motivation is exploring the non-perturbative aspects of QFT.

We study the processes of self-energy (SE) and vacuum polarization (VP). The expression for the energy shift caused by one-loop SE reads

$$\Delta E_{SE} = \frac{\alpha}{\pi}\int \frac{\mathrm{d}^4 k_F}{k^2}\langle\psi_{at}|\gamma_\mu \frac{1}{\gamma\cdot(\Pi-k)-m}\gamma_\mu|\psi_{at}\rangle\,. \tag{1}$$

Here $\mathrm{d}^4k_F = i(2\pi)^{-2}\mathrm{d}^4k$, ψ_{at} is the wafefunction of the bound electron, Π is the four-momentum of the electron in an external Coulomb field $\Pi = \left(E+\frac{Z\alpha}{r},\vec{p}\right)$, where Z is the nuclear charge. For the energy shift caused by one-loop VP one has

$$\Delta E_{VP} = \langle\psi_{at}|V_{VP}|\psi_{at}\rangle, \tag{2}$$

where

$$-\nabla^2 V_{VP} = \rho_{VP} \qquad \text{and} \qquad \rho_{VP} = -i\int\frac{\mathrm{d}E}{2\pi}\langle\vec{r}|\gamma_0\frac{1}{\gamma\cdot\Pi-m}|\vec{r}\rangle. \tag{3}$$

The usual evaluation of these expressions is done by making use of the expansion of the electron propagators around the free particle solutions, e.g.

$$\frac{1}{\gamma\cdot(\Pi-k)-m} = \frac{1}{\gamma\cdot(p-k)-m} + \frac{1}{\gamma\cdot(p-k)-m}\gamma\cdot(\Pi-p)\frac{1}{\gamma\cdot(p-k)-m}+\ldots. \tag{4}$$

For SE this leads to infrared divergencies; calculations have to be matched with low energy calculations. With increasing order of $Z\alpha$ the complexity grows fast. For VP, there are no infrared problems, but the calculation is impractical. Another approach is based on partial wave expansion [2], which works for high Z but not low.

Our idea is to take advantage of known solution of the Dirac equation for Coulomb potential first and only then perform any expansion. For VP the calculation is relatively straightforward, for SE it has to be supplemented with the relativistic multipole expansion [3], which consists of two steps. Firstly, rewrite the fraction from (1)

$$\frac{1}{\gamma\cdot(\Pi-k)-m} = \frac{1}{k^2-2k\cdot\Pi+\mathscr{H}}\left[\gamma(\Pi-k)+m\right], \tag{5}$$

where $\mathscr{H}$ is the second order Dirac hamiltonian. Secondly, expand fraction (5) as follows

$$\frac{1}{k^2-2k\cdot\Pi+\mathscr{H}} = \frac{1}{k^2-2k\cdot\varepsilon+\mathscr{H}} + \frac{1}{k^2-2k\cdot\varepsilon+\mathscr{H}}2k\cdot(\Pi-\varepsilon)\frac{1}{k^2-2k\cdot\varepsilon+\mathscr{H}}+\ldots, \tag{6}$$

where $\varepsilon = (m,\vec{0})$. The idea behind the expansion is that the dominant contribution to SE comes from the virtual states where canonical four-momentum is dominated by the electron mass.

Once the renormalization of the electron mass and charge is made no divergencies are encountered. The calculation is analytic up to the very end. What remains are 1D integrals for SE and 2D for VP which have to be calculated numericaly. For light hydrogen-like atoms the results [3] for SE and VP are either the most accurate obtained so far or are competitive with the most accurate ones.

References

[1] R. Pohl et al, Nature **466**, 213 (2010). See also A. Antognini et al, J. Phys.: Conf. Series **312**, 032002 (2011); R. Pohl, R. Gilman, G. A. Miller and K. Pachucki, Annu. Rev. Nucl. Part. Sci. **63**, 175 (2013).

[2]U. D. Jentschura, P. J. Mohr and G. Soff, Phys. Rev. Lett. **82**, 53 (1999). See also U. D. Jentschura, P. J. Mohr and G. Soff, Phys. Rev. A **63**, 042512 (2001); U. D. Jentschura and P. J. Mohr, ibid. **69**, 064103 (2004).

[3] V. Patkóš and J. Zamastil, Phys. Rev. A **91**, 062511 (2015). See also J. Zamastil and V. Patkóš, Phys. Rev. A **88**, 032501 (2013); J. Zamastil and D. Šimsa, submitted to Phys. Rev. A (2016).

Precision Test of Many-Body QED in the Be^+ 2*p* Fine Structure Doublet Using Short-Lived Isotopes

Wilfried Nörtershäuser
Institut für Kernphysik, Technische Universität Darmstadt, D-64289 Darmstadt, Germany

Christopher Geppert[1,2], Andreas Krieger[1,2], Krzysztof Pachucki[3], Mariusz Puchalski[3,4], Klaus Blaum[5], Mark L. Bissell[6], Nadja Frömmgen[2], Michael Hammen[2], Magdalena Kowalska[7], Jörg Krämer[1], Kim Kreim[5], Rainer Neugart[2], Gerda Neyens[6], Rodolfo Sánchez[8], Deyan T. Yordanov[5]

1. Institut für Kernphysik, Technische Universität Darmstadt, D-64289 Darmstadt, Germany
2. Institut für Kernchemie, Johannes Gutenberg-Universität Mainz, D-55128 Mainz, Germany
3. Faculty of Physics, University of Warsaw, Pasteura 5, 02-093 Warsaw, Poland
4. Faculty of Chemistry, Adam Mickiewicz University, Umultowska 89b, 61-614 Poznań , Poland
5. Max-Planck-Institut für Kernphysik, D-69117 Heidelberg, Germany
6. Instituut voor Kern- en Stralingsfysica, KU Leuven, B-3001 Leuven, Belgium
7. CERN, Physics Department, CH-1211 Geneva 23, Switzerland
8. GSI Helmholtzzentrum für Schwerionenforschung GmbH, D-64291 Darmstadt, Germany

Absolute transition frequencies of the $2s\ ^2S_{1/2} \rightarrow 2p\ ^2P_{1/2,3/2}$ transitions in Be^+ were measured for the isotopes $^{7,9\text{-}12}$Be. The fine structure splitting of the 2*p* state and its isotope dependence are extracted and compared to results of ab initio calculations using explicitly correlated basis functions, including relativistic and quantum electrodynamics effects at the order of $m\alpha^6$ and $m\alpha^7 \times \ln \alpha$. Laser spectroscopy was performed using quasi-simultaneous frequency-comb based collinear and anticollinear laser spectroscopy at CERN/ISOLDE. Since the extraction of the fine-structure splitting of the stable isotope ^{9}Be is hampered by the unresolved hyperfine structure in the $2s\ ^2S_{1/2} \rightarrow 2p\ ^2P_{3/2}$ transition, we have also studied the radioactive isotopes ^{10}Be and ^{12}Be with lifetimes of 1.6×10^6 years and 20 ms, respectively. These even-even isotopes do not exhibit nuclear spin and are therefore free of hyperfine splitting. Measured fine-structure splitting of all isotopes, including the halo isotope ^{11}Be, were combined after correcting with the calculated splitting isotope shifts, to improve the accuracy of the ^{9}Be fine structure splitting by another factor of 4. In total accuracy has been improved in both the theory and experiment by 2 orders of magnitude, and reasonable agreement is observed. This represents an accurate test of quantum electrodynamics for many-electron systems, being insensitive to nuclear uncertainties [1].

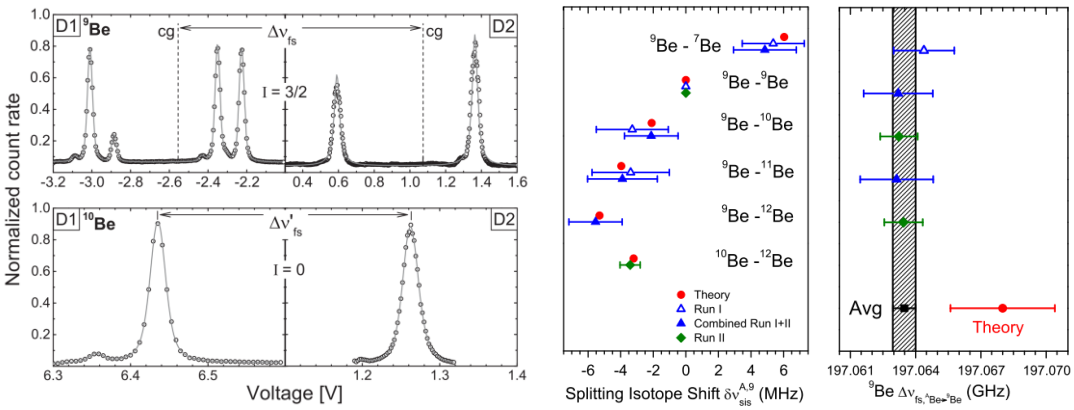

Fig. 1 Left: Fluorescence spectra of ^{9}Be (top row) and ^{10}Be (bottom row) in the $2s\ ^2S_{1/2} \rightarrow 2p\ ^2P_{1/2}$ (left) and the $2s\ ^2S_{1/2} \rightarrow 2p\ ^2P_{3/2}$ (right) transition as a function of the Doppler-tuning voltage. The distance corresponding to the 2*p* fine structure splitting $\Delta\nu_{fs}$ is indicated. Right: Experimental results and comparison with theory for the splitting isotope shift (left column) and for the fine structure splitting of all isotopes transferred to ^{9}Be (right column)..

.

References

[1] W. Nörtershäuser *et al.*, *Precision Test of Many-Body QED in the Be+ 2p Fine Structure Doublet Using Short-Lived Isotopes*, Phys. Rev. Lett. **115**, 033002 (2015).

Spectral and Spatial Properties of Bright Squeezed-Vacuum States of Light

O. V. Tikhonova[1], P. R. Sharapova[1;2], M. V. Chekhova[1;3;4], A. Perez[3] , S. Lemieux[5], G. Leuchs[3,4]

1 - *Physics Department, Lomonosov Moscow State University, Leninskie Gory, 1, 119991, Moscow, Russia*
2 - Department of Physics, University of Paderborn, Warburger Straße 100, D-33098 Paderborn, Germany
3 - Max-Planck Institute for the Science of Light, Bau 24, Erlangen D-91058, Germany
4 - Department of Physics, University of Erlangen-Nuremberg, Guenther-Scharowsky Strasse 1, 91058 Erlangen, Germany
5 - Department of Physics and Max Planck Centre for Extreme and Quantum Photonics, University of Ottawa, 25 Templeton Street, Ottawa, Ontario K1N 6N5, Canada

Squeezed states of light are very attractive and perspective non-classical subjects for scientific investigation in modern quantum optics. They are known to be characterized by strong correlations or "entanglement" between photons both in the frequency and space domain. Many papers are aimed to describe theoretically the spatial and frequency correlations of photons in a bi-photon pair with the perturbation theory being used. In the case when the nonlinear signal is stimulated by a rather intensive pump a bright squeezed vacuum state (BSV) can be generated. This state is referred to as a macroscopic non-classical state of light since the number of photons is huge and numerous correlations between many photons take place. In such "high-gain" regime the perturbation theory is no more valid and new theoretical approaches able to describe strong correlations between many photons are of great importance. To develop a theoretical description under these conditions the collective frequency modes (called broadband modes) were introduced in a set of papers [1-3]. This approach usually leads to a system of integro-differential equations that, in a rigorous way, should be solved numerically and hardly can clarify the physical mechanisms of experimentally observed effects [2,3]. Thus the theoretical description of collective correlations observed in BSV remains still an open question.

In our work we investigate both theoretically and experimentally the spectral and spatial features and correlations in macroscopic (bright) squeezed quantum states of light generated in high-gain parametric down-conversion and referred to as bright squeezed vacuum (BSV). To describe theoretically these states we develop a generalized fully analytical approach, based on the concept of independent collective (Schmidt) modes and valid for the cases of both weak and strong nonlinear interaction. Such possibility is based on the known Schmidt decomposition procedure. In the frame of the Heisenberg representation we obtain the fully analytical solution for the evolution of the photon-creation operators in Schmidt modes and calculate different characteristics measured in experiment. We present the comparison of our theoretical results with the properties of bright squeezed vacuum observed in experiments performed in the Max-Planck Institute and demonstrate a very good agreement. In addition we show the possibility to vary and control the spatial and spectral features of BSV and the number of modes using a nonlinear interferometer based on two nonlinear crystals separated by a certain medium. If a medium with group velocity dispersion is used it is possible "to play" with the spectral properties of the BSV light by changing the time delay between the pump pulse and the nonlinear signal amplified in the second crystal (for example by varying the length of the medium). At the same time significantly different BSV spectra are obtained for the case of rather low and high intensity of the pump pulse (See Fig. 1).

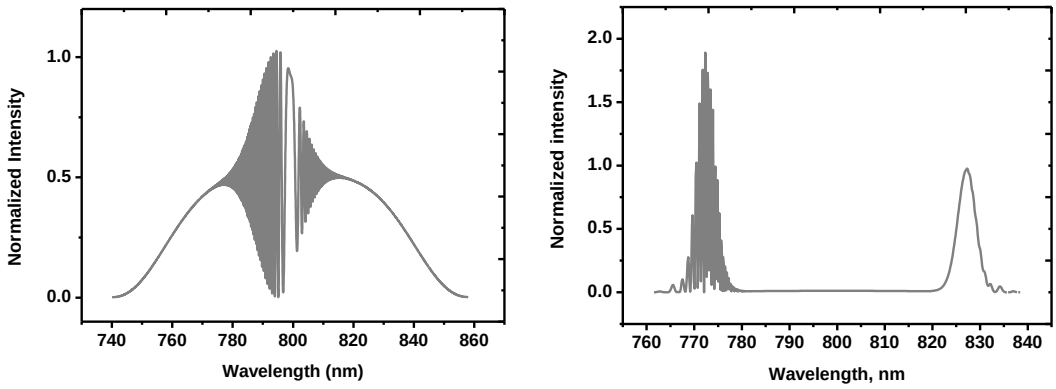

Fig. 1 BSV spectrum obtained for low (left) and high (right) pump intensity.

References

[1] B. Dayan, Phys. Rev. A **76**, 043813 (2007).
[2] A. Christ, B. Brecht, W. Mauerer, and C. Silberhorn, New J. Phys. **15**, 053038 (2013).
[3] A. Eckstein, B. Brecht, and C. Silberhorn, Opt. Express **19**, 13770 (2011).

Quantum States with High Angular Momentum Entanglement

R. Fickler[1,2,3], S. Lemiuex[3] M.V. Chekhova[4,5], G. Leuchs[4,5], R.W. Boyd[3,6], A. Zeilinger[1,2]

1. *Institute for Quantum Optics and Quantum Information (IQOQI), Austrian Academy of Sciences, 1090 Vienna, Austria*
2. *Faculty of Physics, University of Vienna, 1090 Vienna, Austria*
3. *University Ottawa Max Planck Centre for Extreme and Quantum Photonics, University of Ottawa, Ottawa, K1N 6N5, Canada*
4. *Max-Planck Institute for the Science of Light, 91058 Erlangen, Germany*
5. *University of Erlangen-Nürnberg, 91054 Erlangen, Germany*
6. *Institute of Optics, University of Rochester, Rochester, 14620, USA*

Photonic quantum states have always played a vital role in investigating fundamental properties of nature and testing possible limitations of quantum theory. From first experimental demonstrations of quantum entanglement and quantum teleportation to quantum physics-boosted cryptography and computation, photons have always been at the forefront of cutting edge research [1]. Starting with a seminal work in 2001 [2] the transverse spatial degree of freedom of photons, more precisely the orbital angular momentum (OAM) connected to a twisted phase front, has been used to open up a novel field of investigations: quantum optics using spatial structures. Since the state space of such quantum states is in principle unbounded, they serve as a physical realization of high-dimensional quantum states and enlarge the information content per single quantum carrier. However, they also can be used to test possible limitations of quantum physics by means of generating quantum entanglement of high angular momenta [3]. In the following we describe and propose experiments pursuing this goal.

In a recent serious of experiments, we succeeded to entangle a photon with up to 10010$\hbar$ of OAM with the polarization of its partner photon. We start with polarization entanglement and coherently transfer one of the two photons to the largest OAM states possible. By taking advantage of a recently introduced technique to generate high OAM states, namely spiral phase mirrors [4], we are able to entangle up to 10010 angular momentum quanta (see Fig 1 a). Thereby we are not only increasing the complexity of spatial structures imprinted on single photons, but also generating a quantum state with the largest quantum number experimentally observed (to our best knowledge). The latter one demonstrates nicely that an assumed existence of a quantum-classical transition for increasing quantum numbers is often misinterpreted. Additionally, such high OAM states are known to be advantageous for enhanced angular sensing experiments.

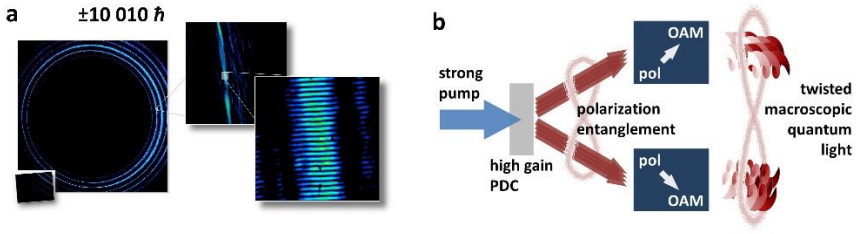

Fig. 1: a) False colour recordings of the intensity of a superposition ±10010$\hbar$ OAM. After zooming in twice the characteristic paddle structure becomes visible. b) Sketch of the proposed setup to generate highly twisted macroscopic quantum light.

In addition to bi-partite entanglement, we investigate possible extensions to multi-photon quantum states with high OAM values. For this we are developing a scheme to generate twisted bright squeezed vacuum (BSV), often referred to as macroscopic quantum light [5], due to its large number of photons and quantum properties like reduced noise. More importantly, it was shown recently that BSV can be used to generate polarization entangled pulses with up to 10^5 photons [6]. We are currently developing techniques to use such polarization-entangled multi-photon states and transfer them, following ideas describe above, into states that have high OAM quanta. Since each photon would carry a high OAM quanta, a successful transfer will lead to entanglement of unprecedented high OAM values. Such states are not only interesting from a fundamental point of view but also to enable enhanced interactions of quantum states of light with massive systems or improve quantum metrology schemes.

References

[1] A. Zeilinger, G. Weihs, T. Jennewein, M. Aspelmeyer *Happy centenary, photon.* Nature **433**, 230 (2005).
[2] A. Mair, A. Vaziri, G. Weihs, A. Zeilinger *Entanglement of the orbital angular momentum states of photons.* Nature **412,** 313 (2001).
[3] R. Fickler, R. Lapkiewicz, W.N. Plick, M. Krenn, C. Schaeff, S. Ramelow, A. Zeilinger *Quantum entanglement of high angular momenta.* Science **338**, 640 (2012).
[4] G. Campbell, B. Hage, B. Buchler, P.K. Lam *Generation of high-order optical vortices using directly machined spiral phase mirrors.* Appl.Opt. **51** 873 (2012).
[5] M.V. Chekhova, G. Leuchs, M. Żukowski *Bright squeezed vacuum: Entanglement of macroscopic light beams.* Opt.Comm. **337**, 27 (2015).
[6] T.S. Iskhakov, I.N. Agafonov, M.V. Chekhova, G. Leuchs *Polarization-entangled light pulses of 10^5 photons.* PRL **109,** 150502 (2012).

Superflourescent-like Behaviour of an Ensemble of Thermal Stronitum Atoms with Cavity-Enhanced Interaction

Stefan A. Schäffer[1], Bjarke T. R. Christensen[1], Stefan M. Rathmann[1], Martin R. Henriksen[1], Matthew Norcia[2], James K. Thompson[2], Jun Ye[2], Jan W. Thomsen[1]

1. The Niels Bohr Institut, University of Copenhagen, Blegdamsvej 17, DK-2100 København Ø, Denmark

2. JILA, National Institute of Standards and Technology and University of Colorado, Boulder, Colorado 80309-0440, USA

Quantum metrology and ultra stable optical atomic clocks rely on the frequency stability of reference lasers [1-3]. These lasers have linewidths down to tens of mHz [4], relying heavily on stabilization to ultra stable reference cavities [5] whose fractional frequency stability is currently limited by the Brownian motion in the mirror substrates [6]. The possibility of using cavity-enhanced spectroscopy on narrow transition lines has been studied [7] and it has been proposed to use the direct emission of radiation from atoms with such narrow lines instead [8]. It could be possible to use radiation emitted on such narrow lines directly as a reference laser. This, however, requires a large sample in order to generate considerable intensity during the long transition relaxation times. This picture changes significantly if one considers the case of superradiant or superfluorescent emission of light. In this case the photon emission flux can be considerably increased by collective atomic decay, while simultaneously achieving a narrowing of the emitted light compared to the transition linewidth [9,10]. Some advances have already been made in connection with proof of principle quasi-continuous superfluorescent systems [9] using atoms loaded into an optical lattice at very low temperatures.

We report the observation of Superfluorescent-like behaviour of an ensemble of strontium atoms freely moving at temperatures of about 4 mK. The atoms have a strong collective coupling to a single cavity mode, significantly enhanching their cooperativity, and allowing them to emit a coherent flash into the cavity mode, see Fig. 1.

The Strontium atoms are cooled with a single-stage MOT, resulting in about $N = 2 \cdot 10^7$ atoms overlapping with the cavity mode. We obtain a collective cooperativity of $C_N = 1.1 \cdot 10^4$. In the cavity mode an optical field detuned one free spectral range, $\Omega = 781$ MHz, ensures that the cavity is kept on resonance with the atoms. Additionally this allows for resonant seed light by means of sideband generation at $\nu = \nu_0 \pm \Omega$. We inject a resonant pi-pulse of light at an angle of 45° with respect to the cavity axis, see Fig. 1. The pulse causes all ground-state atoms to be excited, and collectively emit a burst of light into the cavity mode stimulated by the seed light with a delay τ_D.

The initial burst of photons is followed by a periodic ringing attesting the possible coherent behaviour of the system. The current width of the emission peaks is limited by the linewidth $\kappa = 2\pi \cdot 520$ kHz of the cavity mode. The cavity linewidth acts as a low-pass filter with a characteristic time of $\tau_{LP} = 310$ ns.

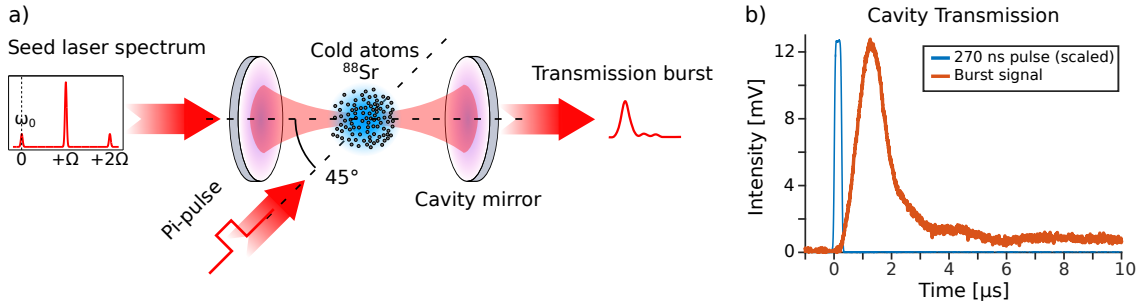

Fig. 1 a) System setup. **b)** Pi-pulse followed by a Superfluorescent-like burst in the cavity transmissison.

Superfluorescence in the bad cavity regime is an interesting alternative approach towards an ultra narrow continuous laser source. The narrowing of the linewidth in the superfluorescent light means that such a device could significantly increase the stability and accuracy of reference lasers for use in optical atomic clocks.

References

[1] B. J. Bloom, T. L. Nicholson, et al., *An Optical lattice clock with Accuracy and Stability at the 10^{-18} level*, Science **506**, 71 (2014).
[2] R. Le Targat, L. Lorini, et al., *Experimental realization of an optical second with strontium lattice clocks*, Nat. Commun. **4**, 2109 (2013).
[3] I. Ushijima, M. Takamoto, et al., *Cryogenic optical lattice clocks*, Nat. Phot. **9**, 185 (2015).
[4] M. Bishof, X Zhang, et al., *Optical Spectrum Analyzer with Quantum-Limited Noise Floor*, Prys. Rev. Lett. **111**, 093604 (2013)
[5] T. Kessler, C. Hagemann, et al., *A sub-40-mHz-linewidth laser based on a silicon single-crystal optical cavity*, Nat. Phot. **6**, 687 (2012).
[6] G. D. Cole, W. Zhang, et al., *Tenfold Reduction of Brownian noise in high-reflectivity optical coatings*, Nature Phot. **7**, 644 (2013).
[7] B. T. R. Christensen, M. R. Henriksen , et al., *Nonlinear Spectroscopy of Sr Atoms in an Optical Cavity for Laser Stabilization*, Physical Review A., **92**, 053820 (2015).
[8] J. Chen, *Active optical clock*, Chin. Sci. Bull. **54**, 348 (2009).
[9] J. G. Bohnet, Z. Chen, et al., *A steady-state superradiant laser with less than one intracavity photon* **484**, 78 (2012).
[10] W. Zhuang, and J. Chen, *Active Faraday optical frequency standard*, Opt. Lett. **39**, 21 (2014).

Robust Optical Fiber Interface for NV Center Nanodiamonds

Stepan Bolshedvorskii[1,2,4], Vadim Vorobyov[1,2,4], Vladimir Soshenko[1,2,3], Javid Javadzade[2,4] , Nikolay Lebedev[2,4], Vadim Sorokin[1,2], Andrey Smolyaninov[3], Alexey Akimov[5,1,2]

[1]Lebedev Physical Institute RAS, 53 Leninskij Prospekt, Moscow 119991, Russia

[2]Russian Quantum Center, 100 Novaya Str., Skolkovo, Moscow 143025, Russia

[3]Photonic Nano-Meta Technologies, Str. Nobel b.7, The territory of Skolkovo Innovation Center, Moscow, 143026, Russia

[4]Moscow Institute of Physics and Technology, 9 Institutskiy per., Dolgoprudny, Moscow Region, 141700, Russia

[5]Texas A&M University, College Station, TX 77843, USA

Recent time there are some promising systems which are considered as a candidates for building blocks of quantum computer, nitrogen vacancy (NV) center in diamond is one of them. This time with NV center were demonstrated substantial milestones in long-lifetime quantum memories, heralded entanglement, single short readout of the quantum state [1-3]. Besides application for computation, NV center could be utilized as a stable room temperature true single photon source.

Nowadays handling of the NV center rely on complicated and often low efficient technics. There were several attempts to build a robust optical interface to NV center: by using tapered fibers and AFM setups, photonics crystal fibers and placing nanocrystals inside air holes; by making waveguides within bulk diamond substrate [4,5].

Here we present novel and robust fiber based technology of spin photon interface for the NV center nanodiamonds. Our approach is easy, reproducible and cryogenic-temperature compatible [6].

We carefully studied parasitic fluorescence of the fiber (Fig 1 (c)) and methods to reduce it below the level of NV center emission. With our technic we were able to collect 3 times the number of photons from NV center collected with confocal microscope (0.5% collection efficiency) in one side of the fiber 1.5% or 3% in two sides. It is not limit for our technology, NV-fiber coupling may be more effective, because we use hand-made fiber connectors that limited transmission of the optical fiber line from NV center to detector level of 10%. This way we can suppose, that collection efficiency at tapered section of the fiber was about 15% from one side (30% from two sides). We expect that using manufactured fiber connectors will give us opportunity to reach mentioned above collection efficiency from single NV center nanodiamonds. Our approach could be further developed using recently demonstrated idea of utilizing fiber Bragg cavity [7]. This way one could use power of cavity quantum electrodynamics within relatively simple technics. This way our approach may become basis for many applications with NV centers in diamond.

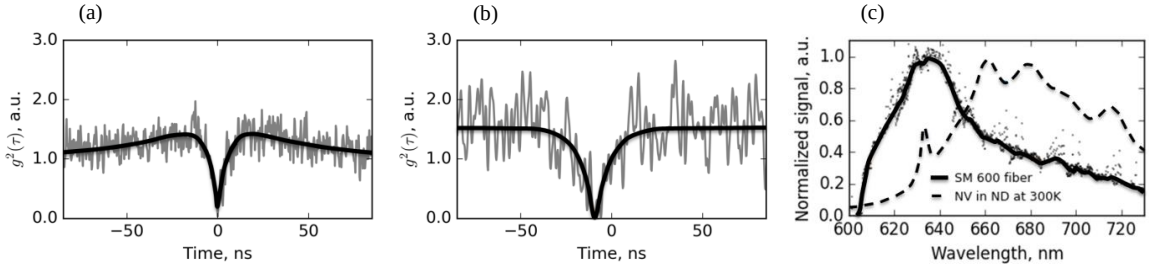

Fig. 1 (a) Second order autocorrelation function (G2) of the single NV on tapered fiber, collected with objective; (b) G2 function collected with tapered fiber; (c) Spectra of parasitic fiber fluorescence versus NV fluorescence.

References

[1] H. Bernien, B. Hensen, W. Pfaff, G. Koolstra, M. S. Blok, L. Robledo, T. H. Taminiau, M. Markham, D. J. Twitchen, L. Childress, & R. Henson, *Heralded entanglement between solid-state qubits separated by three metres*, Nature **497**, 86-90 (2013).

[2] Neumann,P.,Beck, J., Steiner, M., Rempp, F., Fedder, H., Hemmer, P.R., Wrachtrup, J., Jelezko, F., *Single-Shot Readout of a Single Nuclear Spin*, Science **329**, 542-544 (2010).

[3] Sen Yang, Ya Wang, D. D. Bhaktavatsala Rao, Thai Hien Tran, S. Ali Momenzadeh, Roland Nagy, M. Markham, D. J. Twitchen, Ping Wang, Wen Yang, Rainer Stoehr, Philipp Neumann, Hideo Kosaka, Joerg Wrachtrup, *High fidelity transfer and storage of photon states in a single nuclear spin*, arxiv: **1511.04939** (2015).

[4] Schröder T, Schell AW, Kewes G, Aichele T, Benson O., *Fiber-integrated diamond-based single photon source* ,Nano Lett. **11**, 198-202

[5] Michael J. Burek, Yiwen Chu, Madelaine Liddy, Parth Patel, Jake Rochman, Srujan Meesala, Wooyoung Hong, Qimin Quan, Mikhail D. Lukin & Marko Lončar, *High quality-factor optical nanocavities in bulk single-crystal diamond*, Nature Communications **6718** (2014).

[6]Masazumi Fujiwara, Hong-Quan Zhao, Tetsuya Noda, Kazuhiro Ikeda, Hitoshi Sumiya and Shigeki Takeuchi, *Ultrathin fiber-taper coupling with nitrogen vacancy centers in nanodiamonds at cryogenic temperatures*, arxiv: **1601.06188** (2010).

[7] Andreas W. Schell, Hideaki Takashima, Shunya Kamioka, Yasuko Oe, Masazumi Fujiwara, Oliver Benson & Shigeki Takeuchi, *Highly Efficient Coupling of Nanolight Emitters to a Ultra-Wide Tunable Nanofibre Cavity*, Scientific Reports **5**, 9619 (2015).

A loophole-free violation of Bell's inequality with single atoms entangled over a large distance

Wenjamin Rosenfeld[1], Daniel Burchardt[1], Kai Redeker[1], Robert Garthoff[1], Norbert Ortegel[1], Markus Rau[1], Harald Weinfurter[1,2]

1. Fakultät für Physik, Ludwig-Maximilians Universität München, D-80799 München, Germany
2. Max-Planck Institut für Quantenoptik, D-85748 Garching, Germany

Bell's inequality allows to test whether nature can be described in a local-realistic way. An experimental test of Bell's inequality can be performed by measuring correlations of two entangled particles. A conclusive test requires a high detection efficiency for the particles as well as strict space-like separation of the measurement events. These demanding requirements enforced additional assumptions (loopholes) in previous experiments and could be coped with only very recently [1].

Here we present our approach for achieving this task using heralded entanglement of two neutral ^{87}Rb-atoms [2]. The atoms are stored in two independently operated optical traps separated by 400 m (Fig. 1). In each trap a single photon is generated whose polarization is entangled with the spin of the respective atom. The two photons are coupled into single-mode fibers and overlapped on a beam splitter. Coincident detection of the two photons constitutes a Bell-state measurement (BSM) and thus projects the two atoms onto an entangled state.

To close the locality loophole the individual measurement results on both sides have to be obtained independently from each other. This means that the whole process including choice and selection of the measurement setting and the subsequent readout must be finished in a time shorter than 1.33 μs. By employing a fast quantum random number generator (QRNG) combined with polarization switching by means of AOMs the measurement setting takes $\sim$ 300 ns. The atomic state readout itself is based on a state-selective ionization scheme and subsequent detection of fragments by means of channel-electron multipliers (CEMs) [3]. The fragments are detected with an efficiency of ~ 0.99 enabling a readout fidelity of > 0.95. The time until the result of the readout appears at the output is $\sim$ 700 ns and thus the two measurement processes are space-like separated. Since a measurement result will be reported each time the BSM arrangement heralds the availability of an entangled pair, the detection efficiency equals to unity thereby closing also the detection loophole.

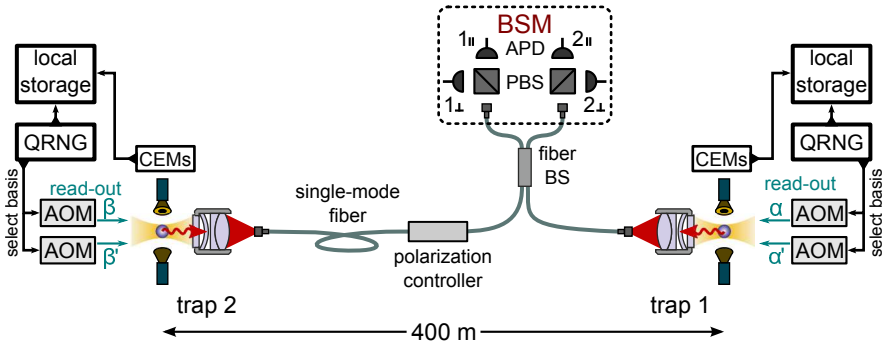

Fig. 1 Simplified scheme of the experiment.

We present results on a loophole-free violation of Bell's inequality. First measurements have shown a violation by two standard deviations, $S = 2.30 \pm 0.15$, corresponding to a p-value of $p = 0.0265$. Current work is on increasing the measurement statistics to achieve even lower p-values. A reliable violation of Bell's inequality would form the basis for certified generation of random numbers and device-independent quantum key distribution.

References

[1] B. Hensen et al., Nature **526**, 682 (2015); M. Giustina et al., Phys. Rev. Lett. **115**, 250401 (2015); L.K. Shalm et al., Phys. Rev. Lett. **115**, 250402 (2015).

[2] J. Hofmann et al., *Heralded entanglement between widely separated atoms*, Science **337**, 72 (2012).

[3] F. Henkel et al., Highly Efficient State-Selective Submicrosecond Photoionization Detection of Single Atoms, Phys. Rev. Lett. **105**, 253001 (2010).

Interaction effect on the thermodynamic parameters of rotating condensate boson

Ahmed S. Hassan, Azza M. El-Badry

Department of Physics, Faculty of Science, Minia University, El Minia, Egypt

Recently Bose-Einstein condensation becomes a model system for the study of vortex matter. Quantized vortices play a key role in many physical branch, such as superfluidity and superconductivity. Many open questions remain, predominantly related to exploring the effects of interparticle interactions on the behaviour of these systems under different circumstances [1]. These include, but are not limited to:

In this work a conventional semiclassical approach, Hartree-Fock approximation, is used to investigate the interaction effect on the temperature dependence of the thermodynamic parameters. We calculate the condensate fraction, entropy, heat capacity, effective *in situ* radii, Moment of inertia and vortices number is considered. The obtained results provide useful qualitative theoretical results for future Bose Einstein condensation experiments in a rotating traps [2].

References

[1] S. Stringari, Phys. Rev. Lett. **76**, 4725 (1996); S. Kling and A. Pelster, Phys. Rev. A **76**, 023609 (2007); A. L. Fetter, Phys. Rev. A **64**, 063608 (2001). N. R. Cooper, Adv. Phys **57**, 539 (2008); N. Tammuz, R. P. Smith, R. L. D. Campbell, S. Beattie, S. Moulder, J. Dalibard, and Z. Hadzibabic, Phys. Rev. Lett. **106**, 230401 (2011)

[2] J. Abo-Shaeer, C. Raman, J. Vogels, and W. Ketterle, Science **292**, 476 (2001); K. W. Madison, F. Chevy, V. Bretin, and J. Dalibard, Phys. Rev. Lett. **86**, 4443 (2001); P. Haljan, I. Coddington, P. Engels, and E. Cornell, Phys. Rev. Lett. **87**, 210403 (2001).

One-Dimensional Bose-Einstein Condensation of Photons in a Microtube

Alex Kruchkov†
Laboratory for Quantum Magnetism (LQM), École Polytechnique Fédérale de Lausanne (EPFL), Station 3, CH-1015 Lausanne, Switzerland

This study [1] considers a quasiequilibrium one-dimensional Bose-Einstein condensation of photons trapped in a microtube. Light modes with a cut-off frequency (a photon's "mass") interact through different processes of absorption, emission, and scattering on molecules and atoms. In this study, I discuss the conditions for the one-dimensional condensation of light and the role of photon-photon interactions in the system. The technique in use is the Matsubara's Green's functions formalism modified for the quasiequilibrium system under study.

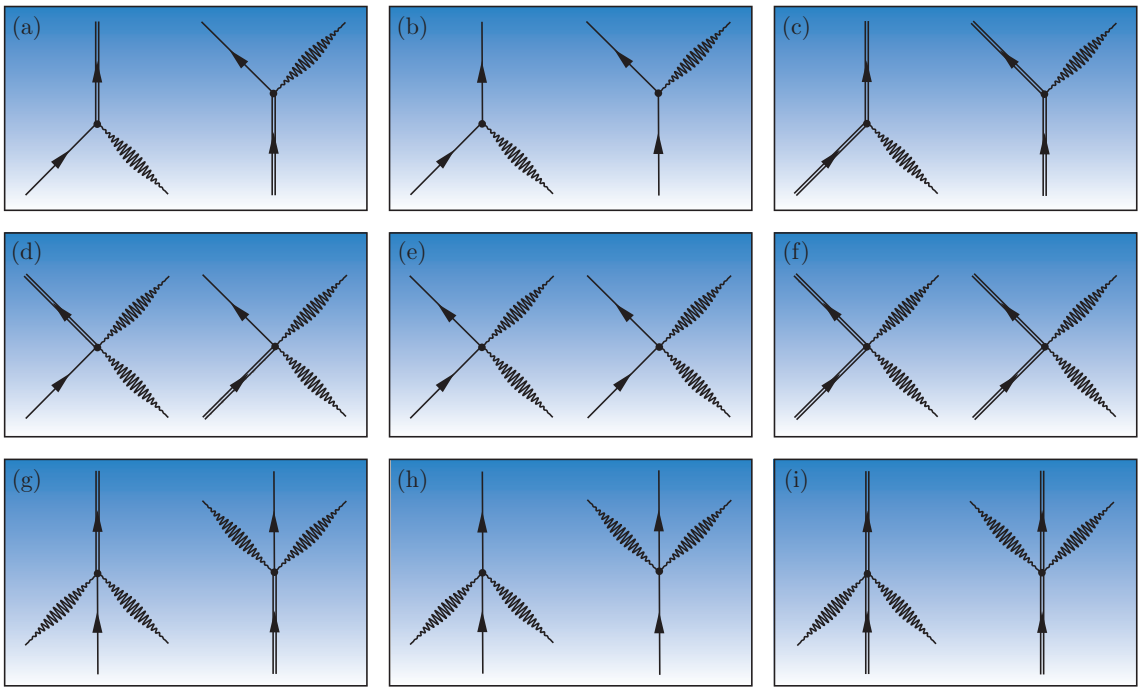

Figure 1: Photon-atom interaction processes (up to the first order in fine structure constant): (a)-(c) One-photon processes; (d)-(i) Two-photon processes. A single line designates a ground-state atom; a double line designates an excited-state atom; a curly line designates a photon.

In 2010, the group of German physicists led by M.Weitz reported an observation of quasiequilibrium Bose-Einstein condensate (BEC) of light in a flat cavity [2,3], and recently the experiment was reproduced by an independent group led by R.Nyman [4]. What is important, is that in these studies photons behave as effectively two-dimensional particles and under some conditions they can condense. The impact of these experiments was quite high, motivated by possible applications of the BEC of light both as a new light source and as an intermediate step in the efficient conversion mechanism of light energy in solar cells. However, the choice of the systems is so far restricted to the microcavity with spherically curved walls, where the condensation of photons happens in the two-dimensional reciprocal space [2-5].

In this study [1], I consider the one-dimensional condensation of photons. As it follows from my calculations, it can be observed in a long microtube with a specific shape under certain conditions. This results will be of interest both for the experimentalists and theorists.

References

†Email: alex.kruchkov@epfl.ch

[1] A. Kruchkov, Phys. Rev. A [accepted 11-03-2016].
[2] J. Klaers, J. Schmitt, F. Vewinger, and M. Weitz, Nature, 468 (2010) 545.
[3] J. Klaers, J. Schmitt, T. Damm, F. Vewinger, M. Weitz, Applied Physics B, 105, 1 (2011).
[4] J. Marelic and R. A. Nyman, Phys. Rev. A 91 033813 (2015).
[5] A. Kruchkov, Phys. Rev. A 89, 033862 (2014).

Stable vortex solitons in microwave-coupled atomic condensates

Guangjiong Dong

State Key Laboratory of Precision Spectroscopy, East China Normal University, Shanghai, China

Stable quantum solitons with large values of embedded vorticity S are not only a subject of fundamental interest, but are also required by various applications, such as quantum information processing and storage, and rotation sensing. However, in conventional atomic Bose-Einstein condensates (BECs) vortex solitons with S>1 cannot be stable. Here, we demonstrate that robust solitons with any S (at least, up to 5) can be created in the trap- and rotation-free two-dimensional space by means of the local-field effect (the feedback of BEC on the propagation of electromagnetic waves) in a condensate of two-level atoms coupled by a microwave (MW) field, as well as in a gas of MW-coupled fermions with spin 1/2. Furthermore, the vortex solitons remain stable in the presence of arbitrarily strong repulsive contact interactions (in that case, solitons can be constructed by means of the Thomas-Fermi approximation), as well as under moderately strong attractive contact interactions (ACI) between the atoms (which, by itself, would lead to collapse). We find, in numerical and analytical forms, a threshold strength of the ACI up to which the stable solitons exist. The solitons with higher S are more robust against the ACI-induced collapse. When the ACI strength is close to the threshold value, an internal mode is readily excited in the solitons.

Spinor quantum gases with narrow-line control

M. Robert-de-Saint-Vincent[1,2], **E. Maréchal**[1,2], **P. Pedri**[2,1], **L. Vernac**[2,1], **O. Gorceix**[2,1], **B. Laburthe-Tolra**[1,2]
1. CNRS, UMR 7538, Laboratoire de Physique des Lasers, 99 avenue Jean-Baptiste Clément, F-93430 Villetaneuse, France
2. Université Paris 13, Sorbonne Paris Cité, LPL, 99 avenue Jean-Baptiste Clément, F-93430 Villetaneuse, France

Degenerate atomic gases provide a new realization of magnetic systems, which permits to revisit questions encountered in condensed matter while also providing access to a new range of physical situations. Alkali-earth species combine the attractive properties of large-spin fermionic isotopes, and of narrow spectroscopic lines commonly used in the context of metrology. Our project aims at taking full advantage of the spectroscopic properties of Strontium 87 to study the many-body physics of a 10-component spinor fermionic gas in lattice geometry [1]. In particular, the 7 kHz wide ${}^1S_0 \rightarrow {}^3P_1$ transition will be used for a state transfer and detection method marrying single site selectivity with full spin sensitivity. The mHz wide "clock" transition ${}^1S_0 \rightarrow {}^3P_0$ offers prospects for the optical control of interactions [2] and for the preparation of metastable magnetic impurities [3]. The optical frequency reference from the optical clocks at Observatoire de Paris, disseminated to Laboratoire de Physique des Lasers through a fiberized link [4], will permit to assess the frequency stability of the laser sources involved in narrow-line control of this many-body system. In parallel to experimental progresses, we will introduce theoretical considerations on the production of correlated magnetic systems by direct cooling of the magnetic degree of freedom.

References

[1] A. V. Gorshkov, M. Hermele, V. Gurarie, C. Xu, P. S. Julienne, J. Ye, P. Zoller, E. Demler, M. D. Lukin, and A. M. Rey, Nature Phys. **6**, 289-295 (2010).
[2] P. O. Fedichev, Y. Kagan, G. V. Shlyapnikov, and J. T. M. Walraven, Phys. Rev. Lett. **77**, 2913 (1996).
[3] M. Foss-Feig, M. Hermele, and A. M. Rey, Phys. Rev. A **81**, 051603(R) (2010).
[4] F. Kéfélian, H. Jiang, P. Lemonde, and G. Santarelli, Opt. Lett. **34**, 1575-1575 (2009).

Coulomb-Explosion Imaging of Ultracold ^{6}Li Molecules using Intense Laserpulses

Niels Kurz[1], **Christoph Bogda**[1], **Thomas Pfeifer**[1], **Alexander Dorn**[1]
1. Max-Planck-Institute for Nuclear Physics, Saupfercheckweg 1, 69117 Heidelberg, Germany

This project aims to develop a new experimental imaging technique for studying few-body physics in ultracold Fermi gases. Therefore, a fermionic sample of ^{6}Li atoms will be prepared in an optical dipole trap. Adjusting the interaction strength of the atoms via a Feshbach resonance to positive values leads to the binding of atom pairs in different spin-states to bosonic molecules. In this way a molecular BEC of weakly bound ^{6}Li dimers is formed. The spatial size of the molecules can be tuned in the vicinity of the Feshbach resonance from a few up to ten thousand Bohr radii. The inter-atomic distance distribution will be measured by Coulomb explosion imaging (CEI). Therefore, an intense femtosecond laser pulse is focused into the ensemble ionizing both atoms of the dimer. From their repulsion the ions will gain kinetic energy which will be measured and allows to conclude on their initial separation at the instant of ionization. For this purpose a recoil ion momentum spectrometer is used where all the ions are imaged onto time- and position-sensitive detectors such that their momentum vectors can be reconstructed as it is routinely done for atomic ionization reactions using reaction microscopes or the COLTRIMS technique. With a momentum resolution better than 0.05 a.u. for an ultra cold target gas in a small source volume, we expect to be able to resolve spatial separations of a few micrometers and below.

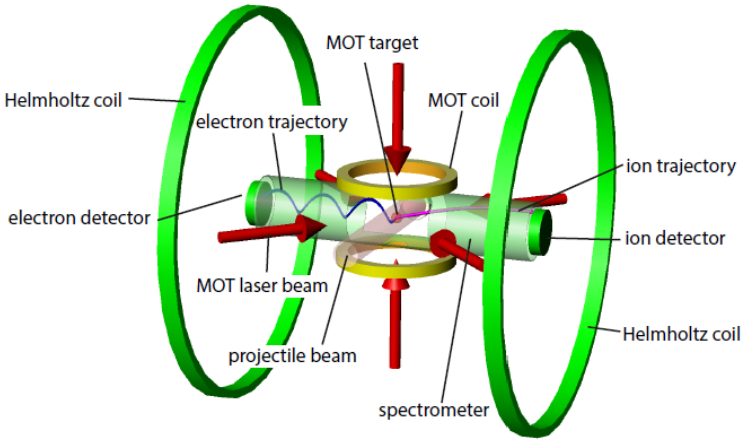

Fig. 1 Schematic of a MOT Remi, i.e. a recoil ion spectrometer with a cloud of cold atoms as a target, trapped in a magneto-optical trap (MOT). After successful MOT trapping, the atoms will be transferred to an optical dipole trap to further cool the atomic sample by evaporative cooling.

A further prospect of cold atomic samples of ^{6}Li atoms in a reaction microscope is the possibility of RF association of Efimov trimers [1] and subsequent use of CEI to directly map their geometrical structure. In principle this method can be applied to study the physics of arbitrary few particle fermion systems which can be produced deterministically, e.g., in optical microtraps using the so-called spilling technique [2].

References

[1] T. Lompe, T. B. Ottenstein, F. Serwane, A. N. Wenz, G. Zürn and S. Jochim, Science **330**, 6006, (2010).
[2] F. Serwane, G. Zürn, T. Lompe, T. B. Ottenstein, A. N. Wenz and S. Jochim, Science **332**, 6027 (2011).

Experimental and theoretical studies of three different EIT-type resonances formed in a nanocell containing ^{87}Rb vapor

Arevik Amiryan[1,2], Armen Sargsyan[1], Emmanuel Klinger[2], David Sarkisyan[1], Leah Margalit[3], Arlene Wilson-Gordon[3], Yevgenya Pashayan-Leroy[2], Claude Leroy[2]

1. Institute for Physical Research, NAS of Armenia, 0203 Ashtarak-2, Armenia

2. Laboratoire Interdisciplinaire Carnot de Bourgogne, UMR CNRS 6303, Université de Bourgogne - Franche-Comté, 9 avenue Alain Savary, BP 47870, 21078 Dijon Cedex, France

3. Department of Chemistry, Bar-Ilan University, 5290002 Ramat Gan, Israel

The electromagnetically induced transparency (EIT) phenomenon is studied experimentally and theoretically for D_1 line of ^{87}Rb atomic vapor using $L = 795$ nm thickness cell. The EIT resonance is recorded in three different atomic configurations - 1. Λ-system with two hyperfine ground levels, 2. Λ-system realized in Zeeman sublevels and 3. V-system. From all above mentioned configurations the linewidth of the EIT-resonance formed in the Λ-system (where the ground levels are separated with the hyperfine splitting ~ 6835 MHz, denoted as EIT$_H$-resonance) is the smallest ~ 10 MHz [1]. The linewidth of the EIT-resonance realized on the second Λ-system ($F_g = 2 \rightarrow F_e = 1$ Zeeman transition, denoted as EIT$_Z$-resonance) is ~ 14 MHz [2]. The last one, denoted as EIT$_V$-resonance and formed in V-system has the largest linewidth ~ 40 MHz. We demonstrate that EIT phenomena can be formed in different types of Λ-systems even for $L < 1000$ nm thicknesses.

It is also recorded the splitting of the EIT$_Z$-resonance into two components (each with 12 MHz linewidth) in an external transverse magnetic field and presented in Fig.1. The theoretical model calculated for EIT$_Z$ is in a good agreement with the experimental results.

Research conducted in the scope of the Marie Curie International Research Staff Exchange Scheme Fellowship within the 7th EC Framework Programme COSMA and the International Associated Laboratory IRMAS (CNRS-France & SCS-Armenia).

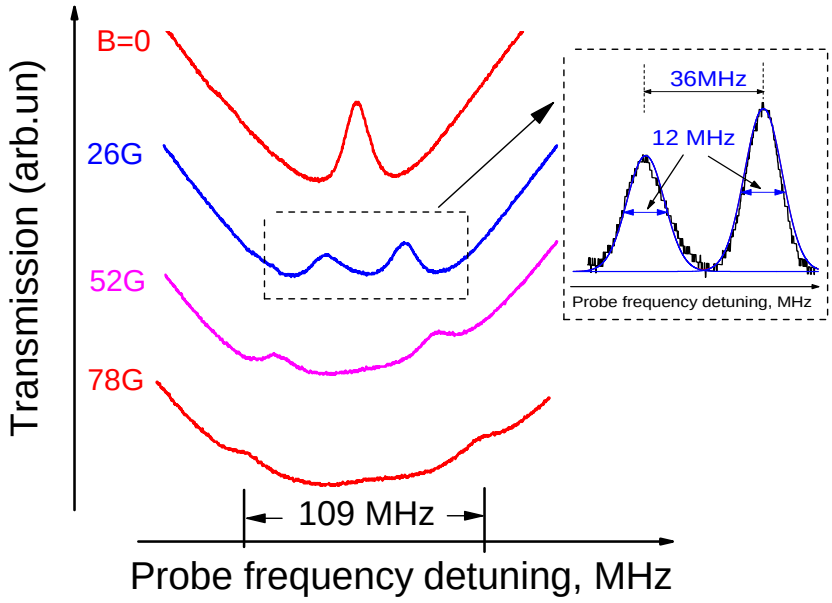

Fig. 1 The splitting of EIT$_Z$ resonance in external magnetic field. In the inset presented the fitting in $B = 26$ G field. Each component has 12 MHz linewidths.

References

[1] Armen Sargsyan, Yevgenya Pashayan-Leroy, Claude Leroy, Stefka Cartaleva and David Sarkisyan, *J. Mod. Opt.*, **62**, (769) (2015).

[2] Nemi Gavra, Michael Rosenbluh, Tzurit Zigdon, Arlene Wilson-Gordon, Harry Friedmann, *Opt. Commun.*, **280**, (374) (2007).

A Sharp Resonance of Collective-Effect Origin in the L-shell Photodetachment from the Negative Silicon Ion

Galina Schrange

St. Petersburg Polytechnical University, Russia, e-mail: gkashenock@yahoo.de

The theoretical investigation on the inner-shell single-photodetachment from the Si^- ($1s^2 2s^2 2p^6 3s^2 3p^3\ ^4S^o$) negative ion will be presented. The partial and total cross sections, the photoelectron phaseshifts, and the parameters of angular anisotropy are calculated in the framework of Many-Body Theory for L-shell photodetachment from Si^- ion in the experimentally accessible range of photon energies (7.5-14 *Ry*). Comparison is made between the calculations of the response of the ionic many-electron system Si^- to an electromagnetic field at the different levels of approximation: the "frozen-field" Random Phase Approximation with Exchange (RPAE), and the static relaxation approximation [1]. The existence of both limits of the "3p↓" state - as a bound state, or Feschbach resonance, in the "frozen-core" approximation and as a quasi-bound state, shape resonance, in the static relaxation approximation - allow us to suppose that the real situation is subtler. The optimal analysis is made when the dynamic relaxation and polarization are included within the Dyson Equation Method (DEM) simultaneously with the RPAE corrections (RPAE&DEM approach [2,3]). It is predicted that the photoexcitation to a resonance state « 3p↓ » of complex "shape-Feschbach" nature in the open p-shell reveals itself as a prominent resonance structure in the photodetachment cross sections in the energy range of the 2s and 2p inner shell thresholds similar to that in the well-studied 1s inner-shell photodetachment from C^- [3,4]. The system Si^- is more complex compared to C^- where the resonance of "shape-Feschbach" hybrid nature is primarily formed by the one-channel contribution. Here we need to consider the partial cross sections for four close spin-polarized inner subshells (six phototransitions): 2p↑→εs↑, 2p↑→ εd↑, 2p↓→εs↓, 2p↓→ εd↓, 2s↑→εp↑, 2s↓→ n,εp↓. The Si^- photodetachment dynamical characteristics clearly demonstrate the significance of all the considered collective effects within the RPAE&DEM approach, however the total photodetachment cross section is dominated by a strong resonance peak just after the 2s threshold (fig.1). Dynamical relaxation (screening) is identified as a decisive factor in the formation of this resonance, however the total response of the whole system is shown to be emphatic collective.

The results provide a convincing demonstration of the importance of representing subtle core-electron correlation effects for near-threshold photodetachment spectra in an understudied ion. The possible experimental evidence for the prominent resonance structure predicted in the present study could be of a great interest.

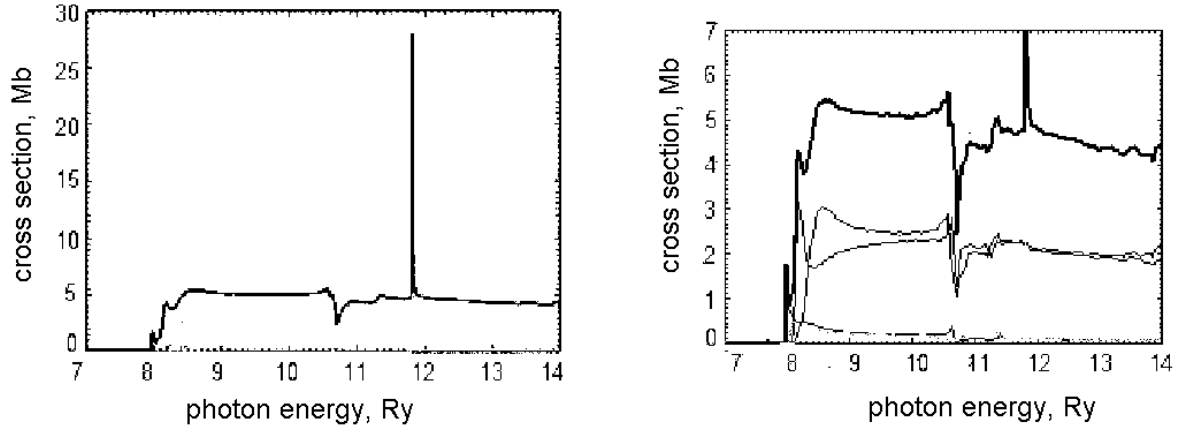

Fig. 1 The results of calculations within the RPAE&DEM approach – the dynamical relaxation, polarization and interchannel interaction are included – the thick line is the total photodetachment cross section. The 2p partial cross sections (thin lines), where the additional peculiarities of the Fano-profile type appear as a result of electronic correlation interaction with the resonance channel 2s↓→ « 3p↓ »,εp↓, are also depicted on the right panel.

References

[1] M.Ya. Amusia, *Atomic Photoeffect*. Plenum Press (1990).
[2] G.Schrange-Kashenock, *Collective Effects in Negative Ion Photodetachment. Many-Body Theory*. LambertAcademicPublishing (2015).
[3] G.Yu.Kashenock and V.K.Ivanov, J.Phys.B: At.Mol.Opt.Phys. **39,** 1379 (2006).
[4] C.W.Walter, N.D.Gibson, R.C.Bilodeau, N.Berrah , J.D.Bozek , G.D.Ackerman and A.Aguilar, Phys.Rev.A **73,** 062702 (2006).

Laser Induced Fluorescence Spectroscopy of Atomic Vanadium in the Wavelength Range of 760 nm to 840 nm

Günay Başar[1], Gönül Başar[2], İpek K. Öztürk[2], Feyza Güzelçimen[2], Alev Er[2], Sophie Kröger[3]

[1]*Istanbul Technical University, Faculty of Science and Letters, Physics Engineering Department, 34469 Maslak, Istanbul, Turkey*

[2]*Istanbul University, Faculty of Science, Physics Department, Tr-34134 Vezneciler, Istanbul, Turkey*

[3]*Hochschule für Technik und Wirtschaft Berlin, Fachbereich 1, Wilhelminenhofstr. 75A, D-12459 Berlin, Germany*

This work is a continuation of investigation about hyperfine structure on atomic vanadium (VI) [1-3]. In the previous studies [1-3] Fourier transform spectra have been analysed, whereas in the present work laser spectroscopic method is applied.

Vanadium is one of the iron-group elements which are important for astrophysics. The spectrum of V is characterized by a broad hyperfine structure caused by the large nuclear magnetic dipole moment of the stable isotope ^{51}V with nuclear spin of $I = 7/2$ and natural abundance 99%.

Laser induced fluorescence spectroscopy was applied to investigate the hyperfine structure of selected spectral lines of atomic vanadium in the wavelength range from 760 nm to 840 nm. Experiments were performed in the Laser Spectroscopy Laboratory of the Istanbul University by using a tunable single mod Ti:Sa laser (MBR-110, Coherent, output power of 4 W) which is pumped with a cw solid state laser (Verdi 18 W). The relative frequency reference is acquired by a home-made temperature stabilized confocal Fabry-Perot Interferometer with a free spectral range of 299.0010 (8) MHz. A hollow cathode discharge lamp cooled with liquid nitrogen running with a current about 60-70 mA in a Ne atmosphere of 1.3 mbar was used to evaporate vanadium and to excite the freeV atoms.

The hyperfine structure of altogether 20 transitions have been measured. All lines have already been listed and classified in the wavelength list of Thorne [4]. The spectral profiles of all lines were fitted with Voigt profiles using the program Fitter [5] in order to obtain the magnetic dipole hyperfine constants A of upper and lower levels. As results of this work, new experimental magnetic dipole hyperfine structure constants A and electric quadrupole hyperfine structure constants B will be presented.

References

[1] Güzelçimen F., Başar Gö., Öztürk I.K., Kröger S., Ferber R., Jarmola A., Tamanis M., Başar Gü., *Hyperfine Structure of the 3d34s4p 6G Multiplet of Atomic Vanadium,* Journal of Physics B: Atomic, Molecular and Optical Physics, **44**, 21 (2011)

[2] Güzelçimen F., Yapıcı B., Demir G., Er A., Öztürk I.K., Başar Gö., Kröger S., Tamanis M., Ferber R., Docenko D., Başar Gü., *Hyperfine Structure Constants of Energetically High-Lying Levels of Odd Parity of Atomic Vanadium,* The Astrophysical Journal Supplement Series, **214**, 1 (2014)

[3] Güzelçimen F., Er A., Öztürk I.K., Başar Gö., Kröger S., Tamanis M., Ferber R., *Investigation of the Hyperfine Structure of Weak Atomic Vanadium Lines by Means of Fourier Transform Spectroscopy,* Journal of Physics B: Atomic, Molecular and Optical Physics, **48**, 11 (2015)

[4] Thorne, A. P., Pickering, J. C., Semeniuk, J., *The Spectrum and Term Analysis of V I,* The Astrophysical Journal Supplement Series, **192**, 11 (2011)

[5] Guthöhrlein G., *Program Fitter*, University of Bundenswehr Hamburg (unpublished) (2004)

Measurement of the pion mass from X-ray spectroscopy of exotic atoms

M. Trassinelli[1], D. F. Anagnostopoulos[2], G. Borchert[3], A. Dax[4], J.-P. Egger[5], D. Gotta[3], M. Hennebach[3], P. Indelicato[6], Y.-W. Liu[4], B. Manil[6], N. Nelms[7], L. M. Simons[4], A. Wells[7]

1. Institut des NanoSciences de Paris, CNRS, Sorbonne Universités UPMC Univ Paris 06, Paris, France
2. Dept. of Materials Science and Engineering, University of Ioannina, Ioannina, Greece
3. Institut für Kernphysik, Forschungszentrum Jülich GmbH, Jülich, Germany
4. Laboratory for Particle Physics, Paul Scherrer Institut, Villigen PSI, Switzerland
5. Institut de Physique de l' Université de Neuchâtel, Neuchâtel, Switzerland
6. Laboratoire Kastler Brossel, CNRS, Sorbonne Universités UPMC Univ. Paris 06, ENS, Paris, France
7. Dept. of Physics and Astronomy, University of Leicester, Leicester, England

X-ray spectroscopy of exotic atoms allows the determination of the mass of short-lived negatively charged unstable particle like muons, pions, or kaons from the energies of characteristic X-ray radiation. Pions are captured by the target atoms in a highly excited state and a de-excitation cascade takes place accompanied by Auger and radiative emission. Auger emission is dominant at the beginning of the cascade process, with the shell by shell ejection of the electrons, when the X-ray emission take place mainly for lower level de-excitation. The mass of the pion is extracted by the accurate measurement of X-ray photons corresponding to transitions between levels neither affected by strong-interaction effects nor by remaining electrons. The best conditions are found in the medium part of medium Z atoms which corresponds to the few keV range for X-ray transitions.

The actual reference value of the pion mass from the Particle Data Group [1] has an accuracy of 2.5 parts per million (ppm) and is based on two high-accuracy crystal spectroscopy of pionic magnesium and pionic nitrogen. In the case the πMg, the use of a solid target induces a continuous electron refilling during the de-excitation cascade and an assumption on the number of remaining electrons has to be done to extract the pion mass value from the $(4f-3d)$ transition energy measurement [2]. This is not the case when a gaseous target is used as in the measurement of πN atoms where the $(5g-4f)$ energy transition was measured with respect to Cu Kα fluorescence radiation [3]. In this case, the accuracy was limited by the complex structure of the broad copper calibration line.

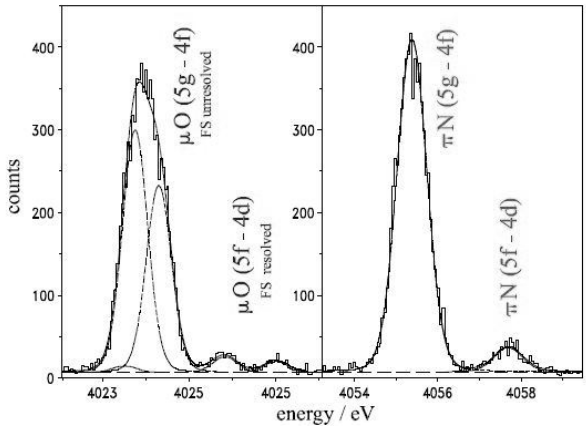

Fig. 1 $(5g-4f)$ transitions in muonic oxygen (calibration) and pionic nitrogen obtained by the X-ray spectrometer equipped with a bent silicon crystal.

Here we present a new experiment performed at the Paul Scherrer Institut that resumes the strategy of the gas target measuring the πN $(5g-4f)$ transition but exploiting the almost coinciding narrower μO $(5g-4f)$ transition as reference. With an uncertainty of 0.033ppm, the mass of the muon provides a very high accuracy of the reference energy (1 meV). The πN and μO transitions are measured simultaneously with a Johann-type spectrometer equipped with a spherically bent Si(220) crystal and a dedicated array of 6 x-ray CCDs. The simultaneous measurement minimizes possible systematic shifts during the unavoidably long measuring periods. Pionic and muonic atoms are formed in a gas cell containing an O_2/N_2 mixture and positioned inside the cyclotron trap. The muons stem from pion decay. A new value of the pion mass is obtained with an uncertainty of 1.3ppm, half of the world average value [4]. The final accuracy is limited only by statistics due to the limited production of muonic atoms and line broadening from Coulomb explosion.

References

[1] K.A. Olive and Particle Data Group, Chinese Physics C, **38**, 090001 (2014).
[2] B. Jeckelmann *et al.*, Phys. Rev. Lett., **56**, 1444-1447 (1986), B. Jeckelmann *et al.*, Phys. Lett. B, **335**, 326-329 (1994).
[3] S. Lenz *et al.*, Phys. Lett. B, **416**, 50-55 (1998).
[4] M. Trassinelli *et al.*, in preparation for Phys. Lett. B.

Relative intensities of M-x-ray satellite lines by electron impact ionization

Takeshi Mukoyama
Institute for Nuclear Research of the Hungarian Academy of Sciences (ATOMKI), Bem tér 14/c, H-4026 Debrecen, Hungary

Since early days of x-ray spectroscopy extensive investigations for K- and L-shell x-ray emission spectra have been performed both theoretically and experimentally. On the other hand, studies on M-x-ray spectra are rather scarce because of low fluorescence yields and of complex structure of emission lines. For M-shell ionization, the primary vacancy created in one of M subshells can migrate to other M subshells through Coster-Kronig (CK) transitions. This fact makes it complicate to analyze experimental data and we need knowledge of some atomic parameters, such as CK coefficients, subshell fluorescence yields, and radiative level widths.

With advance in x-ray spectrometers and strong radiation sources, experimental measurements for M-x-ray emission spectra have been reported. However, most of them are restricted only for diagram lines and the number of experimental studies on M-x-ray satellite lines has not been so large. Recently Limandi *et al.* [1] observed the satellite lines in Mα and Mβ spectra for heavy elements by electron impact ionization and measured relative intensities and energies of the satellite lines. These satellite lines are considered due to the vacancy transition from the M subshell to the N subshell with additional vacancies in N subshells. In the case of soft collisions, such as low-energy electron impact ionization, the mechanisms for production of such additional vacancies can be ascribed to the following two reasons, (1) electron shakeoff and shakeup processes following M-shell ionization and (2) the Auger and CK transitions during decay of the initial vacancy.

In the present work, the theoretical model for relative intensity of $L\beta_2$ satellite line for photoionization with synchrotron radiation [2] was extended to the case of M-shell satellite lines by electron impact. From the experimental energy shifts of the satellite lines, we assumed that only one additional vacancy exists in one of N subshells. The x-ray intensities of the Mα and Mβ diagram and satellite lines by 15-keV electron impact were calculated and the intensity ratios of satellite lines to diagram lines were obtained for Bi and Th. For this purpose, M-subshell ionization cross sections by electron impact were calculated with the analytical expression of Bote *et al.* in the distorted Born approximation [3]. The total N-shell shakeoff and shakeup probabilities accompanying M-subshell ionization were obtained from the tables of Mukoyama [4]. The CK coefficients and the M-subshell fluorescence yields were taken from the tabulated values by Chauhan and Puri [5] and by McGuire [6]. The total subshell radiative widths and the partial widths for Mα and Mβ x-ray emission in Bi and Th were calculated with the Dirac-Fock-Slater method [7]. The change in the subshell fluorescence yields due to additional N-shell vacancy was taken into account for satellite intensities.

Table 1 Calculated relative intensities of M-x-ray satellite lines for Bi and Th produced by 15-keV electron impact are compared with the experimental values of Limandi *et al*. [1].

Element	E (keV)	Mα		Mβ	
		Exp	Cal	Exp	Cal
Bi	15	0.270 ± 0.007	0.241	0.19 ± 0.04	0.179
Th	15	0.201 ± 0.007	0.244	0.16 ± 0.02	0.168

The calculated relative intensities of the Mα and Mβ satellite lines for Bi and Th are shown in Table 1 and compared with the experimental values of Limandi *et al.* [1]. The present results are in good agreement with the experimental values of Mβ satellite lines both for Bi and Th. In the case of Mα satellite the calculated value is slightly smaller than the measured one for Bi and larger for Th.

References

[1] S. P. Limandi, J. C. Trincavoelli, R. D. Bonettto, and A. C. Carreras, *Structure of the Pb, Bi, Th, and U M x-ray spectra*, Phys. Rev. A **78**, 022518 (2008).
[2] H. Oohashi, Y. Ito, T. Tochio, A. M. Vlaicu, and T. Mukoyama, *Evolution of Au $L\beta_2$ visible satellites around thresholds*, Phys. Rev. A **73**, 022507 (2006).
[3] D. Bote, F. Salvat, A. Jablonski, and C. J. Powell, *Cross sections for ionization of K, L and M shells of atoms by impact of electrons and positrons with energies up to 1 GeV: Analytical formulas*, At. Data Nucl. Data Tables **95**, 871 (2009).
[4] T. Mukoyama, *Electron shake probabilities of heavy elements as a result of M-shell vacancy production*, X-Ray Spectrom. **44**, 7 (2015).
[5] Y. Chauhan and S. Puri, *M_i (i=1-5) subshell fluorescence and Coster-Kronig yields for elements with $67 \leq Z \leq 92$*, At. Data Nucl. Data Tables **94**, 38 (2008).
[6] E. J. McGuire, *M-shell Auger and Coster-Kronig Electron Spectra*, Phys. Rev. A **5**, 1052 (1972).
[7] T. Mukoyama and H. Adachi, *M-shell X-ray emission rates for rare earth elements*, J. Phys. Soc. Jpn **53**, 984 (1984).

Cavity-enhanced frequency up-conversion in rubidium vapour

Rachel F. Offer[1], Johnathan W. C. Conway[1], Erling Riis[1], Sonja Franke-Arnold[2], Aidan S. Arnold[1]

1. Department of Physics, SUPA, University of Strathclyde, Glasgow G4 0NG, UK

2. School of Physics and Astronomy, SUPA, University of Glasgow, Glasgow G12 8QQ, UK

The resonant enhancement of nonlinear processes in atomic vapours allows efficient wave mixing to be carried out even with low intensity, continuous wave, pump beams. In rubidium vapour, four wave mixing can be used to frequency up-convert near-infrared light (780 and 776 nm) to blue light (420 nm) [1-4]. We report the first use of a ring cavity to both enhance the output power and dramatically narrow the linewidth of blue light generated by four wave mixing in a rubidium vapour cell.

For a single pass, 780 nm and 776 nm pump beams can be converted to 420 nm light, with conversion efficiencies of up to 260 %/W reported [4]. We have recently investigated, for the first time, the effect of adding a ring cavity to this system [5]. We find that a low finesse cavity, singly resonant with the blue light, not only more than doubles the blue output power, but also significantly narrows the linewidth of the blue light produced. Figure 1 (a) compares the single pass and cavity-enhanced blue output power as a function of pump laser detuning. With the cavity, the output power more than doubles when the blue light, whose frequency scans with the pump laser, is resonant with the cavity. There is additional scope for increasing the cavity-enhanced output power by reducing the large parasitic losses (around 20%) in our current ring cavity. The linewidth of the generated blue light, measured by performing a beat note with a 420 nm laser, is shown in figure 1 (b). For a single pass the generated blue light has a significantly power broadened linewidth of around 33 MHz. With the cavity however, this is narrowed to < 1MHz. Unlike the single pass setup, the cavity allows high output power and narrow linewidth to be achieved concurrently.

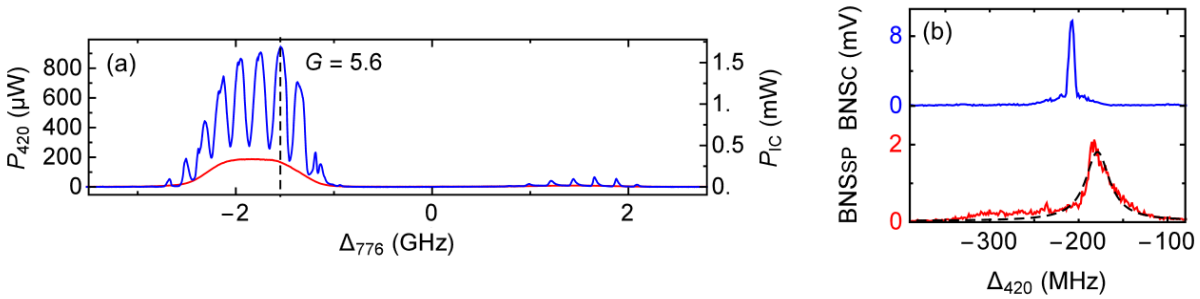

Fig. 1 (a) Blue output power as a function of 776 nm pump detuning for a single pass (red) and with the cavity (blue). (b) Beat note of the generated blue light against a 420 nm ECDL for a single pass (red) and with the cavity (blue). Offer et. al. 2016 [5]

We have also shown that the generated blue light is widely tunable over the ^{85}Rb $5S_{1/2}$ to $6P_{3/2}$ transitions. As a result we suggest that this light source would have applications in ultracold atomic gases, for example in second-stage laser cooling of rubidium, or for enhanced resolution imaging. Furthermore, for single pass four wave mixing, it has been demonstrated that transverse phase structure, for example orbital angular momentum, can be transferred between the near-IR pump beams and the generated blue light [6]. Our ring cavity may allow this process to be carried out more efficiently, which would be important for applications such as higher dimensional quantum information processing.

References

[1] A. S. Zibrov, M. D. Lukin, L. Hollberg, and M. O. Scully, *"Efficient frequency up-conversion in resonant coherent media,"* Phys. Rev. A **65**, 051801 (2002).

[2] A. M. Akulshin, R. J. McLean, A. I. Sidorov, and P. Hannaford, *"Coherent and collimated blue light generated by four-wave mixing in Rb vapour."* Opt. Express **17**, 22861–22870 (2009).

[3] T. Meijer, J. D. White, B. Smeets, M. Jeppesen, and R. E. Scholten, *"Blue five-level frequency-up conversion system in rubidium."* Opt. Lett. **31**, 1002–1004 (2006).

[4] A. Vernier, S. Franke-Arnold, E. Riis, and A. S. Arnold, *"Enhanced frequency up-conversion in Rb vapor."* Opt. Express **18**, 17020–17026 (2010).

[5] R. F. Offer, J. W. C. Conway, E. Riis, S. Franke-Arnold, A. S. Arnold, *"Cavity-enhanced frequency up-conversion in rubidium vapour."* Opt. Lett **41**, 2177-2180 (2016).

[6] G. Walker, A. S. Arnold, and S. Franke-Arnold, *"Trans-spectral orbital angular momentum transfer via four-wave mixing in Rb vapor,"* Phys. Rev. Lett. **108**, 243601 (2012).

Zeeman resolved spectra of rubidium 5*S*-5*D* two-photon excitation

Yuta Komiyama[1], Takuma Ito[1], Taro Mashimo[1], Kosuke Shibata[1], Satoshi Tojo[1]
1. Department of Physics, Chuo University, 1-13-27 Kasuga, Bunkyo, 112-8551, Tokyo, Japan.

Two-photon transition spectroscopy is one of powerful tools for observation of non-linear phenomena, which is applied for localized spaces with Doppler free measurement [1]. Recently, non-linear phenomena including collision broadenings observed in Rb two-photon spectra in the condition of high density of atoms [2].

We study two-photon spectroscopy in the high-power excitation regime which makes novel quantum conditions, such as dressed states of atoms with the strong laser field. The atoms are excited from the $5S_{1/2}$ ground state to the $5D_{5/2}$ excited state via off-resonant $5P_{3/2}$ state. We observe the fluorescence at 420 nm of 6*P*-5*S* transition from the 5*D*-6*P* cascade decay as shown Fig. 1 (a). In order to observe intensity dependence, the laser intensity is controlled in the range from 50 to 300 mW. We confirm that the signal intensity of the two-photon transition spectra are proportional to the square of the excitation laser intensity. Zeeman splitting exposed to magnetic field resolve a degeneracy of hyperfine structure [3].We derive the two-photon spectra with magnetic sublevels resolved by Zeeman splitting under an applied magnetic field in the range from 0 to 42 G. Figure 1 (b) shows two-photon transition spectra in a homogeneous magnetic field of 9 G and exciting laser intensity of 100 mW at the temperature of 357 K.

We observe line broadning and frequency shift and estimate the broading due to the power broadening effect. We have found the observed line broadenings and the light shift can be quantitatively explained by laser power broadening and different coupling strength of magnetic sublevels, respectively. In addition we will also report on the Zeeman and Paschen-Back effects of the two-photon transition by changing in the applyed magnetic field strength and the light intensity.

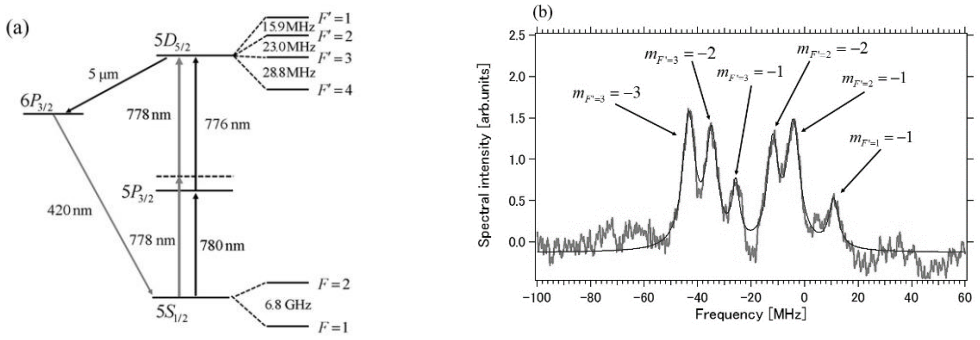

Fig. 1 (a) Energy level diagram for ^{87}Rb in $5S_{1/2} - 5D_{5/2}$ excitation. (b) Zeeman spectra $5S_{1/2}$ ($F = 1$) – $5D_{5/2}$ ($F' = 1, 2, 3$) with magnetic sublevels resolved.

References

[1] A. J. Olson, E. J. Carlson and S. K. Mayer, Am. J. Phys. **74**, 218-223 (2006).
[2] F. Nez, F. Biraben, R. Felder, and Y. Millerioux, Opt. Comm. **102**, 432-438 (1993).
[3] L. Windholz and M. Musso, Z. Phys. D **8**, 239-249 (1988).

Specific Excitation at the Stereocenter of the Chiral Molecule Halothane

Martin Pitzer[1,2], Phillip Burzinsky[1], Gregor Kastirke[1], Miriam Weller[1], Markus Waitz[1], Daniel Metz[1], Jonathan Neff[1], Till Jahnke[1], Reinhard Dörner[1], Markus Schöffler[1]

1. Institut für Kernphysik, Goethe-Universität, Max-von-Laue-Str. 1, 60438 Frankfurt am Main, Germany
2. Experimentalphysik IV, Universität Kassel, Heinrich-Plett-Str. 40, 34132 Kassel, Germany

Determining the absolute configuration of chiral molecules, i.e. their microscopic handedness, is still a challenge for many species. For several decades, anomalous X-ray diffraction as introduced by Bijvoet et al. [1] had been the only method for this purpose that did not rely on theoretical input or semi-empirical rules. Recently, Coulomb Explosion Imaging has been shown to be a promising approach for the direct determination of small molecules' absolute configuration [2,3]. For this technique, the molecule is multiply ionized within a time-scale that is short compared to structural changes. The positively charged ion cores subsequently repel each other due to Coulombic forces so that their momentum vectors carry information on the initial structure. This momentum vectors can be measured for single molecules in coincidence, e.g. with a COLTRIMS setup (Cold Target Recoil Ion Momentum Spectroscopy) [4].

In this contribution, we extend the method to the chiral ethane derivative halothane ($CF_3CHClBr$). Its increased complexity is an important step to test the method's suitability for larger molecules. Multiple ionization was induced by single-photon excitation at the energy of the carbon K-shell and subsequent relaxation processes. We compare various fragmentation pathways in order to investigate which break-ups carry a signature of handedness and to evaluate their reliability for the determination of absolute configuration.
In addition, the different halogenes attached to the carbon atoms lead to significant energy shifts of the respective carbon K-shell. This enables us to post-select the primary ionization site via the photoelectron energy and to compare fragmentation patterns for the photo-ionization of the two different carbon atoms. These results help to identify ionization energies and fragmentation pathways that are promising for the determination of absolute configuration of larger molecules.

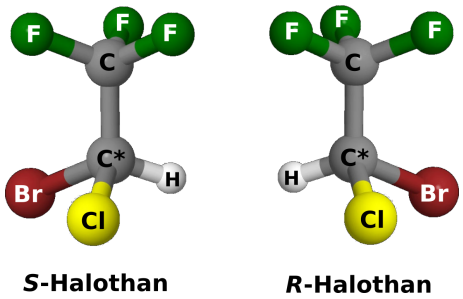

Fig. 1 Structure model of the *S*- and *R*-Enantiomers of Halothan. The stereocenter is marked with an asterisk.

References

[1] J.M. Bijvoet, A.F. Peerdeman, and A.J. van Bommel *Determination of the Absolute Configuration of Optically Active Compounds by means of X-rays*, Nature **168**, 271 (1951).
[2] M. Pitzer, M. Kunitski, et al. , *Direct Determination of Absolute Molecular Stereochemistry in Gas Phase by Coulomb Explosion Imaging*, Science **341**, 1096 (2013).
[3] Ph. Herwig, K. Zawatzky, et al. , *Imaging the Absolute Configuration of a Chiral Epoxide in the Gas Phase*, Science **342**, 1084 (2013).
[4] R. Dörner, V. Mergel, et al. , *Cold Target Recoil Ion Momentum Spectroscopy: a 'momentum microscope' to view atomic collision dynamics*, Phys. Rep. **330**, 95 (2000).

Study of Selenium Molecular Beam by Electron Impact

Anatoly Zavilopulo, Otto Shpenik, Pavlo Markush, Olha Pylypchynets

Institute of Electron Physics, Ukrainian National Academy of Sciences, Universitetska str. 21, Uzhgorod, 88017 Ukraine, e-mail: gzavil@gmail.com

This study was aimed at obtaining new data on the process of formation of selenium ions at electron ionization of selenium molecular beam by mass spectrometry at different temperatures of the initial material evaporation and energies of the bombarding electrons. For this purpose we performed a detailed investigation of mass spectra of selenium molecular beam in the temperature range T = 420–500 K and measured energy dependences of the ion formation. The experiment was carried out at a setup using an MX 7304A monopole mass spectrometer as an analytical device with the mass resolution better than ΔM = 1 Da [1]. The selenium molecular beam was formed by an effusion type source providing the concentration of molecules in the region of intersection with the electron beam in the range of 10^{10}–10^{11} cm^{-3}. The ion source with electron ionization was operating in electron current stabilization mode and enabled the electron beams with fixed energy of 5 to 90 eV at currents of 0.05 – 0.5 mA and the energy spread ΔE = 300 meV to be obtained. The mass scale calibration was performed for Ar and Xe isotopes, and the electron energy scale was calibrated using the initial part of the atomic ionization cross sections of Kr atom and N_2 molecule. The experiment was carried in two stages: first the mass spectra were studied, and at the second stage the energy dependences of relative cross sections of dissociative ionization were measured.

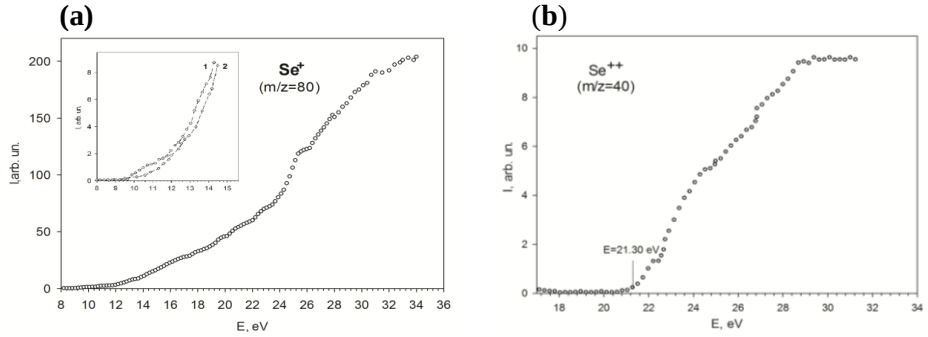

Fig. 1 Ionization efficiency curves for Se^+ ions (left panel, the inset showing comparison our data for the initial part of Se relative ionization cross section (**1**) with those of Viswanathan et al [2] (**2**)) and Se^{2+} ions (right panel).

After configuring the mass spectrometer for the separation of a certain mass, relative cross-sections of formation of different selenium ions in Se^{n+} (n = 1–4) were measured from the process threshold to 36 eV. The energy dependences of formation of Se^+ and Se^{2+} ions are shown in Fig. 1. The possible channels of Se formation are the following:

electron ionization of the selenium atom: $Se + e^- = Se^+ + 2e^-$ (1)

dissociative ionization of selenium molecules: $Se_n + e^- = Se^+ + Se_{n-1} + 2e^-$. (2)

Selenium atoms in the gaseous state appear at temperatures above 700 K, hence at our experimental conditions (T = 420–500 K) their concentration is low. This means that the formation of Se^+ ions at such conditions basically follows the reaction (2) due to the processes of dissociative ionization of Se_5–Se_7 molecules similarly to the processes studied earlier for sulfur [1]. The general trend of the threshold area for Se^+ is similar to the data of [2]; however, we observed two small steps at 10.50 and 11.40 eV which may arise as a result of dissociative decay and excitation [3] of certain molecular components, or due to the onset of the autoionization channel in the dissociation process. We first measured the relative ionization cross section of doubly charged selenium ion Se^{2+} (Fig. 1), the most probable channel of its formation being the reaction (1). Features at 22.5, 24.8, and 26.8 eV observed in the ionization efficiency curve, evidence for the onset of an additional dissociation channel resulting in this ion formation. From the threshold segments of the energy dependences, using the least square method we determined the appearance energies for the Se^+ (E=9.81 eV), Se_2^+ (E=9.04 eV), Se_3^+ (E=10.35 eV), Se_4^+ (E=10.25 eV), and Se^{2+} (E=21.30 eV) fragment ions.

References

[1] A.N. Zavilopulo, P.P. Markush, O.B. Shpenik and M.I. Mykyta, *Electron Impact Ionization and Dissociative Ionization of Sulfur in the Gas Phase*, Technical Physics, **59**, No. 7, pp. 951–958. (2014).

[2] R. Viswanathan, R. Balasubramanian, D. Darwin Albert Raj, M. Sai Baba, T.S. Lakshmi Narasimhan, *Vaporization studies on elemental tellurium and selenium by Knudsen effusion mass spectrometry*, Journal of Alloys and Compounds **603**, pp.75–85. (2014).

[3] Yu. Smirnov, *Dissociative excitation of selenium atoms in collisions of electrons with Se_2 molecules*, TVT, **44**. (5), pp. 664–672. (2006).

Self-referenced, accurate and sensitive optical frequency comb spectroscopy with VIPA spectrometer

Grzegorz Kowzan[1], Kevin F. Lee[2], Mateusz Borkowski[1], Piotr Ablewski[1], Szymon Wójtewicz[1], Kamila Stec[1], Daniel Lisak[1], Martin E. Fermann[2], Ryszard S. Trawiński[1], Piotr Masłowski[1]

1. Institute of Physics, Faculty of Physics, Astronomy and Informatics, Nicolaus Copernicus University in Toruń, Grudziadzka 5, 87-100 Toruń, Poland

2. IMRA America, Inc., 1044 Woodridge Ave., Ann Arbor, MI, USA 48105

Direct frequency comb spectroscopy combines the sensitivity and resolution of laser spectroscopy with the speed of broadband spectroscopy, replacing single-line wavelength scanning with a parallel measurement over a large frequency bandwidth. For emerging applications such as human breath analysis and industrial process monitoring, exceptional sensitivity and accuracy are required. Here, we demonstrate a spectrometer using a high-finesse optical enhancement cavity [1] to achieve high absorption sensitivity, and dispersing the frequency comb spectrum with a virtually imaged phase array (VIPA) etalon, diffraction grating, and HgCdTe camera for sensitive multiplexed detection.

The measurement system is based on an Er:fiber laser with repetition rate of 250 MHz, operating in the 1.5-1.6 μm range. Comb teeth are locked to a high-finesse enhancement cavity (F = 8500) either by a low bandwidth (~20 Hz) swept locking scheme [2] or a two-point Pound-Drever-Hall scheme [3]. The transmission spectrum is resolved by a VIPA etalon and a diffraction grating, which results in 38-nm wide spectrum with 600 MHz frequency resolution. A Vernier scheme [4] is implemented to obtain higher repetition rate (4 GHz), which allowed us to resolve single comb modes and calibrate the frequency axis of the VIPA spectrometer with them. As a demonstration we obtain broadband spectra of the second overtone rovibrational band of carbon monoxide (P branch) and carbon dioxide (R branch) diluted in argon with both locking schemes.

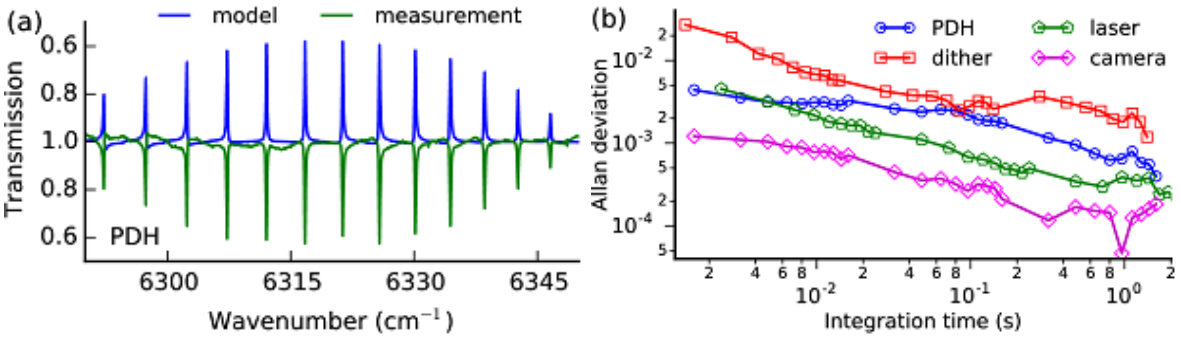

Fig. 1 (a): Measurements of CO 0-3, P branch transitions with PDH locking scheme and simulated spectrum based on the HITRAN database [5]. The spectral line shapes distortions caused by interplay of molecular dispersion and cavity resonances are clearly visible. (b): Fractional Allan deviation of single spectral element intensity for two locking schemes, laser beam bypassing the cavity and photodetector array noise.

We present a careful comparison and analysis of the performance of both locking schemes with obtained absorption enhancement, noise averaging and noise-equivalent absorption included. For the PDH scheme we obtain NEA of 9.9×10^{-10} cm^{-1} and 7.4×10^{-11} cm^{-1} per spectral element. For swept locking we obtain 5.3×10^{-9} cm^{-1} and 1.5×10^{-9} cm^{-1} per spectral element. A calibration scheme based on known VIPA dispersion formulas [6] and data points with precisely known frequencies (obtained through the Vernier scheme) is shown. Comparison with other calibration schemes is presented and it is verified that the calibration scheme is limited only by the camera pixel size.

References

[1] Grzegorz Kowzan, Kevin F. Lee, Magdalena Paradowska, Mateusz Borkowski, Piotr Ablewski, Szymon Wójtewicz, Kamila Stec, Daniel Lisak, Martin E. Fermann, Ryszard S. Trawiński, and Piotr Masłowski, *Self-referenced, accurate and sensitive optical frequency comb spectroscopy with a virtually imaged phased array spectrometer*, Opt. Lett. **41**, 974-977 (2016).

[2] Michael J. Thorpe, David Balslev-Clausen, Matthew S. Kirchner, and Jun Ye, *Cavity-enhanced optical frequency comb spectroscopy: application to human breath analysis*, Opt. Express **16**, 2387 (2008).

[3] A. Foltynowicz, P. Masłowski, A. J. Fleisher, B. J. Bjork, and J. Ye, *Cavity-enhanced optical frequency comb spectroscopy in the mid-infrared application to trace detection of hydrogen peroxide*, Appl. Phys. B **110**, 163–175 (2012).

[4] Christoph Gohle, Björn Stein, Albert Schliesser, Thomas Udem, and Theodor W. Hänsch, *Frequency Comb Vernier Spectroscopy for Broadband, High-Resolution, High-Sensitivity Absorption and Dispersion Spectra*, Phys. Rev. Lett. **99**, 263902 (2007).

[5] L. S. Rothman et al., *The HITRAN2012 molecular spectroscopic database*, J. Quant. Spectrosc. Radiat. Transf. **130**, 4–50 (2013).

[6] Shijun Xiao, Andrew M. Weiner, and Christopher Lin, *A dispersion law for virtually imaged phased-array spectral dispersers based on paraxial wave theory*, Quantum Electron. IEEE J. Of **40**, 420–426 (2004).

The spectroscopy of ground and electronic excited states in chemmotology and method of identifications the atomic-molecular structure of hydrocarbons

A.E. Obukhov
Head of laboratory «The physical methods investigation of combustive-lubricating materials», FAE «25th State Research Institute of Chemmotology the Ministry Defence of the Russian Federation», Moscow 121467 Molodogvardeyskaya street, 10. Russia.

The atomic and molecular electronic and spatial structure of the multiatomic compounds, hydrocarbons and lubricants in chemical composition in the ground state, and using the full energy spectrum of singlet and triplet electronic excited states of different orbital nature of complexes the spectral methods of studies. Based on the mechanisms the hyperfine of electron-nuclear interaction proposed large-scale classification of all types of hydrocarbons by the orbital-spin characteristics the study. Examples the spatial and electronic structure and spectral characteristics of quantum-chemical methods LCAO-MO SCF extended-CI INDO/S of calculations (Figure 1). The directions research works on study the spectroscopy of parameters of hydrocarbons on the basis of developing of quantum-optical theories of combustion and explosion [1-4]. The ElExSt spectroscopy studies of organic and inorganic compounds and their complexes in extreme conditions for achieving (exceeding) of the ionization potential by exposure: thermal, chemical, radiation, electrical, optical or ion types of pump sources. The performance properties of lubricants defined spectral mechanisms of hyperfine electron-nuclear interaction of high-spin many-electron multiatomic compounds, which form a complex chemical composition of substances in the fuel and, thus, are determined by the electronic and spatial structure of the compounds in the ground state and the full energy spectrum of the electronic singlets and triplets excited states of different spin and orbital nature in different aggregate conditions, when exposed various characteristics of the external environment, as well as different types of pump sources. The figure 1 shows that the spectral characteristics (the oscillator strengths, frequency and polarization) of different types the electronic discrete multistep of nonoptical transitions in the full spectra of STElExSt form the characteristics the experimental bands of the spectra: absorption, Raman-scattering and luminescence, emission and radiation are presented [1-3].

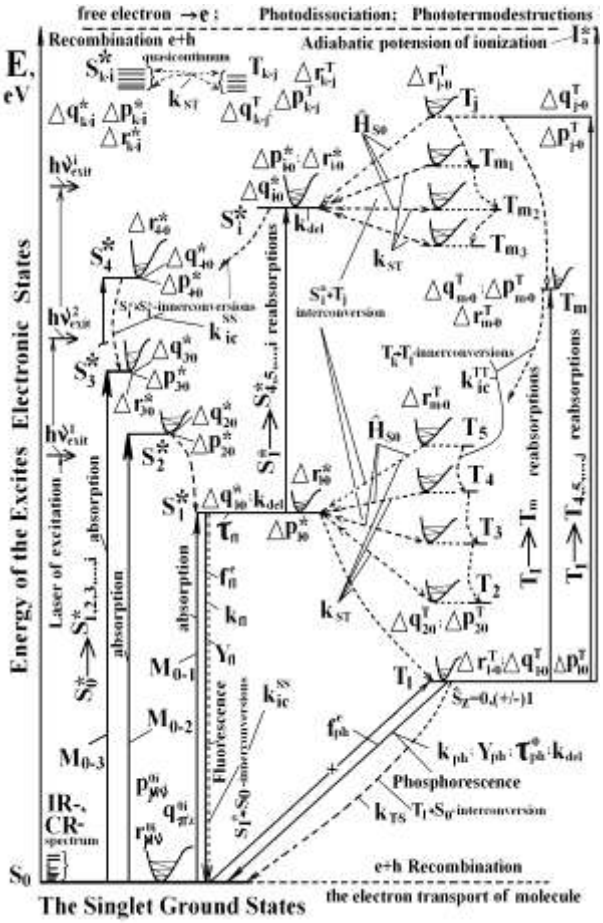

Figure 1. The optical and of the non-optics transition between the systems of the ground states and between the full spectra of singlets and triplets of the ElExS S^*_i and T_j (for the molecule-ion and radical is the quartet Q_n and the duplets D_m). The now scheme non-optical transition from the working S^*_1 states through active vibrations $\{n\}$ term T_f, $\{l\}$ is quasi-continuum inactive in none-radiations transition of oscillatory levels of term T_m, V_n is the matrix elements (MtEl) the mechanism of spin-orbital interactional (SpOrIn). Here $\Delta\rho_{\mu\nu}$, $\Delta p_{\mu\nu}$ and $\Delta r_{\mu\nu}$ is values the MtEl of the total electronic density from the atoms, matrix the order, and length of bonding in structure of molecules, corresponds.

References

[1]. Obukhov, A.E. 1997 *Laser Physics* **7(5) 1102**.
[2]. Obukhov A.E. Spectroscopy of Ground and Excited States of the Multiatomic Molecules in Variation of Condisions. Izd-vo. «Sputnik+». Russia. Moscow. 2010. - 274 p.
[3]. Obukhov. A.E. 1999 *Laser Physics* **9(3) 723**

E-mail: aobukhov@fo.gpi.ru
aobukhovAuthor.One@DomainOne.edu

Experimental and Theoretical Studies on the Electronic State Spectroscopy of Methanol

Emanuele Lange[1], Denis Duflot[2], Filipe Ferreira da Silva[1], Paulo Limão-Vieira[1]

1. Faculdade de Ciência e Tecnologia,, Universidade Nova de Lisboa, 2829-516 Caparica, Portugal.

2. Univ. Lille, CNRS, UMR 8523 – PhLAM – Physique des Lasers, Atomes et Molécules, F-59000 Lille, France

Methanol (CH_3OH), the simplest of the alcohols is a vital molecule within the interstellar chemistry because the UV photodissociation of condensed methanol is thought to be the main mechanism that drives the formation of more complex molecules which are incorporated into the protoplanetary disks of new solar systems[1–5]. The current societal needs to use alcohols as renewable energy sources lead to an increase in the emissions of such species into the lower atmosphere making the interaction of alcohols with UV radiation extremely relevant from the environmental point of view [6].

In this study we have been measured high-resolution VUV photoabsorption cross section of methanol in the 5.9 – 10.6 eV energy range and compare these results against theoretical calculation of the excited estates (valence and Rydberg) using time dependent density functional theory for two different basis set. Excitation of particular vibrational modes are fully investigated. .

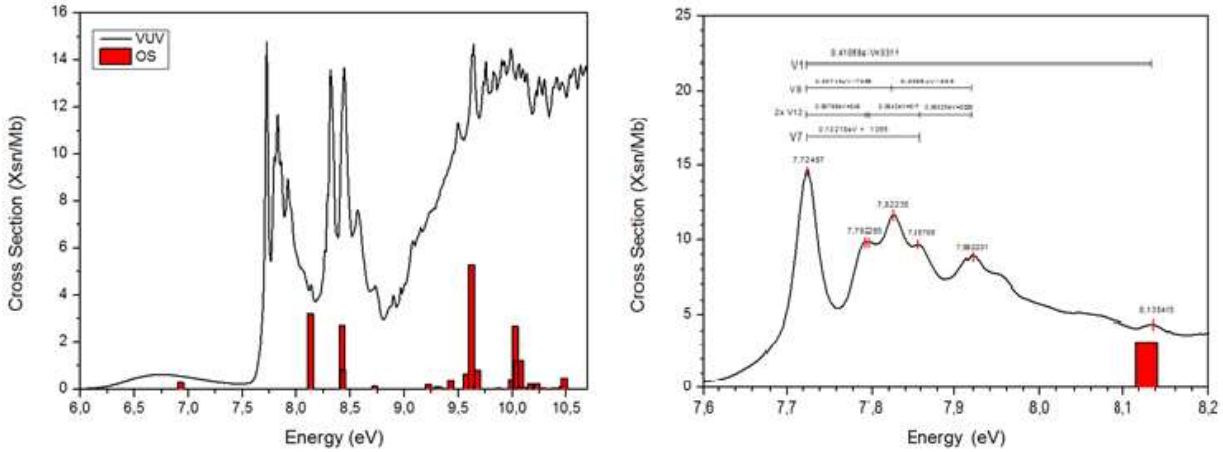

Fig. 1 Left: The entire VUV photoabsorption cross section of methanol with the red bars indicating the calculated oscillator strengths of each transition. Right: The VUV photoabsorption cross section between 7.6-8.2 eV with assignment of the vibrational progressions.

Theoretical calculations were performed to obtain the first thirty singlet and triplet transitions using Gaussian 09 package [7] by means of TD-DFT/LC-ωPBE calculations in association with the-aug-cc-pVTZ and aug-cc-pVQZ basis sets, augmented with (5s5p2d) diffuse functions.

High-resolution VUV photoabsorption spectrum of methanol was recorded at the UV1 beam line of the ASTRID synchrotron facility, ISA at the Aarhus University, Denmark. [8].

References

[1] M. P. Bernstein, S. A. Sandford, L. J. Allamandola, S. Chang, and M. A. Scharberg, *Organic Compounds Produced by Photolysis of Realistic Interstellar and Cometary Ice Analogs Containing Methanol*, Astrophys. J, **454**, 327 (1995).

[2] P. Ehrenfreund and S. B. Charnley, O*rganic Molecules in the Interstellar Medium, Comets, and Meteorites: A Voyage from Dark Clouds to the Early Earth*, Annu. Rev. Astron. Astrophys., **38**, 427 (2000).

[3] R. T. Garrod, S. L. W. Weaver, and E. Herbst, *Complex Chemistry in Star- forming Regions: An Expanded Gas- Grain Warm- up Chemical Model*, Astrophys. J., **682**, 283 (2008).

[4] K. I. Öberg, R. T. Garrod, E. F. van Dishoeck, and H. Linnartz, *Formation rates of complex organics in UV irradiated CH 3 OH-rich ices,* Astron. Astrophys., **504**, 891 (2009).

[5] J. C. Laas, R. T. Garrod, E. Herbst, and S. L. Widicus Weaver, *Contributions From Grain Surface And Gas Phase Chemistry To The Formation Of Methyl Formate And Its Structural Isomers*, Astrophys. J., **728**, 71 (2011).

[6] M.-T. Lee, G. L. C. de Souza, L. E. Machado, L. M. Brescansin, A. S. dos Santos, R. R. Lucchese, R. T. Sugohara, M. G. P. Homem, I. P. Sanches, and I. Iga, *Electron scattering by methanol and ethanol: a joint theoretical-experimental investigation.*, J. Chem. Phys., **136**, 114311, (2012).

[7] M. J. Frisch et al., *Gaussian 09 Rev*. D.01.,Gaussian, Inc., Wallingford, CT, USA, (2009)

[8] S. Eden, P. Limão-Vieira, S. V. Hoffmann, and N. J. Mason, *VUV photoabsorption in CF3X (X=Cl, Br, I) fluoro-alkanes*, Chem. Phys., **323**, 313 (2006).

Multi fragment vector correlation imaging - A search for hidden dynamical symmetries in many-particle molecular fragmentation processes

Florian Trinter[1], Lothar Ph. H. Schmidt[1], Till Jahnke[1], Markus S. Schöffler[1], Ottmar Jagutzki[1], Achim Czasch[1], Julian Lower[1], Timur A. Isaev[2], Robert Berger[2], Allen L. Landers[3], Thorsten Weber[4], Reinhard Dörner[1], and Horst Schmidt-Böcking[1]

1. Institut für Kernphysik, Goethe-Universität Frankfurt, Max-von-Laue-Straße 1, D-60438 Frankfurt, Germany
2. Clemens-Schöpf Institute for Organic Chemistry and Biochemistry, TU Darmstadt, Petersenstraße 22, D-64287 Darmstadt, Germany
3. Department of Physics, Auburn University, Auburn, Alabama 36849, USA
4. Lawrence Berkeley National Laboratory, Chemical Sciences, Berkeley, California 94720, USA

State-of-the-art multi-fragment imaging techniques like the COLTRIMS reaction microscope unveil the complete momentum pattern in low energy atomic and molecular many-particle fragmentation processes much like the bubble chamber in high energy particle physics. The excellent momentum resolution far below 1 $m_e a_0 E_h/\hbar$ (1 a.u.) and the high multi-fragment detection efficiency of the COLTRIMS technique reveal the dynamic correlation of bound many-particle systems as they are fragmented into the continuum. For the fragmentation process of carbon monoxide following carbon K-shell ionization using 306 eV photons (right and left circularly polarized) $h\nu + CO \Rightarrow e_{photo} + O^+ + C^+ + e_{K\text{-}Auger}$, the vector correlations between all fragments were measured in coincidence for each event. According to the common view of this process, the photoelectron and Auger electron emission probe different aspects of the time dependent fragmentation process, i.e. the "time evolution" of fragmentation. Based on measured vectors and vector combinations (e.g. vector products) of (1) the absorbed photon, (2) the emitted photoelectron and (3) ions, the Auger electron emission can be investigated with respect to axes and planes defined by these vector combinations for each event in order to explore dynamical symmetries in multi-particle systems.

In our approach all momenta of the charged fragments are measured in coincidence and are stored for each interaction in an event list (k,l,m,n). This way of data storing ensures that the photoelectron of event (k,l,m,n) is only correlated to fragments of the same event and never to any proceeding or subsequent events (k,l,m,n±i). Therefore, one can calculate for each event the vector products and project the measured Auger distributions on axes or planes defined by these vector products. One example is the vector product $\boldsymbol{Z} = \boldsymbol{A}_{photon} \times \boldsymbol{p}_{ephoto}$. When mirroring the time from $t \Rightarrow -t$ this new vector $\boldsymbol{Z}$ does not change its direction. That means that $\boldsymbol{Z}$ is even under time reversal (T-even). On the other hand, under spatial inversion, $\boldsymbol{r} \Rightarrow -\boldsymbol{r}$, the vector $\boldsymbol{Z}$ is odd (P-odd). The Auger electron emission should show with respect to this $\boldsymbol{Z}$ direction a perfect symmetrical distribution, if time is reversible in the Auger process. Measuring the Auger electron distribution for $\boldsymbol{A}_{photon}(t)$ and $\boldsymbol{p}_{ephoto}(t)$ as well as for $\boldsymbol{A}_{photon}(-t)$ and $\boldsymbol{p}_{ephoto}(-t)$, i.e. for left and right polarized photons and photoelectrons emitted in opposite directions, respectively, one can test the time inversion symmetry. The then inversed Auger spectrum ($-t$) should be identical with the one of (t). In Table 1, other interesting combinations of vector products and scalar products with different behavior under P- and T-reversal are presented (with $\boldsymbol{n}$ being the molecular vector pointing from the carbon nucleus to the oxygen nucleus).

Vector product	$t \Rightarrow -t$	$\boldsymbol{r} \Rightarrow -\boldsymbol{r}$
$\boldsymbol{Z} = \boldsymbol{A}_\gamma \times \boldsymbol{p}_{ephoto}$	$\boldsymbol{Z}(t) = +\boldsymbol{Z}(-t)$	$\boldsymbol{Z}(\boldsymbol{r}) = -\boldsymbol{Z}(-\boldsymbol{r})$
$\boldsymbol{Z'} = (\boldsymbol{A}_\gamma \times \boldsymbol{p}_{ephoto}) \times \boldsymbol{p}_{K\text{-}Auger}$	$\boldsymbol{Z'}(t) = -\boldsymbol{Z'}(-t)$	$\boldsymbol{Z'}(\boldsymbol{r}) = +\boldsymbol{Z'}(-\boldsymbol{r})$
$S = (\boldsymbol{A}_\gamma \times \boldsymbol{p}_{ephoto}) \cdot \boldsymbol{n}$	$S(t) = +S(-t)$	$S(\boldsymbol{r}) = +S(-\boldsymbol{r})$

Table 1 Vector products with respect to time and parity symmetries.

References

[1] Florian Trinter et al., *Multi-fragment vector correlation imaging. A search for hidden dynamical symmetries in many-particle molecular fragmentation processes*, Mol. Phys. Vol. **110**, Nos. 15-16, 1863 (2012).

Ultrafast molecular three-electron Auger decay

R. Feifel[1], J.H.D. Eland[1,2], R.J. Squibb[1], M. Mucke[3], S. Zagorodskikh[1,3], F. Tarantelli[4], P. Kolorenc[5], and V. Averbukh[6]

[1]*Department of Physics, University of Gothenburg, 421 59 Gothenburg, Sweden*
[2]*Department of Chemistry, Oxford University, Oxford OX1 3QZ, United Kingdom*
[3]*Department of Physics and Astronomy, Uppsala University, 751 21 Uppsala, Sweden*
[4]*Dipartimento di Chimica, Universita di Perugia and ISTM-CNR, 06123 Perugia, Italy*
[5]*Institute of Theoretical Physics, Charles University in Prague, 180 00 Prague, Czech Republic*
[6]*Blackett Laboratory, Imperial College London, London SW7 2AZ, United Kingdom*

A new class of many-electron Auger transitions in atoms, schematically illustrated in Fig. 1, was initially proposed over 40 years ago [1,2], but the first tentative evidence for its real existence was only adduced by Lee *et al.*[3] in 1993, on the basis of the resonant Auger spectrum of Kr. Using a multi-electron coincidence technique with synchrotron radiation, we unambiguously showed very recently that the transition suggested by Lee *et al.* [3] in Kr really does take place, but with a rather small branching ratio [4].

Related inter-atomic three-electron transitions in rare gas clusters were recently predicted by Averbukh and Kolorenč [5] and demonstrated by Ouchi *et al.* [6]. From consideration of the energy levels involved it seems that the basic three-electron process could occur in molecules too, wherever a double inner-valence shell vacancy lies at a higher energy than the molecular triple ionisation onset.

Multi-electron coincidence experiments on CH_3F based on a magnetic bottle [7] reveal for the first time the existence of this new decay pathway there, and theoretical calculations also show that despite its three-electron nature, its effective oscillator strength is surprisingly orders of magnitudes higher than in atoms, allowing an efficient competition with both molecular dissociation and two-electron decay channels on the ultrafast time scale. The dramatic enhancement of the molecular three-electron Auger transition can be explained in terms of a partial breakdown of the molecular orbital picture of ionization [8].

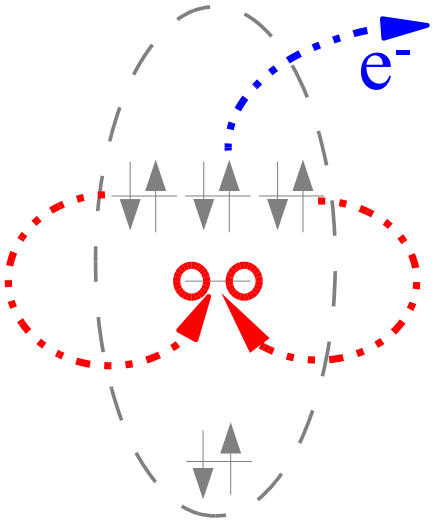

Figure1: Illustration of intra-atomic collective decay of a double inner-shell vacancy. Two valence electrons recombine into the empty orbital producing enough energy for a third electron to be ejected.

We predict that the collective decay pathway will be significant in a wide variety of molecules ionised by extreme UV and soft X-rays, particularly at Free-Electron-Lasers where double inner-shell vacancies can be created efficiently by two-photon transitions. Molecules containing heteroatoms will be especially susceptible.

References

1. G.N. Ogurtsov, I.P.Flaks and S.V. Avakyan, Sov. Phys. Tech. Phys. **15**, 1656 (1971).
2. V.V. Afrosimov, Yu. S. Gordeev, A.N. Zinoviev, D.H. Rasulov and A.P Shergin, JETP Lett. **21**, 249 (1975).
3. I. Lee, R. Wehlitz, U. Becker and M. Ya. Amusia, J. Phys. B: At. Mol. Opt. Phys. **26**, L41 (1993).
4. J.H.D. Eland, R.J. Squibb, M. Mucke, S. Zagorodskikh, P. Linusson, and R. Feifel, New J. Phys. **17**, 122001 (2015).
5. V. Averbukh and P. Kolorenč, Phys. Rev. Lett. **103**, 183001 (2009).
6. T. Ouchi *et al.*, Phys. Rev. Lett. **107**, 053401 (2011).
7. R. Feifel, J.H.D. Eland, R.J. Squibb, M. Mucke, S. Zagarodskikh, P. Linusson, F. Tarantelli, P. Kolorenc, and V. Averbukh, Phys. Rev. Lett. **116,** 073001 (2016).
8. L. Cederbaum, W. Domcke, J. Schirmer, and W. von Niessen, Adv. Chem. Phys. **65**, 115 (1986).

Formation and destruction of molecular ions in cold ion-atom hybrid traps

Humberto da Silva Jr, Mireille Aymar, Maurice Raoult, and Olivier Dulieu

Laboratoire Aimé Cotton, CNRS, Université Paris-Sud, ENS Cachan, Université Paris-Saclay, 91405 Orsay Cedex, France

Radiative emission during cold collisions between trapped laser-cooled Rb atoms and alkaline-earth ions (Ca^+, Sr^+, Ba^+ and Yb^+, and between Li and Ca^+ and Yb^+, are studied theoretically, using accurate effective-core-potential based quantum chemistry calculations of potential energy curves and transition dipole moments of the related molecular ions. Radiative association of molecular ions is predicted to occur for all systems with a cross section two to ten times larger than the radiative charge transfer one. Partial and total rate constants are also calculated and compared to available experiments. Narrow shape resonances are expected, which could be detectable at low temperature with an experimental resolution at the limit of the present standards. Vibrational distributions are also calculated, showing that the final molecular ions are not created in their ground state level [1].

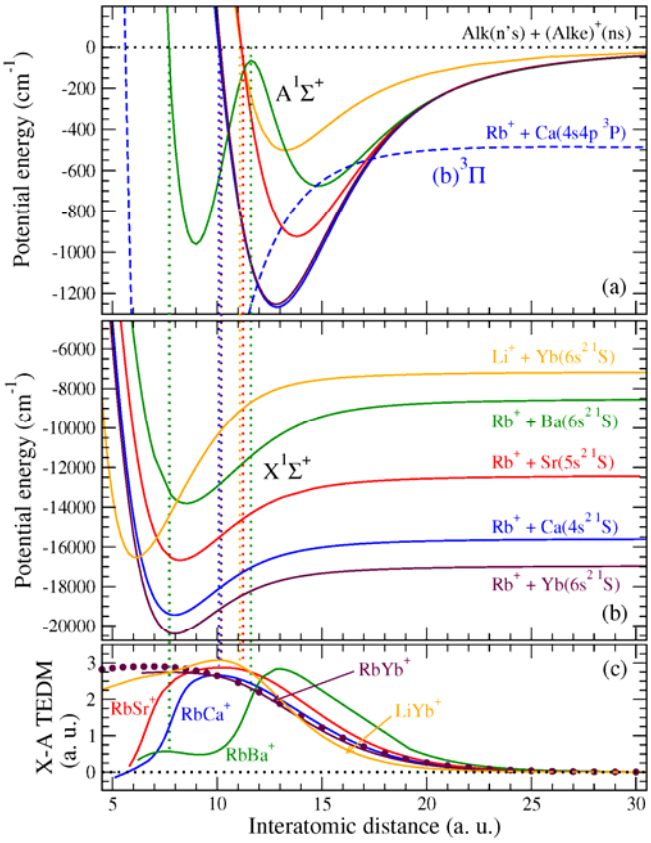

Fig. 1 Potential energy curves of (a) the $A^1\Sigma^+$ state, and (b) of the $X^1\Sigma^+$ state, for the [(Alk)-(Alke)]$^+$ molecules, with (Alk)=Li or Rb (n'=2, 5), and (Alke) = Ca, Sr, Ba, and Yb (n=4, 5, 6, 6). The origin of energies is taken at the dissociation of the $A^1\Sigma^+$ potential curve for all systems. The lowest $^3\Pi$ potential curve of Rb-Ca$^+$ is also displayed for completeness. (c) Transition electric dipole moments between the X and A states. The vertical dotted lines tag the inner turning points of the incoming continuum wave function -- in the entrance channel -- with the respective points in the exit channel and the transition dipole moment magnitude at that position..

We carried further calculations of photodissociation cross sections of the created molecular ions induced by the presence of the various lasers present in the experimental setups. The destruction of the molecular ion due to cold collisions with surrounding neutral atoms will also be discussed.

References

[1] Humberto da Silva Jr, Mireille Aymar, Maurice Raoult, and Olivier Dulieu, New J. Phys. **17**, 045015 (2015)

Dynamic dipole polarizabilities of heteronuclear alkali dimers: optical response, trapping and control of ultracold molecules

R. Vexiau, D. Borsalino, M. Lepers, M. Aymar, O. Dulieu and N. Bouloufa-Maafa
Laboratoire Aimé Cotton, CNRS, Université Paris-Sud, ENS Cachan, Université Paris-Saclay, 91405 Orsay Cedex, France

We theoretically study optical response of heteronuclear alkali dimers when trapped in optical lattices and determine optimal frequencies of those lattices allowing optimal transfer to the absolute ground state of initially weakly bound molecules. For each of the ten molecules composed of two of (^{7}Li,^{23}Na,^{39}K,^{87}Rb,^{133}Cs) alkali atoms, dynamic dipole polarizabilities are computed as a function of the frequency of the oscillating electric field [1]. Combining precise experimental and theoretical molecular potential curves and electronic transition dipole moment we make an extensive investigation of both low and optical frequency regimes. In particular we discuss suitable wavelength for the trapping of the studied molecules. When they exist we determine the so called "magic frequencies" giving the same ac Stark shift and thus the same viewed trap depth for both weakly bound and lowest bound level of the ground state. Our results are of interest for experiments aiming to control those cold polar molecules. In addition we propose an approximate analytical formula to determine the dynamic dipole polarizabilities, based only on a few parameters. This approximation is checked against recent experimental measurements on Rb_2, revealing a very good agreement [2].

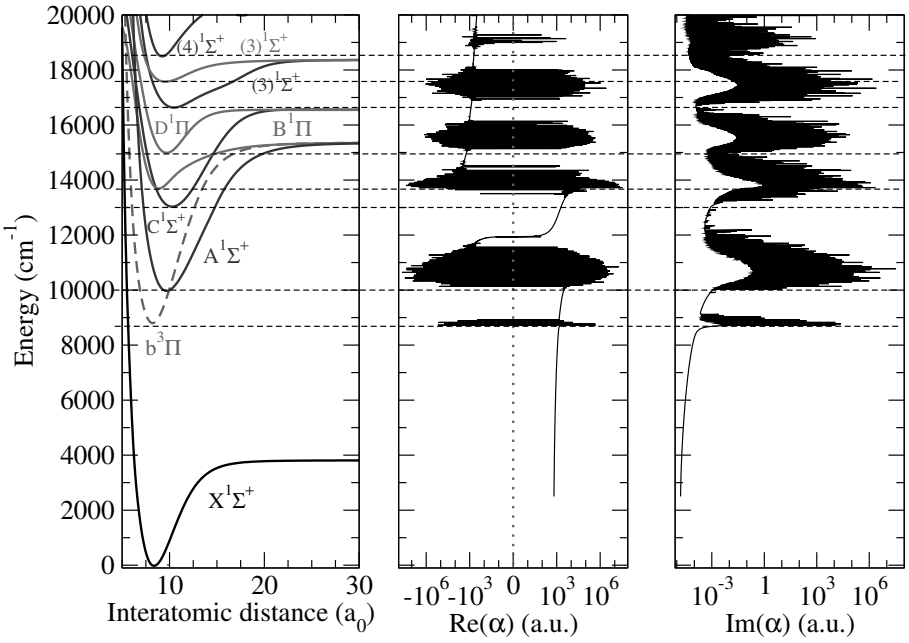

Fig. 1 Potential energy curves of RbCs as a function of the interatomic distance (left panel). Real part (middle panel) and imaginary part (right panel) of the polarizability of a $X^1\Sigma^+; v = 0$ RbCs molecule as a function of the energy of the laser.

References

[1] R. Vexiau, D. Borsalino, M. Lepers, M. Aymar, O. Dulieu and N. Bouloufa-Maafa, submitted.
[2] Markus Deiß, Björn Drews, Johannes Hecker Denschlag, Nadia Bouloufa-Maafa, Romain Vexiau, and Olivier Dulieu, New J. Phys. **17**, 065019 (2015)

Observation of Atom-Surface Interaction in Evanescent Field Using Ultracold Atoms

Yutaka Kobayashi[1], Satoshi Asahi[1], Kosuke Shibata[1], Satoshi Tojo[1]
1. Department of Physics, Chuo University, 1-13-27 Kasuga, Bunkyo, 112-8551, Tokyo, Japan.

Precise manipulation of laser-cooled atoms near surfaces is a powerful technique for investigation of atoms-surface interactions [1, 2]. We have studied higher-order interactions between laser-cooled atoms and an optical near-field. Neutral atoms have high-operationality due to high-sensitive to light and magnetic fields. Therefore, by using laser-cooled atoms having locality as a probe, we explore phenomena in the local vicinity of the surface.

We have prepared laser-cooled Rb atoms and loaded them into a focus region of Far-Off Resonance Trap (FORT). We have realized to transport trapped atoms into the region of several micrometers from a glass surface with 10^5 atoms at below 50 μK, which is implemented by changing in the focus position of the FORT (10 W , 1064 nm) precisely controlled by a submicrometer stage as shown in Fig. 1(a).

Optical lattices are formed by the interference between counter-propagating laser beams of FORT generating periodic deep potential when the laser-cooled atoms are manipulated close to the glass surface [2]. The generated potential of the optical lattice can be approximated to the harmonic oscillator with its characteristic trap frequency in the near focus region. Figure 1(b) shows a dependence of trapped number-of-atoms on the modulation frequency in the parametric resonance experiment and trapped atoms decrease in the characterictic frequency owing to forming optical lattices. The result indicates that the laser-cooled atoms exist the region within some dozen of micrometer from the surface. We will report on interaction phenomena of cold atoms in an evanescent light field.

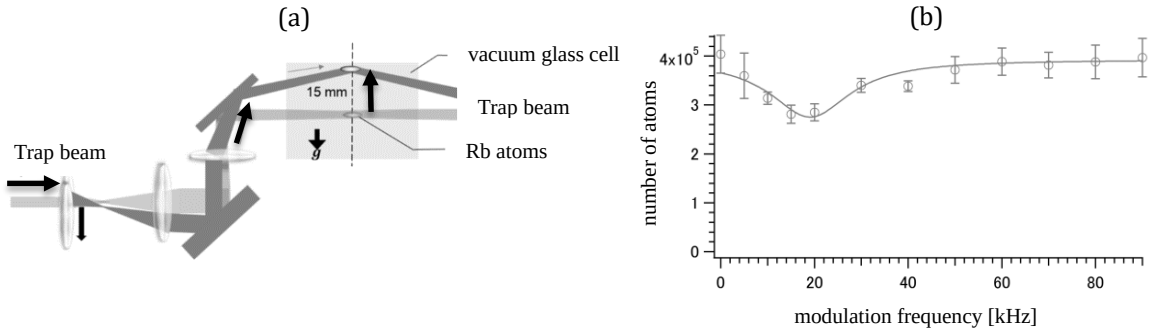

Fig. 1 (a) Schematic representation of experimental manipulation of cold atoms into the vicinity of the glass surface. (b) Dependence of trapped number-of-atoms on the modulation frequency.

References

[1] H Bender, Ph W Courteille, C Marzok, C Zimmermann, and S Slama, Phys. Rev. Lett. **104**, 083201 (2010).
[2] J. I. Gillen, W. S. Bakr, A. Peng, P. Unterwaditzer, S. Fölling, and M. Greiner, Phys. Rev. A **80**, 021602(R) (2009).

Resonances in the rotational constants spectrum of excited molecules analysed with an improved LeRoy-Bernstein formula and a 2-channel model-comparison with the vibrational quantum defect method

Laurence Pruvost[1] **, Haikel Jelassi**[2]

1. Laboratoire Aimé Cotton, CNRS, Université de Paris Sud, ENS-Cachan, Université Paris Saclay, 91405, Orsay, France.

2. Laboratoire de Recherche Energie et Matière pour les Développement des Sciences Nucléaires & Direction de la Recherche sur l'Energie et la Matière, National Center for Nuclear Science and Technology, Sidi Thabet Technopark 2020 Ariana Tunisia

The quantum defect theory is a well-known approach used for Rydberg atoms, to characterize a Rydberg series and to reveal any coupling between Rydberg series. The signature appears in the change of the quantum defect progression of the levels.

In order to identify coupling between molecular potentials, available to give routes to form molecules from cold atoms via weakly-bound molecules, we have investigated the spectrum analysis by introducing the vibrational quantum defect (VQD). This quantity issues from the analogy between the Rydberg law and the LeRoy-Bernstein one. VQD-graphs obtained with data of high-resolution photoassociation spectroscopy exhibit resonances that have been associated to coupling between molecular potentials [1, 2, 3] and analyzed by a 2 channel model, providing the coupling parameters.

Another signature of the coupling exists in the progression of the rotational constants B_v (B_v-spectrum) with resonances in the vicinity of the perturbing levels. We propose an improved-B_v-Formula associated to a 2-channel model to explain both the Lorentzian-shape of the resonances and the background and to fit the B_v-spectrum of $6s_{1/2}$-$6p_{1/2}$ 0_g^- given in [4]. Fitting parameters give the coupling parameters in agreement with the VQD method [5].

References

[1] H. Jelassi, B. Viaris de Lesegno, and L. Pruvost, Phys. Rev. A **73**, 032501 (2006).

[2] H. Jelassi, B. Viaris de Lesegno, and L. Pruvost, M. Pichler, W. C. Stwalley, Phys. Rev. A. **78**, 022503 (2008).

[3] L. Pruvost and H. Jelassi, J. Phys. B: At. Mol. Opt. Phys. **43**, 125301 (2010).

[4] H. Lignier, A. Fioretti, R. Horchani, C. Drag, N. Bouloufa, M. Allegrini, O. Dulieu, L. Pruvost, P. Pillet, and D. Comparat, Phys. Chem. Chem. Phys. **13** (2011)18910.

[5] H. Jelassi and L. Pruvost, submitted.

Two-structural distribution of cold atoms in quantum regimes

Roman Ilenkov[1,2], Aleksey Taichenachev[1,2], Valery Yudin[1-3]

[1]Institute of Laser Physics SB RAS Ac. Lavrentyev's prosp., 13/3, 630090 Novosibirsk, Russia
[2]Novosibirsk State University, ul. Pirogova 2, 630090 Novosibirsk, Russia
[3]Novosibirsk State Technical University, pr. Karla Marksa 20, 630073 Novosibirsk, Russia

Invention such precise and powerful tool as a laser has opened before scientists a wide range of capabilities for atom manipulation: acceleration, deceleration, localization, deflection, and focusing. So laser cooling has become an integral part of both fundamental science and many practical applications (high-precision frequency and time standards, nanolithography, quantum information etc.)

The theoretical description of the kinetics of neutral atoms in the polarized light fields with all the atomic levels, the coherence, the recoil effect is both important and challenging problem. The first step toward understanding mechanisms of interaction between atoms and light was called quasi-classical approach. [1,2] It lies in the fact that the equations for the density matrix can be reduced to the Fokker-Planck equation for the Wigner function in the phase space. Later quantum methods were developed [3], for example, the secular approach which describes cooling and localization of atoms in the optical potential. At a fixed depth of the optical potential this approximation is valid in the limit of large detuning, and thus, for a given configuration is disrupted in a deep optical potential. Secular approximation fails high vibrational levels.

We have developed an own quantum method [4] to obtaining the stationary distribution of two-level atoms in a standing wave of arbitrary intensity, allowing full account the recoil effect. Using this method kinetics of atoms in light fields of varying intensity was investigated. The new and most important result was mode which we called the anomalous localization. In strong standing wave (Rabi frequency greater than the constant spontaneous relaxation) was detected a anomalous behavior of atoms, namely, the concentration at the peaks of the optical potential.

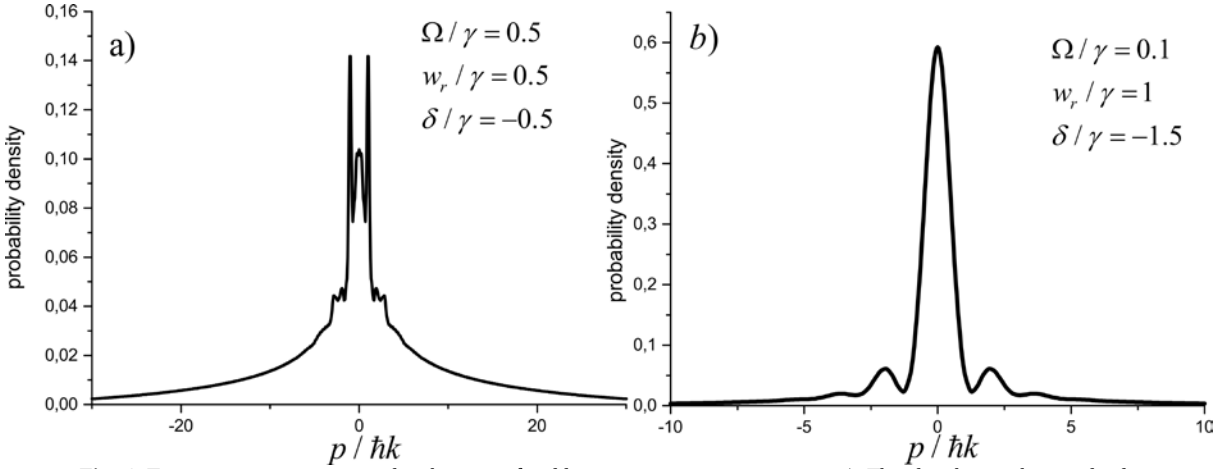

Fig. 1 Two-structure momentum distributions of cold atoms in quantum regimes: a) The distribution has a clearly expressed narrow peaks which width of order a single photon momentum. b) The distribution has narrow structure of cold atoms and wide wings. Parameters of the problem are located on graphs.

The next important step was to study the quantum modes for different parameters of the problem. The next important step was to study the quantum modes for different parameters of the problem. It is known that the quasi-classical approach gives Gaussian shape momentum distributions of and is completely inapplicable to the quantum regimes. The results of quantum calculation are shown in **Fig.1**. There is a two-structural distribution - the narrow central peak and a broad substrate. Selecting parameters and cutting off the hot atoms, can be obtained temperatures below the Doppler cooling limit.

The work was supported by the Ministry of Education and Science of the Russian Federation (State Assignment No. 2014/139, Project No. 825), by the Russian Foundation for Basic Research (Grants No. 14-02-00712, 14-02-00939, 15-02-08377, 15-32-20330).

References

[1] V.G. Minogin, V.S. Letokhov, *Laser Light Pressure on Atoms*, Gordon and Breach, New York, 1987.
[2] A. P. Kazantsev, G. I. Surdutovich, and V. P. Yakovlev, *Mechanical Action of Light on Atoms*, World Scientific, Singapore, 1990.
[3] A. Aspect, E. Arimondo, R. Kaiser, N. Vansteenkiste, and C. Cohen-Tannoudji, *Laser Cooling below the One-Photon Recoil Energy by Velocity-Selective Coherent Population Trapping*, Phys. Rev. Lett. **61**, 826 (1988).
[4] O. N. Prudnikov, R. Ya. Il'enkov, A. V. Taichenachev, A. M. Tumaikin, V. I. Yudin, *Steady state of a low-density ensemble of atoms in a monochromatic field taking into account recoil effects*, JETP, Volume **112**, 939-945 (2011).

Beyond the Landau-Zener model: perturbation theory for non-adiabatic losses from RF-dressed cold atom traps

Kathryn A Burrows[1], Dany Ben Ali[2], Germán A Sinuco-Leon[1], Hélène Perrin[2], and Barry M Garraway[1]

[1] Department of Physics & Astronomy, University of Sussex, Brighton, BN1 9QH, UK
[2] CNRS, UMR 7538, Université Paris 13, Sorbonne Paris Cité, Laboratoire de physique des lasers, 99 avenue J.-B. Clément, F-93430 Villetaneuse, Paris, France

Ultracold atoms can be trapped using spin dependent adiabatic potentials, formed by the atomic interaction with a static position dependent magnetic field and a radio frequency (RF) magnetic field. This type of cold atom trap, known as a RF-dressed trap, offers a high degree of versatility over the trapping potential by tuning the static magnetic field gradient, RF field amplitude and RF field frequency of oscillation. This allows the coherent manipulation of atoms, which is of high importance for applications such as atom interferometry. RF-dressed cold atom traps have a range of potential applications as sensors, with the possibility of miniaturisation using atom chip technology. However, non-adiabatic effects, which occur due to a coupling of internal and translational degrees of freedom, could limit the trap lifetime when the RF field amplitude is small or the static magnetic field gradient is large.

A theory is presented for non-adiabatic losses from RF-dressed cold atom traps providing a prediction of the decrease in the number of trapped atoms with time. Fermi's Golden Rule is used to determine decay rates for dressed spin state changes which lead to losses as the atoms no longer feel the adiabatic trapping potential. The obtained decay rates are compared with experimental data recorded in the regime of weak RF field amplitude in which non-adiabatic losses have a significant effect.

Agreement is found with experimental data when heating processes induced by fluctuations in the currents which generate the trapping magnetic fields are taken into consideration. Investigations show that the Landau-Zener model, which is currently used to determine the rate of non-adiabatic transitions to untrapped spin states, significantly underestimates non-adiabatic effects. This implies tighter restrictions must be imposed on the static magnetic field gradient and RF field amplitude for a given trap lifetime.

Optoelectrical cooling of polar molecules to submillikelvin temperatures

Martin Ibrügger[1], Alexander Prehn[1], Rosa Glöckner[1], Martin Zeppenfeld[1], and Gerhard Rempe[1]
1. Max-Planck-Institut für Quantenoptik, Hans-Kopfermann-Str. 1, 85748 Garching, Germany

Due to their rich internal level structure and their electric dipole moment, polar molecules cooled to ultracold temperatures (T< 1mK) offer a wide range of intriguing applications. These include quantum simulation with degenerate quantum gases, investigation of collisions and quantum controlled chemistry or hybrid quantum devices for quantum information processing. Realizing these exciting applications requires advanced cooling techniques for polar molecules.

Here we present direct cooling of formaldehyde (H_2CO) to the microkelvin regime [1]. Our approach is optoelectrical Sisyphus cooling which is a simple and robust scheme as it only requires a single laser, a single microwave source and a single radiofrequency source. Molecules are electrically trapped [2] and cooled by a dissipative cooling method relying only on generic properties of polar molecules making it applicable to a large variety of molecule species. After a first demonstration with methyl fluoride (CH_3F) [3] we now produce an ultracold ensemble of about $3 \cdot 10^5$ formaldehyde molecules by reducing the temperature by three orders of magnitude to about 420μK. The phase space density is increased by roughly a factor of 10^4. In addition to our control over the motional degrees of freedom we have good control over the internal degrees of freedom of our molecules [4]: by optical pumping they are prepared within a single rotational state with a purity higher than 80%. This record-large ensemble of ultracold formaldehyde provides an ideal starting point for future experiments. Ultracold collision studies and fountain experiments now seem feasible. Furthermore, it brings within reach the investigation of sympathetic or evaporative cooling.

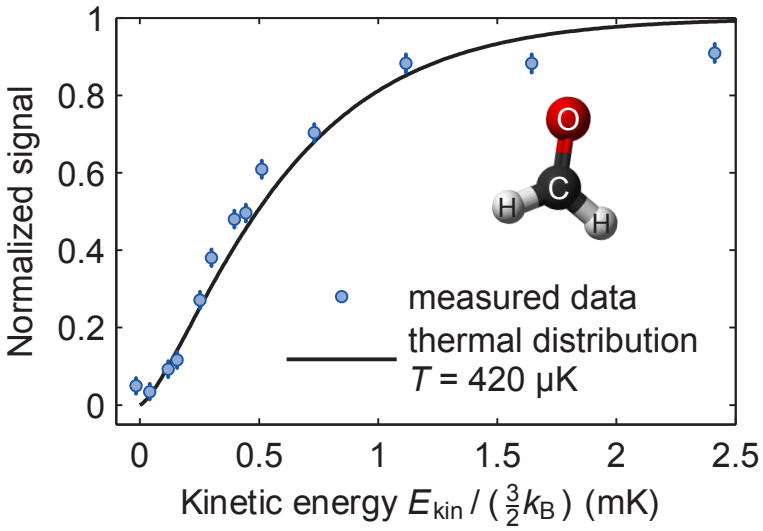

Fig. 1 Measured integral of the kinetic energy distribution of formaldehyde molecules in our trap. The solid curve shown corresponds to a theoretical thermalized sample with a temperature of 420μK.

References

[1] Alexander Prehn, Martin Ibrügger, Rosa Glöckner, Gerhard Rempe, and Martin Zeppenfeld, *Optoelectrical Cooling of Polar Molecules to Submillikelvin Temperatures*, Phys. Rev. Lett. **116**, 063005 (2016).
[2] Barbara G. U. Englert, Manuel Mielenz, Christian Sommer, Josef Bayerl, Michael Motsch, Pepijn W. H. Pinkse, Gerhard Rempe, and Martin Zeppenfeld, *Storage and Adiabatic Cooling of Polar Molecules in a Microstructured Trap*, Phys. Rev. Lett. **107**, 263003 (2011).
[3] Martin Zeppenfeld, Barbara G. U. Englert, Rosa Glöckner, Alexander Prehn, Manuel Mielenz, Christian Sommer, Laurens D. van Buuren, Michael Motsch, and Gerhard Rempe, *Sisyphus cooling of electrically trapped polyatomic molecules*, Nature **491**, 570-573 (2012).
[4] Rosa Glöckner, Alexander Prehn, Barbara G. U. Englert, Gerhard Rempe, and Martin Zeppenfeld, *Rotational Cooling of Trapped Polyatomic Molecules*, Phys. Rev. Lett. **115**, 233001 (2015).

Study on the Effective Rotational Temperature Dependence of the Reaction-Rate Constants between Cold Ions and Slow Polar Molecules

Yusuke Takada[1] and Kunihiro Okada[1]

1. Department of Physics, Sophia University, 7-1 Kioicho, Chiyoda, Tokyo 102-8554, Japan

Reaction-rate constants between molecular ions and polar molecules at low temperatures are important for studying the synthesis of interstellar molecules [1]. Extensive laboratory measurements, however, have not been performed owing to the condensation of polar gases at low temperatures.

In the above context, we have recently constructed a new experimental setup to measure reaction-rate constants at translational temperatures lower than 10 K in ultrahigh vacuum conditions [2]. In brief the setup consists of a Stark-velocity filter for producing slow polar molecules and an ion trap apparatus for generating cold ion targets, which are sympathetically cooled by laser-cooled Ca^+ ions. In addition to the original design of the setup [3], we introduced a cooled gas nozzle for injection of polar gases into the Stark-velocity filter in order to observe the rotational state dependence of reaction rates. Figure 1(a) shows snapshots of the laser induced fluorescence images of mixed-ion Coulomb crystals consisting of Ca^+ and Ne^+ ions before/after $CH_3CN + Ne^+ \rightarrow$ *products* reactions. The dark area occupied with Ne^+ ions progressively decreases with increasing the reaction time mainly due to the progress of the $CH_3CN + Ne^+ \rightarrow CH_3CN^+ + Ne$ reactions. The relative number of Ne^+ ions (N_{rel}) is obtained by calculating the volume of the dark area in the LIF images by assuming the cylindrical column distribution of Ne^+ ions as well as the constant number density, which are reasonable assumptions in our experimental conditions [4].

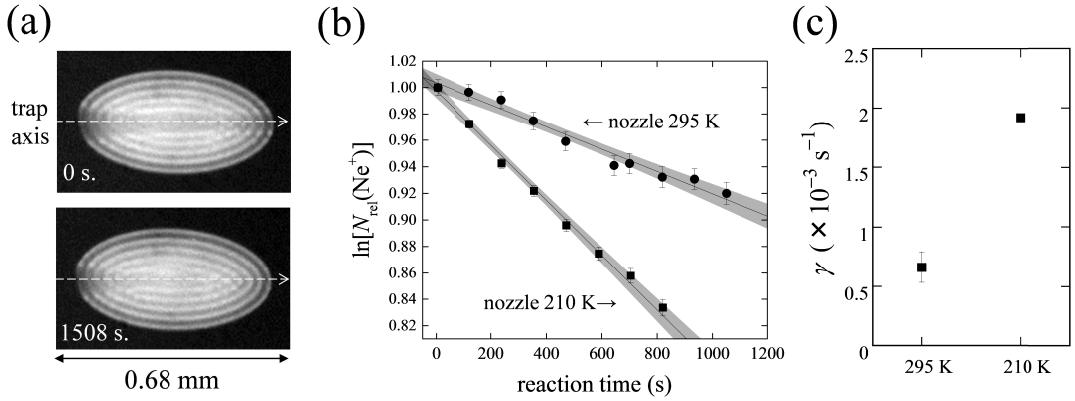

Fig. 1 (a) LIF images of mixed-ion Coulomb crystals consisting of Ca^+ (bright are) and Ne^+ (dark area near the trap axis) before/after introducing slow CH_3CN molecules. (b) Plots of the relative number of sympathetically cooled Ne^+ ions embedded in Ca^+ Coulomb crystals during $CH_3CN + Ne^+ \rightarrow$ *products* reactions at lower temperatures than 10 K. The upper and lower traces were taken when the gas nozzle temperature was set to 295 K and 210 K, respectively. The coloured areas show the 95% confidence intervals. (c) Plot of the average reaction rates at the nozzle temperatures of 295 K and 210 K.

Figure 1(b) shows plots of the relative number of sympathetically cooled Ne^+ ions embedded in Ca^+ Coulomb crystals as a function of the reaction time at different nozzle temperatures. The average reaction rates γ over many times were given in Fig.1(c). There are two reasons why the reaction rate becomes faster at the low nozzle temperatures. The first one is the increase of the slow CH_3CN density at the ion trap, and the second is possibly due to the increase of the reaction-rate constant at a lower effective rotational temperature of CH_3CN.

In the presentation the details of the experimental setup and the method will be reported. We will also discuss the effective rotational temperature dependence of reaction-rate constants for $CH_3CN + Ne^+$ and $CH_3CN + N_2H^+$ reaction systems.

References

[1] V. Wakelam *et al*., *Reaction networks for interstellar chemical modelling: Improvements and challenges*, Space Sci. Rev. **156**, 13

[2] K. Okada *et al*., *Cold ion-polar-molecule reactions studied with a combined Stark-velocity-filter-ion-trap apparatus*, Phys. Rev. A **87**, 043427 (2013).

[3] S. Willitsch *et al*., *Cold Reactive Collisions between Laser-Cooled Ions and Velocity-Selected Neutral Molecules*, Phys. Rev. Lett. **100**, 043203 (2008).

[4] K. Okada *et al*., *Quasiequilibrium Characterization of Mixed-Ion Coulomb crystals*, Phys. Rev. Appl. **4**, 054009 (2015).

The nature of anisotropic interactions and emergence of quantum chaos in ultracold Er and other lanthanide gases

V. V. Flambaum[1], **G. F. Gribakin**[2]
1. School of Physics, University of New South Wales, Sydney, New South Wales 2052, Australia
2. School of Mathematics and Physics, Queen's University Belfast, Belfast BT7 1NN, United Kingdom

Unlike the alkali-metal atoms, which are simple, spherically symmetric and were the first to be cooled and Bose-condense, lanthanide atoms, such as Er and Dy, have large electrons spins and are nonspherical. The origin of this is the partially filled, "submerged" $4f$ orbital surrounded by two nominally spherical $6s$ electrons, in the atomic ground state configuration $4f^{\nu}6s^2$. As a result, the interaction between such atoms can be highly anisotropic. This leads to mixing between partial waves with different orbital angular momenta, and results in a dense spectrum of Fano-Feshbach resonances observed as a function of magnetic field in ultracold scattering of Dy and Er [1,2]. Moreover, analysis of statistical properties of the resonance spectra has indicated [2,3] that the diatomic systems is in a quantum chaotic regime (with similar signatures of chaos observed recently in a much simpler system [4]).

Quantum chaos is characterised by absence of quantum numbers that can be used to classify the energy levels, apart from the exact total angular momentum and parity (see, e.g., Ref. [5] which studied quantum chaos in electronic spectra of rare-earth atoms). It is convenient to consider the onset of quantum chaos by starting from a simpler, integrable system, whose levels are mixed by a lower-symmetry perturbation. For quantum chaos to occur in cold-atom collisions, the anisotropic part of the interatomic interaction which mixes the partial waves, should be sufficiently strong. In this work we analyse the nature and degree of anisotropy of this interaction. We also derive a criterion for chaotic mixing, which explains the results of numerical calculation of the resonant spectra [3].

The nonspherical shape of the lanthanide atoms such as Er $4f^{12}6s^2$ or Dy $4f^{10}6s^2$, is induced by the quadrupole moment of the $4f^{\nu}$ electrons. For the atomic ground state (governed by the Hund rule), it is given by [6]

$$Q_{zz} \equiv Q_L = \pm \frac{|e|\,\overline{r^2}}{(2l-1)(2l+3)}\,\nu(2l-\nu+1)(2l-2\nu+1), \tag{1}$$

where $\overline{r^2}$ is the mean-squared radius of the $4f$ orbital ($l=3$), and the upper sign is used for $\nu \le 2l+1$, while for $\nu > 2l+1$ one uses the lower sign and replaces the number of electrons by the number of holes. Using $\overline{r^2} \approx 0.8$ a.u., one obtains the quadrupole moment of the $4f$ subshell as $Q \approx -0.5$ and 0.2 a.u., for Er and Dy, respectively. These values are 1–2 orders of magnitude greater and have opposite signs to the atomic quadrupole moments from calculations which include electron correlations [2,7,8]. This shows the extent of quadrupole polarization of the $6s$ orbital, which screens the bare $4f$ quadrupole. We show that a similar induced contribution to the quadrupole polarisability exceeds greatly the quadrupole polarisability of the $4f^{\nu}$ electrons. This effect is critical for determining the degree of orientational anisotropy ΔC_6 of the van der Waals coefficient C_6.

Numerical calculations [3] show that the mixing of the atomic states with different orbital angular momenta l (and the ensuing chaos) is primarily due to the anisotropic part of the van der Waals interaction W. Estimating the quadrupole-polarisability-induced mixing matrix element between atomic bound states with near-zero energies E_l and $E_{l'}$ in the criterion of strong, chaotic mixing ($\langle l'|W|l\rangle / |E_{l'} - E_l| > 1$), yields the condition

$$\Delta C_6/C_6 > 2\sqrt{2\pi}\,(\Delta_{l'l}/n_{l'l})^{3/2}\,, \tag{2}$$

where $\Delta_{l'l} = (l'-l)(l+l'+1)$, $n_{l'l} = (E_{l'} - E_l)/E_{\rm vdW}$, and $E_{\rm vdW} = \hbar^2/(2M\sqrt{2MC_6})$ is the characteristic van der Waals binding energy (M being the reduced mass). For $l'-l=2$ and $n_{l'l} \sim 100$ [9], we obtain $\Delta C_6 > 0.05 C_6$ for small l, which is similar to the sizes of anisotropy that produced quantum chaotic spectra in Er and Dy [3].

References

[1] K. Baumann, N. Q. Burdick, M. Lu, and B. L. Lev, *Observation of low-field Fano-Feshbach resonances in ultracold gases of dysprosium*, Phys. Rev. Lett **89**, 020701 (2014).
[2] A. Frisch, M. Mark, K. Aikawa, F. Ferlaino, J. L. Bohn, C. Makrides, A. Petrov, and S. Kotochigova, *Quantum chaos in ultracold collisions of gas-phase erbium atoms*, Nature **507**, 475 (2014).
[3] T. Maier *et al.*, *Emergence of chaotic scattering in ultracold Er and Dy*, Phys. Rev. X **5**, 041029 (2015).
[4] D. G. Green, C. L. Vaillant, M. D. Frye, M. Morita, and J. M. Hutson, *Quantum chaos in ultracold collisions between Yb($^1S_0$) and Yb($^3P_2$)*, Phys. Rev. A **93**, 022703 (2016).
[5] V. V. Flambaum, A. A. Gribakina, G. F. Gribakin, and M. G. Kozlov. *Structure of compound states in the chaotic spectrum of the Ce atom: localization properties, matrix elements, and enhancement of weak perturbations*, Phys. Rev. A **50**, 267 (1994).
[6] Eq. (1) corrects the mistake in §75, Problem 3, Eq. (6) of L. D. Landau and E. M. Lifshitz, *Quantum Mechanics* (Pergamon, Oxford, 1977).
[7] S. Kotochigova and A. Petrov, *Anisotropy in the interaction of ultracold dysprosium*, Phys. Chem. Chem. Phys. **13**, 19165 (2011).
[8] C. Harabati, V. A. Dzuba, and V. V. Flambaum, *Effect of the atomic electric quadrupole moment on positron binding*, Phys. Rev. A **90**, 014501 (2014).
[9] B. Gao, *Zero-energy bound or quasibound states and their implications for diatomic systems with an asymptotic van der Waals interaction*, Phys. Rev. A **62**, 050702 (2000).

Double Differential Electron-Emission Cross Sections of DNA constituents induced by protons at Bragg Peak Energies

Benedikt Rudek[1], Daniel Bennett[1], Marion Bug[1], Mingjie Wang[1], Woon Yong Baek[1], Ticia Buhr[1], Gerhard Hilgers[1], Christophe Champion[2], Hans Rabus[1]

1. Physikalisch-Technische Bundesanstalt (PTB),Bundesallee 100, 38116 Braunschweig, Germany

2. Université de Bordeaux, CNRS/IN2P3, Centre d'Etudes Nucléaires de Bordeaux Gradignan, 33 175 Gradignan Cedex, France

Radiation damage in human tissue can be attributed to either direct damage by the ionizing particle or to indirect effects following the emission of secondary electrons. Indirect effects are estimated to contribute two thirds of the overall damage. The vast majority of secondary electrons carry kinetic energies of only few electron volts and thus their inelastic mean free path amounts to only a few nanometers. To simulate damage in the DNA, which is considered to be the most radiosensitive target within the cell, it is therefore necessary to consider secondary electron emission not only from the surrounding water molecules but also from the DNA constituents themselves [1]. In proton beam therapy, the highest probability for electron emission occurs at the end of the proton trajectory, the so called Bragg peak, when the proton beam has been decelerated from kinetic energies of initially several MeV to about 100 keV. Our incentive was to quantify the electron emission from DNA constituents in this energy range and implement the data into the MC trajectory simulation toolkit Geant4 DNA [2], which should eventually lead to a better estimation of the relative biological effectiveness (RBE) of proton beams.

In detail, double differential cross sections were measured for the electron emission from vapor-phase pyrimidine, tetrahydrofuran and trimethyl phosphate that are structural analogues to the base, the sugar and the phosphate residue of the DNA, respectively. The range of proton energies was from 75 keV to 135 keV, the angles ranged from 15◦ to 135◦, and the electron energies were measured from 10 eV to 200 eV. Single differential and total electron emission cross sections are derived by integration over angle and electron energy and compared to a semi-empirical and a quantum mechanical calculation, both within the first Born approximation. The CB1 calculation provides the best prediction of double and single differential cross section for electron energies larger than 60 eV. The total emission cross sections of the three samples are proportional to their total number of valence electrons.

The measurements were part of the EMRP Joint Research Project BioQuaRT [3, 4] which aimed to determine the physical properties of ionizing particle track structure on molecular and nanoscopic scales, and to correlate these track structure properties at the cellular level with the biological effects of radiation.

While proton beam therapy has the advantage of a superior localization of dose compared to the standard use of therapeutic x-rays, it still involves a significant dose to healthy tissue. In an attempt to improve the therapeutic index, high-Z contrast agents have been introduced into tumor cells as effective electron emitters in cell experiments. The experimental dose enhancement factors have not yet been verified by simulations due to the lack of experimental input data. At our presentation, we would like to discuss ideas, challenges and first results for measuring the electron emission spectra of gold nanoparticles.

References

[1] M. U. Bug, *Nanodosimetric particle track simulations in water and DNA media*, Dissertation, University of Wollongong, Australia (2014), URL http://ro.uow.edu.au/theses/4150/.

[2] S. Incerti, G. Baldacchino, M. Bernal, R. Capra, C. Champion, Z. Francis, P. Guèye, A. Mantero, B. Mascialino, P. Moretto, P. Nieminen, C. Villagrasa, and C. Zacharatou, *The GEANT4-DNA project*, International Journal of Modeling, Simulation, and Scientific Computing, **01**, 157–178 (2010).

[3] H. Rabus, H. Palmans, G. Hilgers, P. Sharpe, M. Pinto, C. Villagrasa, H. Nettelbeck, D. Moro, A. Pola, S. Pszona, and P. Teles, *Biologically weighted quantitiesin radiotherapy: an EMRP joint research project*, EPJ Web of Conferences, **77**, 00021 (2014).

[4] H. Palmans, H. Rabus, A. L. Belchior, M. U. Bug, S. Galer, U. Giesen, G. Gonon, G. Gruel, G. Hilgers, D. Moro, H. Nettelbeck, M. Pinto, A. Pola, S. Pszona, G. Schettino, P. H. G. Sharpe, P. Teles, C. Villagrasa, and J. J. Wilkens, *Future development of biologically relevant dosimetry*, The British Journal of Radiology, **88**, 1045 (2015).

Near edge X-ray absorption mass spectrometry of gas phase proteins: the influence of protein size

Dmitrii Egorov, Ronnie Hoekstra, Thomas Schlathölter

University of Groningen, Zernike Institute for Advanced Materials, Nijenborgh 4, 9747AG Groningen, Netherlands

Only very recently, interactions of soft X-ray photons with gas phase protonated proteins and peptides have been investigated for the first time, using synchrotron radiation [1,2]. The first studies indicated, that multiply protonated peptides and proteins in the gas phase can respond to near edge X-ray absorption in two different ways: i) Non dissociative ionization and ionization accompanied by loss of small neutrals dominates for proteins with masses in the 10 kDa range [1]. ii) Photofragmentation leading to formation of small sidechain related fragments such as immonium ions dominates for peptides in the 1 kDa range [2]. Backbone scissions that can deliver protein sequence information are weak for both, low and higher masses.

In order to investigate the transition between the two regimes, we have studied carbon 1s photoexcitation and photoionization for a series of peptides and proteins with masses covering the range from 0.5 kDa to more than 10 kDa. The gas phase protonated molecules where trapped in a radiofrequency ion trap and exposed to synchrotron radiation. Measurements were carried out at the U49/2-PGM1 beamline at Helmholtz-Zentrum Berlin. Time of flight mass spectrometry was employed for investigation of the photoionization and photofragmentation process. The transition from the photofragmentation regime to the non-dissociative photoionization regime turns out to be smooth. The observed mass spectra are most complex in the few kDa regime, where non-dissociative ionization, backbone scission and immonium ion formation coexist.

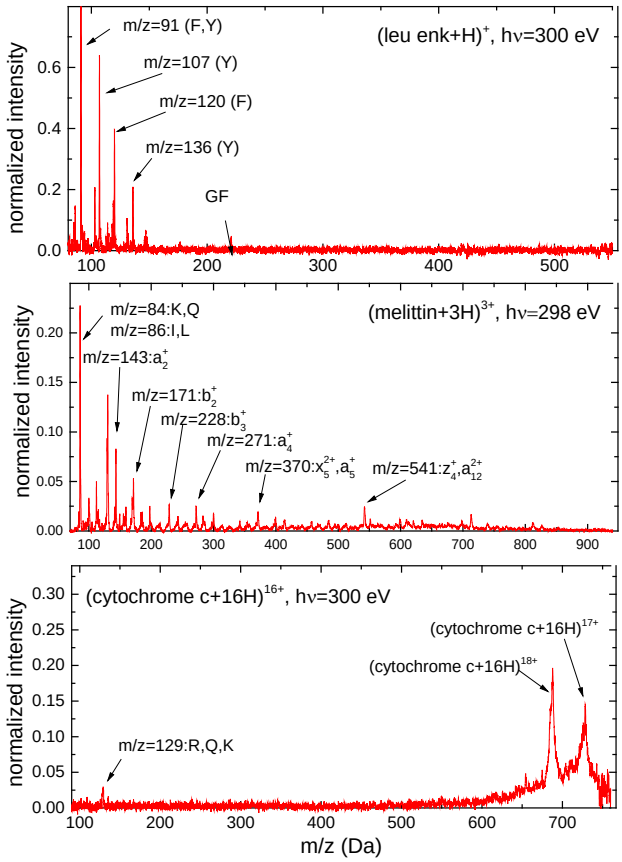

Fig. 1 Photoionization spectra for leu-enkephalin (M=555 Da), melittin (M=2.85 kDa), cytochrome c (M=12 .4 kDa).

The dependence of ionization and fragmentation dynamics on protein mass will be discussed in the light of statistical fragmentation models and local charge/excitation driven fragmentation.

References

[1] A. R. Milosavljević, F. Canon, C. Nicolas, C. M. L. Nahon and a. A. Giuliani, *Gas-Phase Protein Inner-Shell Spectroscopy by Coupling an Ion Trap with a Soft X-ray Beamline*, J. Phys. Chem. Lett., **3**, 1191 (2012).

[2] O. Gonzalez-Magaña, G. Reitsma, M. Tiemens, L. Boschman, R. Hoekstra and T. Schlathölter, *Near edge X-ray absorption mass spectrometry of a gas-phase peptide*, J. Phys. Chem. A, **116**, 10745 (2012)

Electron-Collision Induced Ionization and Fragmentation in Hydrated Biomolecule Clusters

Xueguang Ren, Alexander Dorn
Max-Planck-Institute for Nuclear Physics, 69117 Heidelberg, Germany

In recent years it became apparent that for the transition from isolated molecules to clusters or solid phases of matter, a wealth of new energy and charge transfer phenomena emerge which are absent for isolated molecules like the intermolecular Coulombic decay (ICD) [1]. An important role in this respect plays water which is ubiquitous on earth and surrounds all biological matter. Water and hydrated biomolecule (water-mixed) clusters have been the subjects of intense studies due to their importance in life and environmental sciences [2].

In the present work, we report an experimental study on the electron-collision induced fragmentation and intermolecular processes in clusters consisting of water and bio-relevant molecules like DNA constituents. We use the multi-particle coincidence technique (reaction microscope) [3, 4] in which the momentum vectors and, consequently, the kinetic energies of all final state particles (electrons and ions) are measured in coincidence. The bio-molecule employed here is tedrahydrofuran (THF, C_4H_8O) which is often regarded as being the simplest molecular analog of deoxyribose, part of the DNA backbone linking the phosphate groups and the DNA bases. Figure 1 presents the measured fragment ion time-of-flight (TOF) spectra for both THF and hydrated THF clusters induced by electron ionization (65 eV). Compared to the fragmentation of isolated THF molecule where the most abundant fragment ion is identified as $C_3H_6^+$ [3], the observed major species for cluster fragmentation are $(C_4H_8O)H^+$, $(C_4H_8O)C_2H_4O^+$ and $(C_4H_8O)_2H^+$ for the THF clusters and $(C_2H_4O)H_2O^+$, $(C_4H_8O)(H_2O)H^+$, $(C_4H_8O)(H_2O)_2H^+$ and $(C_4H_8O)(H_2O)_3H^+$ for the hydrated THF clusters. We observe that the fragmentation processes are modified by the presence of the water molecule. From the measured kinetic energies of two outgoing electrons and one fragment cluster ion, the binding energy for each fragmentation channel is obtained. By comparing the correlation spectra of binding energy and fragment species between clusters and the isolated molecule, we can investigate in detail the role of neighbor for the modification of the biomolecular fragmentation. In addition, the measurements of two fragment ions in coincidence with ejected electrons are also obtained to investigate ICD and other related processes in hydrated biomolecule systems as predicted by theory in [5]. Detailed results will be presented at the conference.

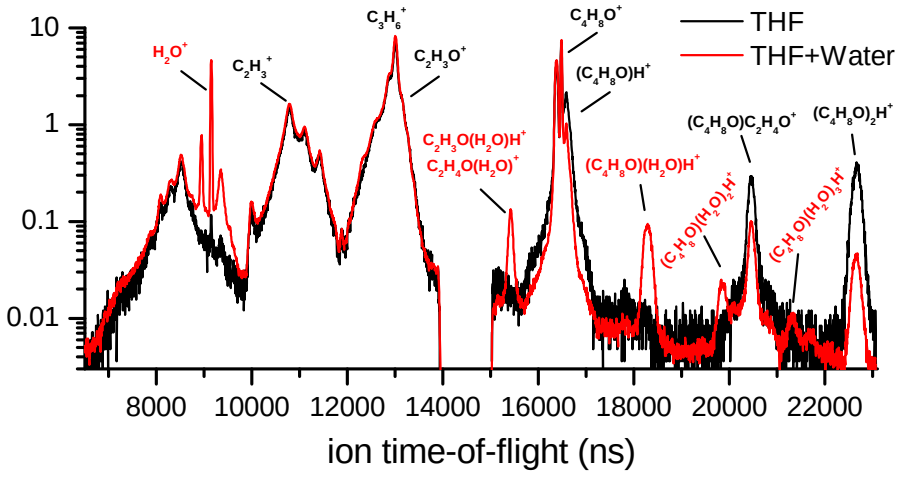

Fig. 1 Measured fragment ion time-of-flight spectra of THF and hydrated THF clusters induced by electron ionization (65 eV).

References

[1] L. S. Cederbaum, J. Zobeley, and F. Tarantelli, *Giant Intermolecular Decay and Fragmentation of Clusters*, Phys. Rev. Lett. **79**, 4778 (1997).

[2] S. Thürmer *et al.*, *On the nature and origin of dicationic, charge-separated species formed in liquid water on X-ray irradiation*, Nature Chem. **5**, 590 (2013).

[3] X. Ren *et al.*, *An (e, 2e + ion) study of low-energy electron-impact ionization and fragmentation of tetrahydrofuran with high mass and energy resolutions*, J. Chem. Phys. **141**, 134314 (2014).

[4] X. Ren *et al.*, *Direct evidence of two interatomic relaxation mechanisms in argon dimers ionized by electron impact*, Nat. Commun. **7**, 11093 (2016). DOI: 10.1038/ncomms11093

[5] S. D. Stoychev *et al.*, *Intermolecular Coulombic decay in small biochemically relevant hydrogen-bonded systems*, J. Am. Chem. Soc. **133**, 6817 (2011).

Determination of Energy-Transfer Distributions in Ionizing Ion-Molecule Collisions

S. Maclot[1], R. Delaunay[1], D.G. Piekarski[2], A. Domaracka[1], B.A. Huber[1], L. Adoui[1], F. Martín[2], M. Alcamí[2], L. Avaldi[3], P. Bolognesi[3], S. Díaz-Tendero[2], and P. Rousseau[1]

[1]Normandie Université, CIMAP, UMR6252 (CEA/CNRS/ENSICAEN/UNICAEN), Boulevard Henri Becquerel, BP5133, 14070 Caen cedex 5, France

[2]Departamento de Química, Módulo 13, Universidad Autónoma de Madri , 28049 Madrid, Spain

[3]CNR - Istituto di Struttura della Materia, Area della Ricerca di Roma 1, Monterotondo Scalo, Italy

Dynamics of different relaxation processes, reflecting energy and charge flow processes in complex systems that can imply a vast number of relaxation pathways (e.g. evaporation, structural reorganization, fragmentation). In the present work, we study response of tymidine molecule (nucleoside, component of DNA molecule) after interaction with ions or photons in the gas phase. Moreover, we have coupled the experimental investigations with quantum theoretical calculations to obtain a complete picture of charge and energy flow transfers in the case singly ionized thymidine molecules.

The experiments have been performed with two different crossed beam devices relaying on mass spectrometry coincidence measurements: valence shell ionization (GASPHASE beamline, Elettra synchrotron, Trieste, Italy) and low-energy ions (ARIBE facility of the GANIL, Caen, France). Quantum chemistry calculation has been performed using the GAUSSIAN09 package (UAM, Madrid, Spain).

The thymidine cation, produced in collisions with 48 keV O^{6+} ions, hardly survives (see Fig. 1). It dissociates via the glycosidic bond cleavage, an important mechanism in the radiation damageof DNA molecule. Interestingly, an intramolecular H-transfer is observed when the charge is localized on the base part yielding $(B+1)^+$ ions. This does not occur when the charge is localized on the sugar part (S^+). From the quantum chemistry calculations it has been shown that such products are the most stable ones. A very small amount of fragments heavier than the base or sugar parts are also observed, i.e. loss of neutral fragments keeping intact the glycosidic bond. This is due to the large distribution of impact parameters in the case of ion collisions [1] which leads to energy transfers, spanning from few meV to few tens of eV and involves a distribution of vibrational energy transfer and electron captures in various electronic states. Thus, the knowledge of the distribution of the energy transferred to the molecule plays a key role to unravel its fragmentation dynamics. It is difficult to assess experimentally this energy distribution even if translational spectroscopy can provide it in the case of multiple electron capture [2].

The photoelectron-photoion coincidence method (PEPICO) was used to investigate the fragmentation dynamics as a function of the electronic excitation energy. Particularly, the comparison of the PEPICO mass spectrum with the calculated orbitals shows the strong dependence of the charge localization on the excited orbitals. Combining such state-of- the-art techniques, we provide a complete picture of the charge localization and the excitation energy distribution in complex molecular systems after interaction with ionizing radiation. More importantly, it becomes possible to determine the energy deposited in the target as a result of an ionizing collision with ions, which is the primary process associated with radiation damage.

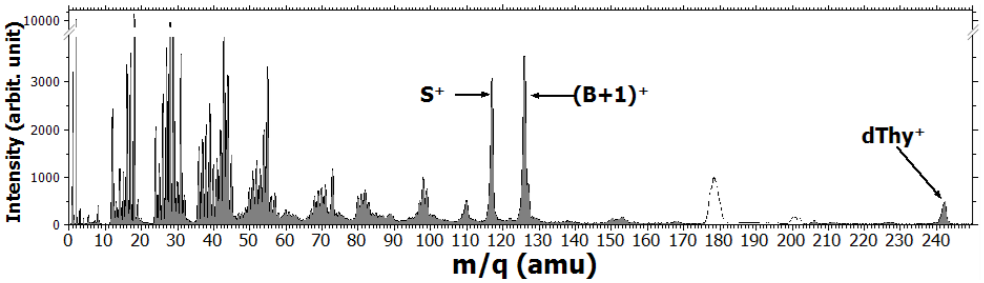

Fig. 1 Mass spectrum of thymidine molecule after interaction with 48 keV O^{6+} ions.

Acknowledgements: Research was conducted in the framework of the CNRS-International Associated Laboratory (LIA) DYNAM and the COST actions XLIC and Nano-IBCT. Financial support from the PHC Galilée/Galileo (G12-44 project "New light on radiosensitisers") is acknowledged.

References

[1] G. Martinet, S. Díaz-Tendero, M. Chabot, K. Wohrer, S. D. Negra, F. Mezdari, H. Hamrita, P. Désesquelles, A. L. Padellec, D. Gardés, L. Lavergne, G. Lalu, X. Grave, J. F. Clavelin, P.-A. Hervieux, M. Alcamí, F. Martín, Phys. Rev. Lett. **93**, 063401 (2004).

[2] L. Chen, S. Martin, J. Bernard, R. Bredy, Phys.Rev. Lett. **98**, 193401 (2007); R. Brédy, J. Bernard, L. Chen, G. Montagne, B. Li, S. Martin, J. Chem. Phys. **130**, 114305 (2009).

Spectroscopy of Highly Charged Ions with Applications for Metrology and Tests of Variation of the Fine-Structure Constant

Hendrik Bekker[1], **Alexander Windberger**[1,2], **José R. Crespo López-Urrutia**[1]
1. Max-Planck-Institut für Kernphysik, Saupfercheckweg 1, 69117 Heidelberg, Germany
2. Advanced Research Center for Nanolithography, Science Park 110, 1098 XG Amsterdam, Netherlands

In recent years, various highly charged ions with optical transitions have been proposed for implementation in next generation optical frequency standards, for example by Berengut *et al.* [1]. The precision reached by current ones suffers from shifts caused by external fields [2]. The compact wavefunctions of HCI are much less sensitive to these perturbations. Due to the reordering of atomic subshells near level crossings, two or more electronic configurations become nearly degenerate in certain HCI. Hence, many optical transitions can exist, such as is the case for Nd-like Ir^{17+} ($Z = 77$) at the $4f$–$5s$ level crossing [1,3]. Furthermore, increased relativistic effects in the nearly full $4f$ subshell of this HCI enhance the sensitivity of certain transitions to a possible variation of the fine-structure constant α. Unfortunately, the complex many-electron couplings reduce the accuracy achieved by predictions to a level unsuitable for laser spectroscopic searches.

In order to resolve this issue, we produced and trapped Re^{15+}, Os^{16+}, Ir^{17+}, and Pt^{18+} ions of the Nd-like isoelectronic sequence in the Heidelberg electron beam ion trap (EBIT). Ionization and excitation of the ions was achieved through electron impact, subsequent emission spectra were measured with spectrometers sensitive in the optical and the extreme ultraviolet (EUV) range [3, 4]. Several optical transitions could be identified by their known scaling with the atomic number Z^2. Identifications were also based on the characteristic line shapes due to the Zeeman splitting of involved fine-structure levels in the strong magnetic field (8 T) of the EBIT, see Fig. 1.

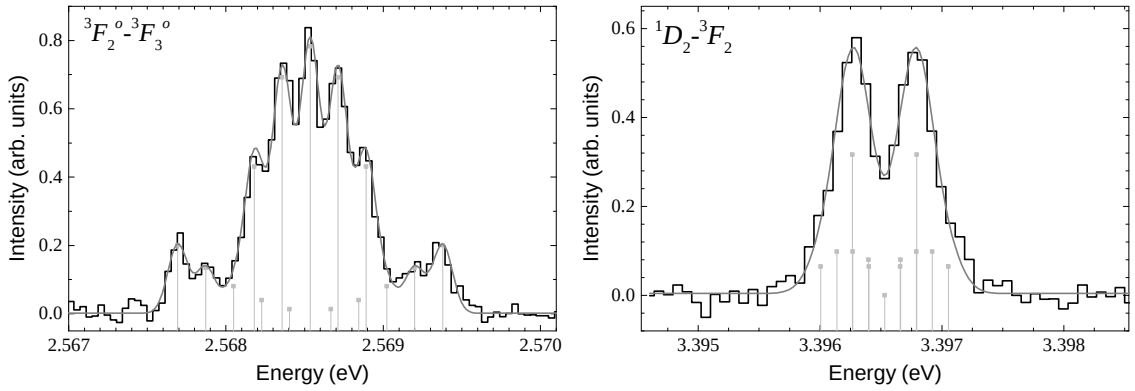

Fig. 1 Two examples of well resolved M1 lines of Ir^{17+} that could be identified by their characteristic Zeeman line shapes. The smooth gray line shows a fit of the Zeeman line shape model to the data (black). The vertical lines show the energies of the individual Zeeman components.

The interpretation of the EUV spectra in the range from approximately 16 to 23 nm was supported by predictions from a collisional-radiative model. In this manner, several of the lines in the dense spectra could be identified. In the Pm-like iso-electronic sequence Re^{14+}, Os^{15+}, Ir^{16+}, and Pt^{17+} the long sought-after alkali-like $5s_{1/2}$–$5p_{3/2}$ transitions could be identified. Further identifications in both Pm-like and Nd-like ions could be used to benchmark and improve the accuracy of atomic theory for these complex, not well-understood, systems. Moreover, the obtained results are an important step towards future precision laser spectroscopy that could be performed with sympathetically cooled HCI in cryogenic Paul traps such as CryPTEx [5].

References

[1] J.C. Berengut, V.A. Dzuba, V.V. Flambaum, and A. Ong, *Electron-Hole Transitions in Multiply Charged Ions for Precision Laser Spectroscopy and Searching for Variations in* α Phys. Rev. Lett. **106**, 210802, May 2011.
[2] A.D. Ludlow, M.M. Boyd, J. Ye, E.Peik, and P.O.Schmidt, *Optical atomic clocks*, Rev. Mod. Phys. **87**, 637–701, Jun 2015.
[3] A. Windberger *et al.*, *Identification of the Predicted* $5s$–$4f$ *Level Crossing Optical Lines with Applications to Metrology and Searches for the Variation of Fundamental Constants*, Phys. Rev. Lett. **114**, 150801, Apr 2015.
[4] H. Bekker *et al.*, *Identifications of* $5s_{1/2} - 5p_{3/2}$ *and* $5s^2 - 5s5p$ *EUV transitions of promethium-like Pt, Ir, Os and Re*, J. Phys. B **48**, 144018 (2015).
[5] L. Schmöger *et al.*, *Coulomb crystallization of highly charged ions*, Science **347**, 1233 (2015).

Laser cooling of stored relativistic heavy ion beams

Danyal Winters
GSI Helmholtzzentrum Darmstadt, Germany

Danyal Winters[1], Tobias Beck[2], Gerhard Birkl[2], Oliver Boine-Frankenheim[1,2], Christina Dimopoulou[1], Lewin Eidam[2], Volker Hannen[3], Daniel Kiefer[2], Thomas Kühl[1,4], Matthias Lochmann[1], Markus Löser[5,6], Xinwen Ma[7], Lijun Mao[7], Fritz Nolden[1], Wilfried Nörtershäuser[2], Benjamin Rein[2], Rodolfo Sanchez[1], Ulrich Schramm[5,6], Mathias Siebold[5], Peter Spiller[1], Markus Steck[1], Thomas Stöhlker[1,4,8], Sascha Tichelmann[2], Johannes Ullmann[1,2], Thomas Walther[2], Hanbing Wang[7], Weiqiang Wen[7], Daniel Winzen[3], Jiancheng Yang[7], Youjin Yuan[7], and Michael Bussmann[5]

1.GSI Helmholtzzentrum Darmstadt
2.Technische Universität Darmstadt
3.Westfälische Wilhelms-Universität Münster
4.Helmholtz-Institut Jena
5.Helmholtz-Zentrum Dresden-Rossendorf
6.Technische Universität Dresden
7.Institute of Modern Physics, Lanzhou, China
8.Friedrich-Schiller-Universität Jena

Laser cooling is a very powerful method to obtain very cold ensembles of particles (atoms, ions, sometimes even molecules). However, concerning charged particles, this is mostly true for light ions in low charge states and at low velocities. We prefer to address the opposite sides of these cases, i.e. heavy ions in high charge states and at very high velocities. Laser cooling is then not used to slow down the particles to rest (as in traps), but to strongly reduce their longitudinal temperature (velocity spread) at a fixed velocity, which is close to the speed of light [1]. At the same time, atomic transitions in these exotic ions, which are otherwise not accessible, can be reached using normal laser systems by exploiting the huge Doppler shift. In this research field, atomic physics meets accelerator physics and laser physics, and the best of all fields is required to obtain the 'coolest' results.

An overview of recent laser cooling activities with relativistic heavy ion beams at the ESR (GSI, Darmstadt, Germany) [2,3] and the CSRe (IMP, Lanzhou, China) [4] storage rings will be given. In the light of these latest results new developments concerning an xuv-detector system and cw and pulsed laser systems will be discussed. Finally, plans for laser cooling at the Facility for Antiproton and Ion Research (FAIR) in Darmstadt will be addressed [1,5].

References

[1] M. Bussmann, ICFA Beam Dynamics Newsletter **No. 65**, 8 (2014).
[2] M. Bussmann *et al.*, JACOW Conf. Proc. COOL 2009 **MOA1MCIO01** 22 (2009).
[3] M. Bussmann *et al.*, GSI Scientific Report **2010**, 339 (2011).
[4] W. Wen *et al.*, Nucl. Instr. Meth. Phys. Res. A **736** 75 (2014).
[5] D. Winters *et al.*, Phys. Scr. **T166** 014048 (2015).

High resolution spectroscopy in HCI using high-order harmonic generation

Janko Nauta[1], Andrii Borodin[1], Peter Micke[1,2], Lisa Schmöger[1,2], Maria Schwarz[1,2], Julian Stark[1], José R. Crespo López-Urrutia[1], Thomas Pfeifer[1]

1. Max-Planck-Institut für Kernphysik, Saupfercheckweg 1, 69117 Heidelberg, Germany
2. Physikalisch-Technische Bundesanstalt, Bundesallee 100, 38116 Braunschweig, Germany

Highly charged ions (HCI) are very abundant atomic systems in the Universe and also of interest for both theoretical and experimental studies. As an example, HCI with just a few tightly bound electrons offer many advantages over neutral and singly charged ions for probing fundamental physics. These HCI have much larger contributions from QED effects and show in most cases a reduction of the complexity of the electronic structure in comparison with many-electron systems. Furthermore, they are intrinsically more sensitive to variation of the fine-structure constant α. Their low polarizability makes them practically insensitive to black body radiation and laser-induced shifts. For these reasons they have been recently proposed as candidates for novel frequency standards in several works (cf. [1]).

Recent progress in trapping HCI in a cryogenic linear quadrupole trap, and sympathetically cooling them down to the mK regime with Be^+ ions [2] paved the way for performing high resolution laser spectroscopy of HCI. In order to expand the future applications of this technique towards higher photon energies, we have started a new project. It aims at performing ultra-high resolution laser spectroscopy of cold HCI in the extreme ultraviolet (XUV) regime, where they possess many interesting transitions. Those were so far only accessible at low resolution either in emission studies or using free-electron lasers [3]. To this end, we are developing an enhancement cavity (shown in Figure 1) to amplify femtosecond pulses from a phase-stabilized infrared frequency comb.

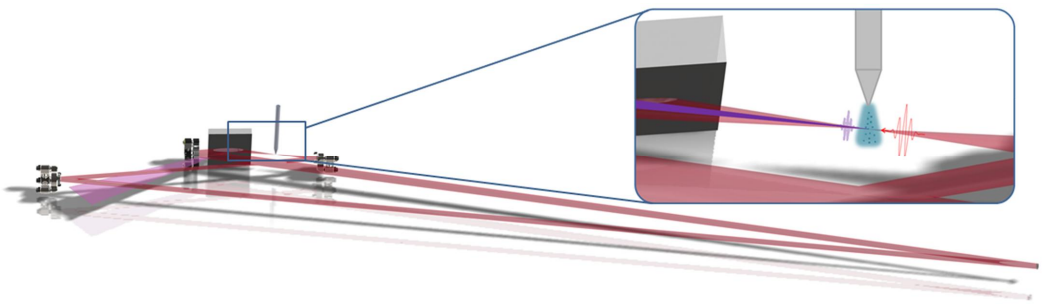

Fig. 1 Overview of the enhancement cavity, which consists of four mirrors and a small period diffraction grating. The inset shows the region around the focus, where higher harmonics are generated and coupled out of the cavity via the grating.

High order harmonics will be generated at the location of the tight focus in the cavity, and can be used for direct frequency comb spectroscopy of HCI to determine absolute transition energies.

References

[1] Andrei Derevianko, V. A. Dzuba, and V. V. Flambaum, *Highly Charged Ions as a Basis of Optical Atomic Clockwork of Exceptional Accuracy*, Phys. Rev. Lett. **109**, 180801 (2012).

[2] L. Schmöger, O. O. Versolato, M. Schwarz, M. Kohnen, A. Windberger, B. Piest, S. Feuchtenbeiner, J. Pedregosa-Gutierrez, T. Leopold, P. Micke1, A. K. Hansen4, T. M. Baumann, M. Drewsen, J. Ullrich, P. O. Schmidt, J. R. Crespo López-Urrutia1, *Coulomb crystallization of highly charged ions*, Science **347**, 6227 (2015).

[3] S. Bernitt, G. V. Brown, J. K. Rudolph, R. Steinbrügge, A. Graf, M. Leutenegger, S. W. Epp, S. Eberle, K. Kubiček, V. Mäckel, M. C. Simon, E. Träbert, E. W. Magee, C. Beilmann, N. Hell, S. Schippers, A. Müller, S. M. Kahn, A. Surzhykov, Z. Harman, C. H. Keitel, J. Clementson, F. S. Porter, W. Schlotter, J. J. Turner, J. Ullrich, P. Beiersdorfer, J. R. Crespo López-Urrutia, *An unexpectedly low oscillator strength as the origin of the Fe XVII emission problem*, Nature **492**, 225–228 (2012).

Penning trap experiments for precision optical and microwave spectroscopy of highly charged ions

M.S. Ebrahimi[1], G. Birkl[2], A. Martin[2], T. Murböck[1,2], W. Nörtershäuser[3], W. Quint[1,4], S. Schmidt[1,3], N. Stallkamp[1,5], M. Vogel[1], M. Wiesel[1,2,4]

1. GSI Helmholtzzentrum für Schwerionenforschung, 64291 Darmstadt, Germany
2. Institut für Angewandte Physik, TU Darmstadt, 64289 Darmstadt, Germany
3. Institut für Kernphysik, TU Darmstadt, 64289 Darmstadt, Germany
4. Physikalisches Institut, Ruprecht Karls-Universität Heidelberg, 69120 Heidelberg, Germany
5. Helmholtz-Institut Jena, 07743 Jena, Germany

We present the status of the two Penning trap experiments SpecTrap and ARTEMIS located at the HITRAP facility at GSI, Germany, and show first measurements. The SpecTrap experiment is designed for optical precision spectroscopy of confined highly charged ions cooled by laser-cooled Mg^+ ions [1]. We have performed Doppler laser cooling of Mg^+ ions and studied the formation of ion crystals by imaging with a CCD camera. The typical cloud size of several thousands of ions leads to the formation of mesoscopic Coulomb crystals which display a particular shell structure in good agreement with theory. The applied combination of buffer gas cooling and laser cooling allows to cool the ions' motion from several hundreds of eV to below micro-eV within seconds. We compare the experimental results to theory and discuss the potential for sympathetic cooling of highly charged ions.

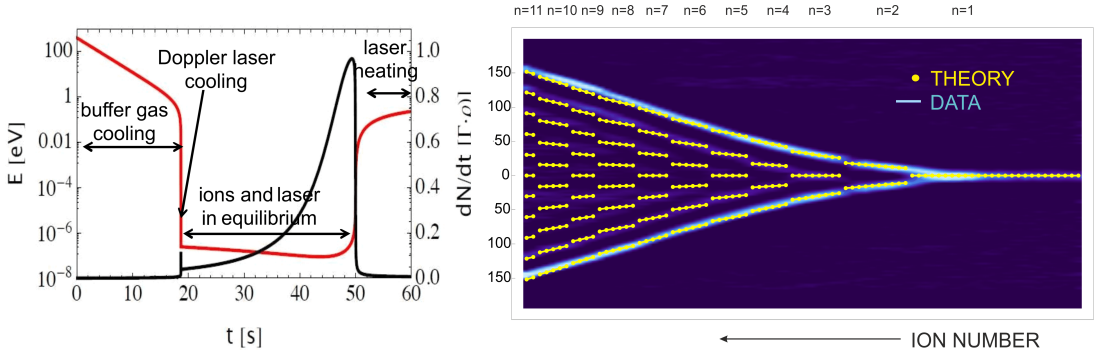

Fig. 1 Left: ion energy vs. time (theory), right: crystal shell number vs. ion number (experiment and theory.)

The ARTEMIS experiment is designed for precision microwave spectroscopy of confined highly charged ions to the end of measuring the magnetic moments of bound electrons with high precision. This allows tests of calculations in the realm of QED in strong fields, and adresses the topic of higher-order Zeeman effects [2]. Presently, the setup features an in-trap source for highly charged ions, which has been operated to produce argon ions up to Ar^{16+}. These ions have been cooled by resistive cooling and stored for several days, indicating a vacuum of better than 10^{-13} mbar. The resistive cooling and ion detection is achieved by use of superconducting resonators, the behaviour of which has been characterized in detail by measuring their properties in external fields between zero and 6 Tesla. Currently, spectroscopic measurements of the fine structure splitting in Ar^{13+} are being prepared.

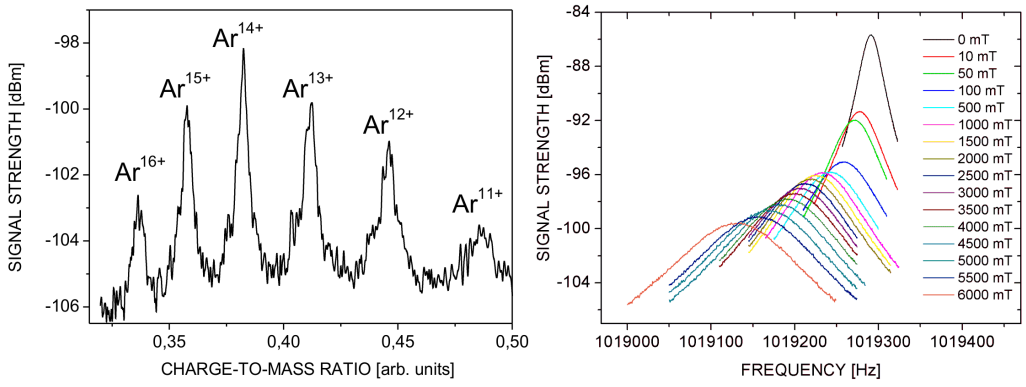

Fig. 2 Left: charge state spectrum of highly charged argon, right: resonator behaviour vs. magnetic field strength.

References

[1] Z. Andelkovic et al., Phys. Rev. A **87**, 033423 (2013).
[2] D. von Lindenfels et al., Phys. Rev. A **87**, 023412 (2013).

APPA R&D — BMBF Collaborative Research at FAIR

Stefan Schippers[1] **and Thomas Stöhlker** [2,3] **on behalf of the APPA collaborations**
1. I. Physikalisches Institut, Justus-Liebig-Universität Gießen, 35392 Giessen, Germany
2. GSI Helmholtzzentrum für Schwerionenforschung, 64291 Darmstadt, Germany
3. Helmholtz-Institut Jena, 07743 Jena, Germany

The research collaboration APPA R&D [1] comprises the German university groups who have set out to perform scientific research at the future international accerlator complex FAIR (Facility for Antiproton and Ion Research) under the umbrella of APPA (Atomic, Plasma Physics and Applications). The FAIR-installations are currently under construction at the site of the GSI Helmholtz Center for Heavy Ion Research in Darmstadt, Germany. APPA is one of the four research pillars of FAIR hosting the international research collaborations BIOMAT (biophysics and material research), FLAIR (physics with low-energy antiprotons), HEDgeHOB/WDM (plasma physics), and SPARC (atomic physics) who focus on investigations of matter under extreme conditions such as strong fields, high densities, high pressures, and high temperatures [2].

The APPA R&D research collaboration pursues coordinated research projects in the area of accelerator based experiments with heavy ions at the future FAIR-installation. Central issues are i) further development of the the experimental infrastructure, in particular, research and development for enhancing the scientific capabilities of the existing installations and of the future accelerator and detector systems including the respective base technologies, and ii) set-up of the APPA experiments of the modules 0-3 of the modularized start version of FAIR.

APPA R&D is funded by the German Federal Ministry for Education and Research (BMBF) within the collaborative-research frame work (‘Verbundforschung’).

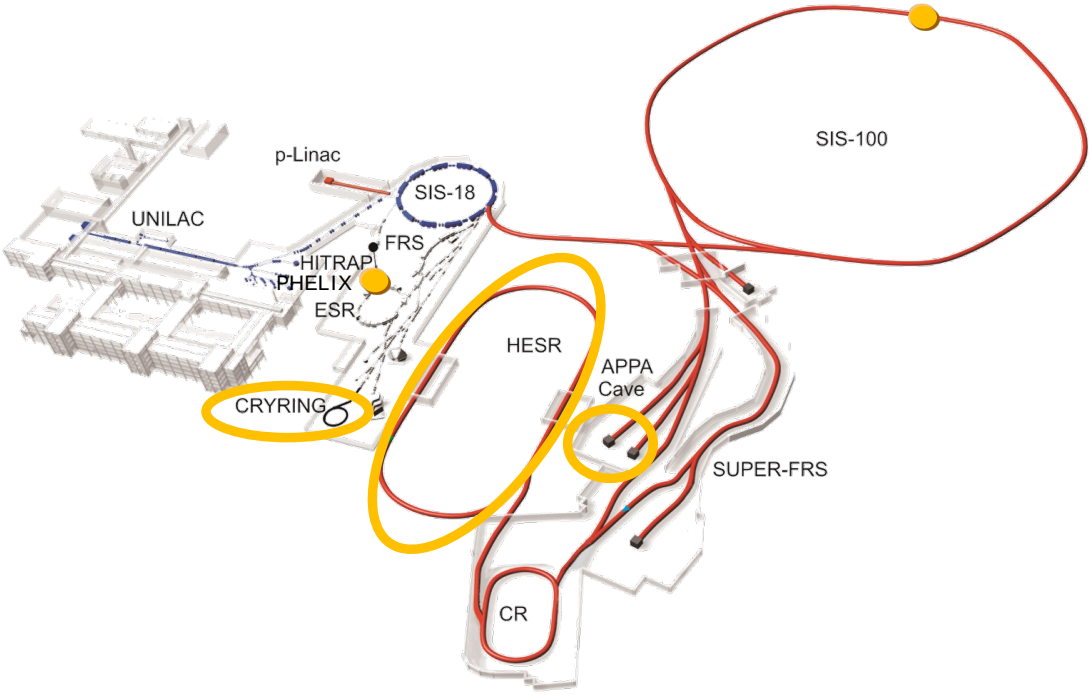

Fig. 1 APPA-experiments (marked in yellow) at the future FAIR accelerator complex.

References

[1] `http://appa-rd.fair-center.eu`
[2] Th. Stöhlker, V. Bagnoud, K. Blaum, A. Blazevic, A. Bräuning-Demian, M. Durante, F. Herfurth, M. Lestinsky, Y. Litvinov, S. Neff, R. Pleskac, R. Schuch, S. Schippers, D. Severin, A. Tauschwitz, C. Trautmann, D. Varentsov, and E. Widmann on behalf of the APPA Collaborations, *APPA at FAIR: From Fundamental to Applied Research*, Nucl. Instrum. Methods B **385**, 680 (2015).

On the influence of the MD-method on the emittance of ion beams extracted from the Frankfurt 14GHz Electron-Cyclotron-Resonance-Ion-Source

J.C. Müller, F. King, R. Dörner, K.E. Stiebing

Institut für Kernphysik der Goethe Universität Frankfurt am Main (IKF), Max von Laue Straße 1, 60438 Frankfurt am Main

Electron-Cyclotron-Resonance-Ion Sources (ECRIS) are widely used as injectors of highly charged ions into linear accelerator structures. Substantial experimental and theoretical effort has been made to improve this type of ion source with regard to their high charge state performance. One of these methods is the use of a special layer with a well-defined metal-dielectric transition at the inner wall of the plasma chamber (MD-method), which has been developed and tested in detail in a series of dedicated experiments at the 14GHz ECRIS of the IKF in Frankfurt. The use of this method does not only strongly increase the output of highly charged ions, but also allows reducing the injected RF-Power for a given intensity or to reduce the X-ray load on source components. Dedicated measurement have shown that the effect is due to an increase of density and temperature of the plasma electrons as compared to the standard source with stainless steel walls, and hence can also be used to generate a reproducible change of the plasma EEDF for diagnostic purposes.
It is well known that it is one drawback of ECRIS`s that they have a relatively large emittance. In this contribution we report on dedicated experiments on the influence of the MD method on the emittance of extracted beams from the Frankfurt ECRIS.

Observation of the Efimov State of the Helium Trimer

M. Kunitski[1], S. Zeller[1], J. Voigtsberger[1], A. Kalinin[1], L. Ph. H. Schmidt[1], M. Schöffler[1], A. Czasch[1], W. Schöllkopf[2], R. E. Grisenti[1], T. Jahnke[1], D. Blume[3] and R. Dörner[1]

1. Institut für Kernphysik, Goethe-Universität Frankfurt am Main, Max-von-Laue-Straße 1, 60438 Frankfurt am Main, Germany

2. Department of Molecular Physics, Fritz-Haber-Institut, Faradayweg 4-6, 14195 Berlin, Germany

3. Department of Physics and Astronomy, Washington State University, Pullman, WA 99164-2814, USA

In 1970 Vitali Efimov predicted remarkable counterintuitive behaviour of a three-body system made up of identical bosons. Namely, a weakening of pair interaction in such a system brings about in the limit appearance of infinite number of bound states of a huge spatial extent [1]. The helium trimer has been predicted to be a molecular system having an excited state of this Efimov character under natural conditions without artificial tuning of the attraction between particles by an external field.

Here we report experimental observation of the Efimov state of $^4He_3$ by means of Coulomb explosion imaging of mass-selected clusters [2]. Helium trimers were prepared under supersonic expansion of the gaseous helium through a 5 µm nozzle. The clusters were selected from the molecular beam by means of matter wave diffraction [3]. Each atom of a trimer was singly ionized by a strong ultrashort laser field resulting in Coulomb explosion of the cluster. The momenta, the ions acquired during Coulomb explosion, were measured by COLTRIMS. These momenta were utilized for reconstruction of the initial spatial geometry of the neutral trimer at the instant of ionization using Newton's equation of motion.

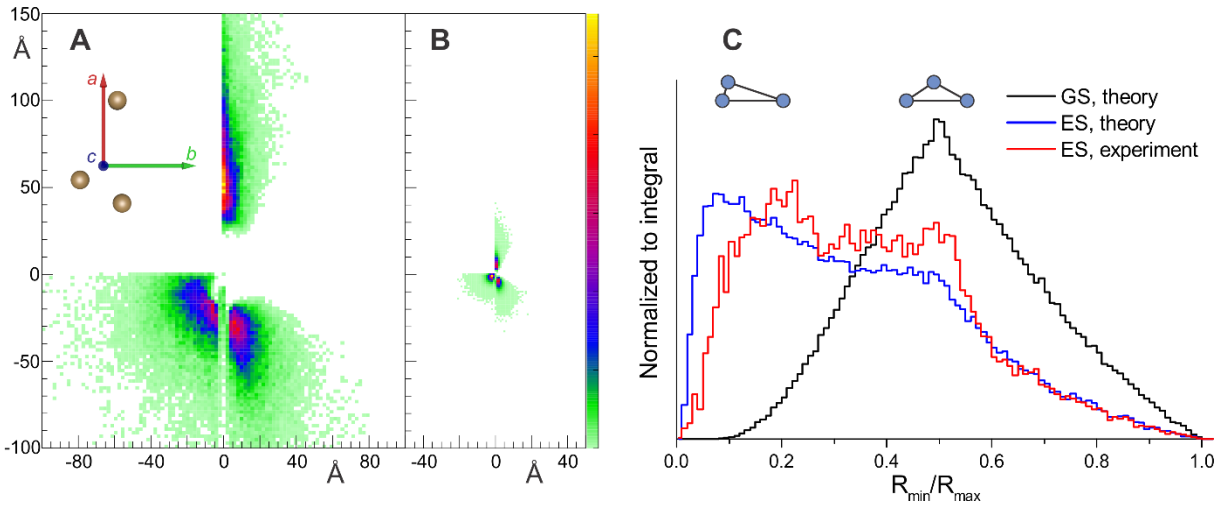

Fig. 1 Structures of the helium trimer: A – excited state, experimental, B – ground state, theoretical. Three helium atoms of each trimer are plotted in the principal axis frame *abc*. C: Distributions of the ratio of the shortest interparticle distance to the longest interparticle distance for ground state structures (black), theoretical excited state structures (blue) and experimental excited state structures (red).

Structures of the excited Efimov state of the $^4He_3$ (Fig. 1A) are about eight times larger than those of the ground state (Fig. 1B), which is in accordance with theory. Whereas the ground state corresponds to an almost randomly distributed cloud of particles [4], the excited Efimov state is dominated by configurations in which two atoms are close to each other and the third one farther away (Fig. 1C).

References

[1] V. Efimov, *Energy Levels Arising from Resonant Two-Body Forces in a Three-Body System*, Phys. Lett. B **33**, 563 (1970).

[2] M. Kunitski, S. Zeller, J. Voigtsberger, A. Kalinin, L. P. H. Schmidt, M. Schöffler, A. Czasch, W. Schöllkopf, R. E. Grisenti, T. Jahnke, D. Blume, and R. Dörner, *Observation of the Efimov State of the Helium Trimer*, Science **348**, 551 (2015).

[3] W. Schöllkopf, J. P. Toennies, *Nondestructive Mass Selection of Small van der Waals Clusters*, Science **266**, 1345 (1994).

[4] J. Voigtsberger, S. Zeller, J. Becht, N. Neumann, F. Sturm, H.-K. Kim, M. Waitz, F. Trinter, M. Kunitski, A. Kalinin, J. Wu, W. Schöllkopf, D. Bressanini, A. Czasch, J. B. Williams, K. Ullmann-Pfleger, L. P. H. Schmidt, M. S. Schöffler, R. E. Grisenti, T. Jahnke, and R. Dörner, *Imaging the Structure of the Trimer Systems $^4He_3$ and $^3He^4He_2$*, Nat. Comm. **5**, 5765 (2014).

Photoabsorption cross section in the frame of local plasma frequency model for semiconductor nanoparticles on example of In_2O_3

Valery Astapenko[1], Sergey Sakhno[1], Mordko Kozhushner[2], Vladimir Posvyanskii[2], Leonid Trakhtenberg[1,2,3]

1. Moscow Institute of Physics and Technology, 9 Institutsky Lane, 141700 Dolgoprudnyi, Russia

2. Semenov Institute of Chemical Physics of RAS, 4 Kosygin St., 119991Moscow, Russia

3. SSC RF "Karpov Institute of Physical Chemistry", 10 Vorontsovo Pole St., 105064Moscow, Russia

One of the main characteristics of photoabsorption is cross section, through which we can express some parameters of the nanoparticle interaction with different external fields. The calculation of photoabsorption cross section is based on the spatial and energy distribution of charge in spherical semiconductor nanoparticles. The dependencies of conduction electrons densities from the radius at different temperatures and various radii of the nanoparticles were obtained from the first principles [1].

The total photoabsorption cross section is equal to the sum of three values:

$$\sigma = \sigma_c + N_\upsilon \sigma_\upsilon + N_s \sigma_s , \qquad (1)$$

whereσ_c is cross section of photoabsorptionby free electrons , σ_υ – by electrons at donors and σ_s – by the electrons on surface oxygen atoms; N_υ, N_s are the numbers of corresponding electrons.

The cross sections σ_υ and σ_s were calculated using the methodic [2]. The value σ_c was obtained using so-called local plasma frequency model [3] (this model also known as Brandt-Lundquist model) and results on spatial distribution of the charge in the nanoparticle.

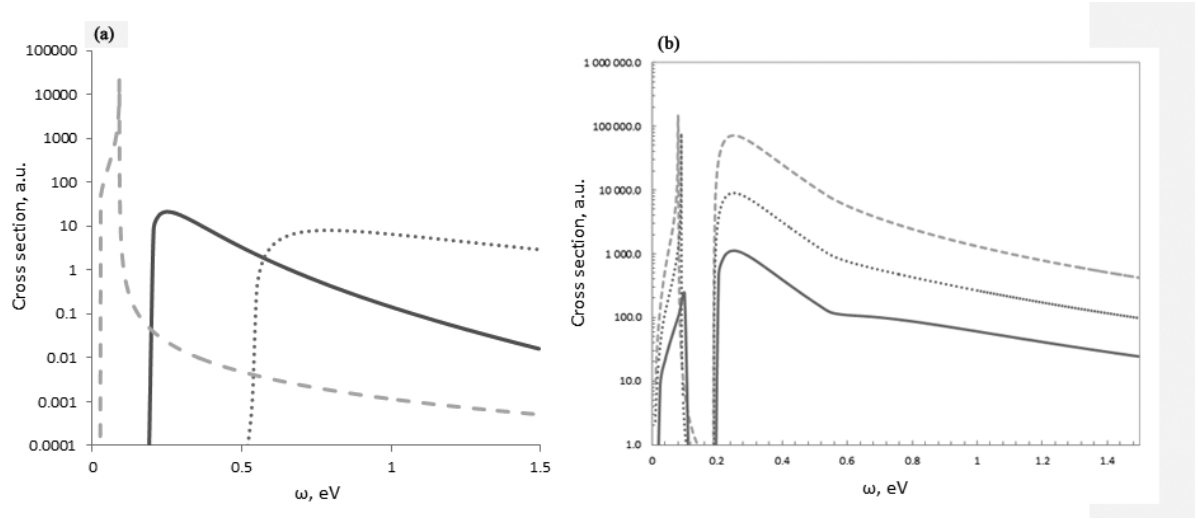

Fig. 1 Spectrum of photoabsorption cross section for In_2O_3 nanoparticles: a) partial photoabsorption cross sections for R = 10 nm, b) total photoabsorption cross sections for different radii of nanoparticles: dotted line – R = 10 nm, dashed line – R = 20 nm, solid line – R = 35 nm.

As an example the spectrum of the photoabsorption cross section of In_2O_3 nanoparticles of radius R = 10 nm was calculated. Fig. 1a shows the dependence of the partial sections: the dotted line corresponds to the cross section of the photoabsorption by free electrons, the solid curve – to the electrons in the traps in the volume of nanoparticles, and the dotted curve – by the electrons trapped on its surface.

Fig. 2b shows the dependence of total photoabsorption cross sections for various radii of nanoparticles; the calculations made by the formula (1). The graph shows that with increasing the radius of nanoparticles, increases also the magnitude of cross section. Besides, the main contribution to the formation of photoabsorption cross section of In_2O_3 nanoparticle give the scattering cross section of free electron (left peak) and electrons in the traps in volume of nanoparticles (right peak).

It should be kept in mind that the contribution to the photoabsorption of electrons in traps on the nanoparticle surface, due to their small number, makes a small contribution to the total cross section and almost not observed in the final graph.

References

[1] M. A. Kozhushner, B. V. Lidskii, I. I. Oleynik, V. S. Posvyanskii, L. I. Trakhtenberg, *Inhomogeneous Charge Distribution in Semiconductor Nanoparticles*, J. Phys. Chem. C, **119**, 16286−16292 (2015).

[2] S. Chaudri, *Optical-transition cross sections involving impurities in semiconductors*. Phys. Rev. B., **26**, P. 6593-6602 (1982).

[3] W. Brandt, S. Lundqvist, *Atomic Oscillations in the Statistical Approximation*. Phys. Rev., **139**, p. A612-A617 (1965).

XUV atomic lasers in noble gases and clusters at the FLASH free-electron laser

L. Mercadier[1], C. Weninger[1], M. Blessenohl[2], B. Langbehn[3], D. Rupp[3], C. Bomme[4], B. Erk[4], C. Bostedt[5], M. Bucher[5], A. Nelde[3], H. Bekker[2], S. Bernitt[2], S. Dobrodey[2], A. Sanchez-Gonzalez[6], A. Przystawik[4], T. Laarmann[4], P. Schmidt[7], M. Wilke[7], A. Knie[7], R. Steinbrügge[2], A. Rudenko[8], Z. Yin[4], A. Sorokin[4], A. Ehresmann[7], D. Rolles[8], T. Möller[3], J. R. Crespo Lopez-Urrutia[2], N. Rohringer[1]

1. Max Planck Institute for the Structure and Dynamics of Matter, Luruper Chaussee 149, 22761 Hamburg, Germany

2. Max-Planck-Institut für Kernphysik, Saupfercheckweg 1, 69117 Heidelberg, Germany

3. Institut für Optik und Atomare Physik, Technische Universität Berlin, 10623 Berlin Germany

4. Deutsches Elektronen-Synchrotron DESY, Notkestraße 85, 22607 Hamburg, Germany

5. Argonne National Laboratory, 9700 Cass Ave, Lemont, IL 60439, USA

6. Department of Physics, Imperial College London, London SW7 2AZ, United Kingdom

7. Institut für Physik, Universität Kassel Heinrich-Plett-Straße 40, 34132 Kassel, Germany

8. MacDonald Laboratory, Kansas State University, Manhattan, KS 66506, USA

When an intense, ultrashort x-ray free-electron laser (XFEL) beam is focused onto matter, inner-shell electrons are photo-ionized and the subsequent relaxation processes can lead to population inversion between two highly energetic states: the basic ingredient for an atomic x-ray laser. We present recent experiments performed at FLASH on XUV lasers in xenon and krypton. First, we demonstrate lasing of the two noble gases in an elongated target at sub-atmospheric pressure. The photo-ionization of the xenon 4d shell by the focused XFEL beam creates a vacancy that rapidly decays via various Auger channels. This results in the creation of long-lived population inversion within the n=5 shell. Three extremely narrow, stimulated emission lines in the XUV domain are observed in the XFEL propagation direction, with gain spanning over 4 orders of magnitude. Similar decay processes lead to the observation of one lasing line in krypton from the n=4 shell.

In a second experiment, probing the same lasing schemes, we study the transition from a homogeneous gaseous medium to an ensemble of clusters with sizes comparable to the lasing wavelength. Are the nano-emitters coherently adding up to the lasing signal? Are they comparable to random lasers of small scattering centers, where the stimulated light gets multiply scattered from nanoparticle to nanoparticle? Can lasing be observed from one single, big cluster?

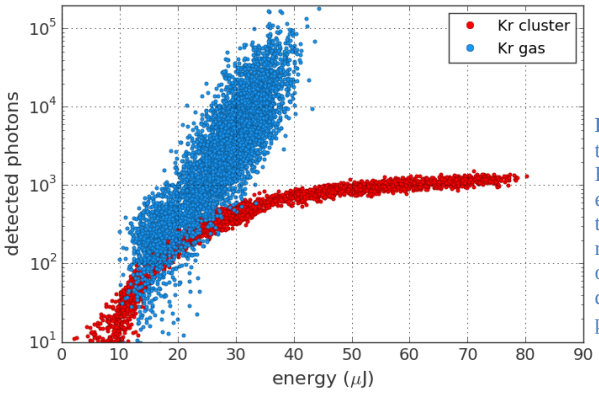

Fig. 1. Lasing intensity of the Kr^{2+} transition as a function of incoming FEL pulse energy. The FEL photon energy is 100 eV and the lasing transition energy is 23 eV. Saturation is reached earlier in the case of clusters, one of the many characteristics that differentiate these nano-emitters from a purely homogeneous medium.

We show that it is possible to stimulate emission lines from xenon and krypton clusters, and that the lasing signal exhibits striking differences with its gaseous counterpart. At the so-called xenon 4d giant resonance (92 eV), the strong energy coupling creates dense nanoplasmas and high charge states that quench the lasing process and broaden the emission lines. At higher photon energies (136 eV), the lasing gain is linear as opposed to exponential in the gas phase. In addition, lasing intensity increases with cluster size, showing a clear difference from a homogeneous medium. We characterize the charge states by fluorescence spectroscopy and the size of emitters by small angle scattering and discuss the effects of the various parameters that control the size and density of the emitters.

A multi-reflection time-of-flight mass spectrometer for the investigation of atomic clusters

Paul Fischer[1], Gerrit Marx[1], Madlen Müller[1], Marco Rosenbusch[1], Birgit Schabinger[1], Lutz Schweikhard[1] and Robert Wolf[2]

1. Institut für Physik, Ernst-Moritz-Arndt Universität Greifswald, Felix-Hausdorff-Str. 6, 17489 Greifswald, Germany

2. Max-Planck-Institut für Kernphysik, Saupfercheckweg 1, 69117 Heidelberg, Germany

Based on the experience at the ISOLTRAP experiment at ISOLDE/CERN [1–5] in precision mass spectrometry of exotic radionuclides, a new multi-reflection time-of-flight mass spectrometer (MR-ToF MS) has been developed for the investigation of atomic clusters. Multiple reflections lead to a long ion flight path and, thus, to a high mass resolving power, which will be exploited for the analysis of the composition of big atomic clusters. In addition, from samples of clusters of the same size, single mass components can be separated and selected, i.e. highly purified ensembles will be provided for the study of laser-cluster interactions such as photo-fragmentation or photoelectron-spectroscopy investigations.

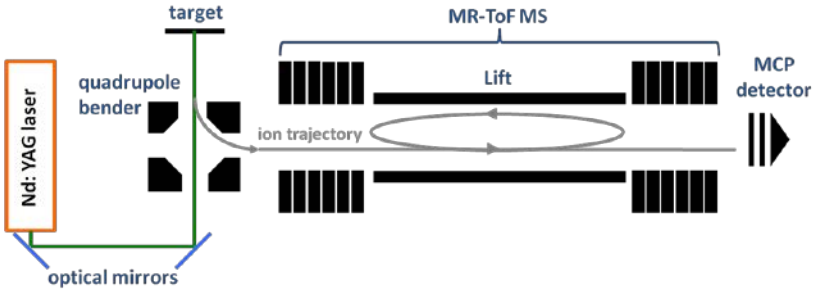

Fig. 1. Schematic overview of the multi-reflection time-of-flight mass spectrometer for cluster investigations.

At the present setup (Fig. 1) cluster ions are produced by laser irradiation of metal targets. These ions are guided by various ion optical elements (not shown) through an electrostatic quadrupole ion-beam bender to the MR-ToF analyzer, where they are captured by an in-trap lift [6]. After several reflections between the two ion optical mirrors they are ejected (again by the by the in-trap lift) towards a microchannel plate for detection.

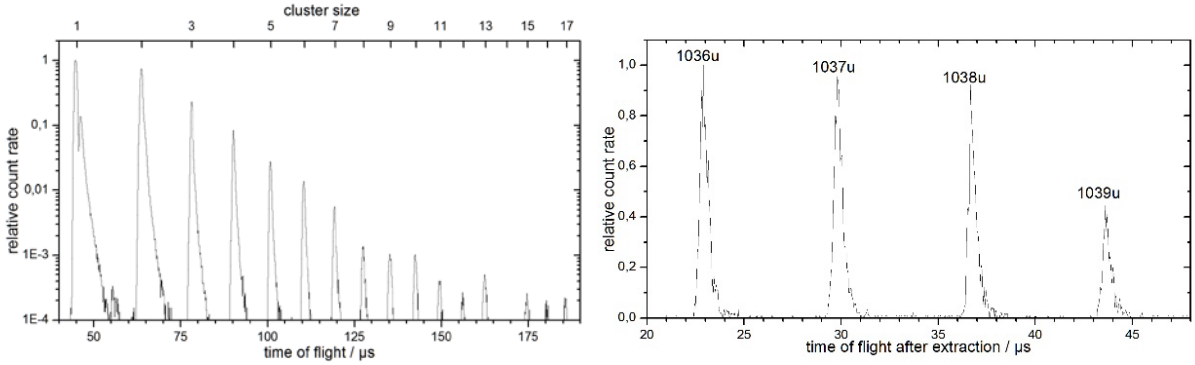

Fig. 2. Single-path ToF spectrum of lead clusters Pb_n^+ (left) and multi-reflection ToF spectrum of Pb_5^+ isotopologues (right).

Figure 2 shows a single-pass spectrum of lead clusters with a prominent signal of Pb_{13}^+ compared to the neighboring cluster sizes – in particular no counts at Pb_{14}^+ – as well as a zoom at the mass region of Pb_5^+, which indicates the capabilities of the device: After 132 laps in the MR-ToF analyzer, i.e. a storage time of 14 ms, the resolving power is $m/\Delta m(FWHM) \approx 14000$, i.e. the Pb_5^+ cluster isotopologues at mass numbers 1036 to 1039 are clearly separated. These test measurements have just started and the limits of the setup are yet to be explored.

References

[1] R. Wolf *et al.*, *ISOLTRAP's Multi-Reflection Time-of-Flight Mass Separator/Spectrometer*, Int. J. Mass Spectrom. **349-350**, 123 (2013).

[2] R. Wolf *et al.*, *Plumbing neutron stars to new depths with the binding energy of the exotic nuclide ^{82}Zn*, Phys. Rev. Lett. **110**, 041101 (2013).

[3] F. Wienholtz *et al.*, *Masses of exotic calcium isotopes pin down nuclear forces*, Nature **498**, 346 (2013).

[4] M. Rosenbusch *et al.*, *Probing the N = 32 shell closure below the magic proton number Z = 20: Mass measurements of the exotic isotopes $^{52,53}K$*, Phys. Rev. Lett. **114**, 202501 (2015).

[5] D. Atanasov *et al.*, *Precision mass measurements of $^{129-131}Cd$ and their impact on stellar nucleosynthesis via the rapid neutron capture process*, Phys. Rev. Lett., Phys. Rev. Lett. **115**, 232501 (2015).

[6] R. Wolf *et al.*, *Static-mirror ion capture and time focusing for electrostatic ion-beam traps and multi-reflection time-of-flight mass analyzers by use of an in-trap potential lift*, Int. J. Mass Spectrom. **313**, 8 (2012).

Spontaneous decay of Ag_n^- clusters

Emma K. Anderson[1], Magdalena Kaminska[1,2], Kiattichart Chartkunchand[1], Gustav Eklund[1], Klavs Hansen[3], Henning Zettergren[1], Henning T. Schmidt[1] and Henrik Cederquist[1]

1. Department of Physics, Stockholm University, Alba Nova University Centre, SE-106 91 Stockholm, Sweden

2. Institute of Physics, Jan Kochanowski University, 25-369 Kielce, Poland

3. Department of Physics and Astronomy, Aarhus University, Ny Munkegade, DK 8000 Aarhus C, Denmark

The Double ElectroStatic Ion Ring ExpEriment (DESIREE) has been used to observe the spontaneous neutral particle emission rate from small silver cluster anions, Ag_n^-, $n = 2$ to 6. DESIREE operates at ~ 13 K and has an extreme high vacuum, $\sim 10^{-14}$ mbar, allowing for long storage times of tens of minutes [1]. This allows the investigation of the spontaneous decay of anions over long times before collisions with the background gas limits further measurements. For an ensemble of anionic clusters with a broad internal energy distribution we expect the decay rate to follow a power law t^{-p} where $p \approx 1$ [2].

A caesium sputter ion source was used to produce a beam of Ag_n^- anions with a broad distribution of excitation energies. The ions are accelerated to 10 keV, injected into the ring after mass selection and stored in one of the two storage rings of DESIREE. Neutral particle emission is detected as a function of time by a MCP detector along the line of sight from one of the straight sections of the ring (see inset of Fig. 1).

Previous studies of small silver clusters (Ag_n^- with $n = 4$ to 9) have been made using the storage ring ELISA, Aarhus University, and report short characteristic times for photon emission from the $n = 4, 6$ and 8 clusters of less than 20 ms [2]. This characteristic time is when the decay curve deviates from a t^{-p} behaviour and may indicate radiative cooling of the cluster. The characteristic (radiative) relaxation time for Ag_5^- was concluded to be at least 50 ms by K. Hansen *et al.*[2]. Observations of the decay at later times was not possible due to collisions with the background gas in ELISA [2].

The extreme high vacuum in DESIREE allows us to observe the decay of the Ag_n^- clusters to much longer time than has been previously possible [1,3]. In Fig. 1, we show how the rate of neutrals emitted from Ag_5^- ions stored in DESIREE changes as a function of time after injection. At early times the neutral particle emission follows a power law, at ~ 100 ms the curve deviates from this law and at ~ 1.5 s the signal reaches the collisional background rate. The extreme high vacuum in DESIREE allows the following new observations: the Ag_5^- ions deviate from a power-law decay at a characteristic time of the order of 250 ms, the Ag_4^- neutral production rate is significantly lower than many of the other clusters (e.g. Ag_5^-) but its radiative cooling time is in fact very long.

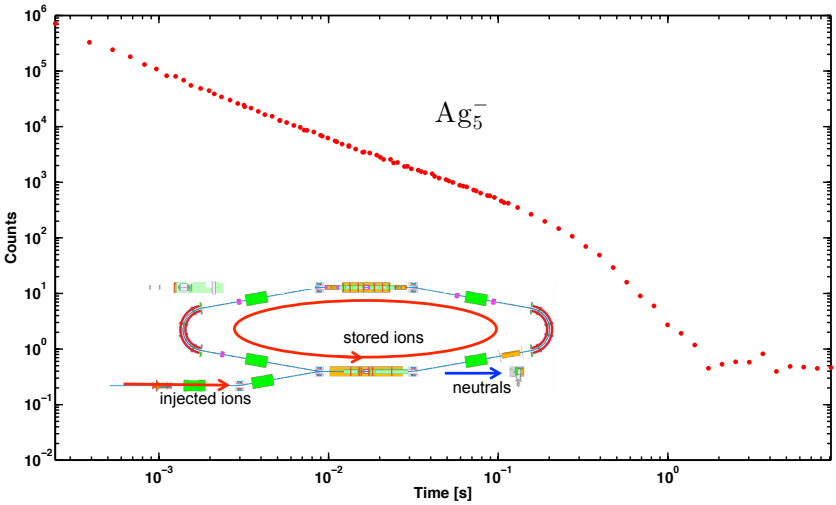

Fig. 1 Rate of neutral particle emission from a stored Ag_5^- beam as a function of time after injection. A t^{-p} power law is observed for the first ~ 100 ms, at later times we see a deviation from this law. A schematic of the apparatus is inset.

References

[1] H. T. Schmidt, R. D. Thomas, M. Gatchell, S. Rosén, P. Reinhed et al., *First storage of ion beams in the Double Electrostatic Ion-Ring Experiment: DESIREE*, Rev. Sci. Instrum. **84**, 055115 (2013).

[2] K. Hansen, J. U. Andersen, P. Hvelplund, S. P. Møller, U. V. Pedersen, and V. V. Petrunin, *Observation of a 1/t decay law for hot cluster and molecules in a storage ring*, Phys. Rev. Lett. **87**, 124401 (2001).

[3] E. Bäckström, D. Hanstorp, O. M. Hole, M. Kaminska, R. F. Nascimento, M. Blom, M. Björkhage, A. Källberg, P. Löfgren, P. Reinhed, S. Rosén, A. Simonsson, R. D. Thomas, S. Mannervik, H. T. Schmidt and H. Cederquist, *Storing keV Negative Ions for an Hour: The Lifetime of the Metastable $^2P^o_{1/2}$ level in $^{32}S^-$*, Phys. Rev. Lett. **114**,143003 (2015).

Kinetic-energy release distributions of fragment anions from collisions of potassium atoms with D-ribose and tetrahydrofuran

A. Rebelo[1], T. Cunha[1], M. Mendes[1],
G. García[2], P. Limão-Vieira[1] and F. Ferreira da Silva[1]

[1] *Laboratório de Colisões Atómicas e Moleculares, CEFITEC, Departamento de Física, Faculdade de Ciências e Tecnologia, Universidade NOVA de Lisboa, 2829-516, Caparica, Portugal*

[2] *Instituto de Física Fundamental, Consejo Superior de Investigaciones Científicas (CSIC), Serrano 113-bis, 28006 Madrid, Spain*

Electron transfer in atom-molecule collision experiments is mediated by the crossing of the covalent (K + AB) and ionic (K^+ + AB^-) potential energy surfaces, where the electron donor is an alkali atom (K) and AB an electron acceptor molecule. At large atom-molecule distances, the ionic potential-energy surface lies above the covalent whilst at smaller distances, due to the Coulomb interaction, a crossing seam may be reached, meaning that both potential surfaces have the same value [1]. In this type of processes a positive ion K^+ and a temporary negative ion (TNI) (or molecular anion $(AB^-)^{\#}$) is formed, allowing access to states which are not attained by electron attachment experiments. In particular, states with a positive electron affinity can be formed, and the role of vibronic excitation can be studied [2], as well as the distribution of the translational energy of the fragment anions formed upon electron transfer in potassium molecule collisions.

In this communication we present Kinetic-energy release distributions obtained from the width and shapes of the time-of-flight (TOF) negative ion mass peaks in collisions of fast potassium atoms with D-Ribose and tetrahydrofuran (THF) molecules. In the case of D-Ribose the most intense signal is due to OH^- [3] whereas in the case of THF is due to O^- [4] formation. The kinetic energy release for a molecule dissociating into to fragments with masses m_1 and m_2, is obtained as

$$\varepsilon_d = \frac{1}{8\mu}\left(F.\Delta t\right)^2$$

were μ is the reduced mass of the m_1 and m_2 system, Δt the extraction time and F extracting field. The kinetic energy release distribution is obtained by

$$D(\varepsilon_d) = \frac{1}{A}\left[1 + \frac{3}{4}\frac{v_m^2}{v_o^2} + \ldots\right]\Delta t.I(\Delta t)$$

References

[1] A. W. Kleyn and A. M. C. Moutinho, *Negative ion formation in alkali-atom-molecule collisions,* J. Phys. B **34**, R1 (2001).
[2] A. W. Kleyn, J. Los, and E. A. Gislason, *Vibronic coupling at intersections of covalent and ionic states***,** Phys. Rep. **90**, 1 (1982).
[3] D. Almeida, F. Ferreira da Silva, G. García, and P. Limão-Vieira, *Dynamic of negative ions in potassium-D-ribose collisions*, J. Chem. Phys. **139**, 114304 (2013).
[4] D. Almeida, F. Ferreira da Silva, S. Eden, G. García, and P. Limão-Vieira, *New Fragmentation Pathways in K–THF Collisions As Studied by Electron-Transfer Experiments: Negative Ion Formation,* J. Phys. Chem. A **118**, 690 (2014).

Classification of the $4p^5n_1l_1n_2l_2$ Metastable States in Rb

Viktoriya Roman[1], Gintaras Kerevičius[2], Alicija Kupliauskienė[2], Alexander Borovik[1,3]

1. Department of Electron Processes, Institute of Electron Physics, Universitetska 21, 88017 Uzhgorod, Ukraine

2. Institute of Theoretical Physics and Astronomy, Vilnius University, Saulėtekio Ave. 3, 10222 Vilnius, Lithuania

3. Faculty of Physics, Uzhgorod National University, Voloshina 54, 88000 Uzhgorod, Ukraine

The energy structure of the $4p^5n_1l_1n_2l_2$ autoionizing states in Rb atoms has been studied both experimentally [1] and theoretically [2]. In particular, accurate spectroscopic classification has been performed for the levels in $4p^55s^2$, $4p^55s5p$, $4p^54d5s$ and $4p^55s6s$ configurations. However, the existing data on classification of metastable states essentially contradict each other [3, 4]. For example, the lowest metastable state initially was identified as $4p^54d(^3F)5s\ ^4F_{9/2}$ state at 15.8 eV [3], whereas in a subsequent study [4] it was assigned as $4p^55s(^3P)5p\ ^4D_{7/2}$ state at 16.77 eV. Single configuration Hartree-Fock calculations [5] could not clarify this situation. Meanwhile, the incident electron energy-loss spectroscopy is known as the most reliable source of direct data on excitation energies and cross sections of atomic states. In the present work, the energy-loss spectrum at 25.5 eV impact energy and an energy resolution of 0.12 eV was measured simultaneously with the ejected-electron spectrum of $4p^5n_1l_1n_2l_2$ states located between 15.7 and 19.2 eV. Both spectra are shown in Fig. 1.

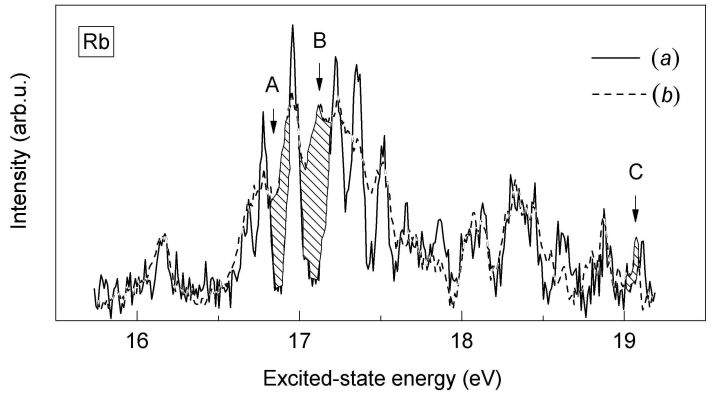

Fig. 1 The ejected (*a*) and energy-loss (*b*) electron spectra of Rb observed at 54.7° to an incident electron beam of 25.5 eV.

Comparative analysis of the spectra (*a*) and (*b*) reveals the presence of three energy regions A, B and C where the minimum intensity in ejected-electron spectrum corresponds to the maximum intensity in energy-loss spectrum. Since the former reflects only the excitation of autoionizing and quasimetastable states, the reason for such a difference can be the presence of energy-loss lines in these energy regions which reflect the excitation of metastable states. Indeed, the fitting of spectrum (*b*) revealed three lines at 16.82, 17.13 and 19.07 eV energy loss which are very close to the calculated excitation thresholds of $5s(^3P)5p\ ^4D_{7/2}$, $4d(^3F)5s\ ^4F_{9/2}$ and $5s(^3P)5d\ ^4F_{9/2}$ states with autoionization probabilities $A^a \sim 10^6\ s^{-1}$ [2] (see Table 1). This data completes the spectroscopic classification of $4p^5n_1l_1n_2l_2$ levels in Rb atoms.

Table. 1 Experimental E_{exp} and calculated E_{cal} excitation energies (in eV), and autoionization probabilities A^a ($\times 10^6\ s^{-1}$) for $4p^55snl\ LSJ$ metastable states in Rb atoms.

Feature	Classification	E_{exp}	E_{cal} [2]	A^a [2]
A	$5s(^3P)5p\ ^4D_{7/2}$	16.72	16.463	2.88
B	$4d(^3F)5s\ ^4F_{9/2}$	17.13	17.097	4.76
C	$5s(^3P)5d\ ^4F_{9/2}$	19.07	18.957	0.73

References

[1] A. Borovik, V. Roman, and A. Kupliauskienė, *The $4p^6$ autoionization cross section of Rb atoms excited by low-energy electron impact*, J. Phys. B: At. Mol. Opt. Phys. **45**, 045204 (2012).

[2] A. Kupliauskienė and G. Kerevičius, *Theoretical study of the $4p^5nln'l'$ autoionizing states of Rb excited by electron impact*, Phys. Scripta **88**, 065305 (2013).

[3] P. Feldman and R. Novick, *Auto-Ionizing States in the Alkali Atoms with Microsecond Lifetimes*, Phys. Rev. **160**, 143 (1967).

[4] R. Novick, G. Sprott, and T. Lucatorto, *Identification of the lowest metastable autoionizing level in Rb from rf spectroscopic studies*, Phys. Rev. A **14**, 273 (1976).

[5] M. W. D. Mansfield, *A New Interpretation of the Rb I 4p Subshell Excitation Spectrum between 15 and 19 eV*, Proc. R. Soc. Lond. A **364**, 135 (1978).

Collision-induced dissociation of protonated water clusters

F. Berthias*, L. Feketeová*, H. Abdoul-Carime*, B. Farizon*, M. Farizon*, and T. D. Märk#

* Université de Lyon; Université Claude Bernard Lyon1; Institut de Physique Nucléaire de Lyon, CNRS/IN2P3 UMR 5822, 69622 Villeurbanne Cedex, France

Institut für Ionenphysik und Angewandte Physik, Leopold Franzens Universität, 6020 Innsbruck, Austria

Collision-induced dissociation (CID) has been studied for protonated water clusters $H^+(H_2O)_n$, with n = 2–8, colliding with argon atoms at a laboratory energy of 8 keV [1]. The experimental data have been measured with the recently apparatus developed at the Institut de Physique Nucléaire de Lyon; 'Dispositif d'Irradiation d'Agrégats Moléculaire,' DIAM [2,3]. It includes an event-by-event mass spectrometry detection technique, COINTOF (correlated ion and neutral fragment time of flight). The latter device allows, for each collision event, to detect and identify in a correlated manner all produced neutral and charged fragments.

For all the studied cluster ions, it has allowed us to identify branching ratios for the loss of i=1 to i=n water molecules, leading to fragment ions ranging from $H^+(H_2O)_{i=n-1}$ all the way down to the production of protons. Using a corresponding calibration technique we determine total charged fragment production cross sections for incident protonated water clusters $H^+(H_2O)_n$, with n=2–7. Observed trends for branching ratios and cross sections, and a comparison with earlier data on measured attenuation cross sections for water clusters colliding with other noble gases (He and Xe), give insight into the underlying dissociation mechanisms.

References

[1] F. Berthias *et al* 2014 *Phys. Rev. A* **89** 062705
[2] C. Teyssier *et al* 2014 *Rev. Sci. Instrum.* **85** 015118
[3] G. Bruny *et al* 2012 *Rev. Sci. Instrum.* **83** 013305

A Set-Up for Angle-Resolved Spectroscopy of Electron Emissions by Chiral Molecules

Jan Dreismann[1], **Alfred Müller**[2], **Daniel Paul**[1], **Sandor Ricz**[3], **Stefan Schippers**[1]
1. I. Physikalisches Institut, Justus-Liebig-Universität Gießen, Leihgesterner Weg 217, 35392 Giessen, Germany
2. Institut für Atom- und Molekülphysik, Justus-Liebig-Universität Gießen, Leihgesterner Weg 217, 35392 Giessen, Germany
3. Institute for Nuclear Research, Hungarian Academy of Sciences, Bem tér 18, 4026 Debrecen, Hungary

The chirality of a molecule can be a decisive property determining its ability to take part in biochemical reactions. According to the current understanding in chemistry this is related to the different spatial arrangements of the atomic constituents in the two enantiomers. It is, however, much less understood in how far the electronic structure and dynamics in a molecule is influenced by chirality. One approach to this question is to study collisions of chiral molecules with chiral probes such as circularly polarized photons (see e.g. [1]) or spin-polarized electrons (see, e.g. [2]).

For analysis of electron spectra from such reactions we plan to use an electron spectrometer ESA-22 [3-5]. A schematic view of the setup is given in Fig. 1. Electrons emitted in the scattering plane pass electrostatic electrodes for energy separation and then are detected on 22 channel-electron-multipliers. Changes to the existing setup had to be adapted for a molecular gas target and an electron-projectile beam instead of a photon beam.

We present first experimental spectra of methyl lactate ($C_4H_8O_3$) with unpolarized electrons. In the future we will use spin-polarized electrons from PEGASUS facility which is currently under construction at GSI in Darmstadt, Germany.

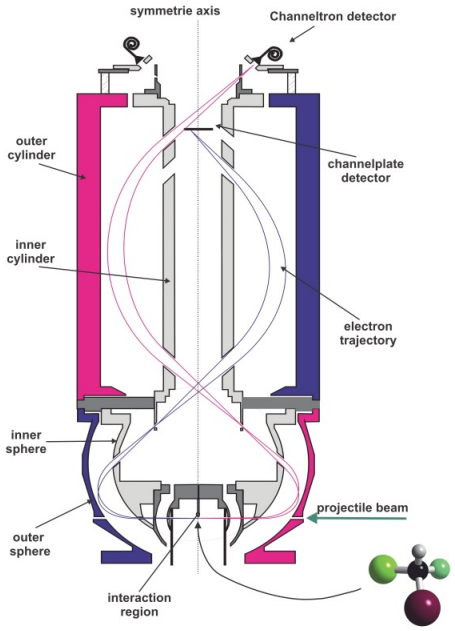

Fig. 1 Schematic view of the rotational symmetric spectrometer setup. A molecular gas beam is crossed with the projectile beam at the spectrometers interaction point. Electrons emitted in the horizontal plane are focused and energy selected by a spherical mirror analyser followed by an cylindrical mirror analyser. Either a channel plate detector or a ring array of channeltron detectors can be used.

References

[1] M.H.M. Janssen, and I. Powis, *Detecting chirality in molecules by imaging photoelectron circular dichroism*, Phys. Chem. Chem. Phys. **16**, 856-871 (2014).
[2] J.M. Dreiling, F.W. Lewis, J.D. Mills, and T.J. Gay, *Anomalously Large Chiral Sensitivity in the Dissociative Electron Attachment of 10-Iodocamphor*, Phys. Rev. Lett. **116**, 093201 (2016).
[3] S. Ricz, Á Kövér, M. Jurvansuu, D. Varga, J. Molnár, and S. Aksela, *High-resolution photoelectron-Auger-electron coincidence study for the L_{23} -M_{23} M_{23} transitions of argon*, Phys. Rev. A **65**, 042707 (2002).
[4] D. Varga, I. Kádár, S. Ricz, J.Végh, Á. Kövér, B. Sulik and D. Berényi, *A spherical mirror-double cylindrical mirror electron spectrometer for simultaneous energy and angular distribution measurements: design, construction and experiences*, Nucl. Instrum. Methods A**313**, 162-172 (1992).
[5] L. Ábrók, T. Buhr, Á. Kövér, R. Balog, D. Hatvani, P. Herczku, S. Kovács, and S. Ricz, *A method for intensity calibration of an electron spectrometer with multi-angle detection*, Nucl. Instrum. Methods B**369**, 24-28 (2015).

Importance of inelastic processes in cold reactions involving polyatomic molecules

Krzysztof Jachymski[1], Michał Hapka[2], Justinas Jankunas[3] and Andreas Osterwalder[3]
1. Faculty of Physics, University of Warsaw, Pasteura 5, 02-093 Warsaw, Poland
2. Faculty of Chemistry, University of Warsaw, Pasteura 1, 02-093 Warsaw, Poland
3. Institute for Chemical Sciences and Engineering, Ecole Polytechnique Fédérale de Lausanne (EPFL), 1015 Lausanne, Switzerland

Low energy reaction dynamics can strongly depend on the internal structure of the reactants. Here we explore the role of rotationally inelastic processes competing with chemical reactions in cold collisions involving polyatomic molecules. We present theoretical analysis of recent experiments [1-3] in which merged beam technique was used to study Penning ionization reaction of CHF_3 and NH_3 by metastable helium and neon in a range of collision energies from < 1 to about 100K. We introduce a simple theoretical model based on quantum defect theory which is able to describe the reaction dynamics of all these systems. We find that the combination of a broad range of collision energies and the relatively small rotational constants of CHF_3makes rotationally inelastic collisions a crucial factor in the total reaction dynamics [1]. Quantitative agreement between theory and experiment is only obtained if the energy-dependent probability for rotational excitation is included in the calculations, in stark contrast to NH_3 [2,3] and H_2 [4] where classical scaling laws are able to qualitatively describe the results.

References

[1] J. Jankunas, K. Jachymski, M. Hapka, and A. Osterwalder, *Importance of rotationally inelastic collisions in low-energy CHF_3 Penning ionization*, submitted (2016)
[2] J. Jankunas, K. Jachymski, M. Hapka, and A. Osterwalder, *Observation of orbiting resonances in He (3S1)+ NH3 Penning ionization*, Journ. Chem. Phys 142, 164305 (2015)
[3] J. Jankunas, B. Bertsche, K. Jachymski, M. Hapka, and A. Osterwalder, *Dynamics of gas phase Ne*+ NH3 and Ne*+ ND3 Penning ionisation at low temperatures*, Journ. Chem. Phys. 140, 244302 (2014)
[4] Y. Shagam, A. Klein, W. Skomorowski, R. Yun, V. Averbukh, C. Koch, and E. Narevicius, *Molecular hydrogen interacts more strongly when rotationally excited at low temperatures leading to faster reactions*, Nature Chem. **7**, 921 (2015)

Collisions Between Ions and Biomolecules. A Geometric Screening Model for the Calculation of Electron Removal Cross Sections within the Independent Atom Model

Hans Jürgen Lüdde[1], Alexander Achenbach[2], Thilo Kalkbrenner[3], Hans-Christian Jankowiak[3], Tom Kirchner[4]

1. Institut für Theoretische Physik, J. W. Goethe-Universität, Max-von-Laue-Str. 1, 60437 Frankfurt am Main, Germany
2. Frankfurt Institute for Advanced Studies, Ruth-Moufang-Str. 1, 60438 Frankfurt am Main, Germany
3. Center for Scientific Computing, J. W. Goethe-Universität, Max-von-Laue-Str. 1, 60437 Frankfurt am Main, Germany
4. Department of Physics and Astronomy, York University, Toronto, Ontario, Canada M3J 1P3

A recently introduced model to account for geometric screening corrections in an independent-atom-model description of ion-molecule collisions [1] is applied to proton collisions from amino acids and DNA and RNA nuclobases. Based on the independent-atom-model the cross sections for net ionization and capture are represented by

$$\sigma_{mol}^{netx} = \sum_{j=1}^{N} s_j \sigma_j^{netx} ,$$

where x stands for ionization or capture, the sum runs over the N constituents of the target molecule, and $0 \leq s_j \leq 1$ are screening coefficients. The latter are obtained from using a pixel counting method (PCM) for the exact calculation of the effective cross sectional area that emerges when the molecular cross section is pictured as a structure of (overlapping) atomic cross sections. This structure varies with the relative orientation of the molecule with respect to the projectile beam direction and, accordingly, orientation-independent total cross sections are obtained from averaging the pixel count over many orientations.

We present net capture and net ionization cross sections over wide ranges of impact energy and analyze the strength of the screening effect by comparing the PCM results with Bragg additivity rule (AR) cross sections and with experimental data where available.

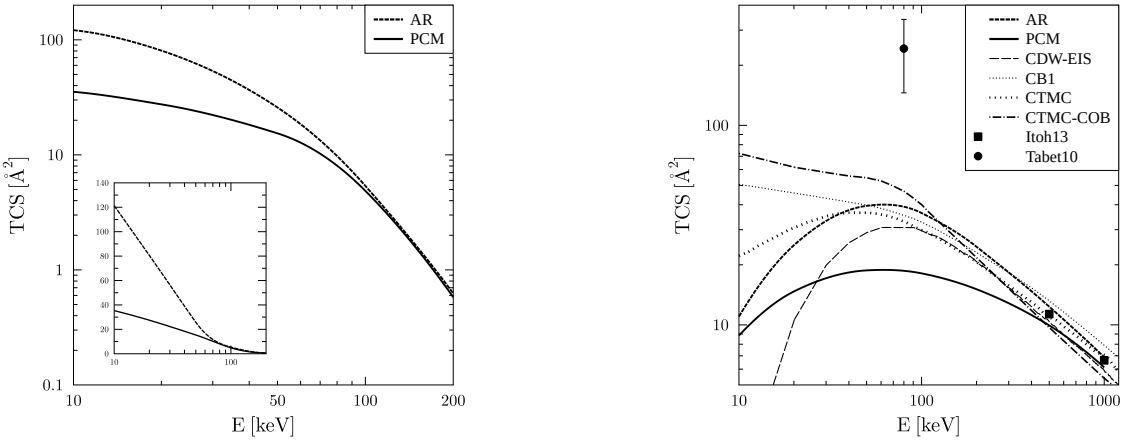

Fig. 1 Total cross sections for net capture (left panel) and net ionization (right panel) in p-$C_4H_4N_2O_2$ (uracil) collisions as function of impact energy. CDW-EIS, CB1, and CTMC-COB results are taken from [2], CTMC [3]. Experiments: Itoh et. al [4], Tabet et al. [5]

References

[1] Hans Jürgen Lüdde, Alexander Achenbach, Thilo Kalkbrenner, Hans-Christian Jankowiak and Tom Kirchner, *An Independent Atom Model Description of Ion Molecule Collisions Includiong Geometric Screening Corrections*, Eur. Phys. J. **D 70**, 82 (2016).

[2] C. Champion, M. E. Galassi, P. F. Weck, S. Incerti, R. D. Rivarola, O. Fojn, J. Hanssen, Y. Iriki and A. Itoh, *Proton Induced Ionization of Isolated Uracil Molecules: A Theory/Experiment Confrontation*, Nucl. Inst. Meth. Phys. Res. Sec. **B 314**, 66 (2013).

[3] L. Sarkadi, *Classical Treatment of the Electron Emission from Collisions of Uracil Molecules with Fast Protons*, Phys. Rev. **A 92**, 062704 (2015).

[4] A. Itoh, Y. Iriki, M. Imai, C. Champion and R. D. Rivarola, *Cross Sections for Ionization of Uracil by MeV-Energy Proton Impact*, Phys. Rev. **A 88**, 052711 (2013).

[5] J. Tabet, S. Eden, S. Feil, H. Abdoul-Carime, B. Farizon, M. Farizon, S. Ouaskit and T. D. Märk, *Absolute Total and Partial Cross Sections for Ionization of Nucleobases by Proton Impact in the Bragg Peak Velocity Range*, Phys. Rev. **A 82**, 022703 (2010).

Resonances in positron-lithium system

Muhammad Umair, Svante Jonsell
Department of Physics, Stockholm University, SE-10691 Stockholm, Sweden)

Theoretical investigation of atomic resonances relating to positrons and positronium∼(Ps) atoms has gained significant interest over the past several years. For Ps formation in positron-lithium scattering, the loosely bound valence electron is involved in the transitions. The e^+-Li system can be modelled as a three-body system: a frozen core, a positron and an electron. The interaction between the Li^+ core and the active electron is Coulombic only at very long range. At shorter distances the nuclear charge is only partially screened, which makes it necessary to employ some sort of model potential for the e^--Li^+ interaction. More generally this interaction should also include electron exchange, but this has not been explicitly included in our study. The e^+-Li interaction is, like the e^+-H interaction, at long distances dominated by the polarizability of the atom, giving a potential $\propto r^{-4}$. The polarizability of lithium atom is however larger than that of H, which allows the formation of a truly bound state of the e^+-Li system [1]. Furthermore, the hydrogen atom has energy levels degenerate with respect to orbital angular momentum (neglecting fine structure) whereas the alkali atoms do not. Another characteristic of a positron-lithium system are that the ionization energy is smaller than the binding energy of Ps (0.25 a.u.), allowing for positronium formation even at zero impact energy.

The method of complex scaling is used to calculate *S*-, and *P*-wave resonance energies and widths below the $\mathrm{Li}(3s,3p,4s,4p)$ excitation thresholds and positronium($n=2$) formation threshold in the positron-lithium system. We used two different types of model potentials to determine the interaction between the core and the valence electron. A dipole series of resonances are found under Ps($n=2$) threshold, furthermore, these resonances were found to agree well with an analytically derived scaling law [1]. The presented results are compared with other theoretical calculations [3-7].

Explicitly correlated Gaussian trial functions expressed in Jacobi coordinates spanning all three rearrangement channels have been employed to include the correlation effects between the outer electron, the positron and the core. The complex scaling method has been used. Two different types of analytical model potentials are used to represent the interaction between the core and outer electron. Of the earlier works, our method is most similar to the stabilization method [4,5,7], but allows more accurate description of resonances by going into the complex plane. It is also different in the coordinate system and functional forms it uses for representing the wave-function, allowing relatively large basis sets to be used.

References

[1] J Mitroy, M W J Bromley and G G Ryzhikh, J. Phys. B. **35**, R81 (2002).
[2] A Temkin and J F Walker 1965, Phys. Rev. A. **140**, A1520 (1965).
[3] S J Ward, J. Phys. B **22**, 3763 (1989).
[4] U Roy and Y K Ho, J. Phys. B **35**, 2149 (2002).
[5] H Han *et al.*, Phys. Rev. A **78**, 044701 (2008).
[6] F Liu, Y Cheng, Y Zhou, and L Jiao, Phys. Rev. A **83**, 032718 (2011).
[7] U Roy and Y K Ho, Nuclear Instruments and Methods in Physics Research B **221**, 36 (2004).

The role of fullerene shell upon stuffed atom polarization potential

Miron Ya Amusia[1,2], Larissa V. Chernysheva[2]

1. Racah Institute of Physics, the Hebrew University of Jerusalem, 91904 Jerusalem, Israel

2. A. F. Ioffe Physical-Technical Institute, 194021 St. Petersburg, Russian Federation

We have demonstrated that the polarization of the fullerene shell considerably alters the polarization potential of an atom, stuffed inside a fullerene. This essentially affects the electron elastic scattering phases as well as corresponding cross-sections. We illustrate the general trend by concrete examples of electron scattering upon endohedrals Ne@C_{60} and Ar@C_{60}.

To obtain the presented results, we have suggested a simplified approach that permits to incorporate the effect of fullerenes polarizability into the Ne@C_{60} and Ar@C_{60} polarization potentials. By applying this approach, we obtained numeric results that show strong variations in shape and magnitudes of scattering phases and cross-sections due to effect of fullerene polarization upon the endohedral polarization potential.

At first glance, the addition of a single relatively small atom inside a fullerene should not affect essentially the electron elastic scattering cross-section of the latter, since the presence of an additional atom inside alters negligibly the total size of the system under consideration. As it was demonstrated recently in [1] and [2], the quantum interference changes the situation impressively, so that the total phase $\delta_l^{A@C_N}$ of the partial wave l of an electron scattered upon endohedral A@C_N is with good accuracy equal to the sum of scattering phases δ_l^A and $\delta_l^{C_N}$ of electrons upon atom A, stuffed inside the fullerene C_N, and the C_N itself. It means, counterintuitively, that a single atom contribution is quite big as compared to the background of C_N cross-section.

In calculations presented in this talk we treat the Ne and Ar atoms. The polarization potential is calculated in the random phase approximation with exchange (RPAE) frame, while C_{60} is represented by a static square well potential, which parameters are chosen to represent the experimentally known electron affinity of C_{60}^-, and low- and medium energy photoionization cross-sections of C_{60}. We take into account the polarization potential of the fullerene.

It appeared that the property of additivity discussed in [1] and [2] is accurate enough only if the effect of the fullerene shell upon atomic polarization interaction is small. In fact, however, already the inclusion of polarization interaction, but with endohedral instead of pure atom's A wave functions, considerably affects the scattering phases and cross-sections. Each step in increasing the accuracy of our approach leads to prominent changes in the cross-section.

It apeared that due to alteration of the inner atom polarization potential by the fullerene, the cross-sections acquire a very big resonance at low energy, perhaps even at $E \to 0$ and a deep minimum at $E \approx 0.1$ Ry. In atomic scattering such a minimum is called Ramsauer minimum.. Note that this variation of the cross-section does not exist for pure fullerene, or even in the simpliest version of RPAE for the endohedral.

Using concrete examples we have demonstrated that the elastic scattering of electrons upon endohedrals is an entirely quantum-mechanical process, where addition of even a single atom can qualitatively alter the multi-particle cross-section.

Even the crudest account of the fullerene influence upon the caged atom polarization potential that is achieved by using endohedral's electron wave functions to describe the intermediate atomic states, alters the phases and cross-sections impressively.

Surprisingly enough, the fullerenes shell dynamic polarization strongly modifies the stuffed atom polarization potential.

Only further clarification of the polarization potential can permit to make a decisive conclusion on the existence of either a low-energy scattering resonance or an extra bound state between an incoming electron and an endohedral.

References

[1] M. Ya. Amusia and L. V. Chernysheva, JETP Letters, **101**, 7, 503-506 (2015).

[2] V. K. Dolmatov, C. Bayens, M. B. Cooper, and M. E. Hunter, Phys. Rev. **A 91**, 062703 (2015).

Positronium Collisions with Noble-gas Atoms

A. R. Swann, G. F. Gribakin
School of Mathematics and Physics, Queen's University Belfast, University Road, Belfast BT7 1NN, United Kingdom

Positronium (Ps) is a hydrogen-like system of an electron and positron bound together. Recent experiments have revealed insteresting phenomena, e.g., that Ps scatters from atoms in a similar way to how electrons scatter from atoms [1], and that the cross section for Ps-atom scattering becomes very small at low Ps energies [2]. These phenomena still await a rigorous theoretical explanation.

Ps-atom scattering has historically been difficult to research theoretically, since both the target and projectile are composite objects. The modern generation of calculations began in the 1990s, using such methods as close coupling [3], stochastic variational [4], and pseudopotential [5], in a variety of approximations, such as static-exchange, frozen-target, and including the long-range van der Waals interaction. The various approaches have shown limited agreement with each other and with experiment, particularly at low Ps energies.

We present a new way of studying low-energy Ps scattering from closed-shell atoms. We confine the entire Ps-atom system inside an impenetrable spherical cavity of radius R_c. A B-spline basis is used to calculate electron and positron states in the static (Hartree-Fock) field of the atom. The two-particle Ps wave function is then written as an expansion in these single-particle wave functions. By diagonalizing the Ps Hamiltonian in this basis, we obtain the energy levels of the Ps in the cavity. We select the states which correspond to Ps($1s$), and find the scattering phase shifts δ_L from the boundary condition at the wall, viz. [6], $\tan\delta_L(K) = J_{L+1/2}[K(R_c-\rho(K))]/Y_{L+1/2}[K(R_c-\rho(K))]$, where J_ν (Y_ν) is the Bessel (Neumann) function, L is the orbital quantum number for the centre-of-mass motion, K is the centre-of-mass momentum, and $\rho(K)$ is the 'collisional radius' of Ps($1s$), which can be determined by investigating states of Ps in an otherwise empty cavity [7]. This gives the phase shifts at certain discrete values of K, and we use calculations for a range of $R_c = 10$–16 a.u. and effective-range-theory-type fits [6] to determine the phase shifts at a general value of K, whence the cross section can be found.

This 'frozen-target' approach fully accounts for distortion of the Ps, but the target atom remains in its ground state. We can alleviate this by including the long-range van der Waals potential between the Ps and target with a suitable cutoff function, viz., $V_W(R) = -(C_6/R^6)\{1-\exp[-(R/R_0)^8]\}$, where C_6 is the van der Waals coefficient for the system (which is known [8]), R is the distance between the atomic nucleus and the Ps centre of mass, and R_0 is a cutoff radius. This approach was used recently in the pseudopotential Ps-atom scattering calculations [5].

The results for He through to Xe are qualitatively similar. Figure 1 shows our frozen-target and van der Waals cross sections for Ps scattering on Ar in comparison with experimental data [2]. Including the van der Waals potential results in smaller cross sections, as it partially cancels the static Ps-atom repulsion. The present results are model-dependent and at variance with experiment for any cut-off radius. We intend to remedy this using many-body theory in the near future, and obtain the most accurate picture of low-energy Ps-atom scattering thus far.

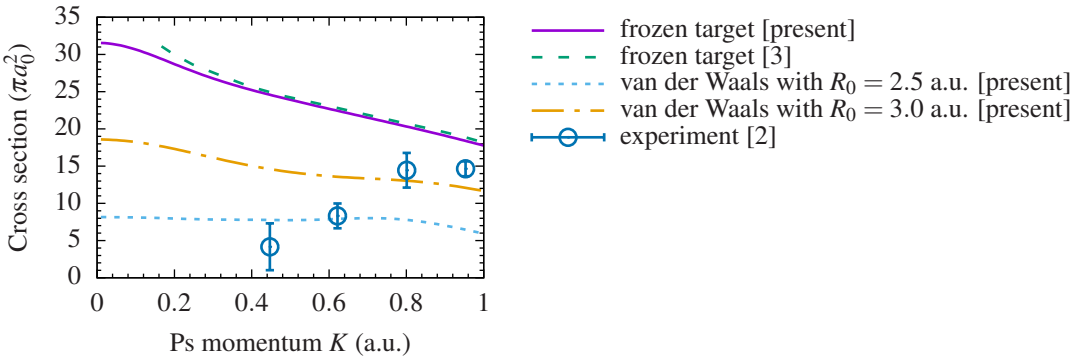

Fig. 1 Cross sections for Ps scattering on Ar, in the frozen-target and van der Waals approximations.

References

[1] S. J. Brawley *et al.*, *Electron-like Scattering of Positronium*, Science **330**, 789 (2010).
[2] S. J. Brawley *et al.*, *Positronium Production and Scattering below Its Breakup Threshold*, Phys. Rev. Lett. **115**, 223201 (2015).
[3] J. E. Blackwood *et al.*, *Positronium Scattering by Ne, Ar, Kr and Xe in the Frozen Target Approximation*, J. Phys. B **35**, 2661 (2002).
[4] J. Mitroy and I. A. Ivanov, *Positronium Scattering from Closed-shell Atoms and Ions*, Phys. Rev. A **65**, 012509 (2001).
[5] I. I. Fabrikant and G. F. Gribakin, *Positronium-Atom Scattering at Low Energies*, Phys. Rev. A **90**, 052717 (2014).
[6] P. G. Burke, *Potential Scattering in Atomic Physics* (Plenum Press, New York, 1977).
[7] R. Brown, Q. Prigent, A. R. Swann, and G. F. Gribakin, *Effect of Confinement on the Radius of Positronium*, unpublished.
[8] A. R. Swann *et al.*, *van der Waals Coefficients for Positronium Interactions with Atoms*, Phys. Rev. A **92**, 012505 (2015).

Quantum chaos in ultracold collisions between Yb($^1S_0$) and Yb($^3P_2$).

Dermot. G. Green[1], Christophe L. Vaillant[2], Matthew D. Frye[2], Masato Morita[2] and Jeremy M. Hutson[2]
1. School of Mathematics and Physics, Queen's University Belfast, University Road, Belfast BT7 1NN, United Kingdom
2. Joint Quantum Centre (JQC) Durham-Newcastle, Department of Chemistry, Durham University, South Road, Durham DH1 3LE, United Kingdom

Signatures of quantum chaos have recently been observed in ultracold collisions of the complex atoms Er and Dy in magnetic fields [1-3]. Such chaos may have very important consequences for ultracold physics: it is likely to make it impossible to assign quantum numbers to resonances and near-threshold states, and may make it impossible even in principle to determine interaction potentials by fitting to observed resonances. In addition, it may cause long-lived 2-body collisions that result in fast 3-body loss [4]. It is thus important to understand the nature of chaos in ultracold collisions, and delineate when it occurs.

We calculate and analyse Feshbach resonance spectra for ultracold Yb($^1S_0$) + Yb($^3P_2$) collisions as a function of an interatomic potential scaling factor λ and external magnetic field [5]. Even in this remarkably simple system, which has strong anisotropy but only 3 electronic curves correlating with the $^3P_2$ threshold, we find strong signatures of chaos that appear when a magnetic field is applied (see Fig. 1). In addition, we show that the resonances in magnetic field in the experimentally accessible range 400 to 2000 G are chaotically distributed, with strong level repulsion that is characteristic of quantum chaos [5].

The results demonstrate that an electronic structure of the complexity of Er+Er or Dy+Dy is not a prerequisite for chaos in ultracold collisions. They also suggest that chaos is likely to be widespread in ultracold collisions, which will have important consequences for the lifetimes of ultracold species.

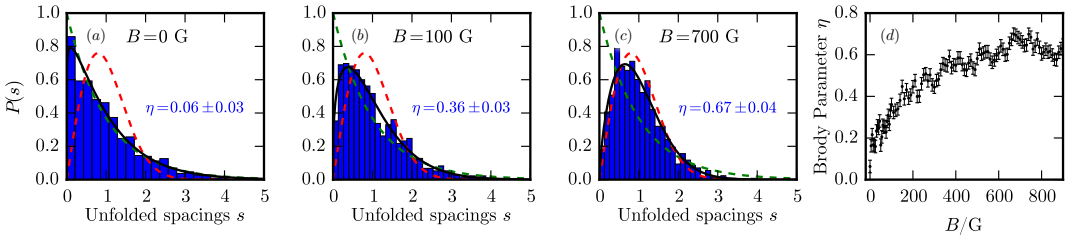

Fig. 1 Statistical analysis of Feshbach resonance positions in ultracold Yb($^1S_0$) + Yb($^3P_2$) collisions with respect to potential scaling factor λ. (a), (b) and (c) show the nearest-neighbour distributions $P(s)$, which is the probability density of two neighbouring levels having the spacing s (on a dimensionless scale in which the levels have unit number density). The nearest-neighbour spacing distribution of a randomly distributed set of levels is of Poisson type, while that of a chaotically distributed set is of Wigner-Dyson type. The Wigner-Dyson distribution exhibits strong level repulsion, i.e., vanishingly small probabilities of finding levels that coincide. The Brody distribution interpolates between Poisson and Wigner-Dyson ones, via a single parameter that takes values between zero (Poisson) and unity (Wigner-Dyson). Coupled-channel results (blue histograms); fitted Brody distributions (black lines, with the corresponding Brody parameters stated); Poisson and Wigner-Dyson distributions (green and red dashed lines, respectively). (d) shows the calculated Brody parameter as a function of magnetic field. Figure adapted from that appearing in [5].

References

[1] A. Frisch *et al.*, *Quantum chaos in ultracold collisions of gas-phase erbium atoms*, Nature London **507**, 475 (2014).
[2] T. Maier *et al.*, *Emergence of Chaotic Scattering in Ultracold Er and Dy*, Phys. Rev. X **5**, 041029 (2015).
[3] T. Maier *et al.*, *Broad universal Feshbach resonances in the chaotic spectrum of dysprosium atoms*, Phys. Rev. A **92**, 060702 (2015).
[4] M. Mayle, B. P. Ruzic, and J. L. Bohn, *Statistical aspects of ultracold resonant scattering*, Phys. Rev. A **85**, 062712 (2012).
[5] D. G. Green, C. J. Vaillant, M. D. Frye, M. Morita and J. M. Hutson, *Quantum chaos in ultracold collisions between Yb($^1S_0$) and Yb($^3P_2$)*, Phys. Rev. A. **93**, 022703 (2016).

Autler-Townes effect in the formation of Feshbach resonances at the collision of two atoms in laser radiation filed.

E.A. Gazazyan, A.D. Gazazyan
Institute for Physical Research, NAS of Armenia, Ashtarak, Armenia

Autler-Townes effect is considered in the formation of metastable molecular states (Feshbach resonances[1]) at the resonance scattering of two atoms in the laser radiation field. Expressions for metastable level populations and resonance scattering cross section are received. In the case of exact resonance of laser radiation and due to the Autler-Townes effect[2], graphics for populations and resonance scattering cross section, which have two peaks, are produced. These results are important role in the study of controlled chemical reactions, in the understanding of the processes in the quantum systems of the Bose-Einstein condensate at low temperatures, and in various optical processes in atomic gases. Fig. 1 shows that the population of the levels ground and excited occurs in two ways. The population of level ground occurs by a direct transition from the continuous state of incident particles to the state $|g\rangle$ and by a transition from the continuous state to the excited state $|e\rangle$ followed by a transition to the state $|g\rangle$. The population of the state $|e\rangle$ also occurs in two ways. These transitions interfere with each other and cause the Autler-Townes effect. The double peak is also observed in the cross sections of resonant scattering [3]. The splitting is based on the Autler-Townes effect. When q=0 the peaks coincide, and when q increases, the peaks separation.

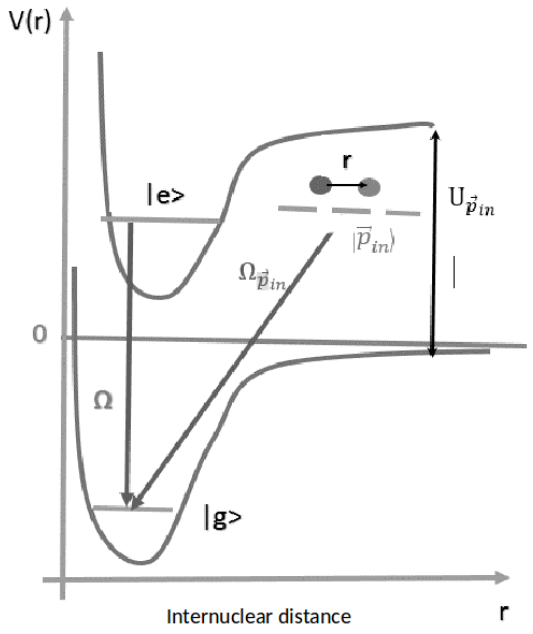

Fig. 1 Schematic diagram of atom-atom collision in the laser radiation fields

The work was supported by the Ministry of Education and Science of Armenia, State Committee of Science (15 T-1S066) and IRMAS project.

References

[1]H. Feshbach, *Ann. Phys.*, **19**, 287 (1962)
[2] S.H. Autler and C.H. Townes, *Phys Rev.* **100**, 703 (1955).
[3] Emil A. Gazazyan, Alfred D. Gazazyan, and Vigen O. Chaltykyan, *Eur. Phys. J. D*, **67**, 197 (2013).

The influence of electrostatic field on resonance charge-exchange

Anna Artamonova[1], Alexander Devdariani[1,2]

1. Dept. Optics and Spectroscopy, St. Petersburg University, Ulyanovskaya str. 3, 198504 St. Petersburg 1, Russia

2. Dept. Theoretical Physics, Herzen University, Moyka emb. 48, 191186, St. Petersburg Russia

The aim of the present work is to study the influence of electrostatic field on resonance charge exchange taking the $H^-+H \rightarrow H+H^-$ reaction as a typical example. The motivation is that charge exchange seems to be one of the basic processes in plasma and, in particular, determines transport properties in plasma. In the same time electric field is always present in plasma.
In the frame of diabatic approach the reaction can be contemplated in terms of transition of an electron between two identical atomic cores [1]. The external electric field destroys the initial resonance and decreases the probability of charge exchange. As the first step we have determined the value of the blocking field, that is the field that blocks the electron transition at some interatomic distance R. The interaction of the electron with atomic cores can be described by two zero-range potentials (or δ-potentials), which is well suited to describe negative ions [2]. Then the blocking field can be found from the Equation

$$\alpha A \leq \frac{1}{2} ER ,$$

where E is a strength of the field, α is a capacity of δ-potentials and $A=\Psi^*(0)\cdot\Psi(R)$, where Ψ are the one-electron wave functions in the electric field.
The result is shown on Fig.1. In this plot the blocking field is area above the graph.

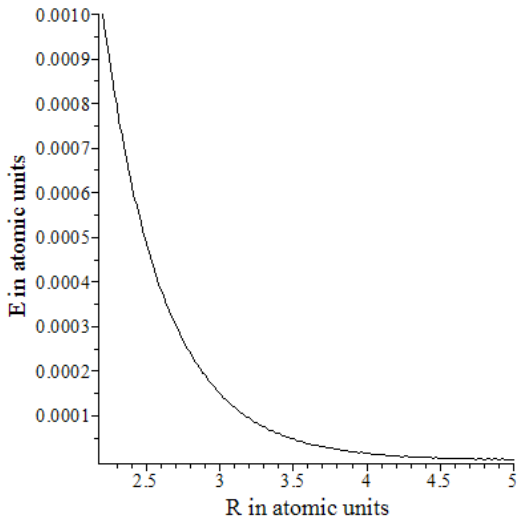

Fig. 1 The electric field as a function of distance between atoms for hydrogen in atomic units

As the next step we are aimed at calculating the dependence of charge-exchange cross-section on the strength of electric field.

References

[1] Bransden B.H., McDowell M.R.C. *Charge Exchange and the Theory of Ion-Atom Collisions,*Claredon Press - 474 p (1992)
[2] Demkov U. N, Ostrovskii V. N. *Zero-range potentials and their application in Atomic Physics*, Plenum Press, 287 p. (1975)

Straggling of Energy Loss at Collisions of Fast Ions with Atoms

D.N. Makarov and V.I. Matveev

Northern (Arctic) Federal University, Severnaya Dvina Emb. 17, 163002 Arkhangelsk, Russia

The energy losses and energy loss straggling of fast charged particles interacting with various materials are investigated both experimentally and theoretically in many scientific centers. Theories currently used for energy losses are developed "synchronously" with experimental investigations, whereas theoretical investigations of energy loss straggling of fast heavy ions on bound atomic electrons are far behind the experimental needs [1], particularly for fast highly charged ions. There have been only a few attempts to improve the result obtained by Bohr [2, 3] for energy loss straggling. The first quantum-mechanical generalization of the Bohr formula was the Livingston–Bethe formula [4] based on perturbation theory. The more widely used modification of this formula was proposed by Fano [5]. However, perturbation theory cannot be used because of the strong fields of highly charged ions. Using the Bloch approach and Bethe–Bloch formula [6] beyond perturbation theory, Titeica [7] obtained the formula for straggling. But his result is incorrect for large charges of ions and leads to significant numerical errors. Thus the Fano formula is commonly accepted as a strict result in the framework of perturbation theory. The relativistic quantum-mechanical generalization of the Bohr formula that is obtained in [8] using the exact solution of the Dirac equation for the scattering of free electrons in the Coulomb field of a heavy ion is also commonly accepted. At the same time, both exact and approximate commonly accepted nonperturbative approaches for energy loss straggling of heavy highly charged ions on bound atomic electrons are still absent [1]. In this case, various semiquantitative formulas with fitting parameters determined experimentally are used.

In this work, energy loss straggling of fast charged particles colliding with atoms are considered using the eikonal approximation in the region of applicability of the nonrelativistic eikonal approximation. In the region of applicability, these calculations can be treated as exact (more precisely, they introduce a standard, negligibly small error). At the same time, eikonal calculations are technically complicated. We show that the Titeica formula is obtained only under certain approximations in eikonal calculations. The errors from these approximations have not yet been estimated. A nonperturbative correction is introduced to the Titeica formula, and a formula for estimating it is proposed. It is shown that straggling calculated with allowance for nonperturbative effects at large Coulomb parameters $\eta = Z/v$ are significantly different (by an order of magnitude) from the results obtained by the Titeica formula. This explains why the Titeica formula is unpopular for the using. The energy losses of fast highly charged ions on copper atoms are calculated and compared to experimental data. It is shown that the inclusion of nonperturbative corrections noticeably improves agreement with the experimental data compared to the Bohr and Titeica formulas. This undoubtedly reduces the number of fitting parameters in various modifications of these formulas that are usually determined semiempirically.

References

[1] P. K. Sigmund, Ion Beam Science: Solved and Unsolved Problems, Ed. by P. Sigmund, Dan. Vidensk. Selsk. Mat. Fys. Medd. 52 (Spec. Iss.), 557 (2006).
[2] N. Bohr, Mat.-Fys. Meddr. Dansk. K. Vidensk Selsk. 18 (1948).
[3] N. Bohr, Selected Works (Nauka, Moscow, 1970), Vol. 1 [in Russian].
[4] M. S. Livingston and H. Bethe, Rev. Mod. Phys. 9, 245 (1937).
[5] U. Fano, Ann. Rev. Nucl. Sci. 13, 1 (1963).
[6] F. Bloch, Ann. Phys. 16, 285 (1933).
[7] S. Titeica, Bul. Soc. Roman. Phys. 38, 81 (1939).
[8] J. Lindhard and A. Sorensen, Phys. Rev. A 53, 2443 (1996).

Influence of renormalization plasma shielding on the electron-impact ionization in dense plasmas

Myoung-Jae Lee[1], Young-Dae Jung[2]

1. Department of Physics, Hanyang University, Seoul 04763, South Korea
2. Department of Applied Physics and Department of Bionanotechnology, Hanyang University, Ansan, Kyunggi-Do 15588, South Korea

The renormalization shielding effects on the electron-impact ionization process are investigated in dense plasmas. The effective projectile-target interaction Hamiltonian and the semiclassical trajectory method are employed to obtain the transition amplitude as well as the ionization probability as functions of the impact parameter, the collision energy, and the renormalization parameter. It is found that the renormalization shielding effect suppresses the transition amplitude for the electron-impact ionization process in dense partially ionized plasmas. It is also found that the renormalization effect suppresses the differential ionization cross section in the peak impact parameter region. In addition, it is found that the influence of renormalization shielding on the ionization cross section decreases with an increase of the relative collision energy. The variations of the renormalization shielding effects on the electron-impact ionization cross section are also discussed.

A Powerful New Electron Gun for Electron-Ion Crossed-Beams Experiments

Benjamin Ebinger [1], **Alexander Borovik Jr.**[1], **Stefan Schippers**[1], **and Alfred Müller**[2]
1. I. Physikalisches Institut, Justus-Liebig-Universität Gießen, 35392 Giessen, Germany
2. Institut für Atom- und Molekülphysik, Justus-Liebig-Universität Gießen, 35392 Giessen, Germany

The experimental sensitivity of an electron-ion crossed-beams experiment is mainly determined by the densities of both beams in the interaction region. Aiming at the extension of the available range of accessible electron energies and densities, a new high-power electron gun has been developed and fabricated. It delivers a ribbon-shaped beam with high currents at variable energies between 10 and 3500 eV [1,2]. The design goals of the gun are being met by the utilization of a variety of electrodes, all of which are insulated from each other: Cathode and collector, focusing and defocusing electrodes, four controlling electrodes, and the segmented interaction region 1 and 2 (Fig.1). This electrode configuration allows for a variety of possible operational modes and, thus, provides a high versatility concerning the optimization of the electron-beam properties depending on the purpose of a given experiment. The most important modes of operation are the high-energy mode, different high-current modes (with higher voltages at the controlling electrode 1 in order to obtain high electron currents at low energies) and modes without a potential trap in the interaction region (by applying a negative potential on the controlling electrodes 2 and 3 with respect to the interaction region).

Here, we report on performance tests of our newly developed electron gun. First experiments have demonstrated the expected high electron currents in the interaction region and very good beam transmission. Meanwhile, the tests have entered the final phase as the electron gun has been integrated into the experimental crossed-beams setup in Giessen. Employing the *animated crossed-beams* technique [3], first ionization cross sections were measured. Several challenging issues associated with space-charge effects in the high-density electron beam are currently being investigated.

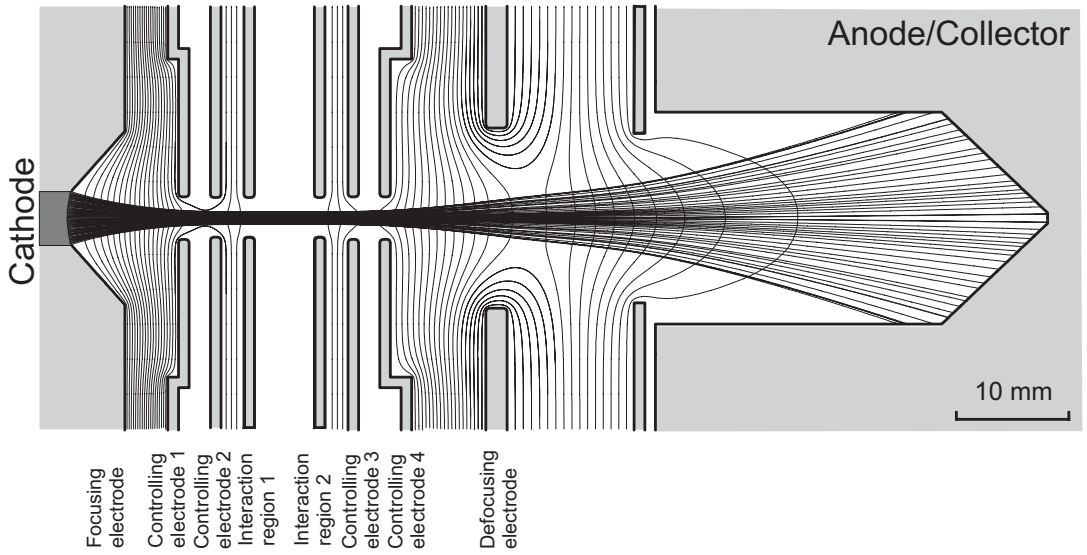

Fig. 1 Geometrical sketch of the electron gun with its various electrodes as well as the trajectories of the electrons for the high-energy mode. Small losses on the electrodes are unavoidable but the majority of electrons reaches the collector.

References

[1] Wei Shi, Jörg Jacobi, Holger Knopp, Stefan Schippers, and Alfred Müller, *A high-current electron gun for electron–ion collision physics*, Nucl. Instr. Meth. Phys. Res. B **205**, 201-206 (2003).

[2] Alexander Borovik Jr., Wei Shi, Jörg Jacobi, Stefan Schippers, and Alfred Müller, *High-power electron gun for electron-ion crossed-beams experiments*, J. Phys.: Conf. Ser. **488**, 142007 (2014).

[3] Alfred Müller, Kurt Huber, Klaus Tinschert, Reinhard Becker, and Erhard Salzborn, *An improved crossed-beams technique for the measurement of absolute cross sections for electron impact ionisation of ions and its application to Ar^+ ions*, J. Phys. B. **18**, 2993-3009 (1985).

Electron-Impact Ionization Cross Section and Rate Coefficient of Se^{18+}

Erdi A. Bleda[1], Zikri Altun[1]

1. Marmara University, Department of Physics, Ziverbey 34722, Istanbul, Turkey

The ionization of atoms by electron impact is one of the most fundamental electron collision processes and plays an important role in many areas of research. The modeling and diagnostic of astrophysical and laboratory plasmas need atomic data characterizing the various collision processes that might occur in them. In this study, we investigate the electron-impact ionization of Se^{18+} and calculated the cross section and rate coefficients. Direct ionization cross section of 2s,2p,3s, and 3p subshells were calculated within the semireletavistic Configuration-average distorted wave (CADW) method[1]. The excitation-autoionization contributions originating from the inner shell excitations of the type $2s^22p^63s^23p^4 \rightarrow 2s^22p^53s^23p^4nl$, $2s^12p^63s^23p^4nl$ for Se^{18+} ($n = 4-8, l = 0-3$) were calculated using both CADW and semirelativistic level-resolved distorted-wave (LLDW) method[2]. Branching ratios for the radiation damping of the autoionizing configurations and levels are included. $2s^22p^63s^13p^4nl$ excitations are found to be all below the first ionization threshold. The rate coefficients are also calculated. Total CADW cross sections are also calculated using the codes developed at the Los Alamos National Laboratory[3] and presented along with our own total CADW cross section.

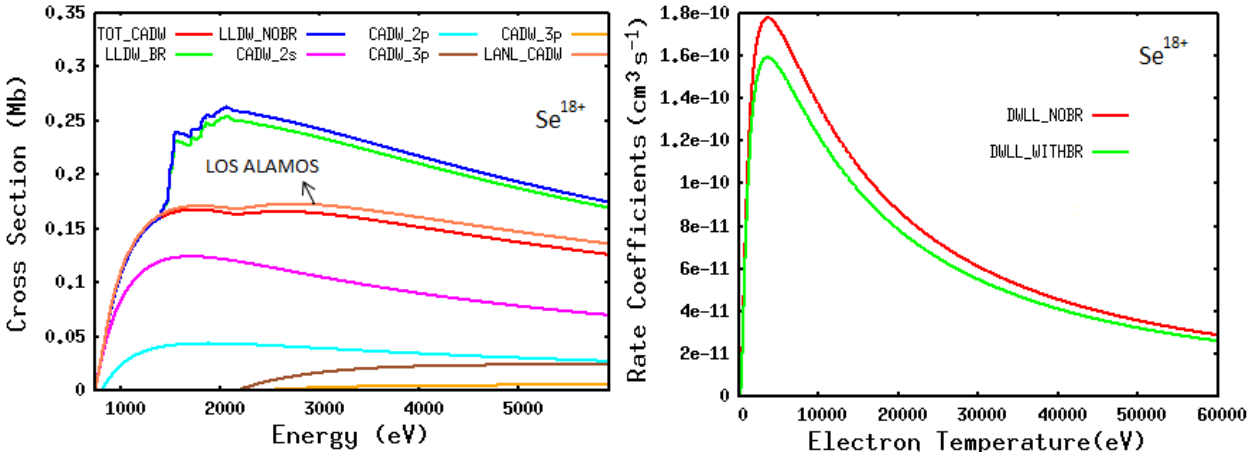

Fig. 1 Cross sections(a) and rate cofficients (b) for Se^{18+}.

The results are shown in Figure 1a and 1b. In Figure 1a CADW direct cross sections for 2s,2p,3s, and 3p electrons are labeled as CADW_2s, CADW_2p, CADW_3s, and CADW_3p, respectively. The purpose of this calculation is to show the contributions from various subshell to the total cross sections. Total CADW cross section is labeled as TOT_CADW in Figure 1a. Total LLDW cross section with branching and unit branching are labeled as LLDW_BR and LLDW_NOBR in Figure 1a. As it can be seen from the figure radiation damping of autoionizing levels did not change the magnitude of the cross section dramatically. The curves labeled as LOS ALAMOS in Figure 1a represents total configuration-average direct electron-impact ionization cross sections within distorted-wave approach calculated using the codes developed at the Los Alamos National Laboratory[3]. The agreement between our total direct CADW results and the Los Alamos curve is quite good. The cross-section results from LLDW_BR and LLDW_NOBR calculations were converted into temperature dependent rate coefficients by performing a Maxwellian integration. The results are shown in Figure 1b.

Acknowledgement

We thank BABKO of Marmara University and National Energy Research Scientific Computing Center (NERSC) in Oakland, California for computational support

References

[1] M. S. Pindzola, D. C. Griffin, and C. Bottcher, 1986, Atomic Processes in Electron-Ion and Ion-Ion Collisions, ed. F. Brouillard, NATO ASI B 145, 75

[2] Cowan R.D., 1981, The Theory of Atomic Structure and Spectra. Berkeley CA: University of California Press

[3] Los Alamos National Laboratory, USA, http://aphysics2.lanl.gov/tempweb/lanl/

Potential Electron Scattering by the Bi and Rn Atoms

Vladimir Kelemen[1], Shandor Demesh[1,2], Eugene Remeta[1]

1. Institute of Electron Physics, National Academy of Sciences of Ukraine, Universitetska St. 21, 88017 Uzhhorod, Ukraine

2. Institute for Nuclear Research of the Hungarian Academy of Sciences (ATOMKI), Bem tér 18/c, 4026 Debrecen, Hungary

We used the optical potential approach to calculate elastic electron scattering by the Bi and Rn atoms at the same impact energies, which are neighboring atoms of the Periodic Table's 6th period. The local relativistic parameter-free real optical potential approximation (RSEP LA) is used [1]. It contains static, relativistic local exchange, local correlation-polarization, scalar-relativistic and spin-orbit potentials. The relative values of differential cross sections (DCSs) are measured for e+Bi scattering for a wide energy range 5-1200 eV in [2] for scattering angles from 30° to 155°. The absolute values of DCSs and integral cross section (ICS) values are measured experimentally for e+Bi scattering at 40 eV in [3], when the bismuth beam is obtained around 1000°C and contains Bi atoms (86%) and Bi_2 molecules (14%). Worth noting, that the polarisation in electron scattering by Hg, Tl, Pb and Bi (and Bi_2) atoms were measured in [4] for energies 6-180 eV and angles from 30° to 130°.

As an example we present the DCSs for e+Bi at 10 and 40 eV impact energies in Fig.1 (a) and (b). Our DCS is compared at 40 eV with the experimental data [3], where the DCSs are measured with ±20% accuracy and ICS with an uncertainty factor 2. Note here, that the ICS for e+Bi, Bi_2 at 40 eV in [3] is equal $45.0 \cdot 10^{-20}$ m^2, while our value for e+Bi is $14.04 \cdot 10^{-20}$ m^2. Fig.1 (c) and (d) show the DCSs for e+Rn at 10 and 30 eV impact energies. In this case the ICS at 30 eV is equal $19.52 \cdot 10^{-20}$ m^2.

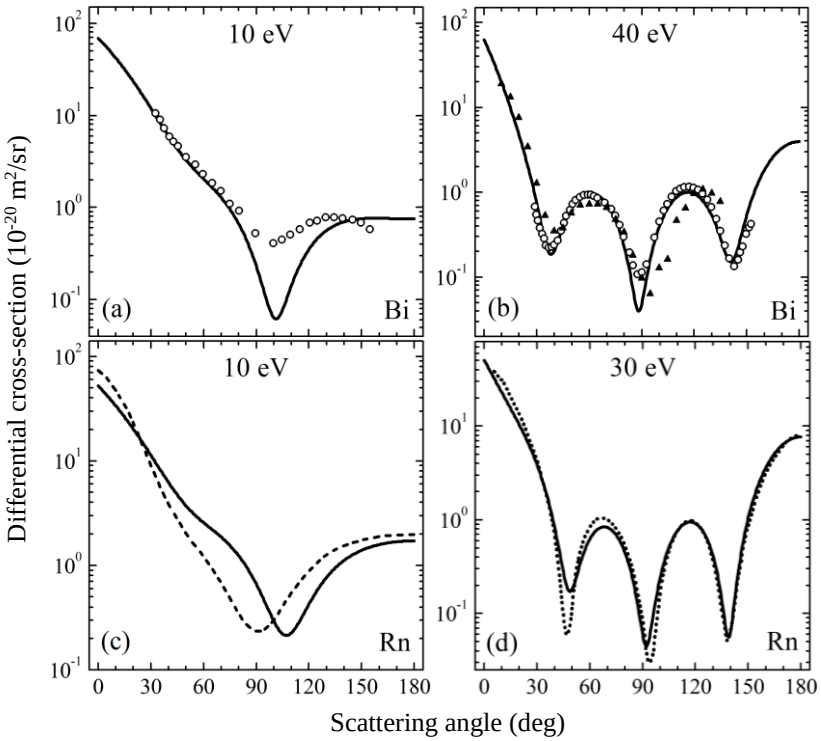

Fig. 1 Differential elastic cross sections for e+Bi scattering at 10 eV (a) (○ [2]) and 40 eV (b) (○ [2], ▲ [3], normalized by our DCSs at 120°) and for e+Rn scattering at 10 eV (c) (--- [5]) and 30 eV (d) (··· [6]).

References

[1] V.I. Kelemen and E.Yu. Remeta, *Critical minima and spin polarization in the elastic electron scattering by the mercury atoms*, J. Phys. B: At. Mol. Opt. Phys. **45**, 185202 (2012).

[2] R. Haug, *Elastische Sreuung langsamer Elektronen an einem Bi-Atomstrahl*, Z. Physik. **215**, 350 (1968).

[3] W. Williams, S. Trajmar and D.G. Bozinis, *Elastic and inelastic scattering of 40 eV electrons from atomic and molecular bismuth*, J. Phys. B: At. Mol. Phys. **8**, L96 (1975).

[4] F. Kaussen, H. Geesmann, G.F. Hanne and J. Kessler, *Study of spin polarisation in elastic scattering of electrons from Hg, T1, Pb and Bi atoms*, J. Phys. B: At. Mol. Phys. **20**, 151 (1987).

[5] Neerja, A.N. Tripathi, and A.K. Jain, *Spin polarization and cross sections in elastic scattering of electrons from Yb, Rn, and Ra atoms*, Phys. Rev. A **61**, 032713 (2000).

[6] L.T. Sin Fai Lam, *Relativistic effects in electron scattering by atoms 111. Elastic scattering by krypton, xenon and radon*, J. Phys. B: At. Mol. Phys. **15**, 119 (1982).

Non-radioactive source of electrons at atmospheric pressure

Matúš Sámel, Michal Stano, Štefan Matejčík
Faculty of mathematics, physics and informatics, Comenius University in Bratislava, Mlynská dolina F2, 842 48 Bratislava, Slovakia

Electron guns are devices used to generate electron beams. The electron guns are used in plenty of applications, such as ion sources in Mass Spectrometry (MS), electron welding, electron microscopy and many others. The electron guns are operated in vacuum. At atmospheric pressure, electrons interact with the gas and undergo ionisation, excitation reactions and subsequent thermalisation. Most common source of the electrons at atmospheric pressure is a photocathode irradiated by UV light of suitable wavelength [1]. Recently, vacuum electron guns with nanomembrane vacuum-atmosphere interface (window) of 300 nm thickness were developed, which allow transport of keV electrons from vacuum to atmosphere [2 - 4]. Such electron sources are suitable as replacement of radioactive ion sources based on β radiation and could be applied for Atmospheric Pressure Ionization (API) in MS, Ion Mobility Spectrometry (IMS) or other analytical methods at atmospheric pressure (e.g. excitation fluorescence, electron swarm experiments…)[5].

We developed similar non-radioactive Source of Electrons at Atmospheric Pressure (SEAP), which allows transmission of electrons at lower energies as reported in previous studies [2 - 4]. We used two types of windows Si_3N_4 with thickness 100 and 150 nm. Our main results are shown in Figure 1. As we can see in the Figure 1 a), accelerated electrons start penetrate window at energies around 3 keV (depends on thickness of window) and generate ion current in the order of units of nanoamps. The authors in study [3] reported ion current of 50 nA generated by 8.6 keV electrons, this comparison indicated, that present SEAP reach almost 20 times higher current at the same acceleration voltage. Figure 1 b) shows dependence of ion current for both windows at atmospheric pressure on the electron emission current from the tungsten filament in vacuum chamber. This measurement confirms us, that ion current is generated by accelerated electrons and the most efficiency is near to the edge of the curves, so emission current of 25μA was used in all subsequent measurements.

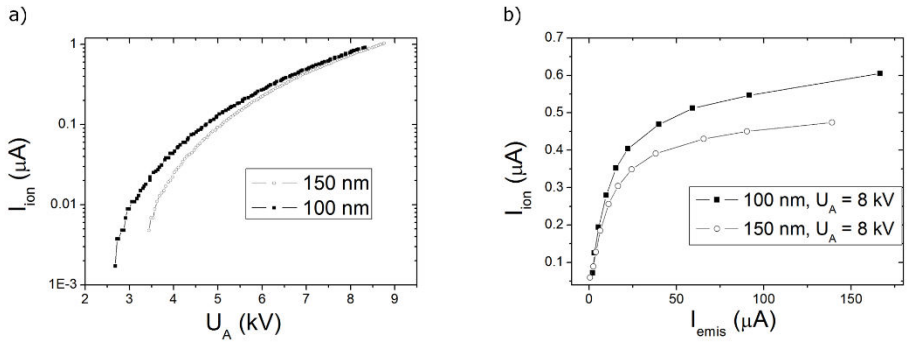

Fig. 1 Dependences of produced ion current at atmospherics pressure on the acceleration voltage a) and emission current of electrons b) in vacuum chamber.

We carried out set of measurements with vacuum on both sides of window, to determine penetration of electron current through window. Final goal of our study is to apply SEAP as ion source for MS and IMS.

This work was supported by the Slovak Research and Development Agency, project Nr. APVV0733-11 and the grant agency VEGA, project Nr. 1/0417/15. This project has received funding from the European Union's Horizon 2020 research and innovation programme under grant agreement No 692335.

References

[1] de Urquijo-Carmona J, *Ion mobilities and clustering in SF6 at high pressures*, J. Phys. D: Appl. Phys., **16**, 1603-1609 (1983).
[2] Gunzer F, Ulrich A and Baether W, *A novel non-radioactive electron source for ion mobility spectrometry*, Int. J. Ion Mobil. Spec. **13**, 9-16 (2010).
[3] Cochems P, Langejuergen J, Heptner A and Zimmermann S, *Towards a miniaturized non-radioactive electron emitter with proximity focusing*, Int. J. Ion Mobil. Spec. **15**, 223-229 (2012).
[4] Cochems P, Runge M and Zimmermann S, *A current controlled miniaturized non-radioactive electron emitter for atmospheric pressure chemical ionization based on thermionic emission*, Sensors and Actuators A**206**, 165– 170 (2014).
[5] Ulrich A, HeindlT, Krücken R, Morozov A, Skrobol C, Wieser J, *Electron beam induced light emission,* Eur. Phys. J. Appl. Phys. **47**, 22815 (2009).

Interactions of low energy electrons with 2,4,6-Trichloroanisole

Michal Lacko[1], Michal Stano[1], Zuzana Lichvanová[1], Peter Papp[1], Štefan Matejčík[1]

1. Department of Experimental Physics, Faculty of Mathematics, Physics and Informatics, Comenius University in Bratislava, Mlynská dolina F2, 842 48 Bratislava, Slovak republic

The compound 2,4,6-trichloroanisole $C_7H_5Cl_3O$ (TCA) is considered to be the main reason of the 'off-flavor' of taint wine [1]. The unpleasant odor of taint wine resembles to wet cardboard, mushrooms or earthy smell. Various analytical methods are in use for detection of TCA including gas chromatography-mass spectrometry [2], single drop ionic liquid microextraction coupled with multicapillary column separation [3], ion mobility and mass spectrometry [4]. New knowledge on electron interactions with this molecule and on its electronic structure may help to develop new analytical methods or improve the existing ones.

In the present work we study formation of positive and negative ions by electron collisions of isolated TCA molecules with low energy electrons. In addition, electronic structure of the TCA molecule is investigated by ultraviolet photoelectron spectroscopy and by OVGF quantum chemical calculations.

Electron impact ionization and electron attachment reactions are studied under single collision conditions by means of crossed electron/molecular beam apparatus [5]. Electron beam was created by trochoidal electron monochromator with resolution ~150 meV. Molecular beam was generated by sublimation of the solid sample in high vacuum. Produced ions were mass analyzed using a quadrupole mass spectrometer and detected by channeltron electron multiplier. Ionization energy of TCA molecule and appearance energies of fragment ions were determined. Investigation of electron attachment to TCA revealed that dominant reaction is formation of Cl- with maximum cross section at 0.25 eV. All remaining anionic products were wormed at significantly lower intensities. All electron attachment reactions occurred in the narrow energy range between 0 eV and 2 eV.

Electronic structure of TCA was investigated using HeI photoelectron spectrometer. Photons of 58.4 nm (21.22 eV) were generated in an electrical discharge in He and transmitted to a target chamber through a capillary. The isolated TCA molecules were ionized in a gas phase. Photoelectrons generated by the ionization exit the target chamber through a narrow slit and their energy was analyzed using a cylindrical electrostatic analyzer coupled to a channeltron detector. The ionization energy from the highest and from molecular orbitals was determined.

The molecular energy levels of the TCA were calculated by means of OVGF method [6] in Gaussian 09. Good agreement between the calculated energy levels and the PES experiment allowed to attribute most of the structures observed in the PES spectrum to the molecular orbitals and to experimentally determine the ionization energies from the respective molecular orbitals.

This work was supported by the Slovak grant agency VEGA, project nr. 1/0417/15. This project has received funding from the European Union's Horizon 2020 research and innovation programme under grant agreement No 692335.

References

[1] M.A. Sefton, R.F. Simpson, *Compounds causing cork taint and the factors affecting their transfer from natural cork closures to wine – a review*, Australian Journal of Grape and Wine Research, **11** (2005) 226-240.

[2] H. R. Buser, C. Zanier, and H. Tanner, *Identification of 2,4,6-trichloroanisole as a potent compound causing cork taint in wine J. Agric. Food Chem.*,**30**, no. 2, (1982) 359–362.

[3] I. Márquez-Sillero, S. Cárdenas, and M. Valcárcel, *Direct determination of 2,4,6-tricholoroanisole in wines by single-drop ionic liquid microextraction coupled with multicapillary column separation and ion mobility spectrometry detection*, *J. Chromatogr. A*,**1218**, no. 42, (2011) 7574–80.

[4] Z. Lichvanová, V. Ilbeigi, M. Sabo, M. Tabrizchi, S. Matejčík, *Using corona discharge-ion mobility spectrometry for detection of 2,4,6-Trichloroanisole*, Talanta,**127** (2014) 239-43.

[5] M. Stano, S. Matejcik, J.D. Skalny, T.D. Märk, *Electron impact ionization of CH 4 : ionization energies and temperature effects*, Journal of Physics B: Atomic, Molecular and Optical Physics, **36** (2003) 261.

[6] J. V. Ortiz, *Electron binding energies of anionic alkali metal atoms from partial fourth order electron propagator theory calculations* J. Chem. Phys., **89**, (1988) 6348-52.

Nonlocal model of vibrational dynamics of the lowest autodetachment state of water anion

Martin Čížek, Karel Houfek
Institute of Theoretical Physics, Faculty of Mathematics and Physics, Charles University in Prague, V Holešovičkách 2, 180 00 Praha, Czech Republic

We construct a nonlocal resonance model [1] of the vibrational dynamics of the water anion taking into account nonadiabatic dynamics of electron autodetachment. The construction is done in several steps. First, we have calculated the global ground potential energy surface of the H_2O^- ion with the MRCI method and a large basis (this extends the previous work of Werner et al. [2]). We have also identified a region close to the equilibrium geometry of the neutral water molecule, where the ion is metastable and the electron can escape through the process of autodetachment.

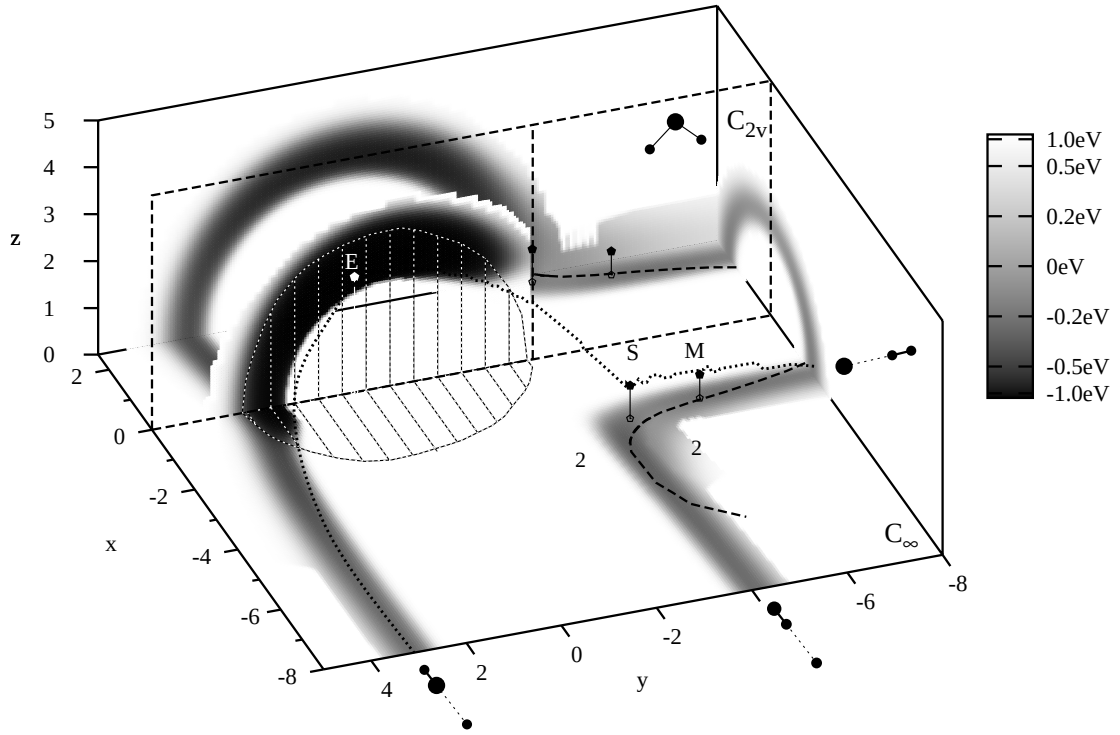

Fig. The ground state potential of the water anion in Johnson coordinates [3]. The O^-+H_2 energy is chosen as zero in energy scale. The planes $z = 0$ and $x = 0$ correspond to linear molecule (C_∞ symmetry) and symmetric stretch (C_{2v} group) respectively. The O^-+HH, OH^-+H and HO^-+H asymptotes are indicated with dot diagrams at the edges. The net of lines marks the autodetachment region, where the ion decays to H_2O+e. The minimum energy reaction path from the O^-+HH to HO^-+H channels through special points M (minimum), S (saddle point), E (equilibrium H_2O geometry) is marked.

For the molecular geometries inside and close to the autodetachment region we have also performed the R-matrix calculations of the electron scattering. The special attention was paid to select the model of correlation energy inside the R-matrix calculation that is consistent with the MRCI calculation of the potential energy surface [4]. The scattering eigenphase sums are than used to fit parameters of the nonlocal resonance model taking into account the full dimensionality of the problem.

The preliminary attempts to use the model for description of the process of vibrational excitation and dissocitive attachment to the water molecule near the threshold are discussed. We predict that new structures will occur for electron scattering from vibrationaly excited water molecule close to dissociative attachment threshold.

References

[1] W. Domcke, Phys. Rep. **208** (1991) 97.
[2] H.-J. Werner, U. Manz, P. Rosmus, J. Chem. Phys. **87** (1987) 2913.
[3] B. R. Johnson, J. Chem. Phys. **73** (1980) 5051.
[4] K. Houfek, M. Čížek, Eur. Phys. J. D, in press.

Unravelling interatomic coulombic decay and radiative charge transfer in electron ionization of the argon dimer

Xueguang Ren [1,2], Elias Jabbour Al Maalouf [3], Alexander Dorn[1], Stephan Denifl[3]

1. Max-Planck-Institut für Kernphysik, 69117 Heidelberg, Germany

2. Physikalisch-Technische Bundesanstalt, 38116 Braunschweig, Germany

3. Institut für Ionenphysik und Angewandte Physik, Universität Innsbruck, Technikerstrasse 25, 6020-Innsbruck, Austria

In recent years, the interatomic Coulombic decay (ICD) has become known as an important decay process in weakly bonded systems, like for example in the Ar dimer studied here. In ICD the excess energy is transferred by exchange of a virtual photon to a neighbouring atom, thereby, ionizing it by emitting an ICD electron [1]. In addition, the relaxation process of radiative charge transfer (RCT) may occur in the Ar dimer in which one atom is doubly ionized, and an electron is transferred from a neighbour-atom to the doubly charged Ar^{2+} ion. The system can relax by emitting a photon. Both ICD and RCT processes can result in two repulsive Ar^{+} ions and hence the separation of both processes is highly challenging in an experiment.

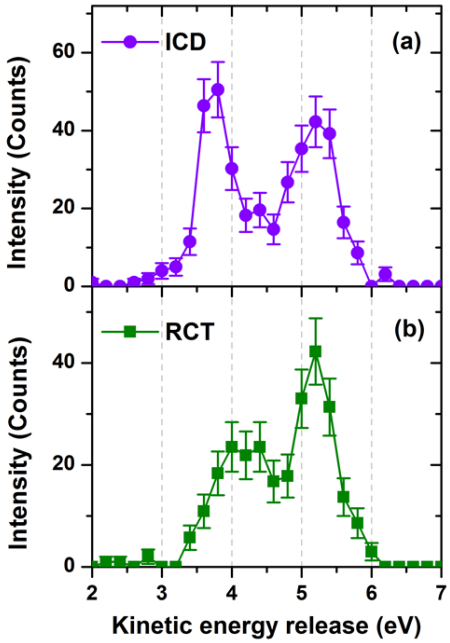

Fig. 1 Contribution of (a) ICD and (b) RCT processes, respectively, to the kinetic energy release distribution of the Ar^{+} - Ar^{+} ions. [2]

In the present work [2], we study the electron ionization of the Ar dimer using a reaction microscope in which the kinetic energies of all final state particles are measured with the multiple particles coincidence method. From the measured kinetic energies of the five particles emitted in the ionization event (two Ar^{+} ions and three electrons), the binding energy or ionization energy for each channel are obtained. Thereby, we can clearly identify the two decay channels (ICD vs. RCT) in the ionization of the Ar dimer (see Fig.1) and determine the relative contributions as function of the observed kinetic energy release (KER).

This work was supported by DFG (FOR1789) and FWF (I1015).

References

[1] Uwe Hergenhahn, *Interatomic and intermolecular coulombic decay: The early years*, J. Elect Spec. Real. Phen. **184**, 78 (2011)

[2] Xueguang Ren, Elias Jabbour Al Maalouf, Alexander Dorn, Stephan Denifl, *Direct evidence of two interatomic relaxation mechanisms in argon dimers ionized by electron impact*, Nature Communications, DOI:10.1038/NCOMMS11093 (2016).

Bose-Einstein Condensate of thulium atoms

A.V. Akimov[1,2,3], I.S. Cojocaru[2,4], S. Pyatchenkov[2], S. Snigirev[2,5], I. Luchnikov[2,4], E. Davletov[2,3,4],V. Tsyganok[2,4], D.N. Kublikova[2,4], V. Bushmakin[2,4], D. Sukachev[2,6], E. Kalganova[2,3], G. Vishnyakova[2,3], V.N. Sorokin[2,3]

[1] Texas A&M University, Department of Physics, 4242 TAMU, College Station, TX, 77843, USA
[2]Russian Quantum Center, 100, Novaya st., Skolkovo, Moscow Reg., 143025, Russia
[3]P. N. Lebedev Institute of Russian Academy of Sciences, 53 Leninsky prospect, Moscow, 119991, Russia
[4]Moscow Institute of Physics and Technology, 9 Institutskiy per., Dolgoprudny, Moscow Region, 141700, Russia
[5]Max Planck Institute of Quantum Optics, Hans-Kopfermann-Straße 1, 85748 Garching bei München, Germany
[6]Harvard University, Department of Physics, 17 Oxford Street, Cambridge, MA 02138, USA

E-mail: akimov@physics.tamu.edu

Since the first demonstration of Bose-Einstein Condensates (BEC) [1] the variety of an atoms for which BEC is reached constantly grows. Today BEC became a powerful tool for many research directions. Among those quantum simulations take a very special place. Utilizing the analogies between complicated materials and cold atoms in optical lattices this simulators promise to resolve many open questions in understanding of complex materials. Due to their unique properties, rare-earth elements are of great interest for quantum simulations. For example, such a systems allow low-field Feshabach resonances enabling tunability in long-range interactions. In particular, thulium atom has one vacancy in the 4f shell therefore having orbital moment of 3 in the ground state, and magnetic moment of 4 Bohr magnetons in ground state. While magnetic moment of the thulium atom is less than that of Erbium [2] or Dysprosium [3] which were already cooled to BEC temperature thulium has simpler level structure and the possibility to capture it at the tight optical lattice operating at 532 nm. This way thulium provide similar level of magnetic dipole-dipole interactions as Erbium of Dysprosium in conventional lattice operating at 1 μm, but due to simplicity of level structure and a bit lower orbital moment can benefit from less dens Feshbach resonances and more predictable behaviour [4]. This make thulium atom an extremely attractive subject for quantum simulations.

In this contribution, I will report on our experimental efforts on reaching BEC for Thulium atom. In particular, I will focus on our studies of light assisted collisions and low field Feshbach resonances as well as on our efforts of evaporative cooling of thulium atom.

References

[1] K. B. Davis, M.-O. Mewes, M. R. Andrews, N. J. van Druten, D. S. Durfee, D. M. Kurn, and W. Ketterle, Phys. Rev. Lett. **75**, 3969 (1995).
[2] K. Aikawa, A. Frisch, M. Mark, S. Baier, A. Rietzler, R. Grimm, and F. Ferlaino, Phys. Rev. Lett. **108**, 1 (2012).
[3] M. Lu, N. Q. Burdick, S. H. Youn, and B. L. Lev, Phys. Rev. Lett. **107**, 1 (2011).
[4] A. Frisch, M. Mark, K. Aikawa, F. Ferlaino, J. L. Bohn, C. Makrides, A. Petrov, and S. Kotochigova, Nature **507**, 475 (2014).

Studying two-dimensional Fermi and Bose gases in a single experiment

Andrey Turlapov
Institute of Applied Physics, Russian Academy of Sciences, ul. Ulyanova 46, Nizhniy Novgorod, Russia

Neither long-range order nor Bose condensation may appear in uniform 2D systems at finite temperature. Despite that, 2D superconductors, such as cuprates, are among the systems with highest critical temperatures. 2D quantum systems remain intriguing, and their understanding is incomplete despite huge progress seen in the recent decades. Ultracold atoms are a platform for studying 2D physics. Using tunability of atomic gases, we have realized a crossover between a 2D gas of Fermi atoms and a 2D gas of weakly-bound diatomic Bose molecules by varying s-wave interactions in the gas. Between these two asymptotic states, there is a regime of strong interactions, whose quantitative description is challenging, e. g., a mean field of Cooper pairs fails to describe the crossover even qualitatively, unlike in 3D gases. At the lowest achievable temperatures, $\sim 10\%$ of the Fermi energy, the pressure is measured in the whole Fermi-to-Bose crossover and compared with the available theoretical models, including those which appeared over the last year. In the Fermi regime of weak interactions, the pressure is systematically above a Fermi-liquid-theory prediction, which maybe due to mesoscopic effects. Alternatively, this upshift is partially reproduced within a recent mean-field theory supplemented with fluctuations. On the Bose side of the crossover, the molecules easily condense, which is found in interferometric measurements. On one hand, such condensation is expected because the gas is held in a nearly harmonic trap, which favors condensation unlike the uniforms space. On the other hand, each molecule is locally in a flat potential, which is the sum of the trap and the strong repulsive mean field, and this should inhibit the condensation.

Controlled formation of cold molecules in their absolute ground state

Nadia Bouloufa-Maafa
In collaboration with the Theomol group

Laboratoire Aimé Cotton, CNRS, Université Paris-Sud, ENS Cachan, Université Paris-Saclay, 91405 Orsay Cedex,France

The ability to create in the laboratory dilute atomic gases at ultracold temperatures ($T = E/k_B << 1$ mK), where particles are almost at standstill, represents one of the most spectacular recent developments of atomic physics, which lead to the observation of quantum degeneracy in ultracold atomic gases twenty years ago. When particles possess an intrinsic electric dipole moment, like heteronuclear bialkali molecules, anisotropic long-range interaction dominate the evolution of the ultracold gas, opening the way toward fascinating prospects such as precision measurements, test of fundamental theories, quantum simulation, or ultracold chemistry. However, due to their inherent complexity, creating a dense gas of ultracold polar molecules is still a challenge.

In this talk, I will describe the way which has led to a successful creation of such gases in the case of KRb [1], RbCs [2,3], NaK [4], and NaRb [5] based on a Raman adiabatic transfer of the population from an initial weakly-bound molecular level to their absolute ground state level. In particular, I will emphasize on the crucial importance of the knowledge of the molecular properties based on a delicate combination of available spectroscopic data with our calculations of potential energy curves, transition dipole moments, dynamic polarizabilities, and hyperfine structure to design optimal paths for the adiabatic transfer. I will discuss the examples of RbCs, NaRb, and KCs molecules, to illustrate the variety of situations that can be encountered.

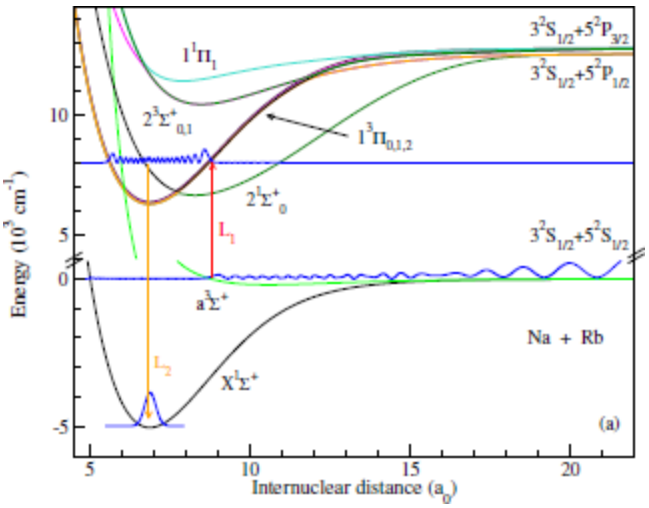

Fig. 1 STIRAP scheme used to transfer NaRb Feshbach molecules to the absolute ground state. The scheme is based on up to date molecular data

References
[1] S. Ospelkaus, K.-K. Ni, D. Wang, M. H. G. de Miranda, B. Neyenhuis, G. Quéméner, P. S. Julienne, J. L. Bohn,D. S. Jin, and J. Ye, Science **327**, 853 (2010)
[2] T. Takekoshi, L. Reichsöllner, A. Schindewolf, J. M. Hutson, C. R. Le Sueur, O. Dulieu, F. Ferlaino, R. Grimm,and H.-C. Nägerl, Phys. Rev. Lett.**113**, 205301 (2014).
[3] P. K. Molony, P. D. Gregory, Z. Ji, B. Lu, M. P.Köppinger, C. R. Le Sueur, C. L. Blackley, J. M. Hutson, and S. L. Cornish, Phys. Rev. Lett.**113**, 255301 (2014).
[4] J. W. Park, S. A. Will, and M. W. Zwierlein, Phys. Rev.Lett.**114**, 205302 (2015).
[5] Mingyang Guo, Bing Zhu, Bo Lu, Xin Ye, Fudong Wang, Romain Vexiau, Nadia Bouloufa-Maafa, Goulven Quéméner, Olivier Dulieu, and Dajun Wang, accepted for publication in PRL (2016)

Laser Cooling and Magneto-Optical Trapping of Diatomic Molecules

M. R. Tarbutt
Centre for Cold Matter, Blackett Laboratory, Prince Consort Road, Imperial College London, London SW72BW, UK.

Cold molecules can be used to test fundamental physics [1-4], process quantum information [5,6], explore cold chemistry [7] and study strongly-interacting many-body quantum systems [8]. Laser cooling is difficult to apply to molecules because their vibrational structure precludes closed electronic transitions. However, for some molecules only a small number of vibrational branches need to be addressed for laser cooling to succeed [9]. I will discuss our experiments on laser slowing and cooling of CaF molecules. With just two laser wavelengths, we use radiation pressure to slow a beam of these molecules to low velocity and greatly compress their distribution of forward velocities. We account for the changing Doppler shift as the molecules slow down either by chirping the laser frequency or by broadening the laser linewidth. These cooled, slowed molecules are then delivered to a magneto-optical trap (MOT) where we aim to trap and cool them into the micro-Kelvin regime.

MOTs for atoms usually use an electronic transition where the angular momentum of the excited state is greater than that of the ground state. For molecules, the laser cooling transition does not have this property. This complicates the MOT because the molecules tend to be optically pumped into dark Zeeman sub-levels, which weakens the trapping force. The force is further weakened if the excited state has a small magnetic moment, which it usually does for the favoured laser cooling transition in molecules [10]. I will discuss two methods for producing stronger MOT trapping forces. The first uses a *dual frequency effect*, where the MOT beams contain two oppositely-polarized laser components, one red-detuned and one blue-detuned [11]. In the second, known as the *rf MOT*, the laser polarizations and magnetic field direction are rapidly and synchronously switched [12].

References

[1] The ACME Collaboration, *Order of Magnitude Smaller Limit on the Electric Dipole Moment of the Electron*, Science **343**, 269 (2014).
[2] J. J. Hudson, D. M. Kara, I. J. Smallman, B. E. Sauer, M. R. Tarbutt and E. A. Hinds, *Improved measurement of the shape of the electron* Nature **473**, 493 (2011).
[3] E. R. Hudson, H. J. Lewandowski, B. C. Sawyer, and J. Ye, *Cold molecule spectroscopy for constraining the evolution of the fine structure constant*, Phys. Rev. Lett. **96**, 143004 (2006).
[4] S. Truppe, R. J. Hendricks, S. K. Tokunaga, H. J. Lewandowski, M. G. Kozlov, C. Henkel, E. A. Hinds and M. R. Tarbutt, *A search for varying fundamental constants using Hz-level frequency measurements of cold CH molecules*, Nat. Commun. **4**, 2600 (2013).
[5] D. DeMille, *Quantum computation with trapped polar molecules*, Phys. Rev. Lett. **88**, 067901 (2002).
[6] A. André. *et al.*, *A coherent all-electrical interface between polar molecules and mesoscopic superconducting resonators*, Nature Phys. **2**, 636 (2006).
[7] R. V. Krems, *Cold controlled Chemistry*, Phys. Chem. Chem. Phys. **10**, 4079 (2008).
[8] A. Micheli, G. Brennen, and P. Zoller, *A toolbox for lattice-spin models with polar molecules*, Nature Phys. **2**, 341 (2006).
[9] M. D. Di Rosa, *Laser cooling molecules*, Eur. Phys. J. D **31**, 395 (2004).
[10] M. R. Tarbutt, *Magneto-optical trapping forces for atoms and molecules with complex level structures*, New J. Phys. **17**, 015007 (2015).
[11] M. R. Tarbutt and T. C. Steimle, *Modeling magneto-optical trapping of CaF molecules*, Phys. Rev. A **92**, 053401 (2015).
[12] E. B. Norrgard, D. J. McCarron, M. H. Steinecker, M. R. Tarbutt and D. DeMille, *Sub-millikelvin dipolar molecules in a radio-frequency magneto-optical trap*, Phys. Rev. Lett. **116**, 063004 (2016).

Ultrafast Electron Dynamics Initiated in Molecules by Attosecond Pulses

Francesca Calegari
Institute for Photonics and Nanotechnologies, National Research Council of Italy, IFN-CNR, P.zza Leonardo da Vinci 32, 20133 Milano, Italy

Dynamical processes in molecules occur on an ultrafast temporal scale, ranging from picoseconds to femtoseconds when concerning with a structural change, down to attoseconds when dealing with electrons. Electron dynamics plays a very important role in bond-formation and bond-breakage, thus determining the final chemical reactivity of the molecule. Recently, theoretical studies have pointed out that after sudden ionization of a large molecule very efficient "charge migration" can occur along the molecular backbone on a temporal scale ranging from few femtoseconds down to tens of attoseconds [1]. Attosecond science is nowadays a well-established research field, and it potentially offers formidable tools for the investigation of this charge migration process [2].

In this work I will first show that XUV attosecond pulses in combination with NIR/VIS few-cycle pulses can be used to investigate with extreme time-resolution the dissociative ionization dynamics of molecular nitrogen. The time-dependent measurements reveal the presence of NIR/VIS-induced transitions between N_2^+ ionic states together with an interference pattern that carries the signature of the potential energy curves activated by the XUV pulse. We show that the sub-fs characterization of the interference pattern is essential for a semi-quantitative determination of the repulsive part of these curves [3].

I will then discuss the use of an XUV attosecond pump - NIR/VIS femtosecond probe approach to investigate charge migration in more complex molecules such as aromatic amino acids [4]. By measuring the time evolution of the yield of the doubly charged immonium ion for phenylalanine (Phe) and tryptophan (Trp) we were able to identify the presence of fast modulations of the dication yield with periodicities of 4.17 fs for Phe and 4.34 fs for Trp (see **Fig. 1**). To better understand the observed ultrafast dynamics, numerical calculations have been performed. For both Phe and Trp, the calculated hole density around the amino group displays beatings characterized by oscillation frequencies in good agreement with the experimental results. The main beating frequency for Phe around 0.24 PHz is originated from the coherent superposition of the A25 and the A28 molecular orbitals, resulting in charge migration between the amino group and the carboxylic functional group. In the case of Trp, the main beating frequency around 0.23 PHz is originated from the coherent superposition of the A29 and the A31 molecular orbitals. In this case this coherent superposition of electronic states is responsible for charge oscillations mainly between the amino group and the indole group of the molecule.

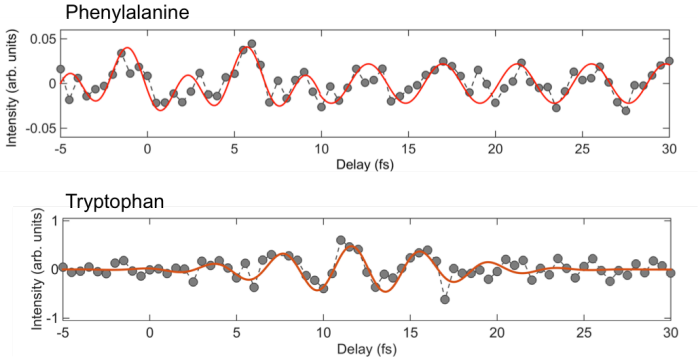

Fig. 1 Doubly charged immonium ion yield measured as a function of the pump-probe delay and obtained after subtraction of the slow femtosecond decay for Phe (top panel) and for Trp (bottom panel).

Finally, I will show that the same experimental approach allowed us to measure in real-time hydrogen migration occurring in 5-halo-uracils. In the case of 5FU, the XUV pulse ionizes the molecule catalyzing the hydrogen migration from C6 to C5 at the first step of the reaction, leading to the fragment m/z=44. The pump-probe measurement reveals that at early times, the NIR-VIS pulse inhibits the hydrogen migration process thus resulting in a sudden reduction of fragments m/z=44, and a consequent increase of fragment m/z=43.

References

[1] L. S. Cederbaum et al Chem. Phys. Lett. **307**, 205 (1999)
[2] P. B. Corkum & F. Krausz, Nature Physics **3**, 381-387 (2007)
[3] A. Trabattoni et al., Phys. Rev. X **5**, 041053 (2015)
[4] F. Calegari et al., Science **346**, 336 (2014)

Real-time wavepacket dynamics through a conical intersection: the primary event of vision

Giulio Cerullo[1], Dario Polli[1], Marco Garavelli[2]

1. IFN - CNR - Dipartimento di Fisica, Politecnico di Milano, Piazza Leonardo da Vinci 32, 20133 Milano, Italy

2. Dipartimento di Chimica ''G. Ciamician'', Università di Bologna, V.F. Selmi 2, 40126 Bologna, Italy.

Since the conversion of the 11-cis retinal chromophore to its all-trans form in rhodopsin was identified as the primary photochemical event in vision [1], experimentalists and theoreticians have tried to unravel the molecular details of this process. The high quantum yield of 0.65 and the production of the primary ground-state rhodopsin photoproduct within a mere 200 fs all suggest a paradoxically fast and efficient photoactivated one-way reaction. Rhodopsin's unique reactivity is generally attributed to a conical intersection between the potential energy surfaces of the ground and excited electronic states and thereby enables the efficient and ultrafast conversion of photon energy into chemical energy. Obtaining direct experimental evidence for the involvement of a conical intersection is challenging: the energy gap between the electronic states of the reacting molecule changes significantly over an ultrashort timescale, calling for observational methods that combine high temporal resolution and a broad spectral observation window. Here we show that ultrafast transient absorption spectroscopy with sub-20-fs time resolution and spectral coverage from the visible to the near-infrared allows us to follow rhodopsin isomerisation in real time [2]. We track coherent wave-packet motion from the photoexcited Franck–Condon region to the photoproduct by monitoring the loss of reactant stimulated emission and the subsequent appearance of photoproduct absorption (Fig. 1), and find excellent agreement between the experimental observations and molecular dynamics calculations that involve a true electronic states crossing, occurring within ≈100 fs. Taken together, these findings constitute the most compelling evidence to date for the existence and importance of conical intersections in visual photochemistry.

When probing the 9-*cis* analog isorhodopsin, the scenario changes completely [3]: we find that the reaction path, starting from the Frank-Condon region, suddenly branches towards two competitive deactivation paths involving two different conical intersection funnels: the first is rapidly accessed (within ≈160 fs), but is unproductive; the second (displaying a twist about the C9=C10 double bond) is accessed later (within ≈280 fs), but is the only one able to produce the all-trans photoproduct, although on longer times than in rhodopsin. This path branching explains the strongly non-exponential decay of the stimulated emission and is the reason for the reduced quantum yield and slower isomerization rate that is observed in isorhodopsin compared to rhodopsin.

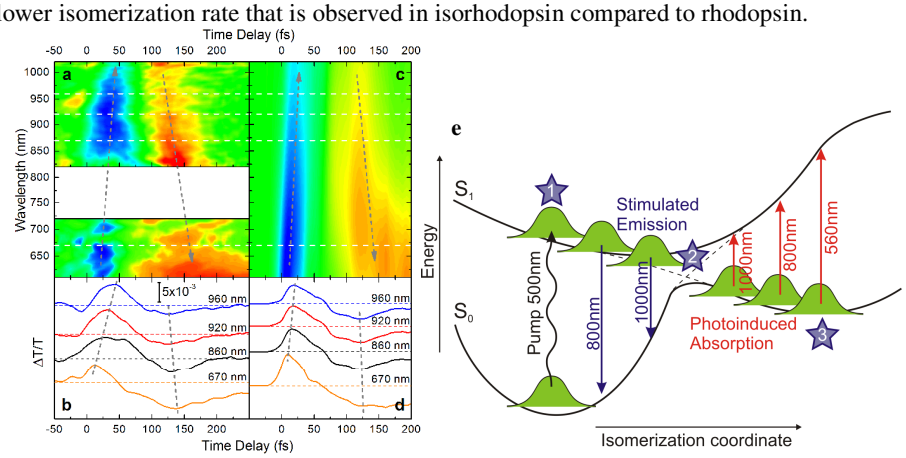

Fig. 1 Wavepacket dynamics through the rhodopsin conical intersection. Experimental (a) and simulated (c) differential transmission (ΔT/T) map as a function of probe delay and wavelength in the visible and NIR spectral regions. Gray lines are a guide to the eye highlighting the shifts of the stimulated emission and photoinduced absorption signals in time. Experimental (b) and simulated (d) time traces at selected probe wavelengths (as indicated). Sketch of the ground- and excited-state potential energy surfaces of the chromophore in rhodopsin as a function of the isomerization coordinate, showing that stimulated emission from the excited state of the parent molecule and photo-induced absorption from the hot photoproduct can monitor the wavepacket dynamics through the conical intersection.

References

[1] T. Yoshizawa and G. Wald, *Pre-lumirhodopsin and the bleaching of visual pigments*, Nature **197**, 1279 (1963).

[2] D. Polli, P. Altoè, O. Weingart, K.M. Spillane, C. Manzoni, D. Brida, G. Tomasello, G. Orlandi, P. Kukura, R.A. Mathies, M. Garavelli, and G. Cerullo, *Conical Intersection Dynamics of the Primary Photoisomerization Event in Vision*, Nature **467**, 440-443 (2010).

[3] D. Polli, O. Weingart, D. Brida, E. Poli, M. Maiuri, K.M. Spillane, A. Bottoni, P. Kukura, R.A. Mathies, G. Cerullo, M. Garavelli, *Wavepacket splitting and two-pathway deactivation in the photoexcited visual pigment isorhodopsin*, Angew. Chem. Intl. Ed. **53**, 2504-2507 (2014).

Extreme Ultraviolet Free Induction Decay Controlled with Strong IR Pulses

Johan Mauritsson
Department of Physics, Lund University, P.O. Box 118, SE-221 00 Lund, Sweden

We present an experimental study of controlled Free Induction Decay (cFID) in the extreme ultraviolet (XUV) regime. An attosecond pulse train is used to coherently promote argon to a superposition of the ground state ($[Ne]3s^2 3p^6$) and a series of excited states ($[Ne]3s^1 3p^6 np^1$), which are embedded in the $[Ne]3s^2 3p^5$ continuum. This superposition coherently emits light with the same directionality and divergence as the incoming XUV light. Applying a strong infrared probe pulse either break the coherence, or control the direction and phase of the emitted light.

When an ensemble of atoms is exposed to a short, coherent light pulse it will respond collectively and the excited atoms will start to act as oscillating dipoles. These dipoles may continue to oscillate coherently for a long time after the excitation pulse has passed resulting in forward scattered light known as Free Induction Decay (FID) [1,2]. This forward scattered light has the same spatial properties as the excitation pulse, but the phase is shifted by π. The overlap between the two fields will therefore yield the normal absorption spectrum observed in optical spectroscopy. FID has been observed from THz radiation to the optical regime, but it is more challenging when shorter wavelengths are used.

We present a method to observe FID at even shorter wavelengths in the extreme ultraviolet (XUV) regime. The coherent XUV light is generated using high-order harmonic generation from a carrier-wavelength tunable Ti:Sapphire laser. The laser system is a conventional chirped pulse amplification Ti:Sapphire based laser with a programmable acousto-optic filter in the amplification chain to minimize gain-narrowing. By restricting the bandwidth of the seed for the amplification chain the carrier wavelength of the output can be tuned from 770-820 nm, while maintaining sub-40 fs pulses.

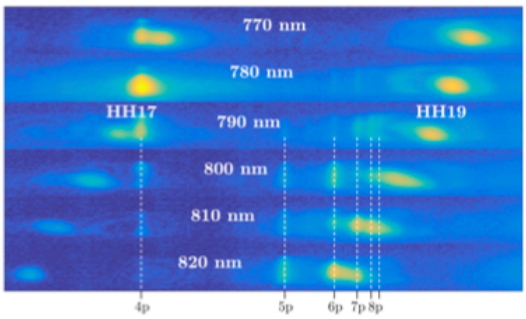

Fig. 1. Harmonics 17 and 19 transmitted through argon as a function of carrier-wavelength of the infrared laser. A number of window resonances in the absorption cross-section of the $[Ne]3s^2 3s^5$ continuum are observed [3].

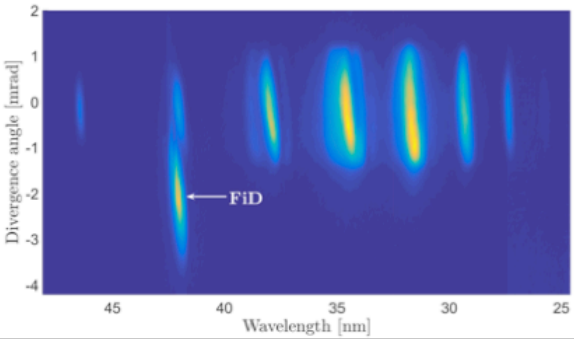

Fig. 2. The spectrum transmitted through argon under the influence of a strong non-collinear infrared probe pulse. The probe pulse modulates the spatial phase of the excited dipoles, thus modifying the directionality and divergence of the FiD.

Figure 1 demonstrates the tunability of the XUV light. Harmonics generated in an argon gas jet are refocused into a second pulsed gas jet of argon; the light transmitted through the second jet is then recorded by a flat-field spectrometer. Whenever parts of the harmonic light spectrally overlap with inner-shell transitions in argon, a coherent wave packet is excited, which emits light with similar directionality and divergence as the incoming XUV light.

In order to overcome the challenges of observing FID in the XUV region we use a short IR pulse to change the direction of the light emitted by the ensemble of oscillating dipoles. We demonstrate that the spatial phase of the FID can be controlled if an IR probe pulse is focused at the ensemble at a small non-collinear angle, illustrated in Fig. 2. In addition to these snapshots we will present time-evolution of these dipoles as a function of the pump-probe delay.

References

[1] R. G. Brewer and R. L. Shoemaker, Phys. Rev. A **6**, 2001-2007 (1972)
[2] F. A. Hopf, R. F. Shea, and M. O. Scully, Phys. Rev. A 7, 2105-2110 (1973)
[3] S. L. Sorensen *et al,* Phys. Rev. A **50,** 1218-1230 (1994)

Isolated attosecond pulses with controlled polarization

Carlos Hernández-García[1,2], Charles Durfee[1,3], Daniel D. Hickstein[1], Tenio Popmintchev[1], Amanda Meier[3], Margaret Murnane[1,4], Henry C. Kapteyn[1,4], Íñigo J. Sola[2], Agnieszka Jaron-Becker[1,4], and Andreas Becker[1,4]

1. JILA, University of Colorado at Boulder, Boulder, CO 80309-0440 USA

2. Grupo de Investigación en Aplicaciones del Láser y Fotónica, University of Salamanca, E-37008, Salamanca, Spain

3. Department of Physics, Colorado School of Mines, Golden, CO 80401, USA

4. Department of Physics, University of Colorado at Boulder, Boulder, CO 80309-0440 USA

High-order harmonic generation (HHG) is a breakthrough source of coherent radiation extending from the EUV to the soft X-ray regime, in the form of attosecond bursts. It is simply understood in semiclassical terms: an electron is tunnel ionized from an atom by an intense linearly polarized laser field, then accelerated, and finally driven back to its parent ion, releasing the kinetic energy acquired form the field in the form of EUV/X-ray radiation upon recollision. If driven by a circularly polarized field, the electronic wavepacket does not recollide with the parent ion, and it was believed impossible to generate bright circularly polarized EUV light by HHG. This precluded many applications such as X-ray magnetic circular dichroism.

In the early 2000s, the production of circularly polarized EUV harmonics was proposed through HHG driven by two-color, collinear, counter-rotating circularly polarized pulses [1]. This technique enabled the first tabletop implementation of X-ray magnetic circular dichroism measurements [2,3]. Recently, a novel scheme to produce circularly polarized harmonics has been demonstrated through noncollinear mixing of counter-rotating circularly polarized drivers of the same color (NCP-HHG) [4]. In contrast to the previous existing technique, this scheme simultaneously produces separate beams of right circular and left circular polarization for each harmonic.

In this contribution we perform advanced theory to propose two schemes capable of generating isolated attosecond pulses of controlled polarization, using the NCP-HHG technique. Our results show that in this set-up, isolation of a single attosecond pulse can be achieved either by restricting the driver pulse duration to a few cycles or by temporally delaying the two crossed driver pulses. We further propose to optimize the NCP-HHG technique by compensating the temporal walkoff between the pulses across the focal spot using angular spatial chirp. The isolation of pure circularly polarized attosecond pulses, along with the opportunity to select their central energy and helicity in the NCP-HHG technique, opens new perspectives to study ultrafast dynamics in chiral systems and magnetic materials.

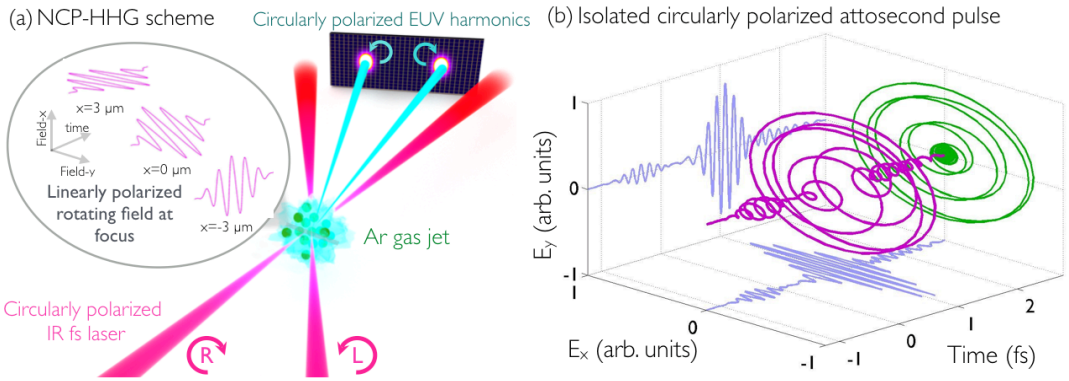

Fig. 1 (a) Scheme of NCP-HHG: 800 nm R circular and 800 nm L circular crossed beams are focused into a gas jet, producing L and R circular harmonic beams. (b) Isolated circularly polarized attosecond pulse produced by NCP-HHG, using few-cycle (3 fs) laser pulses.

References

[1] D. B. Milosevic, W. Becker, and R. Kopold, *Generation of circularly polarized high-order harmonics by two-color coplanar field mixing*, Phys Rev A **61**, 063403 (2000).

[2] O. Kfir, P. Grychtol, E. Turgut, R. Knut, D. Zusin, D. Popmintchev, T. Popmintchev, H. Nembach, J. M. Shaw, A. Fleischer, H. Kapteyn, M. Murnane and O. Cohen, *Generation of bright phase-matched circularly- polarized extreme ultraviolet high harmonics,* Nature Phot. **9**, 99 (2015).

[3] T. Fan, P. Grychtol, R. Knut, C. Hernández-García, D. D. Hickstein, D. Zusin, C. Gentry, F. J. Dollar, C. A. Mancuso, C. W. Hogle, O. Kfir, D. Legut, K. Carva, J. L. Ellis, K. M. Dorney, C. Chen, O. G. Shpyrko, E. E. Fullerton, O. Cohen, P. M. Oppeneer, D. B. Miloševic, A. Becker, A. A. Jaron -Becker, T. Popmintchev, M. M. Murnane, and H. C. Kapteyn, *Bright circularly polarized soft X-ray high harmonics for X-ray magnetic circular dichroism,* Proc. Natl. Acad. Sci. USA **112**, 14206-14211 (2015).

[4] D. D. Hickstein, F. J. Dollar, P. Grychtol, J. L. Ellis, R. Knut, C. Hernández-García, C. Gentry, D. Zusin, J. M. Shaw, T. Fan, K. M. Dorney, A. Becker, A. Jaroń-Becker, H. C. Kapteyn, M. M. Murnane, and Ch. G. Durfee, *Angularly separated beams of circularly polarized high harmonics*, Nature Phot. **9**, 743 (2015).

[5] Carlos Hernández-García, Charles Durfee, Daniel D. Hickstein, Tenio Popmintchev, Amanda Meier, Margaret Murnane, Henry C. Kapteyn, Íñigo J. Sola, Agnieszka Jaron-Becker, and Andreas Becker, *Schemes for generation of isolated attosecond pulses of pure circular polarization*, submitted.

Quantum mechanics in the negative mass reference frame.

E. S. Polzik[1]

[1]Niels Bohr Institute, University of Copenhagen, Copenhagen,Denmark
E-mail: polzik@nbi.dk

Measurement of motion with precision beyond the vacuum state uncertainty in *both* position and momentum is possible if it is carried out in a quantum reference frame with an effective negative mass [1,2]. This approach has been put in a broad quantum information perspective in [3]. Following these works, recently the proposals involving the negative mass approach were extended to BEC [4] and to pure mechanical systems [5]. A negative mass oscillator can have the first excited state energy lower than the ground state energy. The role of the negative mass reference frame can be played by an atomic spin oscillator [6]. Here we will report progress of an experiment where we track the motion of a mechanical oscillator in the reference frame of the spin oscillator by probing the combined hybrid system with light. The mechanical oscillator is a macroscopic object, a membrane of a millimeter size. Due to exceptionally high quality factor achieved via phononic bandgap engineering [7], the back action of the measurement of the mechanical motion can be observed. We demonstrate that coherent back action of the measurement induced by just a few photons on the two systems has opposite signs and cancels out. The negative mass reference frame physics opens the way towards measurements where entanglement allows for practically unlimited measurement precision of the disturbance on two non-commuting variables of a system. Applications include fundamental physics of entangled macroscopic objects, force and acceleration measurements, and clock synchronization beyond the projection noise limit [8].

References

[1] K. Hammerer, M. Aspelmeyer, E.S. Polzik, P. Zoller. *Phys. Rev. Lett.* 102, 020501 (2009).
[2] E.S. Polzik and K.Hammerer. *Annalen der Physyk*. 527, No. 1–2, A15–A20 (2015).
[3] M. Tsang and C. Caves, *Phys. Rev. Lett.* 105(12), (2010).
[4] K. Zhang, P. Meystre, and W. Zhang, Physical Review A **88**(4), 043632 (2013).
[5] M. J. Woolley and A. A. Clerk, Physical Review A **87**(6), 063846 (2013).
[6] G. Vasilakis, H. Shen, K. Jensen, M. Balabas, D. Salart, B. Chen, and E. S. Polzik. Nature Physics, doi:10.1038/nphys3280 (2015).
[7] Y. Tsaturyan, A. Barg, A. Simonsen, L. G. Villanueva, S. Schmid, A. Schliesser, and E. S. Polzik. Optics Express, Vol. 22, Issue 6, pp. 6810-6821 (2014).
[8] E. S. Polzik and J. Ye. PhysRevA.93.021404 (2016).

Nonlinear quantum optics mediated by Rydberg atoms

C. Tresp,[1] I. Mirgorodskiy,[1] H. Gorniaczyk,[1] A. Paris-Mandoki,[1] and S. Hofferberth[1,*]

[1] *5. Phys. Inst. and Center for Integrated Quantum Science and Technology, Universität Stuttgart, Pfaffenwaldring 57, 70569 Stuttgart, Germany*

Mapping the strong interaction between Rydberg excitations in ultracold atomic ensembles onto single photons via electromagnetically induced transparency (EIT) enables the realization of optical nonlinearities which can modify light on the level of individual photons.

This novel approach opens the possibility of photonic gates operated by single control photons. We present experimental demonstration of a single-photon transistor, where a single gate photon controls the transmission of many source photons and of a single-photon absorber, where exactly one photon is subtrated from an arbitrary input state.

In parallel to these optical information processing applications, this system combining quantum optics and atomic physics gives access to a variety of phenomena such as non-equilibrium dephasing dynamics and high-precision spectroscopy of Rydberg pair-state resonances.

* s.hofferberth@physik.uni-stuttgart.de

Multicomponent slow light

Gediminas Juzeliūnas[1], **Julius Ruseckas**[1], **Ite A. Yu**[2]
1. Institute of Theoretical Physics and Astronomy, Vilnius University, Vilnius, Lithuania
2. Department of Physics, National Tsing Hua University, Hsinchu, Taiwan

Slow and stationary light is expected to play an important role in the quantum information processing and nonlinear optics at a few photon level [1]. Most of the existing studies are restricted to a single component slow and stationary light, which is usually created using Lambda or double Lambda atom-light coupling schemes. In the present talk we shall analyze a two component slow light produced by means of a double tripod atom-light coupling scheme [2-5]. The setup involves two pairs of control laser beams, as well as a pair of probe beams. All the beams couple resonantly three atomic ground states to two excited states. This enables one to create a two-component slow or stationary light exhibiting a number of distinct properties, such as the neutrino type oscillations between components of the slow light [3-5]. Under certain conditions the two-component slow light can be described by a relativistic equation of the Dirac-type for particles of a finite mass [2,3]. We shall discuss an experimental observation of the two-component slow light at the NTHU in Hsinchu [5]. Finally we shall consider effects of the atom-atom interaction on the two-component slow light [6]. The atom-atom interaction introduces a two-photon detuning leading to mixing between components of the two component slow light. It is shown that a generated second component of the slow light can be highly non-classical.

References

[1] M. Fleischhauer, A. Imamoglu and J. P. Marangos, *Electromagnetically induced transparency: Optics in coherent media*, Rev. Mod. Phys. **77**, 633 (2005).
[2] R. G. Unanyan, J. Otterbach, M. Fleischhauer, J. Ruseckas, V. Kudriašov, and G. Juzeliūnas, *Spinor Slow-Light and Dirac Particles with Variable Mass*, Phys. Rev. Lett. **105**, 173603 (2010).
[3] J. Ruseckas, V. Kudriašov, G. Juzeliūnas, R. G. Unanyan, J. Otterbach, and M. Fleischhauer, *Photonic-band-gap properties for two-component slow light*, Phys. Rev. A **83**, 063811 (2011).
[4] J. Ruseckas, V. Kudriašov, I. A. Yu, and G. Juzeliūnas, *Transfer of orbital angular momentum of light using two-component slow light*, Phys. Rev. A **87**, 053840 (2013).
[5] M.-J. Lee, J. Ruseckas, C-Y. Lee, V. Kudriašov, K.-F. Chang, H.-W. Cho, G. Juzeliūnas and I. A. Yu, *Experimental demonstration of spinor slow light*, Nat. Commun. 5, 5542 (2014).
[6] J. Ruseckas, I. A. Yu and G. Juzeliūnas, in preparation.

Conical Intersections and Non-Adiabatic Transitions in Ultracold Gases

S. Wüster[1,2], **K. Leonhardt**[1], **A. Eisfeld**[1] **and J. M. Rost**[1]
1. Max Planck Institute for the Physics of Complex Systems, Nöthnitzer Strasse 38, 01187 Dresden, Germany
2. Department of Physics, Bilkent University, Ankara 06800, Turkey

We propose ultracold assemblies of Rydberg atoms as accessible laboratory platform for the simulation of quantum chemical phenomena on much inflated length scales.

Conical intersections (CIs) of electronic energy surfaces are a generic feature of large molecules [1,2] and recently also attracted the attention of the cold-atom community. The intersections provide fast *intra-molecular* transition channels between electronic states and can thus affect the outcome of (photo-) chemical processes. Radiation-less de-excitation of large bio-molecules proceeds through these channels and yields enhanced photo-stability that might have been crucial for the development of life on earth [3]. Modern techniques allow to model quantum dynamics at conical intersections of large molecules in detail. However experiments usually monitor such dynamics only *indirectly*, e.g., through reactant fractions or fluorescence spectra.

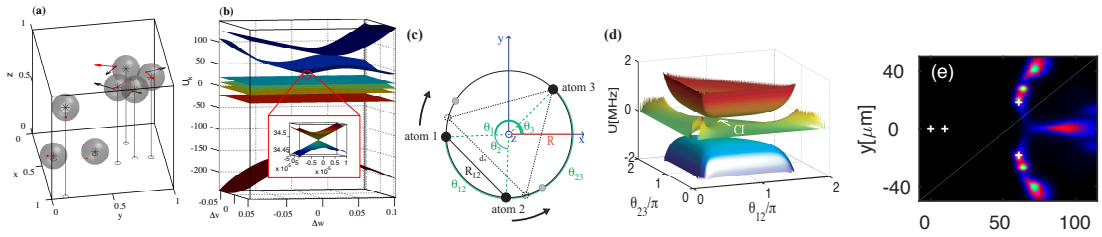

Fig. 1 (a) Random configurations of ultracold Rydberg atoms are usually near a conical intersection configuration (within the grey sphere). (b) Dipole-dipole energy surfaces for (a) with marked CI. (c,d) The pictures is clearer for a Rydberg-trimer constrained on a ring, with CI at the equilateral triangle position. (e) However, also free atomic motion in 3D can involve a CI with signatures of non-adiabatic splittings on multiple BO surfaces clearly evident in the corresponding atom position distributions.

The *direct* observation of many-body densities could be realized near conical intersections in ultracold Rydberg gases. As we demonstrate [4], intersections are ubiquitous between Born-Oppenheimer (BO) surfaces of *inter-atomic* (or molecular) transition dipole-dipole interactions, such as

$$\hat{H} = -\sum_{n,m;n\neq m}^{N} \frac{C_3}{|\mathbf{r}_n - \mathbf{r}_m|^3} |\pi_n\rangle\langle\pi_m|, \tag{1}$$

where r_n are atomic positions and $|\pi_n\rangle \equiv |g\cdots e\cdots g\rangle$ denotes a state with only the n'th atom excited.

Due to the exaggerated properties of Rydberg atoms, the characteristic length-scales for these Born-Oppenheimer surfaces is μm, and the time-scale tenths of μs, both much more accessible than their counterparts in quantum chemistry. Through recent advances in Rydberg atom detection, a versatile laboratory platform where the quantum many-body dynamics around conical intersections is observable in detail comes within reach [8].

Proposed features are the direct visualisation of geometric phases [4], exploitation of intersections as switches for excitation transport [5,6] or, possibly, experimentally accessible scenario for the study of vibrational relaxation across a CI. The latter would additionally require coupling to a dissipative reservoir, which is typically naturally present in cold gases [7]. Experimental signatures of non-adiabatic effects in the unconstrained 3D motion of atoms could already be attained in state-of-the art experiments [8].

References

[1] D. Yarkony, *Conical Intersections: The New Conventional Wisdom*, J. Phys. Chem. A **105**, 6277 (2001).
[2] G. A. Worth and L. S. Cederbaum, *Beyond Born-Oppenheimer: Molecular Dynamics Through a Conical Intersection*, Annu. Rev. Phys. Chem. **55**, 127 (2004).
[3] S. Perun, A.L. Sobolewski, and W. Domcke, *Ab Initio Studies on the Radiationless Decay Mechanisms of the Lowest Excited Singlet States of 9H-Adenine*, J. Am. Chem. Soc. **127**, 6257 (2005).
[4] S. Wüster, A. Eisfeld and J. M. Rost , *Conical intersections in an ultracold gas*, Phys. Rev. Lett. **106**, 153002 (2011).
[5] K. Leonhardt, S. Wüster and J. M. Rost, *Switching exciton pulses through conical intersections*, Phys. Rev. Lett. **113**, 223001 (2014).
[6] K. Leonhardt, S. Wüster and J. M. Rost, *Orthogonal flexible Rydberg aggregates*, Phys. Rev. A **93**, 022708 (2016).
[7] D. Schönleber, A. Eisfeld, M. Genkin, S. Whitlock, S. Wüster, *Quantum Simulation of Energy Transport with Embedded Rydberg Aggregates*, Phys. Rev. Lett. **114**, 123005 (2015).
[8] K. Leonhardt, S. Wüster and J. M. Rost, *Exciton induced directed motion of unconstrained atoms in an ultracold gas*, http://arxiv.org/abs/1602.01032

Laser-subcycle control of double-ionization and electron recapture processes

Markus Kitzler[1]

1. Photonics Institute, Vienna University of Technology, Gusshausstrasse 27, A-1040 Vienna, Austria

No abstract available.

Classical-quantum correspondence in atom ionization by mid-infrared pulses

C. Lemell[1], N. I. Shvetsov-Shilovski[2], D. G. Arbo[3], S. Nagele[1], M. Lein[2], K. Tökesi[4], J. Burgdörfer[1]

1. Institute for Theoretical Physics, Vienna University of Technology, A-1040 Vienna, Austria, EU

2. Institut für Theoretische Physik and Centre for Quantum Engineering and Space-Time Res., Leibniz University Hannover, D-30167 Hannover, Germany, EU

3. Instute for Astronomy and Space Physics, 1428 Buenos Aires, Argentina

4. Institute of Nuclear Research of the Hungarian Acadademy of Sciences, Debrecen, and ELI-HU Nonprofit Ltd., Szeged, Hungary, EU

In recent years, the investigation of the photoionization process has gained renewed interest due to the development of few-cycle light sources with high intensity ($I \sim 10^{14}$ W/cm^2) and improved observation tools for the fragmentation process. In parallel to experimental advances also refined theoretical methods have been developed to interpret the experimental results.

While the solution of the time-dependent Schrödinger equation (TDSE), usually in single particle approximation can be compared directly with measured data, the applicability of quantum methods is limited by computational resources. Multiple ionization and large quiver amplitudes $\alpha = F_0/\omega^2$ of electrons in mid-infrared fields remain a major challenge.

Therefore, to support quantum simulations and provide a more intuitive interpretation of quantum results, (semi-)classical algorithms have been conceived which show a surprisingly good agreement with experimental [1] and with quantum results (e.g., the distribution of energies and angular momenta shown in Fig. 1 [2]) also in regimes where the applicability of classical methods is far from obvious.

In this presentation I will give an overview over of our investigations on quantum-classical correspondence over a wide range of intensities and wavelengths [1,2] and discuss the extension of classical-trajectory Monte-Carlo (CTMC) simulations to also account for the semiclassical phase accumulated along the electron trajectory resulting in the observation of interferences in photoelectron spectra with near-perfect agreement between TDSE and CTMC results. These developments will allow for analysis of the photoionization process in parameter regimes not easily accessible to full solutions of the TDSE.

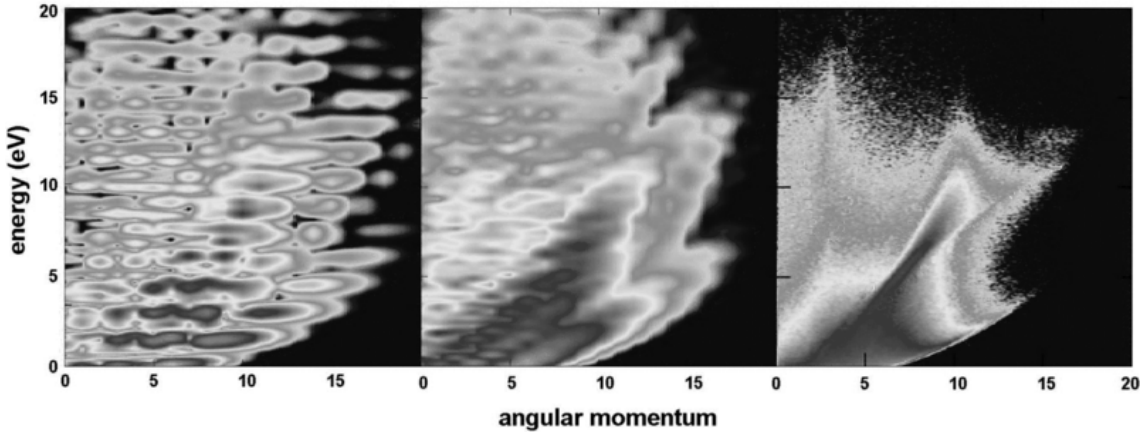

Fig. 1 Electron energy versus angular momentum as calculated by TDSE and CTMC on a logarithmic color scale covering four orders of magnitude in intensity. The TDSE results have been calculated without (left panel) and with intensity averaging (center panel). CTMC results including intensity averaging are shown in the right panel. Adapted from [2].

References

[1] B. Wolter, C. Lemell, M. Baudisch, M. G. Pullen, X.-M. Tong, M. Hemmer, A. Senftleben, C. D. Schröter, J. Ullrich, R. Moshammer, J. Biegert, and J. Burgdörfer, Phys. Rev. A **90**, 063424 (2014).

[2] D. G. Arbó, C. Lemell, S. Nagele, N. Camus, L. Fechner, A. Krupp, T. Pfeifer, S. D. López, R. Moshammer, and J. Burgdörfer, Phys. Rev. A **92**, 023402 (2015).

[3] N. I. Shvetsov-Shilovski, M. Lein, L. B. Madsen, E. Räsänen, C. Lemell, J. Burgdörfer, D. G. Arbó, and K. Tökési, submitted to Phys. Rev. A (2016).

The interaction of metastable neon with a few cycle laser pulse

J. E. Calvert[1], Han Xu[1], A. J. Palmer[1], R. D. Glover[2], D. E. Laban[1], X. M. Tong[3], V. K. Dolmatov[4], A. S. Kheifets[5], K. Bartschat[1,6], I. V. Litvinyuk[1], D. Kielpinski[1] and R. T. Sang[1]

1. Australian Attosecond Science Facility and Centre for Quantum Dynamics, Griffith University, Brisbane, Queensland 4111, Australia
2. Institute for Atomic and Nuclear Physics, University of Liege, Liege 4000, Belgium
3. Graduate School of Pure and Applied Sciences, and Center for Computational Science, University of Tsukuba, Tsukuba, 305-8571, Japan
4. Department of Physics and Earth Science, University of North Alabama, Florence, AL 35632, USA
5. Research School of Physics and Engineering, The Australian National University, Canberra ACT 0200, Australia
6. Department of Physics and Astronomy, Drake University, Des Moines, IA 50311, USA

The interaction of matter with few cycle (< 3) laser pulses is a rapidly expanding field. These interactions generate nonlinear effects such as high harmonic generation (HHG), above threshold ionisation and several higher order ionisation processes [1].

In atomic gases these nonlinear effects occur when the pulse is tightly focussed, and the high electric field strength causes the Coulomb potential that binds the valence electron to the atomic core to be suppressed. This allows the valence electron to escape by tunnelling, or by entering the continuum state over the barrier. Once the electron is free of the ionic core, it's trajectory is determined by the laser field. Therefore it is necessary to have a deep understanding of the ionisation principles in order to understand the nonlinear processes described above.

This work examines the effects of few cycle laser pulses on the $^3P_2$ metastable state of neon, hereafter referred to as Ne*. Ne* is an excellent candidate for this study as it allows the effects that different atomic states have on the ionisation process to be examined. This can be achieved through the comparison of ionisation rates to ground state neon, or as we show in this work, by comparing results from spin-polarised target hyperfine states of Ne*. This work provides two measurements. The first is a comparison of Ne* ion yield to ion yield as predicted by Ammosov-Delone-Krainov (ADK) theory [2] and ion yield as predicted by an approximated solution to the TDSE for the system [3]. The second measurement is a comparison of experimental ion yield for Ne* that are spin polarised in the $m_j = -2$ state compared to the $m_j = +2$ state.

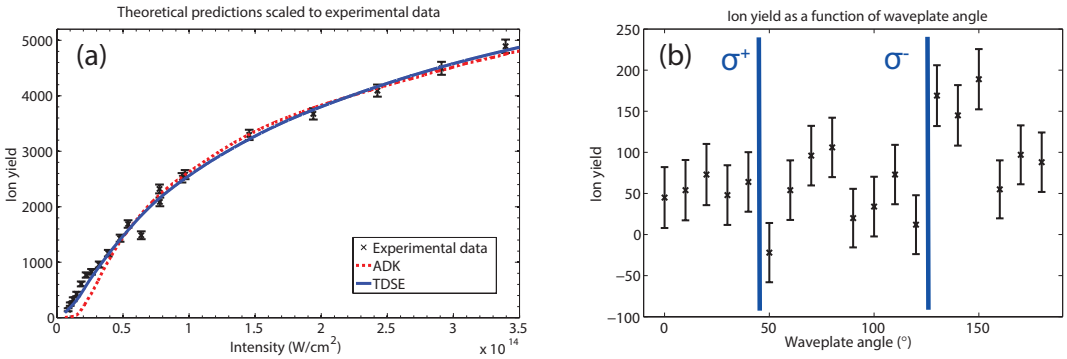

Fig. 1 (a) shows theoretical predictions of ion yield scaled to match the experimental ion yield. The scaling equation is $y = A \times \text{spline}(\nu x)$ where spline is an interpolating Matlab function. For the ADK theory, $\nu = 3.89$ and for the TDSE theory, $\nu = 1.59$. (b) depicts the ion yield as the function of the angle of the fast axis of a quarter waveplate with respect to a linear polariser used in an optical setup to pump Ne* atoms into spin polarised ensembles. The locations where the light is fully σ^+ and σ^- polarised are indicated, which correspond to a peak in $m_j = +2$ and $m_j = -2$ atoms, respectively.

The TDSE provides a better fit to the experimental data than ADK theory. This is due to the inability of ADK theory to correctly predict ions generated by OBI processes at low ionisation potentials. It is also noted that there is an asymmetry in the ion yield when comparing Ne* targets in different m_j states. We propose that this is a result of different m_j states having ionisation potentials due to different exchange interactions that the valence electron has with core electrons, depending upon the value of the electron's spin. The ionisation potentials are calculated to be $I_{p(m_j=+2)} = 4.75$eV and $I_{p(m_j=-2)} = 4.66$eV [4].

References

[1] T. Brabec and F. Krausz, Rev. Mod. Phys. **72**, 545 (2000).
[2] M. V. Ammosov, N. B. Delone and V. P. Krainov, Sov. Phys. JETP **64**, 425 (1986).
[3] X. M. Tong, K. Hino and N. Toshima, Phys. Rev. A **74**, 031405(R) (2006).
[4] J. E. Calvert *et al*, arXiv pre-print:1601.03786 (2016).

Unraveling the Principles Governing the Stability of Endohedral and Exohedral Fullerenes

Yang Wang[1,2], **Sergio Díaz-Tendero**[1,3], **Manuel Alcamí**[1,2], **Fernando Martín**[1,2,3]
1. Departamento de Química, Módulo 13, Universidad Autónoma de Madrid, 28049 Madrid, Spain
2. Instituto Madrileño de Estudios Avanzados en Nanociencia (IMDEA-Nanociencia), Cantoblanco, 28049 Madrid, Spain
3. Condensed Matter Physics Center (IFIMAC), Universidad Autónoma de Madrid, 28049 Madrid, Spain

Recent experimental evidences have confirmed that in nature fullerenes are much more abundant than expected [1]. In addition to neutral species, cationic and hydrogenated fullerenes are naturally present in outer space. On the other hand, fullerene anions, as well as endohedral and exohedral fullerenes, play important roles in material science, biomedicine and astrophysics [2,3]. An unusual behavior of charged, endohedrally and exohedrally derivatized fullerenes is that the isomer stability is often substantially different from that of their neutral counterparts [2,3]. The well established stability rules for neutral fullerenes, such as isolated-pentagon rule (IPR), are no longer valid for many experimentally observed structures (see Fig. 1 for an example).

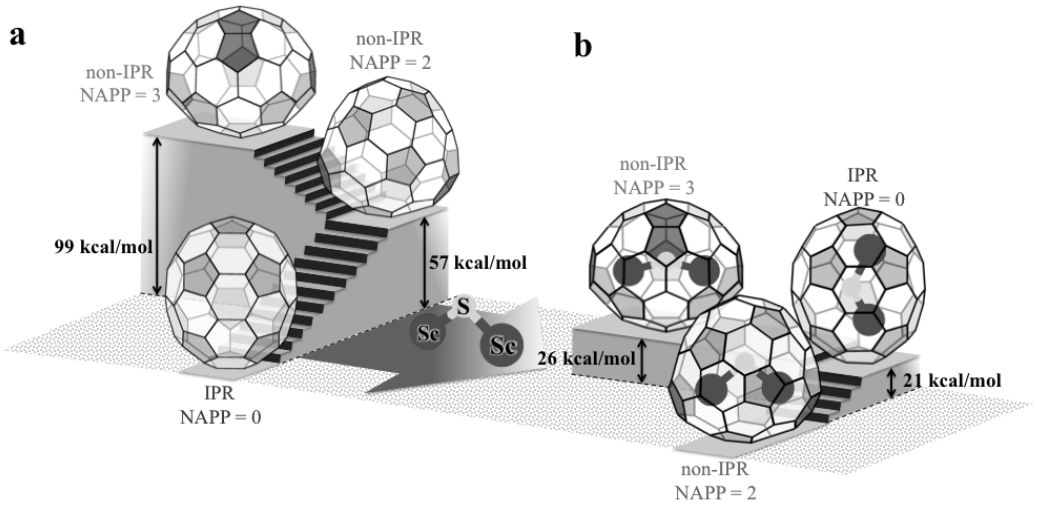

Fig. 1 Relative energies of three isomers of C_{70} containing 0, 2 and 3 adjacent pentagon pairs. (a) For neutral pristine C_{70}, the only isomer isolated experimentally follows the isolated pentagon rule (NAPP = 0). (b) For endohedral fullerene $Sc_2S@C_{70}$, the only isomeric form isolated experimentally so far is the one containing two adjacent pentagon pairs (NAPP = 2).

Which are then the underlying principles that govern the stability of charged and derivatized fullerenes? The answer to this question is not only of fundamental importance, but is also practically useful to predict experimentally producible fullerene structures, which are only a few among the enormous number (millions or billions or more) of possible cage isomers and regioisomers.

In this presentation, we propose a simple and unified model, based on the concepts of cage connectivity and frontier π orbitals [4], to fully understand the stability of charged, endohedrally and exohedrally derivatized fullerenes. Requiring only the knowledge of fullerene topology, the model permits a rapid determination of stable structures, among a huge number of possible isomers, without performing elaborate quantum chemistry calculations [4,5]. These predictions are relevant in fields as diverse as astrophysics, electrochemistry and supramolecular chemistry.

References

[1] Ewen K. Campbell, Matthias Holz, Dieter Gerlich, and John Paul Maier, *Laboratory confirmation of C_{60}^+ as the carrier of two diffuse interstellar bands*, Nature **523**, 322 (2015).
[2] Alexey A. Popov, Shangfeng Yang, and Lothar Dunsch, *Endohedral Fullerenes*, Chem. Rev. **113**, 5989 (2013).
[3] Yuan-Zhi Tan, Su-Yuan Xie, Rong-Bin Huang, and Lan-Sun Zheng, *The Stabilization of Fused-Pentagon Fullerene Molecules*, Nature Chem. **1**, 450 (2009).
[4] Yang Wang, Sergio Díaz-Tendero, Manuel Alcamí and Fernando Martín, *Cage Connectivity and Frontier π Orbitals Govern the Relative Stability of Charged Fullerene Isomers*, Nature Chem. **7**, 927 (2015).
[5] Yang Wang, Sergio Díaz-Tendero, Manuel Alcamí and Fernando Martín, *Key Structural Motifs to Predict the Cage Topology in Endohedral Metallofullerenes*, J. Am. Chem. Soc. **138**, 1551 (2016).

Coherent Control of Bond Making

Coherent control of chemical reactions has been suggested more than 30 years ago. However, its experimental demonstration remains an open challenge until today. I will review progress toward coherent control of chemical reactions and explain why it has proven so difficult. Focussing on coherent control of bond making, I will present our recent results on femtosecond photoassociation of hot magnesium atoms [1] and its coherent control [2].

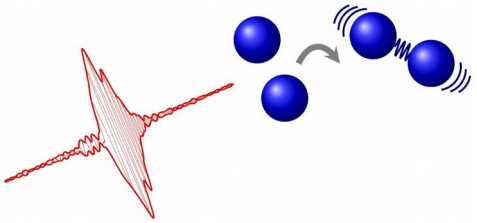

[1] L. Rybak et al., Phys. Rev. Lett. 107, 273001 (2011).
[2] L. Levin et al., Phys. Rev. Lett. 114, 233003 (2015).

Imaging Macromolecules with X-ray Laser pulses

Henry N. Chapman[1,2,3]

1. Center for Free-Electron Laser Science, DESY, Notkestrasse 85, 22607 Hamburg, Germany

2. Department of Physics, University of Hamburg, Luruper Chaussee 149, 22761 Hamburg, Germany

3. Centre for Ultrafast Imaging, Luruper Chaussee 149, 22761 Hamburg, Germany

The pulses from X-ray free-electron lasers are a billion times brighter than the brightest synchrotron beams available today. When focused to micron dimensions, such a pulse destroys any material, but the pulse terminates before significant atomic motion can take place. This mode of "diffraction before destruction" yields high-resolution structural information from proteins that cannot be grown into large enough crystals or are too radiation sensitive for high-resolution crystallography [1,2]. This has opened up a new methodology of serial femtosecond crystallography for radiation damage-free structures without the need for cryogenic cooling of the sample. Consequently, it is possible to carry out high-resolution diffraction studies of dynamic protein systems with time resolutions ranging from below 1 ps to milliseconds, from samples under physiological temperatures and other conditions [3]. Dynamical processes in these samples can be induced with a laser pulse, for example, or by rapid mixing of reactants.

The extremely high intensity of the X-ray pulses and their high spatial coherence has also been of interest for imaging non-crystalline samples, such as virus particles and single molecules [4]. Such single-particle imaging is being developed but is challenging due to the very low signal levels (compared to background sources) of tiny non-crystalline particles. There is a very significant advantage of measuring continuous diffraction from non-crystalline objects since it contains vastly more information than is encoded by the Bragg peaks in diffraction patterns of crystals. The increase in information makes it possible to directly determine the diffraction phases, overcoming the well-known phase problem in crystallography.

One way to address the low diffracted signals of single molecules is to place many oriented particles into the beam so that their diffraction signals sum to give a measurable pattern. Laser fields can be used to orient molecules, for example [5]. Disordered crystals also provide a way to obtain a large number of oriented molecules at high density. Translational disorder of molecules in a crystal gives rise to random phases in the scattering from those molecules that destroy the formation of Bragg peaks, and instead gives access to their continuous diffraction patterns. We have found that crystals of large macromolecules such as membrane proteins possess such translational disorder. This has previously limited the achievable crystallographic resolution (largest scattering angles of Bragg peaks) in many cases, but we have managed to measure the much weaker continuous diffraction from crystals of photosystem II, shown in Fig. 1, that extends far beyond visible Bragg peaks. We have reconstructed an image of this macromolecular complex using the phasing approach of single-molecule diffraction [6] (see Fig. 1).

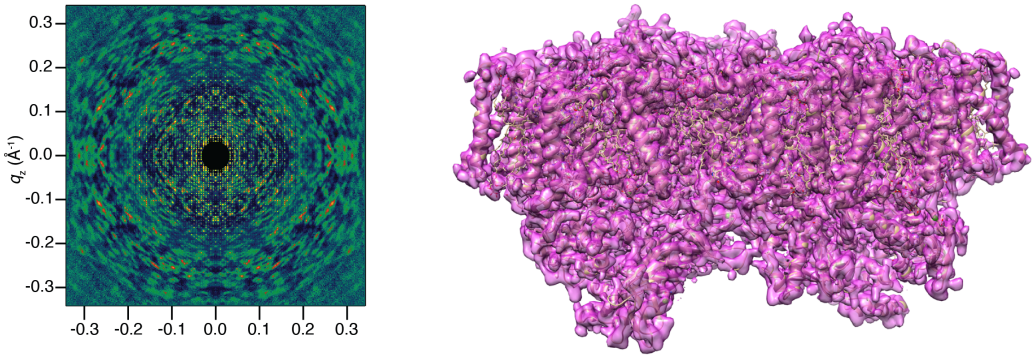

Fig. 1 Continuous "single molecule" diffraction measured from photosystem II crystals with translational disorder (left) and the three-dimensional electron density map that was reconstructed directly from the diffraction using iterative phasing (right). From [6].

References

[1] H.N. Chapman *et al.*, *Femtosecond x-ray protein nanocrystallography*. Nature **470**, 73–77 (2011).
[2] S. Boutet *et al.*, *High-resolution protein structure determination by serial femtosecond crystallography*, Science **337**, 362–364 (2012).
[3] K. Pande *et al.*, *Femtosecond structural dynamics drives the trans/cis isomerization in photoactive yellow protein*. Science **352**, 725–729 (2016).
[4] M. M. Siebert *et al.*, *Single mimivirus particles intercepted and imaged with an x-ray laser*, Nature **470**, 78–81 (2011).
[5] J. Küpper *et al.*, *X-ray diffraction from isolated and strongly aligned gas-phase molecules with a free-electron laser*. Phys. Rev. Lett. **112**, 083002 (2014).
[6] K. Ayyer *et al.*, *Macromolecular diffractive imaging using imperfect crystals*, Nature **530**, 202–206 (2016).

An Atomically Thin Matter-Wave Beam Splitter

Christian Brand[1], Michele Sclafani[1,2], Christian Knobloch[1], Yigal Lilach[3], Thomas Juffmann[1,4], Jani Kotakoski[5], Clemens Mangler[5], Andreas Winter[6], Andrey Turchanin[6], Jannik Meyer[5], Ori Cheshnovsky[3,7], and Markus Arndt[1]

1. University of Vienna, Faculty of Physics, VCQ, Boltzmanngasse 5, 1090 Vienna, Austria
2. ICFO - Institut de Ciènces Fotòniques, 08860 Castelldefels (Barcelona), Spain.
3. The Center for Nanosciences and Nanotechnology at Tel Aviv University
4. Department, Stanford University, 382 Via Pueblo Mall, Stanford, California 94305-4060, USA.
5. Faculty of Physics, University of Vienna, PNM, Boltzmanngasse 5, A-1090 Vienna, Austria
6. Friedrich Schiller University Jena, Institute of Physical Chemistry, Lessingstrasse 10, D-07743 Jena, Germany
7. Tel Aviv University, School of Chemistry, The Raymond and Beverly Faculty of Exact Sciences, Tel Aviv 69978, Israel

Matter-wave interferometry has matured into a highly sensitive tool for fundamental tests in physics, sensing miniscule forces and tiny length deviations. A requirement for any interferometric study is the coherent splitting of the incident wave in two or more parts which experience different phase shifts before they are recombined. Due to their internal level structure, refined laser schemes as used in atom interferometry cannot be applied to large polyatomic molecules. An alternative approach is based on nano-patterned mechanical gratings where the diffraction process is independent from the internal complexity of the diffracted object [1,2]. However, the universality of this approach is limited by the attractive van der Waals interactions between the matter-wave and the grating.

Here, I will present how to reduce the van der Waals interaction by minimizing the grating thickness to its ultimate limit - a single atomic layer [3]. We managed, for the first time, to pattern free-standing single layer graphene membranes with a period as small as $d = 100$ nm over large areas to diffract massive organic dye molecules. In a comprehensive study we compare the performance of several gratings with a thickness ranging between 0.3 and 90 nm. From the relative population of the individual far-field diffraction orders we deduce surprisingly large van der Waals interactions for these ultra-thin masks. For thick gratings we observe a matter-wave separation between the extreme orders of up to $18\,h/d$, corresponding to about $140\,\hbar$k for an alkali atom. This may allow to build compact rugged interferometers in the future. For the thinnest conceivable grating, however, the van der Waals interaction is minimized and only the zeroth and first diffraction orders are sizeably populated. This facilitates the high contrast diffraction of complex molecules. Furthermore, we find conditions which lead to the formation of nanoscrolls from single layer graphene ribbons. These optimize opening fraction of the grating, leading to an additional reduction in the van der Waals attraction.

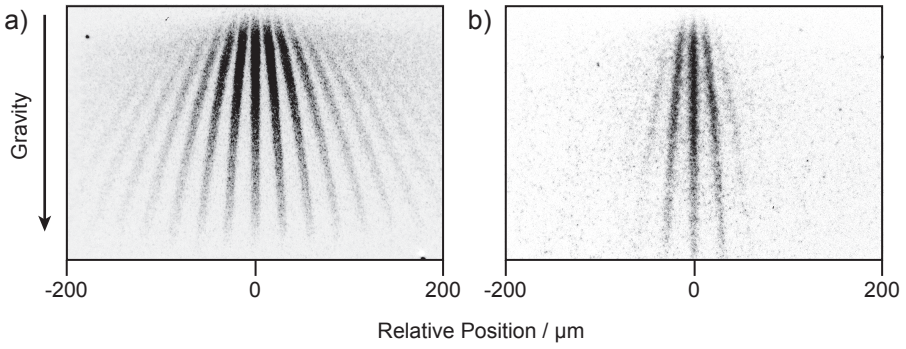

Fig. 1 Molecular diffraction at a 90 nm thick silicon nitride grating results in a population of up to the $\pm 9.th$ diffraction order (a). The observation of only three dominant diffraction orders for single layer graphene (b) illustrates the strong reduction in the attractive interaction between the grating and the matter-wave.

References

[1] D. W Keith, M. L. Schattenburg, H. I. Smith and D. E. Pritchard, *Diffraction of Atoms by a Transmission Grating*, Phys. Rev. Lett. **61**, 1580 (1988).
[2] Wieland Schöllkopf and Jan-Peter Toennies, *Nondestructive Mass Selection of Small Van der Waals Clusters*, Science **266**, 1345 (1994).
[3] Christian Brand, Michele Sclafani, Christian Knobloch, Yigal Lilach, Thomas Juffmann, Jani Kotakoski, Clemens Mangler, Andreas Winter, Andrey Turchanin, Jannik Meyer, Ori Cheshnovsky, and Markus Arndt, *An atomically thin matter-wave beamsplitter*, Nat. Nanotechnol. **10**, 845 (2015).

Development of a multi species cold atom interferometer

Clément Diboune
ONERA, DMPH, BP 80100, 91123 Palaiseau, France

Alexis Bonnin[1], Nassim Zahzam[1], Yannick Bidel[1], Alexandre Bresson[1], Malo Cadoret[1,2]
[1]ONERA, DMPH, BP 80100, 91123 Palaiseau, France
[2]Conservatoire National des Arts et Métiers (CNAM), 75003 Paris, France

Atom interferometry is now proven to be a very efficient technique to achieve highly sensitive and absolute inertial sensors. As a matter of fact gyroscopes or gravimeters based on this technique by using cold atoms have already been developed and give now very promising performance.
Our work concerns particularly the development of a multi species atom interferometer addressing mainly the topics of onboard applications such as navigation or geophysics, but also fundamental physics. At ONERA a double species – ^{87}Rb / ^{85}Rb – cold atom interferometer has already been developed and allowed the first atomic test of the weak equivalence principle with simultaneous measurements. We have also pointed out the interest of using more than one atomic species in the instrument through the development of original concepts to improve inertial measurements. We are currently working on the implementation of a third atomic species – ^{133}Cs – to go further into these concepts and get rid of the dead times measurements inherent to the use of a single species atomic interferometer. It could also be of interest for the equivalence principle test by comparing the free fall between cesium and rubidium.
The first step towards the triple species – ^{87}Rb / ^{85}Rb / ^{133}Cs – cold atom interferometer is the development of the laser needed for the cesium's cooling and manipulation**.** We are currently building a fibered laser system using an original approach potentially well suited for onboard applications.
We will present the ongoing progress concerning the laser development and also the different concepts of use of the multi species atom interferometer.

Disruption of Spin-Echo due to Atom Interactions

Cyrille Solaro[1], Alexis Bonnin[1], Matthias Lopez[1], Xavier Alauze[1], Franck Pereira Dos Santos[1]
1. SYRTE, Observatoire de Paris, PSL Research University, CNRS, Sorbonne Universités, UPMC Univ. Paris 06, LNE, 61 avenue de l'Observatoire, 75014 Paris, France
Frédéric Combes[2], Jean-Noël Fuchs[2,3], Frédéric Piéchon[2]
2. Laboratoire de Physique des Solides, CNRS UMR 8502, Univ. Paris-Sud, F-91405 Orsay Cedex, France
3. Laboratoire de Physique Théorique de la Matière Condensée, CNRS UMR 7600, Univ. Pierre et Marie Curie, 4 place Jussieu, 75252 Paris Cedex 05, France

We use spin echo and Ramsey interferometry on an ultracold ^{87}Rb ensemble confined in an optical dipole trap. The spin-echo technique is used to restore the coherence of the spin ensemble by cancelling out phase inhomogeneities. However, at high atomic densities, we observe the opposite behavior: a spin-echo pulse, placed at the middle of a Ramsey interferometer, accelerates the dephasing of the spin ensemble leading to a faster contrast decay of the interferometer.

Varying the atomic densities in the $10^{11} - 10^{12}$ at/cm^{-3} range, we observe a modulation of the Ramsey contrast with and without spin echo as the density increases [Fig.1]. We understand this phenomenon as a subtle competition between the spin-echo technique and a rephasing mechanism based on the identical spin rotation effect (ISRE). In trapped atomic clocks, ISRE, originating from particle indistinguishability, was shown to enhance the clock's coherence via the so-called spin self-rephasing mechanism, up to several tens of seconds![1] We propose here a model that reproduces well the experimental data and offers clear insight into this remarkable interplay between spin echo and spin self-rephasing [Fig.1].

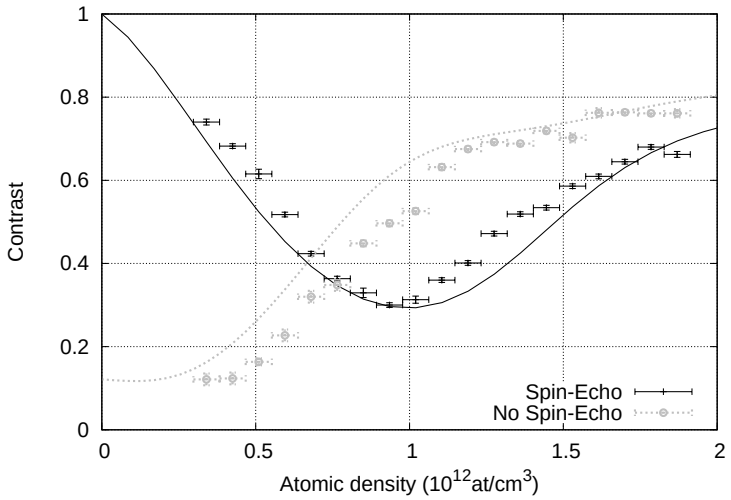

Fig. 1 Ramsey fringe contrast with (dots) and without (circles) spin-echo technique as a function of atomic density. The free precession time is 400ms. Solid (dotted) lines are simulations from our model of the Ramsey contrast with (without) spin-echo.

References

[1] C. Deutsch, F. Ramirez-Martinez, C. Lacroûte, F. Reinhard, T. Schneider, J. N. Fuchs, F. Piéchon, F. Laloë, J. Reichel, et P. Rosenbusch. *Spin Self-Rephasing and Very Long Coherence Times in a Trapped Atomic Ensemble* Phys. Rev. Lett. **105**, 020401 (2010)

Design of a miniaturized atomic gyroscope with an inductively coupled ring trap: advantages and challenges

German A. Sinuco-Leon, Kathryn A. Burrows, Barry M. Garraway
Department of Physics and Astronomy, University of Sussex, Brighton, BN1 9QH, United Kingdom

In view of their impressive sensitivity, atom interferometers have wide applicability ranging from testing fundamental physical laws to engineering applications. However, in designing portable atom-interferometric devices, it remains an important challenge to realize such advantages out of the laboratory. Here we describe advances in the design of a miniaturised atomic gyroscope with an atom-chip configuration. After introducing general operational principles, we provide an overview of our miniaturization strategy, which can be modified for other interferometric applications. Then, we describe in detail some elements of the proposed system. Firstly, we explain how an interferometer closed path can be defined by inductive effects over a micro-engineered conducting loop [1], and demonstrate that, operating at microwave frequencies, this scheme creates a ring trap for heavy alkali atoms atoms such as Rb and Cs. Secondly, we present various schemes for coupling the trapping conducting loop to microwave radiation. Thirdly, we outline a protocol that induces state-dependent transport, which is required to guide the atoms during an interferometric sequence [2,3]. Finally, we present a qualitative discussion of the atomic dephasing due to trap inhomogeneities and atomic interactions and its impact on the gyroscope performance.

References

[1] G.A. Sinuco-Leon, K.A., Burrows, A.S. Arnold, and B.M. Garraway, *Inductively coupled circuits for ultracold dressed atoms*. Nature Communications **5**, 5289 (2014).
[2] R. Stevenson, M. R. Hush, T. Bishop, I. Lesanovsky, and T. Fernholz, *Sagnac Interferometry with a Single Atomic Clock*. Physical Review Letters **115**, 163001 (2015).
[3] D. Siedel and J.G. Muga, *Ramsey interferometry with guided ultracold atoms*. The European Physical Journal D**41**, 71 (2007).

Investigation of Clock Transition at $\lambda = 1.14\,\mu$m in Cold Thulium Atoms

Gulnara Vishnyakova[1,2,3], Elena Kalganova[1,2,3], Artem Golovizin[1,2,3], Dmitry Tregubov[1,2,3], Denis Sukachev[1,3], Alexey Akimov[1,2,3], Ksenia Khabarova[1,3], Nikolay Kolachevsky[1,2,3], Vadim Sorokin[1,3]

1. P. N. Lebedev Physical Institute of RAS, 53 Leninsky prosp., Moscow 119991, Russia
2. Moscow Institute of Physics and Technology, 9 Institutsky per., Dolgoprudny, Moscow region, 141700, Russia
3. Russian Quantum Center, 100 Novaya st., Skolkovo, Moscow region 143025, Russia

Precise measurements of time and frequency are important both in fundamental problems and in applications such as navigation systems and telecommunications. Rapid development of optical frequency standards was stimulated by creation of femtosecond optical frequency synthesisers [1] and development of new methods of cooling, capturing and exciting atomic ensembles. The standards on single ions and on ensembles of neutral atoms trapped in optical lattices [2] are developing very actively. The optical frequency reference on a single aluminium ion has the systematic inaccuracy of $\sim 8.6 \times 10^{-18}$ [3], whereas for the optical frequency standard on strontium atoms in JILA [4] the total relative error is 6.4×10^{-18}. Moreover, due to a large number of interrogated atoms, systems on neutral atoms possess a substantially lower level of quantum projection noise, which provides the relative frequency instability of 10^{-17} for the measuring duration of 100 s [4].

We propose to use the magnetic-dipole transition $4f^{13}(^2F^o)6s^2\ (J = 7/2) \rightarrow 4f^{13}(^2F^o)6s^2\ (J = 5/2)$ between fine components of Tm ground state as a clock transition in optical atomic clock. It has width of 1.2 Hz and is shielded from external electric fields and collisions due to filled outer shields $5s^2$ and $6s^2$. This transition is in optical domain and has wavelength of $\lambda = 1.14\,\mu$m.

We detected clock transition in cloud of cold thulium atoms in (i) magneto-optical trap [5], (ii) optical lattice at 532 nm [6] and (iii) without any trapping fields [6]. The temperature of cloud is $10 \div 20\,\mu$K and the number of atoms is $10^5 \div 10^6$. Linewidth observed in optical lattice depends on power of trapping laser and determined mostly by inhomogeneity of trapping potential, tensor polarizability of clock levels and residual magnetic fields. The minimum linewidth was observed in the case (iii) and amounts to $\Delta\nu = 0.6$ MHz. Also we detected the shift of clock transition in the optical lattice due to nonzero differential polarizabilities of clock levels.

To prove that the clock transition is indeed narrow and suitable for optical clocks we have measured the clock level lifetime of thulium atoms in the optical lattice. From the exponential fit we determine clock level lifetime to be $\tau = 112 \pm 4$ ms which corresponds to the total linewidth of 1.4 Hz.

In order to choose "magic" wavelength of optical lattice (at which shifts of both clock levels are equal to each other) we calculate dynamic polarizabilities of the corresponding clock levels in a broad spectral range and start spectroscopy of clock transition in optical lattice at the wavelength in the range of $750 \div 850$ nm.

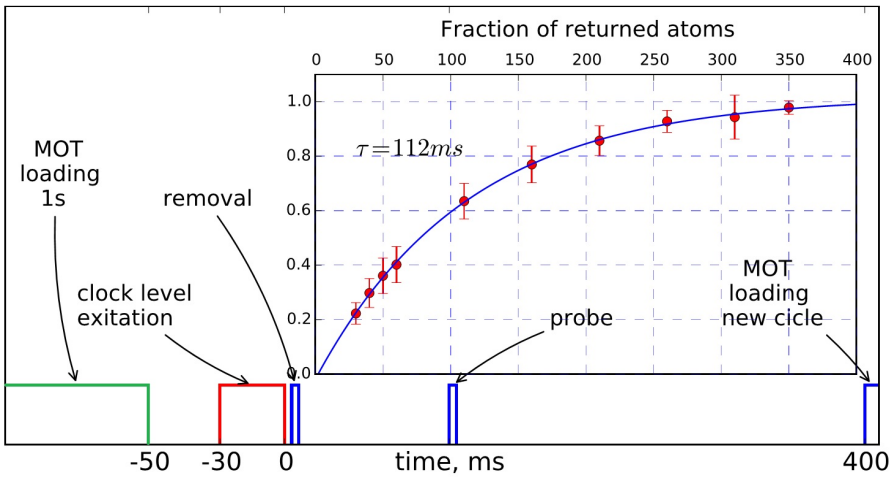

Fig. 1 Measurement of the lifetime of the $J = 5/2$ level. The normalized number of atoms decayed to the ground $J = 7/2$ level in dependence of time is shown.

References

[1] Udem Th. et al., Opt. Lett. **24** (13), 881 (1999).
[2] Katori H., Nat. Photonics **5**, 203 (1999).
[3] Chou C.W., Hume D.B., Koelemeij J.C.J., Wineland D.J., Roseband T., Phys. Rev. Lett. **104**, 070802 (2010).
[4] Bloom B.J. et al., Nature **506**, 71 (2014).
[5] Golovizin A. et al., Quant. Electron. **45** (5), 482 (2015).
[6] Vishnyakova G. et al., Phys. Usp. **59**, (2016).

Observation of Atom-Wave Beats Using a Kerr Modulator for Atom Waves

Boris Décamps, Jonathan Gillot, Jacques Vigué, Alexandre Gauguet, and Matthias Büchner

Laboratoire Collisions Agrégats Réactivité-IRSAMC, Université de Toulouse-UPS and CNRS UMR 5589, Toulouse, France

Wave beating is a very important phenomenon in physics: it was discovered with acoustic waves and is commonly used in electromagnetics, from the radio frequency to the laser domain. Obviously, wave beating can be extended to matter waves if a coherent superposition of quantum states with different kinetic energies can be achieved. ***This is precisely what we have observed with our lithium atom interferometer!***

We modulate the phase of an atom wave by applying time dependent, sinusoidal varying electric fields, i.e. we realize the equivalent of a Kerr modulator for atom waves [1]. These sinusoidal phase modulations are detectable in the interference signal, shown in Fig. 1. This signal exhibits time dependence, i.e. the fingerprint of atom wave beats. A Fourier analysis reveals the presence of the beat frequency and its harmonics. We varied the phase modulation depth (Fig.2) and the amplitude of the p^{th} harmonics modulation shows a Bessel-like behavior, in good agreement with theory.

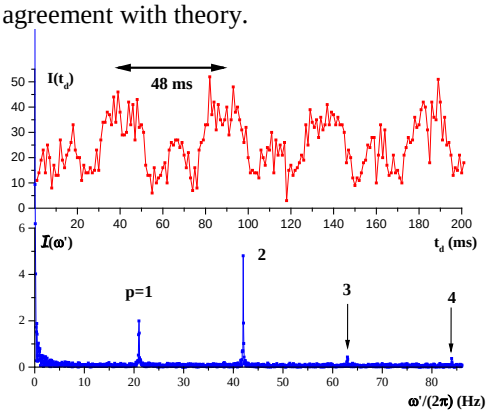

Fig. 1: The interferometer signal in the presence of a phase modulation oscillating at a frequency $\omega/(2\pi)= 21$ Hz.
Top panel: Direct recording of the interferometer signal.
Bottom panel: Modulus of the Fourier transform of a 16.4 s-long record of the signal.

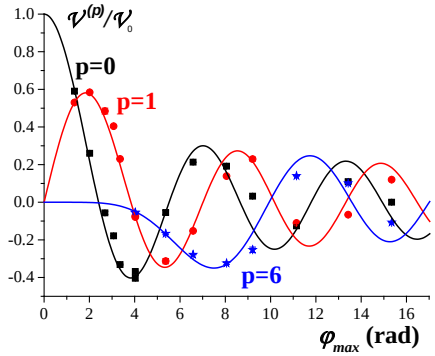

Fig. 2: Amplitude of modulation of the p^{th} harmonics as a function of the amplitude φ_{max} of the phase modulation. The curves are our theoretical results with no free parameters and the symbols (p=0: squares; p=1: bullets; p=6: stars) our measurements.

We have also made experiments with the two arms modulated with different frequencies. Each modulation is too fast to be detected, but we observe the beat at the frequency difference and its harmonics: this is a heterodyne experiment with matter waves.

Our method to create phase modulation can be extended to other matter waves. Especially its extension to electron waves can open fascinating opportunities. In electron holography microscopy, it should make it possible to measure the response of a sample with very high spatial and temporal resolutions.

We also used our set-up for educational goals, i.e. we transmit information by phase modulations. Fig. 3 shows a digitalized image, we have transmitted pixel per pixel by atom wave phase modulation [1].

Fig.3: Image [2] transmitted by atom wave phase modulation: ca. 96000 pixels were transmitted at 200 pixels/second with an error rate below 0.1%.

References

[1] B. Décamps, J. Gillot, J. Vigué, A. Gauguet, and M. Büchner, *Observation of Atom-Wave Beats Using a Kerr Modulator for Atom Wave* Phys.Rev. Lett. **116, 053004 (2016),** **http://dx.doi.org/10.1103/PhysRevLett.116.053004**

[2] Original image: Peter August Böckstiegel,Westphalian expressionist,, Self-portrait, 1917/1918; wood-cut; http://www.paboeckstiegel.de/

A self-interfering clock as a "which path" witness

Yair Margalit[a], Zhifan Zhou[a], Shimon Machluf[b], Daniel Rohrlich[a], Yonathan Japha[a], Ron Folman[a]

[a] *Department of Physics, Ben-Gurion University of the Negev, Beer-Sheva 84105, Israel*

[b] *Present address: Van der Waals-Zeeman Institute, University of Amsterdam, Science Park 904, 1090 GL Amsterdam, The Netherlands*

In Einstein's general theory of relativity, time depends locally on gravity; in standard quantum theory, time is global—all clocks "tick" uniformly. We demonstrate [1] a new tool for investigating time in the overlap of these two theories: a self-interfering clock, comprising two atomic spin states. We prepare the clock in a spatial superposition of quantum wave packets, which evolve coherently along two paths into a stable interference pattern. If we make the clock wave packets "tick" at different rates, to simulate a gravitational time lag, the clock time along each path yields "which path" information, degrading the pattern's visibility. In contrast, in standard interferometry, time cannot yield "which path" information. This proof-of-principle experiment may have implications for the study of time and general relativity and their impact on fundamental effects such as decoherence and the emergence of a classical world.

---

[1] Y. Margalit, Z. Zhou, S. Machluf, D. Rohrlich, Y. Japha, and R. Folman, Science **349**, 6253 (2015).

Photoionization and Photofragmentation of $Lu_3N@C_{80}^{q+}$ Ions (q = 1, 2, 3)

Jonas Hellhund[1], Alexander Borovik Jr.[2], Kristof Holste[2], Stephan Klumpp[3], Michael Martins[3], Sandor Ricz[4], Stefan Schippers[2], and Alfred Müller[1]

1. Institut für Atom- und Molekülphysik, Justus-Liebig-Universität Gießen, 35392 Giessen, Germany
2. I. Physikalisches Institut, Justus-Liebig-Universität Gießen, 35392 Giessen, Germany
3. Institut für Experimentalphysik, Universität Hamburg, 22761 Hamburg, Germany
4. Institute for Nuclear Research, Hungarian Academy of Sciences, Debrecen, H-4001, Hungary

We have measured cross sections for photoionization and photofragmentation of endohedral fullerene ions $Lu_3N@C_{80}^{q+}$ (q=1,2,3) [1] employing the photon-ion merged-beams technique at the PIPE end-station [2] of beamline P04 of the PETRA III synchrotron at DESY in Hamburg, Germany. The photo-reaction channels $Lu_3N@C_{80}^{q+} \rightarrow Lu_3N@C_{80-2r}^{p+}$ [q=1,2,3; p=2,3,4,5,6; r=0,1,3,4] were investigated in the photon energy ranges 280–330 eV around the carbon K-shell threshold, 380–435 eV around the nitrogen K-Shell threshold, and 1500–1700 eV around the lutetium M-shell threshold. The present work extends recent studies on (endohedral) fullerenes [3-6] to a heavier and more complex species as well as to higher photon energies.

In the energy range between 280 and 330 eV we could identify the same group of resonances in all investigated reaction channels. Since this group of resonances seems to make up for the most prominent structures in all spectra, we attempted to model each spectrum (for examples see Fig. 1) as a sum of seven Fano line shapes (full lines), a threshold feature (dashed line), and a constant background (dash-dotted line). The relative strengths of the resonance peaks (labeled 1 through 7) are given by the vertical blue bars in the insets of the figure. In the multiple ionization channels, a threshold can be observed at about 294 eV, in addition. We observe a shift of the ionization threshold towards higher photon energies when comparing double ionization of $Lu_3N@C_{80}^{2+}$ with double ionization of $Lu_3N@C_{80}^{+}$. We can determine the size of the endohedral fullerene ion based on this threshold shift. The cross sections measured at higher photon energies of 380–435 eV and of 1500–1700 eV show no structures and decrease with increasing photon energy.

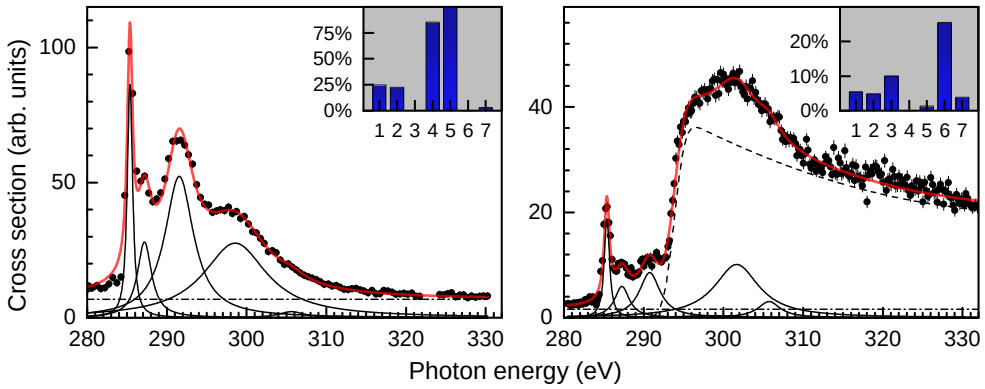

Fig. 1 Measured (symbols) and fitted (lines) cross sections for single (left) and double (right) photoionization of $Lu_3N@C_{80}^{+}$.

References

[1] J. Hellhund, A. Borovik Jr., K. Holste, S. Klumpp, M. Martins, S. Ricz, S. Schippers, and A. Müller, *Photoionization and photofragmentation of multiply charged $Lu_3N@C_{80}$ ions*, Phys. Rev. A **92**, 013413 (2015).

[2] S. Schippers, S. Ricz, T. Buhr, A. Borovik Jr., J. Hellhund, K. Holste, K. Huber, H.-J. Schäfer, D. Schury, S. Klumpp, K. Mertens, M. Martins, R. Flesch, G. Ulrich, E. Rühl, T. Jahnke, J. Lower, D. Metz, L. P. H. Schmidt, M. Schöffler, J. B. Williams, L. Glaser, F. Scholz, J. Seltmann, J. Viefhaus, A. Dorn, A. Wolf, J. Ullrich, and A. Müller, *Absolute cross sections for photoionization of Xe^{q+} ions ($1 \leq q \leq 5$) at the 3d ionization threshold (J. Phys. B Highlight 2014)*, J. Phys. B **47**, 115602 (2014).

[3] K. K. Baral, N. B. Aryal, D. A. Esteves-Macaluso, C. M. Thomas, J. Hellhund, R. Lomsadze, A. L. D. Kilcoyne, A. Müller, S. Schippers, and R. A. Phaneuf, *Photoionization and photofragmentation of the C_{60}^{+} molecular ion*, Phys. Rev. A **93**, 033401 (2016).

[4] R. A. Phaneuf, A. L. D. Kilcoyne, N. B. Aryal, K. K. Baral, D. A. Esteves-Macaluso, C. M. Thomas, J. Hellhund, R. Lomsadze, T. W. Gorczyca, C. P. Ballance, S. T. Manson, M. F. Hasoglu, S. Schippers, and A. Müller, *Probing confinement resonances by photoionization of Xe inside a C_{60}^{+} cage*, Phys. Rev. A **88**, 053402 (2013).

[5] A. L. D. Kilcoyne, A. Aguilar, A. Müller, S. Schippers, C. Cisneros, G. Alna'Washi, N. B. Aryal, K. K. Baral, D. A. Esteves, C. M. Thomas, and R. A. Phaneuf, *Confinement resonances in photoionization of $Xe@C_{60}^{+}$*, Phys. Rev. Lett. **105**, 213001 (2010).

[6] A. Müller, S. Schippers, M. Habibi, D. Esteves, J. C. Wang, R. A. Phaneuf, A. L. D. Kilcoyne, A. Aguilar, and L. Dunsch, *Significant redistribution of Ce 4d oscillator strength observed in photoionization of endohedral $Ce@C_{82}^{+}$ ions*, Phys. Rev. Lett. **101**, 133001 (2008).

Multiple Ionization of Ne^+ Ions by Photoabsorption Near the K Edge

A. Müller[1], D. Bernhardt[1], A. Borovik Jr.[1,2], T. Buhr[1,3], J. Hellhund[1], K. Holste[1,2], A. L. D. Kilcoyne[4], S. Klumpp[5], M. Martins[5], S. Ricz[1,6], J. Viefhaus[7], S. Schippers[1,2]

1. Institut für Atom- und Molekülphysik, Justus-Liebig-Universität Giessen, Germany
2. I. Physikalisches Institut, Justus-Liebig-Universität Giessen, Germany
3. Physikalisch-Technische Bundesanstalt, Braunschweig, Germany
4. Advanced Light Source, Lawrence Berkeley National Laboratory, Berkeley, California, USA
5. Institut für Experimentalphysik, Universität Hamburg, Germany
6. Institute of Nuclear Research of the Hungarian Academy of Sciences, Debrecen, Hungary
7. FS-PE, DESY, Hamburg, Germany

Single, double and triple photoionization of Ne^+ ions by a single photon have been investigated using the photon-ion spectrometer PIPE [1] at the PETRA III synchrotron radiation source in Hamburg. Absolute cross sections were measured (see Fig. 1) employing the photon-ion merged-beams technique [2]. In the course of photon-energy calibration measurements, high-resolution K-shell ionization spectra were also measured for neutral neon by employing an ionization chamber. Natural widths of several prominent lines of neutral Ne and of Ne^+ ions including the Ne K_α transitions could be determined with high accuracy. For comparison with existing theoretical calculations photoabsorption cross sections were inferred by summing the measured partial ionization channels. Agreement between theory and experiment is of mixed quality. It is remarkable, though, that the available R-matrix calculations nicely reproduce fine details in the photoabsorption cross section where interference of double excitations with the channel of direct photoionization occurs. The observed resonances in the different final ionization channels reveal the presence of complex Auger-decay mechanisms. The ejection of three electrons from the lowest K-shell-excited $Ne^+(1s2s^22p^6\ ^2S_{1/2})$ level, for example, requires cooperative interaction of at least four electrons in a single event even if the final charge state is reached via a cascade of Auger decays. The statistical quality, the energy range and the number of channels investigated in the present experiment are unique in the context of K-shell excitation and ionization of ions [3]. Only a previous experiment with C^+ ions [4] has provided a similarly comprehensive, high-quality set of absolute cross section data for photon-ion interactions in the energy range around the K edge (vertical bars in Fig. 1 show the onsets of photoionized K-vacancy levels).

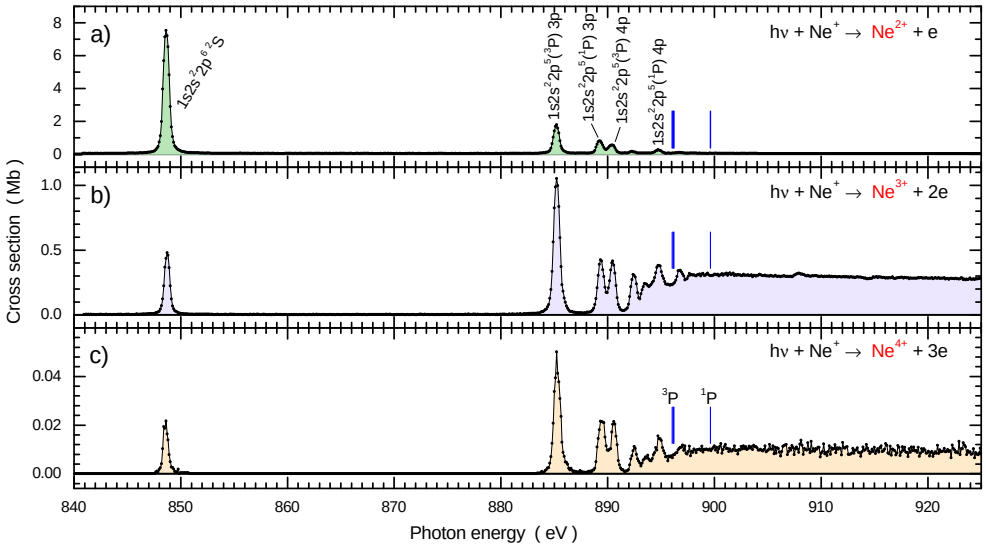

Fig. 1 Photoionization cross sections of Ne^+ near the K edge: Single ionization a), double ionization b), triple ionization c).

References

[1] S. Schippers, S. Ricz, T. Buhr, A. Borovik Jr., J. Hellhund, K. Holste, K. Huber, H.-J. Schäfer, D. Schury, S. Klumpp, K. Mertens, M. Martins, R. Flesch, G. Ulrich, E. Rühl, T. Jahnke, J. Lower, D. Metz, L. P. H. Schmidt, M. Schöffler, J. B. Williams, L. Glaser, F. Scholz, J. Seltmann, J. Viefhaus, A. Dorn, A. Wolf, J. Ullrich, and A. Müller, *Absolute cross sections for photoionization of Xe^{q+} ions ($1 \le q \le 5$) at the 3d ionization threshold (J. Phys. B Highlight 2014)*, J. Phys. B **47**, 115602 (2014).

[2] R. A. Phaneuf, C. C. Havener, G. H. Dunn, A. Müller, *Merged-beams experiments in atomic and molecular physics*, Rep. Prog. Phys. **62**, 1143 (1999).

[3] A. Müller, *Precision studies of deep-inner-shell photoabsorption by atomic ions*, Phys. Scr. **90**, 054004 (2015).

[4] A. Müller, A. Borovik Jr., T. Buhr, J. Hellhund, K. Holste, A. L. D. Kilcoyne, S. Klumpp, M. Martins, S. Ricz, J. Viefhaus, S. Schippers, *Observation of a four-electron Auger process in near-K-edge photoionization of singly charged carbon ions (Editors's Suggestion)*, Phys. Rev. Lett. **114**, 013002 (2015).

The effect of cluster sizes on the probability of ICD

Ltaief Ben Ltaief[1], Andreas Hans[1], Philipp Schmidt[1], Xaver Holzapfel[1], Philipp Reiss[1], Catmarna Küstner-Wetekam[1], Florian Wiegandt[2], Till Jahnke[2], Reinhard Dörner[2], Arno Ehresmann[1] and André Knie[1]

1. Universität Kassel, Institut für Physik, Heinrich-Plett Straße 40, D-34132 Kassel, Germany

2. Institut für Kernphysik, J. W. Goethe-Universität, Max-von-Laue-Str. 1, 60438 Frankfurt am Main, Germany

Relaxation processes occurring in excited weakly bound systems, e.g. van-der-Waals clusters, have been subject of several recent studies. Among these processes is the well-known ultrafast mechanism of energy transfer between two sites, i.e. the interatomic or molecular Coulombic decay (ICD) [1]. Here, the excess energy of the excited atom or molecule is transferred to a neighboring site, thereby, ionizing it. The important aspect of ICD is that the energy from an electronic transition is used to eject a low kinetic energy electron (the ICD electron) from the neighboring site. It was shown that these electrons are genotoxic and may induce irreparable damage in living tissues [2]. Recently, we have successfully demonstrated a first unambiguous proof of ICD by undispersed measurements of the emitted vacuum ultraviolet (VUV) photons from 2s-excited neon clusters for $\langle N \rangle \approx 20$ as mean cluster size [3]. Here, we report the effect of cluster size on ICD by means of the same fluorescence detection method. The present experiments were performed for the prototypical neon clusters covering the size range from monomers up to a few thousand atoms/cluster. The idea of the present work is to resonantly photoexcite a 2s inner valence electron of a neon atom within a cluster to an unoccupied orbital (nl). Then, this electronically excited state can relax via ICD which gives rise to the emission of a slow ICD electron (0 to 10 eV kinetic energy) from a neighboring neon atom. After the occurrence of ICD, a part of the excess energy remains at the initially excited atom. This excess energy is not sufficient to ionize the system further and is released by emission of a photon. This is the emitted photon that we measure in order to study the effect of cluster size on ICD. The overall process we investigate is as follow.

$$Ne_N(2s^2 2p^6) + h\upsilon \rightarrow Ne(2s^1 2p^6 nl)Ne_{N-1}(2s^2 2p^6)$$

$$\rightarrow Ne(2s^2 2p^5 nl)Ne^+(2s^2 2p^5)Ne_{N-2}(2s^2 2p^6) + e^-_{ICD}$$

$$\rightarrow Ne(2s^2 2p^6)Ne^+(2s^2 2p^5)Ne_{N-2}(2s^2 2p^6) + e^-_{ICD} + h\upsilon'$$

It has been shown theoretically that the ICD life time drops with increasing the number of nearest neighbors of the excited center [4, 5], implying that bulk sites are mostly sensitive to the occurrence of ICD. Our experimental results show the dependence of the ICD probability on the amount of neighboring atoms for a large range of cluster sizes.

References

[1] L.S. Cederbaum, J. Zobeley and F. Tarantelli, *Giant intermolecular decay and fragmentation of clusters*, Phys. Rev. Lett. **79**, 4778-4781 (1997).

[2] B. Boudaiffa, P. Cloutier, D. Hunting, M. A. Huels and L. Sanche, *Resonant formation of DNA strand breaks by low-energy (3 to 20 eV) electrons*. Science **287**, 1658-1660 (2000).

[3] A. Knie, A. Hans, M. Förstel, U. Hergenhahn, P. Schmidt, P. Reiß, Ch. Ozga, B. Kambs, F. Trinter, J. Voigtsberger, D. Metz, T. Jahnke, R. Dörner, A.I. Kuleff, L.S. Cederbaum, P.V. Demekhin and A. Ehresmann, *Detecting ultrafast interatomic electronic processes in media by fluorescence*, New. J. Phys. **16**, 102002 (2014).

[4] R. Santra, J. Zobeley and L.S. Cederbaum, *Electronic decay of valence holes in clusters and condensed matter*, Phys. Rev. B **64**, 245104 (2001).

[5] R. Santra and L.S. Cederbaum, *Coulombic Energy Transfer and Triple Ionization in Clusters*, Phys. Rev. Lett. **90**, 153401 (2003).

Chemical Bond Reformation Subsequent To Resonant Auger Decay

Esko Kokkonen[1], Matti Vapa[1,2], Kari Jänkälä[1], Klemen Bučar[3], Wei Cao[1], Matjaz Žitnik[3] and Marko Huttula [1]

1. Nano and Molecular Systems research unit, University of Oulu, P.O. Box 3000, FIN-90014, Oulu, Finland

2. Department of Theoretical Chemistry and Biology, School of Biotechnology, KTH Royal Institute of Technology, SE-10691, Stockholm, Sweden

3. Jožef Stefan Institute, P.O. Box 3000, SI-1001, Ljubljana, Slovenia

Wide usage of chlorinated hydrocarbons (CHCs) as industrial chemicals leads to their eventual release to nature and to the atmosphere. While in the atmosphere, CHCs can decompose and initiate catalytic processes, which involve free chlorine radicals, leading to ozone depletion. It is therefore important to understand the effects of these molecules as a function of external perturbation, such as sunlight. Electronic structure is a key component in the dynamical processes the compounds experience when ionized by sunlight, making it an important aspect for study. [1]

In this work we explore the chemical bond reformation after an X-ray induced core-shell excitation. In the chloromethane (CH_3Cl) molecule, a Cl 2*p* electron initially excited to an unoccupied antibonding σ* orbital leads to a resonant Auger decay. Following the initial excitation, multiple fragmentation pathways are opened for the system, with their relative probability depending on the exact electronic final state that is reached. Specific Auger final states leads to a new chemical bond formation between one hydrogen and the chlorine atom, forming stable HCl^+ ion.

This bond reformation was experimentally and computationally explored. The experiments involved an electron-energy-resolved fragment-ion coincidence measurement. The coincidence procedure allows us to link the exact Auger final states to the produced ion fragments. In the technique utilized in the coincidence setup at University of Oulu (further information in refs [2, 3] and references therein), the measurement of the kinetic energy of the Auger electron initiates the measurement of the masses of the resulting ions. Several fragmentation pathways are found following the Cl $2p \rightarrow \sigma^*$ excitation. Specific interest was in the underlying mechanism of the reformation of HCl^+ ion. Fig. 1 shows an example of a coincidence spectrum of Cl^+ and HCl^+ cations together with the traditional Auger electron spectrum recorded in the σ* resonance. Photon energy dependence of HCl^+ appearance was further studied by changing the photon energy in a large energy range. The HCl^+ appearance was confirmed to occur only the σ* resonance when viewed in coincidence with the Auger electrons [4]. This dependence and the appearance with respect to the Auger phenomenon was additionally studied using quantum chemical calculations.

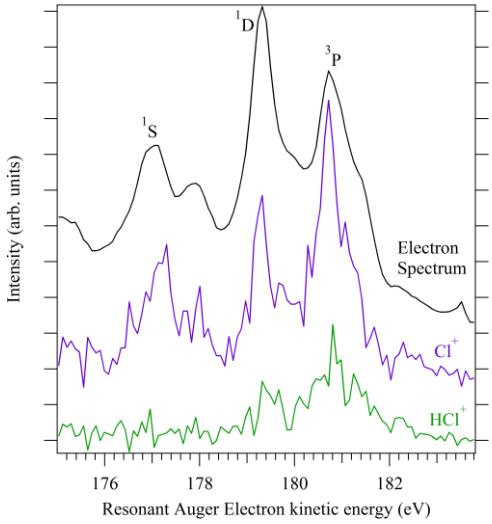

Fig. 1 An example of electron ion coincidence spectrum of Cl^+ and HCl^+ cations from CH_3Cl recorded in coincidence with the Auger final states (top curve)

References

[1] M. J. Molina, *Role of chlorine in stratospheric chemistry*, Pure Appl. Chem., **68**(9), 1749 (1996)
[2] E. Kokkonen, *et al. Fragmentation of mercury compounds under ultraviolet light irradiation*, J. Chem. Phys., **143**, 074037 (2015)
[3] E. Kokkonen, *et al. Spin-orbit mediated molecular dissociation*, J. Chem. Phys., **140**, 184304 (2014)
[4] C. Miron, *et al. Multipathway dissociation dynamics of core-excited methyl chloride probed by high resolution electron spectroscopy and Auger-electron–ion coincidences* J. Chem. Phys., **128**, 154314 (2008)

Molecular Double Core Hole Spectroscopy: The Role of Electronic and Nuclear Dynamics in Carbon Monoxide

Solène Oberli[1], Nicolas Sisourat[1], Patricia Selles[1], Stéphane Carniato[1]

1. Sorbonnes Universités, UPMC Univ Paris 06, CNRS, Laboratoire de Chimie Physique Matière et Rayonnement, F-75005, Paris, France

X-ray photoelectron spectroscopy (XPS) is a well-known sensitive and selective mean to access electronic and structural properties of molecules: the binding energy of a core electron is both characteristic of the atomic species and sensitive to the molecular chemical environment. Higher sensitivity may be reached using double core hole (DCH) spectroscopy, in which two inner-shell electrons are ejected from a molecule. The chemical shift is significantly enhanced when the two core holes are located on different atoms (two-site DCHs) [1,2] compared to the single-site DCH configuration, where a single atom is doubly ionized in the core shell. As a consequence, two-site DCH states formation allows to probe equivalent atoms, which may be indistinguishable by conventional XPS.

Study of doubly core-ionized molecules received a strong impetus since 2009 through the recent and rapid development of X-ray free electron lasers (XFELs). Despite the very small cross sections of DCH states compared to singly ionized species, XFELs open the possibility to produce DCH states by sequential X-ray two-photon absorption [3], as shown in Fig. 1. The theoretical description of this X-ray two-photon photoelectron spectroscopy (XTPPS) is challenging owing to the competition between x-ray photon absorption, nuclear dynamics and electronic relaxation by Auger decay which all occur at similar timescales. Therefore, a full time-dependent treatment of these processes is required, but previous studies are limited to classical rate-equation models for describing the time evolution in the different ionization channels [3,4].

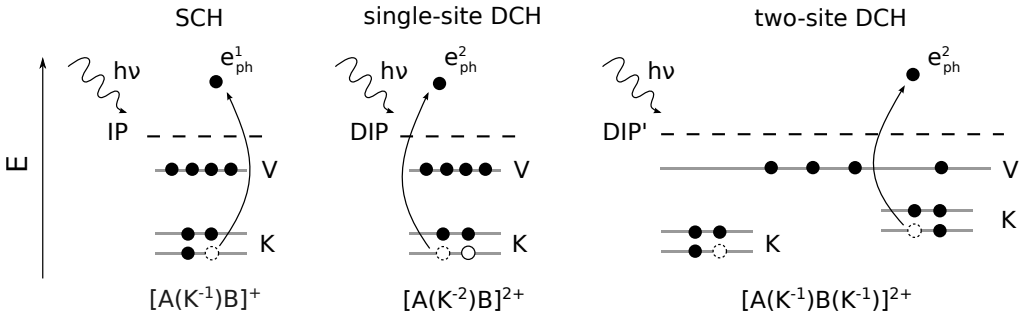

Fig. 1 Single-site and two-site DCH formation by the successive absorption of two X-ray photons of energy $h\nu$, which is higher than the double ionization potential DIP of the diatomic molecule AB. K and V denote the K- and valence shells, respectively.

In this work, we present the methodology and the numerical implementation of a complete description of XTPPS. Our model takes into account for the first time all competitive processes. Vibrationally resolved photoelectron spectra of singly and doubly ionized isolated carbon monoxide are calculated using a full quantum description of the nuclear motion, which includes explicitly the laser pulse and the Auger decay of the unstable core-ionized states.

References

[1] L. S. Cederbaum, F. Tarantelli, A. Sgamellotti and J. Schirmer, *On double vacancies in the core*, J. Chem. Phys. **85**, 6513-6523 (1986).

[2] L. S. Cederbaum, *Many-body theory of multiple core holes*, Phys. Rev. A **35**, 622 (1987).

[3] R. Santra, N. V. Kryzhevoi and L. S. Cederbaum, *X-ray two-photon photoelectron spectroscopy: a theoretical study of inner-shell spectra of the organic para-aminophenol molecule*, Phys. Rev. Lett. **103**, 013002 (2009).

[4] C. Buth, J.-C. Liu, M. H. Chen, J. P. Cryan, L. Fang, J. M. Glownia, M. Hoener, R. N. Coffee and N. Berrah, *Ultrafast absorption of intense x rays by nitrogen molecules*, J. Chem. Phys. **136**, 214310 (2012).

Absolute Cross Sections for the One-Photon Detachment of O^-

Matthieu Génévriez[1], Kevin M. Dunseath[2], Mariko Terao-Dunseath[2], Alain Cyr[2], Arnaud Dochain[1], Xavier Urbain[1]

1. Institute of Condensed Matter and Nanosciences, Université Catholique de Louvain, Louvain-la-Neuve B-1348, Belgium
2. Institut de Physique de Rennes, UMR 6251 CNRS–Université de Rennes 1, Campus de Beaulieu, F-35042 Rennes cedex, France

The photodetachment of the negative ion of oxygen O^-, although a seemingly simple process, is the subject of a long lasting discrepancy between theory and experiment. The cross section was determined experimentally in the 60's by Smith and Branscomb *et al.* [1, 2], and was later confirmed by two other measurements, although on much narrower energy ranges [3, 4]. It is considered as a reference, and has thus been used to put other relative measurements on an absolute scale. In the meantime, theories have tackled the challenging task of computing the photodetachment cross section for an open-shell ion. However even the latest *ab-initio* calculation significantly differs from the experiments, both in shape and magnitude [5]. This long lasting discrepancy between theory and experiment, and the use of the latter for calibration purposes, calls for further study.

We present a joint experimental and theoretical study of the one-photon detachment of O^-. The experiment has been performed using the animated-crossed-beam method [6], which allows to avoid the determination of the interaction volume and therefore requires much less assumptions than other methods. This is made possible by repeatedly sweeping the laser beam across the ion beam while recording easily measurable quantities: the ion current, the laser power and the number of neutral atoms produced. The theoretical work is twofold. The residual oxygen atom is described by a CI expansion that is voluntarily restricted in order to keep the photoionization calculations simple, yet including enough correlation to reproduce the electron affinity of the $O^-(1s^2 2s^2 2p^5\ ^2P^o)$ initial state and the polarizability of the $O(1s^2 2s^2 2p^4\ ^3P)$ ground state with sufficient precision. The CI description is then used to perform *ab initio*, non-perturbative *R*-Matrix Floquet calculations (*R*MF).

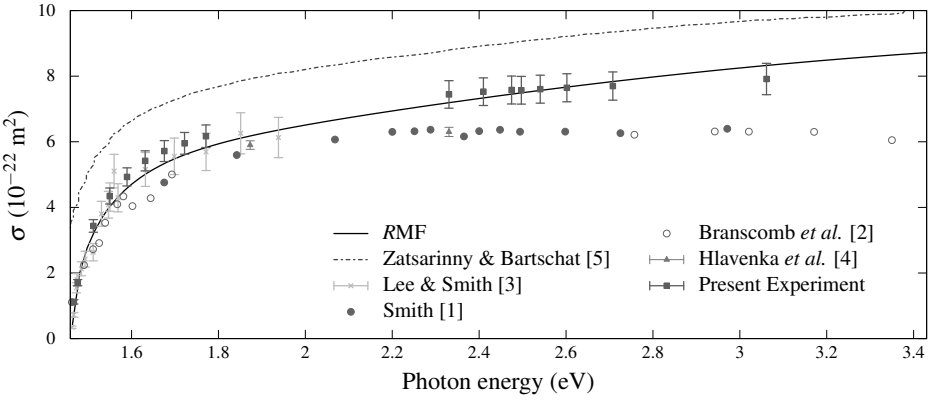

Fig. 1 Cross section for the one-photon detachment of O^-.

The present results are shown in figure 1 together with previous studies. They lie some 15% lower than the extensive calculation of Zatsarinny and Bartschat [6]. The discrepancy with previous measurements [1-4] is small close to threshold but becomes more pronounced as the photon energy increases, reaching 20% in the plateau region above 2.2 eV. The present theoretical and experimental results are in reasonable agreement over the whole photon energy range. A long-standing discrepancy between theory and experiment is thus resolved. The present values are also important for other photodetachment cross sections that were calibrated using the value of Smith, *e. g.*, for the C^- ion [7].

References

[1] S. J. Smith, Proceedings of the 4th International Conference on Ionization Phenomena in Gases (ICPIG) (1959).
[2] L. M. Branscomb, S. J. Smith and G. Tisone, *Oxygen Metastable Atom Production Through Photodetachment*, J. Chem. Phys. **43**, 2906 (1965).
[3] L. C. Lee and G. P. Smith, *Photodissociation and photodetachment of molecular negative ions. VI. Ions in $O_2/CH_4/H_2O$ mixtures from 3500 to 8600 A*, J. Chem. Phys. **70**, 1727 (1979).
[4] P. Hlavenka, R. Otto, S. Trippel, J. Mikosch, M. Weidemüller, R. Wester, *Absolute photodetachment cross section measurements of the O^- and OH^- anion*, J. Chem. Phys. **130**, 061105 (2009).
[5] O. Zatsarinny and K. Bartschat, *Low-energy photodetachment of O^-* Phys. Rev. A **73**, 022714 (2006).
[6] M. Génévriez and X. Urbain, *Animated-beam measurement of the photodetachment cross section of H^-*, Phys. Rev. A **91**, 033403 (2015).
[7] M. L. Seman and L. M. Branscomb, *Structure and Photodetachment Spectrum of the Atomic Carbon Negative Ion*, Phys. Rev. **258**, 1602 (1962).

Collective excitations and their impact on plasmon-assisted double ionizationfrom fullerenes

Michael Schüler[1], **Yaroslav Pavlyukh**[1], **Paola Bolognesi**[2], **Lorenzo Avaldi**[2], **Jamal Berakdar**[1]
1. Institut für Physik, Martin-Luther-Universität Halle-Wittenberg, 06099 Halle, Germany
2. CNR-ISM, Area della Ricerca di Roma 1, CP10, 00016 Monterotondo Scalo, Italy

The correlated release of an electron pair from a sample upon absorbing one photon, called double photoemission (DPE), is a process that is particularly sensitive to the effective electron-electron interaction. As a prototypical example we consider the C_{60} molecule. We analyse its strongly pronounced collective many-body excitations (plasmons) using ab initio calculations based on the time-dependent density-functional theory (TDDFT). Utilizing the nonnegative matrix factorization method, the individual plasmon modes are isolated and characterized by their multipolar and spatial distribution of the associated charge-density oscillations. This allows to construct a new model for the density-density response function and the effective electron-electron interaction that accurately describes typical experiments such as electron-energy loss spectroscopy (EELS) (see **Fig**. 1(a). Using our model parameterization of screened interaction and further ab initio calculations, we compute the electron-pair coincidence spectrum of C_{60}. Both theory and experiment underpin the new features arising from the dynamically screened interaction mediating the effective electron-electron interaction (see **Fig**. 1(b)) and thus endorse DPE as a powerful tool for tracing electron pair correlations in complex many-body systems [2].

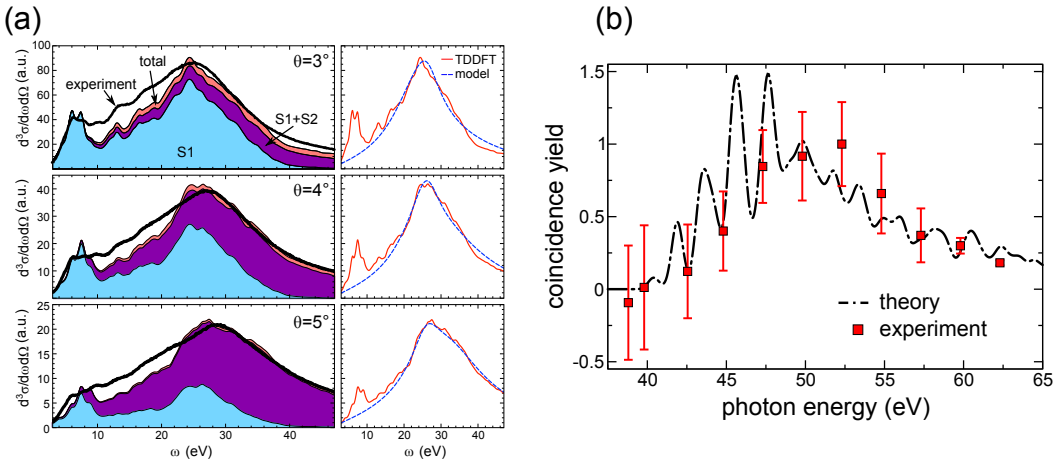

Fig. 1 (a) EELS cross section as computed by our TDDFT approach and resolved with respect to the individual plasmon modes S1 (symmetric surface plasmons), S2 (anti-symmetric surface plasmons), and the full signal including volume plasmons, as well, vs. experimental results. The panels on the right-hand side compare the model predicitions with the TDDFT results. (b) DPE coincidence yield as a function of the photon energy as measured in recent experiments, along with the theoretical prediction [2].

References

[1] Michael Schüler, Jamal Berakdar and Yaroslav Pavlyukh, *Disentangling multipole contributions to collective excitations in fullerenes*, Phys. Rev. A **02**, 021403(R) (2015).

[2] Michael Schüler,Yaroslav Pavlyukh, Paola Bolognesi, Lorenzo Avaldi and Jamal Berakdar,*Electron pair escape from fullerene cage via collective modes*, Sci. Rep. **accepted** (2016).

Two-photon ionization of the 3p shell of Ar

Ivan D. Petrov[1], Boris M. Lagutin[1], Victor L. Sukhorukov[2], André Knie[3], Arno Ehresmann[3]

1. Rostov State University of Transport Communications, 344038 Rostov-on-Don, Russia

2. Institute of Physics, Southern Federal University, 344090 Rostov-on-Don, Russia

3. Institut für Physik, Universität Kassel, D-34132 Kassel, Germany

The generalized two-photon ionization cross section of the 3p shell of Ar were calculated in the lowest order of perturbation theory (LOPT) and with taking into account many-electron correlations. The photoionization amplitudes were calculated using the correlation functions, obtained by the method similar to the Dalgarno-Lewis one [1]. We implemented noniterative numerical procedure for solving respective inhomogeneous integro-differential equations provided their convergence at energies close to the energy of intermediate resonances, where the usual Dalgarno-Lewis method diverges.

In our calculation we took into account many-electron correlations, similar to those considered in [2]. The inclusion of those correlations results in close agreement between the photoionization cross sections calculated in the length and velocity forms of electric-dipole operator. One of the strong correlations is the following:

$$3p^6 \dashrightarrow 3p^5\varepsilon' l' \longrightarrow 3p^4\varepsilon l\varepsilon' l' \dashrightarrow 3p^5\varepsilon l,$$

where the dashed arrows denote electric dipole interaction and the solid arrow denotes Coulomb interaction.

The influence of many-electron correlations is shown in Fig. 1a where the partial two-photon ionization cross section to the $3p^5\varepsilon p(^1S)$ channel is presented.

In addition to the discussed above many-electron correlations the influence of the polarization of the atomic core induced by the outgoing electron [3] was also considered. Accounting for this effect increases the theoretical two-photon ionization cross section near the threshold by approximately 17% and provides an excellent agreement between computed and measured energies of the intermediate resonances. In Fig. 1b the core polarization effect is demonstrated for the total 3p two-photon ionization cross section of Ar.

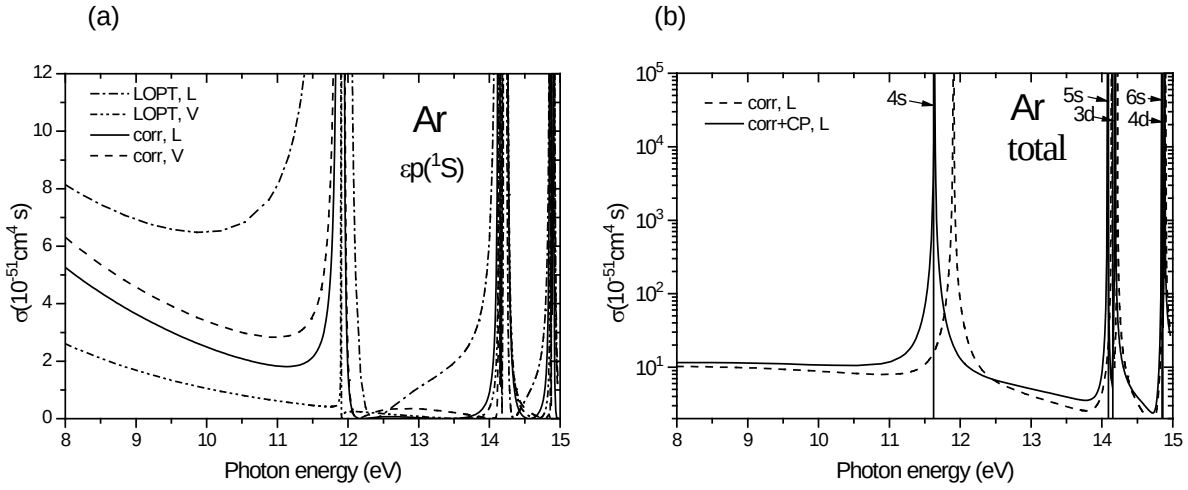

Fig. 1 (a) The 3p partial generalized two-photon ionization cross section for the transition to the $3p^5\varepsilon p(^1S)$ channel and for linearly polarized incoming radiation calculated in LOPT and with taking into account many-electron correlations (corr). Both length (L) and velocity (V) forms are presented.
(b) The 3p total generalized two-photon ionization cross section in the length (L) form for linearly polarized incoming radiation calculated with taking into account many-electron correlations (corr) and, in addition, polarization of the atomic core by the photoelectron (corr + CP). Vertical lines: experimental energy positions of the intermediate resonances.

References

[1] A. Dalgarno and J. Lewis, *The exact calculation of long-range forces between atoms by perturbation theory*, Proc. R. Soc. London **233**, 70 (1955).

[2] C. Pan, B. Gao, and A. F. Starace, *Two-photon ionization of the ar atom and detachment of the F^- ion*, Phys. Rev. A **41**, 6271 (1990).

[3] I. D. Petrov, V. L. Sukhorukov, and H. Hotop, *The influence of core polarization on photo-ionization of alkali and metastable rare gas atoms near threshold*, J. Phys. B: At. Mol. Opt. Phys. **32**, 973 (1999).

A Single Atom Antenna

Florian Trinter[1], Joshua B. Williams[1], Miriam Weller[1], Markus Waitz[1], Martin Pitzer[1], Jörg Voigtsberger[1], Carl Schober[1], Gregor Kastirke[1], Christian Müller[1], Christoph Goihl[1], Phillip Burzynski[1], Florian Wiegandt[1], Robert Wallauer[1], Anton Kalinin[1], Lothar Ph. H. Schmidt[1], Markus S. Schöffler[1], Ying-Chih Chiang[2], Kirill Gokhberg[2], Till Jahnke[1], and Reinhard Dörner[1]

1. *Institut für Kernphysik, J. W. Goethe-Universität Max-von-Laue-Strasse 1, D-60438 Frankfurt am Main, Germany*
2. *Theoretische Chemie, Universität Heidelberg, Im Neuenheimer Feld 229, D-69120 Heidelberg, Germany*

In radio technology antennas are used to efficiently collect energy from the electromagnetic field. In the optical regime nano-scale antennas have been developed [1] and in nature specialized antenna molecules efficiently collect the visible light for light harvesting. Schematically all these systems consist of the antenna itself which couples to the radiation field, a receiver which uses the energy and a route to transport the energy between them.

Here we demonstrate the smallest possible implementation of such an antenna-receiver complex which consists of a single (helium) atom acting as the antenna and a second (neon) atom acting as a receiver [2,3]. We investigate the ionization of HeNe from below the He 1s3p excitation to the He ionization threshold. We observe $HeNe^+$ ions with an enhancement by more than a factor of 60 when the He side (the antenna atom) of the antenna couples resonantly to the radiation field. The energy transfer occurs via Interatomic Coulombic Decay (ICD) [4]. The $HeNe^+$ ions are an experimental proof of a two-center resonant photoionization mechanism predicted by Najjari et al. [5]. Furthermore, our data provide electronic and vibrational state resolved decay widths of interatomic Coulombic decay in HeNe dimers. We find that the interatomic Coulombic decay lifetime strongly increases with increasing vibrational state.

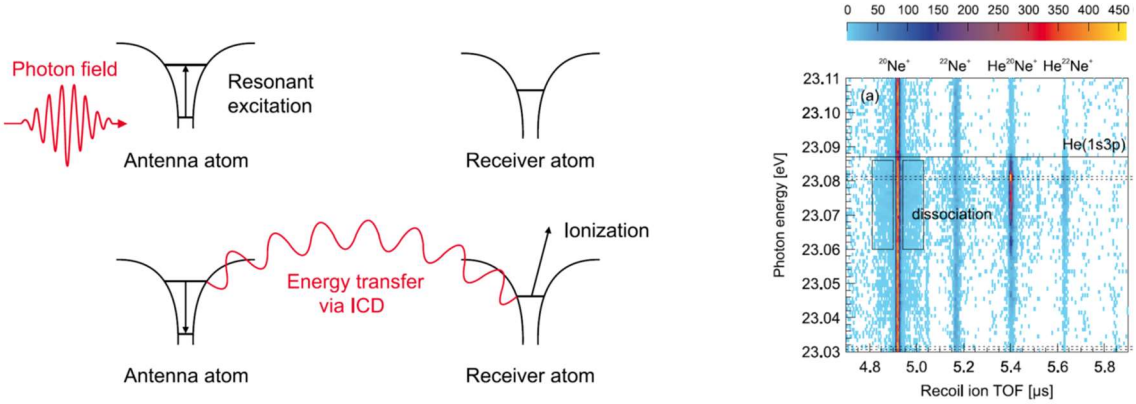

Fig. 1 Schematic of the antenna mechanism and experimental results: Ion time of flight versus photon energy in the vicinity of the He(1s3p) resonance.

References

[1] L. Novotny and N. van Hulst, *Antennas for light*, Nat. Photonics **5**, 83 (2011).
[2] F. Trinter et al., *Vibrationally Resolved Decay Width of Interatomic Coulombic Decay in HeNe*, Phys. Rev. Lett. **111**, 233004 (2013).
[3] G. Jabbari et al., *Ab initio calculation of ICD widths in photoexcited HeNe*, J. Chem. Phys. **140**, 223305 (2014).
[4] L. S. Cederbaum, J. Zobeley, and F. Tarantelli, *Giant Intermolecular Decay and Fragmentation of Clusters*, Phys. Rev. Lett. **79**, 4778 (1997).
[5] B. Najjari, A. B. Voitkiv, and C. Müller, *Two-Center Resonant Photoionization*, Phys. Rev. Lett. **105**, 153002 (2010).

The interaction of metastable neon with a few cycle laser pulse

J. E. Calvert[1], Han Xu[1], A. J. Palmer[1], R. D. Glover[2], D. E. Laban[1], X. M. Tong[3], V. K. Dolmatov[4], A. S. Kheifets[5], K. Bartschat[1,6], I. V. Litvinyuk[1], D. Kielpinski[1] and R. T. Sang[1]

1. Australian Attosecond Science Facility and Centre for Quantum Dynamics, Griffith University, Brisbane, Queensland 4111, Australia
2. Institute for Atomic and Nuclear Physics, University of Liege, Liege 4000, Belgium
3. Graduate School of Pure and Applied Sciences, and Center for Computational Science, University of Tsukuba, Tsukuba, 305-8571, Japan
4. Department of Physics and Earth Science, University of North Alabama, Florence, AL 35632, USA
5. Research School of Physics and Engineering, The Australian National University, Canberra ACT 0200, Australia
6. Department of Physics and Astronomy, Drake University, Des Moines, IA 50311, USA

The interaction of matter with few cycle (< 3) laser pulses is a rapidly expanding field. These interactions generate nonlinear effects such as high harmonic generation (HHG), above threshold ionisation and several higher order ionisation processes [1].

In atomic gases these nonlinear effects occur when the pulse is tightly focussed, and the high electric field strength causes the Coulomb potential that binds the valence electron to the atomic core to be suppressed. This allows the valence electron to escape by tunnelling, or by entering the continuum state over the barrier. Once the electron is free of the ionic core, it's trajectory is determined by the laser field. Therefore it is necessary to have a deep understanding of the ionisation principles in order to understand the nonlinear processes described above.

This work examines the effects of few cycle laser pulses on the $^3P_2$ metastable state of neon, hereafter referred to as Ne*. Ne* is an excellent candidate for this study as it allows the effects that different atomic states have on the ionisation process to be examined. This can be achieved through the comparison of ionisation rates to ground state neon, or as we show in this work, by comparing results from spin-polarised target hyperfine states of Ne*. This work provides two measurements. The first is a comparison of Ne* ion yield to ion yield as predicted by Ammosov-Delone-Krainov (ADK) theory [2] and ion yield as predicted by an approximated solution to the TDSE for the system [3]. The second measurement is a comparison of experimental ion yield for Ne* that are spin polarised in the $m_j = -2$ state compared to the $m_j = +2$ state.

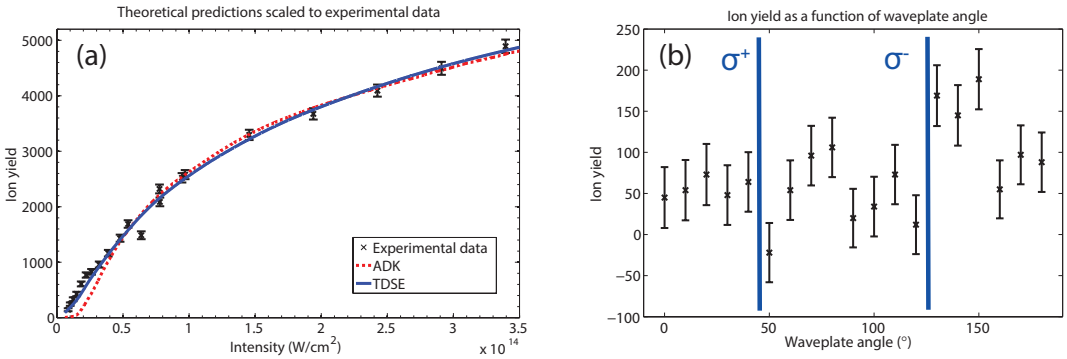

Fig. 1 (a) shows theoretical predictions of ion yield scaled to match the experimental ion yield. The scaling equation is $y = A \times \text{spline}(\nu x)$ where spline is an interpolating Matlab function. For the ADK theory, $\nu = 3.89$ and for the TDSE theory, $\nu = 1.59$. (b) depicts the ion yield as the function of the angle of the fast axis of a quarter waveplate with respect to a linear polariser used in an optical setup to pump Ne* atoms into spin polarised ensembles. The locations where the light is fully σ^+ and σ^- polarised are indicated, which correspond to a peak in $m_j = +2$ and $m_j = -2$ atoms, respectively.

The TDSE provides a better fit to the experimental data than ADK theory. This is due to the inability of ADK theory to correctly predict ions generated by OBI processes at low ionisation potentials. It is also noted that there is an asymmetry in the ion yield when comparing Ne* targets in different m_j states. We propose that this is a result of different m_j states having ionisation potentials due to different exchange interactions that the valence electron has with core electrons, depending upon the value of the electron's spin. The ionisation potentials are calculated to be $I_{p(m_j=+2)} = 4.75$eV and $I_{p(m_j=-2)} = 4.66$eV [4].

References

[1] T. Brabec and F. Krausz, Rev. Mod. Phys. **72**, 545 (2000).
[2] M. V. Ammosov, N. B. Delone and V. P. Krainov, Sov. Phys. JETP **64**, 425 (1986).
[3] X. M. Tong, K. Hino and N. Toshima, Phys. Rev. A **74**, 031405(R) (2006).
[4] J. E. Calvert *et al*, arXiv pre-print:1601.03786 (2016).

Enhancing high-order harmonic generation in light molecules by using chirped pulses

M. Lara-Astiaso[1], R. E. F. Silva[1], A. Gubaydullin[1], P. Rivière[1], C. Meier[2] and F. Martín[1,3,4]

1. Departamento de Química, Universidad Autónoma de Madrid, 28049 Madrid, Spain

2. Laboratoire de Collisions Agrégats Réactivité, IRSAMC, UMR CNRS 5589, Université Paul Sabatier, 31062 Toulouse, France

3. Instituto Madrileño de Estudios Avanzados en Nanociencia 28049 Madrid, Spain

4. Condensed Matter Physics Center (IFIMAC), Universidad Autónoma de Madrid, 28049 Madrid, Spain

The process of generating high-order harmonics is a result of the non-linear response of the electrons in a strong laser field, leading to the emission of light of much higher frequency than that of the driving laser [1]. One of the most appealing applications of this technique is the generation of attosecond pulses of light, which can in be used in time-resolved pump-probe experiments, to resolve physical processes at such timescales. The typical harmonic emission spectrum consists of a series of peaks at odd multiples of the driving laser frequency and exhibits a plateau region followed by a sharp cut-off at an energy approximately given by $E_{max} = I_p + 3.17\ \mathrm{I}_0\ \lambda^2/4$, being I_p the ionization potential and I_0, λ, the intensity and wavelength of the driving field, respectively [2].

Nowadays, extending the harmonic cut-off to increasingly high energies while maintaining the efficiency of the high harmonic emission represents an important challenge to the state-of-the art of high harmonic generation technology [3]. In this work, we show that the combined effect of linearly chirped pulses and nuclear dynamics in light molecules allows one to achieve this goal. The effect is only observed for down chirps and for IR pulses that are long enough to induce nuclear wave packet dynamics able to bring the molecule well outside the Franck-Condon region. We also show that, by varying the pulse duration or by performing isotopic substitution while keeping the pulse duration constant, one can control the extension of the the harmonic plateau.

The observed extension and enhancement of the HHG spectrum derives from an adequate timing of the low-frequency cycles with respect to the molecular stretching, since the HHG spectrum of H_2^+ arising from down-chirped pulses is more intense and extends to much larger harmonic orders than that resulting from unchirped or up-chirped pulses. This is a consequence of the laser-induced nuclear dynamics that drives the system to large internuclear distances, where the trailing long-wavelength cycles can efficiently ionize the molecule. By varying the pulse duration or the mass of the nuclei, one can tune the time at which ionization by the long wavelengths occurs and thus control the extension of the harmonic cut-off. Similar effects are expected in other molecules containing light nuclei.

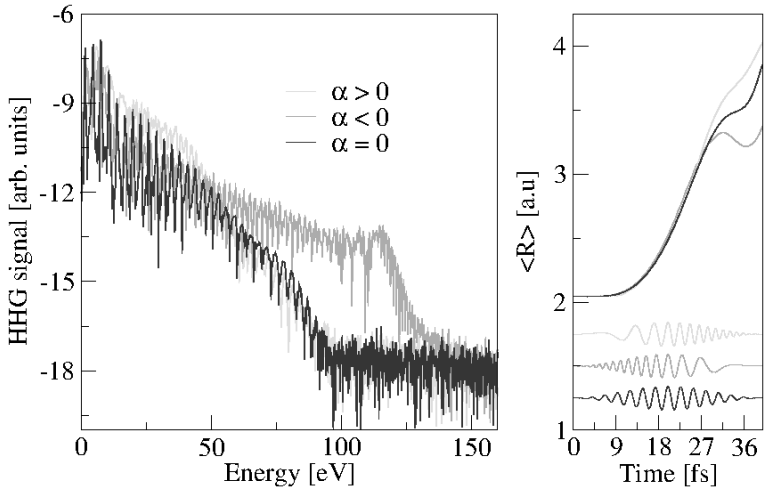

Fig. 1 (Left) High harmonic spectra of H_2^+ obtained with chirped pulses ($\alpha \neq 0$) of 40 fs, which correspond to an unchirped pulse ($\alpha = 0$) of 15 cycles of $\lambda = 800$ nm and peak intensity $\mathrm{I}_0 = 3 \times 10^{14}\mathrm{W/cm^2}$. The pulse is said to be up-chirped if $\alpha > 0$ or down-chirped if $\alpha < 0$. The carrier-envelope phase is always set to $\delta_0 = 0$. The right panel displays the pulses used to obtain the corresponding harmonic spectra as well as the mean value of the internuclear distance $< R >$ as functions of time.

References

[1] Anne L'Huillier and Philippe Balcou, *High-order harmonic generation in rare gases with a 1-ps 1053-nm laser*, Phys. Rev. Lett. **70**, 774 (1993).

[2] Paul B. Corkum, *Plasma perspective on strong field multiphoton ionization*, Phys. Rev. Lett. **71**, 1994 (1993).

[3] Carsten Winterfeldt, C. Spielmann, and Gustav Gerber, *Optimal control of high-harmonic generation*, Rev. Mod. Phys. **80**, 117 (2008).

Real-time imaging of the tunneling process via ionization

Johann Förster and Alejandro Saenz

Institut für Physik / AG Moderne Optik, Humboldt-Universität zu Berlin, Newtonstr. 15, 12489 Berlin

We explore the possibility to image the umbrella motion of ammonia to, e.g., create a real-time movie of a tunneling in a double well potential. The ionization behavior of the ammonia molecule as a function of the inversion coordinate is investigated. Different theoretical approaches for obtaining the ionization yield are compared, all of them showing a strong dependence of the ionization yield on the inversion coordinate, especially at long wavelengths ($\geq$ 800 nm). We show how this effect can be exploited to create and probe nuclear wave packets in neutral ammonia. Furthermore, we propose dedicated experiments to image this motion by measuring the ionization yield or high-harmonic spectra.

Rotation of "Rotationless" Helium Clusters by Intense Ultrashort Laser Pulses

Holger Maschkiwitz, Jörg Hahnenbruch, Maksim Kunitski and Reinhard Dörner
Institut für Kernphysik, Goethe-Universität Frankfurt am Main
Max-von-Laue-Straße 1, 60438 Frankfurt am Main, Germany

Helium clusters are unique quantum mechanical systems. The van der Waals interaction between two helium atoms is extremely weak, so that only single bound state exists in ^{4}He dimer. This tiny interaction is responsible for the existence of the Efimov state in the helium trimer [1]. Both helium dimer and trimer are believed to not have any excited rotational states [2], since the centrifugal term related to these states is larger than the binding energy of the clusters. What happens to such "rotationless" systems upon a "kick" by an ultrashort intense laser pulse?

In order to answer this question we are planning the following experiment. The helium clusters will be produced under supersonic expansion of helium gas into vacuum through a tiny 5μm nozzle (Fig. 1). The clusters will be selected by the matter wave diffraction [3] and then subjected to an ultrashort laser pump pulse. In this way an angular momentum will be transferred to the cluster system. The subsequent time evolution of the clusters will be probed by the Coulomb Explosion Imaging [4] initiated by the second laser pulse inside the COLTRIMS spectrometer [5].

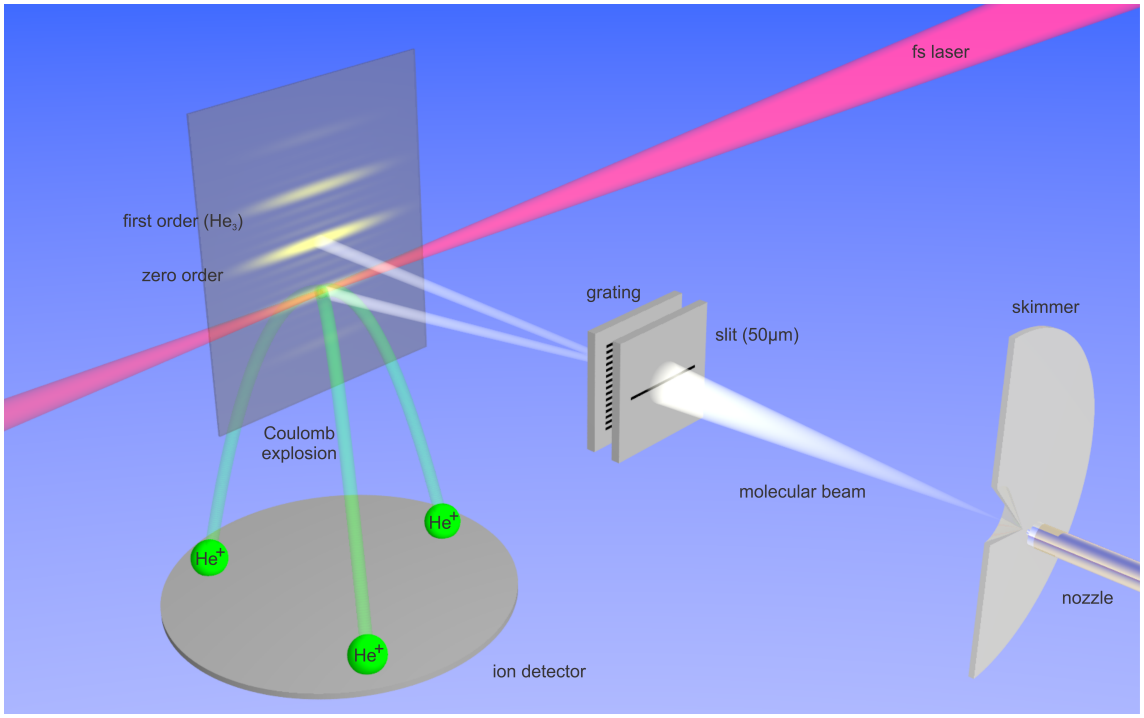

Fig. 1 Experimental Setup.

References

[1] M. Kunitski, S. Zeller, J. Voigtsberger, A. Kalinin, L. Ph. H. Schmidt, M. Schöffler, A. Czasch, W. Schöllkopf, R. E. Grisenti, T. Jahnke, D. Blume, R. Dörner, *Oberservation of the Efimov state of the helium trimer*, Science **348**, 6234, (2015).
[2] A.V. Matveenko and E.O. Alt, *Does the Helium Trimer Have Bound Rotational States?*, Hyperfine Interactions **138**: 421-425, (2001).
[3] W. Schöllkopf, J. P. Toennies, *Nondestructive Mass Selection of Small van der Waals Clusters*, Science **266**, 5189, (1994).
[4] Z. Vager, R. Naaman, E. P. Kanter, *Coublomb Explosion imaging of Small Molecules*, Science **244**, 4903, (1989).
[5] J. Ullrich, R. Moshammer, A. Dorn, R. Dörner, L. Ph. H. Schmidt and H. Schmidt-Böcking, *Recoil-ion and electron momentum spectroscopy: reaction-microscopes*, Rep. Prog. Phys. **66**, 1463, (2003).

Coherent Control Of Atomic Ionization By Two-Color Laser Fields

Nicolas Camus[1], Lutz Fechner[1], Diego G. Arbó[2], Christoph Lemell[3], Stefan Nagele[3]
Joachim Ullrich[1,4], Thomas Pfeifer[1], Sebastian D. López[2], Joachim Burgdörfer[3], Robert Moshammer[1]
1. Max-Planck-Institut für Kernphysik, Heidelberg, 69117, Germany, EU
2. Institute for Astronomy and Space Physics, IAFE (Conicet-UBA), Buenos Aires, Argentina
3. Institute for Theoretical Physics, Vienna University of Technology, Austria, EU
4. Physikalisch-Technische Bundesanstalt, 38116 Braunschweig, Germany, EU

Strong-field ionization of atoms with near infra-red laser pulses reveals a rich structure in the momentum distribution of the liberated electron. The patterns observed (Fig. 1) arise from the interferences of multiple pathways leading to the same final momentum state. They retain precise information about the creation of electron wavepackets in the laser field and the phase they accumulate during the propagation in the combined laser and ionic Coulomb field [1].

We present experimental results and a theoretical analysis of the ionization process of argon interacting with linearly polarized two-color fields. These laser pulses are formed by the combination of 800 nm laser pulses and their frequency-doubled component (400 nm). By controlling the relative phase between the red and blue carrier waves, we can control the ionization rate via the temporally modified electric field strength. More importantly, this shaped field controls also the trajectories of the ionized electron and the accumulated phase leading to modified interference structures in the 3-dimensional momentum distributions. We precisely monitor the modifications of the interference structures.

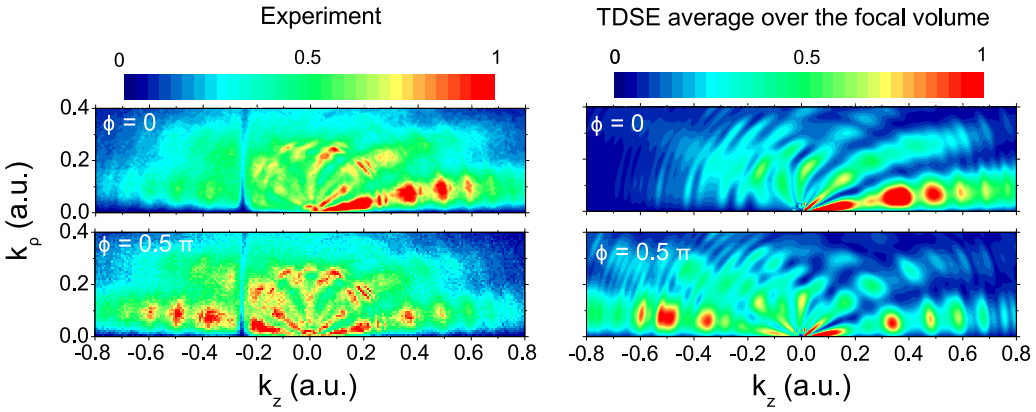

Fig. 1 Measured (left column) and calculated (right column) electron momentum distributions for fixed two-color phases: $\phi = 0$ and $\phi = 0.5\pi$.

Electron momentum distributions are recorded with a reaction microscope. The results are compared to simulated spectra that were obtained by using strong-field and Coulomb-Volkov approximations as well as ab-initio solutions of the Time Dependent Schrödinger Equation (TDSE). The comparison enables us to determine the influence of the ionic Coulomb potential on the ejected electron. In addition, this allows for characterization of unknown experimental parameters such as the absolute value of the relative two-color phase ϕ. We also perform a study of classical-quantum correspondence in the simulation of laser-atom interactions. We find a surprisingly good agreement between Classical Trajectory Monte Carlo (CTMC) analysis and TDSE simulations which might open the pathway for an improved understanding of previously unexplained features observed in experimental spectra.

References

[1] Diego G Arbó, Shuhei Yoshida, Emil Persson, Konstantinos I. Dimitriou and Joachim Burgdörfer, *Interference Oscillations in the Angular Distribution of Laser-Ionized Electrons near Ionization Threshold*, Phys. Rev. Lett. **96**, 143003 (2006).

[2] Diego G. Arbó, Christoph Lemell, Stefan Nagele, Nicolas Camus, Lutz Fechner, Andreas Krupp, Thomas Pfeifer, Sebastian D. López, Robert Moshammer and Joachim Burgdörfer, *Ionization of argon by two-color laser pulses with coherent phase control*, Phys. Rev. A **92**, 023402 (2015).

Strong Field Ionization of N_2 Molecules in Two-Colour Circularly Polarized Laser Field

Xiao-Min Tong[1,2], **Nobuyuki Toshima**[2]
1. Center for Computational Sciences, University of Tsukuba, Tsukuba 305-8571, Japan
2. Graduate School of Pure and Applied Science, University of Tsukuba, Tsukuba 305-8571, Japan

Strong field ionization of atoms in two-color circularly polarized fields has been one of the hot topics because the process can be used to generate a circularly polarized extreme ultraviolet high harmonics [1]. Different from atoms, diatomic molecule provides one more freedom – alignment between the molecular axis with the polarization plane of the laser field. Therefore, the photoionization of a diatomic molecule in the two-color circularly polarized laser field may provide more physical insight. To study the process theoretically by solving the time-dependent Schrödinger equation (TDSE) is still very challenge because it is a full 3-dimensional time-dependent problem.

We develop a new method to solve the full 3-dimensional TDSE using a fast fourier transfromation (FFT) method. To remove the fast oscillation of wave function near the atomic center, we employ non-local pseudo-potentials to replace the electron parent-core interactions. This procedure allows us to remove the Coulomb singularity and use a large grid step even in the inner region near the atomic center [2]. With this newly developed method, we can study the dynamical processes of atoms, molecules and clusters with the total number of the space grids more than 10^8.

As the first example, we investigated the photoelectron momentum distribution of N_2 molecules in a two-color (800 nm + 400 nm) counter-rotating circularly polarized laser field. Here we choose the laser polarization plane on the $xy-$plane with one thousand grid points on each direction and one hundred grid points on the $z-$direction. therefore, we employed 10^8 grid points in the real space. As shown in Fig. 1, when the molecular axis is on the polarization plane ($xy-$plane), the electron is mainly ionized along the molecular axis (left panel of Fig. 1). When the molecular axis is perpendicular to the polarization plane, the electron is ionizated along the three directions (right panel of Fig. 1), which represent the three-leaf clover structure of the laser field peaks due to the combination of the two-color laser fields [3]. When the molecular axis is aligned at 45° with the polarization plane, the results are close to three-leaf clover structure with one strong leaf. The detail of the numerical method and the more results of how the photoelectron momentum distribution depends on the ratio of the two laser intensities will be presented in the conference.

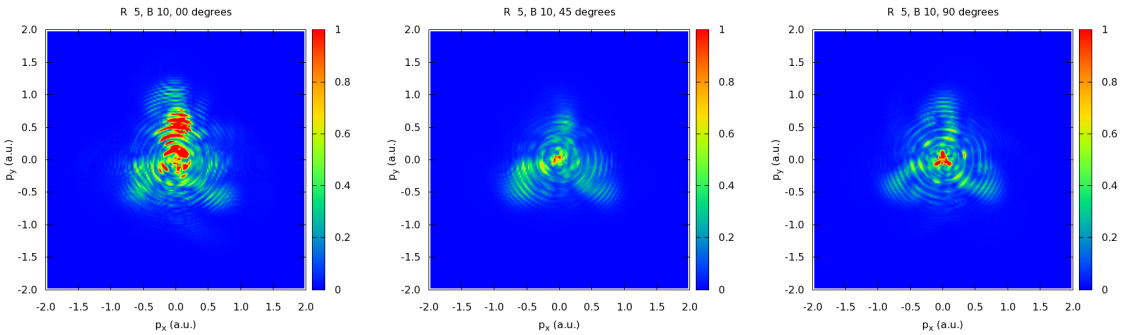

Fig. 1 Photoelectron momemtum distribution of N_2 molecules in a two-color counter-rotating circularly polarized laser field on the polarization plane with the molecular axis on the plane (left panel), perpendicular to the plane (right panel) and 45° to the plane (middle panel).

References

[1] Ofer Kfir, et. al., *Generation of bright phase-matched circularly-polarized extreme ultraviolet high harmonics*, Nature Photonics. **9**, 99-105 (2015).
[2] Xiao-Min Tong,Georg Wachter, Shunsuke A. Sato, Christoph Lemell, Kazuhiro Yabana, and Joachim Burgdörfer, , *Application of norm-conserving pseudopotentials to intense laser-matter interactions*, Phy. Rev. A **92**, 043433 (2015).
[3] Christopher A. Mancuso, et. al., *Controlling electron-ion rescattering in two-color circularly polarized femtosecond laser fields*, Phys. Rev. A **93**, 053406 (2016).

Time Delay in Photoionization with Light Carrying Orbital Angular Momentum

Jonas Wätzel[1], Jamal Berakdar[1]

1. Institut für Physik, Martin-Luther Universität Halle-Wittenberg, Karl-Freiherr-von-Fritsch Str.3, 06112 Halle, Germany

The pioneering experiment of Schultze *et al.* [1] on time delay in photoemission triggered substantial experimental and theoretical activities with the aim to understand and quantitatively reproduce the results of the measurements [2-4]. Up to date various mechanisms and calculation techniques were put forward, yet disputable some differences between theory and experiment remain despite the relative simplicity of the considered targets.

To add yet a new aspect to time delay in photoemission we considered using a twisted light beam, also called optical vortex. Such a beam has a phase singularity at its centre and carries orbital angular momentum (OAM) characterized by the topological charge. The spatial inhomogeneity makes it possible to transfer OAM and therefore a torque to an electron. The amount of transferable OAM is controlled by the topological charge. The use of OAM XUV laser beams to trigger photoionization implies a complete new set of optical selection rules [5] that optical transitions tuneable by the choice of the beam topological charge.

We present results of calculations of the atomic time delay of the photoionization process of the argon *3p* subshell initiated by a twisted light XUV pulse. We show that in different directions either the co-rotating electron (relative to the field) or the counter rotating electron dominates photoionization amplitude. Furthermore the corresponding time delays are completely different in magnitude and sign, and depend sensitively on the position of the atom in the laser beam spot. Therefore, the time delay represents an interesting measure to identify the origin of the photoelectron with respect to the initial magnetic (sub-)state as well as the position in space of the ionized atom.

References

[1] M. Schultze *et al.*, *Delay in photoemission*, Science **328**, 1658 (2010).
[2] J. Wätzel *et al.*, *Angular resolved time delay in photoemission*, J. Phys B: At. Mol. Opt. Phys. **48**, 025602 (2015) and references therein.
[3] J. Dahlström *et al.*, *Theory of attosecond delays in laser-assisted photoionization*, Chem. Phys. **414**, 53 (2013).
[4] A. S. Kheifets, *Time delay in valence-shell photoioinzation of noble-gas atoms*, Phys. Rev. A **87**, 063404 (2013).
[5] A. Picón, *Photoionization with orbital angular momentum beams*, Opt. Expr. **18**, 3660 (2010).

Ultrafast correlated electronic and nuclear motions in molecules interacting with strong laser fields

Antoine Desrier[1], Jérémie Caillat[1], Richard Taieb[1]

1. Sorbonne Universités, UPMC Univ Paris 06, CNRS, Laboratoire Chimie Physique Matière et Rayonnement, F-75005, Paris, France

Attosecond-resolved spectroscopy has expanded for the last 15 years, mainly through processes and technologies involving **High Harmonic Generation** (HHG). This nonlinear phenomenon of interaction between light and matter, well described by the so-called three step model at the single atom level [1], enables to carry out time-resolved measurements of **ultrafast** nuclear and electronic **dynamics** in atoms and molecules [2].
Besides, **Conical Intersection** and more generally **vibronic coupling** [3] is one of the famous signature of **nuclear-electron correlations**. It has been subject to numerous time-resolved studies because of the ultrafast **nuclear dynamics** (~ 10 fs) in such region of the potential energy surfaces (PES). More precisely, two PES of different electronic states (obtained with **Born-Oppenheimer approximation**) can cross each other and exchange some population and energy.
As a result, in order to follow and explain those ultrafast correlated motions, one has to take into account several degrees of freedom, resulting in very long computation time, even for small molecular systems.
In this work, we theoretically investigate ultrafast dynamics of small molecules (Conical Intersection in SO_2 for example) using a **versatile reduced dimension model**. Indeed, we have developed an approach based on scattering theory. We consider one or more **ionization channels**, each defining the ionization of one electron from one considered orbital. For instance, we can then look at the vibronic coupling between the ground state (ionization of one electron from the HOMO) and an excited state (ionization of one electron from the HOMO-2) of the molecular ion. These channels are coupled by some model couplings depending on physical consideration [4]. Our model of **1D** for electron and **1D** for nuclei enables to reproduce mainly the total wavefunction behaviour, at a reduced cost.
The one active electron approximation, valid for **ionization and high harmonic generation,** opens the way to tracking and investigating the influence of such correlations on **light matter interactions** (**photoelectron** and **High Harmonic Spectroscopies**).

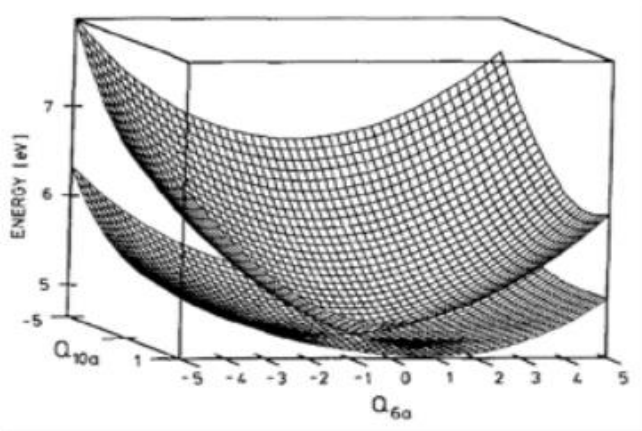

Fig. 1 Example of Conical Intersection in pyrazine [5].

References

[1] Lewenstein M et al. Phys. Rev. A **49**, 2117 (1994).
[2] M. Drescher et al. Nature 419, 803 (2002).
[3] G.A. Worth, L.S. Cederbaum, *Beyond Born-Oppenheimer : Molecular dynamics through a conical intersection*, Annual Review of Physical Chemistry, (2004)
[4] A.Ferretti et al. J.Phys.Chem, **104**, 5517-5527 (1996)
[5] C. Woywod et al. J. Chem. Phys. **100**, 2 (1994)

Continuum extension of quantum chemistry tools: the photoionization of neon.

Carlos Marante[1], Tor Kjellsson,[2] Jesús González-Vázquez[1], Inés Corral[1], Markus Klinker[1], Luca Argenti[1], Eva Lindroth[2], Fernando Martín[1,3,4]

1. Departamento de Química, Universidad Autónoma de Madrid, Cantoblanco 28049, Madrid, Spain
2. Department of Physics, Stockholm University, Alba Nova University Center S-106 91, Stockholm, Sweden
3. Instituto Madrileño de Estudios Avanzados en Nanociencia (IMDEA-Nanociencia), Cantoblanco 28049, Madrid, Spain
4. Condensed Matter Physics Center (IFIMAC), Universidad Autónoma de Madrid, Cantoblanco 28049, Madrid, Spain

Recent breakthroughs in the generation of extreme ultraviolet (XUV) and x-ray attosecond pulses [1, 2], have made it possible to study electron dynamics at its natural time scale. Many numerical approaches can accurately reproduce the ionization processes triggered by these pulses in small atomic and molecular targets [3-6]. Problems arise, however, when tackling more complex systems, due to the correlated short-range structure of polyelectronic functions. Whereas sophisticated methods to compute the electronic structure of bound molecular states are implemented in standard quantum chemistry packages (QCP) (e.g., MOLCAS [7]), equivalent general tools for the electronic continuum are not available yet.

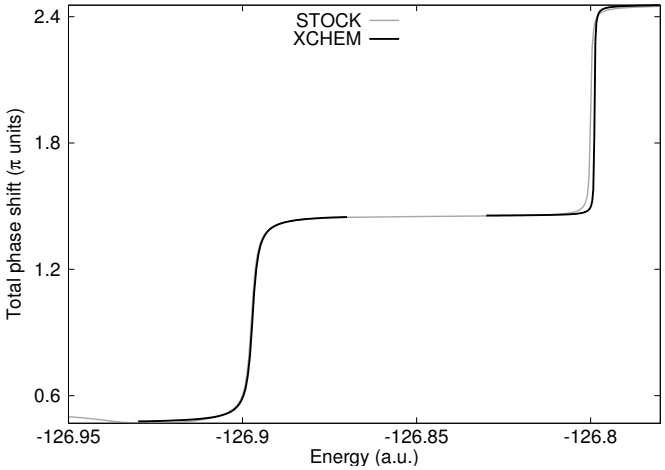

Fig. 1 Total $^1S^e$ phase shift of the neon atom in the proximity of its two first autoionizing states, computed with the XCHEM code and compared with the results from the STOCK code, as a reference.

To tackle this problem we are developing a merge between existing QCPs and current numerical scattering methods (XCHEM code). In our approach, the electronic configuration space is separated in a short-range region, which can host all the interacting electrons, and a long-range region in which one outer electron interacts with a finite number of correlated parent ions. This outer electron is expressed in terms of a hybrid basis (GABS) which combines short-range Gaussian functions, compatible with standard QCPs, with B-splines [8], which are appropriate to represent the continuum. Using this approach, we have already obtained good results for He and H_2, whose parent ions contain a single electron. Here, we illustrate the capabilities of the XCHEM code for the neon atom, a more complex system with multi-electronic parent ions. We use XCHEM to compute multichannel eigenphases as well as the photoionization cross section, and find good agreement with the results obtained using the STOCK code [9].

References

[1] Michael Chini, Kun Zhao, and Zenghu Chang, *The generation, characterization and applications of broadband isolated attosecond pulses*, Nature Photonics **8**, 178 (2014).
[2] Tenio Popmintchev, et al, *The attosecond nonlinear optics of bright coherent X-ray generation*, Nature Photonics **4**, 822 (2010).
[3] Álvaro Jiménez-Galán, Luca Argenti, Fernando Martín, *Modulation of Attosecond Beating in Resonant Two-Photon Ionization*, Phys. Rev. Lett. **113**, 263001 (2014).
[4] Christian Ott, et al, *Reconstruction and control of a time-dependent two-electron wave packet*, Nature **516**, 374 (2014).
[5] Giuseppe Sansone, et al, *Electron localization following attosecond molecular photoionization*, Nature **465**, 763 (2010).
[6] D. Dowek, et al, *Circular Dichroism in Photoionization of H_2*, Phys. Rev. Lett. **104**, 233003 (2010).
[7] Gunnar Karlström, et al, *MOLCAS: a program package for computational chemistry*, Comput. Mater. Sci. **28**, 222 (2003).
[8] Carlos Marante, Luca Argenti, Fernando Martín, *Hybrid Gaussian–B-spline basis for the electronic continuum: Photoionization of atomic hydrogen*, Phys. Rev. A **90**, 012506 (2014).
[9] T. Carette, *Multiconfigurational Hartree-Fock close-coupling ansatz: Application to the argon photoionization cross section and delays*, Phys. Rev. A **87**, 023420 (2013).

Stimulated Raman Excitation of Hydrogen by Short XUV Radiation Pulses

Henri Bachau[1], Mihai Dondera[2], Viorica Florescu[2]
1. CELIA, Université de Bordeaux-CNRS-CEA, 33405 Talence Cedex, France
2. Department of Physics and Centre for Advanced Quantum Physics, University of Bucharest, MG-11, Bucharest-Măgurele, 077125 Romania

Recent progress achieved in the direction of shortening the high frequency (XUV or soft X-rays) pulses duration [1] motivate theoretical studies of processes due to the *finite* spectral bandwidth of the radiation field [2], i.e., processes that would not be observed in the case of a single monochromatic electromagnetic field. Besides the basic interest of such processes, their study can be very useful in order to characterize the radiation pulse itself.

The present contribution follows a previous work on stimulated Compton Scattering [3], it refers to the stimulated Raman excitation of H(1*s*). This is a two-photon process involving the excitation of H(*nl*) bound states during the interaction of the hydrogen atom with a XUV (or soft X-ray) short radiation pulse. We investigate the process using numerical results based on the integration of the time dependent Schrödinger equation (TDSE) and on the lowest order semiclassical perturbation theory (LOPT), i.e., second order in $\mathbf{A}\cdot\mathbf{P}$ terms and first order in $\mathbf{A}^2$, where $\mathbf{A}(\mathbf{r},t)$ is the vector potential that describes the electromagnetic field of the pulse. In TDSE calculations the field is taken as a $\cos^2$ pulse with a finite duration τ, linearly polarized, while for LOPT calculations we also use Gaussian pulses. Transitions to the final states nlm ($n = 2-10$) are considered.

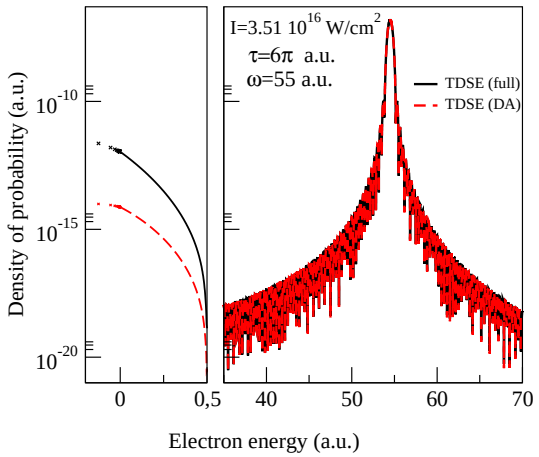

Fig. 1 Energy spectrum at the end of the pulse for the electron energy ranges [-0.125,0.5] a.u. (left panel) and [35.,70.] a.u. (right panel). The left panel shows the stimulated Compton and Raman excitation of low continuum and bound states, respectively. The right panel shows the peak associated to one-photon absorption. The laser parameters are indicated in the figure, the pulse duration τ is close to 0.45 femtoseconds. Calculations with the full Hamiltonian (labelled full in the figure) and in dipole approximation (labelled DA). In left panel we note that calculations with full Hamiltonian and dipole approximation differ by orders of magnitude.

We present numerical results for the excitation probabilities in the case of pulses with central frequency ω_0 in the range of tens of eV to keV, sub-femtosecond duration, and peak intensity of the order of 10^{16} W/cm^2. We analyze these results by varying the pulse parameters, either the frequency (for a fixed number of oscillations), or the pulse duration (for several fixed frequencies). Our numerical results show that in the lower part of the considered frequency range the contribution of $\mathbf{A}\cdot\mathbf{P}$ terms is more important than that of $\mathbf{A}^2$. Results will be presented at the conference, as well as calculations at shorter wavelengths (55 a.u.) (see Fig. 1), where nondipole effects dominate, and also for the intermediate regime.

References

[1] E. Hemsing , G. Stupakov, D. Xiang, and A. Zholents, Rev. Mod. Phys. **86**, 897 (2014).
[2] S. Miyabe and P. Bucksbaum, Phys. Rev. Lett. **114**, 143005 (2015).
[3] H. Bachau, M. Dondera and V. Florescu, Phys. Rev. Lett. **112**, 073001 (2014).

Selective enhancement of resonant multiphoton ionization with strong laser fields

Min Li, Peng Zhang, Siqiang Luo, Yueming Zhou, Qingbin Zhang, Pengfei Lan, and Peixiang Lu

School of Physics and Wuhan National Laboratory for Optoelectronics, Huazhong University of Science and Technology, Wuhan, 430074, China

Email :mli@hust.edu.cn

Above-threshold ionization (ATI) has attracted considerable attention since its first observation more than 30 years ago [1]. Generally, ATI is interpreted as multiphoton absorption via nonresonant or resonant states when the Keldysh parameter is larger than 1 [2]. At a specific laser intensity, both resonant ionization and nonresonant ionization can significantly contribute to the final electron momentum spectrum, and their contributions will mix with each other in the momentum spectrum. Because of the mixture of different contributions, the photoelectron angular distributions of one process will be modified by the other process which affects the precision of the phase reconstruction using the photoelectron interference fringes.

By measuring laser-intensity-resolved photoelectron energy spectrum with a COLTRIMS setup, we isolated the resonant multiphoton ionization from the nonresonant contributions [3]. The isolation is based on the fact that the nonresonant ATI peak shifts towards lower energy with the increase of the laser intensity whereas the resonant ionization is independent of the laser intensity. We also calibrated the laser peak intensity precisely with an uncertainty less than 5% using the intensity-resolved photoelectron spectrum.

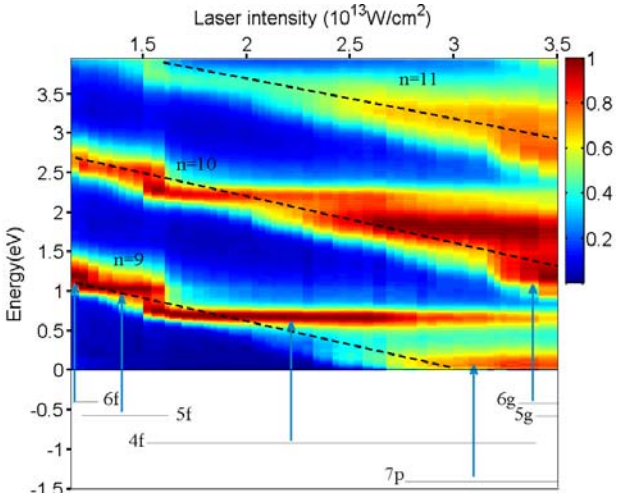

Fig. 1 Normalized intensity-resolved photoelectron energy distributions for the intensities from $1.1*10^{13}$ to $3.5*10^{13}$ W/cm^2. The dashed lines denote the *n*-photon ATI peaks. The solid horizontal lines with negative energy show the energy level of the resonant states involved in the experiment.

We further precisely measured the two-dimensional photoelectron momentum distributions of Xe at lower laser intensities using a homebuilt VMI spectrometer, which has a better signal-to-noise ratio compared with the COLTRIMS setup [4]. We find that the contribution of the resonant ionization is dominant over that of the nonresonant ionization at low laser intensities. The recorded velocity map shows a distinct double-ring structure at certain laser intensities resulting from resonant multiphoton excitation of multiple Rydberg states. Varying the laser intensity, we can selectively control different atomic Rydberg states via which the resonant multiphoton ionization occurs (Fig. 1).

References

[1] P. Agostini, F. Fabre, G. Mainfray, G. Petite, and N. K. Rahman, *Free-free transitions following six-photon ionization of xenon atoms*, Phys. Rev. Lett. **42**, 1127 (1979)

[2] R. R. Freeman, P. H. Bucksbaum, H. Milchberg, S. Darack, D. Schumacher, and M. E. Geusic, *Above-threshold ionization with subpicosecond laser pulses*, Phys. Rev. Lett. **59**, 1092 (1987).

[3] Yun Shao, Min Li, et al. *Isolating resonant excitation from above-threshold ionization*, Phys. Rev. A **92**, 013415 (2015).

[4] Min Li, et al. *Selective enhancement of resonant multiphoton ionization with strong laser fields*, Phys. Rev. A **92**, 063404 (2015).

The exact single-electron picture of strong field processes

Axel Schild* and E.K.U. Gross
Max-Planck Institut für Mikrostrukturphysik, Weinberg 2, 06120 Halle, Germany

It is possible to factor an *N*-particle wavefunction as a product of an *M*-particle marginal wavefunction and an *(N-M)*-particle conditional wavefunction. The equation of motion for the marginal wavefunction is a standard *M*-particle Schrödinger equation with an effective scalar and vector potential.[1,2]

We recently used this factorization to obtain an exact single-electron Schrödinger equation for multi-electron systems.[3] Starting from the exact factorization, we devised an adiabatic approximation for the computation of strong-field processes and sucessfully tested it on a 2-electron model for high-order harmonic generation.

Here, we report on the properties of the exact single-electron potentials for 2- and 3-electron models in strong laser fields. This study helps both conceptually and computationally: It provides theoretical tools for analysis of experiments and raises, for example, the question whether single-electron potentials can be used for strong-field processes in a similar way as nuclear potential energy surfaces are used for molecular dynamics. It helps to explain the success of approximate single-electron theories for the description of strong field processes by comparison with the exact one. Finally, it also provides new ways to include multi-electron effects while still retaining the virtues of single-electron approaches.

[1] G. Hunter, Int. J. Quant. Chem. 1975, 8, 237
[2] A. Abedi, N.T. Maitra and E.K.U. Gross, Phys. Rev. Lett. 2012, 137, 22A530
[3] A. Schild, E.K.U. Gross, arXiv:1602.00259

Frustrated double ionization in triatomic molecules

A. Emmanouilidou
Physics and Astronomy, University College London, U.K.
chenahaiphysics@gmail.com

Abstract: We explore the formation of highly excited neutral fragments during the break-up of strongly-driven triatomic molecules. We consider the kinetic energy release of the ion fragments (KER) as well as the break-up patterns of the fragments.

We consider D_3^+ when it is strongly driven by a linearly polarized infrared laser field. To do so we use a 3-dimensional semiclassical model that is described in detail in [1,3]. Our model accounts for tunnelling during the propagation and in that sense it is a semiclassical model. We explore the formation of highly excited neutral fragments in the triatomic molecule. We find that as for Frustrated Double Ionization (FDI) in strongly-driven diatomics, see [2], two pathways contribute to the formation of frustrated double ionization in strongly-driven triatomics [3]. In one pathway the initially bound electron tunnel ionizes gaining energy from the laser field but at the end of the laser field it does not have enough energy to ionize and remains captured. In the other pathway the initially tunnel ionizing electron returns to re-collide with the bound electron, transferring energy to it. At the end of the pulse the bound electron escapes while the re-colliding electron remains captured.

We find that the kinetic energy release of the fragments (nuclei), see Fig.1, are in good agreement with experimental results [4]. To compare with the experimental results at a field strength of E_0 =0.56 a.u we account for the focal volume effect. That is we average over all field strengths up to the maximum field strength of E_0 =0.56 a.u.. The agreement is very good for the FDI process while for DI our KER distribution peaks at a higher energy than the experimental one [4]. Moreover, we find that with increasing intensity the mechanism that underlies FDI is no longer tunnel-ionization [3]. In addition, we obtain the break-up patterns for DI which has a three-lobe structure as is the case in previously obtained experimental results. We also obtain the break-up for FDI which also has a three-lobe structure as for DI but it is less symmetric, i.e. the contribution of each of the three lobes is not the same for the FDI process.

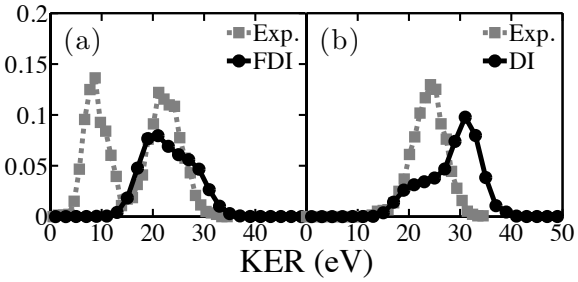

Fig.1. Intensity averaged KER distributions for FDI (a) and DI (b) for a maximum field strength of E_0 =0.56 a.u.. The grey dashed lines show the relevant experimental results from [4].

References

[1] H. Price, C. Lazarou, and A. Emmanouilidou, Phys. Rev. A **90**, 053419 (2014).
[2] A. Emmanouilidou, C. Lazarou, A. Staudte and U. Eichmann, Phys. Rev. A**, 85 (R),** 011402 (2012).
[3] A. Chen, H. Price, A. Staudte and A. Emmanouilidou (to be submitted).
[4] J. McKenna, A. M. Sayler, B. Gaire, N. G. Kling, B. D. Esry, K. D. Carnes, and I. Ben-Itzhak, New J. Phys. 14, 103029 (2012).

Laser-sub-cycle Control of Sequential Double Ionization Dynamics of Helium

Markus S. Schöffler,[1] Xinhua Xie,[1] Philipp Wustelt,[2,3] Max Möller,[2,3] Stefan Roither,[1] Ondrej Hort[1], Daniil Kartashov,[1] Andrius Baltuska,[1] Gerhard G. Paulus,[2,3] and Markus Kitzler[1]

1. Photonics Institute, Vienna University of Technology, Gusshausstrasse 27, A-1040 Vienna, Austria
2. Institute of Optics and Quantum Electronics, Friedrich-Schiller-University Jena, D-07743 Jena, Germany
3. Helmholtz Institute Jena, D-07743 Jena, Germany

One of the most fundamental benchmark processes that is used in both experiments and theory for the investigation of dynamical electron-electron correlation effects is the removal of both electrons from the strongly correlated ground state of the helium atom. Here we report on experiments that investigate the dynamics of two-electron removal from helium on sub-laser-cycle time-scales using intense, near-circularly polarized few-cycle laser pulses. In our experiments, the relative timing between the two emission steps can be controlled by the duration and peak intensity of the laser pulse: While for long pulses the second electron can be emitted with a considerable delay, uninfluenced by the first ionization event, i.e., in an uncorrelated manner, we show that for high intensity pulses with sub-two-cycle durations the emission dynamics of the two electrons is squeezed into sub-cycle intervals. We obtain experimental access to this fast emission dynamics by applying the concept of angular streaking introduced by Maharjan *et al.* [1], now also known as the attoclock technique [2].

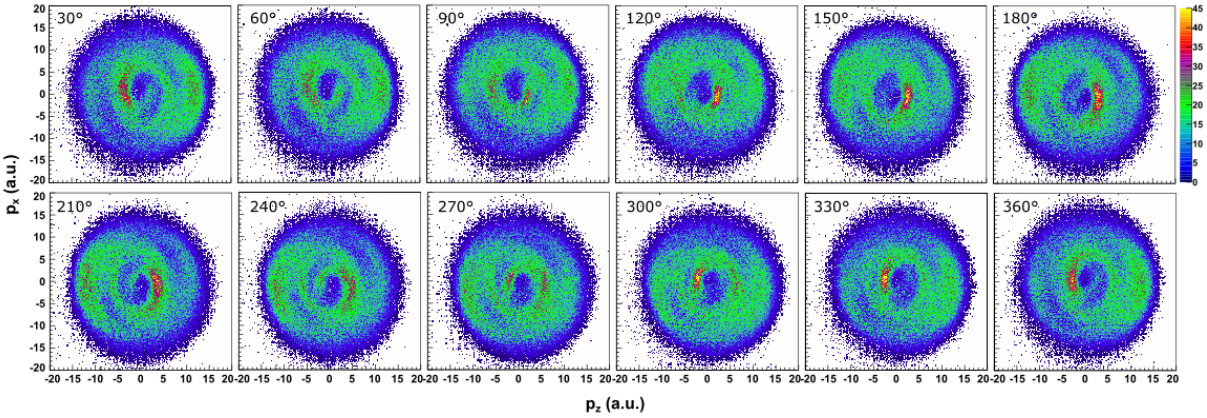

Fig. 1: He^{2+} momentum distributions in the polarization plane of near-circularly polarized laser pulses (ellipticity $E_\perp/E_\parallel$=0.95) with a constant FWHM pulse duration of 4.5 fs and a peak intensity of 10^{16} W/cm^2 for different values of the CEP (as indicated in the panels).

We demonstrate that sub-half-cycle temporal resolution of the two-electron emission dynamics can be obtained if the different contributions to the He^{2+} momentum distribution from the separate half-cycle ionization bursts can be disentangled. The separate bursts and their attosecond evolution can be clearly identified in the CEP-resolved He^{2+} momentum distributions, exemplarily shown in Fig. 1 for a He^{2+} momentum distribution observed with a 4.5fs-long pulse with a peak intensity of 10^{16} W/cm^2. By comparison to a semi-classical model [3] we can (with only few exceptions) unambiguously assign each peak and segment in the distributions shown in Fig. 1 to a certain two-electron emission dynamics. Thus, attosecond timing information on the two emission steps can be extracted from the measured distributions.

We find that for the shortest pulse durations (1.8 laser cycles) and not too high intensities (≈6×10^{15} W/cm^2) the two electrons are dominantly emitted with a sub-laser-cycle delay between the two emission steps. The sequential double ionization dynamics can be sensitively controlled with the pulse duration and the laser peak intensity, and the delay between the two electron emission steps can be tuned. We observe that the two electrons are surprisingly likely emitted in between the peaks of the laser field oscillations rather than at the field maxima. Such double ionization emission dynamics has to our knowledge not been observed so far. The reason for this is yet to be identified. Moreover, several structures in the He^{2+} momentum distributions are not reproduced by the semi-classical model. This is surprising since it could reproduce measured distributions for neon in the long-pulse limit remarkably well [3].

References

[1] Maharjan, C., Alnaser, A., Tong, X., Ulrich, B., Ranitovic, P., Ghimire, S., Chang, Z., Litvinyuk, I. & Cocke, C. Momentum imaging of doubly charged ions of Ne and Ar in the sequential ionization region. *Phys. Rev. A* **72,** 041403 (2005).
[2] Pfeiffer, A. N., Cirelli, C., Smolarski, M., Dörner, R. & Keller, U. Timing the release in sequential double ionization. Nat. Phys. 7, 428 (2011).
[3] Wustelt, P., Möller, M., Rathje, T., Sayler, A. M., Stöhlker, T. & Paulus, G. G. Momentum-resolved study of the saturation intensity in multiple ionization. Phys. Rev. A 91, 031401 (2015).

Optical Tunneling and Quantum Entanglement

Attila Czirják[1,2], Szilárd Majorosi[2], Szabolcs Hack[1], Mihály G. Benedict[2]

1. ELI-ALPS, ELI-HU Non-Profit Ltd., Dugonics tér 13, H-6720 Szeged, Hungary

2. Department of Theoretical Physics, University of Szeged, Tisza L. krt. 84-86, H-6720 Szeged, Hungary

Optical tunneling plays a fundamental role in attosecond physics [1]: a suitably strong laser pulse enables an electron to tunnel out from its atomic bound state into the continuum [2], which is the first step of the very successful three-step model [3] underlying our understanding of high-order harmonic generation [4]. Currently, the resulting experimental techniques enable to measure the electrons' dynamics in atoms and molecules with attosecond time resolution [5, 6]. However, this new quantum metrology demands more theoretical knowledge about the fundamental quantum features of these processes.

The above strong-field process can also create quantum entanglement between the liberated electron and the parent ion-core, which has a time-dependence closely related to that of the driving laser pulse [7, 8], thereby opening the possibility to control their pair entanglement by the features of the laser pulse.

In this contribution, we present 3D simulation results of an atom with a single active electron, driven by a strong, linearly polarized few-cycle laser pulse, which were computed with a novel numerical solution of the Schrödinger equation [9]. We compare these results with earlier works based on different 1D atomic model potentials [7], using quantum phase space methods. We address the problems of the tunneling time and the electron's exit momentum, and we also show how pair entanglement [8] is created during the process.

Based on our 3D simulations, and in accordance with the Hohenberg-Kohn theorems [10], we suggest a novel 1D model potential which can be used in the TD-DFT simulation of a model helium atom, and we show how the electron-electron entanglement is governed by the linearly polarized driving laser pulse.

This research has been granted by the Hungarian Scientific Research Fund OTKA under contract No. T81364. Partial support by the ELI-ALPS project is also acknowledged. The ELI-ALPS project (GOP-1.1.1-12/B-2012-000, GINOP-2.3.6-15-2015-00001) is supported by the European Union and co-financed by the European Regional Development Fund.

References

[1] F. Krausz and M. Ivanov, Rev. Mod. Phys. **81**, 163 (2009).
[2] L. V. Keldysh, Sov. Phys.- JETP **20**, 1307-14 (1965).
[3] P. B. Corkum, Phys. Rev. Lett. **71**, 1994 (1993).
[4] M. Lewenstein et al., Phys. Rev. A **49**, 2117 (1994).
[5] M. Uiberacker et al., Nature **446**, 627 (2007).
[6] A. N. Pfeiffer et al., Phys. Rev. Lett. **109**, 083002 (2012).
[7] A. Czirják et al., Opt. Com. **179**, 29-38 (2000); Phys. Scr. **T153**, 014013 (2013).
[8] M. G. Benedict et al., J. Phys. A: Math. Theor. **45**, 085304 (2012).
[9] Sz. Majorosi et.al., "Fourth Order Real Space Solver for the Time-Dependent Schrödinger Equation with Singular Coulomb Potential", submitted.
[10] P. Hohenberg and W. Kohn, Phys. Rev. **136**, B864 (1964).

Correlated High-Harmonic Spectra from Time-Dependent Two-Particle Reduced Density Matrix Theory

Fabian Lackner[1], Iva Březinová[1], Takeshi Sato[2], Kenichi L. Ishikawa[2], Joachim Burgdörfer[1]
1. Institute for Theoretical Physics, Vienna University of Technology,Wiedner Hauptstraße 8-10/136, 1040 Vienna, Austria, EU
2. Department of Nuclear Engineering and Management, School of Engineering, The University of Tokyo, 7-3-1 Hongo, Bunkyo-ku, Tokyo 113-8656, Japan

High-harmonic generation (HHG) is one of the fundamental processes in strong field physics whose applications range from attosecond metrology [1], tunable table-top XUV/Soft X-ray sources [2] to high precision spectroscopy [3] and orbital imaging [4]. On the atomic level the theoretical description of HHG is challenging due to the difficulty to describe the many-electron dynamics. While simple models like the single active electron approximation (SAE) or time-dependent Hartree-Fock (TDHF) are suited to describe qualitative features of HHG [5] advanced theories capable of correctly treating electron correlation are needed for a realistic description [6]. Approaches along two lines seem to be most promising. Wavefunction based methods such as the multi-configurational time-dependent Hartree-Fock (MCTDHF) method reduce the computational complexity by solving the Schrödinger equation within a subset of the full Hilbert space. A different approach is to abandon the full wavefunction and propagate time-dependent reduced densities instead. Great success along this line has been achieved by time-dependent density functional theory (TDDFT) [7]. However, accurate calculations in TDDFT face the difficulty of unknown exchange-correlation functionals. Going beyond the limitations of TDDFT we propagate the time-dependent two-particle reduced density matrix (TD-2RDM). Our closure scheme [8] is capable of conserving all symmetries of the Hamiltonian and includes contributions from three-particle correlations. To asses the role of correlation in the high-harmonic generation we compare the results obtained by the (exact) MCTDHF method to TDDFT and TD-2RDM.

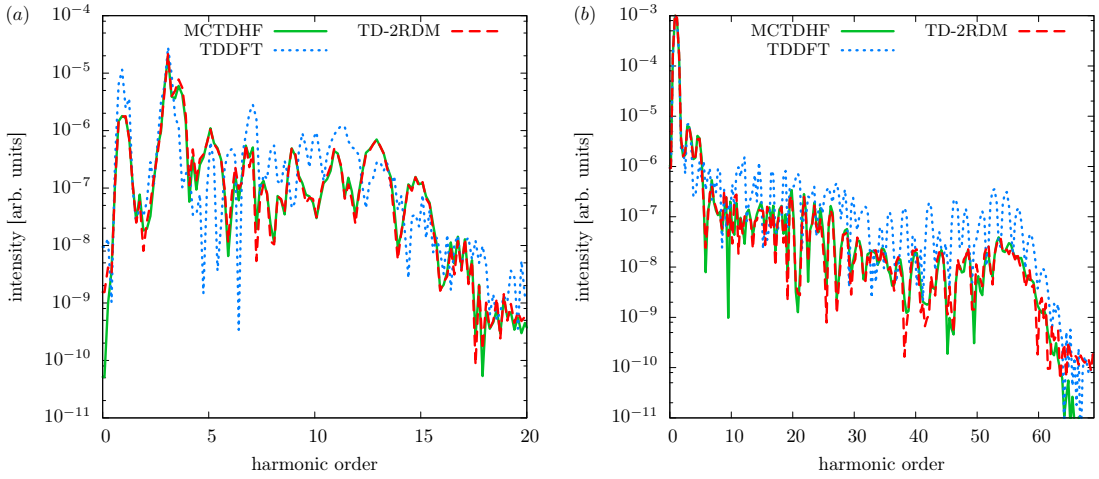

Fig. 1 HHG spectrum of Beryllium subject to (a) a 6-cycle laser pulse with $I = 0.5 \times 10^{14}\mathrm{W/cm^2}$ and (b) a 3-cycle laser pulse with $I = 4.0 \times 10^{14}\mathrm{W/cm^2}$.

We find that electronic correlation as measured by the difference between the TDHF and the MCTDHF calculation has a strong influence on the height and the structure of the HHG peaks (see Fig. 1). The TDDFT approach using the local density approximation is not able to account for this correlated contribution. The good performance of the TD-2RDM method shows that a correct treatment of two-particle correlations is essential to obtain accurate HHG spectra. This gives new insight into the many-body nature of the mechanisms underlying HHG that is inaccessible from calculations within the SAE approximation.

References

[1] M. Hentschel et al., *Attosecond metrology*, Nature **414**, 509 (2001)
[2] Ph. Zeitoun et al., *A high-intensity highly coherent soft X-ray femtosecond laser seeded by a high harmonic beam*, Nature **431**, 426 (2004)
[3] A. D. Shiner et al., *Probing collective multi-electron dynamics in xenon with high-harmonic spectroscopy*, Nature Phys. **7**, 464 (2001)
[4] J. Itatani et. al, *Tomographic imaging of molecular orbitals*, Nature **432**, 867 (2004)
[5] K. C. Kulander et. al, *High-order harmonic generation from atoms and ions in the high intensity regime*, Phys. Rev. Lett. **68**, 3535 (1992)
[6] S. Sukiasyan et. al, *Multielectron Correlation in High-Harmonic Generation: A 2D Model Analysis*, Phys. Rev. Lett. **102**, 223002 (2009)
[7] X. M. Tong et al., *Application of norm-conserving pseudopotentials to intense laser-matter interactions*, Phys. Rev. A **92**, 043422 (2015)
[8] F. Lackner et al., Propagating two-particle reduced density matrices without wave functions, Phys. Rev. A **91**, 023412 (2015)

Strong-field photoionization of H_2^+ at mid-infrared wavelength

Max Möller[1,2], Philipp Wustelt[1,2], A. Max Sayler[1,2], Stefanie Gräfe[3], Gerhard G. Paulus[1,2]

1. Institute for Optics and Quantum Electronic and Abbe Center of Photonics, Friedrich Schiller University Jena, Max-Wien-Platz 1, 07743 Jena Germany

2. Helmholtz Institute Jena, Fröbelstieg 3, 07743 Jena Germany

3. Institute of Physical Chemistry and Abbe Center of Photonics, Friedrich Schiller University Jena, Helmholtzweg 4, 07743 Jena Germany

Increasing the driving laser wavelength into a region above 1 µm has led to a number of interesting phenomena and applications in the field strong-field interactions [1] of atoms such as the of the discovery of low-energy structures [2] or the generation or high harmonics with photon energies above 1 keV [3]. Due to the nuclear degree of freedom, strong-field photoionization of small molecules induces more complex dynamics such as charge-resonant enhanced ionization [4], or laser-induced electron diffraction [5].

Here, the fragmentation of an H_2^+ ion beam by a strong mid-infrared laser field is studied experimentally as a function of intensity for the first time. Three-dimensional coincidence imaging in combination with a well collimated ion beam and high pondermotive potential of the laser allows to perform a kinematic complete experiment where the momentum of the two protons, p_1 and p_2, are measured directly and the electron momentum, p_e, is inferred based on momentum conservation. The experimental results show a double-peak structure in the kinetic energy release (KER) spectrum that indicates a strong dependence of the ionization yield on the inter-nuclear distance, R, see Fig. 1 a) and b). It is found that this structure is very sensitive to the intensity. 2D-plots of the ionization yield as function of KER and the electron energy show that the electron energy is sensitive to the nuclear energy, see Fig. 1 c). This modulation is also apparent after conversion from KER to R as illustrated by Fig. 1 d). It is a signature of coupling between the electronic and nuclear dynamics during the ionization process. Solutions of the time-dependent Schrödinger equation are used in conjunction with quasi-static ionization models to gain insight into the physical mechanisms.

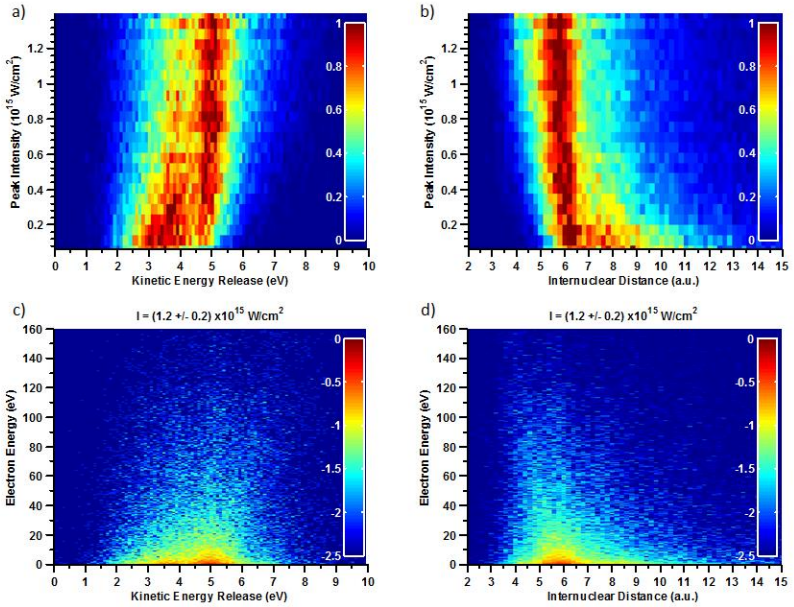

Fig. 1 a) Intensity dependence of the kinetic energy release (KER) spectrum. b) Intensity dependence of the ionization yield as function of internuclear distance after conversion from KER to R. c) shows the distribution of the electron energy as function of KER for a fixed intensity on a log scale. d) shows the same data as c) after conversion to internuclear distance. Note that in a) and b), the monotonous increase of the count rate for increasing intensity has been removed in order to emphasize the shape of the distributions.

References

[1] P. Colosimo, *et al*, *Scaling strong-field interactions towards the classical limit*, Nat. Phys. **4**, 386-389 (2008).
[2] C. I. Blaga, *et al*, *Strong-field photoionization revisited*, Nat. Phys. **5**, 386-389 (2009).
[3] T. Popmintchev, *et al*, *Bright Coherent Ultrahigh Harmonics in the keV X-ray Regime from Mid-Infrared Femtosecond Lasers*, Science **336**, 1287-91 (2012).
[4] T. Zuo and A. D. Bandrauk, *Charge-resonance-enhanced ionization of diatomic molecular ions by intense lasers*, Phys. Rev. A **52**, 2511-2514 (1995).
[5] C. I. Blaga, *et al*, *Imaging ultrafast molecular dynamics with laser-induced electron diffraction*, Nature **483**, 194-197 (2012).

Quantum Trajectory resolved high harmonic spectroscopy

Pengfei Lan[1], Lixin He[1], Chuanyang Zhai[1], Feng Wang[1],Xiaosong Zhu[1], Qingbin Zhang[1], Peixiang Lu[1,2]

1.School of Physics and Wuhan National Laboratory for Optoelectronics, Huazhong University of Science and Technology, Wuhan, 430074, China

2. Laboratory of Optical Information Technology, Wuhan Institute of Technology, Wuhan 430073, China

Recent progress of high harmonic spectroscopy has opened pathways to probe the structure and dynamics of molecules [1-3]. The physics underlying high harmonic generation (HHG) is usually explained by the three-step model : the electron is first freed by tunneling ionization, then is accelerated in the laser field and finally recombines with the parent ion by emitting high order harmonics. The recommbination time depends on the kinetic energy i.e., the photon energy of HHG. This is so-called atto-chirp, which enables one to link the harmonic photon energy to time and thus to probe the electronic dynamics with an resolution of 100 attoseconds [2,3]. However, according to the three-step model, there are two trajectories in each half optical cycle. Therefore, to guarantee a one-to-one map between the harmonic frequency and time, only the short trajectory is selected in experiment [3]. Even though this can be easily realized, the information of the long trajectory is completely wasted; one straightforward shortage is the emission time (i.e., the temporal measurement range) of the short trajectory is limited within half-cycle of the laser field. Moreover, the chirp of the long trajectory is smaller than that of the long trajectory, thus giving a better temporal resolution.

In this work, we experimental demonstrate a trajectory resolved high harmonic spectoscopy method to disentangle the contribution of short and long trajectories. Figure 1(a) shows a high harmonic spectrum generated by focusing an intense laser on Ar gas. In our experient, a Ti-sapphire driving laser with a central wavelength of 800 nm is adopted. The pulse duration is 30 fs and the pulse energy is changed from 1 mJ to 2.5 mJ. Different from the normal discrete odd harmomics, one can see a double peak structe for each odd harmonics. The right peak has a divergence angle less than 3 mrad. In contrast, the left peak shows a large divergence of about 8 mrad. Based on the numerical simulations, we can show that the spectrum splitting is due to the transient phase matching of different quantum trajectories and the left and right peaks correspond to the long and short trajectories, respectively. This double peak structure and spatial profiles provide a useful way to disentangle the short and long trajectories. Moreover, as increasing the laser intensity, the harmonic yields of the left and right peaks are modulated and the central wavelengths are shifted as shown in Fig. 1(b). The measured frequency shift and harmonic yield enables us to retrieve the atomic dipole phases and reveal the atto-chirps both for the short and long trajectories. By take advantage of the trajectory resolved atto-chirps, the nucleus dynamics of H_2 and D_2 can be probed in a full optical cycle.

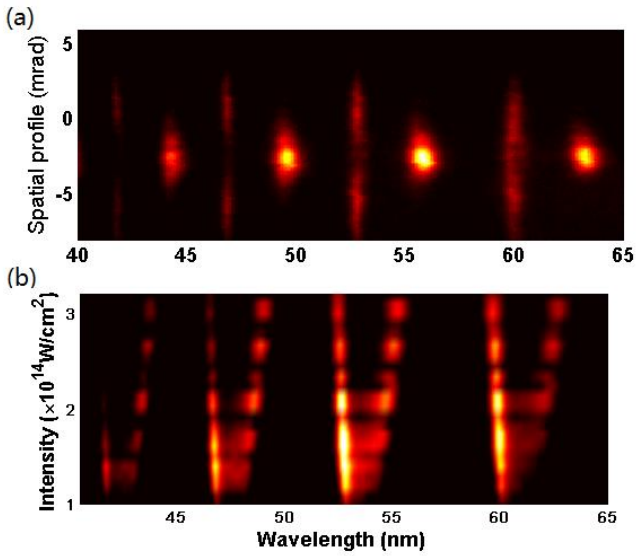

Fig. 1 (a) Measured high harmonic spectrum. (b) The intensity dependence of high harmonic spectra.

References

[1]J. Itatani, et al., Nature **432**, 867 (2004)
[2] M. Lein, Phys. Rev. Lett. **94**, 053004(2005)
[3] S. Baker et al., Science **312**, 424(2006).

Intratrajectory interference in High-order Harmonic Generation

Stefanos Carlström[1], **Jana Preclíková**[2], **Esben Witting Larsen**[1], **Christoph M. Heyl**[3], **Kenneth. J. Schafer**[4], **Johan Mauritsson**[1]

1. Division of Atomic Physics, Lund University, Lund, Sweden
2. Technical University of Liberec, Liberec, Czech Republic
3. JILA institute, Unversity of Colorado at Boulder, Boulder, USA
4. Department of Physics and Astronomy, Baton Rouge, Louisiana State University, USA

We observe farfield interference of light generated from high-order harmonic generation (HHG). Normally interference in the HHG spectrum is attributed to contributions from different classes of quantum paths—the so-called short and long trajectories. For each short trajectory there is also one long trajectory that leads to the same final energy; they may therefore interfere on-axis in the farfield, since they overlap spatially there. Here we show that in addition to this, electrons following distinct long trajectories leading to the same final energy may also interfere. This is due to the quantum path acquiring different phases depending on the generating field intensity distribution. The ability to actually observe these interference fringes is solely due to the excellent stability of our HHG setup [1], since even the smallest fluctuations would wash out the interference pattern completely.

The acquired data also allows us to test the validity of the often used approximation for the amplitude of the single-atom harmonic field:

$$E_q(t,r) = I^{\frac{n}{2}}(t,r)\sum_j \exp[\mathrm{i}\alpha_{q,j}I(t,r)],$$

where n is a non-linearity parameter, j corresponds to the different trajectories contributing to the emission and $\alpha_{q,j}$ are constants describing the intensity-dependence of the harmonic phase. Using this model to describe the single-atom harmonic response can only partly explain the observed phenomena. Instead calculating the single-atom response using the Strong-Field Approximation [2], and using a Hankel transform to calculate the farfield harmonic distribution, we are able to get a qualitatively better match with the experiments.

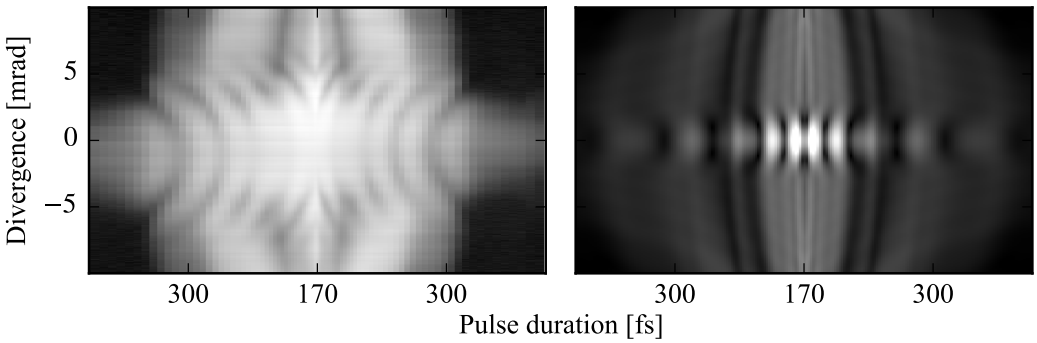

Fig. 1 Left panel: Quantum path interference as observed experimentally for harmonic 17 of 1030 nm as a function of pulse duration. On-axis, interference between the long and short trajectories can be observed, whereas off-axis, interference of the long trajectory with itself can be observed. Right panel: Quantum path interference as calculated using the Strong-Field Approximation.

References

[1] Eleonora Lorek, Esben Witting Larsen, Christoph M. Heyl, Stefanos Carlström., David Paleček, Donatas Zigmantas, & Johan Mauritsson. *High-order harmonic generation using a high-repetition-rate turnkey laser*, Rev. Sci. Instr. **85**(12), 123106, (2014). doi:10.1063/1.4902819

[2] Maciej Lewenstein, Philippe Balcou, Mikhail Y. Ivanov, Anne L'Huillier, & Paul B. Corkum. *Theory of high-harmonic generation by low-frequency laser fields*,. Phys. Rev. A **49**(3), 2117, (1994). doi:10.1103/PhysRevA.49.2117

Probing ultrafast dynamics of chiral molecules with photoelectron circular dichroism

S. Beaulieu[1,2], A. Comby[1], A. Ferré[1], R. Géneaux[3], R. Canonge[1], D. Descamps[1], B. Fabre[1], N. Fedorov[1], G. Garcia[4], F. Légaré[2] L. Nahon[4], S. Petit[1], T. Ruchon[3], B. Pons[1], V. Blanchet[1], Y. Mairesse[1],

[1] *Université de Bordeaux - CNRS - CEA, CELIA, UMR5107, F33405 Talence, France*
[2] *ALLS/LSF, INRS-ÉMT, 1650 Boulevard Lionel-Boulet, Varennes, Qc, Canada*
[3] *LIDYL, CEA, CNRS, Université Paris-Saclay, CEA Saclay 91191 Gif-sur-Yvette, France*
[4] *Synchrotron SOLEIL, Saint Aubin, BP 34, 91192 Gif-sur-Yvette, France*

Chiral molecules exist as two forms – enantiomers – which are mirror images of each other but are non superimposable. Two enantiomers can only be distinguished through their interaction with another chiral object. The enantiospecificity of chemical processes plays a crucial role in biology because most of the basic constituents of life are chiral. Understanding the fundamental processes at play in chiral reactivity requires measuring the dynamics of chiral molecules on their natural timescales – femtoseconds to attoseconds. Circularly polarized light can be used to identify enaniomers, through chiroptical processes. However, the vast majority of these processes are forbidden within the electric dipole approximation and are thus extremely weak. This makes their application to study ultrafast dynamics in the gas phase difficult. Photoelectron circular dichroism (PECD) is the exception to this rule and opens a new route to ultrafast time-resolved chirality measurements.

PECD has first been studied in single-photon ionization by extreme ultraviolet (XUV) radiation [1,2]. It consists of a strong (up to $20-30\%$) forward/backard asymmetry in the angular distribution of electrons ionized from *randomly aligned* chiral molecules by circularly polarized light. Many studies of PECD using synchrotron light have shown its high sensitivity to electronic structure [3], vibrational excitation [4] and conformation [5,6]. PECD is thus a perfect candidate for time-resolved experiments. However, this requires circularly polarized fs light pulses. Even though a few free-electron lasers are able to produce circular XUV fs pulses, a table top laser-based optical set-up, for instance based on high-order harmonic generation, would be of huge interest. Unfortunately, the harmonic generation efficiency strongly decays as the laser ellipticity increases, and the emission generally remains only weakly elliptical. We have found out that resonant high order harmonic generation could solve this problem. Using either bound resonances (Rydberg states in argon) or continuum resonances (shape resonances in SF6), we showed that bright, highly elliptical femtosecond pulses could be produced. We have used this source to measure PECD from fenchone molecules and observed a strong forward/backward asymmetry in the photionization [7].

Femtosecond visible and UV laser pulses are an interesting alternative for PECD measurements. The extension of PECD to the multiphoton ionization regime was demonstrated in 2012. Lux *et al.* [8] measured a large PECD ($\sim 15\%$) resulting from (2+1) resonance-enhanced multiphoton ionization (REMPI) of fenchone. Since this pioneering experiment, REMPI-PECD has been measured in other compounds, still in a (2+1) configuration [9,10,11]. Recently Lux *et al.* observed PECD in the first above threshold ionization (ATI) peak in a (2+2) scheme [12]. We performed a *complete* study of PECD using ultrashort light pulses in different ionization regimes: one photon absorption, resonant and non-resonant MPI, including ATI, and tunnel ionization. We show that PECD is a universal effect in ionization of chiral molecules by circularly polarized radiation, with different sensitivities depending on the regime. We intepret this universality by using a classical analysis of the ionization process, which gives an intuitive picture of the ongoing dynamics.

On the basis of all these experiments, we have performed the first (to our knowledge) experimental investigation on time-dependent chiral dynamics by PECD. We have followed the relaxation of Rydberg wavepackets, showing that PECD revealed dynamics invisible in the angle-integrated photoelectron spectra. This confirms the interest and sensitivity of PECD to probe ultrafast dynamics of chiral molecules

References

[1] B. Ritchie, Phys. Rev. A 13, 1411 (1976).
[2] N. Bowering, T. Lischke, B. Schmidtke, N. Muller, T. Khalil, and U. Heinzmann, Phys. Rev. Lett. 86, 1187 (2001).
[3] I. Powis, C. J. Harding, G. A. Garcia, and L. Nahon, Chem. Phys. Chem. 9, 475 (2008).
[4] G. A. Garcia, L. Nahon, S. Daly, and I. Powis, Nat. Comm. 4 (2013).
[5] M. Tia, B. Cunha de Miranda, S. Daly, F. Gaie-Levrel, G. A. Garcia, I. Powis, and L. Nahon, J. Phys. Chem. Lett. 4, 2698 (2013).
[6] S. Turchini, D. Catone, N. Zema, G. Contini, T. Prosperi, P. Decleva, M. Stener, F. Rondino, S. Piccirillo, K. C. Prince and M. Speranza, Chem. Phys. Chem. 14, 1723 (2013)
[7] A. Ferre, C. Handchin, M. Dumergue, F. Burgy, A. Comby, D. Descamps, B. Fabre, G. Garcia, R. Geneaux, L. Merceron, E. Mevel, L. Nahon, S. Petit, B. Pons, D. Staedter, S. Weber, T. Ruchon, V. Blanchet and Y. Mairesse, Nat. Photon. 9, 93 (2015)
[8] C. Lux, M. Wollenhaupt, T. Bolze, Q. Liang, J. Kochler, C. Sarpe and T. Baumert, Angew. Chem. 51, 5001 (2012)
[9] C. S. Lehmann, N. B. Ram, I. Powis, and M. H. M. Janssen, J. Chem. Phys. 139, 234307 (2013).
[10] M. M. R. Fanood, M. H. M. Janssen, and I. Powis, Phys. Chem. Chem. Phys. 17, 8614 (2015).
[11] C. Lux, M. Wollenhaupt, C. Sarpe, and T. Baumert, Chem. Phys. Chem. 16, 115 (2015).
[12] C. Lux, A. Senftleben, C. Sarpe, M. Wollenhaupt and T. Baumert, J. Phys. B 49, 02LT01 (2016)

CEP Effects for Multiple-cycle Laser Pulses of Arbitrary Length

Klaus Renziehausen[1], Kilian Hader[2], Volker Engel[2]

1. Max Planck Institute of Microstructure Physics, Weinberg 2, 06120 Halle (Saale), Germany

2. Institute for Physical and Theoretical Chemistry, University of Würzburg, Campus Hubland Nord, Emil-Fischer-Str. 42, 97074 Würzburg, Germany

The carrier envelope phase (CEP) of a laser pulse is usually assumed to be effective only for ultrashort pulses with a length of few oscillation cycles (for examples, see [1–3]). However, this restriction on the pulse length can be lifted if a special two-pulse-scheme is used. For this scheme, a first pulse is applied which is temporally as short as necessary to excite wave packets in several electronic states. The subsequent second laser pulse is spectrally small, and its temporal length can be chosen *unconditionally large*. It is shown that there are observables which depend on the CEP of the second pulse but not on the CEP of the first pulse, thus, a CEP effect is measurable.

The two-pulse scheme can be used for the control of asymmetry effects for the dissociation of molecules of the A_2^+-type [4,5] (see figure 1(a)). Moreover, the localization in a double well potential can be controlled by this pulse scheme [6,7] (see figure 1(b)).

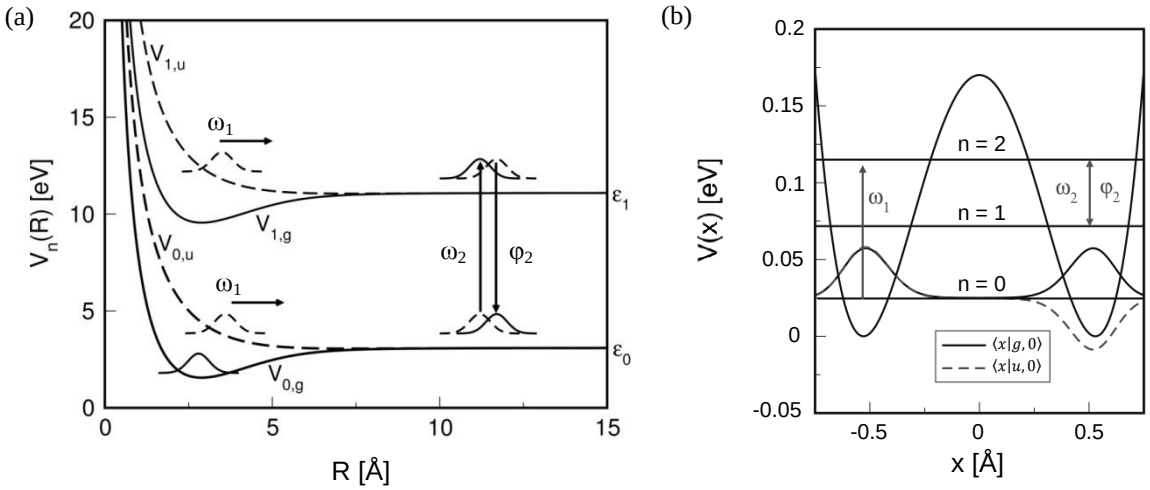

Fig. 1 (a): Illustration of the two-pulse scheme for a A_2^+-type molecule. Shown are two potentials $V_{0,g}(R)$, $V_{1,g}(R)$ for states $|0,g\rangle, |1,g\rangle$ of gerade parity (continuous lines) and two potentials $V_{0,u}(R)$, $V_{1,u}(R)$ for states $|0,u\rangle, |1,u\rangle$ of ungerade parity (dashed lines). Starting from the electronic ground state $|0,g\rangle$, a first spectrally broad pulse (ω_1) prepares outward-moving wave packets in the excited ungerade states $|0,u\rangle, |1,u\rangle$. Upon reaching the fragmentation channel, a second, resonant interaction (ω_2) creates nuclear wave packets in the gerade states $|0,g\rangle, |1,g\rangle$ due to one-photon transitions. The CEP φ_2 of this second pulse has measurable effects on the fragmentation of the A_2^+-type molecule.
(b): Illustration of the two-pulse scheme for a double-well potential. Starting from different initial states which are coherent superpositions or mixtures of the $|0,g\rangle, |0,u\rangle$ lowest eigenstates, a first laser pulse (ω_1) prepares a wave packet. A second interaction (ω_2) couples eigenstates belonging to excited vibrational states where the CEP φ_2 of the second pulse enters. The vertical lines correspond to the energies $E_{n,g}$, $E_{n,u}$ with different quantum numbers (n), where energies of states with gerade (g) and ungerade (u) symmetry are nearly degenerated. Moreover, the wave functions $\langle x|0,g\rangle$ (solid line) and $\langle x|0,u\rangle$ (dashed line) are shown. The CEP φ_2 influences the probability to find the system in the right or left potential well.

References

[1] Gerhard G. Paulus, Felix Grasbon, Herbert Walther, Paolo Villoresi, Mauro Nisoli, Salvatore Stagira, Enrico Priori, Sandro De Silvestri, *Absolute-phase Phenomena in Photoionisation with Few-cycle Laser Pulses*, Nature **414**, 182 (2001).

[2] Lev Chuntonov, Avner Fleischer, Zohar Amitay, *Weak-field Multiphoton Femtosecond Coherent Control in the Single-cycle Regime*, Optics Express **19**, 6865 (2011).

[3] Vladimir Roudnev, Brett D. Esry, *General Theory of Carrier-envelope Phase Effects*, Phys. Rev. Lett. **99**, 220406 (2007).

[4] Klaus Renziehausen, *Dissertation: Interaction of Molecules with Laser Pulses: Researches on the Numerical Implementation of Time-dependent Perturbation Theory and on Carrier Envelope Phase Effects for Laser Pulses of Arbitrary Length*, University of Würzburg (2014).

[5] Klaus Renziehausen, Kilian Hader, Werner Jakubetz, Volker Engel, *Weak-field, Multiple-cycle Carrier Envelope Phase Effects in Laser Excitation*, ChemPhysChem **14**, 1464 (2013).

[6] Kilian Hader, Klaus Renziehausen, Volker Engel, *Carrier Envelope Phase Effects Induced by Weak Multicycle Pulses: Localized Quantum Dynamics in Double Well Potentials*, Chem. Phys. Lett. **579**, 23 (2013).

[7] Kilian Hader, Volker Engel, *Coherent and Incoherent Contributions to the Carrier-envelope Phase Control of Wave Packet Localization in Quantum Double Wells*, J. Chem. Phys. **140**, 184316 (2014).

The ALPHA Experiment: Towards 1S-2S Laser Spectroscopy of Antihydrogen Atoms

D. Maxwell[1], and the ALPHA Collaboration
1. Swansea University, Singleton Park, Swansea, Wales, SA2 8PP, UK

In 2011, the ALPHA collaboration at CERN demonstrated the trapping of antihydrogen atoms for 1000s [1]. The long confinement time opened up the possibility of performing precision measurements of the properties of antihydrogen. A property of particular interest is the transition frequency of the 1S-2S transition. The corresponding transition in hydrogen is known to a precision of 4 parts in 10^{14} [2]. A measurement in antihydrogen would therefore provide a direct, high-precision comparison between matter and antimatter, and a test of CPT (charge-parity-time) symmetry [3].

Over recent years, the ALPHA collaboration has been upgrading its apparatus to perform laser spectroscopy of the 1S-2S transition in antihydrogen. A number of factors mean that the experiment is extremely technically challenging. Typically, only two antihydrogen atoms are trapped per experimental cycle. In addition to this, the low available laser power at the 1S-2S transition wavelength of 243nm means that observing the transition in antihydrogen is very difficult. To overcome these issues, a resonant optical cavity has been built in the ALPHA cryogenic atom trap.

The first spectroscopy measurements began in 2015, and will continue in the 2016 antiproton run. We present the current state of the experiment, including a detailed description of the ALPHA apparatus.

References

[1] ALPHA Collaboration, *Confinement of Antihydrogen for 1,000 seconds*, Nature Physics **7**, 558 (2011).
[2] A. Matveev et al, *Precision Measurement of the Hydrogen 1S-2S Frequency via a 920-km Fiber Link*, Phys. Rev. Lett. **110**, 230801 (2013).
[3] T. Hansch et al, *Laser spectroscopy of hydrogen and antihydrogen*, Hyperfine interact. **76**, 47-57 (1993).

Higher-order perturbative relativistic calculations for few-electron atoms and ions

Dmitry A. Glazov[1,2], Andrey V. Volotka[3], Aleksei V. Malyshev[1,2], Vladimir M. Shabaev[1], Ilya I. Tupitsyn[1], Guenter Plunien[4]

1. Department of Physics, St. Petersburg State University, Universitetskaya nab. 7/9, 199034 St. Petersburg, Russia
2. State Scientific Centre "Institute for Theoretical and Experimental Physics" of National Research Centre "Kurchatov Institute", B. Cheremushkinskaya st. 25, 117218 Moscow, Russia
3. Helmholtz-Institut Jena, Fröbelstieg 3, D-07743 Jena, Germany
4. Institut für Theoretische Physik, Technische Universität Dresden, Mommsenstraße 13, D-01062 Dresden, Germany

An effective computational method is developed for evaluation of the perturbation theory terms for few-electron atoms and ions on the basis of the Dirac-Coulomb-Breit Hamiltonian. One-electron finite basis set is constructed within the DKB approach [1]. Many-electron wave functions are represented by the Slater determinants. The recursive formulation of the perturbative series provides an efficient access to the higher-order contributions of the interelectronic interaction. The presented approach is applied to evaluation of the binding and transition energies, g-factors and hyperfine splittings in lithiumlike and boronlike systems. The results obtained are in agreement with the large-scale configuration interaction Dirac-Fock-Sturm method and other all-order calculations. For the g-factor of lithiumlike ions the accuracy of the total theoretical values [2] is improved, which strengthens the agreement with the recent experimental data for $^{28}Si^{11+}$ [3] and $^{40,48}Ca^{17+}$ [4].

References

[1] V. M. Shabaev, I. I. Tupitsyn, V. A. Yerokhin, G. Plunien, and G. Soff, Phys. Rev. Lett. **93**, 130405 (2004).
[2] A. V. Volotka, D. A. Glazov, V. M. Shabaev, I. I. Tupitsyn, and G. Plunien, Phys. Rev. Lett. **112**, 253004 (2014).
[2] A. Wagner *et al.*, Phys. Rev. Lett. **110**, 033003 (2013).
[3] F. Köhler *et al.*, Nature Communications **7**, 10246 (2016).

Casimir-Polder effect of atoms and molecules in the near field of a hot surface: Energy level shifts and quantum energy transfer

J.C. de Aquino Carvalho [1], A. Laliotis [1], P. Chaves de Souza Segundo[1,2], I. Maurin [1], B. Darquié[1], S.K. Tokunaga[1], D. de Sousa Meneses[3], P. Echegut [3], M. Ducloy [1], D. Bloch [1]

1. Laboratoire de Physique des Lasers, UMR 7538 CNRS, Université Paris13-Sorbonne Paris Cité, 93430 Villetaneuse, France

2. Universidade Federal de Campina Grande, Cuité, PB, Brésil

3. CNRS, CEMHTI UPR3079, Université d'Orléans, F-45071 Orléans, France

The modification of quantum and thermal fluctuations by a surface of finite reflectivity shifts the energy levels of quantum objects, such as atoms and molecules, and changes their radiative properties. This phenomenon is referred to as the Casimir-Polder effect. At nanometric distances away from a surface (near field) electromagnetic fluctuations are dominated by evanescent polariton modes, whose thermal excitation creates intense, but evanescently decaying electromagnetic fields. This was shown to have profound effects on the near field thermal emission of a hot surface making it almost coherent and monochromatic compared to the well-known black-body radiation [1]. We recently demonstrated the effects of near field thermal emission on the Casimir-Polder interaction of a $Cs(7D_{3/2})$ atom near a sapphire surface [2]. Using selective reflection spectroscopy that probes atoms ~100 nm away from the surface we showed that the C_3 coefficient (in the near field the energy shift of a given level is given by $-C_3/z^3$) increases almost by a factor of 2 for temperatures ranging from 500 K to 1000 K. This increase is due to the thermal excitation of the sapphire polariton modes at 12.2 µm that couple to the $7D_{3/2} \rightarrow 5F_{5/2}$ transition at 10.8µm. We are currently performing spectroscopic measurements on the second resonance of Cs, at 459 nm and 455 nm for $Cs(7P_{1/2})$ and $Cs(7P_{3/2})$ respectively. Our theoretical predictions show that in the case of $Cs(7P_{1/2})$ the C_3 coefficient shows a sharp increase with temperature due to the very resonant coupling of the $7P_{1/2} \rightarrow 6D_{3/2}$ transition at (12.15µm) with the sapphire polariton whereas in the case of $Cs(7P_{3/2})$ the $7P_{3/2} \rightarrow 6D_{5/2}$ transition at 14.6µm is responsible for a slow decrease of the C_3 coefficient with temperature. Our predictions are corroborated by a preliminary but extended set of experimental measurements. In order to refine our theoretical predictions of the C_3 coefficient we are experimentally measuring the dielectric constant of both the ordinary and the extra-ordinary axis of sapphire at various temperatures. Our measurements are performed on superpolished windows (identical to the ones used for the selective reflection experiment) and they should provide useful information on the exact position and temperature dependence of the sapphire polariton resonances.

The extremely resonant coupling of the $7P_{1/2} \rightarrow 6D_{3/2}$ transition to the sapphire polariton also means that $Cs(7P_{1/2})$ atoms can directly absorb energy from the thermally excited polariton. Near field heat transfer has been explored rather extensively with classical nanoparticles, but here we present our ongoing efforts towards an experimental demonstration of near field energy transfer to objects that are distinctly quantum. Direct absorption of energy from the polariton modes on the $7P_{1/2} \rightarrow 6D_{3/2}$ transition also implies a distant-dependent transition linewidth which should have measurable effects on the shape and amplitude of the selective reflection spectra. However, quantifying all other broadening mechanisms, such as atomic collisions or even conventional, far-field, black-body radiation would be valuable for the analysis of our selective reflection measurements. Even though these mechanisms do not inherently depend on the distance from the surface (our experiments are conducted in an oven at thermal equilibrium) they could influence our measurements. Towards this end, independent fluorescence experiments allow us to estimate the importance of the collisional broadening of $Cs(7P_{1/2})$ as well as its dependence on temperature.

We also discuss the possibility of measuring the Casimir-Polder interaction of molecules by means of selective reflection spectroscopy. Molecule-surface interactions have a fundamental interest mostly linked to the complex geometry of molecules (chirality and anisotropy [3]) but there also of extreme importance in physical chemistry. Here we present preliminary experiments on an SF_6 vapour at room temperature, using a CO_2 as well as a tuneable Quantum Cascade Laser at 10.6 µm. Selective reflection measurements are possible, despite the inherent difficulties of molecular spectroscopy (weak rovibrational transitions and molecular partition in rotational levels).

Joao Carlos de Aquino Carvalho receives a grant from the Brazilian program 'Ciências sem fronteiras'.

References

[1] J-J. Greffet, R. Carminati, K. Joulain, J-P. Mulet, S. Mainguy and Y. Chen *Coherent emission of light by thermal sources* Nature **416**, 61 (2002).

[2] A. Laliotis, T. Passerat de Silans, I. Maurin, M. Ducloy and D. Bloch *Casimir-Polder interactions in the presence of thermally excited surface modes*, Nat. Commun **5**, 5634 (2014).

[3] D.T. Butcher S.Y. Buhmann and S. Scheel, *Casimir–Polder forces between chiral objects* New J. Phys. **14**, 113013 (2012); P. Thiyuam et al. *Anisotropic contribution to the van der Waals and the Casimlir-Polder energies for CO_2 and CH_4 molecules near surfaces and thin films* Phys. Rev. A **92**, 052704 (2015).

Precision determination of properties of $^{138}Ba^{+}$ ion

N. Valappol, E. A. Dijck, A. Mohanty, J. O. Grasdijk, O. Böll, K. Jungmann, L. Willmann
Van Swinderen Institute, University of Groningen , Zernikelaan 25, 9747AA, The Netherlands

The weak interaction manifests itself in atomic spectra in electric dipole transition amplitudes and associated light shifts between states of same parity. A quantitative measurement of the magnitude of these Atomic Parity Violation (APV) effects permits the extraction of $\sin^2\Theta_W$, where Θ_W is the weak mixing angle. This approach is complementary to the studies of weak interaction at high energies. The best measurement at the lowest accessible momentum transfer was performed in atomic Cs with a precision of 1.3% in $\sin^2\Theta_W$ [1]. Single trapped heavy ions open the path to a new signature of APV by studying differential light shifts [2]. We investigate laser cooled Ba^+ and Ra^+ ions which have been identified as ideal candidates for this approach. The experimental setup is equivalent to an ion based atomic clock promising a relative uncertainty in the range of 10^{-18} [3].

Measurements on a single trapped $^{138}Ba^+$ ion for the detailed understanding of atomic structure to a percent level are presented here. The lowest levels of Ba^+ form a Λ-configuration. The two major laser cooling transitions provide a coherent coupling between the $^2S_{1/2}$ and $^2D_{3/2}$ levels leading to Raman resonances in the spectrum. The one-photon and two-photon components of the line shape are extracted using an eight-level optical Bloch model. This results in an absolute accuracy of the transition frequency of the $^2S_{1/2}$-$^2P_{1/2}$ transition of 200 kHz and for the $^2D_{3/2}$-$^2P_{1/2}$ transition of 100 kHz which is an improvement by two orders of magnitude over previous determinations [4]. The spectrum shows the 5d $^2D_{3/2}$ – 6p $^2P_{1/2}$ transition of $^{138}Ba^+$ ion in excellent agreement with the calculations from the optical Bloch equations (Fig.(a)). In order to extract matrix elements we determine the lifetime of the $^2D_{5/2}$ state employing quantum jump spectroscopy [5] (Fig.(b)). The very long lifetime makes it sensitive to probe any effects that influence the long term performance of the experiment (i.e. several hours to days). Furthermore, light shifts permit the mapping of weak interaction effects onto the energy splitting between the magnetic sublevels (Fig.(c)). They are well suited to determine the relevant matrix element in the Ba^+ system. The differential light shift of magnetic substates is proportional to square of the matrix element and the intensity of the laser. All of these measurements are required for the execution of an APV measurement in a single trapped ion.

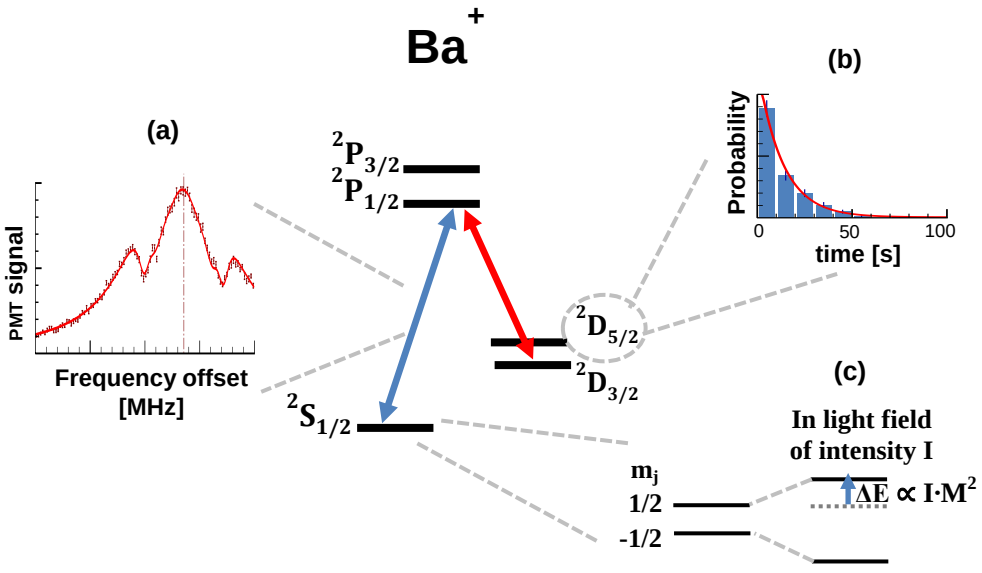

Fig: Level scheme of Ba^+ with insets (a) Transition frequency measurement with Raman resonances (b) A typical lifetime measurement (c) Light shift measurement, M is matrix element.

References

[1] S. C. Bennett and C. E. Wieman, Phys. Rev. Lett. 82, 2484 (1999).
[2] E. N. Fortson, Phy. Rev. Lett. 70, 2383 (1993)
[3] M. Nuñez Portela, E.A. Dijck, A. Mohanty, H. Bekker, J. E. van den Berg, G. S. Giri, S. Hoekstra, C. J. G. Onderwater, S. Schlesser, R. G. E. Timmermans, O. O. Versolato, L.Willmann, H. W. Wilschut, & K. Jungmann, Appl. Phys. B 114, 173 (2014)
[4] E. A. Dijck, M. Nunez Portela, A. T. Grier, K. Jungmann, A. Mohanty, N. Valappol, L. Willmann, Phys. Rev. A 91, 060501(R) (2015).
[5] A. Mohanty, E.A. Dijck, M. Nunez Portela, A.T.Grier, N.Valappol, T.Meijknecht, L.Willmann, K.Jungmann, Hyp. Int. 233, 113 (2015).

Radiation power of a moving nanoparticle

Vahid Ameri[1], **Mohammad Eghbali-Arani**[2]
1. Department of Physics, Faculty of Science, Hormozgan University, Bandar-Abbas, Iran
2. Department of Physics, University of Kashan, Kashan, Iran

Starting from a Lagrangian, the electromagnetic field is quantized in the presence of a nanoparticle moving parallel to a semi-infinite substrate. Response functions and fluctuation-dissipation relations are obtained. Radiation power of moving nanoparticle is obtained in terms of dyadic Green's tensor [1].

$$\langle \mathscr{P} \rangle = \frac{\hbar}{2\pi c^2} \int_0^\infty \frac{d^2 k_\parallel}{(2\pi)^2} \int_0^\infty d\omega\, \omega^3 \Big[2\mathrm{Im}\alpha(\omega - k_x V_0)[a_T(\omega - k_x V_0) - a_{T_0}(\omega)] \\ \big[\mathrm{Im}\, D_{xx}(z,z',\omega) + \mathrm{Im}\, D_{yy}(z,z',\omega) + \mathrm{Im}\, D_{zz}(z,z',\omega)\big] \Big], \quad (1)$$

where D_{ij} is dyadic Green's tensor and $a_T(\omega) = \coth(\hbar\omega/2k_BT) = 2[n_T(\omega) + \frac{1}{2}]$. Using the small radius expansion of the Mie scattering coefficient $(a/\lambda \ll 1)$, we have $\alpha(\omega) \approx a^3 \frac{\varepsilon(\omega)-1}{\varepsilon(\omega)+2}$.

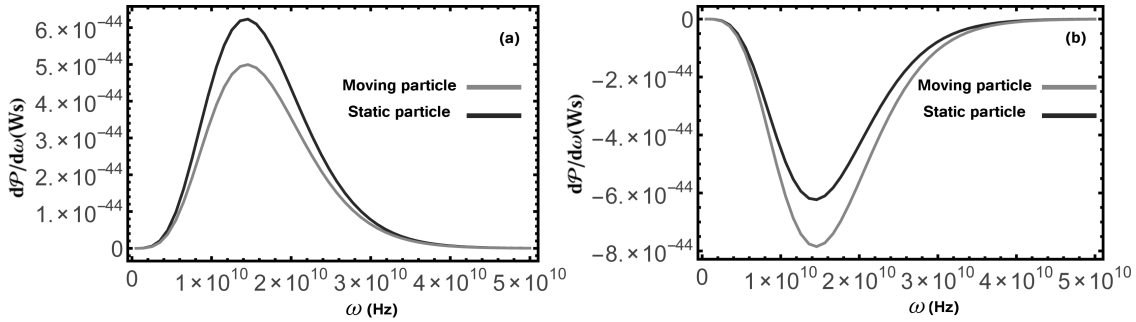

Fig. 1 The spectrum of radiation power for a gold nano-particle with $a = 10nm$ and $(\sigma_0 \approx 1.6 \times 10^7 \Omega^1 m^{-1})$. The temperatures of the particle and its medium are assumed to be (a) 0.11 K and 0.12 K and (b) 0.12 K and 0.11 K, respectively.

As a consequence, the motion of nanoparticle doesn't change the radiation power in vacuum (absence of semi-infinite substrate) as we expect to do not. Also the frictional radiation vanishes when the temperatures are zero where it approved by previous results [2].

Fig.1 shows the spectrum of radiation power for two situations. First we consider the case where the nanoparticle is colder than the environment (Fig.1a). In such situation the particle absorbs the thermal radiation (positive spectrum) while the spectrum of frictional radiation is always negative which it causes a smaller peak for total radiation of moving nanoparticle with respect to the static one. Fig.1b shows the spectrum of radiation power for the case where the particle is a bit hotter than the environment. In this case, particle has negative spectrum for thermal and frictional radiation power. So the total radiation power of moving particle is considerably higher than the static particle.

We can consider the case where the moving particle and environment have same non zero temperature. So there is no thermal radiation and one can find the spectrum of frictional radiation power which it has same frequency spectrum around $\omega = K_BT/\hbar$.

The aim of this work is to show that there is a frictional radiation combined to the thermal radiation of particle with same spectrum. While in comparison to a rotating nanoparticle where we had two different spectrum for mechanical radiation power and also the thermal one [3], here we don't have any mechanical radiation power which is obviously acceptable to don't have it.

References

[1] Maradudin, A. A., and Mills, D. L. *Scattering and absorption of electromagnetic radiation by a semi-infinite medium in the presence of surface roughness* Physical Review B **11.4**, 1392 (1975).
[2] Dedkov, G. V., and Kyasov, A. A. *Vacuum friction and heat exchange of a nano-and a microparticle with a solid surface* Technical Physics **53.4**, 389-398 (2008).
[3] Kheirandish, Fardin, and Vahid Ameri. *Electromagnetic field quantization in the presence of a rotating body* Physical Review A **89.3**, 032124 (2014).

Imaging the He_2 quantum halo state using a free electron laser

S. Zeller*,[1] M. Kunitski,[1] J. Voigtsberger,[1] A. Kalinin,[1] A. Schottelius,[1] C. Schober,[1] M. Waitz,[1] H. Sann,[1] A. Hartung,[1] T. Bauer,[1] M. Pitzer,[1] F. Trinter,[1] C. Goihl,[1] C. Janke,[1] M. Richter,[1] G. Kastirke,[1] M. Weller,[1] A. Czasch,[1] M. Kitzler,[2] M. Braune,[3] R. E. Grisenti,[1, 4] W. Schöllkopf,[5] L. Ph. H. Schmidt,[1] M. Schöffler,[1] J. B. Williams,[6] T. Jahnke,[1] and R. Dörner*[1]

1. Institut für Kernphysik, J. W. Goethe-Universität, Max-von-Laue-Str. 1, 60438 Frankfurt am Main, Germany

2. Photonics Institute, Vienna University of Technology, Gußhausstraße 27, 1040 Vienna, Austria

3. Deutsches Elektronen-Synchrotron DESY, Notkestraße 85, 22607 Hamburg, Germany

4. GSI Helmholtz Centre for Heavy Ion Research, Planckstraße 1, 64291 Darmstadt, Germany

5. Department of Molecular Physics, Fritz-Haber-Institut, Faradayweg 4-6, 14195 Berlin, Germany

6. Department of Physics, University of Nevada, 1664 N. Virginia Street, Reno, NV 89557, USA

We report on Coulomb explosion imaging of the wavefunction of the quantum halo system He_2. Each atom of this system is ionized by tunnel ionization in a femto second laser pulse and in a second experiment by single photon ionization employing a free electron laser. We visualize the exponential decay of the probability density of the tunneling particle over distance for over two orders of magnitude up to an internuclear distance of 250 Å. By fitting the slope of the density in the tunneling regime we obtain a binding energy of 151.9 ± 13.3 neV, which is in agreement with most recent calculations [1].

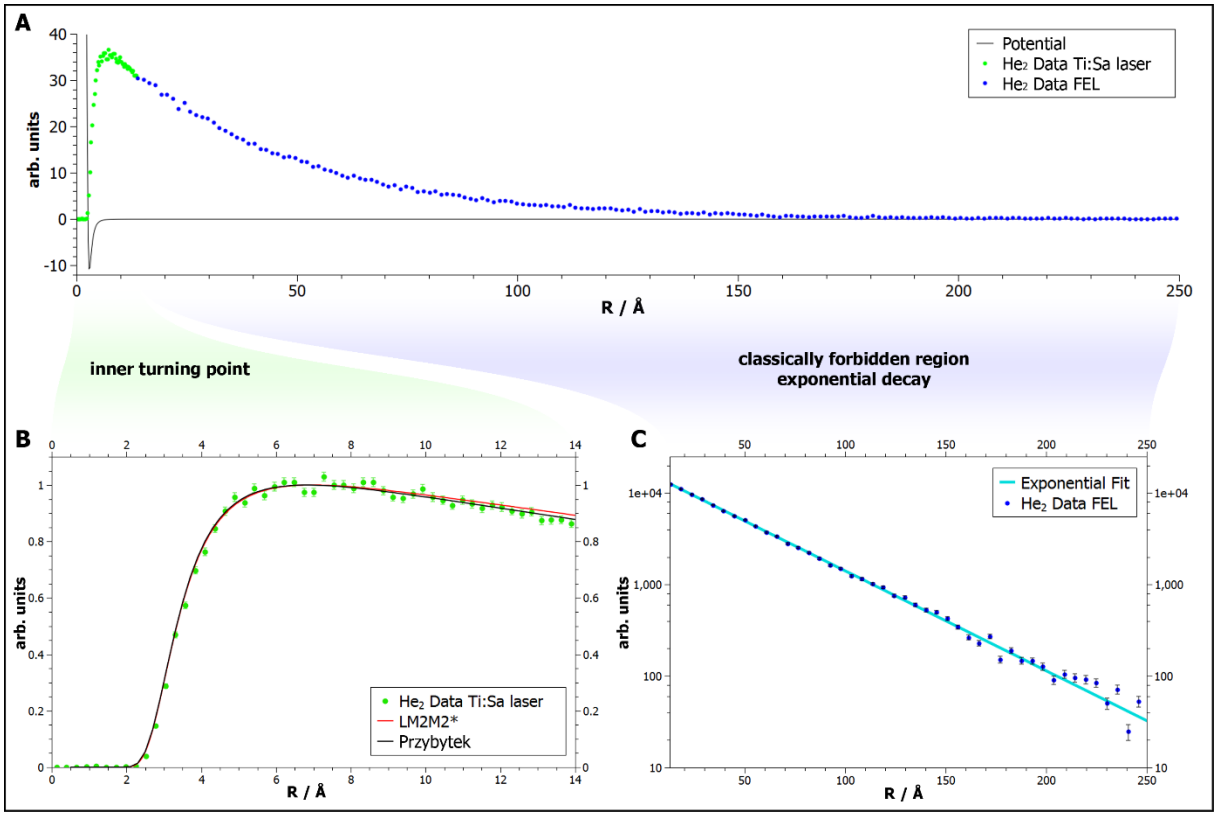

Fig. 1 Measurement of the helium dimer wavefunction (A). Two detailed views show the important features of this quantum system: The region of the inner turning point (B) is in agreement with theoretical predictions LM2M2*[2] and Przybytek[1], and the exponential decay in the classical forbidden region (C). A helium dimer binding energy of 151.9 ± 13.3 neV is obtained from the exponential slope. The electron recoil has to be taken into account to conclude from the slope shown in C to the value of the binding energy.

References

[1] M. Przybytek, W. Cencek, J. Komasa, G. Lach, B. Jeziorski, and K. Szalewicz, *Relativistic and Quantum Electrodynamics Effects in the Helium Pair Potential*, Phys. Rev. Lett. **104**, 183003 (2010).

[2] F. Luo, G. Kim, G. C. McBane, F. C. Giese, and W. R. Gentry, *Influence of retardation on the vibrational wave function and binding energy of the helium dimer*, J. Chem. Phys. **98**, 9687 (1993).

From a loophole-free Bell test to a global quantum network

Andreas Reiserer [1,2],

1. *Qutech and Kavli Institute of Nanoscience, Lorentzweg 1, 2628CJ Delft, The Netherlands*
2. *Max-Planck-Institute of Quantum Optics, Hans-Kopfermann-Str. 1, 85748 Garching, Germany*

Bas Hensen, Hannes Bernien, Anaïs Dréau, Norbert Kalb, Machiel S. Blok, Koen J.M. van Bemmelen, David Elkouss, Stephanie Wehner, Tim H. Taminiau, Ronald Hanson

Qutech and Kavli Institute of Nanoscience, Lorentzweg 1, 2628 Delft, The Netherlands

Entanglement is one of the most intriguing phenomena in quantum science. The outcomes of independent measurements of the quantum state of entangled objects are correlated, even if the objects are space-time separated. This property, often called quantum non-locality, cannot be explained by classical physics and is a unique resource for quantum information processing and quantum communication.

Fifty years after its derivation, many experiments have tested Bell's famous inequality [1]. However, all of these experiments relied on additional assumptions in order to obtain a violation, most prominently the absence of communication between the entangled particles, and fair sampling of the full dataset when using inefficient detectors. Closing the 'loopholes' that arise from these assumptions has been one of the major fundamental research goals of experimental quantum physics, with applications [2] such as device-independent quantum key distribution to the generation of provably random numbers.

In [3], we have demonstrated the first experiment that is free of any such additional assumption. We have entangled two electronic spins in diamond at a separation of 1.3 km via an optical fiber channel. We have used an event-ready scheme in combination with efficient and fast spin read-out (to avoid the fair-sampling assumption) and fast random basis-selection (to ensure the required locality conditions). A second run of the loophole-free Bell experiment has further improved statistical evidence [4].

To enable further fundamental tests, as well as numerous applications in quantum communication, computation and measurement, we plan to extend the separation as well as the number of entangled particles, aiming for the realization of a global-scale quantum network [5]. This will be feasible by embedding the diamond samples into high-quality optical resonators, as pioneered with cold atoms [6]. In addition, unavoidable inefficiencies in photon transmission require the implementation of a quantum memory that is robust under failed remote entanglement attempts.

We have demonstrated individual control and readout of five nuclear spin qubits via the hyperfine interaction with a close-by electronic spin. By encoding quantum states into a decoherence-protected subspace of two nuclear spins we show that quantum coherence can be maintained for over 1000 repetitions of a remote entangling protocol [7]. These results and insights pave the way towards remote entanglement purification [8] and the realization of a quantum repeater [9] using nitrogen-vacancy center quantum network nodes. I will present our recent results in this respect.

References

[1] J.S. Bell, *On the Einstein Podolsky Rosen Paradox*, Physics **1**, 195 (1964) .

[2] N. Brunner, D. Cavalcanti, S. Pironio, V. Scarani, and S. Wehner, *Bell nonlocality*, Rev. Mod. Phys. **86**, 419 (2014).
A. Ekert and R. Renner, *The ultimate physical limits of privacy*, Nature **507**, 443 (2014).

[3] B. Hensen, H. Bernien, A. E. Dréau, A. Reiserer, N. Kalb, M. S. Blok, J. Ruitenberg, R. F. L. Vermeulen, R. N. Schouten, C. Abellán, W. Amaya, V. Pruneri, M. W. Mitchell, M. Markham, D. J. Twitchen, D. Elkouss, S. Wehner, T. H. Taminiau, and R. Hanson, *Loophole-free Bell inequality violation using electron spins separated by 1.3 kilometres*, Nature **526**, 682 (2015).

[4] B. Hensen, N. Kalb, M. S. Blok, A. Dréau, A. Reiserer, R. F. L. Vermeulen, R. N. Schouten, M. Markham, D. J. Twitchen, K. Goodenough, D. Elkouss, S. Wehner, T. H. Taminiau, and R. Hanson, *Loophole-free Bell test using electron spins in diamond: second experiment and additional analysis*, arXiv:1603.05705 (2016).

[5] H. J. Kimble, *The quantum internet*, Nature **453**, 1023 (2008).

[6] A. Reiserer and G. Rempe, *Cavity-based quantum networks with single atoms and optical photons*, Rev. Mod. Phys. **87**, 1379 (2015).

[7] A. Reiserer, N. Kalb, M. S. Blok, K. J. M. van Bemmelen, D. J. Twitchen, M. Markham, T. H. Taminiau, and R. Hanson, *Robust quantum-network memory using decoherence-protected subspaces of nuclear spins*, arXiv:1603.01602 (2016).

[8] C. H. Bennett, G. Brassard, S. Popescu, B. Schumacher, J. A. Smolin, and W. K. Wootters, *Purification of Noisy Entanglement and Faithful Teleportation via Noisy Channels*, Phys. Rev. Lett. 76, 722 (1996).

[9] H.-J. Briegel, W. Dür, J. I. Cirac, and P. Zoller, *Quantum Repeaters: The Role of Imperfect Local Operations in Quantum Communication*, Phys. Rev. Lett. 81, 5932 (1998).

Storage and retrieval of a single photon emitted by a quantum memory on a highly excited Rydberg state

Emanuele Distante[1], Pau Farrera[1], Auxiliadora Padrón-Brito[1], David Paredes-Barato[1], Georg Heinze[1] and Hugues De Riedmatten[1,2]

1. ICFO-Institut de Ciencies Fotoniques, The Barcelona Institute of Science and Technology, 08860 Castelldefels (Barcelona), Spain
2. ICREA-Institució Catalana de Recerca i Estudis Avançats, 08015 Barcelona, Spain

The possibility to control the interaction between photons provided by highly nonlinear media is a key ingredient to the goal of quantum information processing using photons and a unique tool to study the dynamics of many-body correlated systems [1]. Many different systems showing high nonlinear optical response at the single-photon level have been studied during the past years ranging from resonators coupled to single atoms, atomic ensembles, to artificial two-level atoms. A promising strategy to perform different quantum information processing tasks using photons as carriers is the combination of electromagnetically induced transparency (EIT) and Rydberg atoms. Using EIT one maps the state of the photons into atomic coherence in the form of slow travelling Rydberg dark-state polaritons (DSPs) by means of an auxiliary coupling field. By switching off and back on the coupling field, photons can be stored as Rydberg excitations and retrieved at later time [2-4]. The strong Rydberg dipole-dipole (DD) interaction between neighbouring excitations provide an effective interaction between photons which can be exploited to implement single-photon switches, transistors as well as π phase shift controlled with single-photon level pulse [5-8]. The achievable non-linear interaction between single photons can be exploited to implement deterministic Bell state measurement which would be beneficial for quantum teleportation and quantum repeater scheme boosting the rate of entanglement distribution over long distance.

All the experiments with Rydberg EIT so far have been carried out with weak coherent input pulse. Here we present the first experiment of storage and retrieval of a heralded single photon in highly excited Rydberg state. To couple single photons with a cold atomic Rydberg ensemble the challenge is to generate the photons with the appropriate spectral width to match the Rydberg EIT memory bandwidth (in the sub MHz regime). To fulfil this requirement, we produce high quality single photons by means of a cold atomic quantum memory based on the Duan Lukin Cirac and Zoller (DLCZ) scheme [9]. Here the cold atomic cloud is illuminated with a weak write pulse which creates probabilistically a photon by Raman scattering (*write photon*). The detection of this photon heralds the presence of a single collective excitation in the atomic cloud. After a programmable storage time, the excitation can be mapped out as single photon (*read photon*) with controllable temporal shape [10] by means of a read laser pulse. The read photon is then sent to a second separated cold atomic cloud where it is converted to a Rydberg DSP by means of EIT and successively stored by switching off the coupling beam on the Rydberg state $|60S_{1/2}\rangle$. After a storage time $t_{s,R}$, the excitation is read out by switching on the coupling beam and the photon is detected with a single photon detector. The cross correlation function between the write and the stored and retrieved read photon is measured as a function of the storage time in the DLCZ cloud $t_{s,DLCZ}$ or in the Rydberg state $t_{s,R}$ and non-classical correlations are found to persist up to $t_{s,DLCZ} = 30\,\mu$s and up to $t_{s,R} = 5\,\mu$s.

Our experiment paves the way to study the interaction between single photons mediated by the Rydberg atoms. The ability to store the state of a single-photon as a Rydberg excitation is beneficial to study the photon-photon interaction as well as to implement photon-photon gates, transistor and switch. Moreover, our experiment is a building block for a future quantum repeater scheme based on cold atomic quantum memory and deterministic Bell state measurement.

References

[1] Darrick E. Chang, Vladan Vuletić, Mikhail D. and Lukin, *Quantum nonlinear optics — photon by photon*, Nature Photonics **8**, 685, (2014).
[2] J. D. Pritchard, D. Maxwell, A. Gauguet, K. J. Weatherill, M. P. A. Jones and C. S. Adams, *Cooperative Atom-Light Interaction in a Blockaded Rydberg Ensemble*, Phys. Rev. Lett. **105**, 193603, (2010).
[3] T. Peyronel, O. Firstenberg, Q. Y Liang, A. V. Gorshkov, S. Hofferberth, T. Pohl, M. D. Lukin and V. Vuletić *Quantum nonlinear optics with single photons enabled by strongly interacting atoms*, Nature **488**, 57, (2012)
[4] D. Maxwell,D. J. Szwer, D. Paredes-Barato, H. Busche, H., J. D. Pritchard, A. Gauguet, K. J. Weatherill, M. P. A. Jones and C. S. Adams. *Storage and Control of Optical Photons Using Rydberg Polaritons*. Phys. Rev. Lett. **110**, 103001, (2013).
[5] S. Baur,D. Tiarks,G. Rempe and S .Dürr *Single-Photon Switch Based on Rydberg Blockade*, Phys. Rev. Lett. **112**, (2014).
[6] D. Tiarks, S. Baur, K. Schneider, S.Dürr, and G. Rempe, *Single-Photon Transistor Using a Förster Resonance*, Phys. Rev. Lett. **113**, (2014).
[7] H. Gorniaczyk, C. Tresp, J. Schmidt, H. Fedder, and S. Hofferberth, *Single-Photon Transistor Mediated by Interstate Rydberg Interactions*, Phys. Rev. Lett **113**, (2014).
[8] D. Tiarks, S.Schmidt, G. Rempe, S. Dürr, *Optical Pi Phase Shift Created with a Single-Photon Pulse*, arXiv:1512.05740 [quant-ph], (2015).
[9] L. M. Duan, M. D. Lukin, J. I. Cirac and P. Zoller, *Long-distance quantum communication with atomic ensembles and linear optics*, Nature **414**, 413, (2001).
[10] P. Farrera, G. Heinze, B. Albrecht, M. Ho, M. Chávez, C. Teo, N. Sangouard and Hugues de Riedmatten, *Generation of single photons with highly tunable wave shape from a cold atomic quantum memory*, arXiv:1601.07142, (2016)

Generation of single photons with highly tunable wave shape from a cold atomic quantum memory

Pau Farrera[1], Georg Heinze[1], Boris Albrecht[1], Melvyn Ho[2], Matías Chávez[2], Colin Teo[3,4], Nicolas Sangouard[2], and Hugues de Riedmatten[1,5]

1. ICFO-Institut de Ciencies Fotoniques, The Barcelona Institute of Science and Technology, 08860 Castelldefels (Barcelona), Spain
2. Department of Physics, University of Basel, Klingelbergstrasse 82, 4056 Basel, Switzerland
3. Institute for Quantum Optics and Quantum Information of the Austrian Academy of Sciences, A-6020 Innsbruck, Austria
4. Institute for Theoretical Physics, University of Innsbruck, A-6020 Innsbruck, Austria
5. ICREA-Institució Catalana de Recerca i Estudis Avançats, 08015 Barcelona, Spain

A vast range of experiments in quantum information science and technology rely on single photons as carriers of information. Single photon sources are thus key components and have been continuously improved over the past years [1]. The spectrum and temporal shape of the emitted photons are important parameters of such sources. The generation of ultra-long single photons is for example an essential requirement for precise interactions with media exhibiting a sharp energy structure like trapped atoms, ions, or doped solids, which have been proposed as quantum memories for light [2] and also with cavity optomechanical systems [3].

We report on a single photon source with highly tunable photon shape based on a cold ensemble of Rubidium atoms [4]. We follow the DLCZ scheme [5] to implement an emissive quantum memory, which can be operated as a photon pair source with controllable delay. We find that the temporal wave shape of the emitted read photon can be precisely controlled by changing the shape of the driving read pulse (see Fig. 1). We generate photons with temporal durations varying over three orders of magnitude up to $10\,\mu$s without a significant change of the read-out efficiency. We prove the non-classicality of the emitted photons by measuring their antibunching, showing near single photon behavior at low excitation probabilities. We also show that the photons are emitted in a pure state by measuring unconditional autocorrelation functions. Finally, to demonstrate the usability of the source for realistic applications, we create ultra-long single photons with a rising exponential or doubly peaked wave shape which are important for several quantum information tasks.

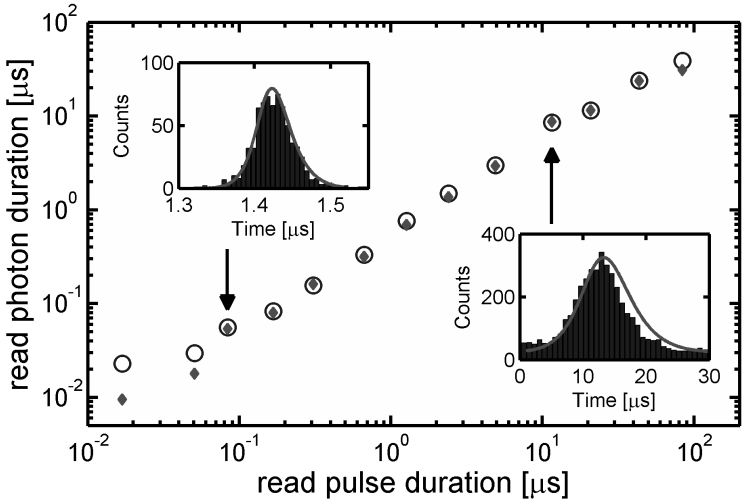

Fig. 1 Temporal duration (FWHM) of the emitted read photon vs the duration of the driving read pulse. Experimental data (open circles, errorbars smaller than symbol size) are compared with numerical simulations (diamonds). The insets show two examples of the read photon wave shape as reconstructed from the number of counts and arrival times in the single photon detectors (histograms) as well as the simulated wave shapes (solid lines) for which we allowed at most 10% adjustment of the input parameters to account for experimental inaccuracies.

References

[1] M. D. Eisaman, J. Fan, A. Migdall, S. V. Polyakov, *Invited Review Article: Single-photon sources and detectors*, Rev. Sci. Instrum., **82**, 071101 (2011).
[2] M. Afzelius, N. Gisin, H. de Riedmatten, *Quantum memory for photons*, Physics Today, **68**, 42 (2015).
[3] M. Aspelmeyer, T. J. Kippenberg, F. Marquardt, *Cavity optomechanics*, Rev. Mod. Phys., **86**, 1391 (2014).
[4] P. Farrera, G. Heinze, B. Albrecht, M. Ho, M. Chávez, C. Teo, N. Sangouard, H. de Riedmatten, *Generation of single photons with highly tunable wave shape from a cold atomic quantum memory*, arXiv:1601.07142 (2016).
[5] L. M. Duan, M. D. Lukin, J. I. Cirac, P. Zoller, *Long-distance quantum communication with atomic ensembles and linear optics*, Nature **414**, 413 (2001).

Automated Search for new Quantum Experiments

Mario Krenn[1,2], Mehul Malik[1,2], Robert Fickler[1,2,3], Radek Lapkiewicz[1,2,4], and Anton Zeilinger[1,2]

1. Vienna Center for Quantum Science and Technology (VCQ), Faculty of Physics, University of Vienna, Boltzmanngasse 5, A-1090 Vienna, Austria.

2. Institute for Quantum Optics and Quantum Information (IQOQI), Austrian Academy of Sciences, Boltzmanngasse 3, A-1090 Vienna, Austria.

3. present address: Department of Physics and Max Planck Centre for Extreme and Quantum Photonics, University of Ottawa, Ottawa, K1N 6N5, Canada.

4. present address: Faculty of Physics, University of Warsaw, Pasteura 5, 02-093 Warsaw, Poland.

Quantum mechanics predicts a number of at first sight **counterintuitive phenomena**. It is therefore a question whether our intuition is the best way to find new experiments. Here we report the development of the computer algorithm MELVIN [1] which is able to **find new experimental implementations** for the creation and manipulation of **complex quantum states**. And indeed, the discovered experiments extensively use unfamiliar and asymmetric techniques which are challenging to understand intuitively. The results range from the first implementation of a high-dimensional Greenberger-Horne-Zeilinger (GHZ) state, to a vast variety of experiments for **asymmetrically entangled quantum states** – a feature that can only exist when both the number of involved parties and dimensions is larger than 2. Additionally, new types of high-dimensional transformations are found that perform cyclic operations. MELVIN **autonomously learns from solutions** for simpler systems, which significantly speeds up the discovery rate of more complex experiments (Fig. 1 shows the working principle).

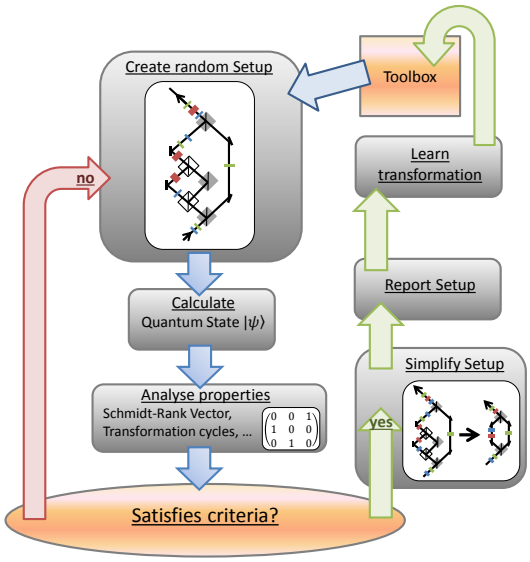

Fig. 1: Working principle of the algorithm. First, an experiment is created using elements from a basic toolbox. Then, the quantum state is calculated, and subsequently its properties are analyzed. Those properties are compared with a number of criteria. If these criteria are not satisfied, the algorithm starts over again. However, if the criteria are satisfied, the experiment is simplified and reported, together with all relevant information for the user. Useful solutions can be stored and used in future experiments, which significantly increases the discovery rate of more complex experiments. The orange boxes (toolbox and criteria) are adapted when a different type of quantum property is investigated, while the rest of the algorithm stays the same.

The large number of discoveries reveals a way to investigate new families of complex entangled quantum systems in the laboratory. Several of these experiments **have already been successfully built in our labs** [2, 3], and hopefully many more will follow. The ability to automate the design of a quantum experiment can be applied to many quantum systems and allows the physical realization of quantum states **previously thought of only on paper**.

References

[1] Mario Krenn, Mehul Malik, Robert Fickler, Radek Lapkiewicz, and Anton Zeilinger, *Automated Search for new Quantum Experiments*, Phys. Rev. Lett. **116**(9), 090405 (2016).

[2] Mehul Malik, Manuel Erhard, Marcus Huber, Mario Krenn, Robert Fickler, Anton Zeilinger, *Multi-photon entanglement in high dimensions*, Nature Photon. in press, arXiv:1509.02561.

[3] Florian Schlederer, Mario Krenn, Robert Fickler, Mehul Malik, Anton Zeilinger, *Cyclic transformation of orbital angular momentum modes*, New J. Phys. in press, arXiv:1512.02696.

Entanglement of Two Hybrid Optomechanical Cavity Composed of BEC Atoms Under Bell Detection

Mohammad Eghbali-Arani[1], **Vahid Ameri Seyahooei**[2]
1. Departement of Physics, University of Kashan, Kashan, Iran
2. Depertment of Physics, Faculty of Science, Hormozgan University, Bandar-Abbas, Iran

In this paper, firstly, we exploit two bipartite entanglement of output optical field, moving mirror, and the lowest band of a one dimensional BEC inside a driven optomechanical cavity. We consider atomic collision on the behaviour of the BEC in the weak photon-atom coupling, and use Bogoliubov approximation for the condensate. Secondly under above conditions, we propose a scheme for entanglement swapping which involves tripartite systems. In our investigation, we consider a scenario where BECs, mirrors, and field modes are given in a Gaussian state with a covariance matrix (CM). By applying the Bell measurement to the output optical field modes (See Fig. 1), we show how the remote entanglement between two BECs, two mirrors, and BEC-mirror modes in different optomechanical cavity can be generated.

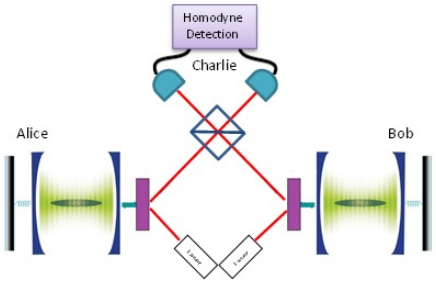

Fig. 1 Scheme of the entanglement swapping protocol.

Entanglement dose not describe all of the non-classical properties of quantum correlations. So, finally we measure all of non-classical correlations beyond entanglement by analysing the quantum discord. Recent studies have shown that some separable - and also some mixed systems, which despite being unentangled - might also contain correlations that classically unexplainable [1] and quantum discord was introduced as a measure of all quantum correlations, which is including-but not restricted to-entanglement [2, 3]. Thus as the entanglement dose not include all of the quantum correlations, we investigate the effect of Bell measurement to generation quantum discord between subsystems.
Entanglement between the different bipartite systems formed by BEC, mechanical, and output optical modes, which is important from a practical point of view because any quantum-communication application involves the manipulation of travelling optical fields. It has been shown that the Stokes output mode is strongly entangled with the BEC, and mechanical modes, and also there is no entanglement between the mechanical and BEC modes. Entanglement swapping protocol can be implemented using two distant hybrid optomechanical system. We considere two remote optomechanical cavity composed of one dimensional ultracold atoms inside the cavity and performe Bell measurement for entangling two same or different remote systems. Bell measurement entangles all of the subsystems except the BEC and mechanical mode in the position of each node. We showe that the qualitative manner of quantum discord is very similar to that of the entanglement, But here Bell measurement can create quantum discord between BEC and mechanical mode in the position of each node.

References

[1] L. Henderson and V. Vedral, J. Phys. A: Math. Gen., 34, 6899 (2001).
[2] W. H. Zurek, Annalen der Physik (Leipzig), 9 (2000).
[3] H. Ollivier and W. H. Zurek, Phys. Rev. Lett, 88, 017901 (2001).

Consequence of interaction on the moment of inertia and vortices number of a rotating condensate boson

Ahmed S. Hassan and Azza M. El-Badry
Department of Physics, Faculty of Science, Minia University, El Minia, Egypt.

We employ a developed Hartree-Fock approximation semiclassical. We provide a general and systematic method for including effects of interaction on rotating condensate boson. We have calculated the thermodynamic potential for this system. Thereby, we investigate the interaction effect on the moment of inertia and vortices number.

A story of geometry and fluctuations in the stage of condensates

Arko Roy, D. Angom
Physical Research Laboratory, Navrangpura, Ahmedabad-380009, Gujarat, India

We investigate the structural transformation of the low-lying spectral modes in Bose-Einstein condensates, especially the Kohn mode, from radial to circular topology as harmonic confining potential is modified to a toroidal one, and this corresponds to a transition from simply to multiply connected geometry. For this we employ the Hartree-Fock-Bogoliubov theory to examine the evolution of low energy quasiparticles. We, then, use the Hartree-Fock-Bogoliubov theory with the Popov approximation to demonstrate the two striking features of quantum and thermal fluctuations. At $T = 0$, the non-condensate density due to interaction induced quantum fluctuations increases with the transformation from pancake to toroidal geometry. The other feature is, there is a marked change in the density profile of the non-condensate density at finite temperatures with the modification of trapping potential. In particular, the condensate and non-condensate density distributions have overlapping maxima in the toroidal condensate which is in stark contrast to the case of pancake geometry.

References

[1] A. Griffin, Phys. Rev. B **53**, 9341 (1996).
[2] A. Roy and D. Angom, arXiv:1511.08655 (2015).
[3] A. Roy and D. Angom, Phys. Rev. A **92**, 011601(R) (2015).

Efficient Technique to Evaluate the Lindhard Dielectric Function

Lorenzo Ugo Ancarani[1], **Hervé Jouin**[2]
1. Equipe TMS, SRSMC, UMR CNRS 7565, Université de Lorraine, 57078 Metz, France
2. Université de Bordeaux, CNRS, CEA, CELIA, UMR 5107, 33400 Talence, France

Since the pioneering work of Lindhard, the dielectric response function obtained in [1] from first principles within the Random Phase Approximation (RPA) has been and is widely used in many areas of Physics such as Solid State Physics, Plasmonics, Plasma Physics, Atomic Physics in plasmas and Nuclear Physics. Indeed, the dielectric function is the fundamental ingredient for many theories related to the response of matter to an external perturbation. In all the above applications the Lindhard dielectric function has to be evaluated many times (for given values of a real parameter λ, and for given temperature T). It is notorious that the integral defining its real part presents a logarithmic divergency which renders the calculation delicate and time consuming. In this contribution we propose a simple way to avoid, in all cases, this mathematical difficulty [2].

For a given Fermi temperature T_F and chemical porential μ, let $t = T/T_F$ be the reduced temperature and $\alpha(t) = \mu/E_F$ the reduced chemical potential which depends only on the reduced temperature t. The calculation of the real part of the Lindhard dielectric function involves the following integral (to make our proposal as general as possible, and simpler to treat mathematically, we use the dimensionless variable X)

$$\int_0^\infty X\, f(X)\, \ln\left|\frac{X+1}{X-1}\right| dX \tag{1}$$

with the Fermi-Dirac distribution function

$$f(X) = \frac{1}{1+\exp(AX^2-B)} \tag{2}$$

where A and B are real constants ($A = \lambda^2/t$ is always positive while $B = \alpha(t)/t$ can take either negative or positive values). Clearly an integrand divergency appears for $X = 1$, as illustrated for three cases in the upper panels of Figure 1. It may lead to serious loss of accuracy when performing the integration.

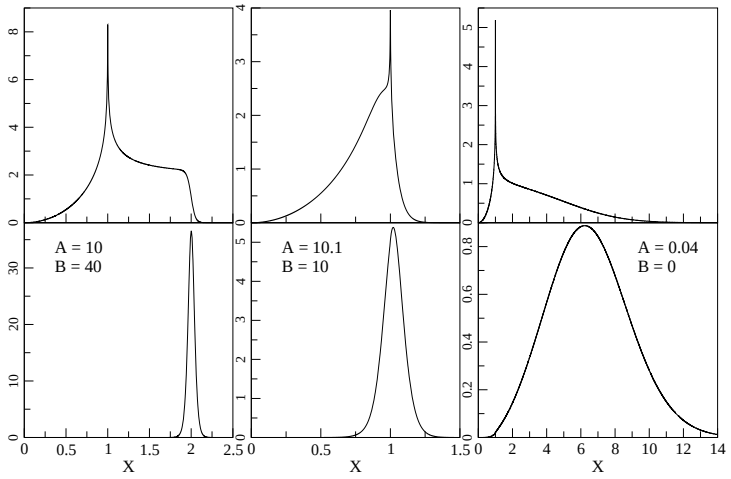

Fig. 1 The integrand of equation (1) (upper) and the transformed one (lower) are shown as a function of the dimensionless variable X, for three cases: (left) $A = 10$, $B = 40$; (middle) $A = 10.1$, $B = 10$; (right) $A = 0.04$, $B = 0$.

Through a simple but very efficient mathematical trick (integral by parts) we were able to remove the well known logarithmic singularity and obtain a useful integral expression which is trouble-free, i.e., it can be dealt with any standard numerical quadrature [2]. In all cases (i.e., any combination of A and B values), one finds well behaved integrands over the whole X range, as illustrated in the Figure (bottom panels).

Due to the very wide use of the Lindhard dielectric function (and its extensions) in many branches of Physics, we believe that the present work should be useful to many researchers.

References

[1] J. Lindhard 1954 *K. Dan. Vidensk. Selsk. Mat. Fys. Medd.* **28** 8 (1954).
[2] Lorenzo Ugo Ancarani and Hervé Jouin, *Efficient technique to evaluate the Lindhard dielectric function*, Eur. Phys. J.-Plus, in press (2016).

Rosensweig Instability and Droplets in a Quantum Ferrofluid of Dysprosium Atoms

Matthias Schmitt, Holger Kadau, Matthias Wenzel, Igor Ferrier-Barbut, Tilman Pfau
5. Physikalisches Institut and Center for Integrated Quantum Science and Technology, Universität Stuttgart, Pfaffenwaldring 57, 70569 Stuttgart, Germany

Ferrofluids exhibit unusual hydrodynamic effects due to the magnetic nature of their constituents. A striking example in a classical ferrofluid happens when the magnetization is increased beyond a critical magnetization as this triggers a Rosensweig instability which is characterized by the appearance of self-organized structures or droplet crystals.
In the experiment we observe a similiar behavior in a sample of ultracold dysprosium atoms, a quantum ferrofluid. By controlling the short-range interaction with a Feshbach resonance we can induce a finite-wavelength instability due to the dipolar interaction, in close similarity to the Rosensweig instability.
Subsequently, we observe the spontaneus transition from an unstructured superfluid to an ordered arrangement of droplets by in situ imaging, shown in figure 1. These patterns are surprisingly long-lived and show hysteretic behavior. This stability of the observed droplets is unexpected and in contradiction with the theoretical predictions.

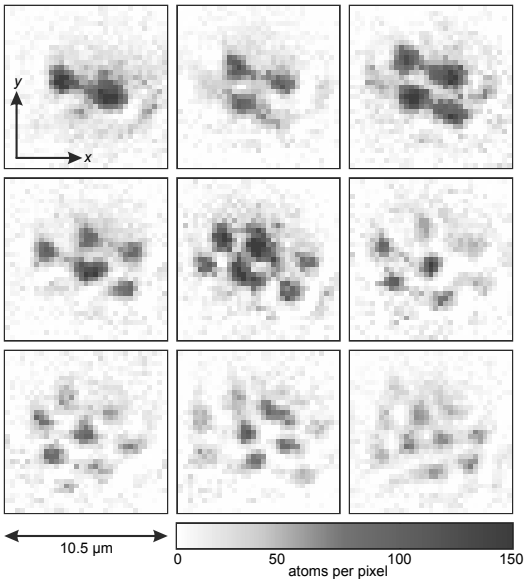

Fig. 1 Single-shot in situ images of droplet patterns with droplet numbers ranging from two to ten [1].

To investigate the mechanisms involved in the droplet stability, we transferred the sample to a waveguide configuration. In this waveguide we are able to observe isolated droplets as well as interacting chains of droplets. As opposed to a Bose-Einstein condensate which expands along the waveguide direction, these droplets remain self-confined.
Using novel techniques to measure the density and its scaling behaviour with interactions, we were able to demonstrate that quantum fluctuations constitute the stabilization mechanism. In addition, time-of-flight measurements allowed us to observe interference between droplets [2].

References

[1] Holger Kadau, Matthias Schmitt, Matthias Wenzel, Clarissa Wink, Thomas Maier, Igor Ferrier-Barbut & Tilman Pfau, *Observing the Rosensweig instability of a quantum ferrofluid*, Nature **530**, 194-197 (2016).
[2] Igor Ferrier-Barbut, Holger Kadau, Matthias Schmitt, Matthias Wenzel & Tilman Pfau *Observation of quantum droplets in a strongly dipolar Bose gas*, arXiv: 1601.03318, accepted in Phys. Rev. Lett. (2016).

Recent experiments with dipolar quantum gases: realization of spin models and new cooling methods

Bruno Naylor[1,2], Aurélie de Paz[1,2], Etienne Maréchal[1,2], Paolo Pedri[1,2], Bruno Laburthe-Tolra[1,2], Laurent Vernac[1,2] and Olivier Gorceix[1,2],

1. LPL, CNRS, UMR7538, F-93430 Villetaneuse, France

2. Laboratoire de Physique des Lasers, Université Paris 13, Sorbonne Paris Cité, F-93430 Villetaneuse, France

Ultracold atom gases stand as exquisitely controllable systems to investigate quantum many-body physics. We use high-spin dipolar chromium atoms in optical lattices to simulate quantum magnetism. Our systems enable the analysis of out-of-equilibrium spin dynamics as described through Hubbard models including long-range interactions between distant lattice sites [1]. We have studied the interplay between super-exchange mechanisms and dipolar spin exchanges as the quantum gas is driven from the Mott insulating phase to the superfluid phase [2] showing the intricate coupling of spin dynamics and transport. These studies are prone to be extended to dipolar Fermi seas using the recently demonstrated degenerate gases made of ^{53}Cr fermionic atoms [3].
In a complementary set of experiments, we proposed and demonstrated a new cooling method for Bose-Einstein condensates by spin distillation [4]. Rapid demagnetization and spin filtering of our Cr BEC held in an optical trap resulted in a new type of evaporative cooling with a significant reduction of the entropy of the trapped gas (by a factor of two in one cooling cycle). Technical reasons (B-field stability, signal-to-noise ratio, …) and one issue specific to chromium, that a Cr-BEC depolarizes below a critical B-field, limited the achievable temperature in our experiment to 140nK. Nevertheless, applying the cooling method of spin distillation to Na BECs is expected to result into temperatures well below 1nK.
This work is supported by Ministère de l'Enseignement Supérieur et de la Recherche (within Contrat Plan Etat Région - CPER) and by Conseil Régional Ile-de-France (within IFRAF / DIM Nano-K). BN thanks INP/CNRS for support.

References

[1] A. de Paz et al., Phys. Rev. Lett. **111**, 185305 (2013)
[2] B. Naylor et al., Phys. Rev. A **93**, 021603 Rapid (2016)
[3] B. Naylor et al., Phys. Rev. A **91**, 011603 Rapid (2015)
[4] B. Naylor et al., Phys. Rev. Lett. **115**, 243002 (2015)

High-Contrast and Narrow Magneto-Optical Resonance in Rb Vapour Cell

Denis Brazhnikov[1,2], Alexey Novokreshchenov [1], Alexey Taichenachev[1,2], Valeriy Yudin[1–3], Christina Andreeva[4], Vasiliy Entin[2,5], Igor Ryabtsev[2,5], Stepan Ignatovich[1], Nikolai Kvashnin[1], and Mikhail Skvortsov[1]

1. Institute of Laser Physics SB RAS, pr. Lavrentieva 13/3, Novosibirsk 630090, Russia
2. Novosibirsk State University, ul. Pirogova 2, Novosibirsk 630090, Russia
3. Novosibirsk State Technical University, pr. K. Marksa 20, Novosibirsk 630073, Russia
4. Institute of Electronics, Tzarigradsko chaussee blvd 72, Sofia 1784, Bulgaria
5. Rzhanov Institute of Semiconductor Physics SB RAS, pr. Lavrentieva 13, Novosibirsk 630090, Russia

Electromagnetically induced transparency (EIT) resonances caused by coherent population trapping (CPT) have been found to be useful in many directions of laser physics, nonlinear optics and, especially, quantum metrology. The resonances of the opposite sign (electromagnetically induced absorption – EIA) have far less applications due to some problems. Indeed, buffer-gas-filled or antirelaxation-coated cells are exploited everywhere for improving the properties of EIT. Unfortunately, these methods are useless in the case of EIA in standard observation schemes [1,2] due to collisional depolarization of excited state. There are several "non-standard" methods for observing EIA signals, but it is still very hard to get simultaneously narrow (~kHz) and high-contrast (> 50%) EIA resonances.

We study EIA in the Hanle configuration with the help of a new scheme proposed previously [3]. This resonance usually appears as a subnatural-width dip in the laser-wave transmission signal from a vapour cell, when the magnetic field is being scanned. The new scheme allows us using a buffer gas for improving the properties of EIA. The method implies using pump and probe counterpropagating waves with the same frequency and orthogonal linear polarizations. We considered the D_1 line of ^{87}Rb atom (λ=795 nm, $\gamma=2\pi\times5.57$ MHz), whose dipole transitions are open (i.e. the branching ratio of a particular transition differs from unity). It is well known that the openness of a transition suppresses the amplitudes of EIT as well as EIA resonances in standard schemes of observation. In our scheme the openness played crucial and positive role and led to the great increase of the contrast of the nonlinear resonance. In particular, the theory showed that the contrast can reach values up to 100% at kHz or even sub-kHz width (Fig.1a).

Our experimental result is shown in Fig.1b. A buffer-gas-filled cell with the natural mixture of rubidium isotopes was used (Ar pressure ≈ 5 Tor). The cell was placed in a two-layer magnetic shield (without the end caps) that suppressed the inhomogenity of the stray magnetic field down to approximately 8 mG. The cell dimensions were 60 x 30 mm. The diameter of the laser beams was 0.9 mm. We observed the contrast of 50-85%, depending on the atomic transition, pump beam power and temperature of the cell. The EIA resonance in Fig.1b has the width of about 20 mG (≈15 kHz), which is determined mainly by the power broadening and inhomogeneous stray magnetic field. We expect that further improvements of the setup (adding the third magnetic layer with the end caps, increasing the diameter of the pump beam) will bring better results. We are also going to test the proposed method using an antirelaxation-coated vapour cell.

The work was supported by the RFBR (15-02-08377, 15-32-20330, 14-02-00712, 14-02-00939), the RF Ministry of Education and Science (order no. 2014/139, project no. 825), the Presidium of SB RAS, and the EU project FP7-PEOPLE-2011-IRSES №295264 "COSMA".

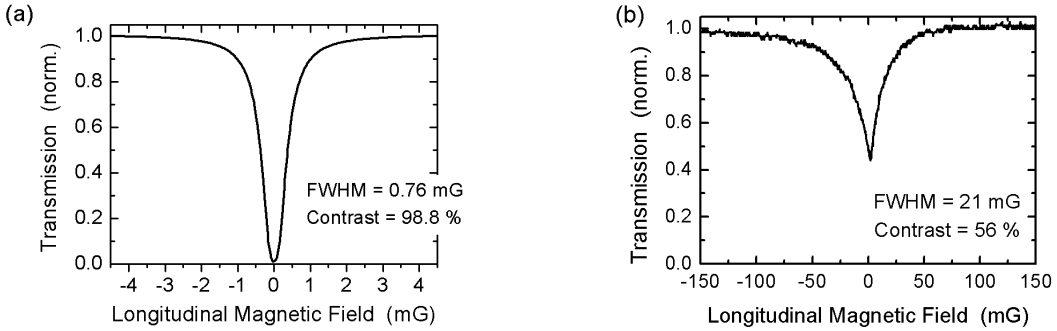

Fig. 1 EIA resonance in the probe-wave transmission through a buffer-gas-filled cell: a) Numerical calculation for the atomic transition $F_g=1\rightarrow F_e=1$, b) Experimental result with P_{pump} = 340 μW, P_{probe} = 4.4 μW, and T_{cell} = 374 K.

References

[1] A.M. Akulshin, S. Barreiro, A. Lezama, Phys. Rev. A **57**, 2996 (1998).
[2] Y. Dancheva, G. Alzetta, S. Cartaleva, M. Taslakov, Ch. Andreeva, Opt. Commun. **178**, 103 (2000).
[3] D.V. Brazhnikov, A.V. Taichenachev, A.M. Tumaikin, V.I. Yudin, Laser Phys. Lett. **11**, 125702 (2014).

Theoretical and experimental studies of selective reflection effect in a nanocell filled with alkali vapor

E. Klinger[1], **A. Amiryan**[1,2], **Y. Pashayan-Leroy**[1], **C. Leroy**[1], **A. Sargsyan**[2], **D. Sarkisyan**[2], **A. Papoyan**[2]

1. Laboratoire Interdisciplinaire Carnot de Bourgogne, UMR CNRS 6303,
Université de Bourgogne - Franche-Comté, 9 avenue Alain Savary, BP 47870, 21078 Dijon Cedex, France
2. Institute for Physical Research, NAS of Armenia, 0203 Ashtarak-2, Armenia

Numerous applications have been found using selective reflection of light from the interface of a dielectric surface and resonant atomic vapor [1]. This effect is known to be an efficient spectroscopic tool for studies of high-density vapor, atom-surface interaction, etc. Extension of this technique to the case of nanometric-thickness cells having a space between windows of the order of resonant radiation wavelength is promising both for deeper understanding of fundamental processes underlying interaction of laser radiation with atomic system and for new applications such as magnetic-field controlled tunable locking of laser frequency to atomic resonance lines [2]. Meanwhile, unlike the case of ordinary cells, theoretical treatment of selective reflection from nanocells is significantly elaborated, involving additional effects, which has to be taken into account. Preliminary experimental studies demonstrate that the reflection spectrum indeed exhibits dramatic rapid oscillations with thickness L.

We have analyzed possible influence of the concomitant effects inherent to resonant interaction of laser radiation with atoms confined in nanocells on selective reflection spectra in order to develop an appropriate theoretical model, which will be further verified and elaborated through experimental realization. The following processes are considered: velocity-anisotropic contribution of atoms and velocity-selective optical pumping; coherent Dicke narrowing occurring at $L = (2n+1)\lambda/2$ thickness; and interplay of forward and backward beams (Fabry-Pérot behavior) observed with $L = n\lambda/2$ period. Findings of this work will be used to define conditions of experimental studies using Rb or Cs nanocells with variable thickness.

Research conducted in the scope of the International Associated Laboratory IRMAS (CNRS-France & SCS-Armenia).

References

[1] A. Badalyan, V. Chaltykyan, G. Grigoryan, A. Papoyan, S. Shmavonyan, M. Movsessian, *Eur. Phys. J. D* **37**, 157-162 (2006).
[2] E.A. Gazazyan, A.V. Papoyan, D. Sarkisyan, A. Weis, *Laser Phys. Lett.* **4**, 801-808 (2007).

E1 transitions and lifetimes for Kr VIII

Gültekin Çelik

Selcuk University, Faculty of Science, Department of Physics, 42075 Konya, Turkey

Transition probabilities are very sensitive to the different interaction schemes used in studies of the atomic structure, allowing verification of their validity. In addition, spectroscopic data are related to the common interest to investigate the characteristics of excited atoms and ions, and for checking of the validity of the new methods of calculation. Transition probabilities and lifetimes for states of Cu I and Cu iso-electronic sequence are important for the determination of impurity concentration in high temperature plasmas [1]. In the Cu-like ions, the transitions from satellite lines to the brightest Ni-like ions and are of great importance for M-shell diagnostics of heavy ions.

We have determined allowed transition probabilities and lifetimes of excited levels for Cu-like krypton. The weakest bound electron potential model (WBEPM) theory and the quantum defect orbital (QDO) theory have been used. The accuracy of the evaluated spectroscopic parameters such as transition probabilities and lifetimes depends upon the energies of initial and final levels and the ionization potential E_{limit} of the atom in all of semi-empirical methods. We employed experimental energy values and theoretical expectation values of radii in these calculations. Previously, two study for Cu and Cu-like Zn have been done using the WBEPM theory and the QDO theory [2,3]. The calculated transition probabilities and lifetimes have been compared with available theoretical results [4-6]. A good agreement with results in literature has been obtained. Moreover, some transition probability and the lifetime values not existing in the literature for some highly excited levels have been obtained using these methods.

References

[1]E. Biemont, F. Fryczynski, P. Palmeri, P. Quinet, C.J. Zeippen. J. Quant. Spectrosc. Radiat. Transfer **55**, 215 (1996).
[2]G. Çelik, E. Erol, E. and M. Taşer, J.Quant. Spec.Radiat.Trans. **129,** 263(2013)
[3]G. Çelik, Ş. Ateş, and E. Erol, Canadian Journal of Physics, **93,** 1015 (2015)
[4]A. Lindgard, L.J. Curtis, I. Martinson and S.E. Nielsen, Physica Scripta, **21**, 47(1982)
[5]H.S. Chou and W.R. Johnson Physical Review A, **56,** 2424 (1997)
[6]A.E. Livingston, L.J. Curtis, R.M. Schertman and H.G. Berry Physical Review A, **21(3),** 771(1980)

Bayesian Statistics for Atomic Physics

MartinoTrassinelli[1]
1. Institut des NanoSciences de Paris, CNRS, Sorbonne Universités UPMC Univ Paris 06, Paris, France

In certain cases of analysis of experimental data, the standard probability theory reaches its limitations. As an example, in the low statistics atomic spectrum with unresolved peaks as in Fig. 1 left, how can we objectively determine the number of contributions? A model with additional parameters corresponds often to a lower value of χ^2 (or higher likelihood) due to additional degrees of freedom that allow us to better fit the data. But what is the plausibility for having four peaks instead of three? In other words, given a set of experimental data, how can we test different hypothesis and assign them a probability? This is a general question for many situations where data modelling is not univocal and the model parameters have to be evaluated. This type of problem is often encountered, like in particular in astrophysics and cosmology where experiments cannot be repeated, as in the recent discovery of gravitational waves, where only one observation is available (at present). In this domain as in many others, a different approach to define probability has to be applied using data analysis methods based on the work of Th. Bayes, P.-S. Laplace, H. Jeffreys, etc. commonly called *Bayesian statistics* [1-4].

We present here some practical uses of Bayesian methods for cases often encountered in atomic physics. In particular, we will show how it is possible to calculate, for low-statistic data presented in Fig. 1 (left), the most likelihood number of peaks from the calculation of the probability of each hypothesis (number of peaks) using the Bayes' theorem and the *Bayesian evidence* (also discussed in Ref. [5]). Moreover, considering a non-trivial line profile from a spectrometer, we will show how to choose the correct shape to be adopted and how to extract accurately its position (with the associated uncertainty) even if the choice of the shape is not unambiguous. In all examples, we use a newly developed computational tool called `Nested_fit` that will be presented as well. This program is based on the nested sampling algorithm [6]; for a given data set and chosen model, it provides (i) the *Bayesian evidence* for the comparison of different hypotheses and (ii) the parameter probability and correlation distributions. In Figure 1, we show some typical outputs of `Nested_fit` for the low-statistic spectrum discussed before, assuming a four-peak model. On the left, the predictions corresponding to the most probable parameter set are compared to the experimental data. On the right, the 2D histogram of the probability distribution of the first and second peak positions is shown.

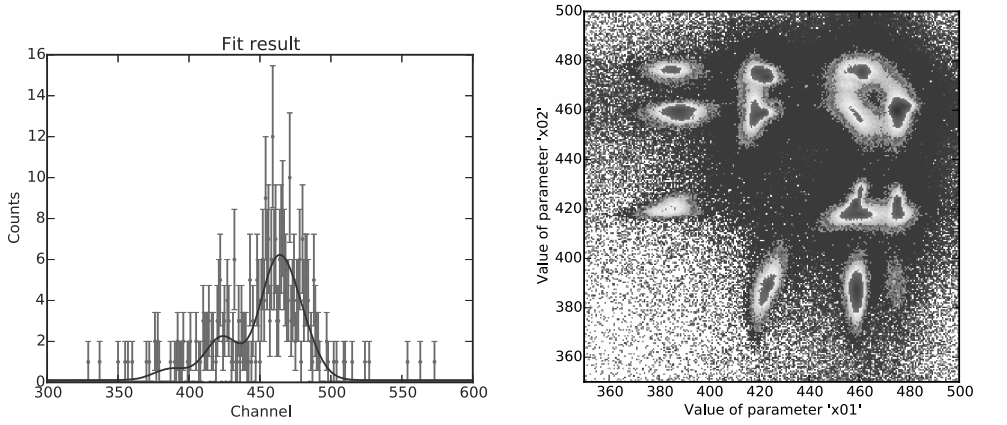

Fig. 1 Left: High-resolution X-ray spectrum of $1s2p\ ^3P_2 \rightarrow 1s2s\ ^3S_1$ helium-like uranium intrashell transition from Ref. [7] and the result of the fit assuming the presence of four peaks. Right: 2D histogram of the probability distribution of two parameters corresponding to the positions of two different peaks. As we can see, the two positions are strongly correlated and they can assume four possible different value.

References

[1] M. Bayes and M. Price, Philosophical Transactions **53**, 370-418 (1763).
[2] P.S. Laplace, *Essai philosophique sur les probabilités*, Bachelier (1825).
[3] H. Jeffreys, *Theory of Probability*, Oxford, U.K.: Oxford University Press (1961).
[4] E.T. Jaynes and G.L. Bretthorst, *Probability Theory: The Logic of Science*, Cambridge Univ. Press (2003).
[5] D.S. Sivia and C.J. Carlile, The Journal of Chemical Physics **96**, 170-178 (1992).
[6] J. Skilling, Bayesian Anal. **1**, 833-859 (2006), D.S. Sivia and J. Skilling, *Data analysis: a Bayesian tutorial*, Oxford Univ. Press (2006).
[7] M. Trassinelli *et al.*, Eur. Phys. Lett. **87**, 63001 (2009).

Transition probabilities abd oscillator strengths for Nitrogen like Fluorine

Murat Yıldız
KaramanogluMehmetbey University, Faculty of Science, Department of Physics, Karaman, Turkey

Transitions in ions of the nitrogen isoelectronic sequence are frequently observed in the spectra of astrophysical sources as well as in tokamak and laser-produced plasmas [1]. Because of the importance in astrophysics and plasma physics many of theoretical and experimental study has been performed for nitrogen sequence.

In this study, the transition probabilities and oscillator strengths have been calculated using weakest bound electron potential model theory (WBEPMT) for Nitrogen like Fluorine. In the determination of relevant parameters, we employed theoretical expectation values of radii and the necessary energy values have been taken from experimental energy data in the literature [2]. The calculated transition probabilities and oscillator strengths have been compared with available results from the literature. The WBEPM theory is especially useful when large numbers of transition probabilities, oscillator strengths and lifetimes are required. Because wave functions and matrix elements are computed quickly and automatically using only energy level, ionization potential data and the expectation values of radii belonging to levels as inputs. Moreover, spectroscopic parameters belong to higher excited levels can be readily obtained using this method. It is generally considered that the choice of the WBEPM theory is justified for transitions involving high–energy unperturbed highly excited states. Previously, the many of studies obtained using the WBEPM theory were done and very satisfactory ionization potential, transition probability, oscillator strength and lifetime results were obtained for both allowed and forbidden transitions [3-6].

References

[1]P.Ruynkun, P. Jönsson, G.Gaigalas, F. F. Fischer At. Data Nucl. Data Tables 100 2 315-402 (2014)
[2]A. Kramida, Yu, Ralchenko, J.Reader and NIST ASD Team (2015) http://physics.nist.gov/asd
[3] M.Yıldız, Y. Gökçe Can. J. Phys. **92**, 1 82-85 (2014)
[4] M.Yıldız Acta Physica Polonica A **123**, 1 25-30 (2013)
[5] G. Celik, Y. Gokce, M. Yildiz At. Data Nucl. Data Tables **100** 3 792-801 (2014)
[6] G. Çelik, E. Erol and M.Taşer J. Quant. Spectrosc. Radiat. Transfer **129** 263-271 (2013)

Design of mechanically compensated Penning trap for the study of ions in extreme laser field

Sugam Kumar[1], S. Ringleb[2], Nils Stallkamp[2], M. Vogel[3], W. Quint[4], Th. Stöhlker[2], C.P. Safvan[1]

1. Inter-University Accelerator Centre, Aruna Asaf Ali Marg, New Delhi, India.

2. Helmholtz-Institut Jena, 07743 Jena, Germany

3. GSI Helmholtzzentrum für Schwerionenforschung, 64291 Darmstadt, Germany

4. Physikalisches Institut, Ruprecht Karls-Universität Heidelberg, 69120 Heidelberg, Germany

We have designed and constructed a mechanically compensated Penning trap[1] as a tool to confine atomic ions in static electric and magnetic fields for the study of non-linear processes such as multi-photon ionization (MPI) from well-defined initial charged states and with a large range of photon energies by non-destructive observation. During the interaction of ions with extreme laser fields it is also possible to realize above-threshold ionization (ATI), tunneling ionization (TI) and above-the-barrier ionization (ABI) processes.

The experimental setup consists of a cylindrical Penning trap with 20mm inner diameter located at the magnetic field centre of a dry superconducting magnet which can produce homogeneous magnetic fields up to 6 T. In the region of ±10mm from the centre of magnet bore the homogeneity of magnetic flux density is better than $\pm 10^{-4}$ T [2]. A pulse-tube cooler is used to cool the trap electrodes, cryo-electronics and radiation shields. The trap will be cooled down to 4.2K and as a result the background pressure in the trap is expected to be 10^{-12} Torr. We have chosen a 3-pole open-endcap (figure 1) cylindrical Penning trap with geometric compensation which consists of ring electrode and a pair of endcap electrodes with a separation distance of 17.4mm with an additional set of capture electrodes (length 20mm) on either side of endcap electrodes for dynamic capture of ions into the trap. These electrodes have a conical opening to accept laser beams up to an aperture of f/5. This geometry leads to a ring electrode with a large axial extension, such that ions in the trap centre are efficiently coupled to the ring. The detection of ion motions is done through Fourier-transform ion cyclotron resonance (FT-ICR). Since the ring electrode will be used for FTICR as well as for the purpose of Rotating wall drive, the ring electrode is split into 8 segments of which 4 are 30^0 segments which will be used for rotating wall drive while the remaining 4 segments are of 60^0 and used for pick up of radial signal (FTICR). A Gap of 0.25mm separation between each segment has been kept. Segmented ring electrodes are separated from other with rectangular pieces of sapphire blocks as shown in figure 2. Two high quality factor resonators with resonant frequencies of 457kHz and 702kHz are employed to measure the axial frequencies whereas a helical resonator which amplifies multiples of fundamental frequencies is the used to measure cyclotron frequencies.

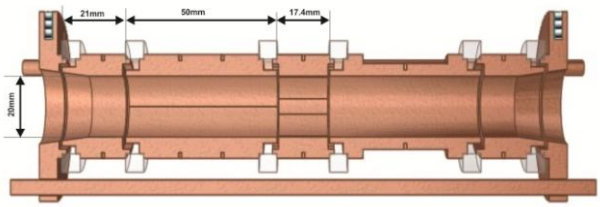

Fig. 1 Cross section geometry of 3-pole mechanically compensated Penning trap with pair of capture electrodes with conical opening.

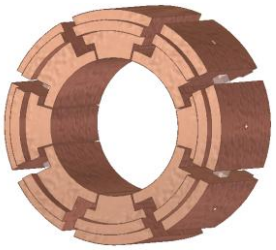

Fig. 2 Three dimensional schematic view of the segmented ring electrode

The FLASH Laser facility at DESY, Germany may be used as a source of high-intensity photons. It has the capability to produce photons with wavelengths down to 4.5 nm (275 eV) in pulses of a few femto-seconds duration resulting in a peak power of around 5GW with repetition rate of 10Hz. This allows photo-ionization studies well inside the non-linear regime. The plan also includes the use of the PHELIX laser with wavelength 1053 nm at GSI and POLARIS (1030 nm) and JETI (800 nm) at Jena, Germany with intensities up to order 10^{21}W/cm^2.

References

[1] G. Gabrielse, L. Haarsma and S.L. Rolstone, *Open-endcap Penning Traps for high precision experiments*, Int. J. Mass Spectr. Ion Proc. **88**, 319 (1989).

[2] M.Vogel, W. Quint, G.G. Paulus and Th. Stöhlker, *A Penning trap for advance studies with particles in extreme laser fields*, NIMB **285**, 65 (2012).

Interaction of the $D0_u^+$ and $\beta 1_g$ Ion–Pair States in Free Iodine Molecule

Vera V. Baturo, Igor N. Cherepanov, Sergey S. Lukashov, Vitaly V. Muravyev, Sergey A. Poretsky, Anatoly M. Pravilov

Department of Physics, Saint-Petersburg State University, SPbSU, 7/9 Universitetskaya nab., St. Petersburg, 199034 Russia

We present the results of analysis of perturbations between $D0_u^+$ and $\beta 1_g$ ion-pair states in free I_2 molecule. The electronic states of opposite g/u symmetry may be coupled only by the hyperfine interaction (magnetic-dipole (MD) and electric-quadrupole (EQ) interactions, primarily).

Spectroscopic characteristics of the both states are well known [1, 2]. Preliminary analysis has shown that the following pairs of vibronic states contain close-lying rotational levels satisfying selection rules $|\Delta\Omega| \leq 1$, $|\Delta J| = \leq 1$ for the *MD* and $|\Delta\Omega| \leq 2$, $|\Delta J| \leq 2$ for the *EQ* interactions:

$\beta 1_g$, 13, $J_\beta \sim D$, 12, J_D, $J_D = J_\beta + 2, +1, 0$;
$\beta 1_g$, 28, $J_\beta \sim D$, 28, J_D, $J_D = J_\beta + 2, +1, 0$;
$\beta 1_g$, 47, $J_\beta \sim D$, 48, J_D, $J_D = J_\beta + 2, +1, 0$.

Coupling among all the pairs was studied after optical-optical double resonance population of the β rovibronic levels. We did not find any mixing corresponding to ΔJ=2, so we assume that there is no EQ hyperfine coupling between the states.

Analysis of integral $D \rightarrow X$ and $\beta \rightarrow A$ luminescence intensities allowed us to estimate the electronic matrix element of the interaction between β and *D* states, $H_{hf}^{el}(\beta, D)$. It was found to be about 0.05 cm^{-1}, close to $H_{hf}^{el}(1_u, 2_g)$ = 0.048(6) cm^{-1} obtained for the $1_u(^1D)$ and $2_g(^1D)$ rovibronic states in [3]. On the other hand, this value is ten times smaller than those for the valence 0_g^+ and 1_u(bb) as well as 0_g^+ and $0_u^-(bb)$ states [4].

This work continues the series of studies on perturbations between iodine I_2 valence and IP states. Heterogeneous and hyperfine interactions between valence states correlating with the $I(^2P_{1/2})$ + $I(^2P_{1/2})$ (*bb*) dissociation limit and heterogeneous perturbation of the $I_2(D0_u^+$ and $\delta 2_u)$ states described in the second order of perturbation theory have been observed and studied in [4, 5].

References

[1] J.P. Perrot, M. Broyer, J. Chevaleyre, B. Femelat, *Extensive study of the $1_g(^3P_2)$ ion pair state of I_2*, J. Molec. Spectrosc, **98,** 161 (1983).
[2] J. Tellinghuisen, *The D state of I_2: a case study of statistical error propagation in the computation of RKR potential curves, spectroscopic constants, and Franck–Condon factors*, J. Molec. Spectrosc, **217,** 212 (2003).
[3] Y.Nakano, H.Ukeguchi, T.Ishiwata, *Observation and analysis of the $2_g(^1D)$ ion-pair state of I_2: The g/u mixing between the $1_u(^1D)$ and $2_g(^1D)$ states*, J. Chem. Phys., **121,** 1397 (2004).
[4] V.V. Baturo, I.N. Cherepanov, S.S. Lukashov, S.A. Poretsky, A.M. Pravilov, A.I. Zhironkin, *Heterogeneous and hyperfine interactions between valence states of molecular iodine correlating with the $I(^2P_{1/2}) + I(^2P_{1/2})$ dissociation limit* (sent to J. Chem. Phys.).
[5] V.V. Baturo, S.S. Lukashov, S.A. Poretsky, A.M. Pravilov, O.S. Vasyutinskii, *Mixing of the $D0_u^+$ and $\delta 2_u$ ion-pair states of iodine molecule*, Chem. Phys. Letts. **638**, 244 (2015).

Time Resolved Spectroscopy of Excited Neutrals in Low Temperature Afterglow Plasmas

Ábel Kálosi[1], Petr Dohnal[1], Radek Plašil[1], Juraj Glosík[1]

1. Department of Surface and Plasma Science, Faculty of Mathematics and Physics, Charles University in Prague, V Holešovičkách 2, 18000 Prague, Czech Republic

Excited neutrals have major influence on thermalization of electrons in low temperature afterglow plasmas [1]. The electron temperature is a crucial parameter in afterglow ion-electron recombination experiments. These experiments are usually carried out in different mixtures of neutral gases depending on the studied ion. The aim of our current study is to confirm the fast removal of long-lived sources of energy that could heat the electron gas in afterglow plasmas.

We have studied experimentally the time evolution of highly excited argon atoms and helium excimers in afterglow plasmas by means of cavity ring-down absorption spectroscopy (for further details see [2]). These molecules are produced in low temperature discharges in pure helium and helium with small admixtures of argon. In afterglow recombination experiments helium is used as the buffer gas and argon is added to remove undesired helium metastable atoms [3].

In our present experiments we focus on the case of the He/Ar mixture to construct a scheme of relevant processes that lead to the thermalization of the afterglow plasma. He/Ar gas mixtures are also used in analytical applications where metastable states play a crucial role in the excitation scheme [4,5]. Preliminary results at neutral gas temperature of 300 K show similar dependence of time evolution of absorption by excited Ar and He_2 neutrals on Ar number density as in our previous studies in He/Ar/H_2 gas mixtures [6]. Examples of measured data are shown in Fig. 1.

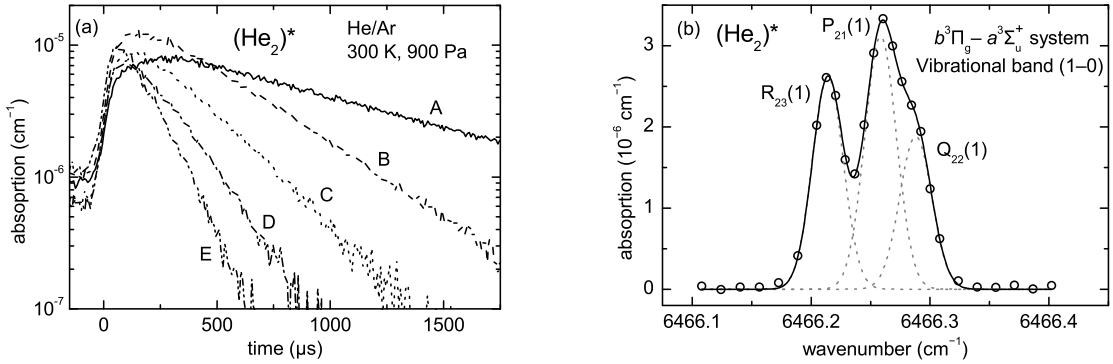

Fig. 1. Panel (a): Time evolutions of the absorption coefficients of an $(He_2)^*$ absorption line (transition $R_{23}(1)$) measured in mixtures of He/Ar at different Ar number densities. Capital letters A, B, C, D, and E indicate [Ar] = 0, 7.5, 15, 29, and 56×10^{12} cm^{-3}, respectively. The time is set to zero at the beginning of the afterglow. Panel (b): Absorption line profiles of the $(He_2)^*$ transitions originating from the ground vibrational state of the $a^3\Sigma_u^+$ electronic state that correspond to the measured time evolutions in panel (a). For spectroscopic notation see Ref. [7]. The lines were fitted by Gaussian line profiles.

In H_3^+ recombination experiments we are using He/Ar/H_2 gas mixtures, where we observed a dependence of the measured time evolution of absorption by excited Ar and He_2 molecules on the Ar and H_2 number densities in the gas mixture [6]. From these observations we concluded that the most likely sources of these excited neutrals in the afterglow are metastable helium atoms produced during the discharge, which at typical experimental conditions are removed from the afterglow within 100 μs.

References

[1] I. Korolov, R. Plašil, T. Kotrík, P. Dohnal, O. Novotný, and J. Glosík, *Measurements of EEDF in Helium Flowing Afterglow at Pressures 500 – 2000 Pa*, Contrib. Plasma Phys. **48**, 461 (2008).

[2] P. Macko, G. Bánó, P. Hlavenka, R. Plašil, V. Poterya, A. Pysanenko, O. Votava, R. Johnsen, and J. Glosík, *Afterglow studies of H_3^+ ($v = 0$) recombination using time resolved cw-diode laser cavity ring-down spectroscopy*, Int. J. Mass. Spectrom. **233**, 299 (2004).

[3] J. Glosík, P. Dohnal, P. Rubovič, Á. Kálosi, R. Plašil, Š. Roučka, and R. Johnsen, *Recombination of H_3^+ ions with electrons in He/H_2 ambient gas at temperatures from 240 K to 340 K*, Plasma Sources Sci. Technol. **24**, 065017 (2015).

[4] K. Wagatsuma, *Emission Spectroscopic Study on Gas–Gas Interactions in Glow Discharge Plasmas Using Several Binary Gas Mixtures*, Anal. Sci. **26**, 303 (2010).

[5] S. Mushtaq, E. B. M. Steers, J. C. Pickering,and K. Putyera, *Selective and non-selective excitation/ionization processes in analytical glow discharges: excitation of the ionic spectra in argon/helium mixed plasmas*, J. Anal. At. Spectrom. **29**, 681 (2014).

[6] Á. Kálosi, P. Dohnal, L. Augustovičová, Š. Roučka, R. Plašil, and J. Glosík, *Monitoring the removal of excited particles in He/Ar/H_2 low temperature afterglow plasma at 80 – 300 K*, Eur. Phys. J. Appl. Phys., in press (2016).

[7] C. Focsa, P.F. Bernath, and R. Colin, *The Low-Lying States of He_2*, J. Mol. Spectrosc. **191**, 209 (1998).

Measurements of the second overtone P branch carbon monoxide transitions in argon by cavity ring-down and broadband comb spectroscopy

Kamila Stec[1], Vinicius Silva de Oliveira[2], Mikołaj Zaborowski[1], Agata Cygan[1], Grzegorz Kowzan[1], Szymon Wójtewicz[1], Piotr Wcisło[1], Roman Ciuryło[1], Daniel Lisak[1], Axel Ruehl[1], Ingmar Hartl[1], Ryszard S. Trawiński[1], Piotr Masłowski[1]

1. Institute of Physics, Faculty of Physics, Astronomy and Informatics, Nicolaus Copernicus University in Toruń, Grudziadzka 5, 87-100 Toruń, Poland

2. Deutsches Elektronen-Synchrotron (DESY), Notkestrasse 85, 22607 Hamburg, Germany

Cavity ring-down spectroscopy (CRDS) is an established technique based on measurements of dependence of light decay time constant on the gas sample composition inside the cavity. Its insensitivity to laser power fluctuations and negligible influence of the instrumental line shape function makes it a powerful tool for sensitive trace gas detection and detailed spectral line-shape analysis.

Absorption spectroscopy based on direct interaction of optical frequency comb (OFC) beam with a gas sample, so called direct frequency comb spectroscopy (DFCS), allows for measurements of molecular absorption spectra in wide spectral range and with high signal-to-noise ratio. It removes the limitations of cw-laser spectroscopy caused by time consuming tuning and limited frequency range. Fourier transform spectrometers (FTS) coupled with OFC provide broadband spectral bandwidth and acquisition times orders of magnitude shorter than traditional ones with FTS coupled with thermal sources [1]. The resolution of FTS with OFC is not limited by the maximum optical path difference between the interferometer arms [2], which makes it suitable for simultaneous acquisition of tens of molecular lines in wide pressure range.

We present measurements of the P branch transitions from the CO second overtone in wide pressure range, performed with both CRDS and OFC-FTS system. The first setup is a frequency-stabilized Pound-Drever-Hall-locked CRDS spectrometer [3], linked to the OFC. The enhancement cavity with finesse of 13000 and high SNR of the spectra enable it to reach noise-equivalent absorption of $7\ 10^{-11}$ cm^{-1}. The frequency accuracy of the system is 30 kHz. The broadband system is based on an Er:fiber frequency comb, locked with two-point PDH locking scheme [4] to an enhancement cavity with finesse of 8500. The lines measured with the CRDS system are: P2, P4, P6, P9 and P14 in five pressures from 10 to 700 Torr. Line centers, line shifting and broadening parameters were retrieved, with line center position uncertainties from 130 kHz to 330 kHz. We obtained for the first time line shifting coefficients of the second overtone CO transitions in argon and observed MHz-level departures from linear behaviour. We also report line broadening coefficients of these transitions with significantly lower uncertainties than previously [5] and provide fitted coefficients of an empirical formula allowing to calculate line broadening of lines not measured in this work. The results of measurements of the same gas sample with OFC-FTS spectrometer will be presented and will include a comparison of the accuracy of the mixing ratio determination as well as the accuracy and precision of retrieved absolute line positions.

References

[1] J. Mandon, G. Guelachvili and N. Picqué, *Fourier transform spectroscopy with a laser frequency comb*, Nature Photonics **3,** 99-102 (2009).

[2] P. Maslowski, K. F. Lee, A. C. Johansson, A. Khodabakhsh, G. Kowzan, L. Rutkowski, A. A. Mills, C. Mohr, J. Jiang, M. E. Fermann and A. Foltynowicz, *Surpassing the path-limited resolution of Fourier-transform spectrometry with frequency combs*, Physical Review A **93**, 021802 (2016).

[3] A. Cygan, S. Wójtewicz, J. Domysławska, P. Masłowski, K. Bielska, M. Piwiński, K. Stec, R. S. Trawiński, F. Ozimek, C.Radzewicz, H. Abe, T. Ido, J. T. Hodges, D. Lisak and R. Ciuryło *Spectral line-shapes investigation with Pound-Drever-Hall-locked frequency-stabilized cavity ring-down spectroscopy*, The European Physical Journal Special Topics **222**, 2119–2142 (2013).

[4] A. Foltynowicz, P. Masłowski, A. J. Fleisher, B. J. Bjork, and J. Ye, *Cavity-enhanced optical frequency comb spectroscopy in the mid-infrared application to trace detection of hydrogen peroxide*, Appl. Phys. B **110**, 163–175 (2012).

[5] J. P. Bouanich and C. Haeusler, *Linewidths of carbon monoxide self-broadening and broadened by argon and nitrogen*, JQSRT 12, 695–702 (1972)

Controlled OCS molecules for the investigation of ultrafast dynamics in the molecular frame

Sebastian Trippel[1,2], Terence Mullins[1], Andrea Trabattoni[1], Joss Wiese[1], Nele Müller[1], Jens Kienitz[1,3], Jochen Küpper[1,2,3]

1. Center for Free-Electron Laser Science, DESY, 22607 Hamburg, Germany

2. Center for Ultrafast Imaging, University of Hamburg, 22761 Hamburg, Germany

3. Department of Physics, University of Hamburg, 22761 Hamburg, Germany

State-selected, strongly aligned and oriented molecular ensembles serve as ideal samples to study ultrafast chemistry in the molecular frame [1]. Possible probing mechanisms include the investigation of molecular-frame photoelectron angular distributions [2] or the measurement of structure-solved dynamics via X-ray or electron diffraction [3,4]. We have developed techniques to manipulate the motion of molecules in cold supersonic beams using strong inhomogeneous electric and laser fields [5]. State-selected molecules are aligned by strong laser fields or oriented in combination of laser fields and static electric fields. The laser pulse duration can be varied continuously between 50 fs and 500 ps. This allows for the manipulation of the rotational degrees of freedom of the molecules non-adiabatically (impulsively), as well as adiabatically and in the intermediate regime.

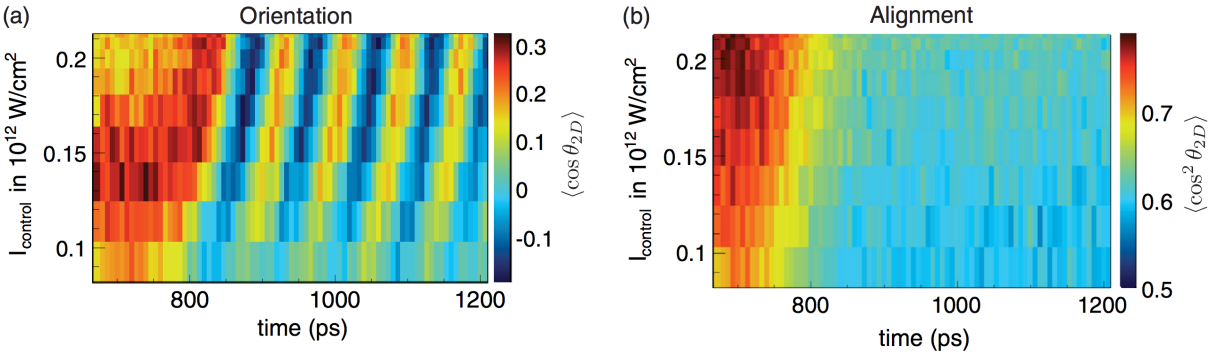

Fig. 1 (a) Degree of orientation of OCS molecule as a function of the relative delay between the orientation and probe laser pulses and the control laser peak intensity. (b) Degree of alignment extracted from the same data set as (a). Adapted from [7].

Here we present our work on the alignment and orientation of carbonyl sulphide (OCS). We have created a coherent superposition of pendular states in the strong field of the alignment laser and follow its propagation as a function of time [6]. The (non) adiabaticity of the alignment and orientation of OCS will be discussed. Furthermore we were able to obtain strong laser-field-free orientation of absolute-ground-state OCS molecules [7]. The molecules were oriented by the combination of a 485-ps-long non resonant laser pulse and a weak static electric field. The edges of the laser pulse create a coherent superposition of two rotational states resulting in revivals of strong transient molecular orientation after the laser pulse. The degree of orientation we measured corresponds to the theoretical maximum for mixing of the two states.

References

[1] J. Hansen, et al., Phys. Rev. Lett. 106, 073001 (2011).
[2] L. Holmegaard et al., Nature Physics, 6, 428 (2010).
[3] Filsinger et al., Phys. Chem. Chem. Phys.13, 2076–2087 (2011).
[4] C. J. Hensley, J. Yang, and M. Centurion, Phys. Rev. Lett. 109, 133202 (2012).
[5] S. Trippel et al., Mol. Phys. 111, 1738 (2013).
[6] S. Trippel et al., Phys. Rev. A 89, 051401(R) (2014).
[7] S. Trippel et al., Phys. Rev. Lett. 114, 103003 (2015).

Spectroscopic investigation of the $3^1\Pi_u$ state in Rb_2 molecule

Wlodzimierz Jastrzebski[1], Pawel Kowalczyk[2]

1. Institute of Physics, Polish Academy of Sciences, Al. Lotników 32/46, 02-668 Warszawa, Poland

2. Institute of Experimental Physics, Faculty of Physics, University of Warsaw, ul. Pasteura 5, 02-093 Warszawa, Poland

Development of techniques of photoassociation and magnetoassociation has renewed interest in the investigation of excited electronic states of alkali dimers. Their detailed knowledge may help to establish effective ways to transfer populations from the translationally cold, but vibrationally hot states resulting from association of two cold atoms to the molecular absolute ground state. Rubidium has been widely used in laser cooling experiments but experimental knowledge of excited electronic states of Rb_2 molecule is limited. Recently we have reported spectroscopic characterisation of two such states, $5^1\Sigma^+_u$ and $5^1\Pi_u$ as well as *ab initio* calculations of the manifold of states up to the Rb(5s) + Rb(5f) atomic limit [1].

In this contribution we present the first experimental observation of the $3^1\Pi_u$ state of rubidium dimer by recording spectra of the $3^1\Pi_u \leftarrow X^1\Sigma^+_g$ band system with the V-type optical-optical double resonance polarisation spectroscopy technique [2]. This state dissociates into Rb(5s) and Rb(6p) atoms and up to now has been known only from theoretical calculations. A wide range of rovibrational levels $0 \le v \le 50$, $25 \le J \le 173$ was observed. By using the pointwise Inverted Perturbation Approach (IPA) method [3] to our experimental data (ca. 1500 energy levels in $^{85}Rb^{85}Rb$ and $^{85}Rb^{87}Rb$ isotopologues) we obtained a rotationless potential energy curve of the $3^1\Pi_u$ state which reproduces the observed energy levels with a standard deviation of 0.08 cm^{-1}. The examples of the spectra and details of their analysis will be shown.

References

[1] W. Jastrzebski, P. Kowalczyk, J. Szczepkowski, A.R. Allouche, P. Crozet, A.J. Ross, *High-lying electronic states of the rubidium dimer – ab initio predictions, and experimental observation of the $5^1\Sigma^+_u$ and $5^1\Pi_u$ states of Rb_2 by polarization labelling spectroscopy*, J. Chem. Phys. **143**, 044308 (2015).

[2] W. Jastrzebski and P. Kowalczyk, *The $3^1\Pi_u$ and $3^1\Sigma^+_u$ states of K_2 studied by polarization labelling spectroscopy technique*, Phys. Rev. A **51**, 1046 (1995).

[3] A. Pashov, W. Jastrzębski, P. Kowalczyk, *Construction of potential curves for diatomic molecular states by the IPA method*, Comput. Phys. Commun. **128**, 622 (2000).

Mass-selective Circular Dichroism after Femtosecond Laser Ionization

Tom Ring, Alexander Kastner, Stefanie Züllighoven, Tobias Grabsch, Cristian Sarpe, Christian Lux, Arne Senftleben, Thomas Baumert

Institut für Physik und CINSaT, Universität Kassel, Heinrich-Plett-Straße 40, 34132 Kassel, Germany

Multi Photon Ionization grants access to Circular Dichroism (CD) with circularly polarized laser pulses. The analysis via time of flight mass spectra provides a mass-selective tool to distinguish chiral molecules in the gas phase [1, 2]. Hence, mixtures of chiral molecules as well as CD effects on fragments can be investigated.
Introducing a twin mass peak setup allows circumventing shot-to-shot fluctuations in laser pulse intensity, gas density or ion detection. Two foci with a small spatial displacement result in time-separated mass spectra; a change in helicity from focus to focus implements a self-referencing system [1]. Our in-line optical setup allows to combine this with femtosecond laser pulses, whose broad bandwidth promises new possibilities in chiral control. Besides the advantages of this setup we present recent findings on prototype chiral molecules.

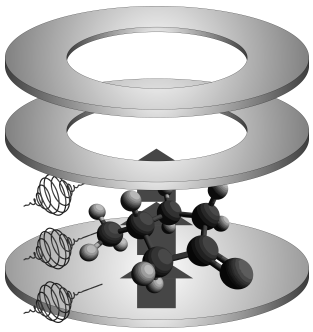

Fig. 1 Multi Photon Ionization of 3-methyl-cylopentanone within a Wiley-McLaren setup.

References

[1] Christoph Logé, Alexander Bornschlegl, and Ulrich Boesl, *Twin mass peak ion source for comparative mass spectrometry: Application to circular dichroism laser MS*, Int. J. Mass Spectrom. **281**, 134 (2009).

[2] Philipp Horsch, Gunter Urbasch, and Karl-Michael Weitzel, *Analysis of Chirality by Femtosecond Laser Ionization Mass Spectrometry*, Chirality **24**, 684 (2012).

Sub-One Per Cent Enantiomeric Excess Sensitivity using Femtosecond Photoelectron Circular Dichroism

Alexander Kastner, Christian Lux, Tom Ring, Stefanie Züllighoven, Cristian Sarpe, Arne Senftleben and Thomas Baumert

University of Kassel, Institute of Physics and Center for Interdisciplinary Nanostructure Science and Technology (CINSaT), Heinrich-Plett-Str. 40, D-34132 Kassel, Germany

Photoelectron circular dichroism (PECD) is investigated experimentally on chiral specimen with a varying amount of enantiomeric excess (e.e.). As a prototype we measure and analyze the photoelectron angular distribution from randomly oriented fenchone molecules in the gas phase resulting from ionization with circularly polarized femtosecond laser pulses. The quantification of these measurements shows a linear dependence with respect to e.e. [1]. In addition, a distinction of differences in the e.e. (denoted as detection limit) below one per cent for nearly enantiopure samples as well as for almost racemates is demonstrated. In combination with a reference the assignment of absolute e.e. values is possible. The present measurement time is a few minutes but can be reduced further. This table-top laser-based approach facilitates a widespread implementation in chiral analysis.

References

[1] A. Kastner et al., *Sub-One Per Cent Enantiomeric Excess Sensitivity using Femtosecond Photoelectron Circular Dichroism*, ChemPhysChem **17**, DOI: 10.1002/cphc.201501067 (2016).

Dissociative Ionization of Molecules PTCDA by Electron Impact

Olha Pylypchynets, Anatoly Zavilopulo

Institute of Electron Physics, Ukrainian National Academy of Sciences, Universitetska str. 21, Uzhgorod, 88017 Ukraine
E-mail: gzavil@gmail.com

The study of thin organic films has much actuality due to their wide potential applications and also they have fundamental importance in elementary-particle physics [1]. The 3,4,9,10-perylenetetracarboxilic dianhydride (PTCDA) molecule consist of perylene core (5 benzene rings) and anhydride groups which containing three atoms of O_2 and most often used as the organic film. Due to its unique optical and electronic properties, and the ability to form thin layers of the crystalline structure on various surfaces, PTCDA molecules have great prospects of practical application in photovoltaic energy converters and light-emitting devices. The aim of this work was to study the ionization functions of fragment ions PTCDA molecule resulting from dissociation by electron impact. The experiment was performed on the setup with a monopole mass spectrometer MX 7304A with a mass resolution of no worse than $\Delta M = 1$ Da [2]. Molecular beam of the PTCDA molecules was formed with a multichannel effusion source. The density of molecules in the interaction area with the electron beam was 10^{10}-10^{11} cm^{-3}. The ion source with electron ionization worked in the electronic current stabilization mode and permits electron beams with fixed energy of 5 to 90 eV at currents of 0,05 – 0,5 mA and an energy spread $\Delta E = 300$ meV. Calibration of the mass scale was performed on isotopes of Ar and Xe atoms, and the electron energy scale – for the initial part of the cross sections ionization of N_2 molecule. The experiment was conducted in two phases: on the first phase the mass spectrum was studied (mass number range 0-290 a.m.u.), and on the second the energy dependence of cross sections of dissociative ionization was measured.

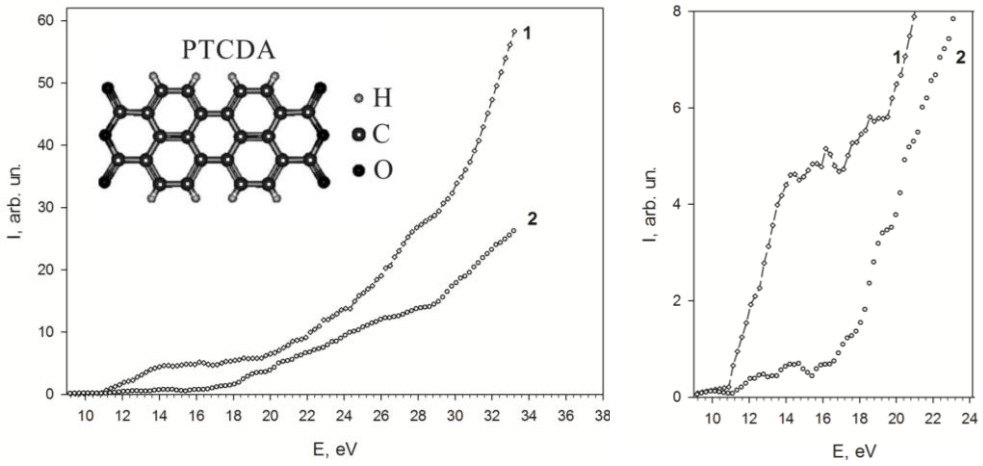

Fig. 1 The relative cross sections for ions O^+ (m/z = 16) - the curve **1** and CO^+ (m/z = 28) curve **2**.

After configuring the mass spectrometer to the allocation of a certain weight, relative cross-sections formation of fragment ions that arise in the process of dissociative ionization of PTCDA molecules was measured from threshold to 36 eV with the temperature of the source T = 470 K. The energy dependences of the O^+ and CO^+ ions formation are shown in Fig. 1. There are a number of features which are especially well manifested in the threshold area (fig.1, on the right) which can be seen on these curves. It should be noted that observed peaks with m/z = 28 and 44 in the mass spectrum correspond to the formation of CO and CO_2 molecules and indicated that the interaction of electrons with the molecules PTCDA leads to the separation and decomposition of the carboxyl groups, and the appearance of atomic oxygen (m/z = 16) means the evidence of the CO_2 molecules dissociation ($CO_2 = CO+O$). On the other hand the presence of CO and CO_2 molecules should be considered as a result of the fragmentation of unstable dicarboxylic group C_2O_3. Thus, the presence of various competitive processes is displayed on the energy dependence, particularly in the threshold energies area (Fig. 1). Energy appearance fragment ions O^+ and CO^+ were defined on the threshold areas of energy dependence by the least-squares method ($E = 10.61$ eV for O^+); ($E = 11.54$ eV for CO^+).

References

[1] A. G. Ramonova, I. V. Tvauri, S. A. Khubezhov, et. al, *Photoinduced Decomposition of PTCDA Molecules and Desorption of Their Fragments from the Films Formed on the GaAs(110) Surface*, Russian Journal of Phys. Chemistry A, **89**, No. 10, pp. 1944–1947 (2015).
[2] A.N. Zavilopulo, P.P. Markush, O.B. Shpenik and M.I. Mykyta, *ElectronImpact Ionization and Dissociative Ionization of Sulfur in the Gas Phase*, Technical Physics, **59**, No. 7, pp. 951–958. (2014).

Creation of a strongly dipolar gas of ultracold ground-state $^{23}Na^{87}Rb$ molecules

Romain Vexiau[1], Mingyang Guo[2], Bing Zhu[2], Bo Lu[2], Xin Ye[2], Fudong Wang[2], Dajun Wang[2,3], Nadia Bouloufa-Maafa[1], Goulven Quéméner[1], Olivier Dulieu[1]

1. Laboratoire Aimé Cotton, CNRS, Université Paris-Sud, ENS Cachan, Université Paris-Saclay, 91405 Orsay Cedex, France

2. Department of Physics, The Chinese University of Hong Kong, Hong Kong, China

3. The Chinese University of Hong Kong Shenzhen Research Institute, Shenzhen, China

We report the successful production of an ultracold sample of absolute ground-state $^{23}Na^{87}Rb$ dipolar molecules with a large induced electric dipole moment [1]. Starting from weakly-bound Feshbach molecules formed via magneto-association, the lowest rovibrational and hyperfine level of the electronic ground state is populated following a high efficiency stimulated Raman adiabatic passage (STIRAP). We performed a theoretical analysis of possible transfer routes and expected structure of the intermediate level using state-of-the-art molecular potentials, spin-orbit couplings and transition dipole moments. The most efficient path was determined after performing one-photon high-resolution spectroscopy of the mixed excited ($A^1\Sigma^+$ - $b^3\Pi$) molecular states. Based on an effective Hamiltonian model, a detailed interpretation of the hyperfine structure of the chosen intermediate level is achieved (Fig.1). With an external electric field, we have induced an effective dipole moment over one Debye, enough to provide strong long-range dipolar interactions. Our results pave the way toward investigation of ultracold molecular collisions in a fully controlled manner, and possibly to quantum gases of ultracold bosonic molecules with strong dipolar interactions.

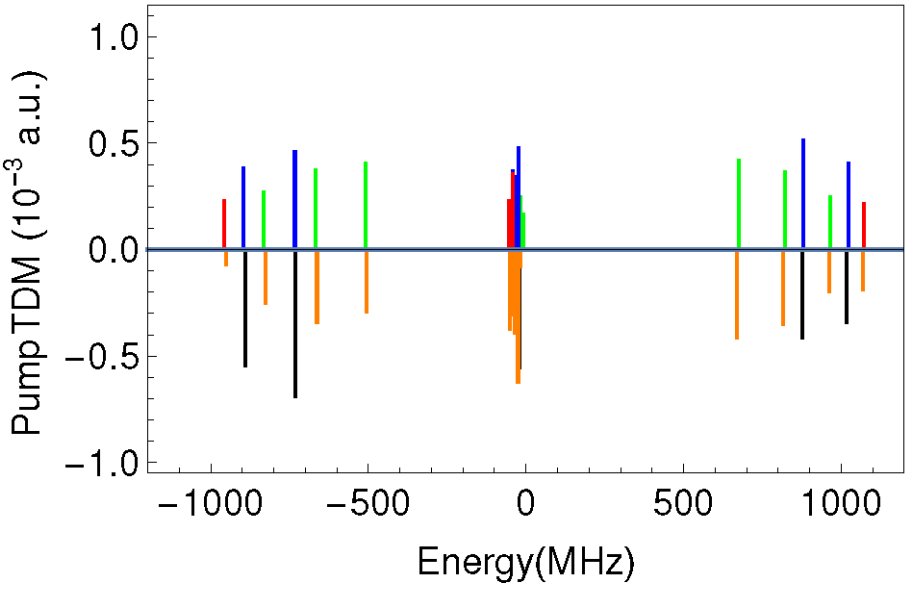

Fig. 1 Hyperfine structure of the chosen intermediate level for STIRAP. Top panel : computed spectra. Bottom panel : observed spectra.

References

[1] M. Guo, B. Zhu, B. Lu, X. Ye, F. Wang, R. Vexiau, N. Bouloufa-Maafa, G. Quéméner, O. Dulieu, D. Wang, arXiv:1602.03947, Phys. Rev. Lett., accepted}

Using ultracold atoms to operate a deterministic ion source

Cihan Sahin, Jens Benary, Andreas Müllers, Herwig Ott
Technische Universität Kaiserslautern, Erwin-Schrödinger-Str. 46, 67663 Kaiserslautern, Germany

Minimal energy spread and good control in combination with high repetition rates are desirable properties for ion sources in experiments and technical applications like precise ion implantation or ion interferometry/spectrometry.

We present a deterministic ion source using ultracold atoms in a magneto-optical trap (MOT). ^{87}Rb atoms are photoionized from the $5P_{3/2}$ state with a 405 nm laser or a 480 nm LED. The ionization fragments are detected with Channel Electron Multipliers. The electrons serve as triggers for the ions, enabling us to predict and control the latter. Correlations between electrons and ions are obtained by the normalized $g^{(2)}$-function and used for the appropriate operation of the corresponding optics. Repetition rates from a few ions to 10^3 ions per second are currently possible.

After the first characterization phase with the current setup, an upgrade of the ion detector to a position sensitive Multi Channel Plate with a Delay Line Detector is scheduled. This will allow for the measuremnet of the momentum spread of the ions and give insight to the reaction dynamics during the photoionization. Also the photoionization scheme will be upgraded from two photon ionization to three photon ionization with only NIR lasers. This will lead to a minimal energy transfer during the ionization process as well as to a reduced background electron rate due to the photoelectric effect.

Chip-scale MOT for Microsystems Technology

Argyrios T. Dellis, Matthew T. Hummon, Songbai Kang, Elizabeth A. Donley, John Kitching

National Institute of Standards and Technology, Boulder, Colorado 80305, USA

Magneto-optical traps (MOT) are the first stage for a plethora of cold atoms instruments and sensors. The miniaturisation of instruments and sensors based on laser-cooled atoms is hindered by the large pumps needed to maintain the vacuum requirements (<10^6 Torr)**.** Currently all the laser cooled atom systems require some kind of actively pumping in order to operate. We are developing a micro-fabricated platform to support the creation of laser cooled samples for chip-scale instruments.

Our micro-fabricated vacuum chamber is shown in Fig. 1a. It is made of silicon and glass. The silicon part, which is 4 mm thick and 28mm x 28mm wide, is etched and two glass windows are anodically bonded to it to form a cavity. One of the windows has a hole and a silicon washer is anodically bonded to it. A glass to metal adaptor is anodically bonded to this washer in order to connect the cell to a 2 L/sec ion pump and an alkali dispenser which provides the source for ^{85}Rb atoms. We use six independent beams and a pair of anti-helmholtz coils for cooling and trapping the atoms. Each beam has a 3mm diameter (FWHM) [1] and ~1mw power. The light source is a DBR laser, frequency locked via saturation absorption spectroscopy. The repumping light was produced by directly modulating the laser current at 2.927GHz.

Our cell has only two windows and all the beams must enter the science chamber in the <111> configuration. After balancing the intensity of the laser beams and carefully align them so that their intersection overlaps with the zero of the quadrature field we were able to observe a MOT of about 5×10^5 atoms as shown in Fig. 2 by using a fluorescence imaging system. The imaging system which is similar to the one used in [2] has a resolution of about 200 atoms.

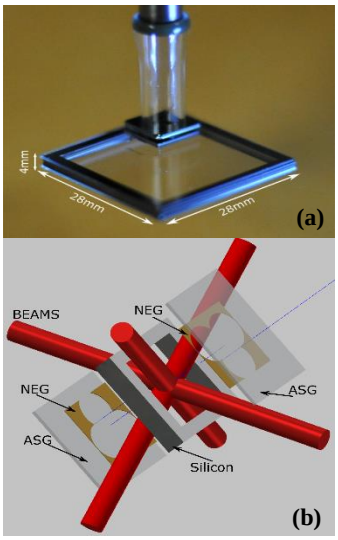

Fig. 1 (a): The actively pumped chip-scale cell used for cooling and trapping ^{85}Rb atoms. The cell is connected to a 2L/sec ion pump through a glass to metal adaptor. **(b)**: Design of the passively pumped chip scale cell.

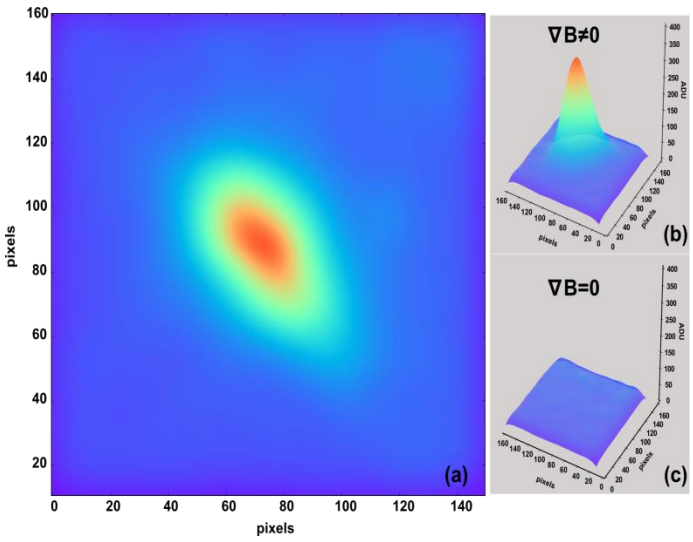

Fig. 2 (a): Signal of the MOT after background subtraction and smoothing. **(b), (c):** Comparison of the signal coming from the CCD camera when the magnetic field is on and off.

We have shown that we can trap about 5×10^5 atoms in a chip-scale actively pumped cell by using off the shelf components. We are currently moving towards replacing the ion pump by passively pumping elements such as non-evaporable getters (NEG) which are deposited on the glass windows in thin film form (Fig. 1b). In addition to NEGs we are also using windows made of alumino-silicate glass (ASG), which can reduce significantly the helium permeation [3], compared to borosilicate glasses, and can also be anodically bonded to silicon.

The miniaturization of laser cooled instruments will enable the use of laser cooled atoms in microsystems. Future instruments and sensors based on this technology will include accurate atomic clocks, atom interferometers and gyroscopes and many others.

References

[1] G. W. Hoth, E. A. Donley, and J. Kitching, *Atom number in magneto-optic traps with millimeter scale laser beams*, Optics letters 38 (2013), no. 5, 6613.

[2] S. Pollock, *Integration of Magneto Optical Traps in Atom Chips*, Imperial College (2010).

[3] A. T. Dellis, V. Shah, E. A. Donley, S. Knappe, J. Kitching, *Low Helium Permeation Cells for Atomic Microsystems Technology*, submitted

Multiparticle losses in a linear Paul trap

Ilya Semerikov
P.N. Lebedev Physical Institute of the Russian Academy of Sciences, 53, Leninskiy Prospekt, Moscow, Russia

Ilya Semerikov[1,2], Ilya Zalivako[1,2,3], Timofey Shpakovsky[1,2], Alexandr Borisenko [1,2,3], Ksenia Khabarova[1,2,4], Vadim Sorokin[1,2], Nikolay Kolachevsky[1,2,3,4]
1. P.N. Lebedev Physical Institute of the Russian Academy of Sciences, 53, Leninskiy Prospekt, Moscow 119991, Russia
2. Russian Quantum Center, 100 Novaya St., Skolkovo, Moscow 143025, Russia
3. Moscow Institute of Physics and Technology,9 Institutsky per., Dolgoprudny, Moscow region, 141700, Russia
4.National Research Institute for Physical-Technical and Radiotechnical Measurements, Mendeleevo, Moscow Region, 141570 Russia.

For many physical problems, such as time and frequency metrology, precision spectroscopy, quantum simulation, it is necessary to isolate the object of study from the influence of surrounding fields and particles, and to minimize its speed. To localize particles - ions, atoms and molecules, one should apply confinement field or gradient of fields.
In the case of neutral particles that field or field gradient must be large, since they weakly interact with external fields due to absence of charge. The presence of the external field may lead to the shifts in the atomic level structure. Due to ions have an electrical charge, they could be easily trapped with small RF fields, which makes them to be an interesting object for many applications. It is possible to trap ensembles of ions as well as single ions. Localization in a small volume allows one to use laser cooling effectively, and long lifetimes provide an opportunity to work with the most narrow spectral line without limitation on light-ion interaction time.
There are several factors, which limiting the lifetime of the ions in the trap: charge exchange with buffer gas, phase shift on trapping electrodes, contact potential on electrodes, and other heating mechanisms, which lead to increase of the average kinetic energy of the ions.[1-3] In an ensemble of trapped ions it is necessary to take into account the interaction between the ions by Coulomb force, which leads to additional frequencies in the motion spectrum. Since the depth of the potential in the ion trap may reach 20 eV, they can trap particles with a kinetic energy corresponding to a temperature well above room temperature. In this case, the interaction of the ions by the Coulomb force can be a major reason for the reduction of life time of the ensemble in the trap and make it difficult to hold a large number of particles.
In this work we discuss the multiparticle loses in a linear RF Paul trap, designed for Mg and Al ions. We made an experiment on living time of hot ions in the trap. We also modeled dynamics of hot ions in the trap.

The work is supported by Russian scientific foundation grant # 16-12-00096

References

[1] Harmon T. J., Moazzan-Ahmadi N., and Thompson R. I., *Instability heating of sympathetically cooled ions in a linear Paul trap*, Phys. Rev. A, **67**, 013415 (2003)
[2] Berkeland D. J., Miller J. D., Bergquist J. C., Itano W.M., Wineland D. J., *Minimization of ion micromotion in a paul trap*, J. of Appl. Phys., vol. **83**, no. 10, p. 5025 (1998).
[3]Andelkovic, Z. et al., *Laser cooling of externally produced Mg ions in a Penning trap for sympathetic cooling of highly charged ions*, Phys.Rev. A, **87**, 033423 (2013).

Laser cooling of thulium atoms for investigation of cold collisions

Elena Kalganova[1,2,3], Gulnara Vishnyakova[1,2,3], Artem Golovisin[1,2,3], Dmitry Tregubov[1,2,3], Denis Sukachev[1,3], Ksenia Khabarova[1,3], Alexey Akimov[1,2,3], Nikolay Kolachevsky[1,2,3], Vadim Sorokin[1,3]

1. P. N. Lebedev Physical Institute of RAS, 53 Leninsky prosp., Moscow 119991, Russia

2. Moscow Institute of Physics and Technology,9 Institutsky per., Dolgoprudny, Moscow region, 141700, Russia

3. Russian Quantum Center, 100 Novaya St., Skolkovo, Moscow 143025, Russia

Thulium is a rare-earth element with one vacancy in inner $4f$ shell. Along with other lanthanides with unfilled $4f$ shell it has a large magnetic dipole moment of a ground state ($4\mu_B$), that makes it a promising object for study dipole-dipole interaction and for quantum simulations. Furthermore, thulium is expected to possess a lot of low-field Feshbach resonances. Our group deals with laser cooling and trapping of thulium atoms for the purpose of its collisional properties investigation.

The first step towards observation of cold collisions is a preparation of an ultracold atomic ensemble. For this we perform a two-stage laser cooling of thulium atoms in a magneto-optical trap (MOT) [1]. For the first-stage cooling and Zeeman slowing we use a strong transition $4f^{13}(^2F^o)6s^2, J_g = 7/2, F_g = 4 \rightarrow 4f^{12}(^3H_5)5d_{3/2}6s^2, J_e = 9/2, F_e = 5$ at the wavelength 410.6 nm with a natural linewidth $\gamma_{blue} = 10$ MHz. The second-stage cooling is performed on transition $4f^{13}(^2F^o)6s^2, J_g = 7/2, F_g = 4 \rightarrow 4f^{12}(^3H_6)5d_{5/2}6s^2, J_e = 9/2, F_e = 5$ at the wavelength 530.7 nm with a natural linewidth $\gamma_{green} = 350$ kHz. The dependence of an atomic cloud shape and a temperature on a second-stage cooling light detuning is shown on Fig 1(a). The lowest obtained temperature is about 9 μK.

It is seen that a temperature levels off at large detunings. That is a feature of laser cooling at weak transition: at large detuning a MOT trapping force becomes lower than gravitation force, so atomic cloud falls dawn until energy levels shifts caused by MOT magnetic field compensate an increase of cooling light detuning. As a result, a change of light detuning leads only to change of cloud position and shape while effective light frequency detuning and cloud temperature remain constant. Another specific for a narrow-line cooling phenomenon we observe is so called momentum-space crystals, which are formed by blue detuned MOT light. Fig. 1(b,c) shows a picture of a cloud after 3 ms time of flight which expands as eight separate groups. This behaviour indicates the appearance of momentum-space crystals [2,3].

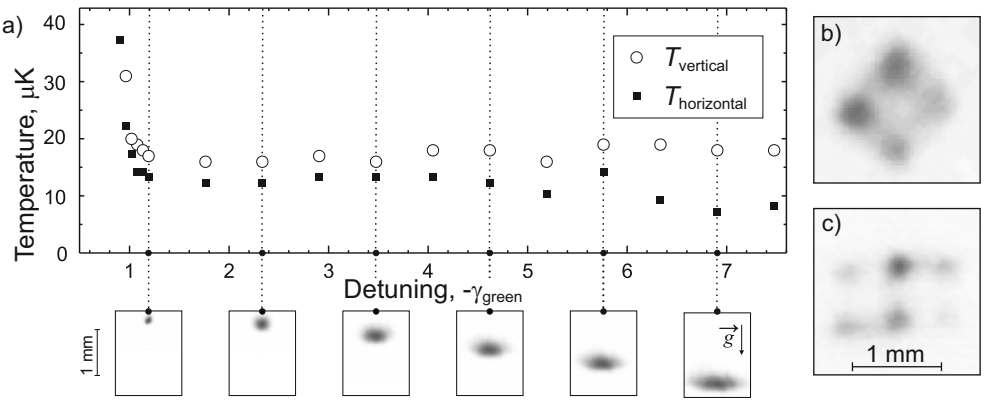

Fig. 1 a) Temperature and position of atomic cloud vs. light detuning. b,c) Picture of atomic cloud after 3 ms time of flight, top (b) and side (c) view. Cloud shape displays momentum-space crystals formation.

After cooling, thulium atoms are recaptured in an optical lattice formed by a focused laser beam at wavelength 532 nm with a power up to 8 W. It is focused into the atomic cloud, providing confinement potential with a depth of 100 μK. An efficiency of recapture amounts to 60%.

Thus, we demonstrate a deep laser cooling of thulium atoms on a narrow transition in MOT and effective atoms recapture into an optical lattice. An ensemble of 10^5 atoms with a temperature $T = 20\mu$K was obtained. Now we are working on a further decrease of cloud temperature by evaporative cooling which is expected to allow observation of low-field Feshbach resonances.

References

[1] Gulnara Vishnyakova et al, *Two-stage laser cooling and optical trapping of thulium atoms*, Laser Phys. **24**, 074018 (2014).

[2] Gulnara Vishnyakova et al, *Ultracold lanthanides: from optical clocks to quantum simulators*, Phys. Usp. **59**, (2016).

[3] Thomas H. Loftus et al, *Narrow line cooling and momentum-space crystals*, Phys. Rev. A **70**, 063413 (2004).

Confinement-Induced Resonances in Ultracold Atom-Ion Systems

Vladimir Melezhik[1], **Antonio Negretti**[2]

1. Bogoliubov Laboratory of Theoretical Physics, Joint Institute for Nuclear Research and State University "Dubna", Dubna, Moscow Region 141980, Russian Federation

2. Zentrum für Optische Quantentechnologien and the Hamburg Centre for Ultrafast Imaging, Universität Hamburg, Luruper Chaussee 149, 22761 Hamburg, Germany

We have investigated confinement-induced resonances (CIR)s in a system composed by a tightly trapped ion and a moving atom in a waveguide [1]. The conditions for the appearance of such resonances were determined for a broad region – from the "long-wavelength" limit to the opposite case when the typical length scale of the atom-ion interaction R^* essentially exceeds the transverse waveguide width $a_\perp$. We have found considerable dependence of the resonance position on the atomic mass which, however, disappears in the "long-wavelength" limit $R^*/a_\perp \to 0$, where the well known result [2] for the atom-atom CIR position $a_\perp/a_{3D} = 1.46$ is reproduced (see Fig.1). We have also derived an analytic formula for the CIR position in the "long-wavelength zero-energy" limit.

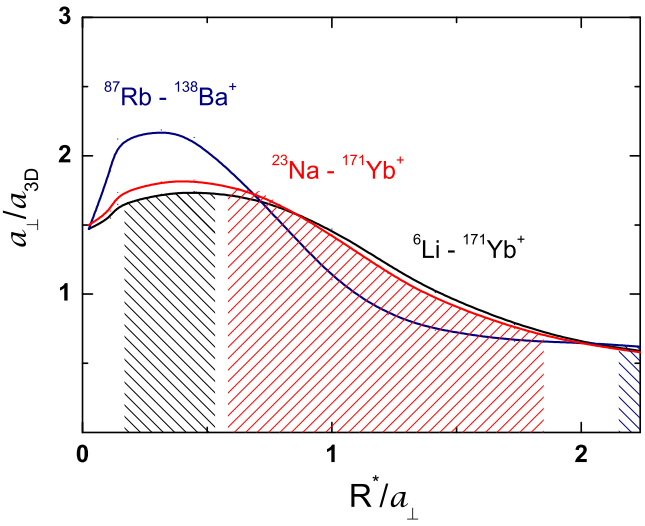

Fig. 1 The ratio $a_\perp/a_{3D}$ of the waveguide width $a_\perp = \sqrt{\hbar/(\mu\omega_\perp)}$ to the free-space atom-ion scattering length a_{3D} in the points of the CIR as a function of $R^*/a_\perp$. Shaded areas indicate the range $\omega_\perp = 2\pi \times (10-100)$kHz for the atomic trap frequencies which are reachable in current experiments.

Our results can be used in current experiments for searching atom-ion CIRs with the aim of measuring the atom-ion scattering length, determining the temperature of the atomic gas in the presence of an ion impurity, manipulating the effective atom-ion interaction in confined systems. In particular, the control of the atom-ion interaction could be exploited to control the atom-phonon coupling in a solid-state quantum simulator [3], to investigate more exotic quantum phases in low dimensional systems, where the trap width is tuned in such a way that simultaneously an atom-atom and an atom-ion CIR are generated and a strongly correlated atom-atom and the atom-ion system is created, or, by exploiting the effect of the complete reflection of the confined atom from the ion in the CIR, to realise a device for triggering the confined atom flow, similarly to a single atom transistor [4].

References

[1] V.S. Melezhik, and A. Negretti, *Confinement-Induced Resonances in Ultracold Atom-Ion Systems*, arXiv: 1602.05550 (2000).

[2] M. Olshanii, *Atomic Scattering in the Presence of an External Confinement and a Gas of Impenetrable Bosons*, Phys. Rev. Lett. **81**, 938 (1998).

[3] U. Bissbort, D. Cocks, A. Negretti, Z. Idziaszek, T. Calarco, F. Schmidt-Kaler, W. Hofstetter, and R. Gerritsma, *Emulating Solid-State Physics with a Hybrid System of Ultracold Ions and Atoms*, Phys. Rev. Lett. **111**, 080501 (2013).

[4] A. Micheli, A.J. Daley, D. Jaksch, and P. Zoller, *Single Atom Transistor in a 1D Optical Lattice*, Phys. Rev. Lett. **93**, 140408 (2004).

Anderson localization of a one-dimensional Bose-Einstein Condensate after long-time expansion

Stefan Donsa[1] **, Harald Hofstätter**[1]**, Othmar Koch**[2]**, Joachim Burgdörfer**[1]**, Iva Březinová**[1]
1. Institute for Theoretical Physics, Vienna University of Technology, Vienna, Austria, EU
2. Faculty of Mathematics, University of Vienna, Vienna, Austria, EU

Anderson localization is an interference effect of non-interacting particles in disordered systems which leads to suppression of transport [1]. It is still an open question whether Anderson localization occurs in interacting systems. In recent experiments Bose-Einstein condensates were used to investigate Anderson localization in a highly controllable setup [2]. A Bose-Einstein condensate initially trapped in a harmonic potential was released and its expansion in a weak disorder potential was monitored. The observed suppression of its expansion was explained assuming that the initially interacting system becomes non-interacting for long expansion times [3]. We test this assumption and examine the long-time influence of pair interactions by calculating the expansion with and without inter-particle interaction.
In the experiment [2], a Bose-Einstein condensate was formed out of a cloud of ultra-cold atoms (in the present case ^{87}Rb atoms) that interact with each other via van der Waals interactions. At very low temperatures these interactions can be described as point-like interactions. The many-body dynamics can be described on the mean-field level within the Gross-Pitaevskii equation

$$i\hbar\frac{\partial}{\partial t}\Psi(x,t) = \left[-\frac{\hbar^2}{2m}\frac{\partial^2}{\partial x^2} + V(x) + g\,|\Psi(x,t)|^2\right]\Psi(x,t)\,, \tag{1}$$

which assumes that the motion of all atoms is fully coherent at all times and can be described effectively by one wavefunction with self-interaction (Eq. 1).

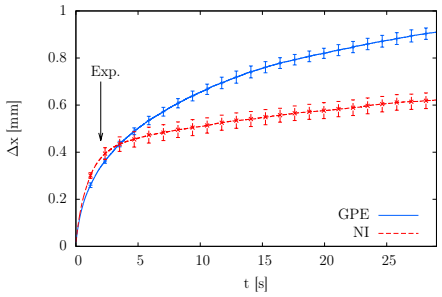

Fig. 1 (a) Comparison of the width Δx of a Bose-Einstein condensate that is interacting throughout the simulation (solid line - GPE) with the case where interactions are turned off after an initial expansion period where most of the interaction energy is converted into kinetic energy (dashed line - NI). We show the mean value and the standard deviation over 30 different realizations of the disorder potential. The arrow denotes the experimentally investigated time span [2].

We compare the scenario[2,3] of non-interacting (NI) particles with a calculation in which the condensate is interacting at all times (GPE). In the first case (NI), we switch off interactions when most of the initial interaction energy is converted into kinetic energy. Monitoring the width Δx of the Bose-Einstein condensate for the two scenarios, we observe a difference for $t > 5$ s (Fig. 1). This is a time scale long compared to the experiment in which observations stopped at $t \approx 2$ s [2].
In contrast to the interpretation of the experiment that the condensate is sufficiently dilute during the propagation and can therefore be treated as non-interacting we show that the effect of interactions becomes increasingly visible after long propagation times. We propose to revisit this problem experimentally and are confident that the influence of interactions on Anderson localization at long expansion times can be observed.

References

[1] P. Anderson, *Absence of Diffusion in Certain Random Lattices*, Phys. Rev. **109**, 1492 (1958).
[2] J. Billy et al., *Direct observation of Anderson localization of matter waves in a controlled disorder*, Nature **453**, 891 (2008).
[3] L. Sanchenz-Palencia et al., *Disorder-induced trapping versus Anderson localization in Bose-Einstein condensates expanding in disorder potentials*, New Journal of Physics **10**, 045019 (2008).

Towards negative La laser cooling

Giovanni Cerchiari[1], Elena Jordan[1], Alban Kellerbauer[1]

1. Max-Planck-Institut für Kernphysik, Saupfercheckweg 1, 69117 Heidelberg, Germany

One of the yet missing milestones in negative ion physics is a successful application of the laser cooling technique. Finding a negative ion species that can be brought to ultracold temperature by lasers [1] would open up the possibility to perform a wide range of low-temperature experiments with anions, including a precision gravity measurement on antimatter. Our research group aims to directly laser cool a negatively charged ion cloud in a radiofrequency trap. To reach this goal we first performed high-resolution spectroscopy on the few atomic anions predicted and in some cases experimentally confirmed to be suitable for laser cooling [2,3]. The experimental studies were pursued in a collinear spectroscopy setup, where the resonant transition was probed via a two-step excitation process [4,5]. The presence of the intermediate excited state was revealed by an enhanced detachment rate of the excess electron when the laser frequency was tuned into resonance. A suitable transition in La^- was identified from the spectroscopy, which might be used to cool the ion via Doppler laser cooling.

Currently we are commissioning a double trap experiment improving the already existing apparatus to achieve laser cooling. First the anion beam will be stopped in a Penning trap and mixed with electrons. After this pre-cooling stage the atomic anions will be transferred to a linear radiofrequency trap where interaction with the laser will take place.

References

[1] A. Kellerbauer, J. Walz, *A novel cooling scheme for antiprotons*, New Journal of Physics **8** (2006) 45

[2] S. M. O'Malley, D. R. Beck, *Lifetimes and branching ratios of excited states in La^-, Os^-, Lu^-, Lr^-, and Pr^-*, Phys. Rev. A **81**, 032503 (2010)

[3] C. W. Walter, N. D. Gibson, D. J. Matyas, C. Crocker, K. A. Dungan, B. R. Matola, and J. Rohlén, *Laser cooling of a negative ion: Observations of bound-bound transitions in La^-*, Phys. Rev. Lett. **113**, 063001 (2014)

[4] U. Warring, M. Amoretti, C. Canali, A. Fischer, R. Heyne, J. O. Meier, Ch. Morhard, and A. Kellerbauer, *High-resolution laser spectroscopy on the negative osmium ion*, Phys. Rev. Lett. **102**, 043001 (2009)

[5] E. Jordan, G. Cerchiari, S. Fritzsche, A. Kellerbauer, *High-resolution spectroscopy on the laser-cooling candidate La^-*, Phys. Rev. Lett. **115**, 113001 (2015)

TILDA-V: A full-differential code for proton tracking in biological matter

Christophe Champion[1], Michele A. Quinto[2], Juan M. Monti[2], Philippe F. Weck[3], Omar A. Fojón[2], Jocelyn Hanssen[2], Roberto D. Rivarola[2]

1. Université de Bordeaux, CNRS/IN2P3, Centre d'Etudes Nucléaires de Bordeaux Gradignan, Gradignan, France

2. Instituto de Física Rosario, CONICET and Universidad Nacional de Rosario, Argentina

3. Sandia National Laboratories, Albuquerque, NM 87185, USA

Understanding the radiation-induced effects at the cellular level is of prime importance for predicting the future of irradiated biological organisms. Thus, whether it is in radiobiology to identify the DNA critical lesions or in medicine to adapt the radio-therapeutic protocols, an accurate knowledge of the numerous interactions induced by charged particles in living matter is required. To do that, Monte-Carlo track-structure codes represent the most suitable and powerful tools, in particular for modeling the full slowing-down of ionizing particles in biological matter. However, it is worth mentioning that such numerical codes are reliable only if the input database used for modeling the charged particle induced interactions is precise and complete. In this context, the literature reports several numerical codes for proton and electron transport in water, the latter being commonly used as surrogate of the living medium.

The current work aims at going beyond this artifice with the development of an *event-by-event* Monte Carlo code - called *TILDA-V* - based on a complete set of multiple-differential and total cross sections for describing all the inelastic and elastic processes occurring throughout the slowing-down of protons in water and DNA [1]. *TILDA-V* (an acronym for Transport d'Ions Lourds Dans Aqua & Vivo) refers to an extension of the *TILDA* code previously developed by Champion *et al.* [2]. It is based on a complete set of quantum-mechanical cross sections for all the electron- and proton/hydrogen-induced interactions in water as well as in biological targets including the DNA nucleobases and the sugar-phosphate backbone [3-5]. Furthermore, a realistic description of the biological medium has been considered by modeling a typical nucleotide equivalent unit of hydrated DNA, namely, a nucleobase-pair plus a sugar phosphate group both surrounded by a hydration shell composed by 18 water molecules.

A detailed description of the Monte Carlo code will be presented in this work as well as intra-comparisons between water and hydrated DNA in terms of proton range and stopping power (see Figure 1). The obtained results indicate that the approach commonly used in the existing Monte Carlo studies, which consists in rescaling the water based track-structure simulations by a realistic density is clearly inappropriate for mimicking the biological reality and, more importantly, leads to an underestimation of the proton-induced energetic cartography. These findings may have relevant consequences on both radiation damage predictions and radiotherapeutical treatment planning.

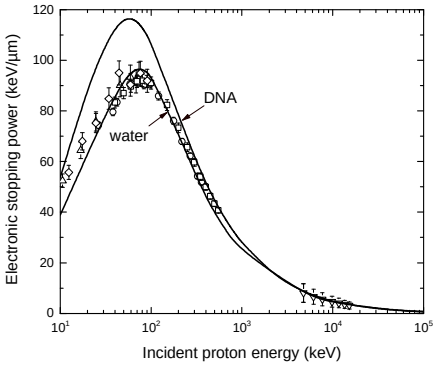

Fig. 1 Electronic stopping power (induced by H^+/H^0) in water and hydrated DNA.

References

[1] Michele A. Quinto, Juan M. Monti, Marielle E. Galassi, Philippe F. Weck, Omar A. Fojón, Jocelyn Hanssen, Roberto D. Rivarola and Christophe Champion, *Proton track structure code in biological matter*, J. Phys. Conf. Ser. **583**, 012049 (2015).

[2] Christophe Champion, Alain L'Hoir, Marie-Françoise Politis, Pablo D. Fainstein, Roberto D. Rivarola and Annie Chetioui, *A Monte Carlo code for the simulation of heavy-ion tracks in water*, Radiat. Res. **163**, 222-231 (2005).

[3] Marielle E. Galassi, Christophe Champion, Philippe F. Weck, Roberto D. Rivarola, Omar Fojón and Jocelyn Hanssen, *Quantum-mechanical predictions of DNA and RNA ionization by energetic proton beams*, Phys. Med. Biol. **57**, 2081-2099 (2012).

[4] Christophe Champion, Philippe F. Weck, Hacène Lekadir, Marielle E. Galassi, Omar Fojón, Paula Abufager, Roberto D. Rivarola and Jocelyn Hanssen, *Proton-induced single electron capture on DNA/RNA bases*, Phys. Med. Biol. **57**, 3039-3049 (2012).

[5] Juan M. Monti, Carmen A. Tachino, Jocelyn Hanssen, Omar A. Fojón, Marielle E. Galassi, Christophe Champion and Roberto D. Rivarola, *Distorted wave calculations for electron loss process induced by bare ion impact on biological targets*, Appl. Radiat. Isotopes **83**, 105-108 (2014).

Partial ionization cross sections for positive fragments produced by electron impact on biomolecules

Peter J. M. van der Burgt, Marcin L. Gradziel, Melissa Dunne and Michael Brown
Department of Experimental Physics, National University of Ireland Maynooth, Maynooth, Co. Kildare, Ireland

We have measured mass spectra of positive ions for electron impact on various biomolecules, with electron energies ranging from 0 to 100 eV in steps of 0.5 eV. Ions have been collected and detected using a reflectron time-of-flight mass spectrometer. Details about the experiment and the data analysis can be found in [1-3], which present results obtained for electron impact on cytosine, thymine and adenine. Preliminary results have been reported on uracil [4].

An effusive beam of biomolecules is generated by a resistively heated oven mounted in an expansion chamber, and the forward section of the beam effusing from a capillary in the oven passes through a skimmer into the collision chamber, where the beam is crossed by a 0.5 μs pulsed electron beam. Positively charged fragments are mass resolved and detected using a reflectron time-of-flight mass spectrometer. LabVIEW based data acquisition techniques are used to accumulate time-of-flight spectra as a function of electron impact energy. Ion yield curves are normalized by comparing the sum of the ion yields to the average of calculated total ionization cross sections. Appearance energies are determined by fitting onset functions to the ion yield curves.

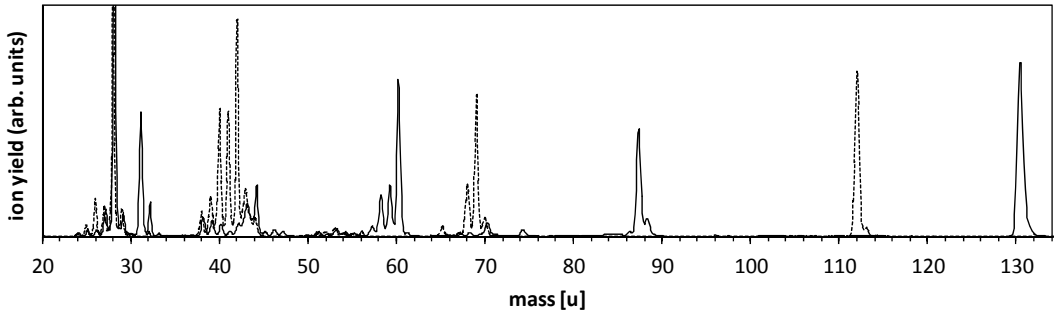

Figure 1. Time-of-flight mass spectra of uracil and fluorouracil.

Published experimental results [1-3] have been obtained using a Stanford DG535 digital pulse generator and a FastComtec 7886S multichannel scaler. We are in the process of replacing both these components with a single CompactRIO device (National Instruments model cRIO-9075). All the code for the time-of-flight spectrometer pulsing and the time-resolved data acquisition has been developed in LabVIEW, with time-critical functions implemented on the integrated field-programmable gate array (FPGA). Initial tests have produced results that are in excellent agreement with measurements taken with the multichannel scaler. Using the CompactRIO device a factor 2 is gained in data acquisition efficiency.

The current work focuses on uracil, fluorouracil, and a few of the smaller polycyclic aromatic hydrocarbons. First results will be presented at the conference.

References

[1] Peter J. M. van der Burgt, *Electron impact fragmentation of cytosine: partial ionization cross sections for positive fragments*, Eur. Phys. J. D **68**, 135 (2014).
[2] Peter J. M. van der Burgt, Francis Mahon, Gerard Barrett, and Marcin L. Gradziel, *Electron impact fragmentation of thymine: partial ionization cross sections for positive fragments*, Eur. Phys. J. D **68**, 151 (2014).
[3] Peter J. M. van der Burgt, Sinead Finnegan, and Samuel Eden, *Electron impact fragmentation of adenine: partial ionization cross sections for positive fragments*, Eur. Phys. J. D **69**, 173 (2015).
[4] S. Diskin, S. Eden, and P. J. M. van der Burgt, *Partial ionization cross sections for positive fragments produced by electron impact on uracil*, J. Phys: Conf. Ser. **635**, 072057 (2015).

Mass-Spectrometric Studies of the Valine Molecule Fragmentation by Electron Impact

Alexander Papp[1], Vasyl Vukstich[1], Liudmila Romanova[1], Jelena Tamuliene[2], Laura Baliulyte[2], Alexander Snegursky[1]

[1] *Institute of Electron Physics, Ukr. Nat. Acad. Sci., 21 Universitetska str., 88017 Uzhgorod, Ukraine*
[2] *Vilnius University, Institute of Theoretical Physics and Astronomy, 12 A. Goštauto str., 01108, Vilnius, Lithuania*

The new data on the electron-impact fragmentation of the amino acid valine molecule ($C_5H_{11}NO_2$) obtained by using a mass-spectrometric technique are presented being related to the formation of the ionized products due to the influence of low-energy ionizing radiation on the above molecule. An extensive DFT-theory based theoretical approach enabled the main pathways of the valine molecules fragmentation to be elucidated. A series of fragments produced have been identified. For some of them the absolute appearance energies have been both measured experimentally and calculated theoretically. The data of the experimental studies and theoretical calculations are compared and analyzed.

Figure 1 shows the valine molecule mass-spectrum that illustrates the general pattern of the yields of the initial molecule ion fragments. In general, our spectrum is close to those quoted in the NIST database for the valine, D- and DL-valine molecules obtained by different authors [1]. The main difference is the largest relative intensity of the ion yields measured by us in the mass range *m/z*=27–30 a.m.u.

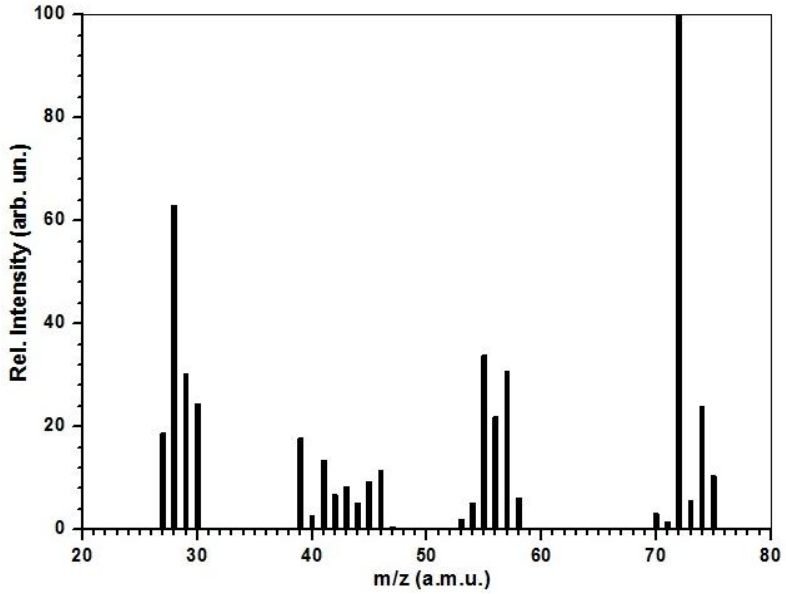

Fig. 1 Valine molecule mass-spectrum measured at the 70 eV incident electron energy.

We have both measured and calculated the absolute appearance potential values for several most intense ion fragments of the initial molecule. Comparison of our results with those published in [2] shows the best coincidence in case of the *m/z*=57 and *m/z*=28 ions. Table 1 presents our data on the appearance energies for the differently charged $C_4H_{10}N$ fragment calculated for two main valine molecule conformers I and II.

Table 1. Appearance energies (eV) for differently charged $C_4H_{10}N$ fragment conformers of the valine molecule.

$C_4H_{10}N$ fragment charge	Conformer I	Conformer II
+1	7.94	7.80
0	11.53	11.53
–1	12.31	12.34

According to the results obtained for the neutral and ionized conformers, certain skeleton bonds become weaker under the electron impact ionization, while some of them become stronger. Variations of the bond lengths and the orders of the ionized conformers indicate the highest probability of the C-C_α bond dissociation. Hence, it is not surprising that the most abundant ion in our spectrum is the $C_4H_{10}N^+$ one (*m/z*=72 a.m.u.) formed due to the C-C_α bond cleavage. Thus, this main valine molecule dissociation pathway is similar to that inherent in the most of the α-amino acids. This means that the most probable valine dissociation process is related to the carboxyl group detachment.

References

[1] National Institute of Standards, Standard Reference Database: Chemistry Webbook – http://webbook.nist gov.
[2] Peter Papp, Pavel Shchukin, Jaroslav Kočišek, and Štefan Matejčik, J.Chem.Phys. **137**, 105101 (2012).

Schottky Diagnostics for Precision Laser Spectroscopy of Bi^{82+} and Bi^{80+} at the Storage Ring ESR

C. Trageser[1,3], C. Brandau[2,3], C. Geppert[3], Yu.A. Litvinov[3], J. Meisner[4], A. Müller[1], W. Nörtershäuser[5], R. Sanchez[3], S. Sanjari[3], S. Schippers[2], M. Schmidt[4], J. Ullmann[5,6]

1. Institut für Atom- und Molekülphysik, Justus-Liebig-Universität Giessen, 35392 Giessen, Germany
2. I. Physikalisches Institut, Justus-Liebig-Universität Giessen, 35392 Giessen, Germany
3. GSI-Helmholtzzentrum für Schwerionenforschung, 64291 Darmstadt, Germany
4. Physikalisch-Technische Bundesanstalt, 38116 Braunschweig, Germany
5. Institut für Kernphysik, Technische Universität Darmstadt, 64289 Darmstadt, Germany
6. Helmholtz-Institut Jena, 07743 Jena, Germany

Schottky diagnostics of ions in storage rings and circular accelerators is a well established method to assess beam properties in a non-destructive way [1]. In addition, Schottky techniques are nowadays used for precision mass spectroscopy and for nuclear decay studies of highly charged radioisotopes and of nuclear isomers via the so-called Schottky Mass Spectroscopy (SMS) and Time-resolved Schottky Mass Spectroscopy (TRSMS) [2].

In support of a new high-quality Schottky probe that was installed in 2010 in the storage ring ESR of the GSI-Helmholtzzentrum für Schwerionenforschung in Darmstadt [3] a new broadband, continuous data acquisition system (NTCAP-DAQ) that rapidly samples (”time-captures”) the Schottky signal was commissioned recently [4]. Recording of the Schottky signal demodulated to its in-phase (I) and quadrature (Q) components with rates exceeding $35 \cdot 10^6$ IQ-Samples s^{-1} (data rate 140 MByte s^{-1}) was demonstrated, allowing several harmonics of the circulating beam to be recorded simultaneously and at high frequency resolution.

In the present contribution, we report about the use of this NTACP-DAQ system as a high precision ”beam logbook” in assistance of storage ring laser spectroscopy experiments of Bi^{82+} and Bi^{80+} at the ESR [5]. In these laser spectroscopy studies the knowledge about the ion velocity is crucial [6]. A precision high-voltage divider [7] provided by the Physikalisch-Technische Bundesanstalt, Braunschweig, was installed to measure the voltage of the ESR electron cooler and consequently, via electron cooling, the ion beam velocity. During the laser data taking the ion beam needs to be bunched and hence decoupled from the cooling process. Using the Schottky frequency technique the constancy of beam quality, e.g., stability of ion beam momentum $\Delta p_i/p_i$, its momentum spread $\delta p_i/p_i$ or energy deviations $\Delta E_i/E_i$ down to relative changes of $< 10^{-7}$ can be monitored and compared to the conditions during electron cooling phases (Fig. 1).

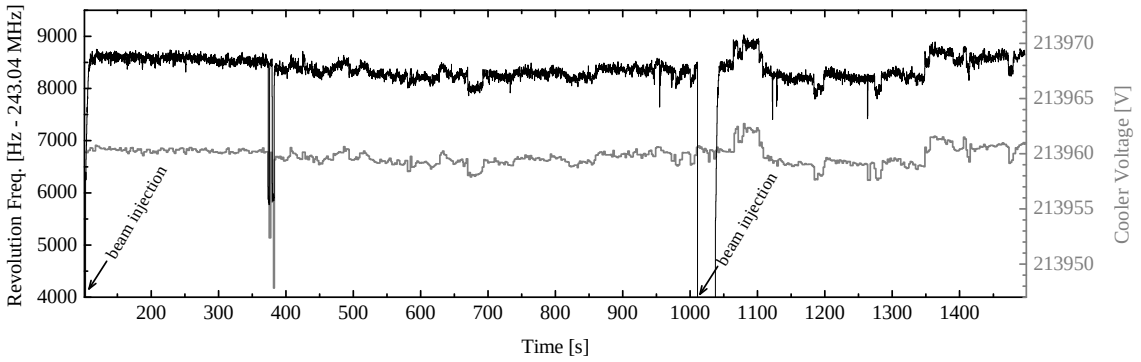

Fig. 1 Revolution frequency (124th harmonics) of Bi^{82+} ions in the storage ring ESR (black line, left y-axis) and corresponding cooler voltage (grey line, right y-axis). Due to the electron cooling force the revolution frequency of the ions almost immediately adjusts to the small fluctuations ($< 10^{-5}$) of the cooler voltage.

References

[1] D. Boussard, *Schottky noise and beam transfer function diagnostics*, in: S. Turner (Ed.), Proc. CERN Accelerator School: 5th Advanced Accelerator Physics Course, Rhodes, Greece, 20 Sept - 1 Oct 1993, ed. S. Turner, CERN 95-06, p. 749ff (1995).

[2] F. Bosch, Yu.A. Litvinov and Th. Stöhlker, *Nuclear physics with unstable ions at storage rings*, Prog. Part. Nucl. Phys. **73**, 84 (2013).

[3] F. Nolden, P. Hülsmann, Yu.A. Litvinov et al., *A fast and sensitive resonant Schottky pick-up for heavy ion storage rings*, Nucl. Instrum. Meth. A **659**, 69 (2011).

[4] C. Trageser, C. Brandau, C. Kozhuharov et al., *A new data acquisition system for Schottky signals in atomic physics experiments at GSI's and FAIR's storage rings*, Phys. Scr. **T166**, 014062 (2015).

[5] J. Ullmann, Z. Andelkovic, A. Dax et al., *An improved value for the hyperfine splitting of hydrogen-like* $^{209}Bi^{82+}$, J. Phys. B: At. Mol. Opt. Phys. **48**, 144022 (2015).

[6] M. Lochmann, R. Jöhren, C. Geppert et al., *Observation of the hyperfine transition in lithium-like bismuth* $^{209}Bi^{80+}$*: Towards a test of QED in strong magnetic fields*, Phys. Rev. A **90**, 030501(R) (2014).

[7] J. Hällström, A. Bergmann, S. Dedeoğlu et al. *Performance of a wideband 200-kV HVDC reference divider module*, IEEE Trans. Instrum. Meas. **63**, 2264 (2014)

The FISIC Project for N-body Quantum Dynamics Study in Fast Ion - Slow Ion Collisions: Status and Progress

***E. Lamour*[*], *T. Stöhlker*[§], *J. Rangama*[‡], *A. Gumberidze*[(•)†], *L. Adoui*[‡], *A. Bräuning-Demian*[†], *H. Bräuning*[†], *J.Y. Chesnel*[‡], *R. Geithner*[§], *C. Hahn*[§], *A. Lévy*[*], *S. Macé*[*], *A. Méry*[‡], *C. Prigent*[*], *P. Rousseau*[‡], *J.-P. Rozet*[*], *U. Spillmann*[†], *S. Steydli*[*], *N.A. Tahir*[†], *M. Trassinelli*[*], *D. Vernhet*[*], *G. Weber*[§]**

** INSP Sorbonne Universités, CNRS, UPMC Univ Paris 06, Paris, France*

§ Friedrich-Schiller-Universität Jena, Helmholtz-Institut, Jena, Germany

‡ CIMAP, CEA/CNRS/ENSICAEN/Université de Caen Basse-Normandie, Caen, France

† GSI, (•) ExtreMe Matter Institute, Darmstadt, Germany

Knowledge of fundamental electronic mechanisms at play in fast ion – slow ion collisions can provide a real breakthrough in the understanding of energy transfer in various plasmas such as inertial confinement fusion plasmas, stellar/interstellar plasmas and also in material damages. Indeed, when a few MeV/u ions collide with a few keV/u ions, a hitherto unexplored collision regime is reached: a regime where the ion energy transfer is at its maximum. There, all the primary electronic processes, like electron capture, loss and excitation, reach their optimum leading, for instance, to possible interference effects. Measurements and reliable theoretical predictions are completely lacking in this intermediate collision regime corresponding therefore to a real "terra incognita" for atomic physics.

Crossing two multicharged ion beams, under well controlled conditions, has always been a very challenging task, whatever the domain of physics under consideration. So far, ion-ion collisions for atomic physics have been performed mainly in the context of magnetically confined plasmas, using a crossed beam device [1] in the low-energy domain where the charge transfer is the dominant process. The forthcoming availability of MeV energy, intense and stable ion beams of high optical quality at French and German Large Scale Facilities (GANIL/SPIRAL2 and FAIR/CRYRING) opens new opportunities towards the intermediate collision regime. With the FISIC project [2], we propose an experimental crossed-beam arrangement with an ultimate control of experimental conditions to measure absolute cross sections. The goal is to span from a pure three-body problem (collision between a bare ion and a hydrogenic target) to a collision system between dressed partners (study of the effect of a controlled number of additional electrons). For the realization of such a challenging experimental project, a lot of technical barriers have to be overcome. Solution/progress for several of them will be presented at the conference, namely:

- The *stripping issue* of intense ion beams delivered by the SPIRAL2 accelerator. First, an upstream work has been accomplished to extend the ETACHA code [3] so as to determine the most appropriate stripper nature and thicknesses with respect to the desired ion charge state. Second, the technical issue of the stripper thermal load during beam irradiation will be overcome by fixing the thin solid strippers on a rotating wheel [4].
- The *collision chamber* has been designed in order to ensure UHV conditions and to monitor the intensity profile of the high-energy ion beam upstream and downstream from the interaction zone. A specific setup will be used to tag the signals coming from the true physical events of interest.
- The *high energy ion detectors*. New detector prototypes capable to cope with some MHz count rates and to withstand the accompanying radiation damage are required. Solutions that rely on polycrystalline diamond devices and crystal scintillators such as YAP:Ce are currently tested.
- The *control and detection of the slow ion charge state*. An arrangement of two 180° spherical electrostatic analyzers used as a purification system, prior to the interaction, has been designed. A charge state analyzer, which includes movable electrodes and/or movable detectors, necessary to cover the wide range of slow ions we want to investigate, is currently under study.

References

[1] S. Meuser, F. Melchert, S. Krüdener, A. Pfeiffer, K. von Diemar, and E. Salzborn, *"Crossed-beams arrangement for the investigation of charge-changing collisions between multiply charged ions"* Rev. Sci. Instrum. **67** (1996) 2752.

[2] E. Lamour et. al, *Fast ion-slow ion collisions-FISIC project*, at http://www.agence-nationale-recherche.fr/?Project=ANR-13-IS04-0007 and http://pro.ganil-spiral2.eu/spiral2/instrumentation/s3/working-documents/loi-day-1-experiments

[3] E Lamour, P D Fainstein, M Galassi, C Prigent, C A Ramirez, R D Rivarola, J.-P. Rozet, M. Trassinelli and D. Vernhet, *"Extension of charge state distribution calculations for ion-solid collisions towards low velocities and many-electron ions"* Physical Review A **92** (2015) 042703.

[4] N.A. Tahir, V. Kim, E. Lamour, I.V. Lomonosov, A.R. Piriz, J.P. Rozet, Th. Stöhlker, V. Sultanov and D. Vernhet, *"Two–Dimensional Thermal Simulations of Aluminum and Carbon Ion Strippers for Experiments at SPIRAL2 Using the Highest Beam Intensities*", NIM B **290** (2012) 43-47.

Forward-angle electron spectroscopy in heavy-ion atom collisions studied at the Experimental Storage Ring

Pierre-Michel Hillenbrand[1], **Siegbert Hagmann**[1], **Yuri Litvinov**[1], **and Thomas Stöhlker**[1,2,3]
1. GSI Helmholtzzentrum für Schwerionenforschung, Planckstrasse 1, 64291 Darmstadt, Germany
2. Helmholtz-Institut Jena, Fröbelstieg 3, 07743 Jena, Germany
3. Institut für Optik und Quantenelektronik, Friedrich-Schiller-Universität Jena, Max-Wien-Platz 1, 07743 Jena, Germany

In collisions of heavy highly-charged projectile ions with atomic targets, the energy distribution of the emitted electrons is a characteristic observable for the underlying elementary charge-transfer processes. At the experimental storage ring ESR of the heavy-ion accelerator facility GSI, a dedicated magnetic electron spectrometer was installed downstream from the gas-jet target, which enables the measurement of high-energetic electrons emitted in ion-atom collisions with velocities similar to the projectile velocity within a small cone in the forward direction. This provides the ability to extend the well known study of cusp electrons towards heavy-ion atom collisions at near-relativistic projectile energies. Through the electron-loss-to-continuum cusp, double-differential cross sections of projectile ionization can be studied even for the heaviest few-electron projectiles. But also a new channel opens up, the radiative electron capture to continuum, which can be directly compared to its non-radiative counterpart. Using the electron spectrometer in combination with detectors for emitted x rays and charge-exchanged projectiles, the study of the collision system $U^{88+} + N_2$ @ 90 MeV/u revealed three processes, each characterized by a unique shape of the electron cusp [1]:

(a) The process of **electron loss to continuum** (ELC) corresponds to the ionization of an electron from the projectile into the projectile continuum during the collision with the target, $U^{88+} + N_2 \rightarrow U^{89+} + [N_2]^* + e^-$. For the ELC, the measured spectrum is compared to first-order perturbation theory using fully-relativistic Dirac wavefunctions [2].

(b) The process of **electron capture to continuum** (ECC) corresponds to the capture of a target electron into the projectile continuum, while the excess energy is carried away by the recoil of the generated target ion: $U^{88+} + N_2 \rightarrow U^{88+} + \left[N_2^+\right]^* + e^-$. For the ECC, the measured spectrum is compared to calculations in the impulse approximation using semi-relativistic Sommerfeld-Maue wavefunctions, and to calculations in the continuum-distorted-wave (CDW) approach [3].

(c) The process of **radiative electron capture to continuum** (RECC) corresponds to the capture of a target electron into the projectile continuum, while the excess energy is carried away by a photon: $U^{88+} + N_2 \rightarrow U^{88+} + \left[N_2^+\right]^* + e^- + \gamma$. This process can be seen as the high-energy endpoint of bremsstrahlung studied in inverse kinematics. For the RECC, the measured spectra are compared to calculations using fully-relativistic Dirac wavefunctions, and to calculations in the impulse approximation using semi-relativistic Sommerfeld-Maue wavefunctions [4].

Furthermore, the process of ELC was investigated for **multi-electron projectiles** in the collision systems

$$U^{28+} + H_2 \rightarrow U^{29+} + [H_2]^* + e^-, \quad U^{28+} + N_2 \rightarrow U^{29+} + [N_2]^* + e^-, \quad \text{and} \quad U^{28+} + Xe \rightarrow U^{29+} + Xe^* + e^-.$$

The experimental data revealed a significant electron cusp asymmetry, which increases towards heavier targets. This behavior is not yet consistent with presently available theories based on first-order perturbation using fully-relativistic wavefunctions [5].

As a next step, an experimental study of ELC for U^{89+} colliding with different gaseous target is envisaged, at a projectile energy just above the threshold for electron impact ionization. For these collision systems, relativistic CDW calculations predict a deviation of the electron energy distribution from first-oder perturbation due to the effect, that the electron emitted by the projectile is attracted by the target nucleus.

References

[1] P.-M. Hillenbrand *et al.*, *Forward-angle electron spectroscopy in heavy-ion atom collisions studied at the ESR*, J. Phys. Conf. Ser. **635**, 012011 (2015).
[2] P.-M. Hillenbrand *et al.*, *Electron-loss-to-continuum cusp in $U^{88+} + N_2$ collisions*, Phys. Rev. A **90**, 042713 (2014).
[3] P.-M. Hillenbrand *et al.*, *Electron-capture-to-continuum cusp in $U^{88+} + N_2$ collisions*, Phys. Rev. A **91**, 022705 (2015).
[4] P.-M. Hillenbrand *et al.*, *Radiative-electron-capture-to-continuum cusp in $U^{88+} + N_2$ collisions and the high-energy endpoint of electron-nucleus bremsstrahlung*, Phys. Rev. A **90**, 022707 (2014).
[5] P.-M. Hillenbrand *et al.*, *Strong asymmetry of the electron-loss-to-continuum cusp of multi-electron U^{28+} projectiles in near-relativistic collisions with gaseous targets*, Phys. Rev. A, submitted (2016).

High-Precision X-ray Spectroscopy of Highly-Charged Ions at Storage Rings Using Silicon Microcalorimeters

S. Kraft-Bermuth[1], V. Andrianov[1,2,3], A. Bleile[3,4], A. Echler[1,3,4], P. Egelhof[3,4], P. Grabitz[3,4], C. Kilbourne[5], D. McCammon[6], P. Scholz[1]

[1] Institute for Atomic and Molekular Physics, Justus-Liebig-University, 35392 Giessen, Germany
[2]Lomonosov Moscow State University,119991 GSP-1, Moscow, Russia
[3] GSI Helmholtz Center, 64291 Darmstadt, Germany
[4] Institute of Physics, Johannes-Gutenberg University, 55099 Mainz, Germany
[5]NASA/Goddard Space Flight Center, Greenbelt, USA
[6]Department of Physics, University of Wisconsin, Madison, USA

The precise determination of the energy of the Lyman-α lines in hydrogen-like heavy ions provides a sensitive test of quantum electrodynamics in very strong Coulomb fields. However, one limitation of the current accuracy of such experiments is the energy resolution of available X-ray detectors [1]. To improve this accuracy, a novel detector concept, namely the concept of "microcalorimeters", is now exploited for such measurements.

Microcalorimeters detect the temperature change of an absorber after an incoming particle or photon has deposited its energy as heat. This operation principle provides considerable advantage over conventional detectors with respect to energy resolution, detection efficiency, energy threshold and radiation hardness. For the detection of X-rays, a large dynamic range and a high absorption efficiency as well as sufficient detector solid angle are mandatory. Therefore, the microcalorimeters used in the present experiments consist of silicon thermometers, ensuring a high dynamic range, and of absorbers made of high-Z material to provide high X-ray absorption efficiency. The desired detector solid angle is obtained by detector arrays, because the size of individual microcalorimeters is limited by constraints on their heat capacity. With such detectors, a relative energy resolution of about 1 per mille is obtained in the energy regime of 1–100 keV.

The application of microcalorimeters for hard X-rays, based on silicon thermistors and tin absorbers, for the determination of the 1s Lamb Shift in hydrogen-like heavy ions has been pursued our collaborating groups for more than two decades. Two detector arrays have been successfully applied in two experiments at the Experimental Storage Ring (ESR) of the GSI Helmholtz Center for Heavy Ion Research to determine the 1s Lamb Shift of hydrogen-like lead and gold [2]. An excellent agreement with theory has been obtained. Based on these experiments, a larger detector array with 6 times the active detector area in a new, cryogen-free cryostat is currently in preparation.

In this contribution, we will briefly introduce the detection principle, then we will present the ESR experiments and their results. In addition to the new detector array for experiments at the future FAIR facility, perspectives for other high-precision experiments, i.e. spectroscopy of inner-shell transitions, will be discussed.

References

[1] Th. Stöhlker et al., Lecture Notes in Physics **745**, 151, Springer-Verlag Berlin, Heidelberg (2008)
[2] S. Kraft-Bermuth et al., Phys. Scr. **T166** (2015) 014028

X-ray Laser Spectroscopy with Highly Charged Ions at Ultrabrilliant Light Sources

Sven Bernitt[1,2], René Steinbrügge[1], Stepan Dobrodey[1], Jan K. Rudolph[1,3], Sascha W. Epp[4], Peter Micke[1,5], Thomas Stöhlker[2], José R. Crespo López-Urrutia[1]

1. Max-Planck-Institut für Kernphysik, Saupfercheckweg 1, 69117 Heidelberg, Germany
2. Institut für Optik und Quantenelektronik, Friedrich-Schiller-Universität, Max-Wien-Platz 1, 07743 Jena, Germany
3. Institut für Atom- und Molekülphysik, Justus-Liebig-Universität, Leihgesterner Weg 217, 35392 Giessen, Germany
4. Max-Planck-Institut für Struktur und Dynamik der Materie, Luruper Chaussee 149, 22761 Hamburg, Germany
5. QUEST Institute, Physikalisch-Technische Bundesanstalt, Bundesallee 100, 38116 Braunschweig, Germany

By resonantly exciting electronic transitions with monochromatic light and recording the induced fluorescence as a function of the light wavelength, a technique commonly known as laser spectroscopy, it is possible to directly probe the electronic structure of atoms, molecules and ions. Laser spectroscopy with optical lasers is one of the most precise experimental methods available today, and is widely applied in physics and chemistry. In recent years, the advent of the newest generation of ultrabrilliant light sources has enabled the application of those techniques in the previously unaccessible X-ray regime.

The transportable electron beam ion trap FLASH-EBIT [1] has been used in a number of experiments to provide targets of trapped highly charged ions for VUV and X-ray radiation from the free-electron lasers FLASH [1,2] and LCLS [3], as well as the synchrotron light sources BESSY II [4] and PETRA III [5,6,7]. By observing resonantly excited fluorescence we were able to measure transition energies [1,2,5,7], relative oscillator strengths [3] and natural line widths [5,6]. By simultaneously detecting changes of ion charge states, caused by resonant photoionization [4], we were also able to deduce branching ratios and absolute radiative and Auger decay rates [6].

Our measurements have provided valuable atomic data for the interpretation of astrophysical X-ray spectra [3]. Furthermore, the study of high-Z few-electron systems provided tests of atomic theory on the level of QED contributions [5,7].

Based on the methods explored with the FLASH-EBIT, we now develop a novel compact electron beam ion trap based on permanent magnets, which will be used to investigate new applications of X-ray laser spectroscopy with highly charged ions for metrology and polarimetry.

References

[1] Sascha W. Epp *et al.*, *Soft X-Ray Laser Spectroscopy on Trapped Highly Charged Ions at FLASH*, Phys. Rev. Lett. **98**, 183001 (2007)
[2] Sascha W. Epp *et al.*, *X-ray laser spectroscopy of highly charged ions at FLASH*, J. Phys. B: At. Mol. Opt. Phys. **43**, 194008 (2010)..
[3] Sven Bernitt *et al.*, *An unexpectedly low oscillator strength as the origin of the Fe XVII emission problem*, Nature **492**, 225-228 (2012).
[4] Martin C. Simon *et al.*, *Resonant and Near-Threshold Photoionization Cross Sections of* Fe^{14+}, Phys. Rev. Lett. **105**, 183001 (2010).
[5] Jan K. Rudolph *et al.*, *X-Ray Resonant Photoexcitation: Linewidths and Energies of* $K\alpha$ *Transitions in Highly Charged Fe Ions*, Phys. Rev. Lett. **111**, 103002 (2013).
[6] R. Steinbrügge *et al.*, *Absolute measurement of radiative and Auger rates of K-shell-vacancy states in highly charged Fe ions*, Phys. Rev. A **91**, 032502 (2015).
[7] Sascha W. Epp *et al.*, *Single-photon excitation of* $K\alpha$ *in heliumlike* Kr^{34+}*: Results supporting quantum electrodynamics predictions*, Phys. Rev. A **92**, 020502(R) (2015).

Unraveling the Principles Governing the Stability of Endohedral and Exohedral Fullerenes

Yang Wang[1,2], **Sergio Díaz-Tendero**[1,3], **Manuel Alcamí**[1,2], **Fernando Martín**[1,2,3]

1. Departamento de Química, Módulo 13, Universidad Autónoma de Madrid, 28049 Madrid, Spain

2. Instituto Madrileño de Estudios Avanzados en Nanociencia (IMDEA-Nanociencia), Cantoblanco, 28049 Madrid, Spain

3. Condensed Matter Physics Center (IFIMAC), Universidad Autónoma de Madrid, 28049 Madrid, Spain

Recent experimental evidences have confirmed that in nature fullerenes are much more abundant than expected [1]. In addition to neutral species, cationic and hydrogenated fullerenes are naturally present in outer space. On the other hand, fullerene anions, as well as endohedral and exohedral fullerenes, play important roles in material science, biomedicine and astrophysics [2,3]. An unusual behavior of charged, endohedrally and exohedrally derivatized fullerenes is that the isomer stability is often substantially different from that of their neutral counterparts [2,3]. The well established stability rules for neutral fullerenes, such as isolated-pentagon rule (IPR), are no longer valid for many experimentally observed structures (see Fig. 1 for an example).

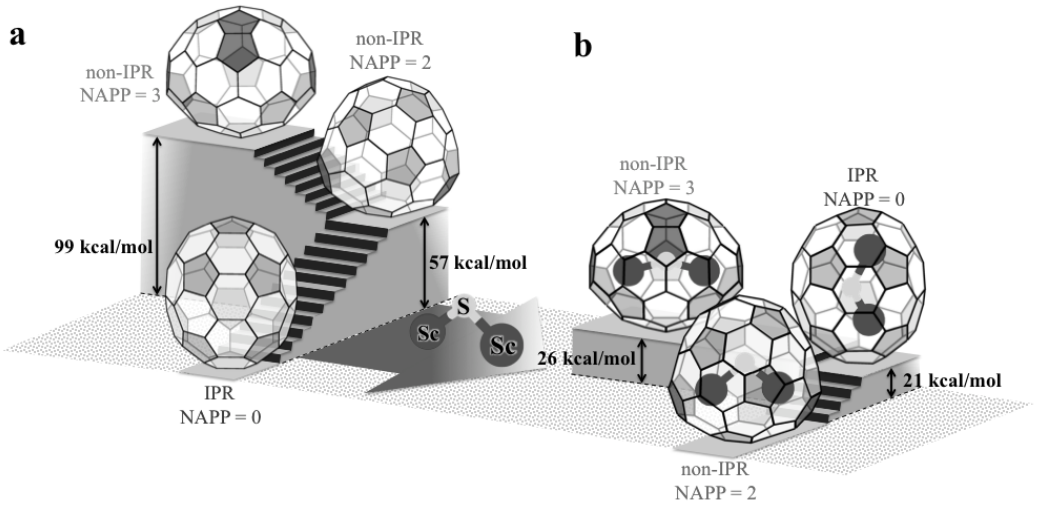

Fig. 1 Relative energies of three isomers of C_{70} containing 0, 2 and 3 adjacent pentagon pairs. (a) For neutral pristine C_{70}, the only isomer isolated experimentally follows the isolated pentagon rule (NAPP = 0). (b) For endohedral fullerene $Sc_2S@C_{70}$, the only isomeric form isolated experimentally so far is the one containing two adjacent pentagon pairs (NAPP = 2).

Which are then the underlying principles that govern the stability of charged and derivatized fullerenes? The answer to this question is not only of fundamental importance, but is also practically useful to predict experimentally producible fullerene structures, which are only a few among the enormous number (millions or billions or more) of possible cage isomers and regioisomers.

In this presentation, we propose a simple and unified model, based on the concepts of cage connectivity and frontier π orbitals [4], to fully understand the stability of charged, endohedrally and exohedrally derivatized fullerenes. Requiring only the knowledge of fullerene topology, the model permits a rapid determination of stable structures, among a huge number of possible isomers, without performing elaborate quantum chemistry calculations [4,5]. These predictions are relevant in fields as diverse as astrophysics, electrochemistry and supramolecular chemistry.

References

[1] Ewen K. Campbell, Matthias Holz, Dieter Gerlich, and John Paul Maier, *Laboratory confirmation of C_{60}^+ as the carrier of two diffuse interstellar bands*, Nature **523**, 322 (2015).

[2] Alexey A. Popov, Shangfeng Yang, and Lothar Dunsch, *Endohedral Fullerenes*, Chem. Rev. **113**, 5989 (2013).

[3] Yuan-Zhi Tan, Su-Yuan Xie, Rong-Bin Huang, and Lan-Sun Zheng, *The Stabilization of Fused-Pentagon Fullerene Molecules*, Nature Chem. **1**, 450 (2009).

[4] Yang Wang, Sergio Díaz-Tendero, Manuel Alcamí and Fernando Martín, *Cage Connectivity and Frontier π Orbitals Govern the Relative Stability of Charged Fullerene Isomers*, Nature Chem. **7**, 927 (2015).

[5] Yang Wang, Sergio Díaz-Tendero, Manuel Alcamí and Fernando Martín, *Key Structural Motifs to Predict the Cage Topology in Endohedral Metallofullerenes*, J. Am. Chem. Soc. **138**, 1551 (2016).

Ab initio-based Potentials for Studying Ion Hydration

Rita Prosmiti[1], **Daniel J. Arismendi-Arrieta**[1]
1. Institute of Fundamental Physics (IFF-CSIC), CSIC, Serrano 123, 28006 Madrid, Spain

Despite numerous experimental and theoretical studies, a molecular-level understanding of how ionic species are hydrated, and the extent to which differences in the local hydration structure can result in different solution properties has just started emerging [1]. In this context, the investigation of structural, thermodynamic, and spectroscopic properties of small $X^{\pm}(H2O)_n$ clusters (with X being a halide or alkali ion) represents the first step toward the development of a molecular-level understanding of the hydration properties of ionic solutions in different environments and conditions.

In this study, we describe the development of *ab initio*-based potential energy functions representing the interactions between halide or alkali ions and water molecules [2,3]. These potentials include an explicit treatment of two-body repulsion, electrostatics, and dispersion energy, with many-body effects being taken into account through classical polarization within an extended version of the Thole-type model (TTM). All parameters of the potential functions are obtained from *ab initio* CCSDT(T)-F12 and DFT data. By construction, the ion-water functional form is compatible with any many-body (rigid/flexible) TTM-based water potentials. The accuracy of the potentials is validated through an extensive analysis and comparisons, of both energies and structures of $X^{\pm}(H2O)_{n=1-8}$ clusters, with *ab initio* data from CCSD(T)-F12, DF-MP2, and DFT calculations, as well as with results obtained using modern polarizable force fields. We found that as the cluster size increases, different hydrogen bond patterns start emerging, with the H_2O molecules either forming a single hydration shell around the ion or developing a multishell structure, with the halide ions preferentially reside on the surface of the clusters, accepting hydrogen bonds from the water molecules located in the first hydration shell (see Figure 1).

Importantly, the agreement obtained with the *ab initio* data suggests that the potentials developed in this study provide an accurate and efficient representation of halide/alkali–water interactions, which correctly include many-body effects, representing an accurate and efficient alternative to DFT+D models that can be used in molecular dynamics simulations to characterize the structural, thermodynamic, and dynamical properties of ionic solutions. Currently, such simulation studies are in progress focused on the characterization of the hydration properties of speficic ions from clusters to bulk aqueous ionic solutions.

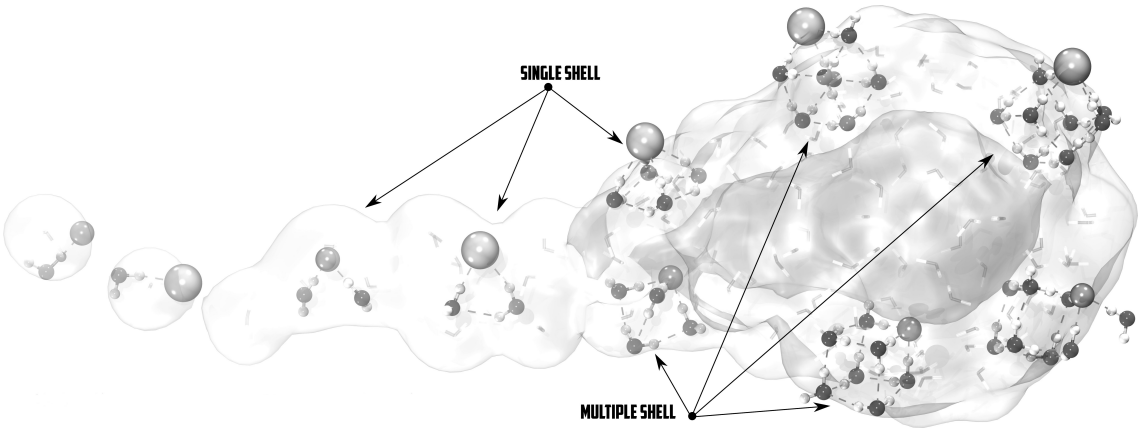

Fig. 1 Schematic representation of halide/alkali ion hydration from finite-size systems to bulk aqueous solutions.

References

[1] A.A. Hassanali, J. Cuny, V. Verdolino, and M. Parrinello, *Aqueous Solutions: State of the Art in Ab Initio Molecular Dynamics* Philos. Trans. R. Soc. A **372**, 20120482 (2014),

[2] D.J. Arismendi-Arrieta, R. Prosmiti, and F. Paesani, *Modeling the water-halide ion interactions*, J. Phys.: Conf. Ser. **635**, 032008 (2015); *The i-TTM Model for Ab Initio-Based Ion-Water Interaction Potentials. I. Halide-Water Potential Energy Functions*, J. Phys. Chem. B **120**, 1822 (2016).

[3] D.J. Arismendi-Arrieta, and R. Prosmiti, to be submitted (2016).

Hydrogen Beam Irradiation of Suspended Mono and Bilayer Graphene

X. Urbain[1], P.-L. Bourgeois[1], M. Génévriez[1], A. Dochain[1], N. Reckinger[2], C. N. Santos[1], B. Hackens[1]

1. Institute of Condensed Matter and Nanosciences, Université catholique de Louvain, 1348 Louvain-la-Neuve, Belgium

2. Research Group on Carbon Nanostructures (CARBONNAGe), University of Namur, 5000 Namur, Belgium

The transmission of charged particles through thin targets has attracted new attention recently with the possibility to study true 2D materials like graphene. These particles may trigger structural modification of the ordered material through their interaction with individual carbon atoms. They may also capture one or several electrons, as demonstrated for highly charged ions transmitted by carbon nanomembranes [1]. In this work, the irradiated samples consist of few- layers graphene grown by chemical vapour deposition on copper substrates, and transferred on top of metallic TEM grids (part of the samples were bought from Ted Pella, Inc.).

The impact of a well-collimated beam of protons, deuterons, H^- or D^- on single- and double-layer graphene was studied at incident energies ranging from 500 to 7000 eV. The charge-state distribution of transmitted particles was determined by means of an electrostatic quadrupole analyser. The measured yield for neutralization is significantly lower than what is predicted in the literature [2], which cannot be solely attributed to the imperfect coverage of the supporting grid. The velocity distribution was characterised by time-of-flight analysis when operating with a pulsed ion beam. Substantial energy loss and straggling is observed (Fig.1), far beyond what may be anticipated from the reduction of areal density of the target when compared to thick samples. The linear growth of that energy loss with incident energy does however qualitatively agree with the predictions of TDDFT-MD calculations [3].

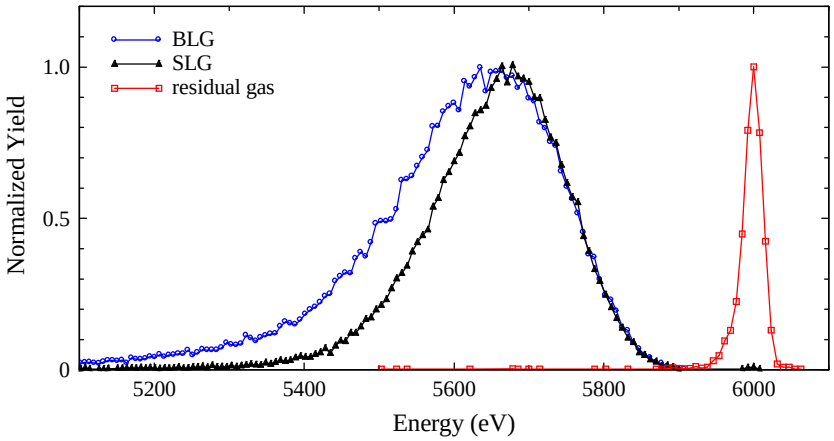

Fig. 1 Energy distribution of emerging H atoms for 6 keV proton bombardment of single- (SLG) and bi-layer (BLG) graphene. The narrow peak in the absence of graphene is a result of charge exchange with the residual gas.

Another aspect of the ion beam interaction with a suspended graphene sheet is the generation of defects in the graphene crystal lattice. Raman microspectroscopy is an appropriate technique in this framework: the D peak, located at a Raman shift around ~1350 cm^{-1}, is a direct probe of the lattice defect density. We investigated in particular the evolution of graphene D and G bands as a function of the ion beam parameters (type of ion, energy, fluence) and found a regime of stagnation of their intensity ratio I_D/I_G with the irradiation fluence, in agreement with previous reports [4]. From these data, we extract the defect density [5], and examine its correlation with the irradiation parameters. From the defect density and irradiation fluence, one can deduce the probability of sputtering a C atom through atomic collision with the incident ions, and discuss the agreement with simulation results [6].

References

[1] R. A. Wilhelm, E. Gruber, R. Ritter, R. Heller, S. Facsko, and F. Aumayr, *Charge Exchange and Energy Loss of Slow Highly Charged Ions in 1 nm Thick Carbon Nanomembranes*, Phys. Rev. Lett. **112**, 153201 (2014)

[2] G. Labaigt, A. Dubois, and J. P. Hansen, *Electron capture imaging of two-dimensional materials*, Phys. Rev. B **89**, 245438 (2014)

[3] A. V. Krasheninnikov, Y. Miyamoto, and D. Tománek, *Role of Electronic Excitations in Ion Collisions with Carbon Nanostructures*, Phys. Rev. Lett. **99**, 016104 (2007)

[4] S. Mathew, T.K. Chan, D. Zhan, K. Gopinadhan, A.-R. Barman, M.B.H. Breese, S. Dhar, Z.X. Shen, T. Venkatesan, and J. T.L. Thong, *The effect of layer number and substrate on the stability of graphene under Mev proton beam irradiation*, Carbon **49**, 1720 (2011).

[5] A. C. Ferrari and D. M. Basko, *Raman spectroscopy as a versatile tool for studying the properties of graphene*, Nat. Nano. **8**, 235 (2013).

[6] R. C. Ehemann, P. S. Krstic, K. Dadras, P.R.C. Kent, and J. Jakowski, *Detection of hydrogen using graphene*, Nano. Res. Lett. **7**, 198 (2012).

Tracking Interatomic Processes in Prototypical Noble Gas Clusters Using Time- and Spectrally Resolved Luminescence Detection

Andreas Hans[1], Philipp Schmidt[1], Christian Ozga[1], Xaver Holzapfel[1], Florian Wiegandt[2], Marko Förstel[3], Ltaief Ben Ltaief[1], Till Jahnke[2], Reinhard Dörner[2], Uwe Hergenhahn[4], Arno Ehresmann[1], André Knie[1]

1. Institut für Physik, Universität Kassel, Heinrich-Plett-Str. 40, 34132 Kassel, Germany
2. Institut für Kernphysik, J. W. Goethe-Universität, Max-von-Laue-Str. 1, 60438 Frankfurt am Main, Germany
3. Department of Chemistry, University of Hawaii at Manoa, Honululu, HI 96822, USA
4. Leibniz-Institut für Oberflächenmodifizierung e.V., Permoserstr. 15, 04318 Leipzig, Germany

The investigation of weakly bound structures such as van-der-Waals clusters or hydrogen-bonded systems in recent years revealed the omnipresence of non-local autoionization and related processes like Interatomic Coulombic Decay (ICD), Electron Transfer Mediated Decay (ETMD), and Radiative Charge Transfer (RCT) [1]. It is currently actively discussed whether the impact of these mechanisms extends beyond the scope of experimentally prepared samples to natural chemically and biologically relevant processes. They have been suggested to play a role in radiation damage and could therefore be utilized in radiation therapies. The early experimental exploration focused on the detection of charged particles. Although tremendous progress has been made in combining techniques like electron and ion spectroscopy with dense samples as liquids or jets of large clusters, the probing of bulk sites remains challenging because of the short escape length of charged particles in dense matter. Recently, it was demonstrated that photon detection can be used as complementary detection method for a resonant ICD process in neon clusters [2]. Here, we report on progress in experiments using photon detection as tool to investigate interatomic mechanisms in prototypical noble gas clusters.

Absolute cross sections for decay paths following photon absorption are an essential quantity to include those processes into theoretical models and to estimate the relevance in natural environments. Since an experimental noble gas cluster jet typically is only partially condensed, the intensity of measured cross sections for fluorescence emission from clusters after photon excitation can be compared to atomic emission and thereby be calibrated to absolute values. In a proof-of-principle experiment, we demonstrated this method and determined absolute cross sections for the resonant ICD process investigated earlier [2].

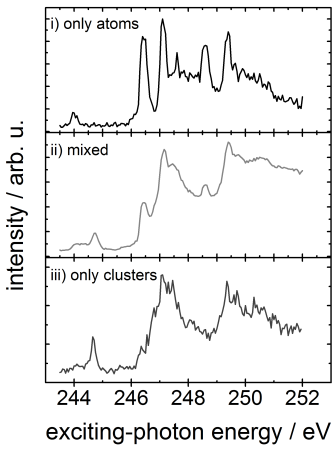

Fig. 1 Disentangling the cluster signal (panel iii) in the argon 2p excitation range from the pure atomic signal (panel i) by applying a time filter to the mixed signal (panel ii).

One main experimental challenge is to separate the signal of interest from side effects, such as remaining monomers in a cluster jet or the gas halo surrounding a liquid. Already in the early experiment [2], it was shown that signals from monomers and clusters can be identified by different radiative lifetimes. In the energy range around the argon 2p edge, signals from monomers and clusters can not be separated by their excitation energy but overlap heavily (Fig. 1b, panel ii). By applying a time filter we demonstrated the complete discrimination of contributions from clusters (Fig. 1b, panel iii) in this energy range. This validates time resolved photon detection as a suitable tool to experimentally separate signals stemming from monomers and clusters.

References

[1] Till Jahnke, *Interatomic and intermolecular Coulombic Decay: the coming of age story*, J. Phys. B **48**, 082001 (2015).
[2] André Knie *et al.*, *Detecting ultrafast interatomic electronic processes in media by fluorescence*, New J. Phys. **16**, 102002 (2014).

Fano-CI method for the computation of decay widths of electronic resonances in medium-sized atomic and molecular systems

Tsveta Miteva[1], **Sévan Kazandjian**[1], **Nicolas Sisourat**[1]

1. Sorbonne Universites, UPMC Univ Paris 06, CNRS, Laboratoire de Chimie Physique Matière et Rayonnement, F-75005, Paris, France

A resonance state of an atom or a molecule is a metastable state with a finite lifetime and sufficient energy to break up into subsystems [1]. Resonances are of great interest in many fields of chemistry and physics [1]. In the recent years, they have attracted attention also in connection with novel electronic decay processes such the interatomic Coulombic decay (ICD) and ICD-related phenomena [2, 3].

Resonance states are characterized with a complex energy whose real and imaginary parts represent the position and the decay width of the resonance, respectively. The theoretical description of resonance processes requires as a first step the calculation of these quantities. In the case of the Auger and ICD processes, which are the focus of our work, the metastable states can be considered as bound states interacting with a continuum of states [4, 5]. The total decay width of such resonances can then be calculated as a sum of the partial decay widths expressed as coupling elements between the bound Φ and the continuum parts $\chi_{\beta,\varepsilon_\beta}$ of the resonance

$$\Gamma = 2\pi \sum_{\beta=1}^{N_c} |\langle \Phi | \hat{H} - E_r | \chi_{\beta,\varepsilon_\beta} \rangle|^2$$

Within the Fano-ADC-Stieltjes approach [6, 7], these two parts are constructed using the Algebraic Diagrammatic Construction (ADC) technique [8, 9]. However, due to the computational costs of the ADC method, the Fano-ADC method is applicable to relatively small systems, for example, small rare-gas and metal-water clusters [6, 7, 10-12].

In order to extend the methodology to larger systems, we present a novel approach to the calculation of decay widths of resonances in singly-ionized systems. In our approach, the bound part of the resonance is approximated at the zeroth order as a one-hole configuration. The final states of the decay are obtained after diagonalization of the Hamiltonian matrix in the space of all two-hole-one-particle (2h1p) configurations with a fixed virtual orbital. The obtained CI final states are an approximation to the true continuum final states. Finally, the Stieltjes procedure is applied to recover the true decay width. The Fano-CI method can be applied to the computation of both total, as well as partial decay widths. Furthermore, it has fairly low computational costs and can thus be employed for investigating medium-sized atomic and molecular systems.

To check the validity of our method, we present benchmark calculations of the Auger and ICD widths of small rare-gas clusters. Comparison with available theoretical and experimental data shows that a satisfactory estimate of the decay width can be achieved with a relatively small basis set, which is of importance for the application of the method to larger systems.

References

[1] N. Moyseev, *Quantum theory of resonances: calculating energies, widths and cross-sections by complex scaling*, Phys. Rep. **302**, 211 (1998).
[2] V. Averbukh *et al.*, *Interatomic electronic decay processes in singly and multiply ionized clusters*, J. Electron Spectrosc. Relat. Phenom. **183**, 36 (2011).
[3] T. Jahnke, *Interatomic and intermolecular Coulombic decay: the coming of age story*, J. Phys. B: At. Mol. Opt. Phys. **48**, 082001 (2015).
[4] G. Howat, T. Åberg and O. Goscinski, *Relaxation and final-state channel mixing in the Auger effect*, J. Phys. B: Atom. Mol. Phys. **11**, 1575 (1978).
[5] U. Fano, *Effects of Configuration Interaction on Intensities and Phase Shifts*, Phys. Rev. **124**, 1866 (1961).
[6] V. Averbukh and L. S. Cederbaum, *Ab initio calculation of interatomic decay rates by a combination of the Fano ansatz, Green's-function methods, and the Stieltjes imaging technique*, J. Chem. Phys. **123**, 204107 (2005).
[7] P. Kolorenč, V. Averbukh, K. Gokhberg and L. S. Cederbaum, *Ab initio calculation of interatomic decay rates of excited doubly ionized states in clusters*, J. Chem. Phys. **129**, 244102 (2008).
[8] J. Schirmer, *Beyond the random-phase approximation: A new approximation scheme for the polarization propagator*, Phys. Rev. A **26**, 2395 (1982).
[9] J. Schirmer, L. S. Cederbaum and O. Walter, *New approach to the one-particle Green's function for finite Fermi systems*, Phys. Rev. A **28**, 1237 (1983).
[12] S. Kopelke, Y.-C. Chiang, K. Gokhberg and L. S. Cederbaum, *Quenching molecular photodissociation by intermolecular Coulombic decay*, J. Chem. Phys. **137**, 034302 (2012).
[11] P. Kolorenč and N. Sisourat, *Interatomic Coulombic decay widths of helium trimer: Ab initio calculations*, J. Chem. Phys. **143**, 224310 (2015).
[10] V. Stumpf, K. Gokhberg and L. S. Cederbaum, *The role of metal ions in X-ray-induced photochemistry*, Nature Chem. **8**, 237 (2016).

Two-Step Autoionization in Ejected-Electron Spectra of Ba

Vasyl Hrytsko[1], Gintaras Kerevičius[2], Alicija Kupliauskienė[2], Alexander Borovik[1,3]

1. *Department of Electron Processes, Institute of Electron Physics, Universitetska 21, 88017 Uzhgorod, Ukraine*
2. *Institute of Theoretical Physics and Astronomy, Vilnius University, Saulėtekio Ave. 3, 10222 Vilnius, Lithuania*
3. *Faculty of Physics, Uzhgorod National University, Voloshina 54, 88000 Uzhgorod, Ukraine*

Our recent studies of excitation and decay processes of the $5p^5 n_1 l_1 n_2 l_2 n_3 l_3$ autoionizing states in Ba [1] showed that the decay channel with formation of Ba^+ in $5p^6 6s_{1/2}$ ground state is predominant for the states lying above 21 eV. However, large excitation cross sections predicted for these states both theoretically [1] and experimentally [2, 3] contradict the observed low intensities of corresponding lines in ejected-electron spectra (see group of lines B in Fig. 1).

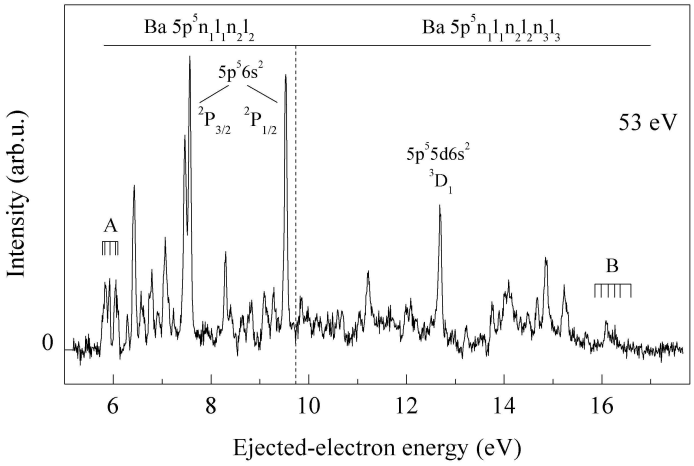

Fig. 1 The ejected-electron spectrum of barium vapour observed at 54.7° to an incident electron beam of 53 eV.

Moreover, by analyzing the spectrum in Fig. 1 one can see that there are no lines at ejected-electron energies above 16.6 eV. A possible reason for this is the existence of additional decay channels for high-lying atomic autoionizing states to the low-lying ionic states $5d^2(^3F)\ ^4D_{1/2,3/2,5/2}$, $5d(^3P)6s\ ^4P_{3/2,5/2}$ and $5d(^3P)6s\ ^2P_{1/2,3/2}$ [4] which is the first step of two-step autoionization process [5, 6], i. e.

$$Ba^*(5p^5 n_1 l_1 n_2 l_2 n_3 l_3) \rightarrow Ba^{+*}(5p^5 n_1 l_1 n_2 l_2) + e^1_{ejc} \quad (1)$$

$$\searrow\ Ba^{++}(5p^6) + e^2_{ejc} \quad (2)$$

Calculations [1] show that the probability of the decay process (1) with formation of Ba^+ in the $5p^5 5d^2$ states is about 10^{12} s^{-1}, i. e. of the same order as for the decay to the $5p^6 nl$ Ba^+ states, but it is by an order of magnitude higher for transitions with formation of Ba^+ in the $5p^5 5d6s$ states. In the latter case the branching ratios *B* for $5p^6 nl$ decay channels decrease from three up to five times. The dominance of the process (1) explains (i) the low intensity of lines B, (ii) the complete absence of lines in spectra above 16.6 eV ejected-electron energy and (iii) the high intensity of lines related to the process (2) (see group of ionic lines A in Fig. 1). Note that two-step autoionization is at the bottom of two well-known anomalies in Ba atoms, i. e. the high double ionization rate when Ba atoms are excited by 584.3 Å radiation [6] and a sharp rise of the total ionization cross section above 21 eV electron impact energy [7].

References

[1] V. Hrytsko, G. Kerevičius, A. Kupliauskienė, and A. Borovik, *The 5p autoionization spectra of Ba atoms excited by electron impact: Identification of lines*, J. Phys. B: At. Mol. Opt. Phys. (2016, submitted).
[2] M. A. Baig, J. P. Connerade, C. Mayhew, and K. Sommer, *New high-resolution studies of the 5p spectrum of Ba*, J. Phys. B: At. Mol. Phys. **17**, 371 (1984).
[3] S. Trajmar and W. Williams, *Electron-Metal Atom Collision Cross Section*, Physics of Ionized Gases ed. B. Navinsek (Yugoslavia: J Stephen Institute), 199 (1976).
[4] J. Nienhaus, O. I. Zatsarinny, and W. Mehlhorn, *Experimental and Theoretical Auger and Autoionization Spectra for Electron Impact on Laser-Excited Ba Atoms*, Phys. Essays **13**, 307 (2000).
[5] H. Hotop and D. Mahr, *On the 584.3 Å photoelectron spectrum of Ba*, J. Phys. B: At. Mol. Phys. **8**, L301 (1975).
[6] J. E. Hansen, *Interpretation of the 21.2 eV photoelectron spectrum of atomic Ba*, J. Phys. B: At. Mol. Phys. **8**, L403 (1975).
[7] L. A. Vainshtein, V. I. Ochkur, V. I. Rakhovskii, and A. M. Stepanov, *Absolute Values of Electron Impact Ionization Cross Sections for Magnesium, Calcium, Strontium and Barium*, Sov. Phys. JETP **34**, 271 (1972).

Velocity distributions of a molecule evaporated from mass-selected water nanodroplet

H. Abdoul-Carime*, F. Berthias*, L. Feketeová*, F. Calvo[$], B. Farizon*, M. Farizon*, and T. D. Märk[#]

[*] Université de Lyon; Université Claude Bernard Lyon1; Institut de Physique Nucléaire de Lyon, CNRS/IN2P3 UMR 5822, 69622 Villeurbanne Cedex, France
[$] Univ Grenoble 1, CNRS, LIPhy UMR 5588, F-38041 Grenoble, France
[#] Institut für Ionenphysik und Angewandte Physik, Leopold Franzens Universität, 6020 Innsbruck, Austria

The velocity of a molecule evaporated from a mass-selected protonated water nanodroplet ($H^+(H_2O_{n=2-8})$ is measured by velocity map imaging in combination with the recently developed COINTOF technique [1-4]. The measured velocity distributions allow probing statistical energy redistribution in water nanodroplets after ultrafast electronic excitation induced by a single collision. We show that even for ultimately small nanodroplets consisting of a few water molecules, a large amount of energy can be evenly redistributed over the droplet prior to molecular evaporation. As the droplet size increases, the velocity distribution of the evaporated molecules rapidly approaches the behaviour expected for macroscopic droplets. However, a distinct high-velocity contribution provides evidence of molecular evaporation before complete energy redistribution, corresponding to non-ergodic events

References

[1] F. Berthias *et al* 2014 *Phys. Rev. A* **89** 062705
[2] C. Teyssier *et al* 2014 *Rev. Sci. Instrum.* **85** 015118
[3] G. Bruny *et al* 2012 *Rev. Sci. Instrum.* **83** 013305
[4] H. Abdoul-Carime *et al* 2015 Angewandte Chemie International Edition: DOI: 10.1002/anie.201505890, Angew. Chem. Int. Ed., **54**, 14685 –14689

Associative detachment in Li^-+H and Li+H^- collisions

Jan Dvořák, Martin Čížek, Karel Houfek
Institute of Theoretical Physics, Faculty of Mathematics and Physics, Charles University in Prague, V Holešovičkách 2, 180 00 Praha, Czech Republic

Lithium is the heaviest element present in significant amount in the early Universe. The processes involving lithium atoms and ions thus contribute to molecular composition of the early Universe [1, 2]. The cross sections for the processes of associative detachment

$$\begin{aligned} \mathrm{Li}^- + \mathrm{H} &\rightarrow \mathrm{LiH} + e^- \\ \mathrm{Li} + \mathrm{H}^- &\rightarrow \mathrm{LiH} + e^- \end{aligned}$$

are not know very well and the reaction rates for the production of the LiH molecule are only estimated.

Based on MRCI calculation of the potential energy curves for both neutral LiH and negative ion LiH^- together with R-matrix calculation of the electron scattering from LiH we construct the nonlocal model for the above mentioned associative detachment processes. In construction of the model we follow the procedure of Čížek et al. [3]. We then calculate cross sections and reaction rates of the associative detachment processes. We also estimate the accuracy of the calculations and we study the influence of various uncertainties of the model on the final data.

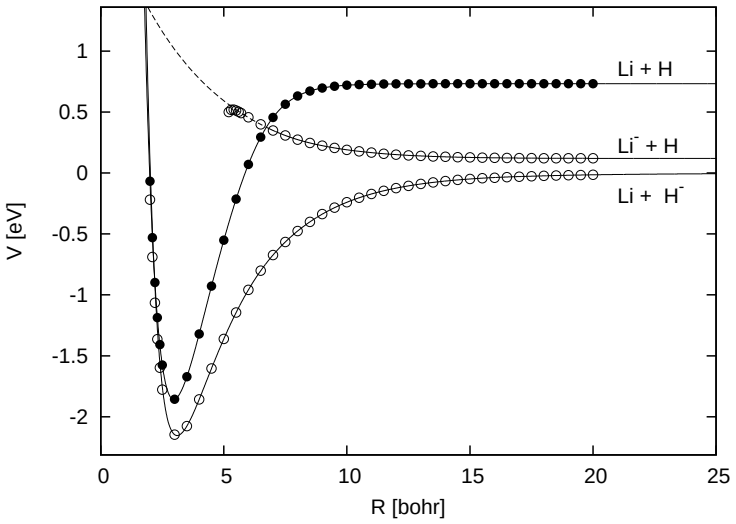

Fig. 1 Potential energy curves for the neutral molecule LiH and the anion LiH^-.

References

[1] S. Lepp, P. C. Stancil, A. Dalgarno, J. Phys. B **35** (2002).
[2] S. C. O. Glover, J. Chluba, S. R. Furlanetto, J. R. Pritchard, D. W. Savin, Advances in AMO Phys. **63** (2014).
[3] M. Čížek, J. Horáček, W. Domcke, J. Phys. B **31** (1998) 2571.

Lifetime Measurements of Excited States in Atomic Negative Ions I: Ni^- and Pt^-

KC Chartkunchand[1,2], M. Kamińska[1,3], O. M. Hole[1], R. F. Nascimento[1,4], M. Blom[1], M. Björkhage[1], A. Källberg[1], P. Löfgren[1], P. Reinhed[1], S. Rosén[1], A. Simonsson[1], R. D. Thomas[1], S. Mannervik[1], V. T. Davis[2], P. A. Neill[2], J. S. Thompson[2], D. Hanstorp[5], H. T. Schmidt[1], and H. Cederquist[1]

1. Department of Physics, Stockholm University, AlbaNova, SE-106 91 Stockholm, Sweden
2. Department of Physics, University of Nevada, Reno, Nevada 89557, USA
3. Institute of Physics, Jan Kochanowski University, 25-369 Kielce, Poland
4. Centro Federal de Educação Tecnológica Celso Suckow da Fonseca, Petrópolis 25620-003, Rio de Janeiro, Brazil
5. Department of Physics, University of Gothenburg, SE-412 96 Gothenburg, Sweden

Negative ions are ideal systems for probing the subtle behavior of electronic structure and dynamics on the atomic scale. Measurements of properties such as binding energies and lifetimes of negative ion excited states yield insight on the electron correlation effects that allow these fragile entities to exist. Such measurements provide stringent tests of theories that attempt to accurately describe these interactions.

We present preliminary studies of excited state lifetimes for the platinum negative ion Pt^- using the cryogenic ion beam storage ring DESIREE [1, 2]. By cooling the storage ring down to 13 K, pressures on the order of 10^{-14} mbar are achieved, greatly reducing ion beam losses due to collisions with residual gases (dominated by H_2 [2]). The cold environment also mitigates photodetachment losses due to thermal blackbody radition, an important consideration for loosely-bound states such as those under study here. Pt^- has two excited states: a $5d^9\ 6s^2\ ^2D_{3/2}$ excited fine-structure level sharing the same electron configuration as the ground state and a higher-lying $5d^{10}\ 6s\ ^2S_{1/2}$ state. This makes Pt^- one of the few atomic negative ions to support an excited state of differing electron configuration from the ground state.

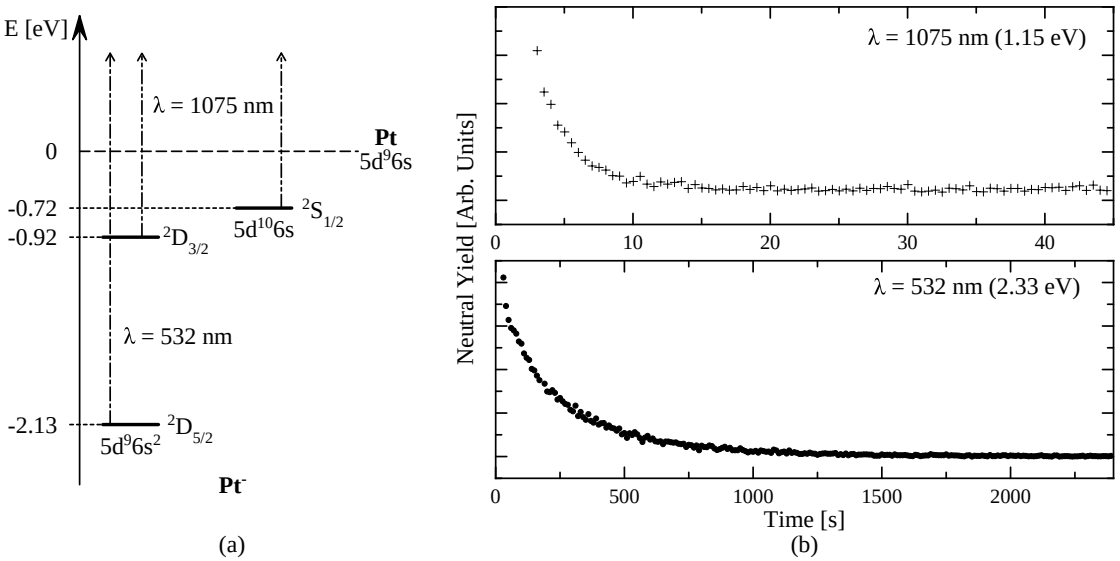

Fig. 1 (a) Pt^- energy level diagram indicating state energies in relation to the $5d^9\ 6s\ ^3$D Pt ground state. (b) Pt^- decay curves measured at photon wavelengths of 1075 nm (only excited states detached), and 532 nm (all states detached); note the differing time scales of the two panels.

Lifetime measurements were performed using two different laser wavelengths: 532 nm, which allowed detachment from all states of Pt^-, and 1075 nm, which allowed detached from only the excited levels in Pt^-. Platinum anions were stored with ion beam storage lifetimes on the order of 300 s and the excited state lifetimes determined through measurement of neutral Pt yield as functions of time after ion injection into the storage ring for photon wavelengths of 1075 nm (upper panel, Fig. 1 (b)) and 532 nm (lower panel, Fig. 1 (b)). Preliminary analysis and results will be presented and comparisons made to recent measurements of the lifetime of the $3d^9\ 4s^2\ ^2D_{3/2}$ excited state in the nickel negative ion Ni^- [3], which is a member of the same periodic group as platinum.

References

[1] R. D. Thomas *et al.*, *The double electrostatic ion ring experiment: A unique cryogenic electrostatic storage ring for merged ion-beams studies*, Rev. Sci. Instrum. **82**, 065112 (2011).
[2] H. T. Schmidt *et al.*, *First storage of ion beams in the Double Electrostatic Ion-Ring Experiment: DESIREE*, Rev. Sci. Instrum. **84**, 055115 (2013).
[3] M. Kamińska *et al.*, *Lifetime of the bound excited level in Ni^-*, Phys. Rev. A **93**, 012512 (2016).

Radiative Association of Metastable Helium He(2^3P) with Lithium Cations

Martina Zámečníková[1], Wolfgang P. Kraemer[2], Pavel Soldán[1]
1. Department of Chemical Physics and Optics, Faculty of Mathematics and Physics, Charles University in Prague, Ke Karlovu 3, CZ-12116 Prague 2, Czech Republic
2. Max-Planck-Institute for Astrophysics, Postfach 1317, D-85741 Garching, Germany

Fully quantum-mechanical approach [1] has been employed on the investigation of radiative association of metastable He(2^3P) with lithium cations. The aim is to calculate cross-sections and rate coefficients for both the spontaneous (with zero termodynamic temperature of the background) and stimulated (with the non-zero background temperature) processes.

The first part of the study focused on electronic states $a^3\Sigma^+$, $b^3\Sigma^+$, and $c^3\Sigma^+$ [2], while the second part also includes $1^3\Pi$ state. For the processes involving triplet-Π symmetry, the Hönl-London coefficients for dipole moment transitions are derived. Then, the cross-sections and rate coefficients of the following processes are computed: starting from the continuum states of $1^3\Pi$ and going to a ro-vibrational bound state of $1^3\Pi$, $c^3\Sigma^+$, $b^3\Sigma^+$, and $a^3\Sigma^+$; starting from the continuum states of $c^3\Sigma^+$ and going to a ro-vibrational bound state of $1^3\Pi$.

First, potential energy curves, dipole moment and transition dipole moments have been calculated by *ab initio* method and subsequently inter- and extrapolated by the one-dimensional reciprocal power reproducing kernel Hilbert space method. Secondly, the ro-vibrational states (of $1^3\Pi$, $c^3\Sigma^+$, $b^3\Sigma^+$, and $a^3\Sigma^+$) and resonances (of $1^3\Pi$ and $c^3\Sigma^+$) have been generated by program LEVEL7.7 [3]. Energy-dependant cross-sections are computed by an in-house programme for these processes: $1 \to 1$, $1 \to$ c, $1 \to$ b, $1 \to$ a and c $\to 1$. Besides, the allowed changes of the total molecular moment is $\Delta\Omega = 0$ or ± 1, which is a consequence of selection rules. Last, the temperature-dependant rate coefficients for spontaneous and stimulated processes are calculated by an in-house programme.

The current results are compared with those in ref. [2]. It turns out that some processes involving $1^3\Pi$ state have a hump in their cross-sections for low collisional energies. The cross-sections of the processes restricted to the triplet-Σ manifold, however, fall down in the whole range of collisional energies except for the regions with resonances.

References

[1] Bernard Zygelman, Alexander Dalgarno, *The Radiative Association of* He^+ *and* H, Astrophys. J. **365**, 239 (1990).
[2] Lucie Augustovičová, Martina Zámečníková, Wolfgang P. Kraemer, Pavel Soldán, *Radiative association of* He(2^3P) *with lithium cations*, Chem. Phys. **462**, 65 (2015).
[3] Le Roy, *LEVEL 7.7: A Computer Program for Solving the Radial Schrödinger Equation CPRR-66*, (2005).

Real time simulation of 1 MeV proton microbeam transmission through an insulating macrocapillary

Gyula U.L. Nagy, István Rajta and Károly Tőkési

Institute for Nuclear Research, Hungarian Academy of Sciences (Atomki), 4026 Debrecen Bem tér 18/c, Hungary

Charged particle beams are able to pass through insulating capillaries keeping their initial kinetic energy and charge state, even if the capillary target is tilted with respect to the direction of the incident beam and thus preventing the geometrical transmission. The phenomenon is called ion guiding and caused by the self-organized charge-up of the insulating material. At the beginning the incident beam hits the inner capillary wall and deposits its charge on it (see Figure 1 for our recent case), which will repulse the ions arriving later due to the Coulomb interaction. Once a dynamical equillibrium is established between the charges being put on the surface and the leakage currents flowing away, a stable transmission is realized. The fraction of the beam which is guided through the capillary with the help of these charge patches keeps its original energy and charge state.

After successful experimental investigation of the transmission of 1 MeV proton microbeam through a Teflon macrocapillary in Atomki [1–3], we started to develop a classical trajectory Monte-Carlo simulation code to reproduce our experimental data in order to study the key processes responsible for the guiding of the swift ion beam. The target is a poly(tetrafluoroethylene) (PTFE, known as Teflon) macrocapillary. The angle between the axis of the beam and the capillary is 1° which ensures the geometrical non-transparency due to the small beam divergence (< 0.3° half opening angle) and the large aspect ratio of the target (length to diameter > 55).

The simulation counts with the protons implanted into the insulating material, with the Coulomb forces act on the projectile ions and with the charge relaxation along the surface and into the bulk. Scattering of the incident ions by the surface atoms is also taken into account. We found highly consistent results with our experiments, thus we have become able to gain new information that we could not extract from our experiments.

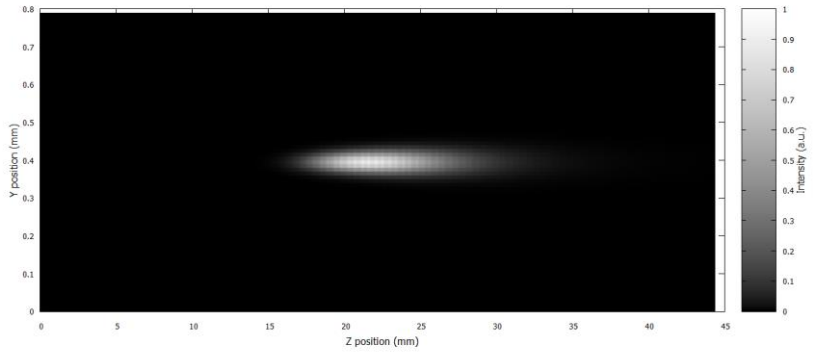

Fig. 1 Charge distribution on the inner capillary wall (YZ section) deposited by the focused proton microbeam with well known spot size (FWHM ≈ 1μm) and divergence (<0.3° and <0.1° in the X and Y plane, respectively).

References

[1] G.U.L. Nagy, I. Rajta, R.J. Bereczky, K. Tőkési, *Experimental setup for studying guiding of proton microbeam*, AIP Conf. Proc. **1525,** 40 (2013).

[2] G.U.L. Nagy, I. Rajta, R.J. Bereczky, K. Tőkési, *Incident beam intensity dependence of the charge-up process of the guiding of 1 MeV proton microbeam through a Teflon microcapillary*, EPJ D **69,** 102 (2015).

[3] I. Rajta, G.U.L. Nagy, R.J. Bereczky, K. Tőkési, *Interaction of proton microbeam with the inner surface of a polytetrafluoroethylene macrocapillary*, NIM B **354,** 328 (2015).

MOCCA: a 4k-pixel molecule camera for the position and energy resolved detection of neutral molecular fragments

Lisa Gamer[1], Christian Enss[1], Andreas Fleischmann[1], Loredana Gastaldo[1], Sebastian Kempf[1], Claude Krantz[2], Oldřich Novotný[2], Dennis Schulz[1], Andreas Wolf[2]

1. Kirchhoff Institute for Physics, Heidelberg University, INF 227, 69120 Heidelberg, Germany

2. Max Planck Institute for Nuclear Physics, Saupfercheckweg 1, 69117 Heidelberg, Germany

Stored beams of molecular ions at kinetic energies of some tens or hundreds of keV are widely used in molecular collision physics, and a mass spectroscopic identification of fragmentation products is often a key requirement for unambiguous data interpretation. For the reconstruction of the kinematics of electron-ion collisions at the Cryogenic Storage Ring (CSR, MPIK Heidelberg) we developed MOCCA, a new large-area 4096-pixel detector based on magnetic micro-calorimeters. Here, the kinetic energy deposited by a fragmented reaction product in one of the pixels is a measure of its mass, as all fragments have roughly the speed of the initial molecular ion. This calorimetric approach allows for identification of all fragments, in particular including neutrals. MOCCA has an active area of 45mm x 45mm, which is segmented into 64 x 64 absorbers, each 700µm x 700µm in size.

We discuss design considerations and present micro-fabricated detectors. We discuss the results of first tests with x-ray photons, including the uniformity of the detector response, cross-talk, multi-hit capability and the energy resolution for photons and for the massive particles. Including all effects, we expect MOCCA to easily resolve mass differences down to 1*u* for molecules with a few hundred mass units at CSR [1,2].

References

[1] MOCCA: A 4k-Pixel Molecule Camera for the Position and Energy-Resolving Detection of Neutral Molecule Fragments at CSR, L. Gamer, D. Schulz, C. Enss, A. Fleischmann, L. Gastaldo, S. Kempf, C. Krantz, O. Novotny, D. Schwalm, A. Wolf, J. Low Temp. Phys. (2016)

[2] Cryogenic micro-calorimeters for mass spectrometric identification of neutral molecules and molecular fragments, O. Novotný, S. Allgeier, C. Enss, A. Fleischmann, L. Gamer, D. Hengstler, S. Kempf, C. Krantz, A. Pabinger, C. Pies, D. W. Savin, D. Schwalm and A. Wolf , J. Appl. Phys. 118, 104503 (2015)

Dynamics of N_2 dissociative ionization by electron impact

X. Wang, Y. Zhang, D. Lu, R. Hutton, Y. Zou and B. Wei

Institute of Modern Physics, Fudan University, Shanghai 200433, China
brwei@fudan.edu.cn

In recent years, the combination of three dimensional (3D) momentum measurement with the coincident detection technique has rendered the kinetic energy release (KER) measurement possible [1, 2], which can provide an important and efficient tool to retrieve information concerning molecular ion geometry and structure, reaction energetics and dynamics.

Dissociative single, double and triple ionizations of N_2 by 200, 400 and 1000 eV electron impact are studied using cold target recoil-ion momentum spectroscopy technique in Shanghai [3]. Kinetic energy distributions are determined for different dissociation channels including dissociative excitation ($N_2^+ \rightarrow N^+ + N$, $N_2^{2+} \rightarrow N^{2+} + N$) and Coulomb explosion ($N_2^{2+} \rightarrow N^+ + N^+$, $N_2^{3+} \rightarrow N^{2+} + N^+$) channels. Possible ionic state of corresponding parent ion in each channel is identified. It is uncovered that electron ionization from different orbitals (outer and inner valence orbitals) of N_2 can result in different fragmentation channels with different kinetic energy releases, also different variation tendency of corresponding kinetic energy distributions with electron collision energies increasing from 200 to 1000 eV.

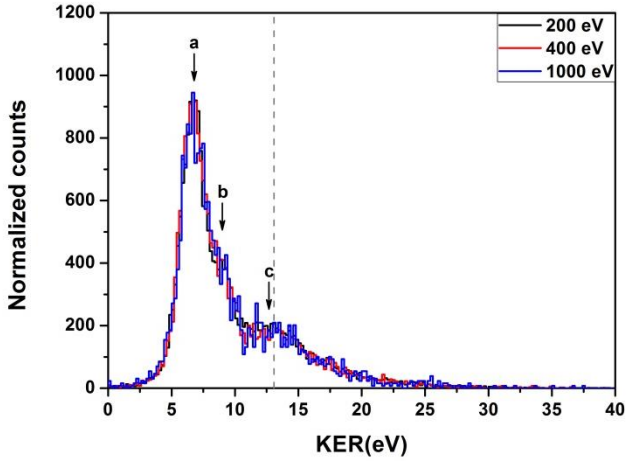

Fig. 1 Normalized KER spectra for the charge symmetric dissociation ($N_2^{2+} \rightarrow N^+ + N^+$) channel of N_2^{2+} taken at three different incident electron energies. The vertical solid line (position 13.08 eV) indicates the KER predicted by the Coulomb explosion model.

For the unstable dications, there are two breakup channels， via charge symmetric dissociation (CSD, $N_2^{2+} \rightarrow N^+ + N^+$) or charge asymmetric dissociation (CAD, $N_2^{2+} \rightarrow N^{2+} + N$) channel. As demonstrated in Figure 1 , the KER for CSD of N_2^{2+} exhibits three major contributions, namely two peaks *a* and *b* at 6.9, 9.2 eV and a "shoulder" *c* at 12.5 eV. It is interesting to notice that in contrast to that of the kinetic energy distribution of N^+ changing with electron energy increasing from 200 to 1000 eV, the profile of KER for CSD of N_2^{2+} does not change. More detail will be provided at the conference.

References

[1] J. Ullrich, R. Moshammer, A. Dorn, R. Dörner, L. P. H. Schmidt, and H. Schmidt-Böcking, Rep. Prog. Phys. 66, 1463 (2003).
[2] B. Wei, Y. Zhang, X. Wang, D. Lu, G. C. Lu, B. H. Zhang, Y. J. Tang, R. Hutton, and Y. Zou, J. Chem. Phys. 140, 124303 (2014).
[3] Y. Zhang, X. Wang, D. Lu, B. Wei, B. H. Zhang, Y. J. Tang, R. Hutton, and Y. Zou, Nucl. Instr. and Meth. B 337, 39 (2014)

Many-Body Theory of Positronium-Atom Scattering

D. G. Green, A. R. Swann, G. F. Gribakin
School of Mathematics and Physics, Queen's University Belfast, University Road, Belfast BT7 1NN, United Kingdom

Recent experiments on positronium (Ps) scattering on atoms and molecules have revealed interesting phenomena, e.g., above the Ps break-up threshold, this composite particle scatters in a way similar to how electrons scatter from atoms [1], while at low energies the Ps-noble-gas-atom cross section becomes very small [2]. Calculations using the simple impulse approximation provided an explanation of the electron-like Ps scattering [3]. In contrast, at low energies the dynamics of both the projectile and the target become important, and the outcome depends on a subtle cancellation of the static Ps-atom repulsion and the van der Waals-type attraction [4,5].

We propose a new method to describe Ps interaction with many-electron atoms and calculate Ps-atom scattering phase shifts and cross sections. It is based on many-body theory which provides an accurate description of electron [6,7,8] and positron [9] interaction with noble-gas atoms. We first solve the Dyson equation $\left(\hat{H}_0^{\pm}+\hat{\Sigma}^{\pm}\right)\psi^{\pm}=\varepsilon^{\pm}\psi^{\pm}$, to obtain the electron $(-)$ and positron $(+)$ wavefunctions in the field of the atom. Here $\hat{H}_0^{\pm}$ is the zeroth-order Hamiltonian in the static (Hartree-Fock) field of the atom, $\hat{\Sigma}^{\pm}$ is the self-energy, which represents the electron/positron nonlocal correlation potential (shown diagrammatically in Fig. 1). We confine the system in a spherical cavity and use a B-spline representation of the electron/positron basis states.

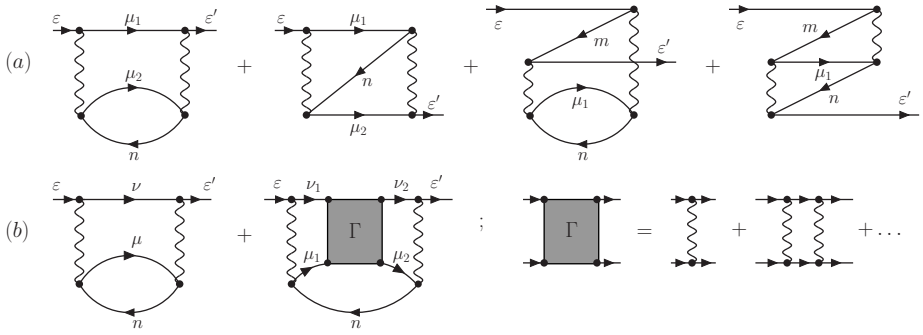

Fig. 1 Main contributions to the (a) electron and (b) positron self-energies $\Sigma^{\pm}$. External lines represent the electron or positron in the static field of the atom; internal lines directed to the right and labelled μ (ν) represent excited electron (positron) states; lines directed to the left represent holes; wavy lines are the Coulomb interactions; the Γ-block is the virtual Ps contribution.

The Ps wavefunction (in the cavity) is obtained as an expansion $\Psi=\sum_{\mu,\nu}C_{\mu\nu}\psi_{\mu}^{-}\psi_{\nu}^{+}$, substituted in the two-particle Dyson equation $\left(\hat{H}_0^{-}+\hat{\Sigma}_{\varepsilon}^{-}+\hat{H}_0^{+}+\hat{\Sigma}_{\varepsilon}^{+}+\tilde{V}\right)\Psi=E\Psi$. Here $\tilde{V}$ is the *dressed* electron-positron interaction (see Fig. 2), which accounts for the screening of the electron-positron interaction by the atom (cf. Ref. [10]).

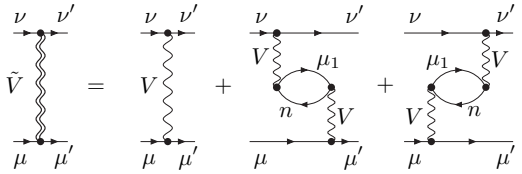

Fig. 2 The main contributions to the dressed electron-positron Coulomb interaction $\tilde{V}$ (double wavy line) in Ps are the bare Coulomb interaction V (wavy line) and the two screening diagrams shown.

The Ps energy eigenvalues, taken together with the boundary condition at the cavity wall, will provide the scattering phase shifts and hence, the cross sections [5]. Overall, the method should enable the most accurate treatment of Ps-noble-gas-atom scattering to date, and allow a comparison with the recent measurements [2].

References

[1] S. J. Brawley *et al.*, *Electron-like Scattering of Positronium*, Science **330**, 789 (2010).
[2] S. J. Brawley *et al.*, *Positronium Production and Scattering below Its Breakup Threshold*, Phys. Rev. Lett. **115**, 223201 (2015).
[3] I. I. Fabrikant and G. F. Gribakin, *Similarity between positronium-atom and electron-atom scattering*, Phys. Rev. Lett. **112**, 243201 (2014).
[4] I. I. Fabrikant and G. F. Gribakin, Positronium-atom scattering at low energies, Phys. Rev. A 90, 052717 (2014).
[5] A. R. Swann and G. F. Gribakin, *Positronium collisions with noble-gas atoms* (unpublished).
[6] M. Ya. Amusia *et al.*, *Elastic scattering of slow electrons by atoms*, Zh. Eksp. Teor. Fiz. **68**, 2023 (1975) [Sov. Phys. JETP **41**, 1012 (1975)].
[7] M. Ya. Amusia *et al.*, *Slow-electron elastic scattering on argon*, Phys. Rev. A **25**, 219 (1982).
[8] W. R. Johnson and C. Guet, *Elastic scattering of electrons from Xe, Cs^+, and Ba^{2+}*, Phys. Rev. A **49**, 1041 (1994).
[9] D. G. Green, J. A. Ludlow, and G. F. Gribakin, *Positron scattering and annihilation on noble-gas atoms*, Phys. Rev. A **90**, 032712 (2014).
[10] V. A. Dzuba, V. V. Flambaum, and M. G. Kozlov, *Combination of the many-body perturbation theory with the configuration-interaction method*, Phys. Rev. A **54**, 3948 (1996).

Ions colliding with clusters of small hydrocarbon chains — a pathway to aromatic rings?

Michael Gatchell[1], Henning Zettergren[1], Rudy Delaunay[2,3], Arkadiusz Mika[2,3], Giovanna D'Angelo[1], Kostiantyn Kuliyk[1], Alicja Domaracka[3], Patrick Rousseau[2,3], Bernd A. Huber[3], and Henrik Cederquist[1]

1. Department of Physics, Stockholm University, SE-106 91 Stockholm, Sweden

2. Université de Caen Basse-Normandie, Esplanade de la Paix, F-14032 Caen, France

3. Centre de Recherche sur les Ions, les Matériaux et la Photonique (CIMAP), CEA-CNRS-ENSICAEN, Boulevard Henri Becquerel, F-14070 Caen Cedex 05, France

Energetic ions colliding with loosely bound molecular clusters can lead to the growth of new and larger molecular species, even in clusters consisting of very stable and unreactive molecules like Polycyclic Aromatic Hydrocarbons (PAHs) [1] or C_{60} fullerenes [2]. There the key mechanism is the prompt knockout of atoms from molecules in the cluster by the impacting keV projectile [3,4]. This produces radical species that can efficiently form covalent bonds with neighboring molecules with little or no reaction barriers [1,2].

Here we present results for keV ions colliding with loosely bound clusters of small hydrocarbon molecules. An experimental mass spectrum from collisions between 3 keV Ar^+ ions and clusters of C_4H_6 (butadiene) molecules is shown in Fig. 1. We see clear evidence of molecular growth and the formation of new larger molecules with up to at least nine C atoms. Compared to the broad range of growth products observed with PAH clusters [1] we see here that certain specific products $C_{n>4}H_x$ are much more abundant than others. In particular, the peaks corresponding to $C_5H_7^+$ and $C_6H_7^+$ stand out, indicating that they are "magic" and more stable than other similarly sized species.

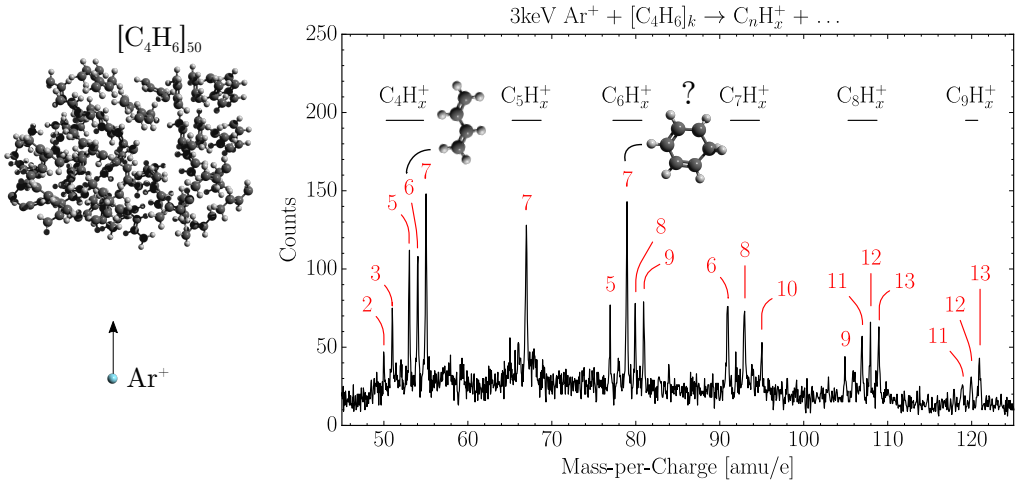

Fig. 1 Experimental mass spectrum for 3 keV Ar^+ ions colliding with weakly bound clusters of C_4H_6. The labels above each group of peaks indicate their molecular formula $C_nH_x^+$. The numbers in red indicate the numbers of H atoms for $n = 4$, 5, 6, 7, 8, and 9 carbon atoms in the fragmentation/growth products. The insets show the structures of intact $C_4H_6^+$ and the most stable form of $C_6H_7^+$.

We will also present results from our classical and quantum chemical molecular dynamics simulations of the same $Ar^+ + [C_4H_6]_k$ collisions. The classical simulations show that the knockout process could initiate growth inside the butadiene clusters similar to what has been observed for PAH [1] and fullerene [2] clusters. However, more work is required to fully understand the roles that the internal energy and charge of the molecules have on the growth in the present case. Our pilot quantum chemical calculations suggest that one of the most intense peaks in our mass spectrum (see Fig. 1), that of $C_6H_7^+$, may correspond to a cyclic structure — protonated benzene. If this is the case, this type of processing may be important for the formation and growth of large aromatic molecules, like for example PAHs, in the interstellar medium [5].

References

[1] R. Delaunay *et al.*, *Molecular Growth Inside of Polycyclic Aromatic Hydrocarbon Clusters Induced by Ion Collisions*, J. Phys. Chem. Lett. **6**, 1536–1542 (2015).

[2] H. Zettergren *et al.*, *Formations of Dumbbell C_{118} and C_{119} inside Clusters of C_{60} Molecules by Collision with α Particles*, Phys. Rev. Lett. **110**, 185501 (2013).

[3] M. H. Stockett *et al.*, *Nonstatistical fragmentation of large molecules*, Phys. Rev. A **89**, 032701 (2014).

[4] M. Gatchell *et al.*, *Non-statistical fragmentation of PAHs and fullerenes in collisions with atoms*, Int.. J. Mass **365–366**, 260–265 (2014).

[5] A. G. G. M. Tielens, *The molecular universe*, Rev. Mod. Phys. **85**, 1021–1081 (2013).

Mass-spectrum of product ions from the collision of 450eV N_2^+ with hydrocarbon covered surface of tungsten

Sunil Kumar[a], Bhupendra Singh[a], Suman Prajapati[a], B.K.Singh[a], and R.Shanker[a]
[a] Atomic Physics Laboratory, Department of Physics, Banaras Hindu University, Varanasi-221005
email: shankerorama@gmail.com

The process of low energy ion-surface interaction has attracted a growing interest in recent years in the scientific community, particularly, in the researches in controlled magnetically confined thermonuclear fusion devices, like ITER [1]. The tungsten has been considered to be one of the preferred candidates as a material for the first wall and the diverter targets of the plasma vacuum vessel due to its characteristic properties. It is hence of considerable interest to perform a dedicated laboratory experiment in order to understand the mechanism of interaction and to obtain the product ions that are generated under bombardment of low-energy ions relevant to edge plasma with polycrystalline tungsten surfaces. Keeping in view of the above objectives, a well characterized 450eV N_2^+ ion beam has been produced by using a Colutron ion source in our laboratory [2]. We have studied the mass spectra of various product ions resulting from the interaction of N_2^+ ions with hydrocarbons covered surface of a polycrystalline tungsten metal using a TOF mass spectrometry technique .
The spectra of product ions are found to consist of not only the reflected and dissociated primary ions but also several sputtered ions of tungsten and hydrocarbons along with a few contaminants of the basic material. In addition, we have also observed the formation of tungsten nitride, namely WN^+ with measurable intensities. Details of experimental setup and that of results derived from the experiments will be presented and discussed.

Keywords: *colutron ion source, ion-surface interaction, tungsten nitrite*

References

1. G.Meisl et.al. New Journal of Physics 16 (2014) 093018
2. Sunil Kumar et.al. Int. J. Mass. Spectrom 32 (2015) 385

Evolution of energy-loss-spectrum profile with projectile mass in impulsive ion-molecule collisions at hyperthermal energies

Masato Nakamura
College of Science and Technology, Nihon University, Narashinodai, 2748501 Funabashi Japan

Atsushi Ichimura
Institute of Space and Astronautical Science, JAXA, Yoshinodai, Chuo-ku 2298510 Sugamihara, Japan

In large angle scattering of ions by molecules at hyperthermal energies, a short range repulsive force plays a dominant role. In these collisions, sudden-limit models, the hard-shell model for rigid rotor [1] and the hard-potential model [2] for vibrating rotor, well describes the mechanism of the energy transfer from the translational motion to the molecular internal motions. We study how the profile of the energy-loss spectrum varies with the projectile taking a common interaction potential.

Figure 1 shows energy-loss spectra in the center-of-mass system of H^+ and K^+ ions scattered from an N_2 molecule. We take an incident energy E of 1 atomic unit (= 27 eV) and the scattering angle θ of 180°. In the figure, the horizontal axis represents the scaled energy-loss $y = (4M/m)\delta E/E$, where m and M are the reduced masses of inter- and intra-molecular motions, respectively, and δE denoting the energy loss; the vertical axis represents a convoluted energy-loss spectrum $f(y)$. The spectra are obtained by the classical trajectory (CT) calculation and compared with the hard-shell model and the hard-potential model. For a projectile much lighter than the target, the vibrational and rotational excitation occurs in such a way that the hard-potential model predicts, producing a spectral profile with double peaks shown in the left panel of the figure. As the projectile mass increases, the vibrational suddenness is degraded so that the vibrational excitation becomes quenched, while the spectral profile still shows a double peak structure explainable with the hard-shell model. Subsequently as the projectile mass further increases, the rotational suddenness is also degraded so that the spectrum indicates a profile departing far from the prediction of the hard-shell model. Eventually, the deeply inelastic peak collapses and the nearly elastic peak dominates as shown in the right panel of Fig. 1. Comparison with an experimental result [4] for $Na^+ - N_2$ collisions is made.

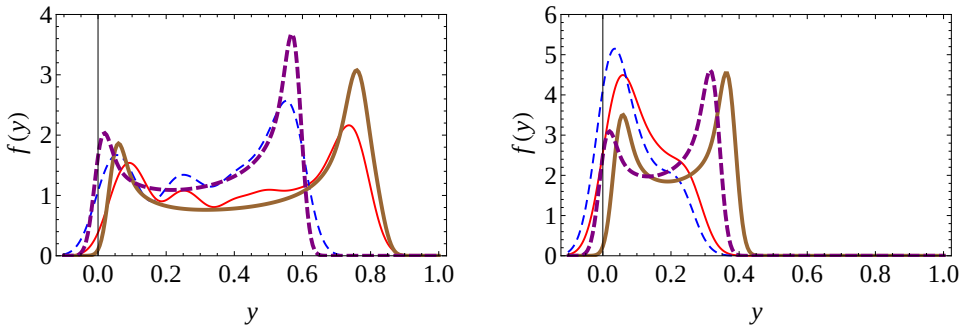

Fig. 1 Energy-loss spectrum of an H^+ (K^+) ion scattered from a N_2 molecule in the left (right) panel. The spectra with the hard-potential model and those with the hard-shell model are shown by thick-solid curves and thick-dashed curves, respectively. The spectra by the CT calculation for a vibrating-rotor molecule and those for a rigid-rotor molecule are shown by thin-solid curves and thin-dashed curves, respectively.

.

References

[1] D. Beck, U. Ross, and W. Schepper, Z. Phys. A**293** 107 (1979), A**299** 97 (1981).
[2] A. Ichimura and M. Nakamura, Phys. Rev. A **69** 022716 (2004).
[3] M. Nakamura and A. Ichimura, Phys. Rev. A**71** 062701 (2005).
[4] M. Nakamura, S. Kita, and T. Hasegawa, J. Phys. Soc. Jpn. **56** 3161 (1987).

Electron-impact Ionization of W^{19+} Ions

Alexander Borovik, Jr.[1,2], Benjamin Ebinger[1], Daniel Schury[2,3], Stefan Schippers[1] and Alfred Müller[2]

1. I. Physikalisches Institut, Justus-Liebig Universität Gießen, Leihgesterner Weg 217, 35392 Giessen, Germany

2. Institut für Atom- und Molekülphysik, Justus-Liebig Universität Gießen, Leihgesterner Weg 217, 35392 Giessen, Germany

3. GSI Helmholtzzentrum für Schwerionenforschung GmbH, Planckstraße 1, 64291 Darmstadt, Germany

For its unique properties tungsten has been chosen as the material for plasma-facing elements in tokamaks. Due to an extreme sustainability of this material the erosion of the surfaces due to enormous particle fluxes is to be minimized. The sputtering of tungsten from the surfaces, however, cannot be prevented completely and certain limited amounts of tungsten are to be expected to penetrate the tokamak plasma. This may result in significant energy losses up to preventing the tokamak plasma from ignition. At the same time, highly-charged tungsten ions can serve for diagnostics of the plasma [1]. In both cases, extensive modeling of the tokamak plasma is needed requiring sets of accurate data on atomic processes involving tungsten ions, among others, on electron-impact ionization.

We present an extensive study of electron-impact ionization of nineteenfold ionized tungsten ions aimed at inferring accurate plasma rate coefficients using both experimental and theoretical approaches [2]. The Giessen crossed-beams apparatus has been used to measure electron-impact ionization cross sections in the energy ranges from the observed ionization onsets up to 1000 eV. The setup incorporates both the animated crossed-beams method for measurements of the absolute cross-section values and the fine-step scan technique to uncover fine structures in the measured cross sections. Configuration-averaged distorted-wave method calculations were used for theoretical estimation of contributions of various ionization mechanisms, namely direct ionization and excitation-autoionization processes involving different electron subshells.

The figure shows the plasma rate coefficients for electron-impact single ionization of W^{19+} ions inferred from the experimentally measured cross section and its theory-based extrapolation to higher energies. The solid and dashed curves represent results for ions in the ground- and first excited electron configurations, respectively. The dots are previous data calculated by Loch et al [3]. The present data exceed the calculations of Loch et al. by approximately 30%. This discrepancy arises from strong contributions of excitation-autoionization processes involving excitations of autoionizing states with principal quantum numbers beyond 8, which were not included in the calculations of Loch et al.

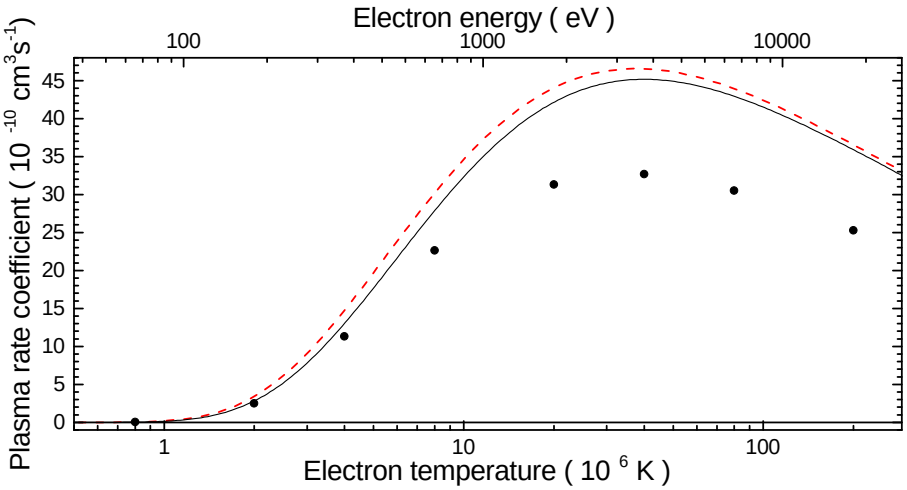

Fig. 1 Inferred plasma rate coefficients for electron-impact ionization of W^{19+} ions. The dashed and solid lines are the present results for the first excited and the ground configuration, respectively. Dots represent the data of Loch et al. [3].

References

[1] P. Beiersdorfer, *Highly charged ions in magnetic fusion plasmas: research opportunities and diagnostic necessities*, J. Phys. B **48** 144017 (2015).

[2] A. Borovik, Jr., B. Ebinger, D. Schury, S. Schippers, and A. Müller, *Electron-impact single ionization of W^{19+} ions*, Phys. Rev. A **93**, 012708 (2016).

[3] S. D. Loch, J. A. Ludlow, and M. S. Pindzola, A. D. Whiteford, D. C. Griffin, *Electron-impact ionization of atomic ions in the W isonuclear sequence*, Phys. Rev. A **72**, 052716 (2005).

Quantum Statistical Theory of Electron Recombination in Highly Charged Ions via Chaotic Many-Electron States

Julian Berengut[1], Celal Harabati[1], Vladimir Dzuba[1], Victor Flambaum[1], Gleb Gribakin[2]
1. School of Physics, University of New South Wales, Sydney, NSW 2052, Australia
2. School of Mathematics and Physics, Queen's University, Belfast BT7 1NN, Northern Ireland, United Kingdom

Electron recombination with highly charged ions that have open f shells (e.g. Au^{25+} and W^{20+}) is dominated by chaotic many-electron resonances [1]. In these systems the strong mixing of the many-electron basis states results in very large numbers of complex, chaotic eigenstates which can only be described using a statistical theory. Electron capture into these 'compound resonances' is orders of magnitude more efficient than direct radiative recombination, and furthermore cannot be described by standard theories of dielectronic recombination [2].

In the many-body quantum chaos (MBQC) statistical theory, the problem is treated as capture into dielectronic 'doorway' states which then spread into the chaotic compound resonances. Once the compound resonance has formed, the energy is distributed among the many valence electrons, which suppresses autoionization. The capture into these states therefore leads to long-lifetime trapping of the incident electron, allowing the radiative decay and hence recombination to occur.

We have developed the theory of many-body quantum chaos to accurately describe the both the initial electron capture process and the subsequent radiative decay or autoionization. A 'level-resolved' statistical theory that considers electron capture into doorway states with fixed angular momentum, projection and parity is presented [3]. We find very good agreement with the 'configuration-average' MBQC statistical theory used in previous works, where the effects of spectator electrons and angular momentum conservation are not included. The theory shows excellent agreement with experimental recombination rate coefficients in a range of ions with open f-shells[4].

References

[1] V. A. Dzuba, V. V. Flambaum, G. F. Gribakin, C. Harabati, and M. G. Kozlov, *Electron Recombination, Photoionization, and Scattering via Many-Electron Compound Resonances*, Phys. Rev. A **88**, 062713 (2012).

[2] N. R. Badnell, C. P. Ballance, D. C. Griffin, and M. O'Mullane, *Dielectronic Recombination of W^{20+} ($4d^{10}\,4f^8$): Addressing the Half-Open f Shell*, Phys. Rev. A **85**, 052716 (2012).

[3] J. C. Berengut, C. Harabati, V. A. Dzuba, V. V. Flambaum, and G. F. Gribakin, *Level-resolved quantum statistical theory of electron capture into many-electron compound resonances in highly charged ions*, Phys. Rev. A **92**, 062717 (2015).

[4] S. Schippers, D. Bernhardt, A. Müller, C. Krantz, M. Grieser, R. Repnow, A. Wolf, M. Lestinsky, M. Hahn, O. Novotný, and D. W. Savin, *Dielectronic Recombination of Xenonlike Tungsten Ions*, Phys. Rev. A **83**, 012711 (2011).

Potential Electron Scattering by the Bi_2 Molecule

Shandor Demesh[1,2], Vladimir Kelemen[1], Eugene Remeta[1]

1. Institute of Electron Physics, National Academy of Sciences of Ukraine, Universitetska St. 21, 88017 Uzhhorod, Ukraine

2. Institute for Nuclear Research of the Hungarian Academy of Sciences (ATOMKI), Bem tér 18/c, 4026 Debrecen, Hungary

We used the optical potential approach [1] to calculate various cross-sections for e+Bi_2 elastic scattering in the independent atom model (IAM) [2,3]. The local relativistic parameter-free real optical potential approximation (RSEP LA) is used for e+Bi scattering. It contains static, relativistic local exchange, polarization (local correlation-polarization), scalar-relativistic and spin-orbit potentials [1].

The differential cross section (DCS) for potential electron scattering by a two-atomic homonuclear molecule in the IAM framework is given: $d\sigma_{\mathrm{el}}/d\Omega = (2d\sigma_{\mathrm{el,A}}/d\Omega)[1+\sin(sr_{12})/sr_{12}]$. Here $s = 2k\sin(\theta/2)$, θ – scattering angle, $k = \sqrt{2E}$ (in a.u.), E – electron's energy; r_{12} – distance between the atoms, $d\sigma_{\mathrm{el,A}}/d\Omega$ – DCS for electron scattering by an individual atom. The NIST value for the r_{12} interatomic distance of Bi_2 molecule is equal 2.6596 Å. Integral elastic, momentum transfer and viscosity cross sections are calculated from the DCSs by integration in scattering angles.

As an example we present the DCSs at 10 and 40 eV impact energies in Fig. 1 (a) and (b). Our DCS is compared at 40 eV with the experimental data [4], where the DCSs are measured with ±20% accuracy and ICS with an uncertainty factor 2 (the bismuth beam contains Bi atoms (86%) and Bi_2 molecules (14%)). The integral elastic and momentum transfer cross sections are presented in Fig.2 (a) and (b). Note here, that integral elastic cross section at 40 eV in [4] is equal $45.0\cdot10^{-20}$ m^2, while we obtained a value $35.24\cdot10^{-20}$ m^2 for this.

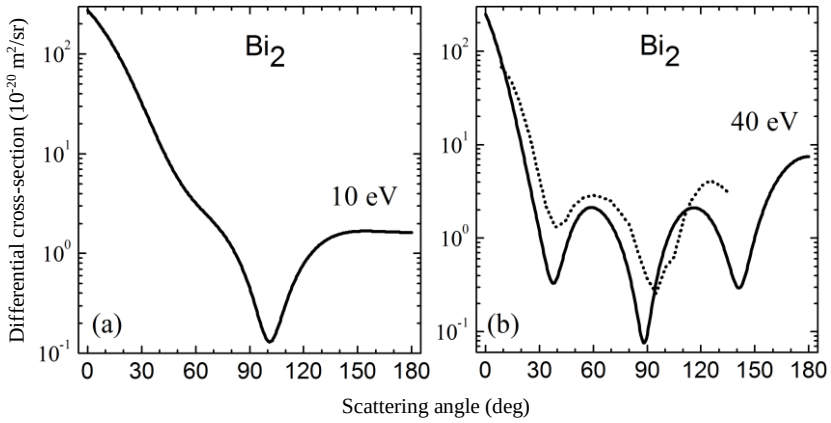

Fig. 1 Differential elastic cross sections for e+Bi_2 scattering at 10 eV (a) and 40 (b) eV (··· [4])

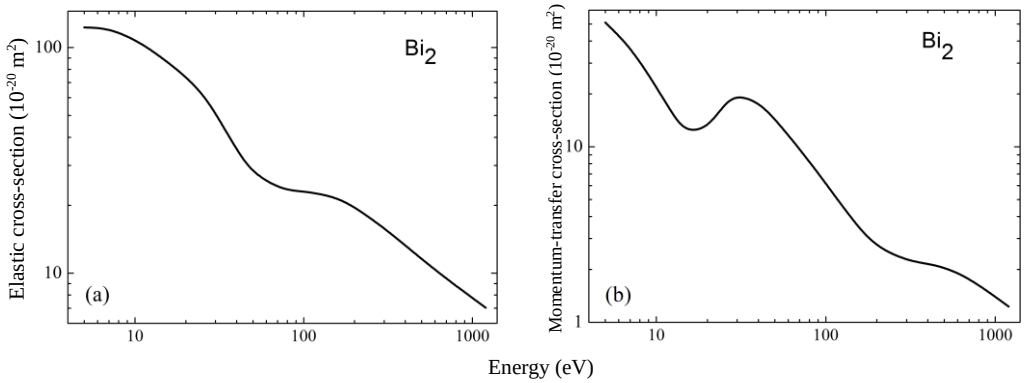

Fig. 2 Integral cross sections for e+Bi_2 scattering. Elastic (a) and momentum transfer (b).

References

[1] Sh. Demesh, E. Remeta and V. Kelemen, *Elastic Electron Scattering on Molecule in Optical Potential Approach*, CEPAS-6 (Bratislava, Slovakia) 65 (2014).

[2] D. Raj, *A Note of the Use of the Additivity Rule for Electron-Molecule Elastic Scattering*, Phys. Lett. A **160**, 571 (1991).

[3] P. Możejko, B. Żywicka-Możejko and C. Szmytkowski, *Elastic Cross-Section Calculations for Electron Collisions with XY_4 (X=Si, Ge; Y=H, F, Cl, Br, I) molecules*, Nucl. Instr. Meth. B. **196**, 245 (2002).

[4] W. Williams, S. Trajmar and D.G. Bozinis, *Elastic and inelastic scattering of 40 eV electrons from atomic and molecular bismuth*, J. Phys. B: At. Mol. Phys. **8**, L96 (1975).

Electron Interactions with Iron Pentacarbonyl Molecules and Clusters

Dušan Mészáros[1], Peter Papp[1], Michal Lacko[1], Michal Stano[1], Štefan Matejčík[1]

1. Department of Experimental Physics, Faculty of Mathematics, Physics and Informatics, Comenius University in Bratilsava, Mlynská dolina F2, 842 48 Bratislava, Slovakia

The Iron pentacarbonyl FEBID (Focused Electron Beam Induced Deposition) [1] precursor was studied in the past using the crossed electron/molecular beams apparatus (CEMBA) [2] built at the Comenius University in Bratislava. Interactions of low energy electrons (0 – 30 eV) with $Fe(CO)_5$ molecules were performed [2] to describe the side effects during FEBID, products were detected with quadrupole mass analyzer. The primary beam in FEBID with keV energy electrons produces a high yield of secondary electrons with kinetic energies below ~50 eV which interact with the precursor in the volume close to deposited surface. This has unexpected effects of broadening and contamination of the deposited layer/structure.

We have carried out several measurements of the ion efficiency curves of positive and negative ions produced via electron/molecular reactions with $Fe(CO)_5$ in the gas phase. The most pronounced products can be characterised with sequential loss of CO group form $Fe(CO)_n$, both in cationic and anionic reaction channels. Several doubly charged fragments and fragments with dissociated carbonyl can be found in the spectrum as well. These studies were recently extended with cluster measurements of gas phase $Fe(CO)_5$ in argon gas, electron/cluster beams apparatus equipped with quadrupole mass analyzer [3]. Similarly to the observations from CEMBA experiment, the more carbonyls were dissociated the higher ion yield of $Fe(CO)_n^+$ was obtained up to the final decomposition to Fe^+. Contrary to the monomolecular spectrum from CEMBA several doubly ionised cluster peaks contribute to the monomolecular part of the spectrum (below m/z 196) obtained from CLUSTER. The opposite trend was observed for negative ions where the ion yield of $Fe(CO)_4^-$ is the dominant with low energy resonance at ~0 eV and the more carbonyls are dissociated the higher the resonance energy is but with decreasing ion yield, with final decomposition to Fe^- at ~6 eV. In the cluster spectrum measured recently we have identified the $[Fe(CO)_5]_n$ cluster with n=2, 3 and 4 (which was at the detection limit of the analyzer). The electron induces not only ionization of the cluster, but fragmentation as well. Therefore several sequences of CO, Fe and $Fe(CO)_m$ (1, 2 up to 4) attached with the molecular clusters were found in the spectrum. This feature is however independent on the charge which is carried on the cluster, the products mentioned above were detected both for positive and negative ions via electron ionisation and dissociative electron attachment. No molecular clusters with the carrying Ar gas were detected in the spectrum. These results demonstrate the important role of low energy electrons (with kinetic energies from 0 eV up to 20 eV used in this work) which produce a high yield of several molecular or cluster fragments of $Fe(CO)_5$ precursor in the FEBID.

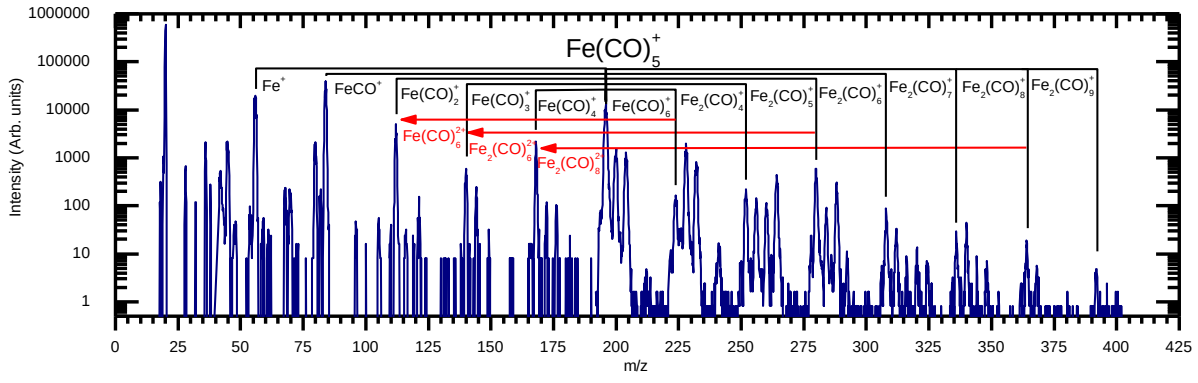

Fig. 1 Part of the electron induced mass spectrum of $Fe(CO)_5$ clusters in Ar gas, incident electron energy 80 eV.

This work was supported by the Slovak Research and Development Agency under Contract No. APVV-0733-11 and the Slovak grant agency VEGA 1/0417/15. This work was conducted within the framework of the COST Action CM1301 (CELINA). This project has received funding from the European Union's Horizon 2020 research and innovation programme under grant agreement No 692335.

References

[1] Ivo Utke, Patrik Hoffmann and John Melngailis, *Gas-assisted focused electron beam and ion beam processing and fabrication*, J. Vac. Sci. Technol. B **26**, 1197 (2008).

[2] Michal Lacko, Peter Papp, Karol Wnorowski and Štefan Matejčík, *Electron-induced ionization and dissociative ionization of iron pentacarbonyl molecules*, Eur. Phys. J. D **69**, 84 (2015).

[3] Oddur Ingolfsson, Fritz Weik, Eugen Illenberger, *The reactivity of slow electrons with molecules at different degrees of aggregation: gas phase, clusters and condensed phase*, Int. J. Mass. Spec. **155**, 1 (1996).

Insight into the effects of polarization in e + A@C_{60} elastic scattering

Miron Ya. Amusia[1,2], Larissa L. Chernysheva[2], Valeriy K. Dolmatov[3]

1. Racah Institute, Hebrew University, 91904 Jerusalem, Israel

2. A. F. Ioffe Physical-Technical Institute, 194021 St. Petersburg, Russia

3. Department of Physics and Earth Science, University of North Alabama, Florence, Alabama 35632, U.S.A.

A deeper insight into a complicated multi-faceted problem of low-energy electron elastic scattering off endohedral fullerenes, labelled *A*@C_{60}, where *A* is an atom encapsulated inside the hollow interior of a C_{60} fullerene, is unravelled. The "zeroth order" insight into the problem was provided earlier [1, 2] in the framework of a model static-exchange approximation. Important corrections to results of works [1, 2] were introduced and probed in another model approximation [3] by evaluating the impacts of dynamical polarizability of only the atom *A*, surrounded by *static* C_{60}, on $e + A@C_{60}$ scattering. In the present work, we provide a deeper insight into $e + A@C_{60}$ scattering by utilizing the approximation which accounts for polarization of both C_{60} and atom *A* by an incident electron. The emphasis is not only on the study of the polarization effects themselves, but on their sensitivity to the size and polarizability of the encapsulated atom *A* (*A* = Ne, Ar, Xe and Ba) as well.

Key points of the utilized approximation could be outlined as follows. A static part $V_s(r)$ of the C_{60} potential is approximated by an attractive square-well (in the radial coordinate *r*) potential of certain depth U_0, inner radius r_0 and thickness Δ, as in [1-3]. The polarization potential $V_F(r)$ of C_{60} is approximated as $V_F(r) = -\alpha/[2(r^2+b^2)^2]$, where α is the static polarization of C_{60}, *b* is a parameter of the order of r_0, as in [4]. The impact of dynamical polarizability of the atom *A* on electron scattering is accounted for with the help of the concept of a self-energy part of the one-electron Green function, similar to [3], but modified in the present work by accounting for coupled interactions between electrons of the atom A and electrons of C_{60} as well, as in [4].

For illustration only, calculated data for a partial *s*-electron elastic scattering cross section off Ba@C_{60}, obtained at different levels of approximation, are depicted in Fig. 1. Significant differences between electron scattering off empty C_{60}, off free Ba and off Ba@C_{60} are seen along with the revealed dramatic impact of polarization of Ba@C_{60} on the scattering process and its sensitivity to a probed level of approximation.

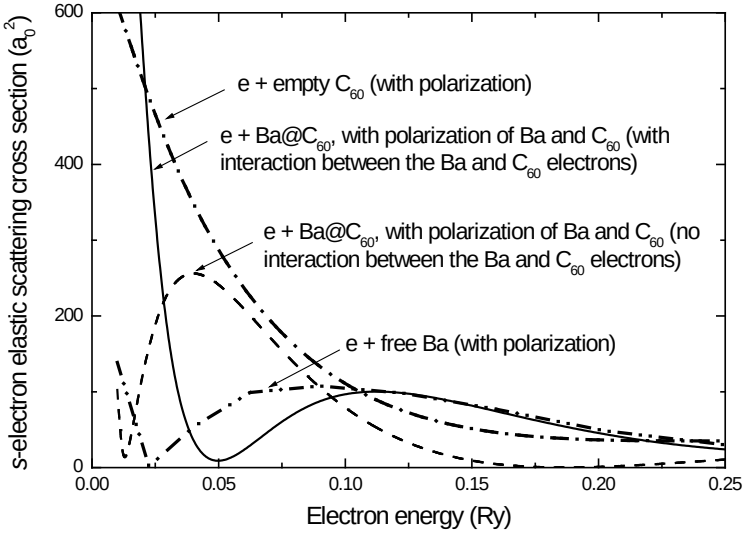

Fig. 1 Partial *s*-electron elastic scattering cross sections for $e + C_{60}$, *e* + free Ba and e + Ba@C_{60} calculated with account for target-polarization impacts upon the scattering process, at different levels of approximation, as marked.

VKD acknowledges the support of NSF under the grant No. PHY-1305085.

References

[1] V. K. Dolmatov, M. B. Cooper, and M. E. Hunter, *Electron elastic scattering off endohedral fullerenes A@C_{60}: The initial insight*, J. Phys. B **47**, 115002 (2014).

[2] M. Ya. Amusia and L. V. Chernysheva, *On the behaviour of scattering phases in collision of electrons with multi-atomic objects*, JETP Lett. **101**, 703 (2015).

[3] V. K. Dolmatov, M. Ya. Amusia, and L. V. Chernysheva, *Electron elastic scattering off A@C_{60}: the role of atomic polarization under confinement*, Phys. Rev. A **92**, 042709 (2015).

[4] M. Ya. Amusia and L. V. Chernysheva, *The role of fullerene shell upon stuffed atom polarization potential*, JETP Lett. **103**, 286 (2016).

Trend of the properties of the Lyman-alpha$_{1,2}$ emission along the H isoelectronic sequence following radiative recombination

Mohammed reda Boufatah[1], Latifa Bettadj[1], Kemal Mokhtar Inal [1]

1. Laboratoire de Physique Théorique, Département de Physique, Universié de Tlemcen, 13000 Tlemcen, Algeria

In this work, we explore how the intensity and polarization of the Lyman-alpha emission of H-like ions is affected in a plasma by the radiative recombination (RR) of bare ions when compared with the electron-impact excitation.

We have considered the case of RR of bare nuclei involving a single-electron system, with colliding electrons assumed to be unidirectional and monoenergetic. We have treated the RR process in the framework of a fully relativistic theory for the motion of the electrons and the electron-photon coupling [1]. The calculations of Ly-α_1 ($2p_{3/2} \rightarrow 1s_{1/2}$) polarization as well as the intensity ratio of Ly-α_1 to Ly-α_2 ($2p_{1/2} \rightarrow 1s_{1/2}$) lines have been performed for various recombined H-like ions with atomic numbers in the range $10 \leq Z \leq 54$. Our results are presented in the table below for the polarization degree $P_{Ly\text{-}\alpha1}$ and intensity ratio $I_{Ly\text{-}\alpha1} / I_{Ly\text{-}\alpha2\ (+M1)}$ calculated for the five H-like ions Ne^{9+}, Ar^{17+}, Fe^{25+}, Mo^{41+}, and Xe^{53+} at the same incident-electron energy in threshold units, ε=1.078 x E_I, E_I being the ionization threshold of the corresponding H-like ion. Calculations have been performed at the ionization-recombination balance. The values of the abundance ratios ρ of bare to hydrogen-like ions at such a balance are also presented in the table together with the branching ratios B_{M1}. Comparison was made between the theoretical calculations which include contributions from the RR process (columns labeled ``IE+RR") with those that account for the electron-impact excitation process alone (columns labeled ``IE"). As seen from the table below, in the near-threshold region the contribution of the RR process to the intensity ratios and polarization parameters remains very weak for all the considered ions, although the abundance ratio ρ changes by three orders of magnitude from Ne to Xe. One can understand this behavior by noting that both excitation and ionization cross-sections σ^{IE} and σ^{II} decrease approximately as $(1/Z)^4$ with increasing Z, while radiative recombination cross-sections σ^{RR} are nearly independent of Z. This leads finally to a similar Z-dependence of σ^{IE} and $\rho\ \sigma^{RR}$, which implies that the relative contribution of RR remains almost constant along the isoelectronic sequence.

Ion	ε(keV)	ρ	B_{M1}	$P_{Ly\text{-}\alpha1}$(%)		$I_{Ly\ \alpha1} / I_{Ly\ \alpha2\ (+M1)}$	
				IE	IE+RR	IE	IE+RR
Ne^{9+}	1.47	1.38[+1]	3.05[-3]	34.4	34.3	2.24	2.23
Ar^{17+}	4.77	1.31	3.17[-2]	34.3	34.2	2.18	2.16
Fe^{25+}	10.0	2.93[-1]	1.28[-1]	34.2	34.1	2.02	2.00
Mo^{41+}	26.5	4.33[-2]	7.71[-1]	33.9	33.8	1.57	1.54
Xe^{53+}	44.5	1.55[-2]	9.81[-1]	33.5	33.4	1.35	1.32

Table. 1 The effect of the RR process on the polarization degree $P_{Ly\alpha1}$ and intensity ratio $I_{Ly\alpha1} / I_{Ly\alpha2\ (+M1)}$ for several H-like ions at one incident electron energy, ε=1.078 x E_I, where E_I is the ionization threshold of the corresponding H-like ion. Also given are the bare to H-like abundance ratio ρ at the ionization balance and the branching ratio B_{M1}.

References

[1] Latifa Bettadj, Mokhtar Kemal Inal, Andrew Surzhykov and Stephan Fritzsche, *Effects of the radiative recombination on the intensity and polarization of the Ly-α emission of hydrogen-like ions*, Nuclear. Methods Phys. Res. B. (**268**), 3509 (2010).

Low Energy Molecular Collisions in Merged Neutral Beams

Andreas Osterwalder
Ecole Polytechnique Fédérale de Lausanne (EPFL), Switzerland

Chemical reactions at temperatures below 1 K can be studied by merging two supersonic expansions, using electric and magnetic guides. This technique has been developed in the past few years and was used to study several fundamentally important aspects of low-energy Penning ionization. To this date it is the only experimental approach that can yield sub-Kelvin collision energies in atomic and molecular beams.

In this presentation I will present our recent studies where we targeted low-energy scattering dynamics with a particular focus on polyatomic molecules. In these systems, in contrast to atom+atom and atom+diatom collisions, one not only has access to effects due to rotational structure but also to the specific dynamics owed to the strongly anisotropic interaction potentials between the reactants. These can lead to multiple reaction channels that can be distinguished via the selective detection of reaction products, and they can be linked to stereodynamical effects that in turn can be studied selectively by using oriented reactants. Furthermore, when the mass of the molecules is increased the rotational level structure is compressed, leading to many more states accessible to inelastic scattering at any given energy.

Taming Molecular Collisions

Sebastiaan Y.T. van de Meerakker

Radboud University, Institute for Molecules and Materials, Heijendaalseweg 135, 6525 AJ Nijmegen, Netherlands

The study of molecular collisions with the highest possible detail has been an important research theme in physical chemistry for decades. Over the last years we have developed methods to get improved control over molecules in a molecular beam [1]. With the Stark decelerator, a part of a molecular beam can be selected to produce bunches of molecules with a computer-controlled velocity and with longitudinal temperatures as low as a few mK. The molecular packets that emerge from the decelerator have small spatial and angular spreads, and have almost perfect quantum state purity. These tamed molecular beams allow for crossed beam scattering experiments with unprecedented levels of precision and sensitivity [2,3].

I will discuss our most recent results on the combination of Stark deceleration and velocity map imaging. The narrow velocity spread of Stark-decelerated beams results in scattering images with an unprecedented sharpness and angular resolution. This has facilitated the observation of diffraction oscillations in the state-to-state differential cross sections for collisions of NO with rare gas atoms [4,5], and the observation of scattering resonances at low-energy inelastic NO-He collisions [6].

References

[1] S.Y.T. van de Meerakker, H.L. Bethlem, G. Meijer, *Nature Physics* **4**, 595 (2008).
[2] J.J. Gilijamse, S. Hoekstra, S.Y.T. van de Meerakker, G.C. Groenenboom, G. Meijer, *Science* **313**, 1617 (2006).
[3] M. Kirste, X. Wang, H.C. Schewe, G. Meijer, K. Liu, A. van der Avoird, L.M.C. Janssen, K.B. Gubbels, G.C. Groenenboom, S.Y.T. van de Meerakker, *Science* **338**, 1060 (2012).
[4] A. von Zastrow, J. Onvlee, S.N. Vogels, G.C. Groenenboom, A. van der Avoird, S.Y.T. van de Meerakker, *Nature Chemistry* **6**, 216 (2014).
[5] S.N. Vogels, J. Onvlee, A. von Zastrow, G.C. Groenenboom, A. van der Avoird, S.Y.T. van de Meerakker, *Phys. Rev. Lett.* **113**, 263202 (2014).
[6] S.N. Vogels, J. Onvlee, S. Chefdeville, A. van der Avoird, G.C. Groenenboom, S.Y.T. van de Meerakker, *Science* **350**, 787 (2015).

Electron Induced Decomposition of Thiopyrimidine Nucleobases

Janina Kopyra[1], Hassan Abdoul-Carime[2]

1. Siedlce University, Faculty of Sciences, 3 Maja 54, 08-110 Siedlce, Poland

2. Université de Lyon, F-69003, Lyon, France; Université Lyon 1, Villeurbanne; CNRS/IN2P3, UMR5822, Institut de Physique Nucléaire de Lyon

Recent years have witnessed a remarkable growth of interest in the studies of low energy electron (LEE) interactions with biomolecules. This has been mainly stimulated by the seminal experiment performed by the group of Sanche [1] in which it has been shown that low energy electrons can effectively cause strand breaks already at energy below the ionization threshold of DNA macromolecule. This observation is of particular importance since the deposition of energy by primary high energy particles in (biological) medium produces secondary electrons with energy below 20 eV [2,3] as the most abundant species [4]. Hence reactions induced by these secondary electrons are considered as important initial and decisive steps in the molecular description of radiation damage to biological systems [5,6,7].

The detrimental effect of LEEs on DNA can in fact be useful when considering a radiation therapy treatment to remove or at least reduce the tumor tissue. In particular, interesting results have been obtained by combining the incorporation of chemical agents (e.g., 5-fluorouracil and cisplatin) with radiation. In the case of cisplatin LEEs with almost no excess energy (≈0 eV) can cause a release of both chlorine atoms from the target molecule [8] facilitating the formation of cisplatin-DNA complexes, which can cause the inhibition of DNA replication. By contrast, an increase of the cross section for dissociative electron attachment (DEA) is observed in the case of 5-fluorouracil or 5-bromouracil that undergoe incorporation into the DNA and therefore can act as radio-sensitizer. Sulphur containing nucleobases are also effectively used as anticancer drugs [9]. In general, the incorporation of such analogues of the canonical nucleobases enables a variety of uses including the exploration [10] and modification [11] of their structures, functionalities or their interaction [12] with proteins. In particular, the thiolated nucleobases attract much attention in synthetic biology [13] that contributes to the health care improvement, for instance, towards immunodeficiency viruses [14]. There is, however, lack of knowledge on the degradation of these molecules by ionizing radiation.

In this contribution, the dissociation of 2-thiothymine and 2-thiouracil induced by the impact of low energy electrons will be discussed. It will be shown that the fragmentation of the sulphur analogue of canonical nucleobases arise mainly at the sulphur site of the molecule.

References

[1] B. Boudaıffa, P. Cloutier, D. Hunting, M.A. Huels and L. Sanche, *Science* **287,** 1658 (2000).
[2] M. Mucke et al., *Nature Phys.* **6,** 143 (2010).
[3] S.M. Pimblott J.A. LaVerne, *Radiat. Phys. Chem.* **76,** 1244 (2007).
[4] M. Kimura, N. Inokuti, M.A. Dillon, in *Advances in Chemical Physics*, I. Prigogine, S.A. Rice (Eds.),vol. LXXXIV, Wiley, (1993).
[5] L. Sanche, *Eur. Phys. J. D* **35**, 367 (2005) (Review).
[6] I. Baccarelli, I. Bald, F.A. Gianturco, E. Illenberger and J. Kopyra, *Phys. Rep.* **508,** 1 (2011).
[7] L. Sanche, *Nature* **461,** 358 (2009).
[8] J. Kopyra, C. Koenig-Lehmann, I. Bald, E. Illenberger, *Angew. Chem. Int. Ed.* **48,** 7904 (2009).
[9] G.B. Elion, *Science* **244,** 41 (1989).
[10] M.J. Rist, J.P. Marino, *Curr. Org. Chem.* **6,** 775 (2002).
[11] J.M. Layzer et al., *RNA* **10,** 766 (2004).
[12] Y. Tor, *Pure Appl. Chem.* **81**, 263 (2009).
[13] W.W. Gibbs, *Sci. Am.* **290,** 74 (2004).
[14] T. Elbeik et al. *J. Clin. Microbiol.* **42,** 3120 (2004).

Collision Experiments with Hydrogenated PAHs

Nathalie de Ruette[1], Michael Gatchell[1], Michael Wolf[1], Linda Giacomozzi[1], Mark H. Stockett[1,2], Henning T. Schmidt[1], Henning Zettergren[1], and Henrik Cederquist[1]

1. Department of Physics, Stockholm University, 106 91 Stockholm, Sweden.

2. Department of Physics and Astronomy, Aarhus University, Ny Munkegade 120, DK 8000 Aarhus C, Denmark.

Polycyclic Aromatic Hydrocarbons (PAHs) are likely to be important components of interstellar dust and gas. They are commonly believed to contribute to strong emission bands in the IR spectra of interstellar environments [1]. How these molecules could survive and evolve in harsh environments, such as in planetary nebulae with strong UV radiation fields or in shock-heated outflows of supernovae [2] is not fully understood.

It has recently been suggested that the hydrogenation of PAHs, where extra H atoms are added to PAH molecules, may protect these molecules from carbon backbone breakage [3]. A recent study of hydrogenated coronene cations $C_{24}H^+_{12+m}$ (m = 0–7) ionized further by carbon K-shell X-ray absorption [3] showed that fewer of the twelve native H atoms were lost when the molecule was hydrogenated than when it was in its native form (m = 0). This protective effect grew stronger as the degree of hydrogenation increased. The reasoning behind this is that the additional H atoms are rather weakly bound to the PAH molecule, and can easily be emitted when the molecule is heated, thus cooling the rest of the system.

Here, we report experimental results [4] on collisions between pyrene or hydrogenated pyrene cations ($C_{16}H^+_{10+m}$ with m = 0, 6, and 16) and He atoms at center-of-mass energies of 20–200 eV. These energies are typical for particles in supernova shock waves [2]. Measuring absolute cross sections, we find that additional hydrogen atoms do not protect the carbon backbone from fragmentation. Rather, we observe that the carbon-backbone fragmentation cross section increases with the degree of hydrogenation. The increased heat capacity stabilizes the system while the weakening of the C-C bonds causes destabilization, as is shown by means of quantum chemical molecular dynamics simulations [4]. We find that the latter, weakening, effect takes the upper hand and is particularly significant for m = 16 yielding non-aromatic $C_{16}H^+_{26}$ molecules.

In order to shed more light on this issue, we have in addition measured absolute single carbon loss cross sections for native or hydrogenated pyrene cations as functions of the collision energy [5]. We find that collision induced carbon backbone fragmentation is governed by very different processes when pyrene is hydrogenated and when it is not. For native pyrene individual carbon atoms may be knocked out of the molecule promptly (fs timescale) in billiard-ball like collisions. This may also occur for hydrogenated pyrene, but here it is also possible to break the carbon backbone through much slower statistical CH_x-loss processes, which have much lower dissociation energies for hydrogenated than for native PAHs. This is shown explicitly in Fig. 1 through direct observations of significant CH_x-loss cross sections far below classical Molecular Dynamics threshold energies for carbon knockout at E^{th} = 35.4 ± 0.7 eV and 29.3 ± 0.7 eV for $C_{16}H_{16}$ and $C_{16}H_{26}$, respectively. In contrast, such simulations reproduce the experimental results in the threshold region quite well for native pyrene $C_{16}H^+_{10}$. Thus, the weakening of the carbon backbone is a much more important effect than the increase in heat capacity for hydrogenated pyrene indicating that hydrogenation *does not* protect PAHs from fragmentation.

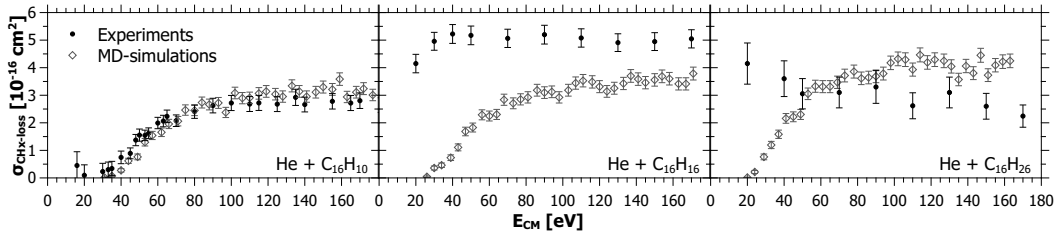

Fig. 1 Experimental CH_x-loss (filled symbols) and Molecular Dynamics (MD) simulations of CH_x-knockout (open symbols) absolute cross sections for $C_{16}H^+_{10+n}$ (n = 0, 6 and 16) + He collisions as functions of the center-of-mass collision energy E_{CM}.

References

[1] A. G. G. M. Tielens, *The molecular universe*, Rev. Mod. Phys. **85**, 1021 (2013).

[2] E. R. Micelotta, A. P. Jones, and A. G. G. M. Tielens, *Polycyclic Aromatic Hydrocarbon Processing in Interstellar Shocks*, Astron. & Astrophys., **510**, A36 (2010).

[3] G. Reitsma, L. Boschman, M. J. Deuzeman, O. Gonzàlez-Magaña, S. Hoekstra, S. Cazaux, R. Hoekstra, and T. Schlathölter, *Deexcitation Dynamics of Superhydrogenated Polycyclic Aromatic Hydrocarbon Cations after Soft-x-Ray Absorption*, Phys. Rev. Lett., **113**, 053002 (2014).

[4] M. Gatchell, M. H. Stockett, N. de Ruette, T. Chen, L. Giacomozzi, R. F. Nascimento, M. Wolf, E. K. Anderson, R. Delaunay, V. Vizcaino, P. Rousseau, L. Adoui, B. A. Huber, H. T. Schmidt, H. Zettergren, and H. Cederquist, *Failure of Hydrogenation in Protecting Polycyclic Aromatic Hydrocarbons from Fragmentation*, Phys. Rev. A **92**, 050702(R) (2015).

[5] M. Wolf, L. Giacomozzi, M. Gatchell, N. de Ruette, M. H. Stockett, H. T. Schmidt, H. Cederquist, and H. Zettergren, *Hydrogenated pyrene: Statistical single-carbon loss below the knockout threshold*, Eur. Phys. J. D (in press).

Astrophysics and Chemistry Induced by Ion Collisions

Alicja Domaracka

Centre de recherche sur les Ions, les MAtériaux et la Photonique CIMAP (CEA/CNRS/ENSICAEN/UCN), Bd Henri Becquerel, 14070 Caen, France

We are living in a molecular Universe [1] which contains both simple dihydrogene molecules and more complex fullerenes. However, the routes to form small grains in space and the rich molecular inventory of our universe are still not well understood. Therefore, the knowledge about growth mechanism, starting from individual molecular building blocks (e.g. small carbon molecules) is required.

The present work combines experimental and theoretical studies of the collisions between keV ions and pyrene clusters (simple polycyclic aromatic hydrocarbon, PAH, molecules) [2]. We have shown that low-energy ion collisions lead to intra-cluster molecular growth processes resulting in the formation of a wide range of new molecules with masses larger than that of pyrene molecule (see Fig. 1). By comparing the interaction with different low-energy ions (H^+, He^+, N^{3+}, O^{2+}, Ar^{2+}) and using coincidence mass spectrometry technique, it has been shown that the molecular growth process is triggered by nuclear stopping. The experimental results are well-reproduced by classical molecular dynamics simulation, which emphasize the role of prompt knockout of C and/or H atoms from one or several molecules in the cluster due to interaction with the projectile. Subsequently, reactive fragments may interact with intact neighbouring molecules.

The present results are relevant to understand the physical chemistry of the PAH-rich upper atmosphere of Saturn's moon Titan, indicating that ions can play an important role in particle growth. Furthermore, this opens new perspective to study the molecular growth from linear hydrocarbons to cyclic ones and PAHs in an astrophysical environment.

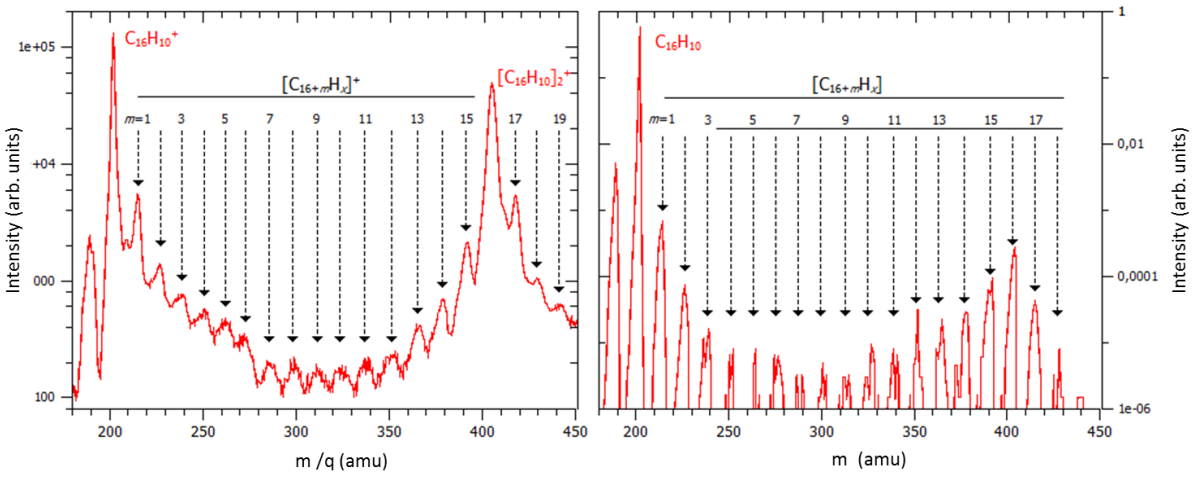

Fig. 1 a) Mass spectrum of cationic products after 24 keV O^{2+} ions interaction with pyrene clusters. b) Simulated mass spectrum.

Acknowledgment. The experimental studies have been performed at the lowenergy ion beam facility ARIBE at GANIL (Caen, France). The simulations have been performed at Stockholm University, Sweden and at the Universidad Autónoma de Madrid, Spain. Research was conducted in the framework of the International Associated Laboratory (LIA) "Fragmentation DYNAmics of complex Molecular Systems" DYNAMO" and the COST actions "XUV/X-ray light and fast ions for ultrafast chemistry" (XLIC - CM1204).

References

[1] A. G. G. M. Tielens, Rev. Mod. Phys. 85, 1021 (2013).
[2] R. Delaunay et al, J. Phys. Chem. Lett. 6, 1536 (2015).

Studying Ion Atom Collisions Using MOTRIMS

Daniel Fischer

Missouri University of Science and Technology, Rolla, MO 65409, US

Max-Planck-Institut für Kernphysik, Saupfercheckweg 1, 69117 Heidelberg, Germany

The fragmentation of simple atoms due to charged particle impact provides insight in the dynamics of correlated few-particle Coulomb-systems, and thus advances our understanding of the fundamentally important few-body problem. On the experimental side, kinematically complete information of ion-atom collisions processes became available with the development of 'Reaction Microscopes', often referred to as cold target recoil ion momentum spectroscopy (COLTRIMS) about two decades ago. Experiments using this technique provide the most detailed data sensitively testing theoretical models. However, earlier ion-atom collision experiments focussed almost exclusively on the fragmentation of ground-state helium and other rare gas atoms, because these targets can easily be prepared at the required temperatures (below 1K) using supersonic gasjets.

In the last five years a novel experiment has been developed where a magneto-optical trap (MOT) is used to prepare a lithium target at mK temperatures in a Reaction Microscope (REMI) [1,2]. The new apparatus has several benefits over conventional Reaction Microscopes. First, the temperatures achievable by laser cooling are at least 2 orders of magnitude lower than the temperatures in gasjets which results in an improved momentum resolution. Second, lithium becomes available as target for multiple differential collision experiments. Lithium is particularly appealing, because it is the simplest atom with an optically active electron. Due to its relatively simple 'hydrogen-similar' structure with only three electrons, a theoretical description of the target is well manageable. Moreover, the initial target state can easily be prepared with lasers allowing for excited and even polarized target atoms. This provides unique possibilities to study the dependence of the dynamics on the initial target state and orientation.

Several experiments have been performed in the ion storage ring TSR at the Max-Planck Institute for Nuclear Physics in Heidelberg. The experiment delivered fully differential cross sections for the ionization of the 1s, 2s, and 2p initial target states. Along with theoretical models, the new results provide detailed insights into the collision dynamics and the influence of the initial target state and orientation [3,4] as well as electronic correlations [5]. In future experiments it is planned, to further exploit the possibilities of laser cooling and manipulation of the target atoms, and to extent the studies of target ionization to strong-field interactions.

References

[1] D. Fischer, D. Globig, J. Goullon, M. Grieser, R. Hubele, V.L.B. de Jesus, A. Kelkar, A. LaForge, H. Lindenblatt, D. Misra, B. Najjari, K. Schneider, M. Schulz, M. Sell, X. Wang, *Ion-Lithium Collision Dynamics Studied with a Laser-Cooled In-Ring Target*, Phys. Rev. Lett. **109**, 113202 (2012).

[2] R. Hubele, M. Schuricke, J. Goullon, H. Lindenblatt, N. Ferreira, A. Laforge, E. Brühl, V.L.B. de Jesus, D. Globig, A. Kelkar, D. Misra, K. Schneider, M. Schulz, M. Sell, Z. Song, X. Wang, S. Zhang, D. Fischer, *Electron and recoil ion momentum imaging with a magneto-optically trapped target*, Rev. Sci. Instrum. **86**, 033105 (2015)

[3] R. Hubele, A. LaForge, M. Schulz, J. Goullon, X. Wang, B. Najjari, N. Ferreira, M. Grieser, V.L.B. de Jesus, R. Moshammer, K. Schneider, A.B. Voitkiv, D. Fischer, *Polarization and Interference Effects in Ionization of Li by Ion Impact*, Phys. Rev. Lett. **110**, 133201 (2013)

[4] E. Ghanbari-Adivi, D. Fischer, N. Ferreira, J. Goullon, R. Hubele, A. LaForge, M. Schulz, D. Madison, (submitted)

[5] M.D. Śpiewanowski, L. Gulyás, M. Horbatsch, J. Goullon, N. Ferreira, R. Hubele, V.L.B. de Jesus, H. Lindenblatt, K. Schneider, M. Schulz, M. Schuricke, Z. Song, S. Zhang, D. Fischer, T. Kirchner, *Target electron ionization in Li^{2+}-Li collisions: A multi-electron perspective*, J. Phys.: Conf. Series **601**, 12010-12017 (2015)

Nanoparticles in proton and heavy ion therapy

Sandrine Lacombe[1]

1. *Institut des Sciences Moléculaires d'Orsay (ISMO), Univ. Paris Sud, CNRS, Université Paris Saclay, Orsay Cedex*

At the moment of printing, no abstract was submitted

Ions collisions to suppress the thermal hysteresis in magnetocaloric thin films

Sophie Cervera[1], Martino Trassinelli[1], Louis Bernard Carlsson[1], Mahmoud Eddrief[1], Victor Etgens[1], Vasilica Gafton[1,2], Emily Lamour[1], Anna Lévy[1], Stéphane Macé[1], Massimiliano Marangolo[1], Christophe Prigent[1], Jean-Pierre Rozet[1], Sébastien Steydli[1] and Dominique Vernhet[1]

1. Institut des NanoSciences de Paris (INSP), Sorbonne Universités, UPMC Univ. Paris 06, CNRS, UMR 7588, 4 Place Jussieu, 75005 Paris, France

2. Alexandru Ioan Cuza University, Faculty of Physics, 11 Carol I Blv, Iasi 700506, Romania

Magnetic materials with giant magnetocaloric effect are promising for application in magnetic refrigeration. But they all exhibit a first-order phase transition and suffer from a large thermal hysteresis which reduces significantly the efficiency of the refrigeration cycle. Several studies aimed at getting rid of the thermal hysteresis but it was to the detriment of the other magnetic properties, inducing for instance a collapse of the refrigerant power [1,2]. Another approach consists of using ion collisions to modify material properties. Nevertheless, most of those studies were focused on magnetic materials with second-order phase transition and using singly charged ions.
Recently, our group demonstrated that the thermal hysteresis of the MnAs thin film can be entirely suppressed by impact of Ne^{9+} at 90 keV whereas other structural and magnetic properties are barely affected [3]. In addition, we show this modification to be stable in time [4], but mechanisms at the origin of the thermal hysteresis suppression were not completely understood.

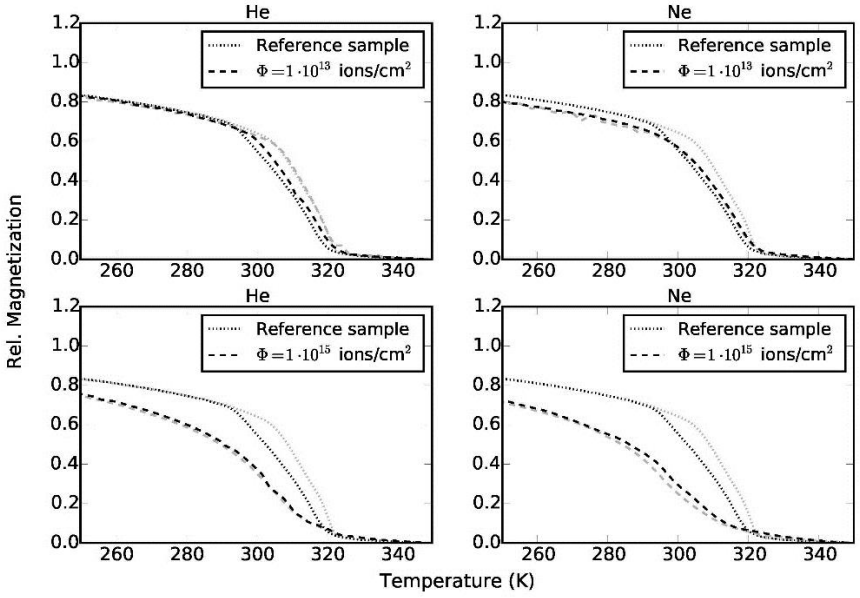

Fig. 1 Relative magnetization of MnAs thin film as a function of temperature for the reference (dotted lines) and for the irradiated samples (dashed lines) with He and Ne ions at two fluences. Data obtained by a temperature increase (grey) and decrease (black).

Trying to disentangle ion implantation effect from and ion collision-induced defects, we investigated the role of different parameters like the projectile mass and energy, and the ion fluence. As displayed in figure 1, comparing helium and neon ion impact at different fluences but with the same penetration depth, the ion mass is playing the major role. This indicates that the binary collision kinematics, at the origin of induced-defects, seems to be the key parameter responsible for the thermal hysteresis suppression. Further investigations are in progress and will be presented at the conference.

References

[1] Jian Liu, et. al., *Giant magnetocaloric effect driven by structural transitions*, Nat. Mater. **11**, 620-626 (2012)

[2] Ariana De Campos, et. al. *Ambient pressure colossal magnetocaloric effect tuned by composition in Mn1-xFexAs*, Nat. Mater. **10**, 802-804 (2006)

[3] Martino Trassinelli, et. al. , *Suppression of the thermal hysteresis in magnetocaloric MnAs thin film by highly charged ion bombardment*, Appl. Phys. Lett. **104**, 081906 (2014)**.**

[4] Sophie Cervera, et.al., *Hints on the origin of the thermal hysteresis suppression in giant magnetocaloric thin films irradiatied with highly charged ions*, J. Phys.: Conf. Ser. **635**, 012028 (2015).

Determination of Energy-Transfer Distributions in Ionizing Ion-Molecule Collisions

S. Maclot[1], R. Delaunay[1], D.G. Piekarski[2], A. Domaracka[1], B.A. Huber[1], L. Adoui[1], F. Martín[2], M. Alcamí[2], L. Avaldi[3], P. Bolognesi[3], S. Díaz-Tendero[2], and P. Rousseau[1]

[1]Normandie Université, CIMAP, UMR6252 (CEA/CNRS/ENSICAEN/UNICAEN), Boulevard Henri Becquerel, BP5133, 14070 Caen cedex 5, France

[2]Departamento de Química, Módulo 13, Universidad Autónoma de Madri , 28049 Madrid, Spain

[3]CNR - Istituto di Struttura della Materia, Area della Ricerca di Roma 1, Monterotondo Scalo, Italy

Dynamics of different relaxation processes, reflecting energy and charge flow processes in complex systems that can imply a vast number of relaxation pathways (e.g. evaporation, structural reorganization, fragmentation). In the present work, we study response of tymidine molecule (nucleoside, component of DNA molecule) after interaction with ions or photons in the gas phase. Moreover, we have coupled the experimental investigations with quantum theoretical calculations to obtain a complete picture of charge and energy flow transfers in the case singly ionized thymidine molecules.

The experiments have been performed with two different crossed beam devices relaying on mass spectrometry coincidence measurements: valence shell ionization (GASPHASE beamline, Elettra synchrotron, Trieste, Italy) and low-energy ions (ARIBE facility of the GANIL, Caen, France). Quantum chemistry calculation has been performed using the GAUSSIAN09 package (UAM, Madrid, Spain).

The thymidine cation, produced in collisions with 48 keV O^{6+} ions, hardly survives (see Fig. 1). It dissociates via the glycosidic bond cleavage, an important mechanism in the radiation damageof DNA molecule. Interestingly, an intramolecular H-transfer is observed when the charge is localized on the base part yielding $(B+1)^+$ ions. This does not occur when the charge is localized on the sugar part (S^+). From the quantum chemistry calculations it has been shown that such products are the most stable ones. A very small amount of fragments heavier than the base or sugar parts are also observed, i.e. loss of neutral fragments keeping intact the glycosidic bond. This is due to the large distribution of impact parameters in the case of ion collisions [1] which leads to energy transfers, spanning from few meV to few tens of eV and involves a distribution of vibrational energy transfer and electron captures in various electronic states. Thus, the knowledge of the distribution of the energy transferred to the molecule plays a key role to unravel its fragmentation dynamics. It is difficult to assess experimentally this energy distribution even if translational spectroscopy can provide it in the case of multiple electron capture [2].

The photoelectron-photoion coincidence method (PEPICO) was used to investigate the fragmentation dynamics as a function of the electronic excitation energy. Particularly, the comparison of the PEPICO mass spectrum with the calculated orbitals shows the strong dependence of the charge localization on the excited orbitals. Combining such state-of- the-art techniques, we provide a complete picture of the charge localization and the excitation energy distribution in complex molecular systems after interaction with ionizing radiation. More importantly, it becomes possible to determine the energy deposited in the target as a result of an ionizing collision with ions, which is the primary process associated with radiation damage.

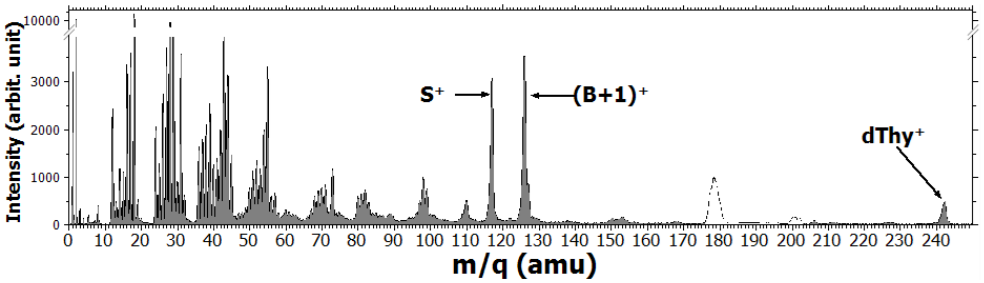

Fig. 1 Mass spectrum of thymidine molecule after interaction with 48 keV O^{6+} ions.

Acknowledgements: Research was conducted in the framework of the CNRS-International Associated Laboratory (LIA) DYNAM and the COST actions XLIC and Nano-IBCT. Financial support from the PHC Galilée/Galileo (G12-44 project "New light on radiosensitisers") is acknowledged.

References

[1] G. Martinet, S. Díaz-Tendero, M. Chabot, K. Wohrer, S. D. Negra, F. Mezdari, H. Hamrita, P. Désesquelles, A. L. Padellec, D. Gardés, L. Lavergne, G. Lalu, X. Grave, J. F. Clavelin, P.-A. Hervieux, M. Alcamí, F. Martín, Phys. Rev. Lett. **93**, 063401 (2004).

[2] L. Chen, S. Martin, J. Bernard, R. Bredy, Phys.Rev. Lett. **98**, 193401 (2007); R. Brédy, J. Bernard, L. Chen, G. Montagne, B. Li, S. Martin, J. Chem. Phys. **130**, 114305 (2009).

Control and dynamic x-ray imaging of ultrafast nanoplasma dynamics

Thomas Fennel

Institute of Physics, University of Rostock, Albert-Einstein-Str. 23, 18059 Rostock, Germany

The interaction of intense laser light with condensed matter leads to the ultrafast generation of finite plasmas. Understanding the underlying complex many-particle dynamics promises a fundamental route to controlling laser-driven plasmas – with implication for a broad spectrum of application, ranging from nanomachining over medical applications to particle acceleration with laser plasmas. Atomic clusters provide an ideal model system to explore the underlying ultrafast physical processes in the resulting transient nanoscale plasmas [1]. Several new pathways in ultrafast nanoplasma science have been opened up with the availability of intense XUV and x-ray laser fields – two of them will be discussed in detail in this talk.

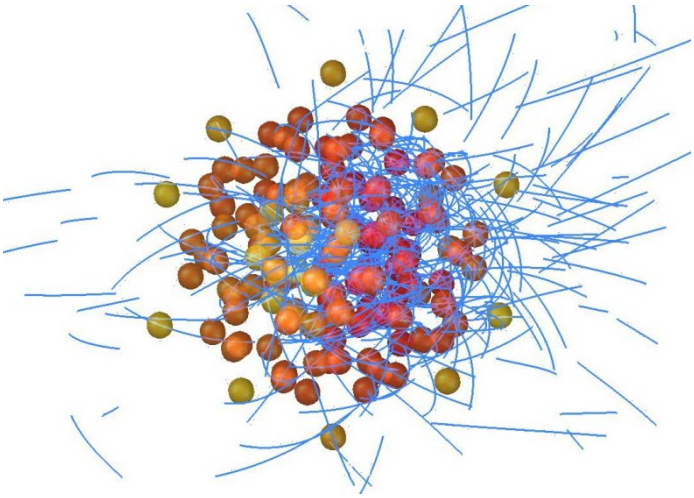

One major promise of current x-ray science at free electron lasers is the realization of unprecedented imaging capabilities for resolving the structure and ultrafast dynamics of matter with nanometer spatial and femtosecond temporal resolution or even below via single-shot x-ray diffraction. Laser-driven atomic clusters and nanoparticles provide an ideal platform for developing and demonstrating the required technology to extract the ultrafast transient spatiotemporal dynamics from the diffraction images [3].

In the first part of this talk, the perspectives and challenges of dynamic x-ray imaging will be discussed based on complete self-consistent microscopic electromagnetic simulations of IR pump x-ray probe imaging. The results of the microscopic particle-in-cell simulations (MicPIC) enable the simulation-assisted reconstruction of corresponding experimental data [3]. This capability is demonstrated by converting recently measured LCLS data into a ultrahigh resolution movie of laser-induced plasma expansion. Possible routes towards reaching attosecond time resolution in the visualization of complex dynamical processes in matter by x-ray diffraction will be discussed.

As a second aspect, it will be shown that the combination of IR and XUV fields open new pathways to control ultrafast electron and ion dynamics in laser-driven nanoplasmas via seeded avalanching [4]. The resulting control capabilities mark a new frontier in ultrafast nanoscience.

References

[1] T. Fennel, K.-H. Meiwes-Broer, J. Tiggesbäumker, P.G. Reinhard, P. M. Dinh, and E. Suraud, *"Laser-driven nonlinear cluster dynamics"*, Rev. Mod. Phys. **82**, 1793 (2010)

[2] T. Gorkhover *et al.*, "Femtosecond and nanometre visualization of structural dynamics in superheated nanoparticles", Nature Photon. **10**, 93 (2016)

[3] C. Peltz, C. Varin, T. Brabec, T. Fennel, *"Time-resolved x-ray imaging of anisotropic nanoplasma expansion"*, Phys. Rev. Lett. **113**, 133401 (2014)

[4] B. Schütte, M. Arbeiter, A. Mermillod-Blondin, M.J.J. Vrakking, A. Rouzee, and T. Fennel, *"Ionization avalanching in clusters ignited by extreme-ultraviolet driven seed electrons"*, Phys. Rev. Lett. **116**, 033001 (2016)

Time-dependent two-particle reduced density matrix theory: Application to high-harmonic generation

Iva Březinová[1], Fabian Lackner[1], Stefan Donsa[1], Takeshi Sato[2], Kenichi Ishikawa[2], Joachim Burgdörfer[1]
1. Institute for Theoretical Physics, Vienna University of Technolog, Wiedner Hauptstrasse 8-10/136, 1040 Vienna, Austria, EU
2. Photon Science Center, Graduate School of Engineering, The University of Tokyo, 7-3-1 Hongo, Bunkyo-ku, Tokyo 113-8656, Japan

Calculating the time-dependent dynamics of correlated quantum many-body systems is one of the great challenges of modern theoretical physics. Several approaches are frequently employed each of which featuring advantages and drawbacks. On one hand, the time-dependent density functional theory (TDDFT) allows for the treatment of hundreds of particles due to its favorable scaling with particle number. The drawback lies in the drastic approximations for the correlation Hamiltonian which have no universal validity and do not allow for systematic improvement. On the other hand, the multi-configurational time-dependent Hartree Fock (MCTDHF) ansatz (for a review see e.g. [1]) allows for an, in principle, exact treatment but is in practice limited to only small systems due to the factorial scaling with particle number.
Motivated by recent progress in ground state calculations in which the two-particle reduced density matrix (2RDM) has been used as starting point (see e.g.[2]), we attempt to bridge the gap between TDDFT and MCTDHF by developing a time-dependent quantum many-body theory which uses the 2RDM as the fundamental variable. In doing so we fully incorporate two-particle correlations. The equations of motion for the 2RDM depend on the three-particle reduced density matrix which has to be approximated to obtain the equations of motion in closed form. This typically goes hand in hand with neglecting three-particle correlations completely [3,4]. Through a new ansatz [5] and using the Yasuda-Nakatusji approximation [6] we manage to reconstruct parts of the three-particle correlations. The key advantage of our theory is the polynomial rather than factorial scaling with particle number.

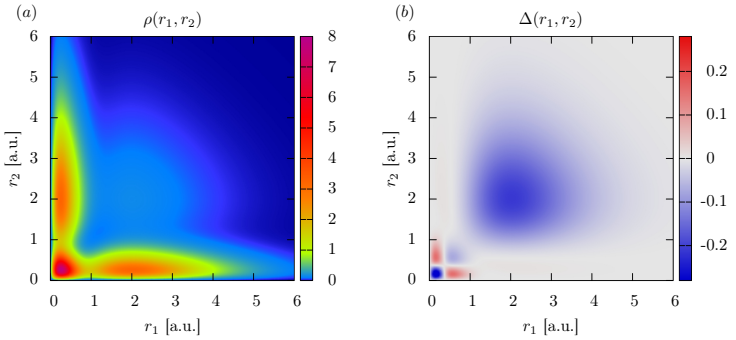

Fig. 1 (a) The 2RDM of the ground state of Be averaged over angular degrees of freedom and spin. (b) Two-particle correlations of the ground state as measured by the two-particle cumulant.

In this talk we will report on first remarkably successful applications of our theory to several atomic systems. We focus on high-harmonic generation (HHG) in strong fields. While two-particle correlations play an important role and must be included (see Fig.1) three-particle correlations turn out to be small and reasonably well approximated within our approach. As a benchmark we use the MCTDHF method converged in orbital number. To access the effect of correlations for HHG we compare to time-dependent Hartree Fock which neglects correlations altogether and TDDFT within the local density approximation where two-particle correlations are taken into account only approximatively. We identify features in the high-harmonic spectrum that sensitively probe correlation effects.
In the talk we will also give an outlook to applications in the field of ultra-cold fermionic lattice systems.

References

[1] D. Hochstuhl, C.M. Hinz, and M. Bonitz, *Time-dependent multiconfiguration methods for the numerical simulation of photoionization processes of many-electron atoms*, Eur. Phys. J. Special Topics **223**, 177–336 (2014)
[2] David A. Mazziotti, *Two-Electron Reduced Density Matrix as the Basic Variable in Many-Electron Quantum Chemistry and Physics*, Chem. Rev. **112**, 244 (2012)
[3] A. Akbari, M. J. Hashemi, A. Rubio, R. M. Nieminen, and R. van Leeuwen, *Challenges in truncating the hierarchy of time-dependent reduced density matrices equations* Phys. Rev. B **85**, 235121 (2012)
[4] B. Schäfer-Bung and M. Nest, *Correlated dynamics of electrons with reduced two-electron density matrices*, Phys. Rev. A **78**, (2008)
[5] Fabian Lackner, Iva Březinová, Takeshi Sato, Kenichi L. Ishikawa, and Joachim Burgdörfer, *Propagating two-particle reduced density matrices without wave functions*, Phys. Rev. A **91**, 023412 (2015)
[6] Koji Yasuda and Hiroshi Nakatsuji, *Direct determination of the quantum-mechanical density matrix using the density equation. II.*, Phys. Rev. A **56**, 2648 (1997)

Slow electrons from intense fields

Jan Michael Rost[1,2]

1. Max-Planck-Institut für Physik komplexer Systeme, Nöthnitzer Straße 38, 01187 Dresden, Germany

2. PULSE Institute, Stanford University and SLAC National Accelerator Laboratory, 2575 Sand Hill Road, Menlo Park, California 94025, USA

At the moment of printing, no abstract was submitted

Time-dependent restricted-active-space self-consistent-field theory: Formulation, application, and extension by space-partition concept

Haruhide Miyagi and Lars Bojer Madsen
Department of Physics and Astronomy, Aarhus University, 8000 Aarhus C, Denmark

As emphasis is shifting towards more detailed and fundamental analyses of non-perturbative electron dynamics in atoms and molecules, intense efforts have been deployed to develop time-dependent (TD) many-electron theories to support experiments of strong-field and attosecond science. The muticonfigurational TD Hartree-Fock (MCTDHF) method (see, e.g., Ref. [1]) is among the most accurate and widely recognized methodologies in this research area. Expanding the wave function in terms of the TD configuration-interaction (CI) coefficients with the Slater determinants comprising TD orbitals, the MCTDHF method achieves high accuracy with relatively small computational costs. With increasing the number of electrons, however, the number of electronic configurations exponentially increases, due to the full-CI expansion, deterring the method from being easily applicable to large systems containing more than ten electrons. This difficulty motivated us to generalize the MCTDHF method and develop the TD resctricted-active-space self-consistent-field (TD-RASSCF) method [2-4]. The use of the RAS scheme instead of the full-CI expansion extends the numerical efficiency while retaining a reasonable accuracy, because of a large reduction in the number of electronic configurations. However, the calculation of every TD orbital composed of many orbital-angular momentum states in a large simulation volume still requires a considerable amount of computational overhead and stands in the way of further numerical applications. To break this computational limitation, we propose an incorporation of the space-partition concept as in *R*-matrix-related theories (see, e.g., Ref. [5]). Abandoning the treatment of all electrons over the large simulation volume is the key to reduce the computational cost.

As an example, consider single- or double-ionization of an N_e-electron atom in light fields with moderate intensity. Introducing a spherical surface Σ centered at the nucleus, we divide the configuration space into its inner and outer regions, and construct the N_e-electron wave function in a piecewise manner:

$$|\Psi(t)\rangle \equiv \sum_{\gamma=0}^{\Gamma} |\Psi_\gamma(t)\rangle \equiv \sum_{\gamma=0}^{\Gamma} \sum_{\boldsymbol{I}_\gamma \in \mathscr{V}_\gamma}^{\mathrm{RAS}} C_{\boldsymbol{I}_\gamma}(t) |\Phi_{\boldsymbol{I}_\gamma}(t)\rangle, \tag{1}$$

where $\Gamma(\leq N_\mathrm{e})$ is the maximum number of electrons in the outer region, $|\Psi_\gamma(t)\rangle$ denotes an N_e-electron state consisting of $N_\mathrm{e}-\gamma$ electrons in the inner region and γ electrons in the outer region. Each $|\Psi_\gamma(t)\rangle$ is then expanded in terms of the CI coefficients $C_{\boldsymbol{I}_\gamma}(t)$ and the Slater determinants $|\Phi_{\boldsymbol{I}_\gamma}(t)\rangle$ multi-indexed by $\boldsymbol{I}_\gamma$ and composed of TD orbitals: $N_\mathrm{e}-\gamma$ chosen from $\{\phi_i(\boldsymbol{r},t)\}_{i=1}^{M}$ domained in the small inner region and γ from $\{\varphi_i(\boldsymbol{r},t)\}_{i=1}^{N}$ defined in the large outer region. The RAS scheme, $\sum_{\boldsymbol{I}_\gamma \in \mathscr{V}_\gamma}^{\mathrm{RAS}}$, takes into account electron excitations within the inner region and also from the inner to the outer region up to the maximum number, Γ. Setting $r_\Sigma = 20$–50 a.u. and $M \approx 2N_\mathrm{e}$ will enable accurate description of the complex electronic structure of the atom. On the other hand, correlations among the two photoelectrons in the outer region will be well captured by setting $\Gamma = 2$ and $N \approx 2\Gamma$. We will present more details of the formulation and numerical applications, and discuss the strengths as well as still-remaining problems of the TD-RASSCF method extended by the space-partition concept.

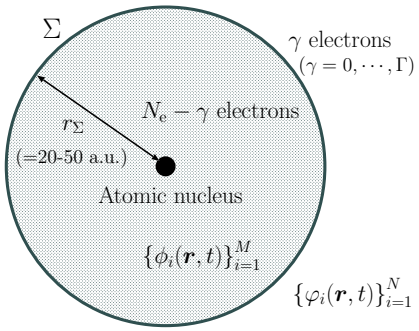

Fig. 1 Division of the configuration space into the inner and outer regions by a spherical surface Σ. See text for details.

References

[1] J. Caillat, J. Zanghellini, M. Kitzler, O. Koch, W. Kreuzer, and A. Scrinzi, Phys. Rev. A **71**, 012712 (2005).
[2, 3] H. Miyagi and L. B. Madsen, Phys. Rev. A **87**, 062511 (2013); *ibid.* **89**, 063416 (2014).
[4] H. Miyagi and L. B. Madsen, J. Chem. Phys. **140**, 164309 (2014).
[5] H. W. van der Hart. Phys. Rev. A **89**, 053407 (2014).

Towards nanoparticle enhanced radiotherapy

Fred Currell

Centre for Advanced and Interdisciplinary Radiation Research and Centre for Plasma Physics, School of Mathematics and Physics, Queen's University Belfast, BT7 1NN, UK

Cutting-edge forms of radiotherapy, such as heavy ion therapy or nanoparticle-enhanced therapy, are amenable to a bottom-up description grounded in atomic and molecular physics. This bottom-up description usually takes the form of Monte Carlo radiation transport simulations designed to capture the essential physics at work. From the Monte Carlo simulation a description of the particles created, their energies and the energy they deposit in the sample is derived and then post-processed to predict biological outcome. While this procedure is well established for heavy ion therapy, it is still a matter of on-going research for nanoparticle-enhanced therapies.

This talk will present progress on developing an understanding of nanoparticles as radiosensitizers. The 10-year research program has sought to understand the basic mechanisms underpinning radiosensitization by nanoparticles in biological systems through both experimental and computational approaches. Nanoscale energy deposition effects, based on Auger emission, have been shown to be of critical importance [1]. Furthermore new chemical effects have been observed [2] along with photoionization-driven DNA damage effects [3]. Combining ideas from atomic collision physics and chemical kinetics, these effects have now been placed in a unified data-fitting framework, at least for irradiated nanoparticle colloids, in terms of analytical descriptions of pathways A, B and C (see figure 1). This framework and the match to experimental results will be reported. Ideally one would like a full bottom-up description of these pathways in terms of the underlying atomic and molecular physics without recourse to data fitting. In the final part of this talk, the future atomic and molecular physics data needs for this domain of research will be briefly reviewed along with a discussion about how such data might be obtained.

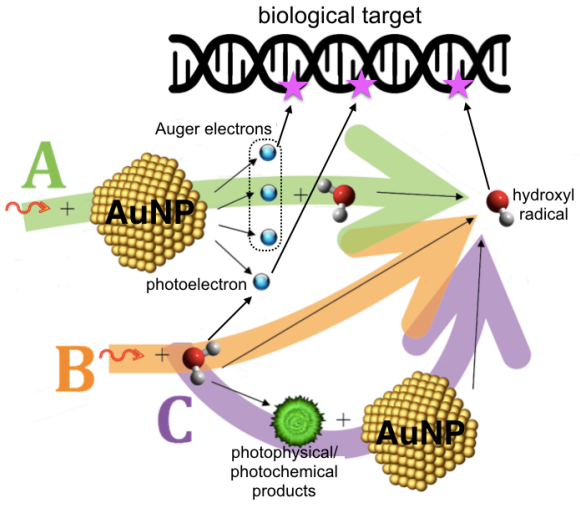

Fig. 1 Graphical summary of the atomic and molecular processes involved in nanoparticle enhancement. Adapted from [2]

References

[1] McMahon,SJ; Hyland,WB; Muir,MF; Coulter,JA; Jain,S; et al. *Biological consequences of nanoscale energy deposition near irradiated heavy atom nanoparticles,* Nature Sci Rep **1** 00018 DOI:10.1038/srep00018 (2011).

[2] Sicard-Roselli, C; Brun, E; Gilles, M; Baldacchino, G; Kelsey, C; el al. *A New Mechanism for Hydroxyl Radical Production in Irradiated Nanoparticle Solutions* Small **10(16)** 3338-3346 DOI: 10.1002/smll.201400110 (2014).

[3] McQuaid, Harold N.; Muir, Mark F.; Taggart, Laura E.; et al. *Imaging and radiation effects of gold nanoparticles in tumour cells* Nature Sci Rep **6** 19442; doi: 10.1038/srep19442 (2016).

Resonant Auger driven Interatomic Coulombic Decay

Kirill Gokhberg
Theoretische Chemie, Physikalisch-Chemisches Institut, Universität Heidelberg, INF 229, 69120 Heidelberg, Germany

Absorption of X-ray photons by atoms and molecules results in populating of core excited or core ionised states which decay in isolated species by the resonant or normal Auger processes. In clusters or bulk media the local Auger decay still predominates but it is often accompanied by the non-local electronic decay processes: interatomic Coulombic decay (ICD), and electron transfer mediated decay (ETMD).

In the energy transfer driven ICD process an electronically excited species de-excite by singly ionising a neighbouring atom or molecule emitting a slow (up to few tens eV) electron. In this talk I will discuss a scheme [1], whereby the location of ICD process as well as the energies of ICD electrons can be controlled. It consists of resonant X-ray absorption followed by the resonant Auger decay populating a number of ionisation satellites which in turn decay by ICD with the neighbouring atoms or molecules. This scheme relies firstly on the high sensitivity of resonant core excitations to the nature and chemical environment of different atoms which allows energy deposition at selected location in an extended system. Secondly, by varying the energy of initial excited state one controls which satellites are populated in the resonant Auger decay, therefore, controlling the energies of ICD electrons. The feasibility of this control mechanism has been demonstrated experimentally [2] and by accurate *ab initio* calculations [3] in Ar_2 and ArKr clusters.

Electronic decay triggered by X-ray photoabsorption is an important source of radiation damage in complex systems such as biomolecules. Both the location of the photon impact and the presence of low energy electrons are crucial in causing the damage to molecules. Therefore, the ability to control the ICD process is thought to be important for controlling the damage itself. In biological systems the X-ray absorption often results in more complicated cascades. For example, the excitation of an 1s-electron of a solvated metal cation leads to an electronic decay cascade involving multiple interatomic decay steps [4]. However, as I will show, the control scheme described above can still be applied to steer damage in such systems.

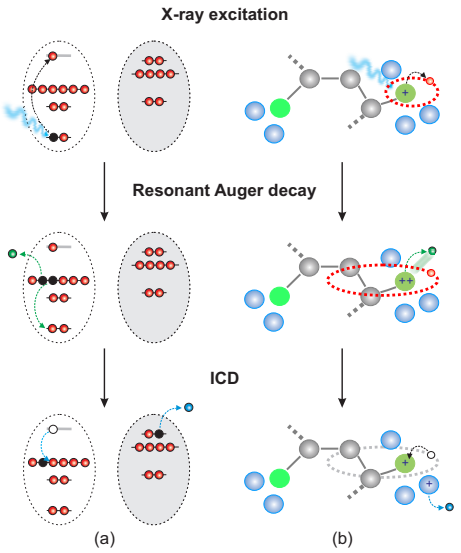

Fig. 1 Schematic description of the resonant Auger - ICD cascade.

References

[1] K. Gokhberg, P. Kolorenč, A.I. Kuleff & L.S. Cederbaum, *Site- and energy-selective slow-electron production through intermolecular Coulombic decay*, Nature **505**, 651 (2014); F. Trinter et al., *Resonant Auger decay driving intermolecular Coulombic decay in molecular dimers*, Nature **505**, 664 (2014).

[2] P. O'Keeffe et al., *The Role of the Partner Atom and Resonant Excitation Energy in Interatomic Coulombic Decay in Rare Gas Dimers*, J. Phys. Chem. Lett. **4**, 1797 (2013); K. Kimura et al., *Controlling Low-energy Electron Emission via Resonant-Auger-induced Interatomic Coulombic Decay*, J. Phys. Chem. Lett. **4**, 1838 (2013);

[3] T. Miteva et al., *Interatomic Coulombic decay following resonant core excitation of Ar in argon dimer*, J. Chem. Phys. **141**, 064307 (2014); T. Miteva et al., *The effect of the partner atom on the spectra of interatomic Coulombic decay triggered by resonant Auger processes*, J. Chem. Phys. **141**, 164303 (2014).

[4] V. Stumpf, K. Gokhberg & L.S. Cederbaum, *The role of metal ions in X-ray-induced photochemistry*, Nat. Chem. **8**, 237 (2016)

Atomic Processes in Laser Produced Plasmas for EUV Nanolithography

Oscar Versolato[1], Dmitry Kurilovich[1,2], Francesco Torretti[1,2], Joris Scheers[1,2], Alexander Windberger[1,3], José Crespo López-Urrutia[3], Wim Ubachs[1,2], Ronnie Hoekstra[1,4]

1. Advanced Research Center for Nanolithography (ARCNL), Science Park 110, 1098 XG Amsterdam, The Netherlands

2. Department of Physics and Astronomy, and LaserLaB, Vrije Universiteit, De Boelelaan 1081, 1081 HV Amsterdam, The Netherlands

3. Max-Planck-Institut für Kernphysik, Saupfercheckweg 1, 69117 Heidelberg, Germany

4. Zernike Institute for Advanced Materials, University of Groningen, Nijenborgh 4, 9747 AG Groningen, The Netherlands

We experimentally investigated the propulsion and shaping of a liquid indium-tin micro-droplet in a laser-produced-plasma source driven by a nanosecond-pulsed Nd:YAG laser. We found that the droplet propulsion can be accurately described in terms of plasma pressure, and we provide a scaling law for the imparted momentum that enables the optimization of the laser-droplet coupling (Fig.1 a,b). Comparing our findings to those from evaporation-accelerated mm-sized water droplets, we demonstrate, together with the Physics of Fluids group at the University of Twente, the scalability of the hydrodynamic response of impacted droplets independent on the propulsion mechanism. To obtain a better understanding of the atomic processes within the laser generated plasma itself we performed charge-state-resolved spectra of highly charged Sn ions using the electron beam ion traps (EBIT) at the Max Planck Institute for Nuclear Physics in Heidelberg. The tuneable electron beam energy of the EBIT enabled us to obtain the energy dependence of the fluorescence intensity of spectral lines originating from magnetic dipole transitions and, thus, to assign them to their respective charge states (Fig. 1 c). Significant contributions from meta-stable states are suggested by the doubly-peaked structures appearing at potentials below the required ionization potential (Fig. 1 d). Our results enable a more accurate determination of ground state energy configurations than possible to date. Comparison with previous work suggests that line identifications in the EUV need to be revisited. These results are of particular interest for EUV light sources with nanolithographic applications.

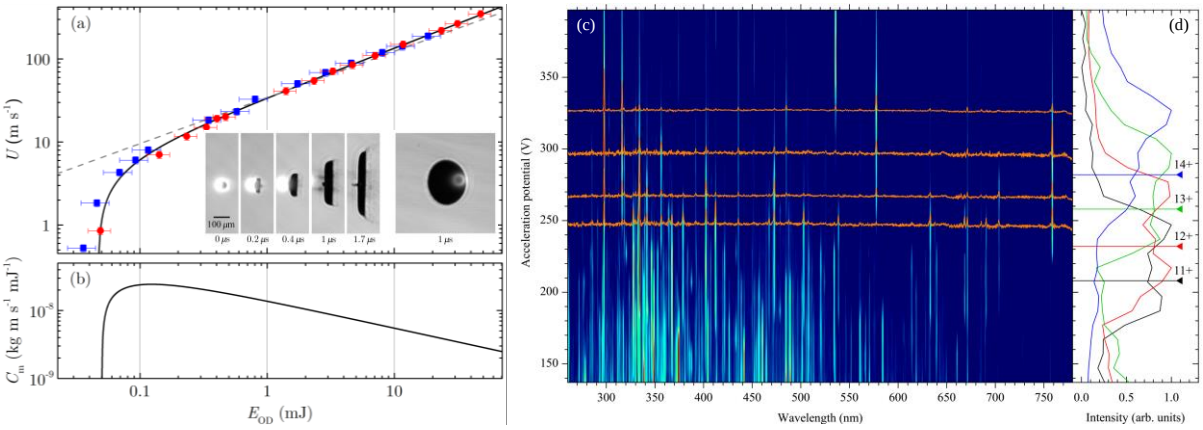

Fig. 1 (a) Propulsion velocity U of In-Sn droplets as a function of total laser pulse energy impinging on the droplet E_{OD} for two different focusing conditions. A single offset power law accurately describes all data. The inset shows five side- and a single front view shadowgrams of expanding droplets. (b) Momentum coupling coefficient C_m. (c) Composite spectral map from EBIT spectroscopy of Sn ions. The orange lines represent spectra of $Sn^{11+...14+}$ ions. (d) Fluorescence yield for each charge state as a function of EBIT potential.

Structure and Dynamics of Clusters Probed by Synchrotron Radiation Based X-ray Spectroscopies

Minna Patanen
Nano and Molecular Systems Research Unit, Faculty of Science, P. O. Box 3000, 90014 University of Oulu, Finland

The research of the electronic structure of clusters have often been justified by an (academic) interest to see how clusters bridge the gap between infinite solid and an isolated atom. However nowadays one could claim that the cluster research is more timely and topical than ever: clusters' unique, size-scalable properties are exploited in industrial applications and they have found to be ubiquitous in nature with impact on human health and climate. Whether it is a catalysis application or naturally occurring chemical reactions involving atmospheric clusters, it is the electronic structure of the surface of these clusters which essentially govern their reactivity and physical chemistry. Therefore, the studies of the structure of the first monolayers of nanomaterials are of utmost importance, and there is no other like soft x-ray photoelectron spectroscopy, when it comes to surface sensitive techniques probing the electronic structure of matter. In nature, clusters and nano-sized matter is often in gas-phase, like volatile organic compounds of biogenic origin, sea-salt clusters from oceans, soot from forest fires, sulfate clusters of volcanic activity. Recently, these tiny aerosol particles have gained a lot of attention in a context of climate change as they remain the lowest confidence contributor for climate models [1]. Thus, it is important to study them in their natural environment as free-standing isolated species, since deposition on substrates may change their properties and induce other undesired effects like charging.

Third generation synchrotron radiation facilities have enabled studies of more and more diluted samples. New instrumentation, like fast-readout position sensitive detectors and wide acceptance angle hemispherical electron analysers, make it possible to obtain reasonable resolution with high count rates. I will introduce some of the recent soft X-ray spectroscopy studies of very dilute clusters species, mostly carried out at PLEIADES beamline at Synchrotron SOLEIL (Saint-Aubin, France). Advances in lightsources, beamlines, and analysers have opened a way to perform systematic studies requiring stable experimental conditions over a long period of time. Such kind of experiment is needed for example to study bond contraction on the surface of free-standing clusters [2], evolution of crystal structure of small salt clusters [3], or photoemission anisotropy telling about the inelastic and elastic scattering processes within clusters. Core-level electron spectroscopy is a powerful tool when it comes to structural information: owing to coordination-dependent polarization screening inducing different chemical shifts in electron spectra, even the different surface sites (e.g. corner vs. face) can be distinguished.

Element specificity of soft X-ray spectroscopy was used in a study of fragmentation of small size-selected ammonium bisulphate clusters [4]. Cationic clusters created with an electrospray ion source were trapped to an ion trap and excited with synchrotron light at S, N, and O edges. The mass analysis of fragments revealed a favourable Coulomb explosion route after the electronic relaxation of the core excitation. Ammonium bisulfate clusters are important in nucleation processes in the atmosphere, and the resonance induced X-ray fragmentation can be used to probe details of hydrogen bonding and intramolecular protolysis within such clusters.

Besides analysing electron and ion emissions separately, these signals can be detected in coincidence, giving a more complete picture of a photoionization event. In the end, I will discuss shortly some specificities of coincidence experiments of free-standing clusters. As an outlook to the future, the prospects of synchrotron radiation excited soft X-ray spectroscopy of free-standing clusters will be discussed in a light of new openings at MAX IV laboratory in Lund, Sweden, especially related to atmospherically important aerosol clusters and their reactivity.

References

[1] T.F.Stocker, D. Qin, G.-K. Plattner, M. Tignor, S.K. Allen, J. Boschung, A. Nauels, Y. Xia, V. Bex, and P.M. Midgley (eds.). *IPCC 2013, Climate Change 2013: The Physical Science Basis*, Contribution of Working Group I to the Fifth Assessment Report of the Intergovernmental Panel on Climate Change, Cambridge University Press, Cambridge, United Kingdom and New York, NY, USA (2013).

[2] M. Patanen, S. Benkoula, C. Nicolas, A. Goel, E. Antonsson, J. J. Neville, and C. Miron, *Interatomic scattering in energy dependent photoelectron spectra of Ar clusters*, J. Chem. Phys. **143**, 124306 (2015).

[3] L. Hautala, K. Jänkälä, M.-H. Mikkelä, M. Tchaplyguine, and M. Huttula, *Surface site coordination dependent responses resolved in free clusters: applications for neutral sub-nanometer cluster studies*, Phys. Chem. Chem. Phys. **17**, 7012 (2015).

[4] M. J. Ryding, A. Giuliani, M. Patanen, J. Niskanen, G. Simões, G. B. S. Miller, E. Antonsson, T. Jokinen, C. Miron, O. Björneholm, K. Hansen, K. J. Børve, and E. Uggerud, *X-ray induced fragmentation of size-selected salt cluster-ions stored in an ion trap*, RSC Advances **4**, 47743-47751 (2014).

Precision measurements of fundamental properties of atomic particles in Penning traps

***Klaus Blaum*[1]**

1. Max-Planck-Institut für Kernphysik, Saupfercheckweg 1, 69117 Heidelberg, Germany

This plenary lecture will provide an overview on recent applications of precision measurements with cooled and stored ions in Penning traps. One the one hand, precision Penning-trap mass measurements provide indispensable information for atomic, nuclear and neutrino physics as well as for testing fundamental symmetries [1,2]. On the other hand, in-trap measurements of the bound-electron *g*-factor in highly-charged hydrogen-like ions allow for better determination of fundamental constants and for constraining Quantum Electrodynamics [3,4,5]. Furthermore, ongoing preparations for the experimental comparison of the proton and antiproton *g*-factors will allow us to achieve a crucial test of the Charge-Parity-Time reversal (CPT) symmetry [6,7]. Among others, a 13-fold improvement of the atomic mass of the electron by combining a very accurate measurement of the magnetic moment of a single electron bound to a carbon nucleus with a state-of-the-art calculation in the framework of bound-state Quantum Electrodynamics [4], as well as the most stringent test of CPT symmetry on the baryonic sector by a charge-to-mass ratio comparison of the proton and antiproton [8], will be presented.

References

[1] E.G. Myers *et al*., *Atomic Masses of Tritium and Helium-3*, Phys. Rev. Lett. **114**, 013003 (2015).
[2] S. Eliseev *et al*., *Direct Measurement of the Mass Difference of ^{163}Ho and ^{163}Dy Solves the Q-Value Puzzle for the Neutrino Mass Determination*, Phys. Rev. Lett. **115**, 062501 (2015).
[3] S. Sturm *et al*., *g Factor of Hydrogenlike $^{28}Si^{13+}$*, Phys. Rev. Lett. **107**, 023002 (2011).
[4] S. Sturm *et al*., *High-precision measurement of the atomic mass of the electron*, Nature **506**, 467 (2014).
[5] F. Köhler *et al*., *Isotope dependence of the Zeeman effect in lithium-like calcium*, Nature Comm. **7**, 10246 (2016).
[6] J. DiSciacca *et al*., *One-Particle Measurement of the Antiproton Magnetic Moment*, Phys. Rev. Lett. **110**, 130801 (2013).
[7] A. Mooser *et al*., *Direct high-precision measurement of the magnetic moment of the proton*, Nature **509**, 597 (2014).
[8] S. Ulmer *et al*., *High-precision comparison of the antiproton-to-proton charge-to-mass ratio*, Nature **524**, 196 (2015).

Attosecond Molecular Dynamics

Fernando Martín[1,2,3]

1. Departamento de Química, Módulo 13, Universidad Autónoma de Madrid, 28049 Madrid, Spain

2. Instituto Madrileño de Estudios Avanzados en Nanociencia (IMDEA Nano), Campus de Cantoblanco, 28049 Madrid, Spain.

3. Condensed Matter Physics Center (IFIMAC), Universidad Autónoma de Madrid, 28049 Madrid, Spain.

Attosecond laser pulses allow one to probe the inner workings of atoms, molecules and surfaces on the timescale of the electronic motion. For example, in molecules, sudden ionization by an attosecond pulse is followed by charge redistribution on a time scale from a few-femtoseconds down to hundreds attoseconds, which is usually followed by fragmentation of the remaining molecular cation. Such complex dynamics arises from the coherent superposition of electronic states covered by the broadband attosecond pulse and from rearrangements in the electronic structure of the molecular cation due to electron correlation. To investigate these ultrafast processes, attosecond pump-probe and transient absorption spectroscopies have been shown to be very valuable tool [1-7]. In this talk I will present the results of molecular attosecond pump-probe experiments and theoretical simulations in which several molecules, from the simplest H_2 one to the aminoacids phenylalanine and tryptophane, are ionized with a single attosecond pulse (or a train of attosecond pulses) and are subsequently probed by one or several infrared or xuv few-cycle pulses. In all cases, the evolution of the electronic and nuclear densities in the photo-excited molecule or remaining molecular ions can be inferred from the measured (or calculated) ionization or fragmentation yields with attosecond time-resolution, and can be visualized by varying the delay between the pump and probe pulses. The results of these pioneering works will certainly serve as a guide of future experimental efforts in more complicated molecules and may open the door to the control of charge transfer in biologically relevant processes.

References

[1] G. Sansone, F. Kelkensberg, J. F. Pérez-Torres, F. Morales, M. F. Kling, W. Siu, O. Ghafur, P. Johnsson, M. Swoboda, E. Benedetti, F. Ferrari, F. Lépine, J. L. Sanz-Vicario, S. Zherebtsov, I. Znakovskaya, A. L'Huillier, M. Yu. Ivanov, M. Nisoli, F. Martín, and M. J. J. Vrakking, *Nature* **465**, 763 (2010).

[2] S. E. Canton, E. Plésiat, J. D. Bozek, B. S. Rude, P. Decleva, and F. Martín, *Proc. Natl. Acad. Sci.* **108**, 7302 (2011)

[3] A. González-Castrillo, A. Palacios, H. Bachau and F. Martín, *Phys. Rev. Lett.* **108**, 063009 (2012)

[4] A. Palacios, A. González-Castrillo and F. Martín, *Proc. Natl. Acad. Sci.* **111**, 3973 (2014).

[5] F. Calegari, D. Ayuso, A. Trabattoni, L. Belshaw, S. De Camillis, S. Anumula, F. Frassetto, L. Poletto, A. Palacios, P. Decleva, J. Greenwood, F. Martín, and M. Nisoli, *Science* **346**, 336 (2014)

[6] C. Ott, A. Kaldun, L. Argenti, P. Raith, K. Meyer, M. Laux, Y. Zhang, A. Blättermann, S. Hagstotz, T. Ding, R. Heck, J. Madroñero, F. Martín, and T. Pfeifer, *Nature* **516**, 374 (2014)

[7] P. Ranitovic, C. W. Hogle, P. Rivière, A. Palacios, X.-M. Tong, N. Toshima, A. González-Castrillo, L. Martina, F. Martín, M. M. Murnane, and H. Kapteyn, *Proc. Natl. Acad. Sci.* **111**, 912 (2014)

Optoelectrical cooling of polar molecules to submillikelvin temperatures

Martin Ibrügger[1], Alexander Prehn[1], Rosa Glöckner[1], Martin Zeppenfeld[1], and Gerhard Rempe[1]
1. Max-Planck-Institut für Quantenoptik, Hans-Kopfermann-Str. 1, 85748 Garching, Germany

Due to their rich internal level structure and their electric dipole moment, polar molecules cooled to ultracold temperatures (T< 1mK) offer a wide range of intriguing applications. These include quantum simulation with degenerate quantum gases, investigation of collisions and quantum controlled chemistry or hybrid quantum devices for quantum information processing. Realizing these exciting applications requires advanced cooling techniques for polar molecules.

Here we present direct cooling of formaldehyde (H_2CO) to the microkelvin regime [1]. Our approach is optoelectrical Sisyphus cooling which is a simple and robust scheme as it only requires a single laser, a single microwave source and a single radiofrequency source. Molecules are electrically trapped [2] and cooled by a dissipative cooling method relying only on generic properties of polar molecules making it applicable to a large variety of molecule species. After a first demonstration with methyl fluoride (CH_3F) [3] we now produce an ultracold ensemble of about $3 \cdot 10^5$ formaldehyde molecules by reducing the temperature by three orders of magnitude to about 420μK. The phase space density is increased by roughly a factor of 10^4. In addition to our control over the motional degrees of freedom we have good control over the internal degrees of freedom of our molecules [4]: by optical pumping they are prepared within a single rotational state with a purity higher than 80%. This record-large ensemble of ultracold formaldehyde provides an ideal starting point for future experiments. Ultracold collision studies and fountain experiments now seem feasible. Furthermore, it brings within reach the investigation of sympathetic or evaporative cooling.

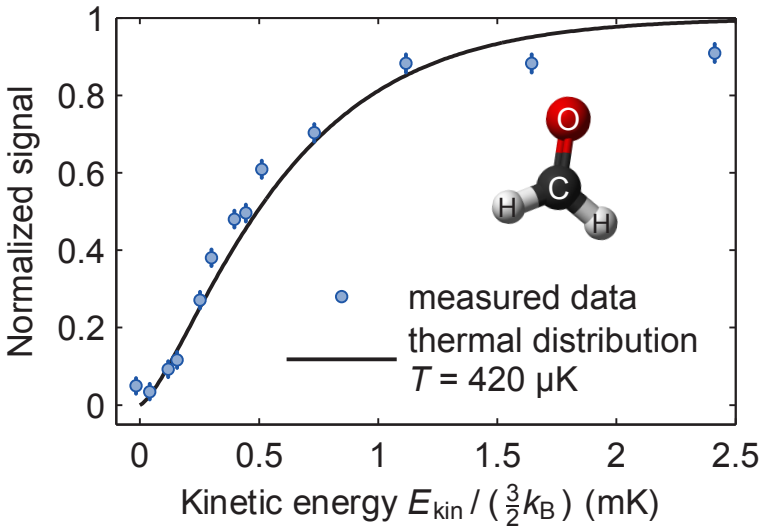

Fig. 1 Measured integral of the kinetic energy distribution of formaldehyde molecules in our trap. The solid curve shown corresponds to a theoretical thermalized sample with a temperature of 420μK.

References

[1] Alexander Prehn, Martin Ibrügger, Rosa Glöckner, Gerhard Rempe, and Martin Zeppenfeld, *Optoelectrical Cooling of Polar Molecules to Submillikelvin Temperatures*, Phys. Rev. Lett. **116**, 063005 (2016).
[2] Barbara G. U. Englert, Manuel Mielenz, Christian Sommer, Josef Bayerl, Michael Motsch, Pepijn W. H. Pinkse, Gerhard Rempe, and Martin Zeppenfeld, *Storage and Adiabatic Cooling of Polar Molecules in a Microstructured Trap*, Phys. Rev. Lett. **107**, 263003 (2011).
[3] Martin Zeppenfeld, Barbara G. U. Englert, Rosa Glöckner, Alexander Prehn, Manuel Mielenz, Christian Sommer, Laurens D. van Buuren, Michael Motsch, and Gerhard Rempe, *Sisyphus cooling of electrically trapped polyatomic molecules*, Nature **491**, 570-573 (2012).
[4] Rosa Glöckner, Alexander Prehn, Barbara G. U. Englert, Gerhard Rempe, and Martin Zeppenfeld, *Rotational Cooling of Trapped Polyatomic Molecules*, Phys. Rev. Lett. **115**, 233001 (2015).

The Magnetic Moment of the Proton and a High-Precision Comparison of the Proton to Antiproton Charge-To-Mass Ratio

Andreas Mooser[1], Klaus Blaum[2], James Harrington[1], Takashi Higuchi[1,3], Nathan Leefer[4], Yasuyuki Matsuda[3], Hiroki Nagahama[1,3], Georg Schneider[1,5], Stefan Sellner[1], Christian Smorra[1,6], Toya Tanaka[1,3], Wolfgang Quint[7], Jochen Walz[4,5], Yasunori Yamazaki[8], Stefan Ulmer[1]

1. Ulmer Initiative Research Unit, RIKEN, 2-1 Hirosawa, Wako, Saitama 351-0198, Japan
2. Max-Planck-Institut für Kernphysik, Saupfercheckweg 1, 69117 Heidelberg, Germany
3. Graduate School of Arts and Science, University of Tokyo, 3-8-1 Komaba, Meguro-ku, Tokyo 153-8902 Japan
4. Helmholz-Institut Mainz, Johann-Joachim-Becher-Weg 36, 55128 Mainz, Germany
5. Institut für Physik, Johannes Gutenberg-Universität Mainz, Staudingerweg 7, 55128 Mainz, Germany
6. CERN, CH-1211 Geneva 23, Switzerland
7. Atomphysik, GSI-Helmholzzentrum für Schwerionenforschung, Planckstraße 1, 64291 Darmstadt, Germany
8. Atomic Physics Laboratory, RIKEN, 2-1 Hirosawa, Wako, Saitama 351-0198, Japan

The Standard Model (SM) of particle physics is known to be incomplete. This inspires various searches for physics beyond the SM, among those, direct high-precision tests of the invariance under the simultaneous transformations of charge conjugation, parity inversion and time reversal (CPT). The goal of the BASE collaboration is to perform such CPT-tests by comparing with highest precision the magnetic moment $\mu_{p,\bar{p}}$ and the charge-to-mass ratio of single protons and antiprotons stored in cryogenic Penning traps at low energy [1].
In a Penning trap the measurement of $\mu_{p,\bar{p}}$ is based on the determination of two frequencies, the Larmor and the cyclotron frequency. Based on a statistical detection of spin transitions we measured the Larmor frequency on a single proton for the first time [2], which resulted in a direct determination of μ_p with a fractional precision at the parts-per-million level [3]. The precision was improved significantly by using a double Penning-trap technique [4]. This required the detection of single spin flips, which was achieved with an improved apparatus and by using Bayesian data analysis [5]. Our developments ultimately culminated in the most precise and first direct high-precision measurement of the proton magnetic moment with a relative precision of 3.3 parts per billion [6].
This method can be directly applied to measure the magnetic moment of the antiproton, to provide one of the most stringent tests of CPT invariance using baryons. Thus we constructed the BASE experiment at the antiproton decelerator of CERN. In our first experimental campaign with the newly implemented apparatus we developed a novel fast measurement procedure for cyclotron frequency comparisons of two individual particles. This enabled us to compare the charge-to-mass ratio of the proton and the antiproton with a fractional precision of 69 parts per trillion, which is the most precise test of CPT-invariance using baryons [7]. Our measurements were performed at cyclotron frequencies of about 30 MHz, which means that in this case CPT symmetry holds at the atto-electronvolt scale. Currently the apparatus is beeing prepared for magnetic moment measurements. A major part of the required techniques has been implemented. In the contribution I will summarize the achievements and give an outlook on future perspectives.

References

[1] Christian Smorra *et al.*, *BASE - The Baryon Antibaryon Symmetry Experiment*, Eur. Phys. J. ST **224**, 14 (2015).
[2] Stefan Ulmer *et al.*, *Observation of Spin Flips with a Single Trapped Proton*, Phys. Rev. Lett **106**, 253001 (2011).
[3] Cricia Rodegheri *et al.*, *An experiment for the direct determination of the g-factor of a single proton in a Penning trap*, New J. Phys. **14**, 063011 (2012).
[4] Andreas Mooser *et al.*, *Demonstration of the Double Penning Trap Technique with a Single Proton*, Phys. Lett. B **723**, 78 (2013).
[5] Andreas Mooser *et al.*, *Resolution of Single Spin-Flips of a Single Proton*, Phys. Rev. Lett **110**, 140405 (2013).
[6] Andreas Mooser *et al.*, *Direct high-precision measurement of the magnetic moment of the proton*, Nature **509**, 596 (2014).
[7] Stefan Ulmer *et al.*, *High-precision comparison of the antiproton-to-proton charge-to-mass ratio*, Nature **524**, 196 (2015).

Gravity tests and precision measurements with a cold atom gradiometer based on Raman and Bragg transitions

Gabriele Rosi[1], Luigi Cacciapuoti[2], Fiodor Sorrentino[3], Marco Prevedelli[4], Giulio D'Amico[1], Marco Menchetti[5] and Guglielmo M. Tino[1]

1. Dipartimento di Fisica e Astronomia & LENS, Università di Firenze, INFN Sezione di Firenze, via Sansone 1, I-50019 Sesto Fiorentino (FI), Italy

2. European Space Agency, Keplerlaan 1, 2201 AZ Noordwijk, The Netherlands

3. Dipartimento di Fisica e Astronomia, Universitá di Bologna, Via Berti-Pichat 6/2, I-40126 Bologna, Italy

4. INFN Sezione di Genova, Via Dodecaneso 33, I-16146 Genova, Italy

5. National Physical Laboratory, Hampton Road, Teddington, TW11 0LW, UK

In this talk we are going to present some of the latest results recently obtained with our cold atom gravity gradiometer.

In the first part a measurement of the gravity curvature generated by nearby source masses using three conjugated atom interferometers [1] is presented. The ability to detect gravity gradient variations can be crucial for the interpretation of survey data [2]. The possibility to use such scheme for a new atom inteferometry-based measurement of the Newtonian constant of gravitation is also discussed [3].

In the second part a novel tests of the Weak Equivalence Principle on quantum states is reported, thanks to the recent implementation of high-order Bragg diffraction transitions for the interferometers. The ability of our scheme to accurately test the universality of free fall on quantum objects could be crucial for future WEP quantum formulations [4].

References

[1] *Atom Interferometry*, Proceedings of the International School of Physics "Enrico Fermi," Course CLXXXVIII, edited by G. M. Tino and M. A. Kasevich (IOS Press,Amsterdam, 2014).

[2] D. A. G. Nowell, *Gravity terrain corrections-an overview*,J. of Appl. Geophysics **42**, 117134 (1999).

[3] G. Rosi, L. Cacciapuoti, F. Sorrentino, M. Menchetti, M. Prevedelli, and G. M. Tino, *Measurement of the Gravity-Field Curvature by Atom Interferometry*, Phys. Rev. Lett. **114**, 013001-1/013001-5 (2015).

[4] M. Zych and C. Brukner, *Quantum formulation of the Einstein Equivalence Principle* arXiv:1502.00971 [gr-qc] (2015).

Two particle interference with cold atoms

Christoph Westbrook, Raphael Lopes, Almazbek Imanaliev, Alain Aspect, Marc Cheneau, Denis Boiron
Laboratoire Charles Fabry, Institut d'Optique Graduate School, CNRS, Université Paris-sud, 2 avenue Fresnel, Palaiseau, 91127 France

The quantum theory has introduced physicists to two major counter-intuitive concepts. On the one hand, there is wave-particle duality, expressing the idea that objects normally described as particles can also behave as waves, while entities primarily described as waves, such as light, can behave as particles. This revolutionary idea nevertheless relies on concepts borrowed from classical physics, either waves or particles evolving in an ordinary space-time. On the other hand, entanglement can lead to interferences between the amplitudes of multi-particle states, which are described via Hilbert space and have no classical counter-part.

This fundamental feature has of course been strikingly demonstrated by the violation of Bell's inequalities. There is however, a conceptually simpler situation in which the interference between two-particle amplitudes entails a behavior impossible to describe by any classical model. This is the celebrated Hong Ou and Mandel experiment, in which two photons arriving simultaneously in the input channels of a beam-splitter always emerge together in one of the output channels. This effect has been extensively used to characterize the quality of non-classical light sources.

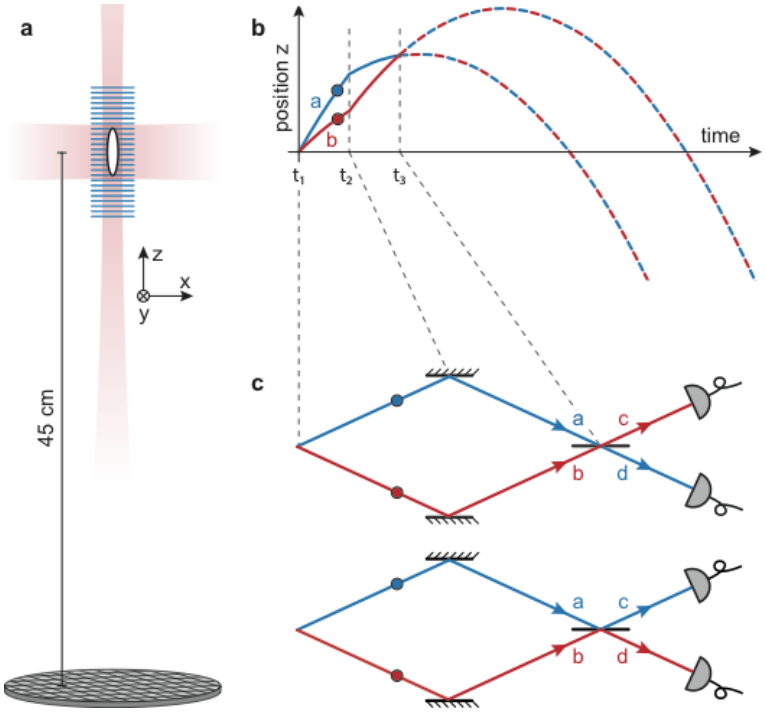

Fig. 1 (a) Schematic diagram of the experiment. Atom pairs are produced in an optical lattice with different momenta along the z axis, and fall to a single particle detector below. (b) Representation of the atomic trajectories along the vertical axis as a function of time. The pairs are produced at time t_1. At time t_2 a laser standing wave induces Bragg diffraction exchanging. the atomic momenta. At time t_3 a second standing wave acts as a beam splitter, mixing the two momentum components. (c) Representation of the atomic trajectories in the center of mass frame. Two input ports a and b and two output ports c and d are shown. The two possibilities that are displayed correspond to quantum amplitudes with opposite signs. They thus interfere destructively causing the cross correlation signal of ports c and d to vanish.

Our group in Palaiseau has recently realized a Hong-Ou-Mandel experiment using metastable helium atoms [1]. A schematic diagram of the apparatus is shown in Fig. 1. We monitor the cross correlation signal between the two output ports $\langle \hat{n}_c \hat{n}_d \rangle$ as a function of the time t_3 of application of the beam splitter. At this time we observe a 65% reduction in the cross correlation. This degree of supression cannot be explained by either a wavelike or particlelike description of the atoms.

References

[1] R. Lopes, A. Imanaliev, A. Aspect, M. Cheneau, D. Boiron, C. I. Westbrook, *Atomic Hong-Ou-Mandel Experiment*, Nature **520**, 66 (2015).

Observation of the Efimov State of the Helium Trimer

M. Kunitski[1], S. Zeller[1], J. Voigtsberger[1], A. Kalinin[1], L. Ph. H. Schmidt[1], M. Schöffler[1], A. Czasch[1], W. Schöllkopf[2], R. E. Grisenti[1], T. Jahnke[1], D. Blume[3] and R. Dörner[1]

1. Institut für Kernphysik, Goethe-Universität Frankfurt am Main, Max-von-Laue-Straße 1, 60438 Frankfurt am Main, Germany

2. Department of Molecular Physics, Fritz-Haber-Institut, Faradayweg 4-6, 14195 Berlin, Germany

3. Department of Physics and Astronomy, Washington State University, Pullman, WA 99164-2814, USA

In 1970 Vitali Efimov predicted remarkable counterintuitive behaviour of a three-body system made up of identical bosons. Namely, a weakening of pair interaction in such a system brings about in the limit appearance of infinite number of bound states of a huge spatial extent [1]. The helium trimer has been predicted to be a molecular system having an excited state of this Efimov character under natural conditions without artificial tuning of the attraction between particles by an external field.

Here we report experimental observation of the Efimov state of $^4He_3$ by means of Coulomb explosion imaging of mass-selected clusters [2]. Helium trimers were prepared under supersonic expansion of the gaseous helium through a 5 µm nozzle. The clusters were selected from the molecular beam by means of matter wave diffraction [3]. Each atom of a trimer was singly ionized by a strong ultrashort laser field resulting in Coulomb explosion of the cluster. The momenta, the ions acquired during Coulomb explosion, were measured by COLTRIMS. These momenta were utilized for reconstruction of the initial spatial geometry of the neutral trimer at the instant of ionization using Newton's equation of motion.

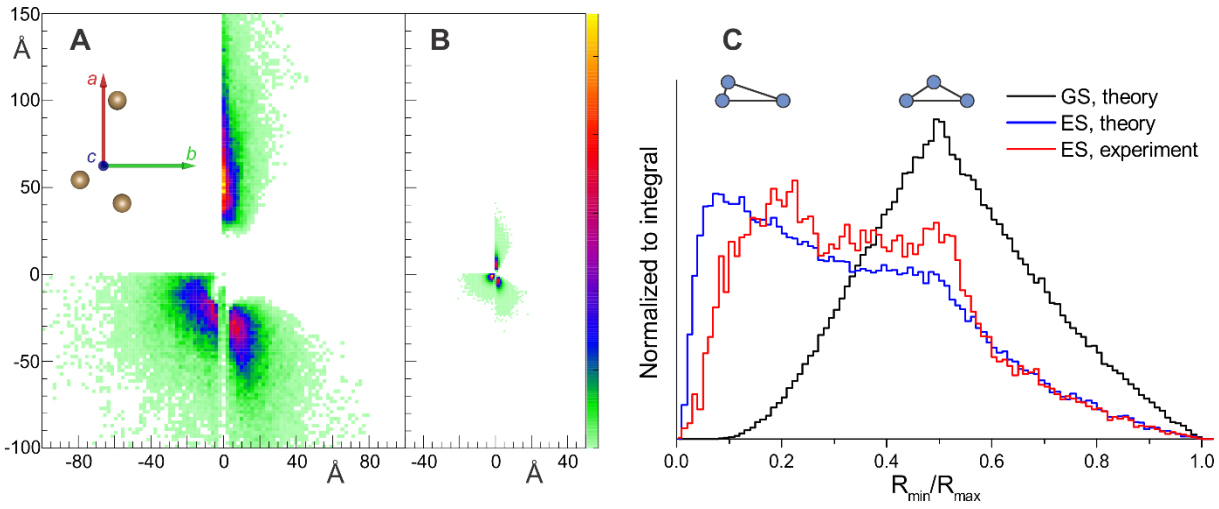

Fig. 1 Structures of the helium trimer: A – excited state, experimental, B – ground state, theoretical. Three helium atoms of each trimer are plotted in the principal axis frame *abc*. C: Distributions of the ratio of the shortest interparticle distance to the longest interparticle distance for ground state structures (black), theoretical excited state structures (blue) and experimental excited state structures (red).

Structures of the excited Efimov state of the $^4He_3$ (Fig. 1A) are about eight times larger than those of the ground state (Fig. 1B), which is in accordance with theory. Whereas the ground state corresponds to an almost randomly distributed cloud of particles [4], the excited Efimov state is dominated by configurations in which two atoms are close to each other and the third one farther away (Fig. 1C).

References

[1] V. Efimov, *Energy Levels Arising from Resonant Two-Body Forces in a Three-Body System*, Phys. Lett. B **33**, 563 (1970).

[2] M. Kunitski, S. Zeller, J. Voigtsberger, A. Kalinin, L. P. H. Schmidt, M. Schöffler, A. Czasch, W. Schöllkopf, R. E. Grisenti, T. Jahnke, D. Blume, and R. Dörner, *Observation of the Efimov State of the Helium Trimer*, Science **348**, 551 (2015).

[3] W. Schöllkopf, J. P. Toennies, *Nondestructive Mass Selection of Small van der Waals Clusters*, Science **266**, 1345 (1994).

[4] J. Voigtsberger, S. Zeller, J. Becht, N. Neumann, F. Sturm, H.-K. Kim, M. Waitz, F. Trinter, M. Kunitski, A. Kalinin, J. Wu, W. Schöllkopf, D. Bressanini, A. Czasch, J. B. Williams, K. Ullmann-Pfleger, L. P. H. Schmidt, M. S. Schöffler, R. E. Grisenti, T. Jahnke, and R. Dörner, *Imaging the Structure of the Trimer Systems $^4He_3$ and $^3He^4He_2$*, Nat. Comm. **5**, 5765 (2014).

Photoionization and Photofragmentation of $Lu_3N@C_{80}^{q+}$ Ions (q = 1, 2, 3)

Jonas Hellhund[1], Alexander Borovik Jr.[2], Kristof Holste[2], Stephan Klumpp[3], Michael Martins[3], Sandor Ricz[4], Stefan Schippers[2], and Alfred Müller[1]

1. Institut für Atom- und Molekülphysik, Justus-Liebig-Universität Gießen, 35392 Giessen, Germany
2. I. Physikalisches Institut, Justus-Liebig-Universität Gießen, 35392 Giessen, Germany
3. Institut für Experimentalphysik, Universität Hamburg, 22761 Hamburg, Germany
4. Institute for Nuclear Research, Hungarian Academy of Sciences, Debrecen, H-4001, Hungary

We have measured cross sections for photoionization and photofragmentation of endohedral fullerene ions $Lu_3N@C_{80}^{q+}$ (q=1,2,3) [1] employing the photon-ion merged-beams technique at the PIPE end-station [2] of beamline P04 of the PETRA III synchrotron at DESY in Hamburg, Germany. The photo-reaction channels $Lu_3N@C_{80}^{q+} \rightarrow Lu_3N@C_{80-2r}^{p+}$ [q=1,2,3; p=2,3,4,5,6; r=0,1,3,4] were investigated in the photon energy ranges 280–330 eV around the carbon K-shell threshold, 380–435 eV around the nitrogen K-Shell threshold, and 1500–1700 eV around the lutetium M-shell threshold. The present work extends recent studies on (endohedral) fullerenes [3-6] to a heavier and more complex species as well as to higher photon energies.

In the energy range between 280 and 330 eV we could identify the same group of resonances in all investigated reaction channels. Since this group of resonances seems to make up for the most prominent structures in all spectra, we attempted to model each spectrum (for examples see Fig. 1) as a sum of seven Fano line shapes (full lines), a threshold feature (dashed line), and a constant background (dash-dotted line). The relative strengths of the resonance peaks (labeled 1 through 7) are given by the vertical blue bars in the insets of the figure. In the multiple ionization channels, a threshold can be observed at about 294 eV, in addition. We observe a shift of the ionization threshold towards higher photon energies when comparing double ionization of $Lu_3N@C_{80}^{2+}$ with double ionization of $Lu_3N@C_{80}^{+}$. We can determine the size of the endohedral fullerene ion based on this threshold shift. The cross sections measured at higher photon energies of 380–435 eV and of 1500–1700 eV show no structures and decrease with increasing photon energy.

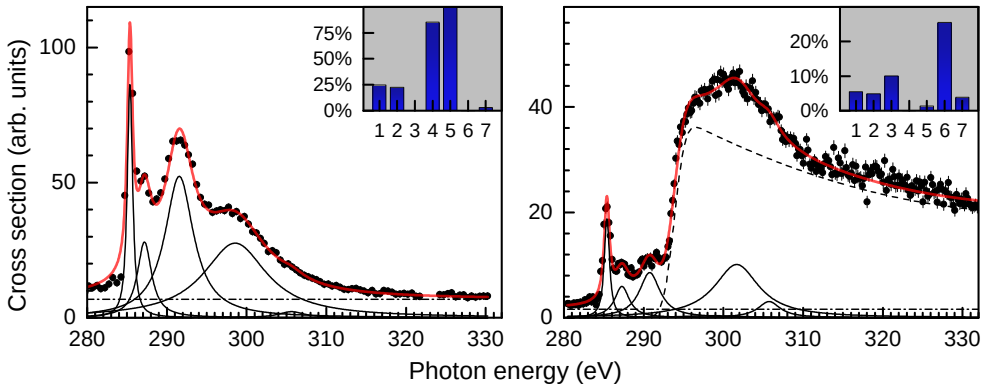

Fig. 1 Measured (symbols) and fitted (lines) cross sections for single (left) and double (right) photoionization of $Lu_3N@C_{80}^{+}$.

References

[1] J. Hellhund, A. Borovik Jr., K. Holste, S. Klumpp, M. Martins, S. Ricz, S. Schippers, and A. Müller, *Photoionization and photofragmentation of multiply charged $Lu_3N@C_{80}$ ions*, Phys. Rev. A **92**, 013413 (2015).

[2] S. Schippers, S. Ricz, T. Buhr, A. Borovik Jr., J. Hellhund, K. Holste, K. Huber, H.-J. Schäfer, D. Schury, S. Klumpp, K. Mertens, M. Martins, R. Flesch, G. Ulrich, E. Rühl, T. Jahnke, J. Lower, D. Metz, L. P. H. Schmidt, M. Schöffler, J. B. Williams, L. Glaser, F. Scholz, J. Seltmann, J. Viefhaus, A. Dorn, A. Wolf, J. Ullrich, and A. Müller, *Absolute cross sections for photoionization of Xe^{q+} ions ($1 \leq q \leq 5$) at the 3d ionization threshold (J. Phys. B Highlight 2014)*, J. Phys. B **47**, 115602 (2014).

[3] K. K. Baral, N. B. Aryal, D. A. Esteves-Macaluso, C. M. Thomas, J. Hellhund, R. Lomsadze, A. L. D. Kilcoyne, A. Müller, S. Schippers, and R. A. Phaneuf, *Photoionization and photofragmentation of the C_{60}^{+} molecular ion*, Phys. Rev. A **93**, 033401 (2016).

[4] R. A. Phaneuf, A. L. D. Kilcoyne, N. B. Aryal, K. K. Baral, D. A. Esteves-Macaluso, C. M. Thomas, J. Hellhund, R. Lomsadze, T. W. Gorczyca, C. P. Ballance, S. T. Manson, M. F. Hasoglu, S. Schippers, and A. Müller, *Probing confinement resonances by photoionization of Xe inside a C_{60}^{+} cage*, Phys. Rev. A **88**, 053402 (2013).

[5] A. L. D. Kilcoyne, A. Aguilar, A. Müller, S. Schippers, C. Cisneros, G. Alna'Washi, N. B. Aryal, K. K. Baral, D. A. Esteves, C. M. Thomas, and R. A. Phaneuf, *Confinement resonances in photoionization of $Xe@C_{60}^{+}$*, Phys. Rev. Lett. **105**, 213001 (2010).

[6] A. Müller, S. Schippers, M. Habibi, D. Esteves, J. C. Wang, R. A. Phaneuf, A. L. D. Kilcoyne, A. Aguilar, and L. Dunsch, *Significant redistribution of Ce 4d oscillator strength observed in photoionization of endohedral $Ce@C_{82}^{+}$ ions*, Phys. Rev. Lett. **101**, 133001 (2008).

An Atomically Thin Matter-Wave Beam Splitter

Christian Brand[1], Michele Sclafani[1,2], Christian Knobloch[1], Yigal Lilach[3], Thomas Juffmann[1,4], Jani Kotakoski[5], Clemens Mangler[5], Andreas Winter[6], Andrey Turchanin[6], Jannik Meyer[5], Ori Cheshnovsky[3,7], and Markus Arndt[1]

1. University of Vienna, Faculty of Physics, VCQ, Boltzmanngasse 5, 1090 Vienna, Austria
2. ICFO - Institut de Ciènces Fotòniques, 08860 Castelldefels (Barcelona), Spain.
3. The Center for Nanosciences and Nanotechnology at Tel Aviv University
4. Department, Stanford University, 382 Via Pueblo Mall, Stanford, California 94305-4060, USA.
5. Faculty of Physics, University of Vienna, PNM, Boltzmanngasse 5, A-1090 Vienna, Austria
6. Friedrich Schiller University Jena, Institute of Physical Chemistry, Lessingstrasse 10, D-07743 Jena, Germany
7. Tel Aviv University, School of Chemistry, The Raymond and Beverly Faculty of Exact Sciences, Tel Aviv 69978, Israel

Matter-wave interferometry has matured into a highly sensitive tool for fundamental tests in physics, sensing miniscule forces and tiny length deviations. A requirement for any interferometric study is the coherent splitting of the incident wave in two or more parts which experience different phase shifts before they are recombined. Due to their internal level structure, refined laser schemes as used in atom interferometry cannot be applied to large polyatomic molecules. An alternative approach is based on nano-patterned mechanical gratings where the diffraction process is independent from the internal complexity of the diffracted object [1,2]. However, the universality of this approach is limited by the attractive van der Waals interactions between the matter-wave and the grating.

Here, I will present how to reduce the van der Waals interaction by minimizing the grating thickness to its ultimate limit - a single atomic layer [3]. We managed, for the first time, to pattern free-standing single layer graphene membranes with a period as small as $d = 100$ nm over large areas to diffract massive organic dye molecules. In a comprehensive study we compare the performance of several gratings with a thickness ranging between 0.3 and 90 nm. From the relative population of the individual far-field diffraction orders we deduce surprisingly large van der Waals interactions for these ultra-thin masks. For thick gratings we observe a matter-wave separation between the extreme orders of up to $18\,h/d$, corresponding to about $140\,\hbar$k for an alkali atom. This may allow to build compact rugged interferometers in the future. For the thinnest conceivable grating, however, the van der Waals interaction is minimized and only the zeroth and first diffraction orders are sizeably populated. This facilitates the high contrast diffraction of complex molecules. Furthermore, we find conditions which lead to the formation of nanoscrolls from single layer graphene ribbons. These optimize opening fraction of the grating, leading to an additional reduction in the van der Waals attraction.

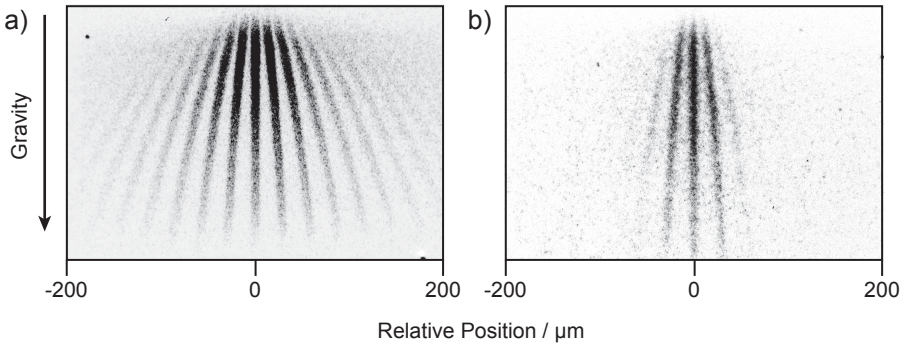

Fig. 1 Molecular diffraction at a 90 nm thick silicon nitride grating results in a population of up to the $\pm 9.th$ diffraction order (a). The observation of only three dominant diffraction orders for single layer graphene (b) illustrates the strong reduction in the attractive interaction between the grating and the matter-wave.

References

[1] D. W Keith, M. L. Schattenburg, H. I. Smith and D. E. Pritchard, *Diffraction of Atoms by a Transmission Grating*, Phys. Rev. Lett. **61**, 1580 (1988).
[2] Wieland Schöllkopf and Jan-Peter Toennies, *Nondestructive Mass Selection of Small Van der Waals Clusters*, Science **266**, 1345 (1994).
[3] Christian Brand, Michele Sclafani, Christian Knobloch, Yigal Lilach, Thomas Juffmann, Jani Kotakoski, Clemens Mangler, Andreas Winter, Andrey Turchanin, Jannik Meyer, Ori Cheshnovsky, and Markus Arndt, *An atomically thin matter-wave beamsplitter*, Nat. Nanotechnol. **10**, 845 (2015).

Observation of Atom-Wave Beats Using a Kerr Modulator for Atom Waves

Boris Décamps, Jonathan Gillot, Jacques Vigué, Alexandre Gauguet, and Matthias Büchner

Laboratoire Collisions Agrégats Réactivité-IRSAMC, Université de Toulouse-UPS and CNRS UMR 5589, Toulouse, France

Wave beating is a very important phenomenon in physics: it was discovered with acoustic waves and is commonly used in electromagnetics, from the radio frequency to the laser domain. Obviously, wave beating can be extended to matter waves if a coherent superposition of quantum states with different kinetic energies can be achieved. ***This is precisely what we have observed with our lithium atom interferometer!***

We modulate the phase of an atom wave by applying time dependent, sinusoidal varying electric fields, i.e. we realize the equivalent of a Kerr modulator for atom waves [1]. These sinusoidal phase modulations are detectable in the interference signal, shown in Fig. 1. This signal exhibits time dependence, i.e. the fingerprint of atom wave beats. A Fourier analysis reveals the presence of the beat frequency and its harmonics. We varied the phase modulation depth (Fig.2) and the amplitude of the p^{th} harmonics modulation shows a Bessel-like behavior, in good agreement with theory.

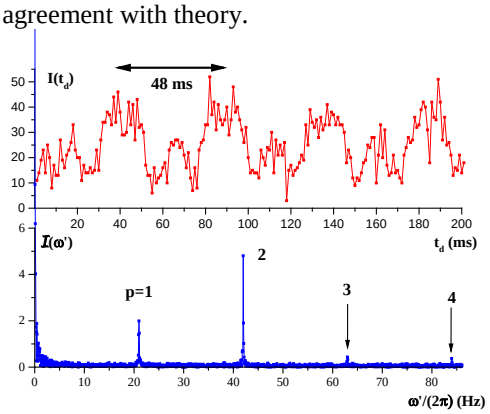

Fig. 1: The interferometer signal in the presence of a phase modulation oscillating at a frequency $\omega/(2\pi)= 21$ Hz.
Top panel: Direct recording of the interferometer signal.
Bottom panel: Modulus of the Fourier transform of a 16.4 s-long record of the signal.

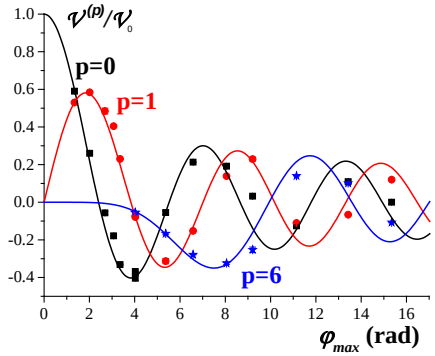

Fig. 2: Amplitude of modulation of the p^{th} harmonics as a function of the amplitude φ_{max} of the phase modulation. The curves are our theoretical results with no free parameters and the symbols (p=0: squares; p=1: bullets; p=6: stars) our measurements.

We have also made experiments with the two arms modulated with different frequencies. Each modulation is too fast to be detected, but we observe the beat at the frequency difference and its harmonics: this is a heterodyne experiment with matter waves.

Our method to create phase modulation can be extended to other matter waves. Especially its extension to electron waves can open fascinating opportunities. In electron holography microscopy, it should make it possible to measure the response of a sample with very high spatial and temporal resolutions.

We also used our set-up for educational goals, i.e. we transmit information by phase modulations. Fig. 3 shows a digitalized image, we have transmitted pixel per pixel by atom wave phase modulation [1].

Fig.3: Image [2] transmitted by atom wave phase modulation: ca. 96000 pixels were transmitted at 200 pixels/second with an error rate below 0.1%.

References

[1] B. Décamps, J. Gillot, J. Vigué, A. Gauguet, and M. Büchner, *Observation of Atom-Wave Beats Using a Kerr Modulator for Atom Wave* Phys.Rev. Lett. **116, 053004 (2016),** **http://dx.doi.org/10.1103/PhysRevLett.116.053004**

[2] Original image: Peter August Böckstiegel,Westphalian expressionist,, Self-portrait, 1917/1918; wood-cut; http://www.paboeckstiegel.de/

$\overline{\mathrm{H}}^+$ production from Collisions between Positronium and keV Antiprotons for GBAR

Paul-Antoine Hervieux[1] **,** ***Pauline Comini***[2]

1.Institut de Physique et Chimie des Matériaux de Strasbourg, CNRS and Université de Strasbourg, F-67000 Strasbourg, France

2. ETH Zurich, Institute of Particle Physics, Zurich, Switzerland

The GBAR experiment (Gravitational Behavior of Antihydrogen at Rest) [1] was recently accepted at CERN at its Antiproton Decelerator facility. The aim of the experiment is to perform the free fall of antihydrogen atoms $\overline{\mathrm{H}}$ to test the weak equivalence principle for antimatter. In order to reduce the uncertainty on the initial $\overline{\mathrm{H}}$ velocity, ultra-cold antihydrogen atoms of a few neV are required. The key idea of the GBAR experiment is to use $\overline{\mathrm{H}}^+$ ions that can be cooled with techniques established for ultra-cold atoms [2]. The $\overline{\mathrm{H}}^+$ ions will be produced from collisions between keV antiprotons $\overline{\mathrm{p}}$ and a positronium Ps cloud through two successive reactions: (1) $\overline{\mathrm{p}} + \mathrm{Ps}(n_p, l_p) \rightarrow \overline{\mathrm{H}}(n_h, l_h) + \mathrm{e}^-$ (3-body reaction) and (2) $\overline{\mathrm{H}}(n_h, l_h) + \mathrm{Ps}(n_p, l_p) \rightarrow \overline{\mathrm{H}}^+ + \mathrm{e}^-$ (4-body reaction). A theoretical study of reactions (1) & (2) has been undertaken in order to optimize the $\overline{\mathrm{H}}^+$ production by choosing accurately the energy of the $\overline{\mathrm{p}}$ beam and the Ps excited states (n_p, l_p). An exhaustive set of cross sections has been obtained for both reactions, from Ps(*1s*) to Ps(*3d*) and considering $\overline{\mathrm{H}}$ states up to $n_h = 4$. Contrary to reaction (2), reaction (1) has been already widely investigated, mainly through the reverse reaction of Ps formation (see for instance [3-4]), but for the sake of theoretical consistency, it has been decided to apply the same theoretical model, namely the Continuum Distorted Wave – Final State model (CDW-FS), to compute the cross sections of both reactions at the same level of approximation [5]. Concerning reaction (2), the highly correlated system formed by $\overline{\mathrm{H}}^+$ has been treated carefully, using three different wave functions proposed for H^- [6]. In the case of reaction (1), the results show an enhancement of the $\overline{\mathrm{H}}$ production toward low $\overline{\mathrm{p}}$ kinetic energies, when n_h and n_p increase. This agrees with experimental data [7] and previous calculations [3]. For reaction (2), a nearly resonant behavior close to threshold is observed for excited positronium, when $\overline{\mathrm{H}}$ is in its ground state. For both reactions, above 1 keV $\overline{\mathrm{p}}$ energy, the highest cross sections are obtained with Ps(*2p*).

In order to estimate the $\overline{\mathrm{H}}^+$ production in the reaction chamber of the GBAR experiment and optimize other experimental parameters such as laser power for Ps excitation and delays between pulses, a simulation based on the present cross sections, solving Bloch equations to compute the Ps populations, has been implemented. This highlights the challenges to be solved in this critical part of GBAR.

References

[1] The GBAR Collaboration 2011 CERN-SPSC-2011-029, SPSC-342.
[2] P. Perez et al., Hyperfine Interactions **233**, 21 (2015).
[3] J. Mitroy, Phys. Rev. A **52**, 2859 (1995).
[4] A. S. Kadyrov, C. M. Rawlins, A. T. Stelbovics, I. Bray, and M. Charlton, Phys. Rev. Lett. **114**, 183201 (2015).
[5] P. Comini and P. –A. Hervieux, New Journal of Physics **15**, 095022 (2013).
[6] C. Le Sech, J. Phys. B **30**, L47 (1997).
[7] J. P. Merrison et al., Phys. Rev. Lett. **78**, 2728 (1997).

Coulomb Crystallization of Highly Charged Ions

Lisa Schmöger[1,2], O. O. Versolato[1,2], M. Schwarz[1,2], M. Kohnen[2], A. Windberger[1], B. Piest[1], S. Feuchtenbeiner[1], J. Pedregosa[3], T. Leopold[2], P. Micke[1,2], A. K. Hansen[4], T. M. Baumann[1], M. Drewsen[4], Thomas Pfeifer[1], J. Ullrich[2], P. O. Schmidt[2,5], J. R. Crespo López-Urrutia[1]

1. Max-Planck-Institut für Kernphysik, Saupfercheckweg 1, 69117 Heidelberg, Germany

2. Physikalisch-Technische-Bundesanstalt, Bundesallee 100, 38116 Braunschweig, Germany

3. Aix-Marseille Université, Centre universitaire de St Jerome - Case C21, Ave Escadrille Normandie-Niémen, 13397 Marseille, France

4. Aarhus University, Department of Physics and Astronomy, Bygning 1520, Ny Munkegade, 8000 Aarhus C, Denmark

5. Institut für Quantenoptik, Leibniz Universität, Welfengarten 1, 30167 Hannover, Germany

With the ability to simultaneously control both the excitation and the motional degrees of freedom of individual quantum objects, atomic physics has reached a degree of accuracy without peer among the experimental sciences. Immediate practical consequences are the development of atomic and optical clocks. These are meanwhile capable of measuring subtle effects of relativity and even of setting upper limits to possible variations of fundamental constants. In principle, the binding energy of atomic electrons in their ground state is sensitive to all levels of Standard Model physics. Their wavefunction adapts to all small contributions arising from all known interactions. This universal pattern of sensitivity is expected to appear again if forces beyond the Standard Model were to exist.

In highly charged ions (HCIs), the wavefunction of the optically E1-forbidden active electron is much reduced in size. This implies magnified sensitivity to electron-nucleus interactions and QED terms in general, and an extremely suppressed sensitivity to external field perturbations. Further, E1 forbidden optical transitions found near level crossings in HCIs are extremely sensitive to possible drifts in the fine structure constant. This favorable combination of properties has been widely recognized as an advantage for precision studies with HCIs and the development of HCI based clocks in many recent theoretical works. However, there has been a persistent experimental problem hindering improved photonic studies with HCIs: All known sources of HCIs produce them at high temperatures, typically in the MK regime. Bringing these translational temperatures down to the mK scale has been a long and elusive target of various experimental groups.

We have developed an experiment for retrapping, cooling and high-precision laser spectroscopy of HCIs [1]. It is based on continuously laser-cooled Be^+ Coulomb crystals in a linear cryogenic Paul trap [2] for stopping the motion of externally produced HCIs and sympathetically cooling them below 250 mK. This cooling induces the formation of stable mixed crystals – down to a single HCI cooled by a single co-trapped Be^+ ion [3]. The strongly suppressed thermal motion of the embedded HCIs offers novel possibilities for investigation of questions regarding the time variation of fundamental constants, parity non-conservation effects, and quantum electrodynamics. Our current work aims at high-precision spectroscopy of the $^2P_{1/2}$ - $^2P_{3/2}$ M1 transition at 441 nm in cold Ar^{13+} ions. Adding HCIs to the quantum toolbox is the ultimate goal within the scope of next-generation experiments, which are currently being set up. One aims at applying quantum logic schemes to HCIs and developing an HCI optical clock, the other one at direct VUV frequency comb spectroscopy of transitions in HCIs.

References

[1] L. Schmöger et al., *Deceleration, precooling, and multi-pass stopping of highly charged ions in Be+ Coulomb crystals*, Rev. Sci. Instrum. **86**, 103111 (2015)

[2] M. Schwarz et al., *Cryogenic linear Paul trap for cold highly charged ion experiments*, Rev. Sci. Instrum. **83**, 083115 (2012)

[3] L. Schmöger, O. O. Versolato, M. Schwarz, M. Kohnen, A. Windberger, B. Piest, S. Feuchtenbeiner, J. Pedregosa-Gutierrez, T. Leopold, P. Micke, A. K. Hansen, T. M. Baumann, M. Drewsen, J. Ullrich, P. O. Schmidt and J. R. Crespo López-Urrutia , *Coulomb crystallization of highly charged ions* , Science **347**, 1233 (2015).

New methods and approaches in high-resolution spectroscopy of ultracold atoms and ions

Alexey Taichenachev[1,2], Valeriy Yudin[1,2], and Sergey Bagayev[1,2]

1. Institute of Laser Physics, Novosibirsk, Russia
2. Novosibirsk State University, Novosibirk, Russia

Presently, laser spectroscopy and fundamental metrology are among the most important and actively developed directions in modern physics. Frequency and time are the most precisely measured physical quantities, which, apart from practical applications (in navigation and information systems), play critical roles in tests of fundamental physical theories (such as QED, QCD, unification theories, and cosmology) [1,2]. Now, laser metrology is confronting the challenging task of creating an optical clock with fractional inaccuracy and instability at the level of 10^{-17} to 10^{-18}. Indeed, considerable progress has already been achieved along this path for both ion-trap- [3,4] and atomic-lattice-based [5,6] clocks.

Work in this direction has stimulated the development of novel spectroscopic methods such as spectroscopy using quantum logic [7], magnetically induced spectroscopy [8], hyper-Ramsey spectroscopy [9], spectroscopy of "synthetic" frequency [10] and others [11]. Part of these methods was developed in order to excite and detect strongly forbidden optical transitions. The other part fights with frequency shifts of various origins. In the present talk we will review both parts with a special emphasis on methods developed and studied in Institute of Laser Physics SB RAS, Novosibirsk. The history and present status of experimental works devoted to the optical frequency standards will be discussed.

Our work is supported by Russian Foundation for Basic Research (grants nos. 14-02-00712, 14-02-00806, 14-02-00939, 15-02-08377, 15-32-20330), Ministry of Education and Science of Russian Federation (State Assignment № 2014/139 project № 825), Russian Academy of Sciences, and by a grant of President of RF (NSH-4096.2014.2).

References

[1] S. N. Bagayev *et al.*, Appl. Phys. B **70**, 375 (2000).
[2] S. A. Diddams *et al.*, Science **306**, 1318 (2004).
[3] T. Rosenband *et al.*, Science **319**, 1808 (2008); C.W. Chou *et al.*, Phys. Rev. Lett. **104**, 070802 (2010).
[4] N. Huntemann *et al.*, Phys. Rev. Lett. **116**, 063001 (2016).
[5] T. Akatsuka,M. Takamoto, and H. Katori, Nature Physics **4**, 954 (2008).
[6] N. Hinkley *et al.*, Science **341**, 1215 (2013); B.J. Bloom *et al.*, Nature **506**, 71 (2014).
[7] P. O. Schmidt *et al.*, Science **309**, 749 (2005).
[8] A. Taichenachev *et al.*, Phys. Rev. Lett. **96**, 083001 (2006); Z. Barber *et al.*, Phys. Rev. Lett. **96**, 083002 (2006).
[9] V. Yudin *et al.*, Phys. Rev. A **82**, 011804(R) (2010); N. Huntemann *et al.*, Phys. Rev. Lett. **109**, 213002 (2012).
[10] V. Yudin *et al.*, Phys. Rev. Lett. **107**, 030801 (2011).
[11] V. Yudin *et al.*, Phys. Rev. Lett. **113**, 233003 (2014).